

**ABSTRACTS OF THE THIRTY-FIRST ANNUAL  
MID WINTER RESEARCH MEETING  
OF THE**

---

**A**ssociation for  
**R**esearch in  
**O**tolaryngology

---

**February 16-21, 2008**

**Phoenix, Arizona, USA**

**Peter A. Santi, PhD**  
*Editor*

Association for Research in Otolaryngology  
19 Mantua Road, Mt. Royal, NJ 08061 USA

## CONFERENCE OBJECTIVES

After attending the Scientific Meeting participants should be better able to:

1. Understand current concepts of the function of normal and diseased ears and other head and neck structures.
2. Understand current controversies in research methods and findings that bear on this understanding.
3. Understand what are considered to be the key research questions and promising areas of research in otolaryngology.

ISSN-0742-3152

The *Abstracts of the Association for Research in Otolaryngology* is published annually and consists of abstracts presented at the Annual MidWinter Research Meeting. A limited number of copies of this CD and previous books of abstracts (1978-2007) are available.

Please address your order or inquiry to:  
**Association for Research in Otolaryngology**  
19 Mantua Road  
Mt. Royal, NJ 08061 USA

**General Inquiry**  
Phone (856) 423-0041 Fax (856) 423-3420  
E-Mail: [headquarters@aro.org](mailto:headquarters@aro.org)

**Meetings**  
E-Mail: [meetings@aro.org](mailto:meetings@aro.org)

This book was prepared from abstracts that were entered electronically by the authors. Authors submitted abstracts over the World Wide Web using Mira Digital Publishing's PaperCutter™ Online Abstract Management System. Any mistakes in spelling and grammar in the abstracts are the responsibility of the authors. The Program Committee performed the difficult task of reviewing and organizing the abstracts into sessions. The Program Committee Chair, Dr. John Middlebrooks and the President, Dr. P. Ashley Wackym constructed the final program. Mira electronically scheduled the abstracts and prepared Adobe Acrobat pdf files of the Program and Abstract Books. These abstracts and previous years' abstracts are available at: <http://www.aro.org>.

Citation of these abstracts in publications should be as follows:

**Authors, year, title, Assoc. Res. Otolaryngol. Abs.: page number.**

For Example:

Moore, Brian C.J., 2007, Using Psychoacoustics to Explore Cochlear Function: Basic Mechanisms and Applications to Hearing Aids, Assoc. University of Cambridge, Abs.: 942.



General Chair

P. Ashley Wackym, MD (2007-2008)

Program Organizing Committee

John C. Middlebrooks, PhD, *Chair* (2005-2008),  
*Council Liaison* (2007-2008)

David P. Corey, PhD (2006-2009)

J. David Dickman, PhD (2005-2008)

Robert Frisina, PhD (2006-2009)

Timothy E. Hullar, MD (2007-2010)

Bronya J. Keats, PhD (2007-2010)

Sharon G. Kujawa, PhD (2005-2008)

Sandra McFadden, PhD (2006-2009)

Xiaoqin Wang, PhD (2005-2008)

Jeffrey J. Wenstrup, PhD (2007-2010)

Tom C.T. Yin, PhD (2005-2008)

Program Publications

Peter A. Santi, PhD, *Editor* (2000-2009)

Animal Research

Michael Anne Gratton, PhD, *Chair* (2006-2009)

Kumar N. Alagramam, PhD (2007-2010)

Elisabeth Glowatzki (2005-2008)

Cornelis Jan Kros, MD, PhD (2006-2009)

Charles J. Limb, MD, PhD (2007-2010)

Charles A. Miller, PhD (2006-2009)

John S. Oghalai, MD (2007-2010)

Paul Popper, PhD (2005-2008)

Edward J. Walsh, PhD (2006-2009)

Award of Merit Committee

Donata Oertel, PhD, *Chair* (2006-2009)

Robert A. Dobie, MD (2006-2009)

Edwin M. Monsell, MD, PhD (2007-2010)

J. Christopher Post, MD, PhD (2007-2010)

William S. Rhode, PhD (2005-2008)

Murray B. Sachs, PhD (2005-2008)

Historian David Lim, MD, *Council Liaison* (2007-2008)

Diversity & Minority Affairs

Vishakha W. Rawool, PhD, *Chair* (2007-2010)

David Z.Z. He, MD, PhD (2006-2009)

Ivan A. Lopez, PhD (2007-2010)

Robert M. Raphael, PhD (2007-2010)

Lina A. Reiss, PhD (2006-2009)

Barbara G. Shinn-Cunningham, PhD (2006-2009)

Ebenezer Nketia Yamoah, PhD (2006-2009)

Editor Advisory

Peter A. Santi, PhD, *Chair* (2000-2009)

Gerald Popelka, PhD, *Past Editor*

John C. Middlebrooks, PhD, *Program Committee Chair*

Darla M. Dobson, *Executive Director*

Education Committee

Alan G. Micco, MD *Chair* (2005-2008)

Ann Eddins, PhD, *Co-Chair* (2006-2009)

David J. Brown, MD (2005-2008)

David M. Harris, PhD (2006-2009)

Timothy E. Hullar, MD (2005-2008)

Brian M. McDermott, PhD (2007-2010)

Christina Runge-Samuels, PhD (2007-2010)

Neil Segil, PhD (2006-2009)

John C. Middlebrooks, PhD, *Council Liaison* (2007-2008)

Government Relations Committee  
**Maureen Hannley, PhD, Chair (2007-2010)**  
**H. Alexander Arts, MD (2007-2010)**  
**Marian J. Drescher, PhD (2006-2009)**  
**Gay R. Holstein, PhD (2005-2008)**  
**Walt Jesteadt, PhD (2006-2009)**  
**Cliff A. Megerian, MD (2007-2010)**  
**Ted A. Meyer, MD, PhD (2007-2010)**  
**Richard T. Miyamoto, MD (2005-2008)**  
**Jay T. Rubinstein, MD, PhD (2005-2008)**  
**Nigel K. Woolf, ScD (2006-2009)**  
**David J. Lim, MD, Council Liaison, ex officio (2007-2008)**

Graduate Student Travel Awards  
**Paul Popper, PhD, Chair (2007- 2010)**  
**Paul J. Abbas, PhD (2006-2009)**  
**Deniz Baskent, PhD (2006-2009)**  
**Janet L. Cyr, PhD (2006-2009)**  
**Larry F. Hoffman, PhD (2007-2010)**  
**Suhua Sha, MD (2006-2009)**  
**Katherine Shim, PhD (2007-2010)**

International Committee  
**Karen B. Avraham, PhD Chair (2005-2008)**  
**Barbara Canlon, PhD, Sweden (2007-2010)**  
**Lin Chen, PhD, China (2006-2009)**  
**Chunfu Dai, MD, PhD, China (2005-2008)**  
**Bernhard Gaese, PhD, Germany, (2005-2008)**  
**Timo Petteri Hirvonen, MD, PhD, Finland (2005-2008)**  
**Philip X. Joris, MD, PhD, Belgium (2006-2009)**  
**Glenis R. Long, PhD, USA (2006-2009)**  
**David McAlpine, United Kingdom (2006-2009)**  
**Seung Ha Oh, MD, PhD, Korea (2007-2010)**  
**HongJu Park, MD, Korea (2005-2008)**  
**Nicolas Perez, MD, Spain (2005-2008)**  
**Allesandro Rinaldo, MD, Italy (2007-2010)**  
**Shu Hui Wu, MD, Canada (2005-2008)**  
**Karen B. Avraham, PhD, Council Liaison (2007-2008)**

JARO Editorial Board  
**Ruth Anne Eatock, PhD, Editor-in-Chief (2011)**  
**J. David Dickman, PhD (2009)**  
**Paul A. Fuchs, PhD (2009)**  
**Matthew C. Holley, PhD (2007)**  
**Gary D. Housley, PhD (2007)**  
**Marci M. Lesperance, MD (2009)**  
**Paul B. Manis, PhD (2009)**  
**Teresa A. Nicolson, PhD (2009)**  
**Andrew J. Oxenham, PhD (2009)**  
**Jay T. Rubinstein, MD, PhD (2007)**  
**Mario A. Ruggero, PhD (2007)**  
**Alec N. Salt, PhD (2009)**  
**Terry T. Takahashi, PhD (2009)**  
**Tom C. T. Yin, PhD (2007)**  
**Fan-Gang Zeng, PhD (2009)**

JARO (Publications Committee)  
**Debara L. Tucci, MD, Chair (2007- 2010)**  
**Catherine E. Carr, PhD (2008-2011)**  
**Monita Chatterjee, PhD (2006-2009)**  
**Richard A. Chole, MD, PhD (2005-2008)**  
**Donna M. Fekete, PhD (2006-2009)**  
**Rick A. Friedman, MD, PhD (2007- 2010)**  
**Keiko Hirose, MD (2004-2010)**  
**Clifford R. Hume, MD, PhD (2008-2011)**  
**Marlies Knipper, PhD (2004-2008)**  
**Christine Koepl (2006-2009)**  
**Jian-Dong Li, MD, PhD (2005-2008)**  
**Zhijun Shen, MD (2008-2011)**  
**Dennis R. Trune, PhD, MBA (2007- 2010)**  
**D. Bradley Welling, MD, PhD (2007- 2010)**  
**Eric D. Young, PhD (2008-2011)**  
**Ruth Anne Eatock, PhD, JARO Editor, ex officio**  
**Joseph E. Burns, Springer Representative, ex officio**  
**Peter A. Santi, PhD (2007-2008), Council Liaison**  
**Steven Rauch, MD, Secretary/Treasurer, ex officio**

Long Range Planning Committee  
**Robin L. Davis, PhD Chair (2005-2008)**  
**Barbara Canlon, PhD (2005-2008)**  
**Thomas E. Carey, PhD (2007-2010)**  
**Paul A. Fuchs, PhD (2005-2008)**  
**Steven H. Green, PhD (2005-2008)**  
**Timothy E. Hullar, MD (2007-2010)**  
**Manuel S. Malmierca, MD, (2006-2009)**  
**Marci M. Lesperance, MD (2007-2010)**  
**J. Christopher Post, MD, PhD (2005-2008)**  
**Yehoash Raphael, PhD (2006-2009)**  
**Dan H. Sanes, PhD (2005-2008)**  
**Donna S. Whitlon, PhD (2006-2009)**  
**Amy Donahue, PhD - NIDCD Rep.**  
**Paul A. Fuchs, PhD, Council Liaison (2007-2008)**  
**Karen B. Avraham, PhD, Chair, International Cmte (2005-2008)**

Media Relations  
**Lawrence R. Lustig, MD, Chair (2005-2008)**  
**Ben Bonham, PhD (2006-2009)**  
**Daniel J. Lee, MD (2005-2008)**  
**Anne E. Luebke, PhD (2007- 2010)**  
**Cliff A. Megerian, MD (2007-2010)**  
**Yael Raz (2007-2010)**  
**Ana Elena Vazquez, PhD (2006-2009)**  
**Edward J. Walsh, PhD (2003-2007)**  
**John Williams, Ex officio AAO-HNS Dir. Congr Rel**  
**Steven Rauch, MD, Council Liaison (2007-2008)**

Membership Committee  
**Karen Jo Doyle, MD, PhD, Chair (2006-2009)**  
**David R. Friedland, MD, PhD (2007-2010)**  
**Daniel Lee, MD (2007-2010)**  
**Jennifer J. Lister, PhD (2006-2009)**  
**Virginia M. Richards, PhD (2006-2009)**  
**Tatsuya Yamasoba, MD, PhD (2006-2009)**

Nominating Committee  
**Robert V. Shannon, PhD, Chair (2007-2008)**  
**Douglas A. Chotanche, PhD (2007- 2008)**  
**Saumil N. Merchant, MD (2007- 2008)**  
**Edwin M. Monsell, MD, PhD (2007- 2008)**  
**William F. Sewell, PhD (2007- 2008)**

Patient Advocacy Group Relations  
**Charles J. Limb, MD, Chair (2006-2009)**  
**Daniel I. Choo, MD (2007-2010)**  
**Sandra Gordon-Salant, PhD (2006-2009)**  
**Akira Ishiyama, MD (2007-2010)**  
**J. Tilak Ratnanather, Dphil (2005-2008)**  
**Peter S. Steyger, PhD (2006-2009)**  
**D. Bradley Welling, MD, PhD (2007-2010)**  
**Susan L. Whitney, PhD, PT (2006-2009)**  
**Steven Rauch, MD, Council Liaison (2007-2008)**

Physician Research Training  
**David R. Friedland, MD, PhD, Chair (2005-2008)**  
**Timothy E. Hullar, PhD (2006-2009)**  
**Joseph Kerschner, MD (2007-2010)**  
**Charles J. Limb, MD (2006-2009)**  
**Saumil N. Merchant, MD (2005-2008)**  
**Yael Raz (2005-2008)**  
**Claus-Peter Richter, MD, PhD (2005-2008)**  
**Konstantina M. Stankovic, MD, PhD (2007- 2010)**  
**Ebenezer Nketia Yamoah, PhD (2007- 2010)**  
**James F. Battey, MD, PhD, NIDCD Director ex-officio**  
**Maureen Hannley, PhD, Exec VP Rsch, ex-officio**  
**P. Ashley Wackym, MD, Council Liaison (2007-2008)**

Research Forum Co-Chairs  
**John S. Oghalai, MD (2005-2008)**  
**J. Christopher Post, MD (2004-2007)**

## President's Message 2008

Welcome to Phoenix – the Valley of the Sun – for the 31<sup>st</sup> Annual MidWinter Meeting of the Association for Research in Otolaryngology. While this is the second time the meeting has been convened away from water; we have moved to a much warmer location. Phoenix is an enjoyable city with great restaurants, interesting museums and for those of us who find Frank Lloyd Wright an interesting and creative force, Taliesin West is an easy day trip from the meeting site. For the first time we are also able to hold the meeting in a convention center and have our organization committed to six different hotels – each with a range of room rates. The meeting space and meeting environment will likely prove to be the best that we have experienced in several decades, which I personally look forward to experiencing again.



Also this year, for the first time, the Council began a strategic planning process that should help in charting the course for ARO for the next five to ten years. In addition to discussing challenges facing our membership in their professional lives, we focused on issues that represent opportunities and threats to our community. We reviewed, considered and discussed the mission and vision of the ARO, which also incorporated the perspectives of the focus groups who helped provide membership input. Finally, we focused efforts on defining measurable goals for the next two to three years that will advance the mission of our organization.

Thanks to the strong response from our members, we have scheduled many interesting and innovative symposia, including: A Memorial to the Contributions of Merle Lawrence, Gene Expression and Regulation in the Auditory System, Emerging Approaches for Inner Ear Drug Delivery, Ear and Brain: Influences of Sex Hormones on Auditory Processing, State Dependence of Neural Processing in Central Auditory System and Music and Deafness. The Presidential Symposium Sunday morning is entitled, Translational Research in Otolaryngology.

This year we have been able to continue to offer travel awards to research trainees, thanks to generous donations from the AAO-HNSF, DRF, and the AAAF. These funds allow for an important function of the MidWinter meeting: introducing young people to the network of scientists and researchers of the ARO. Young researchers are vital to the health of the organization, as “new blood” invigorates both the scientific and social interactions made possible by the meeting. I still remember my first ARO meeting in 1989 and the impact it had on my career. We welcome all new attendees and look forward to their ongoing participation in the ARO.

Brian C. J. Moore has been selected to receive the Award of Merit this year. The title of Brian's Presidential Lecture will be Using Psychoacoustics to Explore Cochlear Function: Basic Mechanisms and Applications to Hearing Aids. Many former students and colleagues will participate in this tribute to Brian and his great influence on auditory neuroscience.

Ruth Anne Eatock has not only assumed the editorship of JARO, she is actively taking the journal to an entirely different level expanding the scope of the journal to reflect the diversity of our field. The Council is confident in the future of the journal with Ruth Anne's leadership. She deserves our thanks and admiration for her commitment to our community. This year I asked Dr. Debara Tucci to serve as the new Chair of the Publications Committee not only because of her experience as a clinician-investigator, but also because of her journal oversight experience that she has held with her role on the Board of Otology and Neurotology, Inc. – the business entity responsible for overseeing the journal of the same name. I have served with her in that capacity and based on what I have observed of her expertise, she will be invaluable as we consider the relationship with our current publisher and determine what will be best for ARO as we renegotiate and determine which publishing house will best serve the interests of the ARO in the future. I have no doubt that ARO will benefit from the negotiation with whoever the next publisher of JARO will be.

Members of the ARO Council deserve special thanks for their role in organizing this meeting: Paul Fuchs (President-Elect), Bob Shannon (Past-President), Steve Rauch (Secretary/Treasurer), Peter Santi (Editor), David Lim (Historian), Laurel Carney, John C. Middlebrooks, and Karen Steel. The ARO continues to benefit from the expert organizational activities of the Talley Management Group. Darla Dobson and Lisa Astorga provide outstanding guidance and support for the ARO. We are very fortunate to have them as a part of our team. Members of the Council are working

with Lisa Astorga on identification of future meeting sites. We want to keep room prices and expenses down so that as many people as possible can participate in the meeting. At the same time, we want to select cities and hotels that will be appropriate, fun and synergistic for convening our meetings.

I expect we will have another fun and productive MidWinter meeting this year. Attendance and membership in the ARO has remained strong over recent years, despite the difficulties associated with venue changes. The numbers of registrants and the number of submitted abstracts have been stable over the last six years. As the MidWinter Meeting moves to new locations in the future, members remain strongly committed to the meeting and to the organization. It is clear that the ARO is much more than an organization – it is a community that is vital, growing and evolving. I am proud to be a member of this community and I look forward to discussing new ideas with colleagues, expanding my perspective, meeting new people, and renewing friendships in Phoenix.

A handwritten signature in black ink, reading "P. Ashley Wackym". The signature is fluid and cursive, with the first letter of each word being capitalized and prominent.

P. Ashley Wackym



**Brian C. J. Moore**  
**2008 Award of Merit Recipient**

Brian C. J. Moore

2008 Recipient of the Award of Merit

Brian Moore has made exceptional contributions to auditory science. Many of us are most familiar with his contributions to the understanding of the basic processes underlying normal hearing, and how these are affected by sensory hearing loss, but at least equal to these are the practical implementations of his research both in clinical and non-clinical settings. This encomium will start with a couple of examples of how he combines these approaches to provide unique insights into the functioning of the auditory system and the alleviation of hearing loss.

One area in which Brian has successfully combined basic, clinical, and applied research techniques is in the area of pitch perception. Because changes in the frequency of a sound are accompanied by changes both in which auditory nerve fibers are excited and in the temporal pattern of those responses, untangling the influence of these “place” and “phase locking” cues is a major challenge. Brian has shown that that “time is the key”: his research has demonstrated that the place of excitation cues are much too small to account for our exquisite ability to detect minute frequency changes, and that, for impaired listeners, the size of these “place” cues does not correlate with the ability to detect frequency shifts. Nowadays, nearly all accounts of both simple and complex pitch perception are based on the timing cue. It’s a sign of his lasting influence that a simple qualitative model, introduced in a textbook in 1982, provided the inspiration for the most popular class of pitch model used today. An innovative aspect of that model is the suggestion that, although phase-locking cues are paramount, it may also be important that they are conveyed by auditory nerve fibers that are tuned (more or less) to the frequency of that phase locking. Evidence in favor of this proposal has recently come from his work with hearing-impaired patients. In the process of developing a clinical tool, involving the diagnosis of patients with so-called “dead regions” – portions of the basilar membrane devoid of inner hair cells. Playing a tone at the frequency of a listener’s dead region can give rise to a highly unusual percept, with a weak pitch, consistent with the temporal cues appropriate to one region of the basilar membrane being encoded solely in neurons that synapse on receptor cells occupying quite different regions. More recently, as part of a collaboration with Christian Lorenzi and Kathryn Hopkins, he has provided evidence that sensory hearing loss involves not only impairments of frequency selectivity and of absolute sensitivity, but also in the temporal representation of the waveform fine structure.

A second area in which Brian’s research has made an enormous impact concerns the perception of loudness. Some of his basic research showed that the steeper growth of loudness with stimulus level in impaired ears is due primarily to a loss of peripheral compression, rather than to a growth in the spread-of-excitation. This loss of compression results in a substantially smaller dynamic range in impaired than in normal ears, and must be corrected by hearing aids. Brian developed a novel form of automatic gain control (AGC), incorporating separate time constants to control for short- and long-term changes in level, which has formed the basis for the AGC in a number of digital hearing aids and which has been incorporated into the Clarion cochlear implant. His basic research also led to his development of a loudness model that has been adopted as an American National Standard, and proposed as an ISO standard. Furthermore, an extension of the model to account for the effects of sensory hearing loss has been implemented into a method for fitting hearing aids. Outside the clinic, the model has been refined so that it can predict the reduction in loudness of one sound by another, and the software implementing this model (developed by Brian in collaboration with Brian Glasberg) is used by major international companies such as Boeing, Nokia, Dolby and Bose.

Brian's influence extends beyond his own research. His introductory textbook, now in its 5<sup>th</sup> edition, has become widely adopted in undergraduate and graduate courses world-wide, and has been translated into Polish and Japanese. His lab is a happy one, often supplemented by visiting scientists who have come to benefit from his expertise, and many of his graduate students and post-docs have subsequently ventured forth alone into the cut-throat (and somewhat daredevil) world of psychophysics. He wears his fame lightly, and is renowned among friends for his fondness for clever jokes, fine wines, and willing renditions of Tom Lehrer songs.

Brian Moore's contributions to auditory science have been honored many times; he is a Fellow of the Royal Society, received the Silver Medal of the Acoustical Society of America in 2003, and each visit to his office requires increasingly careful navigation of impressive silverware and framed awards. The Order of Merit is a major recognition of his work, and one that he richly deserves.

BOB CARLYON



# Association for Research in Otolaryngology

Executive Offices

19 Mantua Road, Mt. Royal, NJ 08061 USA

Phone: (856) 423-0041 Fax: (856) 423-3420

E-Mail: [headquarters@aro.org](mailto:headquarters@aro.org)

Meetings E-mail: [meetings@aro.org](mailto:meetings@aro.org)

## *ARO Council Members 2007-2008*

**President:** P. Ashley Wackym, MD  
Medical College of Wisconsin  
Department of Otolaryngology &  
Communicative Sciences  
9000 West Wisconsin Avenue  
Milwaukee, WI 53226

**Secretary/Treasurer:** Steven Rauch, MD  
Harvard Medical School  
Massachusetts Eye and Ear Infirmary  
243 Charles Street  
Boston, MA 02114

**President Elect:** Paul A. Fuchs, PhD  
John Hopkins University of Medicine  
521 Traylor Research Building  
720 Rutland Avenue  
Baltimore, MD 21205

**Editor:** Peter A. Santi, PhD  
University of Minnesota  
Department of Otolaryngology  
Lions Research Bldg., Room 121  
2001 Sixth St. SE  
Minneapolis, MN 55455

**Past President:** Robert V. Shannon, PhD  
House Ear Institute  
Auditory Implant Research  
2100 W. Third Street  
Los Angeles, CA 90057

**Historian:** David J. Lim, MD  
House Ear Institute  
2100 W. Third St., Fifth Floor  
Los Angeles, CA 90057

## *Council Members at Large*

Karen P. Steel, PhD, FMed  
Wellcome Trust Sanger Institute  
Wellcome Trust Genome  
Campus  
Hinxton  
Cambridge CB 10 1SA, UK

John C. Middlebrooks, PhD  
University of Michigan  
Kresge Hearing Research  
Institute  
1301 East Ann Street  
Ann Arbor, MI 48109-0506\

Laurel Carney, PhD  
Syracuse University  
Institute for Sensory Research  
Biomedical & Chemical  
Engineering  
Syracuse, NY 13244

# Association for Research in Otolaryngology

Executive Offices

19 Mantua Road, Mt. Royal, NJ 08061 USA

Phone: (856) 423-0041 Fax: (856) 423-3420

E-Mail: [headquarters@aro.org](mailto:headquarters@aro.org)

Meetings E-mail: [meetings@aro.org](mailto:meetings@aro.org)

## Past Presidents

1973-74	David L. Hilding, MD
1974-75	Jack Vernon, PhD
1975-76	Robert A. Butler, PhD
1976-77	David J. Lim, MD
1977-78	Vicente Honrubia, MD
1978-80	F. Owen Black, MD
1980-81	Barbara Bohne, PhD
1981-82	Robert H. Mathog, MD
1982-83	Josef M. Miller, PhD
1983-84	Maxwell Abramson, MD
1984-85	William C. Stebbins, PhD
1985-86	Robert J. Ruben, MD
1986-87	Donald W. Nielsen, PhD
1987-88	George A. Gates, MD
1988-89	William A. Yost, PhD
1989-90	Joseph B. Nadol, Jr., MD
1990-91	Ilsa R. Schwartz, PhD
1991-92	Jeffrey P. Harris, MD, PhD
1992-93	Peter Dallos, PhD
1993-94	Robert A. Dobie, MD
1994-95	Allen F. Ryan, PhD
1995-96	Bruce J. Gantz, MD
1996-97	M. Charles Liberman, PhD
1997-98	Leonard P. Rybak, MD, PhD
1998-99	Edwin W. Rubel, PhD
1999-00	Richard A. Chole, MD, PhD
2000-01	Judy R. Dubno, PhD
2001-02	Richard T. Miyamoto, MD
2002-03	Donata Oertel, PhD
2003-04	Edwin M. Monsell, MD, PhD
2004-05	William E. Brownell, PhD
2005-06	Lloyd B. Minor, MD
2006-07	Robert V. Shannon, PhD

## Award of Merit Recipients

1978	Harold Schuknecht, MD
1979	Merle Lawrence, PhD
1980	Juergen Tonndorf, MD
1981	Catherine Smith, PhD
1982	Hallowell Davis, MD
1983	Ernest Glen Wever, PhD
1984	Teruzo Konishi, MD
1985	Joseph Hawkins, PhD
1986	Raphel Lorente de Nó, MD
1987	Jerzy E. Rose, MD
1988	Josef Zwislocki, PhD
1989	Åke Flóck, PhD
1990	Robert Kimura, PhD
1991	William D. Neff, PhD
1992	Jan Wersäll, PhD
1993	David Lim, MD
1994	Peter Dallos, PhD
1995	Kirsten Osen, MD
1996	Ruediger Thalmann, MD & Isolde Thalmann, PhD
1997	Jay Goldberg, PhD
1998	Robert Galambos, MD, PhD
1999	Murray B. Sachs, PhD
2000	David M. Green, PhD
2001	William S. Rhode, PhD
2002	A. James Hudspeth, MD, PhD
2003	David T. Kemp, PhD
2004	Donata Oertel, PhD
2005	Edwin W. Rubel, PhD
2006	Robert Fettiplace, PhD
2007	Eric D. Young, PhD
2008	Brian C. J. Moore, PhD

# Table of Contents

## Abstract Number

### Presidential Symposium

A:	Translational Research in Otolaryngology .....	1-6
Symposium		
B:	Gene Expression and Regulation in the Auditory System .....	7-13
C:	Non-Auditory Modulation of Auditory Processing in the Inferior Colliculus .....	14-18

### Poster

D1:	Middle Ear: Pathophysiology.....	19-31
D2:	Inner Ear Genetics I .....	32-43
D3:	Inner Ear Genetics II.....	44-50
D4:	Genetics.....	51-71
D5:	Servicing the Inner Ear .....	72-80
D6:	Hair Cell Channels & Cell Biology .....	81-99
D7:	Development I .....	100-115
D8:	Regeneration I.....	116-132
D9:	Hair Cell Prestin & Tuning I .....	133-144
D10:	Inner Ear Damage and Prevention I .....	145-152
D11:	Inner Ear Damage and Prevention II.....	153-171
D12:	Inner Ear Mechanics .....	172-179
D13:	Otoacoustic Emissions I: Generation and Measurement.....	180-196
D14:	Hair Cell Synapses .....	197-215
D15:	Cochlear Innervation .....	216-219
D16:	Physiology, Modeling and Non-Acoustic Stimulation .....	220-234
D17:	Vestibular: Clinical.....	235-250
D18:	Clinical Otolaryngology.....	251-260
D19:	Protection and Treatment Strategies.....	261-273
D20:	Auditory Prosthesis: Alternatives to Cochlear Implants .....	274-280
D21:	Auditory Prosthesis: Bilateral and Spatial.....	281-288
D22:	Auditory Prosthesis: Miscellany .....	289-296
D23:	Auditory Brainstem: Structure and Functional Markers.....	297-308
D24:	Auditory Brainstem: Cellular Mechanisms in Cochlear Nucleus .....	309-321
D25:	Midbrain I .....	322-336
D26:	Auditory Cortex and Thalamus: Circuits, Development and Plasticity .....	337-356
D27:	Central Changes, Behavior and Psychoacoustics .....	357-368
D28:	Auditory Cortex and Thalamus: Imaging and Human Studies .....	369-387
D29:	Clinical Audiology I .....	388-396
D30:	Psychophysics: Frequency and Pitch.....	397-402
D31:	Psychophysics: Scene Analysis.....	403-414
D32:	Speech .....	415-426

### Workshop

E:	NIDCD Workshop .....	427-428
----	----------------------	---------

### Patient Advocacy Group Workshop

F:	Music and Deafness: Perception, Performance and Progress .....	429-434
----	--	---------

### Podium

G:	Development.....	435-449
----	------------------	---------

### Symposium

H:	Emerging Approaches for Inner Ear Drug Delivery.....	450-455
----	--	---------

### Podium

I:	Psychophysics .....	456-468
----	---------------------	---------

Symposium	J:	Noise-Induced Hearing Loss: From Molecules to Man.....	469-475
	K:	State Dependence of Neural Processing in Central Auditory System.....	476-482
Podium	L:	Hair Cell Development & Transduction .....	483-497
	M:	Inner Ear Mechanics .....	498-507
Symposium	N:	A Memorial to the Contributions of Merle Lawrence, Ph.D.: Vascular Physiology and Cell Communication in the Cochlea: Pathways and Barriers.....	508-514
Poster	O1:	Clinical Audiology II.....	515-526
	O2:	Middle Ear: Mostly Mechanics .....	527-546
	O3:	Regeneration II.....	547-560
	O4:	Regeneration III.....	561-571
	O5:	Development II.....	572-587
	O6:	Inner Ear Modeling .....	588-597
	O7:	Inner Ear Physiology Podium .....	598-604
	O8:	Mutations and Cochlear Function .....	605-611
	O9:	Receptors, Drugs, and Cochlear Function .....	612-626
	O10:	Cochlea: Imaging and Fine Structure .....	627-639
	O11:	Cochlear Mechanisms and Changes .....	640-649
	O12:	Inner Ear Stereocilia & Transduction.....	650-666
	O13:	Hair Cell Prestin & Tuning II.....	667-684
	O14:	Otoacoustic Emissions II .....	685-693
	O15:	Cochlear Stress Mechanisms.....	694-701
	O16:	Mechanisms of Noise Damage.....	702-710
	O17:	Prevention of Noise Damage .....	711-719
	O18:	Mechanisms of Ototoxicity .....	720-729
	O19:	Inner Ear Ototoxicity Prevention .....	730-738
	O20:	Damage and Protection: SGNs and Synapses.....	739-747
	O21:	SGN Development and Survival: Molecular Biology and Anatomy .....	748-759
	O22:	Vestibular: Receptors .....	760-777
	O23:	Vestibular: Afferents and CNS.....	778-796
	O24:	Auditory Prosthesis: Nerve, Telemetry, and Tonotopy.....	797-807
	O25:	Auditory Prosthesis: Music and Speech .....	808-818
	O26:	Auditory Brainstem: Physiology of Cochlear Nucleus.....	819-831
	O27:	Auditory Brainstem: Efferents and Evoked Potentials.....	832-843
	O28:	Auditory Brainstem: Binaural Pathways.....	844-856
	O29:	Sound Localization: Neural Mechanisms and Complex Environments .....	857-867
	O30:	Midbrain II.....	868-875
	O31:	Sound Localization: Behavior and Spatial Cues .....	876-890
	O32:	Auditory Cortex and Thalamus: Physiology .....	891-908
	O33:	Psychophysics: Complex Sounds .....	909-915
	O34:	Psychophysics: Binaural and Spatial.....	916-922
	O35:	Psychophysics: Methodology.....	923-934
	O36:	Psychophysics: Time.....	935-941
Presidential Lecture	P:	Presidential Lecture and Award Ceremony .....	942
Symposium	Q:	Hair Cell Afferent Synaptic Transmission.....	943-951
Podium	R:	Vestibular: Molecules to Behavior.....	952-964
Symposium	S:	Ear and Brain: Influences of Sex Hormones on Auditory Processing.....	965-970
Podium	T:	Auditory Prosthesis.....	971-983
	U:	Auditory Cortex and Thalamus .....	984-996
	V:	Genetics.....	997-1008

## **1 Is Our Research Community on Track with the Development of Translational Research?**

**<sup>1</sup>P. Ashley Wackym.**

*<sup>1</sup>Department of Otolaryngology and Communication Sciences, Medical College of Wisconsin, Milwaukee, Wisconsin, 53226.*

Early on in Dr. Zerhouni's leadership of the National Institutes of Health, he established the innovative NIH Roadmap Initiative. Within this context, he emphasized the need to enhance translational research in various ways because of the recognition that to improve human health, scientific discoveries must be translated into practical applications, and that such efforts usually require a multi-disciplinary team of scientists and clinicians. Toward this end, a range of methods have been introduced to enhance the effectiveness of the clinical research enterprise, recognizing the bidirectional nature of discovery (the familiar bench to bedside, but also bedside to bench). This presentation will outline some of these mechanisms and review how the otolaryngology research community has responded to this imperative. I will also summarize recent funding trends across individual NIH Institutes, which reflect where we stand in comparison to other clinical disciplines, and review some factors that continue to impede further progress. Each of the presentations that follow in the symposium will focus on several aspects of the re-engineering effort, which are needed to create greater opportunity for catalyzing the development of the discipline of clinical and translational science.

## **2 Basic Scientist or Translational Scientist? Changing Roles of Physician-Scientists in Biomedical Research**

**Carey D. Balaban<sup>1</sup>**

*<sup>1</sup>Departments of Otolaryngology, Neurobiology, Communication Sciences & Disorders, and Bioengineering, University of Pittsburgh 15213.*

Over the previous thirty years, there has been considerable concern that, despite our best efforts, the physician-scientist is "an endangered species." This presentation reviews the role of physician-scientists from an historical perspective and issues that impact on our current efforts to develop translational biomedical research.

Since ancient times, practitioners of Western medicine have balanced two distinct traditions, practice on the empiricism and rational scientific principles. Empirical medicine required (1) recognition of a disease and (2) application of the time-honored treatment. Dogmatic (or scientific) medicine required an understanding and articulation of scientific principles or models underlying diagnosis and treatment. the ideal physician was regarded as a scholar with expertise in both realms. the ancient challenge of merging empiricism and biomedical science is precisely the challenge that we face in fostering the development of clinician-investigators for disease oriented research, patient oriented research and basic research. Claude Bernard's late 19<sup>th</sup> century articulation of the goals of experimental medicine provides a framework for considering the mission of modern translational research: the articulation of principles linking basic scientific findings with clinical practice. This is an information synthesis that can be accomplished well by researchers immersed in the realities of clinical practice, the physician-scientist, but our academic programs must provide environment that fosters the development of the necessary scientific wisdom for creative

translational research. the components of this environment include rigorous clinical and basic science training, modifications in career development expectations, and appropriate weighting of translational significance in peer-review.

## **3 High-Throughput Molecular Genetics**

**J. Christopher Post,<sup>1</sup> Fen Z. Hu,<sup>1</sup> Benjamin Janto<sup>1</sup>, Garth D. Ehrlich<sup>1</sup>**

*<sup>1</sup>Center for Genomic Sciences, Allegheny Singer Research Institute, Allegheny General Hospital, Pittsburgh, PA.*

Techniques such as high-throughput (HT) DNA sequencing, tissue microarrays (TMA) and proteomic analyses are fundamentally changing biomedical research. These highly automated techniques produce a massive and continuous data flow that cannot be interpreted without reliance upon software. Most HT techniques are highly parallel processes, producing thousands or millions of results simultaneously. When applied to DNA sequencing they provide for the analysis of complex, biologically meaningful genomic regions and even whole genomes quickly and inexpensively. an entire bacterium can now be sequenced in a day, and we will soon achieve the goal of the "\$1000 human genome" through technology such as nanopore sequencing, direct imaging by atomic force or electron microscopy. Similarly, TMAs, particularly useful in cancer research, reveal the cellular localization, prevalence and clinical significance of candidate genes products by the visualization of molecular targets in thousands of tissue specimens within a few hours, thereby facilitating transcriptomics-based diagnostics and drug discovery targets. Proteomics involves studying proteins that a tissue or organism expresses under certain conditions, and how those proteins interact. Many entire genomes have already been sequenced, including animals, plants and their bacterial pathogens, as well as unculturable microbes. the routine sequencing of individual human genomes will usher in an era of personalized medicine. Our Center has sequenced over 90 bacterial genomes in 30 months, providing the data to model the core and supragenomes of numerous human pathogens and to develop the distributed genome hypothesis. HT genetic techniques, together with powerful gene clustering algorithms and metabolomic reconstructions, when combined with STEM-enhanced confocal laser microscopy and precise strain phenotyping enable us to understand the nutrient, waste, and energy fluxes within complex microbiomes and polymicrobial communities.

Supported by NIDCD grants DC05659, DC04173 and DC02148.

## **4 Clinical Trials and Outcomes Research**

**Steven D. Rauch<sup>1</sup>**

*<sup>1</sup>Harvard Medical School, Mass. Eye & Ear Infirmary*

Clinical trials and outcomes research are critical steps in the path from basic science investigation to improved health. Despite the fact that such studies are desperately needed, few have been done in our field. One explanation for the shortfall in clinical research may be the logistical problems encountered in trying to study diseases that are low incidence and/or low prevalence, a common situation in Otolaryngology. Another explanation may be the short supply of clinical investigators in Otolaryngology with expertise and experience in the field of clinical trials and outcomes research. Another may be the very limited epidemiologic research done to date that would lay the groundwork for clinical trials. Still another may be the fact

that clinical trials are very expensive compared to typical basic science projects. In an effort to maintain support for the basic scientists in our field, few resources are allocated for clinical trials. There is good reason to believe that, in the long run, this may be a self-defeating strategy. This presentation will review some of the methodological, infrastructural, societal, and financial factors that are relevant to the conduct of clinical trials and outcomes research. Specific examples will be drawn from the ongoing NIH-supported Sudden Sensorineural Hearing Loss Treatment Trial.

## 5 Stem Cells: Current Challenges and Future Promise

James F. Battey, Jr.<sup>1</sup>

<sup>1</sup>National Institute on Deafness and Other Communication Disorders, Bethesda, Maryland, 20892-2320.

Stem cells have two remarkable properties that make them a unique resource for biomedical research. They can either renew themselves, or differentiate into one or more of the several hundred different types of adult cells. Stem cells derived from the human embryo are particularly remarkable in that they appear to have an unlimited capacity to self renew in cell culture, and, because they are derived from the inner cell mass of an embryo at the blastocyst stage, have the capacity to differentiate into all of the many hundred different adult cell types. Human embryonic stem cell lines are an enabling resource that is proving invaluable for elucidating the molecular mechanisms that determine adult cell fate, generating cellular models for discovery of new drugs, and creating populations of differentiated cells for novel transplantation therapies. Scientists have made remarkable recent progress towards developing sources of pluripotent cells that do not involve embryos. The National Institutes of Health (NIH) has identified some of the rate limiting steps to realizing the full potential of stem cells to revolutionize regenerative medicine, and has provided funding initiatives to accelerate research progress. These research challenges and enabling resources will be discussed in this address. Given the remarkable potential, high priority

## 6 Translational Research within an Academic Medical Center in an Era of the Clinical and Translational Science Awards

Howard J. Jacob<sup>1</sup>

<sup>1</sup>Department of Physiology and Pediatrics, Medical College of Wisconsin, Milwaukee, Wisconsin, 53226.

Over the last decade, the NIH has increased the number of training programs for clinicians e.g. K01, K08, K12, but these have not met the growing need for clinical scientists. The development of the CTSA program recognizes that each institution has its own set of limitations preventing the expansion of clinical/translational research. The fundamental goal of the program is to reengineer the infrastructure required to enable a larger number of clinical investigators and allied healthcare personnel to participate in research. The program has also engendered the feeling that a CTSA award is a credentialing step for the major Academic Medical Centers (AMCs). It is this latter component that has generated the most interest in the leadership of many if not all the AMCs, including our own, which is leading to significant changes in how we conduct translational research.

Our goals are:

- To increase the critical mass of clinical-translational investigators in our environment, including the recruitment of new individuals—our cluster hires and “new faculty”;
- To create new investigators from existing CTSI faculty through education, and most important, removing the obstacles facing the investigator entering the complex maze of clinical/translational research; and
- To capitalize on the steps achieved through our planning grant to implement our research Metropolis.

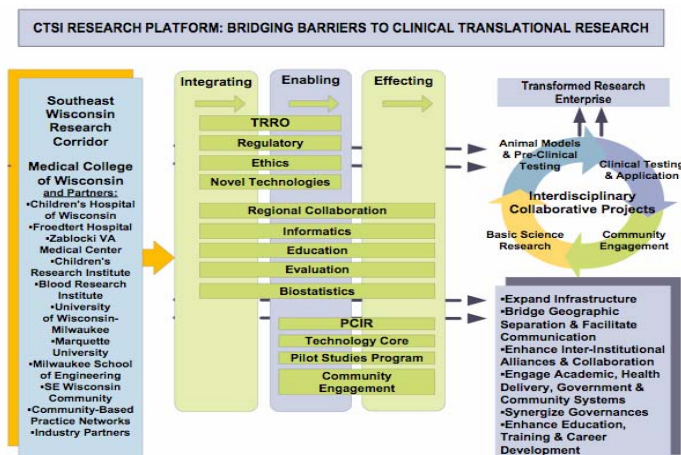
The included figure outlines our CTSI, which I will discuss in the context of a Department.

## 7 Using High-Throughput Data to Understand Cellular Response Pathways

Ernest Fraenkel<sup>1</sup>

<sup>1</sup>Department of Biological Engineering, Massachusetts Institute of Technology, Cambridge, MA, USA

Systems biology techniques provide a wealth of data, but these are often difficult to interpret. In this talk I will describe our recent efforts to unravel mechanisms of transcriptional regulation and signaling changes from diverse high-throughput data including mRNA levels, genetic data and genome-wide chromatin immunoprecipitation experiments. I will present evidence that although tissue-specific transcription is typically highly conserved between human and mouse, the mechanisms of transcriptional regulation show a surprising level of divergence. I will also discuss new techniques that we have developed to integrate high-throughput genetic screens with expression arrays to reveal components of the cellular response that are not detectable by either method alone.



for NIH support to advance research using stem cells is warranted for the foreseeable future. Supported by NIDCD, NIH.

## **[8] Expression Profiling and Pathway**

### **Analysis in the Inner Ear**

**Michael Lovett<sup>1</sup>**, David Alvarado<sup>1</sup>, Samin Sajan<sup>1</sup>, Mark Warchol<sup>1</sup>

<sup>1</sup>*Washington University in St Louis*

We have developed detailed, statistically robust, expression profiles of the developing inner ear during mouse and chicken embryonic development. These profiles span all the stages from the early otic cup until later stages when the major structures of the ear are fully developed. Microdissected substructures (such as the saccule, cochlea and utricle) were separately profiled. We have also measured gene expression changes as chicken inner ear sensory epithelia (SE) regenerate. This regenerative process does not occur in mammals and the resulting loss of inner ear function is a major cause of deafness. Comparisons between these datasets reveals interesting commonalities and overlapping pathways, including changes in circadian rhythm genes and various nuclear receptor signaling pathways during development and regeneration. in order to further dissect developmental and regenerative gene expression signatures we have tested individual genes by RNAi knockdowns in regenerating avian SE. for example, we have identified components of AP1 and PAX signaling that are necessary for early proliferative events in regeneration. by reiteratively profiling gene expression changes after each gene knockdown (and profiling tissues from various mouse knockout and/or microdissected structures) we have placed many of these components into probable networks and pathways. by a combination of these inferential methods and more direct tests of gene interactions we hope to compile a gene network diagram of the developing/regenerating inner ear SE in avians and mammals.

## **[9] Understanding Mechanisms of MicroRNA Regulation and Function**

**Noam Shomron<sup>1</sup>**

<sup>1</sup>*Massachusetts Institute of Technology*

MicroRNAs (miRNAs) are short ~21nt non-coding RNAs that negatively regulate a large portion of the transcriptome through binding to the mRNA 3'UTR. My talk will focus on three aspects of miRNA biology that together shed light on their roles in molecular biology and evolution. ANNOTATION: We completed the miRNA registry with hundreds of mammalian high-confidence miRNA homologs using our own developed homologous miRNA gene finder (termed miRNAMiner; also available as a web-server) and looked into their genomic organization and regulation. ROLE: Canalization is a design principle wherein extremely robust developmental pathways are stabilized to increase phenotypic reproducibility and to result in stereotyped outcomes. We proposed a new function for miRNAs in buffering stochastic perturbations and thereby conferring robustness to developmental genetic programs. TARGETING: in order to better understand miRNA targeting rules, and to assess a variety of potential miRNA targeting determinants, we analyzed the effects of miRNA under- and over-expression on global

mRNA and protein regulation. We deciphered determinants of targeting by endogenous and exogenous miRNAs taking targeting a leap forward and revealing additional principals that enhance seed match-associated mRNA repression. Together, our studies seek to better understand the mechanism governing miRNA regulation and the role it plays in molding the transcriptome and thus affecting cellular fate.

## **[10] Expression and Function of Micornas in the Inner Ear**

**Michael Weston<sup>1</sup>**, Marsha Pierce<sup>1</sup>, George Enniful<sup>1</sup>, Bernd Fritsch<sup>1</sup>, **Garrett Soukup<sup>1</sup>**

<sup>1</sup>*Creighton University*

MicroRNAs (miRNAs) are small regulatory RNAs that mediate interaction of the RNA-Induced Silencing Complex (RISC) with target mRNAs to cause post-transcriptional gene silencing. It is estimated that approximately one third of mammalian gene expression might be subject to regulation by miRNAs. in support of such pervasive miRNA influence in biology, miRNAs have been demonstrated to play crucial roles in animal development and disease by affecting cell proliferation, differentiation, and function. to begin to understanding how miRNAs affect ear biology we have used a variety of techniques to assess miRNA expression in the mouse inner ear that include microarray analysis, cloning, quantitative RT-PCR, and *In Situ* hybridization. These studies have revealed that a substantial number of miRNAs are expressed in the inner ear and in the cochlea. in particular, miRNA-183 family members (miR-183, miR-96, and miR-182) demonstrate mechanosensory hair cell expression that follows specification by Atoh1. the extraordinary conservation of miRNA-183 family member sequence and expression in neurosensory organs of vertebrate and invertebrate organisms suggest their importance in the development of ciliated sensory cells. Moreover, we have investigated the function of miRNAs in inner ear development by examining the effect of conditional *Dicer* knockout in the mouse inner ear, where Dicer is required for miRNA processing and function. Results from these studies demonstrate that depletion of miRNAs early in inner ear development results in severe defects in morphogenesis, histogenesis, and innervation. Understanding individual miRNA regulatory functions in pathways and processes important to sensory epithelial development will be critical to implementing therapeutic strategies that make use of small RNAs as tools or targets in the inner ear.



## **11 An ENU-Induced Mutation of a Mirna Associated with Progressive Hearing Loss**

Morag Lewis<sup>1</sup>, Elizabeth Quint<sup>2</sup>, Agnieszka Rzadzinska<sup>1</sup>, Anne Kent-Taylor<sup>1</sup>, Helmut Fuchs<sup>3</sup>, Martin Hrabé De Angelis<sup>3</sup>, Cordelia Langford<sup>1</sup>, Stijn Van Dongen<sup>1</sup>, Anton Enright<sup>1</sup>, Nick Redshaw<sup>4</sup>, Tamas Dalmay<sup>4</sup>, **Karen Steel**<sup>1</sup>

<sup>1</sup>Wellcome Trust Sanger Institute, Hinxton, UK, <sup>2</sup>MRC Institute of Hearing Research, Nottingham, UK, <sup>3</sup>GSF National Center for Environment and Health, Munich, Germany, <sup>4</sup>University of East Anglia, Norwich, UK

Progressive hearing loss is very common in the human population, but relatively little is known about the molecular or genetic basis. We report here a new ENU-induced mouse mutant called *diminuendo* (*Dmdo*), inherited in a semi-dominant manner. Heterozygotes show progressive loss of auditory responses and hair cell degeneration. Homozygotes show no cochlear responses and have extensive hair cell loss by 4 weeks after birth. Hair cells in homozygotes have reduced apical surfaces and hair bundles show anomalies soon after birth. However, interstereocilia links appear unaffected at early stages despite progressive loss of the staircase organisation. We mapped the mutation to a 4.5 Mb region of chromosome 6 containing 40 genes, and resequenced the majority of exons within this region. Eventually, we found a single base change in the seed region of a microRNA, miR-96. This miRNA is expressed in sensory hair cells from an early stage, and we are currently investigating candidates for its target sites to elucidate the mechanism of action.

## **12 Molecular Signaling Pathways in Hair Cell Development**

**Matthew Kelley**<sup>1</sup>, Elizabeth Driver<sup>1</sup>, Chandrakala Puligilla<sup>1</sup>, Norio Yamamoto<sup>1</sup>, Alain Dabdoub<sup>1</sup>

<sup>1</sup>NIDCD/NIH

Hair cells and supporting cells are derived from a subset of epithelial cells within the otocyst. During development these cells initially become competent to develop as any cell type within the sensory epithelium through a process of prosensory specification. Once specified, individual prosensory cells become restricted to either a hair cell or supporting cell fate. Our understanding of the molecular signaling pathway(s) that direct cells into the prosensory lineage and ultimately to either a hair cell or supporting cell fate is limited. But recent results have identified at least part of the signaling cascade. the first definitive indicator of prosensory specification is expression of Jagged1 and activation of the notch pathway. the factors that regulate expression of Jagged1 are unknown, but inhibition of the hedgehog signaling pathway induces ectopic expression of Jagged1 and formation of prosensory cells. Inactivation of notch signaling through deletion of *Jagged1* or *Rbp-j* leads to a marked decrease in the number of prosensory cells and in expression of the prosensory marker Sox2. in contrast, Sox2 is up-regulated in response to activated Notch. Forced expression of Sox2 induces Prox1, a second transcription factor that is expressed in most prosensory cells, and Prox1 expression is lost in Sox2 mutants. Atoh1 expression is also lost in Sox2 mutants, however forced expression of Sox2 or Prox1 does not

induce Atoh1, suggesting the existence of parallel pathways. Atoh1 expression initiates a hair cell differentiation program. However a subset of cells are able to increase their relative level of Atoh1, leading to expression of Jag2 and Dll1 and reactivation of the notch signaling pathway in neighboring cells. But at this stage, notch acts to inhibit the hair cell fate through direct antagonism of Atoh1. Prosensory cells in which Atoh1 is antagonized are induced to develop as supporting cells through interactions with surrounding hair cells through an unknown pathway.

## **13 Molecular Networks Underlying Hair Cell Development and Physiology Deciphered by Human Deafness Gene Products and Their Ligands**

Nicolas Michalski<sup>1</sup>, Vincent Michel<sup>1</sup>, Gaëlle Lefèvre<sup>1</sup>, Elisabeth Verpy<sup>1</sup>, Michel Leibovici<sup>1</sup>, Dominique Weil<sup>1</sup>, Jean-Pierre Hardelin<sup>1</sup>, Richard J Goodyear<sup>2</sup>, Guy P Richardson<sup>2</sup>, Paul Avan<sup>3</sup>, **Christine Petit**<sup>4</sup>

<sup>1</sup>Institut Pasteur, <sup>2</sup>University of Sussex, <sup>3</sup>Université d'Auvergne, <sup>4</sup>Institut Pasteur, Collège de France, INSERM

To identify the genes causative for deafness in humans, in a first step, we selected genes exclusively or preferentially expressed in the cochlea. They turned out to be a valuable source of candidate genes. in a second step, in order to understand the role of their encoded proteins, we searched for their ligands by using the yeast two-hybrid technique. Data obtained from all screenings were crossed to further the putative molecular complexes.

Today, both the deafness gene products and their ligands can be integrated in molecular mechanisms underlying specific developmental or physiological processes. As an example, the hair bundle links composition, anchoring and functioning will be discussed.

The obstacles and the limits of this approach and the way to test the *In Vivo* relevance of these interactions will be addressed. As expected, the genes encoding these ligands are today a source of deafness genes too.

1INSERM UMRS587, Unité de Génétique des Déficits Sensoriels, Institut Pasteur, 25 rue du Dr Roux, 75724 Paris cedex 15, France.

2 School of Life Sciences, University of Sussex, Falmer, Brighton, UK.

3Laboratoire de Biophysique Sensorielle, Faculté de Médecine, Clermont-Ferrand, France

## **14 Cholinergic Pathways to the Inferior Colliculus**

**Brett R. Schofield**<sup>1</sup>, Susan D. Motts<sup>1</sup>

<sup>1</sup>Northeastern Ohio Univ. Coll. Med.

Acetylcholine (ACh) alters the response properties of most cells in the inferior colliculus (IC). Further, ACh has been implicated in the effects of auditory cortical stimulation on IC responses. Our understanding of the cholinergic effects has been hampered by lack of information on its source. We combined fluorescent retrograde tracers to identify cells that project to the IC with immunohistochemistry against choline acetyltransferase to identify cholinergic



cells. We identified two nuclei in the midbrain tegmentum – the pedunculo pontine (PPT) and laterodorsal (LDT) tegmental nuclei – as the sources of ACh in the IC. the projections are bilateral, with more cells projecting ipsilaterally than contralaterally. On both sides, more PPT cells than LDT cells project to the IC. the PPT and LDT are well known for their cholinergic projections to the thalamus and for collateral projections from individual cells to multiple targets. We combined multi-label retrograde tracing with immunohistochemistry to identify cholinergic cells that project to multiple auditory targets. Our results show multiple patterns of projection from PPT and LDT cells, including bilateral projections to the IC, projections to one IC and one medial geniculate (MG); one IC and one cochlear nucleus; one IC and both MGs, or both ICs and one cochlear nucleus.

The PPT and LDT are best known for their projections to the thalamus, where they play a role in arousal. the projections from these nuclei raise the possibility of a similar role for acetylcholine in the IC. the collateralization of the cholinergic axons to multiple auditory nuclei suggests that such effects may be exerted on multiple auditory areas simultaneously.

Supported by NIH DC04391, DC08463.

## **15 A State-Dependent Auditory Filter: Measuring Serotonin Levels in Behaving Animals**

**Laura Hurley<sup>1</sup>**

<sup>1</sup>*Indiana University*

The neuromodulator serotonin is linked with mood and anxiety disorders, but this widespread signaling molecule regulates neural networks throughout the brain, including those within the auditory system. the inferior colliculus (IC) has a dense network of serotonergic fibers originating mainly in the dorsal and median raphe nuclei, which also innervate other brain regions. Recent work in our laboratory has focused on how different serotonin receptor types translate the release of serotonin into specific effects on auditory response properties in the IC. the behavioral contexts in which these effects are likely to be relevant are not yet well understood, although previous studies of the serotonergic system have suggested that serotonin levels in the IC should respond to changes in behavioral arousal or to environmental stressors. We have recently begun to investigate the role of behavioral context on serotonergic activity by using carbon fiber electrodes to voltammetrically measure serotonin in the IC of behaving mice. These experiments have confirmed that the amount of serotonin is regulated by the firing rates of raphe neurons and the local reuptake and degradation of released serotonin. These processes combine to create fluctuations in the level of serotonin in response to changes in behavioral state or sensory stimuli. During the transition from anesthesia to waking, serotonin levels steadily increase and then plateau. Preliminary results also suggest that smaller and more variable increases in serotonin occur in awake animals in response to the presentation of noise bursts and flashes of light. Some behavioral events such as the presentation and consumption of food, however,

evoke no change in serotonin level. These findings support a model of serotonin as a state-dependent filter for auditory processing, signaling particular types of internal or external events and creating specific modulations in the auditory circuitry of the IC.

## **16 Integration of Ascending Auditory and Somatosensory Information in the External Nucleus of the Inferior Colliculus**

**Susan Shore<sup>1</sup>**

<sup>1</sup>*University of Michigan*

The external nucleus of the inferior colliculus (ICx) receives ascending projections from both auditory and somatosensory nuclei. the combined use of retrograde and anterograde tracing, immunohistochemistry and electrophysiology allowed us to elucidate the extent of interactions between auditory and somatosensory representations in the IC.

Injections of anterograde tracers into either the cochlear nucleus (CN) or spinal trigeminal nucleus (Sp5) resulted in terminal labeling in ICx primarily on the contralateral side. Most projection fibers from Sp5 terminated within the ventrolateral ICx, the ventral border and the ventromedial edge of IC (collectively termed “the ventrolateral border region of IC”, ICxV). Injecting different tracers into both Sp5 and CN in the same animals indicated overlapping areas of convergent projections from Sp5 and CN in the ICxV, with less intense dual labeling in the rostral part of ICx. Some of these projection terminals were glutamatergic, co-labeling with vesicular glutamate transporters. Injections of retrograde tracers into ICx resulted in fusiform and multipolar cell-labeling in the contralateral CN, as well a variety of cells in the pars interparialis and caudalis of Sp5. This convergence of projection fibers from CN and Sp5 provides an anatomical substrate for multimodal integration in the ICx.

Single unit recordings from ICxV revealed bimodal integration similar to that observed in the dorsal CN (Shore, Eur. J. Neurosci, 2005), with most neurons showing suppression of acoustically driven responses by trigeminal stimulation. This indicates that the bimodal processing initiated in the dorsal CN is passed on to the next level for integration by the extra-lemniscal system.

## **17 Visual and Saccade-Related Signals in the Primate Inferior Colliculus**

**Jennifer Groh<sup>1</sup>, David Bulkin<sup>1</sup>, Kristin Porter<sup>2</sup>**

<sup>1</sup>*Duke University*, <sup>2</sup>*Dartmouth*

The inferior colliculus (IC) is normally thought of as a predominantly auditory structure, due to its early position in the ascending auditory pathway. Recent work has suggested that the IC may also bear a responsibility for mediating visual influences over hearing. the IC receives anatomical projections from several visual areas such as the retina, visual cortex, and the superior colliculus. in barn owls, neurons in the external nucleus of the IC (ICx) alter their auditory tuning properties when the visual scene is displaced with prisms. in primates, we have previously shown that many IC neurons are sensitive to eye position,

a key signal necessary for the integration of visual and auditory information (Groh et al. 2001; Porter et al. 2006).

in this study, we assessed the visual responsiveness of IC neurons in monkeys performing a task involving a visual stimulus, a saccade, and a sound presentation. We found that a majority of IC neurons (64% of 180 neurons) in awake monkeys carried visual and/or saccade-related signals in addition to their auditory responses. the response patterns included excitatory and inhibitory visual responses, increased activity time-locked to the saccade, and slow rises in activity time-locked to the onset of the visual stimulus.

Based on several previous studies in species other than primates, it has been suggested that the ICX plays a role in multisensory processing but the ICC (central nucleus) does not. to see if this was true for visual signals, we conducted a series of mapping experiments in which assessed multiunit activity at regular intervals throughout the IC. We found visual responses in both putative ICX and putative ICC, in approximately equal proportions. This suggests that in the primate, both of these subregions of the IC play a role in integrating visual and auditory information. More broadly, our results show that interactions between sensory pathways can occur at very early points in sensory processing streams. This in turn implies that multisensory integration may be a low-level rather than an exclusively high-level process.

## **[18] Who is Saying What to Whom: The Amygdala and the Inferior Colliculus Talk**

**Jeffrey Wenstrup<sup>1</sup>, Diana Peterson<sup>1</sup>, Donald Gans<sup>1</sup>**

<sup>1</sup>*Northeastern Ohio Universities College of Medicine*

Inferior colliculus (IC) projections to the auditory thalamus lay groundwork for multiple auditory inputs to the amygdala. This limbic center evaluates biological/emotional significance of sensory stimuli and orchestrates an animal's responses to emotion-laden stimuli. the amygdala in turn influences auditory processing through several routes. Here we consider functional properties and connections of a direct pathway from the basolateral amygdala to IC in bats, species with multiple highly developed acoustic behaviors. to identify acoustic conditions under which the amygdala is activated, we presented a variety of sounds while recording activity in the amygdala. Most amygdalar neurons that respond to acoustic stimuli (~92%) are highly selective for one or a few vocal communication signals. About half display time locked responses to auditory stimuli, but over half displayed a prolonged firing pattern. Prolonged firing patterns were characterized by onset latencies usually exceeding one second and continuous discharge that lasts up to several tens of seconds. These response properties and firing patterns should have a significant impact on target neurons in the IC. Axonal transport studies show that the IC receives a mostly ipsilateral amygdalar projection originating from the magnocellular subdivision of the basal nucleus. in IC, the projection neurons have fine axons with en passant endings. Glutamate/aspartate application or electrical stimulation of the amygdala affects nearly all IC recording sites. At some sites it evokes action potentials, while at others it suppresses background

discharge. At most recording sites, amygdalar stimulation alters responses to acoustic stimuli (increase or decrease), often depending on the match between tuning at the IC recording site and the test frequency. Amygdalar activation may thus alter the responses of IC neurons to emotion-laden sounds. Supported by NIDCD grants RO1 DC 00937 (JJW) and F32 DC007786 (DCP).

## **[19] The History of Serous Otitis Media Parts II & III**

**Robert Ruben<sup>1</sup>**

<sup>1</sup>*Albert Einstein College of Medicine*

Serous otitis media (SOM) is a condition which has always affected humankind but it was not a significant problem the last half of the 20th century. the following will trace the ways in which SOM was considered and cared for during the 20th and 21st centuries. the first part of the 20th century saw little change in the recognition or care of SOM. Our current 21st century conceptualization and concern of SOM has come about from four advances; antibiotics, the re discovery of the tympanostomy tube, the clinical use of middle ear impedance and the association of a history of otitis with linguistic deficiency. Eagle, 1946, documents the marked increase in SOM seen over an 11 year's period (1935 -1946). Armstrong, 1954, reported five cases that the insertion of a vinyl tube through a myringotomy was successful in treating chronic secretory otitis media. Zwislocki's development, 1957, of a physical method to measure the impedance of the tympanic membrane in a living human allowed for its clinical application. This was developed into an instrument by Masden in 1960. Jerger reported his results in 1970 and a suggested classification has been widely accepted. the 1967 report of Holm Kunze found that children with fluctuating hearing losses from otitis media preformed significantly worse than controls in 8 of 12 cognitive /linguistic measures which required the receiving or processing of auditory stimuli or the production of verbal response. the four in which there was no differences were all dependent on visual and motor skills. the historical study of SOM exemplifies the way in which disease is recognized, how prevalence changes and the role it plays in human health. There was developed technology, otoscopy and impedance which facilitated the accurate diagnosis of SOM. the observations and documentation in the 1950's clearly show that the prevalence of SOM greatly increased, probably due to antibiotics, and, as we are now learning, by the formation biofilms. the assumption that SOM was always as prevalent as it is now and that the care of SOM is a 'fashion' is not sustained. This is a disease which appears to be made more prevalent by the change in the bacterial environment from the use and over use of antibiotics.

## **[20] Activation of NF-Kb and Serine Phosphorylation by Otitis Media Pathogens and TNF in Epithelial Cells**

Sung Moon<sup>1</sup>, Jeong-Im Woo<sup>1</sup>, Huiqi Pan<sup>1</sup>, Haa-Yung Lee<sup>1</sup>, Robert Gellibolian<sup>1</sup>, David Lim<sup>1</sup>

<sup>1</sup>House Ear Institute

NF-kB is a eukaryotic transcription factor, required for regulating genes related to inflammation. Five different subunits of Rel/NF-kB proteins have been identified such as p65 (Rel-A), c-Rel, Rel-B, NF-kB1 (p105/p50), and NF-kB2 (p100/p52). the most prevalent activated form of NF-kB is a heterodimer of p65, in complex with p50 or p52. Recently, we showed that activation of p65 is involved in nontypeable *Haemophilus influenzae* (NTHi)-induced monocyte chemotactic protein 1 up-regulation in the spiral ligament fibrocytes (Moon et al, 2007). the purpose of this study is to elucidate the specific subunits of NF-kB that are activated upon exposure to TNF and otitis media (OM) pathogens such as NTHi and *S. pneumoniae* (SP) and to identify the phosphorylated serine residue of the NF-kB subunits involved. Luciferase assay was performed with vectors containing multiple copies of the NF-kB consensus sequence, demonstrating that NTHi, SP and TNF activate NF-kB. Immunolabeling showed that p65 and p105 were translocated to the nucleus upon exposure to NTHi, SP or TNF. Immunoblotting showed that Ser536 of p65 and Ser933 of p105 are phosphorylated upon exposure to NTHi, SP or TNF. Interestingly, Ser468 and Ser276 of p65 were phosphorylated by SP or TNF, but not by NTHi. TNF showed a faster kinetics in activating NF-kB than NTHi or SP. Taken together, it is suggested that NTHi activates host inflammatory genes through a different NF-kB activation pathway than SP or TNF. the next phase of this project is identifying the specific subunit of NF-kB – with its associated phosphorylation sites – in the presence of OM pathogens or TNF, which enables us to better understand host-pathogen interactions.

## **[21] Macrophage Phagocytosis, Intracellular Killing and Cytokine Production During Otitis Media is Impaired in the Absence of TNF and MyD88**

Anke Leichtle<sup>1</sup>, Michelle Hernandez<sup>2</sup>, Kwang Pak<sup>3</sup>, Friedrich Bootz<sup>4</sup>, Allen F. Ryan<sup>3</sup>, Stephen I. Wasserman<sup>5</sup>

<sup>1</sup>Department of Surgery, Division of Otolaryngology, UCSD School of Medicine, USA and Bonn, Germany,

<sup>2</sup>Department of Pediatrics, Division of Allergy & Immunology, UNC School of Medicine, <sup>3</sup>Department of Surgery, Division of Otolaryngology, UCSD School of Medicine, <sup>4</sup>Department of Surgery, Division of Otolaryngology, University of Bonn, Germany,

<sup>5</sup>Department of Medicine, Division of Rheumatology, Allergy & Immunology, UCSD School of Medicine

Rationale: Toll-like receptors (TLRs) shape innate immunity to pathogens and trigger the production of inflammatory cytokines, such as tumor necrosis factor (TNF), and chemokines. All TLRs except TLR3 are linked to the adaptor molecule MyD88 to downstream signaling. We previously found that middle ear (ME) bacterial

clearance was impaired in mice deficient in these molecules. We therefore evaluated the role of TLR signaling and TNF in cytokine/chemokine production and macrophage behavior during otitis media (OM).

Methods: the MEs of MyD88 <sup>-/-</sup>, TNF <sup>-/-</sup> and WT mice were inoculated with NTHi and assessed histologically from 0-21days for neutrophil and macrophage recruitment. Gene expression of NTHi-infected ME mucosa was evaluated by DNA microarray analysis and real-time PCR. Phagocytosis and intracellular killing by MyD88 <sup>-/-</sup>, TNF <sup>-/-</sup> and WT macrophages was assessed *In Vitro*, using cells derived from bone marrow stem cells.

Results: Neutrophil and macrophage recruitment to the ME was delayed and then prolonged in MyD88 <sup>-/-</sup> and TNF <sup>-/-</sup> mice. Moreover, the capacity for phagocytosis and intracellular killing was impaired in both MyD88 <sup>-/-</sup> and TNF <sup>-/-</sup> macrophages. Expression of IL1b, IL6, IL10, CXCL2 and CCL3 was observed in TNF <sup>-/-</sup> prior to NTHi administration, indicating ongoing inflammation. While in WT mice these genes were rapidly induced by NTHi, peaking at 6 hours, most transcripts in TNF <sup>-/-</sup> mice were hyporesponsive to NTHi.

Conclusions: in the absence of either a key signaling molecule or a key effector of innate immunity, OM chronicity is increased due to deficits in phagocyte recruitment and function. Moreover hyporesponsiveness of cytokine/chemokine expression, presumably reflecting TLR tolerance, contributes to these deficits.

(Supported by grants DC00129 (AR) and DC006279 (SW))

## **[22] Correlation of Middle and Inner Ear Cytokine Gene Expression in Mouse Otitis Media Models Suggests Inflammatory Factors Contribute to Sensorineural Hearing Loss**

Dennis Trune<sup>1</sup>, Jiaqing Pang<sup>1</sup>, Beth Kempton<sup>1</sup>, Carol MacArthur<sup>1</sup>, De-Ann Pillers<sup>1</sup>

<sup>1</sup>Oregon Health & Science University

The inner ear is at risk in both acute and chronic otitis media (OM), but the mechanisms underlying the transient and permanent sensorineural hearing loss are unknown. Previous DNA array screening studies showed cytokine genes might be upregulated in the cochleas of BALB/c mice given transtympanic heat-killed bacteria and in cochleas of C3H/HeJ mice with chronic middle ear inflammation. This implied the inner ear could manifest a direct inflammatory response to OM that may cause local damage. Therefore, to better understand inner ear cytokine gene expression during OM, quantitative RT-PCR was performed on these mouse models to measure and correlate middle and inner ear mRNA levels of inflammatory and remodeling cytokines.

in acute OM (Balb/c mice, transtympanic *S. pneumo* inoculation, 3 day survival), significant elevation in middle ear mRNA was seen for IL-1a, IL-1b, IL-6, TNFa, and BMP7 (p<0.01), some several fold. Cochlear tissues significantly expressed these same cytokines, as well as FGF1, TGFb, and VEGF (p<0.01). RT-PCR of our chronic OM mouse model (C3H/HeJ) also showed significant

middle ear mRNA expression of BMP6, BMP7, FGF1, IL-1a,b, TGFb, TNFa, and VEGF ( $p<0.01$ ). Inner ear mRNA was significantly elevated for the same cytokines, as well as IL-6 ( $p<0.01$ ). Thus, both transient and chronic OM caused both the middle ear and inner tissues to express cytokine genes. Furthermore, these cytokines induce tissue remodeling (TNFa, FGF, BMP) and angiogenesis (VEGF), as well as inflammatory cell proliferation (IL-1a,b, IL-2, IL-6).

These studies show tissues within the cochlea are capable of expressing cytokine mRNA, which explains its inflammation and remodeling during middle ear disease. This provides a molecular basis for the transient and permanent sensorineural hearing loss often reported with acute and chronic OM.

(Supported by NIH-NIDCD R01 DC05593 & DC005593-S1, NIH-NIDCD R21 DC007443, and NIH-NIDCD P30 DC005983).

## **[23] Mucin Gene 19 (MUC19) Response to Inflammatory Cytokine Exposure in Middle Ear Epithelium**

**Joseph Kerschner<sup>1</sup>**, Pawjai Khampang<sup>1</sup>

<sup>1</sup>*Medical College of Wisconsin*

Title: Mucin gene 19 (MUC19) response to inflammatory cytokine exposure in middle ear epithelium

Otitis media (OM) is the most common diagnosis in pediatric patients who visit physicians for illness in the United States. Mucin production in response to otitis media causes significant sequelae including hearing loss and the need for surgical intervention. MUC19 is a recently identified mucin gene which produces the largest identified mucin protein to date. In addition, MUC19 is a gel-forming mucin. As gel-forming mucins increase middle ear fluid viscosity and inhibit mucociliary clearance these mucin products warrant investigation into their role in middle ear pathophysiology.

We investigated the expression of MUC19 in human middle ear epithelium (HMEEC) in response to inflammatory cytokines important in OM pathogenesis. Time-dependent experiments demonstrated a significant difference in MUC19 expression from HMEEC with maximum expression after exposure to tumor necrosis factor alpha (TNF- $\alpha$ ) at 2 hours ( $p<0.001$ ). In addition, at the 2-hour time point, MUC19 expression after exposure to 100ng/ml of TNF- $\alpha$  was significantly increased compared to control HMEEC ( $p<0.008$ ). Exposure of HMEEC to interleukin-1 $\beta$  (IL-1 $\beta$ ), interleukin-6 (IL-6) and interleukin-8 (IL-8) also demonstrated a significant time-dependent expression with maximum expression at 1 hour (all  $p<0.001$ ).

These studies further elucidate the expression of MUC19 in HMEEC and demonstrate that its expression is time-dependent with respect to inflammatory cytokines which also have the potential to up-regulate expression of this mucin gene. Further studies with respect to the overall function of this mucin gene product in the middle ear and its role in the pathogenesis of OM are warranted and ongoing.

## **[24] Comprehensive Evaluation of 16 Functional Candidate Genes for Chronic Otitis Media with Effusion and/or Recurrent Otitis Media (COME/ROM)**

**Michele Sale<sup>1</sup>**, Miranda Marion<sup>2</sup>, Peter Perlegas<sup>2</sup>, Fernando Segade<sup>3</sup>, Dax Allred<sup>2</sup>, Stephen Rich<sup>1</sup>, Kathleen Daly<sup>4</sup>

<sup>1</sup>*University of Virginia Charlottesville*, <sup>2</sup>*Wake Forest University*, <sup>3</sup>*University of Pennsylvania*, <sup>4</sup>*University of Minnesota*

Variants in genes involved in the innate immune response, secondary response to infection, and anatomical development may confer susceptibility to chronic otitis media with effusion and/or recurrent otitis media (COME/ROM). We evaluated single nucleotide polymorphisms (SNPs) in 16 functional candidates, a total of 145 SNPs encompassing 447 kb, selected using HapMap data, were successfully genotyped on the Sequenom platform in 142 families (619 subjects) from the Minnesota COME/ROM Family Study. Data were analyzed for association with COME/ROM using the Pedigree Disequilibrium Test (PDT). Single SNP and 2- and 3-SNP haplotype analyses were performed. Three single SNPs, five 2-SNP haplotypes and six 3-SNP haplotypes exhibited nominal ( $P<0.05$ ) evidence for association with COME/ROM. Variants in toll-like receptor 4 (TLR4) were associated with COME/ROM: SNP rs2770146 ( $P=0.026$ ) and three haplotypes (rs2770146 and rs5030717,  $P=0.017$ ; rs12377632, rs2770146 and rs5030717,  $P=0.014$ ; rs11536857, rs11536857 and rs12377632,  $P=0.025$ ). The Interleukin 10 (IL10) SNP rs3021094 ( $P=0.040$ ), and three haplotypes were also associated with COME/ROM (rs3021094 and rs1800872,  $P=0.039$ ; rs3024509 and rs1554286,  $P=0.012$ ; rs1800896, rs1800893 and rs1800890,  $P=0.017$ ). Associations in the mucin 5 gene region were seen with SNP rs2735733 ( $P=0.019$ ) and a two-SNP haplotype containing rs2735733 ( $P=0.046$ ). Two non-overlapping 3-SNP haplotypes in surfactant protein D ( $P\sim 0.025$ ) and a single 3-SNP haplotype in interleukin 1- $\beta$  ( $P=0.040$ ) were also associated. Genes that did not contain variants that were associated with COME/ROM were: lactotransferrin, toll-like receptor 2, interleukin 8,  $\beta$ -defensin 1, surfactant proteins A1 and A2, voltage-gated sodium channel type 1  $\beta$ , mucin 2, mannose-binding lectin precursor, CD14, and ecotropic viral integration site 1. These analyses have focused attention on specific regions of five genes that warrant further evaluation for a role in COME/ROM susceptibility.

**[25] Identification of Nasopharyngeal Biofilms with Middle Ear Pathogens in Otitis-Prone Children Utilizing Scanning Electron Microscopy and Fluorescent *In-Situ* Hybridization Confocal Microscopy**

Michael Hoa<sup>1</sup>, Emily Kingsley<sup>2</sup>, Lisa Christensen<sup>3</sup>, Luanne Hall-Stoodley<sup>4</sup>, Paul Stoodley<sup>4</sup>, Garth D. Ehrlich<sup>4</sup>, J. Christopher Post<sup>4</sup>, Richard Berk<sup>5</sup>, James Coticchia<sup>3</sup>

<sup>1</sup>*Dept. of Otolaryngology-Head and Neck Surgery (HNS), Wayne State University (WSU) School of Medicine,*

<sup>2</sup>*Wayne State University School of Medicine,* <sup>3</sup>*Div. of Pediatric Otolaryngology, Dept. of Otolaryngology-HNS, WSU School of Medicine,* <sup>4</sup>*Center for Genomic Sciences, Allegheny-Singer Research Institute,* <sup>5</sup>*Department of Immunology and Microbiology, Wayne State University School of Medicine*

**Objectives:** Biofilms have been implicated in the development of infections. Protection from overcrowding and altered oxygen tension, poor antibiotics diffusion through the biofilm matrix, and creating an effective milieu for gene transfer and subsequent antibiotic resistance are some ways in which biofilms mediate recalcitrant infections. Nasopharyngeal (NP) biofilms may serve as a middle ear pathogen reservoir, allowing for recurrent infections of the middle ear. We sought to demonstrate middle ear pathogens in nasopharyngeal biofilms using scanning electron microscopy (SEM) and fluorescent *In-Situ* hybridization (FISH) confocal laser microscopy.

**Study Methods:** Comparative micro-anatomic investigation of adenoid mucosa using SEM and FISH imaging from patients with RAOM.

**Results:** All otitis-prone children demonstrated biofilm presence greater than 85% by SEM. FISH Confocal imaging also demonstrated dense biofilms by staining techniques. All biofilms contained middle ear pathogens and were frequently in polymicrobial distributions. 67%, 67% and 50% of samples contained *Haemophilus influenzae*, *Streptococcus pneumoniae* and *Moraxella catarrhalis*, respectively.

**Conclusions:** Previous investigators have demonstrated the development of negative middle ear pressure in children with viral upper respiratory infections. Aspiration of planktonic middle ear pathogens existing in resistant NP biofilms during a viral URI may be an important event in the development of AOM.

**[26] Effects of Streptococcus Pneumoniae Proteins, Pspa and Pneumolysin, on the Sensorineural Hearing Loss in a Chinchilla Model of Otitis Media**

Vladimir Tsuprun<sup>1</sup>, Sebahattin Cureoglu<sup>1</sup>, Patricia Schachern<sup>1</sup>, Michael Paparella<sup>2</sup>, Steven Juhn<sup>1</sup>

<sup>1</sup>*University of Minnesota,* <sup>2</sup>*University of Minnesota, Paparella Ear, Head and Neck Clinic*

*Streptococcus pneumoniae* is the most frequent bacterium in acute and recurrent otitis media (OM). Temporary or permanent sensorineural hearing loss (SNHL) is known to be a sequela of pneumococcal OM. the pathogenesis of the SNHL is thought to arise from

passage of bacterial products and inflammatory mediators from the middle ear through the round window membrane (RWM) into the inner ear. the purpose of this study was to find the effects of pneumococcal proteins, pneumococcal surface adhesion protein (PspA), and pneumolysin (Ply) of *S. pneumoniae*, on inner ear and SNHL in a chinchilla model of OM. Twenty eight days after instillation of ~ 40 CFU of live wild-type pneumococci, a frequency-specific ABR test (1-32 kHz) showed threshold changes of 10-15 dB for 4-32 kHz, and more than 20 dB for 1-2 kHz. Histological analysis showed no fluid, inflammatory cells or bacteria in the middle ear, indicating that hearing loss was sensorineural. in all other groups of animals, normal hearing was observed after instillation of the same or even higher dose of isogenic *S. pneumoniae* mutants of PspA or Ply proteins, or saline injection, after the same period of 28 days. Based on these data, we hypothesize that in addition to the bacteria survival and middle ear inflammation, these two pneumococcal proteins may contribute to the inner ear inflammation and SNHL. These findings suggest that using PspA and Ply proteins for vaccination may have positive effects for prevention of the middle and inner ear inflammation, and SNHL.

Supported by: NIDCD R01DC006452

**[27] Screening of Nontypeable Haemophilus Influenzae-Specific Molecules Responsible for Inducing DEFB4**

Jeong-Im Woo<sup>1</sup>, Sung Moon<sup>1</sup>, Huiqi Pan<sup>1</sup>, Haa-Yung Lee<sup>1</sup>, Robert Gellibolian<sup>1</sup>, David Lim<sup>1</sup>

<sup>1</sup>*House Ear Institute*

Nontypeable *Haemophilus influenzae* (NTHi) is a clinically important pathogen because it causes exacerbating chronic obstructive pulmonary disease in adults, and otitis media in children. Recently, we showed that NTHi molecules up-regulate DEFB4 in epithelial cells (Moon et al, 2006). However, the specific identity of these molecules remains unknown. to remedy this, we decided to perform proteomic analyses of the fractionated NTHi molecules to identify specific inducers of DEFB4, binding to pathogen pattern recognition receptors (PPRRs). We showed that NTHi's ability to induce DEFB4 expression was inhibited by heat treatment, indicating the involvement of tertiary structure of proteins. Moreover, this ability to induce DEFB4 was inhibited by lysozyme (muramidase), but not by lipase. the soluble fraction of NTHi molecules showed increased capacity to up-regulate DEFB4 compared to other fractions. Interestingly, IL-8 was highly induced by the periplasmic fraction, suggesting the presence of inducers specific to the target genes. 1-D gel electrophoresis showed different protein separation profiles between the fractions. Mass spectrometry was performed on specific isolated bands in the soluble fraction, and potential candidate proteins in DEFB4 induction identified and listed. We are currently screening this list using the luciferase-expressing vector with the DEFB4 promoter and the PPRR-expressing vectors. Identification of specific DEFB4 inducers will enable us to better understand host-pathogen interactions and the molecular pathogenesis leading to otitis media.

**[28] Microarray Analysis of Keloid Versus Normal Skin Cells and Fibroblasts: Up-Regulation of the TGF-Beta Pathway**

Selena Heman-Ackah<sup>1</sup>, David Hom<sup>2</sup>, Jizhen Lin<sup>1</sup>

<sup>1</sup>University of Minnesota, <sup>2</sup>University of Cincinnati

Microarray Analysis of Keloid versus Normal Skin Cells and Fibroblasts: Up-regulation of the TGF-beta pathway

**BACKGROUND:** Keloids are benign dermal tumors that occur in response to tissue injury. Keloids are characterized by the proliferation of dermal fibroblasts, overproduction of extracellular matrix components, expansion beyond the original boundaries of the injury and recurrence of disease. Recent studies indicate that transforming growth factor (TGF)- $\beta$  pathway may play an essential role in the pathogenesis of keloids by inducing and sustaining activity of keloid fibroblasts. the exact mechanism is not well understood. **OBJECTIVES:** the objective of this study is to identify sites within the TGF- $\beta$  pathway which are up-regulated or down-regulated in keloid fibroblasts when compared to normal skin cells from scar tissue and normal fibroblasts **METHODS:** a microarray assay was performed evaluating genes within the TGF- $\beta$  pathway. the following samples were evaluated: 2 samples of normal scar tissue from human subjects, 3 samples of cultured human dermal fibroblasts, and 2 samples of keloid tissue from human subjects. **RESULTS:** a total of 104 genes related to the TGF- $\beta$  pathway were evaluated. Statistically significant differences were observed in the TGF- $\beta$  pathway (scored at 62.12) between keloids and controls (human dermal fibroblasts and normal scar cells). a better understanding of these mechanisms underlying keloid formation could lead to more effective treatment of this disease process.

**[29] Glucocorticoid and Mineralocorticoid Suppression of Acute and Chronic Otitis Media in Mice**

Carol MacArthur<sup>1</sup>, J Beth Kempton<sup>1</sup>, Jacqueline DeGagne<sup>1</sup>, Dennis Trune<sup>1</sup>

<sup>1</sup>OHSU

Glucocorticoid and Mineralocorticoid Suppression of Acute and Chronic Otitis Media in Mice

Although middle ear inflammation from acute otitis media (AOM) generally subsides after 5-7 days, suppression of this response would help alleviate suffering and minimize risk to the inner ear. Also, chronic otitis media (COM) causes considerable middle ear inflammation and puts the inner ear at risk for hearing loss. Thus, suppression of inflammation in both AOM and COM is critical. Glucocorticoids and mineralocorticoids have differential effects on inflammation and fluid absorption, but little is known of their control of middle and inner ear manifestations of AOM and COM. Therefore, various steroids were investigated for their ability to reduce these middle ear inflammatory sequelae to determine the potential for therapeutic approaches to their control. **AOM:** Balb/c mice were inoculated transtympanically with heat-killed *Streptococcus pneumoniae*. oral steroid treatments (prednisolone, dexamethasone, fludrocortisone,

aldosterone) were begun the day before inoculation and middle ears were assessed after 3 or 5 days for suppression of fluid area, inflammatory cells, and tympanic membrane (TM) thickness. **COM:** C3H/HeJ mice with COM were tested for baseline ABR thresholds and then given the same steroids. Thresholds were remeasured after 2 and 4 weeks of treatment. At 4 weeks study animal ears were processed for histopathology. **AOM:** ANOVA showed significant steroid effects at both 3 and 5 days in reduction of fluid area, cell number and TM thickness in the middle ear. Glucocorticoids were most effective in controlling inflammation. **COM:** ANOVA showed significant steroid treatment effects on ABR thresholds at all frequencies except 8 kHz. Both glucocorticoids and mineralocorticoids caused some degree of hearing recovery. These studies offer insight into the potential steroid control of middle and inner ear disease during acute and chronic otitis media. Steroid control of middle ear disease may be useful in alleviating symptoms faster and reducing risk to the inner ear.

Supported by NIH-NIDCD R01 DC05593 & DC005593-S1, NIH-NIDCD R21 DC007443, and NIH-NIDCD P30 DC005983.

**[30] Fungus Infection of the Middle Ear in a Cetacean**

*Withdrawn*

**[31] Improvement in Hearing Following Occipital Nerve Injection**

Neil Cherian<sup>1</sup>

<sup>1</sup>Neurological Institute at the Cleveland Clinic

Normal hearing function is the product of a number of discrete events including mechanical conduction of vibrational energy in the middle ear, electrochemical stimulation in the cochlea and various converging and diverging pathways in the brainstem on its way to the auditory cortex. Additional mechanisms including middle ear muscle responses and outer hair cell (efferent) pathways play a role in further shaping and filtering hearing function. the following is a discussion regarding a patient whose hearing function improved after a trigger point injection of the greater occipital nerve. A 53 year-old woman experienced the onset of a fluctuating left-sided hearing loss over time. She noted intermittent hearing fluctuation at times with vertigo starting at age 34. She was diagnosed as Meniere's disease though did not respond to diuretic therapy. No response to endolymphatic sac shunt surgery. Eight years ago she started to experience drop attacks. Upon evaluation in my office, I noted an improvement of left-sided hearing with neck flexion against resistance. Cervical spine exam revealed a derangement of upper cervical spine biomechanics. a greater occipital nerve trigger point injection was performed on the left using marcaine (anesthetic) and triamcinolone (steroid). Immediately afterward patient noted a significant

improvement in her hearing. Responses were correlated with audiometry.

The improvement in hearing in response to neck flexion against resistance suggests the erroneous co-contraction of middle ear muscles upon the activation of neck musculature. the patient's response to the trigger point injection suggests an inhibition of the hyperexcitability of the middle-ear musculature. Although she may, indeed, have an otogenic syndrome, it appears that her hearing deficit is multifactorial.

### **[32] Hearing in Women with Turner Syndrome: Studies on Peripheral and Central Hearing Function**

*Withdrawn*

### **[33] Isolation and Characterization of Genomic DNA from Archival Human Temporal Bones**

**Jose Fayad, MD<sup>1</sup>**, Orlando Valentino<sup>1</sup>, Ana Cortez<sup>1</sup>, Fred Linthicum, Jr, MD<sup>1</sup>, Robert Gellibolian, PhD<sup>1</sup>

<sup>1</sup>*House Ear Institute*

**Objectives:** to quantitatively extract and measure concentrations of genomic DNA in archived celloidin preserved human temporal bones that have been stored for different periods of time. to study the effects of storage and digestion times on the concentrations and quality of extracted DNA.

**Study Design:** 50 mg of each 20 microns celloidin embedded section was measured out. Digestion was done using Proteinase K (20mg/ml) using the RecoverAll™ Total Nucleic Acid Isolation kit (Ambion, Inc.). Genomic DNA was measured with a Beckman 650 spectrophotometer, and was then amplified using whole genome amplification (WGA). Concentrations of WGA-DNA were measured and subsequently used for sequence analyses.

**Methods:** Tissue samples from formalin-fixed, celloidin embedded archival human temporal bones that have been stored for various times (5 to 30 years) were digested for different amounts of time (48 to 120 hours). Concentrations and quality of genomic DNA isolated under these conditions were compared using spectrophotometric analyses, PCR and sequencing.

**Results:** in general, the yield of genomic DNA isolated from temporal bone samples increased with longer digestion times. Specimen stored longer than 20 years yielded the lowest concentrations of DNA, with longer digestion times exhibiting little or no improvements in the yield of nucleic acid. However, specimen stored for less than 10 years yielded higher concentrations of genomic DNA.

**Conclusions:** Age of specimen and duration of storage as well as digestion time are important factors in yielding higher concentration of DNA.

**Key Words:** Genomic DNA, celloidin embedded human temporal bones, whole-genome amplification, PCR.

### **[34] Expression of Telomerase and Cytomegalovirus in Vestibular Schwannoma**

**Andrew Patel<sup>1</sup>**, Joni Doherty<sup>1</sup>

<sup>1</sup>*University of California, San Diego*

**Background and Objectives:** Vestibular schwannomas (VS) present significant management challenges both in patients with sporadic tumors and in patients with neurofibromatosis type 2 (NF2). Telomerase, the enzyme that stabilizes telomere length, is reactivated with almost all cancer types, and investigating genes involved in maintenance of genomic integrity might deepen understanding of VS progression. Telomerase activity in VS is clinically relevant because the presence of the enzyme suggests that these benign-appearing tumors may contain a population of immortal cells. the expression of hTERT, the human telomerase catalytic subunit gene, is a rate-limiting determinant of the enzymatic activity of human telomerase. in addition, it has recently been shown that human cytomegalovirus (HCMV) initiates infection by interacting with epidermal growth factor receptor (EGFR) and inducing intracellular signaling through glycoprotein B (gB), its principal envelope glycoprotein. Members of the ErbB receptor family are over-expressed in several types of human tumors, and we hypothesize that ErbB signaling may be up-regulated in VS. HCMV infection may thus mediate increased ErbB signaling via this pathway.

This study sought to determine the relationship between vestibular schwannomas and telomerase and cytomegalovirus expression.

**Methods:** Tissue from surgically removed vestibular schwannomas of 40 patients was analyzed. Tumor samples were stored immediately after surgery in liquid nitrogen until RNA extraction. Real-Time RT-PCR was then performed with quantification of and normalization to transcripts of the human cyclophilin gene as the endogenous RNA control and final results expressed as N-fold differences in hTERT and HCMV gB gene expression. **Results and Conclusions:** in patients with VS with and without NF2, the role of infection with the neurotropic HCMV and expression of telomerase in the pathoetiology of the disease will be investigated.



### **[35] ABR Latency Prolongation in CIC-2**

#### **Knockout Mice**

Adrian Münscher<sup>1</sup>, Hannes Maier<sup>1</sup>, Judith Blanz<sup>2</sup>, Michaela Schweizer<sup>3</sup>, Christian Hübner<sup>4</sup>, Thomas Jentsch<sup>5</sup>  
<sup>1</sup>ENT Dept, Hamburg University Medical School, Germany, <sup>2</sup>Dept of Biochemistry, Kiel, Germany, <sup>3</sup>ZMNH, Hamburg, Germany, <sup>4</sup>Dept. of Clinical Chemistry, Jena, Germany, <sup>5</sup>Max-Delbrück Center, Berlin, Germany

CIC-2 is a broadly expressed plasma membrane Cl<sup>-</sup> channel of the CLC family. the subgroup, which includes CIC-2 is responsible for genetic diseases as myotonia congenita (CIC-1) and Bartter syndrome (CIC-Kb or its beta-subunit barttin). in mice CIC-2 disruption led to blindness and male infertility (Bösl et al., 2001; Nehrke et al. 2002) presumably based on changes of the ionic environment.

To determine the significance of CIC-2 for hearing, auditory evoked brainstem responses (ABR) to clicks were recorded in anesthetized animals (16mg/kg xylazine hydrochloride, 120mg/kg ketamine hydrochloride) by subdermal silver wire electrodes (vertex, forehead and mastoids). Alternating clicks were applied at a rate of 21/s and averaged 400 to 2000 times. Stimulus intensities started at 117 dB pe SPL and were varied in increments of 20 dB except near threshold where 5 dB steps used. Latency analysis was performed at 117 dB pe SPL blinded.

Auditory brainstem responses showed statistically indistinguishable hearing thresholds at the ages 3, 5, 12 and 24 weeks of wild types and CLC2<sup>-/-</sup>. Inter peak intervals (IPIs) between waves I and III were significantly increased in 5 and 12 weeks old animals KO while IPis between wave III and V were unchanged. These findings indicate a slowed nerve conductance and/or impaired synaptic transmission before the cochlear nucleus.

Although we found a severe and widespread spongiform vacuolation of the white matter and spinal cord neurological deficits were mild in CIC-2 KO mice. Hearing thresholds determined by clicks were unchanged in CIC-2 KO mice and showed a comparable degree of age-related hearing loss. Only IPis between wave I and III of auditory brainstem responses were significantly increased in older animals indicating a decreased nerve conductance in KO animals. Our findings correlate with the progressive vacuolation found in the white matter including the brainstem while peripheral nerves were unaffected.

### **[36] MAP: Mouse Auditory Proteomics**

Kumar Alagramam<sup>1</sup>, Daniel H.-C. Chen<sup>1</sup>, Qing Zheng<sup>1</sup>, Shuqing Liu<sup>2</sup>, Ming-Zhong Sun<sup>2</sup>, Mark Chance<sup>2</sup>

<sup>1</sup>Department of Otolaryngology-HNS, School of Medicine, Case Western Reserve University, <sup>2</sup>Center for Proteomics and Mass Spectrometry, School of Medicine, Case Western Reserve University

INTRODUCTION: Mouse mutants have served as excellent models to understand the genetic basis of hereditary inner ear disorders, including those linked to Usher syndromes. Though the Usher models have been available for many years none of them have been utilized for proteomic studies. Our ultimate aim is to establish a

mouse auditory protein database and biomarkers for hearing impairment. Here we report data from a pilot study. the aim of this pilot study is to identify biomarkers of sensory cells and ear pathogenesis in the mouse model for deafness in Usher 1F by comparing the global protein expression changes between normal and mutant mouse cochlea. METHOD: the affected and normal cochlea of mice at 1 month of age were dissected on ice and homogenized with the aid of liquid nitrogen. the protein was then extracted by using 7M urea plus 2M thiourea and 4% chaps with the aid from water bath sonication. the soluble proteins extracted from the cochlea were then labeled by Cys-dye, prefractionated by the 2-D DIGE, digested by trypsin and analyzed by MALDI-OTOF (prOTOFM 2000) and MDLC LTQ systems. DeCyder software 6.5 was used to quantify the protein spots on the 2D gel. PRELIMINARY DATA: in this pilot study, 2D-difference gel electrophoresis (DIGE) technique combined with mass spectrometry analysis was performed to compare protein expression profiles of the affected and normal cochlea at 1 month of age, a time point when most of the hair cells in the mutant cochlea have degenerated. a successful and reproducible method for protein extraction with stable yield has been established. the soluble proteins were analyzed by the 2D-DIGE system newly established at the Case Center for Proteomics and Mass Spectrometry. the analytic gel resolved more than 2000 protein spots. Over 20 protein spots showed significant changes by the difference in gel analysis (DIA). the biological variation analysis (BVA) experiments are in process. the interesting proteins will be picked, digested and identified both by MALDI-OTOF and MDLC LTQ, and the relevant results will be presented. the proteomic discovery of biomarkers and the establishment of potential regulation pathway are of clinical relevance to the prevention and treatment of hearing diseases.

### **[37] Mouse Models for Usher Syndrome Have a Protein Translocation Defect in Photoreceptors, and are Susceptible to Light-Induced Photoreceptor Cell Degeneration**

You-Wei Peng<sup>1</sup>, Weimin Wang<sup>1</sup>, Marisa Zallocchi<sup>1</sup>, Dominic Cosgrove<sup>1</sup>

<sup>1</sup>Boys Town National Research Hospital

Usher syndrome is characterized by congenital deafness associated with delayed onset and progressive retinitis pigmentosa (RP). Mouse models exist for most of the nine known genes associated with Usher syndrome. All mouse models examined to date show a common phenotype in cochlear hair cells where disorganized and dysmorphic stereocilia are associated with deafness. the retinas appeared to be unaffected in these mice. Recently there have been reports of a subtle and markedly delayed retina phenotype associated with USH1F mice and most recently USH2A mice. Current thinking suggests that the mouse may not be an appropriate species for studying Usher syndrome-related RP. Translocation of visual cycle proteins arrestin and transducin occurs in opposite directions between the inner and outer segments of photoreceptors as a function of both light and dark



adaptation. Using mouse models of Usher syndrome 1B, 1F, and 2A, we show that usher syndrome mouse models are defective in this translocation process. Upon continuous exposure to light at 2500 lux illumination (standing outside on a sunny day is >5000 lux illumination), we show that USH2A and USH1B mouse models show significantly greater loss of photoreceptors (as quantified by counting nuclei in the outer nuclear layer) than wild type littermates. These findings suggest that usher mouse models do indeed possess a robust retinal phenotype, which has likely been masked due to low light conditions in animals housing facilities. Further these data show a common molecular defect in protein translocation for all usher models tested, likely reflecting a common pathway of retinal pathology.

Supported by R01 DC004844 and P20 RR018788

### **[38] Autoimmune Patient Sera Bind to Recombinant Human CTL2 Protein**

**Thankam Nair**<sup>1</sup>, Pavan Kommareddi<sup>1</sup>, Mounica Vallurupalli<sup>1</sup>, Steven Telian<sup>2</sup>, Alexander Arts<sup>2</sup>, Hussam ElKashlan<sup>2</sup>, Thomas Carey<sup>1</sup>

<sup>1</sup>Kresge Hearing Research Institute, <sup>2</sup>University of Michigan

We have previously shown that choline transporter like protein 2 (CTL2) is a target of antibody induced hearing loss and suspected to be one of the target antigens in autoimmune sensorineural hearing loss. Here we report preliminary findings of autoimmune sera binding to recombinant human CTL2 (rHuCTL2) produced using the Invitrogen Bac-Bac Baculovirus expression system. Sera from patients previously shown to have antibodies to guinea pig inner ear supporting cells and to the corresponding 68-72 kDa protein were tested on purified rHuCTL2. CTL2 protein in guinea pig is a 68-72 kDa glycoprotein with a core protein mass of 62 kDa. In insect cells rHuCTL2 is expressed as 62, 66 and 70kDa proteins where the 62 kDa is the core protein and the other two are glycosylated. We screened 12 autoimmune sera and 12 control sera for rHuCTL2 protein binding on western blots. Six autoimmune sera and two control sera exhibited binding with immunoprecipitated rHuCTL2 protein. Further analysis of positive sera with nickel NTA column-purified, histidine-tagged rHuCTL2 revealed that the autoimmune sera were most reactive with the core protein and showed less binding with the glycosylated 66 and 70kDa proteins. The same sera also gave positive binding with deglycosylated rHuCTL2 protein on western blot and by ELISA on 96 well dishes coated with rHuCTL2 purified antigen. This preliminary result strongly indicates that rHuCTL2 produced through an insect cell system can be used for investigation of autoimmune patient sera.

Supported by the Townsend Fund, NIH R01 DC03686, NIH T32 DC00011, and NIH P30 DC05188

### **[39] Bisphosphonates Inhibit Bone Remodeling in the Otic Capsule of Osteoprotegerin Deficient Mouse, an Animal Model of Otosclerosis**

**Osamu Adachi**<sup>1</sup>, Konstantina M. Stankovic<sup>1</sup>, Arthur G. Kristiansen<sup>1</sup>, Joe C. Adams<sup>1</sup>, Sharon G. Kujawa<sup>1</sup>, Michael J. McKenna<sup>1</sup>

<sup>1</sup>Massachusetts Eye & Ear Infirmary

The otic capsule remodels minimally if at all under normal physiologic conditions. Under pathologic conditions, like otosclerosis, the otic capsule can undergo substantial remodeling. Bone remodeling is regulated by the osteoprotegerin (OPG)-receptor activator of nuclear factor kappa b (RANK) - RANK ligand (RANKL) system. We have previously shown that OPG knockout (ko) mice exhibit pathologic bone remodeling reminiscent of otosclerosis, and that these mice present the best animal model to date for otosclerosis, a common cause of acquired hearing loss. Here, we test whether pharmacologic inhibition of otic capsule remodeling in OPG ko mice is possible with bisphosphonates, which are potent inhibitors of bone resorption and remodeling. Three week old OPG ko mice were treated by intraperitoneal injection of zoledronate (100 microgram/ kg/ day, 6 days, or 500 microgram/ kg/ day, 6 days) or risedronate (1.6 mg/ kg/ time, 5 times/ week, for 14 weeks) and sacrificed 9 and 18 weeks later. Prior to sacrifice, hearing was evaluated with auditory brainstem evoked response and distortion product otoacoustic emissions. Temporal bones were processed for histological analysis and stained with Azure or tartrate resistant acid phosphatase stain, which evaluates osteoclast activity. Both zoledronate and risedronate dramatically suppressed otic capsule remodeling and resorption, and reduced hearing loss. Our results suggest that bisphosphonates may be helpful in preventing hearing loss associated with otosclerosis.

### **[40] Intercellular Glucose Transport Mediated by Gap Junctions in the Cochlea is Compromised in Connexin30-Deficiency Mice**

**Qing Chang**<sup>1</sup>, Wenxue Tang<sup>1</sup>, Shoeb Ahmad<sup>1</sup>, Xi Lin<sup>1</sup>

<sup>1</sup>Emory University School of Medicine

Mutations in connexin26 (Cx26) and Cx30, which are the major protein subunits to form gap junction (GJ) intercellular channels in the cochlea, cause deafness in both human patients and mouse models. Deficit in GJ mediated K<sup>+</sup> recycling in the cochlea has been considered as one underlying mechanism. However, recent studies showed that Cx26 mutations exerting little effect on ionic coupling were sufficient to cause deafness in human patients. These results suggested that GJ-mediated biochemical coupling is also essential for normal hearing. Indeed, immunolabeling showed that extensive Cx26 homomeric GJ plaques were still present in the cochlea of Cx30<sup>-/-</sup> mice, and cellular patterns of these homomeric Cx26 GJs suggested that intercellular conduits for K<sup>+</sup> diffusion were not disrupted. To compare the extent of biochemical coupling among various types of cochlear cells (Claudius, Hensens, Outer sulcus epithelial and

marginal cells), we used a modified whole-mount cochlear preparation in which the cochlear lateral wall was preserved during dissections. Using such an *In Situ* preparation, we found that cochlear GJs allowed both negative and positive charged fluorescent dyes to pass, including propidium iodide, lucifer yellow and 2-NBDG (a non-hydrolyzable analogue of D-glucose). These molecules readily moved between different types of cochlear supporting cells, but stayed in single marginal cells. Significantly, we found that both the rate and extent of dye diffusion were significantly decreased in the cochlea of Cx30<sup>-/-</sup> mice. Deficiency in GJ-mediated intercellular diffusion of 2-NBDG further suggested that GJ-facilitated intercellular diffusion of glucose in the cochlear supporting cells and fibrocytes in the lateral wall is affected in the mutant mice. This study provided the first directly experimental evidence supporting that targeted deletion of Cx30 in mice compromised intercellular transport of metabolically-important molecules among cochlear cells that are connected by GJs.

#### **41 Mechanisms of Hearing Loss and Cell Death in the Cochlea of Connexin Mutant Mice**

**Wenxue Tang<sup>1</sup>**, Qing Chang<sup>1</sup>, Shoeb Ahmad<sup>1</sup>, Yuhua Li<sup>1</sup>, Xi Lin<sup>1</sup>

<sup>1</sup>Emory University School of Medicine

Mutations in connexin26 (Cx26) and Cx30 are the most common genetic defects linked to non-syndromic deafness in human. In order to understand the underlying molecular mechanisms, we have used Cx30 null mutation (Cx30<sup>-/-</sup>) mouse model to investigate pathological changes in the cochlea. Cx mutant mice never developed normal hearing and severe hearing loss across all frequency range was found at postnatal day 17 (P17) in all animals. This is in sharp contrast to a limited outer hair cell (HC) loss found mostly at the basal turn at P17 and a slow progression of HC death with a basal to apical gradient that lasted for 3-4 months after births. These results indicated that HC death was not the direct cause of deafness and it is unlikely that the slow HC deaths were caused by disruption to the K<sup>+</sup> recycling since a high endolymphatic K<sup>+</sup> and hearing were never developed. Because the morphology of other cochlear cells appeared to be normal in Cx30<sup>-/-</sup> mice, the absence of EP seems to be the direct cause of hearing loss. Western blot analyses using tissue isolated from stria vascularis showed significant reduction in expressions of KCNQ1 and KCNE1 before the establishment of EP at P10. The two types of K<sup>+</sup> channels are known to be required for endolymphatic K<sup>+</sup> secretion and generation of EP. We subsequently performed microarray and proteomics analyses comparing cochlear gene expressions in wild type and Cx30<sup>-/-</sup> mice. Results suggested dysfunction of mitochondria resulted from oxidative stress, activation of inflammation signaling pathways in the mutant mice. Our data suggested that deficits in gap junction (GJ) facilitated cochlear functions required for full expressions of KCNQ1 and KCNE1 at developmental stages before the maturation of EP is directly responsible for deafness in Cx30 null mice.

#### **42 Intracochlear Injection of Adenovirus Vector to a Mouse Model Created by a Conditional Knockout of *Gjb2* Gene**

**Takashi Iizuka<sup>1</sup>**, Sho Kanzaki<sup>2</sup>, Ayako Inosita<sup>1</sup>, Osamu Minowa<sup>3</sup>, Tetsuo Noda<sup>4</sup>, Kaoru Ogawa<sup>2</sup>, Katsuhisa Ikeda<sup>1</sup>

<sup>1</sup>Department of otolaryngology, Juntendo university, graduate school of medicine, <sup>2</sup>Department of Otorhinolaryngology, Keio University, <sup>3</sup>Mouse Functional Genomics Research Group, Riken, <sup>4</sup>Department of Molecular Biology, Cancer Institute

Hereditary deafness affects about 1 in 2,000 children and mutations in the *GJB2* gene are the major cause in various ethnic groups. In order to establish the fundamental therapy of congenital deafness, we generated targeted disruption of *Gjb2* using Cre recombinase controlled by P0. Using this animal model, we examined the potential of gene therapy in the inner ear, using the homozygous mutant mice and the heterozygous mutant mice.

In the mouse, three main routes of delivery are possible, namely scala media approaches (via a cochleostomy), semicircular canal approaches and round window membrane approaches. We chose scala media approaches and round window approaches to examine the expression of virus vector in organ of Corti and lateral wall. Adenoviral vectors carrying the green fluorescent protein (GFP) gene were injected into the scala media through the lateral wall and into the scala tympani through the round window of cochlea, respectively. Auditory brainstem responses were measured before and after treatment.

The scala media approach resulted in considerable hearing loss, whereas the round window approach caused elevation of auditory brainstem responses thresholds by less than 10 dB. The expression of GFP was noted in the organ of Corti of the inner ear in both the homozygous and the heterozygous mutant mice by the treatment of the scala media. On the other hand, by the round window approach, the expression of GFP was noted only in the mesothelial cells in the perilymph in both the homozygous and the heterozygous mutant mice.

The injection technique for hearing preservation should be considered. However, our data suggest that the adenovirus-mediated gene transfer may be successful in the inner ear of *Gjb2* knockout mice.

#### **43 Silencing of Prosaposin in Mouse Cochlea by Rnai**

**Christopher Weber<sup>1</sup>**, Omar Akil<sup>1</sup>, Shi-Nae Park<sup>1</sup>, Lawrence R. Lustig<sup>1</sup>

<sup>1</sup>Department of Otolaryngology-HNS, UCSF

Prosaposin is a precursor of four glycoprotein activators (saposin A-D) for lysosomal hydrolases and has been shown to have both lipid transfer properties and neurotogenic activity. Within the organ of Corti, prior work has shown that prosaposin localizes to the inner hair cells, supporting cells, inner pillar cells, synaptic region of the outer hair cells and Deiters' cells, and may interact with the nicotinic acetylcholine receptor  $\alpha 10$ . Additionally, a prosaposin knockout mouse showed deafness by P25, reduced DPOAE emissions from P15 onward, and afferent

and efferent neuronal proliferation, among other aberrations (Akil et al 2006). However since this research was conducted using a systemic knockout, it is not known whether this observed phenotype occurs as a direct consequence of prosaposin disruption within the cochlea, or from the broader neurologic sequelae that are also seen in this mouse (Sun et al, 2002, 2007). Further, insight into the molecular mechanisms that induce the observed neuronal proliferation seen in the knockout could prove important for emerging clinical applications.

To better characterize the role of prosaposin in the cochlea as well as explore a potentially novel strategy for cochlear neuronal proliferation, we have employed a transient prosaposin siRNA delivery method to the round window membrane (RWM) in mice. *In Vitro*, the prosaposin siRNA constructs are able to eliminate >75% of prosaposin mRNA. *In Vivo* Application to the RWM involves a transcervical approach to the bulla. Prosaposin siRNA is pipetted directly onto the RWM and then gelfoam-impregnated siRNA is placed adjacent to the RWM to maintain saturation within the cochlea over a several day period. We demonstrate that this approach preserves hearing while knocking down prosaposin mRNA within the cochlea. This technique not only demonstrates the feasibility of prosaposin siRNA application in the cochlea, but can easily be applied to other mRNA targets where knockdown of function is desirable.

#### **[44] The Highly Expressed Genes in the Inner Ear - Localization, Possible Functions, and Clinical Relevance**

**Shin-ichi Usami<sup>1</sup>**, Nobuyoshi Suzuki<sup>1</sup>, Hiroaki Suzuki<sup>1</sup>, Aki Oshima<sup>1</sup>, Shigenari Hashimoto<sup>1</sup>, Yutaka Takumi<sup>1</sup>, Satoko Abe<sup>2</sup>, Akira Sasaki<sup>3</sup>, Atsushi Matsubara<sup>3</sup> *Shinshu University School of Medicine, <sup>2</sup>Division of Advanced Technology and Development, BML, Inc., <sup>3</sup>Hiroaki University School of Medicine*

Genes that are expressed specifically in auditory tissues are likely to be good candidates to screen for genetic alterations in patients with deafness. We have been continuously examining 52 genes specifically or exclusively expressed in the human inner ear, revealed by cDNA microarray analysis (Abe et al. 2003), and have successfully identified possible disease causing mutations in them (Abe et al. 2003a,b, Asamura et al., 2005, van Camp 2006). In order to explore the sites within the cochlea where the proteins encoded by these genes are functioning, localization of the proteins encoded by CRYM, COL9A1, COL9A3, KIAA1199, UBA52 was immunocytochemically investigated in mouse and rat cochleae using specific antibodies. Immunocytochemical results indicated that  $\mu$ -crystallin was distributed within fibrocytes of the lateral wall, which are known to be potassium-ion recycling. It may be that  $\mu$ -crystallin is involved in the system crucial for ion homeostasis. UBA52 protein was distributed in the stria marginal cells and vestibular dark cells, which regulate the endolymphatic ion homeostasis. KIAA1199 protein was preferentially distributed in the Deiters' cell region, suggesting that this molecule may have specific function in this area. Type IX collagen is distributed in the tectorial membrane, where it

co-localizes with type II collagen, indicating that type IX collagen may contribute to the integrated structure of type II collagen. Mice with targeted disruption of the col9a1 gene were shown through assessment by auditory brain stem response to have hearing loss, suggesting an important role of type IX collagen in maintaining normal hearing. The present study also summarized our series of mutation screening study, and discussed clinical relevance of these genes. In conclusion, the coordinated actions of various molecules distributed in different parts of the cochlea are essential for maintenance of auditory processing in the cochlea.

#### **[45] Transcriptome and Proteome Analysis of Mouse Inner Ears**

**Qing Zheng<sup>1</sup>**, Shuqing Liu<sup>1</sup>, Chunling Gu<sup>1</sup>, Kumar Alagramam<sup>1</sup>, Ming-Zhong Sun<sup>1</sup>, Heping Yu<sup>1</sup>

<sup>1</sup>Case Western Reserve University

The many available mouse models for human hereditary hearing disorders offer extraordinary tools for molecular pathway studies and drug discoveries (www.jax.org). The use of single mutation mouse models with well-characterized phenotypes on genetically defined backgrounds allows us to use gene and protein expression profiling to identify molecular pathways involved in inner ear structure and function. The transcriptomic and proteomic differences between mutant and wildtype mouse ears are primarily specific to inner ear origin. Here we report several new mutations of transcription factor genes that cause reduced inner ear structures. 2D-difference gel electrophoresis (DIGE) technique combined with mass spectrometry analysis was performed to compare protein expression profiles of the mutant and wildtype mouse ears. We have successfully run two-dimensional gel electrophoresis on triple labeled gels using the inner ear samples of these mutants and their littermate controls. We have identified over 200 protein spots that are significantly differentially expressed between mutants and controls. Pyruvate dehydrogenase (lipoamide) beta is identified to be down-regulated in both ddl mutant and math1 mutant ears. We have identified over 100 proteins by Deca XP Mass Spectrometry and 85 proteins by LTQ-MDLC Mass Spectrometry. We have selectively validated several proteins that are expressed in mouse ears by western blot analysis. These proteomic data will lead to the identification of key novel molecules involved in deafness. These molecules may be potential therapeutic targets.

Research supported by NIH NIDCD R01DC007392 (QYZ)

#### **[46] Clarin-1 is Expressed in Auditory Hair Cells and Localizes to the Base of the Stereocilia**

**Dominic Cosgrove<sup>1</sup>**, Marisa Zallocchi<sup>1</sup>, Suneetha Garige<sup>1</sup>, You-Wei Peng<sup>1</sup>, Charles Askew<sup>2</sup>, Michael Anne Gratton<sup>2</sup>

<sup>1</sup>Boys Town National Research Hospital, <sup>2</sup>University of Pennsylvania

The Usher syndrome type 3 (USH3) gene encodes a protein called clarin-1, which is a member of the tetraspanin family of transmembrane proteins. Although

identified more than 5 years ago, very little is known about its localization or function in sensory epithelial cells. the protein is expressed as two known isoforms, a 50 kDa isoform that contains the transmembrane domains, and a 25 kDa isoform that does not. the two are created by alternative splicing of the second exon. We developed antibodies against clarin-1 and used them to characterize expression of the protein in the cochlea and the retina. Both isoforms of the protein are found in extracts of cochlea and neuroretina by western blot. in the retina, clarin-1 localizes to the connecting cilia and inner segments of photoreceptors and to the ribbon synapses in adult mice, much like that reported for most other usher proteins (Reiners et al., *Exp Eye Res.*, v.83, p.97, 2006). in the cochlea, we observe abundant clarin-1 in the stereocilia of P0 mice. Immunostaining of mid-modiolar sections reveal the staining is concentrated at the base of the stereocilia, much like that reported for VLGR1 and the transmembrane isoform of usherin. We did not observe clarin-1 immunostaining in adult mouse cochlea, suggesting a developmental regulation in hair cells. We examined clarin-1 expression in the immortalized hair cell line OC-1. Expression was markedly induced upon differentiation of these cells, suggesting clarin-1 is activated during terminal cytodifferentiation of hair cells. Collectively these data suggest that clarin-1 is transiently expressed in cochlear hair cells and localizes to the base of stereocilia. in both photoreceptors and hair cells, clarin-1 shows a highly specific sub-cellular co-localization with other usher proteins.

Supported by R01 DC004844 and R01 DC 006442

#### **[47] A Mouse Model with Postnatal Endolymphatic Hydrops and Hearing Loss**

Cliff Megerian<sup>1</sup>, Maroun Semaan<sup>1</sup>, Saba Aftab<sup>1</sup>, Lauren Kisley<sup>1</sup>, Qing Zheng<sup>1</sup>, Karen Pawlowski<sup>2</sup>, Charles Wright<sup>2</sup>, Kumar Alagramam<sup>1</sup>

<sup>1</sup>Case Western Reserve University, University Hospitals Case Medical Center, <sup>2</sup>University of Texas Southwestern Medical Center

Endolymphatic hydrops (ELH), hearing loss and neuronal degeneration occur together in a variety of clinically significant disorders, including Meniere's disease (MD). However, the sequence of these pathological changes and their relationship to each other are not well understood. in this regard, an animal model that spontaneously develops these features postnatally would be a valuable research tool. a search for such a model led us to the PhexHyp-Duk mouse, a mutant allele of the Phex gene causing X-linked hypophosphatemic rickets. the hemizygous male (PhexHyp-Duk/Y) was previously reported to exhibit various abnormalities during adulthood, including thickening of bone, ELH and hearing loss. the reported inner-ear phenotype was suggestive of progressive pathology and spontaneous development of ELH postnatally. the focus of this report is to further characterize the inner ear phenotype in PhexHyp-Duk/Y mice and to test the hypothesis that a) the PhexHyp-Duk/Y mouse develops ELH and hearing loss postnatally and b) the development of ELH in the PhexHyp-Duk/Y mouse is associated with obstruction of the endolymphatic duct (ED)

due to thickening of the surrounding bone. Auditory Brainstem Response (ABR) recordings at various times points and histological analysis of representative temporal bones reveal that PhexHyp-Duk/Y mice typically develop adult onset, asymmetric, progressive hearing loss closely followed by the onset of ELH; frequency specific ABR tests suggest that mutants tend to acquire low frequency hearing loss sooner than high frequency hearing loss. ABR and histological data show that functional degeneration occurs prior to structural degeneration. Hearing deterioration with age appears to correlate better with the loss of spiral ganglion cells as opposed to the loss of hair cells or severity of hydrops. Further, PhexHyp-Duk/Y mice develop ELH without evidence of ED obstruction, supporting the idea that ELH can be induced by a mechanism other than the blockade of longitudinal flow of endolymphatic fluid and that occlusion of ED is not a pre-requisite for the development of ELH in patients.

#### **[48] Constitutive ERK and PI3-K Activity Each Promote Proliferation in Vestibular Schwannoma Cells While Constitutive JNK Activity and P75<sup>NTR</sup> Signaling Protect Against Apoptosis**

Erika a Woodson<sup>1</sup>, J Jason Clark<sup>1</sup>, Ninyong Xu<sup>1</sup>, Matthew J Provenzano<sup>1</sup>, Marlan R Hansen<sup>1</sup>

<sup>1</sup>University of Iowa Hospitals and Clinics, Department of Otolaryngology

Vestibular schwannomas (VS) are benign tumors arising from Schwann cells (SC) lining the vestibular nerve. They result from defects in the tumor suppressor gene, *merlin*. the merlin protein suppresses multiple intracellular kinase signaling cascades implicated in tumor formation, including Ras-extracellular signal-regulated kinase (ERK), phosphatidylinositol-3 kinase (PI3-K)/AKT, and c-Jun N terminal kinase (JNK). the extent to which these kinases contribute to the proliferation and survival of VS cells is unknown.

Here we demonstrate that ERK, PI3-K, and JNK are constitutively active in human VS cells. Signaling via ErbB2, a receptor tyrosine kinase that promotes VS cell proliferation, appears to at least partially contribute to the activation of ERKs and PI3-K, since inhibition of ErbB2 reduces ERK and AKT phosphorylation in cultured VS cells. by selective inhibition, we find that ERK and PI3K signaling primarily promote cell proliferation while JNK promotes cell survival. Pro-neurotrophin growth factor, a high-affinity p75-neurotrophin receptor (p75<sup>NTR</sup>) ligand that induces apoptosis in normal SCs, protects VS cells from death induced by JNK inhibition. Using quantitative real-time reverse-transcriptase polymerase chain reaction, we find that VSs express three fold higher levels of p75<sup>NTR</sup> mRNA compared with normal vestibular nerve, suggesting that p75<sup>NTR</sup> signaling may contribute to the increased survival potential of VS cells.

Thus, the effect of merlin dysfunction on the formation of VSs likely involves activation of multiple signaling pathways, including ErbB2, Ras-ERK, PI3-K, and JNK. These pathways differentially promote survival or proliferation of VS cells. Paradoxically, p75<sup>NTR</sup> and

JNK signaling appear to promote VS cell survival, in contrast to their known pro-apoptotic effects on normal SCs.

#### **[49] Postnatal Developmental Expression in *gjb2* Transgenic Mice of the Organ of Corti**

**Ayako Inoshita<sup>1</sup>, Takashi Iizuka<sup>1</sup>, Hiro-oki Okamura<sup>1</sup>, Katsuhisa Ikeda<sup>1</sup>**

<sup>1</sup>*Juntendo University, Department of Otorhinolaryngology-Head and Neck Surgery*

Congenital hearing loss is one of the most prevalent inherited human birth defects, affecting 1 in 1000. a strikingly high proportion (50%) of congenital bilateral nonsyndromic sensorineural deafness cases have been linked to mutations in the *GJB2* coding for the connexin26. It has been hypothesized that gap junctions in the cochlea, especially connexin26, provide an intercellular passage by which K<sup>+</sup> are transported to maintain high levels of the endocochlear potential essential for sensory hair cells excitation. We reported the generation of a mouse model carrying human connexin26 with R75W mutation and analyzed the mice (R75W+ mice) at postnatal days 14 (P14). However, the endocochlear potential was remained within a normal range and the auditory brainstem response (ABR) revealed that the mice at P14 showed severe to hearing loss. the tunnel of Corti was not detected and the shapes of outer hair cells were peculiar but no obvious structural change was observed in the stria vascularis or spiral ligament in the R75W+ mice at P14. These results suggested that the *GJB2* mutation disturbs homeostasis of cortilymph, an extracellular space surrounding the sensory hair cells, due to impaired K<sup>+</sup> transport by supporting cells, resulting in degeneration of the organ of Corti, rather than affecting endolymph homeostasis in mice.

The present study was aimed to evaluate postnatal development of the organ of Corti in the R75W+ mice. ABR revealed that R75W+ mice at P11 had already showed severe to profound hearing loss. Histological examinations was analyzed P5-14. Tunnel of Corti was insufficient to be created and inner and outer pillar cells shows hypoplastic changes, presumably due to poor formation of microtubules in R75W+ mice at P8. in the late stages of inner ear developmet, the outer hair cell-Deiters complex was collapsed and future Nuel's space is occupied by bulky processes of Deiters cells in R75W+ mice.

This study suggests that *GJB2* mutation disturbs an extracellular space surrounding the sensory hair cells, which may be associated with cytoskeletal structure change of the organ of Corti.

#### **[50] The Usher Protein Complex Exists *In Vivo* and is Primarily Localized in the Vesicular Subfraction of Ciliated Tracheal Epithelial Cells.**

**Marisa Zallocchi<sup>1</sup>, Joseph Sisson<sup>2</sup>, Dominic Cosgrove<sup>1</sup>**

<sup>1</sup>*Boys Town National Research Hospital,* <sup>2</sup>*University of Nebraska Medical Center*

Usher syndrome is an autosomal recessive disorder characterized by congenital sensorineural hearing loss or deafness associated with delayed onset and progressive retinitis pigmentosa. There are nine known Usher proteins encoded by the family of Usher genes, many of which are expressed as multiple isoforms in both photoreceptors and cochlear hair cells. Many of the Usher proteins are expressed developmentally in cochlear hair cells during the period when hair cells undergo terminal cytodifferentiation. Localization of Usher proteins in stereocilia and abnormal stereocilia in Usher mouse models suggest a critical role in stereocilia development and maintenance. a wealth of protein interaction studies using expressed domains of Usher proteins suggest the existence of a Usher protein complex comprised of several transmembrane proteins, scaffolding proteins and an unconventional myosin motor protein. Such a complex is inconsistent with stereociliary localization studies and has not been demonstrated *in vivo*. Here we show that all of the Usher proteins are expressed in ciliated nasal and tracheal epithelial cells. We employed cell fractionation studies using sucrose gradients and found the Usher proteins in the buoyant membrane fractions. TEM studies revealed these fractions were primarily comprised of 100 to 200 nm vesicles. When the vesicles were lysed in the presence of a chemical chaperone and resedimented, all of the Usher proteins were identified in the 40-70S fraction, consistent with what is expected for a very large protein complex. We further demonstrated that the Usher proteins would co-immunoprecipitate from the vesicular fraction using antibodies specific for usherin, VLGR1, or SANS proteins. These data demonstrate that the Usher protein complex exists *In Vivo* and is present principally in 100-200 nm vesicles. Understanding the biological function of the protein complex in these vesicles may reveal the mechanistic link underlying Usher syndrome pathologies of ciliated neuroepithelial cells of the cochlea and retina.

#### **[51] Molecular Analysis of the *GJB2*, *GJB6* and *SLC26A4* Genes in Korean Deaf Patients**

**Kyu Yup Lee<sup>1</sup>, Soo Young Choi<sup>2</sup>, Jae Woong Bae<sup>2</sup>, Hae Jin Lee<sup>2</sup>, Sung Hee Kim<sup>3</sup>, Un Kyung Kim<sup>2</sup>, Sang Heun Lee<sup>1</sup>**

<sup>1</sup>*Department of otolaryngology-Head and Neck Surgery, Kyungpook National University, Daegu, Korea,* <sup>2</sup>*Deptment of Biology, Kyungpook National University,* <sup>3</sup>*Department of Otorhinolaryngology, Daegu Fatima Hospital, Daegu, Korea*

Mutations in the *GJB2* (connexin 26) and *SLC26A4* (Pendrin) genes are a frequent cause of deafness in a number of populations. However, little is known about the genetic causes of hearing loss in the Korean population. We sequenced the *GJB2* and the closely related *GJB6*

genes to examine the role of mutations in these genes in deafness in Koreans. We also sequenced the SLC26A4 gene in a group of Korean patients with enlarged vestibular aqueduct (EVA). Coding sequence mutations in GJB2 were identified in 17% of the patients screened. Four different mutations, 235delC, V37I, E47K and T86R were found in five unrelated patients. the 235delC was the most prevalent mutation with an allele frequency of 8.3% in our patient group. Three different variants of SLC26A4 were identified in the EVA patients, including one novel mutation. All EVA patients carried two mutant alleles of SLC26A4, and at least one allele in all patients was the H723R mutation, which accounted for 75% of all mutant alleles. Combined with information from previous studies, the H723R mutation accounts for approximately 40% of SLC26A4 mutations in Korea, similar to the 53% reported in Japanese patients. Our results suggest that GJB2 and SLC26A4 mutations are together responsible for about 30% of sensorineural hearing loss (SNHL) in the Korean population. the cause of the remaining 70% has remained elusive. Further studies may be able to identify other common variants that account for a significant fraction of hearing loss in the Korean population.

## **[52] Prevalence of GJB2 Causing Recessive Non-Syndromic Profound Hearing Impairment in Japanese Subjects**

**CHIERI HAYASHI<sup>1</sup>**, Manabu Funayama<sup>2</sup>, Yuanzhe Li<sup>3</sup>, Atsushi Kawano<sup>4</sup>, Mamoru Suzuki<sup>4</sup>, Nobutaka Hattori<sup>3</sup>, Katsuhisa Ikeda<sup>5</sup>

<sup>1</sup>Department of Otorhinolaryngology, <sup>2</sup>Research Institute for Diseases of Old Age, <sup>3</sup>Department of Neurology, Juntendo, <sup>4</sup>Department of Otorhinolaryngology, Tokyo Medical, <sup>5</sup>Department of Otorhinolaryngology, Juntendo University School of Medicine

GJB2 (connexin 26) and GJB6 (connexin 30) are gap junction protein genes that have been implicated in most cases of autosomal recessive non-syndromic hearing impairment (ARNSHI). GJB2 is the most common mutation gene, and GJB6 is the most common deletion gene in many racial groups. to clarify the correlation between children who are congenitally severely hard of hearing and GJB2- related deafness, we conducted mutation screening for GJB2 and GJB6 in 111 probands with profound non-syndromic hearing impairment (HI) and a control group of 150 Japanese adults with normal hearing. We found the highest-frequency mutation (16.7%) to be c.235delC, which is the same as in previous studies. However, in our research, we identified only two subjects with the single heterozygous for V37I, the second most frequent mutation. the allele frequency was 0.9%, the same as in the control group. the next highest frequency mutations were the following: R143W (5.0%), G45E/Y136X (3.6%), and 176-191del (2.7%). the R143W mutation is a missense mutation and may have an important correlation with severe hearing impairment.

We detected two novel mutations: p.R32S (c.94C>A) and p.P225L (c.674C>T). in this study, no cases of c.35delG or c.167delT were found; nor were the two major deletions in GJB6 observed.

No reports of screening for GJB6 deletions in deaf Japanese subjects have been published; thus, our report is an important study of GJB2 and GJB6 in congenitally profoundly deaf Japanese children.

## **[53] Identification of 10 Novel USH2A Mutations in American Patients with Usher Syndrome Type II**

**Xiaomei Ouyang<sup>1</sup>**, D. Michael Patterson<sup>1</sup>, Li Lin Du<sup>1</sup>, Samuel G Jacobson<sup>2</sup>, Denise Yan<sup>1</sup>, Xue Zhong Liu<sup>1</sup>, <sup>1</sup>Department of Otolaryngology, University of Miami, Miami, FL, <sup>2</sup>Scheie Eye Institute, University of Pennsylvania, Philadelphia, PA

Usher syndrome type II is an autosomal recessive disorder characterized by moderate to severe hearing impairment and progressive visual loss due to retinitis pigmentosa (RP). to identify novel mutations and determine the frequency of Usher Syndrome Type II (USH2) mutations as a cause of USH2A, we have carried-out mutation screening of all 72 coding exons and exon-intron splice sites of the USH2A gene. a total of 25 probands of American descent who presented with clinical USH2A were analyzed using single Strand Conformational Polymorphism Analysis (SSCP) and direct sequencing. Fifteen unique USH2A mutations were identified in 76% (19/25) of the probands, ten of which have not been reported previously. the detected mutations include 6 missense, 4 frame shifts, and 4 non-sense mutations, with 2299delG mutation being the most frequent (18% of alleles), and accounting for 34.6% (9/26) of the pathologic alleles. Two cases were homozygotes, three cases were compound heterozygotes and one case had complex allele with three variants. in 13 probands, only one USH2A mutation was detected and no pathologic mutation was found in the remaining 6 individuals. Altogether, our data support the fact that 2299delG is indeed the most common mutation found in USH2 patients from European Caucasian ethnic background. Thus, if screening for mutations in USH2A is considered, it is reasonable to screen for the 2299delG mutation first.

*This work is supported by NIH DC 05575*

## **[54] Mutations in Otoferlin (OTOF) Causing DFNB9 Deafness in Pakistan**

**Byung Yoon Choi<sup>1</sup>**, Zubair Ahmed<sup>1</sup>, Saima Riazuddin<sup>1</sup>, Munir a Bhinder<sup>2</sup>, Mohsin Shahzad<sup>2</sup>, Tayyab Husnain<sup>2</sup>, Sheikh Riazuddin<sup>2</sup>, andrew Griffith<sup>1</sup>, Thomas Friedman<sup>1</sup>

<sup>1</sup>Laboratory of molecular genetics, NIDCD/NIH, Rockville, USA, <sup>2</sup>National Center of excellence in Molecular Biology, University of the Punjab, Lahore, Pakistan

Mutations in OTOF, encoding Otoferlin, cause non-syndromic recessive hearing loss at the DFNB9 locus. the goal of our study was to define the identities and frequencies of OTOF mutations in a model population. We screened a cohort of 557 large consanguineous Pakistani families segregating recessive deafness for linkage to

DFNB9. Affected individuals were first screened for homozygosity at short tandem repeat (STR) markers linked to DFNB9. Co-segregation of deafness with DFNB9 markers was confirmed in the remaining family members. We thus identified 13(2.3%) of 557 families segregating DFNB9 deafness. We are performing bidirectional nucleotide sequence analysis of the 48 known coding exons of *OTOF* in affected members of the 13 DFNB9 families. We have currently completed the analysis of 46 of 48 exons. We found 10 potentially pathogenic alleles, including 9 novel alleles, in 11 families. The mutant alleles comprised four nonsense mutations (p.R425X, p.W536X, p.R708X, and p.Y1603X), one frameshift mutation (c.1104delGGinsC), one splice site mutation (IVS9-3C>T), three missense mutations (p.L573R, p.A1090E, p.E1733K) and one single amino acid deletion (p.E780del). Six of these alleles are predicted to affect only the long otoferlin isoforms, whereas the other four are predicted to affect both long and short isoforms. We are currently confirming the pathogenicity of the alleles by sequence analyses of normal Pakistani control samples. We are also completing mutation analyses of the two remaining *OTOF* exons in the DFNB9 families. Thus far, *OTOF* mutations account for deafness in 11 (1.97%) of the 557 Pakistani families. This estimate will increase if we find additional mutations in the remaining two *OTOF* exons in the other two DFNB9 families. Given the extensive genetic heterogeneity of nonsyndromic deafness, our study indicates that *OTOF* mutations are a significant contributor to the genetic load of deafness in Pakistan and, probably, other populations.

## **[55] Mutations in the WFS1 Gene are a Frequent Cause of Autosomal Dominant Nonsyndromic Low-Frequency Hearing Loss in Japanese**

**Hisakuni Fukuoka<sup>1</sup>, Shin-ichi Usami<sup>1</sup>**

<sup>1</sup>*Shinshu University School of Medicine*

Mutations in *WFS1* are reported to be responsible for two conditions with distinct phenotypes; DFNA6/14/38 and autosomal recessive Wolfram syndrome. They differ in their associated symptoms and inheritance mode, and although their most common clinical symptom is hearing loss, it is of different types. While DNFA6/14/38 is characterized by low frequency sensorineural hearing loss (LFSNHL), in contrast, Wolfram syndrome is associated with various hearing severities ranging from normal to profound hearing loss that is dissimilar to LFSNHL. to confirm whether within non-syndromic hearing loss patients *WFS1* mutations are found restrictively in patients with LFSNHL and to summarize the mutation spectrum of *WFS1* found in Japanese, we screened 206 Japanese autosomal dominant and 64 autosomal recessive (sporadic) non-syndromic hearing loss probands with various severities of hearing loss. We found three independent autosomal dominant families associated with two different *WFS1* mutations, A716T and E864K, previously detected in families with European ancestry. Identification of the same mutations in independent families with different racial backgrounds, suggests that both sites are likely to be mutational hot spots. All three

families with *WFS1* mutations in this study showed a similar phenotype, LFSNHL, as in previous reports. in this study, one-third (3 out of 9) autosomal dominant LFSNHL families had mutations in the *WFS1* gene, indicating that in non-syndromic hearing loss *WFS1* is restrictively and commonly found within autosomal dominant LFSNHL families.

## **[56] Connexin Gene Variants are Not Common Causes of Presbycusis in European Americans**

**Patricia Libby<sup>1</sup>, Michelle Koplitz<sup>1</sup>, Frances Mapes<sup>2</sup>, Susan Frisina<sup>2</sup>, David Eddins<sup>3</sup>, Robert Frisina<sup>3</sup>, Dina Newman<sup>1</sup>**

<sup>1</sup>*Rochester Institute of Technology*, <sup>2</sup>*International Center for Hearing and Speech Research*, <sup>3</sup>*University of Rochester School of Medicine & Dentistry*

Presbycusis (age-related hearing loss) affects the lives of millions of elderly people. Although the disorder is partially genetic, no susceptibility alleles have yet been discovered in humans. Mutations in connexin genes, critical for cochlear gap junctions and K<sup>+</sup> cycling, are the most common cause of non-syndromic deafness, so we hypothesized that variation in these genes might cause the related phenotype of presbycusis. Specifically, we examined *GJA1*, *GJB2*, *GJB6* and *GJB3*, which code for connexins found in the inner ear and have been associated with deafness. Over 800 subjects (98% white) were tested at ICHSR with a series of audiometric tests focusing on both peripheral and central auditory system functions. for each of the 4 genes, 20-24 European American subjects were sequenced to screen for variants in the exons and upstream regulatory regions. No common amino acid changes were found in any of these genes (*GJB2* V27I, L90P and *GJB6* S199T were each observed at 2% frequency). We observed 12 single nucleotide polymorphisms (SNPs) in *GJB2*, 7 in *GJB6*, 22 in *GJB3* and 13 in *GJA1*. in the 1 kb upstream region of *GJA1*, 9 rare variants were observed, 7 only in presbycusic subjects and not in controls. to investigate whether this discrepancy was statistically significant, 100 additional samples were sequenced. Fifty of those samples had the lowest pure-tone average thresholds (PTA2: 1, 2, 4 kHz threshold average) and 50 had the highest PTA2 thresholds in the subgroup of 600 subjects (all over age 58, European American, no history of hearing-related/neurological diseases or head/ear trauma). All 8 variants found were low frequency, and no significant difference was observed between the 2 subject groups. Preliminary genotyping of observed SNPs in *GJB2*, *GJB6* and *GJB3* has shown no association with presbycusis; additional samples are being added. Taken together, these data suggest that connexin gene variation is not a major cause of presbycusis, at least in European Americans.



## **[57] A Functional Screening Approach to Investigate the Genetics of ARHL**

Lisa Nolan<sup>1</sup>, Barbara Cadge<sup>2</sup>, Sally Dawson<sup>1</sup>

<sup>1</sup>Centre for Auditory Research, Ear Institute, University College London, <sup>2</sup>Institute of Laryngology and Otology, University College London.

Age related hearing loss (ARHL) is a complex disease caused by both genetic and environmental factors. Our laboratory is undertaking a functional screening approach in an attempt to identify the genetic risk factors for ARHL. Common sequence variants within gene regulatory regions may modify the binding of transcription factors and lead to inter-individual differences in gene expression. We are investigating the effect of such variants in hair cell survival and anti-oxidant genes in the possible pathogenesis of ARHL.

Using genetic variation catalogued in the HapMap and NCBI dbSNP databases we have screened the promoter region of ARHL candidates for common sequence variants that bioinformatic analysis predict to modify transcription factor binding. Subsequent comparative EMSA analysis using nuclear extracts derived from a mouse organ of Corti sensory epithelial cell line shows there are sequence variants in the Barhl1 promoter and SOD2 promoter which modify binding affinity of specific nuclear proteins to variant alleles. Competition analysis with consensus transcription factor binding sites suggests one SOD2 promoter variant modifies binding affinity of an SP1 family transcription factor by at least 4 fold. Supershift analysis with a rabbit polyclonal anti-SP1 antibody confirms this SOD2 promoter variant modifies the binding of SP1. We are currently examining the functional effect of these sequence variants on transcriptional activity and regulation of gene expression using reporter gene assays. In parallel we are genotyping these sequence variants in an ARHL patient cohort for an association study. Ultimately, it is hoped that by identifying the genetic risk factors for ARHL the molecular pathways and environmental cues that lead to hair cell death will help to be elucidated.

## **[58] Characterization of Small RNA Molecules within the DFNA41 Locus**

Denise Yan<sup>1</sup>, Xiaomei Ouyang<sup>1</sup>, Li Lin Du<sup>1</sup>, Xue Zhong Liu<sup>1</sup>

<sup>1</sup>Department of Otolaryngology, University of Miami, Miami, FL

Approximately one in 1000 children are born with functionally significant hearing loss (HL). Over half of these cases are due to genetic factors. the likelihood of developing age-related HL (ARHL) increases during middle age with a prevalence estimated to approximately 50% among the population over 80 years old. ARHL can also be genetic, and several loci have been identified. to date, only protein-coding and tRNA/rRNA-coding mitochondrial genes have been linked to deafness in humans. So far, most consideration of regulation of the mechanosensory transduction and development of the inner ear has focused on cis-promoter elements and transcription factors. Emerging evidence suggests that functional dysregulation in microRNAs, a class of small

“noncoding” posttranscriptional regulatory RNA molecules, can be associated with the etiopathology of hearing loss. We have previously reported the mapping of the DFNA41 locus on chromosome 12q24-qter in a large multi-generational Chinese family. to investigate whether microRNAs play a role in the regulation of the DFNA41 locus, we have used bioinformatic driven approach to identify small RNAs molecules within the DFNA41 interval. Secondary structure characterization of 3 sequences located within the high linkage and association region showed that they fulfill several key criteria of microRNAs features. by applying the microRNAs target predictions programs, we have found putative target sequence for miRNA in the 3'-untranslated (3'UTR) of several candidate genes. Further studies are underway to experimentally validate the microRNA-like molecules and to delineate the relationship between microRNAs and target sites in candidate genes.

*This work is supported by NIH DC 05575*

## **[59] Phenotypic and Genotypic Analyses of Autosomal Dominant Sensorineural Hearing Loss in an Extended Family**

Christina Runge-Samuelson<sup>1</sup>, Ericka King<sup>1</sup>, Michael Olivier<sup>1</sup>, P. Ashley Wackym<sup>1</sup>

<sup>1</sup>Medical College of Wisconsin

The purpose of this study is to characterize, audiometrically and genetically, a family with inherited non-syndromic sensorineural hearing loss (NSHL) identified at our clinic. We hypothesize that this family has a novel, previously uncharacterized genetic mutation causing autosomal-dominant NSHL. There are 17 family members across six generations with NSHL in every generation and is transmitted by both genders, consistent with autosomal dominant transmission. Audiometric data have been obtained for 11 affected family members from three branches. Hearing losses for all affected persons are similar in severity and configuration, with a general pattern of moderate-to-severe hearing loss with a dip at 1000 Hz in the severe-to-profound hearing loss range bilaterally. Preliminary genetic analyses were negative for the common connexin 26 and 30 mutations. Genomic DNA samples from family members are currently undergoing genome-wide single nucleotide polymorphism (SNP) analysis to screen for familial linkage of the genetic mutation associated with the affected phenotype. Using 500k SNP chips, the SNP analyses will allow for designation of a 100-200 kb (approx. 1-2 genes) region where the mutation is located. These results for locus identification will be presented.

Sponsored by intramural funds from the Department of Otolaryngology and Communication Sciences, Medical College of Wisconsin



## **60 Characterization of MYO7A Promoter Haplotypes Segregating in a Large Pedigree with Low-Frequency Hearing Loss**

**Jeremy Kallman<sup>1</sup>, Valerie Street<sup>1</sup>**

<sup>1</sup>*V.M. Bloedel Hearing Research Center*

Inherited deafness is a genetically heterogeneous disorder. Large families segregating monogenic hearing loss provide an opportunity to dissect this genetic complexity. We previously identified a large American pedigree (referred to as the HL2 family, HL for hearing loss) with a myosin VIIA (*MYO7A*) G2164C mutation co-segregating with autosomal dominant, progressive, sensorineural hearing loss first affecting the low and mid-frequency ranges. If the mutant *MYO7A*<sup>G2164C</sup> allele is expressed, the mutation would result in a G722R substitution at an evolutionarily conserved glycine residue in the *MYO7A* head domain. However in mice, *Myo7a* mutations at the DNA level generally result in reduced or absent *Myo7a* protein. If this is also the case in humans, the mutant *MYO7A*<sup>G2164C</sup> allele will not produce a stable protein product and the HL2 family auditory deficit may be a result of haploinsufficiency, i.e. the inner ear can only rely on *MYO7A* protein production from the normal *MYO7A*<sup>G2164</sup> allele. the clinical severity of the *MYO7A*<sup>G2164C</sup> mutation in the HL2 pedigree varies between affected individuals with similar medical and noise-exposure histories, suggesting that a genetic modifier is either rescuing or exacerbating the primary *MYO7A*<sup>G2164C</sup> mutation. If the *MYO7A*<sup>G2164C</sup> mutation leads to haploinsufficiency, one likely modifier candidate would be the *MYO7A*<sup>G2164</sup> allele promoter as certain *MYO7A*<sup>G2164</sup> promoter haplotypes may drive different levels of expression. for example, a strong *MYO7A*<sup>G2164</sup> promoter haplotype may drive more *MYO7A* expression than a weak promoter leading to less severe hearing loss in individuals with the strong promoter. to explore this possibility, we are sequencing the *MYO7A*<sup>G2164</sup> associated promoter in DNA from HL2 family members affected by hearing loss. We anticipate finding specific *MYO7A*<sup>G2164</sup> promoter haplotypes that segregate with mild versus more severe low-frequency hearing loss in the HL2 pedigree.

## **61 Alternative Splice Variants of *Myh9***

**Yan Li<sup>1</sup>, Anil K. Lalwani<sup>1</sup>, Anand N. Mhatre<sup>1</sup>**

<sup>1</sup>*NYU School of Medicine*

*MYH9* encodes a class II nonmuscle myosin heavy chain-A (NMHC-IIA), a widely expressed 1960 amino acid polypeptide, with a translated molecular weight of 220 kDa. the relatively large number of exons (40) that encode NMHC-IIA and the splice variants that have been documented for its two isoforms, *MYH10* and *MYH14*, strongly suggest existence of alternative splicing for *MYH9*. in the current study, we perform a targeted search for *Myh9* splice variants in two separate regions of the heavy chain that encode loop 1 and loop 2 sub-domains within which alternative exons in *MYH10* and *MYH14* splice variants have been identified. the splice variant search was conducted using two strategies: amplification across the suspected exons directly or by amplification of putative splice variants identified through conserved

sequence analysis of suspected intronic regions. within loop 1, two separate insertions of 12 and 41 nucleotides were identified using conserved sequence analysis only. Each of these insertions, located within intron 4, resulted in premature termination of the variant transcript. within loop 2, a 63 nucleotide-long in-frame insertion was identified using both strategies. the insertion is identical in length and displays 65% sequence identity with its *Myh10* counterpart, but differs greatly from the 123 nucleotide-long-insertion within *Myh14* transcript identified in this study. Both loop 1 and loop 2 variants of *Myh9* were detected in the cochlea, with the latter being most abundant in the brain. Expression of loop 1 variants with premature termination codon (PTC) may reflect an alternate mode of regulating *Myh9* expression while the conserved sequence and selective expression of the loop 2 variant highlights its potential biological importance.

## **62 Cochlear and Brainstem Auditory Physiological Responses of Whirler Mice**

**Neil Ingham<sup>1</sup>, Mike Rogers<sup>1</sup>, Karen Steel<sup>1</sup>**

<sup>1</sup>*Wellcome Trust Sanger Institute*

Whirler homozygous mutant mice show no response to sound and have short hair cell stereocilia (Holme et al 2002) due to a lack of the protein, whirlin. Despite this, they appear to have electrophysiologically-functional outer hair cells at early post-natal stages (Stepanyan et al 2006). Earlier recordings from the round window of the cochlea in urethane-anesthetized whirler mice at 20 and 56 days old indicated that homozygotes were deaf, and that heterozygotes had reduced latency of compound action potential (CAP) wave components when compared to control age-matched CBA mice (Rogers 1996). Since these measurements were made, it has become possible to genotype whirler mice following identification of the defect in the whirlin gene of these mutants (Mburu et al, 2003). Physiological comparisons are now possible within the whirler strain rather than between different strains with different genetic backgrounds. Auditory brainstem response (ABR) recordings were made of urethane-anesthetized wildtype (Whrn +/+), heterozygous (Whrn +/-) and homozygous (Whrn wi/wi) whirler mice. Homozygotes were deaf, showing no demonstrable ABR at stimulus frequencies from 6–30 kHz, and had head-bobbing and circling behaviour. in contrast, Whrn +/+ and Whrn +/- mice showed good ABR thresholds across this frequency range and had no discernible behavioural anomalies. Click-evoked ABRs were recorded and the amplitude and latency of the first positive and negative peaks of the waveform were plotted as a function of sound level, relative to threshold. ABR wave peak latency and amplitude are being compared to ask if there are any possible differences in the physiology underlying the sensory transduction process in Whrn +/+ and Whrn +/- mice.

Holme RH et al (2002) J Comp Neurol 450: 94-102

Mburu P et al (2003) Nature Genetics 34: 421-428

Rogers MJC (1996) PhD Thesis

Stepanyan R et al (2006) J Physiol 576: 801-808

### **63 Defining the Range of PMCA2 Expression Critical for Auditory Function**

Claire J Walker<sup>1</sup>, Sarah M Lies<sup>1</sup>, Bruce L Tempel<sup>1</sup>

<sup>1</sup>University of Washington

The *Atp2b2* gene, encoding the plasma membrane calcium ATPase 2 (PMCA2), is critical for auditory transduction. However, the functional contribution of PMCA2 in auditory transduction has yet to be elucidated quantitatively. Our lab has identified and studied several mutations in PMCA2 leading to varying degrees of hearing loss, ranging from mild to very severe. A mutant mouse generated by an ethyl-nitrosyl urea mutagenesis screen has a point mutation in PMCA2 changing a critical lysine at the ATP binding site to a stop codon (*Atp2b2K580Stop*), designated as *dfwENU70*. To characterize the effect of a point mutation in the ATP-binding pocket of PMCA2, we compared three strains of mice: *dfwENU70*, deafwaddler (*dfw*) mice and a strain with a known null allele (*dfw2J*). Auditory characterization of *dfwENU70*, *dfw*, and *dfw2J* mice was performed using auditory-evoked brainstem responses (ABRs) across a range of frequencies from 5.6 to 40 kHz. Western blot analysis and quantitative real-time PCR (qPCR) was used to determine the presence of PMCA2 protein and *Atp2b2* mRNA, respectively, in brain tissue from each strain of mice. Mice heterozygous for the *dfwENU70* allele demonstrate more severe hearing loss at 5 weeks of age than mice heterozygous for the null *dfw2J* allele (+/*dfw2J*) as determined by ABR responses. Mice heterozygous for the *dfw* allele have similar ABR thresholds compared to wild-type littermate controls. This result parallels previous findings from our lab showing that auditory function in 3 week old +/*dfw2J* mice is significantly worse than at 2 and 4 weeks of age, and may be explained by the up-regulation of functional PMCA2 from the wild-type *Atp2b2* gene. Preliminary studies suggest that levels of functional PMCA2 may directly correlate with auditory function in these heterozygous mice. These results suggest that expression differences between these three strains bracket the range of functional PMCA2 necessary for auditory function.

### **64 Functional Analysis of *Grxcr1*, the Gene Affected in the Mouse Deafness Mutant Pirouette**

Kristina L. Hunker<sup>1</sup>, Keith A. Marcus<sup>1</sup>, Lisa A. Beyer<sup>1</sup>, Yehoash Raphael<sup>1</sup>, David C. Kohrman<sup>1</sup>

<sup>1</sup>University of Michigan; Dept. of Otolaryngology/Kresge Hearing Research Institute

The mouse mutant *pirouette* (*pi*) exhibits profound hearing loss and circling behavior inherited as recessive traits. Previous studies have demonstrated abnormally thin, deteriorating stereocilia during sensory cell maturation in the inner ears of *pi/pi* mice. We have identified *pi* mutations in the novel gene *Grxcr1*, which encodes a protein localized to stereocilia. GRXCR1 contains two recognizable domains: a central region of similarity to glutaredoxins, enzymes that reduce oxidized cysteines on cellular proteins; and a putative zinc finger in the C-terminus. These domains exhibit deep evolutionary conservation in likely *Grxcr1* homologs in fly, worm, and

plants. Most classic glutaredoxin enzymes contain two Cys residues at their active sites that are required for reduction-oxidation (redox) activity. GRXCR1 contains only a single Cys in its putative active site, similar to several glutaredoxins that have been characterized in yeast (*Grx3-5*). Redox activity of these glutaredoxins is required for a number of cellular functions, including normal production of Fe-S complexes in the mitochondria, regulation of iron homeostasis, and cellular responses to oxidative stress. We have taken a genetic approach in yeast to determine whether the glutaredoxin domain of GRXCR1 possesses inherent redox activity. We have engineered constructs that express hybrid proteins containing the mitochondrial transport signal of yeast *Grx5* fused to the Grx domain of *Grxcr1*. These will be tested for their ability to complement the growth defects and oxidative stress sensitivity exhibited by a mutant yeast strain that lacks endogenous *Grx5*.

We have also attempted to complement the *Grxcr1* mutation in *pirouette* mice. In preliminary transfection studies, delivery of wild-type, full-length *Grxcr1* to sensory cells in explants from early postnatal *pi/pi* mice results in stereocilia of relatively normal dimensions, consistent with successful correction.

### **65 The *Eya1bor/Bor* Modifier Locus *Mead1*, it's Fine Mapping and the Mechanism of it's Modification**

Haoru Niu<sup>1</sup>, Linna Makmura<sup>1</sup>, Rick Friedman<sup>1</sup>

<sup>1</sup>House Ear Institute

The *Eya1<sup>bor/bor</sup>* mouse exhibits genetic-background-dependent variations in phenotypes, such as hearing loss, kidney abnormalities and abnormal behaviors such as circling and head bobbing. Previously, we identified two major modifier loci (*Mead1* and *Mead2*) that account for part of the variations in hearing loss. Here, we report the recent progress in the characterization of the modifier locus *Mead1*.

By measuring a Mendelian trait, the cochlear turn in the *Eya1<sup>bor/bor</sup>* mutants, we narrowed down the *Mead1* locus to a 790 kb-region on chromosome 4, within which only two protein-coding genes are located. Using tissues from the otocyst and the immediate surrounding mesenchyme in E10.5 embryos, we performed RT-PCR analysis for these two genes (*2610301B20* and *Plekha7*). The data shows that both these two genes are expressed in the otocyst and/or surrounding mesenchyme, suggesting that they are both strong candidate genes for the responsible modifier.

In order to figure out the mechanisms of the phenotypic modification, we analyzed the inner ear morphology of the mutant embryos at different developmental stages by paint injection. The study revealed multiple anomalies in the cochlear and vestibular systems in the mutants. However, the *Mead1* locus appears to affect only the growth of the cochlear duct, consistent with the earlier findings on adult mutants.

## **[66] Initial Identification and Characterization of Immune System Associated Proteins in the Mouse Inner Ear**

**Ronna Hertzano**<sup>1</sup>, Janice Babus<sup>1</sup>, Chandrakala Puligilla<sup>2</sup>, Lydia Cardwell<sup>2</sup>, Rani Elkon<sup>3</sup>, Martin Irmeler<sup>4</sup>, Didier Depireux<sup>5</sup>, Matthew W. Kelley<sup>2</sup>, Johannes Beckers<sup>4</sup>, Karen B. Avraham<sup>3</sup>, Scott E. Strome<sup>1</sup>

<sup>1</sup>*Department of Otorhinolaryngology/Head and Neck Surgery, University of Maryland, Baltimore, MD, USA,*

<sup>2</sup>*Section on Developmental Neuroscience, NIDCD, NIH, Bethesda, MD, USA,*

<sup>3</sup>*Department of Human Molecular Genetics and Biochemistry, Tel Aviv University, Tel Aviv, Israel,*

<sup>4</sup>*GSF-National Research Center for Environment and Health, GmbH, Neuherberg, Germany,*

<sup>5</sup>*Department of Anatomy and Neurobiology, University of Maryland, Baltimore, MD, USA*

Transmembrane glycoproteins, also known as cluster of differentiation proteins (CD proteins) expressed on immune cells, are involved in the regulation of various immune responses, including autoimmune diseases. Many of these proteins have also been shown to be expressed on the surface of non-immune system cell types and are upregulated during inflammation. The response of sudden hearing loss as well as autoimmune inner ear disease to corticosteroid treatment suggests an important role of the immune system in these inner ear pathologies. However, the role of CD proteins in the ear is not clear. Identification of the expression pattern of these proteins could shed light on the pathogenesis of these disorders. Moreover, selectively expressed CD molecules may possibly be used as endogenous markers for cell sorting of the mouse sensory epithelia.

We used RNA extracted from early postnatal cochlear and vestibular sensory epithelia to compare the transcriptomes of these two closely related systems. This analysis has identified a group of CD molecules that are expressed in the mouse inner ear sensory epithelia. Several of these genes, such as CD44, were detected as uniquely expressed in either the auditory or vestibular system. We present the initial validation and characterization of expression of these immune related proteins in the mouse inner ear. We further show that CD44 is a new marker for the outer Pillar cell as well as Hensen's cells and present the initial inner ear analysis of the CD44 KO mice.

## **[67] Identification of Proteins That Interact with Transmembrane Channel-Like Gene 1 (TMC1) Protein in the Inner Ear**

**Valentina Labay**<sup>1</sup>, Tomoko Makishima<sup>1</sup>, Andrew Griffith<sup>1</sup>

<sup>1</sup>*National Institute on Deafness and other Communication Disorders/ National Institutes of Health*

Mutations in transmembrane channel-like gene 1 (TMC1) cause hearing loss in humans and mice. Mouse Tmc1 mRNA is expressed in cochlear hair cells and is required for their functional development and survival. TMC1 is a six-pass transmembrane protein localized to the endoplasmic reticulum in heterologous expression systems. In order to elucidate its role in hair cells, we sought to identify proteins that interact with TMC1. We used four bait clones encoding different regions of mouse

TMC1 to screen a yeast two-hybrid library of prey clones derived from P1 mouse inner ear cDNA. We identified 79 positive prey clones in serial high stringency screens. Two genes, FKBP38 and VAP-A, had multiple, overlapping, unique prey clones that interacted with the TMC1 C-terminal bait clone. FKBP38 encodes the 38-kDa FK506-binding protein and VAP-A encodes vesicle-associated membrane protein (VAMP)-associated protein A. We used the STP3 system for *In Vitro* synthesis of the TMC1 C-terminus, FKBP38 and VAP-A. TMC1 could be co-immunoprecipitated with either FKBP38 or VAP-A in this system. We co-expressed epitope-tagged expression constructs for the TMC1 C-terminus and either FKBP38 or VAP-A in COS-7 cells. Immunostaining of the heterologously expressed proteins revealed nearly completely overlapping expression patterns of TMC1 with either FKBP38 or VAP-A. Whereas TMC1 and FKBP38 show a reticular localization pattern when expressed alone, they exhibit a punctate staining pattern when co-expressed. Anti-FKBP38 antibodies stain mouse cochlear hair cells in an intracellular reticular expression pattern. We conclude that TMC1 may interact with FKBP38 *In Vivo* and *In Vitro*. Since FKBP38 is thought to mediate anti-apoptotic signal transduction and negative regulation of sonic hedgehog signaling in neural tissues, a potential interaction with TMC1 may underlie the requirement for TMC1 in hair cell development and survival.

## **[68] A Method for Introducing Sirna Into Specific Inner Ear Tissues**

**Donald Robertson**<sup>1</sup>, Maria Layton<sup>1</sup>, Peter Sellick<sup>1</sup>, Jenny Rodger<sup>1</sup>

<sup>1</sup>*The University of Western Australia*

The overall aim was to investigate the feasibility of using the technique known as RNA interference to manipulate (knockdown) levels of specific proteins in the adult inner ear. It was hoped that the method could be used to elucidate the function of key inner ear proteins involved in the hearing process. In the longer term, success in applying the technique to the inner ear could also provide a basis for gene-related therapies for inner ear disorders.

Introduction of siRNA into the perilymphatic compartment of the cochlea failed to result in uptake into any cells of interest. As a consequence we developed techniques to inject the siRNA into the endolymphatic compartment. We found that this resulted in reproducible uptake of siRNA into the cells of the stria vascularis. We have been able to successfully demonstrate siRNA uptake in the stria of all cochlear turns whilst retaining cochlear function. The method of endolymphatic perfusion that we have developed represents a significant advance on previous work, both because of the extensive uptake we can achieve and because we have monitored cochlear function throughout the process.

Technical difficulties encountered relate to the reproducibility of effects on cochlear function and this has prevented firm conclusions from being drawn at this stage. A number of animals injected with nonsense siRNA that should cause no effect, showed unexplained losses in hearing function. When we compared all such control injections with experiments using specific siRNA chosen to

target two proteins found in stria cells we could not find significant correlations between uptake of these siRNAs into the stria and subsequent measures of cochlear function. Interpretation of these results requires assessment of levels of the targeted proteins.

## **69 Expression of Transcription Factor Nrf2 in LLC-PK1-CL4 Cells**

**Glenn Schneider<sup>1</sup>, Mary D'Souza<sup>1</sup>, Justin Miller<sup>1</sup>, Robert Frisina<sup>1</sup>**

<sup>1</sup>*Univ. Rochester Medical School*

Presbycusis is a common chronic medical condition in the elderly. One of the proposed etiologies of presbycusis involves the dysregulation of oxidative metabolism in the inner ear with age. Over time, the accumulation of reactive oxygen species results in oxidative damage to the cells of the inner ear leading to hearing loss. In order to study oxidative metabolism of the inner ear, real time PCR (qPCR) was used to identify the basal expression of antioxidant genes and transcription factors in the LLC-PK1-CL4 cell line. The LLC-PK1-CL4 cells, which are derived from porcine kidney proximal tubule cells, were used in this study as an approximate model for inner ear cells due to similarities in the structural and biochemical composition of the microvilli brush border between the cells. So far in qPCR studies of this cell line we have found significant expression of the transcription factor Nrf2. Nrf2 has been shown to be activated by oxidative stress as well as being involved in regulating the expression of numerous antioxidant enzymes (Thimmulappa et al. *Cancer Res.* 62: 5196-5203, 2002). We hypothesize that Nrf2 expression in the LLC-PK1-CL4 cells may be linked to expression of antioxidant enzymes. Our ongoing studies will investigate both the protein production and gene expression of antioxidants in the LLC-PK1-CL4 cell line such as Superoxide Dismutase 1 and 2, Glutathione Reductase, and members of the Glutathione Peroxidase family. Hopefully, this knowledge will help provide a basis for inner ear therapeutics involving antioxidants as a means of defending cochlear cells against oxidative stress, to potentially influence the time course of presbycusis.

*[Supported by NIH: NIA, NIDCD, and the Int. Ctr. Hearing Speech Res., Rochester, NY, USA]*

## **70 Connexin-26 Expression in the LLC-PK1-CL4 Epithelial Cell Line**

**Mary D'Souza<sup>1</sup>, Justin Miller<sup>1</sup>, Kathleen McGowan<sup>1</sup>, Glenn Schneider<sup>1</sup>, D. Robert Frisina<sup>2</sup>, Robert Frisina<sup>1</sup>**

<sup>1</sup>*Univ. Rochester Medical School*, <sup>2</sup>*Rochester Institute of Technology*

Connexins comprise a multigene family of conserved proteins, which compose hexameric transmembrane functional channels called gap junctions, that play major roles in intercellular communications. Connexins in the auditory system transport potassium ions in the cochlea, maintaining homeostasis and enabling sensory transduction in hair cells. Single nucleotide polymorphisms in connexin-26 (GJB2) in particular, are known to account for a significant number of births involving genetic sensorineural hearing loss or deafness. The possible role

of connexin-26 in age-related hearing loss – presbycusis, has not yet been elucidated. To begin to explore options for future therapeutic interventions for the inner ear, we are utilizing the LLC-PK1-CL4 cell line model. This cell line is derived from porcine kidney and is epithelial in origin. CL4 was recently used as a cell model to study cochlear structural proteins like espin and myosin, and their possible roles in sensorineural hearing loss and deafness. In the present investigation, using relative real-time PCR, with Taqman primer/probes from ABI we have observed that the LLC-PK1-CL4 epithelial cell line expresses connexin-26. In our ongoing investigations, the LLC-PK1-CL4 cell line is being utilized as a model for detailed molecular analysis of connexin-26 gene regulation and signal transduction, events involved in the direct regulation of potassium ions in the inner ear. These cell culture studies pave the way for *In Vivo* experiments, which are not currently feasible. *[Supported by NIH: NIA, NIDCD, and the Int. Ctr. Hearing Speech Res., Rochester, NY, USA]*

## **71 Microarray Analysis of Keloid Versus Normal Skin Cells and Cultured Human Dermal Fibroblasts: Analysis of Expression within the TGF-Beta Pathway**

**Selena E. Heman-Ackah<sup>1</sup>, Jizhen Lin<sup>1</sup>, David Hom<sup>2</sup>**

<sup>1</sup>*University of Minnesota*, <sup>2</sup>*University of Cincinnati*

**BACKGROUND:** Keloids are benign dermal tumors that occur in response to tissue injury. Keloids are characterized by the proliferation of dermal fibroblasts, overproduction of extracellular matrix components, expansion beyond the original boundaries of the injury and recurrence of disease. Recent studies indicate that transforming growth factor (TGF)-beta pathway may play an essential role in the pathogenesis of keloids by inducing and sustaining activity of keloid fibroblasts. The exact mechanism is not well understood. **OBJECTIVES:** The objective of this study is to identify sites within the TGF-beta pathway which are up-regulated or down-regulated in keloid fibroblasts when compared to normal skin cells from scar tissue and normal fibroblasts. **METHODS:** A microarray assay was performed evaluating genes within the TGF-beta pathway. The following samples were evaluated: 2 samples of normal skin tissue from human subjects, 3 samples of cultured human dermal fibroblasts, and 2 samples of keloid tissue from human subjects. **RESULTS:** A total of 106 genes related to the TGF-beta pathway were evaluated. Differential expression was not observed among the normal skin samples. Statistically significant differences were observed in 25 genes within the TGF-beta pathway within keloid tissue when compared to normal human dermal fibroblasts. Eleven genes were up-regulated within the TGF-beta pathway within the keloid tissue when compared to normal human dermal fibroblasts: ACVR2A, BMP7, CDKN2B, COMP, ID1, ID2, ID3, ID4, SMAD1, SP1, and ZFYVE16. Fourteen genes were down-regulated within the TGF-beta pathway within the keloid tissue when compared to normal human dermal fibroblasts: ACVRL1, DCN, FST, LTBP1, MAPK1, MYC, RHOA, ROCK1, SMAD5, SMURF1, SMURF2, TFDP1, TGFB2, and THBS1. A better understanding of these

mechanisms underlying keloid formation could lead to more effective treatment of this disease process.

## **72 Middle Ear Application of Hyaluronic Acid Gel Loaded with Neomycin in a Guinea Pig Model**

**Amanj Saber**<sup>1</sup>, Goran Laurell<sup>2</sup>, Tobias Bramer<sup>3</sup>, Katarina Edsman<sup>4</sup>, Cecilia Engmer<sup>1</sup>, Mats Ulfendahl<sup>1</sup>

<sup>1</sup>*Department of Clinical Neuroscience, Karolinska Institute, Karolinska University Hospital SE-171 76,* <sup>2</sup>*Department of Clinical Sciences, Umea University, SE-90185 Umea, Sweden,* <sup>3</sup>*Department of Pharmacy, Uppsala University, Box 580, SE-751 23 Uppsala, Sweden,* <sup>4</sup>*Department of Pharmacy, Uppsala University, Box 580, SE-751 23 Uppsala, Sweden*

**Background:** One alternative for controlled drug delivery to the inner ear is application of medication to the middle ear cavity on the promise that it will diffuse through the round window membrane (RWM) into the inner ear.

**Objective:** to evaluate the efficacy of hyaluronic acid gel (HYA) as a vehicle for drugs that are aimed to treat inner ear disorders.

**Methods:** in this study the cochlear hair cell loss and RWM morphology were investigated after topical application. Neomycin was chosen as tracer for drug release and the ototoxic effect was evaluated. HYA, (0.5%) loaded with 3 different concentrations of neomycin, was injected to the middle ear cavity of guinea pigs. the ototoxic effect of neomycin in HYA gel was compared to that of neomycin solution applied to the middle ear cavity. Phalloidin stained surface preparation of the organ of Corti was used to estimate hair cell loss induced by neomycin. the thickness of the midportion of the RWM was measured and compared with that of controls using light and electromicroscope.

**Result:** Neomycin induced a considerable hair cell loss in guinea pigs receiving middle ear injection of HYA loaded with the drug. One week after topical application the thickness of the RWM was dependent upon the concentration of neomycin administered to the middle ear. At 4 weeks the thickness of the RWM had returned to normal.

**Conclusion:** HYA is a safe vehicle for drugs aimed to pass into the inner ear through the RWM. Neomycin was released from HYA and transported into the inner ear as evidenced by hair cell loss. **Key words:** Round window membrane (RWM), hyaluronic acid gel, HYA, hair cell loss, thickness.

## **73 Local Delivery of Dexamethasone to Preserve Residual Hearing Post Cochlear Implantation: Optimisation and Clinical Translation**

**Andrew Chang**<sup>1</sup>, Stephen O'Leary<sup>1</sup>

<sup>1</sup>*University of Melbourne*

**Background:** There is a growing interest in the use of pharmacological agents to protect hearing in the presence of surgical trauma and immune-based inner ear diseases.

Unfortunately at this stage these treatments have a limited clinical efficacy. This is due to issues with the drug delivery method and a limited understanding of the processes involved in hearing loss. Therefore, any developments leading to an increase in hearing protection will have a significant clinical benefit.

This study demonstrates an optimized method for the topical application of anti-inflammatory in a cochlear implantation model, which leads to hearing protection and is applicable to the clinical setting.

**Methods:** a cochlear implantation model using guinea pigs as the experimental subject. the dexamethasone is placed on the round window membrane via a delivery bead (Seprapak) for a different length of time prior to cochleostomy and electrode insertion. All animals had pre-operative and post-operative ABR to measure hearing loss. the animals were sacrificed at a pre-determined time point and cochleae were harvested for histology.

**Results:** Dexamethasone delivered via the round window produced no middle ear pathology and permanently protected inner ear hearing loss post-implantation. the degree of protection appears to be related to the extent of pre-surgery exposure to dexamethasone.. Also, the histology revealed that dexamethasone pre-treatment ameliorated the foreign body reaction to the implanted electrode.

**Conclusion:** Pre-treatment of dexamethasone permanently protects hearing from surgical trauma and the immune responses post-implantation. Topical delivery via the round window is safe and can be easily incorporated into clinical practice. This will benefit future cochlear implant patients and others undergoing otologic surgery.

All Correspondences to Dr. Andrew Chang (MBBS, BEng Hons) ENT Registrar at Level 2, Department of Otolaryngology, Royal Victorian Eye and Ear Hospital, 32 Gisborne Street, East Melbourne 3002. Email: achang@bionicear.org

## **74 Pharmacokinetics of Ganciclovir via Intratympanic Administration**

**Jonette Ward**<sup>1</sup>, Alisa Reece<sup>1</sup>, Edward Acosta<sup>2</sup>, Daniel Choo<sup>1</sup>

<sup>1</sup>*Cincinnati Childrens Hospital Medical Center,* <sup>2</sup>*University of Alabama at Birmingham*

Newborn hearing screening programs are able to identify infants with sensorineural hearing loss (SNHL), of which congenital cytomegalovirus (CMV) infection is one of the most common causes. It is estimated that CMV affects 1% of all newborns in the United States. Children with symptomatic congenital CMV are more likely to have permanent disabilities and the treatments with antiviral drugs have shown hearing improvements. Unfortunately, there are significant risks and side effects when infants are treated systemically with antiviral therapies. Studies have shown that approximately 20% of those with asymptomatic congenital CMV infections have SNHL. However, due to potential adverse effects of parenteral/systemic antivirals, the risk-benefit calculation for treatment is a struggle for clinicians and parents. Finding a safer, more effective

treatment that preserves and/or improves hearing without causing significant adverse effects is the challenge.

Our laboratory is developing a method to deliver antiviral drugs via intratympanic administrations directly to the cochlea. a guinea pig model was used to explore the pharmacokinetics of intratympanic (IT) antiviral drug (ganciclovir) delivery to the inner ear. Four different concentrations of ganciclovir (GCV) were injected into the guinea pig's inner ear, and GCV levels were measured at 24, 48, 72 and 96 hours. Auditory brainstem responses were recorded to identify any ototoxic effects on hearing. Cochlear fluid samples were aspirated for high performance liquid chromatography (HPLC) assays to measure drug levels. After euthanasia, guinea pig temporal bones were harvested and the morphology of the inner ears examined to identify any histologic evidence of toxic effects of the drug.

Initial data demonstrates the rapid access of intratympanic GCV to the perilymph of the scala tympani at pharmacologically relevant levels (and higher). in addition, some GCV was measurable by HPLC in the plasma, indicating absorption of drug, either at the ear level or via drainage down the eustachian tube and into the pharynx. These preliminary data support the investigation of an intratympanic delivery route for antivirals in the setting of CMV-related hearing loss as an efficacious and safe method of treatment.

## **[75] Sustained Release of Lidocaine into the Cochlea via Biodegradable Materials**

**Rie Horie<sup>1</sup>**, Takayuki Nakagawa<sup>1</sup>, Tatsunori Sakamoto<sup>1</sup>, Yayoi S Kikkawa<sup>1</sup>, Kazuya Ono<sup>1</sup>, Yasuhiko Tabata<sup>2</sup>, Jyuichi Ito<sup>1</sup>

<sup>1</sup>Otolaryngology Head and Neck surgery, Graduate School of Medicine, Kyoto University, <sup>2</sup>Biomaterials, Frontier Medical Sciences, Kyoto University

Effective treatment for tinnitus has not been established. Lidocaine is a non-steroidal, anti-inflammatory local anesthetic and intravenous injection of lidocaine has been shown to transiently suppress tinnitus in several double-blind studies. However, transtympanic infusion of lidocaine into the tympanic cavity can cause several vestibular side effects such as vertigo and nausea, making it impractical to use in clinics. Therefore, we developed biodegradable sustained-release materials which has longer and localized release profile, and tested this system *In Vitro* and in vivo. Sustained release of drugs to the inner ear has been achieved by placing these biodegradable materials on the round window membrane (Endo 2005, Tamura 2005, Iwai 2006, Lee 2007). in view of clinical application, we chose gelatin hydrogel and PLGA (poly lactic-co-glycolic acid) as biomaterials for sustained release of lidocaine. *In Vitro* release studies of lidocaine-loaded biomaterials were performed. Results showed no sustained release of lidocaine using gelatin hydrogels. in contrast to hydrogels, PLGA exhibited preferable release profiles of lidocaine *In Vitro*. PLGA particles of which outer diameter was 5  $\mu\text{m}$  showed sustained release of lidocaine over 2 weeks and 100  $\mu\text{m}$ -PLGA particles achieved over 4 week-release of lidocaine. We thus

designed an *In Vivo* study to examine the potential of PLGA particles for sustained delivery of lidocaine into the cochlea fluids using guinea pigs.

## **[76] Intracochlea Infusion in Mice Using an Osmotic Pump**

**Fukuichiro Iguchi<sup>1</sup>**, Julie Harris<sup>1</sup>, Edwin Rubel<sup>1</sup>

<sup>1</sup>Department of Otolaryngology-HNS and VMBHRC, University of Washington

Continuous long-term delivery of experimental drugs to the cochlea of a small animal is one of the essential methods used for auditory research. the technique using an osmotic pump for a guinea pig is often used for this purpose. a small fenestra is made at the base of the cochlea and a catheter tip connected to an osmotic pump is placed into the fenestra. This technique is well established, but when genetic analysis is attempted, mice are more preferable than guinea pigs. Therefore, we applied this technique to mice.

C57BL/6 mice (P21), weighing about 10 g, were used. Tetrodotoxin (TTX, 0.1 mM) was infused to the cochlea. an osmotic pump reservoir was put under the back skin and a catheter was connected to the round window niche. Mice were separated into three groups. in the first group, the stapedial artery was cartelized and TTX was infused. in the second group, the stapedial artery was not cartelized and TTX was infused. in the third group, saline was infused. Each solution was infused continuously at 1 $\mu\text{l/h}$  for 24h. Hearing level was evaluated with ABR prior to and 24h after the operation.

All of the first group became deaf. Most of the second group died. the third group showed about -7 dB threshold shift. Because our method did not make a fenestra on the cochlea, threshold shifts stayed at a minimum without the TTX. to prevent the solution from spreading to the whole body, the stapedial artery should be cartelized. Because this method is not accompanied by big mechanical hearing disturbance and a solution works locally, osmotic pumps can be used for transiently blocking auditory input in mice.

## **[77] An Animal Model of Cochlear Implantation with Perilymphatic Drug Delivery**

**Yann Nguyen<sup>1,2</sup>**, Couloigner Vincent<sup>1,3</sup>, Milan Rudic<sup>1,4</sup>, Alexis Bozorg Grayeli<sup>1,2</sup>, Evelyne Ferrary<sup>1,5</sup>, Olivier Sterkers<sup>1,2</sup>

<sup>1</sup>Inserm, Unit-M 867, Paris, 75018, France, <sup>2</sup>AP-HP, Hôpital Beaujon, Service d'ORL et de Chirurgie cervico-faciale, Clichy, 92118 France, <sup>3</sup>AP-HP, Hôpital Necker-Enfants malades, Service d'ORL et de Chirurgie cervico-faciale, Paris, France, <sup>4</sup>Université Denis-Diderot Paris 7, Paris, France, <sup>5</sup>Institut Fédératif de Recherche Claude Bernard Physiologie et Pathologie, IFR02, Paris, 75018 France

Direct drug delivery to the inner ear is an interesting mean of achieving high local doses while avoiding general side effects. It is also a promising approach to maintain the residual hearing during and after the cochlear implantation. the conception of an animal model is a first step to assess different molecules before human clinical trials. Guinea

pigs with normal hearing were implanted with a prototype electrode carrier that comprised the electrode and a microcatheter that was connected to an osmotic minipump. the tested drug was the antioxydant N-acetylcysteine; artificial perilymph was injected as control. Hearing thresholds were evaluated with auditory brainstem responses (clicks, tone bursts) before, immediately after the implantation, and at day 7 and day 30 postoperatively. CT-scan was used to check the implant position at day 30. in the control group, an ABR threshold shift of  $31 \pm 3.0$  dB in immediate postoperative,  $31 \pm 3.3$  dB at day 7 and  $34 \pm 2$  dB ( $n=10$ ) was observed. This loss was stable as there was no significant threshold shift from immediate post operative to Day 7 and to day 30. N-acetylcysteine did not have any protective effect on hearing preservation. CT-scan images showed that the implants stayed in a stable position in the basal turn during one month. Drug delivery through the implant should be used for chronic treatment for either aetiology of hearing loss or cochlear implant function enhancement. This animal model will be employed to evaluate other components in this approach rather than in decreasing initial cochlear trauma during cochlear implantation.

#### **[78] Scala Tympani Infusion with Dexamethasone Base (Dxmb) in Artificial Perilymph Protects Against Electrode Trauma-Induced Hearing**

**Adrien Eshraghi<sup>1</sup>**, Richard Vivero<sup>1</sup>, Debbie Joseph<sup>2</sup>, Jiao He<sup>1</sup>, Thomas Balkany<sup>1</sup>, Thomas Van De Water<sup>1</sup>

<sup>1</sup>University of Miami, <sup>2</sup>University of FloridaBackground:

*Local treatment of the cochlea with aqueous dexamethasone (sodium phosphate form) can reduce hearing loss initiated by sound trauma, aminoglycosides and electrode insertion trauma (EIT). Recent advances may allow local release of protective molecules from a polymer coating applied to an electrode array. If dexamethasone is to be delivered by a biopolymer, the base form (DXMb) of this synthetic corticosteroid must be used because of its solubility in organic solvents used in formulating biopolymers.*

**Materials and Methods:** a guinea pig model of EIT-induced hearing loss used 41 guinea pigs sub-divided into 3 groups: 1) electron insertion trauma, untreated (EIT only;  $n=14$ ); 2) EIT plus artificial perilymph (EIT + AP;  $n=15$ ); and 3) EIT plus dexamethasone base in AP (EIT + DXMb;  $n=12$ ) with contralateral unoperated cochleae as controls. Auditory brainstem responses (ABRs) to 0.5 – 16 kHz pure tone stimuli were obtained prior to surgery, immediately after, and on post-EIT days 3-30. Nonparametric analysis used the Mann-Whitney U test with a p value of  $< 0.05$  considered significant.

**Results:** Untreated, EIT caused both immediate and progressive losses of hearing thresholds. Perfusion of the scala tympani with artificial perilymph (i.e. EIT + AP) for 8 days following EIT did not prevent either the immediate or progressive losses of hearing thresholds. However, there was a plateau in the degree of hearing loss in these animals. Perfusion of the scala tympani with dexamethasone base (i.e. DXMb-70 micro-g/ml in AP) for

8 days beginning immediately after EIT conserved hearing by preventing the progressive elevation of ABR thresholds, with these EIT + DXMb treated animals recovering to near pre-surgical values. ABR threshold data of all groups was stable at 30 days post-EIT. There were statistical differences ( $p < 0.05$ ) between the hearing thresholds of control and operated ears of the EIT and EIT + AP groups at all frequencies. There were no statistical differences ( $p > 0.05$ ) in the hearing thresholds in the EIT + DXMb vs. control groups at 0.5 - 4 kHz.

**Conclusions:** the absence of significant differences in hearing thresholds of the EIT + DXMb group for pure tone stimuli demonstrates that DXMb was effective in conserving hearing against EIT-induced losses. Therefore, dexamethasone base is a promising molecule for use with biorelease polymers.

#### **[79] Effects of Vestibular Implantation on Hearing in Chinchillas**

**Shan Tang<sup>1</sup>**, Thuy-Anh Melvin<sup>1</sup>, Charles Della Santina<sup>1</sup>

<sup>1</sup>Johns Hopkins School of Medicine

While a vestibular prosthesis should restore labyrinthine sensation after hair cell injury, electrode implantation carries a risk of cochlear damage and hearing loss. We sought to determine how and to what extent implantation of vestibular prosthesis electrodes affects hearing.

The left ears of 8 otherwise normal chinchillas were implanted with 3 bipolar pairs of electrodes (one pair per canal) via fenestra made in the ampullae using a transmastoid approach. Right ears, which served as controls, were subjected to the same mastoid approach without fenestration and implantation. Auditory brainstem response hearing thresholds to free field clicks and tone pips at 2, 4, 6, and 8 kHz were measured bilaterally 3-10 weeks after implantation. Results were compared between sides and against normative data from 6 normal chinchillas.

Five animals suffered significant hearing loss on the implanted side. the threshold difference was  $44.2 \pm 7.3$  dB (left minus right, mean  $\pm$  SD) for clicks,  $32.1 \pm 5.9$  dB for 2 kHz tones,  $48.8 \pm 3.9$  dB for 4 kHz,  $>51.5 \pm 9.8$  dB for 6 kHz, and  $>46.6 \pm 13.9$  dB for 8 kHz ( $p < .01$  for 8kHz,  $p < .001$  for all others). Three animals showed no significant difference in hearing threshold between ears ( $p \geq 0.25$ ). All implants were able to elicit reflexive eye movements during pulsatile electrical stimulation. Right ear control thresholds were 7.7-16.4 dB above normative values across all stimuli ( $p = .08$  for 8kHz,  $p < .05$  for others), demonstrating a small hearing loss due to operative procedures other than electrode implantation. Outcomes did not correlate with surgical experience, duration of anesthesia, or time between implantation and testing.

While a majority of implanted ears suffered hearing loss, these results demonstrate that intralabyrinthine electrode implantation can be performed without significant hearing loss. Future studies should focus on refining electrode design and surgical technique to maximize preservation of hearing.

Supported by NIDCD-K08DC006216



**[80] Adenoviral and AAV-Mediated Gene Transfer to the Inner Ear: Role of Serotype, Promoter, and Viral Load on *In Vivo* and *In Vitro* Infection Efficiencies**

Anne Luebke<sup>1</sup>, Cherokee Rova<sup>2</sup>, Peter Von Doersten<sup>2</sup>, David Poulsen<sup>2</sup>

<sup>1</sup>University of Rochester Medical Center, <sup>2</sup>University of Montana

The lack of effective treatments for many forms of hearing and vestibular disorders has produced interest in virally-mediated gene therapies. However, to develop a gene therapy strategy that would successfully treat inner ear disorders, appropriate viral vectors capable of transfecting cochlear and vestibular cells must be identified. While virally-mediated gene transfer into the inner ear has been accomplished using herpes simplex type 1 virus, vaccinia virus, retroviruses, adenovirus, and adeno-associated virus (AAV), we will restrict our discussion to AAV and adenoviral vectors. Development of a viral vector that facilitates gene delivery and long-term gene expression without ototoxic effects, or subsequent immune reaction as well as correct targeting of desired cochlear cells, is crucial for gene replacement therapy to be clinically used for treating certain forms of deafness. Issues such as vector toxicity, viral serotype and backbone, viral load, and promoter specificity are discussed and contrasted for both *In Vivo* vs. *In Vitro* inner ear gene transfer.

(Supported by NIH DC003086, DC007217)

**[81] Dual-Regulation of ATP on BK Channels in Chick Hair Cells**

Mingjie Tong<sup>1</sup>, R. Keith Duncan<sup>1</sup>

<sup>1</sup>Kresge Hearing Research Institute, University of Michigan  
Large-conductance, Ca<sup>2+</sup>-activated K<sup>+</sup> channels (BK) play important roles in mammalian and non-mammalian vertebrate hair cells. In non-mammalian hair cells, BK channels contribute to an electrical tuning mechanism, by regulating the frequency-dependent responses of hair cells along the tonotopic axis of the cochlea. In various cells, BK channels are post-translationally modified, suggesting that hair cells may modulate channel activity by processes like phosphorylation. In one set of experiments, inside-out patches containing BK channels were excised from hair cells throughout the apical half of the chick basilar papilla. Application of ATP to the intracellular face of BK channels enhanced channel activity, increasing open probability and shifting the half-activation potentials ( $V_{1/2}$ ) to more negative voltages by about 30 mV. Replacing ATP with a nonhydrolysable analog, adenylyl imidodiphosphate (AMP-PNP, 2 mM), failed to mimic excitation by ATP, suggesting that ATP-induced activation is through phosphorylation rather than direct binding to the channels. Activation could be rapidly reversed by removing ATP from the bath. These results indicate that a protein kinase and phosphatase are co-assembled with hair cell BK channels. In contrast to the activation by intracellular ATP, application of 2 mM ATP to the extracellular face inhibited channel activity. Ensemble-averaged recordings of outside-out patches showed that ATP shifted  $V_{1/2}$  to more negative voltages by about 20 mV. Our results reveal a

dual regulatory effect of ATP on BK channel activity, depending on the site of interaction. These data suggest that BK channels may be involved in complex signaling processes in cochlear hair cells. This work has been supported by NIH RO1 DC07432 to RKD and P30 DC0578188.

**[82] A Proteomic Study of BK Partners in Chick and Mouse Cochleae**

Thandavaryan Kathiresan<sup>1</sup>, Margaret Harvey<sup>1</sup>, Lei Chen<sup>1</sup>, Bernd Sokolowski<sup>1</sup>

<sup>1</sup>University of South Florida

Large conductance calcium-activated potassium (BK) channels play a role in auditory signal processing at the level of the hair cells. In turtle cochlea, BK channels contribute to frequency tuning, whereas in chick, BK begins to function at a time when hearing sensitivity increases. In mammals, the role of BK is less clear as these channels are located in extrasynaptic regions. We identified BK interacting partners in both mouse and chicken cochleae in the present study. Anti-BK antibody was used to coimmunoprecipitate membrane and cytoplasmic-related protein partners, which were separated using 2D gel electrophoresis and identified with mass spectrometry (LC-MS/MS). In chick, a total of 132 proteins from both cytoplasmic and membrane fractions were identified as potential BK partners, whereas, in mouse, we identified 123 potential candidates. In both chick and mouse, ~58% of the membrane-derived candidates had been reported as ion channel partners previously. In comparison, ~70% of the cytoplasmic-derived candidates reportedly associated with other types of ion channels. Reciprocal coimmunoprecipitation and colocalization studies revealed interactions not only in sensory-neural tissues but also in supporting cells. Among the putative partners are cytoskeletal, signaling, EF-hand, and myelin-related proteins. These candidates were selected for full-length gene cloning by RT-PCR, using cochlear tissues. Genes were subcloned into the pCMS-EGFP vector for biophysical studies with BK or into the pCS2-Venus vector for FRET analysis with Cerulean-tagged BK. These experiments were pursued to determine if putative BK partners alter channel biophysical characteristics or act during protein assembly.

Supported by grant DC004295 from the NIDCD to BS.

**[83] Arachidonic Acid Depolarizes Guinea Pig Outer Hair Cells Through Inhibiting Kcnq4**

Tao Wu<sup>1</sup>, Alfred Nuttall<sup>1</sup>

<sup>1</sup>Oregon Health and Science University

KCNQ4 is associated with  $I_{K,n}$ , which is activated at hyperpolarization and dominates the membrane conductance at the resting potential of outer hair cell (OHCs). Genetic mutations in the gene for KCNQ4 resulted in non-syndromic hereditary hearing loss. Arachidonic acid (AA) is usually stored within phospholipids of the cell membrane and released into intracellular medium by stimulation of G protein coupled receptors. As second messengers, AA and its active metabolites, such as hydroperoxyeicosatetraenoic acid



(HPETE), prostaglandins (PGs), leukotrienes (LTs), etc, interact with protein kinases and ion channels within the cell. the disturbed AA cascade of OHC has been thought to mediate the tinnitus induced by salicylate, a cyclooxygenase inhibitor. Surprisingly, in the current study with whole cell recordings, extracellular application of AA (100  $\mu$ M) led to substantial depolarization of OHCs by  $7.8 \pm 0.9$  mV (from  $-69.0$  to  $-61.3$  mV,  $n=7$ ), which was completely blocked by linopirdine (100  $\mu$ M), a KCNQ4 channel blocker, in gap-free recordings of current clamp. the depolarized membrane potential recovered to its original with a delay of 3-5 minutes' washing. in gap free recordings of voltage-clamp, AA (100  $\mu$ M) led to a reversible reduction (negatively shift) of  $99.6 \pm 15.6$  pA (70%) in the outward current at the holding voltage ( $V_h$ ) of  $-49$  mV, which was also completely blocked by linopirdine (100  $\mu$ M). in voltage-step recordings for the IV curve, AA (100  $\mu$ M) significantly reduced both the inward current and the outward current by 36.4% at  $-100$  mV and 57.1% at  $0$  mV respectively without a marked change in the kinetics of outward  $I_K$ . the reverse potential of AA sensitive currents, was  $-87.1 \pm 3.0$  mV, indicating a high  $K^+$  selectivity when compared to the theoretical value of  $-88$  mV. in conclusion, Arachidonic acid depolarizes guinea pig outer hair cells through inhibiting KCNQ4.

Supported by NIH-NIDCD DC000141.

#### **[84] Halothane Depolarizes Outer Hair Cells Through Inhibiting Kcnq4**

**Tao Wu<sup>1</sup>**, Alfred Nuttall<sup>1</sup>

<sup>1</sup>Oregon Health and Science University

The mechanism of action of volatile anesthetics is still not completely clear. It has been reported that distortion-product otoacoustic emissions (DPOAE) of birds was very sensitive to volatile anesthetics (Kettembeil 1995): DPOAE disappeared at the onset of deep anaesthesia and recovered to its original magnitude when the anaesthesia was lightened. the underlying molecular and cellular mechanism is unknown. Surprisingly, in the current study with whole cell recordings, extracellular application of halothane (1 mM) led to substantial depolarization of OHCs by  $11.6 \pm 1.6$  mV (from  $-71.0$  to  $-59.4$  mV,  $n=5$ ), which was completely blocked by linopirdine (100  $\mu$ M), a KCNQ4 channel blocker, in gap-free recordings of current clamp. the depolarized membrane potential recovered to its original with a delay of 4-5 minutes of drug washout. Consistent with the findings in current clamp, extracellular application of halothane (1 mM) led to a reversible reduction (negatively shift) by 84.1% (from  $78.7 \pm 12.2$  to  $13.1 \pm 12.1$  pA,  $n=5$ ) in the outward current at the holding voltage ( $V_h$ ) of  $-49$  mV in gap-free recordings of voltage clamp. in voltage-step recordings for the IV curve, halothane (1 mM) significantly reduced both the inward current and the outward current by 17.0 % at  $V_h$  of  $-100$  mV and 46.0 % at  $V_h$  of  $0$  mV respectively without a marked change in the kinetics of outward  $I_K$ . the reverse potential ( $V_r$ ) of halothane sensitive currents was  $-88.6 \pm 4.9$  mV ( $n=5$ ), indicating a high  $K^+$  selectivity when compared to the theoretical  $V_r$  of  $-88$  mV. KCNQ4 has been associated with  $I_{K,n}$ , which is activated at

hyperpolarization and dominates the membrane conductance at the resting potential of OHCs (Housley and Ashmore 1992). We concluded that halothane depolarized guinea pig outer hair cells through inhibiting KCNQ4, which may underlie the findings in vivo.

Supported by NIH-NIDCD DC000141.

#### **[85] KCNQ4 Currents in Spiral Ganglion Neurons of the Mouse Inner Ear**

**Ping Lv<sup>1</sup>**, Dongguang Wei<sup>1</sup>, Tonghui Xu<sup>1</sup>, Kirk W Beisel<sup>2</sup>, Ebenezer N Yamoah<sup>1</sup>, Liping Nie<sup>1</sup>

<sup>1</sup>Center for Neuroscience/Dept. of Otolaryngology, University of California, Davis, Davis, CA 95618,

<sup>2</sup>Department of Biomedical Science, Creighton University, Omaha, NE 68178

in humans, mutations in KCNQ4 channels cause nonsyndromic, sensorineural deafness type 2 (DFNA2), an autosomal dominant form of progressive hearing loss (PHL). One of the hallmarks of DFNA2 is progressive loss of outer hair cells (OHCs) and apparent, subsequent degeneration of spiral ganglion neurons. We have demonstrated that KCNQ4 channels are differentially expressed in hair cells (HCs) and spiral ganglion neurons (SGNs) along the tonotopic axis of the cochlea. in order to gain deeper insight into the etiology of the KCNQ4-associated DFNA2, we determined the properties of KCNQ-currents in primary culture of mouse SGNs. We identified a base-to-apex gradient of KCNQ currents, defined by their sensitivity to linopirdine and retigabine. the presence of KCNQ4 currents in SGNs is consistent with the immunolocalization of KCNQ4 channels reported previously. Also important, we demonstrated that the differential expression of KCNQ currents results in distinct and profound alterations of the membrane properties of the basal versus apical SGNs following blockage of the current. Consequently, inhibition of KCNQ currents in basal SGNs results in altered  $Ca^{2+}$  influx, which may mediate cell death. We propose that the degeneration of SGNs associated with DFNA2 may be one of the primary consequences of dysfunctional KCNQ4 channels, in contrast to the assertion that degeneration of SGNs is secondary to loss of HCs. We are conducting further study to test the present hypothesis. the implications of these findings will be discussed.

This work is supported by the National organization for Hearing Research Foundation grant to L.N. and National Institutes of Health grants DC03828 and DC07592 to E.N.Y.

#### **[86] Expression of Kcna10 in the Mouse Inner Ear and Retina**

**Ayala Lagziel<sup>1</sup>**, Linda Peters<sup>1</sup>, Marissa Reuveni<sup>1</sup>, Gregory Frolenkov<sup>2</sup>, Thomas Friedman<sup>1</sup>, Robert Morell<sup>1</sup>

<sup>1</sup>National Institute on Deafness and Other Communication Disorders, National Institutes of Health, <sup>2</sup>Department of Physiology, University of Kentucky

The inner ear and the retina have complex neuronal networks that require voltage gated potassium (Kv) channels to regulate membrane potential. Kv channels are composed of  $\alpha$  and  $\beta$  subunits. the  $\alpha$ -subunits assemble as tetramers to form a pore, and the  $\beta$ -subunits are auxiliary

subunits which modulate their properties. Functional diversity of the K channel superfamily is achieved through interactions with  $\beta$ -subunits and different subcellular localizations. the *Kcna10* gene is a member of the *shaker* subfamily of voltage-gated potassium channels and encodes an  $\alpha$ -subunit protein of approximately 58 kDa. Our analyses of massively parallel signature sequencing (MPSS) libraries derived from inner ear tissues suggested that *Kcna10* was preferentially expressed in the inner ear. We confirmed inner ear expression of *Kcna10* by RT-PCR. We also amplified *Kcna10* in the mouse retina, but not in other tissues. *In Situ* hybridization experiments revealed that *Kcna10* expression in tissue sections from heads of post-natal day two (P2) and P5 mice was limited to auditory and vestibular hair cells. We generated polyclonal antibodies against a peptide corresponding to an N-terminal region that distinguishes *Kcna10* from other *Kcna* proteins. Immunohistochemistry experiments with our antibodies confirm that *Kcna10* expression is limited to inner and outer hair cells of the organ of Corti and both type I and type II hair cells in the vestibular epithelia. Immunofluorescent staining of *Kcna10* persists during development, becoming more prominent from P21 onward. Our expression analyses provide a starting point for studying the role of *Kcna10* in the inner ear and retina.

### **[87] Molecular Characterization of Hyperpolarization-Activated Conductances in Postnatal Mouse Vestibular Hair Cells**

**Geoffrey C. Horwitz<sup>1</sup>**, Jeffrey R. Holt<sup>1</sup>

<sup>1</sup>University of Virginia

The hyperpolarization-activated current known as  $I_H$  has been previously identified in various cell types of the brain and heart, as well as inner ear hair cells.  $I_H$  can be carried by either homomeric or heteromeric assemblies of any of the four members of the HCN gene family. the channels are permeable to both sodium and potassium and may function to regulate spontaneous activity, input resistance, and resting membrane potential. Recently, HCN1, 2 and 4 have been identified in vestibular hair cells, yet their precise function and the specific molecular composition of hair cell  $I_H$  channels has not been elucidated.

To examine the physiological characteristics of  $I_H$  in mouse vestibular hair cells, we harvested utricular macula from postnatal day 0 to 10 mice (CD-1). We used the whole-cell, tight-seal technique in voltage-clamp mode and recorded  $I_H$  evoked by a standard voltage protocol that featured a family of 2sec steps from a holding potential of -64mV to between -144 and -54mV in 10mV increments followed by a step to -74mV to examine the voltage range of activation. the tissue was bathed in a standard artificial perilymph solution that in some cases contained 500 $\mu$ M BaCl<sub>2</sub> to block other inward rectifier currents.

We recorded robust  $I_H$  ( $I_{\text{Max}} \approx -1$ nA) in both type I and type II vestibular hair cells. the current had properties consistent with previous reports of  $I_H$  which included, a reversal potential of  $\sim -40$ mV, full activation at -140mV and a half activation voltage of -95mV. the magnitude of  $I_H$  was age-dependent and we detected evidence of  $I_H$  as early as P0.

To begin to identify the molecular composition of  $I_H$ , we recorded currents from hair cells of HCN1 knockout mice. Preliminary data revealed little  $I_H$  in either type I or type II hair cells, thus implicating HCN1 as a component of the hair cell  $I_H$ . Nonetheless, a few cells displayed small  $I_H$  ( $I_{\text{Max}} \leq -100$ pA) suggesting that other HCN subunits may also contribute to the hair cell  $I_H$ . (Supported by NIDCD Grant #DC005439)

### **[88] Molecular Cloning of Cyclic Nucleotide-Gated Channel Subunits Expressed in Teleost Saccular Hair Cells**

**Dakshnamurthy Selvakumar<sup>1</sup>**, Marian J. Drescher<sup>1</sup>, Dennis G. Drescher<sup>1</sup>

<sup>1</sup>Wayne State University School of Medicine, Detroit, MI

Cyclic nucleotide gated (CNG) channels are cation-selective channels that open in response to direct binding of cAMP/cGMP and mediate sensory transduction in vision, olfaction and taste. Previously, we determined that mRNA for olfactory subunits CNGA2, CNGA4, CNGB1b and CNGA3 is expressed in cochlear hair cells/organ of Corti, with subunit protein for CNGA2 and CNGA4 immunolocalized to stereocilia (Drescher et al., Mol. Brain Res. 98:1-14, 2002; Drescher et al., ARO Abstr. 24:40-41, 2001). Here, we report the analysis, by RT-PCR with degenerate primers and cloning, of CNG subunit message expressed in a hair cell layer isolated from the trout saccule. CNGA2 (mediating olfactory sensory transduction) and three groups of CNGA3 (mediating cone, olfactory and taste sensory transduction) were detected with CNGA2:CNGA3a:CNGA3b:CNGA3c = 2:8:4:4. the partial aa sequence for CNGA2 covered three putative transmembrane regions, a pore region and cyclic nucleotide-binding domain (CNBD), with 92% identity to zebrafish CNGA5, and  $\sim 86\%$  identity to catfish and human CNGA2. Key amino acids within the pore of hair cell CNGA2 predict cation selectivity and high channel conductance, as for zebrafish CNGA5 (58 pS). the molecular signature for cyclic nucleotide selectivity in the CNBD would specify a cAMP/cGMP-gated CNGA2 channel as opposed to a cGMP-preferring CNG channel. the CNGA3 sequences covered five putative transmembrane regions, a pore region and a CNBD, representing 80% of the cds. CNGA3a and CNGA3c exhibited highest identity (93%, 96%) to zebrafish CNGA3, while CNGA3b was closest (95%) to trout pineal photoreceptor CNGA3. Differences in sequence between CNGA3 subgroups occurred primarily outside transmembrane regions, the pore and CNBD, which were relatively conserved between subgroups in particular for functionally-critical amino acids of the cGMP-preferring CNGA3 channel. CNG channel properties highly depend on specific aa which will impact channel function in hair cells.

## **[89] Action of Capsaicin On the Outer Hair Cells of the Guinea Pig Through Non-TRPV-1 Mechanisms**

Tao Wu<sup>1</sup>, Lei Song<sup>2</sup>, Xiaorui Shi<sup>1</sup>, Zhi-gen Jiang<sup>1</sup>, Joseph Santos-Sacchi<sup>2</sup>, Alfred Nuttall<sup>1</sup>

<sup>1</sup>Oregon Health and Science University, <sup>2</sup>Yale University School of Medicine

The classical action of capsaicin, the active ingredient of many spicy foods, is to activate TRPV-1 receptor and elicit the nociceptive sensation. It was found that TRPV-1 was expressed in the outer hair cells (OHCs) and that capsaicin suppressed cochlear amplification *In Vivo* (Zheng 2003). Activation of TRPV-1 was hypothesized to lead to OHC depolarization resulting in a reduction of receptor potential and subsequent OHC motility. However, in current studies with whole cell recordings, no characteristic TRPV-1 current was found in OHCs. Unexpectedly, we found 1) capsaicin (300  $\mu$ M) was a potent  $I_K$  blocker reducing the outward current by 62.1 % at 0 mV. the reduction was dose-dependent with  $EC_{50}$ =103.1  $\mu$ M and blocked by 4-AP, the specific  $I_K$  blocker. Capsaicin (300  $\mu$ M) also slightly reduced  $I_{K,n}$ , by 10.1 % at -100 mV, which was blocked by  $Ba^{2+}$ , and depolarized OHC by 4.0 mV. the reverse potential ( $V_r$ ) for the capsaicin net current ( $I_{cap}$ ) is -83.6 mV. 2) Capsaicin suppressed a non-selective cation channel in the solutions blocking K channels with the  $V_r$  of  $I_{cap}$  at zero. Gluconate substituting  $Cl^-$  in bath did not significantly shift  $V_r$  of  $I_{cap}$ . the capsaicin response was dose-dependent with  $EC_{50}$ =163.2  $\mu$ M and was reversibly blocked by  $Ca^{2+}$ -free bath and ruthenium red. Blocking or depletion of the ryanodine-sensitive  $Ca^{2+}$  store by ryanodine or caffeine results in a significant reduction of  $I_{cap}$ . Blocking the release of  $IP_3$  sensitive  $Ca^{2+}$  store by 4-APB had no effect on  $I_{cap}$ . by fluorescent imaging of  $Ca^{2+}$ , capsaicin (150  $\mu$ M) slightly and significantly reduced intracellular  $Ca^{2+}$  of OHC. 3) Capsaicin (300  $\mu$ M) had a potent effect on OHC motility by substantially shifting  $V_{p_{kcm}}$  of NLC curve by  $25.0 \pm 1.5$  mV ( $n=5$ ). the shift was dose dependent with  $IC_{50}$ =166  $\mu$ M and was independent of a removal of  $Ca^{2+}$  in both pipette and bath solutions. in conclusion, capsaicin has a strong non-TRPV-1 action on OHCs that underlies the findings in vivo. Supported by NIH-NIDCD DC000141.

## **[90] The Varitint-Waddler (Va) Deafness Mutation in TRPML3 Generates Constitutive, Inward Rectifying Currents and Causes Cell Degeneration**

Keiichi Nagata<sup>1</sup>, Lili Zheng<sup>1</sup>, Thomas Madathany<sup>1</sup>, andrew Castiglioni<sup>1</sup>, James Bartles<sup>1</sup>, Jaime Garcia-Anoveros<sup>1</sup>

<sup>1</sup>Northwestern University

Varitint-waddler (Va) mice are deaf and have vestibular impairment, with inner ear defects that include the degeneration and loss of sensory hair cells. the semidominant Va mutation results in an alanine-to-proline substitution at residue 419 (A419P) of the presumed ion channel TRPML3. We demonstrated that TRPML3 forms channels and that the A419P mutation adds an uncharacteristic sensitivity to hyperpolarizing voltages that

activates the channels at negative potentials. the constitutively active channels generated an inward current, depolarized the cells and caused cell death. Like many other TRP channels, wild-type TRPML3 opened at very positive potentials and thus rectified outwardly. the degeneration-causing TRPML3(A419P) channels displayed an additional inward rectification due to an increase of open probability at negative voltages. Hair cells, marginal cells of stria vascularis and other cells lining the cochlear and vestibular endolymphatic compartments expressed TRPML3. When heterologously expressed in LLC-PK1-CL4 epithelial cells, a culture model for hair cells, TRPML3 accumulated in vesicles as well as in espine-enlarged microvilli that resemble stereocilia. Cells expressing TRPML3(A419P), but not wild-type TRPML3, died and were extruded from the epithelium in a manner reminiscent of degenerating hair cells in Va mice. the reversed voltage sensitivity of TRPML3(A419P), which results in constitutive channel activation at physiological potentials, likely underlies hair cell degeneration in deaf Va mice.

## **[91] Salicylates Decrease AQP6 Expression in the Mouse Organ of Corti**

Simona Tritto<sup>1</sup>, Laura Botta<sup>1</sup>, Umberto Laforenza<sup>1</sup>, Giulia Gastaldi<sup>1</sup>, Paolo Valli<sup>1</sup>, Paola Perin<sup>1</sup>

<sup>1</sup>University of Pavia

Salicylates are well-known for their reversible ototoxic effect. Among their actions in the ear there is a direct inhibition of the OHC molecular motor prestin (Oliver et al. 2001). However, the ear contains other targets for these drugs, notably cyclo-oxygenases (COX; Stjerschantz et al. 2004), which are key enzymes in the synthetic pathway of prostaglandins.

Among the targets of prostaglandins are aquaporins, which form water channels in lipid membranes, thus regulating volume and concentration of cellular and subcellular compartments. Several aquaporins are expressed in the inner ear (Ishiyama et al. 2006), but their role is still largely unclear.

in the present work we have studied the expression of AQP6 in the mouse cochlea, by immunolabeling of paraffin-embedded cochlear sections, in control conditions and after salicylate treatment. AQP6 was observed in the spiral ganglion, and within the organ of Corti at the level of Deiters' and phalangeal cells. After treatment with salicylates, AQP6 labeling of the organ of Corti was dramatically reduced.

This appears interesting, because Deiters' and phalangeal cells represent the "entry points" to epithelial cell gap-junction-coupled systems involved in  $K^+$  recycling (Kikuchi et al. 2000). the role played by AQP6 could involve both water and ionic homeostasis, since this aquaporin isoform displays both water and  $Cl^-$  permeability (Nagase et al. 2007).

## **[92] Slow Motility in Hair Cells of the Frog Amphibian Papilla: Signal Transduction Pathway**

**Nasser Farahbakhsh<sup>1</sup>, Peter Narins<sup>1</sup>**

<sup>1</sup>*UCLA*

Using video, fluorescence and confocal microscopy, quantitative analysis and modeling, we have investigated intracellular processes mediating the calcium/calmodulin ( $\text{Ca}^{2+}/\text{CaM}$ )-dependent slow motility in hair cells dissociated from the rostral region of amphibian papilla, one of the two auditory organs in frogs. the time course of shape and intracellular free calcium ( $[\text{Ca}^{2+}]_i$ ) changes in the rostral amphibian papillar hair cells (RAPHCs) during the period of pretreatment with several specific inhibitors, as well as their response to the calcium ionophore, ionomycin, have been compared. These cells respond to ionomycin with an increase in the  $[\text{Ca}^{2+}]_i$ , followed by a delayed tri-phasic shape change: an initial phase of iso-volumetric length decrease; a period of concurrent shortening and swelling; and the final phase of increase in both length and volume. Our recent work has been focused on the effects of a number of kinase or phosphatase inhibitors on both the  $[\text{Ca}^{2+}]_i$  increase and the initial iso-volumetric shortening. in this presentation we show and compare the effects of the myosin light chain kinase inhibitor, ML-7; antagonists of the multifunctional  $\text{Ca}^{2+}/\text{CaM}$ -dependent kinases, KN-62 and KN-93; the type 1 protein phosphatase inhibitors, calyculin a and okadaic acid; an inhibitor of actin-activated  $\text{Mg}^{2+}$ -ATPase of myosin II, blebbistatin; the MAP kinase kinase (MAPKK or MEK) inhibitor, PD-98059; and the Rho-associated kinases inhibitor, Y-27632. Our results suggest that myosin light chain phosphorylation is required for the iso-volumetric shortening in RAPHCs. However, they do not support a major role for the Rho-kinase - myosin phosphatase pathway in the ionomycin-induced iso-volumetric length change. Supported by NIH grant No. DC00222.

## **[93] Ultrastructural Localization of NMHC-IIa within the Mouse Cochlear Hair Cells**

**Anil Lalwani<sup>1</sup>, Graham Atkin<sup>1</sup>, Jennifer Lee<sup>1</sup>, Dean Hillman<sup>1</sup>, Anand Mhatre<sup>1</sup>**

<sup>1</sup>*NYU SoM*

NMHC-IIA, a nonmuscle myosin heavy chain isoform encoded by MYH9, is expressed in most vertebrate cell types. Mutations of MYH9 are linked to syndromic or nonsyndromic hearing loss. Immunohistochemical studies have identified NMHC-IIA within several different cochlear tissues including the sensory hair cells responsible for transduction of the sound-induced mechanical stimulus. the current study describes ultrastructural immunogold localization of the NMHC-IIa within murine sensory hair cells. the immunogold label was found in the stereocilia, in the cytosol along the plasma membranes and in mitochondria. within the stereocilia, NMHC-IIa is associated with the actin core throughout its length, spanning from the center to the periphery. NMHC-IIa is also associated with the rootlets of the stereocilia that extend into the cuticular plate suggesting a potential role in structural support of these projections. within the sensory

hair cells, NMHC-IIa immunoreactivity was distributed throughout the cytoplasm and localized to the plasma membrane. a novel finding of this study is the presence of NMHC-IIa within the mitochondria, predominantly along its inner membrane. the presence of NMHC-IIa within heterogeneous areas of the hair cell suggests that it may undergo differential post-translational modifications that determine its localization and that it may play a variety of different functional roles in the distinct destinations. Thus, impaired NMHC-IIa function may cause hearing loss by affecting various aspects of hair cell physiology including disruption of stereocilia, disturbing structural and functional integrity of the plasma or mitochondrial membrane, and upsetting cytoplasmic or mitochondrial function.

## **[94] Characterization of Gentamicin-Induced Apoptosis in a Cochlear Cell Line**

**Sung IL Nam<sup>1</sup>, Youn Ho Park<sup>1</sup>, Sun Ho Park<sup>1</sup>, Soon Hyung Park<sup>1</sup>**

<sup>1</sup>*Keimyung University Dongsan Medical Center*

*Department of Otorhinolaryngology*

Aminoglycoside antibiotics are ototoxic. Understanding of the cellular and molecular mechanisms underlying the drug ototoxicity, however, has been hampered by the limited availability. This study was performed to evaluate the mechanism of gentamicin-induced ototoxicity using this cell line. Gentamicin was treated for 3 days in the media containing HEI-OC1 cells. As a result, cell viability was decreased in a gentamicin dose-dependent manner. the cell number was decreased by 50% 3rd day after exposure to 2 mM gentamicin. Penicillin was, however, without any significant effect. FACS analysis revealed that the subG1 arrest representing cellular apoptosis was significantly increased by the treatment with gentamicin, while not by penicillin. Reactive oxygen species (ROS) was also increased in the presence of gentamicin when compared with control or the case of penicillin. Caspase-3 activity was increased accordingly as gentamicin concentration was increased. Expression of the cyclin-dependent kinase inhibitor p27<sup>Kip1</sup> was observed exclusively to be increased after gentamicin treatment. N-acetyl cysteine dose-dependently ameliorated gentamicin-induced cell survival, but not vitamin E and vitamin C. Taken together, HEI-OC1 cell line is a good model to evaluate the mechanism of drug ototoxicity. These results suggest that reactive oxygen species may be involved in gentamicin-induced apoptosis of cochlear cells. the apoptosis may be, at least partially, linked to induction of p27.

## **[95] Using Two-photon, Two-channel, Metabolic Imaging and NADH FLIM to Determine the Metabolic Status of the Cochlea**

**LeAnn Tiede<sup>1</sup>, Alex Bien<sup>2</sup>, Meg Marquardt<sup>1</sup>, Michael Nichols<sup>1</sup>, Richard Hallworth<sup>1</sup>**

<sup>1</sup>*Creighton University*, <sup>2</sup>*University of Nebraska Medical Center*

Metabolism and mitochondrial dysfunction have been proposed to be involved in many different hearing

disorders including noise induced hearing loss. We have employed two-photon fluorescence imaging of electron carriers to study the metabolic status of the different cell types in excised, intact mouse organ of Corti preparations. Reduced nicotinamide adenine dinucleotide (NADH) and the oxidized forms of flavoproteins (Fp) both fluoresce when excited by femtosecond pulses of 740-nm light. Since NADH fluoresces only when reduced and Fp only when oxidized these two intrinsic fluorophores have been used to determine the relative percentages of oxidized and reduced energy equivalents in cells. an evaluation of the hemicochlea and an intact cochlea explant was conducted. Stability of the explanted preparation was improved upon from previous experiments and will be discussed for different turns. Recent studies, however, suggest that intensity based measurements may be prone to error due to changes in fluorescent intensity resulting not from change in concentration but due to change in the lifetime of the fluorophore as a result of changes in the ratio of free and bound populations. to evaluate the impact of these changes we have recently employed two-photon excited NADH Fluorescence Lifetime Imaging. Assessment of the metabolic state by each method will be compared for hair cells of the excised organ of Corti.

## **[96] A Simplified, Atraumatic Technique for *In Situ* Cultures of the Mouse Utricle**

**Henry Ou<sup>1</sup>, Edwin Rubel<sup>1</sup>, Vincent Lin<sup>1</sup>**

<sup>1</sup>VM Bloedel Hearing Research Center, University of Washington, Dept. Otolaryngology-HNS

Traditionally, our *In Vitro* technique for studying hair cells of the mouse utricle involves severing neural connections and removal of the whole utricle from the temporal bone. the utricles are then cultured free floating in media. This technique, while effective, is not ideal due to high variability in the preservation of the sensory epithelium. in addition, there is also a steep learning curve which results in frequent injury of the sensory epithelium in less experienced hands.

We have developed a modification of this technique that minimizes trauma and allows the preparation to be more accessible to other groups hoping to utilize this system. Leaving the temporal bone largely intact, a window from the cranial side is opened in the bony vestibule overlying the mouse utricle. Pigmented epithelium of the membranous labyrinth covering the sensory epithelium is removed to expose the hair cells to culture media. Otoconia are left in place. the entire temporal bone is then placed into culture media. in this manner, the utricle is cultured *In Situ* with essentially no damage to the epithelium, leaving neural attachments intact. Prior to fixation, otoconia can be easily removed. the utricles are then removed from the temporal bone post-fixation.

The technique will be presented with neomycin dose-response curves to demonstrate its value for studying hair cell death.

Supported by NIDCD P30 grant DC004661 and the National organization for Hearing Research

## **[97] A Novel System for Inducible Gene Expression in Mouse Hair Cells Using a Modified Form of the Human Myosin 7a Promoter**

**Yukako Asai<sup>1</sup>, Amy B. Ryan<sup>1</sup>, Heidi Scrabble<sup>1</sup>, Jeffrey Holt<sup>1</sup>, Gwenaelle S.G. Geleoc<sup>1</sup>**

<sup>1</sup>University of Virginia

Gene manipulation *In Vivo* using transgenic or targeted gene deletion can result in embryonic lethality, developmental defects or compensation by other gene products, all of which confound interpretation of normal gene function. Alternate strategies using ear specific promoters and Cre-Lox recombination can circumvent some of these problems but do not allow for on/off control of gene expression. the goal of this project is to design a novel system that allows for precise spatiotemporal control of gene expression which can be used to examine the function of any gene of interest specifically in hair cells. We are constructing a hair cell-specific, inducible gene expression system based on the *lac* operator-repressor regulatory system. in the *lac* system, regulated gene expression results from binding/unbinding of LacI protein to *lac* operator sequences. the operators can be introduced in the promoter sequence to flank the transcriptional start site. in the repressed state LacI is bound and transcription is blocked. in the derepressed state, exposure to the inducer, IPTG, releases LacI from the operators, which turns on transcription. Since the regulation is reversible, addition or removal of IPTG can be used to turn on or off gene expression at any point during development or in the mature animal. We are applying this system to the human Myosin 7a promoter, whose activity in the inner ear is restricted to hair cells. We have tested *lac* operator sequences placed at various positions within the human Myo7a promoter for their ability to regulate gene expression. As an assay we transfect HeLa cells with LacI and *lac* operator-modified Myo7a promoters followed by the gene for luciferase. One of our constructs demonstrated 70% suppression of promoter activity and full recovery in the presence of IPTG. Hair cell-specific, regulatable gene expression will be a valuable tool for understanding gene function during development and age-related hearing loss. (NIDCD Grant #DC008853)

## **[98] Histone Deacetylation Enhances Adenoviral Vector Transduction in Inner Ear Tissues**

**Akiko Taura<sup>1</sup>, Kojiro Taura<sup>2</sup>, Yun-Hoon Choung<sup>3</sup>, Masatsugu Masuda<sup>1</sup>, Kwang Pak<sup>1</sup>, Eduardo Chavez<sup>1</sup>, Allen F. Ryan<sup>1</sup>**

<sup>1</sup>UCSD School of Medicine and VA Medical Center,

<sup>2</sup>UCSD School of Medicine, <sup>3</sup>UCSD School of Medicine and VA Medical Center, Ajou University School Medicine

Adenoviruses (AdVs) are efficient vectors for gene therapy in many tissues. Several studies have demonstrated successful transgene transduction with AdV vectors in the inner ear of rodents. However, toxicity of AdV or lack of tropism to hair cells appear to limit its experimental, and potentially clinical, utility. Histone deacetylase inhibitors (HDIs) are known to enhance AdV-mediated transgene

expression in various organs, but their effects in the inner ear have not been documented. We investigated the ability of one HDI, trichostatin A (TSA), to enhance AdV-mediated transgene expression in vestibular inner ear tissue. We cultured neonatal rat macular explants, and transfected them with an AdV vector encoding GFP for 24hrs. the explants were treated with TSA at the beginning or end of the transfection period, and GFP expression was compared to AdV without TSA. in the absence of TSA, GFP expression was limited, and few hair cells were transduced. TSA did not exert an augmentation effect when given at the beginning of AdV transfection. However, administration of TSA just after AdV increased GFP expression in supporting cells. in addition, more hair cells were also transduced. These results suggest that TSA enhances AdV-mediated transgene expression in the inner ear, and potentially increases successful transduction of hair cells. HDIs, some of which are currently under clinical trials, could be useful tools in overcoming current limitations of gene therapy in the inner ear using AdV vectors.

(Supported by NIH grant DC00139 and the Research Service of the VA)

## **[99] Effect of Dornase Alfa on Isolated Cochlear Outer Hair Cells**

**Dusan Martin**<sup>1</sup>, Kenny H. Chan<sup>2</sup>, You Hyun Kim<sup>1</sup>, Yoon Hwan Kim<sup>1</sup>, Earnest O. John<sup>1</sup>, Timothy T.K. Jung<sup>1</sup>

<sup>1</sup>*Division of Otolaryngology-Head and Neck Surgery, Loma Linda University, Loma Linda, CA,* <sup>2</sup>*Children's Hospital, Denver, CO*

**Background:** Otitis media (OM) is one of the most common diseases. Clinicians have been interested in altering the rheological properties of middle-ear effusion (MEE). Tympanostomy tubes as a treatment of OM are frequently clogged due to thick mucoid MEE. Dornase alfa (Pulmozyme® by Genentech), approved by the FDA since 1994 for treating cystic fibrosis (CF), offers a unique potential for treating OM. It reduces viscoelasticity of sputum by hydrolyzing DNA released by degenerating leukocytes. Many clinical similarities exist between OM and cystic fibrosis. We strongly believe in its potential efficacy in the treatment of OM. Before it can be implemented for a clinical trial, its ototoxicity potential needs to be ruled out.

**Objective:** This study evaluates the potential ototoxicity of dornase alfa by direct exposure to isolated chinchilla cochlear outer hair cells (OHCs).

**Study Design and Methods:** This descriptive study involving morphological changes chinchilla outer hair cells after exposure to dornase alfa. Chinchilla temporal bones and bony otic capsules were harvested after decapitation. Cochleae were dissected under a microscope in standard bathing solution (SBS) and treated with 5 mg/ml solution of trypsin (Sigma, St. Louis, MO, USA) for 15 min. the osmolarity and pH of SBS were closely monitored to be at 305±5 and 7.3-7.4 respectively. OHCs were separated from the organ of Corti by mechanical isolation. with the use of an inverted microscope (Zeiss, Gottingen, Germany) and a camera (Q-Imaging Micropublisher 5.0 RTV, Surrey, BC, Canada), an aliquot of 25µl of OHC suspended SBS was placed on the Petri dish. Upon the

identification of an OHC, they were then exposed to 1:1 Dornase alfa. Images were taken every ten minutes until time of cell death.

**Results:** Toxicity was assessed by time to cell death. the time to cell death was measured every ten minutes until a maximum of 90 minutes. the mean time to cell death was 75 minutes. in control OHCs in SBS time to cell death was similar.

**Conclusion:** Previous studies have demonstrated, when exposed to ototoxic substances, OHC death within the first 20 minutes. in this descriptive study we found that dornase alfa is non-ototoxic, therefore it provides potential therapeutic merits for treating clogged tympanostomy tubes.

## **[100] Tbx2 Plays an Essential Role in Inner Ear Development**

**Jordan D. LeGout**<sup>1</sup>, Angela B. Thompson<sup>1</sup>, Virginia E. Papaioannou<sup>2</sup>, Eri Hashino<sup>1</sup>

<sup>1</sup>*Indiana University School of Medicine,* <sup>2</sup>*Columbia University*

Tbx2 is a member of the T-box family of transcription factors, a family whose members are involved in the developmental regulation of a number of tissues and organs. a previous loss-of-function study revealed that Tbx2 is required for patterning and morphogenesis of the developing heart. However, little is currently known about the role for Tbx2 in inner ear development. Our quantitative RT-PCR analysis with E10-18 mouse otocysts indicated that the Tbx2 expression level is highest at E10, after which it sharply declines and becomes barely detectable by E14. *In Situ* hybridization analysis with E10 embryos showed that strong Tbx2 expression is observed in the ventral region of the otocyst, with a lesser expression in the dorso-medial region. in addition, Tbx2 was expressed in the endolymphatic duct. to elucidate the role for Tbx2 in inner ear development, we analyzed the morphology and gene expression patterns in mutant mice deficient for Tbx2. Since we found the Tbx2 expression domain in the otocyst complementary to the expression domain of Tbx1, a gene known to suppress neurogenesis, we hypothesized that Tbx2 might promote expression of proneural genes in the otocyst. to test this hypothesis, we performed whole-mount *In Situ* hybridization analysis for the neural progenitor markers Ngn1 and Tlx3. We found no noticeable differences in the expression pattern of Ngn1 or Tlx3 between E10 Tbx2 null and heterozygous otocysts, suggesting that Tbx2 is not involved in early neurogenesis of the inner ear up to this stage. However, a distinct phenotype became apparent at E11-12. Severe cranio-facial abnormalities, including a hypoplastic inner ear, were consistently observed in the Tbx2 deficient embryos. in addition, Ngn1 expression was lost entirely in cranio-facial structures, but not in the trunk region of the Tbx2 null embryos. These findings suggest that Tbx2 plays an important role in proper development of the mouse inner ear at stages later than E10.

## **101 The Role of Lmx1a in Histogenesis of the Organ of Corti**

David Nichols<sup>1</sup>, Sarah German<sup>1</sup>, Kathleen Millen<sup>2</sup>, Bernd Fritsch<sup>1</sup>

<sup>1</sup>Creighton Univ. School of Med., <sup>2</sup>University of Chicago

### **The Role of Lmx1a in Histogenesis of the organ of Corti**

There is little molecular data available to explain the origin of the orderly arrangement of cell types in the organ of Corti (OC). Our analysis of the *Lmx1a* mutant (Dreher) mouse cochlea finds the ductus reuniens is missing, and the base of the OC superficially resembles an extension of the saccule. an abrupt transition then separates it from the approximately wildtype apex. *Lmx1a In Situ* hybridizations of E12.5 wildtype embryos demonstrate strong *Lmx1a* expression in the Claudius cell precursors of the outer spiral sulcus along the entire length (i.e., base and apex) of the OC. the basal OC of *Lmx1a* mutants in which heterozygous *Atoh1-lacZ* expression marks hair cells, demonstrate up to 14 rows of stained hair cells, whereas the apex forms an approximately wildtype complement of 4. *In Situ* hybridizations for *Gata3*, a gene expressed in cochlear, not saccular epithelium, labeled the base. Thus the base is related to the OC, not the saccule. This is confirmed by lipophilic dye tracings which find that sensory innervation of the base, though disorganized, originates from the spiral ganglion. Immunohistochemical stains for PROX1 (embryos) and  $\beta$ -tubulin (juveniles) demonstrate that supporting cells do not differentiate into pillar and Deiter's cells in the basal turn, but do so in the apex. in other regions of the embryo, *Lmx1a* expression initiates BMP secretion while a related gene, *Lmx1b*, modulates FGF8 secretion. *Fgf8 In Situ* hybridizations on E18.5 *Lmx1a* mutants show expression specifically located in inner hair cells in the apical OC whereas it is widely expressed in most basal hair cells. Thus our current working hypothesis is that *Lmx1a* expression modulates FGF and possibly BMP secretion gradients, thereby ordering OC histogenesis. Mice lacking both *Lmx1a* and *b* have no OC at all, suggesting that *Lmx1b* covers for *Lmx1a* in the apex of *Lmx1a* mutants.

## **102 Bmp2 is Crucial for the Formation of Semicircular Canals in the Mouse Inner Ear**

Chanho Hwang<sup>1</sup>, Stephen Harris<sup>2</sup>, Doris Wu<sup>1</sup>

<sup>1</sup>NIDCD/NIH, <sup>2</sup>Univ. of Texas Health Science Center at San Antonio

Semicircular canals are parts of the vestibular apparatus within the inner ear that detect angular head movements. the orthogonal arrangement of the three semicircular canals and their exquisite shape allow them to detect three dimensional head motions with precision. in chicken, fibroblast growth factors (FGFs) secreted from the cristae are thought to promote canal development by upregulating *Bmp2* (Development, 131:4201). to further test the role of *Bmp2* in canal formation, we generated *Bmp2* conditional knockout mice through timed matings of *Fogx1-cre*; *Bmp2*<sup>+/-</sup> and *Bmp2*<sup>lox/lox</sup> mice, since *Bmp2* null mice die at an early embryonic stage. Our paint-fill analyses indicated that some of the canal pouches of *Fogx1-cre*; *Bmp2*<sup>lox/-</sup> embryos appeared to be smaller than wildtype at

E11.5. by E13.5, all *Bmp2* conditional knockout inner ears examined have no canals but the three cristae were intact. We are currently investigating whether similar canal genesis zones are present in the mouse inner ear as proposed in the chicken, and whether *Bmp2* functions to maintain these genesis zones in the mouse.

## **103 Roles of BMP Signaling in Inner Ear Development**

Takahiro Ohyama<sup>1</sup>, Makoto Ikeya<sup>2</sup>, Yoshiki Sasai<sup>2</sup>, and Groves<sup>1</sup>

<sup>1</sup>House Ear Institute, <sup>2</sup>RIKEN, Kobe

Bone Morphogenetic Protein (BMP) signaling plays crucial roles during embryonic development such as axis formation and neural induction. Several BMPs are known to be expressed in different areas of the inner ear at different times. Previous studies have shown that BMP signaling regulates formation of the otic capsule and the vestibular sensory patches in chick (Chang, W. et al. Dev. Biol. 251, 2002, Liu, W. et al. Dev. Dyn. 226, 2003, Pujades, C. et al. Dev. Biol. 292, 2006). We analyzed the expression pattern of mouse crossveinless-2 homologue (Cv2) in the inner ear. Cv2, which is a mediator of BMP signaling, has been shown to act as pro-Bmp in the vertebral column, eye and kidney (Ikeya, M. et al. Development 133, 2006). in the inner ear, Cv2 is expressed in the dorsal otocyst from E10.5. Later, the Cv2 expression domain partially overlaps the *Bmp2* domain in the semicircular canals and crista, the *Bmp5* domain in capsule-forming mesenchyme and the *Bmp4* domain in the cochlear duct. in Cv2-null mutant, we observed malformation in the vestibular system and slight delay in maturation of the cochlear hair cells. the maturation delay of the cochlear hair cells is partially rescued in the Cv2-null; *Bmp4*<sup>+/-</sup> compound mutants, suggesting that Cv2 may act as anti-Bmp4 in the cochlear duct.

## **104 The Roles of Notch-Hes1 Pathway in the Formation of Prosensory Region During Mammalian Cochlear Development**

Junko Murata<sup>1</sup>, Toshiyuki Ohtsuka<sup>2</sup>, Akinori Tokunaga<sup>3</sup>, Manabu Tamura<sup>1</sup>, Arata Horii<sup>1</sup>, Katsumi Doi<sup>1</sup>, Hideyuki Okano<sup>3</sup>, Ryoichiro Kageyama<sup>2</sup>

<sup>1</sup>Osaka University School of Medicine, <sup>2</sup>Institute for Virus Research, Kyoto University, <sup>3</sup>Keio University School of Medicine

Notch pathway has a crucial role in the differentiation of hair cells and supporting cells by mediating "lateral inhibition" via the ligands Delta-like1 and Jagged2, and the effectors Hes1 and Hes5 during mammalian inner ear development. Recently, another Notch ligand Jagged1-dependent Notch activation has been revealed to be important for the determination of prosensory region in the earlier stage before cell differentiation. the specification, survival, and the proliferative capacity of auditory sensory precursor cells (ASPCs) are necessary for the determination of prosensory region. Hes1 promotes the progenitor cell proliferation through the transcriptional down-regulation of p27<sup>Kip1</sup> in the thymus, liver, and brain. in this study, we first confirmed that Hes1 expression was



observed from the earlier stage before the cell differentiation, depending on the weak Notch1 activation induced by Jagged1 during mammalian cochlear development. We next analyzed the inner ear of *Hes1*-knockout (KO) mice during the period of prosensory formation to find that the expression level of *p27<sup>Kip1</sup>* was up-regulated, and the number of BrdU-positive, S-phase cell was reduced in *Hes1*<sup>-/-</sup> cochleae. These results implicated that Notch-Hes1 pathway contributes to the adequate proliferation of ASPCs via the transcriptional control of *p27<sup>Kip1</sup>* expression. This crucial role of Notch-Hes1 pathway is interpreted to regulate not simply the total number of ASPCs, but also the proper specification of prosensory region by preventing inappropriately accelerated expression of *p27<sup>Kip1</sup>*.

By contrast, the precocious differentiation of hair cells at E13.5 was not found in *Hes1*<sup>-/-</sup> mutant mice. However, *Math1* expression was diffusely up-regulated at E13.5 in the region where *p27<sup>Kip1</sup>* had already appeared in *Hes1*<sup>-/-</sup> cochleae. This result could be interpreted that the prosensory character is conferred to a wider region at an earlier stage in *Hes1*<sup>-/-</sup> mice compared to wild-type littermates. This work was supported by a grant to J.M. from the Japanese Ministry of Education, Culture, Sports, Science, and Technology (Grant Number: 18591866).

#### **105 The Notch Ligand DNER is Expressed in Hair Cells and Spiral Ganglion Neurons in the Mouse Cochlea**

**Byron H. Hartman<sup>1</sup>**, Olivia Bermingham-McDonogh<sup>2</sup>, Thomas A. Reh<sup>1</sup>

<sup>1</sup>*University of Washington Department of Biological Structure*, <sup>2</sup>*Virginia Merrill Bloedel Hearing Research Center at the University of Washington*

The Notch signaling pathway is known to play key roles in cochlear development. Previous studies have shown that the Notch1 receptor and Notch ligands in the Delta and Jagged families are important for cellular differentiation and patterning of the organ of Corti. Recently, DNER (Delta/Notch-like EGF-related receptor) was identified as a novel Notch ligand expressed in developing and adult CNS neurons (Eiraku et al., 2002). Although the function of DNER is still poorly understood, it has been shown to actively promote morphological and functional maturation of glia through activation of Notch signaling in the cerebellum (Saito and Takeshima, 2006). We have used an antibody against DNER to carry out immunofluorescence studies of the mouse cochlea. We find that DNER is expressed in auditory hair cells at low levels during embryogenesis and is up-regulated during the postnatal period of cellular and morphological maturation, beginning around postnatal day 4. We also find that DNER is expressed in the peripheral processes of spiral ganglion neurons during development and is up-regulated in the synaptic terminals around hair cells during the postnatal period. At present we are continuing immunolabeling studies, as well as performing *In Situ* hybridization analysis to characterize the expression profile of DNER. We are also analyzing the cochlea of DNER-knockout mice, which are known to exhibit motor discoordination (Tohgo et al., 2005), to determine whether

DNER is required for the proper maturation of supporting cells and/or hair cells.

This work is supported by the following grants: RO1 EY13475 to T.A.R. sponsored by NIH/NEI; T32 HD007183-26A1 to B.H.H. sponsored by NIH/NIDCD; and DC005953 to O.B.McD. sponsored by NIH/NIDCD.

#### **106 The Role of Sox1 Group of Transcription Factors and the Antagonistic Relationship Between Sox2 and Atoh1 in the Developing Mouse Cochlea**

**Chandrakala Puligilla<sup>1</sup>**, Alain Dabdoub<sup>1</sup>, Larysa Pevny<sup>2</sup>, Matthew Kelley<sup>1</sup>

<sup>1</sup>*NIH*, <sup>2</sup>*UNC*

Sensory neurons, hair cells and support cells are derived from otic precursor cells during inner ear development. How a group of genes is responsible for delineation of sensory epithelia, proliferation, and differentiation remains unclear. the transcription factors Sox1, Sox2 and Sox3 (Sox1-3) constitute the B1 group of the Sox gene family, are expressed in precursors in the CNS. We examined their role during cochlear development comparing the expression of Sox1-3 proteins. All three SoxB1 proteins overlap in the developing sensory neurons suggesting a role in neurogenesis. Consistent with this, overexpression of Sox2 in cochlear explants results in the formation of *Tuj1* positive cells indicating a role for Sox2 as a proneural gene. in addition, Sox2 is expressed throughout the prosensory domain initially and becomes down-regulated in cells that will develop as hair cells through up-regulation of *Atoh1*. to investigate if downregulation of Sox2 is necessary for hair cell formation, we overexpressed Sox2 in prosensory cells which resulted in inhibition of hair cell formation. Reciprocally, overexpression of *Atoh1* in cells that express Sox2 endogenously resulted in inhibition of Sox2 expression and development of hair cells. Thus an antagonistic relationship between Sox2 and *Atoh1* exists in the cochlea similar to the one between SoxB1 and bHLH proteins in the CNS. for confirmation, we analyzed cochleae from Sox2 hypomorphic mice. At E15 WT cochleae contained a row of inner hair cells and Sox2 hypomorphic cochleae contained 2 rows of outer hair cells and 1 row of inner hair cells indicating that low levels of Sox2 results in early differentiation of hair cells. Furthermore, there was a significant increase in inner hair cell number at E18 in Sox2 hypomorphic cochleae.

Our data suggest that Sox2 plays a dual role in cochlear development both as a proneural and prosensory gene and that the generation of hair cells from progenitors depends on inhibition of Sox2 by *Atoh1*.

#### **107 Sox2 is Essential for Sensory Neuron Survival in the Inner Ear**

Anna Pelling<sup>1</sup>, **Bernd Fritzsche<sup>2</sup>**, Keith Leung<sup>1</sup>, Robin Lovell-Badge<sup>3</sup>, Kathryn Cheah<sup>1</sup>

<sup>1</sup>*University of Hong Kong*, <sup>2</sup>*Creighton University*, <sup>3</sup>*The Ridgeway*

Function of the inner ear requires sensory neurons and sensory epithelia, composed of hair and supporting cells,

that share some common progenitors. Sox2 is required for hair and supporting cell formation, but its role in sensory neurons, which require Neurog1 for specification, is unknown. Sox2, like Neurog1, is transiently expressed in delaminating neuroblasts. In Neurog1 null mice Sox2 is normally expressed. When Sox2 is deficient, Neurog1 is expressed and sensory neurons develop and reach with their processes areas where sensory epithelia would normally develop but soon disappear due to lack of neurotrophic support. Our data implies specification and initiation of differentiation of otic sensory neurons does not require Sox2 and is independent of development of sensory epithelia. Sox2 is however essential for maintenance of innervation and may complement but acts independently of Neurog1. Sox2 may also have a dose-dependent role in regulating the pattern of neuronal fiber outgrowth in the inner ear.

### **108 Sox10 is not Necessary for Auditory Neurons Survival**

Ingrid Breuskin<sup>1</sup>, Morgan Bodson<sup>1</sup>, Nicolas Thelen<sup>1</sup>, Marc Thiry<sup>1</sup>, Philippe Lefebvre<sup>1</sup>, Brigitte Malgrange<sup>1</sup>

<sup>1</sup>CNCM - University of Liege - Belgium

Sox10 is a HMG domain transcription factor required for proper development of neural crest cell derivatives, including melanocytes and peripheral glia. Sox10-null mutations lead to a complete absence of these derivatives, and Sox10 haploinsufficiency results in neural crest defects that causes Waardenburg-Shah syndrome in humans.

Although studies have shown the role of Sox10 in the development of the neural crest cells, its function in auditory system development is unclear. During inner ear development, Sox10 expression is first detected in the otic placode and persisted throughout its development. Sox10 is also expressed in the glial cells of the cochleo-vestibular ganglion and spiral ganglion. In Sox10-null mutant mice, spiral ganglion glial cells and melanocytes are missing. In the absence of these neural crest-derived cells, we have investigated the fate of the otocyst-derived inner ear sensory neurons. Loss of Sox10 function does not alter their morphology and does not cause reduction in their number. Our data demonstrate that as previously described in the peripheral nervous system, the neural crest-derived cells of the inner ear are missing in the Sox10-null mutant mice. But in contrast to the peripheral nervous system, our results also suggest that glial cells and Sox10 do not play a primary role in auditory neurons development and survival in the developing inner ear.

### **109 Functional Analysis of GATA-2 in Auditory and Neuronal System**

Tomofumi Hoshino<sup>1</sup>, Keiji Tabuchi<sup>1</sup>, Ritsuko Shimizu<sup>1</sup>, Masayuki Yamamoto<sup>2</sup>, Akira Hara<sup>1</sup>

<sup>1</sup>University of Tsukuba, <sup>2</sup>Tohoku University

Because inner ear arises from otic vesicle under the regulation of external signal from the neural tube, both otic vesicle and neural tube are important for the inner ear development. Because transcription factor GATA-2 is expressed in both tissues, elucidation of Gata2 gene

regulation is important for the understanding of inner ear development. However, roles of GATA-2 is not clarified yet, because of the embryonic lethal phenotype of Gata2 gene knockout mice. Therefore, we used the conditional knockout (CKO) system to overcome embryonic lethality.

We crossed the Gata2 flox mouse with the Nestin-Cre mouse, in which Cre recombinase is expressed specifically in neural tissues. The Gata2 CKO mice with both Gata2 flox allele and Nestin-Cre transgene were born normally and grew up to adult. We examined the ABR thresholds of 10 weeks old mice. ABR thresholds were significantly higher in Gata2 CKO mice than those of the control mice. Significant reduction of spiral ganglion cells (SGC) was observed in adult Gata2 CKO mice in the histological examination. Surprisingly SGC reduction was clearly observed in newborn pups, indicating that Gata2 CKO mice suffered from hearing impairment. On the other hand, there was no remarkable change in the organ of the Corti and the cochlear nucleus of brain stem. These results indicate that the GATA-2 is important for the inner ear development through the regulation of SGC proliferation in the embryonic period.

### **110 The Role of Gata3 in the Development of Auditory Neurons in Chick Inner Ear**

Jennifer Jones<sup>1</sup>, Mark Warchol<sup>1</sup>

<sup>1</sup>Washington University

During development of the otocyst, neuroblasts delaminate from the anteroventral region of the otic epithelium to form the auditory-vestibular ganglion (AVG) that will innervate the sensory cells of the cochlea and vestibular organs respectively. The molecular basis of cell-fate specification between auditory vs. vestibular neurons is unresolved. It has been reported that the expression of the zinc finger transcription factor Gata3 distinguishes neuroblasts destined for an auditory fate while the bHLH transcription factor, NeuroD, designates vestibular neurons (Lawoko-Kerali et al., 2004). The aim of this study was to examine the potential role of Gata3 in specifying auditory neurons. First, we examined the expression of Gata3 and NeuroD in the AVG at embryonic days E2-E7. During invagination of the otic cup (E2), Gata3 expression was restricted to the lateral wall. Following closure of the otic cup (E2.5-E3.5), Gata3 expression was detected in the lateral wall as well as the anteroventral region of the otocyst, at the site of neuroblast delamination. Notably, we observed two apparently separate populations of neuroblasts (that express either Gata3 or NeuroD) within the region of delaminating cells. As the AVG separates into the auditory ganglion and vestibular ganglion, Gata3 was restricted to auditory neurons while NeuroD was restricted to vestibular neurons. These expression data are consistent with the notion that Gata3 plays a role in specifying auditory neurons. Prior studies of Gata3 null-mutant mice suggest that GATA3 is necessary for the development of auditory neurons (Karis et al., 2001). We are currently investigating the role of Gata3 in the specification of auditory neurons by ectopically expressing Gata3 in the developing chick ear in ovo.

### **111 Expression of POU4F1 and POU4F2 During the Development of Mouse Cochlear-Vestibular Ganglion**

Min Deng<sup>1</sup>, Ling Pan<sup>1</sup>, Xiaoling Xie<sup>1</sup>, Lin Gan<sup>1</sup>

<sup>1</sup>University of Rochester

The Class IV POU-domain transcription factors (POU4Fs) play essential roles in the differentiation and survival of projection neurons within the inner ear, retina, dorsal root and trigeminal ganglia. In the inner ear, otic neurons are derived from the otic epithelium, migrate into the mesenchyme to form the cochlear-vestibular ganglion (CVG), and finally innervate the vestibular and cochlear sensory organs. Here, using immunohistochemistry, we present a detailed analysis of POU4F1 and POU4F2 expression in the CVG, and compare it with the expression of specific otic ganglion cell markers, Neurod1, Gata3 and Islet1, during mouse embryogenesis. At early stages, POU4F1 is colocalized with Islet1 in a majority of the delaminated CVG neurons but not in the otic epithelium cells. Expression of POU4F2 was initially observed in the Neurod1-negative post-mitotic neurons. Later, the expression of POU4F1 and POU4F2 was detected in both vestibular and spiral ganglion cells. Interestingly, while POU4F1 becomes downregulated in a majority of spiral ganglion neurons, POU4F2 expression is expanded. The differential expression of POU4F1 and POU4F2 in the inner ear neurogenesis suggests their potential role in the development of inner ear neuronal cells.

### **112 The Presence and Function of Slit and Robo in the Developing Inner Ear**

Alyssa Hackett<sup>1</sup>, Wei Gao<sup>1</sup>, Yael Raz<sup>1</sup>

<sup>1</sup>University of Pittsburgh

**Background:** Auditory neurons connect the cochlear sensory epithelium with higher brain centers while preserving a precise tonotopic organization. Slit ligands acting via the robo receptors are axon guidance cues which can attract or repel the growth cone. The spatiotemporal distribution of slit and robo as well as preliminary functional data will be presented.

**Methods:** Section and whole mount *In Situ* hybridization of slit1, slit2 and slit3 were performed on E13 to P3 mice. Both *In Situ* and immunohistochemistry of robo1, robo2 and robo3 were performed on E11 to adult mice. Functional studies were carried out using co-cultures of rat spiral ganglion explants. Changes in neurite outgrowth, length, direction, and branching were observed.

**Results:** During the period of neurite outgrowth the three slit homologs have unique but overlapping patterns of expression in the spiral ganglion, adjacent mesenchyme and cochlear epithelium. Robo1 expression was noted as early as E11 in the developing faciostaticacoustic ganglion, and is maintained until birth. Though it is downregulated in the early postnatal period there is widespread expression in the adult cochlea. Robo2 appears to have weak spiral ganglion expression at E13. Robo3 is not expressed in the spiral ganglion. The slits are also expressed in restricted patterns surrounding the cristae as well as the arches of the developing semicircular canals, and utricle. Robo 1 is expressed in the vestibular

nerve endings as they extend towards the vestibular end organs.

**Conclusions:** the expression pattern of slits and robos suggests a role for this axon guidance pathway in regulating cochlear innervation. The expression pattern of slit2 and slit 3 are particularly interesting as potential cues targeting extending neurites to their hair cell targets. Furthermore differential expression of slit ligands amongst the vestibular end organs suggests a possible role in segregating vestibular afferent input.

### **113 Microtubule Associated Protein Tau During Development in the Cochlea and in Spiral Ganglion Cultures**

David Tieu<sup>1</sup>, Sandra Koterski<sup>1</sup>, Mary Grover<sup>2</sup>, Donna Whitlon<sup>2</sup>

<sup>1</sup>Northwestern University, Department of Otolaryngology,

<sup>2</sup>Northwestern University, Department of Otolaryngology, Hugh Knowles Center

Microtubules (MTs) are abundant in spiral ganglion peripheral nerve fibers during normal development but become sparse by P9 and are nearly absent in adult gerbil cochleas. Since MTs are necessary for neurite growth and regrowth, we hypothesized that when neurite growth slows during development, levels of proteins required for generation and/or stabilization of neuronal MTs also decrease. Here we focus on the neuron-specific microtubule associated protein (MAP) tau, a protein that regulates the stability of neuronal MTs. Four different anti-tau antibodies (Abs) were used in this study: Tau-5 and tau 46.1 both recognize all forms of tau; tau-1 recognizes all tau proteins unphosphorylated at amino acids 199-205; AT8 recognizes all tau proteins phosphorylated in the 199-205 amino acid region. Using Abs tau-5, tau46.1 and tau-1, we observed at least two different tau isoforms (50K and 60K) on Western blots of extracts from cochleas aged NB-P6. The ratio of 50K tau-1/neuronal tubulin (t/tu) was highest at birth and decreased by nearly 50% during the first two weeks. The ratio of 60K tau-1 peaked at about a week after birth and decreased about 50% by the end of the second postnatal week. Double immunolabeling of developing cochleas with Tau-1 and tubulin Abs demonstrated expression in spiral ganglion nerve cell bodies and peripheral fibers, particularly in nerve endings at the level of the inner hair cells. No tau-1 labeling was detected in the region of the outer hair cells. In cultures, tau-1 labeled all neurons. The ratio of 50K t/tu was higher in cultures treated with BMP4 than in those treated with LIF. These data demonstrate that the ratio of t/tu changes during development and can be altered *In Vitro* by treatments that alter neuronal morphology. The overall decrease in t/tu during cochlear development is consistent with the overall decrease in MTs observed in peripheral neurites. The results suggest that neurite regrowth after cochlear damage may require alterations in the regulation of tau and other MAPs. (Supported by NIH grant# DC00653, the Hugh Knowles Center and the Department of Otolaryngology, Northwestern University)

### **114 Anti-Paired Helical Filament (PHF) Tau Antibody Recognizes a Developmentally Regulated 220 Kda Protein in the Mouse Cochlea**

Sandra Koterski<sup>1</sup>, Mary Grover<sup>1</sup>, David Tieu<sup>1</sup>, Donna S. Whitlon<sup>2</sup>

<sup>1</sup>Northwestern Feinberg School of Medicine, Dept of Otolaryngology- Head and Neck Surgery, Chicago, IL, <sup>2</sup>1; Northwestern University Hugh Knowles Center & Interdepartmental Neuroscience Program, Chicago, IL

During a developmental study of the molecular forms of the microtubule-associated protein tau in the mouse cochlea (Tieu *et al.*, ARO 2008), we compared the levels of phosphorylated and unphosphorylated tau by Western Blot. to visualize all tau isoforms when they were unphosphorylated between amino acids 199 to 205, we used the monoclonal antibody Tau-1. to visualize the tau isoforms that were phosphorylated in the same region, we used the anti-paired helical filament antibody AT8. We found robust immunoreaction with Tau-1 at its appropriate molecular weight, approximately 55 kDa, but could not detect immunoreactivity with AT8 in the same region. Instead we noticed a single AT8 positive band in the region of 220 kDa. This size is well outside the known molecular weight range of tau. the band was not immunoreactive to the pan tau antibodies Tau-5 or Tau 46.1, indicating that the protein was not tau. the 220 kDa AT8 positive band was detectable in protein extracts taken from whole cochleas during the first postnatal week, but thereafter, declined in intensity. in addition, the 220 kDa AT8 band could be detected in 42-hour cultures of dissociated spiral ganglion. Immunocytochemistry with the AT8 antibody labeled only neurons *In Vitro*. in two separate experiments, concentration by immunoprecipitation of pooled 2-day old cochleas with AT8 allowed for purification of the 220 kDa protein by gel electrophoresis. Analysis by mass spectrometry by the University of Illinois-Chicago Proteomics Laboratory identified both non-muscle myosin IIA and non-muscle myosin IIB. the results raise the possibility that a developmentally regulated form of non-muscle myosin is present in the spiral ganglion and is recognized by the anti-paired helical filament antibody AT8.

Supported by NIH grant #DC00653, Hugh Knowles Center, Northwestern Feinberg School of Medicine Department of Otolaryngology- Head and Neck Surgery.

### **115 Transient Expression of 5-HT in Auditory Brainstem Neurons of the Postnatal MAO a Knockout Mouse**

Ann Thompson<sup>1</sup>

<sup>1</sup>Univ. of Oklahoma Health Sciences Center

Serotonin (5-HT) is essential for the development of central visual and somatosensory projections where neurons transiently accumulate 5-HT. in the perinatal mouse, transient 5-HT expression has been reported in anteroventral cochlear nucleus (AVCN) and lateral superior olive (LSO) neurons. Based on the temporal sequence of this expression and the known projection from

AVCN to LSO, it was hypothesized that 5-HT is involved in the sequential development of the AVCN projection through LSO. As this projection is essential for central auditory function, we studied in more detail the expression of 5-HT in the auditory brainstem postnatally. Brain sections of mice ranging in age from birth to postnatal day (P) 15 were collected and processed immunohistochemically. We used monoamine oxidase a (MAO A) knockout mice to enhance detection of 5-HT neurons.

5-HT-labeled neurons were observed in the cochlear nucleus (CN), LSO, and inferior colliculus (IC) from birth – P6. in CN, labeling was observed infrequently and in fewer neurons at P7 and disappeared at P8. When present, all labeled neurons were located in the dorsal CN and were identified as fusiform cells. a similar timing of labeling was observed in the LSO where 5-HT labeling began to decrease at P7. the decrease was irregular as labeled neurons lingered in the lateral limb until P8. in the IC, labeled neurons were most prominent caudally, outside of the central nucleus and were not observed beyond P7.

These results show the transient expression of 5-HT in the MAO a knockout mouse at birth to P7-8. 5-HT is expressed simultaneously in CN and superior olivary neurons that project directly to the IC. the pattern of expression within the frequency axis of the LSO suggests a later accumulation of 5-HT in neurons that will encode relatively low frequencies in the adult. the timing and transiency of 5-HT expression in these regions indicate 5-HT's role in specific developmental processes before cochlear innervation.

Supported by the Oklahoma Center for the Advancement of Science and Technology (HR-05-118).

### **116 An Efficient Screening Method Using Inner-Ear Derived Spheres for Selection of Compounds That Induce Hair Cell Differentiation**

Masato Fujioka<sup>1</sup>, Makoto Hosoya<sup>2</sup>, Sang-Jun Jeon<sup>1</sup>, Hideyuki Okano<sup>3</sup>, Albert Edge<sup>1</sup>

<sup>1</sup>Eaton-Peabody Laboratory, MEE/Harvard Medical School, <sup>2</sup>School of Medicine, Keio University, <sup>3</sup>Department of Physiology, School of Medicine, Keio University

Math1 is an essential bHLH transcription factor facilitating inner ear sensory epithelium formation. Exogenous transduction of Math1 induces replacement of auditory hair cells even in damaged adult mammalian cochlea. Blockage of Notch/RBP-J signaling by  $\gamma$ -secretase inhibition is an alternative way to induce hair cells *In Vitro*, but studies in other organs have shown that the efficacy of  $\gamma$ -secretase inhibitors is largely dependent on the type of cell and compound used. Since inner ear derived spheres show an increase in hair cell differentiation after  $\gamma$ -secretase inhibitor treatment (Jeon et al abstract, ARO), and the effect occurs through upregulation of Math1, we have developed a method that takes advantage of Math1 upregulation in inner ear-derived spheres to select  $\gamma$ -secretase inhibitors for naïve inner ear cells.

Utricle spheres derived from Math1-nGFP transgenic mice (4th to 6th generation) were used in the assay. After

dissociating spheres, cells were plated onto fibronectin-coated dish in DMEM/F12/B27/N2 overnight. Four candidate  $\gamma$ -secretase inhibitors, DAPT, L-685458, LY411575 and MDL28170 (also a calpain inhibitor), were added to the medium at various concentrations. Five days after incubation, cells were stained with DAPI, and the ratio of nGFP/DAPI positive cells was counted on a microscope using an automated system.

Among the four compounds, MDL28170 and LY411575 had the most profound effect. the dose-response curve suggested that LY411575 was effective at the lowest concentration used (0.1 nM). This is a reliable method for exploring new compounds and allows us to evaluate the effective concentration and the magnitude of the increase and to analyze the results quantitatively. the procedure is straightforward and inter-assay variability is low. in addition, the data suggest that LY411575 has the potential to be used for the treatment of hearing loss by differentiation of inner ear cells into hair cells. Supported by NIDCD grants DC007174 and DC05209.

### **117 Notch Signaling Regulates the Extent of Hair Cell Regeneration in the Zebrafish Lateral Line**

**Eva Ma<sup>1</sup>**, Edwin Rubel<sup>2</sup>, David Raible<sup>3</sup>

<sup>1</sup>*Dept of Biological Structure & MCB Program, University of Washington, Seattle, WA*, <sup>2</sup>*Dept of Oto/HNS & VM Bloedel Hearing Research Center, University of Washington*, <sup>3</sup>*Dept of Biological Structure & VM Bloedel Hearing Research Center, University of Washington*

Mechanosensory hair cells within the zebrafish lateral line spontaneously regenerate after aminoglycoside-induced death. Exposure of 5-day-old larvae to 400  $\mu$ M neomycin for one hour kills almost all mature hair cells within the lateral line neuromasts. Regeneration is rapid, with new hair cells observed by 24 hours after neomycin exposure, and near complete renewal by 72 hours. We previously showed that replacement hair cells primarily arise from proliferating cells, with a transient increase in support cell proliferation occurring between 12 and 21 hours after neomycin damage. We found that expression of Notch signaling pathway members *notch3*, *deltaA*, and *atoh1a* are all upregulated during the time of maximum support cell proliferation. Blocking Notch signaling during regeneration increased the proliferation of support cells, ultimately resulting in an excess of hair cells in each neuromast. Further analysis of the proliferating cells has now revealed two distinct support cell subpopulations that differ in neuromast position, morphology, and temporal pattern of proliferation in response to neomycin exposure. These internal and peripheral support cells also differentially respond to alterations in Notch signaling, suggesting that they are functionally distinct. Proliferation of internal support cells was increased and prolonged with Notch inhibition, while peripheral support cell proliferation decreased. We hypothesize that the internal support cells located centrally within the neuromasts are the proliferative hair cell progenitors, while peripheral support cells may have a separate function.

### **118 Evidence for the Involvement of Planar Cell Polarity (PCP) Signaling During Hair Cell Regeneration in the Avian Ear**

**Mark Warchol<sup>1</sup>**, Mireille Montcouquiol<sup>2</sup>

<sup>1</sup>*Washington University School of Medicine*, <sup>2</sup>*University of Bordeaux*

The otolithic maculae contain two oppositely-oriented populations of hair cells, which are separated by the striolar reversal zone. the orientation of stereocilia is established during embryonic development and involves signaling molecules of the planar cell polarity (PCP) pathway. Hair cells in the maculae of birds can regenerate after ototoxic injury, and *In Vivo* studies have shown that regenerated hair cells are correctly oriented (Dye et al., *Hearing Res* 133: 17, 1999). These findings suggest that PCP information is persevered in the adult maculae and can orient stereocilia during the regenerative process. the present study examined hair cell orientation following regeneration in organ cultures of the chick utricle. Hair cells in cultured utricles were killed by treatment with 1 mM streptomycin. Specimens were then cultured for an additional 7 days, allowing hair cell numbers to recover to about 30% of original levels. Examination of stereocilia revealed that regenerated hair cells were correctly oriented with respect to the reversal zone. We then used a polyclonal antibody raised against Vangl2 to localize this key PCP signaling molecule after hair cell injury and during regeneration. in undamaged specimens, Vangl2 immunoreactivity was confined to cell-cell junctions that were oriented approximately parallel to the reversal zone (e.g., along the anterior-posterior axis). After ototoxic injury, immunoreactivity for Vangl2 was observed at the junctions of remaining supporting cells. Notably, the orientation of Vangl2 expression was unchanged, suggesting that supporting cells retain proper polarity after hair cell loss. the PCP signaling pathway also involves activation of the Jun kinase (JNK). Treatment with the JNK inhibitor SP600125 severely disrupted the orientation of regenerated hair cells but did not affect the patterns of Vangl2 expression. This finding suggests the JNK signaling lies downstream of interactions between PCP molecules.

### **119 Canonical Wnt Signaling Promotes Glutamatergic Specification From Murine Embryonic Stem Cells After Neural Induction**

**Daniel J. Fisher<sup>1</sup>**, Takako Kondo<sup>1</sup>, Angela B. Thompson<sup>1</sup>, Eri Hashino<sup>1</sup>

<sup>1</sup>*Indiana University School of Medicine*

Our recent study demonstrated that canonical Wnt signaling promotes neural differentiation and neuronal subtype specification from bone marrow-derived adult pluripotent stem cells. to test whether Wnt signaling exerts similar effects on embryonic stem (ES) cells and whether the effects are subject to various developmental contexts, we evaluated changes in gene expression in response to the canonical Wnt ligand Wnt1. Mouse ES cells were either maintained as undifferentiated or subjected to a 2-step neural induction protocol, by which cells were directed to form embryoid bodies (EBs) and subsequently exposed

to neural induction medium. Undifferentiated ES cells, those forming EBs and those at neural induction (NI) day 1 (NI-1d) were incubated in the presence or absence of recombinant human recombinant Wnt1 (100-200 ng/mL) for 3 days (ESC, EB, NI-3d) or 7 days (NI-7d). the progression of ES cell differentiation was monitored with ES cell markers (Oct4, Rex1, BMP4 and Sox2) as well as neural markers (Musashi1, HuC, SCG10, TUJ1, NSE and Synaptophysin). We found no significant difference in gene expression except Sox9, a known target gene for canonical Wnt signaling, between Wnt1-treated and untreated ES cells when they are undifferentiated. However, the expression levels of several proneural genes (Ngn1 and NeuroD) as well as AMPA receptor genes (GluR2 and GluR4) in Wnt1-treated ES cells were significantly higher than untreated cells at NI-7d. the coordinated activation of proneural and neural subtype-specific genes after neural induction is consistent with the results obtained from adult stem cells. in addition, the results indicate that Wnt1 exerts context-dependent effects on ES cells despite the presence of all Wnt receptors and effectors regardless of their differentiation status, and suggest the existence of a novel selector gene downstream of the Wnt signaling pathway.

## **120 Canonical Wnt Signaling Promotes Neuronal Differentiation From Somatic Stem Cells Through Activation of Tlx3**

**Takako Kondo<sup>1</sup>**, Eri Hashino<sup>1</sup>

<sup>1</sup>*Indiana University School of Medicine*

We previously showed that the canonical Wnt ligands, Wnt1 and Wnt3a, up-regulate expression of an array of proneural and glutamatergic genes in mouse bone marrow stromal cells (MSCs) in a dose-dependent manner. Since multiple genes were coordinately up-regulated by the Wnt ligands, we speculated that a master selector gene may be involved in Wnt-mediated up-regulation of these neuronal subtype-specific genes. We hypothesized that the T-cell leukemia 3 (Tlx3) gene might be the identity of the selector gene, based on its ability to up-regulate the same combination of glutamatergic marker genes in mouse embryonic stem cells. to test our hypothesis, we first examined whether Wnt1 can up-regulate Tlx3 expression in MSCs. Incubation of MSCs with recombinant human Wnt1 protein for 7 days after neural induction increased the Tlx3 mRNA level and the effects of Wnt1 were dose-dependent. to test whether Tlx3 is sufficient to promote gene expression, MSCs were transfected with pBud-eGFP-Tlx3 or pBud-eGFP control vector using an Amaxa nucleofection kit. MSCs stably expressing Tlx3 were grown in the presence or absence of neural induction medium. the expression levels of Ngn1, NeuroD and Brn3a in Tlx3-expressing MSCs grown in neural induction medium for 4 days were significantly higher than those in MSCs expressing the control vector. At 7days after neural induction, while expression of the proneural genes was down-regulated, VGLUT2 and GluR4 in Tlx3-expressing MSCs significantly increased. in addition, a pan-sodium channel protein was induced in MSCs expressing Tlx3, but not in those devoid of Tlx3. Together, these results identify Tlx3 as a glutamatergic selector gene and a novel

target for the canonical Wnt signaling that promotes neuronal differentiation from bone marrow-derived somatic stem cells.

Supported by NIH R01DC007390

## **121 Antiproliferative Effects of Histone Deacetylase Inhibitors On Avian Utricular Sensory Epithelium *In Vitro***

**Eric Slattery<sup>1</sup>**, Judy Speck<sup>1</sup>, Mark Warchol<sup>1</sup>

<sup>1</sup>*Dept. of Otolaryngology, Washington University, St. Louis, MO, USA*

The inner ear sensory epithelium of non-mammalian vertebrates regenerates after acoustic or ototoxic damage. Gene transcription changes markedly during the regenerative period in chicks (Hawkins et al., 2007) with similar transcriptional trends noted in the developing mammalian inner ear (Sajan et al., 2007). One form of transcriptional regulation comes from histone acetylation, which allows for increased RNA transcription. Enzymes known as histone deacetylases (HDACs) remove histone acetylation acting to decrease transcription. the activity of HDACs is decreased by a variety of compounds known as HDAC inhibitors result in increased histone acetylation, and are shown to effect proliferation and differentiation of many tissues. We examined the effects of the HDAC inhibitors valproic acid, sodium butyrate and trichostatin a on the proliferative ability of the chick utricle sensory epithelium. Dissociated utricular sensory epithelial cells were cultured and exposed to HDAC inhibitors for 24 and 48 hours. Proliferation was quantified by BrdU uptake of S-phase cells and visualized with immunolabeling. All inhibitors demonstrated a marked antiproliferative effect both after 24 and 48 hour exposure that is dose dependent. a similar strong antiproliferative effect by these inhibitors is shown with cultured whole chick utricles treated with HDAC inhibitor following *In Vitro* streptomycin exposure, and then similarly quantified with BrdU uptake. These immunohistologic data show HDAC inhibitors produce an antiproliferative effect on avian inner ear sensory epithelium.

## **122 RNA Interference for P27 Induces Cell Cycle Reentry of Postmitotic Cochlear Supporting Cells**

**Kazuya Ono<sup>1</sup>**, Ken Kojima<sup>1</sup>, Takayuki Nakagawa<sup>1</sup>, Masahiro Matsumoto<sup>1</sup>, Takeshi Kawauchi<sup>2</sup>, Juichi Ito<sup>1</sup>

<sup>1</sup>*Department of Otolaryngology Head and Neck Surgery, Graduate School of Medicine, Kyoto University,*

<sup>2</sup>*Department of Anatomy, Keio University School of Medicine, Tokyo, Japan*

Cell proliferation of supporting cells in mammalian auditory epithelia rarely occurs after birth, which is associated with limited capability of mammalian auditory epithelia for regeneration. Previous studies have demonstrated that p27, a cyclin-dependent kinase inhibitor, plays a crucial role for the maintenance for post-mitotic status of supporting cells in mammalian auditory epithelia. in the present study, we examined the potential of RNA interference (RNAi) of p27 for cell cycle reentry of post-

mitotic supporting cells using organotypic culture of auditory epithelia obtained from postnatal day 3 mice. Short hairpin RNA-expressing vectors targeting p27 coding sequence (sh-p27) was efficiently introduced into supporting cells by electroporation, resulting in deletion of p27 in supporting cells. In contrast, supporting cells introduced short hairpin RNA-expressing scrambled control sequence (sh-scr) exhibited the expression of p27. BrdU-labeling assay demonstrated that cell cycle reentry of supporting cells that had been introduced sh-p27, not sh-scr. These findings indicate that RNAi for p27 has the potential for inducing cell cycle reentry of post-mitotic supporting cells in mammalian auditory epithelia.

## **123 Evaluation of Formulation of Sirna Targeting P27kip1 in the Guinea Pig Cochlea**

**Rende Gu<sup>1</sup>**, Eric Lynch<sup>1</sup>, Huy Tran<sup>1</sup>, James LaGasse<sup>1</sup>, Jonathan Kil<sup>1</sup>

<sup>1</sup>Sound Pharmaceuticals, Inc.

Sensorineural hearing loss affects tens of millions of people in the U.S. the irreversible loss of sensory cells (supporting cells and hair cells) in the organ of Corti is the major cause of many hearing deficits. We are attempting to develop the first therapeutic that can stimulate the regeneration of auditory supporting cells and hair cells as a means to restore auditory function in the deaf and hard of hearing. Previously, we developed and evaluated antisense oligonucleotides (AONs) in cell culture, organ of Corti culture, and *In Vivo* in deafened mammals. Reduction of p27 protein levels by p27 AONs induces supporting cell proliferation and hair cell regeneration both *In Vitro* and in vivo. We have now developed short inhibitory RNAs (siRNAs) that bind and degrade p27 mRNA resulting in a decrease of p27 protein and an increase in cellular proliferation. Current development efforts are determining whether the use of p27 siRNAs represents an improvement over p27 AONs at stimulating proliferative regeneration and a recovery of function in the deafened cochlea of mammals. RNA interference as a means to inhibit gene expression has gained rapid acceptance in large part due to the high potency and limited side effect profile of properly designed and tested sequences. In addition, the ability to knock down gene expression for almost any gene makes RNAi an attractive therapeutic modality. However, as with the previous generations of nucleic acid based molecules antagonists (Antisense Oligonucleotides and Ribozymes), delivery remains a significant concern. Over the past year, SPI has evaluated several drug delivery moieties that when formulated with siRNA molecules, increase their cellular uptake and enhances the RNAi response leading to an increased numbers of proliferating cells in the cochlea and improvements in auditory thresholds when compared to random sense controls.

## **124 Manipulating Cell Cycle Regulation in the Mature Cochlea**

**Ryosei Minoda<sup>1</sup>**, Masahiko Izumikawa<sup>2</sup>, Kohei Kawamoto<sup>2</sup>, Hui Zhang<sup>3</sup>, Yehoash Raphael<sup>4</sup>

<sup>1</sup>Department of Otolaryngology Head and Neck Surgery, Kumamoto University School of Medicine, <sup>2</sup>Department of Otolaryngology Head and Neck Surgery, Kansai Medical University, <sup>3</sup>Department of Genetics, Yale University School of Medicine, <sup>4</sup>Kresge Hearing Research Institute, the University of Michigan

Sensorineural hearing loss, which is often caused by degeneration of hair cells in the auditory epithelium, is permanent because lost hair cells are not replaced. Several conceptual approaches can be used to place new hair cells in the auditory epithelium. One possibility is to enhance proliferation of non-sensory cells that remain in the deaf ear and induce transdifferentiation of some of these cells into the hair cell phenotype. Several genes, including *p27<sup>Kip1</sup>* have been shown to regulate proliferation and differentiation in the developing auditory epithelium. the role of *p27<sup>Kip1</sup>* in the mature ear is not well characterized. We now show that *p27<sup>Kip1</sup>* is present in the nuclei of nonsensory cells of the mature auditory epithelium, not only in the organ of Corti, but also in surrounding regions. Another molecule, Skp2, is an F-box protein that blocks the inhibitory effects of *p27<sup>Kip1</sup>* by ubiquitination, thereby inducing cell division. We analyzed regions adjacent to the organ of Corti in normal (non-deafened) guinea pigs for the effects of forced expression of Skp2. *SKP2* was over-expressed using a recombinant adenovirus vector, Ad.*SKP2*. Assay for presence of new cells using BrdU revealed presence of new cells, but generation of new ectopic hair cells was not found. Forced expression of *Atoh1* (Ad.*Atoh1*, GenVec) has been shown to induce transdifferentiation of supporting cells to hair cells. When both Skp2 and Atoh1 were over-expressed, ectopic hair cells were found in the auditory epithelium in greater numbers than with Atoh1 alone. These findings suggest that the *p27<sup>Kip1</sup>* protein remains in the mature auditory epithelium and therefore *p27<sup>Kip1</sup>* can serve as a target for gene manipulation. the data also suggest that, at least in ectopic locations, induced proliferation, by itself, does not generate new hair cells in the mature cochlea.

Supported by the Williams Professorship, a gift from Berte and Alan Hirschfield, and by NIH/NIDCD Grants DC-01634, DC-05401, DC-03685 and DC05188.

## **125 Localization of Actria and Actriib Receptors in Mature Vertebrate Vestibular and Auditory Sensory Epithelia**

**Jennifer McCullar<sup>1</sup>**, Sidya Ty<sup>1</sup>, Jialin Shang<sup>1</sup>, Elizabeth Oesterle<sup>1</sup>

<sup>1</sup>Dept of Oto-HNS and Virginia Merrill Bloedel Hearing Research Center, University of Washington

The transforming growth factor-beta (TGFβ) signaling pathway regulates cellular proliferation, differentiation, and/or apoptosis through an array of serine/threonine kinase receptor complexes. the type II activin receptors, ActRIIA and ActRIIB, are members of the TGFβ superfamily that have been shown to be involved in



zebrafish fin regeneration, as well as mammalian tooth regeneration and scar formation. the role(s) these receptors play in the regeneration of hair cells in mature inner ear sensory epithelia (SE) is unknown. Using immunocytochemistry (ICC), cryosections of normal posthatch chicken basilar papilla show ActRIIA, but not ActRIIB, expression in auditory sensory epithelium. ICC of the adult mouse ear shows ActRIIA and ActRIIB receptor expression in hair cells and supporting cells of the vestibular and auditory SE. Ligand binding and activation of the receptor complex leads to phosphorylation of specific intracellular mediators known as Smad proteins. to support a role for ActRIIA and ActRIIB signaling in mature inner ear SE, we analyzed for the presence of the Smad proteins through which these receptors are known to signal, specifically, Smad2/3, phosphorylated Smad2 (pSmad2), and phosphorylated Smad1/5/8 (pSmad1/5/8). Smad2/3 localizes to membranes of hair cells in chicken and mouse inner ear SE. pSmad1/5/8 is expressed in nuclei of supporting cells and hair cells in chicken and mouse auditory SE and mouse vestibular SE. These data support ActRIIA and ActRIIB signaling in normal mature inner SE. Putative involvement of activin receptor signaling on cellular proliferation is being further examined in organotypic cultures of posthatch chicken auditory epithelium. Supported by: NIDCD R01 DC03944, NIDCD P30 DC04661, NICHD P30 HD002274, NIDCD DC005361

## **126 Auditory Hair Cell Regeneration in the Zebrafish (*Danio rerio*)**

**Julie Schuck**<sup>1</sup>, Michael Smith<sup>1</sup>

<sup>1</sup>*Department of Biology and Biotechnology Center, Western Kentucky University, Bowling Green, KY 42101*

Fishes are capable of regenerating sensory hair cells in the inner ear after exposure to excessive noise. However, a time course of auditory hair cell regeneration has not been established for zebrafish. Adult zebrafish were exposed to a 100 Hz pure tone at 179 dB re 1  $\mu$ Pa RMS for 36 hours, and then allowed to recover for 0 to 14 days before morphological analysis. Hair cell loss and recovery were determined using phalloidin and DAPI labeling to visualize hair cell bundles and nuclei. Cell proliferation was quantified through BrdU labeling. Immediately following noise exposure, zebrafish saccules exhibited significant hair cell loss in the caudal region. Hair cell counts increased over the course of the experiment, reaching pre-treatment levels at 14 days post-noise exposure. Cell proliferation peaked two days post-noise exposure in the caudal region, and to a lesser extent in the rostral region. Low levels of proliferation were observed in untreated controls, indicating that cells of the zebrafish saccule are mitotically active in the absence of a damaging event. This study establishes a time course of hair cell regeneration in the zebrafish inner ear and demonstrates that cell proliferation is associated with the regenerative process.

## **127 Transcriptional Profiling of Genes Involved in Inner Ear Hair Cell Regeneration in the Adult Zebrafish (*Danio Rerio*)**

**Jin Liang**<sup>1</sup>, Gabriel Renaud<sup>2</sup>, Tyra Wolfsberg<sup>2</sup>, Shawn Burgess<sup>2</sup>

<sup>1</sup>*University of Maryland at College Park*, <sup>2</sup>*National Human Genome Research Institute, NIH*

Sensory hair cells of the inner ear are the mechanotransductive units in the neuroepithelia. in mammals, lost hair cells are not replaced, resulting in various permanent deficiencies in vestibuloauditory sensation. in contrast, zebrafish can replace lost hair cells with new ones throughout adulthood. Our ultimate goal is to understand the molecular mechanism of the inner ear hair cell regeneration in adult vertebrates. As an initial step, we defined the genetic programs used for hair cell regeneration in zebrafish using emerging techniques for gene expression profiling.

We modified a previous noise-exposure protocol, which enabled us to induce constant hair cell loss in the saccular epithelium of the adult zebrafish and characterize the subsequent regeneration process. We determined the inner-ear gene expression profiles at different time points during the regeneration, focusing particularly on those genes with significant increase in expression at the various time points. Here we used a new technique, Sequencing-Based Transcription Profiling (SBTP), to generate the gene expression profiles in an in-depth and high-throughput manner. Similar to SAGE in nature, the technique generates 3 million or more gene "signatures" from the mRNA pool, giving us a very deep view of gene expression at each time point. We have developed and/or utilized various bioinformatic tools for gene assignment, ontological analysis, and pathway analysis. Our preliminary analysis of the SBTP data already yielded results in agreement with our previous profile comparisons using oligomicroarray.

We are now working on refining our data-mining strategy to identify the candidate genes critical for hair cell regeneration in zebrafish. the candidate genes will be further verified with other techniques (e.g. qRT-PCR, *In Situ* hybridization, immunostaining, etc.) to give us the final list. We will also try to explore the interrelationship among the candidate genes, which will give us clues about the intercellular and intracellular pathways involved in the regeneration process.

## **128 Genes Regulated by COUP-TFI**

**Celina Montemayor**<sup>1</sup>, Fernanda R. Ruiz<sup>1</sup>, Haiying Liu<sup>1</sup>, Fred A. Pereira<sup>1</sup>

<sup>1</sup>*Baylor College of Medicine*

Chicken Ovalbumin Upstream Promoter Transcription Factors (COUP-TFs) are orphan members of the nuclear receptor superfamily. Although their ligand and precise function are unknown, the presence of COUP-TF homologues across species and their stunning interspecies similarity indicate that these nuclear receptors play an essential role that has been conserved during evolution. There are two members of this family in mice: COUP-TFI and COUP-TFII, and although they have

overlapping expression patterns, knockout studies have revealed that each has a vital, specific developmental function. of particular interest to our lab, COUP-TFI<sup>-/-</sup> mice exhibit altered inner ear hair cell numbers, having up to 8 rows of outer hair cells (Tang et al. Development 133: 3683-3693, 2006). to better understand the function of this orphan receptor in hair cell differentiation, we have begun to identify *In Vivo* targets of COUP-TFI and its role in the development of mouse inner ear. We have performed microarray gene expression profiles of wild type and COUP-TFI<sup>-/-</sup> inner ear tissue. Real-time RT-PCR analysis of significant gene expression changes confirmed 70% of our top hits, and gene ontology analysis revealed a significant overrepresentation of cell cycle, cell adhesion, myeloid cell differentiation, and lipid metabolism-related genes. We have also performed an independent identification of COUP-TFI target genes using a bioinformatic tool, a Hidden Markov Model (HMM), to search all mammalian genomes for COUP-TFI binding sites. the results were compared to a database of all the published COUP-TFI targets, their binding site sequences, and their global genomic coordinates. Using these tools we have identified candidate COUP-TF binding sites within numerous promoters, including genes implicated in regulation and maintenance of hearing and balance functions. We continue to characterize the direct regulation of these putative COUP-TFI target genes using transient transfections in cultured cells to verify COUP-TFI activation or repression of a luciferase reporter driven by target promoters. This analysis will lead to a better understanding of COUP-TFI in regulation of hair cell development and differentiation.

This work was previously supported by a DC04585 grant to FAP.

## **[129] Differentiation of a Novel Stem Cell for Auditory Neuron Regeneration**

**Ragad El Seady<sup>1</sup>**, Margriet Huisman<sup>1</sup>, Johan Frijns<sup>1</sup>

<sup>1</sup>*Leiden University Medical Center*

**Objectives:** a cochlear implant (CI) benefits many patients, however, speech understanding in noisy situations remains difficult. It is suggested that stem cell-based therapy, by increasing the number of auditory neurons (ANs), will improve the performance of a CI.

Recently, a new type of stem cell has been identified, the epidermal neural crest stem cell (EPINCSC), derived from the bulge of hair follicles from adult mammalian dermis. EPINCSCs are potential candidates for AN regeneration, because they have a similar origin as inner ear cells, their functionality has been proven and autologous transplantation is possible. the aim of this research is to develop a culture technique for the isolation, proliferation and differentiation of this stem cell from mice, guinea pigs and humans. the ultimate goal is EPINCSC cell-based therapy for AN regeneration in different mammals.

**Materials and Methods:** Whiskers of mice, guinea pigs and human leg hair follicles were cultured in a proliferation medium. Subsequently, EPINCSCs were differentiated by supplying neurotrophic support. Quantitative immunohistochemistry was performed to demonstrate the

presence of neural stem cells (nestin), neurons (TUJ1), oligodendrocytes (OSP) and Schwann cells (Krox20).

**Results:** After proliferation, the majority of the cells (90%) were positive for the marker nestin. the average yield per follicle was  $2 \times 10^5$ , while for transplantation purposes  $2-5 \times 10^5$  cells are required. About 70% of the differentiated cells were positive for the neural marker TUJ1. Furthermore, we were able to differentiate EPINCSC into oligodendrocytes and Schwann cells.

**Discussion:** with our culture technique we can obtain sufficient neural stem cells from mice, guinea pig whiskers and human hair follicles for transplantation purposes. Additionally, we could differentiate these stem cells into neurons and glial cells.

## **[130] Cell Therapy for Functional Regeneration of Spiral Ganglion Neurons**

**Takayuki Nakagawa<sup>1</sup>**, Shinpei Kada<sup>1</sup>, Hideaki Ogita<sup>1</sup>, Takatoshi Inaoka<sup>1</sup>, Kyu Yup Lee<sup>2</sup>, Harukazu Hiraumi<sup>1</sup>, Tatsunori Sakamoto<sup>1</sup>, Kazuya Ono<sup>1</sup>, Masahiro Matsumoto<sup>1</sup>, Ryusuke Hori<sup>1</sup>, Rie Horie<sup>1</sup>, Yayoi Kikkawa<sup>1</sup>, Yasuko Fujimoto<sup>3</sup>, Juichi Ito<sup>1</sup>

<sup>1</sup>*Kyoto University*, <sup>2</sup>*Kyungpook National University Hospital*, <sup>3</sup>*Otsu Red Cross Hospital*

Previous studies have indicated the potential of cell therapy for regeneration of spiral ganglion neurons. However, the efficacy of cell transplantation for the functionality of cochleae has not fully been elucidated. the aim of this study was to investigate auditory function in damaged cochleae following cell transplantation. Mouse or monkey ES cells were chosen as a source of transplants. We used the stromal cell-inducing activity established by Kawasaki et al. as a method for neural induction of ES cells. Mouse or monkey ES cell-derived neural progenitor cells were transplanted into cochleae of guinea pigs or macaques, which had been damaged by local ouabain or cisplatin application prior to transplantation. Cell suspensions were injected into the basal portion of cochlear modioli after cochleostomy. in control animals, the culture medium was injected instead of cell suspensions. We measured electrically evoked auditory brain stem responses (eABRs) at various time points following cell transplantation. in guinea pigs, damaged cochleae exhibited significant recovery of eABR thresholds over time following transplantation of mouse ES cell-derived neural progenitors. Differences in eABR thresholds between transplanted and control cochleae were significant. in macaques, cochleae transplanted monkey ES cell-derived neural progenitors exhibited time-dependent recovery of eABR thresholds. an over-all effect of cell transplantation on eABR thresholds was statistically significant. These findings indicate that transplantation of ES cell-derived neurons contributes to functional recovery of damaged cochleae. Future studies must be done to reveal mechanisms underlying functional recovery by cell transplantation.

### **131 Effects of Erythropoietin On Neurite Outgrowth and Survival of Cultured Spiral Ganglion Cells**

**Athanasia Warnecke<sup>1</sup>**, Nurdanat Berkingali<sup>1</sup>, Gerrit Paasche<sup>1</sup>, Thomas Lenarz<sup>1</sup>, Timo Stoeber<sup>1</sup>

<sup>1</sup>Hannover Medical School

Hearing impairment is known to be related to the loss of inner and outer hair cells, followed by degeneration of spiral ganglion cells (SGC). Neuroprotective effects of erythropoietin (EPO) on retinal ganglion cells have been demonstrated recently. Furthermore, the expression of EPO and its receptor has been identified in the guinea pig inner ear. However, its effect on SGC has not been determined. Therefore, we investigated the effects of different concentrations of EPO also in combination with brain-derived neurotrophic factor (BDNF) on spiral ganglion cells *In Vitro* and compared it to the known effect of BDNF.

Freshly isolated SGC from rat pups (P3-5) were cultivated in serum-free medium for 48 and 72 hours. BDNF (50 ng/ml) and/or EPO in concentration from 2.5 to 50 ng/ml were added to the cells. Numbers of surviving cells, diameter of the somata and lengths of the neurites were evaluated and compared between groups.

Treatment with EPO alone had no effect on the number of surviving cells but the surviving cells exhibited a similar neurite growth as BDNF treated cells. In a combined treatment of both factors, the lower concentrations of EPO enhanced the BDNF-induced outgrowth. On average, neurite length doubled when increasing the cultivation period from 48 to 72 hours. Also the number of surviving cells increased indicating, that after 48 hours not all viable cells had formed neurites and were counted.

It can be concluded that EPO induces neurite outgrowth rather than promoting survival. Thus, EPO represents an interesting candidate to enhance and modulate the regenerative effect of BDNF on SGC.

### **132 De-Afferentation Associated Changes in Afferent and Efferent Processes in the Guinea Pig Cochlea with Chronic Intrascalar Brain-Derived Neurotrophic Factor and Acidic Fibroblast Growth Factor Versus Glia Cell-Derived Neurotrophic Factor**

**Rudolf Glueckert<sup>1</sup>**, Josef Miller<sup>2</sup>, Richard Altschuler<sup>2</sup>, Diane Prieskorn<sup>2</sup>, Anneliese Schrott-Fischer<sup>3</sup>

<sup>1</sup>Medical University Innsbruck, <sup>2</sup>University of Michigan, Kresge Hearing Research Institute, <sup>3</sup>Medical University Innsbruck, Department of Otolaryngology

De-afferentation of the auditory nerve from loss of sensory cells is associated with degeneration of nerve fibers and spiral ganglion neurons (SGNs). SGN survival following de-afferentation can be enhanced by application of neurotrophic factors (NTFs); and NTF can induce the regrowth of SGN peripheral processes. Cochlear prostheses could provide targets for regrowth of afferent peripheral processes enhancing neural integration of the implant, decreasing stimulation thresholds and increasing specificity of stimulation. The present study analyzed

distribution of afferent and efferent nerve fibers following deafness in guinea pigs using specific markers (parvalbumin for afferents, synaptophysin for efferent fibers) and the effect of Brain Derived Neurotrophic Factor (BDNF) in combination with Acidic Fibroblast Growth Factor (aFGF) versus Glia Cell-Derived Neurotrophic Factor (GDNF). Histology of the cochlea allowed quantitative analysis of neuron and axonal changes. Chronic BDNF/aFGF resulted in a significantly increased number of afferent peripheral processes. Outgrowth of afferent nerve fibers into the scala tympani were observed and SGN densities were found to be higher than in normal hearing animals. BDNF/aFGF treatment provided no enhanced maintenance of efferent fibers, although some synaptophysin positive fibers were detected at atypical sites suggesting some sprouting of efferent fibers.

GDNF on the other hand didn't show any significant effect on the peripheral processes of the afferent system nor any increase in number and size of spiral ganglion neurons.

Acknowledgements: Support for this study was provided by the European Community Project QL3-CT-2002-01463, NIH grants (NIH-NIDCD R01 DC003820 and P30 DC005188), Austrian Science Foundation FWF project P15948-B05, the General Motors Corporation, and the Ruth and Lynn Townsend Professor of Communication Disorders. AMGEN Corporation generously provided the BDNF.

### **133 Single Molecule Fluorescence Detection of Prestin Oligomerization**

**Ramsey Kamar<sup>1</sup>**, Laurent Cognet<sup>2</sup>, Robert Raphael<sup>1</sup>

<sup>1</sup>Rice University, <sup>2</sup>Centre National de la Recherche Scientifique

Prestin is the putative motor protein that drives outer hair cell electromotility. Several groups have shown evidence of prestin-prestin interactions and prestin oligomerization using biochemical techniques and optical imaging. However, it is unknown what role prestin-prestin interactions or oligomerization play in electromotility or what molecular motifs mediate these interactions. Ensemble optical measurements of prestin self-association cannot provide the molecular level details of prestin-prestin interactions, nor can they measure the oligomeric states they produce. We have thus developed our ability to detect individual prestin-YFP molecules using single molecule fluorescence (SMF) microscopy. We have applied SMF microscopy to measure the distribution of intensities emitted by individual prestin clusters in the HEK cell membrane. The distribution displays peaks spaced at multiples of the unitary intensity which one would expect for a distribution of non-interacting fluorescent emitters. We have resolved the stoichiometries up to tetramers; however it is clear that higher populations also exist. We will explore the effect of membrane cholesterol depletion on the oligomerization of prestin using SMF microscopy to assess whether this treatment dissociates prestin oligomers or simply removes a bulk population of intact oligomers from microdomains. Our development of SMF microscopy for the study of prestin creates the opportunity to investigate previously unexplored aspects of prestin

structure that could not be studied using bulk optical methods.

### **134 FRET as a Method to Demonstrate Prestin Function**

Alexei Surguchev<sup>1</sup>, Joseph Santos-Sacchi<sup>1</sup>, Dhasakumar Navaratnam<sup>1</sup>

<sup>1</sup>*Yale University*

Prestin is a member of the SLC26 family of anion transporters that is responsible for electromotility in outer hair cells. We and others have used FRET using the fluorophores CFP and YFP tagged to the C terminus of separate molecules of prestin that suggests the existence of intermolecular interactions and possible homomultimers of the protein. Here we show FRET data where we tagged a single molecule of prestin at its N and C termini with CFP and YFP respectively. This construct demonstrated more robust FRET than our prior experimental constructs with C terminally tagged prestin. These data suggest that intramolecular interactions between prestin N and C termini or intermolecular interactions between the N terminus of one molecule and the C terminus of another molecule are more robust than the interactions between the C termini of two separate molecules. Furthermore, using this construct we were able to demonstrate a change in FRET co-incident with depolarization induced by the addition of 40mM KCl indicating that a change in conformation of the protein from the relaxed to contracted state is accompanied by a change in the interactions of the intracellular termini of the protein. Moreover, these data indicate a novel method to monitor changes in the proteins conformation independent of measuring non-linear capacitance.

Supported by NIH grants R01 DC 007894 (DSN)  
R01 DC 008130 (JSS)

### **135 Cytoskeleton Mediates Outer Hair Cell Electromotility and Memory Function**

Ning Yu<sup>1</sup>, Hong-Bo Zhao<sup>1</sup>

<sup>1</sup>*Dept. of Surgery-Otolaryngology, University of Kentucky Medical Center, Lexington, KY 40536*

Outer hair cell (OHC) electromotility resides in OHC lateral wall, which is composed of three layers, i.e., plasma membrane (PM), cytoskeletal cortical lattice (CL), and subsurface cisternae. Prestin proteins embed in the PM responsible for OHC electromotility. Here, we report that cytoskeleton in the CL plays an important role in modification on OHC electromotility. the CL is composed of longitudinally oriented spectrins and circumferentially F-actin filaments, which further adhere the PM by a pillar structure. Latrunculin A (LAT-A) is an inhibitor of F-actin polymerization. After intracellular application of LAT-A, OHC electromotility associated nonlinear capacitance remained but the ATP-induced shift on the peak voltage of nonlinear capacitance (V<sub>pk</sub>) was eliminated. the prepulse effect on OHC electromotility, the OHC memory function, also reduced. However, the effect of turgor pressure on OHC electromotility remained; increase in the turgor pressure could still shift the V<sub>pk</sub> of nonlinear capacitance to the depolarizing direction, indicating that the tension

sensitivity of prestin motor protein was not influenced. We also used diamide to destroy the spectrin. After intra- or extracellular application of 5 mM diamide, V<sub>pk</sub>-depolarizing shift induced by ATP was eliminated but the effect of pressure remained. the data indicate that the unique cytoskeletal CL layer in the OHC lateral wall is important for the modification of OHC electromotility.

Supported by NIHDCDC DC05989 to HBZ. NY is partially supported by Chinese Nature & Science Foundation 30600700

### **136 Recruitment of a $\alpha$ II/ $\beta$ Heavy Spectrin Complex in the Cortical Lattice that Sustain Somatic Cochlear Amplification in the Auditory Outer Hair Cells**

Kirian Legendre<sup>1</sup>, Saaid Safieddine<sup>1</sup>, Christine Petit<sup>1</sup>, Aziz El-Amraoui<sup>1</sup>

<sup>1</sup>*INSERM UMRS587, Unité de Génétique des Déficiences Sensoriels, Institut Pasteur, Paris, France*

The sensitivity and frequency selectivity of the mammalian cochlea relies on a mechanical amplification process that involves voltage-dependent contraction-elongation cycles of the outer hair cells' lateral wall, mediated by prestin. So far, very little is known regarding the molecular components of the cortical lattice and how it is coupled to the plasma membrane. Here, we report on a  $\beta$  heavy spectrin subunit,  $\beta$ H that we identified as a binding partner of the myosin VIIa tail in the human and mouse retina. Unlike myosin VIIa,  $\alpha$ II- or  $\beta$ II-spectrins,  $\beta$  heavy spectrin subunit displays a distribution pattern that varies according to the hair cell type. in vestibular hair cells (which lack electromotility),  $\beta$ H spectrin is targeted to cytoplasmic intracellular organelles. in contrast, in the auditory outer hair cells,  $\beta$ H spectrin was concentrated at the cortical lattice, the highly organized cytoskeleton underlying the lateral wall plasma membrane.  $\beta$ II spectrin, however, was restricted to the cuticular plate, a dense apical network of horizontal actin filaments, both in vestibular and auditory hair cells.  $\beta$ H spectrin was progressively recruited into the cortical lattice between postnatal day 2 (P2) and P10 in the mouse, in parallel with prestin membrane insertion that itself parallels the maturation of cell electromotility. Moreover, we show that  $\alpha$ II/ $\beta$ H spectrin directly interacts with F-actin and band 4.1, two components of the cortical lattice. We therefore suggest that the sound-induced somatic electromotility of outer hair cells is based on an  $\alpha$ II/ $\beta$ H spectrin cortical network, and not the conventional  $\alpha$ II/ $\beta$ II spectrin.

### **137 Contribution of the GTSRH Sequence to The Folding of Prestin: Refolding of Transport-Defective Prestin Mutants by Salicylate**

**Shun Kumano**<sup>1</sup>, Koji Iida<sup>1</sup>, Michio Murakoshi<sup>1</sup>, Kouhei Tsumoto<sup>2</sup>, Katsuhisa Ikeda<sup>3</sup>, Izumi Kumagai<sup>1</sup>, Toshimitsu Kobayashi<sup>1</sup>, Hiroshi Wada<sup>1</sup>

<sup>1</sup>Tohoku University, <sup>2</sup>The University of Tokyo, <sup>3</sup>Juntendo University

The electromotility of outer hair cells is believed to be due to the conformational changes of the motor protein prestin. the GTSRH sequence at position 127-131 of the amino acid sequence of prestin is completely conserved in 6 proteins of the solute carrier (SLC) 26 family, to which prestin belongs. a conserved amino acid sequence is considered to be crucial for the SLC26 family. Hence, the purpose of this study was to elucidate the role of the GTSRH sequence in prestin. to this end, characteristics of G127A, T128A, S129A, R130A, H131A and S129T in HEK293 cells were investigated by Western blotting and whole-cell patch-clamp recording. Results showed that mutations in the GTSRH sequence led to insufficient glycosylation of prestin and a defect in its transport to the cell membrane, resulting in a decrease or loss of nonlinear capacitance (NLC), which is a signature of prestin activity. These results imply that the prestin mutants might be misfolded and accumulate in the cytoplasm. Recently, several reports have shown that when misfolded and transport-defective mutants are expressed in cells cultured with cell-membrane permeable molecules strongly bound to such mutants, these mutants are refolded and transported to the cell membrane in an active conformation. Based on those reports, to investigate if the prestin mutants are indeed misfolded, cells expressing prestin mutants were cultured for 24 hours with salicylate, which has cell-membrane permeability and high affinity for prestin. As a consequence, G127A, T128A, S129A and R130A were glycosylated sufficiently and transported to the cell membrane, resulting in an increase of NLC in the patch-clamp recording just after salicylate was washed out of the cells. These results indicate that G127A, T128A, S129A and R130A were misfolded, but refolded by salicylate and then transported to the cell membrane, showing that Gly-127, Thr-128, Ser-129 and Arg-130 play important roles in the folding of prestin.

### **138 Functional Evolution of the SLC26A5, Prestin, Minimal Essential Electromotility Motif**

**Kirk Beisel**<sup>1</sup>, Oseremen Okoruwa<sup>1</sup>, Jason Pecka<sup>1</sup>, Xiaotong Tan<sup>1</sup>, Xiang Wang<sup>1</sup>, Stephen McCleish<sup>1</sup>, Richard Hallworth<sup>1</sup>, David He<sup>1</sup>

<sup>1</sup>Creighton University, Omaha, NE USA

Prestin (SLC26A5) is the molecular motor responsible for cochlear amplification by mammalian cochlear outer hair cells and has the unique combined properties of energy-independent motility, voltage sensitivity and speed of cellular shape change. the ion transport capability, typical of SLC25A members, was exchanged for electromotility

function and is a newly derived feature of the therian cochlea. the minimal essential motif for the electromotility motor (meEM) was identified through the amalgamation of comparative genomic, evolution, and structural diversification approaches. within the highly conserved meEM motif two regions, which are unique to all therian species including monotremes and marsupials, appear to be the last features derived in the therian SLC26A5 peptides. in order to test the functional properties of the evolving meEM, heterologously expressed prestin transporters were electrophysiologically characterized in the HEK cells by measuring the electrical signature of motility, the nonlinear capacitance. Chimeric proteins, engineered from the meEM domains of gerbil, chicken or zebrafish, were assembled. Additional constructs were prepared with swapping of these two regions between the gerbil and chicken prestins. in addition, the platypus SLC26A5 coding sequence, derived from the coding exons of the genomic DNA, was produced. a pEFGP expression plasmid was used in construction of these chimeric and platypus prestins. the results of these experiments will be presented along with a new structural model of the prestin oligomeric transporter protein.

Supported in part by NIH grants – DC5009 (KWB) and DC 004696 (DH).

### **139 A6-Prestin Chimeras Do Not Show NLC**

**Alexei Surguchev**<sup>1</sup>, Jun-Ping Bai<sup>1</sup>, Joseph Santos-Sacchi<sup>1</sup>, Dhasakumar Navaratnam<sup>1</sup>

<sup>1</sup>Yale University

Prestin is a member of the SLC26 anion transporter family responsible for the outer hair cell electromotility. Mammalian cells expressing prestin show non-linear capacitance (NLC) acknowledged as its functional signature. In order to investigate prestin structure-function relationship the group of chimeric proteins with it its closest homologue mouse SLC26A6 were created using overlap extension PCR. These groups included prestin- N terminal-A6 chimera, prestin C-terminal A6 chimera and prestin with AA 70-123 replaced with A6.

All prestin –A6 chimeras were expressed as fusion proteins with YFP, transfected into CHO cells and tested for cell localization and NLC. Although confocal data suggested their preferential localization to the cellular membrane, none of them displayed NLC. These data suggest that the prestins unique properties are a consequence of its particular primary structure. Moreover these data suggest that creating chimeras is a viable method to isolate residues important for prestins function. Supported by R01 DC 007894 (DSN)/R01 DC 008130 (JSS)

## **140 Prestin's Extrinsic Anion Voltage Sensor Model is Untenable**

Joseph Santos-Sacchi<sup>1</sup>, Lei Song<sup>1</sup>, Volodya Rybalchenko<sup>1</sup>

<sup>1</sup>Yale University

The discovery of prestin's monovalent anion sensitivity revealed an important biophysical characteristic of the OHC membrane motor, and provided a potential basis for prestin's voltage sensitivity (Oliver et al., 2001). According to the hypothesis, monovalent anions, notably chloride ions, provide the charged sensors (~1e<sup>-</sup>) which control the two state conformations of prestin when voltage is perturbed. Hyperpolarization would cause intracellularly bound chloride to move through the membrane field forcing prestin motors into the expanded state, which would effect cell elongation.

We provide a host of data that disproves this concept. First, chloride concentration should not, at a fixed clamped voltage, alter the steady state probability of prestin's conformation. We find that it does. Second, multivalent anions should not serve as replacements for the monovalent sensor, without altering the valence of motor charge movement (z) in a predictable manner. We find that di- and trivalent anions can support motor charge movement with no expected change in valence. Third, monovalent anions should remain bound and traverse the membrane field as the motor moves into the expanded conformational state. We find that the affinity of anions depends on the state of prestin that we set with a variety of methods (membrane tension, temperature and voltage), and that movement into the expanded state reduces the affinity of prestin for anions. Consequently, anions are released from prestin during expansion, namely during hyperpolarization. All of these data are in direct conflict with the prevailing notion of prestin's voltage sensing. The most parsimonious explanation is that anions work allosterically on prestin, and that an intrinsic voltage sensor resides within the motor.

(Supported by NIDCD DC 000273 to JSS)

## **141 Creation of a Novel Prestin Knockin Mouse Model with Normal Cochlear and Outer Hair Cell Structure and Mechanical Properties**

Xudong Wu<sup>1</sup>, Jiangang Gao<sup>1</sup>, Jing Zheng<sup>2</sup>, Wendy Cheng<sup>1</sup>, Soma Sengupta<sup>2</sup>, MaryAnn Cheatham<sup>2</sup>, David He<sup>3</sup>, Peter Dallos<sup>2</sup>, Jian Zuo<sup>1</sup>

<sup>1</sup>St. Jude Children's Research Hospital, <sup>2</sup>Northwestern University, <sup>3</sup>Creighton University

The prestin knockout mouse model has provided evidence that prestin-based outer hair cell (OHC) electromotility is required for cochlear amplification. However, the absence of prestin in the OHC lateral membrane significantly reduced the length of OHCs, thus potentially altering the mechanical properties of the cochlea and rendering this model non-definitive. To provide further evidence that somatic motility is the mammalian cochlear amplifier, we created a novel prestin knockin mouse model in which two residues have been replaced (V499G/Y501H; subsequently referred to as "499 mice") near the

presumed junction between the last transmembrane domain and the intracellular C-terminus of prestin. These substitutions were based on previous studies using transfected HEK cells, showing that mutant prestin is still targeted to the plasma membrane but displays significantly diminished functional characteristics (i.e., non-linear capacitance or NLC). 499 homozygous mice appeared normal without obvious behavioral defects. OHCs from the 499 mice have normal lengths. As expected, 499 prestin is normally directed to its location in the lateral membrane of OHCs, and recognized by antibodies targeted against cytoplasmic N- and C-terminus epitopes. 499 prestin forms monomers and dimers with wildtype-like levels and ratios, and the dimer bands disappear after pretreatment with the reducing reagent ethanedithiol. This novel model thus possesses normal cochlear and OHC structure and mechanical properties. Physiological characterization of 499 mice is described in a companion abstract (Cheatham et al.), demonstrating knockout-like auditory characteristics and confirming prestin-based somatic motility as the cochlear amplifier.

This work is supported in part by ALSAC, the Hugh Knowles Center and by NIH grants DC00089 (to P. D.), DC06471, CA023944, and CA21765 (to J. Zuo), DC 006496 (to D.Z.Z.H.), DC006412 (to J. Zheng).

## **142 Prestin-Based Somatic Electromotility is the Cochlear Amplifier**

Mary Ann Cheatham<sup>1</sup>, David Z.Z. He<sup>2</sup>, Charles T. Anderson<sup>1</sup>, Shuping Jia<sup>2</sup>, Xiang Wang<sup>2</sup>, Khurram Naik<sup>1</sup>, Jing Zheng<sup>1</sup>, Jian Zuo<sup>3</sup>, Peter Dallos<sup>1</sup>

<sup>1</sup>Northwestern University, <sup>2</sup>Creighton University, <sup>3</sup>St. Jude Children's Research Hospital

Somatic stiffness of outer hair cells (OHC) obtained from the prestin knockout (ko) mouse is 1/4-1/3 of that of OHCs in wild-type (wt) mice. This implies that the mechanical load on a putative cilia-based amplifier is different in ko and wt mice. Consequently, the prestin ko mouse model cannot be used to discriminate definitively between cilia-based and prestin-based amplification. We created a prestin knockin (ki) mouse in which membrane targeting, cell length, and somatic stiffness is wt-like (see Wu et al.). In addition, patch-clamp recordings from OHCs in the ki hemicochlea demonstrate wt-like transducer currents and fast adaptation. However, at the presumed *In Vivo* membrane potential of OHCs (-70 to -80 mV) the average somatic motility of OHCs is ~7.5% of the average wt motility. Nonlinear capacitance is also dramatically reduced. It is expected that such reduced motility should yield ~55 dB threshold shift if prestin-based motility is the cochlear amplifier. Indeed, compound action potential (CAP) recordings *In Vivo* show threshold shifts of this magnitude, indistinguishable from those obtained in the prestin ko mouse, or in the absence of OHCs. Finally, tuning, as determined by CAP masking tuning curves, is absent in the ki mouse, just as in the ko model.

This work is supported in part by ALSAC, the Hugh Knowles Center and by NIH grants DC00089 (to P. D.), DC06471, CA023944, and CA21765 (to J. Zuo), DC 006496 (to D.Z.Z.H.).

### **143 Effect of Cochlear Microphonics On Limiting Frequency of the Mammalian Ear**

Kuni Iwasa<sup>1</sup>, Bora Sul<sup>1</sup>

<sup>1</sup>NIH

The sensitivity and frequency selectivity of the mammalian ear depend on motile activity of outer hair cells (OHCs). Since electromotility of OHC is likely responsible for this function, its dependence on the receptor potential poses a frequency limit due to the intrinsic low-pass RC filter of the cell. In an earlier report (Ospeck et al, Biophys J 2003) we attempted to find such a frequency limit by imposing the condition that this motility must counteract the shear drag in the gap between the tectorial membrane and the reticular lamina. The value obtained was about 10 kHz, respectable but still short of covering the mammalian auditory frequency.

Here we examine the effect of cochlear microphonics (CM), proposed by Dallos and Evans (Science 1995) for overcoming the RC problem, by considering a simple model, which would set an upper bound. We assume that the receptor current across the plasma membrane generates the receptor potential (RP) and across an external space the CM. Because of the phase difference of  $\sim 180^\circ$ , the CM in turn can enhance the receptor potential of more basal OHCs. Those receiver cells with enhanced RP are, in turn, assumed to convert this electrical energy gain into mechanical energy and transmit back to sustain the vibration of the basilar membrane at the site of the maximal amplitude.

We find that the magnitude of the enhancement indeed exceeds that of RP if the receiver cells are fewer than the generator cells and that this effect may lead up to about 2-fold gain in energy. However, we do not find that this effect extends the previous value of 10 kHz for the frequency limit. The reason is that the previous estimate did not consider an external resistance, which is needed to produce the CM but reduces the RP. Our result therefore indicates that we still need another factor, such as fast voltage-gated K-currents, for high frequency enhancement.

### **144 Efficiency of Outer Hair Cell Somatic Electromotility**

Richard Rabbitt<sup>1</sup>

<sup>1</sup>University of Utah

We often think about the electromechanical behavior of outer hair cell somata under conditions of isometric length where the maximal force production occurs, or under conditions of zero load where the maximum velocity occurs. In both cases, the mechanical work done by the OHC is zero, and the efficiency of the OHC in converting electro-chemical power into mechanical power is zero. This is analogous to skeletal muscle where the efficiency is zero during isometric tetanus and is zero during no-load maximum velocity contraction. The power output is maximum only when the mechanical load is matched to the biological motor – a condition occurring at a contraction velocity and force between the two extremes. We used a biophysically-based model of a single OHC to gain some insight into power efficiency, and how key

dimensions might be tuned to maximize OHC efficiency within specific frequency bands. The model was further used to investigate conditions that would need to be met in order to achieve the maximal OHC power output within the cochlear partition. Results indicate that under best conditions OHCs can convert roughly 50% of the input electrical power entering the soma of the cell (from mechano-electrical transduction) into useful mechanical work. This efficiency is comparable with the most efficient biological motors, but in OHCs has the remarkable capability of functioning from DC to over 50 kHz. The so-called RC paradox is not an issue due to the morphology of OHCs and the fact that electrical charge displacement is directly coupled to motility. Results further suggest that the somatic length of OHCs may vary with place within the mammalian cochlea in order to optimize their power efficiency within the living cochlea. Supported by NIDCD R01 DC04928.

### **145 Hydrogen Peroxide-Induced Stress Pathways in an organ of Corti Cell Line**

Andra E. Talaska<sup>1</sup>, Su-Hua Sha<sup>1</sup>, Candace Liebold<sup>1</sup>, Jochen Schacht<sup>1</sup>

<sup>1</sup>Kresge Hearing Research Institute, University of Michigan

Hydrogen peroxide treatment is a canonical oxidant stress paradigm that has been established in many cell lines and tissues in order to probe oxidant stress-induced signaling pathways. The consequences of direct application of hydrogen peroxide is of particular interest in inner ear insult studies because oxidant stress has proven paramount and primary in auditory pathologies including age-related hearing loss, ototoxic drug responses, and noise trauma, inciting a riot of downstream cellular pathways that parse out their differences to determine the net fate of a cell. Hydrogen peroxide itself is found to be elevated in inner ear tissues *In Vivo* following aminoglycoside treatment or aging (Jiang et al., 2005; Jiang et al., 2007). The HEI-OC1 cell line, derived from the organ of Corti of the immortomouse, has been used to study inner ear pathologies and protection therefrom (Kalinec et al., 2003; So et al., 2005). In this study, we applied hydrogen peroxide to HEI-OC1 cells in order to investigate the particular role of oxidant-generated changes in the inner ear cells. MAPK pathways were induced following hydrogen peroxide treatment. Specifically, p38 and p42/p44 show precipitous phosphorylation, causing induction of the downstream signals, which ultimately lead to cell death. Additionally, hydrogen peroxide treatment caused PTEN phosphorylation and induction of calpain as well as Bcl-2 family proteins, pointing to a highly complex orchestration of variegated stress-induced pathways. In summary, application of hydrogen peroxide to HEI-OC1 cells may shed light on the particular role of reactive oxygen species in redox-regulated signaling pathways in the inner ear. This study was supported by research grant DC-03685 and core grant P30 DC-05188 from the National Institute on Deafness and Other Communication Disorders and by grant AG-025164 from the National Institute on Aging, NIH.



#### **146 1-Cys Peroxiredoxin Attenuates H<sub>2</sub>O<sub>2</sub>-Induced Cell Cycle Arrest in a Mouse organ of Corti Cell Line**

Hye Mi Lee<sup>1</sup>, Joong Ho Ahn<sup>2</sup>, Jung-Eun Shin<sup>3</sup>, Jong Woo Chung<sup>2</sup>, Jhang Ho Park<sup>1</sup>

<sup>1</sup>Asan Institute for Life Science, <sup>2</sup>Department of Otolaryngology, Asan Medical Center, University of Ulsan College of Medicine, <sup>3</sup>Department of Otolaryngology, Konkuk University College of Medicine

Increased amount of reactive oxygen species (ROS) production is one of the major factors associated with the formation of hearing impairment and with senescence of various cell types. Several lines of evidence suggest that changes in the regulation of cell cycle in inner ear cells are involved in age-related hearing loss. 1-Cys peroxiredoxin (1-cysPrx), a member of the peroxiredoxin family with a single conserved cysteine residue, reduces a broad spectrum of hydroperoxides. We examined whether 1-cysPrx was capable of attenuating H<sub>2</sub>O<sub>2</sub>-induced cell cycle arrest in a mouse organ of Corti-derived cell line ((Kalinec et al., 1999). Immunoblot analysis showed that expressions of cell cycle regulatory proteins, such as p21<sup>Cip1</sup>, cyclin dependent kinase (CDK) 2, 4, and 6, and cyclin a and E increased in 250  $\mu$ M H<sub>2</sub>O<sub>2</sub>-treated cells. Meanwhile, human 1-cysPrx transiently overexpressed in cells was able to reduce the expressions of these proteins induced by oxidative stress. Furthermore, FACS analysis showed that 1-cysPrx overexpression rescued H<sub>2</sub>O<sub>2</sub>-induced G1/S arrest in the cells. These results suggest that 1-cysPrx may function as a defensive mediator for hearing loss caused by oxidative stress.

#### **147 Stress-Induced Changes in Mitochondrial Peroxiredoxin in Mouse Cochlear Hair Cells**

Fuquan Chen<sup>1</sup>, Su-Hua Sha<sup>1</sup>, Jochen Schacht<sup>1</sup>

<sup>1</sup>Kresge Hearing Research Institute, University of Michigan, Ann Arbor, MI 48109-0506

Age-, noise-, and drug-dependent hearing loss are accompanied by oxidant stress in the cochlea. a decrease in antioxidants is followed by an upregulation of enzymes that maintain redox homeostasis, in an attempt to counter the oxidative imbalance. Peroxiredoxins are recently characterized components of an antioxidant defense system that catalyze the inactivation of pro-radicals such as hydrogen peroxide and the reduction of protein sulfhydryl groups. the known family of peroxiredoxins is currently comprised of six members of which peroxiredoxin 3 (Prx-3) is a mitochondrion-specific enzyme that acts as a critical regulator of the intracellular redox balance. it's depletion results in increased intracellular levels of H<sub>2</sub>O<sub>2</sub> and sensitizes cells to apoptotic signaling, thus making Prx-3 a crucial mediator of stress-induced apoptosis.

During chronic kanamycin treatment in the mouse, Prx-3 was first upregulated at times when hair cells were still intact and then precipitously decreased preceding outer hair cell death. the rise and fall of Prx-3 was reflected in organ culture. After gentamicin treatment for 8hr, Prx-3 was increased in hair cells and their morphology remained undamaged; by 16hr, Prx-3 decreased significantly and

loss of hair cells ensued. in a mouse model of age-related hearing loss, Prx-3 initially increased with advancing age in the cochlea but decreased around the time of impending hair cell death. a strong correlation between Prx-3 levels and cell fate was underscored by studies of protection. Antioxidant co-treatment (e.g., dihydroxybenzoic acid) with aminoglycosides maintained a high level of Prx-3 in outer hair cells and promoted their survival. These studies suggest a pivotal role for Prx-3 in hair cell death and survival.

This study was supported by research grant DC-03685 and core grant P30 DC-05188 from the National Institute on Deafness and Other Communication Disorders and by grant AG-025164 from the National Institute on Aging, NIH.

#### **148 The Role of Peroxiredoxin III in the Ototoxic Drug-Induced Mitochondrial Apoptosis of Cochlear Hair Cells**

Hoseok Choi<sup>1</sup>, Yoon-Gun Jung<sup>1</sup>, Hun Yi Park<sup>2</sup>, Keehyun Park<sup>2</sup>

<sup>1</sup>Dep. of Otorhinolaryngology, Inha University College of Medicine, <sup>2</sup>Dep. of Otolaryngology, Ajou University School of Medicine

Although the exact mechanism involved in cisplatin and aminoglycoside has not been fully elucidated, reactive oxygen species (ROS) generation that interferes with the antioxidant defense systems of the cochlea have been proposed to play an important role.

Peroxiredoxins (Prxs) are an ubiquitous family of antioxidant enzyme that also control cytokine-induced peroxide levels which mediate signal transduction in mammalian cells. the role of Prx III in the mitochondria of cochlear hair cell lines has not been studied. the aim of the present study is to investigate the protective role of Prx III on the oxidative damage induced by ototoxic agents with the use of RNA interference.

Depletion of Prx III was done by RNA interference in cochlear hair cells (UB/OC-1), and cells were exposed to ototoxic drugs (cisplatin or gentamicin). We then compared the apoptotic signaling between Prx III-depleted and control cells. the depletion of Prx III resulted in increased intracellular ROS levels accompanied by enhanced apoptosis by ototoxic drugs. the Prx III-depleted cells showed mitochondrial membrane potential collapse, cytochrome c release, and caspase activation. We have shown that Prx III is most expressed in UB/OC -1 cells and that the ROS eliminating enzyme defect in mitochondria and the mitochondrial generation of ROS contributes to apoptotic signaling.

The intracellular accumulation of ROS caused by Prx III depletion resulted in acceleration of apoptosis with cytochrome c release and caspase activation. Generation of excessive ROS would overwhelm the antioxidant defense mechanism of the cochlear causing a cascade resulting in apoptosis of hair cells.

in conclusion, we have shown that the ototoxic drug-induced mitochondrial over-generation of ROS contributes to apoptotic signaling in cochlear hair cells and that the

antioxidant protein Prx III is an important ROS-eliminating enzyme in mitochondria.

#### **149 Endocochlear Potentials in Mice with Local Application of 3-Nitropropionic Acid**

**Shinpei Kada<sup>1</sup>, Takayuki Nakagawa<sup>1</sup>, Juichi Ito<sup>1</sup>**

<sup>1</sup>*Graduate School of Medicine, Kyoto University*

The cochlear lateral wall (LW) consists of the stria vascularis (SV) and the spiral ligament (SL), which are crucial components for auditory function. the degeneration of LW, therefore, results in sensorineural hearing loss (SNHL). the SV and the SL play essential roles in generation of endocochlear potentials (EPs). Previously, we reported ABR threshold shifts and the SL degeneration in mice following local application of 3-nitropropionic acid (3-NP), an inhibitor of succinate dehydrogenase in mitochondria. Here, more precise effects of local 3-NP application were investigated by measurements of EPs and further histological evaluations of LW. C57BL/6 mice (6-10 w) were injected with 3-NP (1, 5 or 10 mM; 1.5 µl) or saline (control) into the left posterior semicircular canal. the gap between the hole of the canal and the injection tube was carefully sealed to avoid leakage. ABRs were recorded preoperatively and 1, 7 and 14 days after the administration of 3-NP. EPs at the basal turn of cochleae were measured prior to sacrifice (day 7 or 14). Then, the morphometric analyses of the SV and the SL were carried out. the results demonstrated permanent ABR threshold shifts and significant EP decreases in mice applied with higher dosages of 3-NP. Morphometric analyses revealed significant decrease of the cell density in the SL and reduction of the area of the SV in the basal turn. Immunohistochemistry for connexin 26 demonstrated degeneration of the gap junction network in the SL. the present findings show that local 3-NP application causes functional and histological damage in the LW resulting in profound hearing loss.

#### **150 Over-Expression of XIAP Delays Presbycusis in C57BL/6 Mice**

**Jian Wang<sup>1</sup>, Zhiping Yu<sup>1</sup>, Manohar Bance<sup>1</sup>, David Morris<sup>1</sup>, Craig Moore<sup>1</sup>, George Robertson<sup>1</sup>, Robert Korneluk<sup>2</sup>**

<sup>1</sup>*Dalhousie University*, <sup>2</sup>*University of Ottawa*

Previous studies have demonstrated that apoptosis plays a major role in age-related hearing loss, or presbycusis. in the present study, we evaluated whether over-expression of X-linked Inhibitor of Apoptosis Protein (XIAP) prevented or delayed presbycusis. for this purpose, transgenic mice, on a C57BL/6 genetic background, were used that ubiquitously over-express XIAP using a human *xiap* transgene (ubXIAP). the hearing status and cochlear pathology were compared between the transgenic ubXIAP mice and their wild type (WT) littermates. Hearing status was evaluated using frequency-specific auditory brainstem responses (ABR). the degenerative pathology of the cochleae was evaluated by cochleogram.

Our results demonstrated that WT mice began to show signs of hearing loss at two months of age. the development of hearing loss was slower and significantly smaller in ubXIAP mice than WT controls. This was

observed up to 14 months of age, with ubXIAP mice appearing to have better hearing by 5-30 dB across the frequency range tested. Consistent with these results, cochleograms showed that there was a smaller amount of hair cell loss in the ubXIAP than WT mice. Taken together, these results suggest that XIAP overexpression can delay or reduce age-related hearing loss and cell death in the cochlea. the expression of endogenous *xiap* gene and the transgene was also evaluated in Western Blotting and compared between young versus old and WT versus transgene mice.

#### **151 Effect of Geranylgeranylacetone On Progressive Hearing Loss in a Mouse Model of Age-Related Hearing Loss**

**Takefumi Mikuriya<sup>1</sup>, Kazuma Sugahara<sup>1</sup>, Yoshinobu Hirose<sup>1</sup>, Makoto Hashimoto<sup>1</sup>, Hiroaki Shimogori<sup>1</sup>, Akira Nakai<sup>2</sup>, Hiroshi Yamashita<sup>1</sup>**

<sup>1</sup>*Department of Otolaryngology, Yamaguchi University Graduate School of Medicine*, <sup>2</sup>*Department of Biochemistry and Molecular Biology, Yamaguchi University Graduate School of Medicine*

Mechanisms of age-related hearing loss have not been elucidated as aging processes are extremely complex. Although oxidative stress and apoptotic cell death are involved in progression of ARHL, number of trial to treat ARHL is limited. Heat shock response is characterized by induction of heat shock proteins (HSPs) in response to stresses such as heat shock, which diminishes during aging. HSPs act as molecular chaperones, and some HSPs also inhibit apoptotic pathways. Here, we examined that age-related expression of HSPs in the cochlea of age-related hearing loss model DBA/2J mice and control CBA/N mice. We found that expression of Hsp70 and Hsp110 is constant during aging in the cochlea of CBA/N mice, suggesting that pharmacological induction of HSPs might attenuate age-related hearing loss. We administered DBA/2J mice with food containing Geranylgeranylacetone (GGA) that induces expression of HSPs in the cochlea, and found that its administration suppresses age-related hearing loss examined by ABR threshold and hair cell loss determined by histological examination. in this meeting, we present that these results demonstrate that dietary administration of GGA could be an effective therapeutic strategy for treatment of age-related hearing loss.

#### **152 Effect of Water-Soluble Coenzyme Q10 On Age-Related Hearing Loss in DBA/2J and C57/B6 Mouse**

**Yoshinobu Hirose<sup>1</sup>, Kazuma Sugahara<sup>1</sup>, Takefumi Mikuriya<sup>1</sup>, Makoto Hashimoto<sup>1</sup>, Hiroaki Shimogori<sup>1</sup>, Hiroshi Yamashita<sup>1</sup>**

<sup>1</sup>*Yamaguchi University School of Medicine*

The aging-related hearing loss is the disease that the establishment of the cure is expected. However, the cause of aging-related hearing loss does not yet become clear. the process of age-related hearing loss is associated with many molecular, biochemical and physiological changes. Substantial evidences suggest that reactive oxygen species are produced in aged cochlea and cause cochlear

damage. Therefore age-related hearing loss can be reduced by treatment with antioxidants.

Coenzyme Q10 is one of the antioxidants and vitamin-like substance. the reagent is used for the treatment of disorders of oxidative injury, such as Parkinson's disease, stroke, and ischemic heart disease. in the ear, we reported coenzyme Q10 could protect cochlear from acoustic trauma.

in the present study, we investigated the effect of coenzyme Q10 on acoustic age-related hearing loss in DBA/2J and C57/B6 mouse. the DBA/2J mouse is known as one of the elderly hard hearing model animals because it gets hard hearing at the early stage. Actually, it is reported for hearing to decrease gradually from three weeks. Also C57/B6 are model of aging hearing loss, but more slowly than DBA/2J.

Animals were divided into the three groups: group 1, coenzyme Q10 200mg/day; group 2, coenzyme Q10 20mg/day; group 3, control, mixed into water and given from 4weeks old. We assessed auditory brainstem response (ABR) threshold every 4week in DBA/2J mouse and 8week in C57/B6 mouse. in addition we observed the cochlear hair cell damages.

### **153 Mefloquine-Induced Changes in Apoptotic Gene Expression in Cochlear Basilar Membrane and Spiral Ganglion Neurons**

Haiyan Jiang<sup>1</sup>, Dalian Ding<sup>1</sup>, Richard Salvi<sup>1</sup>

<sup>1</sup>University at Buffalo

in previous studies, we showed that mefloquine damages the cochlear hair cells and auditory nerve fibers in the inner ear by apoptosis; however, the signaling pathways involved are poorly understood. to address this issue, we used quantitative RT-PCR apoptosis-focused gene arrays (96 genes) to assess the changes in gene expression in the basilar membrane (hair cells-supporting cells) and spiral ganglion regions of rat cochlear organotypic cultures treated with 100  $\mu$ M of mefloquine for 3 h. in the basilar membrane, 13 genes increased expression and 13 gene decreased expressions. of these 26 genes, 11 were classified as anti-apoptotic and 15 genes as apoptotic. in spiral ganglion neurons, 21 genes changed significantly; 18 genes showed increased expression and 3 gene showed reduced expression. the apoptotic and anti-apoptotic genes in both basilar membrane and spiral ganglion tissues mainly involved gene associated with p53 signaling, TNF ligand family, CARD family, TNF receptor family, death domain family, and lactate dehydrogenase A. While the gene expression changes in basilar membrane and spiral ganglion tissues showed considerable, some differences were observed which may reflect the unique response of each tissue. These results indicate that mefloquine induces a wide range of apoptotic and anti-apoptotic signals during the early states of ototoxicity. Supported in part by NIH grant R01 DC06630.

### **154 Ototoxicity of Mefloquine in Vestibular organotypic Cultures**

Dongzhen Yu<sup>1</sup>, Dalian Ding<sup>1</sup>, Richard Salvi<sup>1</sup>

<sup>1</sup>University at Buffalo

Mefloquine is an effective and widely used anti-malaria drug; however there are clinical reports suggesting that mefloquine may be neurotoxic and ototoxic. in previous studies, we showed that mefloquine damaged hair cells and neurons in cochlear organ cultures in a dose-dependent manner. Since dizziness and loss of balance are listed as common side effects of mefloquine, we hypothesized the mefloquine might damage the vestibular epithelium. to test this hypothesis, we applied mefloquine to organotypic cultures from postnatal day 3 rat utricles. the macula of the utricle was carefully dissected out, mounted as a flat surface preparation and cultured overnight in serum free medium. Utricular explants were treated with 10, 50, 100, or 200  $\mu$ M mefloquine for 24 h. Some utricles were cultured for 24 h with 50  $\mu$ M mefloquine and the activity of caspase-3, -6, -8, or -9 was evaluated with these fluorogenic caspase inhibitors. Specimens were stained with rhodamine conjugated phalloidin to label the actin in the stereocilia and Topro-3 to visualize the nuclei. Mean vestibular hair cell density was  $65.2 \pm 4.9$  per 0.01 mm<sup>2</sup> in controls. Mefloquine caused a dose-dependent loss of utricular hair cells. Treatment with 10  $\mu$ M caused a slight reduction to 58 per 0.1 mm<sup>2</sup>; 50  $\mu$ M caused a significant decline to  $28.3 \pm 13.4$  per 0.01mm<sup>2</sup> and 200  $\mu$ M destroyed nearly all the hair cells ( $5.2 \pm 3.6$  per 0.01 mm<sup>2</sup>). These results indicate that 10 $\mu$ M of mefloquine is the approximate "threshold" for inducing hair cell loss in postnatal utricular cultures. Hair cell nuclei from mefloquine treated utricles were condensed and fragmented and hair cells were positive for initiator caspases-8, -9 and executioner caspase-3, -6. These results indicate that mefloquine-induced hair cell degeneration in the postnatal rat utricle occurs by apoptosis and is initiated by both membrane and mitochondrial cell death pathways.

Supported in part by NIH grant R01 DC06630-01

### **155 Styrene Ototoxic Effect Depends Mainly On the Exposure Level**

Chiemi Tanaka<sup>1</sup>, Guang-Di Chen<sup>1</sup>, Donald Henderson<sup>1</sup>

<sup>1</sup>SUNY at Buffalo

Campo and colleagues (Campo et al., Hear. Res., 154, 170-180, 2001) reported that styrene-induced hearing loss did not increase with exposure duration. in this experiment, the issue of whether the total dose or the distribution is a key for determining extent of hearing loss was evaluated. Experimental animals (Long-Evans rats) were divided into 4 groups (n=6 rats in each group) to be exposed by gavage to styrene at a dose of 800 mg/kg once a day for 5 days per week for 3 weeks (3w-800 group), at 400 mg/kg for 6 weeks (6w-400 group), at 200 mg/kg for 12 weeks (12w-200 group), and at 100 mg/kg for 24 weeks (24w-100 group). the 3w-800-mg-group developed an up to 35-dB permanent threshold shift (PTS) and an up to 60% OHC loss in the middle turn. the 6w-400 group showed an up to 15-dB PTS and an up to 40% OHC loss, which were

slightly higher than those induced by a 3-week-exposure at a dose of 400 mg/kg. the 12w-200 group showed less than 10% OHC loss and less than 10-dB PTS. the 24w-100 did not show significant damage, although the animals received the same amount of styrene as the other animals. the data indicate that exposure level is critical for styrene ototoxicity and that the ear's propensity to accumulate the toxic styrene is limited. a clinical implication of this research is that short, transient, high-level styrene exposure can be ototoxic.

This study was supported by NIOSH grant 1R01OH008113-01A1.

### **156 Ototoxic Effects of Styrene Exposure During Gestation and Lactation in Rats**

**Manna Li**<sup>1</sup>, Guang-Di Chen<sup>1</sup>, Chiemi Tanaka<sup>1</sup>, Eric Bielefeld<sup>1</sup>, Donald Henderson<sup>1</sup>

<sup>1</sup>SUNY at Buffalo

Styrene is extensively used in industries and many workers, including women, are exposed to styrene. Styrene ototoxicity has been well documented. However, the impact of styrene ototoxicity during gestation and lactation is still unclear. We hypothesize that styrene may induce less ototoxic effect on pregnant rats because of high estrogen levels, but may induce significant ototoxic effects on the development of the babies' auditory system. Five pregnant rats were exposed to styrene by gavage at a dose of 400 mg/kg/day starting from the fourth day of gestation for 5 days per week for 6 weeks. Six male rats were exposed at the same dosage for the same period for comparison. Two pregnant rats were unexposed and their offspring were used as controls. Three days after the last gavage of the 6-week styrene exposure, threshold shift in the mother rats and the male rats was assessed using compound action potential (CAP) recording, and their auditory hair cells were counted. the styrene exposure caused an about 15-20-dB threshold shift and 30-40% outer hair cell (OHC) loss in the mid-frequency region in both groups of the pregnant rats and the males rats. Threshold shifts of the baby rats were measured 2 months after birth by recording of both auditory brainstem response (ABR) and CAP. Significant CAP threshold shift was only observed in those rats from one mother but not the other four mothers. Interestingly, ABR threshold shift was observed in all of the 5 families. Almost all of the baby rats have normal cochlear anatomy, i.e.: no hair cells loss. the mechanism for the hearing loss in the mother rats and the pups is discussed.

This study was supported by NIOSH grant 1R01OH008113-01A1.

### **157 Functional and Structural Changes in the Chinchilla Cochlea and Vestibular System Following Round Window Application of Carboplatin**

**Yide Zhou**<sup>1</sup>, Dalian Ding<sup>1</sup>, Suzanne Kraus<sup>1</sup>, Richard Salvi<sup>1</sup>

<sup>1</sup>University at Buffalo

Carboplatin, a second-generation anticancer drug, has a low level of ototoxicity in most species; however, in

chinchillas carboplatin preferentially destroys inner hair cells (IHC) and type I vestibular hair cells at moderate doses while at higher doses it destroys both IHC and outer hair cells (OHC) and type I and type II vestibular hair cells. to better understand the time course and mechanisms of carboplatin toxicity, carboplatin was applied to the round window membrane (5mg/ml, 50 $\mu$ l) of the right ear and the functional and anatomical consequences were examined at 1, 3, 7, 14 and 30 days post-treatment. Carboplatin caused a significant reduction in distortion product otoacoustic emissions (DPOAE) at all frequencies 3 d post-treatment. the threshold of the compound action potential (CAP) increased significantly from 3 to 7 d post-treatment and after 14 d the CAP was absent. Carboplatin treatment induced spontaneous nystagmus 1 d after carboplatin treatment which disappeared 2-3 d later. Cold caloric stimulation evoked a robust nystagmus response in untreated ears, but the nystagmus response disappeared approximately 3 d after carboplatin treatment. Vestibular dysfunction was associated with a significant reduction of vestibular hair cell density 3 d post-treatment. the early stages of cochlear and vestibular hair cell degeneration were associated with nuclear shrinkage and fragmentation, morphologic features of apoptosis, upregulation of initiator caspase 8 and executioner caspase 3, but absence of caspase 9 labeling. These results indicate that carboplatin rapidly penetrates the round window leading to severe functional deficits arising from programmed hair cell death initiated from the cell death receptors on the surface of cell membrane. Supported by NIH grant R01 DC06630-01

### **158 Effects of Cisplatin-Ethacrynic Acid Cochlear Pathology On DPOAE**

*Withdrawn*

### **159 Selective Damage of Murine Cochlear Cell Types by Varying Concentrations of Ouabain**

**Osamu Adachi**<sup>1</sup>, Konstantina M. Stankovic<sup>1</sup>, Arthur G. Kristiansen<sup>1</sup>, Joe C. Adams<sup>1</sup>, Michael J. McKenna<sup>1</sup>

<sup>1</sup>Massachusetts Eye & Ear Infirmary

Ouabain is a cardiac glycoside that specifically binds to Na/K-ATPase and inhibits its activity. Other authors have established that ouabain induces selective degeneration of spiral ganglion neurons when applied to the round window of gerbils. We wanted to determine whether ouabain can similarly cause selective damage in the murine cochlea. to minimize variability inherent in intratympanic application of pharmacologic agents, we used intralabyrinthine approach to delivered ouabain. a total of 10  $\mu$ l of ouabain at the concentrations 1.0, 0.1 or 0.05mM was injected through a small fenestra in the posterior semicircular canal of 6 week old male CBA/CAJ mice at the volume ratio of 1 $\mu$ l/min after making a release fenestra in the lateral semicircular canal. Mice were sacrificed 10 days after treatment (3 mice for each concentration of ouabain) and their cochleae analyzes histologically using Azure stain, and

immunocytochemically using polyclonal antibodies for Na<sup>+</sup>, K<sup>+</sup>-ATPase, and carbonic anhydrase II (CA II). Ouabain at 0.05mM and 0.1 mM caused selective damage of type I and II fibrocytes of the spiral ligament while spiral ganglion neurons were minimally affected. Ouabain at 1.0 mM caused severe damage of both type I and II fibrocytes of the spiral ligament and spiral ganglion neurons. Our results indicate that ouabain causes selective damage of murine cochlear cell types in a concentration dependent manner, and that selective damage of fibrocytes of the spiral ligament is pharmacologically possible.

## **[160] Effect of Post-Exposure Treatment for Inner Ear Barotrauma**

**Hitoshi Maekawa,MD<sup>1</sup>**, Takeshi Matsunobu,MD<sup>1</sup>, Tetsuya Tanabe,MD<sup>1</sup>, Hitoshi Tsuda,MD<sup>1</sup>, Kaoru Onozato,BS<sup>1</sup>, Yukihiko Masuda,MD<sup>1</sup>, Masami Ogura,MS<sup>1</sup>, Youko Kitagawa,MS<sup>1</sup>, Akihiro Shiotani,MD<sup>1</sup>

<sup>1</sup>National Defense Medical College

**Objective:** in recent year, the free radical species have been proved to be implicated in inner ear disorders such as cisplatin ototoxicity and noise-induced hearing loss . Furthermore, several free radical scavengers have been proved to have protective effect against such inner ear disorders. Edaravone has been proved to be a potent and novel free radical scavenger. Among studies which reported the efficacy of edaravone in inner ear disorders, only one study reported that pre-treatment with edaravone can reduce the incidence of inner ear barotraumas (IEB) , while none reported the efficacy of post-exposure treatment. Present study was conducted to examine the efficacy of post-exposure treatment for IEB using edaravone.

**Methods:** Healthy female guinea pigs with a normal Preyer's reflex were used in this study. We used 18 ears of the control group and 18 ears of the treatment group. Before the pressure loading, auditory brainstem response (ABR) testing was performed. Guinea pigs were exposed to pressure change sufficient to induce IEB, and ABR testing was performed and the threshold shift immediately after the exposure was evaluated. the animals in the treatment group received edaravone intraperitoneally at a dose of 9.0 mg/kg once a day for 5 days. Post-exposure ABR testing was performed 2,3,5 and 7 weeks after the pressure loading. Time course of the amount of ABR threshold shift was compared between the two groups.

**Results:** the time course change of the ameliorations of ABR threshold shift was significantly different between the two groups (repeated measured ANOVA, P=0.0013), and the edaravone group significantly attenuate threshold shift at two weeks after the pressure loading (p=0.0125, unpaired t-test).

**Conclusions:** Post-exposure treatment for IEB using edaravone was proved to be effective. These findings show that edaravone protected the cochlea from IEB and free radical species play as important role in the mechanism of IEB.

## **[161] Dexamethasone Protects Against TNF-Alpha Induced Loss of Auditory Hair Cells in organ of Corti Explants by Altering the Expression Levels of Apoptosis-Associated Genes**

**Christine Dinh<sup>1</sup>**, Scott Haake<sup>1</sup>, Shibing Chen<sup>1</sup>, Kimberly Hoang<sup>1</sup>, Adrien Eshraghi<sup>1</sup>, Thomas Balkany<sup>1</sup>, Thomas Van De Water<sup>1</sup>

<sup>1</sup>University of Miami Ear Institute

**Background:** Apoptosis of a TNF- $\alpha$  damaged cell can involve TNFR1, the Bcl-2 and Bax family of proteins, activation of procaspases and cell cycle regulatory proteins (e.g. p21). Recent *In Vitro* studies demonstrate that TNF- $\alpha$  can initiate apoptosis of auditory hair cells, while another series of studies show that dexamethasone base (DXMb) protects hair cells from TNF- $\alpha$  ototoxicity. However, the mechanisms by which TNF- $\alpha$  kills and DXMb protects hair cells are not fully understood.

**Material and methods:** Total RNA was extracted from 3-day-old rat organ of Corti explants with a Qiagen RNeasy Protect Kit at 0, 12, 24 or 48 hrs *In Vitro* after: 1) no treatment; 2) high dose TNF- $\alpha$  (1 ug/ml); and 3) high dose TNF- $\alpha$  + DXMb (70 ug/ml). Using real-time RT-PCR with SYBR Green, the *mRNAs* were transcribed into *cDNAs* and amplified 40 cycles using primers for: rat *GAPDH* (housekeeping gene); *TNFR1*, *Bcl-2*; *Bax*; *Bcl-xl*; *p53*; and *p21*.

**Results:** *Bax* expression was significantly greater in TNF- $\alpha$  treated as compared to TNF- $\alpha$  + DXMb treated cultures at 48 hrs and was confirmed by mean fold changes in the *Bax/Bcl-2* ratio. These results correlate with the increased expression of *TNFR1* and *p53* in TNF- $\alpha$  cultures at 48 hrs. the otoprotective effects of DXMb in TNF- $\alpha$  cultures were evidenced by up regulation of *Bcl-xl* at 24 and 48 hrs and lower mean fold changes of *Bax*, *TNFR1*, and the *Bax/Bcl-2* ratio. Furthermore, DXMb treatment of TNF- $\alpha$  explants resulted in significant up regulation of *p21* at 24 hrs.

**Conclusions:** TNF- $\alpha$  causes apoptosis of hair cells by: up regulating pro-apoptotic signaling molecules (e.g. *Bax* and *p53*); and down regulating anti-apoptotic signaling molecules (e.g. *Bcl-xl*). DXMb protects auditory hair cells against TNF- $\alpha$  induced apoptosis by: up regulating anti-apoptotic signaling molecules; and down regulating pro-apoptotic signaling molecules. These gene expression results support the use of local dexamethasone treatment to conserve hearing during cochlear implantation.

(Supported by a grant from Advanced Bionics Corporation, Valencia, CA)

## **[162] Glucocorticoid and Mineralocorticoid Induction of Cochlear Mineralocorticoid Receptor-Mediated Proteins**

**Dennis Trune<sup>1</sup>**, Beth Kempton<sup>1</sup>, Barbara Larrain<sup>1</sup>, Fran Hausman<sup>1</sup>

<sup>1</sup>Oregon Health & Science University

Glucocorticoids are used to treat hearing disorders, but little is known of their direct impact on the ear. Besides their immune suppressive function, some glucocorticoids also have strong binding affinity for the mineralocorticoid

receptor that normally binds the hormone aldosterone. Mineralocorticoid receptor-mediated gene products include  $\text{Na}^+, \text{K}^+$ -ATPase and the epithelial sodium channel (ENaC), both of which are involved in endolymph ion homeostasis. This suggests therapeutic glucocorticoids also may be impacting these ion transport functions of the ear to reverse hearing loss. Therefore, to assess glucocorticoid impact on mineralocorticoid receptor functions, mice were given the glucocorticoid prednisolone or mineralocorticoid aldosterone and quantitative sandwich ELISA performed on their cochleas to measure levels of  $\text{Na}^+, \text{K}^+$ -ATPase and ENaC.

Following 24 hours of oral prednisolone (5 mg/kg) or aldosterone (30  $\mu\text{g/kg}$ ), cochleas were harvested, right and left combined, and homogenized with sodium dodecyl sulphate (SDS) to enhance protein recognition by antibodies (SDS-ELISA). Cochlear homogenates (30  $\mu\text{l}$ , 25% of total volume) were applied to 96-well plates coated with capture antibodies for the respective proteins. Following incubation with HRP-conjugated detection antibodies and colorimetric development, optical density was measured and standardized against commercial kidney tissue. Both steroids significantly increased the production of  $\text{Na}^+, \text{K}^+$ -ATPase and ENaC compared to water controls ( $p < 0.0001$ ).

These results revealed that the glucocorticoids have a significant binding affinity for the cochlear mineralocorticoid receptor. Thus, in addition to their cochlear immune suppressive functions, glucocorticoids also can directly affect  $\text{Na}^+$  and  $\text{K}^+$  ion exchange in the endolymph. This suggests cochlear ion homeostatic mechanisms may be relevant in steroid treatments for hearing loss and should be targeted in the design of future therapies.

(Supported by NIH-NIDCD R01 DC05593 & DC005593-S1, NIH-NIDCD R21 DC007443, and NIH-NIDCD P30 DC005983)

### **163 Effects of AAV-Mediated P27 and P53 Sirnas to the Cochlea of Mouse After Kanamycin Treatment**

Laura Pietola<sup>1</sup>, Antti Aarnisalo<sup>1</sup>, Marjo Salminen<sup>2</sup>, Jussi Jero<sup>1</sup>

<sup>1</sup>Dept. of Otorhinolaryngology, Univ. of Helsinki, <sup>2</sup>Institute of Biotechnology, Univ. of Helsinki

Sensorineural hearing loss is a common human deficit, which is often caused by loss of hair cells in the inner ear. Loss of hair cells results in permanent defects in hearing since hair cells are not able to replicate or regenerate. p27<sup>kip1</sup> is a cyclin-dependent kinase-2 inhibitor that acts as a negative regulator in the cell cycle. p53 is a transcription factor that regulates the cell cycle and hence functions as a tumor suppressor.

We have studied the effects of AAV2 mediated p27-GFP-siRNA, p53-GFP-siRNA and p27+p53-GFP-siRNA delivery to the inner ear of a CD-1 mouse. Animals were treated preoperatively with i.p. injections of kanamycin sulphate in order to generate hair cell loss. Vector-siRNA constructs were microinjected into the inner ear through a cochleostomy. Control animals received saline injections.

All operated animals received BrdU for 15 days after microinjections. One month after the vector-siRNA injection the inner ears were removed, fixed and embedded to paraffin. The inner ears were sectioned and further analysed. Transduction efficiency of the vector complexes was determined by fluorescence microscopy. Hair cell regeneration and proliferation was determined immunohistochemically using specific antibodies against BrdU, Ki-67, calbindin, calretinin and parvalbumin.

An uneven GFP-expression was found in the auditory epithelium. p27-GFP-siRNA treated animals had few BrdU stained auditory epithelial cells. Only single BrdU stained auditory epithelial cells were detected after p53-GFP-siRNA or p27+p53-GFP-siRNA injections. It seems that p27-GFP-siRNA and p53-GFP-siRNA promote auditory epithelial cell regeneration after kanamycin treatment.

### **164 Specific Autoimmune Antibodies in Acute Inner Ear Disorders**

Kerstin Ratzlaff<sup>1</sup>, Mark Praetorius<sup>1</sup>, Christina Schlecker<sup>1</sup>, Reinhild Klein<sup>2</sup>, Peter K Plinkert<sup>1</sup>

<sup>1</sup>University of Heidelberg, <sup>2</sup>University of Tuebingen

Introduction: by now the exact pathogenesis of the different forms of acute inner ear disorders like sensorineural hearing loss, sudden deafness, tinnitus and Meniere's disease is still unknown. Disorders of inner ear blood circulation are widely discussed just like viral infections and autoimmune processes.

The aim of this study is to examine specific autoimmune antibodies and their function in occurrence, therapy and prognosis of acute inner ear disorder.

Material and Methods: by now n=70 patients were examined, 32 female and 38 male, suffering from acute inner ear disorder. The average age was about 45.2 years. A general autoimmune disease was not known. Patients underwent a therapy consisting of Prednisone according to Stennert's scheme and Pentoxifylline 3x 400 mg daily. Hearing was examined using pure-tone audiometry at the beginning and 6 weeks after the beginning of therapy. Specific autoimmune antibodies were examined at the beginning and at the end of the therapy using ELISA and immunofluorescence-test (IFL).

Results: Among 70 patients, there were 34 detected with tinnitus (48.57%), 27 with sensorineural hearing loss (38.57%) and 9 with Meniere's disease (12.86%). In about 64% of all patients there was an occurrence of autoimmune antibodies. Antibodies against sarcolemma (ASA) and sinusoids were mostly detected (23%), followed by anti-nuclei-antibodies (ANA; 15.9%). Antibodies against Microsomes, Phospholipids and Laminin were detected each by about 6.5%, and antibodies against anti-Endothelium and smooth muscle (SMA) at about 3% each.

Conclusion: in this study we could demonstrate that there is an occurrence of autoimmune antibodies in acute inner ear disorders. As already described before, this should be considered as one possible mechanism in the pathogenesis of inner ear disease. It is our further aim to examine the effects of these findings in regard to the prognosis and therapeutic treatment of disease.

## **165 Cocksackie-Adenovirus Receptor and Integrin $\alpha_v$ Distributions in the Auditory Epithelium Differ From Adenovirus Transduction Patterns**

**Toru Miyazawa**<sup>1</sup>, Donald Swiderski<sup>2</sup>, Taha Qazi<sup>2</sup>, Masahiko Izumikawa<sup>3</sup>, Shelley Batts<sup>2</sup>, Mark Crumling<sup>2</sup>, Yehoash Raphael<sup>2</sup>

<sup>1</sup>Kanazawa Medical University, <sup>2</sup>Kresge Hearing Research Ins. Univ. Michigan, <sup>3</sup>Kansai Medical University

The cocksackie-adenovirus receptor (CAR) has high affinity for adenoviruses and may be a target for adenoviral binding whereas the integrin  $\alpha_v$  receptor may promote viral entry into cells. We studied CAR and integrin  $\alpha_v$  distribution in mature guinea pig cochleae in normal ears and in ears exposed to ototoxic drugs or intense noise. We also inoculated normal and deafened ears with Ad.GFP and used immunohistochemistry to examine the relationship between expression of these proteins and adenoviral transduction. in normal cochleae, both CAR and integrin  $\alpha_v$  were expressed in sensory hair cells and in many types of supporting cells with the exception of pillar cells. in cochleae deafened with noise or kanamycin/ethacrynic acid, most hair cells are lost, but differentiated supporting cells survive. Expression of CAR and integrin  $\alpha_v$  was noted in both types of surviving cells. in cochleae deafened with neomycin, the organ of Corti was replaced by a flat epithelium, which contained a small sub-population of CAR-positive cells and markedly reduced integrin  $\alpha_v$  expression. in all treatment groups, CAR and integrin  $\alpha_v$  were generally co-localized in the auditory epithelium. in adenovirus inoculated ears, GFP expression pattern only partly corresponded to the CAR/integrin  $\alpha_v$  expression. Notably, hair cells expressed both CAR and integrin  $\alpha_v$  and were GFP-negative, whereas pillar cells appeared to lack both proteins yet were GFP-positive. CAR/integrin and GFP expression in the flat epithelium were limited. Our results indicate that the flat epithelium contains cells which are different from supporting cells in their molecular contents and organization, and that adenovirus entry into some inner ear cell types may not depend on the CAR/integrin pathways.

## **166 Ototoxic Effects On WDR1 Presence in the Avian Inner Ear**

**Henry Adler**<sup>1</sup>

<sup>1</sup>Center of Comparative and Evolutionary Biology of Hearing, University of Maryland

WD repeat-1 protein (WDR1) contains numerous WD40 motifs and demonstrates significant homology to actin-interacting protein 1 (Aip1) in several species such as slime molds. Aip1 binds cofilin/actin depolymerizing factor, suggesting a role of WDR1 in actin dynamics. Also, the chicken gene encoding WDR1 was shifted from hair cells in the normal inner ear to surviving hair cells and supporting cells in the sound-damaged basilar papilla, suggesting a role in inner ear response to acoustic trauma.

Here, we examined WDR1 presence in the inner ears of chicken (21 – 28 days posthatching) following ototoxic treatment. Each bird received a daily subcutaneous

injection of gentamicin (200 mg/kg) for three days, and recovered for 1, 3, or 7 days after the last injection. On the last day of recovery, animals were sacrificed, and their ears processed for two techniques. During reverse transcription - polymerase chain reactions, RNA was isolated from treated and non-treated ears, and its yield for each animal group was normalized to 5  $\mu$ g. Following reverse transcription, cDNA was subjected to PCR with WDR1-specific primers. Each group yielded an expected 510 base-pair band, but it was interesting to detect differences in band intensities among the groups. Both the 1-day and 7-day recovery groups produced the most intense band, more than their age-matched controls, whereas the 3-day control group outshone its 3-day recovery counterpart.

the second technique involved immunocytochemistry with anti-WDR1 antibody on gentamicin-treated and age-matched control ears. Treated and non-treated chicken ears were stained with 1:1,000 rabbit anti-WDR1 Ab and then with 1:1,000 Cy5-conjugated donkey anti rabbit Ab and fluorescein phalloidin. Confocal examinations on those ears showed hair cell loss and disorganized sensory surfaces of surviving hair cells and supporting cells at 1 and 3 days as well as hair cell regeneration at 7 days. These examinations also revealed WDR1 localization in both hair cells and supporting cells in the basilar papilla regions most affected by gentamicin. the observations suggest that WDR1 is involved in inner ear response to stress and that WDR1 is re-localized to supporting cells following ototoxic treatment.

Work supported by NIDCD 000436 and NIH P30-DC04664 (C-CEBH).

## **167 Effect of Montelukast Pre-Treatment On Hearing Loss Induced by Saline Application On the Round Window Membrane**

**You Hyun Kim**<sup>1</sup>, Todd Miller<sup>1</sup>, Dusan Martin<sup>1</sup>, Yoon Hwan Kim<sup>1</sup>, Timothy T.K. Jung<sup>1</sup>

<sup>1</sup>Division of Otolaryngology-Head and Neck Surgery, Loma Linda University, Loma Linda, CA

Background: Saline application to the round window membrane (RWM) has been known to cause hearing loss, but the exact mechanism is unknown. One possible mechanism is the alteration of sodium chloride concentration gradient in normal saline and cochlear perilymph. Montelukast seems to be protective in the group where saline was applied to the RWM. the mechanism of action of montelukast in saline ototoxicity is yet to be discovered.

Objective: the purpose of this study was to determine the effect of treatment with montelukast, a leukotriene (LT) receptor antagonist, on normal saline induced hearing loss.

Study Design and Methods: Two groups were studied using 13 chinchilla ears. the groups are mentioned as follows: substance administered through orogastric tube - substance administered onto the RWM. the two groups consist of: one control group; saline-SALINE (6) and one test group; montelukast-SALINE (7). the montelukast dosage used was 1mg/kg orally diluted in 5ml of normal



saline solution and was administered -24hrs and 0hrs from the time SALINE was placed on the RWM. the same was done with the control group, 5ml of normal saline were administered orally -24hrs and 0hrs from the time SALINE was placed on the RWM. the SALINE was soaked on Gelfoam and placed on RWM. the SALINE was left on the RWM for two hours and then removed. Auditory brainstem response (ABR) thresholds and distortion product ototacoustic emissions (DPOAE) were taken at 0 hrs and after having removed the Gelfoam for the following 6 hours.

Results: ABR measurements showed that hearing loss was at its maximum six hours after SALINE application on the RWM. Both groups had hearing loss when compared but the ABR and DPOAE results show more hearing impairment in the saline-SALINE group than in the montelukast-SALINE group. It seems that montelukast can protect against ototoxicity induced by saline applied on the RWM.

Conclusion: Pre-treatment with montelukast (LT receptor antagonist) was found to prevent hearing loss induced by saline applied on the RWM. LTs may be involved in this ototoxicity.

#### **168 Effects of Prostaglandin E Receptor Agonists On the Inner Ear**

**Ryusuke Hori<sup>1</sup>**, Takayuki Nakagawa<sup>1</sup>, Tatsunori Sakamoto<sup>1</sup>, Takayuki Okano<sup>1</sup>, Yayoi S. Kikkawa<sup>1</sup>, Kazuya Ono<sup>1</sup>, Yoshiko matsunaga<sup>2</sup>, Yuichiro Matsushita<sup>2</sup>, Tsutomu Shiroya<sup>2</sup>, Jyuichi Ito<sup>1</sup>

<sup>1</sup>*Department of Otolaryngology, Head & Neck Surgery, Graduate School of Medicine, Kyoto University,* <sup>2</sup>*ONO PHARMACEUTICAL CO., LTD.*

Prostaglandin E (PGE) has been used for treatment of acute sensorineural hearing loss ; however, actual mechanisms for the effect of PGE have not been fully elucidated. the physiological effects of PGE are mediated by four G protein coupled membrane receptor (EP1, EP2, EP3 and EP4), which are encoded by different genes. EP2 and EP4, in particular, are coupled to adenylate cyclase and generate cyclic adenosine monophosphate (cAMP) that activates the protein kinase (PKA) signaling pathways. Previous reports have involvement of PGE in production of vascular endothelial growth factor (VEGF) and hepatocyte growth factor (HGF) in various types of cells. Zhang et al. have reported that application of PGE induces production of HGF in cultured microglia. Furthermore, it has been indicated that VEGF and HGF induction by PGE may proceed via a cAMP-mediated pathway. in the present study, we investigated the effects of local application of an EP2 or EP4 agonist to inner ears on expression of VEGF and HGF in the mouse cochlea. a content of VEGF or HGF in the cochlea was measured by the EIA method. the results demonstrated significant increase of VEGF following application of EP4 agonists. the level of HGF also exhibited a trend to increase in response to EP4 application, although it was not statistically significant. As HGF and VEGF have a potential for otoprotection, therapeutic effects of PGE might be mediated by increase of these growth factors in the inner

ear. in the future study, we will examine otoprotective effects of EP agonists against hearing impaired animals.

#### **169 Cytoskeletal Inhibitors Block Dying Hair Cell Ejection and Alter Cell Death Progression in organ Cultures of the Chick Cochlea**

**Christina L. Kaiser<sup>1</sup>**, Brittany J. Chapman<sup>1</sup>, Douglas A. Cotanche<sup>1</sup>

<sup>1</sup>*Department of Otolaryngology, Children's Hospital, Boston, MA 02115, USA*

Administration of aminoglycoside antibiotics is known to induce apoptotic death in cochlear hair cells. During the execution phase of apoptosis, the damaged hair cells are ejected out of the sensory epithelium by the surrounding supporting cells. While the exact mechanisms of hair cell extrusion are currently unknown, it is thought that the cytoskeletal proteins actin and myosin may play a role. Previous studies have shown that actin disruption can significantly prevent gentamicin-induced extrusion of bullfrog saccular hair cells and supporting cell scar formation *In Vitro* (Hordichok and Steyger, 2007. *Hear. Res.* 232: 1-19). the purpose of this study is to determine if disruption of actin or myosin cytoskeletal elements can prevent gentamicin-induced hair cell ejection for chick cochleae grown *In Vitro*.

To test this, one-week old birds were sacrificed, and cochleae were dissected in a sterile environment and placed into initial culture medium. After two hours in an incubator, the initial culture medium was replaced and cochleae were incubated in one of three conditions: control culture medium, gentamicin culture medium, or gentamicin culture medium supplemented with cytoskeletal disruption agent (actin—Cytochalasin-D or Latrunculin A; myosin—Y-27632 or ML-9). Following 24 hours of incubation, cochleae were fixed and labeled with myosin VI and phalloidin to visualize hair cells and determine the areas of gentamicin or culture-induced hair cell damage. Preliminary results indicate that the addition of actin disruption agents (in particular Cytochalasin D) to culture medium appears to alter the gentamicin-induced cochlear hair cell damage pattern normally seen *In Vitro*. While this result suggests that actin disruption may prevent gentamicin-induced hair cell ejection in the avian basilar papilla, further studies will be performed to determine if hair cell ejection or rescue does indeed occur.

Supported by NIH NIDCD grants DC01689 (DAC) DC008235 (CLK).

# **170 Functional Interaction Between Mesenchymal Stem Cells (MSC) and Spiral Ligament Fibrocytes Underlies Hearing Recovery After MSC Transplantation Into the Inner Ear**

Guangwei Sun<sup>1</sup>, Hiroko Kouike<sup>1</sup>, Masato Fujii<sup>1</sup>, Tatsuo Matsunaga<sup>1</sup>

<sup>1</sup>National Institute of Sensory organs, National Tokyo Medical Center

Spiral ligament fibrocytes (SLF) play important roles in normal hearing as well as in several types of sensorineural hearing loss attributable to inner ear homeostasis disorders. Our previous study showed when MSC was transplanted into rat inner ear with degenerated fibrocytes, hearing recovery was significantly accelerated compared to control rats without MSC transplantation. In order to learn the characteristics of transplanted MSC and the mechanism of hearing recovery, we investigated the interaction between MSC and SLF *In Vitro*.

Using co-culture system, we investigated the differentiation and proliferation of MSC and SLF. Our results showed the factors secreted by SLF have the ability to promote MSC to transdifferentiate into SLF-like cells. On the other hand, the factors secreted by MSC had a stimulatory effect on proliferation of SLF.

Our results suggest there are two mechanisms of hearing recovery by transplanting of MSC into inner ear. One is transplanted MSC transdifferentiate into SLF-like cells that compensate the lost SLF; the other is transplanted MSC stimulate the regeneration of host SLF. Both mechanisms are considered to contribute functional recovery of spiral ligament.

# **171 Cell Division and Maintenance of Epithelial Integrity in the Deafened Auditory Epithelium**

Young Ho Kim<sup>1</sup>, Yehoash Raphael<sup>2</sup>

<sup>1</sup>Seoul National University, Boramae Hospital, <sup>2</sup>Kresge Hearing Research Institute

Membranous labyrinth cells are quiescent in the normal mammalian cochlea. Loss of hair cells in the organ of Corti is permanent and results in irreversible hearing impairment. Once hair cells are lost, the response of the supporting cells influences possible strategies for therapy. Strategies for future biological therapy will likely be based on insertion of stem cells or induction of transdifferentiation of non-sensory cells to new hair cells. In either case, non-sensory cells that remain in the auditory epithelium of the lesioned cochlea will constitute the substrate for therapy. Administration of neomycin to the perilymph leads to a rapid degeneration of hair cells and flattening of the remaining supporting cells in the auditory epithelium. We now show that robust mitotic activity occurs in the flat epithelium and that dividing cells retain some molecular markers of supporting cells. Mitosis was found to be transient, occurring on the 4th day after the insult. Dividing cells maintained the confluence of tight junctions at the luminal surface. The cell cycle inhibitor, p27Kip1, was present in nuclei of flat epithelial cells, but dividing cells

were negative, suggesting they can spontaneously regulate their cell cycle. The mitotic spindle was parallel to the reticular lamina and its orientation within this plane varied. The average number of dividing cells observed was approximately 50 per cochlea (N=8). Considering that mitosis only lasts 20-60 minutes, the total number of new cells could be hundreds or thousands. Proliferating nuclei were prevalent in basal and second turns, and less frequent in third and apical turns, possibly reflecting the severity of the lesion. These results indicate that the flat epithelium of the cochlea can down-regulate p27Kip1 and divide after a severe lesion, maintaining the epithelial confluence throughout the cochlea. Mitosis in the tissue presents therapeutic opportunities for gene transfer and stem cells therapies.

# **172 In Vivo Effects of Hyperosmotic Perilymph Perfusion On Hair Cell and Neural Potentials**

Greg A. O'Beirne<sup>1</sup>, Robert B. Patuzzi<sup>2</sup>

<sup>1</sup>University of Canterbury, <sup>2</sup>University of Western Australia

The effect of osmotic bias on cochlear potentials was investigated by perfusion of scala tympani with a modified artificial perilymph. The mean osmolality of the artificial perilymph was increased by around 15% (from 303 ± 6 mOsm/kg H<sub>2</sub>O to 349 ± 1 mOsm/kg H<sub>2</sub>O) by addition of sucrose. OHC function was assessed using Boltzmann analysis of the low-frequency CM. Neural thresholds and waveforms were monitored at multiple frequencies, and spontaneous neural noise was monitored via a round-window electrode. The 2-minute perfusions caused a 6 ± 4% increase in the maximal CM amplitude, indicating an increase in OHC basolateral permeability, and an 8 ± 1% increase in MET sensitivity, which may reflect a decrease in OHC axial stiffness. The operating-point shifts recorded were more variable: in healthy animals, the hyperosmotic perfusions caused initial operating point shifts towards scala vestibuli of around 1 – 2 meV that were either followed by a brief undershoot towards scala tympani, or initiated a longer-lasting scala tympani operating point shift. Nonetheless, these operating point shifts were smaller than expected, resulting in a less than ±2 meV deviation from the starting point. Neural thresholds during the perfusion fell (by 20 – 30 dB at 22 kHz), and recovered with a time course consistent with the predicted perilymphatic sucrose concentrations at the corresponding BM place for each frequency. The mechanism of the changes observed with these hyperosmotic perfusions is not known, but its effects were *not* consistent with a simple movement of the reticular lamina towards scala vestibuli. Other data (Marcon and Patuzzi, in preparation) indicate the CAP threshold shifts during these perfusions are most likely mechanical in origin. The experimental results from the guinea pig are compared with simulated perfusions carried out in a mathematical model of cochlear regulation based on the ionic transport mechanisms and motile properties of the outer hair cells.

### **173 Efferent-Induced Changes in Human Cochlear Tuning: Measurements with Stimulus Frequency Otoacoustic Emissions (Sfoaes)**

**Nikolas A. Francis<sup>1</sup>**, John J. Guinan, Jr.<sup>2</sup>

<sup>1</sup>MIT/Health Science & Technology/Speech & Hearing Bioscience & Technology Program, <sup>2</sup>Eaton Peabody Lab/Mass. Eye and Ear Infirmary/Harvard Medical School

in experimental animals, stimulation of medial olivocochlear (MOC) efferents reduces cochlear amplifier (CA) gain thereby making auditory-nerve (AN) tuning curves wider, at least in AN fibers with characteristic frequencies greater than 2 kHz. in humans, it is unknown whether MOC stimulation makes AN tuning wider, and if so, in what frequency range. Filter theory states that a widened filter produces a decreased group delay, so changes in cochlear tuning are expected to be reflected in the group delays of SFOAEs. We hypothesized that in humans, MOC efferent activity would decrease CA gain, widen cochlear tuning and decrease SFOAE group delays. the change in SFOAE group delay was obtained from human ears by measuring the slopes of linear fits to SFOAE phase-versus-frequency functions obtained with and without MOC activity elicited by 60 dB SPL contralateral broad-band noise. SFOAE suppression tests showed that the noise did not evoke middle-ear-muscle contractions. SFOAEs were produced by 40 dB SPL tones in the ipsilateral ear at frequencies 1-8 kHz. in each ear, SFOAE group delays were obtained from SFOAE measurements over 3-7 frequencies spaced 20 Hz apart in a frequency region where the subject had large SFOAEs. the results indicate that contralateral-noise-induced MOC activity (1) produced a phase advance at almost all frequencies, and (2) sometimes

produced decreased group delays, but also sometimes showed no change, or even increased group delays. the phase advance is in accord with the reported MOC-induced phase lead produced in BM motion at low levels. the inconsistent decreases in group delays may indicate that MOC activity does not always widen cochlear tuning.

### **174 Harmonic Distortion of Basilar Membrane Vibration Measured At Two Longitudinal Locations in Living Cochleae**

**Wenxuan He<sup>1</sup>**, Tianying Ren<sup>1</sup>

<sup>1</sup>Oregon Health & Science University

Harmonic distortion of cochlear responses has previously been demonstrated by measuring the cochlear microphonic potential, basilar membrane (BM) vibration, and intracochlear pressure. It remains unclear whether harmonic distortion products propagate inside the cochlea. in this study, the basilar membrane vibration was evoked by pure tones at different frequencies and intensities, and measured at two longitudinal locations using a laser interferometer in sensitive living cochleae. the magnitude transfer function of the BM at the stimulus frequency showed a typical sharp tuning curve and compressive growth at frequencies near the best frequency (BF) of the measured location. the corresponding phase shows a

progressive lag with the frequency. Harmonic distortion products appeared near the BF at stimulus levels as low as 20 dB SPL, and saturated at an intermediate intensity. At low and intermediate intensities, harmonic responses showed a second peak at  $\sim 1/2$  BF for the second harmonics or at  $\sim 1/3$  BF for the third harmonics. At high sound pressure levels, the two peaks merged together and formed a flat response across frequencies. the phase difference between two locations showed that the delay, wave speed, and wavelength of the second harmonic response near  $1/2$  BF were different from those at stimulus frequencies. the data indicate that, at low and intermediate stimulus levels, the harmonics are generated at the BF location of the fundamental tone and travel to harmonic BF locations. At high stimulus levels, harmonic distortion is generated over a wide area along the cochlear partition.

Supported by NIH-NIDCD.

### **175 Longitudinally Propagating Traveling Waves of the Mammalian Tectorial Membrane**

**Roозbeh Ghaffari<sup>1</sup>**, A. J. Aranyosi<sup>2</sup>, Dennis Freeman<sup>1</sup>

<sup>1</sup>Harvard-MIT Division of Health Sciences & Technology,

<sup>2</sup>Research Laboratory of Electronics, Massachusetts Institute of Technology

The remarkable sensitivity and frequency selectivity of the mammalian cochlea depend on traveling waves of motion that propagate along the basilar membrane (BM) and ultimately stimulate the mechano-sensory receptors. the tectorial membrane (TM) plays a key role in this process, but its mechanical function remains unclear. Here we show that the viscoelastic structure of the TM supports traveling waves. Radial forces applied at audio frequencies (2-20 kHz) to isolated TM segments generate longitudinally propagating waves on the TM with velocities similar to those of the BM traveling wave near its best frequency (BF) place. We compute the dynamic shear storage modulus ( $G'$ ) and shear viscosity ( $\eta$ ) of basal ( $G' = 47 \pm 12$  kPa,  $\eta = 0.19 \pm 0.07$  Pa-s;  $n = 5$ ) and apical ( $G' = 17 \pm 5$  kPa,  $\eta = 0.15 \pm 0.04$  Pa-s;  $n = 3$ ) TMs from the propagation velocity of the waves and show that segments of the TM from the basal turn are stiffer than apical segments. Analysis of loading effects of hair bundle stiffness, the limbal attachment of the TM, and viscous damping in the subreticular space suggests that TM traveling waves can occur *In Vivo* (see accompanying poster). These traveling waves can functionally couple a significant longitudinal extent of the cochlea and may interact with the BM wave to greatly enhance cochlear sensitivity and tuning.

### **176 Deflection of IHC Stereocilia by OHC Somatic Electromotility**

**Caio Chiaradia<sup>1</sup>**, Manuela Nowotny<sup>1</sup>, Anthony Gummer<sup>1</sup>

<sup>1</sup>University Tübingen, Section of Physiological Acoustics and Communication

The high sensitivity and precise frequency discrimination of the mammalian cochlea is based on the somatic electromotility of the outer hair cells (OHC). However, the coupling of this motility to the inner hair cells (IHC), the true sensory cells of the cochlea, still remains poorly understood. Nowotny and Gummer (2006) have recently

shown that for pure tones of frequency less than 3 kHz, the somatic electromotility leads to anti-phasic motion of the reticular lamina (RL) and tectorial membrane (TM) in the region of the IHC. This motion is predicted to cause displacement of the fluid inside the subreticular space, the radial component of which is believed to deflect the IHC stereocilia.

We performed experiments in an *In-Vitro* preparation of the guinea-pig cochlea to measure the related displacement of the RL, TM and IHC stereocilia bundle. the organ of Corti was electrically stimulated; the best frequency of the recording location was estimated to be 800 Hz. the resulting transversal vibrations of the RL and TM were measured with a laser Doppler vibrometer, whereas the radial motion of the RL and IHC stereocilia bundle were measured with a fast-line camera (noise floor < 2nm).

The present results show that the RL moves like a rigid body in a combined motion; that is, it not only rotates around a pivot point located close to the pillar cells as Nowotny and Gummer (2006) have shown, but also translates in the radial direction, outward from the modiolus, when the OHCs contract. the deflection of the IHC stereocilia occurs in the same temporal and spatial phase as RL translation, but with larger amplitude. the deflection amplitude of the IHC stereocilia is up to 12 dB larger than RL transversal displacement in the IHC region.

in summary, in addition to high-frequency tuned amplification, there appears to exist a second cochlear amplifying process, operating below 3 kHz, which couples somatic electromotility directly to the IHC stereocilia.

Supported by DFG Gu 194/7-1.

### **177 Trans-Cochlear Sound Pressure Measurements in Human Temporal Bones**

**Hideko Nakajima<sup>1</sup>, Wei Dong<sup>2</sup>, Elizabeth Olson<sup>2</sup>, Michael Ravicz<sup>1</sup>, Saamil Merchant<sup>1</sup>, John Rosowski<sup>1</sup>**

<sup>1</sup>*Eaton-Peabody Lab., Mass. Eye & Ear Inf., Dept. Otology & Laryngology, Harvard Med. Sch., Boston, MA,*

<sup>2</sup>*Columbia Univ., NY, NY*

Intracochlear sound pressures were measured in 6 normal human temporal bone specimens with miniature fiber-optic pressure sensors developed by Olson (1998 JASA 103:3445-3463). the sensors were inserted simultaneously into both scala vestibuli and scala tympani near the oval and round windows and sealed in place. Input sound pressure was measured with a probe-tube microphone near the tympanic membrane. Sound evoked velocities of the stapes and round window were also measured. Precautions were taken to ensure that air was not introduced into the cochlea. the stability of the preparation and of the sensors were determined throughout the procedure.

The sound pressure ratio between scala vestibuli and the ear canal (middle ear gain) was bandpass with maximum gain between 15 and 30 dB at around 0.8-2 kHz. Below 400 Hz, the magnitude had a positive slope of 4-5 dB per octave. the phase was flat below 400 Hz at around 0.2 periods, and decreased approximately ¼ cycle per octave at higher frequencies. the scala tympani pressure gain was

lower than the scala vestibuli by 10 to 20 dB, was flat around 0 dB for  $f < 400$  Hz, and had a bandpass characteristic between 0.6-6 kHz. the phase was 0 at low frequencies, and increased about 0.2 periods around 300-500 Hz, then decreased at ¼ cycle per octave for higher frequencies.

The motion of the cochlear partition is driven by the pressure difference across the partition. the pressure difference between scala vestibuli and scala tympani (normalized to ear canal pressure) had a bandpass characteristic with a peak of 10-28 dB around 1 kHz, and was similar to the scala vestibuli to ear canal pressure gain.

To our knowledge, this is the first time intracochlear pressures have been measured simultaneously in a temporal bone in both scalae. This technique will be valuable in assessing the effects of alterations of middle and inner ear structures (e.g., ossicular lesions, middle ear implants, superior canal dehiscence).

### **178 In-Vivo Impedance of Gerbil organ of Corti From 4 - 20 KHz**

**Wei Dong<sup>1</sup>, Elizabeth Olson<sup>1</sup>**

<sup>1</sup>*Columbia University*

organ of Corti (OC) mechanical impedance was measured from 4 - 20 kHz in the basal turn of the gerbil cochlea. the objective was to quantify the amount of resistance relative to stiffness in the impedance. This is an interesting quantity, as active OHC forces are thought to counteract viscous, resistive forces. We simultaneously measured the basilar membrane (BM) velocity and the scala vestibuli (SV) pressure in the basal turn (best frequency (BF) ~35 kHz) of the cochlea. Pure tones from 200 Hz to 50 kHz were delivered to the ear canal in a closed-field configuration. the BM velocity was measured with a laser interferometer (Polytec) through the transparent round window (RW) membrane, with only a thin layer of covering fluid. the pressure was measured in SV in the region of the cochlear windows, close to the scala media and within ~ 500 micrometers of the BM. Under these conditions the fluid load is relatively small, and at frequencies somewhat less than the BF the measured SV pressure can be considered to be the pressure difference across the OC. Impedance was found by taking the ratio of pressure to velocity. We were able to measure the impedance from ~ 4 to at least 20 kHz. the impedance phase was within 10° of 90° from 4 - 20 kHz, consistent with a stiffness-dominated impedance. the magnitude decreased with frequency, also consistent with a stiffness-dominated impedance. the resistive component of the impedance was relatively small, and in several cases was negative from ~ 4 - 12 kHz. This unexpected finding might be due to a systematic offset in the measurement phase, or something more interesting.

## **179 Impedance Measurements of Isolated Outer Hair Cells**

**Tobias Eckrich<sup>1</sup>**, Manuela Nowotny<sup>1</sup>, Csaba Harasztosi<sup>1</sup>, Marc Scherer<sup>1</sup>, Anthony W. Gummer<sup>1</sup>

<sup>1</sup>*University of Tübingen, Section of Physiological Acoustics and Communication*

The ability of the cochlear partition to amplify and tune sound-induced vibrations is critically dependent on the mechanical impedances of its component structures. Having measured the impedance of the organ of Corti up to 40 kHz (Scherer and Gummer, *Biophys. J.* 2004), we have now investigated the axial impedance of the outer hair cells (OHCs).

OHCs isolated from the basal half of the guinea-pig cochlea had length 20-40  $\mu\text{m}$ . the cells were maintained in Hanks' balanced salt solution (Sigma-Aldrich, modified with 4.17 mM  $\text{NaHCO}_3$  and 10 mM HEPES; osmolarity  $315 \pm 5$  mOsm, pH  $7.35 \pm 0.02$ , RT  $21\text{-}23^\circ\text{C}$ ). a ferromagnetically coated atomic force cantilever (AFL) with length 450  $\mu\text{m}$ , width 35  $\mu\text{m}$ , and thickness 1-2  $\mu\text{m}$  was held against the cuticular plate of the OHC. a frequency independent force was applied to the AFL via a magnetic field. This stimulus contained 30 frequencies (0.12-43.2 kHz) of equal amplitude but uniformly randomized phase. the resulting AFL velocity was measured with a laser Doppler vibrometer (Polytec, Waldbronn, Germany). the cell impedance was calculated from velocity measurements with and without the AFL loaded by the OHC. the effect of axial compression of the cell by the AFL on the impedance values was investigated in 1- $\mu\text{m}$  steps.

The OHC impedance was purely viscoelastic, without inertia and without resonance. the real and imaginary components of the impedance were quantitatively described by a Voigt-Kelvin model, with stiffness  $k$  and damping  $r$  estimated by nonlinear fitting. with increasing axial compression,  $k$  and  $r$  increased, whereas their ratio remained approximately constant ( $r/k = 0.3$ ), independent of compression up to 12  $\mu\text{m}$ . Application of 9-AC (anthracene-9-carboxylic acid; 1 mM), a nonspecific anion channel blocker, led to reversible reduction of  $k$  and  $r$  (by factors of 2-4).

in summary, the transfer function between force generated by the OHC and length change was independent of frequency and compression.

Supported by DFG Gu 194/5-1,2; 7-1.

## **180 Extraction of DPOAE Generator and Reflection Components in the Time Domain in Adults and Infants**

**Glenis Long<sup>1</sup>**, Carrick Talmadge<sup>2</sup>, Beth Prieve<sup>3</sup>, Lisa Lahtinen<sup>3</sup>

<sup>1</sup>*Graduate Center, City University of New York*, <sup>2</sup>*National Center of Physical Acoustics, University of Mississippi*,

<sup>3</sup>*Syracuse University*

DPOAE are believed to consist of two major components: the generator component (short latency) from the region where the primaries overlap on the basilar membrane and the reflection component (longer latency) from the DP region. Because the two components have different

delays, they can be extracted and analyzed separately. When continuously sweeping primaries are used the separate components can be extracted from the sound file using a Least Squares Fit (LSF) analysis that models the sweeping DPOAE. This procedure evaluates the DPOAE components directly from the sound file without the addition of a suppressor. It also avoids the extraction of the components using spectral analysis and reconvolving to the time domain before filtering as is done when the inverse Fourier Transform (IFFT) is used to extract the two components. When a narrow-band LSF analysis with little delay is used with minimal delay, the generator component can be extracted. the reflection component returns too late to fall within the filter. the phase of the reflection component varies more with frequency than does the generator component. This necessitated modifications of the least LSF procedure to permit dynamic fitting of the delay of a given component. This more direct procedure to extract the two components reduces the spectral and temporal splatter, which otherwise can limit the effectiveness the IFFT procedure. the modified LSF procedure was applied to DPOAEs measured from normal-hearing adult and infant ears to permit evaluation of development of the generator and reflection components of DPOAEs.

## **181 Modeling the Distribution of Distortion-Product Otoacoustic Emission Generators in the Cochlea**

Xuedong Zhang<sup>1</sup>, **David C. Mountain<sup>1</sup>**, Allyn E. Hubbard<sup>2</sup>

<sup>1</sup>*Hearing Research Center, Department of Biomedical Engineering, Boston University*, <sup>2</sup>*Hearing Research Center, Department of Electrical and Computer Engineering, Boston University*

It is believed that most distortion product otoacoustic emissions (DPOAE) originate near the peak response region of the higher-frequency primary (F2), and that the generation of the distortion product is determined by the nonlinear electro-mechanical responses of the outer hair cells in that region.

This study explores the generation and propagation of DPOAEs within the cochlea using numerical simulation. in order to understand the relative contribution of different cochlear locations to the DPOAE measured in the ear canal, the nonlinear components that generate the distortion product (DP) in the model were replaced by active sources (generators) that generate responses, which propagate in both directions along the cochlea. the DPOAE measured in ear canal is then a superposition of responses to these distributed individual generators. the ear canal response is determined by three factors: 1) the responses to primaries along the cochlea (NOTE: we use actual experimental data for this step), 2) the relationship between the magnitude and phase of the active sources and the responses to the primaries at the generation sites (generator function), and 3) the transfer function between each generation site and the ear canal.

Our results show that with simple generator functions, the contributions of generators near the peak response region of primaries cancel each other due to the rapid phase

change in this region, and that the positions of the generators that dominate the DPOAE at ear canal change as  $F_1$  changes, when  $F_2$  is fixed. Our results also demonstrate that generator functions more complex than normally assumed are needed to fit the  $F_2$ -fixed DPOAE data (both magnitude and phase).

[Funded by NIDCD grant R01-DC29]

## **182 Vertical Phase Banding in DPOAE Level/Phase Maps is Not Necessarily Indicative of Place-Fixed Emissions**

**Glen Martin**<sup>1,2</sup>, Barden Stagner<sup>1</sup>, Terry Fleck<sup>3</sup>, Paul Fahey<sup>4</sup>, Brenda Lonsbury-Martin<sup>1,2</sup>

<sup>1</sup>VA Loma Linda Healthcare System, <sup>2</sup>Dept of Otolaryngology, Loma Linda Univ Medical Center, Loma Linda CA, <sup>3</sup>Loma Linda Univ School of Medicine, <sup>4</sup>Dept of Physics and Electrical Engineering, Univ of Scranton, Scranton PA

DPOAE level/phase maps were acquired from normal-hearing humans and from rabbits pre- and post-noise exposure. to construct DPOAE ratio vs level and phase maps, DPOAEs were measured in DPOAE-frequency steps of ~44 Hz from 0.5-6 kHz using constant  $f_2/f_1$  ratio sweeps in increments of 0.025 from 1.025-1.5 at various primary-tone levels. DPOAE level was directly plotted, while phase was corrected for primary-tone phase variation and unwrapped before plotting. Maps were collected with and without an interference tone (IT) on alternate trials to minimize time-dependent changes. IT effects were further evaluated by taking vector differences of the maps to obtain a residual. in both humans and rabbits,  $2f_1$ - $f_2$  DPOAEs showed horizontal 'wave-fixed' phase bands at standard  $f_2/f_1$  ratios of 1.21 and 1.25, respectively, and evidence of vertical 'place-fixed' phase banding for closely spaced  $f_2/f_1$  ratios. When present,  $2f_2$ - $f_1$  DPOAEs showed vertical phase bands. ITs placed 44 Hz below  $2f_1$ - $f_2$  or  $2f_2$ - $f_1$  DPOAEs in humans produced the expected residual and decreased fine structure in the related DP-grams but did not eliminate large areas of vertical phase banding. in rabbits ITs placed 44 Hz below  $2f_1$ - $f_2$  or  $2f_2$ - $f_1$  DPOAEs produced minimal or no effects on emissions associated with vertical phase banding. Increasing IT levels in rabbits yielded a residual with horizontal phase bands consistent with effects at the  $f_2$  place. ITs placed at frequencies well above  $f_2$  in rabbits tended to eliminate vertical phase banding, phase ambiguities, and notches in the DPOAE level maps. the resulting residuals were large and had predominately horizontal phase banding. in humans similar effects could be observed but were not as dramatic. the above, as well as the inability of ITs near the DPOAE to affect vertical phase banding in rabbits or to eliminate it in humans were unexpected based upon the 2-source model of DPOAE generation. (Supported by NIDCD DC000613, DC003114, VA/RR&D C4494R).

## **183 Potential Source of Level Dependent Nulls in Rabbit Dpoaes**

**Paul Fahey**<sup>1</sup>, Barden Stagner<sup>2</sup>, Glen Martin<sup>3</sup>

<sup>1</sup>University of Scranton, <sup>2</sup>VA Loma Linda Healthcare, <sup>3</sup>Dept of Otolaryngology Loma Linda Univ Medical Center

Sharp level dependent minimae (nulls) in the distortion product otoacoustic emissions (DPOAEs) have been postulated to be due two different mechanisms. We show here that the level dependent nulls in rabbit  $2f_1$ - $f_2$  DPOAEs carry the signature of the mixing of a third order nonlinear term with a fifth order nonlinear term. That is, the minimae are possibly not due to the mixing of signals from two different physical sites of generation, but rather are due to the nature of the nonlinear response itself. It is shown that several properties of nonlinear input/output functions are indifferent to null production

## **184 Simulating the Propagation of Distortion Product Otoacoustic Emissions in the Human Cochlea**

**Qin Gong**<sup>1</sup>, Huijun Jin<sup>1</sup>, Shixiong Chen<sup>1</sup>, Weiming Song<sup>2</sup>

<sup>1</sup>Tsinghua University, <sup>2</sup>Third Hospital of Peking University

Simulating the propagation of distortion product otoacoustic emissions in the human cochlea

Qin Gong<sup>1</sup>, Huijun Jin<sup>1</sup>, Shixiong Chen<sup>1</sup>, Weiming Song<sup>2</sup>,

<sup>1</sup> Tsinghua University, P.R.China.

<sup>2</sup> Third Hospital of Beijing University, P. R. China

We model the propagation of DPOAEs in the human cochlea on the basis of group delays of distortion-product otoacoustic emissions (DPOAEs) and auditory brainstem responses (ABRs) recorded in the same human ears, and signal front delays obtained from the literature (Ruggero and Temchin, JARO 8: 153-166, 2007). DPOAEs were stimulated by tones  $f_1$  and  $f_2$  ( $f_2 > f_1$ ) presented at 65 and 50 dB SPL, respectively. the group delays of the DPOAEs ( $T_{DPOAE}$ ) were determined from the slopes of  $2f_1$ - $f_2$  phase-vs.-frequency functions using swept- $f_1$  and swept- $f_2$  paradigms. the ABR delays were derived from the peak-V latencies minus the mean  $I-V$  peak interval, corrected for acoustic and synaptic delays. ABRs were stimulated with tones presented at 70dBnHL and frequencies equal to the  $f_2$  frequencies used to stimulate DPOAEs using the swept- $f_2$  paradigm, to permit a direct comparison between DPOAE and ABR delays. in our model,  $T_{DPOAE}$  includes three delays (Ruggero and Temchin, JARO 8: 153-166, 2007): 1) signal-front delay, the forward travel time from the oval window to the DPOAE generation place; 2) filter delay; 3) backward travel time of DPOAEs from the generation place to the oval window. the model produced good fits to the DPOAE experiment data.

**185 Effect of Ear Canal Pressure On Spontaneous Otoacoustic Emissions: Spectral Width of Emissions As a Measure of Inner Ear Signal-To-Noise Ratio**

Pim Van Dijk<sup>1</sup>, Bert Maat<sup>1</sup>

<sup>1</sup>Dpt. of Otorhinolaryngology, University Medical Center Groningen, the Netherlands

The frequency and amplitude of spontaneous otoacoustic emissions depend on ear canal pressure. It is unclear whether this is due to changes in the middle ear transmission, or whether the intra-cochlear source signal depends on the ear canal pressure. Spectral peaks corresponding to a spontaneous emission have a finite width due to the interactions of the emission generators with intra-cochlear noise. If the application of ear canal pressure does not influence the intra-cochlear generator signals, the corresponding spectral peak width is not expected to change. In contrast, if the intra-cochlear generator signals do depend on static pressure, the spectral peak width will correspondingly change as well. We recorded spontaneous otoacoustic emissions in 7 normal hearing subjects. Recordings were performed at various ear canal pressures, ranging from  $p = -200$  daPa to  $+200$  daPa in steps of 50 daPa. The frequency, amplitude and width of 41 peaks in the emission spectra were analyzed. On average, emission frequency was increased 4.4 (s.d. 7.5) Hz at  $-200$  daPa and 1.9 (s.d. 9.1) Hz at  $+200$  daPa. Average amplitude was changed by  $-3.4$  (s.d. 3.5) dB at  $-200$  daPa and  $-4.0$  (s.d. 3.6) dB at  $+200$  daPa. The standard deviations reflect the large range of behaviours observed. Spectral peak widths (FWHM) ranged from 0.24 Hz to 46.2 Hz. In the majority of emission peaks, the width varied with ear canal pressure and was inversely proportional to the emission amplitude for all or a large range of pressures. This behaviour is consistent with that of a mathematical oscillator that interacts with noise: if the oscillator parameters vary such that the oscillation amplitude changes, the spectral peak width of the oscillation signal is inversely proportional to the oscillation amplitude. Therefore our results imply that changing the ear canal pressure changed the intra-cochlear emission source signal.

**186 Stimulus-Frequency Otoacoustic Emissions in Normal Hearing Humans Obtained with a Frequency Sweeping Method Over 0.5 to 8 KHz**

Gerhard W. Hill<sup>1</sup>, Kourosh Parham<sup>1</sup>, Yong-Sun Choi<sup>2</sup>, Duck O. Kim<sup>3</sup>

<sup>1</sup>Div. of Otolaryngology, Dept. of Surgery, Univ. of Connecticut Health Center, Farmington, CT 06030, <sup>2</sup>Dept. of Bio and Brain Eng., Korea Adv. Inst. of Sci. and Tech., Daejeon 305-701, Republic of Korea, <sup>3</sup>Dept. of Neuroscience, Univ. of Connecticut Health Center, Farmington, CT 06030

The present study applied a recently developed efficient method of measuring stimulus-frequency otoacoustic emissions (SFOAEs) over a wide range of frequencies spanning four octaves, 0.5–8 kHz, in adult humans with

normal hearing. This efficient method makes a combined use of continuously swept stimulus frequency and heterodyne analysis originally developed by Choi, Lee, Parham, Neely, and Kim (submitted for publication) where it was initially applied to humans over a limited range of frequencies, 550–1450 Hz. We utilized a similar method and have applied it to an expanded range of frequencies. The advantage of this method is that it provides a high resolution of SFOAE data in a much shorter time than would be required by a conventional method where SFOAEs are measured for one frequency at a time.

In the present study, we used a stimulus where frequency was swept exponentially from 0.5 to 8 kHz. We presented the stimulus at several probe tone levels, 30 to 65 dB SPL re 20  $\mu$ Pa. Using the heterodyne analysis of SFOAE, we examined level and phase of SFOAE as functions of a logarithmic scale of frequency. During this off-line analysis, one can use various frequency resolutions. We chose 500 points per octave as a sufficient resolution to discern the SFOAE fine structures. This resolution corresponds to a frequency spacing of 1.4 Hz at 1 kHz. From these data, we determined the following features of SFOAE fine structures: average peak level, the number of peaks, number of cycles of phase change and energy-weighted group delays. These features for each octave were compared across the four octaves and over different stimulus levels. These observations provide information that can help determine parameters of human cochlear models (e.g., Choi et al.) and provide a normal baseline for future testing of SFOAEs of hearing-impaired humans.

**187 New Procedure for Evaluating Sfoaes Without Suppression or Vector Subtraction**

Glenis Long<sup>1</sup>, Carrick Talmadge<sup>2</sup>, Changmo Jeung<sup>1</sup>

<sup>1</sup>Graduate Center, City University of New York, <sup>2</sup>National Center of Physical Acoustics, University of Mississippi

The SFOAE is generated in the cochlea and has to travel along the basilar membrane before being measured in the ear canal. Cochlear travel times mean that the SFOAE is always delayed relative to the stimulus permitting extraction of the SFOAE based on this delay when continuously sweeping tones are used. The SFOAE delay is frequency dependent. We have modified the continuously sweeping tone procedure developed in our lab for evaluating DPOAE to separate the stimulus and SFOAE. The LSF procedure was modified to permit dynamic fitting of the delay of a given signal component permitting the extraction of the time varying SFOAE. This procedure permits evaluation of the SFOAE without using suppression or vector subtraction. The effects of suppressors on SFOAE obtained in this way were investigated to evaluate local and propagating components of SFOAE. This work was supported by the National organization for Hearing Research foundation (NOHR)



**188 Distortion Product Otoacoustic Emissions: Comparison Between the “Traditional” (Two-Tone) and a Novel (Multi-Tone) Stimulus Paradigm**

**Sebastiaan Meenderink<sup>1</sup>**, Marcel v/d Heijden<sup>1</sup>

<sup>1</sup>*Erasmus MC, Rotterdam, the Netherlands*

When the ear is stimulated by two simultaneous tones having an appropriate frequency ratio, it produces additional frequency components that can be recorded from the ear canal with a sensitive microphone. These so-called distortion product otoacoustic emissions (DPOAEs) are well known, and over the last 3 decades have been an important tool in auditory research and audiological tests. Thus far, this involved the presentation of a two-tone stimulus to evoke DPOAEs. We investigated whether tone complexes consisting of more than two tones are suitable for DPOAE-research, whether such stimuli have added value in terms of measurement efficiency, and whether they allow the derivation of information on cochlear mechanics that cannot be derived from two-tone stimuli.

Recently, irregularly spaced tone complexes (termed *zweis* stimuli) were successfully employed to further the interpretation of neural data in relation to cochlear mechanics [van der Heijden & Joris, (2003), *J. Neurosci.* 23:9194-8]. This stimulus is carefully designed to optimally “survive” the various nonlinear properties of sound transduction within the inner ear, and thus allows the derivation of information from the recorded neural spike train that is not attainable with more traditional stimuli.

We have adapted the *zweis*-stimulus so that it can be used to evoke otoacoustic emissions (i.e. *zweis*-OAEs). To this end, one or both of the primary tones of the customary two-tone stimulus was replaced by a *zweis*-compliant tone complex. Preliminary data show that this novel stimulus paradigm evokes otoacoustic emissions that are very similar to DPOAEs that were evoked by tone pairs. We present data of both “traditional” DPOAEs and various types of *zweis*-OAEs and compare their properties.

**189 Exploring the Optimal Signal Conditions for Recording Quadratic Distortion Product Otoacoustic Emission in Humans**

**Shixiong Chen<sup>1</sup>**, Lin Bian<sup>1</sup>

<sup>1</sup>*Arizona State University*

When our ears are stimulated by two pure tones ( $f_1$ ,  $f_2$ , and  $f_1 < f_2$ ), it can generate a series of distortion product otoacoustic emissions (DPOAEs). Quadratic difference tone (QDT,  $f_2 - f_1$ ) is a major DPOAE component which can be enhanced or suppressed by a low-frequency bias tone as shown in our previous studies in animals. The QDT modulation pattern reflects the compressive nonlinearity of the cochlear transduction and can potentially be applied to the diagnosis of cochlear pathology. Due to its low amplitude, QDT has not been as widely used as the cubic difference tone (CDT,  $2f_1 - f_2$ ) in research and clinical practice. This study is to seek the optimal signal conditions to produce large enough QDT for diagnostic purposes. Experiments were carried out on human subjects, with

levels of  $f_1$  and  $f_2$  swept separately from 54 to 75 dB SPL in 3-dB steps, and  $f_2/f_1$  ratios expanded from 1.2 to 1.8 with an interval of 0.1. Experimental results showed that the largest QDT could be obtained when the frequency ratio equaled 1.4. As the  $f_2/f_1$  ratio increased, the QDT amplitude showed a dip at 1.5 and a limited rise up to 1.6. Large QDT amplitude could be obtained with either higher level of  $f_1$  or  $f_2$  without a preferred  $f_1$  and  $f_2$  level difference. When the level of  $f_1$  or  $f_2$  was fixed, the QDT magnitude grew linearly with the increase in the level of the other tone. The QDT growth pattern was different from that of CDT which exhibited nonlinear input-output relation at high stimulus levels. Larger QDT can be recorded under conditions that are different from those for measuring CDT and its amplitude could be as large as CDT. This indicates that under these new signal conditions QDT could be used as a clinical measure for the diagnosis of hearing disorders due to alterations in cochlear transduction.

*Supported by NIH/NIDCD grant: R03 DC006165*

**190 DPOAE Fine Structure in Human Infants**

**Carolina Abdala<sup>1</sup>**, Sumitrajit Dhar<sup>2</sup>, Sandra Oba<sup>1</sup>, Rebekah Abel<sup>2</sup>

<sup>1</sup>*House Ear Institute*, <sup>2</sup>*Northwestern University*

Distortion product otoacoustic emissions (DPOAEs) measured in human newborns are not adult-like and do not become adult-like until sometime after at least 6 months of age. The underlying source of these age effects has not been fully specified. Recent studies (Abdala & Keefe, 2006; Keefe & Abdala, 2007) have identified outer and middle ear immaturities that only partially explain the differences in DPOAE characteristics between adults and infants. DPOAE fine structure is a pseudo periodic pattern of alternating minima and maxima seen in high-resolution recordings of DPOAE level and group delay. In the case of DPOAEs with characteristic frequency (CF)  $> f_2$ , this pattern reflects constructive and destructive interaction between (at least) two distortion components, one from the overlap region of the stimulus tones and the other from the distortion CF region. Maturation of DPOAE fine structure and the individual distortion components that produce fine structure, has only been preliminarily explored in the literature (Dhar & Abdala, 2007) but may hold important clues into the origin of DPOAE immaturities in human infants. In this study, fine structure prevalence, depth and spacing were examined in a group of newborns and adults. Additionally, the two distortion components were separated and individually compared across age groups and a comparison of fine structure spacing across OAE types was conducted. Fine structure spacing in DPOAEs is thought to be driven by the phase gradient of the CF component which is similar in characteristics to stimulus frequency emissions. Thus, the spacing of DPOAE fine structure is expected to be related to that of stimulus-frequency and spontaneous OAEs.

Results of this study show greater DPOAE fine structure depth, wider spacing and a greater prevalence of non-log-sine morphology in infants compared to adults. Results of DP component analyses and comparisons across OAEs will be reported and discussed. While some of our findings may be explained by an immature outer and

middle ear system in newborns, we argue that some observed findings might be due to remnant immaturities in passive properties of the basilar membrane in the newborn human cochlea.

### **191 Low-Frequency and High-Frequency DPOAE Suppression in Humans**

**Michael Gorga<sup>1</sup>**, Stephen Neely<sup>1</sup>, Darcia Dierking<sup>1</sup>, Judy Kopun<sup>1</sup>, Kristin Jolkowski<sup>1</sup>, Kristin Groenenboom<sup>1</sup>, Hongyang Tan<sup>1</sup>, Bettina Stiegemann<sup>1</sup>

<sup>1</sup>*Boys Town National Research Hospital*

Distortion product otoacoustic emission (DPOAE) suppression was measured with  $f_2 = 500$  and 4000 Hz for ranges of primary levels ( $L_2$ ), suppressor frequencies ( $f_3$ ), and suppressor levels ( $L_3$ ) in 19 normal-hearing subjects. This poster provides a detailed description of the experimental approach that we followed in order to collect comparable data at both  $f_2$  frequencies.  $L_2$  was set relative to each subject's threshold (dB SL), which compensates for differences in forward transmission through the middle ear and helps to equate the "internal" representation of stimuli at the two  $f_2$  frequencies.  $L_1$  was optimized for each  $L_2$ , each  $f_2$  and each subject, which adjusts for variability in optimal stimulus conditions across either frequency or subject. Measurement-based stopping rules with long averaging times (maximum of 210 seconds of artifact-free averaging time per point) were used in efforts to minimize the influence of differences in noise level across frequency. Data were converted to decrements (amount of suppression) by subtracting the response during a suppression condition from the response observed during a control condition when no suppressor was presented. While intersubject variability in absolute DPOAE level was large, within-subject variability was less, with average standard deviations for the control condition of about 2 dB. Slopes of decrement-versus- $L_3$  functions decreased as  $f_3$  increased and were similar at the two  $f_2$  frequencies. Suppression tuning curves (STC) were constructed from decrement functions. As expected, STCs were more sharply tuned at 4000 Hz, but low-frequency tails were more clearly observed at 500 Hz. an accompanying poster describes trends observed in these STCs in relation to cochlear nonlinear processing for low and high frequencies (Neely et al., 2008). [Work Supported by the NIDCD (R01 DC002251 and P30 DC004662)]

### **192 Base-Apex Trends Revealed by DPOAE Suppression Tuning in Humans**

**Stephen Neely<sup>1</sup>**, Michael Gorga<sup>1</sup>, Darcia Dierking<sup>1</sup>, Judy Kopun<sup>1</sup>, Kristin Jolkowski<sup>1</sup>, Kristin Groenenboom<sup>1</sup>, Hongyang Tan<sup>1</sup>, Bettina Stiegemann<sup>1</sup>

<sup>1</sup>*Boys Town National Research Hospital*

Suppression tuning curves (STC) were constructed from distortion product otoacoustic emission (DPOAE) suppression measured with  $f_2 = 500$  and 4000 Hz for ranges of primary levels ( $L_2$ ), suppressor frequencies ( $f_3$ ), and suppressor levels ( $L_3$ ) in 19 normal-hearing subjects. (These data are described in an accompanying poster, Gorga et al., 2008.) STC features are summarized in terms of (1) suppression for on- and low-frequency suppressors,

(2) tip-to-tail differences, (3)  $Q_{ERB}$ , and (4) best frequency. the slope of functions relating suppression "threshold" ( $L_3$  for a 3-dB decrement) to  $L_2$  for off-frequency suppressors provides an estimate of compression that is similar for 500 Hz and 4000 Hz. Tip-to-tail differences,  $Q_{ERB}$  and best frequency decreased as  $L_2$  increased for both  $f_2$  frequencies. However, tip-to-tail difference (an estimate of cochlear-amplifier gain) was greater by 20 dB when  $f_2 = 4000$  Hz, compared to when  $f_2 = 500$  Hz.  $Q_{ERB}$  decreased to a greater extent with  $L_2$  when  $f_2 = 4000$  Hz, but, on a relative frequency scale (octaves), best frequency shifted more when  $f_2 = 500$  Hz.  $Q_{ERB}$  and tip-to tail share the same linear relationship at 500 and 4000 Hz.  $Q_{ERB}$  trends between 500 and 4000 Hz over a 40-dB range in level are similar to trends observed in the level and frequency dependence of tone-burst ABR latencies (Neely et al, 1988). [Work Supported by the NIDCD (R01 DC002251, R01 DC00 8318, and P30 DC004662)]

### **193 Dynamics of Human organ of Corti Homeostasis and Fatigue As Inferred From Post Exposure OAE Fluctuations**

**David Kemp<sup>1</sup>**, Oliver Brill<sup>2</sup>

<sup>1</sup>*UCL Ear Institute London*, <sup>2</sup>*Otodynamics Ltd*

Following short (0.1-2min) exposures to sounds in excess of 80dB SPL human otoacoustic emissions levels exhibit damped oscillation at about 5mHz. These can be well fitted by a simple resonant system model excited at both exposure onset and offset. We report that the fit to the model is substantially improved if a small slow linear downward term is added during exposure and reversed after. We propose the oscillation reveals the transient response of a strong under-damped negative feedback homeostatic system which regulates a key aspect of organ of Corti status and stabilises cochlear amplifier gain. During exposures >60seconds the organ of Corti status is largely restored to a condition where cochlear amplifier gain is 'normal' at the end of exposure. This would help hearing threshold recover rapidly. the observed linear superposition of onset and offset oscillations indicates a system operating within its functional range, not one which is fatigued. the small slow depression accumulating during exposures may be the onset of true fatigue which we propose occurs because restoring 'normal' status during exposure is 'expensive' in metabolic resource.

Only otoacoustic emissions of frequency higher than the exposure frequency are affected indicating that the negative feedback system is excited locally not globally by overstimulation. Travelling wave envelope shape suggests that very low frequency exposures should excite the negative feedback system more strongly at more apical places but we find similar degrees of OAE oscillation over several octaves of OAE frequency. This leads to the possibility that cells at more basal locations are more susceptible to overstimulation. the technique offers a way to parameterise an individual's cochlear homeostatic dynamic performance and its susceptibility to fatigue.

Kevanishvilli Z. et al (2006) Behaviour of evoked otoacoustic emission under low-frequency tone exposure:

### **194 Stimulus-Frequency OAE Phase-Gradient Delays in Non-Human Primates**

**Christopher Bergevin<sup>1</sup>**, Radha Kalluri<sup>2</sup>, Christopher A. Shera<sup>3</sup>

<sup>1</sup>University of Arizona, <sup>2</sup>Massachusetts Eye and Ear Infirmary, <sup>3</sup>Harvard Medical School

Humans have significantly longer stimulus-frequency otoacoustic emission (SFOAE) phase-gradient delays than any other species so far examined. Are human OAE delays truly exceptional? We address this question by examining SFOAEs in old-world monkeys (Cercopithecidae), a family more closely related phylogenetically to humans than other laboratory animals typically used in OAE studies (e.g. cats, guinea pigs, chinchillas). SFOAE phase-gradient delays were measured in anesthetized rhesus monkeys (*Macaca mulatta*, N=6) using moderate stimulus intensities (40-50 dB SPL). Signal-to-noise ratios at frequencies in the range 2-4 kHz were sufficient to permit phase unwrapping and computation of the phase-gradient delay. Preliminary results indicate that delays in the rhesus monkey are typically 4-7 ms, decreasing with frequency. These delays are comparable to (although slightly less than) those of humans and are significantly longer than delays so far measured in other mammalian (and non-mammalian) species, which are typically 0.5-2 ms over the same frequency range. Previous studies have shown that SFOAE phase-gradient delays correlate with physiological measures of cochlear frequency selectivity [Shera, Guinan & Oxenham, PNAS, 2002]. The long delays measured in rhesus monkeys therefore suggest that these old-world monkeys may have relatively sharp auditory tuning, as previously suggested for humans. This notion is consistent with the observation of sharper auditory-nerve-fiber frequency selectivity in old-world monkeys relative to cats [Joris et al., ARO, 2006].

Work supported by NIH grant R01 DC003687.

### **195 Spontaneous and Tone-Evoked Otoacoustic Emissions in Mice**

**Renee Banakis<sup>1</sup>**, Mary Ann Cheatham<sup>1</sup>, Peter Dallos<sup>1</sup>, Jonathan Siegel<sup>1</sup>

<sup>1</sup>Northwestern University

The proliferation of studies using mouse genetics to probe the cellular mechanisms of cochlear mechanics motivated this characterization of otoacoustic emissions evoked by tonal stimuli in mice. Attempts to record spontaneous otoacoustic emissions (SOAEs), stimulus-frequency otoacoustic emissions (SFOAEs) and distortion-product otoacoustic emissions (DPOAEs) were made in thirty-two mice. A group of three SOAEs near 20-25 kHz were recorded in one mouse with especially large SFOAE, but periodic (in frequency) variations in the noise floor in several other animals with large SFOAE, suggested near-spontaneous oscillation. The frequency interval of spectral fluctuations in the noise floor, or between multiple SOAE, was approximately that for which SFOAE phase changed

by one period. SFOAE group delays are consistently near zero for stimuli below 10 kHz, where their amplitudes are relatively small, but continue a trend of decreasing group delay with increasing frequency for higher probe frequencies where SFOAE levels are relatively larger, as noted in other species [i.e., Siegel, et al, J. Acoust. Soc. Am. 118, 2434-2443 (2005)]. The DPOAE  $2f_1$ - $f_2$  recorded in the presence of a suppressor near the DP frequency revealed additional support for the proposed two regions where DPOAE are generated. The component originating in the region of the DP place appears to be largest, relative to that originating in the region of interaction of the stimulus tones, when  $2f_1$ - $f_2$  is in the range of frequencies where SFOAEs are large. This finding suggests that emission generation near the DP place is more prominent in regions of the cochlea that generally produce larger emissions.

Supported by the Hugh Knowles Center and NIDCD grant DC00089.

### **196 Distortion Product Otoacoustic Emissions in the Common Marmoset (*Callithrix jacchus*): Parameter Optimization, Normative and Comparative Findings**

**Michelle D Valero<sup>1</sup>**, Rama Ratnam<sup>1</sup>

<sup>1</sup>University of Texas at San Antonio

Distortion product otoacoustic emissions in the common marmoset (*Callithrix jacchus*): Parameter optimization, normative and comparative findings

Michelle D Valero<sup>1</sup>, Victor Sanchez<sup>1</sup>, Edward G Pasanen<sup>2</sup>, Dennis McFadden<sup>2</sup>, Rama Ratnam<sup>1</sup>

<sup>1</sup>University of Texas at San Antonio, <sup>2</sup>University of Texas at Austin

Distortion-product otoacoustic emissions (DPOAEs) were measured in the common marmoset (*Callithrix jacchus*), a New World primate. The optimal stimulus parameters to generate DPOAEs of maximal amplitude were determined for  $f_2$  frequencies from 3 – 24 kHz. The optimal frequency ratio ( $f_2/f_1$ ) was determined by varying  $f_2/f_1$  from 1.02 – 1.40, using equal-level primary tones. The optimal  $f_2/f_1$  decreased with increasing  $f_2$  frequency between 3 – 17 kHz, but increased at 24 kHz. The optimal  $f_2/f_1$  was positively correlated with increasing primary tone levels from 50 – 74 dB SPL. When all stimulus parameters were considered, the mean optimal  $f_2/f_1$  ranged from 1.21 – 1.24. Varying the difference in level of the primary tones ( $L_1 - L_2$ ) from 0 – 10 dB SPL ( $f_2/f_1 = 1.21$ ) showed that increasing  $L_1 - L_2$  minimally affected DPOAE strength. For comparisons between species, we measured DPOAEs from 3 – 24 kHz in marmosets and from 3 – 18 kHz in humans in 1/5 octave steps. The average DPOAE levels were approximately equal at frequencies up to 4.5 kHz. This study shows that DPOAE characteristics in the marmoset are similar to those of humans and Old World primates, which presumably indicates similarities in cochlear physiology and cochlear structure. Additionally, it suggests that the marmoset is an appropriate human proxy for studying the underlying mechanisms of DPOAE generation.

### **197 The Number of Ribbon Synapses in Mouse Inner Hair Cells Has a Maximum in the Tonotopic Region of Best Hearing and Scales with Exocytosis But Not $\text{Ca}^{2+}$ -Current**

Alexander Meyer<sup>1</sup>, Darina Khimich<sup>1</sup>, Alexander Egner<sup>2</sup>, Yury Yarin<sup>3</sup>, Tobias Moser<sup>1</sup>

<sup>1</sup>InnerEarLab, Dept. of Otorhinolaryngology, University Hospital Göttingen, 37099 Göttingen, Germany, <sup>2</sup>Dept. Nanobiophotonics, Max-Planck-Institute for biophysical Chemistry, 37070 Göttingen, Germany, <sup>3</sup>Dept. of Otorhinolaryngology, Technical University Dresden, 37070 Dresden, Germany

The sensitivity of sound perception to a defined frequency corresponds to a specific tonotopic location in the cochlea. Here, we investigated whether the morphological and physiological properties of the afferent hair cell synapses could contribute to this phenomenon. We found that the number of synaptic contacts per inner hair cell had a maximum in the cochlear region that transmits sounds with highest sensitivity (10-24 kHz). Probing exocytosis by measurements of cell capacitance increments after brief depolarizations, we found that inner hair cells located ~300  $\mu\text{m}$  from the apex released 44% less transmitter than cells located at ~1400  $\mu\text{m}$  from the apex. This functional finding corresponded to a 31% difference in the number of morphologically identified afferent synapses between these locations. Interestingly, size, charge and kinetics of the calcium current did not vary with the tonotopic position of the hair cells. As the IHC  $\text{Ca}^{2+}$  influx may not only depend on the synapse number but also on the active zone size we asked whether the size of presynaptic ribbons and  $\text{Ca}^{2+}$ -channel clusters may vary tonotopically. The Ribbon size distributions at the two tonotopic positions of ~180 and ~1060  $\mu\text{m}$ , as estimated by 4Pi high-resolution optical microscopy, were indistinguishable from each other. Preliminary analysis of the active zone  $\text{Ca}^{2+}$ -channels imaged by STED microscope showed comparable size of the channel clusters.

In conclusion, the cochlea may use a maximum of neural information channels per hair cells in the range of best hearing.

### **198 The origin of Spontaneous Activity in the Developing Auditory System**

Nicolas Tritesch<sup>1</sup>, Eunyong Yi<sup>1</sup>, Jonathan Gale<sup>2</sup>, Elisabeth Glowatzki<sup>1</sup>, Dwight Bergles<sup>1</sup>

<sup>1</sup>Johns Hopkins University, <sup>2</sup>University College London

During development, sensory neurons are electrically active prior to the functional maturation of sensory receptor organs. This experience-independent activity is essential for neuronal survival, as well as the refinement and maintenance of sensory maps in the brain. Intrinsic activity is typically characterized by the synchronous firing of topographically-related neuronal populations. Prior to the onset of hearing, activity occurs in auditory nerves as discrete bursts of action potentials. This activity appears to originate within the cochlea, but the mechanisms responsible for initiating phasic auditory nerve firing in the absence of sound are poorly understood. Our studies indicate that inner hair cells (IHCs) in the developing rat

cochlea undergo rhythmic depolarizations, which trigger the release of glutamate and bursts of action potentials in primary auditory afferents. This spontaneous activity is not intrinsic to IHCs, but is rather initiated by the release of adenosine 5'-triphosphate (ATP) from supporting cells within Kölliker's organ, a columnar epithelium in the inner sulcus that disappears after the onset of hearing. At the developmental ages studied (P7-P10), supporting cell-derived ATP constitutes the only excitatory input to IHCs and is sufficient to synchronize hair cells that share a similar position on the tonotopic axis. Endogenous purinergic signalling also elicits intercellular calcium waves and intrinsic changes in the optical properties of supporting cells in the inner sulcus. Importantly, episodic stimulation of IHCs by ATP ceases after the onset of hearing (P11-P13 in rat), presumably to allow faithful representation of experience-dependent stimuli and minimize spurious, sensory-independent activity. These data indicate that supporting cells in the organ of Corti initiate patterned electrical activity in auditory nerves before hearing, pointing to an essential role for peripheral, non-sensory cells in the development of central auditory pathways.

### **199 Single Calcium Channel ( $\text{Ca}_v1.3$ ) Activity Recorded From Mouse Cochlear Inner Hair Cells**

Valeria Zampini<sup>1</sup>, Stuart Johnson<sup>2</sup>, Sergio Masetto<sup>1</sup>, Walter Marcotti<sup>2</sup>

<sup>1</sup>University of Pavia, <sup>2</sup>University of Sheffield

Voltage-gated  $\text{Ca}^{2+}$  channels expressed in inner hair cells (IHCs) of the mammalian cochlea play a number of key physiological roles in their normal development and sound transduction (Housley et al. 2006, J Memb Biol 209:89-118).  $\text{Ca}^{2+}$  influx into IHCs occurs mainly (>90%) through  $\text{Ca}_v1.3$  L-type  $\text{Ca}^{2+}$  channels (Platzter et al. 2000, Cell 102:89-97; Brandt et al 2003, J Neurosci 23:10832-40). Although some of the macroscopic biophysical properties of  $\text{Ca}_v1.3$   $\text{Ca}^{2+}$  channels are known, their elementary properties have yet to be determined in mammalian IHCs.

Single  $\text{Ca}^{2+}$  channel activity was recorded at body temperature from immature IHCs in cell-attached configuration using acutely dissected mouse organs of Corti. Voltage-dependent  $\text{Ca}^{2+}$  channels were investigated using  $\text{Ba}^{2+}$  in the patch pipette solution as the main charge carrier and Bay K 8644 to resolve the channel openings. Cell-attached recordings confirmed the presence of L-type  $\text{Ca}^{2+}$  channels, which showed a slope conductance of 39.0 pS and 17.6 pS in 70 mM and 5 mM  $\text{Ba}^{2+}$ , respectively. The mean half maximum open probability ( $V_{1/2}$ ) significantly shifted from about -22 mV in 70 mM  $\text{Ba}^{2+}$  to -41 mV in 5 mM  $\text{Ba}^{2+}$ . The voltage threshold for  $\text{Ca}^{2+}$  channel activation was also significantly less hyperpolarized in 70 mM  $\text{Ba}^{2+}$  than in 5 mM  $\text{Ba}^{2+}$ . The maximum and the minimum open probability were: 0.120 and 0.005 in 5 mM  $\text{Ba}^{2+}$  and 0.042 and 0.002 in 70 mM  $\text{Ba}^{2+}$ .

The present results are consistent with mammalian IHCs expressing a homogeneous population of voltage-dependent L-type  $\text{Ca}^{2+}$  channels containing the  $\alpha_1\text{D}$  ( $\text{Ca}_v1.3$ ) subunit. The hyperpolarized activation of these  $\text{Ca}^{2+}$  channels indicate that they are likely to be active at

the presumed resting membrane potential of IHCs, thus supporting spontaneous action potential activity characteristic of pre-hearing IHCs (Marcotti et al. 2003, *J Physiol* 552:743-761).

Supported by: the Royal Society, the Wellcome Trust and Deafness Research UK.

## **[200] Biophysical Properties of the Calcium Current Recorded in Apical and Basal IHCs of the Gerbil Cochlea**

**Stuart Johnson<sup>1</sup>**, Walter Marcotti<sup>1</sup>

<sup>1</sup>*University of Sheffield*

The  $\text{Ca}^{2+}$  current ( $I_{\text{Ca}}$ ) in pre-hearing and mature inner hair cells (IHCs), the primary sensory receptors of the mammalian cochlea, is mainly (>90%) carried by L-type ( $\text{Ca}_v1.3$ )  $\text{Ca}^{2+}$  channels (Platzter et al. 2000, *Cell* 102:89-97; Brandt et al. 2003, *J Neurosci* 23:10832-40). Although these  $\text{Ca}^{2+}$  channels play a crucial role in IHC excitability and trigger the release of neurotransmitter onto auditory afferent fibres (Marcotti et al. 2003, *J Physiol* 552:743-61; Parsons et al. 1994, *Neuron* 13:875-83), there is still an absence of information regarding any change in their biophysical properties as a function of the frequency position along the cochlea.

$I_{\text{Ca}}$  was recorded using whole-cell patch clamp from apical and basal IHCs (P3-P69), maintained near physiological recording conditions (body temperature and 1.3 mM extracellular  $\text{Ca}^{2+}$ ), from acutely dissected gerbil organs of Corti. the size of  $I_{\text{Ca}}$  in adult IHCs was about a third of that in immature cells and was constant along the cochlea at both stages. Changing the temperature from  $\sim 36^\circ\text{C}$  to  $\sim 23^\circ\text{C}$  significantly reduced the size of  $I_{\text{Ca}}$  in both immature ( $Q_{10} = \sim 1.9$ ) and adult ( $Q_{10} = \sim 1.4$ ) IHCs. At body temperature, the activation kinetics of  $I_{\text{Ca}}$  were significantly faster in high-frequency IHCs, moreover, adult cells were more rapidly activating than immature cells. the degree of  $I_{\text{Ca}}$  inactivation was similar along the immature cochlea IHCs ( $\sim 50\%$ ) but larger in high- (58%) than low-frequency (45%) adult IHCs. This inactivation was greatly reduced with barium but not affected by changing the intracellular buffer (BAPTA instead of EGTA).

The results presented here show that while  $I_{\text{Ca}}$  in adult IHCs is best suited to sustain faster and repetitive physiological stimuli, that of immature cells limits the maximum frequency of action potentials to  $\sim 5$  Hz in apical and  $\sim 10$  Hz in basal IHCs.

Supported by: the Wellcome Trust, Deafness Research UK and the Royal Society

## **[201] Developmental Regulation of L-type Current Inactivation in Mouse Inner Hair Cells**

**Frederick Gregory<sup>1</sup>**, Guiying Cui<sup>1</sup>, Françoise Haeseleer<sup>2</sup>, Amy Lee<sup>1</sup>

<sup>1</sup>*Dept. of Pharmacology and Center for Neurodegenerative Disease, Emory University*, <sup>2</sup>*Dept of Ophthalmology, University of Washington*

Presynaptic  $\text{Ca}^{2+}$  influx through  $\text{Ca}_v1.3$  L-type channels is required for transmission of auditory signals by mouse inner hair cells (IHCs). Unlike recombinant systems,  $\text{Ca}_v1.3$  currents in IHCs show relatively little  $\text{Ca}^{2+}$ - or

voltage-dependent inactivation (CDI or VDI, respectively). However, little is known about the factors limiting CDI or VDI in mouse IHCs, and whether they change during development. Here, we compared CDI and VDI in pre-hearing (P4-P7) and post-hearing (P12-18) C57-B/6 (WT) mouse IHCs. Since the calmodulin-like protein, CaBP4, has been implicated in regulating CDI of  $\text{Ca}_v1.3$ , we also analyzed IHCs from mice lacking CaBP4 ( $\text{CaBP4}^{-/-}$ ). Whole-cell patch clamp recordings of IHCs were performed with 10 mM extracellular  $\text{Ca}^{2+}$  or  $\text{Ba}^{2+}$  and 5 mM EGTA in the intracellular recording solution. CDI and VDI were measured from currents carried by  $\text{Ca}^{2+}$  ( $I_{\text{Ca}}$ ) or  $\text{Ba}^{2+}$  ( $I_{\text{Ba}}$ ), respectively, during a double-pulse protocol in which a test current is evoked after a 300-ms conditioning prepulse. CDI and VDI were greater in post-hearing than in pre-hearing WT IHCs (17-37% for  $I_{\text{Ca}}$  and 7-18% for  $I_{\text{Ba}}$  for prepulse voltages -30 to +45 mV). Posthearing, CDI and VDI were weaker ( $\sim 24\%$  for  $I_{\text{Ca}}$  and  $\sim 19\%$  for  $I_{\text{Ba}}$ ) in IHCs from  $\text{CaBP4}^{-/-}$  than from WT mice. However, pre-hearing, CDI was significantly greater ( $\sim 11\%$ ) in  $\text{CaBP4}^{-/-}$  than WT IHCs. These findings suggest dual effects of CaBP4 in enhancing CDI and VDI post-hearing, but inhibiting CDI pre-hearing. the related  $\text{Ca}^{2+}$ -binding protein, CaBP1, is also expressed in mouse IHCs and causes stronger suppression of CDI and VDI than CaBP4. Therefore, CDI and VDI may depend on the net contributions of CaBP1 and CaBP4 in IHCs, which may support the crucial role of  $\text{Ca}_v1.3$  channels in the onset and maintenance of hearing.

Supported by NIH (NS044922 to AL, T32 DA015040 to FG) and Deafness Research Foundation.

## **[202] Cav1.3 $\text{Ca}^{2+}$ Channel Currents in Mature Mouse Inner Hair Cells During and After Mobile Phone Field Exposure**

**Stefan Münkner<sup>1</sup>**, Abdessamad El Ouardi<sup>2</sup>, Sylvia Kasperek<sup>1</sup>, Joachim Streckert<sup>2</sup>, Reinhard Vonthein<sup>1</sup>, Volkert Hansen<sup>2</sup>, **Jutta Engel<sup>1</sup>**

<sup>1</sup>*University of Tuebingen*, <sup>2</sup>*University of Wuppertal*

The increasing use of mobile phones led to an increased public concern with respect to possible health risks involved. in response to those concerns, the WHO orchestrates a world-wide research program to which this study contributes via the "German Mobile Telecommunication Research Programme" organised by the Federal office for Radiation Protection.

During use, mobile phones are in close proximity to the ear and most of their emitted energy is directly absorbed by the area around the ear. We therefore investigated whether mobile phone field exposure had any influence on the functioning of the voltage-activated L-type  $\text{Ca}^{2+}$  channel Cav1.3 in mature mouse inner hair cells. This  $\text{Ca}^{2+}$  channel is driven by the receptor potential of the hair cells, triggers exocytosis and is known to be sensitive to the cells' metabolic state.

$\text{Ca}^{2+}$  channel currents (charge carrier:  $\text{Ba}^{2+}$ ) were measured in whole-cell patch clamp experiments in an acute preparation of the apical organ of Corti of NMRI mice aged  $18 \pm 2$  days.  $\text{K}^{+}$  currents were blocked by extracellular TEA and 4-AP and by intracellular use of  $\text{Cs}^{+}$ .

Ba<sup>2+</sup> currents were recorded for 5 min prior to exposure, during a 20 min exposure phase and for 15 min after exposure (40 min recording time). All recordings were carried out for SAR values corresponding to 0.02, 0.2, 2, 20 W/kg (averaged over the bath volume) and a sham. the exposure conditions were randomised and blinded. Three different exposure signal types simulating GSM 900, GSM 1800 and UMTS communication signals were used, and at least 15 cells were measured for each exposure type and intensity.

Maximum current, voltage of half activation and steepness of activation were extracted from IV relationships and current traces. These parameters were subsequently used in statistical tests to evaluate a possible influence of the exposure on the properties of the Cav1.3 channels.

Supported by the German Federal Ministry of Environment (Federal office for Radiation Protection).

### **[203] Functional Domains of Auxiliary Subunits of Hair-Cell Calcium Channels**

**Corey K. Treadway**<sup>1</sup>, Marian J. Drescher<sup>1</sup>, Steven F. Myers<sup>2</sup>, Dennis G. Drescher<sup>1</sup>

<sup>1</sup>Wayne State University School of Medicine, Detroit, MI,

<sup>2</sup>University of Michigan Flint, Flint, MI

Voltage-gated calcium channels (VGCC), essential for exocytosis of transmitters, consist of a pore-forming  $\alpha 1$  subunit and  $\beta$ ,  $\alpha 2\delta$ , and  $\gamma$  auxiliary subunits that modify channel properties. We have sequenced the full complement of VGCC auxiliary subunits expressed in saccular hair cells of the rainbow trout, a model providing large numbers of sensory cells. of the four known cytoplasmic  $\beta$  subunits,  $\beta 1$  and  $\beta 2a$  are expressed in the hair cell, and these  $\beta$  subunits exhibit structurally a typical PDZ-like region followed by a Src homology 3 and guanylate kinase ( $\beta$ -interaction) domain, both with 80-90% identity to corresponding sequences in higher vertebrates. the  $\beta 2a$  subunit in particular is characterized by an initial N-terminal 16-aa section which can be linked to the plasma membrane via a pair of adjacent cysteines forming thioester bonds with embedded palmitic acid residues. the teleost hair-cell  $\beta 2a$  has a 44-aa deletion in the second variable (V2) region. the  $\alpha 2\delta$  subunit is extracellular, save its sole membrane-crossing  $\delta$  portion. We have identified the  $\alpha 2\delta$  of the teleost hair cell as the  $\alpha 2\delta$ -2 subtype, with 68% identity to mouse  $\alpha 2\delta$ -2 and 54% identity to mouse  $\alpha 2\delta$ -1. the hair-cell  $\alpha 2\delta$ -2 clearly displays binding sites for the anticonvulsant drug, gabapentin, corresponding to a documented subunit specificity for this clinically important medication. Finally, we have sequenced completely the hair-cell  $\gamma 2$  subunit. the  $\gamma 2$  was initially identified as the protein stargazin, mutated in stargazer mice and resulting in a disruption of function, apparently in the inner ear and cerebellum. the hair-cell  $\gamma 2$  consists of 321-aa coding region with an NDS extracellular glycosylation site and an intracellular C-terminal PDZ binding domain (RRTTPV) containing a PKA phosphorylation site. Knowledge of the interactions between the auxiliary subunit functional domains should yield a better understanding of the role of the VGCC in the hair cell.

### **[204] Calcium-Dependent Interaction of Otoferlin with Ca<sub>v</sub>1.3 and Syntaxin 1A**

**Neeliyath A. Ramakrishnan**<sup>1</sup>, Marian J. Drescher<sup>1</sup>, Dennis G. Drescher<sup>1</sup>

<sup>1</sup>Wayne State University School of Medicine, Detroit, MI

Otoferlin, a C2-domain-containing Ca<sup>2+</sup> binding protein, is thought to mediate exocytosis in auditory and vestibular hair cells. Mutations in the gene *OTOF* cause non-syndromic deafness in humans, and it has been shown that *OTOF* knockout mice are deaf (Roux et al., Cell 127: 277-289, 2006). the molecular mechanism underlying synaptic exocytosis in hair cells is not well understood. in the present study, we show that native but not mutated otoferlin domains bind to the voltage-gated calcium channel, Ca<sub>v</sub>1.3, as well as to the SNARE protein, syntaxin 1A. We generated otoferlin fusion proteins that contained two of the same amino acid substitutions detected in DFNB9 patients (Pro1825Ala, Migliosi et al., J Med Genet 39: 502-506, 2002; Leu1011Pro, Tekin et al., Am J Med Genet 138A: 6-10, 2005). We found that the native otoferlin C2F domain bound to syntaxin 1A and to the Ca<sub>v</sub>1.3 II-III loop in a Ca<sup>2+</sup>-dependent manner, with an optimal 100  $\mu$ M free Ca<sup>2+</sup> required for binding. the Pro-Ala mutation in the C2F domain greatly diminished the interaction. Whereas the native C2F domain was capable of binding Ca<sup>2+</sup>, the mutated C2F lacked the Ca<sup>2+</sup>-binding ability. These findings suggest that the C2F domain of otoferlin is important for exocytosis in hair cells because the C2F binds Ca<sup>2+</sup>, interacts with the SNARE protein syntaxin 1A, and requires Ca<sup>2+</sup> for the interaction. We further demonstrated that the otoferlin C2D domain also binds to the Ca<sub>v</sub>1.3 II-III loop in a Ca<sup>2+</sup>-dependent manner, and a Leu-Pro mutation in C2D renders this binding insensitive to Ca<sup>2+</sup> and considerably diminished. Neither the otoferlin C2D domain nor its mutant form was found to interact with syntaxin1A, with or without Ca<sup>2+</sup>. in conclusion, we find that mutations that can cause deafness in humans in the C2 domains of otoferlin impair otoferlin's ability to directly bind and modulate protein components involved in synaptic exocytosis.

### **[205] Calcium- and Otoferlin-Dependent Exocytosis At Ribbon Synapses of Immature Outer Hair Cells**

**Maryline Beurg**<sup>1</sup>, Saaid Saffiedine<sup>1</sup>, Christine Petit<sup>1</sup>, Didier Dulon<sup>1</sup>

<sup>1</sup>INSERM U587 Pasteur Institute Paris and University Bordeaux 2, France

Immature cochlear outer hair cells (OHCs) make transient synaptic contacts (ribbon synapses) with afferent nerve fibers. However, exocytosis of synaptic vesicles has not yet been shown. We thus investigated calcium dependent exocytosis in murine OHCs at postnatal age P2-P3, a developmental stage when calcium current maximum amplitude was the highest. by using time-resolved patch-clamp capacitance measurements, we show that voltage step activation of L-type calcium channels triggers fast membrane capacitance variation. Capacitance variation evoked by long depolarization steps (up to 3000 ms) had two kinetic components, which probably reflect two

functionally distinct pools of synaptic vesicles, a readily releasable pool (RRP) ( $\tau=80$  ms) and a slowly releasable pool (SRP;  $\tau=1200$  ms). the RRP size and maximal release rate were estimated at  $\sim 1200$  vesicles and  $\sim 15000$  vesicles  $s^{-1}$ , respectively. in addition, we found a linear relationship between exocytosis and calcium influx, similar to that reported in mature inner hair cells. These results give strong support to the existence of efficient, calcium dependent neurotransmitter release in immature OHCs. Moreover, we show that immature OHCs, just like immature inner hair cells, are able to produce regenerative calcium dependent action potentials that could trigger synaptic exocytosis in vivo. Finally, the evoked membrane capacitance variation was nearly abolished in P2-P3 OHCs from mutant mice defective for otoferlin, despite normal calcium currents. We conclude that otoferlin, the putative major calcium sensor at inner hair cell ribbon synapses, is essential to synaptic exocytosis in immature OHCs too.

## **[206] Background and Driven Synaptic Activity in the Frog Sacculus Studied *In Vitro*.**

**Mark Rutherford<sup>1</sup>, William Roberts<sup>1</sup>**

<sup>1</sup>*University of Oregon*

Sensitive to seismic vibrations as well as head tilt and airborne sound, the frog sacculus is an inner ear organ with a mixed auditory/vestibular function (J. Lannou and L. Cazin, 1976; J. Christensen-Dalsgaard and P.M. Narrins, 1993; X. Yu et. al., 1991). Individual saccular axons are able to respond to static head position as well as dynamic vibratory/auditory stimuli. to investigate the nature of this mixed sensitivity, we recorded from postsynaptic afferent neurites and their presynaptic hair cells within the sensory epithelium of the isolated frog sacculus without the use of protease or other enzymes known to change hair cell electrical behavior. Steady currents were presented to hair cells in order to mimic the normal resting mechanoelectrical transduction current predicted for a range of static head positions. the resulting hair cell voltage oscillation frequency and amplitude varied with the amplitude of injected current. Hair cells of the tall-skinny morphology exhibited asymmetric spike-like voltage oscillations (up to 60 mV) at low frequencies (4-30 Hz). Short-fat hair cells exhibited smaller symmetric voltage oscillations in the 20-70 Hz range. Differences in oscillatory behavior in current clamp were correlated with different compliments of transmembrane currents measured in voltage clamp which also varied by cell morphology. We speculate that the tall-skinny hair cells in the saccular periphery signal a rate code for head tilt in the frequency range up to 30 Hz for which saccular neurons can respond by discharging on a cycle-by-cycle basis. Furthermore, we propose that the typical saccular afferent is sensitive to both static and dynamic stimuli because it receives input from hair cells of both the tall-skinny and short-fat variety, respectively. Hair cell and afferent neuron responses to dynamic stimuli will also be discussed.

## **[207] Paired Recordings with Capacitance Measurements At the Hair Cell Synapse: Quantal Size and Multiquantal Release**

**Geng-Lin Li<sup>1</sup>, Erica Keen<sup>2</sup>, Daniel andor-Ardó<sup>2</sup>, A. J. Hudspeth<sup>2</sup>, Henrique von Gersdorff<sup>1</sup>**

<sup>1</sup>*The Vollum Institute, Oregon Health & Science University, Portland, OR,* <sup>2</sup>*Howard Hughes Medical Institute and the Rockefeller University, New York, NY*

The excitatory postsynaptic currents (EPSCs) recorded from eighth-nerve afferent terminals include many large signals thought to represent the simultaneous release of several vesicles. We performed paired whole-cell recordings on hair cells and the associated afferent fibers in the amphibian papilla of the adult bullfrog. the amplitudes of spontaneous EPSCs displayed a Gaussian distribution with a mean of  $-129 \pm 24$  pA. the largest signals, with amplitudes exceeding  $-200$  pA, displayed kinetics similar to those only a quarter as large, suggesting that the former stem from the highly synchronized release of multiple vesicles. Holding the hair cells at  $-90$  mV eliminated the large EPSCs, leaving a narrow amplitude distribution with a mean amplitude of  $-55.6 \pm 12.2$  pA and a charge transfer of  $-56 \pm 11$  fC. the inclusion of  $0.4$  mM  $Cd^{2+}$  in the bath solution had a similar effect. During voltage-evoked exocytosis, we compared the synaptic charge transfer into an afferent terminal with the simultaneous increase in membrane capacitance of a hair cell. the resultant regression line, with a consistent slope of  $-1100 \pm 600$  C·F<sup>-1</sup>, implies a single-vesicle capacitance of about  $51$  aF, a value in agreement with the electron-microscopic estimate of  $45$  aF. These results support the hypothesis that the large spontaneous EPSCs are multiquantal.

## **[208] Offset Adaptation in the Inner Hair Cell Synapses is Important for Speech Coding**

**Huan Wang<sup>1</sup>, Werner Hemmert<sup>2</sup>**

<sup>1</sup>*Infineon Technologies,* <sup>2</sup>*Technical University Munich*

One of the most critical processing steps during encoding of sound signals for neuronal processing is when the analog signal is coded into discrete nerve-action potentials. This conversion induces massive information loss -- or to phrase it positive -- information reduction. As any information lost during this process is no longer available for neuronal processing, it is important to understand and model the underlying principles.

Recent pool models of the inner hair cell synapse fail to reproduce a silent period after an intense stimulus. This has important consequences in the next processing step, the cochlear nucleus which receives direct input from auditory nerve fibers (ANFs): Onset Neurons in the ventral cochlear nucleus (VCN), modeled with a detailed Hodgkin-Huxley model (Rothman and Manis, 2003) do not reliably respond to amplitude modulated signals in the frequency region above  $4$  kHz.

We therefore followed the proposal of Zhang and Carney (2005) and included a model of offset adaptation. Responses from the improved model demonstrate superior phase locking characteristics of ANFs to amplitude modulated signals, especially in high frequency regions.



As a direct consequence, modeled Onset Neurons (ONs) driven by ANFs show stronger responses to amplitude modulated signals – we examined especially voiced speech signals - over the whole hearing range.

We also tested coding of sound signals into trains of nerve-action potentials using our full model of human sound processing, which includes outer ear, middle ear, traveling-wave model of the inner ear and a nonlinear compression stage, inner hair cells, the auditory nerve and selected VCN neurons. We used speech in noise (noisy ISOLET database) and a Hidden-Markov speech recognition system to discriminate features derived from spike-trains. We found that onset adaptation substantially improved recognition accuracy of ANF features (the word error rate fell from 20.9% to 12.5%). In addition, when features extracted from VCN ONs were added, recognition scores even further improved.

We conclude that offset adaptation is an important feature of ANF responses which is essential for neuronal processing of auditory signals by Onset Neurons in the VCN. In addition, offset adaptation improves speech coding.

X. Zhang and L. H. Carney. Analysis of models for the synapse between the inner hair cell and the auditory nerve. *J. Acoust. Soc. Am.*, 118:1540–53, 2005.

J. S. Rothman and P. B. Manis, "The roles potassium currents play in regulating the electrical activity of ventral cochlear nucleus neurons," *J. Neurophysiology*, vol. 89, pp. 3097–3113, 2003.

This work was funded by the German Federal Ministry of Education and Research (reference number 01GQ0443).

## **[209] Calcium Channels That Support Acetylcholine Release At the Transient Olivocochlear-Inner Hair Cell Synapse**

**Javier Zorrilla de San Martín**<sup>1</sup>, Carolina Wedemeyer<sup>1</sup>, Paul Fuchs<sup>2</sup>, Ana Belén Elgoyhen<sup>1</sup>, Eleonora Katz<sup>1</sup>

<sup>1</sup>*Instituto de Investigaciones en Ingeniería Genética y Biología Molecular - INGEBI (CONICET)*, <sup>2</sup>*Center for Hearing and Balance, Dept. Otolaryngol-Head and Neck Surgery, Johns Hopkins Univ.*

Before the onset of hearing, inner hair cells (IHC) of the mammalian cochlea are transiently innervated by medial olivocochlear efferent fibers. This synapse is cholinergic, inhibitory and mediated by the  $\alpha 9\alpha 10$  nicotinic cholinergic receptor. During postnatal development, IHC undergo dramatic changes in cholinergic sensitivity, pattern of innervation and expression of key postsynaptic proteins. In developing synapses, synaptic modifications likely take place concurrently in both postsynaptic cells and presynaptic terminals. In mammals, fast synaptic transmission at both central and peripheral synapses is mediated by multiple types of voltage-gated  $\text{Ca}^{2+}$  channels (VGCCs), including N-type (Cav2.2), P/Q (Cav2.1) type and R-type (Cav2.3). So far, nothing is known concerning the VGCCs that support ACh release at the efferent-IHC synapse. Therefore, in this work we evaluated the type/s of  $\text{Ca}^{2+}$  channels coupled to ACh release at this synapse before the onset of hearing. We used the acutely isolated cochlear preparation from mice

and evaluated the effects of different  $\text{Ca}^{2+}$  channel blockers on the quantal content ( $m$ ) of transmitter release and on the amplitude of spontaneous synaptic currents. Postsynaptic cholinergic currents in IHCs, voltage-clamped at  $-90$  mV, were evoked by electrically stimulating the efferent fibers. Both  $\omega$ -conotoxin-GVIA (300 nM), an N-type VGCC blocker, and  $\omega$ -Agatoxin-IVA (200 nM), a P/Q-type VGCC blocker, significantly reduced  $m$  ( $49 \pm 17\%$ ,  $n=5$  and  $52 \pm 8\%$ ,  $n=4$ , respectively). When both toxins were applied together, ACh release was reduced by 96% ( $n=1$ ). Neither of the toxins affected the amplitude of spontaneous synaptic currents ( $n=2-3$ ), indicating that their site of action is only presynaptic. Our results suggest that both N and P/Q-type VGCCs support ACh release at the transient efferent-IHC synapse.

Supported by a grant from NOHR to EK

## **[210] 'Nicotinic' Ach Receptors Activate BAPTA-Sensitive Calcium Stores in Cochlear Hair Cells (*Gallus*)**

**Paul Fuchs**<sup>1</sup>, Ward Yuhas<sup>2</sup>

<sup>1</sup>*Center for Hearing and Balance, Otolaryngology-HNS, Johns Hopkins University School of Medicine*, <sup>2</sup>*Advanced Bionics, Boston, MA*

Vertebrate hair cells are inhibited by acetylcholine (ACh) acting on  $\alpha 9\alpha 10$ -containing ligand-gated cation channels, leading to activation of calcium-dependent, small-conductance (SK) potassium channels that hyperpolarize the membrane. An unresolved issue is whether calcium influx acts alone, or in addition, may trigger calcium-induced calcium release (CICR) from the nearby 'synaptoplasmic cistern'. Evidence in favor of CICR has been largely pharmacological: ryanodine receptor agonists and SERCA pump blockers alter the SK current evoked by ACh in hair cells. A role for calcium entry was suggested originally by the dependence of the SK current on membrane potential (calcium driving force), and by the ability of BAPTA, but not EGTA, to interrupt that activation. The present work shows that CICR from the synaptic cistern of chicken cochlear hair cells has equivalent dependence on membrane potential and BAPTA-sensitivity. That is, SK channel activation by ACh depends on the 'loading-state' of an internal calcium store that in turn depends critically on calcium influx, thereby conferring the same voltage-dependence as expected for direct activation of SK channels by influx through AChRs. Further, the contribution to SK activation from internal calcium stores can be eliminated by BAPTA (but not EGTA), presumably through competition with SERCA pump activity required to maintain the store's calcium load. Surprisingly, ACh-evoked SK currents can be restored, even in 10 mM BAPTA, by voltage-gated calcium loading of the store. Finally, while SERCA blockers can prevent SK activation by ACh, they also temporarily initiate spontaneous transient outward currents (STOCs) with characteristics like those of the ACh-evoked SK currents. STOC-like fluctuations also are observed during prolonged exposure to ACh. The present results show that a synaptic calcium store (the synaptoplasmic cistern) contributes to, indeed is required for, the activation of SK channels by

## **[211] Calcium Induced Calcium Release Contributes to Shaping Action Potentials and Spontaneous Ipscs in Pre-Hearing Mouse Inner Hair Cells**

**Radu Iosub<sup>1</sup>**, Helen J. Kennedy<sup>1</sup>

<sup>1</sup>*Department of Physiology and Pharmacology, University of Bristol, UK*

Pre-hearing mammalian inner hair cells (IHCs) fire spontaneous calcium based action potentials (APs) and receive inhibitory efferent input mediated by  $\alpha 9/\alpha 10$  acetylcholine receptor (AChR). Both processes involve an initial transient increase in intracellular  $\text{Ca}^{2+}$  concentration, which subsequently activates calcium-dependent (SK2-containing) potassium channels. However, it is unclear if these  $\text{Ca}^{2+}$  transients are amplified by calcium-induced calcium release (CICR), a process that can be modulated by the plant alkaloid ryanodine. Here we report that CICR contributes to both AP firing and spontaneous efferent inhibition in neonatal IHCs.

Voltage- and current-clamp recordings were made at 37°C from pre-hearing (P7) mouse IHCs. Ryanodine (Ry) was applied intracellularly to either block (100 $\mu\text{M}$ ) or enhance (1 $\mu\text{M}$ ) CICR. AP recordings were carried out in the presence of 100nM strychnine to block the AChR. Blocking CICR slowed AP repolarization compared to controls (decay: 7.11  $\pm$  0.79 ms, 3.75  $\pm$  0.3 ms respectively) and the effect was cumulative leading to prolonged plateaus during AP firing. These data indicate that blocking CICR reduces activation of SK2 channels, affecting AP repolarization. However, 1 $\mu\text{M}$  Ry did not significantly change AP decay times suggesting that in control experiments the amount of CICR triggered is sufficient to maintain AP firing and further enhancing CICR has no effect.

Spontaneous IPSC amplitudes were significantly increased by 1 $\mu\text{M}$  Ry (54.39  $\pm$  2.39 pA) and reduced by 100 $\mu\text{M}$  Ry (31.54  $\pm$  0.68 pA) compared to controls (35.2  $\pm$  0.65 pA) (holding potential -85 mV). Recent studies show that high concentrations of Ry can act as a positive modulator of AChR gating in hair cells, consequently the reduction in IPSC amplitudes we see in 100 $\mu\text{M}$  Ry may be underestimated.

These experiments demonstrate that CICR is essential for maintaining AP repolarization and forms an important part of the cholinergic inhibition mechanism in IHCs.

## **[212] Role of Nachrs, SK2 Channels, and Intracellular Calcium in ROS Dynamics of Hair Cell-Like Cultures**

**Marc Manix<sup>1</sup>**, Johnvesly Basappa<sup>1</sup>, Douglas Vetter<sup>1</sup>

<sup>1</sup>*Tufts Univ. School of Medicine*

Aminoglycoside-mediated formation of reactive oxygen species (ROS) plays a key role in the cellular events leading to hair cell apoptosis and hearing loss. It is known that  $\text{Ca}^{2+}$  influx plays a role in the toxicity of these antibiotics, but various pathways for  $\text{Ca}^{2+}$  mobilization may be involved. We are investigating the effects of

aminoglycosides on an immortalized organ of Corti cell line, the OC-K3 line, to examine the roles played by the calcium permeable nicotinic receptors, calcium activated potassium channels, and intracellular  $\text{Ca}^{2+}$  stores in the generation of ROS after administration of aminoglycosides.

ROS levels were determined using the 2'-7' dichlorodihydrofluorescein diacetate fluorometric based assay. Administration of the aminoglycoside gentamicin leads to an increase in cellular ROS in OC-K3 cells. But the greatest increase in ROS is seen with the addition of ACh and gentamicin together. Administration of BAPTA-AM results in a large decrease in intracellular ROS for cells exposed not only to gentamicin alone but also in the presence of ACh, indicating ROS generation is dependent on intracellular  $\text{Ca}^{2+}$ . Releasing intracellular calcium stores with thapsigargin first generates a significant increase in ROS levels which decreases with time, indicating that there is protection from ROS generation once the  $\text{Ca}^{2+}$  stores are depleted and blocked from being re-filled. Strychnine blocks the  $\alpha 9/\alpha 10$  nicotinic receptor and decreases the ROS levels normally occurring following ACh and gentamicin. Although the ROS levels are lower, there is still a significant increase when compared to control cells. This result suggests that other channels or receptors may be involved in  $\text{Ca}^{2+}$  influx and generation of ROS. a drop in intracellular ROS normally induced by ACh and gentamicin is observed when the SK2 channel is blocked with apamin., suggesting that SK2 activity plays a critical role in generation of ROS after aminoglycoside administration.

Support by DC6258 (DEV)

## **[213] A Complex Network of Genes Underlie Olivocochlear Synaptogenesis: Developmental Gene Expression Analysis in the $\alpha 9$ Null Mouse Model**

**Sevin Turcan<sup>1</sup>**, Douglas Vetter<sup>2</sup>

<sup>1</sup>*Tufts Univ.*, <sup>2</sup>*Tufts Univ. School of Medicine*

A novel role for the efferent system in olivocochlear synaptogenesis has been uncovered. the function of  $\alpha 9$  and  $\alpha 10$  subunits in synapse formation has been previously established where the loss of either subunit results in changes in olivocochlear function and synapse morphology. While electrophysiological and anatomical studies have facilitated the discovery of this specific role for the efferent system subunits, the molecular mechanisms behind the abnormal synaptic phenotypes have yet to be delineated. in order to reveal the genetic circuitry downstream of  $\alpha 9/\alpha 10$  nAChRs in  $\alpha 9$  null mice, we performed developmental high-throughput genomic studies using the Affymetrix Mouse Expression Set 430 v2 chip. the dynamic properties of synaptogenesis is captured by pooling cochleas from wild type and  $\alpha 9$  null mice at various postnatal ages representing various stages of synapse formation (P3, P7, P10, P13, and P21). We applied traditional bioinformatics analyses to identify preliminary lists of genes with changes in gene expression levels between the normal and the  $\alpha 9$  null mouse at different time points. Data were further analyzed by

inspecting functional sets of genes to discover pathways with subtle changes relevant to synaptogenesis. Temporal gene expression data are clustered to identify groups of genes with similar expression patterns in order to provide further insight into gene-gene interactions downstream of nAChRs. the patterns identified from this global analysis will provide a link to understanding the molecular mechanisms driving olivocochlear synaptogenesis.

Supported by DC006258 (DEV)

## **214 Localization of Synuclein Proteins in the Mice and Rat Cochlea**

**Omar Akil<sup>1</sup>**, Christopher Weber<sup>1</sup>, Shi-Nae Park<sup>1</sup>, Vladimir Buchman<sup>2</sup>, Lawrence Lustig<sup>1</sup>

<sup>1</sup>*Department of Otolaryngology-HNS, UCSF*, <sup>2</sup>*School of Biosciences Cardiff University Museum, UK*

Synucleins are a family of small intracellular proteins expressed mainly in the nervous system. the family includes three known proteins: alpha-synuclein, beta-synuclein and gamma-synuclein. the alpha and beta synuclein proteins are found primarily in neuronal tissue, where they are seen mainly in presynaptic terminals. in contrast gamma-synuclein is found primarily in the peripheral nervous system and retina, and has been associated with the cholinergic system.

Using a yeast-two-hybrid screen with the nicotinic acetylcholine receptor (nAChR) alpha 10 subunit, we demonstrate protein-protein interaction with gamma-synuclein. This binding interaction is further supported by co-immunoprecipitation. RT-PCR of the whole organ of Corti extracts demonstrates gamma-synuclein mRNA expression. Additionally, western blot of organ of Corti protein demonstrated gamma-synuclein protein. Immunofluorescence of mouse and rat organ of Corti shows that gamma-synuclein is localized to the base of the outer hair cell and co-localized with synaptophysin and choline acyl-transferase (ChAT), in the region of the OHC nicotinic acetylcholine receptor. Together, these studies provide strong evidence that the OHC nAChR interacts with gamma-synuclein. Studies are ongoing to determine the nature of this interaction, as well as the role for synucleins in the mammalian organ of Corti

## **215 Expression of Novel Dopamine D2 Receptors in Saccular Hair Cells**

**Maher D. Abu-Hamdan<sup>1</sup>**, Marian J. Drescher<sup>1</sup>, James S. Hatfield<sup>2</sup>, Dennis G. Drescher<sup>1</sup>

<sup>1</sup>*Wayne State University School of Medicine, Detroit, MI*,

<sup>2</sup>*Veterans Affairs Medical Center, Detroit, MI*

Previously, evidence was obtained that dopamine D2L message and receptor protein are expressed in rat organ of Corti, representing a target of olivocochlear dopaminergic lateral efferents (Kewson et al., ARO Abstr. 22:123, 1999; ARO Abstr. 26:619, 2003). We now report that dopamine D2 receptors are also expressed in vestibular epithelia, specifically in hair cells. Degenerate primers targeting dopamine D2 receptor transcript were applied in PCR to cDNA from a model hair cell preparation isolated from the trout saccule. a novel dopamine D2 receptor was amplified, also found in brain. This dopamine

D2L receptor (61% of estimated full-length cds) with highest identity to carp D2 (73%) was accompanied by two variants, both terminating prematurely within the third intracellular loop. a second dopamine D2L receptor (95% cds), representing a previously reported trout dopamine D2L receptor (GenBank Accession No. AJ347729), was also identified in hair cell cDNA, along with its D2S truncated version identified in higher vertebrates (but not previously in trout), characterized by a 29-aa deletion in the third intracellular loop. in summary, two dopamine D2L, one D2S and two truncated D2L transcripts are expressed in the saccular hair cell layer. Consistent with message determinations for the teleost saccule, dopamine D2L receptor protein has been localized to both basal and apical subcuticular sites on hair cells in rat vestibular end organs. the hair cell D2L receptors are hypothesized to be co-expressed with dopamine D1A3 receptors whose message was previously identified in saccular hair cell cDNA (Kewson et al., 2003). Dopamine D1A3 has been immunolocalized to similar sites on hair cells as D2L in rat vestibular end organs. Co-expression of dopamine D2 with dopamine D1 receptors is hypothesized to provide a mechanism for a graded post-synaptic response to dopaminergic efferent input modulating hair cell afferent signaling, differentially effected by expressed D2 variants.

## **216 A Physiological Frequency-Position Map for the Chinchilla Cochlea**

**Marcus Mueller<sup>1</sup>**, Silvi Hoidis<sup>2</sup>, Jean Smolders<sup>2</sup>

<sup>1</sup>*Tübingen Hearing Research Center*, <sup>2</sup>*Neuroscience Center Frankfurt*

We tested the hypothesis that the published frequency place map of the Chinchilla (Eldredge et al., 1981, JASA 69:1091) which was determined from sound damaged ears ("anatomical map") is shifted towards lower frequencies compared to that from intact ears in normal physiological condition ("physiological map").

The hypothesis was based on the observation that the mouse "physiological map" (Mueller et al., 2005, Hear. Res. 202:63) is shifted towards higher frequencies by about an octave compared to the mouse "anatomical map" (Ou et al., 2001, Hear. Res. 145:123). This shift can be explained by sound-trauma-induced shifts of neural frequency tuning (Mueller et al., 2006, Neuroreport 16:1183).

We therefore re-determined the physiological map of the chinchilla by recording the characteristic frequency (CF) of neurons in the cochlear nucleus, followed by iontophoretic application of HRP or biocytine and tracing of labelled auditory nerve fibers towards the hair cells in the organ of Corti. the distance of labelled innervation sites from the basal end of the basilar membrane was determined from serial sections of the cochleae from which a three-dimensional reconstruction of the basilar membrane was derived.

HRP labelling in most cases could be traced up to the spiral ganglion cells only, whereas biocytine also labelled boutons of afferent fibres at the inner hair cells. the physiological frequency-place map was established from labelled boutons for CFs ranging from 0.135 – 24.4 kHz, corresponding to 91 and 0.5% distance from the basal end

of the basilar membrane respectively. the best fit of the map was a linear function of distance as a function of frequency on a logarithmic frequency axis, described by  $d=61.2-42.2\log(f)$  where  $d$  is relative distance from the base (% of total length) and  $f$  is CF in kHz. the data did not indicate "crowding" of frequencies at the apex of the basilar membrane. the slope of the map was 2.53 mm/octave for a mean basilar membrane length of  $20\pm0.9$  mm. the present chinchilla physiological map from sensitive ears was shifted towards higher frequencies compared to the anatomical map from desensitized ears by about half an octave, corresponding to 1.26 mm, as compared to one octave in the mouse, corresponding similarly to 1.25 mm.

We conclude that frequency-place relations on the basilar membrane are dependent on the condition of the cochlea. Desensitization shifts the frequency-place map towards lower frequencies. Furthermore the form of mammalian frequency-place maps appears to be species specific. "Crowding" of low frequencies at the apex of the basilar membrane not a general property.

### **[217] Impact of Neuronal Adhesion Molecule On Wiring and Synaptic Transduction in Spiral Ganglion Neurons**

**Sara Euteneuer<sup>1</sup>**, Gary D. Housley<sup>2</sup>, Matthias Klinger<sup>3</sup>, Allen F. Ryan<sup>4</sup>

<sup>1</sup>University of Luebeck, School of Medicine, Dept. of Otolaryngology, Head and Neck Surgery, <sup>2</sup>Department of Physiology, School of Medical Sciences, Faculty of Medicine, University of New South W, <sup>3</sup>Department of Anatomy, School of Medicine, University of Luebeck, Germany, <sup>4</sup>Department of Surgery, Division of Otolaryngology & Neurosciences, UCSD School of Medicine

**Introduction:** Neuronal cell adhesion molecule (NCAM) has not only shown to serve as a guidance factor for developing neurites but also to impact synapse formation and excitatory synaptic strength in the central nervous system. Recently NCAM has been demonstrated to interact with the GDNF receptor, and with ionotropic glutamate receptors, with a potential impact on neuronal survival and/or glutamate excitotoxicity. the presence of NCAM in the inner ear suggests the potential for a functional role. **Methods:** Inner ear innervation patterns in sections and whole mounts of neonatal NCAM knock out (KO) and wildtype (WT) organ of Corti were compared after labeling spiral ganglion dendrites with tetramethyl rhodamine dextran by retrograde transport. ABRs and DPOAEs were measured in 8- to 9-week old NCAM KO and WT mice, before and after noise exposure. Dendrite morphology after noise exposure (0 and 2 days) was compared by electron microscopy.

**Results:** Preliminary results suggest normal innervation patterns of type I afferent dendrites in neonatal NCAM KO mice. Hearing levels of adult NCAM KO mice were similar to age matched WT animals. Lack of NCAM did not lead to increased sensorineural hearing loss, when compared to threshold shifts observed in WT animals.

**Discussion:** the results suggest that NCAM is not required for the development of normal cochlear innervation

patterns. Moreover, NCAM also appears to lack a functional impact on glutamate excitotoxicity in the inner ear.

Supported by German Research Association (DFG) grant EU 120/1-1(SE), NIH/NIDCD grant DC00139 (AR), the Medical Research (AR) and Rehabilitation Research and Development Services of the VA (AR), and grants supporting the UCSD microscopy core facility NINDS grant NS047101

### **[218] CRHR1 Null Mice Reveal a Role for Stress Hormones in Directing Cochlear Innervation and Glutamate Receptor Expression**

**Christine Graham<sup>1</sup>**, Douglas Vetter<sup>1</sup>

<sup>1</sup>Tufts University School of Medicine

Urocortin, recently discovered in the lateral efferent system of the cochlea, is a neuropeptide related to corticotropin releasing hormone, the major hormone responsible for systemic stress response in other regions of the body. All CRH-like ligands signal through the same two G-protein coupled receptors, corticotropin releasing hormone receptor 1 and 2 (CRHR1 and CRHR2). Genetic ablation of urocortin in mice causes deafness and impaired outer hair cell mechanics, suggesting an important role for this neuroendocrine system in normal cochlear development and function, as well as for protection against acoustic trauma. to further investigate the role of the CRH system in the inner ear, we are examining mice lacking either CRHR1 or CRHR2, both of which are expressed in the cochlea. the present work demonstrates that elimination of CRHR1 results in deafness, abnormal development of both efferent and afferent innervation to the organ of Corti, and misregulation of AMPA receptor subunit expression. Western blot analysis reveals that GluR2/3 and GluR4 are substantially upregulated in CRHR1 null mice compared to wildtypes. Interestingly these results are most pronounced in females, suggesting that this neuroendocrine system influences cochlear development/gene expression differently across genders. Preliminary data further demonstrates that CRHR1 expression is well situated throughout development to act as a guidance cue for fibers innervating the organ of Corti. in addition to the abnormal innervation structure observed in adult mice, postnatal day 7 (P7) females lacking CRHR1 have fewer spiral ganglion radial fibers entering the inner hair cell region, but excessive branching of these fibers compared to age-matched wildtype females. the sexually dimorphic response to the loss of CRHR1 suggests that the molecular mechanisms underlying development of hair cell innervation and receptor expression are differentially sensitive to hormonal regulation in males and females.

## **219** Regeneration of the Cochlear Fibrocytes Leads to Partial Hearing Recovery in a Model of Persistent Hearing Loss Due to Acute Cochlear Energy Failure

Kunio Mizutari<sup>1</sup>, Hideki Mutai<sup>2</sup>, Susumu Nakagawa<sup>2</sup>, Masato Fujii<sup>2</sup>, Kaoru Ogawa<sup>1</sup>, Tatsuo Matsunaga<sup>2</sup>

<sup>1</sup>Keio University School of Medicine, <sup>2</sup>National Institute of Sensory organs, National Tokyo Medical Center

We have reported acute cochlear energy failure using mitochondrial toxin, 3-nitropropionic acid (3-NP), as a model of inner ear disorders such as inner ear ischemia (Hoya et al, 2004, Okamoto et al, 2005). in this model, the main cause of hearing loss was apoptosis of the fibrocytes in the cochlear lateral wall (Kamiya et al, 2007, Mizutari et al, 2007). in the present study, we analyzed the long time prognosis of ABR threshold shift in the permanent threshold shift model, and time course of structural changes in the cochleae in this model. in SD rats treated with 3  $\mu$ l of 3-NP (500 mM) or saline, auditory brainstem response (ABR) recording and histological examination were performed at several time points up to 2 month after surgery. ABR threshold became scale-out at all frequencies 1 day after 3-NP administration, and that hearing level remained until 1 month after surgery. However, after 2 months, ABR showed significant recovery at low frequency (8 kHz) in 4 of 5 3NP treated rats. ABR threshold at 20 kHz occasionally showed some recovery. At high frequency (40 kHz), ABR recovery was not observed. Histological analysis of 3NP treated rats revealed partial regeneration of the lateral wall fibrocytes in the cochlear basal turn 2 month after 3-NP administration despite nearly complete loss of fibrocytes 2w after 3-NP administration. the spiral ganglion cells and the outer hair cells were severely degenerated in the cochlear basal turn. These results indicate that the ABR recovery at low frequency is caused by regeneration of fibrocytes, and continuing ABR threshold shift is mainly caused by degeneration of spiral ganglion cells and outer hair cells. These results suggest that persistent hearing loss may be recovered at least partially by mesenchymal stem cell transplantation into the inner ear which leads to regeneration of lateral wall fibrocytes (Kamiya et al, 2007) .

## **220** Expression of HCN Channels At the Inner Hair Cell Afferent Synapse

Isabelle Roux<sup>1</sup>, Eunyoungh Yi<sup>1</sup>, Elisabeth Glowatzki<sup>1</sup>

<sup>1</sup>Department of Otolaryngology- Head and Neck Surgery, Johns Hopkins School of Medicine, Baltimore, MD

The exquisite temporal precision of hearing relies on the afferent neurons' specialization for rapid and reliable signaling. This led us to investigate the role of postsynaptic voltage-gated ion channels at the inner hair cell afferent synapse, the first synapse in the auditory pathway. Whole cell patch clamp recordings from afferent dendrites of auditory nerve fibers revealed a slowly activating inward current during prolonged hyperpolarizing voltage steps. it's pharmacological profile suggested that this current was mediated by hyperpolarization-activated cyclic nucleotide-gated (HCN) cation channels. These channels are formed

by homo- or heteromeric tetramers of integral membrane proteins encoded by a family of four genes (HCN1-4).

Here, we investigated the differential expression pattern of these proteins in pre- and post-hearing rat cochleae using immunohistochemistry, and studied their colocalisation with calretinin, a calcium binding protein present in both inner hair cells and auditory nerve fibers. Immunoreactivity for HCN-1 and 2 was detected by confocal analyses in afferent dendrites and somata of auditory nerve fibers. HCN expression at afferent dendrites along with electrophysiological data indicate a critical role of HCN channels in regulating synaptic transmission at the inner hair cell afferent synapse.

Supported by EMBO ALTF 952-2006 to IR and NIDCD DC006476 to EG.

## **221** Single-Channel Characterization of Diverse Ion Channel Types in Postnatal CBA/Caj Murine Spiral Ganglion Neurons

Wei Chun Chen<sup>1</sup>, Robin Davis<sup>1</sup>

<sup>1</sup>Department of Cell Biology and Neuroscience, Rutgers University

Spiral ganglion neurons at different cochlear locations display distinctive firing patterns that are shaped by many types and classes of voltage-gated ion channels (Adamson et al., *JCN*, 2002), which are subject to regulation by neurotrophins (Adamson et al., *J. Neurosci.*, 2002). What is not clear, however, is whether the differential distributions that we have noted for Kv1.1, Kv1.2, Kv3.1, Kv4.2, and large  $Ca^{2+}$ -activated  $K^+$  channel (BK) can be solely accounted for by alterations in ion channel subunit density. Other biophysical features, such as calcium sensitivity, inactivation rate, and voltage dependence of activation may also be affected. to address this issue we have begun to characterize the elementary properties of basic channel types in spiral ganglion neurons isolated from known regions of the ganglion. Single-channel patch clamp recordings confirm the current types known to be present in the spiral ganglion (Mo & Davis, *J. Neurophysiol.*, 1997). for example, a small conductance ( $\sim 1.0$  pS) cationic current with long openings evident upon hyperpolarization typifies the  $I_h$  current originally described by DiFrancesco (*Nature*, 1986). Depolarizing voltage pulses reveal both inactivating and non-inactivating conductances ( $21 \pm 1$  pS;  $n = 6$ ), consistent with the A-type currents and delayed rectifiers previously described (Adamson et al., *JCN*, 2002). We also observed intermediate (98 pS) and large ( $166 \pm 17$  pS;  $n = 4$ ) conductance channels, consistent with the presence of  $Ca^{2+}$ -activated  $K^+$  currents. Heterogeneity of the large conductance channels noted in this and previous studies (Bowne-English & Davis, *ARO Abstracts*, 2003) could result from the diversity of BK  $\alpha$ - and  $\beta$ -subunits.

in order to understand better the biophysical properties of ionic currents in the spiral ganglion, we are currently comparing their single-channel properties in different regions of the cochlea and determining how they are regulated by neurotrophins. Supported by NIH NIDCD RO1 DC01856.

## **222 Regional Determinants of Neuronal Excitability in the Murine Spiral Ganglion**

Qing Liu<sup>1</sup>, Robin Davis<sup>1</sup>

<sup>1</sup>Rutgers University

The endogenous firing features of postnatal spiral ganglion neurons vary systematically along the length of the cochlea with local heterogeneity superimposed upon systematic longitudinal changes in action potential number, latency, and onset kinetics. In recent work we have focused on action potential threshold, which is distributed non-monotonically with the greatest sensitivity in the mid-frequency region (Liu & Davis, *J. Neurophysiol.*, 2007). We are currently in the process of determining the underlying mechanisms that regulate neuronal excitability since these features could contribute to frequency sensitivity. Because we also documented a similar non-monotonic distribution of the cationic hyperpolarization activated current ( $I_h$ ), we are testing whether this current contributes in some fashion to the elevated neuronal excitability in the mid-frequency region of the cochlea.

In a preliminary set of experiments, we examined the possibility that  $I_h$  could have a direct effect on action potential threshold. CsCl (5mM) was used to block the  $I_h$  current in cells where constant current injection was used to maintain a membrane potential of -80 mV. Subsequent to measurement of threshold, perfusion of CsCl caused the membrane potential to drop to -106.5 mV ( $\pm$  5.8 mV,  $n=5$ ), but when the current injection was reduced to return the membrane potential to -80 mV, threshold itself was unchanged ( $\Delta = -0.96 \pm 1.5$  mV,  $n=5$ ).

The results from these experiments suggest that two different mechanisms are responsible for determining the sensitivity of spiral ganglion neurons in the mid-frequency region: altered resting potential and firing threshold. Resting potential levels appear to be regulated by  $I_h$  currents, as in other neuronal systems (McCormick and Pape, *J. Physiol.*, 1990). Future studies will extend these preliminary findings and then focus on the underlying ionic currents responsible for threshold regulation in spiral ganglion neurons.

Supported by NIH NIDCD R01 DC-10856.

## **223 Refractoriness Improves Spike-Count Reliability, But Does Not Affect Spike-Timing Precision, of Auditory Nerve Responses**

Michael Avissar<sup>1</sup>, Adam C. Furman<sup>1</sup>, James C. Saunders<sup>1</sup>, Thomas D. Parsons<sup>1</sup>

<sup>1</sup>University of Pennsylvania

Refractoriness, a transient decrease in spike discharge probability following a spike, limits the number of available responses of a sensory neuron to environmental stimuli. Although it constrains the response range of a neuron, refractoriness also reduces the variability of the response to repeated trials of a stimulus. We measured this neural noise in auditory nerve in response to repeated pure tones using three measures of trial-to-trial variability: the jitter of spike timing, the entropy of spike counts, and the entropy of temporal patterns. The effect of refractoriness was examined by using a stochastic point process model and

eliminating discharge history effects. Refractoriness reduced the entropy of spike counts and temporal patterns but did not affect the jitter of spike timing. The effect of refractoriness on temporal patterns was largest at characteristic frequencies between 300 to 400 Hz. We conclude that postsynaptic refractoriness could enhance rate coding by increasing the reliability of spike counts, and temporal coding at select frequencies by increasing the reproducibility of temporal patterns. Given that refractoriness is a property of the postsynaptic fiber, the results also suggest that precision of spike timing is largely determined by presynaptic mechanisms.

This research was supported by awards from the NIDCD (DC000710 - JCS, DC003783 - TDP), the Pennsylvania Lions Hearing Research Foundation (JCS, TDP).

## **224 A Simple Physiological Model to Account for First-Spike Latency and Rate-Level Functions of Auditory-Nerve Fibers and for Perceptual Detection Thresholds**

Heinrich Neubauer<sup>1</sup>, Peter Heil<sup>1</sup>

<sup>1</sup>Leibniz Institute for Neurobiology, 39118 Magdeburg, Germany

The physiological mechanisms underlying first-spike latency (FSL) of auditory-nerve fibers (ANFs) are of considerable interest, because of a close correspondence between perceptual detection thresholds for sounds in quiet and a measure of neuronal thresholds derived from the FSL (Heil & Neubauer, PNAS 2003; Meddis, JASA 2006). Also, the possibility of coding of stimulus attributes by FSL has gained attention (Chase & Young, PNAS 2007 and references therein; Heil, Curr Opin Neurobiol 2004 for review). Here we present a minimal physiological model which accurately explains the dependence of FSL of cat ANFs on amplitude and rise time of tonal stimuli. The model is based on low-pass filtering the stimulus envelope, formation of transmitter release events from the conjunction of  $\alpha \approx 3$  independent sub-events, where the probability of each of those occurring is proportional to the low-pass filtered stimulus amplitude, and probability summation over time. Two of the 5 parameters, viz.  $\alpha$  and the time constant  $\tau$  ( $\approx 1.2$  ms), can be considered constant for the vast majority of ANFs, while the other 3, viz. minimum delay  $L_{\min}$ , spontaneous rate  $R_{\text{spont}}$ , and sensitivity  $k$ , vary in meaningful ways with the ANFs' empirical spontaneous rates. The model also accounts for the distributions of FSLs obtained from the ANFs' responses to repeated presentations of a given stimulus and for the low-level (unsaturated) portions of the rate-level functions. Finally, the model also successfully describes perceptual detection thresholds for tones of different durations and envelopes presented in quiet.

This unifying model further supports a close link between the mechanisms determining the timing of the first (and other) evoked spikes at the level of the auditory nerve and detection thresholds at the perceptual level.

Supported by grants of the Deutsche Forschungsgemeinschaft to P.H. (He1721/5-1, 5-2, 7-1 and SFB-TR 31).

## **[225] Envelope Coding in Auditory-Nerve Fibers Following Noise-Induced Hearing Loss**

Sushrut Kale<sup>1</sup>, Michael Heinz<sup>1</sup>

<sup>1</sup>*Purdue University*

Envelope coding of amplitude modulated sounds has been extensively studied in the normal-hearing auditory system, both neurophysiologically and psychoacoustically. Although, there is evidence for near-normal envelope coding for hearing-impaired listeners from basic psychoacoustical tasks, a thorough study of the neural coding of temporal envelopes in the hearing-impaired auditory periphery has not been performed. Results here represent data collected from individual auditory nerve (AN) fibers in anesthetized chinchillas with normal and impaired hearing. Hearing loss was induced using acoustic overexposure to narrow-band noise centered around 2 kHz.

Envelope coding of sinusoidally amplitude modulated (SAM) tones and single formant stimuli (SFS) was quantified by synchronization index and the modulation depth measured from the response envelope of the period histograms. Synchrony-level and modulation depth-level functions were measured in 5 dB steps in response to SAM tones and SFS stimuli in quiet and in background noise. Temporal modulation transfer functions (TMTFs) were also measured in response to SAM tones.

Preliminary findings suggest that phase locking to the envelope of SAM tones and SFS stimuli is not adversely affected by noise-induced hearing loss, and is in fact enhanced in some ways. the TMTFs for impaired fibers with broader tuning showed strong envelope coding over a wider modulation frequency range (e.g., increased 3-dB cutoffs). Overall modulation gain was slightly higher for impaired fibers. Effects of increasing sound levels and background noise levels on envelope coding of SAM tones and SFS were comparable across the population of normal and impaired fibers.

The overall similarity in envelope coding of the simple stimuli studied here between the populations of normal and impaired fibers is consistent with psychophysical findings that suggest near-normal envelope perception by hearing impaired listeners.

Supported by NIH/NIDCD grant R03-DC007348.

## **[226] Rate-Level and Vector Strength Thresholds Converge in Overstimulated Chick Cochlear Nerve Units**

Evelyn Lazaridis<sup>1</sup>, Michael Avissar<sup>1</sup>, Kirin S. Kennedy<sup>1</sup>, Michael Bilyk<sup>1</sup>, James C. Saunders<sup>1</sup>

<sup>1</sup>*Department of Otorhinolaryngology: Head and Neck Surgery, University of Pennsylvania*

Sound overstimulation causes profound changes in the response properties of chick cochlear nerve units. One well-documented change is a threshold shift in rate level (RL) functions. When phase-locked stimuli are employed it is also possible to calculate vector strength (VS) as a function of stimulus intensity. From this, a VS threshold can be determined. When RL and VS thresholds are compared in control units, VS thresholds are better in low

characteristic frequency units, but this difference declines as frequency increases. the lower VS thresholds are attributed to the entrainment of spontaneous activity to the stimulus phase. the present study compares RL and VS thresholds in units obtained from chicks exposed to an intense pure tone. As expected the RL thresholds exhibited a significant threshold shift. the difference between RL and VS thresholds, however, were much smaller than in the control animals. This difference was attributed to an overstimulation-induced reduction in spontaneous activity, which most likely limited entrainment to the phase-locked stimulus in the exposed units at intensities below RL threshold.

[Supported in part by DC-000710 to JCS and the Neurobiology of Otorhinolaryngology Training Grant to EL.]

## **[227] The Effect of Level On the Distribution of Stimulus Phase Across the Auditory Nerve**

Alan Palmer<sup>1</sup>, Trevor Shackleton<sup>1</sup>

<sup>1</sup>*MRC Institute of Hearing Research, Nottingham, UK*

Direct mechanical measurements at the apex of the cochlear are difficult, so the tendency for action potentials in response to low-frequency stimuli (< 3.5 kHz in the guinea pig; Palmer & Russell, 1986: *Hear Res.*, 24, 1-16) to occur at a specific phase of the stimulus waveform has been used to infer the basilar membrane motion. Van der Heijden and Joris (2006: *J. Neurosci.*, 26, 11462-11473) reported "panoramic measurements" of phase at a single sound level (~ 35 dB above threshold) in the cat using inharmonic tonal complexes to extract the linear component of the response. We confirm and extend these results by recording phase-locked responses, to pure tones over a wide range of frequencies and sound levels, of 186 auditory nerve fibres in the anaesthetised guinea pig (characteristic frequencies [CFs] from 0.071 to 3.227 kHz). Phase lag along the basilar membrane (from base to apex) increased slowly to a frequency position above the frequency of stimulation, beyond which it increased at a much faster rate. These phase distributions are stable over a wide range of sound levels (up to 90 dB SPL) and indicate a change in the propagation rate of the travelling wave. Measurements from individual fibres showed systematic variations in phase with sound level, confirming previous reports (e.g. anderson, Rose, Hind & Brugge, 1971: *J. Acoust. Soc. Amer.*, 49, 1131-1139). We found a "null" frequency (not always at CF) at which no variation in phase occurred with sound level. Away from this null frequency a maximum variation in the phase of 0.2 cycles occurred with sound level: a progressive lag at frequencies below the null and a progressive lead for frequencies above the null. These patterns of response phase are consistent with direct measurements of cochlear mechanics.



## **228 Estimating the Number of Auditory Nerve Fibers Using the Compound Action Potential**

**Brian Earl<sup>1</sup>**, Mark Chertoff<sup>1</sup>, Dianne Durham<sup>1</sup>, Dana Jacobson<sup>1</sup>

<sup>1</sup>*Kansas University Medical Center*

The long-term goal of this research is to develop clinical techniques that characterize hair cell transduction and auditory nerve function in order to provide a greater understanding of the pathophysiology associated with hearing loss. Diagnosis based on pathophysiology will lead to new treatment strategies such as improved signal processing algorithms for hearing aids, and with future developments in hair cell regeneration and genetic therapy, provide tools to target the site for therapeutic agents. the purpose of this study was to determine if the compound action potential (CAP) could be used to estimate the number and health of auditory nerve fibers in impaired ears.

The auditory nerve of Mongolian gerbils was approached by piercing the dorsomedial wall of the round window antrum. a needle electrode was inserted through the hole to deliver current or mechanically damage the nerve. Animals recovered for approximately two months after which CAPs were recorded from an electrode placed on the round window. Stimuli ranged from 1000-16000 Hz with levels ranging from 15-100 dB SPL. Animals were euthanized, histologic sections prepared, and auditory nerve fibers counted using stereologic procedures. Dependent measures were conventional amplitude and latency of N1 and parameters of a convolution model of the CAP. in this initial study the cochlea was spared to avoid confounding effects of cochlear damage.

For normal ears, the average fiber count was 16,587 ( $\pm$  3,172 SD). Lesioned ears had fewer fibers as compared to normal ears and showed normal CAP thresholds with delayed N1 latencies and decreased amplitudes. the frequency parameter from the convolution model, which quantifies the period of N1 oscillation, was approximately half that of normal ( $\sim$ 1000 Hz). These changes indicate that the quantities derived from the CAP are sensitive to the number of auditory nerve fibers and may be able to predict auditory nerve status.

## **229 Measured and Predicted ECAP Response Patterns in the Guinea Pig Auditory Nerve**

**Fuh-Cherng Jeng<sup>1</sup>**, Paul Abbas<sup>2</sup>, Ning Hu<sup>2</sup>, Charles Miller<sup>2</sup>, Kirill Nourski<sup>2</sup>, Barbara Robinson<sup>2</sup>

<sup>1</sup>*Ohio University*, <sup>2</sup>*University of Iowa*

Many of the current cochlear implant speech processors generate trains of amplitude-modulated current pulses in order to deliver the temporal information of speech signals. However, it is not clear to what extent the ECAP response patterns can be predicted from the single-pulse ECAP growth functions. in this study, we used the electrically evoked compound action potential (ECAP) in response to each pulse in a train to evaluate the extent to which the response of the auditory nerve reflects the modulation of

the stimulus train, and also to evaluate to what extent the ECAP response patterns can be predicted from single-pulse ECAP growth functions. Experiments were conducted in guinea pigs that were acutely deafened with intracochlear injections of neomycin to abolish hair cell functionality while leaving an intact auditory-nerve fiber population that could be electrically stimulated. Stimuli were biphasic pulses delivered through a wire electrode placed within the basal turn of the scala tympani. Recordings were made using ball electrodes placed on the auditory nerve. ECAP response patterns were measured using sinusoidally amplitude-modulated pulse trains and were found to be sensitive to modulation depths as low as 5% and were highly distorted from the stimulus envelope at 50% modulation depth or greater. the ECAP response patterns were also predicted from single-pulse ECAP growth functions and exhibited less distortion than the measured ECAP response patterns, particularly at the higher modulation depths. Linear regressions and their residual errors were used to quantify the differences between the measured and predicted data sets. Distortion of the ECAP response patterns was found to be influenced by both the inherent nonlinearity of the single-pulse ECAP growth function and the dynamic nonstationarity of the ECAP, and the dynamic nonstationarity of the ECAP tended to dominate the distortion when higher modulation depths were used.

## **230 Effects of Electrical Stimulation On Acoustically Evoked Cochlear Potentials in Guinea Pigs**

**Christiaan Stronks<sup>1</sup>**, Huib Versnel<sup>1</sup>, Vera Prijs<sup>1</sup>, Sjaak Klis<sup>1</sup>

<sup>1</sup>*Dept. of Otorhinolaryngology, University Medical Center Utrecht, the Netherlands*

Patients with severe to profound high-and mid-frequency hearing loss, but residual low-frequency hearing, are nowadays considered as potential candidates for cochlear implantation. Preservation of residual hearing can improve speech intelligibility and esthetic value of sounds after implantation. However, the improvement by the addition of a hearing aid to a cochlear implant is variable. This raises the issue of how electric and acoustic stimulation interact in the cochlea.

in this study the effects of ipsilateral electric stimuli on acoustically evoked cochlear potentials were examined using a forward masking paradigm in guinea pigs. Cochlear potentials were recorded from the apex of the cochlea, using tone bursts (probes) of variable frequency and level. Electric currents (maskers) preceded the acoustical probe and were presented extracochlearly on the basal turn. Maskers consisted of trains of 10 biphasic pulses at 1 kHz. Masker current level and masker-to-probe interval were varied.

Electrical masking reduced the compound action potential (CAP) amplitude, while effects on cochlear microphonics were limited. in general, CAP masking was maximal using high-frequency probes (8 and 16 kHz) of low acoustical level. Masking increased with current level and decreased with masker-to-probe interval. At high current levels (0.8

mA), masking was evident at masker-to-probe intervals up to 10 ms. At high frequencies of low acoustical level, CAPs were completely masked, increasing the CAP threshold up to 20 dB. CAP latencies of high-frequency probes were increased by 0.2-0.5 ms, even at levels where the CAP was not masked.

Electrical masking of CAPs elicited by low frequencies was limited, probably due to the basal location of the stimulation electrodes on the cochlea. This finding supports the idea that high-frequency cochlear regions can be stimulated electrically, without affecting low-frequency hearing.

This work was supported by the Heinsius-Houbolt Fund, the Netherlands

### **[231] Effects of TRPV Agonists and Antagonists in Optical Stimulation of the Cochlea**

**Eul Suh<sup>1</sup>**, Agnella Izzo<sup>2</sup>, Joseph T. Walsh, Jr.<sup>2</sup>, Claus-Peter Richter<sup>1</sup>

<sup>1</sup>*Department of Otolaryngology, Feinberg School of Medicine, Northwestern University,* <sup>2</sup>*Department of Biomedical Engineering, Northwestern University*

Pulsed infrared lasers can be used to stimulate auditory neurons (Izzo et al., LSM, 2006). It has been suggested that optically radiated neural tissue is stimulated via a thermal mechanism (Wells et al., BiophysJ., 2007). We propose that TRPV channels are activated by the transient temperature increase from the radiation. the TRPV channels are a subfamily of the Transient Receptor Potential (TRP) ion channels, and are known to be thermosensitive. of interest are the TRPV1 and TRPV3 channels, both of which are heat-activated and are believed to interact with each other to form heteromeric receptor channels (Smith et al., Nature, 2002). TRPV1 has an activation threshold of approximately 43°C while TRPV3 has a lower threshold of approximately 39°C (Smith et al., 2002).

Here, we explore the effects that the corresponding agonists and antagonists of these channels may have in the optical stimulation of the gerbil cochlea. Solutions of the following three compounds were applied to the gerbil cochlea in vivo, either through perfusion or direct application to the round window of the cochlea: resiniferatoxin (TRPV1 agonist), capsazepine (TRPV1 antagonist), and ruthenium red (TRPV1-4 channel blocker). Optically and acoustically-evoked compound action potentials (CAP) were measured before and after application of these three compounds.

Preliminary data indicate that the TRPV channels may have an effect on optically evoked neural responses in the cochlea. After perfusing the cochlea with capsazepine, we measured a gradual decline in CAP response to laser stimulation followed by a gradual increase subsequent to ending the perfusion. in addition, when applying capsazepine directly to the round window, we measured a decline in optically-evoked CAP's, followed by an increase after applying the agonist resiniferatoxin.

This project has been funded with federal funds from the National Institute on Deafness and Other Communication

Disorders, National Institutes of Health, Department of Health and Human Services, under Contract No. HHSN260-2006-00006-C / NIH No. N01-DC-6-0006.

### **[232] Evidence Suggesting the Cochlear Compound Action Potential is a Stationary Potential Generated Across the *Dura Mater*** **Daniel J. Brown<sup>1</sup>**, Robert Patuzzi<sup>2</sup>

<sup>1</sup>*Washington University School of Medicine,* <sup>2</sup>*The University of Western Australia*

Our recent studies (Patuzzi et al., 2004a,b,c, Hear Res 190, 75-108) and those by others (Chertoff, 2004, JASA 116, 3022-30; Searchfield et al., 2004, Hear Res 114, 127-38; Sendowski et al., 2006, Hear Res 15, 69-72) have investigated how stochastic and sound-evoked neural activity from the cochlea can be used to diagnose pathologies of the VIII<sup>th</sup> nerve. Several of these studies hypothesised that the extracellular unitary potential (UP), which underlies the compound action potential (CAP; Goldstein and Kiang, 1958, JASA 30, 107-14) and the spectrum of the neural noise (SNN; Dolan et al., 1990, JASA 86, 2167-71) contains components that are the second derivative of the oscillatory intracellular action potential. the present study used differential recordings in guinea pigs, with and without cochlear nerve sectioning, nerve compression, transient focal cooling and pharmacological blockade to investigate further the origins of the CAP. Results showed that the CAP inverted polarity across the internal auditory meatus, was similar throughout the cochlea and after removal of the cochlear nucleus, and was unaltered by sectioning of the efferent neurones. These results suggest the UP is *not* an extracellular analogue of the second derivative of the intracellular action potential, but is almost entirely a volume conducted potential, as first described by Teas et al., (1962, JASA 47, 1527-37). Furthermore, we describe that the UP has properties suggesting that it is a stationary potential, most likely produced by extracellular action currents generating an Ohmic voltage across the *dura mater* as the VIII<sup>th</sup> nerve passes through into the braincase (Moushegian et al., 1962, J Neurophys 25, 515-29; Møller, 1983, Exp Neurol 80, 633-44). As such it can be altered by either the action currents themselves, or by changes in the integrity of the *dura mater* which alter its resistance. This is important in the interpretation and clinical use of the CAP and SNN as diagnostic measures of cochlear pathologies. Supported by Ad-Hoc Scholarship from the University of Western Australia.

### **[233] Comparing Chirp- and Click-Evoked Human Compound Action Potentials**

**Jeffery Lichtenhan<sup>1</sup>**, Mark Chertoff<sup>2</sup>, Marie Willis<sup>2</sup>  
<sup>1</sup>*Eaton-Peabody Laboratory of Auditory Physiology,*  
*Massachusetts Eye and Ear Infirmary,* <sup>2</sup>*University of Kansas Medical Center*

Compound action potentials (CAPs) arise from a stimulus-evoked synchronous discharge of numerous auditory nerve fibers. Transient acoustic stimuli, such as a click, that are commonly used to evoke CAPs are limited to excitation of primarily basal regions of the cochlear

partition. a chirp signal sweeping from low to high frequency at a rate dependent upon the travel time delay of various cochlear frequency places, theoretically excites the entire cochlear partition simultaneously. We thus hypothesized that chirp-evoked and click-evoked CAPs should differ. the purpose of this study was to determine which attributes of CAPs recorded in human subjects to a chirp signal differ from those to a click signal.

Chirp signals were constructed in MATLAB according to Fobel and Dau (2004; JASA, 116(4), 2248-57) using the human cochlear traveling wave delay estimates from Eggermont (1979; JASA, 65(2), 463-70). with a Bio-logic Navigator PRO, CAPs were recorded using a tympanic membrane electrode. Acoustic stimuli varied from 125 to 75 dB pSPL stimuli in 10 dB steps.

The results showed that at low signal levels the chirp-evoked CAPs had larger amplitude than the click-evoked CAPs. At high signal levels the disparity between chirp- and click-evoked CAP amplitudes was less. This suggests that at low signal levels, the chirp stimulus enhances the synchronous discharge among auditory nerve fibers.

Supported by the University of Kansas Medical Center Biomedical Research Training Program.

### **234 Is there an Approach to the Cochlea for Insertion of an Intraneural Electrode with Hearing Preservation?**

**Gerrit Paasche**<sup>1</sup>, Thomas Rau<sup>1</sup>, Markus Pietsch<sup>1</sup>, Timo Stoever<sup>1</sup>, Thomas Lenarz<sup>1</sup>, Omid Majdani<sup>1</sup>

<sup>1</sup>Hannover Medical School Protection of residual hearing gains more and more importance for cochlear implant (CI) patients. Each opening of the cochlea for electrode insertion bears a potential risk for damage to cochlear structures and loss of residual hearing. Therefore, a device for electrical stimulation of the auditory nerve without the risk of damage to the cochlea is of great interest. a possible position for such an electrode could be the modiolar trunk of the auditory nerve. for stimulation at this place compared to stimulation with regular cochlear implant electrodes, much lower thresholds and less interference between simultaneously stimulated electrodes were recently shown (Middlebrooks and Snyder, 2007).

in our current study on fresh frozen human temporal bones, a navigation system was used in order to find possible trajectories for drilling through the bone to the modiolar nerve without damaging any other structures. for this purpose, 5 temporal bones were marked with registration markers (mini osteosynthesis screws), scanned (flat panel Volume CT, General Electric) and the data were transferred to iPlan2.5 image processing and planning software of the navigation system (VectorVision2, BrainLAB). Three main approaches to the modiolar trunk of the auditory nerve were identified. the first possible route is an enlarged posterior tympanotomy to use the space between the basal part of the first turn and the second turn of the cochlea. a second route would be in dorso-medial direction to the cochlea and the third approach could be through the superior semicircular duct.

After scanning and evaluating the temporal bones, only the translabyrinthine approach provides the possibility for a

trajectory going to the modiolar nerve. As a straight approach would then pass a part of the cerebellum, special surgical tools like a laser with optics that allow drilling with an angle have to be used.

### **235 Development of Eye Movement Image Analysis Technique Using Image J**

**Makoto Hashimoto**<sup>1</sup>, Takuo Ikeda<sup>1</sup>, Kazuma Sugahara<sup>1</sup>, Hiroaki Shimogori<sup>1</sup>, Hiroshi Yamashita<sup>1</sup>

<sup>1</sup>Yamaguchi University

Using an infrared CCD camera for recording eye movement is widely accepted and analysis of eye movement is essential for investigating vestibular disturbances. We devised an original eye movement image analysis technique using an infrared CCD camera, a personal computer and public domain software. the analysis was performed using the publish domain software Image J program (developed by the U.S. National Institutes of Health). the video image from an infrared CCD camera was captured at 30 frames per second in 320×240. for analysis of the horizontal and vertical components, the X-Y center of the pupil was automatically calculated using the original macro. for analysis of torsional components, the whole iris pattern, which was rotated each 0.1 degrees, was overlaid with the same area of the next iris pattern, and the angle at which both iris patterns showed the greatest match was calculated. Analysis in eye tracking test, as well as test of optokinetic nystagmus were also applied to this system. Using this technique, it is possible to inexpensively perform eye movement analysis, including in 3-dimension, from video images recorded by many types of infrared CCD cameras.

### **236 Vestibular Function in Patients with Otosclerosis and Balance Disorders**

**Alexis Bozorg Grayeli**<sup>1</sup>, Olivier Sterkers<sup>1</sup>, Michel Toupet<sup>2</sup>

<sup>1</sup>Inserm, UNIT-M 867, APHP Hopital Beaujon, University Paris 7, France, <sup>2</sup>Centre d'Exploration Oto-Neurologique, Paris, France

Introduction: Vestibular function in patients with otosclerosis and balance disorders not related to the immediate postoperative course is rare and seldom described or explored. the aim of this study was to investigate the clinical aspects of these disorders and to assess the audio-vestibular functions of these patients.

Materials and methods: Among 13800 patients examined for balance disorders between 2002 and 2006, 98 (0.7%) presented with otosclerosis. in this group, 73 (28 not operated on, 27 operated on one side, and 18 operated on both sides for hearing rehabilitation) and undergoing audio-vestibular assessment (clinical examination, audiometry, videonystagmography with caloric and rotatory tests, subjective vertical) were included in this retrospective series.

Results: Patients complained of dizziness in 42 cases (58%), symptoms compatible with benign paroxysmal positional vertigo in 38 cases (52%), and rotatory vertigo in 18 cases (25%). in non operated patients labyrinthine the reflectivity measured by the caloric test was highly correlated between left and right ears (R=0.59, P< 0.005,

ANOVA) while there was no left-right correlation for the hearing loss (air and bone conduction pure tone thresholds). This observation suggested that the labyrinthine involvement was bilateral even in patients with unilateral or asymmetrical audiometric signs.

in patients operated on unilaterally, the vestibular reflectivity was lower on the operated side than on the non operated ear suggesting a surgery-induced deficit.

There was no correlation between the sensorineural component of the hearing loss (bone conduction pure tone thresholds) and the vestibular reflectivity. the subjective vertical was not significantly deviated in these patients probably due to the compensation mechanisms.

Conclusions: Balance disorders in patients with otosclerosis can be associated to canal or otolithic dysfunction. Vestibular function as measured by reflectivity remains symmetrical in non operated patients even in cases of unilateral or asymmetrical hearing loss while operated patients with persistent imbalance show vestibular deficit on the side of surgery.

### **[237] Dynamic Subjective Visual Vertical in Vestibular Neuritis During the Recovery Phase**

**Jae Yong Byun<sup>1</sup>, Seung Geun Yeo<sup>1</sup>, Chang Il Cha<sup>1</sup>, Moon Seo Park<sup>1</sup>**

<sup>1</sup>*Kyung Hee University*

Objectives/Hypothesis: by assessing unilateral utricular function at the acute and subacute stages, we sought to determine the ability of the subjective visual vertical (SVV) during eccentric rotation (dynamic SVV) in localizing the site of the lesion in unilateral vestibular neuritis. in addition, we compared the validity of the dynamic SVV with static SVV during the compensated recovery phase.

Methods: the static SVV and dynamic SVV of 19 patients diagnosed with acute unilateral vestibular neuritis and 31 patients diagnosed with the subacute stage of vestibular neuritis were determined in this study. First, the static SVV was measured in a dark booth without rotation. the dynamic SVV was measured during rotation with an eccentric displacement of the head to 3.5 cm from the vertical rotation axis during a constant velocity of 300°/s.

Results: in the acute stage of vestibular neuritis, the static SVV showed an increase in deviation to the side of the lesion compared to findings in normal subjects. in the subacute stage, it did not differ significantly from that of the normal subjects. the dynamic SVV, however, had a statistically significant increase in deviation to the side of the lesion compared to normal subjects in both the acute and subacute stages.

Conclusion: in patients with the compensated phase of unilateral vestibular neuritis, the SVV during eccentric rotation improves both the sensitivity and specificity of otolith function testing. the dynamic SVV would be an effective method in the diagnosis and localization of underlying vestibulopathy, especially compensated unilateral vestibular neuritis.

### **[238] Clinical Significance of Vibration-Induced Nystagmus and Head-Shaking Nystagmus Through the Followup Examinations in Patients with Vestibular Neuritis**

**HongJu Park<sup>1</sup>, JungEun Shin<sup>1</sup>, SangKyun Lim<sup>1</sup>, HyangAe Shin<sup>1</sup>**

<sup>1</sup>*Konkuk University Hospital*

The aims of this study were to verify if vibration-induced nystagmus in patients with vestibular neuritis changed over time and to compare the results of vibration-induced nystagmus test to those of caloric test and head-shaking nystagmus test. We compared vibration-induced nystagmus and head-shaking nystagmus tests with caloric testing results in 23 patients (M:F = 11:12, 15 ~ 67 years old) with acute vestibular neuritis seen at onset and in follow-up for around 2 months. Results of two tests were compared with the caloric test. the eye movement recordings were made and the maximum slow-phase eye velocities were calculated during vibration and after head-shaking. If spontaneous nystagmus was present, it was subtracted from the slow-phase eye velocities of vibration-induced nystagmus and head-shaking nystagmus. Positive value of the slow-phase eye velocities means slow-phase eye movement to the lesioned side.

At the initial assessment, VIN of which SPV was directed towards the lesioned side was observed in 21 (91.3%) of 23 patients (mean 10deg/s, range: -3 ~ 28 deg/s) and the direction of VIN was consistently expectable considering the side of the lesion. SPV of VIN was directed towards the intact side in one patient. At follow-up, SPV of 2nd VIN decreased when compared to those of 1st VIN ( $p < 0.05$ ). VIN (mean 5 deg/s, range: -7 ~ 21 deg/s) appeared in 19 (82.6%), it changed direction in 3 and disappeared in 1. At the initial assessment, HSN to the lesioned side was observed in 22 patients (95.7%, mean 15 deg/s, range: 0 ~ 41 deg/s). At follow-up, SPV of 2nd HSN decreased when compared to those of 1st HSN ( $p < 0.05$ ). HSN to the lesioned side (mean 7 deg/s, range: -12 ~ 25 deg/s) appeared in 17 (73.9%), it changed direction in 5 and disappeared in 1. Correlations between UW in caloric test and the SPV of VIN (average values of SPVs when each mastoid was vibrated) or the SPV of HSN were calculated. Weak, though statistically significant, correlations were observed in between UW & VIN, but not in between UW & HSN.

Both vibration-induced nystagmus and head-shaking nystagmus tests could probe vestibular asymmetry in patients with unilateral vestibular neuritis. Although vibration-induced nystagmus test can predict the severity of vestibular asymmetry in acute and compensated state, head-shaking nystagmus test could not. Our results suggest that VIN might represent the peripheral vestibular asymmetry; however, HSN might represent the stored vestibular asymmetry in velocity storage system induced by peripheral asymmetry.

### **239 Ocular and Cervical Vemps in Superior Canal Dehiscence Syndrome**

John Carey<sup>1</sup>, Miriam Welgampola<sup>2</sup>, Lloyd Minor<sup>1</sup>

<sup>1</sup>Johns Hopkins School of Medicine, <sup>2</sup>University of New South Wales, Sydney, Australia

Diagnosis of superior canal dehiscence syndrome (SCDS) relies upon symptoms and signs such as sound- or pressure-induced vertigo or oscillopsia; demonstration of characteristic upward, contraversive eye movements in response to sound or pressure; and the presence of a defect in the bone overlying the superior semicircular canal on temporal bone CT. Lowered stimulus thresholds for eliciting vestibular-evoked myogenic potentials (VEMPs) provide additional conformation. Our objective was to examine the diagnostic utility of ocular and cervical VEMPs before and after canal plugging for SCDS. VEMPs evoked by air- and bone-conducted 500 Hz tones were measured from the sternocleidomastoid muscles (cVEMPs) and from peri-ocular sites (oVEMPs). Reflex amplitudes and thresholds were recorded from 20 normal volunteers, 10 newly diagnosed subjects with SCDS and 8 subjects who had previously undergone superior canal plugging. In newly diagnosed SCDS ears, thresholds for evoking cervical and ocular VEMPs using air conducted tones were on average,  $83.85 \pm 1.40$  dB SPL (Sound Pressure Level) and  $85.38 \pm 1.32$  dB SPL, 25-30 dB below those of normal controls and unaffected ears. Amplitudes of the cVEMP (although on average, larger in SCDS), overlap with the control values and are unsuitable as a diagnostic measure in SCDS. In contrast, air conducted oVEMP amplitudes in newly diagnosed SCDS did not overlap with those of controls and were consistently greater than 25 microvolts peak to peak (range: 29-111). Therefore, oVEMP amplitudes may be a useful parameter in the diagnosis of SCDS once reference ranges for controls have been documented across age groups. Successful canal plugging with resolution of symptoms resulted in return of reflex thresholds and amplitudes to the normal range. Conclusions: Thresholds for ocular and cervical VEMPs evoked by air conducted sound are equally useful physiological measures in the diagnosis and follow up of SCDS. Stimulus thresholds are consistently lowered upon presentation and normalize following corrective surgery. Amplitude of the ocular VEMP is a promising new measure for SCDS.

### **240 Vestibular Evoked Myogenic Potentials (VEMP): Systematic Survey of Variance**

S.R. Prakash<sup>1</sup>, John G. Guinan<sup>2</sup>, Barbara S. Herrmann<sup>3</sup>, Sharon G. Kujawa<sup>4</sup>, Steven D. Rauch<sup>5</sup>

<sup>1</sup>Harvard-MIT Division of Health Science and Technology,

<sup>2</sup>Eaton-Peabody Laboratory, Mass. Eye & Ear Infirmary,

<sup>3</sup>Dept. of Audiology, Mass. Eye & Ear Infirmary, <sup>4</sup>Dept. of Otology & Laryngology, Harvard Medical School, <sup>5</sup>Dept. of Otolaryngology, Mass. Eye & Ear Infirmary

Vestibular Evoked Myogenic Potentials (VEMP) are inhibitory potentials recorded from the sternocleidomastoid muscle in response to acoustic stimulation of the ipsilateral saccule. Clinical studies have suggested that VEMP is useful in evaluation and monitoring of patients with

Meniere's disease, and in detection of superior semicircular canal dehiscence. The feasibility of using VEMP serially for monitoring progression of disease or response to treatment, and the feasibility of using VEMP to compare across patients, however, depends critically on an understanding and control of the sources of variance in the VEMP measurements. One major source of variance in the VEMP is muscle effort. There is now wide acknowledgement of the need to normalize the recorded potentials relative to muscle effort. Most labs and commercial equipment have implemented a normalization algorithm that uses a pre-stimulus recording epoch of EMG activity to normalize across the entire recording. An alternative is to normalize based upon a running average conducted throughout the data acquisition. In order to systematically explore questions of VEMP variation within and between subjects we have acquired a data set of multiple recording sessions in multiple subjects. In each recording session all raw data are streamed to disk, allowing averages to be made in different ways offline. We use this systematic data set to define the fine temporal characteristics of variation in the pre-stimulus EMG, during the actual VEMP response, and in the immediate post-VEMP EMG. We then use these temporal features to seek normalization algorithms that minimize test-retest variation within subjects and permit valid comparison across subjects.

### **241 Evoked Vestibular Myogenic Potentials: Effect of Electrode Location and Cross-Talking**

Kianoush Sheykholeislami<sup>1</sup>, Julie Bonko<sup>2</sup>, Joseph Carter<sup>2</sup>

<sup>1</sup>Dept. Otolaryngology-Head & Neck Surgery, Univ.

Hospitals of Cleveland, Case Western Reserve Univ.,

<sup>2</sup>Dept. Otolaryngology - Head & Neck Surgery, MetroHealth Medical Center, Case Western Reserve Univ.

A recent technique of assessing vestibular function, the vestibular-evoked myogenic potential (VEMP), is an otolith-mediated, short-latency potential recorded from averaged sternocleidomastoid (SCM) electromyography in response to intense auditory stimuli. Since its initial description, the popularity of this technique (VEMPs) has increased and is now used by investigators worldwide, who thus far have observed characteristic changes in a variety of peripheral and central vestibulopathies. It appears that the VEMPs are affected by the position of the recording electrodes in relation to each other and to the muscle. For instance, placement of the reference electrode on the contralateral non-contracting SCM muscle and the sternoclavicular junction has been reported. Also, it has been reported that the ipsilateral response to monaural air conducted stimulation is larger by 5-19% compared to the response to bilateral stimulation. Plausible explanations for differences in amplitude suggest crossover myogenic potentials that interfere with unilateral measurement of VEMPs during binaural presentation of sound stimuli and activation of the acoustic reflex with high-level binaural stimuli causing attenuation of sound transmission through the middle ear. The purpose of the present investigation was to examine: 1) the role of crossover myogenic potentials on the observed amplitude differences between

monaurally- and binaurally-evoked myogenic potentials and 2) the effect of reference electrode location on the VEMPs.

#### **[242] Stimulus Rate and Vestibular-Evoked Myogenic Potential Thresholds At 250 Hz**

Chizuko Tamaki<sup>1</sup>, R. Steven Ackley<sup>1</sup>

<sup>1</sup>Gallaudet University

Vestibular-evoked myogenic potentials (VEMP) is a measure of the reflexive contraction of the sternocleidomastoid muscles (SCM) in response to high-intensity acoustic stimulation. It has emerged as an effective tool to assess the function of the saccule and the inferior vestibular nerve as well as neural linkages in the brainstem and to the neck (Colebatch & Halmagyi, 1992; Robertson & Ireland, 1995). Rauch et al. (2004) reported usefulness of VEMP threshold patterns in detecting Meniere's disease. Thresholds are not routinely measured mostly because of its lengthy procedure. Previously, an attempt to reduce effective test time by increasing the stimulus repetition rate was made (Tamaki & Ackley, 2007), and found that increasing repetition rate to 13.1/s could yield a threshold within 5 dB of that obtained with a standard rate of 5/s, for 500-, 750-, and 1000-Hz STB, but not at 250 Hz. Since all the stimuli were 4 cycles long (2 cycle on/off ramp), we suspect that the stimulus duration may have been too long for 250-Hz STB. In order to test this theory, a similar group of participants (otologically and neurologically normal participants between the ages of 18 and 40 yrs) were recruited to undergo VEMP threshold testing. The duration of 250-Hz STB will be reduced to 2 cycles (1 cycle on/off ramp), so that the stimulus duration will be equal to a 4-cycle 500-Hz STB. Preliminary results show that the consistency in thresholds obtained at various repetition rates improved by shortening the stimulus duration.

#### **[243] Ion Channels, Transporters, Cotransporters, and Aquaporin Gene Profile Expression in Utricle of Patients with Meniere's Disease**

Luis Beltran-Parrazal<sup>1</sup>, Ivan a Lopez<sup>1</sup>, Gail Ishiyama<sup>1</sup>, Akira Ishiyama Ishiyama<sup>1</sup>

<sup>1</sup>Division of Head and Neck Surgery, David Geffen School of Medicine at UCLA

The regulation of ion concentration in the endolymph (K<sup>+</sup>, Na<sup>+</sup>, Ca<sup>2+</sup> and pH homeostasis) and water permeability are critical for normal function of the vestibular endorgans (VE). Ion channels, transporters, cotransporters and aquaporins are involved in the homeostatic ionic concentration of endolymph. There is very limited information available regarding the gene expression of these membrane proteins in the human VE. The gene expression profile of these molecules was investigated in utricular macula obtained in surgery for acoustic neuroma and compared with utricular macula obtained from patients with Meniere's disease (MD). In the present study, we utilized real time quantitative PCR to obtain the expression of 89 human genes (ion channels, transporters, cotransporters and aquaporins) in utricles of patients with

acoustic neuroma (AN) and intractable MD. When comparing the gene profile from MD vs AN, we found in MD patients an up-regulation of Na<sup>(+)</sup>/K<sup>(+)</sup>-ATPase cotransporter, voltage gated sodium channel, neuronal calcium channel, and potassium neuronal channels. In contrast, we found a down-regulation of chloride channels, voltage gated sodium channel, vesicular monoamine transporters and neurotransmitter transporters to GABA, dopamine, serotonin and glycine. Finally, no significant changes in expression of aquaporins 1, 4 or 6 were detected in utricles from MD patients compared with the AN patients. Our findings help define the molecular mechanism of MD and to identify specific channels alterations in this pathology.

Funded by NIDCD-NIH grants DC005028-05, DC008635-02, and DC005187-05.

#### **[244] The Effects of Cochlear Implantation On the Vestibular System**

Thuy-Anh Melvin<sup>1</sup>, Americo Migliaccio<sup>1</sup>, John Carey<sup>1</sup>, Charles Della Santina<sup>1</sup>

<sup>1</sup>Johns Hopkins Dept. of Otolaryngology - Head and Neck Surgery

We sought to determine the effect of cochlear implantation (CI) on vestibular function, using both objective and subjective assays. Semicircular canal (SCC) function was measured using caloric electronystagmography (ENG), head shake nystagmus (HSN), and head impulse testing (HIT) to assay vestibulo-ocular reflex (VOR) function at low, mid, and high frequency ranges, respectively. Saccular function was measured using vestibular-evoked myogenic potentials (VEMP). Dynamic visual acuity (DVA) was measured during head movement. Patients' subjective assessment was quantified using the Jacobsen Dizziness Handicap Inventory (DHI). CI candidates (N=27, mean age=46) were recruited from the Johns Hopkins Listening Center. All patients were tested prior to implantation; 18 patients to date were tested 6 weeks after implantation. HIT revealed pre-operative unilateral vestibular hypofunction (i.e. VOR gain=eye/head velocity<0.7 in all 3 SCCs on 1 side) in 3 patients, and 1 patient had bilateral vestibular dysfunction (BVD). Post-operatively, 1 of 18 (6%) subjects had a significant reduction in vestibular function in all 3 SCCs on the implanted side. There was no significant pre- to post-op change in ENG (normal caloric asymmetry<25%), HSN (normal is no nystagmus after head shake), VEMP (normal thresholds>75 dB SPL), or DVA (using age-based normal thresholds) for the subset (N=8) of patients undergoing all testing. DHI score decreased in 1 of 18 subjects. Per HIT results, the risk of unilateral vestibular hypofunction in adult CI candidates is 17%. CI carries a 6% risk of iatrogenic vestibular hypofunction in the implanted ear, and thus a 6% risk of BVD if that ear is the only balancing ear pre-operatively; other objective assays revealed no change. Assuming risk to each ear is independent, bilateral CI patients with pre-operatively intact bilateral vestibular function have a 0.3% risk of BVD post-operatively. Funded by AAO-HNS Resident Research Grant, 5T32DC00002717, K08DC006216.

## **[245] Central Derangement of Vestibulo-Ocular Reflex (VOR) Direction May Underlie New Balance Disorder**

**Benjamin Crane<sup>1</sup>**, Junru Tian<sup>2</sup>, Lawrence Yoo<sup>2</sup>, Robert Baloh<sup>2</sup>, Joseph Demer<sup>2</sup>

<sup>1</sup>*Johns Hopkins*, <sup>2</sup>*UCLA*

Performance of VOR has traditionally been quantified in terms of gain or eye velocity relative to the head. Normally, VOR eye velocity is nearly opposite that of the head. Recently a new vertigo and ataxia syndrome has been described with linkage to chromosome 19q13 (Kerber, Jen, Lee, Nelson, & Baloh, Arch Neuro 2007). This syndrome is characterized by episodic vertical oscillopsia which later becomes constant, mild gait ataxia, normal MRI, and onset of symptoms in middle age or older. a 56 yo male with this syndrome was recently tested during whole body rotation in the pitch, roll, right anterior left posterior (RALP), and left anterior right posterior (LARP) planes. This subject had oscillopsia during ambulation, mild limb incoordination and gaze evoked nystagmus. the patient's sister and mother suffered from similar symptoms. Clinical testing revealed decreased vestibular function with very short time constants, minimal caloric responses, and absent rotational responses below 0.2 Hz. Smooth pursuit and OKN were normal. Sudden whole body rotations were conducted at 800°/s to a distance of 45°. the first 80 ms of head rotation prior to quick phases was considered with both a visible target and the lights extinguished immediately prior to rotation. Neither Target visibility nor rotation direction had a effect on the magnitude or direction of the VOR response ( $p > 0.1$  for both). Gain was quantified as axis specific (the component of eye velocity which was compensatory to head velocity vector) and total magnitude (absolute length of eye velocity vector relative to head velocity). the axis difference was the angle of the actual eye velocity axis relative to the ideal axis (opposite that of the head). in pitch VOR axis difference was shifted by  $22 \pm 19^\circ$  (mean  $\pm$  SD) anterior with a magnitude gain of  $0.44 \pm 0.09$  and axis gain of  $0.31 \pm 0.09$ . LARP axis difference was shifted towards roll by  $35 \pm 12^\circ$  with a magnitude gain of  $0.35 \pm 0.9$  and axis gain of  $0.29 \pm 0.10$ . in RALP axis was shifted towards roll by  $80 \pm 18^\circ$  with a magnitude gain of  $0.61 \pm 0.03$  and axis gain of  $0.13 \pm 0.20$ . in roll, the axis difference was shifted rightward by  $156 \pm 3^\circ$  so that the response was effectively in the wrong direction – the same direction as head rotation. in roll, magnitude gain was  $0.87 \pm 11$  and axis gain was  $-0.65 \pm 13$ . These results indicate that peripheral vestibular dysfunction is probably not the primary derangement in this disorder, but rather neural integration of sensory information.

## **[246] Relationship Between Clinical Measures and Performance in a Virtual Grocery Store Environment in Persons with Vestibular Dysfunction**

**Susan Whitney<sup>1</sup>**, Patrick Sparto<sup>1</sup>, Joseph Lacko<sup>1</sup>, Mark Redfern<sup>1</sup>, Joseph Furman<sup>1</sup>

<sup>1</sup>*University of Pittsburgh*

Introduction: People with vestibular disorders often experience difficulty walking in visually complex environments, especially during head movement. the purpose of this study was to determine if there was a correlation between clinical measures of gait and self-report questionnaires versus performance while ambulating in a virtual grocery store in persons with unilateral vestibular hypofunction (UVH) and in control subjects. Methods: Eleven people with UVH (mean age:  $55 \pm 12$ ; 4 women) and 20 age- and control subjects (CON) participated (mean age  $45 \pm 21$ ; 10 women). Subjects attended two sessions of navigating through one aisle of a virtual grocery store. Subjects completed 6 different trials, one of which is reported here consisting of having subjects ambulate on the self-paced treadmill while searching for 2 products randomly placed on fully-stocked shelves. Mean ambulation velocity, distance, and number of products located were recorded. in addition, subjects completed the Dynamic Gait Index (DGI), the Vestibular ADL scale (VADL), the Chambless Mobility Inventory, and the Dizziness Handicap Inventory (DHI). the non-parametric Wilcoxon Signed ranks test was used to compare performance between days and Spearman rho identified relationships between the clinical and virtual reality performance measures. Results: the CON but not the UVH had increased gait velocity, distance traveled, and number of products identified on session 2. There were moderate to strong correlations evident for patients between distance traveled, average velocity, number of products located, and the DGI varying between 0.45-0.97. There was a strong relationship between VADL-functional subscale and the number of products identified ( $r = -0.74$ ;  $p = 0.01$ ) There was no relationship between the Chambless Mobility Inventory or DHI and the virtual reality performance measures. Conclusion: There appear to be moderate to strong relationships between measures of balance and the abilities of people with UVH to ambulate in a virtual grocery store.

Supported by NIH grants DC05384 and DC05205.

## **[247] The Influence of Information-Processing Tasks On Vestibular-Induced Eye Movements in Young and Older Adults**

**Bryan K. Ward<sup>1</sup>**, Mark S. Redfern<sup>1</sup>, Richard Jennings<sup>1</sup>, Joseph M. Furman<sup>1</sup>

<sup>1</sup>*University of Pittsburgh*

The Influence of Information-Processing Tasks on Vestibular-Induced Eye Movements in Young and Older Adults. Attentional processes influence velocity storage in the vestibulo-ocular reflex (VOR), impacting phase lead. the purpose of this study was to further investigate the mechanism of the influence of concurrent information processing tasks on eye movements induced by earth-



vertical axis rotation (EVAR) in young and old participants. Ten young (ages 21-34), ten young-old (ages 65-74) and ten older participants (ages 75-84) each performed five different tasks during sinusoidal EVAR in darkness at 0.02 Hz for three cycles, 0.05 Hz for four cycles, and 0.1 Hz for five cycles, all at a peak velocity of 50 degrees per second. the five tasks differed from one another in terms of their inherent sensory and motor components and were designed to provide insight into the effect of cognitive processing on VOR dynamics. Tasks included frequency and lateralization Disjunctive Reaction Time (DRT) tasks, silent and audible backwards counting, and a question/response control. for the DRT trials, tones were presented to the participant through headphones. Participants were instructed to respond as accurately and as quickly as possible. Eye movements were recorded with electro-oculography and calibrations were performed prior to each trial. Participants had an increase in VOR phase lead while performing DRT tasks as compared to the control task. This result corroborates prior findings. the effect was most noticeable at the 0.02 Hz frequency and in the older age groups. in addition, we observed a decrease in VOR gain while subjects performed the DRT tasks during EVAR at 0.02 Hz, 0.05 Hz and 0.1 Hz as compared to the control and the counting tasks. These results suggest interference between central auditory and vestibular processing primarily at the sensory rather than at the motor level.

Supported by NIH grants AG10009, AG014116, AG021885, AG024827, and DC005205.

#### **[248] Efficacy of the Brainport Balance Device in Patients with Severe Bilateral Vestibular Loss: a Multicenter Trial**

Joel Goebel<sup>1</sup>, Belinda Sinks<sup>1</sup>, Mark Pyle<sup>2</sup>, Robert Brey<sup>3</sup>, Scott Eggers<sup>3</sup>, David Zapala<sup>4</sup>

<sup>1</sup>Washington University School of Medicine, <sup>2</sup>University of Wisconsin-Madison, <sup>3</sup>Mayo Clinic-Rochester, <sup>4</sup>Mayo Clinic-Jacksonville

**STUDY OBJECTIVE:** to evaluate the effect of gravity-specific lingual stimulation upon objective postural control and subjective balance self-assessment in patients with documented severe bilateral vestibular loss (BVL)

**DESIGN:** Prospective, randomized, double-blinded, placebo-controlled multicenter trial

**SETTING:** Four academic tertiary care vestibular function testing and rehabilitation centers

**SUBJECTS:** 26 patients (ages 35-81, mean age 63 years) with absent caloric responses, rotary chair gain <0.3 through 0.5 Hz and repeated free falls on computerized dynamic posturography Sensory organization Tests (SOT) 5 and 6

**INTERVENTION:** Subjects were randomized into an active electrode stimulus group (n=14, ages 35-81 years, mean=62 years) versus random electrode stimulus group (n=12, ages 48-78 years, mean=64 years) and trained on the use of the device which consisted of a head-mounted accelerometer and a 10 x 10 electrode array placed on the tongue. Lingual stimulation was accurately correlated with pitch and roll movement in the active group and random

electrode activation in the placebo group. All subjects received pre-training evaluation and post-training assessment after 8 weeks of structured rehabilitation with the device to evaluate retention.

**OUTCOME MEASURES:** Changes between pre- and post-training tests were measured in the following parameters: 1) SOT Composite Score, 2) Dizziness Handicap Inventory (DHI), 3) Dynamic Gait Index (DGI), and 4) Activities-specific Balance Confidence (ABC) Scale

**RESULTS:** No statistically-significant differences between the active and placebo groups were seen at the 8 week endpoint although the active group demonstrated a trend toward improvement in both objective and subjective measures.

**CONCLUSIONS:** No significant objective or subjective effects were documented in this pilot project with the Brainport balance device although a trend toward improvement was noted with active stimulation. Further investigation is warranted with the device with a larger subject number and longer training period to clarify its clinical utility in rehabilitation of patients with bilateral vestibular loss.

#### **[249] The Brainport® Balance Device As a Potential Training Aid in the Rehabilitation of Balance Following Vestibular Surgery**

Kim Skinner<sup>1</sup>, Monica Metea<sup>1</sup>

<sup>1</sup>Wicab, Inc.

**Title:** the BrainPort® Balance Device as a Potential Training Aid in the Rehabilitation of Balance Following Vestibular Surgery

**Objective:** to investigate the effects of electrotactile sensory substitution using the BrainPort® balance device in improving the balance of patients following acoustic neuroma surgery and perilymphatic fistula repair.

**Methods:** Fifteen subjects with balance problems following either acoustic neuroma resection or traumatic brain injury-related fistulas completed training with the BrainPort® balance device. This device transforms information about the position of the head in space (sensed by an accelerometer) into electrical impulses displayed on the tongue. Subjects use this information to correct their posture and maintain balance. Training sessions consisted of several short trials (1 to 5 minutes) of progressively challenging postural tasks followed by a 20-minute trial while using the device. Subjects were tested at baseline and after the last training session using objective tests and quality of life questionnaires. in addition, both subjective reports and researcher observations were documented.

**Results:** All subjects demonstrated improvement in at least one area. in the subjects with acoustic neuroma resections, after 8 weeks of training with the device, scores on the Sensory organization Test (SOT) improved an average of 22%, Dynamic Gait Index (DGI) scores improved an average of 20%, Berg Balance Scale (BBS) scores improved an average of 13%, Dizziness Handicap Inventory (DHI) scores improved an average of 40%, and Activities-specific Balance Confidence scale (ABC) scores improved an average of 21%. Subjects with perilymphatic fistula repair demonstrated similar improvements after 4

weeks of training with the device. Their average DHI scores improved by 31%, ABC scores by 51%, and Timed Up and Go (TUG) improved by 27%.

Conclusions: These results suggest that electrotactile sensory substitution with the BrainPort® balance device may aid in the rehabilitation and improvement of balance after acoustic neuroma resection and perilymphatic fistula repair.

## **[250] The Impact of Vestibular Physical Therapy On Post-Traumatic Dizziness**

**Kim Gottshall<sup>1</sup>**, Michael Hoffer<sup>2</sup>, Robert Moore<sup>2</sup>, Benjamin Balough<sup>1</sup>

<sup>1</sup>Naval Medical Center San Diego, <sup>2</sup>San Diego Naval Medical Center

Introduction: Current military operational demands in low-intensity conflict environments have increased the number of patients referred for vestibular physical therapy (VPT) with complaints of post-traumatic dizziness (PTD). Few studies have demonstrated the advantages of VPT using objective outcome measures. Moreover, medical therapeutics is an important adjuvant to VPT, but little work has been done engaging novel medical treatments. This study examines the impact of VPT on PTD and explores the role of anti-oxidant therapy.

Materials and Methods: Thirty-four patients with PTD presented to our clinic over a two month period of time. All patients had sustained head injury 3-20 weeks prior to presentation with PTD. All patients received the same migraine prophylaxis. Fifteen of the 34 patients also received oral micronutrients twice daily. Patients completed three income tests to include Computerized Dynamic Posturography (CDP) Sensory organization Test (SOT), the Dynamic Gait Index (DGI). Patients also completed three self-report questionnaires to include the Activities Balance Confidence Scale (ABC), Dizziness Handicap Index (DHI), and Vestibular Disorders Activities of Daily Living Scale (VADL).

The vestibular physical therapist was blinded as to whether the patient was receiving anti-oxidant therapy. Statistical analysis revealed income test scores did not differ significantly between the two groups. Outcome CDP SOT scores for the anti-oxidant group were significantly better than the income measures. Outcome CDP SOT scores for the anti-oxidant group compared to the non-anti-oxidant group were also statistically significant. the DGI scores reached full No other income or outcome test scores were statistically significant from each other for either group.

Summary: This pilot study provides evidence that VPT coupled with micronutrient anti-oxidant therapeutics offers advantages to patients with PTD. a larger double-blind placebo controlled study is warranted.

## **[251] Effect of Japanese Traditional Medicine On Olfactory Behavior After Olfactory Nerve Transection**

**Aigo Yamasaki<sup>1</sup>**, Kazuma Sugahara<sup>1</sup>, Tsuyoshi Takemoto<sup>1</sup>, Hirotaka Hara<sup>1</sup>, Hiroshi Yamashita<sup>1</sup>

<sup>1</sup>Yamaguchi University Graduate School of Medicine

There are reports of the effects of Japanese traditional medicine on the nervous system; however, there have been no behavioral studies of the effect of Japanese traditional medicine on olfactory function. the olfactory system undergoes continuous replacement of sensory neurons. Morphologic and behavioral studies have shown that the olfactory system recovers after bilateral olfactory nerve transection (BNX). However, in the humans, olfactory function does not always recover. in this study, we examined the effect of oral Ninjin-yoei-to (NYT) on behavioral recovery after BNX. Fourteen mice were subjected to BNX. the regular diet was mixed with 2% NYT (NYT diet). Mice were separated into two groups; seven mice were fed the regular diet (control group), and seven mice were fed the NYT diet (NYT group). NYT was administered beginning 7 days prior to BNX and continuing for 35 days after BNX. Mice in both groups had free access to food and water. Olfactory function was evaluated by testing each mouse's ability to avoid cotton balls treated with acetic acid. After BNX, mice lost their ability to avoid cotton balls treated with acetic acid. in the control group, the time for behavioral recovery after BNX was 28 days. in the NYT group, the time for behavioral recovery after BNX was 21 days. NYT hastened behavioral recovery after BNX. NYT may have therapeutic benefits for patients with olfactory disorders.

## **[252] Ipsilateral Laryngeal Pacing for Unilateral Vocal Cord Paralysis in a Swine Model**

**Yongbing Shi<sup>1</sup>**

<sup>1</sup>OHSU

Vocal cord paralysis is a common disorder that usually involves one cord as a result of recurrent laryngeal nerve (RLN) dysfunction. Symptoms include hoarseness and breathiness in voice, loss of voice volume, inability to speak long sentences and aspiration, as a result of incomplete glottic closure. Current treatments mainly involve vocal cord medialization procedures to improve voice quality and reduce aspiration. the results are not always satisfactory, probably because vocal cord medialization is not physiological. Very little has been studied regarding adductive laryngeal pacing, which restore mobility of the paralyzed vocal cord using signals correlated to normal vocal cord activities. the few preliminary studies have demonstrated possibility of pacing the paralyzed vocal cord in canine models using electromyographic (EMG) signals from intrinsic laryngeal muscles on the intact side. the current study is focused on pacing a paralyzed cord using EMG signals from the ipsilateral cricothyroid (CT) muscle in a swine model of unilateral RLN damage. Vocal cord movements were induced by synchronized bilateral vagal nerve stimulation. EMG signals from the ipsilateral CT muscle remained

present following unilateral RLN transection. These signals were successfully used to trigger pacing of the paralyzed vocal cord, generating a movement visually synchronized to the cord on the intact side. Sustaining cord movement was generated with the following pacing stimulus parameters: pulse width 0.5-2 ms, intensity 2-4 mA and frequency 40-100 Hz. However, compared to canine models, swine models are less ideal for this type of studies due to paramedian resting positions of the vocal cords under general anesthesia that limit measurement of cord displacement. Another significant technical challenge is the excessive pacing stimulus artifacts that interfere with accurate sensing of EMG activities from the CT muscle. Conclusion: adductive laryngeal pacing using EMG signals from the ipsilateral CT muscle is feasible, although multiple technical difficulties remain to be resolved. Canine models are superior to swine models in such studies.

### **253 Ototoxicity of Methylosaniline Chloride (Gentian Violet)**

**Hitomi Higuchi<sup>1</sup>**, Takafumi Yamano<sup>1</sup>, Tetsuko Ueno<sup>1</sup>, Mayumi Sugamura<sup>1</sup>, Takashi Nakagawa<sup>1</sup>, Tetsuo Morizono<sup>2</sup>

<sup>1</sup>Fukuoka university, <sup>2</sup>Nishi Fukuoka Hospital

Purpose: the antibacterial and antifungal activity of Gentian Violet (GV) has been well known for more than 60 years. Empirical treatment of chronic otitis externa with GV by many otologists all over the world has shown therapeutic usefulness. to date, however, determination of the ototoxicity of GV by using eighth nerve compound action potentials (CAP) has not been reported. We have examined the ototoxic effects of GV in the guinea pig cochlea, using CAP measurements. Histopathologic study of the temporal bone is also performed. Materials and Methods: Ototoxicity was evaluated in guinea pigs by measuring CAP. The stimulus consisted of click sounds and tone bursts of 4 and 8kHz. the middle ear cavities of the animals were filled with a 5% solution of GV and the reduction in the CAP was measured after 30 minutes, 24 hours and 1week. After all measurements were completed, a histopathologic study of the temporal bones was also made. The bacteriostatic activity of the solution against two strains of MRSA, isolated from ears of patients in our clinic was also studied. Results: No ototoxicity was detected at 30 minutes when using a 5% solution, but the same concentration caused complete abolishment of CAP by 24 hours. a 1.25% solution caused complete abolishment of CAP after 1 week. Solutions of GV between 1.25% and 0.63 % showed marked bacteriostatic activity. Temporal bones examined 6 weeks after application of a 5% solution showed severe middle ear inflammation including massive new bone formations of the middle ear (tympanic bulla).

Conclusions: Although GV has excellent antibacterial and antifungal activity, the use of GV should be limited to the external ear canal. the use of this drug in the middle ear cavity is not recommended.

### **References:**

Spandow O, Anniko M, Moler AR. the round window as access route for agents injurious to the inner ear. *Am J Otolaryngol* 1988;9:327-335

Tom LWC. Ototoxicity of common topical antimicrobial preparations. *Laryngoscope* 2000;110:509-516

### **254 Long-Term Effects of Acetic Acid On the Cochlear Function in the Guinea Pig**

**Takafumi Yamano<sup>1</sup>**, Mayumi Sugamura<sup>1</sup>, Tetsuko Ueno<sup>1</sup>, Hitomi Higuchi<sup>1</sup>, Takashi Nakagawa<sup>1</sup>, Tetsuo Morizono<sup>2</sup>  
<sup>1</sup>Fukuoka University, <sup>2</sup>Nishi Fukuoka Hospital

Purpose: At the previous ARO Meeting in 2006, we reported a concentration dependent ototoxicity of acetic acid in the guinea pig. a significant ototoxic effect was seen for acetic acid solutions at pH3, but not at pH4 or pH5. the acetic acid was applied in the middle ear cavity for only 30 minutes. We have now studied the change in compound action potentials (CAP) at more extended times of 24 hours and at 1 week.

Materials and Methods: Ototoxicity was evaluated in guinea pigs by measuring CAP. the stimulus consisted of click sounds, and tone bursts of 4 and 8kHz. Baseline CAP measurements were first made, then, the middle ears of the animals were filled with an acetic acid solution, 5mols per liter, at either pH4 or 5. CAP compared to baseline was measured at 24 hours or at 1 week. to prevent infection in the middle ear, animals were injected with 30 mg per kg body weight of erythromycin each day.

Results: Acetic acid at pH4 caused complete abolishment of CAP by 24 hours. Acetic acid at pH5 by 24 hours caused a partial reduction in CAP for the tone burst of 4kHz, with no reduction for the tone bursts of 8kHz or for the click stimulus. Acetic acid at pH5 by 1week caused partial reduction in CAP for the tone bursts of 8kHz and 4kHz, with no reduction for the click stimulus.

Conclusion: Our previous report showed that an acetic acid solution at pH4 did not result in any reduction in CAP at 30 minutes whereas the present experiment shows severe ototoxic effects at 24 hours. Obviously, ototoxicity of acetic acid is both concentration and duration dependent. the determination of whether any drug shows ototoxicity relying solely on short term studies can be misleading.

### **255 Delineating the Hearing Loss in Children with Enlarged Vestibular Aqueduct**

**Guangwei Zhou<sup>1</sup>**, **Quinton Gopen<sup>2</sup>**, Margaret Kenna<sup>2</sup>

<sup>1</sup>Diagnostic Audiology, Children's Hospital Boston,

<sup>2</sup>Children's Hospital Boston, Harvard Medical School

Introduction: the association of hearing loss and enlarged vestibular aqueduct (EVA) is well established. Multiple clinical studies have shown that sensorineural hearing loss (SNHL) is the predominant type of hearing loss in EVA. Conversely, some studies have reported that conductive hearing loss (CHL) or mixed hearing loss, indicated by air-bone gap in the audiogram, is frequently noted in patients with EVA. the presence of a conductive component in a child with hearing loss can be easily misinterpreted and lead to mismanagement.

**Methods:** We undertook a retrospective study of children with EVA seen in a pediatric tertiary care facility over the last two years. a total of 54 cases (88 ears) of EVA were identified with complete records, including otologic evaluation, imaging studies and audiologic assessment. the diagnosis of EVA was confirmed by CT scan or MRI of the temporal bone. Hearing status was assessed using behavioral testing or Auditory Brainstem Response (ABR). Tympanometry, acoustic reflexes (AR) and vestibular evoked myogenic potentials (VEMP) testing were also performed when appropriate.

**Results:** 52% of our EVA cases showed bilateral involvement, and 43% of all ears with EVA also had cochlear malformations, such as Mondini dysplasia. SNHL alone was found in 16 ears (20% of the total) with EVA while CHL or mixed loss was found in 66 ears (80% of the total). However, review of all EVA cases with SNHL showed lack of proper bone conduction testing, so air-bone gaps were missed. in spite of air-bone gaps in EVA ears, middle ear pressure and mobility were usually normal, along with present AR. VEMPs were present with abnormally low thresholds.

**Conclusions:** We speculate that air-bone gap would be found in all ears with EVA if both air and bone conduction thresholds are always tested. Normal tympanometry and AR suggest that the conductive component of the hearing loss is due to inner ear, not middle ear, anomalies. Audiologic markers of EVA are also discussed.

## **[256] Spontaneous Brief Unilateral Tinnitus (Sbuts) – Prevalence and Properties li**

**Robert Levine<sup>1</sup>, Yahav Oron<sup>2</sup>, Eui-Cheol Nam<sup>3</sup>, Yehudah Roth<sup>2</sup>, Jennifer Melcher<sup>1</sup>**

<sup>1</sup>*Massachusetts Eye & Ear Infirmary*, <sup>2</sup>*The Edith Wolfson Medical Center*, <sup>3</sup>*Kangwon National University College of Medicine*

Tinnitus refers to a diverse set of phenomena. to understand tinnitus requires an understanding of each of the various types of tinnitus. Progress made in understanding one type of tinnitus may provide further insights into other types of tinnitus.

SBUTs appears to be “a blind spot” in tinnitus research. Despite being the most common form of tinnitus, there are no systematic reports of SBUTs. Previously, we had found that about 76% of normal hearing adults have had SBUTs. There was no obvious association between experiencing SBUTs and age, handedness, or chronic tinnitus. Subjects who had previously experienced tinnitus after a loud sound were more likely to have SBUTs than those who had not. From logging the SBUTs of 5 subjects we tentatively concluded that the rate of occurrence of SBUTs varied from less than 1 per year to over 100 per year. Twice as many SBUTs occur in the right ear than the left ear. the dominant pitch of SBUTs ranges from 100 to 1000 Hz. a pressure feeling usually accompanies SBUTs.

From obtaining four month SBUT logs for another 69 adults, we now conclude that SBUTs are twice as frequent in tinnitus subjects than non-tinnitus subjects. the rate of occurrence of SBUTs varies from less than 1 per year to over 130 per year. SBUTs more commonly occur in the

right than the left ear. the dominant pitch of SBUTs ranges from 100 to 4400 Hz. in about 25% of subjects an ipsilateral ear pressure accompanies all SBUTs, whereas less than 5% of subjects experience an ipsilateral ear pressure with some SBUTs but not with others.

## **[257] Somatosensory Pulsatile Tinnitus Syndrome: Somatic Testing Identifies a Pulsatile Tinnitus Subtype That Implicates the Somatosensory System**

**Robert Levine<sup>1</sup>, Eui-Cheol Nam<sup>2</sup>, Jennifer Melcher<sup>1</sup>**

<sup>1</sup>*Massachusetts Eye & Ear Infirmary*, <sup>2</sup>*Kangwon National University College of Medicine*

We report five cases of non-lateralized pulsatile tinnitus for whom no etiology was found from physical examination or ancillary testing but the pulsations could be suppressed by somatic testing.

The three men and two women ranged in age between 49 and 75. All described their pulsatile tinnitus as high pitched and localized to both ears or in the head. Audiometry was symmetric in all subjects. Auscultation was normal in all. Jugular compression did not modulate any subject's tinnitus. Carotid compression did suppress tinnitus in two subjects, but a similar effect occurred with sternocleidomastoid compression without carotid compression. Imaging studies were all unrevealing including one cerebral angiogram.

All could suppress the pulsations with various strong neck or jaw muscle contractions, or strong pressure on the sternocleidomastoid muscle/carotid artery complex. in some the tinnitus was completely suppressed; in others only the pulsatile component of the tinnitus was suppressed; high pitched non-pulsatile tinnitus remained. with some maneuvers only one side was suppressed.

The non-lateralized quality of the pulsatile tinnitus suggests either a central somatosound or modulation of neural activity of either the central auditory system bilaterally or a level of the auditory system that can affect bilateral auditory perception.

in consideration of (a) negative findings with auscultation and imaging and (b) suppression of the pulsations with activation of the somatosensory system, we suggest the following: some or all of these cases perceive non-lateralized high-pitched pulsatile tinnitus from (1) cardiac modulation of the somatosensory system, which, in turn, (2) modulates the central auditory system, thereby accounting for the pulsatile quality of their high-pitched tinnitus. Our data suggest the sternocleidomastoid muscle/carotid artery complex as a likely source of the somatosensory input.

## **[258] Molecular Approaches to Tinnitus**

**Marlies Knipper<sup>1</sup>**, Rama Panford-Walsh<sup>2</sup>, Lukas Ruettiger<sup>1</sup>, Wibke Singer<sup>1</sup>, HynSoon Geisler<sup>1</sup>, Karin Rohbock<sup>1</sup>, holger Schulze<sup>3</sup>, Ulrike Zimmermann<sup>1</sup>

<sup>1</sup>Hearing Research Center Tuebingen, <sup>2</sup>Haring Research Center Tübingen, <sup>3</sup>University Erlangen

Aberrant neuronal activity is known to lead to changes in neuronal plasticity. However, the molecular changes following sensory trauma and the subsequent response of the central nervous system are only poorly understood. We focused on finding a molecular tool for monitoring the features of excitability which occur following acoustic and ototoxic trauma to the auditory system. of particular interest are genes that alter their expression pattern during activity-induced changes in synaptic efficacy and plasticity. the expression of brain-derived neurotrophic factor (BDNF) and the activity-dependent cytoskeletal protein (Arg3.1/arc) were monitored in the peripheral and central auditory system hours and days following tinnitus-inducing traumatic stimuli or salicylate treatment. Tinnitus induction was monitored in a rodent animal behavior model (Rüttiger et al., 2003, Hear Res). Excitatory input to the rat AI were investigated by local field potential (LFP) post pure-tone acoustic trauma using chronic implantation of multi-channel microelectrode arrays. BDNF and Arg3, were monitored at the mRNA and protein level in the cochlea and subcortical and cortical areas. We present here a summary of recent findings comparing and correlating the expression of activity dependent genes with tinnitus-behavior. the data are discussed in the context of using the monitoring of activity-dependent genes to screen for the pharmacological reversal of tinnitus.

Supported by a grant from the Deutsche Forschungsgemeinschaft Kni-316/3-3.

Acknowledgements: This work was supported by the Deutsche Forschungsgemeinschaft Kni 316/3-2 and Fortüne 816-0-0.

## **[259] Combined Transcranial Magnetic Stimulation (TMS) for the Treatment of Tinnitus**

**Tobias Kleinjung<sup>1</sup>**, Veronika Vielsmeier<sup>1</sup>, Michael Landgrebe<sup>2</sup>, Peter Eichhammer<sup>2</sup>, Goeran Hajak<sup>2</sup>, Juergen Strutz<sup>1</sup>, Berthold Langguth<sup>2</sup>

<sup>1</sup>Department of Otolaryngology, University of Regensburg, Germany, <sup>2</sup>Department of Psychiatry, University of Regensburg, Germany

Objectives: Low-frequency repetitive transcranial magnetic stimulation (rTMS) of the temporal cortex has been proposed as a new treatment strategy for patients with chronic tinnitus. However functional abnormalities in tinnitus patients also involve brain structures relevant for attentional and emotional processing such as the dorsolateral prefrontal cortex and the anterior cingulate. Therefore we developed a new rTMS treatment strategy for tinnitus patients, consisting of a combination of high-frequency prefrontal and low-frequency temporal rTMS.

Study Design: 40 patients received either low-frequency temporal rTMS (10 sessions, 1Hz, left auditory cortex; 2000 pulses/d, 110% motor threshold) or a combination of high-frequency prefrontal and low-frequency temporal

rTMS (10 sessions, at each session 1 Hz rTMS, left auditory cortex, 2000 pulses/d, 110% motor threshold, followed by 20 Hz rTMS, left dorsolateral prefrontal cortex; 2000 pulses/d, 110% motor threshold). Treatment effects were assessed by using a standardized tinnitus questionnaire (TQ).

Results: Both treatment modalities resulted in reduced TQ-scores. Furthermore there was a remarkable advantage for combined prefrontal and temporal rTMS treatment as compared to temporal treatment alone.

Conclusion: These results support recent data suggesting that auditory and non-auditory brain areas are involved in tinnitus pathophysiology.

## **[260] Title: The Role of Physical Therapy in Tinnitus: A Case Report**

**Kay Niedermeier<sup>1</sup>**, Neil Cherian<sup>2</sup>

<sup>1</sup>Physical Medicine and Rehabilitation, the Cleveland Clinic, <sup>2</sup>Neurological Institute, the Cleveland Clinic

Tinnitus is a common disorder with limited treatment options. in the past ten years, research has identified that neck and jaw contractions can influence tinnitus. While treating patients for headaches, dizziness and temporomandibular dysfunction, we have been able to decrease the intensity and/or frequency of tinnitus despite this not being the focus of the interventions. to date there have been no published reports that identify specific physical therapy interventions for improving tinnitus.

This abstract is based on a case description of a 42 year old man who is an avid weight lifter. He works as a line operator at a car manufacturing company. His job requires him to maintain prolonged positions where his head and neck are in flexion and protrusion. His tinnitus was described as a bilateral buzzing and was intermittent. It began six years ago and was worsening. Along with this he complained of headaches, blurry vision and neck tightness.

On his initial evaluation his tinnitus was rated on VAS 4/10. His tinnitus handicap inventory score was 62/100. Evaluation revealed decreased cervical motion as measured by CROM. Resisted muscle contractions of the cervical spine in flexion, extension and rotation increased his tinnitus. Jaw contractions had no effect on his tinnitus. Tenderness of cervical and jaw musculature was noted as well as significant upper cervical spine dysfunction. Physical therapy focused on normalizing cervical spine mechanics via repeated movement assessment, joint mobilization and soft tissue massage.

The patient demonstrated significant improvement in his tinnitus. This was likely due to the noted improvement in cervical spine biomechanics and tone. This improvement was objectively measured by changes in the following disability measures upon discharge: THI, NDI, HDI, DHI.

Given that tinnitus is a complex disorder, along with the lack of consistently effective treatments, it is imperative to identify potential contributions from the cervical spine and temporomandibular region. This may assist in the further understanding of this condition and the subsequent development of effective treatment strategies.

## **261 A Targeted Strategy for Identifying and Evaluating Molecular Candidates of Sensory Hair Cell Protection**

**Valentina Gburcik<sup>1</sup>, Emily Towers<sup>1</sup>, Jonathan Gale<sup>1</sup>, Sally Dawson<sup>1</sup>**

<sup>1</sup>*UCL Ear Institute*

(VG and ET are joint first authors - contributed equally)

The predominant cause of hearing loss is the damage and subsequent death of the sensory hair cells in the inner ear. Our primary aim is to elucidate molecular candidates of survival pathways in hair cells. Several mouse genes have been identified whose deletion produces a phenotype of progressive post-natal hearing loss due to loss of hair cells. Two of these genes are transcription factors; Brn-3c (POU4F3) and Barhl1. the phenotype suggest that they act as key regulators of gene expression at the head of hair cell survival pathways. We performed a subtractive hybridisation screen on OC-2 cells, a cell line derived from the organ of Corti sensory epithelium, comparing gene expression in cells with increased or decreased levels of Brn-3c or Barhl1. This strategy led us to identification of putative Brn-3c and Barhl1 targets. These putative targets were evaluated by a series of experiments. Novel hair cell transcripts were validated using either immunofluorescence during different stages of embryonic and postnatal development or by using qPCR to measure mRNA levels in rodent hair cells obtained from cochlear explants by micropipette aspiration. Altered target gene expression in response to transcription factor levels was confirmed using siRNA technology. Targets may be subject to direct or indirect Brn-3c or Barhl1 regulation. Direct regulation was established in some targets by (i) identification and validation of functional response elements upstream of target genes and (ii) evidence of Barhl1 or Brn-3c mediated activation or repression in reporter gene assays.

in future, we will further examine our candidates by detecting changes in Brn-3c, Barhl1 and target genes expression during hair cell damage. the functional role of those genes will be assessed by manipulating gene expression or protein levels in *ex vivo* explants. This approach may lead to identification of genes that regulate how hair cells respond to damage and thus reveal them as targets for therapeutic or protective intervention.

## **262 Aminoglycoside-Induced Hair Cell Toxicity can be Genetically Modulated in Zebrafish Lateral Line**

**Kelly Owens<sup>1</sup>, Brock Roberts<sup>1</sup>, Katherine Reinhart<sup>1</sup>, Edwin W Rubel<sup>1</sup>, David W. Raible<sup>1</sup>**

<sup>1</sup>*V.M. Bloedel Hearing Research Center*

Loss of mechanosensory hair cells in the inner ear is a leading cause of hearing and balance impairment. Genetic variation contributes markedly to differences in normal disease progression during aging and in susceptibility to ototoxic agents. Exposure to environmental toxins and therapeutic drugs such as aminoglycoside antibiotics and antineoplastic agents contribute to these hearing and balance problems and are provide a tractable approach for inducing hair cell loss. in wildtype zebrafish, *Danio rerio*,

lateral line hair cells are killed by aminoglycosides in a dose-dependent manner. to identify factors that affect hair cell death or survival, we developed an *In Vivo* drug toxicity-interaction screen to uncover genetic modulators of neomycin-induced hair cell death. to date, we have identified five protective mutations with simple Mendelian inheritance. Complementation analysis indicates that these mutations represent distinct genetic loci. Further characterization and identification of the protective mutant, *sentinel* (*snl*), revealed a novel conserved vertebrate gene. the mutation *merovingian* (*mero*) exhibits multiple phenotypes in addition to hair cell protection including inner ear abnormalities. in contrast, the protective mutation *persephone* (*pers*) appears wildtype in the absence of aminoglycoside exposure. Furthermore, *pers* homozygotes are viable and fertile. We are positionally mapping *pers* and *mero* to identify the mutated genes.

## **263 Molecular and Cellular Mechanism of Acute Cochlear Energy Failure and Development of Novel Therapeutic Strategy for Sensorineural Hearing Loss**

**Tatsuo Matsunaga<sup>1</sup>, Kazusaku Kamiya<sup>1</sup>, Guangwei Sun<sup>1</sup>, Yoshiaki Fujinami<sup>1</sup>, Hideki Mutai<sup>1</sup>, Hiroko Kouike<sup>1</sup>, Reiko Nagashima<sup>1</sup>, Daisuke Yamashita<sup>1</sup>, Masato Fujii<sup>1</sup>, Kimitaka Kaga<sup>1</sup>, Kunio Mizutani<sup>2</sup>, Noriyuki Hoya<sup>1</sup>, Yasuhide Okamoto<sup>1</sup>, Seiichi Shinden<sup>1</sup>, Youichiro Takiguchi<sup>1</sup>, Masato Fujioka<sup>2</sup>, Shujiro Minami<sup>2</sup>, Kaoru Ogawa<sup>2</sup>**

<sup>1</sup>*National Institute of Sensory organs*, <sup>2</sup>*Keio University School of Medicine*

in many of patients with acute or sudden sensorineural hearing loss, pathophysiology of hearing loss is unknown and effective treatments are currently limited. One of the major possible causes of hearing loss is cochlear energy failure which is induced by several mechanisms such as cochlear ischemia.

We have recently established a rat model of cochlear energy failure by treatment of cochlea with a mitochondrial toxin, 3-nitropropionic acid (3-NP). in this model, irreversible or reversible hearing loss could be induced depending on the dose of 3-NP and hearing loss was mainly caused by degeneration of cochlear fibrocytes (Hoya et al. 2004, Okamoto et al. 2005). Apoptosis induced by caspase activation was detected in degenerating fibrocytes. Recovery of hearing was related to regeneration of cochlear fibrocytes around the area of degenerated fibrocytes. Several other molecules related to cellular stress were also significantly induced in these fibrocytes. in addition, molecules and cells indicating active inflammation were detected in the cochlear lateral wall of these rats.

Systemic administration of a caspase inhibitor, Z-VAD-FMK, significantly protected deterioration of hearing and degeneration of cochlear fibrocytes in this model (Mizutani et al. 2007). Significant therapeutic effect was also detected with this caspase inhibitor. Furthermore, mesenchymal stem cell transplantation into the inner ear demonstrated significant acceleration of hearing recovery and repair of damaged tissue (Kamiya et al. 2007). in this therapy, cellular interaction between cochlear fibrocytes and mesenchymal stem cells via secreted molecules

appeared to be involved. Expression patterns of marker proteins for each type of cochlear fibrocytes were determined for evaluation of proliferation and differentiation of cochlear fibrocytes.

in conclusion, the present animal model of acute cochlear energy failure contributes clarification of pathophysiology and development of therapeutic strategy for a certain type of sensorineural hearing loss.

#### **[264] Spatial Distribution of Manganese Superoxide Dismutase 2 (Mn SOD2) Expression in Rodent and Primate Spiral Ganglion Cells**

**Yu-Lan Mary Ying<sup>1</sup>**, Carey Balaban<sup>1</sup>

<sup>1</sup>*University of Pittsburgh*

The formation of reactive oxygen species (ROS) appears to play a significant role in sensorineural hearing loss. Manganese superoxide dismutase (Mn SOD2) is a key metabolic anti-oxidant enzyme of the superoxide dismutase family for detoxifying the free radical cascade inside the mitochondria of the cochlea via activation of downstream uncoupling proteins. by contrast, copper/zinc superoxide dismutase (Cu/Zn SOD1) is localized in the cytoplasm. It is well established that hair cells and spiral ganglion cells appear to be more vulnerable to ototoxins at the base of the cochlea than at the apex. Presbycusis also begins with high frequency loss represented at the base of the cochlea. This study examined whether the pattern of expression of these SODs in the cochlea is correlated with the differential cellular vulnerability found in basal versus apical turn of the cochlea. Immunohistochemical methods were used to identify the distribution of Mn SOD2 in paraffin embedded sections of paraformaldehyde fixed formic acid decalcified temporal bones from mice, rats, and macaques; and special archival celloidin-embedded human temporal bone sections. Binding sites of primary rabbit polyclonal antibodies to Mn SOD2 (Abcam Inc., ab13534) were visualized with standard ABC methods and a diaminobenzidine chromogen. Cu/Zn SOD 1 (Abcam Inc., ab13498) was also identified using similar immunohistochemistry in rat and monkey temporal bone sections.

Mn SOD2 immunopositive type 1 spiral ganglion cells were prominent in temporal bone sections from mice, rats, macaques, and humans. in mice, rats and macaques, both the proportion of Mn SOD2 immunopositive spiral ganglion cells and the intensity of immunoreactivity were elevated near the cochlear apex. Fewer stained spiral ganglion cells and weaker staining intensity were observed in the basal cochlear turn. Strongly stained Mn SOD2 type 1 spiral ganglion cells were also observed in archival human temporal bone sections (3 ears from 2 subjects), but more specimens will be needed to substantiate whether expression follows a base to apex gradient. in contrast, the Cu/Zn SOD1 immunopositive type 1 spiral ganglion cells were distributed identically across cochlear turns in rats and macaques. These findings suggest that spiral ganglion cellular responses to ROS exposure may vary along the cochlear spiral, with a lower response capacity in the basal turn. It raises the general hypothesis

that a lower Mn SOD2 anti-oxidative capacity at the cochlear base could contribute to the high frequency hearing loss seen in presbycusis and ototoxin-induced hearing loss. the conservative pattern of Mn SOD2 immunostaining across species further suggests that it may be a fundamental mechanism in ROS metabolism and signaling.

#### **[265] High Potassium Attenuates H2O2-Induced G2-M Arrest and Cell Death in Auditory Cells.**

**Yunha Kim<sup>1</sup>**, Hongseob So<sup>1</sup>, HyungJin Kim<sup>1</sup>, Channy Park<sup>1</sup>, Raekil Park<sup>1</sup>

<sup>1</sup>*Wonkwang University School of Medicine*

Oxidative stress is one of the major factors associated with auditory cell death-related hearing loss. Hydrogen peroxide (H2O2) has been commonly used models of exogenous and intracellular oxidative stress. Exogenous H2O2 treatment resulted in increases of death of HEI-OC1 auditory cells and reactive oxygen species (ROS) generation, which allowed G2-M arrest along with expression changes of cell cycle-related proteins. However, providing of cells with extracellular high potassium (K+) suppressed H2O2-mediated cell death through inhibition ROS production and exit from G2-M arrest. Treatment with high K+ also reduced the protein expression of cyclin B1, cyclin A, Cdc2, and p21/WAF1 whereas it increased the protein level of p27. in addition, exposure of the organ of Corti from newborn SD rats to H2O2 increased the loss of inner hair cells (IHCs) and outer hair cells (OHCs). However, an extracellular high K+ (25 - 75 mM) strongly attenuated the H2O2-induced HCs loss. Taken together, our data suggest that depolarizing condition mimic high K+ may function as a pivotal factor for HC survival against ROS damages.

This work was supported by the Korea Science & Engineering Foundation (KOSEF) through the Vestibulocochlear Research Center (VCRC) at Wonkwang University in 2007.

#### **[266] Down-Regulation of Mapks and NF-Kb Through Nrf2/HO-1 Activation Attenuates Cisplatin-Induced Auditory Cell Damages**

**Hongseob So<sup>1</sup>**, HyungJin Kim<sup>1</sup>, YunHa Kim<sup>1</sup>, Eunsook Kim<sup>1</sup>, Kang-Min Lee<sup>2</sup>, Raekil Park<sup>1</sup>

<sup>1</sup>*Wonkwang University School of Medicine*, <sup>2</sup>*Chonbuk National University*

Recently, we demonstrated that pro-inflammatory cytokines, such as TNF- $\alpha$ , IL-1b and IL-6, played a critical role in cisplatin-induced cochlear injury, and that flunarizine induces a cytoprotective effect against cisplatin cytotoxicity in HEI-OC1 auditory cells and organ of Corti explants by the activation of NF-E2-related factor 2 (Nrf2)/heme oxygenase-1 (HO-1) cascade through PI3K-Akt signaling. We report here that flunarizine markedly attenuates cisplatin-induced the secretion and mRNA transcription of pro-inflammatory cytokine and cisplatin cytotoxicity through the activation of Nrf2/HO-1 and down regulation of NF-kB. Overexpression of Nrf2/HO-1 by gene



transfer and pharmacological approaches attenuated cisplatin-induced cytotoxicity and pro-inflammatory cytokine production. On the contrary, inhibition of Nrf2/HO-1 signaling by pharmacological inhibitors and specific siRNAs significantly abolished the beneficial effects of flunarizine. Flunarizine also attenuated cisplatin-mediated MAPK activation and pharmacological inhibition of MAPKs, especially MEK1/ERK, blocked cisplatin-induced NF-kB activation. Furthermore, WT-Nrf2 overexpression effectively blocked MAPK activation after cisplatin exposure. Finally, oral injection of Sibelium<sup>TM</sup>, the trade name of flunarizine, suppressed the increase of pro-inflammatory cytokines by cisplatin in both serum and cochleas of Balb/c mice, whereas it increased HO-1 expression in cochleas. These results indicate that flunarizine induces a protective effect against cisplatin ototoxicity through the down-regulation of MAPKs and NF-kB by Nrf2/HO-1 activation, and the resulting inhibition of pro-inflammatory cytokine productions.

### **[267] Small Molecule Provides Differential Hair Cell Protection Against Cisplatin and Aminoglycosides in Zebrafish Neuromasts**

**Allison Coffin<sup>1</sup>, Henry Ou<sup>1</sup>, Felipe Santos<sup>1</sup>, Kelly Owens<sup>1</sup>, David Raible<sup>2</sup>, Edwin Rubel<sup>1</sup>**

<sup>1</sup>Virginia Merrill Bloedel Hearing Research Center, Dept of Oto-HNS, University of Washington, <sup>2</sup>Department of Biological Structure, University of Washington

Much progress has been made in the past decade in our understanding of how hair cells die and how we may prevent this process using small molecules or specific biochemical pathway inhibitors. However, the efficacy of these compounds to protect against a wide variety of ototoxic agents, as well as the underlying generality of the cell death pathways activated by specific ototoxic drugs, has not been fully explored. Here, we use a small molecule of the benzothioophene carboxamide family (PROTO1), found to inhibit neomycin-induced hair cell death in a previous chemical screen, to explore cell death and protection with other ototoxic agents in hair cells of the zebrafish lateral line. Five-day-old wildtype zebrafish larvae (AB strain) were exposed to neomycin, gentamicin, or cisplatin at varying concentrations, both in the presence and the absence of PROTO1. Hair cell viability was assessed using the vital dye DASPEI. PROTO1 significantly protects hair cells from neomycin damage (>60% protection) and provides moderate protection from gentamicin (~30% of hair cells survive). However, PROTO1 does not protect against cisplatin-induced hair cell damage. These findings suggest that different ototoxic drugs activate different cell death pathways, and that PROTO1 may be a useful tool for teasing apart the contributions of each pathway. *Supported by T32-DC000018, P30-DC004661, and 5R01-DC005987-05, and by the Virginia Merrill Bloedel Hearing Research Center.*

### **[268] Ebselen Treatment Increases Expression of Antioxidant Enzymes Via ARE Mediated Transcription**

**Eric Lynch<sup>1</sup>, Jim LaGasse<sup>1</sup>, Jonathan Kil<sup>1</sup>**

<sup>1</sup>Sound Pharmaceuticals, Inc.

Ebselen, a small molecule mimic of glutathione peroxidase (GPx), has been shown to increase protein levels of GPx1 in the cochlea following low oral dosing (4 mg/kg) in rats at 5 hrs post intense noise exposure (Kil et al., Hear Res. 2007 Apr;226(1-2):44-51). the spiral ligament and stria vascularis appeared to be among the most affected structures within the noise exposed cochlea and had the highest level of GPx1 protein in both rats and mice. What is unclear is whether the increase in GPx1 protein following Ebselen treatment is due to transcriptional control. We hypothesize that GPx1 expression is modulated by transcriptional control conferred by a near canonical antioxidant response element (ARE) found 92bp 5' to it's ATG start site. to test this, we assayed by TaqMan the expression of EGFP in cells stably transfected with 4X-ARE-TK-EGFP (ARE-GFP) plasmid or TK-EGFP. At 24 hours, 10-50uM Ebselen induced EGFP mRNA by >10x in the ARE-EGFP cell line. the major metabolite of ebselen, glucuronidated ebselen (Gluc-Ebs), showed no induction of EGFP expression under the same conditions. by comparison, 200uM tBHQ, a known inducer of ARE expression, caused a 20x increase in EGFP mRNA at 24hrs. TaqMan analysis of known endogenous ARE responsive genes confirmed induction of NQO1 (4X), GCS1 (4X), GSTA1 (3X). Increases in Nrf2 expression were also observed for ebselen (1.5x) and tBHQ (2.5x). These studies confirm that low uM levels of ebselen induce expression of ARE regulated genes including GPx1. Thus, ebselen induces the transcriptional activation of GPx1. This effect is not observed for Gluc-Ebs possibly due to glucuronide shielding of it's Se moiety. the mechanism of ebselen mediated ARE induction may involve nucleophilic attack by the Se moiety leading to activation of Nrf-2 by disruption of its S-S linkage to Keap1. in addition to its activity as a GPx mimic, ebselen may protect the cochlea following noise or platinum exposure through induction of ARE regulated genes.

### **[269] Bioreleased Dexamethasone Can Prevent TNF-Alpha Induced Apoptosis of Auditory Hair Cells**

**Scott Haake<sup>1</sup>, Christine Dinh<sup>1</sup>, Shibing Chen<sup>1</sup>, Xiaoyun Nong<sup>2</sup>, Adrien Eshraghi<sup>1</sup>, Thomas Balkany<sup>1</sup>, Thomas Van De Water<sup>1</sup>**

<sup>1</sup>University of Miami Ear Institute, <sup>2</sup>Harvard University

Background: Expression of TNF-alpha in the cochlea is linked to trauma-induced inflammation. the expression levels of TNF-alpha and its receptors within the cochlea are up regulated in response to physical trauma. Local treatment of the scala tympani with dexamethasone has been demonstrated to be an effective otoprotective treatment against sound trauma, aminoglycoside ototoxicity and electrode insertion trauma-induced hearing loss in laboratory animals. Both local and/or systemic

corticosteroid therapy have been shown to be effective clinical treatments for sudden sensory neural hearing loss. Material and methods: Three-day-old (P-3) rat organ of Corti explants were used to test for TNF-alpha ototoxicity and the otoprotective efficacy of dexamethasone base (DXMb) treatment. a series of *In Vitro* inhibitor studies using P-3 explants were performed to define the mechanism of action of DXMb, and the efficacy of a biorelease compound (i.e. SIBS) was tested for its ability to deliver DXMb as an otprotective drug against TNF-alpha induced hair cell loss. Hair cell density counts were used as the outcome measure and p values of < 0.05 were considered significant.

Results: TNF-alpha caused the apoptotic cell death of exposed explant hair cells and this cytokine-induced ototoxicity was demonstrated to be preventable by the addition of DXMb to the medium of the explants. the inhibitor studies indicate that DXMb acts through its receptors and that endogenous corticosteroid production, NFkB signaling, PI3 kinase, and Akt are all important factors in the protective effect of DXMb against TNF-alpha induced ototoxicity. It was also determined that DXMb could be effectively bioreleased from SIBS polymer and still retain its otoprotective qualities in TNF-alpha challenged organ of Corti explants.

Conclusions: 1) TNF-alpha is ototoxic to auditory hair cells; 2) DXMb protects hair cells against TNF-alpha induced apoptosis; 3) DXMb acts through its receptors by activating anti-apoptotic signaling pathways (e.g. NFkB and/or Akt); 4) DXMb can be bioreleased and retain its anti-apoptotic activity. These results along with dexamethasone's demonstrated anti-inflammatory activity make this drug an excellent candidate for local delivery (i.e. biorelease from an electrode array) to conserve a patient's residual hearing during the process of cochlear implantation.

(Research supported by Advanced Bionics Corporation, Valencia, CA).

## **[270] P75<sup>NTR</sup> Signaling Promotes IHC-SGN Synapse Regeneration After Excitotoxic Trauma**

**Qiong Wang<sup>1</sup>**, Kelly Rowe<sup>1</sup>, I-chi Liang<sup>1</sup>, Catherine Kane<sup>1</sup>, Eric Wall<sup>1</sup>, Steven Green<sup>1</sup>

<sup>1</sup>Depts. of Biol. Sci. & Otolaryngol., Univ. Iowa, Iowa City, IA 52242, USA.

Excitotoxic trauma disrupts inner hair cell (IHC) to spiral ganglion neuron (SGN) synapses, which subsequently regenerate over several days *In Vivo* and *In Vitro*. the reinnervation is aberrant in that not all of the peripheral SGN axons regenerate and those that do contact multiple IHCs. NT-3 is produced in the IHCs and adjacent supporting cells and promotes synaptic regeneration. the neurotrophin receptor p75<sup>NTR</sup> is expressed in the neonatal rodent cochlea but only in inner pillar cells. However, p75<sup>NTR</sup> is upregulated in IHCs following excitotoxic trauma. We investigated the role of p75<sup>NTR</sup> in synaptic regeneration in 4-6 day old rat organotypic cochlear cultures. p75<sup>NTR</sup> binds unprocessed proneurotrophins with higher affinity than the processed forms so we used <1 nM proNGF to

selectively activate p75<sup>NTR</sup> but not the TrkB or TrkC expressed on SGNs (TrkA is not expressed in the neonatal cochlea). After excitotoxic trauma (exposure to NMDA and kainate, "NK"), cochlear explants were maintained for 3 d in proNGF or control medium. ProNGF significantly increased the number of peripheral processes regenerating and contacting IHCs and significantly increased the number of newly formed synapses. Nevertheless, proNGF had no effect on neurite growth in dissociated cultured SGNs, implying that the action of proNGF on SGNs is indirect. to test whether proneurotrophins might stimulate NT-3 expression or release by cells in the organ of Corti, we maintained NK-treated cultures for 3 d in proNGF and TrkC-IgG, an NT-3 scavenger. TrkC-IgG strongly inhibited the effect of proNGF, indicating that NT-3 is required for the effect of proNGF and suggesting that proNGF promotes regeneration by acting directly on the NT-3-producing cells and only indirectly on SGNs.

Funded by a grant from the AHRF (QW) and NIH R01 DC02961 (SHG).

## **[271] Effect of Diurnal Variation of Serum Corticosterone On Hearing in Mice with Noise Exposure**

**Jong Yang Kim<sup>1</sup>**, Hun Hee Kang<sup>2</sup>, Joong Ho Ahn<sup>3</sup>, Jong Woo Chung<sup>3</sup>

<sup>1</sup>Gangneung Asan Hospital, University of Ulsan College of Medicine, <sup>2</sup>Asan Institute for Life Science, <sup>3</sup>Asan Medical Center, University of Ulsan College of Medicine

Background and Objectives: an acute, short-term activation of the hypothalamic-pituitary-adrenal (HPA) axis can protect the auditory system, while inhibition of the HPA axis can abolish this protection. Corticosterone concentrations of the BALB/c mice HPA axis exhibit circadian variation with lower levels at the onset of the light (inactive) phase and higher levels at the onset of the dark (active) phase. the present study aimed to investigate the difference of the hearing change after noise exposure between BALB/c mice with light (inactive) phase noise exposure and BALB/c mice with dark (active) phase noise exposure.

Materials and Method: the hearing levels of fourteen mice were analyzed with auditory brainstem response before noise exposure, and 1, 3, 5, 7 and 10 day after noise exposure (at 8:00-11:00 or 15:00-18:00). Fourteen mice without noise exposure were used as a hearing control of noise exposed groups. Thirty-six mice were used for serum corticosterone level to avoid the possibility of the increase in serum corticosterone level due to sampling stress in study groups.

Results: the noise exposed group during 8:00-11:00 showed statistically elevated threshold shifts after 1 day and 3 days, compared with noise exposed group during 15:00-18:00 ( $p<0.05$ ). the serum corticosterone value is significantly lower at 8:00-11:00 than at 15:00-18:00. the serum corticosterone value is significantly lower before noise exposure than after noise exposure. the serum corticosterone value is significantly lower at 11:00 after

noise exposure than at 18:00 before noise exposure ( $p < 0.05$ ).

Conclusion: Endogenous serum corticosterone value has a significant effect on hearing after noise exposure. It is necessary to avoid noise exposure at different phase of HPA axis in animal model of noise exposure.

Key words: BALB/c mouse, HPA axis, Corticosterone, Noise, Hearing

## **[272] Notch Signaling Reactivation Following Damage to the Organ of Corti**

**Shelley Batts<sup>1</sup>, Yehoash Raphael<sup>2</sup>**

<sup>1</sup>The University of Michigan, Kresge Hearing Research Institute and the Neuroscience Program, <sup>2</sup>The University of Michigan, Kresge Hearing Research Institute

Notch signaling is responsible for the initial specification and cell patterning of developing tissues, in addition to playing a role in a variety of regenerative processes. In the auditory epithelium, Notch signaling is involved in specification of hair cell versus supporting cell phenotypes. The lack of spontaneous cell regeneration in the organ of Corti motivates studying the expression of Notch1 and its ligands in the mature ear, in normal and lesioned tissue. Using immunocytochemistry and Western analysis, we determined that the mature auditory epithelium has little or no Notch activation, similar to many other mature tissues that use Notch during development. In tissues with regenerative capability such as arteries, muscle cells, intestinal crypt cells and dental pulp cells, Notch has been shown to be reactivated in the wound site, and Delta1 is expressed during the course of regeneration. A similar Notch reactivation pattern has been reported in the regenerating chick ear (Stone et al., 1999). We report that in the damaged mammalian organ of Corti, Notch signaling is reactivated, as evidenced by a significant increase in the activated portion of the Notch1 domain (NICD). While NICD is elevated over the course of a week, protein levels for the intact Notch1 receptor remain unchanged. In many regenerating tissues, including the chick basilar papilla, regeneration is paired with Delta1 expression. However, in the damaged mammalian auditory epithelium, Delta1 is absent and the ligand Jagged1 is confirmed to increase sharply in contrast to normal controls. This suggests differing roles for post-development Notch ligands, with Delta1 possibly facilitating regeneration while Jagged1 mediates supporting cell repair following a lesion. It is therefore possible that Delta1 over-expression may enhance successful hair cell regeneration following trauma to the organ of Corti. In addition, this first report of a re-initiation of Notch activation in the damaged mammalian cochlea suggests that manipulating Notch signaling molecules and its downstream gene targets may be used to influence mature cell fate.

This work has been supported by the Williams Professorship, a gift from Berte and Alan Hirschfield, and NIH/NIDCD Grants DC-01634, DC05188 and T32 DC00011.

## **[273] Contrasting Supporting Cell Mechanisms for Hair Cell Elimination and Epithelial Repair in the Avian Inner Ear**

**Jonathan Bird<sup>1</sup>, Nicolas Daudet<sup>1</sup>, Mark Warchol<sup>2</sup>, Jonathan Gale<sup>1</sup>**

<sup>1</sup>UCL Ear Institute, University College London, <sup>2</sup>Dept. Otolaryngology, Washington University School of Medicine, St Louis, MO

Sensory epithelia help partition the fluid compartments that are necessary for mechano-transduction in the inner ear. Intercellular junctions couple hair cells and supporting cells together to limit paracellular ion flux between the endolymph and perilymph. How the sensory epithelium responds to hair cell damage is thus critical for homeostasis and recovery of inner ear function. We have investigated the cellular events that underlie hair cell removal and epithelial repair in the auditory and vestibular organs of the chick inner ear. Using *In Vitro* 4D time-lapse microscopy of beta-actin EGFP expression mosaics, we found that supporting cells engaged in a remarkable cytoskeletal remodelling that was rapid and organ specific. In utricles exposed to streptomycin, we observed biphasic remodelling of supporting cells surrounding damaged hair cells. At the epithelial surface, supporting cells constricted apically around hair cells to excise and eject the stereocilial bundle within approximately 10 minutes. Basolaterally, the same supporting cells extended lamellipodia to envelop and phagocytose the hair cell somas. Multi-wavelength imaging of beta-actin EGFP and TOTO-3 revealed a close correlation (<5 minutes) between basolateral supporting cell activity and loss of hair cell integrity. In basilar papillae treated with gentamicin, we observed contrasting cytoskeletal events; supporting cell activity was restricted to the basolateral aspect of the hair cell soma only. In this situation, coordinated lamellipodial extension physically ejected the hair cell from the epithelium within 30 minutes. These experiments reveal the highly dynamic nature of supporting cells and clearly demonstrates their essential role in removing damaged hair cells and maintaining epithelial homeostasis.

## **[274] Torque Analysis of Differential Floating Mass Transducer in Static Magnetic Field**

**Il-Yong Park<sup>1</sup>, Min-Woo Kim<sup>1</sup>, Ki-Woong Seong<sup>1</sup>, Eui-Sung Jung<sup>1</sup>, Jin-Ho Cho<sup>1</sup>**

<sup>1</sup>Kyungpook National University

For those who have the sensory neural hearing loss and feel the disadvantages of the conventional hearing devices, the implantable middle ear hearing devices (IMEHDs) have developed in several countries. The IMEHDs can be divided into two groups according to the vibrating transducers. One is a piezoelectric transducer type and the other is an electromagnetic transducer one. As an electromagnetic type, we have developed a differential floating mass transducer (DFMT) based IMEHD. The DFMT has two magnets within one cylindrical coil unlike the Soundbridge's FMT structure. Especially, the DFMT's two magnets are faced to each other with the same pole so that the disturbance due to the environmental magnetic flux can be eliminated. But the

FMT has the disadvantage that unwanted vibration can be generated by the permanent magnet under the environmental magnetic field. the theoretical difference between DFMT and FMT has been announced about the influence by the external magnetic field in other papers. But the detailed simulation results and the experimental demonstration have not been shown up to now.

in this paper, the rotational torque generated by the static magnetic field in two types of the electromagnetic transducers has been calculated through the finite element analysis (FEA) to investigate the effect of the static magnetic field with predefined magnetic flux densities such as 1.5T and 3.0T. Then, the effects by the static magnetic field in both transducers are compared each other through the experiment to identify how much the torque by the external magnetic field can be generated in both transducers of DFMT and FMT.

The simulation and experimental results show that the rotational movement of the FMT is much larger than that of the DFMT. It is expected that the noise by the environmental magnetic field can be reduced as using the IMEHDs with the DFMT.

## **275 Ossicular Stimulation with a Spherical Probe Tip**

**Brian Conn**<sup>1</sup>, James Easter<sup>1</sup>, Marco Ayala<sup>2</sup>, Vikrant Palan<sup>3</sup>, Ben Balough<sup>2</sup>, Herman Jenkins<sup>4</sup>

<sup>1</sup>Otologics, LLC, <sup>2</sup>Naval Medical Center San Diego, <sup>3</sup>Polytec, Inc., <sup>4</sup>University of Colorado Health Sciences Center

Implantable middle ear hearing devices commonly use a clip or a laser ablated hole to assure a constant point of contact between the driver and the ossicular anatomy. Unlike these systems, in this study mechanical stimulation of the incus was achieved through use of a spherical probe tip brought into contact with the superior aspect of the incus and allowed to slide along its surface in response to gross ossicular movement. Stapedial velocity as a function of acoustic and mechanical stimulation was measured using a Laser Doppler Vibrometer (LDV). It was found that the conductive efficiency of the normal acoustic pathway was affected only slightly by the presence of the transducer and probe tip; also, that mechanical efficiency was insensitive to the position of the probe tip relative to the incus. This system holds the promise of permitting direct mechanical stimulation with reduced surgical insult to the ossicles.

## **276 Optical Properties of Tissue in Mid-Infrared: Implications for Laser Stimulation of Cochlea**

Adam Nevel<sup>1</sup>, **Agnella Izzo**<sup>2</sup>, Joseph T. Walsh, Jr.<sup>3</sup>, Claus-Peter Richter<sup>2</sup>

<sup>1</sup>Otolaryngology, Northwestern University, <sup>2</sup>Otolaryngology, Northwestern University; Biomedical Engineering, Northwestern University, <sup>3</sup>Biomedical Engineering, Northwestern University

Recently, pulsed infrared radiation has been shown to be an effective method of nerve stimulation. with this method

come two important questions: what is the spatial distribution of the radiation in tissue, and what are the transmission properties of tissue in the infrared? in the present experiment, the optical properties of tissue were studied in the infrared spectrum (1.85μm) to help answer these questions. Rat muscle, skin, and fat, pig temporal bone, and human modiolar bone samples were irradiated with 250 μs-long pulses at a frequency of 2 Hz. the radiation was delivered via 600μm-diameter optical fiber. the spatial profile of the laser beam and the total amount of energy were measured at varying distances from the distal end of the optical fiber. After differentiating this curve, the resulting Gaussian beam profile was used to calculate the beam width (half max/full width) and the angle by which the beam diverged from the tissue. in addition, the fraction of energy transmitted through the tissue samples was plotted against the thickness of the individual tissue samples. the thickness of tissue that attenuated the laser energy to 1/e was then determined. the spread of the optical beam in to air was found to be negligible (i.e. the beam exiting the optical fiber was collimated). Lactated ringer's solution caused the beam to spread at an average angle of 3.14±0.86°. Pig temporal bone resulted in an average spread angle of 19.46±2.54° (avg±sd). Rat muscle produced a spread angle of 13.23±3.57°. Human cochlear bone produced a spread angle of 13.24±4.95°. Cochlear bone was the only tissue that showed an increase in spread angle with an increase in tissue thickness. the sample size that caused a 1/e attenuation of laser energy for lactated ringer's solution was 1.15mm. Muscle, skin, and fat attenuated the energy to 1/e at 0.90mm, 0.37mm, and 0.80mm respectively. Cochlear bone and temporal bone attenuated the energy to 1/e at 0.70mm and 0.26mm.

This project has been funded with federal funds from the National Institute on Deafness and Other Communication Disorders, National Institutes of Health, Department of Health and Human Services, under Contract No. HHSN260-2006-00006-C / NIH No. N01-DC-6-0006.

## **277 Laser Stimulation of the Cochlea Elicits Neural Activity in the Inferior Colliculus of the Guinea Pig**

**Gentiana I Wenzel**<sup>1</sup>, Hubert H Lim<sup>1</sup>, Ole Massow<sup>2</sup>, Uta Reich<sup>1</sup>, Günter Reuter<sup>1</sup>, Wolfgang Ertmer<sup>3</sup>, Thomas Lenarz<sup>1</sup>

<sup>1</sup>Medical School of Hannover, <sup>2</sup>Laser Zentrum Hannover, <sup>3</sup>University of Hannover

The lack of frequency-specific activation of the cochlea with conventional cochlear implants is an unsolved issue. a new auditory prosthesis that can achieve more localized activation of the auditory pathways may provide improvements in hearing performance. Izzo et al. (2006) demonstrated that laser stimulation of the cochlea can induce cochlear action potentials. We sought to assess if laser-induced cochlear activation could elicit localized neural activation within the central auditory system.

Frequency specific ABRs were recorded in ketamine-anesthetized guinea pigs to confirm normal hearing conditions. an electrode array (16 linear sites) was then

positioned along the tonotopic gradient of the inferior colliculus central nucleus (ICC) based on acoustic-driven responses. Fixing the array to the skull ensured its proper placement before opening the cochlea. a 532 nm Nd:YAG laser (Quantel Brilliant BW, France) was used to deliver 10 ns pulses (300 repetitions, 10 pulses/s) through a 50  $\mu$ m diameter optic fiber that was inserted through the round window membrane and directed towards the basilar membrane of the basal turn. ICC activity was recorded in response to each laser pulse.

Evoked potentials and spike activity were elicited with pulse energy levels between 3-6  $\mu$ J. Activity was present at multiple sites across the tonotopic gradient of the ICC suggesting lack of localized activation. As the energy level was increased up to 12  $\mu$ J, greater activity appeared across all 16 sites. We also observed a decrease of activity for each proceeding pulse and even complete cessation of activity, especially for higher levels. However, neural activity could be elicited again after pausing for several minutes.

We demonstrate herein that central auditory pathways can be activated with laser stimulation of the cochlea. However, appropriate laser parameters and fiber placement locations for safer and more localized activation need to be further investigated.

## **[278] The Auditory Midbrain Implant: Stimulation of the Midbrain Elicits Auditory Sensations But Implant Location Affects Overall Performance**

**Hubert Lim<sup>1</sup>, Minoo Lenarz<sup>1</sup>, Gert Joseph<sup>1</sup>, Rolf-Dieter Battmer<sup>1</sup>, Thomas Lenarz<sup>1</sup>**

<sup>1</sup>Hannover Medical University

The auditory midbrain implant (AMI) is now in clinical trials in which four NF2 patients have been implanted with a single shank array within the auditory midbrain. the motivation for the AMI is to serve as an alternative to the auditory brainstem implant (ABI), which is implanted on the surface of the cochlear nucleus and has not yet performed well in NF2 patients. the intended target was the central nucleus of the inferior colliculus (ICC). However, in the first two patients, the array was positioned into the dorsal cortex of the inferior colliculus (ICD) and near the surface of the lateral lemniscus, respectively. the third patient was implanted into the ICC, while the fourth patient was recently implanted and the array location has not yet been determined. the first three patients (fourth patient not tested yet) obtain various loudness, pitch, temporal, and directional percepts, which are features shown to be important for speech perception and more complex sound processing. However, the patient implanted into the ICD exhibits strong adaptive effects in which the loudness percept decreases over time (dies out completely within tens of seconds) with continuous stimulation. the other two patients exhibit stable auditory sensations with the greatest improvements in hearing performance in the ICC-implanted patient. Generally, our patients achieve performance levels comparable to NF2 ABI patients. These results are encouraging as to the safety and potential of the AMI for hearing restoration. However, it is

apparent that location of midbrain stimulation affects overall hearing performance and we need to identify appropriate regions to implant future patients. Thus far our preliminary human results combined with our previously published animal findings suggest that stimulation of more rostral and lateral regions along the isofrequency laminae of the ICC elicits lower threshold, greater excitatory, enhanced frequency-specific, and more spatially- and temporally-synchronized activation of higher auditory pathways. We hope that placement of our array within this rostral-lateral region in future patients will enable greater improvements in hearing performance. [Funded by Cochlear Ltd.]

## **[279] A Model of Electrode Position in the Auditory Brainstem Implant**

**Arthi Srinivasan<sup>1</sup>, Robert V. Shannon<sup>2</sup>**

<sup>1</sup>Department of Biomedical Engineering, USC,

<sup>2</sup>Department of Auditory Implants and Perception, House Ear Institute

The Auditory Brainstem Implant (ABI) provides auditory sensations to patients with no auditory nerve through electrical stimulation of the cochlear nucleus. the ABI consists of an array of 21 electrodes, which are arranged in a 3 by 7 grid. Due to complex anatomy post-tumor removal, the exact location and orientation of the ABI relative to the cochlear nucleus cannot be precisely determined. However, threshold data collected from patients can indicate the tilt of the array and lateral positioning relative to the cochlear nucleus. We applied a previous model of neural activation (Litvak et al, 2007) to threshold levels from each electrode in the array. We assumed that activation occurred on the surface of the cochlear nucleus and determined the likelihood of the neurons firing and the strength of their response as a function of the current amplitude applied to the electrodes. a fixed neural activation level was assumed to be threshold. an optimization program based on the simplex method was implemented to determine the array location and orientation that led to the best fit of the model given the entire set of current threshold values across electrodes.

## **[280] Comparison of Laminar High Resolution CSDs Evoked by Pure Tones or ICMS Stimulation in Gerbil Primary Auditory Cortex – Implications for Cortical Neuroprostheses**

**Max, F.K. Happel<sup>1</sup>, Marcus Jeschke<sup>1</sup>, Mathias Deliano<sup>1</sup>, Frank, W. Ohl<sup>2</sup>**

<sup>1</sup>Leibniz-Institute for Neurobiology, Magdeburg Germany,

<sup>2</sup>Leibniz-Institute for Neurobiology & Otto-v.-Guericke University, Magdeburg Germany

For modern cortical neuroprosthetic approaches it is important to unravel the generators of the ICMS evoked cortical response. It is highly debated to what amount cortical stimulation is exciting thalamocortical (TC) input by corticothalamic (CT) backpropagating loops. We combined quantitative, high resolution current-source-density

analysis (CSD) with a topical cortical application of the GABA<sub>A</sub>-agonist Muscimol to unravel intracortical and thalamocortical response components of the cortical CSD pattern.

Acoustic stimulation with pure tones reflects a feedforward pattern of cortical activation. Laminar profiles of onset latencies show profound differences by bestfrequency (BF) vs. non-bestfrequency (nonBF)-stimulation in all layers. While granular sinks after BF stimulation are more concise in time and space, supragranular sinks after non-BF stimulation show a faster onset and a reversed laminar gradient reflecting different supragranular inputs for BF vs. non-BF. After blocking intracortical connections with Muscimol the remaining and concise source-sink-source triplatt in layer IV matches with the tonotopic lemniscal TC input. by also blocking the CT feedback-sharpening of TC input, the TC input broadens up over 5 octaves.

By replacing acoustic stimulation with intracortical electrical stimulation (ICMS) we could show profound qualitative similarities between physiological and artificial cortical responses. Quantitative comparison of different parameters shows that ICMS activates the same intrinsic neuronal elements in the same cascade as acoustic stimulation, but in a faster, highly synchronized mode. After blocking intracortical connections by Muscimol we could show that also by stimulating different layers with extensive amplitudes no significant sinks could be evoked. by that, the wide-spread electrically evoked responses after ICMS are based essentially on intracortical neuronal elements. Taking into account the important TC-CT interplay for information transformation in sensory cortex, simple ICMS applied as a sensory neuroprosthetic stimulus might be ineffective.

Acknowledgements: the work was supported by the BioFuture grant 0311891 of the BMBF (German Ministry for Education and Research) and grant XN3590HP/0305M-N3\_OGU of the state Saxony-Anhalt to F.W. Ohl and a scholarship of the Studienstiftung des Deutschen Volkes (German National Academic Foundation) to M.F.K. Happel.

### **[281] Sensitivity to Interaural Time Delays in the Auditory Cortex of Ferrets: Investigating Potential Benefits of Half-Wave Rectified Stimuli to Individuals with Bilateral Cochlear Implants**

**Douglas Hartley<sup>1</sup>**, Amal Isaiah<sup>1</sup>, Jan Schnupp<sup>1</sup>, Johannes Dahmen<sup>1</sup>, James Fallon<sup>2</sup>, Robert Shepherd<sup>2</sup>, andrew King<sup>1</sup>  
<sup>1</sup>Oxford University, UK, <sup>2</sup>Bionic Ear Institute, Melbourne, Australia

Evidence from normal hearing (NH) individuals suggests that sensitivity to interaural time-differences (ITDs) in the modulating envelope of a high frequency carrier can be enhanced using half-wave rectified stimuli. to investigate neural correlates of this phenomenon, and potential benefits of equivalent electrical stimuli to individuals with bilateral cochlear implants (CI), we assessed ITD sensitivity in response to bilateral intracochlear electrical stimulation in the primary auditory cortex and surrounding auditory fields of ferrets. Ferrets were chosen since our

long-term aim is to develop a behavioral model of bilateral CI, for which they are highly suited. Animals were deafened with subcutaneous neomycin administration and, subsequently, stimulated via bilateral intracochlear electrode arrays. Under ketamine anaesthesia, single and multiunit responses were recorded from multichannel electrodes in response to ITDs in the envelope of i) half-wave rectified and ii) sinusoidally-amplitude modulated (SAM) biphasic pulse trains, over a range of modulation frequencies and levels. for comparison, cortical sensitivity to ITDs was assessed in NH animals with half-wave rectified and SAM acoustic carriers.

in NH animals, approximately half of cortical neurons were sensitive to ITDs, regardless of stimulus condition. in response to short duration stimuli (<20ms) a single peak was usually present in the peri-stimulus time histogram, whereas for longer duration stimuli peaks corresponding to the stimulus onset and offset were commonly seen in single units. in these units, ITD sensitivity often changed significantly from the onset- to the offset-response. Cortical sensitivity to ITDs was also seen, albeit less frequently, in the offset-response to bilateral intra-cochlear stimulation. As noted previously in the inferior colliculus recordings from bilaterally implanted cats, this tuning was often found only over a limited range of modulation frequencies and levels.

Supported by the Wellcome Trust & NIDCD No1-DC-3-1005

### **[282] Classification of Cortical Responses to Interaural Time Differences in Cochlear Implant Stimulation: Effect of Congenital Deafness**

**Jochen Tillein<sup>1</sup>**, Peter Hubka<sup>2</sup>, Dorrit Schiemann<sup>2</sup>, Emilie Syed<sup>2</sup>, Silvia Heid<sup>3</sup>, Rainer Hartmann<sup>3</sup>, Andrej Kral<sup>2</sup>  
<sup>1</sup>MedEl Company, Innsbruck, Austria, <sup>2</sup>Institute of Neurophysiology and Pathophysiology, University of Hamburg, Germany, <sup>3</sup>Institute of Physiology II, J.W.Goethe University Frankfurt am Main, Germany

Congenital auditory deprivation leads to deficits in cortical processing demonstrated in single-unit responses, gross synaptic currents and field potentials recorded from congenitally deaf cats (Kral et al., Cereb Cortex 2005; 15:552-62). These deficits are the consequence of an altered developmental sequence and additional degenerative processes. the present work focuses on the question to which extent the naive auditory cortex is able to process binaural cues - specifically, interaural time differences (ITD).

Four adult congenitally deaf cats were used, and four adult hearing cats served as controls. the control animals were acutely deafened by intracochlear application of neomycin. All animals were stimulated with charge-balanced biphasic pulses (200µs/phase) with wide bipolar configuration through a custom made cochlear implant inserted into the scala tympani on either side. Single and multi-unit activity was recorded in the primary auditory field AI by means of microelectrodes and 16 channel electrode arrays respectively (Michigan probes). Sensitivity to interaural time difference in the range of 0-600 µs (ipsilateral ear

leading and lagging) was tested with pulse trains (500 Hz, 3 pulses) at intensities of 0 – 10 dB above the unit's threshold.

According to the shape of the ITD function five different classes of multi-unit responses could be defined using an automatic procedure (Smith & Delgutte, *J Neurosci.* 2007; 27(25):6740-50). the distribution of classified ITD functions differed between the hearing and deaf group: peak (23.2 % vs. 13.66 %), trough (2.19 % vs. 0.62 %), biphasic (17.03 % vs. 5.46 %) and sigmoid (20.31 % vs. 12.85 %), unclassified (=units not classified to either of the previous classes) (26.51 % vs. 24.66 %), nonresponsive (non significant ITD responses) (10.73 % vs. 42.75 %). Significant differences were found for biphasic, sigmoid and the non-responsive class (Mann-Whitney U-test,  $p=0.05$ ). Aside from a different ITD distribution units in deaf animals showed a significantly smaller maximum evoked firing rate when compared to hearing controls.

The data demonstrate a residue of interaural time cue processing in the naïve cortex of congenitally deaf cats; nevertheless the lower number of ITD selective units suggests that congenital absence of hearing experience may significantly affect the ability of the primary auditory cortex to respond to interaural time cues.

Supported by Deutsche Forschungsgemeinschaft (KR 3370/1-1).

### **283 Effects of Intensity On Binaural Processing in the Auditory Brainstem of Children Who Use Cochlear Implants**

**Claire A. Salloum<sup>1</sup>**, Jerome Valero<sup>2</sup>, Blake C. Papsin<sup>2</sup>, Richard van Hoesel<sup>3</sup>, Karen A. Gordon<sup>2</sup>

<sup>1</sup>University of Toronto, <sup>2</sup>The Hospital for Sick Children,

<sup>3</sup>Hearing Cooperative Research Centre

Because behavioral measures in young children can be limited or unreliable, setting cochlear implant stimulation levels can be difficult. This is further complicated in children using bilateral cochlear implants as, ideally, the two devices should provide balanced input. Electrophysiological measures have been proposed as a tool to achieve audible and comfortable stimulation levels in young children. in the present study, we examine the use of the Binaural Difference (BD) component, identified in cats (Smith and Delgutte, 2007), in an adult (Pelizzione, 1990) and a group of pediatric bilateral cochlear implant users (Gordon, 2006), to achieve balanced intensity cues in children receiving a bilateral implant after > 2 years of unilateral experience. In the present study, we recorded bilateral and unilateral electrically-evoked auditory brainstem responses (EABRs) in 15 children using bilateral cochlear implants with  $4.58 \pm 0.48$  years delay between each implantation. BD component was defined as the sum of the left and right unilateral responses minus the bilateral response ((R+L)-B). Stimuli were presented in the upper portion of each child's dynamic range. Unilateral stimuli were presented in increasing steps of 5-10 Clinical Units (CU). the difference in intensity provided by either cochlear implant (Inter-implant Level Difference (ILD)) was varied between 0 and 40 CU.

Unilateral responses increased in amplitude with increased stimulus intensity with little change in latency. BD amplitudes also changed with ILD, with the most maximal amplitude corresponding to the ILD pair with the most similar unilateral amplitudes. Children using two different devices were found to have greater differences between ears than children using the same device.

Our findings suggest that: 1) children using bilateral implants have a measurable BD component which changes with inter-implant level differences 2) ABR amplitudes from unilateral stimulation correspond to changes in intensity and may provide criteria for intensity matching between ears 3) device differences may be important to consider when attempting to optimize binaural interaction.

### **284 ITD Sensitivity in Electrical Hearing: Simulating Channel Interaction Effects in Listeners with Normal Hearing**

**Gary Jones<sup>1</sup>**, Ruth Litovsky<sup>1</sup>, Richard van Hoesel<sup>2</sup>

<sup>1</sup>University of Wisconsin-Madison, USA, <sup>2</sup>CRC HEAR, Melbourne, Australia

Bilateral cochlear implant (BICI) users typically exhibit poor sensitivity to interaural timing differences (ITDs) when listening through their own speech processors. Ongoing work in our lab suggests that ITD JNDs in the tens of microseconds can be achieved by BICI users with postlingual onset of deafness under direct electrical stimulation of a single pair of electrodes. the current project is concerned with channel interaction effects on ITD sensitivity. Specifically, we are examining whether sensitivity to ITDs presented on a single electrode pair predicts performance under more realistic listening conditions, in which there is activation of more than one electrode pair and where more than one ITD may be presented to the auditory system simultaneously. a key consideration in these experiments is that ITD sensitivity of individual cochlear implant patients at specific places along the cochleae can depend on factors such as neural survival and proximity of the electrode contacts to the spiral ganglion. This may have significant implications for binaural sensitivity-based measures of channel interactions. In our current experiments, we simulate presentation of ITDs on binaural pairs of pitch-matched electrodes in normal-hearing listeners. Stimuli for these experiments are bandpass filtered 100 Hz click trains. Specifically, a probe click train presented at 70 dB SPL at a middle frequency is temporally interleaved with an added click train. ITD JNDs for the probe click train are measured while varying the added click train's: a) center frequency, b) level, c) temporal offset from the probe, and d) ITD (matched to probe or fixed at 0  $\mu$ s). We will present results of these experiments and compare them to our findings with BICI users which suggested that stimulation on multiple electrodes can result in a range of interaction effects that may make both positive and negative contributions to binaural sensitivity.

Work supported by NIH-NIDCD (R01 DC003083-09, F31 DC009361).



## **285 Binaural Masking Level Differences in Bilateral Cochlear Implant Users**

Thomas Lu<sup>1</sup>, Ruth Litovsky<sup>2</sup>, Fan-Gang Zeng<sup>1</sup>

<sup>1</sup>University of California, Irvine, <sup>2</sup>University of Wisconsin, Madison

Bilaterally implanted cochlear implant (CI) users experience better speech understanding in noise through redundant cues provided by the second implant. However, the extent to which they can take advantage of true binaural hearing is still under investigation. Because bilateral CI users have two independent speech processors, there is no coordination in stimulation timing nor pitch-matching between pairs of electrodes in the two ears. Previous work suggests that binaural cues are available when presented to single pairs of electrodes. However, this is not a realistic stimulation approach.

In this study, binaural masking level differences (BMLDs) were measured in multiple pairs of electrodes, using 300 ms sinusoids (125, 250, 500 Hz) and 400 ms band-pass noise maskers. Stimuli were presented diotically with the sinusoid either in phase (N0S0) or 180 degrees out of phase (N0S $\pi$ ). The masking noise (N0) was always in phase between ears. BMLD is the difference in signal detection threshold between N0S0 and N0S $\pi$ . Stimuli were presented by computer directly to the line-in jack on a Spear3 processor running a custom program. All subjects were tested using a 3-interval, adaptive procedure. The task was to identify which interval contained the tone (N0S0 or N0S $\pi$  versus N0).

Four bilateral Nucleus 24 implant subjects were tested. BMLDs were measured over basal, middle, and apical pairs of pitch-matched and loudness balanced electrodes. Mean thresholds ranged from 3 to 9 dB SNR (signal to noise ratio) for N0S0 and -9 to 9 dB for N0S $\pi$ . For comparison, normal hearing subjects (N=3) had BMLDs of 7-10 dB SNR. One CI subject showed BMLDs of ~10 dB. Two had BMLD's of ~3 dB. The fourth did not have significant BMLDs. More than one pair of electrodes with significant BMLDs ( $p < 0.05$ ) were obtained in a single subject, suggesting that the binaural unmasking is not confined to a single place of cochlear stimulation. No significant difference in BMLD was found as a function of electrode position. Across subjects, BMLDs were found in all frequencies tested, but there was no clear pattern. Preliminary results using a more realistic approach involving multiple simultaneous pairs of electrodes show BMLDs of ~5 dB. With further study, it may be possible to understand how to better restore true binaural hearing to bilateral CI users.

## **286 Effect of Background Noise and Uncertainty of the Auditory Environment On Localization in Adults with Cochlear Implants**

Smita Agrawal<sup>1</sup>, Ruth Litovsky<sup>1</sup>, Richard Van Hoesel<sup>2</sup>

<sup>1</sup>University of Wisconsin- Madison, <sup>2</sup>CRC HEAR, Melbourne, Australia

An increasing number of deaf patients are receiving bilateral cochlear implants (BiCI). Several studies have compared localization abilities in BiCI users when listening through one vs. two implants. Common concerns are

ceiling effects, and the fact that direct comparisons with unilateral cochlear implant (UCI) users are lacking. The present study is aimed at identifying conditions under which BiCIs provide benefits in high-functioning persons whose deafness was acquired during adult life, in particular, sound localization abilities in more realistic, complex auditory environments. Localization abilities are evaluated under challenging conditions that include interfering environmental stimuli and uncertainty regarding the auditory environment. Both BiCI and UCI users are tested (N=5 in each group), rather than forcing the former group to listen in a unilateral condition that is to them unnatural. Tasks include (1) localizing a known speech token, (2) localizing an unknown speech token, and (3) simultaneously localizing and identifying an unknown speech token. We hypothesize that introducing the aspects of uncertainty in signal and interferers will increase the complexity of the task and identify conditions that are particularly advantageous for BiCI users. This approach enables the evaluation of advantages experienced by BiCI users as compared to UCI users. In addition to these studies, 10 normal hearing listeners are tested on the free-field tasks, since little data are available in this population as well. For the BiCI listeners, sound localization performance in free field is compared with that on binaural sensitivity to interaural time and level difference cues measured using direct electrical stimulation approaches with the Spear 3 device. The extent to which binaural sensitivity measures is predicted from free-field performance will be evaluated.

## **287 Cochlear Implant Modeling: Effect of Spectral Holes On Speech Intelligibility and Spatial Release From Masking**

Soha Garadat<sup>1</sup>, Ruth Litovsky<sup>1</sup>, Fan-Gang Zeng<sup>2</sup>

<sup>1</sup>University of Wisconsin-Madison, <sup>2</sup>University of California-Irvine

Persons with cochlear implants (CIs) typically perform worse than normal hearing listeners (NHLs) tested under comparable conditions. One factor thought to be responsible for this difference is the presence of "dead regions", or "spectral holes" in CI users (Shannon, 2001). A recently growing clinical approach is to provide CI users with bilateral devices (BiCI), but in these users performance is also still poorer than that of NHLs. To understand the limits imposed by the presence of spectral holes on CI users' performance, vocoded speech can be used. In the present study, possible effects of spectral holes were extended for the first time to BiCI simulations. Effects of two types of CI modeling were compared, in which carriers were sinusoid or noise. Prior to processing, stimuli were convolved through HRTFs to provide listeners with spatial cues regarding both target and interferers. Targets were sentences from the Harvard IEEE corpus recorded with a male voice, and convolved through the 0° HRTF. Interferers were 2-female talker sentences, presented from front (0°), right (90°) or left (-90°). Speech reception thresholds (SRTs) were measured adaptively, in quiet and in noise, by varying the level of the target. Spectral holes were created by dropping the frequency information corresponding to two variables: hole size

(6mm and 10 mm) and hole location (base, middle, and apex). Stimuli were presented over headphones under binaural conditions. Results suggest that spectral holes were most disruptive on performance when they occurred in the middle of the simulated electrode array, in particular with the 10 mm size. When comparing the two approaches of CI modeling, no significant differences were found in absence of holes. However, there were effects on SRTs and extent to which spatial cues were useful when spectral holes were introduced. These differences will be discussed as well as their implications to CI studies.

Support provided by the NIH-NIDCD (grant R01 DC003083 to Ruth Litovsky)

### **[288] Sensitivity to Spectral Features for Sound Localization in Cochlear Implant Listeners**

**Matthew Goupell<sup>1</sup>**, Bernhard Laback<sup>1</sup>, Piotr Majdak<sup>1</sup>, Wolf-Dieter Baumgartner<sup>2</sup>

<sup>1</sup>*Austrian Academy of Sciences*, <sup>2</sup>*ENT-Department, University Hospital, Vienna, Austria*

This study determines the feasibility of cochlear implant (CI) listeners to localize sounds in vertical planes by measuring their sensitivity to spectral peaks and notches from an equal-loudness background. Six listeners with a monopolar twelve-electrode implant participated in this study. Three places (low = electrodes 4-6, mid = 7-9, and high = 10-12) and three bandwidths (1, 2, and 3 electrodes) were tested. All conditions were tested with overall level roving absent and present. It was found that the listeners were always sensitive to spectral peaks at any bandwidth and place. Increasing the bandwidth beyond two electrodes showed no significant decrease in the threshold. When level roving was absent, peak detection required a change of 7% of the dynamic range of the electrodes on average. Listeners were much less sensitive to spectral notches, normally requiring changes of 13% of the dynamic range to be detected. Level roving significantly decreased performance. The effect of place was highly variable between listeners. This variability was highly correlated with intensity discrimination thresholds without a background. These results have comparable trends to those found in a similar study for normal hearing (NH) listeners (Moore et al., JASA, 1989); however, peak and notch detection is at least two times worse in CI listeners compared to NH listeners. From these results, a vertical plane sound localization strategy for CI listeners seems realizable and is presently being developed.

### **[289] The Partial Tripolar Cochlear Implant Configuration Assessed by Forward Masking in the Inferior Colliculus**

Julie Bierer<sup>1</sup>, Steven M. Bierer<sup>1</sup>, **John C. Middlebrooks<sup>2</sup>**

<sup>1</sup>*University of Washington*, <sup>2</sup>*University of Michigan*

The partial tripolar configuration allows for systematic variation of electrical field size for cochlear implant stimulation while maintaining a constant locus of activation centered at the active electrode. The physiological correlate of electrical field size is spread of excitation,

which we assessed directly from the spread of activity across the tonotopic axis of the inferior colliculus and indirectly by forward masked thresholds. We recorded from 16 depths in the inferior colliculus of ketamine and xylazine anesthetized guinea pigs. Animals were unilaterally deafened and implanted with an intracochlear array of banded electrodes (Cochlear Corp.). a range of partial tripolar configurations were implemented by varying the fraction of return current ( $\phi$ ) delivered to the flanking electrodes, from  $\phi=0$  (monopolar) to  $\phi=1$  (tripolar). the masker was a 200 ms train of biphasic pulses, presented at a rate of 1017 pulses per second, with a configuration fixed at  $\phi=0.5$ . Following a 10 ms delay, the probe was a single biphasic pulse with varying  $\phi$ . the magnitude of forward masking was measured as the decrease in neural response to the fixed probe as the masker level increased. with decreasing fraction the spread of excitation from the unmasked probe broadened and thresholds decreased. Forward masked tuning curves similarly broadened with decreasing  $\phi$ . Spread of excitation and spread of masking demonstrated in this animal model parallel the functions inferred from our previous psychophysical observations.

### **[290] Effect of Distance Between Stimulating Electrode and Target Neural Tissue/Modiolar Wall On Behavioral Thresholds for Monopolar Electrical Stimulation in the Cat**

**David W. Smith<sup>1</sup>**, Motomichi Sakata<sup>2</sup>, Miriam M. Henson<sup>3</sup>, O.W. Henson, Jr.<sup>4</sup>, Charles C. Finley<sup>3</sup>, Frank Bova<sup>5</sup>, Didier A. Rajon<sup>5</sup>, Gerald E. Loeb<sup>6</sup>

<sup>1</sup>*Dept. of Psychology, Center for Smell and Taste, University of Florida*, <sup>2</sup>*Dept. of Radiology, University of Sapporo*, <sup>3</sup>*Dept. of Otolaryngology, University of North Carolina, Chapel Hill*, <sup>4</sup>*Dept. of Cell Biology and Anatomy, University of North Carolina, Chapel Hill*, <sup>5</sup>*Dept. of Neurosurgery, University of Florida*, <sup>6</sup>*Dept. of Biomedical Eng., Univ. of Southern California*

Convention holds that the closer the stimulating contact is to the target neural tissue, the lower perceptual threshold for electrical stimulation of the cochlea. to more precisely characterize the effect of electrode contact proximity on perceptual thresholds, the implanted ears from four cats with known psychophysical thresholds were removed, fixed and imaged using magnetic resonance microscopy (MRM). a proprietary software program, normally used for planning guided surgical procedures, was then used to form a 3-dimensional (3D) dataset. the program allowed interactive manipulation, slicing, and reconstruction of the temporal bone to visualize the electrode and cochlear features of interest. After segmenting the dataset and extracting the resulting surface (3D model), we measured inter-point distances with 10-um resolution. During extensive psychophysical testing, absolute monopolar thresholds for single, charge-balanced biphasic pulses (50 and 1600 us/phase) were obtained from the cats. These were plotted as a function of the distance from the edge of the stimulating electrode to the modiolar wall and the edge of the nearest spiral ganglion cell (SGC) bodies within the modiolus. in general, for separations of greater than 200 um, there was no discernable relationship between

electrode to target (either modiolar or SGC) distance and psychophysical threshold. In one animal in which a kinking of the electrode forced the contacts closer to the modiolar wall, however, the data suggest that with electrode/neural distances <150  $\mu$ m, thresholds decreased with closer spacing for both stimulus phase durations. Taken together, variations in electrode separation and proximity to surviving neurons cannot account for the observed variations in cochlear implant performance.

This work was supported by NIH R01 DC02832 (DWS). The MRM was conducted at the Duke Center for *In Vivo* Microscopy with significant assistance from Sally Gewalt and Dr. G. Allen Johnson.

## **[291] Pulse Rate in Cochlear Implant Electric Pulse Trains Influences Magnitude of Forward Masking**

**Alana E. Kirby<sup>1</sup>**, John C. Middlebrooks<sup>1</sup>

<sup>1</sup>*University of Michigan*

Fidelity in transmission of temporal features of sound is a prominent achievement of cochlear implants and is particularly necessary for speech recognition. To explore components of this process central to the cochlea, we measured forward masking and gap detection in the guinea pig primary auditory cortex in response to cochlear implant stimulation. Electric pulse trains were presented at 254, 1017, and 4069 pps and masking stimuli lasted 200 ms. Gap detection thresholds shortened with increasing electric pulse rate and increasing stimulus level. Preliminary analysis of electric forward masking data reveals a robust but unexpected dependence of recovery-from-masking time constants on pulse rate. Recovery-from-masking time constants shortened with increasing electric pulse rate, but showed no dependence on masker level.

The observed dependence of gap detection threshold on pulse rate is likely the result of several properties of the auditory system. First, the time course of adaptation of auditory nerve activity has been shown to depend on the electric pulse rate, with significant adaptation occurring at high pulse rates. For that reason, the effective level of the masker at offset may decrease with increasing pulse rates. Another contribution may be found in the shorter recovery time constants at higher pulse rates in forward masking, which is consistent with shorter gap detection thresholds at these pulse rates.

Demonstrating the contributions of the time course of recovery from masking and the effectiveness of the masking stimulus is important for understanding the transmission of temporal information in the auditory system central to the hair cells. These properties may then be used to guide the design of cochlear implants and processors.

Supported by NIH grants R01 DC04312, T32 DC05356, and P30 DC05188

## **[292] Multi-Electrode Spatial Pattern Discrimination with Cochlear Implants**

**Monita Chatterjee<sup>1</sup>**, Kara Schvartz<sup>1</sup>

<sup>1</sup>*Hearing and Speech Sciences, University of Maryland, College Park*

Multi-electrode spatial pattern discrimination was measured in six adult users of the N-24 and Freedom cochlear implants (CIs). Patterns were created by concurrently stimulating 7 contiguous electrodes in the apex (interleaved mode). Each electrode was stimulated by a 300-ms long, 1000-pulses/sec pulse train, resulting in an overall stimulation rate of 7000 pulses/sec. Spatial frequency, spatial contrast, and level of stimulation were varied. Three spatial frequencies were created by stimulating the 7 electrodes with different sequences of high (H) and low (L) amplitude stimuli. The three patterns were HLHLHLH (Pattern 1, 0.71 cycles/mm), HLLHHL (Pattern 2, 0.36 cycles/mm), and HHHLLLH (Pattern 3, 0.24 cycles/mm). For a particular spatial contrast, the H and L levels corresponded to different % dynamic range (DR) levels. Thus, for a 10% DR contrast at 50% DR peak level, the H and L levels were fixed at 50% and 40% of the DR, respectively. These levels were systematically varied to generate different contrasts. The maximum per-channel level was limited by loudness summation. Percent correct scores were obtained in a 3-interval, 3-alternative forced-choice paradigm. The reference pattern was always Pattern 1 (HLHLHLH). For a fixed H level, increasing spatial contrast resulted in improved performance. For a fixed spatial contrast, performance was poorest at low levels. While increases in the level were generally beneficial, performance sometimes declined at the highest levels, possibly due to excessive masking. Patterns 1 and 2 were hardest to discriminate: Patterns 1 and 3 were easiest to discriminate. These results, obtained with electrodes spaced approximately 0.7 mm apart, underscore the role of channel-interaction in multi-channel perception through the CI. We infer that, until CI technology is improved to reduce current spread, only a minority of CI listeners may benefit from the creation of additional, virtual channels between existing electrodes.

## **[293] Effects of Residual Acoustic Hearing On Cochlear Implant Function**

**Stephen Y. Kang<sup>1</sup>**, Deborah J. Colesa<sup>1</sup>, Gina L. Su<sup>1</sup>, Yehoash Raphael<sup>1</sup>, Bryan E. Pfingst<sup>1</sup>

<sup>1</sup>*Kresge Hearing Research Institute, Department of Otolaryngology, University of Michigan*

Earlier in the history of cochlear implants, candidacy was limited primarily to profoundly deaf individuals. More recently, the criterion for cochlear implantation includes patients with some degree of acoustic hearing and efforts are being made to preserve this hearing to supplement electrical hearing provided by the implant. However, studies are needed to determine if the presence of residual acoustic hearing affects the perception of the electrical stimulus. Our objective is to test the hypothesis that the presence of residual acoustic hearing affects temporal processing of the electrical signal. We studied guinea pigs divided into two treatment groups: a control group that was

deafened with cochlear perfusion of neomycin before implantation (n=9) and an experimental group that received a cochlear implant without predeafening (n=13). Psychophysical detection thresholds for electrical pulse trains were measured at pulse rates ranging from 156 pulses per second (pps) to 5000 pps in steps of doubling. We analyzed the shift in electrical threshold per doubling of the pulse rate and found that at pulse rates below 625 pps, the nondeafened animals showed larger decreases in electrical threshold with each doubling of the pulse rate than the control group. to monitor the status of the auditory system in the experimental group, acoustic thresholds and auditory brainstem responses were periodically measured. in both groups, the level of spontaneous activity in the auditory nerve was periodically assessed. Spontaneous activity in the auditory nerve was found only in nondeafened animals. We are processing cochleae for histological analysis to aid in determining the cell survival patterns that might contribute to the differences observed between the two groups. We conclude that the presence of residual acoustic hearing affects temporal response properties to electrical stimulation, specifically temporal integration at low pulse rates.

Supported by NIH grants R01 DC007634, T32 DC005356, and P30 DC05188.

#### **294 Cochlear Implants Stimulate Activity-Dependent CREB Pathway in the Deaf Auditory Cortex: Implications for Molecular Plasticity Induced by Neural Prosthetic Devices**

**Justin Tan<sup>1</sup>, Sandra Widjaja<sup>1</sup>, Jin Xu<sup>1</sup>, Robert Shepherd<sup>1</sup>**

<sup>1</sup>*The Bionic Ear Institute*

Neural activity modulates the maturation of synapses and their organization into functional circuits by regulating activity-dependent signaling pathways. Phosphorylation of cAMP/Ca<sup>2+</sup> responsive element binding protein (CREB) is widely accepted as a stimulus-inducible event driven by calcium influx into depolarized neurons. in turn, phosphorylated CREB activates the transcription of brain-derived neurotrophic factor (BDNF) which is needed for synaptic transmission and long-term potentiation. We examined how these molecular events are influenced by sensorineural hearing loss and long-term re-activation via cochlear implants. Sensorineural hearing loss reduced the expression of phosphorylated CREB and BDNF. in contrast, deafened animals subject to long-term, unilateral intracochlear electrical stimulation exhibited an increased expression of phosphorylated CREB and BDNF in the contralateral auditory cortical neurons, relative to ipsilateral ones. These changes induced by cochlear implants are further accompanied by the activation of the mitogen-activated protein kinase (MAPK) signaling pathway, which has been implicated in long-lasting forms of synaptic plasticity. Because CREB and BDNF are critical modulators of synaptic plasticity, our data describe for the first time possible molecular candidate genes which are altered in the auditory cortex, following cochlear implantation. These findings provide insights to adaptive,

molecular mechanisms recruited by the brain upon functional electrical stimulation by neural prosthetic devices.

Supported by Grant number NO1-DC-3-1005 from the National Institute on Deafness and Other Communication Disorders, the Garnett Passe and Rodney Williams Memorial Foundation, the Freiwillige Akademische Gesellschaft (Switzerland) and Percy Baxter Trust.

#### **295 Across-Site Patterns of Gap and Modulation Detection Thresholds in Cochlear Implant Users**

**Rose Burkholder-Juhasz<sup>1</sup>, Bryan Pflugst<sup>1</sup>**

<sup>1</sup>*University of Michigan*

The psychophysical performance of cochlear implant (CI) users typically varies across stimulation sites when the sites are stimulated individually. Some psychophysical measures such as detection thresholds (Ts) and comfort levels (Cs) show similar across-site patterns suggesting that they rely on common underlying mechanisms. However, across-site patterns of Ts and Cs do not relate to patterns of modulation detection thresholds (MDTs). Here, we examine if across-site patterns of gap detection thresholds (GDTs) match across-site patterns of MDTs. Similar across-site patterns for these temporal-processing skills would suggest that they rely on similar mechanisms. GDTs and MDTs were tested at all active sites (usually 18-21 sites per subject) in adult CI users at 30% of the dynamic range using monopolar stimulation. Test stimuli were 500 msec biphasic pulse trains with a mean phase duration of 50  $\mu$ sec, presented at 1K pps, and separated by a 500 msec ISI. a 2AFC task with flankers and adaptive tracking was used. MDTs were measured using 10 Hz sinusoidal modulation of phase duration. Modulation depth started at 50%. GDTs were measured with an initial gap of 25 msec starting 250 msec after stimulus onset. Across-site patterns of MDTs and GDTs were similar and highly correlated in most subjects. Failure to find this result in some subjects was likely due to ceiling GDTs.

The results suggest that similar mechanisms underlie MDTs and GDTs and their across-site variation. These mechanisms may be different from those affecting across-site variation in Ts and Cs. Pathology affecting neurons activated by each site may cause across-site variation in temporal processing. for example, spatial activation patterns of neurons, the condition and quantity of peripheral and central processes of auditory nerve fibers, and hair cell survival near sites could contribute to across-site variation in temporal processing.

Support: NIH/NIDCD grants R01 DC04312, T32 DC00011 and P30 DC05188.

## **296 Facial Nerve Stimulation after Cochlear Implantation according to types of Nucleus 22-channel electrode arrays**

Joong Ho Ahn<sup>1</sup>, Soo Hee Oh<sup>1</sup>, Jong Woo Chung<sup>1</sup>, Kwang-Sun Lee<sup>1</sup>

<sup>1</sup>Asan Medical Center

**Objective:** to analysis the prevalence of facial stimulation (FNS) after cochlear implantation with Nucleus 22-channel devices according to types of electrodes arrays.

**Materials and Methods:** We retrospectively analyzed medical and mapping records of 394 patients who received cochlear implants (CI) manufactured by Cochlear Corporation from April 1999 to March 2007.

**Results:** Total 26 of 394 (6.6%) patients had FNS (CI24M 4 of 39 [10.3%], CI24RCS 12 of 192 [6.3%], CIRST 9 of 21 [42.9%], CI24RCA 0 of 55 [0.0%], and CI24RE 1 of 87 [1.1%]). in addition, 8 of 331 (2.4%) patients with normal inner ear complained of FNS (CI24M 1 of 33 [3.0%], CI24RCS 6 of 174 [3.5%], CI24RCA 0 of 53 (0.0%), and CI24RE 1 of 71 [1.4%]). We could managed these patients with methods such as decrease of C-level, selective channel turning off, and changes of mapping strategies.

**Conclusion:** in this study, we found that the prevalence of FNS after CI significantly decreased when electrode arrays consisted of half-band electrodes with modiolar facing and curved perimodiolarly for modiolar proximity. Especially, Contour Advance electrodes offered significantly lower incidence of FNS than any other electrode arrays.

## **297 Analysis of Deafferentation-Induced Cell Death in Chick Cochlear Nucleus Using TUNEL Labeling and Laser Capture Microdissection**

Hope Karnes<sup>1</sup>, Doug Girod<sup>1</sup>, Dianne Durham<sup>1</sup>

<sup>1</sup>University of Kansas Medical Center

Neurons in the avian cochlear nucleus, n. magnocellularis (NM) receive exclusive excitatory input from the ipsilateral cochlea. Cochlea removal permanently abolishes this input, and NM neurons undergo rapid ultrastructural, metabolic, and functional changes, ultimately triggering the death of 30% of cells. NM cells destined to die exhibit early indications of cell compromise, including disassembly of ribosomes and degradation of rough endoplasmic reticulum. As a consequence, these "ghost" neurons stain poorly with thionin and can be distinguished from those NM neurons destined to survive deafferentation. Demonstration of caspase upregulation by us and others suggested that the abrupt cell death in NM following cochlea removal is apoptotic. We investigated loss of nuclear DNA integrity, measured by TdT-mediated dUTP Nick-End Labeling (TUNEL). Ten day-old birds underwent unilateral cochlea removal and were sacrificed 6hr to 7days later. Nuclear TUNEL labeling first appears at 6 hours, consistent with apoptosis-mediated DNA fragmentation. We also observed an unusual pattern of diffuse, cytoplasmic TUNEL labeling, beginning 24 hours after deafferentation. This cytoplasmic TUNEL labeling coincides with the number and pattern of "ghost" neurons, which also contain abundant abnormal mitochondria.

Further analysis of the genetic factors that influence cell fate in deafferented NM will include Laser Capture Microdissection (LCM) on thionin-stained sections. We microdissected three subpopulations of neurons: deafferented NM "ghost" cells that stained poorly with thionin; deafferented, surviving NM cells that stained intensely for thionin, and healthy control neurons from contralateral NM. From each subpopulation, RNA is probed against Affymetrix chicken genome microarray chips to identify differences in gene expression between (1) deafferented "ghost" cells and deafferented surviving cells in NM, and (2) deafferented surviving cells and contralateral control cells in NM.

## **298 Role of Metabotropic Glutamate Receptors in Deafferentation-Induced Cell Death in the Chick Cochlear Nucleus**

Kathryn Carzoli<sup>1</sup>, Richard Hyson<sup>1</sup>

<sup>1</sup>Florida State University

The chick auditory brainstem is a useful model system for examining changes that occur as a result of eliminating auditory nerve activity through cochlear ablation. Removal of the basilar papilla (cochlea) results in the death of approximately 30% of neurons in the chick cochlear nucleus, nucleus magnocellularis (NM). One early event in the degradation of NM neurons is the disruption of their ribosomes. This can be visualized as early as 1 h post-cochlea removal using Y10B, a monoclonal antibody that recognizes ribosomal RNA. Previous studies using a brain slice preparation have suggested that metabotropic glutamate receptor (mGluR) activation is necessary to prevent some rapid changes in NM neurons that occur following deafferentation, including the degradation of ribosomal structure and function. Isolating the brain slice in an *In Vitro* preparation, however, may eliminate other potential sources of trophic support for NM neurons. Consequently, it is not known if mGluR activation is truly required for neuronal survival in the intact system. the current experiment evaluates the role of mGluRs *in vivo*. a non-selective mGluR antagonist (MCPG), or vehicle (artificial cerebrospinal fluid) was administered intracerebroventricularly following unilateral cochlea removal. Control subjects replicated the previously reported effect of cochlea removal, showing lighter Y10B-labeling of NM neurons on the deafferented side of the brain compared to those on the intact side of the same section. Blockade of mGluRs *In Vivo* prevented the activity-dependent difference in Y10B labeling, and in some cases, had the reverse effect, yielding darker labeling of the deafferented NM neurons compared to those on the intact side of the brain. These data are consistent with *In Vitro* findings and suggest that mGluR activation plays a vital role in the activity-dependent regulation of NM neuron integrity.

### **299** Changes in Expression and Localization of Vesicular Glutamate Transporters in the Rat Cochlear Nucleus Following Deafness

Bozena Fyk-Kolodziej<sup>1</sup>, Takashi Shimano<sup>1</sup>, Avril Genene Holt<sup>1</sup>

<sup>1</sup>Wayne State University School of Medicine

Quantitative real time PCR (qRT-PCR) was used to examine gene expression of vesicular glutamate transporter(s) (vGluT)s following bilateral cochlear ablation (3 days or 2 months). for qRT-PCR, at each time point there were four normal hearing and four deafness groups, each group containing three animals (n=48 animals). Immunocytochemistry was also used to localize vGluTs within specific regions of the CN (anterior (AVCN) and posterior ventral CN (PVCN), small cell shell/granule cell domain (SCS/GCD), and dorsal CN (DCN)) in normal (n=4), 3 week (n=2) or 2 month (n=2) deafened animals. in normal hearing animals, vGluT1 was highly expressed in the molecular layer of the DCN, the AVCN, and the PVCN. Labeling for vGluT2 was particularly intense in the SCS/GCD region of the CN and in large synaptic terminals surrounding somata. Immunoreactivity for vGluT2 was less impressive in the VCN with labeling still observed in terminals contacting somata, the terminals were smaller. in the DCN, vGluT1 was present in very small densely packed terminals in the molecular layer while in the fusiform and deep layers vGluT1 labeling was localized to medium sized and a few very large terminals. the most prominent vGluT2 labeling in the DCN was in the fusiform layer. Similar vGluT1 and vGluT2 localization has been reported in normal hearing guinea pigs CN (Zhou et al., 2007). Three days following deafening gene expression for vGluT1 showed no change while vGluT2 expression decreased 36% (p < .05). After two-months of deafness, gene expression for vGluT1 significantly decreased (15%; p< .05) and vGluT2 remained decreased (33%;p< .05). in both the AVCN and PVCN vGluT1 labeling was localized to cell bodies and only a few terminals following deafness. While there was no change in the localization of vGluT2 the intensity of labeling was significantly decreased in the deafened groups (95%). in the SCS/GCD vGluT2 labeling increased in intensity (15%) in the deafened group. within the DCN, there were no significant changes.

### **300** Deafferentation Alters the Distribution of Vesicular Glutamate Transporters Associated with Auditory Nerve or Non-Auditory Inputs to the Cochlear Nucleus

Chunhua Zeng<sup>1</sup>, Nishant Nannapaneni<sup>1</sup>, Jianxun Zhou<sup>1</sup>, Susan Shore<sup>1</sup>

<sup>1</sup>University of Michigan

Glutamatergic projections from auditory and non-auditory regions to the cochlear nucleus (CN) are mostly non-overlapping: those originating in non-auditory centers terminate primarily in the granule cell domains (GCD) whereas type I auditory nerve fibers (ANFs) terminate in the magnocellular areas of the VCN (VCNm) and deep layers of DCN. Vesicular glutamate transporters (VGLUTs), which selectively package glutamate into

synaptic vesicles, have different isoforms, VGLUT1 and VGLUT2, that are distinctly associated with synaptic terminals of auditory nerve fibers (ANF), and brainstem somatosensory nuclei, respectively (Zhou et al., 2007). Synaptic vesicle protein2 (SV2), which is a marker of synaptic terminals, decreases following axotomy, and increases with axonal sprouting after injury (Nachman-Clewner and Townes-anderson, 1996). Here we examined the distributions of VGLUT1, VGLUT2 and SV2 expression in the CN following deafferentation by intra cochlear injections of kalamycin (20 ul, 30%), which resulted in profound, unilateral hearing loss. As shown previously (Zhou et al., 2007), the CN regions demonstrating the most intense expression of VGLUT1 and VGLUT2 were largely non-overlapping and were consistent with ANF and somatosensory projections, respectively. One or two weeks following deafening, VGLUT1, which was highly expressed in VCNm and the molecular layer of the dorsal CN in normal animals, was significantly decreased in these regions. On the other hand, VGLUT2, which was predominantly expressed in the GCD in normal animals, was significantly increased in the GCD after deafening. Preliminary results indicate that SV2 was also decreased in VCNm and the molecular layer of the dorsal CN, but increased in the GCD after deafening. the pathway-specific amplification of VGLUT2 expression and the concurrent changes of SV2 in the CN suggests that, in compensatory response to auditory deafferentation, the non-auditory influence on CN is significantly enhanced. Nachman-Clewner M, Townes-anderson E. 1996. Injury-induced remodelling and regeneration of the ribbon presynaptic terminal *In Vitro*. J Neurocytol 25(10):597-613. Zhou J, Nannapaneni N, Shore S. 2007. Vesicular glutamate transporters 1 and 2 are differentially associated with auditory nerve and spinal trigeminal inputs to the cochlear nucleus. J Comp Neurol 500(4):777-787.

### **301** Structural Plasticity in Central Auditory System After Carboplatin Induced Hair Cell Degeneration in the Chinchilla

Suzanne Kraus<sup>1</sup>, Yide Zhou<sup>1</sup>, Dalian Ding<sup>1</sup>, Richard Salvi<sup>1</sup>

<sup>1</sup>University of Buffalo Inner ear damage may lead to structural changes in the central auditory system. in rats, cochleotomy that involves destruction of all hair cells, support cells, neurons and distal olivocochlear axons results in synaptic growth in the ipsilateral ventral cochlear nucleus (VCN), shown by an increased expression of the growth associated protein GAP-43 in synaptic terminals. in this study, we wanted to determine if more limited damage caused by the ototoxic drug carboplatin leads to a similar pattern of central plasticity in the adult chinchilla. to accomplish this goal, we applied a small drop of carboplatin (5mg/ml) to the round window to destroy hair cells. Chinchillas were allowed to survive for 7, 15 or 31 days. After fixation, cochleas were dissected out to determine the degree of hair cell loss. Brainstems including VCN were cut into 30µm thin sections and immunostained for GAP-43.

in general, hair cell lesions increased with survival time. At 7 days post-carboplatin, hair cell loss ranged from modest to approximately 50%, predominantly IHC basally, in the

high frequency region. After 15 days, there was either complete loss of IHC and OHC throughout the cochlea or almost complete loss except in the low frequency region apically. After surviving for 31 days, all hair cells were missing throughout the cochlea. Centrally, GAP-43 expression was strongly increased in the ipsilateral VCN in animals with complete hair cell lesion (15 or 31 days); GAP-43 expression was less in animals with almost complete hair cell lesion (15 days). In one animal, the GAP-43 increase appeared only in the dorsal, high frequency region of the VCN.

These results demonstrate that hair cell loss induced by local carboplatin treatment activates synaptic growth processes centrally. Moreover, hair cell degeneration in the cochlea and GAP-43 up-regulation in VCN follow a high- to low frequency gradient. Supported by NIH grant R01 DC06630

### **[302] Altered Markers of Glycinergic Function in the Dorsal Cochlear Nucleus (DCN) of a Rat Model of Chronic Tinnitus**

**Hongning Wang<sup>1</sup>**, Lynne Ling<sup>1</sup>, Thomas J. Brozoski<sup>1</sup>, Jeremy G. Turner<sup>1</sup>, Jennifer L. Parrish<sup>1</sup>, Larry F. Hughes<sup>1</sup>, Donald M. Caspary<sup>1</sup>

<sup>1</sup>*Southern Illinois University School of Medicine*

Fifteen to 35% of the population in the United States experience tinnitus, a subjective "ringing in the ears". Up to 10% of tinnitus patients report their symptoms are severe and disabling. Tinnitus was induced in FBN rats using one hour, 116 dB (SPL) unilateral octave-band noise exposure centered at 16 KHz via an anesthetized preparation and assessed behaviorally by an operant conditioning paradigm and GAP detection method. Sixteen weeks following noise exposure, young adult (7mos.) rats showed evidence of tinnitus in the 24-32 KHz range while aged (30 mos.) animals showed the greatest evidence of tinnitus at 10 KHz. These results suggest that the frequency characteristics of tinnitus produced by acoustic exposure may be age-dependent. Protein levels of  $\alpha$ 1-3 glycine receptor subunits (GlyRs), gephyrin, BDNF and its receptor TrkB were measured in dorsal cochlear nucleus (DCN) fusiform cells 4 months after exposure using quantitative immunocytochemistry. Young exposed rats showed decreases of GlyR $\alpha$ 1 protein at middle and high frequency regions in DCN while aged exposed rats showed higher  $\alpha$ 1 subunit protein levels in the same DCN regions. The GlyR anchoring protein, gephyrin, was significantly increased in both young and aged exposed rats, suggesting an intracellular receptor trafficking change following acoustic trauma. BDNF and TrkB were also increased over fusiform cells for young and aged exposed rats.

[3H] strychnine binding was used to assess DCN GlyR function following noise exposure. An age-related decrease in GlyR $\alpha$ 1 protein was reflected in a significant age-related down-regulation of Bmax. Young trauma animals showed a significant decrease in Bmax further suggesting a post-exposure reduction of normal adult GlyR function.

These findings suggest that both noise-induced tinnitus and aging are associated with functional GlyR changes in

DCN fusiform cells. Identification of the mechanisms could further the development of novel selective drugs for tinnitus.

### **[303] Revealing the Molecular Layer of the Primate Dorsal Cochlear Nucleus**

**Maria Rubio<sup>1</sup>**, Kathryn Gudsruk<sup>1</sup>, Yolanda Smith<sup>2</sup>, David Ryugo<sup>3</sup>

<sup>1</sup>*University of Connecticut*, <sup>2</sup>*Emory University*, <sup>3</sup>*Johns Hopkins*

The dorsal cochlear nucleus (DCN) receives direct input from the cochlea via the auditory nerve. In nonprimate mammals, the DCN is thought to play a key role in the orientation of the head towards sounds of interest by integrating acoustic and somatosensory information (May, 2000; Davis and Young, 2002). Whether this function pertains to humans and higher primates is unclear because the DCN and granule cell domain of the cochlear nucleus have been reported to undergo pronounced phylogenetic changes in cytoarchitecture across the primate order (Moskowitz, 1969; Moore and Osen, 1979; Moore, 1980; Heiman-Patterson and Strominger, 1985). In this study, we examined the rhesus monkey (cercopithecoid primates) to address the question of whether the superficial DCN of higher primates has similar synaptic components as nonprimate mammals. We used ultrastructural analyses to identify parallel fibers and their synapses, and molecular markers to determine that primates share the main components of excitatory neurotransmission as other mammals. By using immunohistochemistry in combination with light and electron microscopy, we found many unmyelinated, thin axons and en passant glutamatergic synapses on dendritic spines within the molecular layer that are characteristic of parallel fibers. We showed that the primate DCN shares the main molecular components of excitatory neurotransmission. We also found synaptic expression of AMPA and delta glutamate receptor subunits on spines in the molecular layer. Lastly, parallel fibers use VGLUT1 to package glutamate into the synaptic vesicles and to mediate glutamate transport. These observations strongly support the argument that the rhesus monkey DCN has similar neuronal features as other nonprimate mammals. We propose that the DCN of higher primates has the necessary structural organization to integrate multimodal somatosensory information through granule cells.

Support: NIH/NIDCD RO1 DC006881 (M.E.R) and RO1 DC004395 (D.K.R).

### **[304] Topography of Projections from the Lateral Reticular Formation and the Spinal Trigeminal Nucleus in the Guinea Pig Cochlear Nucleus.**

**Yilei Cui<sup>1</sup>**, Susan Shore<sup>1</sup>

<sup>1</sup>*University of Michigan*

The spinal trigeminal nucleus (Sp5) and lateral reticular formation (LRF) are non-auditory structures that convey somatosensory information from the vocal tract, startle reflex and respiratory centers, directly to the cochlear nucleus (CN). Glutamatergic projections from Sp5



terminate primarily in the granule cell domain (GCD) but also in magnocellular regions of ventral CN (VCN; Haenggeli et al., 2005; Zhou et al., 2007; Zhou and Shore, 2004). Recent studies have shown that the LRF also projects to the CN (Shore and Zhou, 2006; Zhan and Ryugo, 2007). It is unclear whether the projections from these two regions have different topographic distributions in the CN. the current study examines the terminal distribution patterns for both LRF and SP5 in the GCD and magnocellular areas of the CN. Two different tracers (Fluoro-ruby and BDA) were injected into each region in the same animal and their respective terminal distributions in the CN were examined.

The LRF projection was mostly distributed across the GCD. the terminal endings were either small, *en passant* boutons (< 2.5µm; (33%)) or large, irregular swellings, suggestive of mossy fibers (≥2.5µm; (67%)). a few endings were also located in the central part of VCN. Likewise, most Sp5 labeled terminals were restricted to the GCD. However, in contrast to the LRF projection, more terminal endings were of the small bouton type (82%), and fewer were of the large, mossy-fiber type (17%). As for the LRF projection, a few endings were located in central VCN.

These findings indicate that the LRF may provide a major mossy fiber input to the GCD, whereas Sp5 provides an input comprised mainly of small boutons. These patterns suggest differences in signal transfer from each nucleus.

Haenggeli CA, Pongstaporn T, Doucet JR, Ryugo DK. 2005. Projections from the spinal trigeminal nucleus to the cochlear nucleus in the rat. *J Comp Neurol* 484(2):191-205.

Shore SE, Zhou J. 2006. Somatosensory influence on the cochlear nucleus and beyond. *Hear Res* 216-217:90-99.

Zhan X, Ryugo DK. 2007. Projections of the lateral reticular nucleus to the cochlear nucleus in rats. *J Comp Neurol* 504(5):583-598.

Zhou J, Nannapaneni N, Shore S. 2007. Vesicular glutamate transporters 1 and 2 are differentially associated with auditory nerve and spinal trigeminal inputs to the cochlear nucleus. *J Comp Neurol* 500(4):777-787.

Zhou J, Shore S. 2004. Projections from the trigeminal nuclear complex to the cochlear nuclei: a retrograde and anterograde tracing study in the guinea pig. *J Neurosci Res* 78(6):901-907.

### **[305] Distribution of Perineuronal Nets in the Human Cochlear Nucleus**

**Randy Kulesza<sup>1</sup>, Jessica Wagoner<sup>1</sup>**

<sup>1</sup>LECOM

The mammalian cochlear nucleus (CN) is a massive aggregation of multiple neuronal subtypes intimately associated with the cochlear division of cranial nerve VIII. in humans, the CN is found mainly along the floor of the 4th ventricle immediately caudal to the inferior cerebellar peduncle and extends rostrally into the middle cerebellar peduncle. the CN is an essential component of the ascending auditory pathway: it is the main target of the auditory nerve and a major site of divergence within the auditory pathway. the CN is traditionally divided into

dorsal (DCN) and ventral (VCN) subdivisions based on cytoarchitectural criteria. Notably, the human DCN lacks the typical laminar organization described in other mammals and the human VCN rather than described as anterior and posterior, is divided into four subregions: an octopus cell area, a central area, a cap region and a rostrally situated spherical cell area (Moore and Osen, 1979).

Certain fast-firing or highly active populations of neurons in the central nervous system are surrounded by a specialized extracellular matrix known as perineuronal nets. Perineuronal nets can be selectively revealed by binding of Wisteria floribunda agglutinin. within the auditory circuits, perineuronal nets are thought to be associated with neurons specifically associated with processing high frequency sounds. within the gerbil cochlear nucleus perineuronal nets are specifically associated with octopus cells and multipolar neurons projecting to the inferior colliculus (Cant and Benson, 2006).

We have used a biotinylated wisteria floribunda to identify sites of perineuronal nets within the human cochlear nucleus. Results from three human brainstems reveal a consistent pattern of labeling. the DCN is generally devoid of labeling; only occasional neurons are revealed. in the VCN, perineuronal nets are found only in distinct regions. Perineuronal nets are found throughout the octopus cell area and around the more rostrally located stellate neurons in the central region. These more rostrally-situated neurons are closely associated with the entering fibers of the cochlear division of CN VIII. in both regions, the perineuronal nets are seen to completely surround the cell bodies and primary dendrites.

### **[306] Comparison and Characterization of Auditory Brainstem Regions in Line H and Line 12 Transgenic Mice**

**Avril Genene Holt<sup>1</sup>, Joseph Rizk<sup>1</sup>, Takashi Shimano<sup>1</sup>, Bozena Fykkolodziej,<sup>1</sup>**

<sup>1</sup>Wayne State University School of Medicine

Throughout the central auditory system many cells can be identified based upon morphology and neurochemistry. Techniques such as Golgi staining and immunohistochemistry have allowed us to make great strides in the characterization of auditory neurons, yet some auditory brain regions contain morphologically homogeneous populations of neurons that display functionally distinct characteristics. We have examined two lines of transgenic mice that each express GFP in subsets of neurons. Line H and Line 12 mice were previously generated to selectively express green fluorescent protein in neurons. the GFP label was expressed throughout the entirety of the neuron from the dendrites and somata to the terminals. Coronal sections (20 micron) were collected from the rostral inferior colliculus (IC) through the most caudal portion of the dorsal cochlear nucleus (DCN). of the brain regions we examined (DCN and ventral cochlear nucleus, dorsal, central, and external nuclei of the IC, dorsal, intermediate and ventral nuclei of the lateral lemniscus, medial nucleus

of the trapezoid body, superior paraolivary nucleus, lateral superior olive, medial superior olive, and primary auditory cortex) Line 12 ( $n = 5$ ) consistently expressed two to twenty times more GFP labeled neurons than Line H ( $n = 4$ ). the exception to this was in the central nucleus of the inferior colliculus where there was no significant difference in the number of neurons selectively expressing GFP across lines. There were virtually no GFP neurons found in the superior olivary complex (five or fewer per nucleus) of Line H mice, while the average number of GFP labeled neurons in the SOC of Line 12 mice ranged from eight to 54. in the DCN similar numbers of GFP labeled neurons were identified in Line H ( $15 \pm 2$ ) and Line 12 ( $17 \pm 3$ ) however, labeled neurons were identified in different layers, e.g. the molecular layer in Line H mice and the fusiform layer in Line 12 mice. We have begun immunohistochemical studies using antibodies for neurotransmitters to further characterize these subsets of neurons. in the future, Line H and Line 12 mice may prove useful in functional or gene expression studies where identifying subpopulations of neurons is critical.

### **[307] Assessment of channelrhodopsin-2 (ChR2) transfected neurons in the auditory pathway**

**Takashi Shimano<sup>1</sup>**, Bozena Fyk-Kolodziej<sup>1</sup>, Zhuo-Hua Pan<sup>1</sup>, Sanford Bledsoe<sup>2</sup>, Mikiya Asako<sup>3</sup>, Avril Genene Holt<sup>1</sup>  
<sup>1</sup>Wayne State University School of Medicine, <sup>2</sup>University of Michigan Kresge Hearing Research Institute, <sup>3</sup>Kansai Medical University

We have delivered an adeno-associated viral vector containing Chop2 fused with GFP (to form the light gated cation channel ChR2), into the dorsal cochlear nucleus (DCN;  $n = 3$ ) or cochlea ( $n = 3$ ). One month later we examined the cochlea, CN, inferior colliculus (IC) and superior olivary complex (SOC) for evidence of transfected cells and found labeled cells and processes in the SOC, CN and IC. We then tested both light and sound driven neuronal activity in the medial and lateral DCN. in the medial DCN the most superficial channels showed gradually increasing activity during the light stimulus rapidly returning to pre-light levels post stimulus. However, the deepest channels showed adaptive responses with neuronal activity immediately increasing to a specific level at the onset of the light stimulus and remaining at that level until the stimulus was removed. in the lateral DCN neuronal activity driven by light was similar to that observed in the medial DCN. the response was not as robust and after removal of the light stimulus several channels exhibited activity that was lower than pre-light stimulus levels. We also examined sound driven responses in the DCN before and after light stimulation. in the medial DCN 87.5% of the 16 channels showed decreased activity in response to sound following light stimulation while 12.5% of the channels showed no change. in the lateral DCN 62.5% of the sites showed increased responses, 12.5% decreased responses and 25% showed no change in sound driven responses following light exposure. Our results indicate obvious distinctions between light mediated responses depending upon the location of the neurons. in addition, sound driven

activity in CN neurons is affected by light mediated activation. Transfecting cells via viral delivery of ChR2 can be useful as a tract tracer and neuronal marker to delineate pathways. in the future ChR2 may be developed as an alternative to electrical stimulation.

### **[308] Glycinergic Inputs to Facilitated Combination-Sensitive Neurons in Inferior Colliculus of Mustached Bat**

**Asuman Yavuzoglu<sup>1</sup>**, Jeffrey Wenstrup<sup>1</sup>

<sup>1</sup>Northeastern Ohio Universities College of Medicine & Kent State University

Combination-sensitive neurons in the mustached bat analyze sonar and social vocalizations. They are facilitated when two sounds of very different frequencies are presented in a specific temporal relationship. Previous work suggests that both high-and low-frequency tuned glycinergic inputs converge on high-frequency regions of the inferior colliculus (IC), creating facilitatory interaction through post-inhibitory rebound excitation. to identify the sources of these glycinergic inputs, we combined retrograde tracing with immunohistochemistry for the neurotransmitter glycine. We deposited retrograde tracer (Fluorogold) into facilitated combination-sensitive recording sites in IC. After transport time, the brain was fixed by perfusion (4% paraformaldehyde) and processed to mark glycinergic cells with green immunofluorescence. We observed the largest number of double-labeled cells in both multipolar and columnar subdivisions of the ipsilateral (IC deposit side) ventral nucleus of the lateral lemniscus (VNLL). This labeling may occur in both high-and low-frequency regions of VNLL. We also observed double labeling in other nuclei, but in fewer numbers: ipsilateral intermediate nucleus of the lateral lemniscus (INLL), ipsilateral lateral and medial superior olives (LSO, MSO); this labeling appeared to be in high-frequency regions. Very few double-labeled cells were located in contralateral cochlear nuclei and some ipsilateral periolivary nuclei. No glycinergic somatic labeling was observed in the dorsal nucleus of the lateral lemniscus (DNLL) and IC. These results suggest that VNLL is the most likely source of low-frequency glycinergic input to combination-sensitive IC neurons. Most likely sources of high-frequency glycinergic input are nuclei of the lateral lemniscus (NLL) (except DNLL) and ipsilateral LSO and MSO. These glycinergic inputs may create selective excitatory responses to complex signals. Supported by NIDCD grant RO1 DC-00937(J.J.W).

### **[309] Biophysical Properties of Neurons From Cat Ventral Cochlear Nucleus**

**Ramazan Bai<sup>1</sup>**, Giyasettin Baydas<sup>1</sup>

<sup>1</sup>Firat University

There are some *In Vivo* studies identifying morphological correlates of most of the principal cochlear nucleus unit types, much of which have been carried out in cats. Oertel and her colleagues have performed complementary studies establishing that physiological response properties are well correlated with underlying morphology in the mouse cochlear nucleus slice preparations (Wu and

Oertel, J. *Neurosci.* 4, 1577, 1984; Hirsch and Oertel, J. *Physiol.* 396, p549, 1988). However, in order to make the *In Vivo* recordings from units of cat cochlear nucleus more meaningful, species-specific characterizations of biophysical properties of cell types should be performed. Therefore, in the present study we aimed to study the intrinsic electrical properties of the neurons in ventral cochlear nucleus slices from cat, using whole-cell patch recordings. Coronal slices (200  $\mu$ m) of the ventral cochlear nucleus (VCN) were made from 7 days old cat. Pipettes contained biocytin so that intrinsic properties could be associated with their particular morphology. Recorded cells were fixed in 4% paraformaldehyde and subsequently processed to visualize biocytin and counterstained with cresyl violet to outline gross structure of the cochlear nucleus.

Whole-cell recordings in the current-clamp configuration were made from one octopus cells, two bushy cells and 15 stellate cells, majority of which were morphologically identified. Octopus cell responded with one large, overshooting action potentials with a slower time course followed by few much smaller action potential-like voltage transients to the depolarizing currents. Similarly bushy cells fired only one action potential in response to depolarizing current pulses. Stellate cells fired trains of action potentials with a slower time course. These preliminary results appear to indicate that responses of the neurons to DC current injections in the ventral cochlear nucleus slices from 7 days old cat are similar to those of mice, but somewhat slower and exaggerated. This might be accounted for by that the neurons in ventral cochlear nucleus is not matured at this age yet.

### **[310] Distribution of Slo 2.1, a Na<sup>+</sup> Activated K<sup>+</sup> Channel, in Neurons of the Cochlear Nucleus**

Joel Cano<sup>1</sup>, Rafael Lujan<sup>1</sup>, Jose Juiz<sup>1</sup>

<sup>1</sup>Med School-Universidad de Castilla-La Mancha

Slo2.1 belongs to a family of potassium channels which are activated by Na<sup>+</sup> influx and therefore may provide neurons with an efficient mechanism to regulate excitability and firing. Although Slo2.1 has been reported to be expressed in neurons of the cochlear nucleus, its distribution pattern is not known, an important piece of evidence to elucidate possible roles of this channel in this auditory brainstem nucleus. Using a combination of high resolution immunocytochemistry techniques we report that in the rat cochlear nucleus, Slo2.1 is present in most major neuronal types in all divisions. Staining intensities in cell bodies vary according to cell type, with octopus cell bodies in the posteroventral division having a lighter staining. Dendritic labeling, on the other hand, is intense and abundant throughout the nucleus. There is no evidence of labeling in axons or synaptic endings. Therefore, the cellular distribution of Slo2.1 is consistent with an important role in the control of high frequency firing in the cochlear nucleus, probably in relation with the entry points of excitatory inputs in the different types of neurons in this nucleus.

Supported by SAN06-009-00, GCS-2006 C15 and BFU2006-13974

### **[311] Localization of Ion Channels That Contain Kv1.1 and HCN1**

Donata Oertel<sup>1</sup>, Shalini Shatadal<sup>1</sup>

<sup>1</sup>University of Wisconsin

To determine where the ion channels that mediate low-voltage-activated potassium (gKL) and hyperpolarization-activated (gh) conductances are located and to what extent gKL and gh are colocalized, we labeled them with antibodies to Kv1.1 and HCN1 respectively and examined their presence with confocal microscopy. Octopus cells were brightly labeled. Antibodies to HCN1 outlined not only cell bodies but also dendrites (Koch et al., 2004). Kv1.1 was colocalized with HCN1 around the cell body and around dendrites and was also detected in the cytoplasm. In addition to being in the octopus cell area, some similar, brightly labeled cells were seen spreading ventrally along the posterior edge of the ventral cochlear nucleus (VCN), indicating that the octopus cell area extends in a ventrocaudal lip. In the multipolar cell area that contains many T stellate cells, labeling for Kv1.1 and HCN1 was weak. In the anterior VCN where most bushy cells are located, Kv1.1 and HCN1 were colocalized around cell bodies and in dendrites. The perinodes of auditory nerve axons were prominently labeled for Kv1.1 in the nerve root and in the anterior VCN. Smaller perinodes were labeled in the posterior VCN, possibly because auditory nerve axons there are finer and have shorter internodes.

gKL sets the sensitivity to rate of depolarization and together with gh sets the resting input resistance of neurons in the VCN. gKL and gh are largest in octopus cells (Bal and Oertel, 2001), vary over an intermediate magnitude in bushy cells (Cao et al., 2007), and are smallest in T stellate cells (Ferragamo and Oertel, 2002; Rodrigues and Oertel, 2006). gKL is mediated through heteromeric ion channels of the Kv1 family with 75% gKL containing a Kv1.1 alpha subunit in octopus and bushy cells (Bal and Oertel, 2001; Cao et al., 2007). gh is mediated through ion channels in the HCN family, many containing HCN1 subunits.

This work was supported by a grant from NIH DC00176.

### **[312] Autonomous Development of Kv3.1b Expression and High-Threshold Outward Currents in Chick Auditory Brainstem Neurons in Primary Culture**

Thomas Kuenzel<sup>1</sup>, Yu Sun<sup>1</sup>, Harald Luksch<sup>2</sup>, Jörg Mey<sup>1</sup>, Hermann Wagner<sup>1</sup>

<sup>1</sup>RWTH Aachen, <sup>2</sup>TU Munich

The nuclei magnocellularis (NM) and laminaris (NL) in the avian auditory brainstem form a neuronal circuit that calculates and provides a first representation of interaural timing delays. The neurons are specialized for very fast action potential (AP) firing, which allows phase-locking to the auditory stimulus at high frequencies (1 kHz). The voltage-gated potassium channel subunit Kv3.1b is implicated in high-frequency APs, because the high-

threshold outward current mediated by these channels is known to speed up the repolarization phase of the AP.

Using a dissociated, low density and serum-free culture system of the embryonic day 7 auditory brainstem of the chicken enriched in NM/NL neurons [Kuenzel T et al., Eur. J. Neurosci. 25 (2007) 974-984], we compared the expression of Kv3.1b and other proteins after 1, 3, 7, and 14 days *In-Vitro* (DIV) to corresponding *In-Vivo* embryonic days with Western-blotting. the development of voltage-activated outward currents was assessed using voltage-clamp whole-cell patch recordings. Progression of synaptogenesis *In-Vitro* was examined physiologically as well as morphologically.

We found a significant 5-fold increase in Kv3.1b protein expression between embryonic days 10 and 14. This increase was paralleled by a significant increase of Kv3.1b protein expression of equal dimension in the culture between E 7 + DIV 3 and E7 + DIV 7. This was corroborated by an increase of a high-threshold outward membrane current with increasing time of cultivation, while the mean width at half-amplitude of the APs was found to be significantly diminishing. in parallel, we found spontaneous and evoked postsynaptic activity in our recordings of neurons aged E7 + DIV7 and older. Functional staining of synaptic zones using the styryl dye FM1-43fx and immunofluorescent labeling of synaptic marker proteins (synapsin I and synaptic vesicle protein 2) was successful in cultures of the same age and older.

Our results imply that synaptogenesis and development of the Kv3.1b protein expression are autonomous processes that take place even under the extreme deafferentation of a dissociated neuronal culture. a causal link between the two processes is suggested.

### **[313] Excitation Differs in Principal Cells of the PVCN, T Stellate and Octopus Cells**

**Xiao-Jie Cao<sup>1</sup>, Donata Oertel<sup>1</sup>**

<sup>1</sup>*Department of Physiology, University of Wisconsin Medical School*

Both major groups of principal cells of the posteroventral cochlear nucleus (PVCN), octopus and T stellate cells, are excited by auditory nerve fibers through glutamate receptors of the AMPA subtype. the time course of miniature excitatory postsynaptic currents (mEPSCs) reflects the properties of AMPA receptors and is indistinguishable in these principal cells (Gardner et al., 1999). We were surprised, therefore, to find that characteristics of evoked EPSCs recorded in whole-cell patch-clamp recordings under voltage-clamp evoked by stimulation of nearby fiber bundles (eEPSCs) differ in octopus and T stellate cells. AMPA receptors involved in responses to shocks in T stellate cells contain more GluR2 subunits than those in octopus cells. Current/voltage relationships of eEPSCs are largely linear, unaffected by intracellular spermine, and insensitive to philanthotoxin in T stellate cells whereas they show rectification, sensitivity to spermine and philanthotoxin sensitivity in octopus cells. Synaptic depression, too, differs in octopus and T stellate cells. Repetitive stimulation resulted in depression of eEPSCs in both cell types but depression was less in T

stellate than in octopus cells. for example, the last response after a train of 8 shocks at 100 Hz, was depressed by 40% in octopus cells but only by 25% in T stellate cells. in these recordings in coronal slices we confirmed the earlier finding that octopus cells receive converging input from many (>60) fibers whereas T stellate cells get converging input from fewer (~6-9 fibers). the small synaptic depression and currents through NMDA receptors in T stellate cell EPSCs presumably contributes to allowing a small number of inputs to produce tonic, "chopper," responses to sounds.

Work was supported by a grant from NIH DC00176.

### **[314] Desensitization and Activity-Dependent Recovery From Depression in the Avian Cochlear Nucleus Angularis**

**Katrina MacLeod<sup>1</sup>, Catherine Carr<sup>1</sup>**

<sup>1</sup>*University of Maryland*

The synaptic properties of the auditory nerve inputs to neurons of the cochlear nucleus are fundamental to the transformation of auditory information. in birds, timing and intensity information used in sound localization are processed in parallel streams beginning with the two divisions of the cochlear nucleus, n. magnocellularis (NM) and n. angularis (NA). Recent results have suggested that differences in the rapid, activity-dependent changes in synaptic strength, known as short-term synaptic plasticity, may contribute to differential transmission of timing and intensity components. At NM synapses, the short-term synaptic depression is due to a mixture of presynaptic effects, such as vesicle depletion, and postsynaptic effects, such as AMPA receptor desensitization. We investigated whether these effects can account for the depression component of synaptic plasticity in NA. We focused on a subset of synapses in NA that appeared to be preferentially depressing, and measured their sensitivity to desensitization blockade and their rate of recovery from depression. We found that although desensitization blockers such as cyclothiazide and aniracetam could prolong the time course of the EPSC, there was negligible effect on the steady state short-term depression during trains of stimuli. Previous experiments have suggested that the EPSC amplitudes may be enhanced due to recovery from depression that may be activity-dependent. We investigated this effect by measuring the recovery rate after low and high frequency stimulation trains and found that the recovery after high frequencies often was similar to or exceeded the recovery after lower frequencies, despite greater steady state depression. in conclusion, short-term depression at NA synapses are due to presynaptic effects, most likely vesicle depletion could also include potential effects like calcium channel inactivation. the preceding activity or degree of depletion strongly influences the recovery from depression. Supported by NIH R01-DC000436, NIH R03-DC007972, and NIH P30 grant DC0466.

### **315 Proximal and Distal Dendrites of Bushy Cells of the Anteroventral Cochlear Nucleus Receive Excitatory and Inhibitory Synaptic Inputs**

**Ricardo Gomez-Nieto<sup>1</sup>, Nathan Maltezos<sup>1</sup>, Maria Rubio<sup>1</sup>**

<sup>1</sup>*University of Connecticut*

Bushy cells (BCs) in the anteroventral cochlear nucleus mediate fast transmission of auditory nerve responses and are involved in early stages of sound localization. One question that remains open is whether BC dendrites play a role in the integration of auditory and non-auditory cues. Revealing the existence of cochlear and non-cochlear inputs on BC dendrites will provide evidence that these neuronal processes are involved in BC activity. to address this issue, we combined retrograde tracing methods with either immunofluorescence for excitatory (VGLUT1) and inhibitory (VGAT) synaptic markers or electron microscopy analysis. BCs and their dendrites were labeled completely after injecting either biotinylated or fluorescent dextrans into the trapezoid body. the confocal microscopic analysis revealed that proximal and distal dendrites of BC were coated with numerous boutons immunolabeled for either VGLUT1 or VGAT. At the electron microscopic level, we observed that retrogradely labeled BC dendrites received synaptic endings having ultrastructural characteristics of excitatory and inhibitory terminals. Morphometric analyses of the excitatory endings on BC dendrites revealed that many of the endings shared the same ultrastructural parameters as the endbulbs of Held. These observations advocate for abundant excitatory and inhibitory synaptic inputs through the entire dendritic tree of BCs. We propose that BC dendrites play a key role in the integration of acoustic information in the ventral cochlear nucleus.

Support: NIH/NIDCD RO1 DC006881 (M.E.R)

### **316 Delayed Release in Mouse Anteroventral Cochlear Nucleus**

**Will C. Hsu<sup>1</sup>, Matthew Xu-Friedman<sup>1</sup>**

<sup>1</sup>*Department of Biological Sciences, University at Buffalo*

Studies at many synapses have found two forms of evoked neurotransmitter release, rapid synchronous release and the elevated quantal release called delayed or asynchronous release that far outlasts synchronous release. Mechanistic studies have demonstrated that delayed release (DR) results from residual calcium in the presynaptic terminal. However, the functional role of DR in information processing is still unclear. to answer this question, we studied DR at the endbulb of Held, the synapse formed by auditory nerve fibers (ANs) onto bushy cells (BCs) in the mouse anteroventral cochlear nucleus (AVCN). BCs are responsible for processing precise acoustic timing information, yet show significant DR. We examined the functional role of DR by performing whole-cell recordings from BCs at 34C in AVCN slices taken from day 15-31 postnatal mice. Delayed release was detected in response to trains of AN stimulation at 100, 200 and 333 Hz. the frequency of DR was significantly increased at higher stimulation frequencies, and for longer duration trains at all ages tested. We confirmed that DR is mediated

by accumulation of residual calcium, using bath application of the calcium chelator EGTA-AM, which reduced DR in a dose-dependent manner. in addition, the magnitude of DR appears to follow a tonotopic organization in AVCN, with more delayed release in high-frequency areas, and little delayed release in low-frequency areas. This suggests that DR plays an important physiological role at the endbulb, which may influence the processing of precise sound timing, especially for high-frequency auditory inputs. We applied a simple model to quantify the amount of delayed release which accounted for the amount of delayed release under a variety of physiological conditions.

### **317 Postnatal Changes of the NMDA Component in Relation to AMPA in Murine Endbulb of Held Synapses During Single Stimuli and Extended Activity**

**Lioudmila Pliss<sup>1</sup>, Matthew Xu-Friedman<sup>1</sup>**

<sup>1</sup>*State University of New York at Buffalo*

The endbulb of Held is an axosomatic synapse formed by auditory nerve fibers on bushy cells (BC) of the anteroventral cochlear nucleus. the endbulb has a prominent, rapidly-decaying AMPA component, as well as a slow NMDA component (half-width 20-30 ms). the balance between AMPA and NMDA and their dynamics during extended activity can affect precision and strength of the endbulb and thus the role of BCs in the processing of temporal information. the NMDA component is often down-regulated at synapses over development. However, the NMDA component usually shows significant summation during extended high frequency activity, such as is found in auditory nerve fibers. to determine the importance of the NMDA component in auditory information processing, we have analyzed endbulb EPSCs during single and high-frequency stimulation in differently aged (P14-30) CBA/CaJ mice.

Initial studies with single stimuli showed that the absolute amplitude of the NMDA EPSC decreased during development, remaining stable after P24. the NMDA/AMPA ratio reached a plateau of ~10% in the oldest animals studied.

During prolonged, high-frequency stimulation, the NMDA EPSC showed considerable temporal summation, while the AMPA component showed depression, resulting in a large relative NMDA component. the NMDA/AMPA ratio in the last EPSC of the train doubled for mice aged P14-17, in comparison to the first EPSC of the train.

We assessed the role of the NMDA component in BC spiking behavior, using current clamp recordings. in the presence of the NMDA receptor antagonist CPP, the probability of spiking decreased at the end of high frequency trains. NMDA receptor block had smaller effect on spike latency and jitter.

We conclude that the NMDA component at the endbulb of Held synapse decreases with age, but does not disappear in CBA/CaJ mice. Furthermore, owing to temporal summation, the NMDA component acts as an amplifier for reliable firing during extended activity.

### **318 Dynamics of Glycinergic Synaptic Transmission From DCN to AVCN in Mouse Cochlear Nucleus**

Ruili Xie<sup>1</sup>, Paul Manis<sup>1</sup>

<sup>1</sup>*Department of Otolaryngology/Head and Neck Surgery, University of North Carolina at Chapel Hill*

Inhibition from the dorsal cochlear nucleus (DCN) helps shape the signal processing of cells of anterior ventral cochlear nucleus (AVCN). to investigate the temporal dynamics of inhibitory synapses from the DCN, we recorded from AVCN neurons while stimulating the DCN deep layer, using a parasagittal brain slice preparation of CBA mouse cochlear nucleus. IPSCs elicited in this manner were largely mediated by glycinergic receptors. IPSCs evoked by DCN stimulation at 1.5 times threshold are small in most neurons, with an average amplitude of  $-180 \pm 102$  pA (mean  $\pm$  SD). in 20% of the neurons, however, IPSC amplitudes are quite large, with an average of  $-1226 \pm 424$  pA. the decay time constant of the evoked IPSC varies widely, from 1.4ms to 45ms (average  $12.6 \pm 12.2$ ms). Neurons with the largest IPSC amplitudes tend to have faster decay time constants, while smaller IPSCs show a wide range of decay time constants. Synaptic dynamics during high frequency activation of inhibitory synapses were also studied. in 25% of AVCN neurons, a 100Hz train evoked an early facilitation (evaluated at 4th-6th IPSCs) followed by a late depression (evaluated at 48th-50th IPSCs). Facilitation was observed in both the early and late stage of the stimulus train in 40% of the neurons, whereas both early and late IPSCs were depressed in the remaining 35% of the neurons. Due to temporal summation, however, the postsynaptic inhibitory currents are sustained at a high level in most neurons. Although asynchronous release is observed later in the stimulus train, it is not as strong or long-lasting as reported for GABAergic synapses.

These results suggest that glycinergic inputs from DCN can exert several different inhibitory effects on AVCN neurons. Inhibition is most frequently potentiated during high frequency synaptic activity, and thus may regulate the firing of AVCN neurons during sustained stimulation.

(Supported by NIDCD grant DC04551)

### **319 Transmission of Complex Spikes within the Cartwheel Cell Network of the Dorsal Cochlear Nucleus**

Michael Roberts<sup>1</sup>, Laurence Trussell<sup>1</sup>

<sup>1</sup>*Oregon Health & Science University*

Complex spikes are brief, high-frequency bursts of action potentials and are characteristic of cartwheel cells (CwCs) of the dorsal cochlear nucleus (DCN) and Purkinje cells of the cerebellum. the relationship between complex spikes and the postsynaptic responses they elicit is not understood. in principle it could depend on multiple factors including the ability of each spike in the burst ("spikelets") to propagate along the axon, reach axon terminals, trigger neurotransmitter release, and activate postsynaptic receptors. Given the short intervals (2-4 ms) separating the spikelets in a complex spike, complex spikes place

high demands on axonal and synaptic machinery, potentially compromising the fidelity of transmission. Recent work in Purkinje cells has in fact shown that somatic complex spikes are transmitted with relatively poor fidelity, such that partway down the axon the second or third spikelets fail (Khaliq and Raman, 2005; Monsivais et al., 2005). Cerebellar anatomy, however, makes it difficult to examine postsynaptic responses to complex spikes, leaving open the question of how the synapse handles this high-frequency information. This question of fidelity of transmission has not been examined in detail in CwCs of the DCN. CwCs form inhibitory synapses onto nearby DCN principal neurons while also forming a local inhibitory network through synapses onto other CwCs. This arrangement makes it possible to record pre- and postsynaptic responses simultaneously, thereby allowing us to examine the effectiveness of both conduction of spikes and synaptic transmission in response to presynaptic complex spikes. Dual whole-cell recordings of synaptically coupled pairs of CwCs were made in which the presynaptic cell was current clamped and the postsynaptic cell was voltage clamped. Pharmacological characterization of CwC evoked IPSCs reveals that the glycine receptor antagonist strychnine blocks the majority of the postsynaptic current, while the GABAA receptor antagonist SR95531 blocks a tiny, remaining, strychnine-resistant current. Previous data from our lab demonstrated that CwC complex spikes result in complex IPSCs in target cells (Tzounopoulos et al., 2004). We now show that the spikelets of CwC complex spikes produce IPSCs in postsynaptic CwCs with very high fidelity for the first 2-3 spikelets, indicating reliable conduction of spikelets, unlike cerebellar Purkinje cells. the presence of IPSCs correlated well with the rate of rise and peak amplitude of presynaptic spikelets. Small, slow spikelets late in the waveform tended not to propagate. As a result, each complex spike reliably generates a high-frequency burst of IPSCs. Thus complex spikes may provide a powerful, failsafe inhibitory signal within the network of CwCs. Support: NIH grant NS028901

### **320 Molecular Components and Synaptic Functions of the Endocannabinoid System in the Dorsal Cochlear Nucleus (DCN)**

YanJun Zhao<sup>1</sup>, Maria Rubio<sup>2</sup>, Thanos Tzounopoulos<sup>1</sup>

<sup>1</sup>*Chicago Medical School, Rosalind Franklin University,*

<sup>2</sup>*University of Connecticut*

Molecular Components and Synaptic Functions of the Endocannabinoid System in the Dorsal Cochlear Nucleus (DCN).

Endocannabinoid (EC) signaling has emerged as one of the most important neuromodulatory systems in the brain. However, the cellular and molecular components of this system have not been determined in the auditory system. Previous studies from our lab have revealed that cell-specific EC signaling in the DCN determines cell-specific synaptic plasticity. the DCN, an auditory brainstem nucleus, integrates acoustic with multimodal sensory inputs from diverse areas of the brain. Excitatory parallel fibers (PFs) carry these diverse signals to the apical, spiny dendrites of fusiform cells (FCs) and cartwheel cells

(CWCs), while auditory nerve (AN) fibers carry acoustic inputs to the basal dendrites of FCs. Here, by using electron microscopy and electrophysiological assays we found that key proteins involved in EC signaling are expressed in the molecular layer, but not in the deep layer of the DCN. Presynaptic CB1 receptors (CB1Rs) are expressed in PFs and in inhibitory terminals synapsing onto CWCs and FCs, while they are absent in AN fibers. 2-arachidonoyl-glycerol (2-AG) and anandamide have been identified as ECs. Diacylglycerol lipase  $\alpha$  (DGL- $\alpha$ ), one of the enzymes synthesizing 2-AG was expressed on dendrites and spines of FC and CWC respectively. by blocking the synthesis of 2-AG with Tetrahydropipstatin (THL, 20  $\mu$ M) or RHC80267 (50  $\mu$ M) depolarization-induced suppression of excitation (DSE), a form of short-term plasticity, was blocked in PF inputs to CWCs, further indicating that 2-AG is the endocannabinoid mediating neuromodulation in the DCN. Depolarization-induced suppression of glycinergic inhibition (DSI) was absent in CWC and FC. However, application of the CB1 receptor agonist WIN 55,212-2 (1 $\mu$ M) resulted in a suppression of glycinergic IPSCs in CWCs. These data suggest that glycinergic terminals in the molecular layer express CB1Rs. Subsequently, EM studies confirmed expression of CB1Rs in glycinergic inhibitory terminals to CWC and FCs.

Determining the anatomical and functional properties of EC signaling in the DCN should not only contribute to an understanding of the generation of auditory neural responses, but will also have a significant impact on our understanding and cures for disorders caused by neural plasticity-like mechanisms, including tinnitus.

(Supported by NIDCD grant DC007905-01A1 to TT)

### **[321] MicroRNA Regulation of Neurotransmitter Levels in the Cochlear Nucleus: Mir-383 and Somatostatin**

**David Friedland<sup>1</sup>, Rebecca Eernisse<sup>1</sup>, Joseph Cioffi<sup>1</sup>**

<sup>1</sup>*Medical College of Wisconsin*

The cochlear nucleus contains a heterogeneous population of neurons utilizing a wide range of neurotransmitters and signaling peptides. Using serial analysis of gene expression, whole genome microarrays, and real-time RT-PCR we identified relatively high levels of transcript for somatostatin (Sst) in the anterior ventral cochlear nucleus (AVCN). Laser capture microscopy allowed us to further localize this expression to spherical bushy cells. Despite high levels of Sst mRNA in these cells, immunohistochemistry failed to identify appreciable levels of somatostatin protein in this region. Recent studies have demonstrated the role of microRNAs in regulating protein translation and we performed *in silico* analyses of potential miRNA regulators of Sst. These analyses predicted the Sst message to be a target of miR-383. We confirmed the presence of miR-383 in the cochlear nucleus with real-time RT-PCR. Further, this quantification demonstrated higher levels of this miRNA modifier in the AVCN as compared to the PVCN and DCN. Gel-shift binding assay between labeled miR-383 and Sst transcript showed specific binding between these molecules. These findings suggest that somatostatin

expression in bushy cells may be regulated by post-transcriptional controls rather than at the level of the genome. Somatostatin has been reported in perinatal rats but the protein expression declines by 3 weeks of age. Further investigations will examine developmental changes in levels of miR-383 and other miRNAs in the cochlear nucleus. MicroRNAs provide an additional mechanism by which the unique morphological and physiological phenotypes of auditory neurons may be developmentally established or secondarily modified by activity dependent plasticity.

This work was supported by NIH/NIDCD K08DC006227.

### **[322] Distribution of Voltage-Dependent Potassium Channels in the Inferior Colliculus of the Guinea Pig**

**David Perez-Gonzalez<sup>1</sup>, Adrian Rees<sup>1</sup>**

<sup>1</sup>*Auditory Group, Institute of Neuroscience, Newcastle University, Newcastle upon Tyne, NE2 4HH, UK*

Voltage-dependent potassium channels ( $K_v$ ) play a key role in controlling the firing of neurons. Intracellular recordings *In Vitro* in the inferior colliculus (IC) show that a transient A-type current, associated with  $K_v1.4$  and the  $K_v4$  family, is only present in pause-build neurons, while onset cells display a high threshold  $K^+$  current characteristic of the  $K_v3$  family.

This correlation of firing pattern with  $K_v$  channels provides a link for understanding the relationship between the functional properties of the IC and its anatomical organisation. We have applied immunocytochemical labelling for  $K_v$  channel subtypes to explore how neurons with different response patterns might be distributed in the IC.

Fresh-frozen brain sections were collected from adult guinea pigs following perfusion under full terminal anaesthesia. Sections were fixed by immersion in paraformaldehyde.  $K_v4.2$  and  $K_v3.1b$  channel subunits were detected using monoclonal and polyclonal antibodies, and were visualized by means of fluorescent secondary antibodies.

Both antibodies produced a weak but consistent labelling of the neuropil in the IC, making it stand out from adjacent ventral structures. the staining was weaker in the more dorsomedial areas. This was most apparent in the case of anti- $K_v3.1b$ , which labelled discrete patches in the caudal and dorsomedial IC.

Some neurons also showed intense staining of the soma. Somas labelled with anti- $K_v3.1b$  were common in the IC, except laterally and dorsally. Anti- $K_v3.1$  also produced strong labelling of the proximal portions of neuronal processes. in the case of anti- $K_v4.2$ , fewer somas were labelled, and these were located mainly in the ventral part of the central nucleus of the IC. Some neurons expressed both  $K_v4.2$  and  $K_v3.1b$ .

The labelled  $K_v$  channels could account for the onset and pause-build firing patterns in the inferior colliculus, but other variants may also contribute to these responses.

Supported by the EPSRC.



### **323 Physiological Characteristics of the Rebound Following Membrane**

#### **Hyperpolarization in Neurons of the Rat's Dorsal Cortex of the Inferior Colliculus**

Hongyu Sun<sup>1</sup>, Shu Hui Wu<sup>1</sup>

<sup>1</sup>*Institute of Neuroscience, Carleton university, Ottawa, ON K1S 5B6 Canada*

The dorsal cortex of the inferior colliculus (ICD) is a major subdivision of the auditory midbrain tectum. It receives a substantial descending projection of fibers from the auditory cortex. There have been relatively few physiological studies of ICD neurons. Our previous results based on patch clamp recordings from ICD neurons in brain slices of young rats have shown that nearly 80% of the cells respond to depolarizing current injection with sustained firing which includes regular, adapting and buildup patterns. More than half (55%) of these sustained neurons exhibit a depolarizing rebound that follows hyperpolarizing current injection. the rebound can be observed in neurons with a regular or adapting firing pattern, but not in those with a buildup pattern. the rebound enhances, suppresses or has little effect on membrane excitability in different ICD neurons.

To understand further how the rebound is generated and how the rebound is affected by the magnitude and duration of membrane hyperpolarization, we made whole cell patch clamp recordings from 82 ICD neurons in brain slices of P10-19 rats. in 45/82 neurons, a rebound depolarization was elicited following hyperpolarization. One to several anode break action potentials could be generated from the rebound. Removal of extracellular  $\text{Ca}^{2+}$  totally eliminated the rebound. Application of  $\text{NiCl}_2$  (100  $\mu\text{M}$ ) reduced the rebound by about 80%. These results suggest that the rebound in ICD neurons is mediated by  $\text{Ca}^{2+}$  primarily through low-threshold T-type  $\text{Ca}^{2+}$  channels. Generation of the rebound and anode break spikes also depended on the magnitude and duration of membrane hyperpolarization. There was a trade off between magnitude and duration for generating the rebound. the rebound could be induced either by a larger and shorter hyperpolarization or a smaller and longer hyperpolarization. Usually a hyperpolarization of -15 to -20 mV for 100-200 ms was enough to generate a large rebound (~15 mV) and spikes. the results suggest that the rebound is one of the neuronal mechanisms for integrating excitatory inputs arriving soon after a period of synaptic inhibition.

Supported by NSERC of Canada

### **324 Proton-Induced Currents in Cultured Neurons of Rat Inferior Colliculus**

Min Zhang<sup>1</sup>, Neng Gong<sup>2</sup>, Guang-Hui Wang<sup>3</sup>, Tian-Le Xu<sup>2</sup>, Lin Chen<sup>1</sup>

<sup>1</sup>*Auditory Research Laboratory, School of Life Sciences, University of Science and Technology of China,* <sup>2</sup>*Institute of Neuroscience, Chinese Academy of Sciences,*

<sup>3</sup>*Laboratory for Neurodegenerative Diseases, University of Science and Technology of China*

Acid-sensing ionic channels (ASICs) are ligand-gated cation channels activated by extracellular protons and

widely distribute in the mammalian brain, the spinal cord and the periphery sensory organs. Abundant experimental evidence shows that ASICs play important roles in physiological/pathological conditions, such as sensory transduction, behavioral memory, retinal function, seizure and ischemia. in the auditory system, however, there are only few studies describing ASICs in hair cells, the spiral ganglion and the vestibular ganglion. in particular, functional ASICs have not been assessed in the central auditory region, although there is evidence to show their expression in the inferior colliculus (IC). in the present study, we first characterized ASIC-like currents in cultured IC neurons with whole-cell patch-clamp technique. an extracellular pH drop induced an amiloride-sensitive transient current in IC neurons with an activation threshold around pH 6.9 and a half activation pH of 5.92. the current was demonstrated to be mainly carried by  $\text{Na}^+$  and partly by  $\text{Ca}^{2+}$ . Extracellular  $\text{Ca}^{2+}$ ,  $\text{Pb}^{2+}$  and spider toxin PcTX1, a specific blocker for homomeric ASIC1a channels, could significantly reduce ASIC-like currents.  $\text{Zn}^{2+}$  could enhance but salicylate had no effects on pH 6.0-activated currents. These results suggest that ASIC-like currents in IC neurons appear to consist of the components generated by homomeric ASIC1a channels and ASIC2a-containing channels. We then demonstrated that ASICs could influence functional activities of IC neurons. Activation of ASICs by a pH drop could evoke neuronal firing in IC neurons. We suggest that ASICs may play a role in auditory information processing in the IC and are probably involved in some pathological processes, such as ischemia and auditory seizures. This work was supported by the National Natural Science Foundation of China (Grants 30270380 and 30470560), the National Basic Research Program of China (Grants 2006CB500803 and 2007CB512306) and the CAS Knowledge Innovation Project (Grant KSCX1-YW-R-36).

### **325 Gain Control by Local Circuits in the Inferior Colliculus**

Ying Xiao<sup>1</sup>, Shobhana Sivaramakrishnan<sup>1</sup>

<sup>1</sup>*Northeastern Ohio Universities College of Medicine*

in the inferior colliculus (IC), neuronal output gain changes in response to auditory input. Gain control is mediated by a changing excitatory-inhibitory balance, and *In Vitro* recordings suggest that much of this balance is achieved through the opposing effects of GABA-ergic inhibition and prolonged NMDA-mediated plateau potentials. the changing shape of synaptic potentials evoked by stimuli of different intensities *In Vitro* and changing response durations *In Vivo* suggests that output gain may be controlled by a secondary activation of local circuits following monosynaptic inputs to the IC from other auditory areas.

Here we use an *In Vitro* brain slice preparation of the IC to examine the control of neuronal gain by local circuits. Firing rates, evoked by stimulating ascending inputs through the lateral lemniscus, were measured before and after inactivation of local circuits, and in NMDA and GABAA receptor antagonists. in control conditions, firing rates increased monotonically with shock strength. When local circuit activity was blocked, the prolonged NMDA-

mediated plateau potentials observed in control conditions were greatly reduced in amplitude and duration, discharge rates were scaled down, and the slopes of the firing rate-depolarization function decreased threefold. Postsynaptic potentials which facilitated in control conditions exhibited synaptic depression in the absence of local circuit activation, and rate-depolarization functions became nonmonotonic. Further, the ratio of NMDA-mediated EPSCs to GABAA-mediated IPSCs decreased when local circuits were blocked. These results indicate that the strength of monosynaptic inputs to the IC through ascending lemniscal inputs is insufficient to counteract the large inhibitory drive that occurs during synaptic recruitment. Local circuits provide the excitatory multiplicative drive necessary to counteract inhibition as well as synaptic depression, and therefore widen the dynamic range of stimulus intensity.

Supported by NIDCD Grant R01DC0008120

### **[326] Time-Dependence of Ipsilateral Inhibition in the Rat's Central Nucleus of the Inferior Colliculus**

Huiming Zhang<sup>1</sup>, Jack Kelly<sup>2</sup>

<sup>1</sup>University of Windsor, Windsor, Ontario, Canada N9B 3P4, <sup>2</sup>Carleton University, Ottawa, Ontario, Canada K1S 5B6

Neurons in the central nucleus of the inferior colliculus (ICC) are sensitive to binaural cues as a result of receiving convergent excitatory and inhibitory inputs that are either monaural or binaural from both ipsilateral and contralateral brainstem auditory structures. In the rat's ICC, most neurons are excited by sounds presented to the contralateral ear and inhibited by sounds presented to the ipsilateral ear. As the excitatory and inhibitory inputs received by the ICC are associated with different neural pathways, and as these inputs are mediated by multiple neurotransmitter receptors with different time courses for activation and inactivation, it is likely that the relative strengths of responses to contralateral excitatory and ipsilateral inhibitory stimuli change over time after the onset of the sounds.

We studied temporal dynamics of excitatory/inhibitory binaural interactions in the ICC by recording responses from single neurons when the interaural-level difference, interaural-time difference, and duration of dichotic stimuli were systematically varied. We found that, for most neurons, the strength of ipsilateral inhibition was reduced after the initial period of the ipsilateral stimulus. Furthermore, inhibitory and/or excitatory responses were observed following the offset of the ipsilateral stimulus in most ICC neurons. The dynamic changes in inhibition and excitation during and after ipsilateral stimulation substantially altered the strength and temporal pattern of responses evoked by contralateral stimulation. This alteration would likely affect the ability to localize sounds in space as well as to recognize sound patterns under binaural stimulus conditions.

Supported by NSERC of Canada and the Hearing Foundation of Canada.

### **[327] Serotonin Levels in the Inferior Colliculus Vary with Behavioral State and Environmental Stimuli**

Ian Hall<sup>1</sup>, Laura M Hurley<sup>1</sup>

<sup>1</sup>Indiana University

Neuromodulation by serotonin plays an important role in the regulation of auditory processing. Although the effect of serotonin on evoked response properties in the inferior colliculus (IC) can be dramatic, little is known about how the level of this neuromodulator changes with behavior. Using voltammetry, a method of electrochemical measurement that allows us to assay extracellular serotonin and its metabolite in behaving animals, we investigated mechanisms that regulate the level of serotonin in the IC.

Serotonin is released by projections from the raphe nuclei whose activity is controlled by the 5-HT<sub>1A</sub> inhibitory autoreceptor. Blocking this autoreceptor with an IP injection of the 5-HT<sub>1A</sub> antagonist WAY100135 increased the level of serotonin, and activating this autoreceptor with the agonist 8-OH-DPAT decreased the level of serotonin. The serotonin reuptake inhibitor imipramine also increased the serotonin level. These results confirm that the amount of serotonin available to activate receptors in the IC is influenced by factors affecting both release and reuptake.

In addition to drugs, the firing patterns of serotonin-releasing neurons change with sleep state and in response to sensory stimuli. We tested two hypotheses based on this knowledge: (1) serotonin levels in the IC reflect the increased activity of serotonergic neurons in awake animals and (2) serotonin levels in the IC change in response to the sensory environment. Preliminary data shows that extracellular serotonin and its metabolite increase over the anesthetized-to-awake transition. Also, auditory and visual stimuli cause small but consistent increases in extracellular serotonin. That these different behavioral conditions are associated with increases in serotonin of different magnitudes suggests that neuromodulation by serotonin occurs in a graded fashion, so that serotonin acts as a rheostat rather than a binary signal in the IC.

### **[328] Topographic Differences in Acoustic Forward Masking Patterns in the Inferior Colliculus Central Nucleus (ICC) of the Guinea Pig**

Olga Stakhovskaya<sup>1</sup>, Matthew C Schoenecker<sup>1</sup>, Russell L Snyder<sup>1</sup>, Ben H Bonham<sup>1</sup>

<sup>1</sup>University of California San Francisco

Physiological studies of forward masking in the auditory nerve have suggested that adaptation that occurs during the masking stimulus is responsible for decreased response to the following probe stimulus, as well as for subsequent suppression of spontaneous activity. Because the level of adaptation is dependent upon the level of response, a corollary of this suggestion is that the best tone masker for activity evoked in any given auditory nerve fiber is a best frequency (BF) tone. It is often assumed

that this is also true of central auditory neurons, however, we have previously reported exceptions to this rule.

in this study, we examined the effects of variable forward masking tones on activity evoked by probe tones that were fixed in level and frequency. Activity was recorded at multiple ICC locations using 16- or 32-channel silicon arrays that were stereotactically inserted into the ICC along a trajectory roughly parallel to the tonotopic axis. the three-dimensional locations of the recording sites were documented and then correlated with their forward masking patterns.

Two general patterns of forward masking were observed, with distinct spatial distributions over planes parallel to isofrequency lamina in the ICC. in caudal ICC locations, probe tone responses were most strongly suppressed by near-BF masking tones regardless of probe frequency -- a masking pattern similar to that observed in the auditory nerve. However, at recording sites in rostral locations, masking was strongest when the frequency of the masker was near the frequency of the probe tone, rather than near the BF of the recording site. This indicates that representation of the sound at the level of the IC is complex and different from that observed in the auditory nerve, and is not homogeneous throughout the inferior colliculus.

Supported by NIDCD NO1-DC21006, NIDCD NO1-DC31006 and Hearing Research Inc.

### **329 Auditory Processing of Changing Sound Characteristics**

Claudia Bentancor<sup>1</sup>, Tamara Liberman<sup>2</sup>, Marisa Pedemonte<sup>3</sup>, **Ricardo A. Velluti<sup>4</sup>**, Ricardo A. Velluti<sup>2</sup>

<sup>1</sup>Facultad de Medicina Universidad de la República,

<sup>2</sup>Facultad de Medicina. Universidad de la República,

<sup>3</sup>Facultad de Medicina. Universidad CLAEH Punta del Este, <sup>4</sup>Facultad de Medicina Universidad de la República Montevideo, Uruguay

The auditory input is continuously changing. How the brain becomes aware of it is part of our questions. Many neuronal networks are involved in processing the differences introduced. We studied two particular processes: the pattern and firing shifts in response to natural call shifts and the relation of changing stimulation rate to hippocampal theta rhythm (Hipp  $\theta$ ). Guinea pigs auditory units were extracellularly recorded at the inferior colliculus central nucleus (ICc). the sound stimulation shifts were: a) pre-recorded guinea pig natural calls (700ms; 2s) played direct or inverted in time; b) pure tone-bursts presented with increasing and/or decreasing rates of sound recurrence. the guinea pigs were studied during wakefulness and sleep with implanted control electrodes.

-Shifts of the natural call stimulation. When the natural call was played backwards,-inverted in time, the neuronal firing changed its pattern and its firing number in waking and sleep. the ICc neuronal response was different when recorded during waking or sleep, i.e., the processing of complex sounds observed in wakefulness, although different, continues to be present in sleep.

-Changes of sound rate recurrence: temporal correlation between ICc unit firing and Hipp  $\theta$ . the cross-correlation

(CC) between an auditory unit and the Hipp  $\theta$  showed a temporal correlation (phase-locking) that appeared in 44% of the recorded units with increasing stimuli recurrence rate. When the stimuli rate was decreasing the phase-locking with Hipp  $\theta$  was 24%. When from some stimulating rate it decreased to silence, the spontaneous firing appeared phase-locked in 6% of the units. in all cases the CC were present during ~ 6s.

Shifts in the stimuli characteristics produce alterations in the processing revealed by auditory units firing rate/pattern and the unit/Hipp  $\theta$  phase-locking, in waking and sleep.

### **330 Local Circuits Shape Rate-Level Functions in the Inferior Colliculus**

**Jason Sanchez<sup>1</sup>**, Shobhana Sivaramakrishnan<sup>1</sup>

<sup>1</sup>Northeastern Ohio Universities College of Medicine

Neurons in the auditory system code a wide range of sound intensities. It is generally believed that a rate-level function (RLF) with a wide dynamic range is a function of high input convergence, but there is no direct evidence for a cause-and-effect relationship between input convergence and the dynamic range of sound intensity. Here we examine the respective roles of input convergence and local circuit activation in determining the dynamic range of sound intensity in the inferior colliculus (IC), where RLFs are monotonic, nonmonotonic or mixed, and dynamic ranges vary between ~20-90 dB SPL.

Neuronal firing rates at different sound intensities were measured extracellularly in the IC of awake mice, in control conditions and with local circuits blocked. RLFs that were monotonic in control conditions became nonmonotonic when local circuits were inactivated, and dynamic ranges narrowed from ~60-80 dB SPL to ~20-40 dB SPL. for neurons that exhibited nonmonotonic RLFs in control conditions, local circuit inactivation either had no effect on the RLF, or decreased overall firing rate without affecting RLF shape or dynamic range. First spike latencies were not affected when local circuits were inactivated.

Our results suggest that most but not all IC neurons are part of local circuits. the conversion of monotonic to nonmonotonic RLFs upon local circuit inactivation, and the lack of effect of local circuit inactivation on nonmonotonic RLFs, indicate that the input to IC neurons is nonmonotonic with increases in sound pressure level, and that those neurons that normally exhibit monotonic RLFs do so because of local circuit activation secondary to input convergence. We conclude that the activation of local circuits in the IC gives single neurons the ability to code a wide range of sound intensities, and further, that input convergence is necessary but not sufficient to widen the dynamic range of sound intensity.

Supported by NIDCD Grant R01 DC0008120

### **[331] Inhibition for Corticofugal Modulation of the Paradoxical Latency Shifts of Inferior Collicular Neurons**

**Xiaofeng Ma<sup>1</sup>, Nobuo Suga<sup>1</sup>**

<sup>1</sup>*Washington University in St. Louis*

The central auditory system creates various types of neurons tuned to different acoustic parameters other than a specific frequency. The response latency of sensory neurons typically shortens with an increase in stimulus intensity. However, ~10% of inferior collicular neurons of the big brown bat show a "paradoxical latency-shift (PLS)": shorter response latencies to weak sounds than to intense sounds. These neurons presumably play an important role in the processing of target distance information carried by a pair of the intense biosonar pulse and its echo (Sullivan 1982). In our current studies, we found that inhibition plays an important role in corticofugal modulation of collicular PLS neurons. Electrical stimulation of cortical auditory neurons evoked two types of changes in the PLS neurons, depending on the relationship in best frequency (BF) between the stimulated cortical and recorded collicular neurons. When the BF was matched between them, the cortical stimulation did not shift the BFs of the collicular neurons and shortened their response latencies at intense sounds, so that the PLS became smaller. When the BF was unmatched, however, the cortical stimulation shifted the BFs of the collicular neurons and lengthened their response latencies at intense sounds, so that the PLS became larger. We also found that wide spread inhibition plays an important role in the corticofugal modulation of response latencies. Our results indicate that the corticofugal feedback is involved in shaping the response properties, such as the spatio-temporal patterns of response, of subcortical auditory neurons through inhibition and facilitation not only in the frequency domain but also in the time domain. (supported by NIDCD research grant DC000175)

### **[332] Sound Level Processing in the Inferior Colliculus of Awake Bats is Modulated by Metabotropic Glutamate Receptors**

**Sergiy Voytenko<sup>1</sup>, Alexander Galazyuk<sup>1</sup>**

<sup>1</sup>*Northeastern Ohio Universities College of Medicine*

Temporally complex sounds such as speech, animal vocal communication calls and pulse-echo echolocating sequences involve a series of sound elements separated by short time intervals. Yet auditory neurons must still analyze these sounds in terms of frequency, amplitude, duration, direction, etc. Since it is well known that metabotropic glutamate receptors (mGluRs) are predominantly active at high rates of stimulation (i.e., short interstimulus intervals), we hypothesize that mGluRs contribute to the encoding of temporally complex sounds. In the present study we conducted extracellular recordings from inferior colliculus (IC) neurons in awake big brown bats. We developed a stimulus paradigm designed to activate mGluRs: a train of 10 sound pulses (tones or downward FM sweeps 4 ms duration each) was presented at the rate of 50Hz at fixed sound levels (50 – 60 dB SPL). A probe stimulus (the same as a pulse from the pulse train)

was presented 100 ms later. Sound level for this pulse was changed from 0 to 80 dB SPL. We then compared rate-level functions (RLF) of IC neurons to a single sound pulse presented alone and to the same pulse following a pulse train. A majority of IC neurons (86%) showed changes in the shape and/or the width of RLF when a single sound pulse was preceded by a pulse train. Such RLF changes could be blocked by iontophoretic application of specific mGluR antagonists. Antagonists for groups I and II but not group III mGluRs had the effect. Our data suggest that mGluRs play a role in processing of sound level in natural sounds where sound elements are separated by short time intervals.

Supported by NIH R01 DC00537.

### **[333] The Contribution of Onset and Sustained Activity in the Neuronal Code for Temporal Periodicity and Acoustic Envelope Shape**

**Yi Zheng<sup>1</sup>, Heather Read<sup>2</sup>, Monty Escabi<sup>1</sup>**

<sup>1</sup>*University of Connecticut, biomedical engineering,*

<sup>2</sup>*University of Connecticut, psychology*

Temporal modulations are an important attribute in many natural sounds including speech. Here we examined the neuronal representation for stimulus periodicity and envelope shape in the central nucleus of the inferior colliculus (ICC) of the anesthetized cat. Specifically we asked whether neurons in the auditory midbrain encode stimulus periodicity or whether they alternately encode the shape of the stimulus envelope in the temporal response pattern. To test this, we used sinusoidal amplitude modulated noise (SAMN, contains repetition and shape), period noise burst (PNB, contains repetition but no shape) and sine ramp noise (SRN, contains shape but no repetition) to examine how stimulus envelope shape and periodicity contribute to the neuronal representation. We developed a shuffled correlation technique that allows us to systematically characterize the temporal response pattern. Neuronal responses to SRN were characterized by onset and sustained response components. The shuffled correlation analysis for these two components showed that they are related to the PNB and SAMN response and consequently contribute to periodicity and envelope shape code, respectively. Conventional rate and synchrony-based analysis was also utilized, and the best modulation frequency for firing rate (rBMF) and synchronization (tBMF) were compared against each other and across SAMN and PNB. No relationship was found between PNB and SAMN. For PNB, the tBMF boundary of most neurons fell consistently around 200Hz, while its rBMF covered a wide frequency range. This result is consistent with the result from shuffled correlation, indicating the ability of repetition rate code is limited to ~200 Hz. Finally, neurons with sustained responses faithfully encode the envelope shape at low modulation frequencies while onset responses can accurately entrain to higher modulation frequencies. These results argue against conventional rate or synchrony based codes and provides two independent but complementary mechanisms by which ICC neurons simultaneously encode envelope

shape and repetition information in complex sounds. (supported by NIDCD R01DC006397-01A1).

### **334 Frequency Selectivity in Frog Auditory Midbrain is Altered by Reversible Unilateral Hearing Loss**

**David Gooler<sup>1</sup>**

<sup>1</sup>*University of Illinois*

Most neurophysiological studies of binaural hearing have focused on the importance of binaural integration to sound localization, but selectivity to sound features is also influenced by binaural interactions. In a previous study frequency selectivity and binaural response properties of neurons in the frog auditory midbrain were modified by acutely reversible, unilateral conductive hearing loss.

The present study addressed the effect of unilateral neural hearing loss on the response properties of neurons in the auditory midbrain. For this purpose, peripheral neural hearing loss was induced unilaterally using a cryoprobe to cool the auditory nerve and produce a reversible block of neural conduction. The advantage of this technique is that response properties of individual central auditory neurons may be evaluated before, during, and after temporary hearing loss.

The cryoprobe was constructed from a coaxial pair of syringe needles with a 250 µm silver wire forming the cooling tip of the probe. Cooled ethanol was pumped through the probe and its temperature monitored. Through a dorsal surgical approach the cryoprobe tip was positioned just above one auditory nerve and neural activity of auditory midbrain neurons contralateral to that nerve was recorded before, during, and after reversible unilateral hearing loss.

Auditory midbrain neurons revealed changes in frequency tuning properties as a result of temporary unilateral neural hearing loss. In some cases neurons that were not driven by acoustic stimulation of the ipsilateral ear became responsive during inactivation of the contralateral auditory nerve. Changes in frequency selectivity of binaural neurons often reflected differences in inhibitory properties from those determined under binaural, ipsilateral monaural, and contralateral monaural intact stimulation.

### **335 Audiological and Behavioral Phenotyping of Mutant Mice Missing the Inferior Colliculus**

**Simone Kurt<sup>1</sup>**, Kristina Vaupel<sup>2</sup>, Markus Moser<sup>2</sup>, Guenter Ehret<sup>1</sup>

<sup>1</sup>*University Ulm*, <sup>2</sup>*Max Planck Institute of Biochemistry, Martinsried*

A way of characterizing the function of brain structures is to generate mouse models with well defined genetic mutations of that structure and to compare the resulting phenotype with that of wild-type controls. Here we present data demonstrating audiological and behavioral phenotypes in mice with complete lack of the inferior colliculus. We recently have generated a mouse mutant of the transcription factor AP-2delta, which is exclusively expressed in the central nervous system. These animals

were kept in a 129Sv/C57BL/6 mixed background. Interestingly, gross anatomical inspection of H&E-stained brain sections revealed a complete lack of the auditory midbrain structure of the inferior colliculus. Despite this profound anatomical defect, AP-2delta deficient mice showed no obvious behavioral defect. We therefore tested the mutants in (a) electrophysiological audiometric measurements of auditory brainstem responses (ABR) and (b) behavioral performance in an auditory discrimination task (shuttle-box, pure tone discrimination, 7 vs. 12 kHz, 80 dB SPL).

The ABR-measurements showed no significant difference in absolute hearing thresholds across the whole hearing range (audiograms) of the mutant mice compared to wild-type controls. Nevertheless, in contrast to control animals, wave V of the ABR was missing in the mutants. In the pure tone discrimination task only subtle differences in the performance between the two groups could be found. In both mutant and wild-type, mice split into good (= fast learning and good discrimination performance after 15 days of training) and bad learners (slow learning and bad discrimination performance). For the good learners, there were no significant differences between mutants and wild-types, but for the bad learners, mutant mice reached a significantly lower discrimination performance than wild-types.

As we found only subtle differences between mutant and wild-type mice despite the large anatomical difference, we conclude from these results that substantial compensatory mechanisms must take place in the mutants during development, possibly a rewiring within the auditory pathway with restoration of inferior colliculus function at some adjacent auditory center.

### **336 Elevated Sound-Evoked Fmri Activation in the Auditory Midbrain of People with Tinnitus and Hyperacusis**

**Jianwen Gu<sup>1</sup>**, Chris Halpin<sup>2</sup>, Eui-Cheol Nam<sup>3</sup>, Robert Levine<sup>2</sup>, Jennifer Melcher<sup>2</sup>

<sup>1</sup>*Massachusetts Institute of Technology*, <sup>2</sup>*Massachusetts Eye and Ear Infirmary*, <sup>3</sup>*Kangwon National University*

Melcher et al. (*Int. Tinnitus Seminar*, 2005) demonstrated elevated sound-evoked activation in the inferior colliculi (IC) of normal hearing tinnitus subjects compared to audiometrically-matched controls without tinnitus. Here, we tested whether the elevated activation is associated with the low tolerance for high-level sound (hyperacusis) experienced by many people with tinnitus.

21 subjects with normal pure tone thresholds underwent behavioral tests followed by fMRI. Subjects were classified according to whether (1) they had tinnitus (10 of 21) and (2) they deemed continuous broadband noise (the stimulus used during fMRI) to be intolerably loud at levels above 90 dB SL. 10 of 21 (8 tinnitus, 2 non-tinnitus) were classified as having "low sound tolerance" by this criterion. 10 slices were imaged in a sparse paradigm to prevent the scanner acoustic noise from contaminating activation measurements. Sound levels were 50, 70, and 80 dB SPL.

A comparison of tinnitus and non-tinnitus subjects (regardless of sound tolerance) showed significantly

greater activation in the tinnitus group at 70 dB SPL (percent change (p.c.) = 1.3 for tinnitus, 1.0 for non-tinnitus;  $p < 0.04$ ), and the same trend at 80 dB SPL (p.c. = 1.3 for tinnitus, 1.1 for non-tinnitus;  $p < 0.1$ ). a comparison of subjects according to sound tolerance (regardless of tinnitus) showed a greater and far more significant difference. At 50, 70, and 80 dB, low sound tolerance subjects showed significantly greater activation (p.c. = 0.94, 1.4, 1.5, respectively) than subjects with high sound tolerance (p.c. = 0.53, 0.91, 1.1;  $p < 0.002$ , 0.00002, 0.007, respectively). a two-way ANOVA indicated a main effect of sound tolerance (50 dB SPL:  $p < 0.004$ , 70 dB SPL:  $p < 0.0004$ ) with no significant effect of tinnitus or interaction. These results suggest that reduced tolerance of high-level sound is associated with, and may arise from, elevated sound-evoked neural activity.

American Tinnitus Association, Tinnitus Research Initiative

### **337 Heterogeneous Short-Term Dynamics of Auditory Thalamocortical Synapses**

**Elliott Merriam<sup>1</sup>, Matthew Banks<sup>2</sup>**

<sup>1</sup>*Dept. of Anesthesiology, Clinical Neuroengineering Training Program, University of Wisconsin-Madison,*

<sup>2</sup>*Department of Anesthesiology, University of Wisconsin-Madison*

**Introduction:** Principal cells in primary auditory cortex (A1) *In Vivo* respond to acoustic stimuli in a manner distinct from their thalamic (MG) inputs. for example, the percentage of cells in A1 using temporal encoding versus rate coding differs from MG, as does the modulation frequency at which rate coding predominates. Short-term plasticity at thalamocortical synapses may contribute to this transformation of response properties. We characterized the short-term dynamics of single (minimally-evoked) thalamic inputs to single neurons in A1 *In Vitro*. **Methods:** Whole-cell recordings with K-gluconate in the patch pipette were obtained from LIII/IV neurons in thalamocortical slices from 2-4 wk CBA/J mice at 34°C. All cells were labeled with biocytin. Single thalamic fibers were activated with bipolar stimulating electrodes, and evoked EPSCs were recorded at a holding potential of -68 mV. Stimulation protocols consisted of single pulses delivered at <0.2 Hz, paired pulses delivered at <0.1 Hz, and pulse trains delivered at <0.033 Hz.

**Results:** Synaptic inputs from MG to A1 show heterogeneous responses to paired pulses, ranging from strong depression (paired-pulse ratio<0.5) to facilitation (paired-pulse ratio>1). Longer stimulus trains show depression after the second pulse, with the rate of depression, the amount of depression at steady state, and the rate of recovery varying across both synapses and stimulus frequencies.

**Conclusion:** Auditory thalamocortical synapses have heterogeneous short-term plasticity properties that might contribute to the thalamocortical transformations of sound representation observed *in vivo*. These data will be useful in future experiments that will use a dynamic clamp system to investigate cortical cells' responses to multiple thalamic spike-train inputs with realistic short-term dynamics.

Supported by NIH (DC006013-01), UW Dept. Anesthesiology. E.M. was supported by NIH (T90DK070079 and R90DK071515).

### **338 Salicylate-Induced Tinnitus: Spectral Changes in Spontaneous Ensemble Activity in Auditory Cortex of Awake Rats**

**Daniel Stolzberg<sup>1</sup>, Jianzhong Lu<sup>1</sup>, Winfried Schlee<sup>2</sup>, Nathan Weisz<sup>2</sup>, Wei Sun<sup>1</sup>, Richard Salvi<sup>1</sup>**

<sup>1</sup>*Center for Hearing and Deafness, University at Buffalo, State University of New York,* <sup>2</sup>*Department of Psychology, University of Konstanz, Germany*

Recent evidence suggests that alpha activity in the EEG directly or indirectly reflects inhibitory processes. When alpha activity is disrupted as a result of reduced thalamocortical afferent inputs such as that caused by peripheral hearing loss, a buildup of synchronous spontaneous neural activity occurs that can give rise to phantom perceptions such as tinnitus. to test this hypothesis, rats were treated with a high dose of salicylate known to produce behavioral evidence of tinnitus. We recorded the ensemble of spontaneous activity (ESA) from a gross electrode chronically implanted on the auditory cortex (AC) of adult rats. to avoid the confounding effects of anesthesia that can disrupt spontaneous and sound evoked neural activity, we recorded the ESA from awake, restrained rats that sat comfortably in a sound attenuating booth. ESA recordings were made before, immediately after and several days following a salicylate treatment (250 mg/kg) that consistently induces tinnitus-like behavior in rats. the ESA data were analyzed offline using wavelet analysis in order to quantify changes in the power spectrum of activity. Preliminary results show that at 1-h post-salicylate, there was a decrease in ESA power from 5-9 Hz (alpha band) and a concomitant increase in power from 15-40 Hz (gamma band). the salicylate-induced change in the ESA spectrum returned to the original baseline levels 1 to 2 days post-salicylate treatment. the changes in the ESA spectrum follow closely the time course for the onset and recovery of salicylate-induced tinnitus measured behaviorally. Supported in part by grant from the Tinnitus Research Consortium, American Tinnitus Association and NIH grant R01DC00909101.

### **339 Nicotine Enhanced Temporal Processing and Auditory Cortex Response**

**Wei Sun<sup>1</sup>, Jianzhong Lu<sup>1</sup>, Erin Landrie<sup>1</sup>**

<sup>1</sup>*University at Buffalo*

Auditory processing plays an important role in language and speech learning. Although central auditory processing disorders in children is one of the important factors leading to learning disabilities, the cause of auditory processing

disorder is not clear. Previous studies indicate that cigarette smoking during pregnancy affects the central nervous system development. Recent human subject studies found maternal smoking caused speech processing deficits in newborns. Animal studies found neonatal nicotine exposure (NNE) on baby rats induced auditory learning deficits when they became adults. To investigate the effect of NNE on temporal processing development and the role of nicotine receptors, we treated new born rats with high dose of nicotine (5 mg/kg, postnatal 8 to 12 days). Gap detection thresholds (GDT) were measured during P20 to P90 using the gap-induced pre-pulse inhibition of the acoustic startle response. Chronic electrodes were implanted into the auditory cortex (AC) of adult rats and sound evoked activities were measured from awake-rats to find the physiological change of the AC related to temporal processing deficits. NNE rats showed a longer GDT than non-nicotine treated rats after P45. An acute injection of nicotine (1 mg/kg) in adult rats induced a significant decrease of GDT and an enhanced AC response in NNE rats. However, the improvement of GDT and AC enhancement induced by nicotine injection only lasted several days. Our results showed NNE induced a temporal processing deficit. Acute nicotine exposure temporarily recovered the deficit presumably through increasing sound evoked AC activity.

Supported by NIH (R03 DC008685) and NOHR

### **340 Salicylate Increases the Gain of the Central Auditory System**

**Jianzhong LU<sup>1</sup>**, Daniel Stolzberg<sup>1</sup>, Edward Lobarinas<sup>1</sup>, Richard Salvi<sup>1</sup>, Wei Sun<sup>1</sup>

<sup>1</sup>University at Buffalo

There is growing evidence that the neural generator that gives rise to the phantom sound of tinnitus may reside in the central auditory system; however, the neurophysiological changes associated with tinnitus are not well understood. To investigate the peripheral and central changes, we treated rats with a high-dose of sodium salicylate that reliably induces tinnitus and hypersensitivity to sounds. Systemic injection of salicylate (250 mg/kg) induced a significant decrease in the amplitude and an increase in threshold of the cochlear compound action potential (CAP). Paradoxically, there was a striking increase in the amplitude of the sound-evoked local field potential from the auditory cortex (AC) of awake-rats. However, when rats were anesthetized with isoflurane, which presumably increases GABA activity, salicylate had little or no effect on AC responses. On the other hand, when rats were given ketamine (136 mg/kg), which blocks NMDA receptors, the salicylate-induced enhancement of the AC response was larger than observed with salicylate alone in conscious rats. When salicylate was applied directly to the round window (RW) of the cochlea of ketamine-acepromazine anesthetized rats, salicylate caused an increase in CAP threshold, a reduction in CAP amplitude and a reduction in AC response amplitude. These results suggest that the salicylate-induced enhancement of AC amplitude does not originate in cochlea, but may originate centrally possibly by down regulation of GABA mediated inhibition. To

determine if the enhancement of the AC response has a behavioral correlate, we measured pre-pulse inhibition (PPI) of the acoustical startle reflex (ASR). After salicylate injection, pre-pulse inhibition (PPI) of ASR significantly increased. This result links the salicylate-induced AC enhancement to behavioral hypersensitivity to sound (hyperacusis) reported by tinnitus patients.

Supported by Grants from the TRC and NIH (R03 DC008685, R01 DC00630, R01 DC009091)

### **341 Acoustic Trauma Induced Auditory Cortex Enhancement and Tinnitus**

**Erin Laundrie<sup>1</sup>**, Lu Jianzhong<sup>1</sup>, Daniel Stolzberg<sup>1</sup>, Edward Lobarinas<sup>1</sup>, Richard Salvi<sup>1</sup>, Wei Sun<sup>1</sup>

<sup>1</sup>University at Buffalo

There is growing evidence that noise-induced cochlear damage may lead to hyperactivity in the central auditory system (CAS) that may give rise to the phantom sound of tinnitus. However, the correlation between the time of onset of the neurophysiological changes in the CAS and behavioral or perceptual onset of tinnitus are not well understood. To investigate this relationship, we implanted chronic electrodes into the auditory cortex (AC) and measured sound evoked activity from awake-rats before and after acoustic overstimulation. The auditory brainstem response (ABR) was used to assess the degree of noise-induced hearing loss. Tinnitus was evaluated by measuring gap pre-pulse inhibition of the acoustic startle response (GPIAS). Rats were exposed monaurally to a high-intensity narrow band or broad band noise at level of 120 dB SPL. After the noise exposure, all the rats developed either permanent (>2 weeks) or temporary (<3 days) hearing loss in the exposed ear; ABR threshold were essentially unchanged in the non-exposed ear. In the rats that developed permanent hearing loss, AC amplitudes increased significantly 4 h after the noise exposure, whereas AC amplitude remained largely unchanged in rats that exhibited only temporary hearing loss. Most of the exposed rats also developed tinnitus-like behavior on GPIAS (decreased GPIAS) 4 h after the noise exposure. Importantly, the post-exposure AC enhancement showed a positive correlation with the amount of hearing loss. However, the onset of tinnitus-like behavior and the onset of AC enhancement did not show a strong correlation.

Supported by grants from the Tinnitus Research Consortium and NIH (R03 DC008685, R01 DC00630, R01 DC009091)

### **342 The Maturation of the Intrinsic and Synaptic Properties of L2/3 Pyramidal Neurons in Primary Auditory Cortex**

**Anne-Marie M. Oswald<sup>1</sup>**, Alex D. Reyes<sup>1</sup>

<sup>1</sup>Center for Neural Science, New York University

We investigated the age dependence of pyramidal cell circuits in L2/3 of primary auditory cortex (AI) in juvenile mice from postnatal day 14 (P14) to P29. In order to characterize the connection architecture, intrinsic and synaptic properties of PCs, we performed simultaneous whole-cell recordings from up to 4 PCs in a thalamocortical



slice preparation. We found that the connections between PCs were highly localized. the probability of connection declined with distance between PC somas but did not vary with age. We then characterized the developmental timeline for the intrinsic and synaptic properties of PCs. At P19, there was a dramatic change in the intrinsic properties of PCs that lead to an overall decrease in neural excitability in older animals. However, no further changes in the intrinsic neural properties occurred between P19 and P29 suggestive of a stable mature state. Likewise, the majority of synapses showed age dependent decreases in synaptic decays and short-term synaptic depression that reached steady state levels by P19. Finally, we show that synaptic decay and short-term synaptic plasticity combine to produce differential synaptic responses that may contribute to differences in auditory processing in young versus older animals. Our results suggest there is a transition in the intrinsic and synaptic properties of L2/3 PCs at P19 that may be indicative of maturation in cortical networks.

Funding: AMO: Robert Leet and Clara Guthrie Patterson Trust Postdoctoral Fellowship in Brain Circuitry; AD: NIH DC005787-01A1

### **343 Development of FM Coding in Chinchilla Auditory Cortex**

**Trecia Brown<sup>1</sup>**, Robert V. Harrison<sup>2</sup>

<sup>1</sup>*Department of Physiology, University of Toronto, Toronto,*

<sup>2</sup>*Departments of Physiology and Otolaryngology - Head & Neck Surgery, University of Toronto, Toronto*

The auditory system has evolved to enable a representation of the external acoustic environment within the brain and to process and interpret a broad variety of environmental sounds. to date, studies on the development of the auditory cortex have primarily focused on the responses to simple tones during maturation and the effects of tonal stimuli on cortical organization. Complex stimuli, such as frequency-modulated (FM) tones, can also be used to further investigate system behaviour. As part of an overall developmental study of FM coding at the cortical level, we have characterized the responses in neurons of the chinchilla auditory cortex using FM stimulation. Anesthetised chinchillas from 4 age groups (P3, P14, P28 and adult) were stimulated monaurally with bidirectional linear FM sweeps (range: 100 Hz - 20 kHz; rates: 0.05-3.28 kHz/ms) presented in the right ear. Responses were obtained from contralateral unit recordings made in the exposed left auditory cortex of each animal. Results from 340 cortical microelectrode penetrations were used for subsequent analysis. Preliminary results indicate that units which demonstrate a strong preference for FM direction (24% of total sampled units) prefer upward FM sweeps. the range of response latencies of these upward FM units was observed to decrease with age (15-40 ms in P3 and P14 groups, 10-30 ms in the P28 group and 10-20 ms in the adult group). the fastest sweep rate (3.28 kHz/ms) was the preferred rate in all age groups with adults showing the strongest preference (45% of sampled units) compared to the other groups (< 25% of sampled units). We hypothesize that these observed preferences for FM direction and sweep

rate are related to early post-natal exposure to a particular acoustic environment. in future, we intend to test this hypothesis by rearing animals in a variety of acoustically modified environments and comparing FM preferences of such animals to the results of our present reference data.

### **344 Mapping the Functional Anatomy of the Neural Network Involved in Tone Detection**

**Kevin Donaldson<sup>1</sup>**, Jonathan Fritz<sup>1</sup>, Shihab Shamma<sup>1</sup>, Elizabeth Quinlan<sup>1</sup>

<sup>1</sup>*University of Maryland, College Park*

Cortical receptive fields are shaped by experience and can be rapidly modulated by the demands of sensory discrimination tasks. We have previously shown that receptive fields in the auditory cortex dynamically change during performance of a tone detection task to enhance response to the target tone frequency (Fritz et al., 2003) and proposed that prefrontal cortex may play a pivotal role in mediating these effects (Fritz et al., 2007). a recent study using immediate early gene (IEG) expression mapping of brain activation during auditory task performance in a positive reinforcement paradigm confirmed activation of both auditory and prefrontal cortices (Bajo et al., 2007). the goal of the present study was to develop a parallel rodent behavioral model system, and use a similar IEG mapping approach to characterize the neural network involved in tone detection. We trained Sprague-Dawley rats, using a conditioned avoidance behavioral paradigm to detect random pure tones from a series of broadband noise stimuli (Fritz et al., 2003). Trained rats learned to perform the tone detection task to behavioral criterion within a week. Experimental control rats were habituated to the training apparatus, and randomly presented with auditory stimuli with no task contingencies. Having successfully trained 4 rats on the random tone detection task, we can now compare the regions of the rodent brain that are activated by the acoustic stimuli using c-fos expression in a behavioral and a non-behavioral context. We will describe the whole brain pattern of c-fos activation in three different experimental groups: sound exposure only in naïve control rats, sound exposure while licking water in naïve control rats and in task performance conditions in trained rats. Mapping of the functional network activated during tone detection will provide the basis for future molecular and physiological studies of auditory behavior using the rodent model system.

### **345 Neural Circuit for Non-Specific Plasticity of Cortical Auditory Neurons Elicited by Pseudoconditioning (Working Hypothesis)**

**Nobuo Suga<sup>1</sup>**, Weiqing Ji<sup>1</sup>

<sup>1</sup>*Washington University in St. Louis*

Conditioning (CS-US), a conditioning tonal stimulus (CS) paired with an unconditioned leg-stimulus (US), evokes tone-specific plastic changes, represented by best frequency (BF) shifts, in the central auditory system, whereas pseudoconditioning, the CS unpaired with the

US, evokes non-specific plastic changes, represented by general augmentation (or sensitization). How can the central auditory system show such dramatically different changes for the CS which is identical in all acoustic properties, but only different by whether it is paired or unpaired? This is neurophysiologically quite an interesting and important question. So, Suga hypothesized (2007) that the CS excites the neural net in the primary auditory cortex and corticofugal feedback loops and elicits a small short-lasting BF shift regardless of whether it is paired or unpaired with the US; that when the delivery of the US to the animal is randomized in time, the response of MGBm neurons to the regularly delivered CS shows little habituation; that the CS unpaired with the US evokes a small short-lasting general augmentation in the auditory cortex by activating the multisensory thalamic nuclei such as the MGBm; and that small general augmentation in the auditory cortex evoked by the multisensory thalamic nuclei is augmented by a non-cholinergic neuromodulator system; and that there are neural mechanisms for selective augmentation of general augmentation or BF shifts. the MGBm is involved in evoking a small short-lasting general augmentation, whereas the MGBv is involved in evoking a small short-lasting BF shift. This hypothesis states only a part of the neural circuit for the general augmentation. It should be noted that the general augmentation occurs in the subcortical auditory nuclei. the Weinberger model states that the MGBm evokes a small BF shift in the auditory cortex only when the CS and US are associated in the MGBm. This model is incorrect in terms of recent neurophysiological findings.

Supported by NIDCD DC000175

### **[346] Non-Specific Plasticity of Cortical Auditory Neurons Elicited by Pseudoconditioning Depends On Neither the Cholinergic Neuromodulator Nor the Activity of the Somatosensory Cortex**

**Wei Qing Ji<sup>1</sup>, Nobuo Suga<sup>1</sup>**

<sup>1</sup>*Washington University in St. Louis*

The response properties of neurons in the auditory system change according to conditioning, pseudoconditioning, etc. the neural circuit for non-specific plasticity (general augmentation or sensitization) elicited by pseudoconditioning must be different from that for tone-specific plasticity (BF shifts) elicited by fear conditioning. We have explored the neural circuit for tone-specific plasticity and have been exploring the neural circuit for non-specific plasticity. in our current study on the big brown bat, we examined changes in the response properties of 71 neurons in the primary auditory cortex elicited by pseudoconditioning: a conditioning tonal stimulus (CS) unpaired with an unconditioned leg-stimulus (US). We found that the unpaired CS-US elicited (1) a heart-rate decrease to tones in a wide range of frequencies; (2) an increase in the auditory response over many different frequencies accompanied with or without an increase in the background discharge; (3) a broadening of frequency-tuning curves; (4) a decrease in the minimum threshold; and (5) a small short-lasting centripetal BF shift

only when the BF of a recorded neuron was 5 kHz higher than the frequency of the CS. a muscarinic cholinergic receptor antagonist, atropine, and a nicotinic cholinergic receptor antagonist, mecamylamine, applied to the auditory cortex had no effect on the development of the general augmentation, but abolished the development of the small short-lasting BF shift. a GABA-A receptor agonist, muscimol, bilaterally applied to the somatosensory cortex (SI) had no effect on general augmentation, but blocked the small short-lasting BF shift. Our current results indicate that the development of non-specific plasticity elicited by pseudoconditioning does not depend on the cholinergic neuromodulator, but the development of tone-specific plasticity elicited by fear conditioning does, and that the SI is not involved in evoking the general augmentation, but in evoking the BF shift.

Supported by NIDCD DC000175

### **[347] Thalamocortical Connections Indicate Multiple Tonotopic Representations in the Ventral Division of the Medial Geniculate Body in the Rabbit**

**Farhad Ardeshtirpour<sup>1</sup>, Douglas C. Fitzpatrick<sup>1</sup>**

<sup>1</sup>*Department of Otolaryngology, University of North Carolina at Chapel Hill School of Medicine*

Each level of the auditory system has a systematic representation of frequency. At the level of the central nucleus of the inferior colliculus (ICc) there is a single tonotopic representation. in contrast, in the auditory cortex there are multiple areas that each contains a separate tonotopic representation. This transformation from a single tonotopic representation to multiple tonotopic representations may occur at the cortical level or at the level of the auditory thalamus. We have chosen to study this question through injections of a bidirectional tracer in two tonotopic areas in the rabbit. the rabbit represents an attractive animal model because the ventral division of the medial geniculate body (MGBv) is a continuous structure throughout the rostrocaudal extent of the MGB that can be readily identified histologically by staining for the presence of calcium binding proteins. in nine rabbits, we injected a tracer, biotinylated dextran amine (BDA), into the primary auditory cortex (AI) or the dorsal anterior region of the cortex (DA). Each injection site was characterized physiologically in unanesthetized rabbits during chronic recording sessions conducted over several months. Injections were made in low (< 1.5 kHz) or high frequency regions of each cortical area. the MGBv was identified with immunocytochemistry for the calcium binding protein parvalbumin. Adjacent sections stained for parvalbumin or BDA were photographed and superimposed so that the BDA labeled cells could be plotted in relation to the parvalbumin staining. the labeled cells from each area showed some overlap with that from the other, but the main labeling from each area was in a distinct part of the MGBv that was separated rostrocaudally. These results suggest that there are at least two tonotopic mappings in the thalamus. Thus, the main transformation from the single

tonotopic map in the ICc to multiple maps in the cortex occurs first in the thalamus.

### **348 Comparison of Primary and Secondary Auditory Fields in Macaques**

**Michael Brosch<sup>1</sup>**, Henning Scheich<sup>1</sup>, Elena Selezneva<sup>1</sup>, Eike Budinger<sup>1</sup>

<sup>1</sup>*Leibniz Institut fuer Neurobiologie*

In the present work we compared various properties of two auditory cortical fields that are considered to be hierarchically related, namely the primary auditory cortical field AI and the caudomedial belt area CM. We analyzed data that we have obtained in our laboratory over the last decade from 10 longtail macaques. In these experiments we assessed (1) neuronal responses to single tones, tone sequences, and click trains (2) cyto- fiber- and chemo-architectural features, and (3) neuronal firing while monkeys performed an auditory categorization task. We found that the two fields had largely overlapping response properties for simple acoustical stimuli. In a best-frequency matched sample of AI and CM, we found similar receptive field bandwidths, first-spike latencies, and rate and temporal modulation transfer functions. Also the two fields had similar sensitivities for the size and direction of frequency steps and their temporal separation. The two fields, however, differed with regard to the time course of these responses, which were more complex and longer lasting in CM than in AI, with regard to neuronal synchronization patterns and that during task performance, task- and decision-related tonic firing was observed in CM only. AI and CM were also different with respect to the laminar patterning of cell bodies, myelinated fibers, parvalbumin-positive neurons, and with respect to the patterns of intrinsic connections. Our results suggest that AI and CM are largely similar with respect to the sound features they represent but that they differ with respect to how the neurons in the two fields encode these features, how the features the neurons respond to are combined, and how non-auditory information affects the two fields during tasks. In conclusion our results challenge the suggestion of hierarchical processing relationships in auditory cortex, at least between areas AI and CM.

### **349 Increased Activity of the Auditory Cortex in a Deaf-Blind Long-Term Cochlear Implant User**

**Yasuhiro Osaki<sup>1</sup>**, Hiroshi Nishimura<sup>1</sup>, Katsumi Doi<sup>1</sup>, Keisuke Enomoto<sup>1</sup>, Takako Iwaki<sup>1</sup>, Yasuyuki Kimura<sup>1</sup>, Katsufumi Kajimoto<sup>1</sup>, Naohiko Oku<sup>1</sup>, Jun Hatazawa<sup>1</sup>, Takeshi Kubo<sup>1</sup>

<sup>1</sup>*Osaka University Graduate School of Medicine*

We previously reported a deaf-blind patient who lost his vision and hearing simultaneously due to meningitis, and regained his hearing by means of a cochlear implant (CI). This patient continued to use the CI for three years, and his listening ability improved gradually. In this study we examined the neural activity of this patient while listening to spoken words (Auditory condition), reading tactile language (Tactile condition), and lying quietly (Resting condition) by means of H<sub>2</sub><sup>15</sup>O PET. We also compared the

results to those of the previous study, which was conducted within 1 year after the surgery. Results from six normal subjects under the same task stimuli were also taken into consideration. Activations of the superior and middle temporal gyri, which were observed in the previous study and in the normal subjects, were also found in this study. Their areas increased bilaterally after the continuous use of the CI, suggesting the recovery of the central auditory system. The occipital cortices of both sides, which were suppressed during the A and T conditions of the previous study, were also deactivated in this study. These results were similar to those of the normal subjects, but were opposite to those of the blind patients studied by other groups. Deaf-blindness with a CI might be a different situation from blindness alone, and a different therapeutic approach might be required for their rehabilitation.

### **350 Differential Effects of Deafening On Dendritic Spine Formation in Pyramidal and Non-Pyramidal Neurons in the Rat Auditory Cortex**

**Scott Schachtele<sup>1</sup>**, Joe Losh<sup>1</sup>, Michael E Dailey<sup>1</sup>, Steven H Green<sup>1</sup>

<sup>1</sup>*University of Iowa*

Pyramidal neurons in cortical layers 2/3 and 5 of the rat auditory cortex rapidly develop dendritic spines, the primary location of excitatory synapses in the central nervous system, between the ages of postnatal day (P)11 and P21. This increase in spine density correlates temporally with both the establishment of mature auditory hair cell thresholds and hearing-evoked activity in central auditory neurons. However, the timing and extent of spine formation in layers 2/3 and 5 pyramidal neurons appears to be an intrinsic property of the brain, independent of auditory input because deafening has no effect on dendritic branching, spine density, spine morphology or occupancy of spines by presynaptic terminals in these neurons in P21 or P42 rats. Layer 4 of the auditory cortex is the recipient of direct projections from the medial geniculate nucleus of the thalamus. We next asked whether dendritic development and dendritic spine formation on layer 4 neurons is susceptible to loss of auditory input (ie, deafening)? We used the lipophilic dye 1,1'-dioctadecyl-3,3,3',3'-tetramethylindocarbocyanine perchlorate (DiI) to label individual neurons in vibratome slices from rat brains fixed in situ. We assessed dendritic and spine morphology separately in layer 4 pyramidal neuron basal and apical dendrites and in non-pyramidal neurons. We used P4, P9, P11, P14, P19, P21 and P21 rats, allowing determination of dendritic and spine morphology from P4, prior to hearing onset, through P21 when hearing is nearly mature. Deafening did not affect elaboration of dendritic branching nor did deafening affect spine morphology in layer 4 neurons. However, there was a significantly increased spine density in deafened rats at P16 and P21 in dendrites of layer 4 non-pyramidal neurons. Dendritic spine density on layer 4 pyramidal neurons, as in layers 2/3 and 5 pyramidal neurons was unaffected by deafening. These data reveal cell-specific

structural effects of sensory deprivation on neuronal development and synaptogenesis in the auditory cortex.

### **351 Hearing Loss Disrupts the Maturation of GABA<sub>A</sub> Receptor $\alpha$ 1 Subunits in the Auditory Cortex**

Vibhakar Kotak<sup>1</sup>, Anne Takesian<sup>1</sup>, Dan Sanes<sup>1</sup>

<sup>1</sup>New York University

Developmental sensorineural loss (SNHL) triggers robust homeostatic adjustments in the supragranular laminae of the gerbil auditory cortex that include an escalation in membrane excitability, heightened glutamatergic activity from the thalamus, and decreased intracortical inhibition. Here, we asked whether decreased GABAergic IPSPs were linked with modification of the  $\alpha$ 1 subunit, a key site of benzodiazepine modulation. SNHL was induced at P10 and zolpidem ( $\alpha$ 1 subunit-specific agonist, 100 nM) was applied to assess the kinetics of spontaneous (s) IPSCs in the thalamoreceptive L2/3 pyramidal neurons 6-9 days after SNHL. Whole-cell voltage-clamp recording were made in the presence of ionotropic glutamate receptor blockers, at a holding potential of -60 mV with high chloride and QX-314 in the internal solution. Zolpidem prolonged sIPSC durations in control neurons, but not in SNHL neurons (control sIPSC durations, mean ms  $\pm$  SEM: before zolpidem, 69  $\pm$  4 vs. after zolpidem, 114  $\pm$  10;  $t=5.6$ ;  $df=9$ ,  $p=0.003$ ; SNHL sIPSC durations before zolpidem, 94  $\pm$  6 vs. after zolpidem, 102  $\pm$  7,  $t=0.8$ ,  $df=9$ ,  $p=0.4$ ). Comparisons of mean sIPSC durations revealed no significant difference between SNHL and pre-hearing (P8-10) neurons, while the control sIPSC duration differed significantly from both groups. (ANOVA,  $F=15.2$ ,  $df=27$ ; sIPSCs durations, mean ms  $\pm$  SEM: pre-hearing, 90.4  $\pm$  6.5 vs. SNHL, 89  $\pm$  4,  $t=0.2$ ,  $df=17$ ,  $p=0.8$ ; pre-hearing, 90.4  $\pm$  6.5 vs. control, 59  $\pm$  3.8;  $t=4.1$ ,  $df=17$ ,  $p=0.0005$ ). This effect was independent of the amplitudes of sIPSCs (ANOVA,  $F=0.2$ ,  $df=20$ ,  $p=0.8$ ). to test whether the reduced sensitivity of the SNHL sIPSCs to the  $\alpha$ 1 subunit agonist mirrors an immature state, the effect of zolpidem was assessed in pre-hearing neurons. Similar to SNHL sIPSCs, pre-hearing sIPSCs displayed no difference in durations after zolpidem treatment ( $t=0.2$ ,  $df=7$ ,  $p=0.8$ ). These results suggest that hearing experience is required for the proper expression of  $\alpha$ 1 subunits at inhibitory synapses in the auditory cortex. (Supported by NIDCD 006864 DHS and VCK.)

### **352 Disruption of Balanced Cortical Excitation and Inhibition by Acoustic Trauma.**

Mike Wehr<sup>1</sup>, Ben Scholl<sup>1</sup>

<sup>1</sup>University of Oregon

Acoustic trauma produces rapid shifts in the frequency response areas of neurons in primary auditory cortex, but the synaptic mechanisms underlying these changes remain unknown. the rapidity of these shifts has led to the suggestion that subthreshold inputs may be unmasked by a selective loss of inhibition. We used *In Vivo* whole cell recordings to directly measure tone-evoked excitatory and inhibitory synaptic inputs in auditory cortical neurons

before and after acoustic trauma. Here we report that acute acoustic trauma disrupted the balance of excitation and inhibition by selectively increasing and reducing the strength of inhibition at different frequencies within the frequency response area. Inhibition was abolished for low frequency stimuli, but was markedly enhanced for high frequency stimuli. These changes led to an expansion of receptive fields towards low frequencies, but not by a simple unmasking process. Rather, membrane potential responses were delayed and prolonged throughout the receptive field, by distinct interactions between synaptic excitation and inhibition. These results demonstrate that the rapid changes caused by acoustic trauma are due to distinct mechanisms at different frequencies within the frequency response area, which depend on differential disruption of excitation and inhibition.

### **353 Experience-Dependent Plasticity of Binaural Interactions in the Primary Auditory Cortex**

Maria Popescu<sup>1</sup>, Daniel Polley<sup>1</sup>

<sup>1</sup>Vanderbilt University Medical School and the Vanderbilt Kennedy Center for Human Development

The functional properties of neural circuits in the primary auditory cortex (A1) are shaped by experience-dependent plasticity processes. Plasticity can promote improved auditory performance, as in the case of auditory perceptual learning, or degraded auditory performance, as exemplified by the effects of auditory deprivation in early life. We have begun to explore the neural and perceptual consequences of auditory deprivation using a rat model for unilateral conductive hearing loss (UHL). UHL was achieved through surgical ligation of the external auditory meatus for a 60 day period beginning on postnatal day 14. ABR analysis was used to confirm that sound levels reaching the deprived ear were attenuated by approximately 50 dB for frequencies above 8 kHz and that these effects were reversible when the ligation was surgically removed prior to neurophysiological recording. UHL was found to disrupt the tonotopic map in A1 contralateral to the deprived ear such that low frequency sounds (1-8 kHz) that were comparatively less attenuated by the ligation were represented over a larger cortical area than maps derived from sham-operated age-matched controls. Tonal receptive fields derived from stimuli delivered to the ipsilateral and contralateral ears were used to calculate a monaural dominance index (MDI), which assigns a value ranging from -1 (completely ipsilateral dominance) to 1 (complete contralateral dominance) according to the quality of tuning to each input source. Compared to sham controls, the MDI was significantly shifted towards negative values in the UHL rats, indicating that many neurons had become preferentially tuned to the developmentally unobstructed ipsilateral ear. Subsequent analysis revealed that this was attributable both to a potentiation of the ipsilateral inputs and a suppression of the normally dominant contralateral inputs. Binaural receptive fields within A1 were also delineated using dichotic stimuli that varied according to interaural level difference (ILD) or interaural time difference (ITD). Although experience-dependent changes

in ILD and ITD tuning were observed, the specific form of these changes did not exactly conform to changes predicted from a model based upon the attenuation and temporal delay of the acoustic signal reaching the deprived cochlea. Ongoing experiments are exploring the effects of UCHL on the neurophysiological responses in A1 in the awake rat and relating these effects to psychophysical discrimination and detection thresholds.

### **354 Intrinsic Projections of Auditory Cortex**

**Kexin Yuan<sup>1</sup>, Christoph Schreiner<sup>1</sup>, Jeffery Winer<sup>2</sup>**

<sup>1</sup>University of California at San Francisco, <sup>2</sup>University of California at Berkeley

About 15-25% of auditory cortex (AC) neurons use gamma-aminobutyric acid (GABA). the projections of these cells are thought to be local from physiological and anatomical studies, but their precise extent and laminar origins are unknown. We investigated the projections of putative primary AC (A1) interneurons with a retrograde tracer (wheat germ apo-HRP conjugated to gold [WAHG]) and the Ca<sup>2+</sup> binding protein, parvalbumin (Pv) as a marker for some GABAergic neurons. We injected 69 nl of WAHG in adult rats, perfused them after a 2-3 day survival and cut sections 30-40 µm thick and processed them for WAHG, Pv, and for colocalization. Single- and double-labeled neurons were plotted in AC and the medial geniculate body (MG) using bright- or darkfield optics. We found that >90% of Pv-WAHG-labeled AC cells were <500 µm from the edge of the deposit in 3 experiments with injections that spanned the pia to the depth of layer VI in A1. All AC layers except layer I contained Pv-WAHG cells. the AC labeling was symmetrical about the dorsal and ventral axes of the deposit and similar in all experiments. the farthest double labeled cell was 1.2 mm away. Thus, in physiologically unguided deposits, the global distribution of Pv-WAHG cells was similar in each case in A1. a positive control was the WAHG-only MG labeling, which was in predicted topographic ventral division loci. a second control was the many WAHG-only AC cells retrogradely labeled up to 6 mm from the deposit sites. AC Pv+ neurons thus serve a local role exclusively which may be parallel to that of the abundant WAHG-only neurons with local axons. We thank Ms. Katie Dorsch and Ms. Anja Dorn for assistance.

Supported by USPHS grants R01 DC02260 (C.E.S.) and DC02319 (J.A.W.).

### **355 Acetylcholine Increases Time-Locking Without Increasing S/N Ratio in *In Vivo* Recordings From the Primary Auditory Cortex of the Anesthetized Rat**

**Justin Nichols<sup>1</sup>, Bryan Roof<sup>1</sup>, Humberto Salgado<sup>1</sup>, Vikram Jakkamsetti<sup>1</sup>, Michael Kilgard<sup>1</sup>, Marco Atzori<sup>1</sup>**

<sup>1</sup>UTD

Acetylcholine is known to greatly affect the excitability of the auditory cortex. From *In Vitro* studies it is known that, at the cellular level, two effects are detectable: an increase in single-cell excitability and a depression of neurotransmitter release. Consequently, acetylcholine increases simultaneously excitation and inhibition. the net

effect of acetylcholine depends on the potency and kinetics of its action on excitatory and inhibitory signals during the presentation of auditory stimuli. We wanted to test the common tenet that the activation of cholinergic receptors increases the S/N ratio.

In order to do so we studied the effect of local applications of carbachol on the auditory responses to trains of broad-band clicks in a ketamine or pentobarbital anesthetized rat preparation. Auditory responses to clicks were studied in control, after the application of a physiological solution alone, or containing increasing concentrations of carbachol.

We found that application of carbachol consistently produced a dose-dependent increase in background spontaneous activity, and a generalized increase in the response to all the stimuli in the click train without increasing the S/N ratio. Carbachol also induced an increase in the firing rate inhibition after the initial burst following the first stimulus in a click train at 12 Hz, partly supporting the S/N ratio increase hypothesis, but had the opposite effect at 5 Hz. Importantly, application of carbachol could better maintain phase locking throughout the entire click train, at all tested frequencies.

We conclude that the net effect of the local activation of cholinergic receptors in the auditory cortex is a generalized increase in the amplitude of the responses without a parallel increase in the S/N, due to the large increase in background firing frequency. This is associated with more effective time-locking of the response to the stimuli.

### **356 Serotonin Modulation of Excitability in the Auditory Cortex Following Sensorineural Hearing Loss**

**Deepti Rao<sup>1</sup>, Gregory Basura<sup>2</sup>, Paul Manis<sup>3</sup>**

<sup>1</sup>Dept. Cell and Molecular Physiology, UNC Chapel Hill,

<sup>2</sup>Dept. Otolaryngology/Head and Neck Surgery, UNC Chapel Hill, <sup>3</sup>Depts. Cell and Molecular Physiology, and Otolaryngology/Head and Neck Surgery, UNC Chapel Hill

Damage to the cochlea or the auditory nerve accounts for 90% of all hearing loss in humans. Brainstem and cortical neurons of animals subjected to hearing loss during development show increased intrinsic excitability. Increased excitability might stem from an effect of hearing loss on serotonin inputs to these neurons, since serotonin can modulate the intrinsic excitability of neurons, and auditory cortex (A1) receives serotonergic inputs early in development. to address whether hearing loss affects the excitability of cortical neurons by affecting serotonin inputs, we pursued three questions: Does serotonin affect excitability in normal A1 neurons? Which serotonin receptors affect excitability? is serotonin-regulated excitability affected by hearing loss?

To assess excitability in A1 neurons we measured firing rate, input resistance (R<sub>in</sub>) and resting membrane potential (RMP) in brain slices from normal 2-3 week old rats using whole cell current-clamp. We applied serotonin (50µM) to neurons and found a decrease in firing rate and R<sub>in</sub> while RMP did not change. to determine which serotonin receptors caused these changes, we used 1µM

ketanserin, a 5HT<sub>2</sub> receptor specific antagonist, during serotonin application. Ketanserin did not block the effect of serotonin on R<sub>in</sub>, but it did block the effect of serotonin on the firing rate. This result suggests two effects of serotonin mediated by different receptors. to study whether serotonin regulation of excitability is altered by hearing loss, we performed bilateral cochlear ablations in 8 day-old rats and raised them for 13 days. in these animals, unlike those with normal hearing, the firing rate, R<sub>in</sub> and RMP of A1 neurons were unaffected by serotonin.

Our results show that serotonin decreases the intrinsic excitability of normal A1 neurons, and that the effects of serotonin involve at least two kinds of receptors. We also find that hearing loss decreases serotonin's effect on excitability.

(Supported by a grant from the Deafness Research Foundation to GB.)

### **[357] Age-Related Changes in the Auditory Physiology of the Fischer 344 Rat**

**Eric Bielefeld<sup>1</sup>**, Donald Coling<sup>1</sup>, Guang-di Chen<sup>1</sup>, Man-na Li<sup>1</sup>, Chiemi Tanaka<sup>1</sup>, Donald Henderson<sup>1</sup>

<sup>1</sup>SUNY at Buffalo

The nature of the age-related hearing loss in the Fischer 344 (F344) rat has been the subject of ongoing investigation for several years. the current studies were undertaken to explore the possible sites of damage at the cochlear level and examine the impact of age on the F344 rat's auditory physiology. the ABR shift begins at 12 months, and by 24 months, there is a 60 dB threshold shift at 40 kHz and a 20 dB loss at 5 kHz. DPOAE amplitudes were depressed in the older (12-24 months) rats. Input-output functions of the compound action potential (CAP) were also depressed across frequency. Evaluation of the endocochlear potential revealed it to be in the 90-100 mV range in the 3 month old rats. All but one of the 24 month old rats' EP was in the +75-85 mV range. Tympanometry revealed Type a tympanograms with peak pressure and peak compliance measures the same in both the young and older rats. the findings suggest cochlear impairment led by damage to the outer hair cells, with secondary influences from damaged stria vascularis and inner hair and/or spiral ganglion cells. Anatomical and biochemical investigations into the nature of cochlear damage are ongoing.

[Research supported by grant #1R01DC00686201A1]

### **[358] Lipoic Acid Rescued DBA Mice From Age-Related Hearing Impairment**

**Joong Ho Ahn<sup>1</sup>**, Hun Hee Kang<sup>2</sup>, Hyun Joon Shim<sup>3</sup>, Jong Woo Chung<sup>1</sup>

<sup>1</sup>Asan Medical Center, <sup>2</sup>Asan Institute for Life Sciences,

<sup>3</sup>Eulji Hospital

**Backgrounds:** Oxidative stress is a pervasive factor in aging and reactive oxygen species (ROS) have been implicated as causative factors in cochlear pathology. Lipoic acid is a sulphur-containing anti-oxidant and is known to have a capability of scavenging ROS.

**Objectives:** the purpose of this study was to prove the effect of lipoic acid in hearing preservation of DBA mice in age-related hearing impairment.

**Materials and Methods:** We fed DBA mice with 0.5% alpha-lipoic acid dissolved in normal saline daily. Total 49 DBA mice were enrolled in this study and they were divided into 4 groups; 2-week, 4-week, and 8-week groups which were fed with lipoic acid from 2-weeks, 4-weeks, and 8-weeks respectively. Mice in control group were not fed with lipoic acid from their birth. We measured the hearing threshold at 4, 8, 16, 32 kHz every week.

**Results:** After 12-week intake of lipoic acid, there were significant hearing decreases in all frequencies, especially in 32 kHz, in control group. the hearing thresholds in all frequencies were preserved in 2- and 4-week group, while hearing thresholds at 8 and 16 kHz were slightly decreased in 8-week group. in immunohistochemical studies, the manifestation of 9-oxoG residues in DNA and 1-cys peroxiredoxin increased more distinctly in the cochlea of mice fed with lipoic acid than in the cochlea of control group.

**Conclusion:** From these results, we could suggest that lipoic acid rescued the hearing of DBA mice from early onset hearing impairment.

### **[359] Evidence for Increased NADPH-Diaphorase-Positive Neurons in the Central Auditory System of the Aged Rat**

**Seung Geun Yeo<sup>1</sup>**, Seok Min Hong<sup>1</sup>, Chang Il Cha<sup>1</sup>, Hyun Joon Shim<sup>2</sup>, Dong Choon Park<sup>3</sup>

<sup>1</sup>Kyung Hee University, <sup>2</sup>Eulji University, <sup>3</sup>Catholic University, Suwon, Korea

**Objectives:** Although NO has been associated with aging, it is unclear whether specific areas of the central auditory system are involved. We therefore assayed aging-related changes in NADPH-d, a selective histochemical marker for NO, in the neurons of the central auditory system and other brain regions.

**Methods:** the numbers of NADPH-d stained neurons and the area and staining density of cell bodies were examined in aged (24 month old) and younger (4 month old) Wistar rats. **Results:** the number of NADPH-d positive neurons in the inferior colliculus was significantly increased in aged rats (p<0.05), whereas the area of NADPH-d positive neurons in all areas did not differ significantly between aged and younger rats (p>0.05). the staining densities of NADPH-d positive neurons in the inferior colliculus, the auditory cortex, and the visual cortex were significantly greater in aged compared with younger rats (p<0.05).

**Conclusions:** the age-related increase in the production of NO suggests that this increase was related to neuron aging and the presbycusis. Additional studies may provide information regarding aging-related changes in the central auditory system.

**Key words:** Nicotinamide adenine dinucleotide phosphate, Aging, Auditory cortex, Cochlear nucleus, Inferior colliculus

**360 Increased Glutamic Acid Decarboxylase in the Auditory Brainstem is Associated with Functional Declines in the Auditory Efferent Feedback System in Tamoxifen-Treated Mice**

Olga Vasilyeva<sup>1</sup>, Xiaoxia Zhu<sup>1</sup>, Daniel Olney<sup>1</sup>, Scott Thompson<sup>1</sup>, Robert Frisina<sup>1</sup>

<sup>1</sup>Univ. Rochester Medical School

The influences of sex hormones on auditory function and aging are controversial. Recently, we reported that blockage of estrogen receptors in young adult female CBA mice negatively affects contralateral suppression (SC) of distortion product otoacoustic emissions (DPOAEs) [Thompson et al., *Otolaryngology- Head & Neck Surgery*. 135:100-105, 2006]. However, the exact mechanism of how estrogen suppression affects the peripheral or central auditory systems is unclear. the primary aim of the present study was to determine neurochemical changes in central auditory regions in mice that had undergone estrogen blockade with tamoxifen - the most commonly used clinical selective estrogen receptor modulator. to accomplish this, the brains were harvested from female CBA mice that underwent 120 days of estrogen receptor blockade: subcutaneous tamoxifen pellet treatment (2x60 day release); age-matched controls received placebo pellets. Brains were harvested from 4 groups of mice: 1) Placebo (5-6 months old, n=4); 2) Tamoxifen (no recovery, 5-6 months old, n=4); 3) Placebo (12 months recovery, 18 months old, n=4); 4) Tamoxifen (12 months recovery, 18 months old, n=4). Brain sections were immunoassayed with anti-glutamic acid decarboxylase antibody (GAD; 1:5000). Relative optical density (ROD) was examined in the superior olivary complex (SOC) and inferior colliculus (IC) to determine GAD expression. Images of these regions were captured under the same optical conditions across animals, and analyzed by using Image Pro Plus (version 5.0). We found that the tamoxifen (no recovery, 5-6 months old) group showed *higher expression* of GAD in the IC, which *significantly declined* after 12 months of recovery. Thus, our results indicate that upregulation of GAD expression in the IC temporally corresponds to efferent feedback decline in estrogen-suppressed animals. More detailed analysis of IC regions is required to obtain more information on precise mechanisms of neurotransmitter changes and auditory feedback deficits in mice undergoing estrogen-suppression therapies.

[Supported by NIH grants: NIA P01 AG09524, NIDCD P30 DC05409; and the International Center for Hearing & Speech Res., Rochester NY, USA]

**361 Estrogen Blockade Impairs Auditory Efferent Feedback Function in Adult Female CBA/Caj Mice**

Xiaoxia Zhu<sup>1</sup>, Scott Thompson<sup>1</sup>, Daniel Olney<sup>1</sup>, Robert Frisina<sup>1</sup>

<sup>1</sup>Univ. Rochester Medical School

Sex hormones can have significant impacts on sensory processing, including age changes that occur in the peripheral and central auditory systems. the present longitudinal study examined the effects of estrogen

suppression on age-related changes in auditory brainstem responses (ABRs), distortion product otoacoustic emissions (DPOAEs) and contralateral suppression (CS) of DPOAEs. Female young adult CBA/Caj mice (6 wk old) were implanted with slow-release, tamoxifen pellets subcutaneously. Tamoxifen is the most commonly used clinical selective estrogen receptor modulator. After 60 days of treatment, these mice displayed an early decrease of CS, (Thompson et al., *Otolaryngology- Head & Neck Surgery*. 135: 100-105, 2006). the present report gives results of this longitudinal study, after the mice stopped the tamoxifen treatments (total treatment duration: 120 days), for a period of 1-year post-treatment. the main discovery is the occurrence of a recovery of CS of DPOAEs upon termination of the tamoxifen treatment. the DPOAE amplitudes and ABRs thresholds were also tracked, and showed predictable age-related deficits with age. Conclusion: Estrogen appears to play an important role in maintaining normal functionality of the auditory efferent feedback (medial olivocochlear bundle) system as animals age.

[Supported by NIH: NIA, NIDCD, and the Int. Ctr. Hearing Speech Res., Rochester, NY, USA]

**362 Aging Affects Nonlinear Features of Post-Excitatory Suppression in the Mouse**

W. Owen Brimijoin<sup>1</sup>, Joseph Walton<sup>1</sup>

<sup>1</sup>University of Rochester

Previously, we reported that post-excitatory suppression (PES) in the inferior colliculus (IC) of the CBA mouse can have two major nonlinear properties: frequency specificity and independence from prior excitation. the frequency specificity of PES manifests itself in a tendency for responses to tones at the edge of the excitatory response area to be preferentially suppressed by preceding tones similar in frequency. Independence from excitation occurs when the excitatory portion of a response to a tone is suppressed by preceding tones but the inhibitory portion that follows is not eliminated. the study reported here compares these nonlinear response properties in young and old CBA mice. Recordings of single-unit and multi-unit clusters were made in the IC in response to a tonal DeBrujin sequence using a 16 channel Michigan Probe. the sequence was centered at the neuron's best excitatory frequency at 30-50 dB above threshold. It was comprised of an equal number of each of 9 tone frequencies and included an equal number of each possible subsequence of 2, 3, and 4 tones. Tone-triggered averaging was used to create spectrotemporal response maps, which displayed excitatory and inhibitory responses to each tone frequency. Excitatory responses were followed by suppression in ~90% of young units and ~76% in old units. Tone-pair-triggered averaging was used to measure responses to each tone pair. the analysis revealed two findings: 1) in old units, the frequency-specificity of PES was reduced relative to young units. 2) in ~60% of young units, suppression following excitatory tones persisted when the excitatory portion of the response had been masked by a previous tone. in the old CBA mouse, this percentage was reduced to ~39%. These findings argue that the nonlinear features of PES, presumably critical in



processing complex sound, are strongly affected by aging. Research supported by NIH/NIA grant PO1 AG09524 and NIDCD P30 grant DC05409

### **363 Neural Correlates of Age-Related Declines in Frequency Selectivity in the Auditory Midbrain**

**U-Cheng Leong<sup>1</sup>, Kathy Barsz<sup>1</sup>, Paul Allen<sup>1</sup>, Joseph Walton<sup>1</sup>**

<sup>1</sup>*University of Rochester*

Impaired frequency selectivity is associated with an age-related decline in speech recognition in background noise and reverberated environments, even in elderly listeners with normal hearing. In order to elucidate the neural correlates of age-related alteration in frequency selectivity, we examined the excitatory frequency response areas (FRAs) of multi-unit clusters in the inferior colliculus (IC) of young (<4 months of age), middle-aged (12-24 months of age), and old (>24 months of age) CBA mice. FRAs were elicited by tone bursts of 25-ms in duration with 5-ms rise/fall times. Each of the 2125 frequency by intensity combinations (2 to 64 kHz in 500 Hz steps, 0 to 80 dB SPL in 5 dB steps) was presented 5 times randomly at a rate of 4/s through a speaker placed at 60° contralateral from the recording site. The FRAs were classified into V-shape, primary-like, multipeak, and closed/complex responses. The rate level functions (RLF) were derived from FRAs at characteristic frequency (CF). In old mice, we found a decrease in the proportion of neurons with high CF (>30 kHz) and in the number of closed/complex FRAs. Intensity coding was also affected by age, as shown in the increase of monotonic RLFs in middle-aged and old animals. In addition to a mild threshold elevation (<15 dB in middle-aged mice, <25 dB in old mice), FRAs from both age groups were broader and more asymmetric in shape as compared to units from young mice. While the decline in estimated spontaneous rate and low-level subthreshold activity began in middle age, reduced driven rates at suprathreshold levels occurred only in units from old mice. This is the first study that reports age-related declines in the neural representation of frequency selectivity as early as middle-age when there is minimal hearing loss involved. These age-related central changes may contribute to more complex sound processing, such as extracting signals in background noise, a major problem found in elderly listeners.

### **364 Far-Field Auditory Evoked Responses to Amplitude Modulated Noise Young and Aged Mice**

**David A. Eddins<sup>1</sup>, Arie Gordin<sup>1</sup>, William O. Brimijoin<sup>1</sup>, Joseph P. Walton<sup>1</sup>**

<sup>1</sup>*Department of Otolaryngology, University of Rochester*

Age-related changes in auditory temporal processing have been documented using a variety of auditory measures. In an effort to identify the mechanisms underlying such age-related changes, a number of comparative models have been used. One of the substantial challenges of such work is that measures of temporal processing in different species often involve different stimuli, presentation

paradigms, and measurement techniques. This is the first in a series of studies designed to mediate these challenges by using identical stimuli, presentation paradigms, and recording techniques in human and animal subjects. The goals of this project were to determine the feasibility of far-field late auditory evoked potential (LAEP) measurements in CBA mice using an acoustic change paradigm successfully implemented with humans, to identify potential differences in the effects of two sedatives, and to identify any age-related changes in auditory temporal processing in the CBA mouse. In the first experiment, late auditory evoked potentials (LAEPs) were obtained in 3 groups of 5 young sedated mice using Avertin® (200 µg/kg), ketamine/xylocaine (120 mg/kg ketamine and 10 mg/kg xylocaine), or chlorprothixene (2.5-6 g/kg). No significant drug effects ( $p > 0.05$ ) were observed. In the second experiment, 8 young (2-5 months) and 8 old (24-27 months) CBA mice were sedated with the ketamine/xylocaine combination. Stimuli were broadband noise bursts 400 ms in duration, the second half of which was 100% sinusoidally amplitude modulated (SAM) at a rates from 20 to 400 Hz presented at 60 to 70 dB SPL. LAEPs included an N1-P2 response to burst onset, N1-P2 response to SAM onset, and an amplitude modulation following response. Significant age effects were observed for all three responses, providing the first evidence of age-related declines in temporal processing using far-field LAEPs in mice. Supported by NIH NIA P01 AG09524, NIDCD P30 DC05409, and the Int. Ctr. Hearing & Speech Res.

### **365 Response to Sweeping Frequency Changes in the CBA/Caj Mouse Model of Presbycusis**

**Paul Allen<sup>1</sup>, Nathaniel Housel<sup>1</sup>, Stephanie Yee<sup>1</sup>, Colleen Zenczak<sup>1</sup>, James Ison<sup>1</sup>**

<sup>1</sup>*University of Rochester*

Speech communication depends on the ability to encode the spectrotemporal patterning of sounds and degradation of this ability with age may contribute to the problems of speech perception common in the elderly with presbycusis. Temporal processing deficits analogous to those seen in elderly humans have been demonstrated in the CBA/Caj mouse model of presbycusis and this study extends these results with a preliminary investigation of spectrotemporal processing in young ( $n=8$ , 3mo) and old mice ( $n=7$ , 22mo).

We use prepulse inhibition (PPI) of the acoustic startle response in a behavioral assessment of the ability of these mice to detect and respond to a change in the frequency of an otherwise continuous 70dB SPL pure tone. The change in frequency is produced by a linear frequency sweep of duration  $dt$  connecting two tone segments ( $f_1$ ,  $f_2$ ). This sweep and frequency change provide the 'prepulse' that is delivered prior to the startle eliciting stimulus by a controlled interstimulus interval (ISI).

In experiment 1, in 3 testing sessions for each young mouse  $df$ ,  $dt$ , and ISI were parametrically varied. With  $dt=20ms$ ,  $df=+/-0.5$  octave, PPI increases with ISI to 100ms then decreases. The magnitude of PPI to Down

sweeps is more than twice that for Up sweeps, and more than 3x for ISI=20ms. Similarly for  $df=\pm 0.5$  octave, ISI=100ms, and  $dt=10, 20, 40$ , and 80ms, Down sweeps produced nearly 3x the level of PPI as Up sweeps. Lastly, with  $dt=20$ ms, ISI=100ms, sweeps of 0.1 and 1 octaves produced equivalent PPI (Down trending larger), while 0.5 octave Down sweeps produced nearly twice the PPI of Up sweeps.

Experiment 2, used the same young mice in a single session with  $dt=20$ ms, ISI=100ms,  $df=0.5$  octave, but  $f1=8, 11, 16, 22$ , or 32 kHz. All sweeps produced significant PPI, but Down sweeps produced more PPI for  $f1=16, 22$ kHz, less for 8kHz, and equivalent for 11 and 32 kHz.

in Experiment 3 the Old mice performed the last session of Exp1. They had slightly less PPI for all Up sweeps than did young mice, but PPI for Down sweeps was more than halved for each of the  $df$  compared to the young, and the PPI produced by the 0.1 octave Down sweep was not significantly different from zero.

Other authors have reported a preference for Up sweeps in human psychoacoustics, animal behavior and physiology. the Down preference seen here for young mice may originate in basilar membrane masking patterns owing to the presence of the continuous  $f1$  prior to the sweep. the age effect seen here is not well accounted for by a simple peripheral explanation, and might arise from central changes in frequency coding with age.

### **[366] Affects of Caloric Restriction and Every Other Day Feeding On Presbycusis in a Mouse Model**

Jennifer L Parrish<sup>1</sup>, Michael S Bonkowski<sup>1</sup>, Larry F Hughes<sup>1</sup>, andrzej Bartke<sup>1</sup>, **Jeremy G Turner<sup>1</sup>**

<sup>1</sup>SIU School of Medicine

Age-related hearing loss, presbycusis, is characterized by a progressive, severe sensorineural hearing loss. Presbycusis is one of the most common problems affecting the elderly population. in addition to peripheral hearing loss, presbycusis is associated with age-related changes to the brain that have been linked to a decline in temporal processing impacting speech perception and understanding. Calorie restriction has been found to help extend longevity in organisms from yeast to mammals (including mice). This dietary regimen is considered a "gold standard" in longevity research and has been shown to either delay or ablate the onset of many age-associated diseases. the current study addressed whether daily calorie restriction and/or every other day ad libitum (AL) feeding could alter the development of presbycusis in the mouse. Female and male mice were reared for approximately 2 years with a diet of either AL food access, 30% daily calorie restriction (CR), or every other day (EOD) AL feeding. Prepulse inhibition was used to assess hearing function at 12, 18 and 24 months of age. Prepulse inhibition testing was conducted using frequencies of 4, 8, 16 and 32 kHz at intensities of 30, 45, 60 and 75 dB SPL to construct a behavioral audiogram. Both males and females developed behavioral evidence of age-related hearing loss by 24 months. Diet interacted significantly with age and gender. While in males, CR and EOD

appeared to hasten presbycusis, females benefited from both CR and EOD, showing improved behavioral evidence of hearing in old age compared to ad libitum fed mice. These studies provide evidence of a sexually dimorphic response of CR and EOD dietary regimens on presbycusis in the mouse.

### **[367] A Cross-Sectional Study of Age-Related Changes in Temporal Gap Detection**

**Robert C. Nutt<sup>1</sup>**, D. Robert Frisina<sup>1</sup>, David A. Eddins<sup>2</sup>

<sup>1</sup>International Center for Hearing & Speech Research, Rochester Institute of Technology, <sup>2</sup>Department of Otolaryngology, University of Rochester School of Medicine & Dentistry

Previous research has revealed declines in various measures of auditory temporal processing with increasing age in adult human and corresponding animal models of aging. Here we report the results of a screening test of auditory temporal processing for 1132 human listeners between the ages of 18 and 97 years. the test was part of a large-scale, cross-sectional study of age-related hearing loss that included measures of pure tone threshold, speech perception in quiet and noise, spatial release from masking, and oto-acoustic emissions. the detection of silent gaps embedded in low-pass (1010 Hz and 4010 Hz) noise bursts was measured in a two-interval, two-alternative, forced-choice paradigm. Gap stimuli were presented at an overall level of 70 dB SPL in a continuous broadband (10,000 Hz) noise background (50 dB SPL). the signal stimulus had a pre-gap duration of 40 ms and a post-gap duration of 100 ms. Two threshold estimates were obtained for each low-pass condition. When categorized by age in decades beginning with the range 18 to 27 years, temporal gap detection thresholds declined with age at a rate of approximately 10% per decade in the 1010 Hz low-pass condition and approximately 20% per decade in the 4010 Hz condition. Pure tone thresholds also increased with age, raising the possibility that the age-related increase in gap detection threshold may be related to decreasing audibility with age. Partial correlations indicated no significant correlation between pure tone and gap detection thresholds when controlling for age, whereas there was a highly significant but relatively weak correlation between age and gap thresholds when controlling for pure tone thresholds. to identify the possible relations among the various auditory measures collected, a series of multivariate statistical analyses will be reported. *Supported by NIH NIA P01 AG09524, NIDCD P30 DC05409, and the International Center for Hearing & Speech Research.*

### **[368] Attention Influences Sensory Integration for Postural Control in Older Adults**

**Mark Redfern<sup>1</sup>**, Martijn Muller<sup>2</sup>, Richard Jennings<sup>1</sup>

<sup>1</sup>University of Pittsburgh, <sup>2</sup>University of Michigan

Attention has been shown to have an influence on standing balance and gait, particularly in older adults and patients with vestibular disorders. We investigated the role of attention in the integration of sensory information

for standing balance in young and older adults. We used a dual-task paradigm, combining postural challenge and information processing tasks. Subjects included 24 older adults (74 +/- 4.3 s.d) and 22 young adults (26 +/- 3.8 s.d), all of whom were healthy with normal vestibular testing. the postural tasks were the six dynamic posturography conditions on a Neurocom Equitest platform performed for a duration of 120 s each. the information processing tasks were a visual choice reaction time (CRT) task and an auditory CRT. the CRT tasks were performed concurrent with the postural tasks, and seated as a control. of particular interest in this study was the effect of postural condition on reaction times. Results showed increases in both auditory and visual CRTs during increasing postural challenge for both young and older adults. When normalized by seated RTs, no age effect was evident. Sway referencing the posture platform was associated with increased RT for both the auditory and visual CRT. Sway referencing the scene caused greater increases in auditory CRTs than in visual CRTs. This study is further evidence that sensory integration during postural control differentially affects attention allocation to vision and hearing. However, this effect was the same for young and older adults. We propose that postural tasks that engage vision (such as in eyes open or visual sway referencing) focus attention on the visual stream and away from the auditory stream, as seen in the increased auditory CRTs for visually challenging postural conditions.

Supported by NIH grants AG14116, AG024827, and DC05205

### **[369] Envelope of Bandpass Filtered Harmonic Tones Alters Tone Height and Neuromagnetic Pitch Response**

**Steffen Ritter**<sup>1</sup>, Hans Guenter Dosch<sup>2</sup>, Hans-Joachim Specht<sup>3</sup>, andré Rupp<sup>1</sup>

<sup>1</sup>Section of Biomagnetism, Dept of Neurology, University Hospital Heidelberg, <sup>2</sup>Institute for Theoretical Physics, University of Heidelberg, <sup>3</sup>Institute of Physics, University of Heidelberg

The neuromagnetic pitch response, a component of the N100-complex, can be isolated by using a continuous auditory stimulation with abrupt pitch changes. in a combined magnetoencephalographic (MEG) and psychoacoustic experiment, we investigated the influence of the envelope of a bandpass filter on the latency of the pitch response and on the perceived tone height. Harmonic complex tones containing either even or odd multiples of the fundamental frequency ( $f_0$ ) were alternated to evoke a pitch change. Tones with two different fundamental frequencies and two widely different central frequencies were applied. Three different bandpass envelopes were tested. Our results approve the relation between perceived tone height and latency if  $f_0$  is varied and the spectral envelope is identical: an increase of the pitch and, correspondingly, of the perceived tone height leads to a decrease of the latency. We also confirm our recent finding that with a fixed  $f_0$  and an increase of the center frequency the latency increases but the perceived tone height increases, too. a reduction of the number of

harmonics also leads to an increase of the latency. Only complete cancellation of harmonics causes this effect, whereas attenuating the harmonics (in bandpass envelopes with rounded corners) has no influence, neither on the latency nor on the perceived tone height.

These results corroborate our conjecture that there is no simple relation between perceived tone height and latency of the pitch response and that also the pitch saliency of the tone is relevant. Reducing the saliency either by increasing the central frequency or by completely eliminating harmonic components causes an increase of the latency.

### **[370] Increased Fmri Responses to Sound in the Inferior Colliculus and Medial Geniculate Body in Patients with Unilateral Tinnitus**

**Cris Lanting**<sup>1</sup>, Emile de Kleine<sup>1</sup>, Pim van Dijk<sup>1</sup>

<sup>1</sup>Dpt. of Otorhinolaryngology, University Medical Center Groningen, the Netherlands

**Objective.** Determine tinnitus related neural activity in the central auditory system of unilateral tinnitus subjects, using fMRI.

**Methods.** Twelve patients with unilateral tinnitus (6 left-sided) and 16 controls without tinnitus were subjected to functional MRI of the central auditory system. All subjects had no or minor hearing deficits in both ears. Experiments were performed on a 3T Philips Intera scanner, using sparse sampling (TR=10 s). Data were acquired of the complete auditory pathway (CN, SOC, IC, MG and auditory cortex) using a resolution of  $2 \times 2 \times 2 \text{ mm}^3$ . Stimuli consisted of right and left ear stimulation with levels of 40 and 70 dB (SPL) of rippled broadband noise. After realignment and normalization to a standard brain template, multiple linear regression was performed using SPM5 in order to identify the response of the brain to the sound stimuli. by a region-of-interest analysis a mean percent signal change was obtained for each stimulus, using the ten percent of the voxels that responded most strongly for each nucleus. in addition, a group analysis was performed on a voxel by voxel basis.

**Results.** We did not observe a difference between tinnitus patients and controls in the fMRI response of the auditory cortex. However there were differences in the medial geniculate body and the inferior colliculus. the responses to stimuli in these nuclei were higher in patients than controls. There was no significant difference in the superior olivary complex and cochlear nucleus between groups. In addition, a difference was observed in the lateral part of the cerebellum in patients. This area responded to sound in left-sided tinnitus patients and not in control subjects.

**Conclusion.** Neural correlates of tinnitus were identified and located in the auditory pathway and in the cerebellum. a larger response was measured, which is in agreement with the hypothesis of a loss of inhibition in the auditory pathway of tinnitus patients.

### **[371] The Effect of Pleasant and Unpleasant Sounding Music in Persons with Hearing Loss and Tinnitus: and Fmri Study**

Nathan Pajor<sup>1</sup>, Barry Horwitz<sup>1</sup>, Fatima Husain<sup>1</sup>

<sup>1</sup>NIDCD/NIH

We studied auditory processing in persons with bilateral hearing loss and tinnitus (TIN) and in persons with normal hearing without tinnitus (NV). to examine group differences in the neural bases of auditory processing as related to emotion, we employed music stimuli that could be classified as either pleasant (consonant) or unpleasant (dissonant) (Blood, et al, Nat. Neurosci., 1999). in a preliminary study, 4 TIN and 4 NV subjects were scanned using an EPI clustered acquisition paradigm in a 3T GE scanner. Subjects listened to 6s of the stimulus, followed by a 3s response period during which the stimuli were rated as pleasant/unpleasant, then a 2s single volume acquisition. the task trials were presented in pseudo-random order with rest trials interspersed. Image volumes were realigned, normalized into standard stereotactic space and smoothed. Multisubject fixed effects analysis was performed in SPM5 with a threshold of  $p < 0.001$  uncorrected. the 2 groups did not differ in their behavioral responses. the average BOLD response for the processing of consonant stimuli produced greater activation than the processing of dissonant stimuli for both groups. for the NV group the consonant greater than dissonant contrast showed activations in the right insula, middle frontal gyrus and dorsolateral frontal gyrus (DMFG). the opposite contrast showed activation only in the left insula. Previous studies have implicated the insula in music processing. for the TIN group, there was no activation in the insula for either contrast. the consonant greater than dissonant contrast showed activations in the nucleus accumbens/putamen, the temporal pole and DMFG. the nucleus accumbens is part of the limbic system and is involved in emotion processing. These preliminary results suggest that although the NV and TIN groups did not differ behaviorally, they invoked different brain regions when responding to emotional auditory stimuli.

Supported by the NIDCD IRP and the Tinnitus Research Consortium

### **[372] Neural Source Configurations of Surface Electric Potentials Elicited by Rapidly Presented Tones in Children, Adolescents, and Adults.**

Elyse Sussman<sup>1</sup>, Mitchell Steinschneider<sup>1</sup>, Valia Gumenyuk<sup>1</sup>, Julia Grushko<sup>1</sup>, Laura Staffaroni<sup>1</sup>, Katharine Lawson<sup>1</sup>

<sup>1</sup>Albert Einstein College of Medicine

Processing rapidly changing acoustic information is fundamental to speech, language, and music perception. Cortical auditory evoked potentials (CAEPs) in children have most often been studied in paradigms using long inter-stimulus intervals (ISIs), which improves signal-to-noise interactions, but does not provide insight into CAEP component development when elicited by stimulus rates commonly encountered in the environment. the present study presented a sequence of pure tone stimuli at four

levels of ISI in children between the ages of 8-11 years, in adolescents, and in young adults. Multiple complementary measures were used to assess effects of maturation and stimulus rate on the obligatory CAEPs. Global field power (GFP) was used to identify the components. an index of global dissimilarity provided a comparison of underlying generator configuration of the CAEP components, along with current source density (CSD) topographic maps computed from the mean amplitude waveforms corresponding to the peak latencies defined by the GFP. the GFP peaks identified P1, P2, and N2 components at the longest rate tested but only P1 and N2 at the shortest rate, in all age groups younger than adult. GFP did not identify activity of the lateral fields (the T-complex), demonstrating dominant field activity of the supratemporal plane for the exogenous potentials. the key effect of rate was the suppression of discrete components. Only the P1 persisted in the waveform regardless of age or stimulus rate, indicating a different refractory period for P1 generators compared to other CAEPs. CSD maps showed homogeneity of topographic configurations for the P1 component across stimulus rates, a frontal distribution for P1 and N2, and central distribution for P2 in the pediatric waveforms. We conclude that both age and stimulus rate are important variables in the assessment of auditory cortex function and maturation.

### **[373] Brain Imaging Studies of Pitch Processing in Human Auditory Cortex.**

Deborah Hall<sup>1</sup>, Christopher Plack<sup>2</sup>, Christopher Brignell<sup>1</sup>, Caroline Witton<sup>3</sup>

<sup>1</sup>Medical Research Council, <sup>2</sup>Lancaster University, <sup>3</sup>Aston University

Data from human fMRI and primate electrophysiological studies suggest that a region near the anterolateral border of primary auditory cortex may be involved in pitch processing. in humans this corresponds to lateral Heschl's gyrus (HG). Collectively, previous findings support the claim for a single region in the central auditory system that is selective for pitch, irrespective of its acoustic characteristics. Most of the human neuroimaging studies addressing this issue have used iterated rippled noise (IRN), a specialized stimulus, to evoke a pitch sensation. We present the results from three neuroimaging studies (fMRI and MEG) in which we have examined the cortical representation of pitch using a range of different pitch-evoking stimuli.

Our fMRI data confirm that, relative to a spectrally matched noise control, IRN did indeed activate lateral HG. the other pitch-evoking stimuli tested, including a variety of pure and complex tones, and Huggins pitch (a binaural pitch dependent on a combination of information from the two ears) did not. in different participants, the responses to the different pitch stimuli were co-located in a variety of brain regions, mostly in planum temporale, but also in the temporo-parieto-occipital junction and prefrontal cortex. a follow-up experiment used MEG to compare the response to a Huggins pitch and a matched noise control. Pitch epochs were predominantly associated with a decrease of oscillatory power in the beta frequency band (14-30 Hz). Beamforming methods for identifying the sources of this

pitch-related desynchronisation revealed a reliable network of brain regions including planum temporale and prefrontal cortex. Additional evidence using a functional connectivity re-analysis of our initial fMRI data also converge on there being a reliable network of these cortical regions, engaged even during passive listening to pitch. We conclude that it may be premature to assign the pitch center to a single region located in lateral HG.

### **374 The Effect of Auditory Selective Attention On the Human Auditory Cortex and Inferior Colliculus**

**Teemu Rinne<sup>1</sup>**, Marja Balk<sup>2</sup>, Sonja Koistinen<sup>1</sup>, Taina Autti<sup>3</sup>, Kimmo Alho<sup>1</sup>, Mikko Sams<sup>4</sup>

<sup>1</sup>*Department of Psychology, University of Helsinki,*

<sup>2</sup>*Advanced Magnetic Imaging Centre, Helsinki University of Technology,* <sup>3</sup>*Helsinki Medical Imaging Center, Helsinki University Central Hospital,* <sup>4</sup>*Laboratory of Computational Engineering, Helsinki University of Technology*

There has been a long-lasting debate on whether attention affects sound processing already in the subcortical auditory pathway. Functional magnetic resonance imaging (fMRI) studies have shown that sound-evoked activations of human auditory cortex (AC) are strongly modulated by attention but attentional modulation in the subcortical auditory pathway remains ambiguous. In the present study, we used fMRI to examine the activation of AC and inferior colliculus (IC) during strictly-controlled auditory attention tasks.

Our subjects (N = 19) were presented with asynchronous left- and right-ear iterated rippled noise bursts (16 iterations, delay 0.5 – 10 ms corresponding to pitch range 2000 – 100 Hz, duration 100 ms) at a rapid rate (onset-to-onset interval within an ear 200 – 390 ms). Subjects were required to selectively attend to sounds in the designated ear in order to detect frequent (about once per second) pitch increases or decreases among the attended sounds and to indicate, by pressing one of the two buttons, the direction of the pitch change. This paradigm allowed us to compare brain activations during Attend Left (ignore right) and Attend Right (ignore left) conditions with similar acoustic inputs.

Behavioral data obtained during the fMRI acquisition showed that, although the task was intentionally difficult, the subjects achieved acceptable performance levels that did not differ between the two tasks. According to initial fMRI data analysis, attentive listening was associated with distinct activations in both AC and IC. Further, both the AC and IC activations were enhanced when attention was focused on the sounds at the contralateral ear as compared with activations during ipsilateral attention.

### **375 Measuring Event Related Auditory Evoked Fields with Beamformers**

**Daniel Wong<sup>1</sup>**, Karen Gordon<sup>1</sup>, Robert Harrison<sup>1</sup>

<sup>1</sup>*University of Toronto*

The aim of the present study was to design an efficient beamformer algorithm that is (a) capable of accurately measuring correlated sources and (b) able to do so without a priori information regarding source location or numbers.

Beamformers are a type of adaptive spatial filter that can produce a tomographic image of cortical activation patterns from neuromagnetic data. This class of source localization algorithms has advantages over traditional equivalent current dipole (ECD) analysis. Beamformers are fairly immune to noise, and when sources are minimally correlated, beamformers avoid the need for a priori knowledge of source numbers and locations. However, when correlated sources exist, their reconstructions show reduced signal intensities and time course distortions.

We utilized a novel and efficient algorithm to locate correlated sources. Then, using a region-suppression algorithm coupled with an event-related synthetic aperture magnetoencephalography beamformer, the sources were reconstructed. The algorithm was validated using simulations, and comparisons to ECD and another proven beamformer (Cheyne et al., 2007). It was then applied to the study of auditory development in 9 normal hearing children and young adults. Auditory evoked responses were moderately correlated; hence their conventional beamformer reconstructions tended to exhibit time course distortions. Results from the developed method show source localizations in Heschl's Gyrus in response to monaural and binaural stimulation consistent with those from ECD. Virtual sensor data show greater contralateral activation in response to monaural versus binaural stimulation and a decrease in response latency with increasing age.

The newly developed beamformer reduces reliance on a priori information. This may be an important tool in future studies examining subjects with disrupted auditory function, including cochlear implants users, in whom source numbers and locations may not be well understood.

### **376 MEG Correlates of Forward Masking of Amplitude Modulation**

**Rebecca Millman<sup>1</sup>**, Gary Green<sup>1</sup>

<sup>1</sup>*York Neuroimaging Centre, the Biocentre, York Science Park, Heslington, YO10 5DG*

Under everyday listening conditions, we typically encounter sounds within the context of a sequence of other sounds. An example of the influence of stimulus context is forward masking, where the presence of one sound (the masker) has the potential to affect the perception of a subsequent sound (the target).

The forward masking of modulated sounds has been investigated both neurophysiologically [Bartlett, E. L. and Wang, X. Q. (2005). "Long-lasting modulation by stimulus context in primate auditory cortex," *J. Neurophysiol.* 94, 83-104] and psychoacoustically [Wojtczak, M. and Viemeister, N. F. (2005). "Forward masking of amplitude modulation: Basic characteristics," *J. Acoust. Soc. Am.* 118, 3198-3210]. However, debate remains about whether masker persistence and/or neural adaptation are the neural mechanisms underlying forward masking. The purpose of the present study was to obtain direct measures of forward masking of amplitude modulation (AM) in humans using magnetoencephalography (MEG). The null hypothesis was that adaptation of the target

modulation depth underlies AM forward masking (Bartlett and Wang, 2005).

The MEG experiment consisted of two stimulus conditions, both containing a masker followed by a target. the masker was either an unmodulated 1-kHz tone or a 6-Hz AM applied to a 1-kHz tone with a modulation depth of 0 dB. the target was a 5-Hz AM imposed on a 1-kHz tone with a modulation depth of -4 dB. the delay between the masker and target was 0 ms. the masker duration was 2.5 s and the target duration was 1.5 s.

Beamforming analysis showed cortical representations of AM forward masking near to the lateral sulcus. Virtual electrodes were placed at these locations. the magnitudes of the Fourier components corresponding to the masker and target modulation frequencies were calculated from the virtual electrode time series. Analyses of these time series suggest that both masker persistence and target adaptation play a role in cortical AM forward masking.

### **[377] An MEG Investigation of Lateralization Effects Based On Temporal Interval Processing**

**Mary Howard<sup>1</sup>, David Poeppel<sup>1</sup>**

<sup>1</sup>*University of Maryland*

Converging evidence suggests that the right and left hemispheres differ in their processing of the temporal dimension of acoustic stimuli and that these differences may critically contribute to left hemisphere dominance in the speech domain. One temporal feature that appears to be particularly important for the construction of elementary auditory representations is the length of the interval separating acoustic events. in the speech domain, for example, discrimination between certain syllables is performed on the basis of interval length. Psychophysical evidence suggests that the interval length that determines whether the order of two events can be reliably distinguished is ~30 ms. a neural correlate of this boundary may be reflected in the M100 response to auditory stimuli, which has an integration window of ~ 32-40ms.

This MEG study examines the hypothesis that interval processing differs in the two hemispheres in a way that would privilege the left hemisphere in distinguishing the order of events separated by a short interval. the study contrasts the evoked response to a brief broadband noise (click) with that evoked by two such stimuli separated by 40ms (click pair). the 40ms interval was selected based on its proximity to both the psychophysical ordering boundary and the upper limit of the M100 integration window. Response patterns in the spatial and temporal domains for both the low-frequency (M50-M100-M200) and the gamma bands are characterized for the two stimuli and these patterns are examined for evidence of hemispheric lateralization. the AEF for the single click is shown to exhibit the same basic features previously observed for a variety of stimuli, including a small but significant hemispheric asymmetry in M100 latency. the AEF for the click pair is examined for evidence that the later click produces a second M100 that is more robust in the left

hemisphere, consistent with superior encoding of order for closely spaced events in the left hemisphere.

### **[378] Cortical Processing of Consonants Occurs in Regions Adjacent to Regions Active in Vowel Processing**

**Roy Patterson<sup>1</sup>, Alexis Hervais-Adelman<sup>1</sup>, timothy Ives<sup>1</sup>, Ingrid Johnsrude<sup>2</sup>, Dennis Norris<sup>3</sup>, William Marslen-Wilson<sup>3</sup>**

<sup>1</sup>*Centre for the Neural Basis of Hearing, Cambridge University, Cambridge UK*, <sup>2</sup>*Queens University, Kingston, Ontario*, <sup>3</sup>*MRC Cognition and Brain Sciences Unit, Cambridge, UK*

Recently, Uppenkamp et al. [NeuroImage 31, 1284-1296 (2006)] used fMRI to localize the initial stages of speech specific processing in the auditory system. They contrasted synthetic vowel sounds with acoustically matched non-speech sounds (referred to as 'musical rain') and demonstrated that regions of the superior temporal gyrus (STG) and the superior temporal sulcus (STS) were more active for the vowel sounds. the current study extended the research in an attempt to locate regions involved in the processing of consonants in syllables, with the hypothesis that the consonant regions would be adjacent to the vowel-processing regions revealed previously. Three classes of consonants (fricatives, sonorants and stops), each with 6-exemplars, were combined with 5 English vowels to create 6 sets of consonant-vowel (CV) and vowel-consonant (VC) syllables. Each set constituted a condition in the experiment, which also included three control conditions, isolated vowels (V), musical rain (MR) and silence. Sets of ten, randomly chosen stimuli, from a single condition were presented during 6.9-s silent intervals between scans (TA: 2.1s, TR: 9s). There were 8 replications of each condition (72 scans), in each of 3 blocks of scans. Twelve normal-hearing, right-handed, native English speakers participated in the study. the results showed that vowels produce more activation than MR in left STS. Consonants produce differential activation along posterior and middle regions of STG on the left; fricatives produced the most activation and sonorants the least. VC stops produced more activation than CV stops in middle left STG. These results support the hypothesis that the initial stages of speech processing occur in regions of STG and STS beyond the primary auditory areas. Research supported by the UK Medical Research Council (G0500221, G9900369) and the VW Foundation (1/97 782)

### **[379] Representation of Temporal Speech Envelope in Human Auditory Cortex**

**Kirill Nourski<sup>1</sup>, John Brugge<sup>1</sup>, Hiroyuki Oya<sup>1</sup>, Hiroto Kawasaki<sup>1</sup>, Matthew Howard<sup>1</sup>**

<sup>1</sup>*The University of Iowa*

Speech comprehension has been related to the ability of the auditory cortex to follow the low-frequency temporal speech envelope (Ahissar et al., 2001, PNAS, 98:13367-72). We investigated spectro-temporal properties of auditory cortical responses to time-compressed speech stimuli in patients undergoing invasive electrophysiological monitoring for pharmacologically refractory epilepsy.

Chronic recordings were made from multi-contact depth electrodes implanted in Heschl's gyrus (HG) and from subdural grid electrodes placed over posterolateral superior temporal gyrus (STG). Experimental stimuli were speech sentences, time-compressed from 0.75 to 0.20 of the natural speaking rate, using an algorithm that preserved the spectral content of the stimuli. Averaged auditory evoked potentials (AEPs) and event-related band power (ERBP), based on the complex Morlet wavelet transform, were obtained at each recording site. ERBP was calculated relative to baseline power over 200 ms before stimulus onset.

Speech stimuli elicited both robust AEPs and increases of ERBP in high (70-130 Hz) and very high (130-210 Hz) gamma frequency bands. Power in both gamma bands was modulated by the speech envelope. a temporal envelope-following response, having a latency of about 100 ms, was localized to posteromedial HG, which is the putative location of the core auditory cortex. Temporal cross-correlation between stimulus and ERBP envelopes decreased with degree of compression. Responses from anterolateral HG and posterolateral STG differed from one another and, unlike posteromedial HG responses, exhibited no envelope following.

Our results identify three functionally distinct auditory areas, place the temporal representation of the speech envelope in the putative auditory core and suggest a relationship between this temporal representation and speech comprehension.

Supported by NIDCD RO1-DC04290, MO1-RR-59 General Clinical Research Centers Program, the Hoover Fund and the Carver Trust.

### **[380] Representation of Interaural Time Delay in Human Cortex**

**Katharina von Kriegstein**<sup>1</sup>, Sarah Thompson<sup>2</sup>, Timothy Griffiths<sup>1</sup>, David McAlpine<sup>3</sup>

<sup>1</sup>Wellcome Functional Imaging Laboratory, Queen Square, London, <sup>2</sup>MRC Cognitive Brain Unit, Chaucer Road, Cambridge, <sup>3</sup>UCL Ear Institute, Gray's Inn Road, London

The representation of interaural time differences (ITDs) is presumed to be one in which sounds leading in time at one ear activate maximally the opposite brain hemisphere. Recent investigations indicate a restricted range of ITD detectors in mammals; no ITD detectors exist beyond  $\frac{1}{2}$  a cycle of the centre frequency of each auditory filter (the  $\pi$ -limit), a notion supported by a recent functional magnetic resonance imaging (fMRI) study demonstrating activation to interaurally-delayed noise in the inferior colliculus (IC) of the midbrain to be greater ipsilateral to the perceived location of the source for ITDs beyond the  $\pi$ -limit (von Kriegstein et al., 2006, Nat. Neurosci. 9, 1096-8). We examined the representation of ITDs in human cortex using fMRI for 400Hz wide bands of noise centred at 500Hz presented over stereo headphones. ITDs of zero, or  $\pm 500\mu\text{s}$  and  $\pm 1500\mu\text{s}$ , corresponding to  $\pm \frac{1}{4}$  or  $\pm \frac{3}{4}$  the period of the 500Hz centre frequency, were imposed on the ongoing waveforms. in accordance with a contralateral representation of auditory space, the contrast  $-500\mu\text{s} > +500\mu\text{s}$  activates right planum temporale (PT) and the reverse contrast activates left PT. However, neither the

contrast  $-1500\mu\text{s}$  vs.  $+1500\mu\text{s}$ , nor the reverse, activate either hemisphere to a greater extent than the other; no significant clusters in PT or Heschl's gyrus were observed. This lack of differential activation can be explained by the bilateral activity in PT/Heschl's gyrus when contrasting  $1500\mu\text{s} > 0\mu\text{s}$ . As expected, the same contrast for short ITDs ( $500\mu\text{s} > 0\mu\text{s}$ ) reveals lateralized activity in PT. the contrast  $\pm 1500\mu\text{s} > \pm 500\mu\text{s}$  activates bilateral primary auditory cortex (TE1.0). the pattern of activation can be understood by the reduced level of interaural correlation for the long ITDs, producing bilateral cortical activation.

### **[381] Musical Training Induced Neuroplasticity in Obligatory Responses to Sound Events in Adolescents**

**Wenjung Wang**<sup>1</sup>, Laura Staffaroni<sup>2</sup>, Errold Reid<sup>2</sup>, Mitchell Steinschneider<sup>2</sup>, Elyse Sussman<sup>2</sup>

<sup>1</sup>City University of New York, the Graduate Center, <sup>2</sup>Albert Einstein College of Medicine

It is known that musical training induces plastic changes in neocortex, while the developmental time course of these changes is less well understood. We initiated this investigation by examining, in adolescents (ages 15-18 years), whether musical training alters the neurophysiological responses to sounds. We tested two groups of adolescents who began playing musical instruments around 10 years old. One group, "musicians", have been playing musical instruments an average of eight hours per week and participating in music groups/classes. the other group, "non-musicians", played instruments an average of 30 minutes per week and did not participate in music groups/classes. We recorded event-related brain potentials (ERPs) and assessed the effects of musical training by measuring the amplitude and latency of the obligatory ERP components (P1, P2, and N2). We found that the amplitude of P1 and N2 were larger and the latency of N2 was earlier in musicians compared to the non-musician adolescents. These results show that musical training that begins in later childhood can modulate neurophysiological responses to sound onsets in adolescence.

### **[382] Auditory-Visual Cross Modal Plasticity in Deaf: Evidence From MEG**

**Myung-Whan Suh**<sup>1</sup>, Hyo Jeong Lee<sup>2</sup>, June Sic Kim<sup>3</sup>, Chun Kee Chung<sup>3</sup>, Ja Hyun Kim<sup>4</sup>, Chong-Sun Kim<sup>1</sup>, Min-Hyun Park<sup>1</sup>, Ho Sun Lee<sup>1</sup>, Jin Hee Lee<sup>1</sup>, Seung Ha Oh<sup>1</sup>

<sup>1</sup>Department of Otorhinolaryngology, Seoul National University College of Medicine, <sup>2</sup>Department of

Otolaryngology, Hallym University College of Medicine,

<sup>3</sup>Department of Neurosurgery, Seoul National University College of Medicine, <sup>4</sup>Department of Biomedical

Engineering, College of Health Science, Yonsei University Although the auditory-visual cross modal plasticity in deaf has been studied in a few fMRI studies, they were not able elucidate the fine temporal relationship between the two cortices due to the low temporal resolution. the purpose of this study was to evaluate the difference in cortical activity propagation in the visual and auditory cortex between deaf and normal controls.



5 post lingual deaf patients and 5 normal controls underwent a MEG study. the stimulation paradigm was a silent video clip of lip movements with (speechreading) or without (gurning) visual phonetics. Latency and amplitude of the dipoles in the visual and auditory cortex were analyzed.

Both group showed a visual cortex activation followed by auditory cortex activation. the latency of the visual cortex activation was about 150 msec which was similar in both groups for both conditions. in speechreading condition, the latency of auditory cortex activation was 237.5 and 259.9 msec in the deaf and control group respectively. in gurning condition, auditory cortex activation was observed in the deaf group but not in the control group. the latency was delayed to 396.1 msec. the amplitude of the dipoles was slightly larger in the control group compared to the deaf group in both conditions.

These finding suggest that deaf subjects can recruit the auditory cortex even in gurning conditions. This may be due to a more comprehensive interpretation of the visual information in order to overcome the deprivation of auditory sensation.

Furthermore, although speechreading and gurning condition both activate the auditory cortex in deaf, they may be processed in the different way. This can be presumed from the big difference in latency between the two conditions. a potentiated connection between the visual and auditory cortex with short latency may be activated by routine speechreading. But gurning may require an additional process before it can be interpreted by the auditory cortex.

### **383 Limitations On Functional Imaging Resolution in Auditory Cortex**

**Thomas L Chen<sup>1</sup>, Paul V Watkins<sup>1</sup>, Dennis L Barbour<sup>1</sup>**

<sup>1</sup>*Washington University*

Sensory neurons typically increase their spiking rates to a point of saturation in response to increasing stimulus intensity. All auditory nerve fibers projecting from the inner ear demonstrate this monotonic spiking behavior, although a large proportion of central auditory neurons do not. These central nonmonotonic neurons are tuned to a specific sound intensity and are suppressed at higher intensities. Because nonmonotonic neurons are not found in auditory nerve fibers, they must be created by central auditory circuits. Despite being extraordinarily common, the physiological role nonmonotonic auditory neurons play in encoding sounds is poorly understood.

Monotonic neurons respond to a wider frequency range than nonmonotonic neurons do, particularly at high intensities. Even a relatively small percentage of monotonic neurons within a brain region would likely dominate a functional image of that region because of their greater overall activity compared with nonmonotonic neurons. to test this hypothesis, we constructed computational models of neuronal function in primary auditory cortex (A1) and stimulated the models with sounds commonly used in functional imaging experiments. Under these conditions computational arrays of monotonic neurons typically demonstrated 10–20 times more

collective activity than arrays of nonmonotonic neurons. This differential was greatest at the highest sound levels. the activity of model monotonic neurons more closely resembled functional imaging data from A1 than did the activity of nonmonotonic neurons, implying that traditional imaging methodologies appear to be measuring predominantly the activity of monotonic neurons. Without methods of filtering out monotonic neuron activity, therefore, functional imaging may be incapable of resolving key characteristics of A1 circuitry.

### **384 Repetitive Transcranial Magnetic Stimulation (rTMS) on Persistent Noise Induced Tinnitus in Rats – a pilot study**

**Edward Lobarinas<sup>1</sup>, Berthold Langguth<sup>2</sup>, Wei Sun<sup>1</sup>, Jianzhong Lu<sup>1</sup>, Richard Salvi<sup>1</sup>**

<sup>1</sup>*University of Buffalo*, <sup>2</sup>*University of Regensburg*

rTMS an innovative method for noninvasive stimulation of the cortex has been proposed as a new treatment option for chronic tinnitus. Here we present first results from a pilot study of rTMS in an animal model of tinnitus

During each rTMS session 100 stimuli were administered with a figure-of-eight Magstim coil at a frequency of 0.5 Hz and with an intensity of 30% of the maximal stimulator output.

In one rat with electrodes implanted in the right auditory cortex rTMS was performed over the implanted auditory cortex. Compared to Baseline there was a reduction of spontaneous and evoked cortical activity ten minutes after rTMS, which returned to baseline levels thirty minutes after rTMS, indicating a transient suppressing effect of low frequency rTMS.

Four rats were exposed to unilateral noise trauma (126 dB SPL, 12,000 Hz NBN, 2h). Subjects were then tested for the presence of persistent tinnitus using gap prepulse inhibition of acoustic startle (GPIAS) at 1, 3, 7, 15, and 30 days post trauma. GPIAS was performed for background noise centered at 6, 12, 16, 20 or 24 kHz. All four subjects tested showed the presence of tinnitus like behavior at 12 and 16 kHz throughout all test sessions. Single sessions of rTMS were performed over the right auditory cortex (contralateral to noise induced hearing loss) and over the left auditory cortex (ipsilateral to noise induced hearing loss). Two of the test subjects showed a partial reversal of tinnitus like behavior indexed by enhanced startle inhibition following rTMS. in one of these two subjects, ipsilateral and contralateral stimulation was equally effective at reducing tinnitus at 12 and 16 kHz. in the other subject, contralateral stimulation was more effective at 12 kHz with little effect at 16 kHz.

These pilot data demonstrate the feasibility of rTMS in animals with evidence of tinnitus. the demonstration of rTMS effects on auditory cortex activity and on tinnitus related behavior are in line with clinical data in humans.

### **385 Auditory Cortical Potentials to Single Feature Changes (Frequency or Intensity) in Continuous Tones.**

**Andrew Dimitrijevic<sup>1</sup>**, Brenda Lolli<sup>2</sup>, Henry Michalewski<sup>1</sup>, Fan-Gang Zeng<sup>1</sup>, Arnold Starr<sup>1</sup>

<sup>1</sup>University of California, Irvine, <sup>2</sup>University of California, San Diego

We examined auditory cortical potentials to 100 ms duration increments of either frequency or intensity of continuous "low" (250 Hz) or of "high" (4000 Hz) frequency tones occurring every 1.4 s. the magnitude of pitch change ( $\Delta f$ ) was randomly set to 0,2,4,10,25, and 50% of the base frequency (250 or 4000 Hz) while the intensity increments ( $\Delta i$ ) varied from 0,2,4,6, and 8 dB. Subjects were normal hearing young adults tested while awake and watching a movie. a 64-channel recording system was used to record the potentials that were then sorted and separately averaged to each of the pitch/intensity changes. the potentials included N100 and P200 components followed by a late a sustained slow potential of maximal amplitude at midline fronto-central electrodes (FCz and Cz). N100 amplitude increased and latency decreased with increasing  $\Delta f$  and  $i$ . Slope functions relating magnitude of frequency change with N100 were significantly different for high and low frequencies. Shallower slopes were seen with higher frequencies compared to low frequencies. However, identical slope functions were seen with  $\Delta i$  for high and low frequencies. These results suggest that cortical pitch change representation differs for high and low frequencies whereas intensity changes do not differ for high and low frequencies. Brain processes encoding pitch and intensity changes are governed by different rules. Work supported by NIH DC-02618.

### **386 Cortical Representations of Multiple Temporal Modulations**

**Juanjuan Xiang<sup>1</sup>**, David Poeppel<sup>1</sup>, Jonathan Z. Simon<sup>1</sup>

<sup>1</sup>University of Maryland

The ability of auditory cortex to represent multiple simultaneous modulations is critical for everyday tasks such as speech perception. for speech perception, both syllabic rates (~ 4 Hz) and phonemic rates (~ 20 Hz) need to be tracked and processed simultaneously. Furthermore, due to the non-linearity of neural processing in auditory cortex, the processing of multiple modulations cannot be reduced to superposition of responses to individual modulations. to investigate the auditory encoding of temporal information in complex sounds, we employ sinusoidally amplitude modulated (SAM) stimuli containing both single and compound modulations. We use magnetoencephalography (MEG) to measure the neural responses of 15 human subjects listening to these modulated stimuli, in order to address three questions: 1) What are the auditory cortical representations of concurrent amplitude modulations? 2) How do the neural representations of concurrent modulations fit into current debates about theories of modulation filter banks? 3) What neural correlate underlies the percept of stimuli with compound modulations? Differences in responses to

broadband carriers and pure tone carriers are also assessed. We find physiological evidence to support the existence of modulation filter banks whose filter bandwidths are band-limited (with respect to modulation rates), allowing syllabic and phonemic modulations to be processed separately. Additionally, we find a neural explanation for specific percepts arising from stimuli with compound modulations.

### **387 Spontaneous MEG Activity in People with and Without Tinnitus**

**Elif Ozdemir<sup>1</sup>**, Hesheng Liu<sup>2</sup>, Robert Levine<sup>1</sup>, Jennifer Melcher<sup>1</sup>

<sup>1</sup>Massachusetts Eye and Ear Infirmary, <sup>2</sup>Massachusetts General Hospital A.Martin Imaging Center

Tinnitus is a common clinical problem for which there are no effective treatments and no proven objective measures. Previously, Weisz et al. (PLoS, 2: e153, 2005) reported abnormalities in the spontaneous cortical activity of tinnitus subjects. Specifically, the power spectrum of spontaneous magnetoencephalographic (MEG) signals was increased at delta frequencies (1.5-4 Hz) and reduced at alpha frequencies (8-12 Hz) in tinnitus subjects compared to non-tinnitus controls. However, the tinnitus subjects had hearing loss whereas the non-tinnitus subjects did not. the present study examines whether the previously reported MEG abnormality is evident when audiometrically matched tinnitus and non-tinnitus subjects are compared.

Spontaneous MEG activity was measured in 17 subjects with normal pure tone thresholds from 250 to 8000 Hz. 9 subjects had chronic tinnitus, which was perceived during MEG. Measurements were made using a 306-channel Neuromag Vectorview system housed in an electrically and magnetically shielded room. Signals were recorded for 10 minutes at a sampling rate of 600 Hz while subjects sat with their eyes closed. Eye blinks registered in the concurrently recorded electro-oculogram indicated that subjects were awake throughout the measurement. the Fourier transform of the MEG signal was averaged across overlapping 8.5-second time windows and across sensors to yield a power spectrum for each subject.

There was no evidence for the previously reported differential effects on delta and alpha activity. Instead, the spectra of tinnitus subjects differed from non-tinnitus subjects only in a global way that may be related to a slight difference in alertness between groups: power was less in delta (1.5-4 Hz,  $p=0.01$ ), theta (4-8 Hz,  $p=0.01$ ), and alpha (8-12 Hz,  $p=0.02$ ). the results suggest that the spectral abnormalities reported by Weisz et al. (2005) are either unrelated to tinnitus or, are related to tinnitus but only when it is accompanied by hearing loss.

### **388 Auditory Screenings in Children with Feeding and Swallowing Disorders**

**Vishakha Rawool<sup>1</sup>**

<sup>1</sup>*West Virginia University*

An interdisciplinary approach is recommended for the general management of children with feeding or swallowing difficulties. However, an audiologist is generally not considered part of the team. the purpose of this report is to provide results of audiological and middle ear screenings of children who were referred to an interdisciplinary feeding and swallowing clinic. Forty four children ranging in age from 3 months to 11 years with feeding and swallowing disorders were included in the study. the hearing screenings consisted of a case-history, otoscopic examination, middle ear screening and audiometric screening. If a child did not pass the hearing screening, whenever possible with reference to time-constraints and child-cooperation, air and bone conduction thresholds were determined for each ear. the current results suggest that up to 50% of the children with feeding and swallowing disorders may suffer from transient or permanent conductive or sensorineural hearing loss. Eighteen of the 33 (55%) children evaluated with tympanometry yielded abnormal findings due to middle ear dysfunction or placement of pressure equalization tubes, suggesting a high prevalence of transient conductive hearing loss. Several connections between feeding and/or swallowing difficulties and hearing were apparent including the connection between ear-infections and swallowing difficulties, malnutrition and ear-infections, medications used for treating ear infections and feeding difficulties, ototoxic medications, micronutrient deficiencies and auditory processing difficulties, deafness and/or blindness and feeding difficulties and syndromes involving both hearing loss and feeding disorders. [Supported by a grant for the LEND Project (#MCJ-549170) from the Maternal and Child Health Bureau (Title V, Social Security Act), Health Resources and Services Administration, Department of Health and Human Services].

### **389 Non organic Hearing Loss in Chinese Teenagers**

**Chunfu Dai<sup>1</sup>**

<sup>1</sup>*Fudan University*

To heighten the physician's awareness of non-organic hearing loss in teenagers in China. We retrospectively conducted cases review of seven patients (6 girls and 1 boy) with sudden hearing loss. the results showed five patients presented with hearing loss bilaterally and 2 patients unilaterally. All patients suffered from severe to profound hearing loss. However, the acoustic reflex test indicated direct and indirect responses were present bilaterally at 1K Hz 100 dB SPL. the results of ABR test revealed hearing threshold within 20 - 30 dBnHL. Further investigations indicated non-organic hearing loss was associated with school stress or environment conflict. Satisfactory outcomes were achieved in all patients. Non-organic hearing loss should be considered when teenagers present with sudden hearing loss while the acoustic reflex is present. School and home stresses are

associated with the occurrence of non-organic hearing loss in the present study.

Key words: non-organic hearing loss, sudden deafness, ABR, acoustic reflex

### **390 Discrepancies of Hearing Examination Results in Patients with Acoustic Neurinoma**

**Teruyuki Sato<sup>1</sup>, Kazuo Ishikawa<sup>1</sup>, Yoshiaki Itasaka<sup>1</sup>, Shin Takahashi<sup>1</sup>**

<sup>1</sup>*Akita university school of medicine*

Discrepancies of Hearing Examination Results in Patients with Acoustic Neurinoma

Mechanisms for pathogenesis of hearing loss caused by acoustic neurinoma has not been sufficiently elucidated. Recently, various audiological test batteries have developed, and were recognized their usefulness to employ as an objective examination.

The aim of our study is to verify the usefulness such as auditory brainstem response (ABR), auditory steady state response (ASSR) and otoacoustic emission (OAE) in acoustic neurinoma patients.

Thirteen patients of acoustic neurinoma patients were reviewed. They are four males, and nine females, ranging from 29-74 years old with an average of 50.7. Three cases were right side, nine cases were left side and one case was bilateral tumor (total fourteen ears). We have compared those audiological results on pure tone audiometry, ABR, ASSR and OAE as objective audiological examinations. Hearing level in pure tone audiometry was equal to that of ABR and ASSR in nine cases. But, hearing level in audiometry was not in line with those of ABR and ASSR in five cases. Some cases with no EOAE had good DPOAE, suggesting that one must be cautious in making final decision on OAE results. Those discrepancies might reflect the complexity of pathogenesis of hearing impairment caused by acoustic neurinoma. Details of those discrepancies were shown, and pathogenesis of hearing disorder by acoustic neurinoma will be discussed, referring pertinent papers.

### **391 Hearing ability in persons with Mild Cognitive Impairment and Alzheimer's Disease**

**Esma Idrizbegovic<sup>1</sup>**

<sup>1</sup>*Inst. of Clinical Science*

The general goal is to study the relationship between hearing ability and dementia in persons in late middle age and in the elderly. a specific goal is to see if an early acoustic stimulation/amplification could slow down cognitive deterioration in persons with Mild Cognitive Impairment (MCI) and Alzheimer's Disease (AD).

Participants are recruited from the Geriatric clinic where persons with memory problems have undergone neurological, cognitive, neuropsychological and behavioural assessment. Depending on the investigation's outcome, persons are divided into three groups: 1) normal cognitive functions; 2) MCI and 3) AD. At the Department of Audiology, the investigation is followed by peripheral and central hearing tests, such as pure tone audiometry,

tympanometry, speech audiometry in quiet and in background noise, dichotic tests and mismatch negativity. Persons with mild to moderate hearing loss are randomly selected for fitting with hearing aids. All participants are followed-up after 6 and 12 months. the preliminary results of this study will be presented.

### **[392] Best-Subsets Linear Regression Analysis of Auditory Measures in Young Adult Cigarette Smokers**

**Kamakshi Gopal<sup>1</sup>**, Richard Herrington<sup>1</sup>, Jacqueline Pearce<sup>1</sup>

<sup>1</sup>*University of North Texas*

Several studies have shown that cigarette smoking is a risk factor for hearing loss. There are, however, no known preclinical predictors of cigarette smoke-induced hearing loss. It is known that cigarette smoking involves exposure to carbon monoxide (CO), and exhaled CO reflects the exposure of smoke to lungs. in this study, the CO level in the subjects' breath was measured with a CO monitor, and was used as the outcome measure. the goal of the study was to investigate if any of the routine auditory test measures can be used as potential predictors of the outcome measure (CO level) in young normal hearing adult smokers.

the study involved 16 normal hearing adult males in the age range of 18-24 years with no history of noise exposure. All subjects had smoked at least a pack of cigarettes daily for the past three years. an auditory test battery consisting of the following tests was administered to all subjects: pure-tone audiometry, acoustic reflex thresholds (ART) for ipsilateral and contralateral stimulation, auditory brainstem response (ABR) latency and amplitude measures, and otoacoustic emissions (OAE) including transient and distortion products. the auditory measures obtained from the above tests were used as predictor variables. Best-subsets linear regression, based on Akaike information criterion (AIC), Bayes information criterion (BIC) and adjusted R-squared model comparison indices, was used in a variable-selection procedure to select an optimal set of linear predictors for the outcome measure. an advantage of using best-subsets regression is that a large group of predictor variables (i.e. auditory measures) obtained on a relatively medium to small sized samples, can be reduced down to a set of variables that have better validity in predicting the outcome measure from new samples (e.g. smaller AIC and adjusted R squared). Results of this approach indicated that the ABR peak V amplitude and distortion product OAEs had the highest predictive value and accounted for most of the variability.

### **[393] Effect of Lipoprostaglandin E1 Treatment On Idiopathic Sudden Sensorineural Hearing Loss Frandomized Control Study**

**Misato Kasai<sup>1</sup>**, Takashi Iizuka<sup>1</sup>, Ayako Inoshita<sup>1</sup>, Chieri Hayashi<sup>1</sup>, Yoko Sakai<sup>1</sup>, Yukiko Itihari<sup>1</sup>, Naoko Yokoi<sup>1</sup>, Hidenori Yokoi<sup>1</sup>, Masayuki Furukawa<sup>1</sup>, Makiko Seki<sup>1</sup>, Katsuhisa Ikeda<sup>1</sup>

<sup>1</sup>*Department of otorhinolaryngology, juntendo university school of medicine*

Glucocorticosteroid is known to be proven as an effective agent for the treatment of idiopathic sudden sensorineural hearing loss (ISSHL). Although lipoprostaglandin E1 (lipo-PGE 1) is expected be effective to ISSHL, few studies have been available so far. We conducted a randomized control trial of lipo-PGE 1 treatment on ISSHL.

Seventy five patients with ISSHL visited at our hospital between 2004 and 2007 were enrolled in the study. the patients were randomly divided into two groups. One group received both 10 µg lipo-PGE 1 and prednisolone (PSL) for 7 days (lipo-PGE 1 plus PSL group) and another group received only PSL for 7 days (PSL group). There were no significant differences between two groups in clinical characteristics. the lipo-PGE 1 plus PSL group showed 83.03±5.5% in recovery rate, which was not significantly differed from the PSL group (81.64±0.7% recovery rate). We also analyzed variations in therapeutic outcomes with respect to age, vestibular symptoms, and time between onset and treatment, which did not affect the clinical effectiveness of lipo-PGE 1. the results failed to prove a beneficial effect of lipo-PGE 1 in the treatment of ISSHL in spite of its higher cure rate.

### **[394] Sound Stimulation During Sleep for the Tinnitus Treatment: Trans-Disciplinary Approach**

**Marisa Pedemonte<sup>1</sup>**, Daniel Drexler<sup>1</sup>, Silvana Rodio<sup>2</sup>, David Pol-Fernandes<sup>2</sup>, Virna Bernhardt<sup>2</sup>

<sup>1</sup>*Facultad de Medicina CLAEH Punta del Este Uruguay,*

<sup>2</sup>*Facultad de Medicina CLAEH University, Punta del Este, Uruguay*

Subjective tinnitus is a sound created by the central nervous system. During wakefulness, different sound stimulation treatments were used (music, white noise, pure tones) with no clear results. Previous research demonstrated that the auditory system processes incoming information during sleep. Then, we may assume that some kind of learning takes place during this stage. It is our tenet that the brain could learn to mask the tinnitus perception with a particular sound stimulation during sleep. Eight patients with subjective idiopathic tinnitus were selected and treated by an otolaryngologist, a psychologist and a sleep medicine expert. the tinnitus was characterized in frequency and intensity and an equivalent sound was recorded in an *ipod* for night stimulation. in 2 patients, 2 Polysomnography (PSG) studies were carried out in order to assess the hypnograms characterizing sleep organization previous to the treatment and after 15 nights of sound stimulation. in other 2 patients, 1 PSG was done -half of the night with sound stimulation and the other

half with silence- to analyze the electroencephalographic power spectra in each sleep stage with and without sound. Psychological interviews and "Tinnitus Handicap Inventory" (THI) tests were done every two months. Preliminary results: 1) sound stimulation at night did not alter sleep while in some patient improved the insomnia of conciliation. 2) All 8 patients improved tinnitus. Two of them with waking periods of total silence. 3) the THI results are independent of the tinnitus improvement. 4) During sound stimulation there was a significant increment in the delta wave power ( 2.5-4 c/s) during slow wave sleep.

Results suggest that the brain processes auditory information during sleep perhaps learning to mask the tinnitus perception. a trans-disciplinary approach is essential to assess the different tinnitus components: the sound perception alteration, attention processes and affective disorders.

### **[395] Development of the Tinnitus Functional Index (TFI): Part 1. Assembling and Testing a Preliminary Prototype.**

**Mary Meikle<sup>1</sup>**, James Henry<sup>2</sup>, Harvey Abrams<sup>3</sup>, Eric Frederick<sup>4</sup>, William Martin<sup>1</sup>, Rachel McArdle<sup>3</sup>, Paula Myers<sup>5</sup>, Craig Newman<sup>6</sup>, Sharon Sandridge<sup>6</sup>, Barbara Stewart<sup>1</sup>, Thomas Creedon<sup>7</sup>, Susan Griest<sup>1</sup>, Dennis Turk<sup>8</sup>  
<sup>1</sup>Oregon Health & Science University, <sup>2</sup>VA National Center for Rehabilitative Auditory Research, <sup>3</sup>Bay Pines VA Healthcare System, <sup>4</sup>Hearing & Speech Institute, <sup>5</sup>James A. Haley VA Medical Center, <sup>6</sup>Cleveland Clinic, <sup>7</sup>editHere.com, <sup>8</sup>University of Washington

In previous work, 18 investigators highly experienced in evaluating tinnitus were surveyed to develop consensus concerning the item content for a new questionnaire designed to optimize validity for both discriminative (diagnostic) and evaluative (outcomes assessment) purposes. From existing questionnaires (175 items) the group selected 69 items that they judged sensitive to treatment effects while addressing all major components or "dimensions" of tinnitus distress. the number of items was then reduced using objective selection procedures to minimize redundancy and maximize responsiveness, resulting in a total of 43 items for use in Prototype 1 of the TFI. Prototype 1 was tested in a multi-center study (5 clinics in Oregon, Ohio, and Florida). Tinnitus patients' responses to TFI Prototype 1, the Tinnitus Handicap Inventory (THI), the Beck Depression Inventory-FastScreen (BDI-FS), and a Visual Analog Scale (VAS) for tinnitus severity were obtained from 327 subjects. Sixty-five subjects provided Follow-up data at 3 months and 39 subjects provided test-retest reliability data. Statistical analyses of the TFI revealed excellent test-retest reliability ( $r=0.92$ ) and internal consistency reliability ( $\alpha=0.99$ ), high intercorrelations for the TFI vs. THI and VAS (0.91 and 0.71 respectively), and expected correlation with BDI-FS (0.59). Various factor analysis models were evaluated; the best (Principal Axis Factoring, oblique rotation) yielded 7 easily-identified factors accounting for 80% of the variance. Three-month follow-up data revealed good effect sizes for both the overall TFI (E.S.=0.79, compared to E.S.=0.71 for the THI) and individual items (most

E.S.>0.70). in summary, Prototype 1 of the TFI exhibits excellent content and construct validity for both discriminative and evaluative purposes, setting the stage for further work to reduce the number of items while retaining maximal sensitivity to treatment-related change. Supported by the Tinnitus Research Consortium

### **[396] Development of the Tinnitus Functional Index (TFI): Part 2. Final Dimensions, Reliability and Validity in a New Clinical Sample.**

**Mary Meikle<sup>1</sup>**, Barbara Stewart<sup>1</sup>, Susan Griest<sup>1</sup>, James Henry<sup>2</sup>, Harvey Abrams<sup>3</sup>, William Martin<sup>1</sup>, Rachel McArdle<sup>3</sup>, Paula Myers<sup>4</sup>, Craig Newman<sup>5</sup>, Sharon Sandridge<sup>5</sup>, Robert Folmer<sup>1</sup>, Dennis Turk<sup>6</sup>

<sup>1</sup>Oregon Health & Science University, <sup>2</sup>VA National Center for Rehabilitative Auditory Research, <sup>3</sup>Bay Pines VA Medical Center, <sup>4</sup>James A. Haley VA Medical Center, <sup>5</sup>Cleveland Clinic, <sup>6</sup>University of Washington

A prior study (Abstract #611, 2008 ARO Midwinter Meeting) identified 43 questionnaire items that are representative of 7 major dimensions of clinically-significant tinnitus. the present research was designed to reduce the number of questionnaire items to the minimum needed for reliable evaluation of those dimensions or subscales. Based on relevant literature, 3-4 items per dimension are required for adequate measurement validity and reliability. Objective selection criteria (to be shown) were therefore applied to the 43-item set, resulting in selection of 23 questions that are well representative of the 7 dimensions or subscales. an additional 7 questions were considered important and had moderate to high factor loadings on more than one factor; these questions were examined using similar criteria, and proved to be interpretable as an eighth factor or subscale characterized as Tinnitus Impact on Quality of Life. Based on data from the prior study, intercorrelations between these eight factors were moderate to high, and all eight showed good or excellent sensitivity to treatment-related change (Effect Sizes of 0.8-1.24 for 6 factors, 0.49 and 0.61 for the other two). the new 30-item TFI will be displayed and responses of over 300 tinnitus patients will be summarized. Intake data are again being obtained from clinics in Oregon, Ohio and Florida, providing a large, diverse patient group. Treatment follow-up results and test-retest reliability are evaluated in smaller subsets. Responses to the TFI, Tinnitus Handicap Inventory, the Beck-Depression Inventory-FastScreen, and a Visual Analog scale for tinnitus severity are being obtained. in clinic use, the 30-item TFI has proven easy for respondents to complete, with very little missing data. Detailed results will be discussed in relation to both discriminative (diagnostic) and evaluative (outcomes assessment) strengths of the new TFI.

Supported by the Tinnitus Research Consortium

### **397 Frequency Discrimination Thresholds in Mongolian Gerbils Indicate Different Mechanisms for Discriminating Pure Tones and Detecting a Mistuned Component in a Complex Stimulus**

**Astrid Klinge<sup>1</sup>**, Georg M. Klump<sup>1</sup>

<sup>1</sup>*University Oldenburg*

Frequency discrimination of pure tones or harmonics within a complex stimulus may rely on different mechanisms indicated by different frequency discrimination thresholds (FDLs). a pure-tone frequency shift can only be detected by a change of the excitation pattern elicited by the tone alone. a tone in a multi-component harmonic complex can be detected by a change in the spectral pattern of excitation elicited by the complex or by the change of the temporal pattern resulting from the interaction of the components.

Mongolian gerbils (*Meriones unguiculatus*) were trained in an operant Go/NoGo procedure with food rewards to report a frequency shift. We measured pure tone FDLs in the range from 200 to 6400 Hz and FDLs for a mistuned component in an otherwise harmonic complex. the complex consisted of 12 harmonics of an 800-Hz fundamental. FDLs were obtained for the 1st, 2nd and 8th harmonic. in one of the experiments all harmonics started at sine phase resulting in a stimulus with a distinct temporal pattern. in the other experiment we provided the gerbils with only spectral patterns as a cue by starting all harmonics at random phase (each stimulus being different).

The FDLs for pure tones decreased from 20.4% (Weber fraction) at 200 Hz to 6.7% at 6400 Hz. FDLs for mistuned harmonics with all components starting in sine phase were significantly lower ranging from 0.06% (1st harmonic) to 0.02% (8th harmonic). FDLs for random phase stimuli ranged from 2.5% (1st harmonic) to 0.2% (8th harmonic). the gerbil's cochlear place-frequency map and the related excitation pattern could account for the pure tone FDLs. Detection of inharmonicity in a complex stimulus must rely on additional processing mechanisms. Providing a complex stimulus with only a spectral pattern gives a 10fold increase in frequency resolution. Supplying a distinct temporal pattern as an additional cue provides for an even higher resolution.

Supported by the DFG (InterGK 591, SFB/TRR 31)

### **398 Processing of a Mistuned Harmonic by the European Starling Auditory System**

**Georg Klump<sup>1</sup>**, Susanne Groß<sup>1</sup>, Naoya Itatani<sup>1</sup>

<sup>1</sup>*Zoophysiology & Behavior Group, Oldenburg University*

Birds were attributed a superior ability to detect mistuned components in a harmonic tone complex and outperform humans by an order of magnitude (Lohr & Dooling, 1998). Recent studies in the Mongolian gerbil, however, suggest that this difference does not apply to birds and mammals in general (Klinge & Klump, ARO 2008). It remains unclear, which functional features of the auditory system enable a superior performance making it desirable to determine the ability to detect mistuned harmonics in a

bird species offering the possibility for a detailed study of auditory processing mechanisms.

European Starlings (*Sturnus vulgaris*) were trained in an operant Go/NoGo procedure with food rewards to report a frequency shift of a 400-ms tone that was either presented alone or as a component of a 400-ms harmonic complex. the complex consisted of the first 12 harmonics of an 800-Hz fundamental. Frequency discrimination limens (FDLs) were obtained for the 1st, 2nd and 6th harmonic. in one experiment all harmonics started at sine phase resulting in a stimulus with a distinct temporal pattern. in another experiment, only spectral patterns were provided as a cue (each stimulus had harmonics in different random phase). Pure tone FDLs were also determined. the FDLs for pure tones decreased from 3.6% (Weber fraction) at 800 Hz to 1.5% at 4800 Hz which is in line with previous measurements. FDLs for a random phase complex ranged from 2.4% (1st harmonic) to 0.2% (6th harmonic). FDLs for mistuned components in a sine phase complex were much lower ranging from 0.11% (1st harmonic) to 0.02% (6th harmonic). the starling data are similar to results obtained in two other bird species (Lohr & Dooling, 1998) and the gerbil (Klinge & Klump, 2008), but indicate a better ability to detect mistuning than found in humans (e.g., Moore, Peters & Glasberg, 1985). the starling data are compared to results from physiological recordings of auditory forebrain neurons.

Supported by the DFG (SFB/TRR 31)

### **399 Perceptual Interactions Between Vibrotactile and Auditory Stimuli: Effects of Frequency**

**E. Courtenay Wilson<sup>1</sup>**, Charlotte M. Reed<sup>1</sup>, Louis D. Braida<sup>1</sup>

<sup>1</sup>*Speech and Hearing Bioscience and Technology Program, MIT, Cambridge, MA*

This research investigates perceptual interactions between vibrotactile and auditory stimuli as a function of the frequency of vibrotactile sinusoidal signals and auditory tones in broadband noise. the vibrotactile stimuli were sinusoidal signals delivered through a single-channel vibrator to the left middle fingertip and the auditory stimuli were pure tones presented binaurally through headphones in a background of broadband noise at an overall level of 50 dB SPL. the stimulating level of the vibrotactile signal was set at 0 dB Sensation Level (SL) based on threshold estimates from an adaptive 3-interval, 2-alternative, forced-choice (3I, 2AFC) procedure. the level of the auditory signals was 0 dB SL relative to detection of tones in the 50-dB SPL broadband noise (again measured with an adaptive 3I, 2AFC procedure). Measurements of *d'* were obtained in a fixed-level 2I, 2AFC procedure using the 0 dB SL signals (set individually for each of four subjects) under the following three conditions: Vibrotactile (V) alone, Auditory (A) alone, and Vibrotactile plus Auditory (V+A). Stimulus duration was 500 msec with 20 msec rise/fall times; in the combined V+A condition, the vibrotactile and auditory signals were presented with simultaneous onset and equal starting phase of 0 degrees. the effect of the relative frequency of the vibrotactile and



auditory stimuli in the V+A condition was examined by (1) holding vibrotactile frequency constant at 250 Hz and varying the frequency of the auditory tone in a range between 125 and 2000 Hz and (2) holding the frequency of the auditory tone constant at 250 Hz and varying the vibrotactile frequency in a range between 50 and 400 Hz. Preliminary results lead to the following observations: (1) that when the stimulating frequency in both modalities is equal at 250 Hz, d' performance through V+A is significantly higher than through either modality alone; (2) that V+A performance decreases systemically as the frequency difference between a and V increases; and (3) that the magnitude of the largest d' scores in V+A conditions is consistent with integration of the two sensory stimuli into a single percept rather than independent sensory processing. [Work supported in part by a Hertz Foundation Fellowship and grants from the National Institutes of Health RO1-DC000126-25 and RO1-DC000117].

#### **400 Complex Pitch Perception Above the "Existence Region" of Pitch**

**Andrew J. Oxenham<sup>1</sup>**, Michael V. Keebler<sup>1</sup>

<sup>1</sup>*University of Minnesota*

This study investigated the roles of peripheral filtering and temporal fine-structure in pitch perception. the first experiment studied fundamental frequency (F0) discrimination as a function of the lowest harmonic number present for complexes consisting of 12 consecutive harmonics, and for F0s between 30 and 2000 Hz. in this and all subsequent experiments, the stimuli were embedded in background noise to mask potential distortion products. We found that earlier findings of a transition from good to poor performance as the lowest harmonic number increased from 9 to 12 held only for F0s of 100 and 200 Hz. At lower and higher F0s, the transition occurred between harmonics 6 and 9 in ways that were difficult to reconcile with models of peripheral filtering. More surprisingly, F0 discrimination remained good in some cases, even when all harmonics present were higher than 6 kHz, i.e., beyond the accepted "existence region" of pitch. This was tested further by measuring pitch matching and melody recognition for complexes with F0s between 1 and 2 kHz, highpass filtered to contain only harmonics above 6 kHz. in both cases, listeners performed well, suggesting that complex pitch perception is possible with resolved harmonics above 6 kHz. the results suggest either that temporal fine structure is not necessary for complex pitch perception, or that some fine structure is available even above 6 kHz.

[Supported by NIDCD grant R01 DC 05216.]

#### **401 Perception of Filtered Iterated Rippled Noise (IRN) Pitch by Normal-Hearing and Hearing-Impaired Listeners**

**Marjorie Leek<sup>1</sup>**, Sarah Melamed<sup>1</sup>, Michelle Molis<sup>1</sup>

<sup>1</sup>*National Center for Rehabilitative Auditory Research*

Iterated rippled noises are aperiodic sounds created by repeatedly copying a wideband noise and adding (positive IRN) or subtracting (negative IRN) an attenuated version

of the copy back to the original noise after some delay. the perceived pitch for the positive IRN corresponds to the reciprocal of the delay time, and the pitch of the negative IRN may be as much as an octave different. the amount of attenuation (or gain) that can be applied while still maintaining the perceived pitch can be used as a metric for the strength of the pitch for a given IRN. One way to establish the importance of temporal fine structure information, as compared with envelope or spectral processes for pitch perception, is to systematically remove the acoustic information in the areas of resolved harmonics (i.e., where auditory bandwidths are relatively narrow) by high-pass filtering. This experiment is designed to evaluate IRN processing with high-pass filtering in normal-hearing (NH) and hearing-impaired (HI) listeners.

NH and HI listeners were asked to discriminate between positive and negative IRNs at delays of 4, 6, 8, and 12 ms, with six high pass cutoff frequencies ranging from .5 to 3 kHz. for all listeners, the strength of the pitches decreased as the cutoff frequency of the high pass filter increased. HI listeners had reduced pitch strength for most conditions, but at the longer delays (lower pitches) there was less difference in pitch strength between groups. the high-pass frequency cutoff at which performance fell was generally lower for hearing-impaired listeners. These results suggest that temporal information may be less available to hearing-impaired listeners and they may be forced to rely on the remaining, although somewhat degraded, spectral cues. If IRN pitch is encoded by fine-structure cues, these results suggest that these are weaker than normal in individuals with hearing loss. [Work supported by NIDCD]

#### **402 The Role of Frequency Selectivity in the Perception of Concurrent Harmonic Sounds.**

**Christophe Micheyl<sup>1</sup>**, Andrew Oxenham<sup>1</sup>

<sup>1</sup>*University of Minnesota* Harmonic complex tones (HCTs) are an ecologically important class of sounds found in both speech and music. in everyday environments where multiple sound sources are present, listeners often have to 'track' HCT-like target sounds that occur concurrently with, and are partially occluded by other such sounds. in this study, we measured how accurately listeners could discriminate changes in the fundamental frequency (F0) of a 'target' harmonic complex tone (HCT) accompanied by an 'interferer', which overlapped with it in frequency and time. the interferer F0 was fixed at -9, 0, or +9 semitones relative to the mean target F0. Depending on the condition, the tones were bandpass-filtered into either of a LOW (800-2400 Hz) or a HIGH (1600-3200 Hz) spectral region, and the mean target F0 was either 100, 200, or 400 Hz. This design yielded different degrees of peripheral resolvability of the harmonics, making it possible to assess the role of frequency resolution on perceptual performance. in additional conditions, the interferer was presented in the contralateral ear only, which introduced a difference in perceived laterality between target and interferer and increased peripheral resolvability, or dichotically with a higher level in the contralateral ear, which also produced a difference in perceived laterality but did not enhance peripheral separation. F0 discrimination performance was dramatically impaired when the interferer



was added into the same ear as the target and there remained no resolved target harmonic in the mixture. Presenting the masker in the opposite ear substantially reduced (but did not eliminate) the interference, while presenting it dichotically did not. These findings provide further evidence for an important role of peripheral separation in the perception of concurrent harmonic sounds, and may shed further light on the selective-listening difficulties of hearing-impaired listeners in cocktail-party situations. [Funded by NIDCD R01DC05216]

#### **403 Multiple Levels of Representation in Auditory Stream Segregation: Evidence From Context Effects**

**Joel Snyder<sup>1</sup>**, Olivia Carter<sup>2</sup>, Erin Hannon<sup>1</sup>, Claude Alain<sup>3</sup>

<sup>1</sup>*University of Nevada, Las Vegas*, <sup>2</sup>*Harvard University*,

<sup>3</sup>*Baycrest Centre for Geriatric Care*

Perception is highly susceptible to influences of prior context. During repeating tone sequences of low (A) and high (B) tones in an ABA pattern, perception of two separate streams ("streaming") increases with greater frequency separation between the a and B tones; in contrast, prior exposure to an ABA context with a large frequency separation results in less streaming, even when the context occurred several seconds earlier. To further investigate this contrastive context effect, we measured streaming after exposure to a variety of different patterns. The context effect occurred at a level of representation with broad frequency tuning and did not depend on an explicit coding of frequency separation. A separate facilitative effect of perceptual context was observed, dissociating stimulus-related and perception-related context effects. Perceiving two objects in a visual analogue to stream segregation had no effect on streaming. These results suggest that auditory-specific processing at multiple levels of representation underlies effects of stimulus and perceptual context on auditory stream segregation.

#### **404 Resetting Effects of a Single Deviant Tone On the Build-Up of Auditory Stream Segregation**

**Nick Haywood<sup>1</sup>**, Brian Roberts<sup>1</sup>

<sup>1</sup>*Aston University*

The tendency to hear a tone sequence as two or more streams (segregated) builds up over time, but a sudden change in properties can reset the percept to one stream (integrated). Resetting following a single deviant tone was explored using a subjective measure of stream segregation. In each experiment, 8 listeners reported the number of streams heard in an ABA-ABA-ABA test sequence (tone duration = 100 ms, tone A frequency = 1 kHz, tone B = 4–14 semitones (ST) higher, – = silence of 100 ms). The test sequence was either presented alone or was preceded by a segregation-promoting induction sequence. The standard inducer comprised 10 tones identical to the A tones in the test sequence, and formed an isochronous sequence with them. This standard inducer was altered in various ways for the other conditions. In experiment 1, the last inducer tone was changed in frequency (–3 ST), level (+12 dB), or duration

(+50 ms), or it was replaced with silence. All these changes resulted in less reported segregation than when all inducer tones were identical, indicating substantial resetting. The extent of resetting was similar across a wide range of frequency changes on the last inducer (–0.5 to –12 ST; Experiment 2), but even smaller and less salient frequency changes produced some resetting (Experiment 3). When either the 4th, 7th or 10th (last) inducer was replaced by silence, reported segregation was reduced only when the last inducer was replaced (Experiment 4). Therefore, the resetting effect of replacement by silence cannot be attributed simply to the reduced number of inducer tones. Perception of the test sequence was unaffected by an earlier deviant tone, because the subsequent inducer tones alone caused enough build-up to obscure the resetting effect before the test sequence began (Experiment 5). Overall, it is concluded that a salient change in a single inducer just before the test sequence can cause substantial resetting in the build-up of stream segregation.

#### **405 Listening to Every Other Word: Testing the Strength of Linkage Variables in Forming Streams of Speech**

**Gerald Kidd Jr.<sup>1</sup>**, Virginia Best<sup>1</sup>, Christine R. Mason<sup>1</sup>

<sup>1</sup>*Boston University*

In a variation on a procedure originally developed by Broadbent (*J. Exp. Psychol.*, 1952), listeners were presented with two sentences spoken in a sequential, interleaved-word format. Thus, sentence one (the target) was composed of the odd-numbered words in the sequence and sentence two (the masker) was composed of the even-numbered words in the sequence. The task of the listener was to report the words comprising sentence one. The goal was to examine the effectiveness of various cues linking the words of the target over time. A variety of such "linkage variables" were examined, including: 1) fixed vs. random talker; 2) fixed vs. random apparent interaural location; and 3) sensible (proper syntactic and semantic structure) vs. nonsensible (random words) sentence form. In general, the linkage variables tested provided a significant performance advantage compared to the standard condition in which the linkage variables were unreliable. The effect of speaking rate was also examined and was found to be very subject dependent. Strong word position effects were found with greater advantages of these linkage variables occurring for the words near the end of the sentence. Overall, this approach appears to be useful for examining interference in speech recognition that has little or no peripheral component. [Supported by AFOSR and NIH/NIDCD]

#### **406 The Build-Up of Streaming Adapts to Sequence Duration**

**Daniel Pressnitzer<sup>1</sup>**

<sup>1</sup>*CNRS Université Paris Descartes & Ecole Normale Supérieure, Paris, France*

The streaming paradigm has been widely used to study the mechanisms underlying auditory scene analysis, both behaviorally and in electrophysiological studies. Typically,

a sequence of two tones of alternating frequencies is used. the first subjective report is usually of a single stream: all sounds seem to originate from a single source. the sequence then splits into two streams after a variable time, that depends on various acoustic parameters such as the frequency difference between tones or their tempo. This dynamic change in perceptual organization has been termed the 'build-up' of streaming. the build-up has a functional role as it imparts some persistence to perceptual organization. Also, it is a landmark feature that neurophysiological studies have sought to discover in single unit and brain-imaging responses. the time required to achieve build-up is thus an important characteristics of streaming.

in this study, we manipulated the duration of the streaming sequences. Sequences of 10s and 60s were used in random presentation order, and human listeners had to report continuously their subjective percepts. Tone duration was 125ms and frequency difference was 6 semitones. in half of the experimental blocks, listeners were cued to the duration of the sequence before hearing them, whereas in the other half they were not. Results showed that build-up was significantly faster for the short sequences when listeners knew the duration in advance (cued). Averaged over the 10s, 34% streaming was observed when the duration was cued but only 25% when not cued. Results were similar when blocking the durations instead of cueing, and for different frequency separations.

These results show that even for simple tone sequences, perceptual organization depends on listeners' expectancies and not only on the signal acoustic parameters. Models based on neural adaptation are compatible with such results if one posits a variable decision threshold after the adaptation process.

#### **407 Temporal Jitter Affects Perceptual Transitions in Auditory Streaming**

**Minae Okada<sup>1</sup>, Makio Kashino<sup>2</sup>**

<sup>1</sup>SHIMOJO Implicit Brain Function Project, ERATO JST,

<sup>2</sup>NTT Communication Science Labs. NTT Corporation, ERATO JST, and Titech

A repeating pattern of low-frequency (L) and high-frequency (H) tones can be perceived as one coherent stream or distinct streams. the perception of auditory streaming is stochastic and transits frequently under appropriate conditions. the dynamics of this phenomenon provides useful information on the neural mechanism of auditory streaming. in this study, the effect of temporal jitter on perceptual transitions was examined. the test sequence was a repeating triplet composed of L tone and H tone with the frequency difference of 6 semitones centered at 1kHz. the duration of each tone was 40 ms. the stimulus onset asynchrony (SOA) of adjacent L and H tones within a triplet was 100 ms, and that of neighboring triplets was 200 ms in the control condition. in the experimental condition, the SOA was randomly modulated following to the Gaussian distribution with the standard deviation (SD) of 1, 5, 10 or 20 ms. Participants reported their perception by touching the corresponding keys of a response box whenever the percept changed. the test sequences were presented for 6 minutes to the left ear

through headphones at 60 dB SPL. It was found that the temporal jitter affected the number of perceptual transitions with the maximum reduction (~30%) at the SD of 20 ms. the result suggests that auditory streaming is dynamically instable.

#### **408 Top-Down Attention Modulates Bottom-Up Streaming Based On Pitch and Location**

**Ross Maddox<sup>1</sup>, Rafael Alvarez<sup>2</sup>, Tim Streeter<sup>1</sup>, Barbara Shinn-Cunningham<sup>1</sup>**

<sup>1</sup>Boston University, <sup>2</sup>Universidad de Puerto Rico, Recinto de Río Piedras

Both pitch and location are useful for forming auditory streams (i.e., connecting events from one source across time). Typically, these two cues work together. However, past studies have explored the relative strengths of pitch and location on streaming by pitting the cues against one another and asking listeners to report the words perceived as one stream. Here, we show that the relative influence of pitch and location on streaming is modulated by which cue the listener is told to attend.

Stimuli consisted of a cue phrase with a random pitch *a* at a random location *X*, followed by a sequence of two concurrent, spoken digit pairs. in each digit pair, one digit had pitch *a* and one had a different pitch, *B*. Similarly, in each pair, one digit was at location *X* and one was from a different location *Y*. Both pitch difference,  $|A - B|$ , and location difference,  $|X - Y|$ , varied from trial to trial, taking on one of three values. Listeners were presented with identical stimuli in two different blocks—only the instructions differed between blocks. in half of the blocks, listeners were instructed to report the two digits whose pitch matched that of the cue. in the other half, listeners were told to report the digits whose location matched that of the cue.

When pitch and location coincided, the task was easy. When the cues opposed one another, listeners could do the task to some degree when attending either pitch or location, but made more errors as the attended cue got smaller or the opposing cue became larger. the most common error was to answer based on the wrong cue, against the instructions for that block.

Results demonstrate the influence of both top-down and bottom-up processes in selecting an auditory stream from a mixture. When the cues oppose one another, errors show that the unattended cue automatically promotes streaming. However, response patterns also depend on which cue the listener attends, demonstrating the influence of top-down attention.

[Work supported by ONR.]

#### **409** Cortical Indices of Auditory Segregation Revealed by Magnetoencephalography: a Parametric Study of Onset Asynchrony and Mistuning

**A.Q. Summerfield<sup>1</sup>**, S.R. Mathias<sup>1</sup>, E.E.M. Knowles<sup>1</sup>, P.T. Kitterick<sup>1</sup>, P.J. Bailey<sup>1</sup>

<sup>1</sup>*Department of Psychology and York Neuroimaging Centre, University of York, UK*

If one component of a harmonic complex tone is perturbed by mistuning its frequency or delaying its onset, the perturbed component may be heard as a sound separate from the other components. Alain et al. (JASA, 2001; 111: 990-5) used electro-encephalography to compare the cortical response to intune and mistuned stimuli. They identified a negative-going peak with a latency of 180ms in the intune-mistuned difference waveform. They named the peak the 'Object-related Negativity' (ORN) and argued that it is an index of automatic processes that segregate a mistuned component as a distinct auditory object. the present experiment tested whether the ORN is a generic index of the segregation of a perturbed component, or a particular index of segregation by mistuning.

The baseline stimulus was a 0.5-s complex tone with a fundamental frequency of 100Hz. Perturbed stimuli were created by mistuning the 6th component by 1%, 3%, or 8%, or by delaying its onset by 40ms, 80ms, or 160ms. the stimulus was presented binaurally with an interaural timing difference (ITD) of 0 $\mu$ s, with the exception of the 6th component which had an ITD of either -150 $\mu$ s or +150 $\mu$ s. Participants were required to report whether the 6th component was lateralised to the left or right on each trial to ensure that they attended to the stimuli. Stimuli were presented to eight adult participants with normal hearing while their brains were imaged with a 248-channel whole-head neuromagnetometer. Neuromagnetic responses to 100 presentations of each stimulus were corrected for ocular and cardiac artefacts, and then averaged. Difference waveforms were computed between the baseline condition and each perturbed condition.

in difference waveforms averaged over subjects, a prominent peak was found over temporal areas of the brain bilaterally, for both mistuning and delay. As mistuning increased from 1% to 3% to 8%, the latency of the peak shortened from 244ms to 187ms to 170ms. As delay increased from 40ms to 80ms to 160ms, the latency of the peak increased from 202ms to 230ms to 309ms. the timing of the peak suggests that it is the neuromagnetic equivalent of the ORN. it's occurrence, 150-250ms after the onset of a mistuned or delayed component, is compatible with the idea that the ORN reflects processes that label a component as a separate auditory object, rather than earlier processes, specific to mistuning or delay, that detect that a component is perturbed.

Acknowledgements: PTK is supported by RNID. MEG data were gathered at the York Neuroimaging Centre.

#### **410** Effects of Context On the Strength of Perceptual Grouping Cues

**Adrian KC Lee<sup>1</sup>**, Barbara Shinn-Cunningham<sup>1</sup>

<sup>1</sup>*Hearing Research Center, Department of Cognitive Neural Systems, Boston University*

often, the amount of energy that an ambiguous sound element (a target) contributes to one auditory object is reduced if there is a competing object that could logically "own" the target. Changing stimulus parameters to favor grouping the target with one object generally increases how much energy the target contributes to that object and decreases the energy it contributes to the other object, resulting in a form of perceptual trading. However, in a recent study in which only spatial cues were manipulated, perceptual trading failed. Here, we measure how an ambiguous target is allocated between two competing objects to better understand when perceptual trading occurs.

Stimuli consisted of a repeated sequence of two pure tones followed by a harmonic complex that was spectrally shaped to sound like a synthetic vowel. Listeners heard a stream of pure tones and a distinct vowel that occurred at one-third the tones' rate. in some trials, listeners identified the tones' rhythm, which depended on whether the target was heard in the tone stream. in other trials, listeners identified what vowel they heard, which depended on how strongly the target contributed to the vowel. in one block, both the spatial cues and relative frequency of tones and target varied to shift how the target contributed to the objects. in another block, only the relative frequency was changed and spatial cues were fixed. in a third block, only the spatial cues changed and the relative frequency was fixed.

in general, the target contributes more to the tones when it contributes less to the vowel, consistent with perceptual trading. However, spatial cues have less influence on how the target is allocated when both frequency and spatial cues are manipulated within a block than when only spatial cues are manipulated. Thus, the relative strength of different grouping cues depends on context, consistent with the idea that perceptual organization depends on top-down processes.

[Supported by ONR N00014-04-1-0131]

#### **411** The Time Course of Cued Informational Masking Trials

**Xiang Cao<sup>1</sup>**, Virginia Richards<sup>1</sup>

<sup>1</sup>*University of Pennsylvania*

The detectability of a tone of known frequency embedded in a multi-tone masker is poor when the frequencies of the masker components are randomly drawn. This informational masking can be reduced if an exact copy of the upcoming masker precedes a yes/no detection trial (masker cue, or MCue). in contrast, a preview of the signal-plus-masker stimulus (SMCue) does not provide a release from informational masking and post-trial presentations of MCue and SMCue are less effective than the pre-trial MCue [Richards *et al.*, 2004; J. Acoust. Soc. Am. 116, 2278–2288]. to explore the effectiveness and persistence of different types of cues, in the first

experiment detection thresholds were obtained as a function of the inter-stimulus interval (ISI) between the cue and the yes/no trial. Four types of cues were tested: MCues or SMCues, with each cue either preceding or following the detection trial. Compared to no cue, (a) the pre-trial MCue provided the largest release of masking, which persisted for as long as 4 seconds; (b) the pre-trial SMCue did not provide a release from masking; (c) the release from masking associated with post-trial cues was moderate. In the second experiment, similar conditions were tested, except in addition to random maskers, the signal, when present, had a frequency that was chosen at random. With signal-frequency randomization, pre-trial masker and signal-plus-masker cues both provided a release from masking relative to no cue. For ISIs longer than 250 ms, the cues were equally effective in reducing masking, but for ISIs less than 250 ms, the MCue gave a larger release from masking. These results suggest that the release from masking associated with pre-trial MCues reflects two processes: a short-term, potentially peripheral, process and a long-term, potentially relatively central, process. Moreover, there was no evidence for a short-term process associated with the SMCue. [Supported by NIH RO1 DC00212].

#### **[412] A Measurement of Dissimilarity for Stimuli Used in Informational Masking Experiments**

**Thomas Lee<sup>1</sup>**, Virginia Richards<sup>1</sup>

<sup>1</sup>*University of Pennsylvania*

Previous experiments have shown that introducing dissimilarity between a signal and a masker leads to a release from the large masking effects found in informational masking. The present study attempts to better understand the nature of this detection threshold reduction by incorporating an independent measure to determine the degree of dissimilarity. In the first experiment, listeners discriminated a multitone complex from each of four qualitatively different stimulus types (pure tone, frequency glide, amplitude-modulated tone, and a series of equal-frequency tone pips). The stimuli were presented in 50 dB SPL pink noise and were equally detectable. Estimates of  $d'$  were found to negatively correlate ( $r = -0.7$ ) with detection thresholds when these four stimulus types were used as signals embedded in a multitone informational masker. In other words, the signal that was most easily discriminated from the multitone complex (the frequency glide) had the lowest detection threshold in an informational masking task. In a follow-up experiment, the relationship between discriminability ( $d'$ ) and detection threshold was explored further by varying the slope of the frequency glide. The preliminary results are consistent with the first experiment and demonstrate that glides with steeper slopes are easier to discriminate from a multitone complex and easier to detect in a multitone masker than glides with shallower slopes. [Supported by NIH DC002012]

#### **[413] Dip-Listening with Vcoded Speech in Steady and Fluctuating Noise**

**Antje Ihlefeld<sup>1</sup>**, Robert P. Carlyon<sup>2</sup>

<sup>1</sup>*MRC Cognition & Brain Sciences Unit; BU Hearing Research Center*, <sup>2</sup>*MRC Cognition & Brain Sciences Unit*

Normal-hearing (NH) listeners are better at identifying target speech in fluctuating noise than in steady noise, a finding attributed to "dip listening". However, this benefit is reduced in cochlear implant (CI) users and in NH subjects listening to "vocode" simulations. Here, we examined whether simple spatial cues can improve the ability to utilize advantageous signal-to-noise ratios (SNR) in the dips of the fluctuating noise for identifying vocoded speech. Using four-band 1) noise-vocoded or 2) sine-vocoded speech (50-Hz envelope cutoff) or 3) unprocessed speech stimuli, we measured speech identification in NH listeners in a series of experiments (Coordinate Response Measure task). Subjects listened over headphones to target speech in their right ear. Noise was played concurrently, either only to the right or to both ears, was spectrally matched to the target speech, and was either steady or square-wave amplitude modulated (AM). Average performance was better for diotic versus monotic presentation of the noise. For unprocessed speech performance was better with AM than steady noise, but this 'modulation advantage' was greatly reduced for noise vocoded stimuli, regardless of whether the masker was monotic or diotic. This suggests that spatial cues by themselves are not sufficient to aid dip-listening. However, a large modulation advantage was obtained for sine-wave-vocoded speech, suggesting that dip-listening can be restored by introducing quality differences between the masker and target [Supported by Otology Research Fund.]

#### **[414] Comodulation Masking Release in the Perception of Vocalizations by Gray Treefrogs**

**Alejandro Velez<sup>1</sup>**, **Mark A. Bee<sup>1</sup>**

<sup>1</sup>*University of Minnesota*

Natural acoustic scenes exhibit correlated ("comodulated") fluctuations in amplitude across the frequency spectrum. Psychophysical studies of comodulation masking release (CMR) and the comodulation detection difference (CDD) in humans and other animals (e.g., European starlings) indicate that the detection of relatively simple signals (e.g., tones and narrowband noises) is improved when maskers are comodulated. While there is some debate about the importance of CMR-like processes to human speech perception, such processes could play potentially important roles in the vocal communication systems of other animals. Gray treefrogs (*Hyla chrysoscelis*) represent a simple but extreme case in which comodulation in natural acoustic scenes may be important in acoustic signal processing. In order to reproduce, females must detect, recognize, localize, and discriminate among male mating calls in the cacophony of a noisy breeding chorus. The gray treefrog peripheral auditory system has two anatomically distinct sensory epithelia that are tuned to separate spectral peaks in male calls (1.3 kHz and 2.6 kHz). The background noise of a chorus is

characterized by two narrow bands of sound that are inherently comodulated due to the obligate production of both spectral peaks in the calls of individual males. Using female phonotaxis toward mating calls as a behavioral assay, we have found that females experience a 5-dB release from masking when two bands of a "chorus-shaped" noise are comodulated over conditions in which the two bands are either unmodulated or incoherently modulated. Given that the two spectral peaks comprising mating signals and chorus noise are largely encoded by separate sensory epithelia in the inner ear, gray treefrogs represent a superb animal model for investigating the contribution of within-channel and across-channel mechanisms to masking release in comodulated noise. [Work supported by NIDCD R03DC008396 to MAB.]

#### **415 Role of Temporal Fine Structure and Spectral Cues in Speech Masking Release**

**Dan Gnansia<sup>1</sup>, Bertrand Philippon<sup>2</sup>, Christian Lorenzi<sup>3</sup>**

<sup>1</sup>CNRS, Paris 5 Univ, ENS, MXM-Neurelec, <sup>2</sup>MXM-Neurelec, <sup>3</sup>CNRS, Paris 5 Univ, ENS

Speech "masking release" (MR) corresponds to the improvement in speech intelligibility in fluctuating compared to steady-state background maskers. This effect is substantial in normal-hearing listeners, reduced in hearing-impaired listeners, and abolished in cochlear implantees. This research attempted to clarify the contribution of temporal fine structure (TFS) and spectral (place of excitation) cues to the MR effect.

To address this issue, MR was assessed in eight normal-hearing listeners using speech and noise stimuli processed in order to degrade independently or jointly spectral and TFS cues between 80 and 8,020 Hz. Stimuli were vowel-consonant-vowel logatomes embedded in a steady-state or fluctuating speech-shaped noise masker. They were presented at a fixed signal-to-noise ratio yielding 50% correct identification in steady noise. Fluctuations were obtained by modulating sinusoidally the amplitude of noise at 8-Hz (100 %). for unprocessed stimuli, maximum MR (performance in fluctuating minus steady noise) was about 35 percentage points.

in a first experiment, spectral cues alone were degraded using a spectral smearing technique attempting to preserve phase information. Results showed that MR dropped by 15 percentage points (from 35 to 20 points) when spectral cues were smeared by a factor of 4.

in a second experiment, TFS cues were degraded using a tone vocoder. Spectral cues were either preserved or degraded by decreasing the number of frequency bands of the vocoder from 32 (1-ERB wide bands) to 8 (4-ERB wide bands) bands. Results showed that MR dropped by 13 percentage points when TFS cues alone were removed (i.e., when 32 bands were used) and was nearly abolished (MR=5 points) when spectral cues were additionally degraded by a factor of 4 (i.e., when 8 bands were used).

The respective and combined contributions of TFS and place cues to MR will be discussed by taking into account potential effects of the spectral smearing technique on TFS transmission.

#### **416 Combinatory Contributions of Temporal Envelope and Fine Structure Cues to Speech Perception in Noise**

**Aparajita Bhattacharya<sup>1</sup>, Emma Moradoghli-Haftevam<sup>1</sup>, Paola Cespedes<sup>1</sup>, Fan-Gang Zeng<sup>1</sup>**

<sup>1</sup>University of California Irvine

Studies on cochlear-implant (CI) users and normal-hearing (NH) listeners tested with CI simulations have shown that envelope (E) cues are sufficient for understanding of speech in quiet. However, the performance degrades sharply in the presence of background noise. One potential reason for poor performance in noise is the lack of temporal fine structure (TFS) information. This study attempts to investigate the relative contributions of temporal envelope and fine structure cues to speech perception in noise.

The stimuli consisted of 16 a/C/a consonants in quiet and in steady-state speech-spectrum-shaped noise at signal-to-noise ratios (SNRs) from -10 dB to +10 dB in 5 dB steps. the 80-8020 Hz signals were band-pass filtered into 16 0.4 octave-wide frequency bands and processed to obtain three kinds of stimuli, intact-speech, E-speech and TFS-speech (Gilbert and Lorenzi, 2006). Hilbert transform was used to decompose signals from each band into E- and TFS-components. the E-components were summed to obtain the E-speech, which was essentially an acoustic simulation of 16-channel cochlear implant. the TFS-components were summed to obtain the TFS-speech.

Six NH listeners were tested on four conditions: Intact, E, TFS and E+TFS, respectively. in the first three conditions, the intact-, E-, or TFS-speech was presented monaurally to the right ear. in the E+TFS condition, speech was presented diotically, with E-speech presented to the right ear and TFS-speech presented to the left ear. the subjects were trained for each condition using stimuli in quiet. Performance with intact speech was higher compared to that with both E-speech and TFS-speech in all conditions. Performance deteriorated with decreasing SNR in all conditions. Performance with E-speech was approximately 10 percentage points higher compared to that with TFS-speech in quiet and also averaged over all noise conditions. Performance in the E+TFS condition was 16 percentage points higher than that in E condition and 26 percentage points higher than that in TFS condition, averaged over all noise conditions. However, the E+TFS performance was still lower than the intact condition, particularly at lower SNRs (approximately 8 percentage points averaged over 0, -5 and -10 dB SNRs). These results showed that E and TFS cues provide independent information and may be linearly combined to contribute to understanding speech in noise. Implications of these results to auditory prostheses will be discussed.

#### **417 Effects of Hearing Impairment and Aging On Speech Intelligibility for Speech At Different Rates**

**Aaron Wolfson<sup>1</sup>, Steve Colburn<sup>1</sup>**

<sup>1</sup>Boston University

Both aging and hearing impairment are known to cause reductions in speech reception; however, in elderly

hearing-impaired subjects, the relative contributions are unknown. Some studies suggest that decreased speech understanding in elderly hearing-impaired listeners is linked to a reduction in binaural processing ability. for those without hearing impairment, age-related declines in temporal processing abilities might be an additional factor causing poor speech understanding. Conducting experiments at accelerated speech rates might expose such factors. in the current study, we aim to separate the effects that aging and hearing impairment have on speech understanding by performing speech intelligibility experiments on young normal, young hearing-impaired, elderly normal and elderly hearing-impaired listeners. the experiments measure monaural and binaural speech reception thresholds for spatially separated speech (80 degrees right of centerline) and speech-shaped noise (at centerline) waveforms. These measurements are made at three speech rates (2, 4, and 6 syllables/second) to investigate the speech-rate dependence of binaural processing. Each sentence consists of four, single-syllable words drawn from four groups of eight words, which allows stable performance with extended testing after familiarity is established. Thresholds are measured adaptively, with target level held constant while masker level is varied. Results to date suggest that speech understanding in elderly hearing-impaired subjects degrades faster than young-normal subjects for the same increase in speech rate. Further, young-normal subjects exhibit a larger two-ear advantage over the elderly hearing-impaired subjects when given binaural information versus monaural information alone. Data comparisons will also include young hearing-impaired and elderly normal subjects.

#### **[418] Modeling the Effects of Selective Hair-Cell Damage On Concurrent Vowel Identification**

**Ananthakrishna Chintanpalli<sup>1</sup>, Michael Heinz<sup>1</sup>**

<sup>1</sup>*Purdue University*

Normal-hearing (NH) listeners have a remarkable ability to understand speech in complex acoustic environments. Psychophysical studies of concurrent vowel identification have shown that NH listeners can take better advantage of differences in fundamental frequency (F0) than listeners with sensorineural hearing loss (SNHL). Several computational models have been proposed for the use of F0 differences in concurrent vowel identification by NH listeners. the present study seeks to predict the effects of selective outer-hair cell (OHC) and inner-hair cell (IHC) damage on the ability to use F0 differences in a concurrent vowel identification task.

This study utilized the same set of vowels used by Assmann and Summerfield (JASA, 1990). in each stimulus, one vowel had F0 = 100 Hz and the other vowel had an F0 that was 0, 0.25, 0.5, 1, 2 or 4 semitones higher. We propose a physiologically realistic model by cascading normal or impaired versions of an auditory-nerve (AN) model (Zilany and Bruce, JASA, 2007) with an F0 segregation algorithm (Meddis and Hewitt, JASA, 1992). the AN model was used to generate four different

hearing conditions: NH, flat losses based on selective OHC or IHC damage and mixed OHC and IHC damage.

Preliminary results show that overall identification and F0 benefit (the difference in identification between 0 and 4 semitones) are both reduced relative to NH for all three hearing losses considered, consistent with previous psychophysical studies. in the case of OHC damage, reduced F0 benefit appears to be related to a reduced ability to segregate the two vowels prior to identification.

Future work involves comparing the specific confusions made in the cases of OHC and IHC damage, which may provide additional insight into the relative contributions of selective hair cell damage to the difficulty listeners with SNHL have in understanding speech in complex acoustic environments.

Partially supported by NIH/NIDCD grant R03-DC007348.

#### **[419] Phoneme Representation in the Human Electrocorticography (Ecog) Signal.**

**Woosung Kim<sup>1</sup>, Nick anderson<sup>1</sup>, Gerwin Schalk<sup>2</sup>, Eric. C. Leuthardt<sup>3</sup>, Dennis. L. Barbour<sup>1</sup>**

<sup>1</sup>*Department of Biomedical Engineering, Washington University, St. Louis, MO, USA,* <sup>2</sup>*Brain-Computer Interface R&D Program, Wadsworth Center, NYS Department of Health, Albany, NY,* <sup>3</sup>*Department of Neurological Surgery, St. Louis Children's Hospital, St. Louis, MO*

Brain computer interfaces (BCIs) provide communication links for patients with neurological or somatic disorders to interact with external devices such as artificial limbs, mobility devices and communications devices. BCIs need robust brain signals in order to transfer the user's intention successfully both for lower bandwidth applications such as simple movement and especially for higher bandwidth applications such as linguistic communication. Electroencephalography (EEG) represents a standard method of detecting brain signals, but suffers several drawbacks in terms of brain signal representation including limited spatial resolution and frequency bandwidth, susceptibility to noise and the need for extensive user training.

An alternative to the EEG is the electrocorticogram (ECoG). ECoG signals are derived from electrodes placed directly on the dural or pial surface. While invasive, ECoG may overcome some of the limitations of and issues with EEG. in the current study, we used ECoG signals recorded in naïve human patients to assess how phoneme identity may be extracted from these brain signals.

Thirty-six consonant-vowel-consonant (CVC) words were delivered to the subjects under ECoG recording conditions. Four different vowels were represented with nine different beginning/ending consonant combinations. the words were presented randomly either in spoken form or spelled out on a computer screen. Subjects were asked to repeat the words, and their verbal responses were recorded, along with the voltage signals from an array of ECoG electrodes distributed at 1 cm spacing in a square grid over the left hemisphere. ECoG signals demonstrated high-frequency activation as a function of the task, with consistent activation of the left anterior and posterior inferior frontal

lobe as well as the left superior temporal lobe. the spatial pattern of activation evolved over the course of the word presentation and repetition.

Speech information is clearly present in ECoG signals at frequencies inaccessible to EEG. ECoG therefore represents a promising modality for extracting communication signals from the brain for use in a BCI.

#### **420 Influence of Musical and Linguistic Experience On Early Cortical Processing of Pitch Contours**

**Bharath Chandrasekaran<sup>1</sup>, Ananthanarayan Krishnan<sup>1</sup>, Jackson Gandour<sup>1</sup>**

<sup>1</sup>*Purdue University*

The relative influence of musical training and experience with linguistically-relevant pitch contours on early cortical processing of pitch contours was evaluated using the mismatch negativity (MMN) component. MMNs were recorded using an oddball paradigm in response to nonspeech (iterated rippled noise, IRN) stimuli under two conditions; 1. homologues of Mandarin tones (T1, 'high level' vs. T2, 'high rising'); and 2. T2L (a linear approximation of T2) vs. T2 'high rising'] from English musicians, English nonmusicians, and Chinese listeners (n=11 per group). We also collected discrimination judgments from the same subjects for the two stimulus pairs (T1/T2, T2L/T2). Irrespective of condition, musicians and Chinese subjects showed larger MMN responses when compared to nonmusicians. That is, both musical and language experience modulate MMN responses to nonspeech pitch contours. Relative to musicians, Chinese subjects showed larger MMN responses for both conditions (T1/T2, T2L/T2). Thus, the domain of experience (language vs. music) influences the degree of modulation. Behaviorally, Chinese were less accurate than musicians or nonmusicians in overt discrimination between T2L and T2. At an attentive level of processing, the difference between the two rising stimuli was judged to be a within-category phonetically irrelevant shift. This disparity between MMN and behavior for the Chinese group argues against top-down modulation of the MMN. Instead, in line with previous findings of enhanced representation of pitch contours at the level of the brainstem for native Chinese speakers and nonnative musicians, we argue for bottom-up modulation of the MMN, the degree of magnitude being determined by the specific nature of experience. Findings are highlighted to address similarities in processing schema between music and language during early preattentive cortical analysis of pitch contours.

#### **421 Preliminary Evidence of a Cortical Network for Spatial Listening in Multi-talker Environments as revealed by Magnetoencephalography (MEG)**

**Padraig T. Kitterick<sup>1</sup>, Isabella Paul<sup>2</sup>, Peter J. Bailey<sup>1</sup>, A. Quentin Summerfield<sup>1</sup>**

<sup>1</sup>*Department of Psychology, University of York,*

<sup>2</sup>*Departments of Clinical Psychology and Neuropsychology, University of Konstanz, Germany*

We are using MEG to address two questions about the processes involved in listening to a single talker in the presence of other talkers: 1) is it possible to identify cortical areas that respond to the onsets of all talkers whether or not they receive attention, and 2) what is the network of cortical regions that are active when attention is sustained to a single talker.

On each trial, a binaural 'spatial' recording of seven 3-s phrases was presented so that a new phrase started every 0.8s. Phrases had the form 'Ready <<CALL-SIGN>>, go to <<COLOUR>> <<NUMBER>> now', with eight possible CALL-SIGNs, four COLOURs, and four NUMBERs. Subjects listened out for the target phrase in each sequence, identified by a unique call-sign, and reported the colour and number coordinates in that phrase by making button presses. the target phrase occurred randomly in either the 3rd, 4th, or 5th slot in each sequence of phrases. Data were recorded from ten normally-hearing young-adult participants using a 248-channel whole-head neuro-magnetometer and were averaged separately for each of the three possible target positions, over trials on which both responses were correct. to identify target-related activity, an average measure of phase coherence was computed for each sensor between the three positional averages synchronised to the start of the target call-sign, from 0.5-4Hz.

Visual inspection identified seven peaks, time-locked to the seven phrase onsets, in sensors over left and right primary auditory areas. High levels of phase coherence were found sequentially in sensors located over three regions: left pre-frontal cortex, and left and right temporal cortex.

These preliminary analyses suggest that pre-attentive responses to all voices in a mixture are found in primary auditory areas. Slow-wave activity, possibly related to the analysis of information-bearing words leading to sustained attention to a talker, occurs first in left-frontal regions and subsequently in left- and right-temporal regions.

**Acknowledgements:** PTK is supported by a studentship from RNID. MEG data were gathered at the York Neuro-imaging Centre.



## **422 Perceptual Clarity of Speech Modulates Activity in Left Temporal-Lobe Regions:**

**Evidence From Fmri for Top-Down Influences**  
Conor Wild<sup>1</sup>, Matthew Davis<sup>2</sup>, Alexis Hervais-Adelman<sup>3</sup>, Ingrid Johnsrude<sup>4</sup>

<sup>1</sup>*Centre for Neuroscience Studies, Queen's University, Kingston, ON, Canada,* <sup>2</sup>*MRC Cognition and Brain Sciences Unit, Cambridge, UK,* <sup>3</sup>*Department of Physiology, Cambridge University, UK,* <sup>4</sup>*Department of Psychology, Queen's University, Kingston, ON, Canada*

Feedback connections within and among auditory cortical regions may allow cognitively 'higher' levels of processing to act predictively on a bottom-up signal in order to perceptually organize and/or 'explain' it. Behavioral evidence supports the idea that perception is guided by mechanisms that compute an input's most probable interpretation. For example, four-band noise-vocoded (NV) speech, which is largely unintelligible to naive listeners, becomes perceptually clear when listeners possess prior knowledge of the signal content – a phenomenon we call 'pop-out'. In the present study, we use fMRI to investigate whether activity elicited in auditory cortex by a noise-vocoded utterance is modulated depending on how coherent and identifiable the stimulus is. Specifically, we employ written 'primes' – matching (M) or non-matching (NM) text strings – to manipulate a subject's perception of single NV words, thereby creating acoustically matched conditions that elicit the perceptions of intelligible or unintelligible speech. Whole brain fMRI data were gathered from 21 right-handed subjects using a Siemens Trio 3-Tesla MRI system, and sparse-imaging procedure (TA = 2 sec; TR = 11 sec). Preliminary analysis reveals multiple regions of statistically significant signal change along the left superior and middle temporal gyri (STG) and superior temporal sulcus (STS) for the interaction contrast (NVM - NVNM) - (ClearM - ClearNM). This activity cannot be due to acoustic differences between NV and clear speech, but is likely to reflect the perceptual clarity resulting from top-down influences. This result is consistent with recent research that shows the posterior STS to be sensitive to the perception of sounds as speech, and not to the complex acoustic features of speech. Future work will explore the network underlying perceptual pop-out by examining how signal within a region, and functional coupling among regions, is modulated by condition type.

## **423 Evaluation of Mandarin-Chinese Tone Production with an Artificial Neural Network**

Ning Zhou<sup>1</sup>, Chao-Yang Lee<sup>1</sup>, Li Xu<sup>1</sup>

<sup>1</sup>*Ohio University*

The purpose of the study was to develop an artificial neural network as an objective tool for evaluating lexical tone production. Speech data consisted of tone tokens recorded from 29 normal-hearing, native Mandarin-speaking adults. The F0 contours of the vowel part of the tone tokens were extracted using an autocorrelation method. The efficacy of the neural network was tested by varying the number of inputs as well as the number of neurons in the hidden layer. The sensitivity of the neural network to speaker variation was tested by 1) using raw F0

data from a number of speakers that varied from 1 to 29 and 2) using raw F0 data from either male- or female-only speakers. Two normalization procedures were compared in their efficacy of reducing speaker variation. The performance of the neural network was compared with that of 10 native Mandarin-speaking listeners. Three inputs and four hidden neurons were found to be sufficient for the neural network to perform at approximately 85% correct using raw speech data. The performance of the neural network was affected by across-speaker, especially between-gender variations. The variations could be effectively reduced after the normalization procedure based on tone 1. Using this normalization procedure, the overall recognition of the neural network and that for each tone achieved human listener-like accuracy. This indicates that the auditory system might use a similar mechanism to normalize tones from different speakers. The success of our neural network in recognizing tones from multiple speakers suggests its potential use for clinical evaluation of tone production.

[Work supported by NIH/NIDCD grant R03-DC006161.]

## **424 Perception of Gestural Information in Words with Deleted Sections**

Pierre Divenyi<sup>1</sup>, Adam Lammert<sup>2</sup>, Barbara Shinn-Cunningham<sup>3</sup>

<sup>1</sup>*VA Northern California Health Care Systems and East Bay Institute for Research and Education,* <sup>2</sup>*East Bay Institute for Research and Education,* <sup>3</sup>*Boston University*

Several years ago, Warren [Science 167, 1970] began a series of studies on intelligibility of speech from which half- or whole-syllable-length segments were cut and replaced with silence or various kinds of noise. Unfortunately, those studies did not obtain the actual confusions for instances of imperfect restoration. The present study employed a variant of Warren's original paradigm to examine the information available in disyllabic English words – words with their middles cut out and replaced with various fillers. The words consisted of both (a) true English spondees and (b) concatenated pairs of true monosyllabic words that are absent from the dictionary in conjunction. They were recorded by two male speakers. Three cut-out widths were examined in four filler conditions: silence, unmodulated speech-spectrum Gaussian noise, the same noise amplitude modulated by the envelope of the cut-out segment, and a low-pass (700 Hz) sawtooth wave having the fundamental frequency of the cut-out speech (zero for unvoiced phonemes). Five normal-hearing young listeners served as subjects. They were told that all stimuli were pairs of true English monosyllabic words and were asked to type what they heard. Talkers and listeners were native American English speakers. Stimuli and responses were transcribed into phoneme sequences and represented as 9 continuous gestures functions (using software developed at Haskins Labs,

[www.haskins.yale.edu/tada\\_download/index.html](http://www.haskins.yale.edu/tada_download/index.html)) a k-means cluster analysis of the results shows that the amount of stimulus-to-response information transmitted differs from one gesture to another, that it increased as the width of the cut-out decreased, and that the gestures continued to persist over periods during which the speech

was cut and/or replaced by fillers. Speech gestures appear to offer a way to represent intelligibility confusions in continuous rather than discretized phonemic form. [Supported by grants from NSF, AFOSR, and the VA Medical Research]

#### **425 Impaired Speech Discrimination in Rats in the Presence of White Noise**

**Benjamin Porter<sup>1</sup>**, Jesse Alaniz<sup>1</sup>, Crystal Engineer<sup>1</sup>, Michael Kilgard<sup>1</sup>

<sup>1</sup>*University of Texas at Dallas*

Masking characteristics of speech and noise are extensively studied topics in humans. Developing a non-human model for the examination of noise effects would lend aid in the development of treatments for multiple types of hearing loss that are not easily studied in humans. the ability to discriminate human speech sounds has been displayed by Sprague-Dawley rats using a go/no-go task with considerable success. Using the same methodology, conditions of speech were tested in the presence of different noise levels. a stimuli set of three females and three males saying the monosyllables /dad/ and /tad/ was generated and shifted one octave higher into the rats hearing range. Two discrimination tasks were created from this stimulus set. One task required the animals to differentiate three males and three females saying the word /dad/ from the same six people saying the word /tad/. a second task divided the stimuli by gender and the animal was required to identify behaviorally if the speaker was male or female. Speech was played at a constant 55 dB while a white noise background was played in intensities varied by block. Gender discrimination had a gentle decline in performance as the noise level increased and were still able to perform above chance when the noise was played at 67 dB. the multi-talker discrimination showed an immediate drop in performance to chance level at the introduction of the lowest level of noise (43 dB). Further physiological and lesion studies will clarify the biological basis for observations.

#### **426 Speech Perception by Humans and Birds: Effects of Syllable Duration**

**Thomas Welch<sup>1</sup>**, Micheal Dent<sup>1</sup>, James Sawusch<sup>1</sup>

<sup>1</sup>*University at Buffalo - SUNY*

in order to test whether knowledge of language is necessary to show typical speaking rate effects in the perception of human speech, budgerigars (*Melopsittacus undulatus*) and zebra finches (*Taeniopygia guttata*) were trained to categorize the endpoint stimuli from four synthetic continua consisting of CV and CVC stimuli, with both short and long syllable-final phoneme durations. This comparative approach aims to shed some light on whether or not knowledge of language has a role in rate normalization effects, such as using duration information as an indicator of speaking rate in human speech perception. Humans and birds were then tested on the exact same sets of full ten-step continua and their performance was compared in terms of their identification of phoneme boundaries along the /b/-/w/ stop-glide continua. Birds were trained to respond differentially to

endpoint syllables beginning with /b/ and /w/. Overall, zebra finches, who are different from budgerigars in that they cannot mimic human speech, were poor at categorizing the human speech tokens and only very few could even categorize two endpoints above criterion performance to move onto testing. Birds that successfully identified endpoint stimuli showed similar identification results to humans when tested on the full continua. the implications of these data and comparisons between birds and humans regarding the effect of phoneme duration (as in human speaking rate) on phonetic boundary placement will be discussed.

#### **427 NIDCD Research Training and Career Development Workshop**

**Daniel Sklare<sup>1</sup>**, Melissa Stick<sup>1</sup>

<sup>1</sup>*National Institute on Deafness and Other Communication Disorders, National Institutes of Health*

This is one of two concurrent workshops conducted by NIDCD staff to provide an overview of the NIH and NIDCD funding opportunities for budding and new investigators. This workshop seeks to help doctoral students, postdoctoral fellows, medical residents and junior faculty members understand the process of application, review, and award of the NIH fellowship (F-series) awards and the career development (K-series) awards for basic scientists and clinician-scientists. the NIH programs providing repayment of educational loans will also be covered. These funding mechanisms will be considered within the continuum of planning and staging one's academic research career. Information needed to help navigate the transition from the training stage to the independent NIH-funded principle investigator career stage will be discussed, particularly how to avoid mistakes commonly observed in the review process. Ample time will be provided for questions of general interest. Individualized, follow-up discussions will be scheduled.

#### **428 NIDCD Grant Funding Workshop for New Investigators Transitioning to an Independent Research Career**

**Bracie Watson<sup>1</sup>**, Shiguang Yang<sup>1</sup>

<sup>1</sup>*NIDCD*

This is one of two concurrent workshops conducted by NIDCD staff. This workshop will provide essential information for junior scientists seeking to obtain their first research project grant. are you a postdoctoral trainee who is now ready to transition to independence? Have you recently transitioned to independence, e.g. accepted a new faculty position, and are in the early stages of establishing your own independent laboratory/research program? If so, this workshop is targeted to you. It is intended for both basic and clinical scientists. We will present an overview of the NIDCD R03 Small Grant Program, review special efforts put forth by NIDCD/CSR to facilitate the most expeditious route to funding possible for New-Investigator initiated R01s, and clarify the roles of NIH program, review, and grants management staff. Furthermore, frequently asked questions and commonly observed mistakes made by new Pis will be covered.

Finally, we will leave ample time to answer your questions about preparation of your application, eligibility and the scientific review process. the goal is for you to gain a better understanding of the process of application, review, and award for the NIDCD Small Grant (R03) and NIDCD New-Investigator R01 award.

#### **429 Music and Deafness**

**J. Tilak Ratnanather<sup>1</sup>**, Charles Limb<sup>1</sup>

<sup>1</sup>*The Johns Hopkins University, Baltimore, MD 21218, USA*

Several notable hearing-impaired individuals ranging from the composer Beethoven to the percussionist Evelyn Glennie have become accomplished musicians. Due in large part to recent advances in technology built upon discoveries in the auditory sciences, it is possible for profoundly deaf children and adults to play and learn music to a degree formerly considered impossible. This is evidenced both by the academic music curriculum at the Mary Hare School for the Deaf in England and the growth of the Adult Musicians with Hearing Loss organization which focuses on issues faced by musicians with hearing loss. These accomplishments raise several questions. How is this degree of musical aptitude possible in the hearing impaired? What can auditory scientists learn from educators of deaf children in teaching music? What can auditory scientists learn from deaf musicians? How have changes in hearing aids and cochlear implants helped deaf individuals to learn music? What are the limitations of hearing aids and cochlear implants observed in the music classroom that need to be studied by the auditory scientists? with these questions as the framework for discussion, the workshop is an opportune time for the auditory scientists to exchange ideas and experiences with both educators of the deaf and deaf musicians. the workshop will also include a couple of performances by deaf musicians.

#### **430 Music and Deafness: an Overview**

**Charles Limb<sup>1</sup>**

<sup>1</sup>*Johns Hopkins University School of Medicine*

Music has generally been regarded as categorically unattainable for individuals with profound hearing impairment. Growing awareness of the capacity of deaf individuals to process musical stimuli, together with the impact of cochlear implantation on auditory rehabilitation, have led to tremendous recent interest in the relationship between music perception and deafness. This presentation will introduce the major issues that will be covered in the symposium on Music and Deafness, and review recent studies on cochlear-implant mediated perception of music.

#### **431 Music Has No Bars – a Deaf Musician's Odyssey**

**Ruth Montgomery<sup>1</sup>**

<sup>1</sup>*Mary Hare Schools for the Deaf, Newbury, England, RG14 3BQ, UK*

Ms. Montgomery became the first profoundly deaf (prelingual) person to obtain a degree in Music. Born into a musical family, and first learning the piano, it wasn't until she went to Mary Hare Grammar School for the Deaf that she began learning the flute. in 2005, she graduated from the Royal Welsh College of Music and Drama with a cum laude degree in Music Studies, having already obtained diplomas in Flute Performance and Teaching. She then performed as soloist with three top orchestras in St.Petersburg, Moscow and London for the Music of Life Foundation.

She will discuss the challenges of music performance as a deaf musician, and those she has faced in the long road to her current position. "How do you know you are in tune with your own instrument and with other instruments?" is a question very frequently asked of Ruth – she will try to explain just how exactly she manages this along with other commonly asked questions. She will also describe how reliant she is on her old analogue hearing-aids as digital replacements have tended to block out sounds other than speech causing the higher flute and other musical frequencies to be cut off.

#### **432 Music Lost and Found**

**Richard Reed<sup>1</sup>**

<sup>1</sup>*C.I. Music*

Music is subjective: one person's comforting old favorite is someone else's noisy torture. This presentation demonstrates, first-hand, music as perceived through one person's cochlear implant. Using a piano or digital keyboard, the pre- and post-activation day auditory experience is simulated in informative and entertaining ways. Attendees will hear the strange aural sensations of environmental sounds and voices- some of them oddly musical- as heard with a CI; and how these sounds improved over time. Sometimes including a Rock & Roll road tale or two- and always a couple of poignant late-deafened stories- the presentation is geared toward an understanding of CI music perception and appreciation. with simple notes and scales, working through melodies, harmonies and whole songs, it's one person's light-hearted (and hopefully uplifting) tale of music lost and found. the soundtrack is mostly old R&B, the encore all Q&A. a Rock & Roll and R&B musician, Richard Reed has played Hammond organ and piano with Junior Walker and the All Stars, Roomful of Blues, Otis Rush, Hubert Sumlin, Earl King, and many others. After losing his hearing to ototoxic meds- with music itself a contributing factor- Richard retired from the music business, and used a succession of increasingly powerful hearing aids. in 2002, cochlear implant surgery allowed him to eventually appreciate and play music again. Richard writes about the CI experience- most recently in the August '07 issue of Esquire Magazine- and is an independent advocate for the international hearing loss community.

### **433 Music Perception with Cochlear**

#### **Implants**

Jay Rubinstein<sup>1</sup>, Ward Drennan<sup>1</sup>, Jillian Crosson<sup>2</sup>, Kaibao Nie<sup>1</sup>, Jong Ho Won<sup>1</sup>, Robert Kang<sup>1</sup>

<sup>1</sup>University of Washington, <sup>2</sup>Cochlear Americas

The Clinical Assessment of Music Perception (CAMP) test has been developed and validated at the University of Washington (Nimmons et al, 2007; Kang et al, submitted). It is being used in two multicenter assessments of music perception in cochlear implant listeners, sponsored by Cochlear Americas and Advanced Bionics. Data from the Cochlear study confirms the validation work in nine centers in the US and Canada. the CAMP test assesses pitch direction discrimination, isochronous melody recognition and musical instrument (timbre) identification. Strong correlations with speech perception in quiet and in noise have been measured. in addition, the multicenter CAMP studies provide the first broad assessment of musical abilities in implant recipients as the target population is much more diverse than the validation group.

(Supported by NIH grant R01DC007525, Cochlear Americas and Advanced Bionics Corporation)

### **434 Teaching Music to Deaf Children in a Deaf School**

Christine Rocca<sup>1</sup>

<sup>1</sup>Mary Hare Schools for the Deaf, Newbury, England, RG14 3BQ, UK

in the United Kingdom, the Mary Hare School for the Deaf ([www.maryhare.org.uk](http://www.maryhare.org.uk)) is the national grammar school for the deaf that prepares academically able deaf children and teenagers for national qualifications permitting them to attend universities or obtain vocational training in the mainstream. Mary Hare is believed to be the only special deaf school in the world to offer music as a fully-fledged academic discipline. in the past 10 years, some 30 deaf children and teenagers of varying degrees of hearing loss have obtained academic qualifications in music in addition to those in traditional subjects.

The music programme at Mary Hare School will be described in some detail focusing on the challenges posed by hearing aids and cochlear implants, music perception by children of a wide range of hearing losses and the benefits for auditory training. Additionally, work in the specific area of music therapy for deaf children with additional handicaps such as autism will be described.

### **435 Role of retinoic acid in anteroposterior axial specification of the inner ear**

Jinwoong Bok<sup>1</sup>, Doris Wu<sup>1</sup>

<sup>1</sup>National Institute on Deafness and other Communication Disorders

Acquisition of axial identities from surrounding tissues is an early step in inner ear development. While recent studies revealed that signals emanating from the hindbrain play a critical role in the specification of dorsoventral axis, tissues and signals responsible for conferring anteroposterior (AP) axial identity to the inner ear are still

elusive. Recently, *Tbx1*, expressed in the posterior otic area, was shown to restrict anterior, neurosensory fate and was proposed to be an important determinant of AP axial identity within the inner ear. Thus, any extra-otic signal that induces/regulates *Tbx1* expression in the otic tissue is likely to be important in specifying the AP axis of the inner ear. Retinoic acid (RA) secreted from the somites is a posteriorizing signal for specifying individual rhombomeres along the AP axis of the hindbrain. Interestingly, RA signaling appears to be active only in the posterior otic cup area, as shown in a RARE-lacZ mouse strain, in which  $\beta$ -gal expression is driven by a retinoic acid responsive element. Thus, to test whether RA plays a role in conferring the posterior identity to the inner ear, we implanted RA soaked beads to the developing otic cup in chicken. We observed an upregulation of *Tbx1* in the anterior region of the implanted ears, as well as downregulation of the anterior, neurosensory markers such as *Lfng* and *NeuroD*. Similar changes were observed in mouse inner ears when RA was administered to pregnant females before otic placodal induction. Conversely, when a bead soaked with Citral, an antagonist of Raldh2 (RA synthesizing enzyme), was implanted posterior to the developing chicken otic cup, *Tbx1* expression was downregulated and *Lfng* and *NeuroD* were ectopically upregulated in posterior otocysts. Based on these results, we propose that RA is an extrinsic signal that confers AP axial identity to the inner ear, most likely by activating *Tbx1*, which in turn restricts neurosensory specification in the anterior otic area.

### **436 The Novel Ig Superfamily Protein Lrig3 Controls Inner Ear Morphogenesis by Regulating Netrin-1 Expression.**

Victoria E. Abraira<sup>1</sup>, Andrew F. Tucker<sup>1</sup>, Lisa V. Goodrich<sup>1</sup>

<sup>1</sup>Department of Neurobiology, Harvard Medical School, Boston MA, USA

Morphogenesis of the complex labyrinths of the inner ear involves precisely regulated cell-cell interactions in the epithelium and mesenchyme of the otic vesicle. in developing semicircular canals, defined regions of the otic epithelium grow towards each other and meet to form the fusion plate. in the fusion plate, the basal lamina breaks down as epithelial cells intercalate to form a single layer of cells. Subsequently, the epithelium disappears and the region is filled with mesenchyme, thereby forming a canal out of an initial pouch structure. a key player in this process is the axon guidance molecule Netrin-1. Netrin-1 is secreted from fusion plate cells into the extracellular matrix where it promotes breakdown of the basal lamina, permitting epithelial-mesenchymal interaction that drive formation of the fusion plate. Hence, when and where Netrin-1 is produced fundamentally affects the complex structure of the vestibular apparatus.

We report that the novel protein Lrig3 controls the timing and extent of fusion in the lateral canal pouch by regulating the expression of Netrin-1. Lrig3 is present in non-fusing regions of the lateral pouch, complementary to Netrin-1 in the fusion plate. in Lrig3 mutant mice, fusion begins prematurely and occurs throughout the lateral pouch, leading to a truncation of the lateral semicircular

canal and circling behavior in adult mice. the fusion defect is accompanied by ectopic breakdown of the basal lamina and expansion of Netrin-1 expression. the canal truncation is rescued when one copy of the Netrin-1 gene is removed, confirming that the Lrig3 mutant phenotype is a result of increased levels of Netrin-1. Lrig3 is a single pass transmembrane protein with 16 leucine-rich repeats and 3 Ig-domains in the extracellular region, and a short cytoplasmic tail with no known motifs. Current studies are aimed at understanding how Lrig3 regulates Netrin-1 expression at the molecular level.

#### **437 Eya1 Acts As a Dosage-Sensitive Regulator for Sensory organ Development in the Mammalian Inner Ear**

**Pin-Xian Xu<sup>1</sup>**, Dan Zou<sup>2</sup>, Christopher Erickson<sup>1</sup>, Eun-Hee Kim<sup>1</sup>, Bernd Fritzsch<sup>3</sup>

<sup>1</sup>Mount Sinai School of Medicine, <sup>2</sup>McLaughlin Research Institute, <sup>3</sup>Creighton University

Haploinsufficiency of the transcription coactivator EYA1 disrupts inner ear development; however, the underlying cause for its dosage requirement and its specific role in sensory cell development are unknown. Here, an allelic series of *Eya1* were generated to study the basis of *Eya1* dosage requirements for sensory organ development. Our results show different threshold requirements for the level of *Eya1* in different regions of the inner ear. Patterning and gene marker analyses indicate that in *Eya1* hypomorphic/null heterozygous mice, a reduction of *Eya1* expression to 21% of normal level causes an absence of cochlear and vestibular sensory formation. to determine whether *Eya1* plays a specific role during sensory cell development, we have carefully assessed the expression of *Eya1* and its relation with *Sox2* expression. *Eya1* is initially expressed in the progenitors throughout the epithelium of all six sensory regions and colocalizes with *Sox2*. During sensory cell differentiation, its expression becomes abundantly restricted to the differentiating hair cells. in the developing cochlear epithelium, in addition to the future organ of Corti, *Eya1* expression extends into the epithelial cells that give rise to inner sulcus, coinciding with a region where the epithelial cells were converted into hair cells by ectopic *Math1* expression. Furthermore, we provide genetic evidence that *Eya1* activity, in a concentration-dependent manner, plays a key role in the regulation of genes that are known to be important for sensory development. Together, our results indicate that *Eya1* may play a specific role in regulating sensory cell specification, hair cell competence and its differentiation. These results also provide a molecular mechanism for understanding how hypomorphic levels of EYA1 cause inner ear defects in humans.

#### **438 Specification of Sensory Epithelia by Dlx3b-4b**

**Dong Liu<sup>1</sup>**, Joseph Christison<sup>1</sup>, Monte Westerfield<sup>1</sup>

<sup>1</sup>Institute of Neuroscience, University of Oregon

We previously determined that both Fgf and Bmp dependent genetic pathways are responsible for otic induction, and demonstrated that *Foxi1* is critical in

establishing the pre-placodal ectoderm (PPE) that is essential for Fgf-mediated otic induction. Unlike its widespread mRNA distribution in non-neural ectoderm of the gastrula, *foxi1* is later restricted to the PPE region of the neurula. We have now discovered that *Foxi1* positively regulates *bmp2b* that highlights the neurula PPE, hence *dlx3b-4b*. Because a loss of *Dlx3b-4b* prevents otic hair cell formation, and a local expansion of *Dlx3b-4b* results in extra otic hair cells, we hypothesize that otic sensory cells are largely dependent on *Dlx3b-4b* function. in support of this hypothesis, we have found that prosensory markers are not expressed in the absence of *Dlx3b-4b*. We have also defined the developmental time window of sensory specification, using transgenic animals expressing genes that either positively or negatively regulate Bmp signaling. Our results provide a new understanding of the genetic pathway that regulates sensory hair cell specification. (Grant support from NIDCD)

#### **439 Exploring the Function of Micrnas in the Specification of Sensory organ and Hair Cell Fates**

**Haiqiong Li<sup>1</sup>**, Wigard Kloosterman<sup>2</sup>, Katherine Byrum<sup>1</sup>, Ronald Plasterk<sup>2</sup>, Donna Fekete<sup>1</sup>

<sup>1</sup>Purdue University, <sup>2</sup>Hubrecht Laboratory of Developmental Biology

The generation of inner ear mechanosensory cells requires progression through a series of developmental states including ectodermal, preplacodal, otic, proneural, prosensory and finally hair cell. the sequential appearance or disappearance of molecular markers accompanies these developmental changes, although the task of connecting such markers to definitive events in cell fate specification remains a challenge. microRNAs (miRNAs) are a class of non-coding short RNA transcripts, which can regulate gene expression level through specific inhibition of messenger RNA translation. Four miRNAs (miR-96, miR-182, miR-183 and miR-200a) were found associated with mechanosensory organs in vertebrate embryos. Their specific expression patterns indicate potential roles in promoting or restricting cell fates during the sensory organ formation. Knockdown of the miRNAs in zebrafish embryos with antisense morpholinos, either alone or in combination, leads to significant reductions (21-60%) in hair cell numbers in the anterior and posterior macula without apparent changes in embryonic stage or sensory organ size. Appearance of hair cells in cristae is also significantly delayed and lateral line neuromasts are abnormally deposited. This contrasts with the phenotypes of embryos injected with exogenous miR-96 duplexes: we find a 28% increase in posterior macular hair cell number and precocious appearance of hair cells in cristae. Ongoing examination of expression patterns of inner ear molecular markers in miRNA-knockdown embryos will reveal potential targets of the miRNAs. These results may offer a novel therapeutic approach to promoting sensory fates and hair cell fates in vivo.

#### **440 FGF20 is a Key Regulator of Sensory Cell Development in the Cochlea**

Toshinori Hayashi<sup>1</sup>, Catherine Ray<sup>1</sup>, Thomas Reh<sup>2</sup>, Olivia Bermingham-McDonogh<sup>1</sup>

<sup>1</sup>Virginia Merrill Bloedel Hearing Research Center  
University of Washington, <sup>2</sup>Department of Biological  
Structure, University of Washington

FGFs, and their receptor tyrosine kinases, are a group of signaling molecules critical for auditory system development. FGFs form a large family of proteins that act as signaling molecules in many key developmental processes, both within the nervous system and in other tissues. There appear to be at least three stages of inner ear development that require FGF signaling: first for the initial determination of the otocyst and early morphogenesis (Ladher et al., 2005; Mansour et al., 1993; Pauley et al., 2003; Pirvola et al., 2000; Wright and Mansour, 2003), second for the establishment of the sensory epithelium precursor pool (Pirvola, 2002) and third for the full differentiation and function of the support cells (Colvin et al., 1996).

We were interested in investigating which FGFs and which FGFRs are expressed at each phase of development. We tested the expression patterns, by *In Situ* hybridization, for Fgf 3, 8, 10, 16, 17, 18 and 20. We found that Fgf20 is highly expressed during the early prosensory phase of development of the cochlea. Sox2, a prosensory marker and Fgf20 are coexpressed in the same region. Fgf20 expression precedes expression of Math1 a marker of differentiating hair cells. We found when we used a blocker of FGFRs, SU5402, in explant cultures at early embryonic ages (earlier than E14) we could inhibit both hair cell and support cell development. This phenotype is similar to the conditional Fgfr1 knockout mouse reported by Pirvola (2002). Treatment of explant cultures from older embryos (E18) did not change the number of hair cells, but the pillar cells failed to develop. When we treated early embryonic cochlear explants with a blocking antibody to FGF20 we found the same block in sensory cell development as found in the SU5402 treated cultures. These results suggest that FGF20 may be a key regulator in sensory cell development in the cochlea.

Supported by NIH grants: DC 005953, P30 DC 004661 and HD002274

#### **441 A Comparative Study of Fgf Signaling in the organ of Corti and Basilar Papilla**

Bonnie Jacques<sup>1</sup>, Matthew Kelley<sup>1</sup>

<sup>1</sup>NIH-NIDCD

The elongated avian cochlea, the basilar papilla (BP), is homologous to the mammalian organ of Corti. Both are characterized by a tonotopically organized sensory epithelium comprised of an array of mechanosensory hair cells and underlying support cells. Fibroblast growth factor receptor 3 (Fgfr3) signaling is a feature common to developing support cells of both the avian and mammalian cochleae. In mouse, Fgfr3 regulates the number and type of support cells that form, the timing of their differentiation and also the positioning of pillar cells. The function of Fgfr3 in avian auditory sensory epithelia is still unknown. Here

we used *In Vitro* organ explant culture systems to determine the function of Fgfr3 within embryonic chick and mouse cochleae. Sensory epithelia from both chick and mouse were grown in culture and treated with the Fgfr antagonist SU5402 or with ectopic Fgf protein. Inhibition of Fgfr3 within the developing organ of Corti results in a reduction in support cell numbers and a subsequent increase in the proportion of cells which develop into hair cells. Similarly, in the basilar papilla, a greater number of hair cells are observed when basilar papillae are treated with Fgfr3 antagonists. A lack of BrdU incorporation suggests that this change in the proportion of hair cells to support cells is the result of trans-differentiation rather than mitoses. It is possible that the lack of regeneration within the mammalian auditory system may be explained by Fgf signaling differences between the quiescent organ of Corti and the dynamic basilar papilla.

#### **442 Role of Hes and Hey Genes in Regulating and Maintaining Supporting Cell Fate**

Angelika Doetzlhofer<sup>1</sup>, Martin Basch<sup>1</sup>, Andrew Groves<sup>1</sup>, Neil Segil<sup>1</sup>

<sup>1</sup>House Ear Institute

In mammals supporting cells do not regenerate hair cells and hair cell loss is permanent leading to deafness and balance disorders. In contrast, avian supporting cells act as hair cell progenitors after trauma and replace lost sensory hair cells either by direct trans-differentiation or following mitosis. The molecular mechanism(s) restricting the progenitor potential of postnatal mammalian supporting cells in the intact organ of Corti is unknown. Since it is believed that Notch signaling restricts hair cell fate during embryonic development of the organ of Corti, we hypothesized that Notch signaling may also reinforce the supporting cell state in the postnatal organ of Corti. We found that Notch signaling is required to keep differentiated supporting cells from trans-differentiating into hair cells. Interestingly, pillar cells resist conversion to hair cells when Notch signaling is interrupted at early postnatal times, whereas neighboring Deiters' cells readily convert into hair cells in the absence of Notch signaling. We will present evidence that the distinct expression pattern of Hes/Hey transcriptional repressors regulates the differential response of supporting cell subtypes to the release of Notch inhibition and discuss the relevance of Notch-dependent and Notch-independent mechanisms in supporting cell differentiation and maintenance.

#### **443 Wnt/B-Catenin Signaling in the Developing Mammalian Cochlea**

Alain Dabdoub<sup>1</sup>, Chandrakala Puligilla<sup>1</sup>, Tingting Gao<sup>1</sup>, Matthew Kelley<sup>1</sup>

<sup>1</sup>NIH

The development of the cochlea and the organ of Corti requires several events including growth, specification of cell fates, proliferation and differentiation. In many systems the Wnt/b-catenin pathway plays a crucial role in determining cell fate, growth and proliferation. Activating this pathway leads to the down regulation of glycogen



synthase kinase-3b (GSK3b) which targets b-catenin for ubiquitin-dependent proteolysis resulting in the accumulation of b-catenin in the cytoplasm. b-catenin migrates to the nucleus, associates with the LEF/TCF transcription factors, and affects transcription of target genes. We identified Wnt signaling elements using a mouse Wnt signaling pathway microarray and screened a total of 96 genes in E13 and P0 sensory epithelia. the expression of a subset of genes detected by gene array was validated. Moreover, using the TOPGAL reporter mouse we demonstrate that this pathway is active in the organ of Corti. We show that inhibition of GSK3b in E13 cochlea results in an increase in inactivated GSK3b and an increase in b-catenin. Since b-catenin functions in cell adhesion in addition to transcription, as a protein interacting with cadherins at the plasma membrane regulating cell-cell contacts and actin cytoskeleton interactions, we activated the Wnt/b-catenin pathway downstream of b-catenin in order to bypass its role in cell adhesion. We show that activating the Wnt/b-catenin pathway at the TCF level in cochlear explant cultures results in the formation of extra hair cells. Furthermore, LEF1 overexpression in P19 murine embryonal carcinoma cells, which normally express endogenous Sox2, results in a significant increase in Sox2 expression. in addition, LEF1 overexpression induced Prox1 expression which is not endogenously expressed in these cells. the induction of Sox2 and Prox1, markers of the prosensory domain in the cochlea, by LEF1 suggests that the Wnt/b-catenin pathway acts upstream of these prosensory genes in cochlear development.

#### **444 Rack1 Interacts with Planar Cell Polarity (PCP) Protein Vangl2 and is Required for PCP-Regulated Processes**

Shuangding Li<sup>1</sup>, Robert Esterberg<sup>2</sup>, andreas Fritz<sup>1</sup>, Ping Chen<sup>1</sup>

<sup>1</sup>Emory University, <sup>2</sup>Emory University

Planar cell polarity (PCP) refers to coordinated polarization of cells within a cell sheet. a distinct example for vertebrate PCP is exhibited by uniform orientation of stereociliary bundles on the apical surface of all the hair cells in the cochlea. in addition to this type of epithelial PCP, planar polarization occurs during convergent extension, a polarized cellular movement that plays an important role in gastrulation and neurulation for generating an extended anterior-posterior body axis and for the extension and closure of the neural tube, respectively. Previously, we and others have shown that a set of conserved membrane proteins, including Frizzled receptors and Vangl2/Ltap, are sorted in a polarized manner along the axis for PCP, presumably to direct downstream cytoskeletal polarization involving JNK. However, the molecular linker between polarized membrane PCP proteins and the cytoskeleton is not clear. Here, we used the C-terminal cytoplasmic domain of Vangl2, and performed a yeast two-hybrid screen with an E15.5 cochlear epithelium cDNA library. We identified the Receptor for Activated Protein Kinase C (Rack1) as a Vangl2-interacting protein. We found that Rack1 is expressed in the developing cochlea during PCP, and forms complexes with Vangl2 in mouse brain and

cochlea *In Vivo* and in transfected cells *In Vitro*. to start assessing a potential role for Rack1 in PCP regulation, we employed morpholino-based gene ablation of Rack1 in zebrafish and showed that the knock down of Rack1 results in specifically a significant reduction of the anterior-posterior body axis. Currently, we are confirming the requirement for Rack1 in convergent extension and testing the genetic epistasis of Vangl2, Rack1, PKC and JNK in PCP signaling in zebrafish. We will further investigate a potential role for Rack1 in the mammalian cochlea.

#### **445 Nonmuscle Myosin II Regulates Cochlear Elongation Through Regulation of Cell Size and Convergent Extension**

Norio Yamamoto<sup>1</sup>, Ma Xuefei<sup>2</sup>, Robert Adelstein<sup>2</sup>, Matthew Kelley<sup>1</sup>

<sup>1</sup>Section on Developmental Neuroscience, NIDCD/NIH,

<sup>2</sup>NHLBI/NIH

The presence of an elongated cochlea plays a key role in both the ability to perceive high frequencies and in frequency discrimination. the developmental and evolutionary mechanisms that directly regulate this elongation are largely unknown although it has been suggested that planar cell polarity (PCP) pathway might affect this regulation through a convergent extension mechanism (Montcouquiol, M et al. 2003, Wang, J et al. 2005).

Nonmuscle myosin II is a conventional myosin found in nonmuscle cells and is involved in cytokinesis, cell motility and cell polarization including the process of convergent extension as it occurs, for example, in *Drosophila* germ band elongation. Three different nonmuscle myosin IIs (II-A, II-B and II-C) have been reported in mammals. Mutations in human nonmuscle myosin II heavy chain genes can cause hereditary deafness but the basis for the auditory defect is unknown. to begin to determine the role of myosin II genes in auditory function, the activity of myosin II was inhibited using two specific myosin II inhibitors, Blebbistatin and Y27632. Treatment of embryonic cochlear explants with either inhibitor disrupted the elongation of cochlear sensory epithelium, resulting in a shorter and wider sensory epithelium compared to control cochlear explants. Moreover, knock-in mice expressing an apparent dominant negative form of non-muscle myosin II-B (R709C) that appears to inhibit the function of other myosin II molecules have shortened cochleae that appear similar to the cochleae from inhibitor experiments. in addition analysis of the size of each cell in the sensory epithelia from dominant negative myosin II-B mice indicated that nonmuscle myosin II also regulates an increase in cell size. These results suggest that convergent extension and cell growth are important processes in cochlear extension and that myosin II plays a key role in regulating these processes.



#### **446 Early Emergence of Type II Spiral Ganglion Neurons in the Embryonic Mouse**

**Lisa Goodrich<sup>1</sup>, Jessica Appler<sup>1</sup>, Edmund Koundakjian<sup>1</sup>**

<sup>1</sup>*Harvard Medical School*

Two types of spiral ganglion neurons are defined by their morphologies and projection patterns. Type I neurons extend radial fibers that innervate one or two inner hair cells. Type II neurons develop long spiral fibers that turn towards the base and connect with many outer hair cells. Neurons are thought to initially contact both inner and outer hair cells, followed by selective pruning, leaving only a small number of Type II neurons. We genetically labeled spiral ganglion neurons using the *Ngn1-CreER<sup>T2</sup>* mouse line, which produces CreER<sup>T2</sup> in all inner ear neurons. *Ngn1-CreER<sup>T2</sup>* mice were crossed to *Z/AP* mice, which express the axonal reporter PLAP after Cre-mediated recombination. Labeling of spiral ganglion neurons was induced by treating pregnant dams with tamoxifen to activate CreER<sup>T2</sup>. Cochleas were collected and stained for PLAP activity, allowing embryonic neurons to be imaged along their entire trajectory. At E12.5, neurons had not yet extended fibers beyond the edge of the spiral ganglion. There was a gradient of development by E15.5, with neurons most mature in the base and least mature in the apex. Young neurons extended multiple branches within the spiral ganglion, whereas neurons in the base elongated radial fibers that traversed the spiral lamina and terminated at the edge of the nascent organ of Corti. One day later, a minority of basal neurons had developed processes capped by a large growth cone that was directly beneath the differentiating outer hair cells and pointed towards the base of the cochlea. These likely represent young Type II spiral ganglion neurons. Indeed, by E18.5, 8% of all labeled neurons had clear Type II morphologies, consistent with their previously reported distribution in the mature cochlea. Neurons with characteristics of both Type I and Type II neurons were not seen. These results suggest that the specification of Type I and Type II spiral ganglion neurons is independent of interactions with the sensory epithelium.

#### **447 Deficiency of the Chromodomain Protein CHD7 Disrupts Gene Expression in the Developing Mouse Vestibular System**

**Elizabeth A. Hurd<sup>1</sup>, Katherine Cheng<sup>1</sup>, Lisa A. Beyer<sup>1</sup>, Yehoash Raphael<sup>1</sup>, Donna M. Martin<sup>1</sup>**

<sup>1</sup>*The University of Michigan*

CHD7 is a chromodomain gene commonly mutated in CHARGE syndrome, a multiple congenital anomaly condition that includes inner ear defects. Mice with heterozygous *Chd7* deficiency (*Chd7<sup>Gt/+</sup>*) exhibit variable, asymmetric lateral and posterior semicircular canal malformations, and defects in posterior sensory epithelia innervation despite the presence of hair cells. Understanding the basis of *Chd7*-deficient inner ear defects has relevance not only for CHARGE but also for conditions that affect hearing and balance in general. In this study, we investigated the underlying mechanisms of these defects within the developing mouse ear. We report that *Chd7* co-localizes with the neuronal marker TuJ1 in

vestibulocochlear ganglia at mid-embryogenesis. Using the neuroanatomical tracer, Dil, to examine the extent of vestibular innervation in embryonic and postnatal *Chd7<sup>Gt/+</sup>* ears, we found variably penetrant defects in innervation of the posterior cristae. In support of this observation, markers of the vestibulocochlear ganglia displayed variable reductions in expression in embryonic *Chd7<sup>Gt/+</sup>* inner ears. Immunofluorescence using BrdU specific antibodies suggest there may be subtle defects in the *Chd7<sup>Gt/+</sup>* inner ear epithelium, indicating that cell proliferation may be partly responsible for the observed *Chd7<sup>Gt/+</sup>* inner ear abnormalities. Several markers of developing cristae were reduced or absent in *Chd7<sup>Gt/+</sup>* embryos, indicative of abnormal developmental signaling pathways. Markers of semicircular canal primordia were also reduced in mid-gestation *Chd7<sup>Gt/+</sup>* embryos. These data indicate that *Chd7* function is essential for normal expression of genes during development of the vestibular sensory epithelia, semi-circular canals and sensory ganglia of the mouse inner ear. Target genes regulated by CHD7 may be candidates for mutation analysis in CHARGE patients, and might also provide important clues for designing therapies to treat other hearing and balance disorders.

Funded by NIH RO1 DC01634, P30 DC06188, the Williams Professorship, the National organization for Hearing Research, a gift from Berte and Alan Hirschfield, and the Center for Hearing Disorders.

#### **448 Canal Cristae Growth and Fiber Extension to the Outer Hair Cells Require Prox1 Activity**

**Bernd Fritsch<sup>1</sup>, Sathish Srinivasan<sup>2</sup>, Natasha Harvey<sup>3</sup>, David Nichols<sup>1</sup>, Guillermo Oliver<sup>2</sup>**

<sup>1</sup>*Creighton University*, <sup>2</sup>*St. Jude Hospital*, <sup>3</sup>*Hanson Institute*

The homeobox gene *Prox1* is required for lens, retina, pancreas, liver, and lymphatic vasculature development. During the development of the mammalian ear, *Prox1* is an early marker of the canal cristae and its expression remains in all supporting cells. In other vestibular organs, *Prox1* is only transiently expressed and it is upregulated late in cochlea development. We have now investigated the role of *Prox1* in the developing mouse ear taking advantage of available standard and conditional *Prox1* mutant mouse strains. A severe reduction in size of the canal cristae but not in the other vestibular organs was identified in the mutant ear. As indicated by *MyoVII* expression, hair cell differentiation appeared normal in E18.5 *Prox1* conditional mutant ears; however, their typical distribution pattern was slightly disorganized in the cochlea. In the cochlea we found that although the innervation of inner hair cells appeared normal, the growth of type II nerve fibers to outer hair cells along *Prox1* expressing supporting cells was severely disrupted. These results identify a dual role of *Prox1* during inner ear development; growth of the canal cristae and fiber guidance along supporting cells in the cochlea.

**449 Conditional Disruption of Atoh1 in the Developing Hindbrain Results in Central Deafness and Reveals a Novel Function of the Cochlear Nucleus in the Maintenance of Neurons in the Brainstem Accessory Auditory Nuclei and Spiral Ganglion**

**Stephen Maricich<sup>1</sup>**, Anping Xia<sup>1</sup>, John Oghalai<sup>1</sup>, Bernd Fritzsch<sup>2</sup>, Huda Zoghbi<sup>1</sup>

<sup>1</sup>Baylor College of Medicine, <sup>2</sup>Creighton University

Atoh1 is a basic helix-loop-helix transcription factor necessary for the specification of cochlear hair cells and multiple neuronal subtypes in the mammalian hindbrain. We used Cre-loxP technology to generate conditional knockouts (CKOs) of Atoh1 specifically in the developing cochlear nucleus (CN). Adult Atoh1 CKO mice are behaviorally deaf, have diminished auditory brainstem evoked responses, disrupted CN morphology, and aberrant afferent and efferent connectivity of the CN, while cochlear structure and hair cell function are normal. Atoh1 CKO mice also lose spiral ganglion cells (SGCs) in the cochlea and neurons of the brainstem accessory auditory nuclei during the first 3 days of life. We demonstrate that NT-3, the most important trophic factor for SGCs, is expressed by cells in the embryonic CN, that NT-3 expression is lost in the CKO, and that the NT-3 receptor (trkC) is found on neurons of the accessory auditory nuclei, suggesting that the neuronal loss is secondary to loss of NT-3-mediated trophic support. Our report provides the first description of a mouse model of pure central deafness and reveals the importance of the CN for support of a subset of peripheral and central auditory neurons.

**450 Positioning the Dose: Materials for Localized Drug Delivery**

**Mark Saltzman<sup>1</sup>**

<sup>1</sup>Yale University

The practice of medicine has changed dramatically in our lifetimes, and even greater changes are anticipated in the next 20 years. Drug delivery is one area of substantial progress. Drugs have long been used to improve health and extend lives, but a number of new modes of drug delivery, which were made possible primarily through the work of biomedical engineers, have entered clinical practice recently. In addition, biomedical engineers have contributed substantially to our understanding of the physiological barriers to efficient drug delivery such as transport in the microcirculation and drug movement through cells and tissues. Still, with all of this progress, many drugs—even drugs discovered using the most advanced molecular biology strategies—have unacceptable side effects. Side effects limit our ability to design drug treatments for cancer, neurodegenerative, and infectious diseases. This lecture will discuss an alternate strategy for drug delivery, which is based on physical targeting, or placement of the delivery system at the target site. The effectiveness of this approach will be illustrated with examples of new treatments for cancer and infectious disease, as well as new approaches for tissue engineering.

**451 Cochlear Hair Cell and Neuronal Regeneration - From the Culture Dish Into the Animal**

**Stefan Heller<sup>1</sup>**

<sup>1</sup>Stanford University

Recent advances in intracochlear gene delivery, novel bioactive compounds, and stem cells have led to a new focus on cochlear cell regeneration and cell replacement. Current research makes use of manipulating the expression of developmentally important genes in the damaged adult cochlea, for example by re-expression of the Atoh1 gene, or by manipulation of intercellular signaling. Likewise, exploration of the potential of inner ear progenitor cells, derived from stem cells, has been given increased attention. Here, I will discuss two directions taken by several laboratories to replace lost cochlear cells in vivo: 1) stem cells and, 2) the utilization of drugs. Different strategies to guide the differentiation of murine and human stem cells toward cell types with features of inner ear progenitor cells will be presented. It will be discussed whether stem cell transplantations and potential drug treatment present feasible future treatment options.

**452 In Vivo Screening for Potentially Therapeutic Drugs**

**Edwin Rubel<sup>1</sup>**, Julian Simon<sup>2</sup>, Felipe Santos<sup>1</sup>, Henry Ou<sup>1</sup>, Lynn Chiu<sup>1</sup>, David Raible<sup>1</sup>

<sup>1</sup>University of Washington, <sup>2</sup>Fred Hutchinson Cancer Research Center

Perhaps the major challenge for application of new methods of drug delivery to the inner ear is selection of safe, robust and readily available therapeutic agents. Whether our goals are regeneration of hair cells or other missing cell types, or protection from damaging effects of aging, aminoglycosides or anti-neoplastic agents, we are still searching for effective agents that work across a range of dosages and genotypes. Toward this end, we have developed a series of screening methods using *In Vivo* imaging of lateral line hair cells in larval zebrafish (*Danio rerio*). These hair cells are highly accessible and easily visualized using fluorescent dyes. Morphological and functional similarity to mammalian hair cells of the inner ear make the zebrafish lateral line a powerful preparation for assessing the modulation of hair cell survival by large numbers of compounds. These methods allow rapid medium-high-throughput screening of drug libraries, followed by efficient analyses of the robustness and breadth of value for any selected compounds. We have now begun screens of large libraries of drug-like compounds and of libraries of FDA-approved drugs. The screens target drugs for protection against aminoglycoside ototoxicity and cisplatin ototoxicity, drugs that influence hair cell regeneration and FDA-approved drugs that cause occult ototoxicity. The strategies we use for each screen will be presented along with data on protection and occult ototoxicity, and initial validation of the strategy by assessment of results from experiments on mature mouse utricle cultures.

Supported by Research, Training and P30 Awards from NIDCD

#### **453 Inner Ear Delivery of Therapeutic Molecules Using Magnetically-Directed Superparamagnetic Nanoparticles**

**Richard Kopke**<sup>1</sup>, Kejian Chen<sup>2</sup>, Kenneth Dormer<sup>3</sup>, Xinsheng Gao<sup>2</sup>, Youdan Wang<sup>1</sup>, Angelica Vasquez-Weldon<sup>4</sup>, Brian Grady<sup>5</sup>, David Bourne<sup>5</sup>

<sup>1</sup>Hough Ear Institute, <sup>2</sup>Hough Ear Institute & INTEGRIS Health, <sup>3</sup>University of Oklahoma Health Sciences Center, <sup>4</sup>Oklahoma Medical Research Foundation, <sup>5</sup>University of Oklahoma

A major challenge for otology is the controlled, efficient delivery of therapeutic molecules to the labyrinth. One novel approach utilizes magnetically-enhanced delivery, across the round window membrane (RWM), of superparamagnetic iron oxide nanoparticles (SPION) incorporated into nanoscale polymer complexes containing therapeutic payload. the payload may include small molecules, proteins, plasmid DNA (pDNA), and RNA. Such particles have been created and characterized with incorporation of pDNA, proteins, and small molecules. RWM delivery of these particles using external magnetic forces has been demonstrated *In Vitro* and *in vivo*. Current accomplishments as well as current challenges and future approaches will be reported.

#### **454 Delivery Strategies for Neurotrophin Delivery Into the Inner Ear for Sgn Protection Following Deafness**

**Robert Shepherd**<sup>1</sup>, Anne Coco<sup>1</sup>, Jacqueline andrew<sup>2</sup>, andrew Wise<sup>1</sup>, Lisa Pettingill<sup>1</sup>

<sup>1</sup>Bionic Ear Institute, <sup>2</sup>Department of Otolaryngology, University of Melbourne

Loss of hair cells following sensorineural hearing loss (SNHL) sets in place degenerative changes within the cochlea including loss of spiral ganglion neurons (SGNs) that has implications for the efficacy of cochlear implants. Exogenous neurotrophins (NT) rescue SGNs from degeneration following a SNHL, however NT administration must be continuous to ensure long-term SGN survival. This has important implications for the safe clinical delivery of these drugs. Potential drug delivery strategies include the use of pumps; the transfer of NT gene(s) into cells within the cochlea; NT release from polymers and nanoparticles; and the use of cell-based therapies. in addition, since greater SGN rescue is observed when NT administration is combined with chronic electrical stimulation (ES), we examine whether chronic ES can maintain SGN survival long after cessation of NT delivery. the implications of this work in relation to the safe clinical application of NTs within the deafened cochlea are discussed.

Support provided by the NIH-NIDCD (NIH-N01-DC-3-1005) and Living Cell Technologies Pty. Ltd.

#### **455 Microfluidic Drug Delivery to the Cochlea**

**Jeffrey Borenstein**<sup>1</sup>, Sharon Kujawa<sup>2</sup>, Mark Mescher<sup>1</sup>, William Sewell<sup>2</sup>, Jason Fiering<sup>1</sup>, Erin Swan<sup>1</sup>, Zhiqiang Chen<sup>2</sup>, Mark Keegan<sup>1</sup>, Marcello Peppi<sup>2</sup>, Brian Murphy<sup>1</sup>, Michael McKenna<sup>2</sup>

<sup>1</sup>Draper Laboratory, <sup>2</sup>Massachusetts Eye and Ear Infirmary  
Microfluidic and Microelectromechanical Systems (MEMS) are revolutionizing diagnostic and therapeutic approaches for the treatment of disease. Existing techniques for drug delivery to the inner ear use inefficient routes and are not capable of precisely metering compounds over extended periods. Alternative approaches rely upon passive modes such as osmotic pumps or degradable release systems, but these are limited in terms of lifetime, accuracy and control. Here we report on the development of microfluidic delivery systems for chronic treatment of hearing loss and other auditory and vestibular diseases. Because they deliver directly to perilymph, these devices will find early application as a tool for investigating the molecular mechanisms associated with inner ear diseases and for the discovery of new therapeutic compounds. Ultimately, we envision that fully implantable devices will provide a new therapeutic modality for programmable, automated and extended delivery of compounds to the cochlea.

The system we have developed for animal studies comprises a micropump with electronic controls mounted in a wearable pack, with a cannula delivering drug to scala tympani for periods of several hours to several months. Initial results using the reciprocating, pulsatile delivery system, demonstrate a safe, robust surgical procedure with place-dependent responses to drugs consistent with kinetic models. Reversible effects of compounds such as CNQX, DNQX and salicylate have been observed over a range of auditory frequencies, providing insights into the pharmacokinetic behaviour and flow dynamics. Microfluidic systems comprising a drug reservoir, valve and pump, and flow sensor, are currently being developed and integrated. Continued miniaturization of the micropump and associated electronic control system will ultimately enable the entire system to be implanted within a cavity in the mastoid for human clinical use.

#### **456 Speech and Nonspeech Auditory Training Enhances Phonological Processing in Children**

**Lorna Halliday**<sup>1</sup>, Jenny Taylor<sup>1</sup>, Kerri Millward<sup>1</sup>, David Moore<sup>1</sup>

<sup>1</sup>MRC Institute of Hearing Research

Auditory training has been shown to be effective in the remediation of language-learning impairments and in enhancing normal language development in children. We examined whether improvements in phonological processing were specific to training in (a) the auditory (speech and nonspeech) or (b) the speech domain. Eighty-six 8- to 10-year-old typically-developing children were divided into four groups. Three of the groups received twelve 30-minutes sessions of either auditory frequency (AFD group), phonemic (PD group), or visual frequency (VFD group) discrimination training over four weeks.

Participants received training on a battery of 11 different stimuli (tone, phoneme, or spatial frequency contrasts), which were delivered via child-friendly computer games using a 3I-3AFC adaptive procedure. The fourth, control (CA) group, did not receive any training. Thresholds on all psychophysical tasks (AFD, PD, and VFD), along with performance on a battery of phonological processing tests were assessed for all groups before and after training. None of the groups showed any change in thresholds on the VFD task from pre- to post-training. However, both the AFD and the PD groups showed significant reductions (improvements) in thresholds on the task upon which they were trained (AFD and PD tasks, respectively), although learning did not transfer to the untrained tasks. Moreover, both the AFD and PD groups – but not the VFD or CA groups – showed modest improvements on the battery of phonological processing tests following training. The results demonstrate transfer of nonspeech (AFD) and speech (PD) auditory learning to ‘higher-level’ phonological processing skills, but without generalization to different auditory or visual discrimination tasks. These findings suggest that speech and nonspeech auditory learning enhance phonological processing abilities through at least partially independent processes, since learning does not transfer to tasks that involve analogous task demands.

#### **457 Auditory Learning is Driven by Dimension-Specific Attention**

**Sygal Amitay<sup>1</sup>, Lorna Halliday<sup>1</sup>, Jenny Taylor<sup>1</sup>, David Moore<sup>1</sup>**

<sup>1</sup>*MRC Institute of Hearing Research*

We have previously shown that frequency discrimination improves following training with physically identical tones that are impossible to discriminate. We used an oddball paradigm wherein listeners were not given explicit instructions to listen to a specific stimulus dimension (i.e. frequency), suggesting that the improvement was either non-specific to stimulus dimension (bottom-up learning) or implicitly influenced by the preceding brief (30 trials) pre-training frequency discrimination threshold assessment (top-down learning). This was tested directly in this study. Forty-eight adult listeners were divided into three groups. Two groups received 8 training blocks (100 each) on an oddball task using 3 identical tones (1-kHz, 60-dB SPL). One group was instructed to base their discrimination on perceived frequency differences (‘which tone had a different pitch?’). The second group was instructed to respond based on perceived intensity differences (‘which tone had a different volume?’). A third group acted as control; listeners completed ‘SuDoku’ puzzles during the training session. Frequency- and intensity-discrimination thresholds were obtained for all groups before and after training. Listeners instructed to attend to pitch differences showed significant learning on the frequency- but not the intensity-discrimination task. Conversely, participants instructed to listen for intensity differences improved on the intensity- but not the frequency-discrimination task. These results suggest that learning is task specific, and therefore influenced by top-down attentional processes which tune listeners to the relevant stimulus dimension for discrimination. Surprisingly, the control ‘SuDoku’ group

also improved on the frequency- but not the intensity-discrimination task. This supports a type of ‘general arousal’ in auditory learning and suggests that it may be more influential in frequency- than intensity-discrimination tasks.

#### **458 Development of Temporal-Interval Discrimination Learning During Adolescence**

**Julia Jones Huyck<sup>1</sup>, Beverly A. Wright<sup>1</sup>**

<sup>1</sup>*Dept. of Comm. Sci. and Disorders, Northwestern University*

Adults are able to improve their performance on many auditory perceptual tasks with training, but little is known about the developmental course of this learning ability, or how that course relates to the development of naïve performance. To investigate these issues, we examined the influence of perceptual training on a temporal-interval discrimination task in normally-developing 11-year-olds (n=8, mean = 11.5 years) and 14-year-olds (n=8, mean = 14.4 years) and compared their data to those of adults (n=6, mean = 21.7 years; data from Wright & Sabin, 2007, *Exp Brain Res*, 180, 727-36). During training, all listeners completed ~15 discrimination threshold estimates each day for 10 days. Patterns of performance over the training days differed markedly across the three age groups. Overall, while the adults improved significantly, the 11-year-olds actually tended to get worse and the 14-year-olds showed no systematic change in performance. However, individually, though half of the 14-year-olds did not improve with training, the other half did, suggesting that adult-like learning on this task emerges in some individuals between 11 and 14 years of age, but is not present in the entire population until sometime after age 14. Notably, most of the adolescents who did not improve with training had similar starting (naïve) thresholds to the adults, indicating that adult-like naïve performance was not a determining factor in whether or not an individual learned. These data suggest that (1) at least on some auditory perceptual tasks, the ability to learn may continue to develop well into adolescence and (2) naïve performance and learning ability may have different developmental courses. [Supported by NIH/NIDCD.]

#### **459 Effects of Visually Guided Endogenous and Exogenous Spatial Attention On Auditory Target Identification**

**Jing Xia<sup>1</sup>, Virginia Best<sup>1</sup>, Barbara Shinn-Cunningham<sup>1</sup>**

<sup>1</sup>*Boston University*

Visual cues may influence auditory perception by 1) enabling listeners to focus endogenous attention on the cued location, 2) causing involuntary shifts of exogenous attention towards the cued location, and 3) causing cross-modal enhancement of a simultaneous auditory event from the cued location. By manipulating the timing and location of a visual cue relative to an auditory target and measuring auditory identification, we find evidence for all three effects.

Subjects identified a target digit presented with four simultaneous, reversed-speech digits. The five simultaneous sources were arrayed from -30 deg to +30

deg; (15 deg separation). the target digit randomly came from -15 deg or +15 deg. in RANDOM blocks, the visual cue was equally likely to come from the target location (RANDOM VALID) or the location symmetrically opposite (RANDOM INVALID), providing no information about the target. in VALID blocks, the visual cue came from the target location. in INVALID blocks, the visual cue came from the location symmetrically opposite the target. in all blocks, the cue-target stimulus onset asynchrony (SOA) was randomly selected on each trial (0, 100, or 300 ms).

Performance for INVALID trials was relatively poor at 0 SOAs, but approached performance for VALID trials at SOAs of 300 ms, suggesting that INVALID cues only direct endogenous attention when enough time is allowed. for SOAs of 100 ms, performance was much better for RANDOM VALID than RANDOM INVALID trials, as if exogenous attention drives spatial attention when delays are too short to allow shifts of endogenous attention. On VALID trials, identification was better for SOAs of 0 than 100 ms, consistent with cross-modal enhancement of a simultaneous auditory signal from the location of a visual cue, an effect that is more rapid than the involuntary shift of exogenous attention seen for the 100-ms SOAs.

Work supported by grants from ONR and NSF.

#### **460 An Investigation of Factors Potentially Responsible for the Degradations of Binaural Detection Measured with Brief, Simultaneously-Presented Signals and Maskers**

**Leslie Bernstein<sup>1</sup>**, Constantine Trahiotis<sup>1</sup>

<sup>1</sup>*University of Connecticut Health Center*

It is well-known that NoSt $\pi$  detection thresholds are substantially elevated when brief signal-plus-masker durations are employed. the primary purpose of this study was to evaluate whether or to what degree such degradations in the efficiency of binaural detection are the result of interactions between the duration of the stimuli and underlying listener-based processing imperfections (often termed "internal noise"). Said differently, the question was whether decreasing the duration of such binaural stimuli would result in changes in the amounts or types of effective internal noise required to account quantitatively for the behavioral data via an interaural correlation-based model. to that end, NoSt $\pi$  detection thresholds at 500 Hz were measured as a function of the level of broadband (100-3000 Hz) masking noise (spectrum levels ranging from -10 to 50 dB) for signal-plus-masker durations between 10 and 320 ms. in separate conditions, St $\pi$  detection thresholds were measured as a function of the interaural correlation of the broadband masking noise. Once again, signal-plus-masker durations ranged between 10 and 320 ms. the empirical findings were that both changes in detection thresholds as a function of the spectrum level of the masker and changes in detection thresholds as a function of the interaural correlation of the masker were essentially independent of the duration of the stimuli. At this time, this suggests to us that the relative inefficiency of binaural detection found with brief stimuli is probably not a manifestation of internal

noise that interacts with duration, i.e., becomes relatively more influential, as duration is decreased.

#### **461 Across-Listener Variation in Naïve Performance As a Potential Predictor of Learning Patterns On Interaural Time and Level Difference Discrimination**

**Yuxuan Zhang<sup>1</sup>**, Beverly A. Wright<sup>2</sup>

<sup>1</sup>*Northwestern Univ Institute for Neuroscience,*

<sup>2</sup>*Northwestern Univ Institute for Neurosci. & Dept. of Comm. Sci. and Disord., Northwestern Univ.*

The pattern in which perceptual performance improves with practice often differs across tasks, even when identical training regimens are employed. Can the learning pattern be predicted? Here, we report data from four auditory training experiments that suggest that the across-listener variation of performance *before training* provides a clue to how performance will change *during training*. Each experiment involved training interaural level difference (ILD) or interaural time difference (ITD) discrimination with either a pure tone or a sinusoidally amplitude modulated tone. for each listener, we obtained multiple threshold estimates before, during, and after training, and examined two within-listener measures of performance at each time point: the lowest estimate (reflecting the best ability) and the standard deviation of all estimates (reflecting the performance consistency). Before training, the lowest threshold estimate varied across listeners for ILD but not ITD discrimination, while the standard deviation differed across listeners for ITD but not ILD discrimination. Most interestingly, this pattern of across-listener variation in naïve performance paralleled that of within-listener improvement through training. That is, when listeners differed in their best ability but not in their performance consistency before training, they acquired higher sensitivity without becoming more consistent during training (ILD conditions). in contrast, when listeners had similar best abilities but differed in performance consistency before training, they improved their consistency but not best ability with training (ITD conditions). Thus, for a given task, the across-listener variation in naïve performance may help foretell the pattern with which performance will improve with practice. (Supported by NIH/NIDCD)

#### **462 Activity Across the Icx Correlates with Behavioral Detection in the Barn Owl (*Tyto alba*)**

**Elizabeth Whitchurch<sup>1</sup>**, Avinash Deep Bala<sup>1</sup>, Brian Nelson<sup>1</sup>, Terry Takahashi<sup>1</sup>

<sup>1</sup>*University of Oregon*

Barn owls can reliably direct saccades toward auditory targets as quiet as -6 dB SPL<sub>A</sub> (re: 20  $\mu$ Pa). Below this level, owls do not always respond, suggesting a failure to detect or an inability to localize such quiet sounds. to distinguish between these possibilities, we measured detection thresholds using the pupillary dilation response which makes use of the reflexive dilation of the pupil when a sound is detected. Detection thresholds to a frozen

broadband noise burst (100ms: 2-12 kHz, also used in saccade behavior) presented directly in front of the bird were found to average -9 dB SPL<sub>A</sub>, suggesting that detection of low-level stimuli may be occurring slightly below saccadic threshold.

The ICx is the first site at which binaural cues are integrated across frequency to represent space. Based on the behavioral findings, we hypothesize that detection and localization may arise from separate codes in the ICx. Extracellular responses from 199 units in the ICx were measured in response to the same broadband noise bursts used in behavioral experiments (above). Measured rate-level-functions described the relationship between a neuron's observed spike rate and the stimulus SPL. Cellular thresholds, defined as the lowest SPL to evoke a statistically-significant response above spontaneous, ranged from -15 to +17 dB SPL<sub>A</sub>. of these thresholds, 29% fell below -5 dB and 12% were below -8 dB SPL<sub>A</sub>.

Behavioral detection thresholds were also measured in the presence of a co-localized masker. in keeping with Weber's Law, detection thresholds scaled with the level of the masker. Cellular rate-level functions in the owl's ICx adapt to masker levels (Keller, unpublished). Cellular thresholds thus provide a neural substrate for the detection behavior observed both with and without an added masker, and activity across the auditory space map may be used to predict stimulus detection in a variety of environmental conditions. (Supported by grant DC03925.)

#### **463 Effect of Type of Maskers in Dichotic Listening Tasks**

**Nandini Iyer**<sup>1</sup>, Douglas Brungart<sup>2</sup>, Brian Simpson<sup>2</sup>

<sup>1</sup>General Dynamics Advanced Information Systems, <sup>2</sup>Air Force Research Laboratory

In diotic listening, speech maskers typically produce less masking than steady-state noise signals presented at the same signal-to-noise ratio. However, it is not clear what, if any, influence type of masker has on performance in dichotic listening tasks. in the current experiment, target identification was measured in four listening tasks: a diotic task with a single target and a single masker; a dichotic "known-ear" task, with one CRM phrase and one masker presented to both ear and location of one of the phrases (target phrase) known; a dichotic "unknown-ear" task, with CRM phrases and maskers in both ears and unknown location of a target phrase; and a dichotic "two-of-two" task where the listener responded to the CRM phrases (targets) presented to both ears simultaneously. Five types of maskers were presented: noise, modulated noise, speech, reversed speech and speech babble. the results show that speech signals produce much less masking than an equivalent level of noise in diotic listening tasks, but that they produced as much or more masking than an equivalent level of noise in the unknown-ear and two-of-two dichotic tasks. the results suggest overt attention is needed to segregate target speech from a speech masker.

#### **464 The Influence of Ambiguous Grouping Cues On an Auditory Object's Perceived Spectral Content and Location**

**Andrew Schwartz**<sup>1</sup>, Barbara Shinn-Cunningham<sup>2</sup>

<sup>1</sup>MIT, <sup>2</sup>Boston University

We constantly make decisions about what acoustic energy we perceive belongs to what source, forming auditory objects or streams from a mixture of sound. Different cues help us determine both what energy an object contains and where it is located. However, these cues can be ambiguous or conflicting.

This research investigates how listeners perceive a mixture containing an ambiguous tone complex that could logically belong to either a "target" or "interfering" stream. We measure both how much of the ambiguous tone energy is allocated to the target stream (Experiment A) and how much the ambiguous tone influences the perceived location of the the target stream (Experiment B). in the Experiment A, listeners use an analog dial to directly set the perceived spectral content of a match stimulus to that of the target in the ambiguous stimulus. in Experiment B, listeners match the perceived laterality of the ambiguous stimulus by controlling the interaural level difference of a pointer stimulus. Finally, we compare the localization results with localization match results in which there is no interfering stream, but the intensity of the ambiguous tone varies.

Data show that the "what" and "where" computations, averaged across subjects, are consistent in that the perceived location of the target in the mixture is well predicted by the perceived location of the single-stream target with an appropriately attenuated ambiguous tone. These results suggest that computations of "what" and "where" operate on the same acoustic energy taken from a sound mixture. However, we are now investigating whether this result is true when individual results are considered.

#### **465 Psychophysical Spectro-Temporal Receptive Fields in an Informational Masking Task**

**Daniel E. Shub**<sup>1</sup>, Virginia M. Richards<sup>1</sup>

<sup>1</sup>Department of Psychology, University of Pennsylvania

A psychophysical method analogous to the physiological methods used to estimate the spectro-temporal receptive fields (STRFs) of neurons was used to investigate informational masking. the stimulus consisted of a signal (a sequence of four 50-ms tone pips of a known frequency) and a spectrally sparse masker (temporally and spectrally random 50-ms tone pips). the method differed from traditional approaches in that the stimulus was continuously presented for approximately five minutes and subjects were asked to respond, with a button press, as quickly as possible whenever a signal was detected. the signal was presented at random times with an expected rate of one signal every 3.2 s. the psychophysical STRF was estimated by temporally aligning, relative to the response times, and averaging the spectrograms of 1-second snippets of the stimulus whenever a *false alarm*

occurred. the analysis of the informational masking task focused on this response-triggered averaged spectrogram for *false alarms* as well as a signal-triggered averaged spectrogram for *misses*. the *false alarm*-spectrogram is similar to a noisy version of the signal; subjects incorrectly responded that there was a signal approximately 700 ms after the masker had power near the signal frequency. the *miss*-spectrogram reveals effects that have not been previously reported. Specifically, the likelihood of a *miss* decreased when the stimulus had power near the signal frequency immediately before or after the signal (mimicking a "long" signal). Further, the likelihood of a *miss* increased when the masker had power at frequencies within one-half of an octave of the signal frequency. the *false alarm*- and *miss*-spectrograms (and the previously unseen effects) reflect a reasonable, although non-optimal, response strategy for this task. an added advantage of the current method is that it provides a means of comparing psychophysical results to physiological STRFs. [Supported by NIH DC002012 and DC005363]

#### **466 Masking Release with Temporal Asynchrony in Children and Adults**

Lori Leibold<sup>1</sup>, Caitlin Rawn<sup>1</sup>

<sup>1</sup>The University of North Carolina

This study examined the degree to which children can use temporal onset/offset differences to improve performance in an informational masking task. Listeners were 16 children (5-10 years) and 8 adults. Masked thresholds were measured for a 1000-Hz tone presented with a random-frequency, 2-tone masker. Maskers were played at an overall level of 60 dB SPL in each interval of a 2IFC adaptive procedure. Onset/offset asynchrony was manipulated across conditions by examining performance for masker durations of 300, 380, 400, 420, 460, and 500 ms. the 300-ms signal, when present, was temporally centered in the masker, resulting in an asynchrony that ranged from 0 to 100 ms. for adults, maximum masking release was achieved with a 40-ms asynchrony. Increasing the duration of the asynchrony beyond 40 ms provided no additional release. for twelve children, masking release was also observed with a 40-ms asynchrony. in contrast to adults, however, approximately half of these children received additional benefit with increasing asynchrony. Four children showed no masking release with any degree of asynchrony examined. These findings suggest that children can use temporal onset/offset differences to perform sound source determination, but often require a longer asynchrony than adults to achieve maximal benefit.

#### **467 The Duration of Infants' and Adults' Temporal Window**

Lynne Werner<sup>1</sup>

<sup>1</sup>University of Washington

The status of auditory temporal resolution during infancy is still in question. Infants are worse than adults at detecting gaps, but their temporal modulation transfer functions are not obviously different from adults'. in this study, the temporal window paradigm was used to further investigate

this issue. the listeners were 11-week-olds, 24-week-olds and young adults. Thresholds for a 20-ms 1-kHz tone were estimated adaptively using an observer-based procedure. a 500-2000 Hz 45 dB N<sub>0</sub> bandpass noise was presented throughout a session. On a trial 4 gaps, 200 ms apart, were introduced in this noise. the duration of the gaps ranged from 0 to 50 ms across conditions. On tone trials, the tone was presented, temporally centered in each gap. On no-tone trials, no tone was presented in the gaps. Listeners learned to respond on tone trials, but not on no-tone trials. the duration of the temporal window is indicated by the improvement in threshold with increasing gap duration. Adults' thresholds were similar to those reported in the literature. Infants' thresholds were higher than adults'. Preliminary analyses indicate, however, that the improvement in threshold with increasing gap duration, and thus, the duration of the temporal window, is similar in infants and adults.

#### **468 Sound Texture Perception Via Synthesis**

Josh H. McDermott<sup>1</sup>, Eero P. Simoncelli<sup>2</sup>, Andrew J. Oxenham<sup>1</sup>

<sup>1</sup>University of Minnesota, <sup>2</sup>New York University

Many natural sounds, such as those produced by rainstorms, fires, insects at night, or birds in a forest, are the result of large numbers of superimposed acoustic events occurring rapidly and randomly. Such "sound textures" are temporally homogeneous, and in many cases do not depend much on the precise arrangement of the component events, suggesting that they might be represented statistically. to test this idea and explore the statistics that might characterize natural sound textures, we designed an algorithm to synthesize sound textures from statistics extracted from real sounds. the algorithm is inspired by those used to synthesize visual textures, in which a set of statistical measurements from a real sound are imposed on a sample of noise. This process is iterated, and converges over time to a sound that obeys the chosen constraints. If the statistics capture the perceptually important properties of the texture in question, the synthesized result ought to sound like the original sound. We tested whether rudimentary statistics computed from the responses of a bank of bandpass filters could produce compelling synthetic textures. Simply matching the marginal statistics (variance, kurtosis) of individual filter responses was generally insufficient to yield good results, but imposing various joint envelope statistics (cross-band correlations, autocorrelations within each band, and cross-band correlations across time) greatly improved the results, frequently producing synthetic textures that sounded natural and recognizable. Synthesizing some classes of textures may necessitate complex "feature detectors", but in many cases, textures with audible features (raindrops, crackles, insect/bird calls) emerge from the imposition of much simpler statistical constraints. the results suggest that the auditory system may rely on surprisingly simple statistics to recognize real-world sound textures. [Supported by NIH grant R01DC07657 and the Howard Hughes Medical Institute].



#### **469 Current Noise Research: Implications for Regulation**

**Donald Henderson<sup>1</sup>**

<sup>1</sup>*Center for Hearing and Deafness, SUNY at Buffalo*

Our current noise standards date back to 1968. In spite of 40 years of new insights, the only substantial change that has been made is the lowering of the "action level" from 90 dBA to 85 dBA. This presentation will review noise exposure phenomena that have the potential to have an impact on the regulation of noise exposure: 1) the "total energy" model underlying current noise standards is inappropriate for exposure to impulse and impact noises. High-level transients can damage the cochlea by causing mechanical failure, and hearing loss is related to the peak level of the noise rather than the total energy of the exposure. 2) Combinations of continuous and impulse/impact noise are particularly hazardous (more than the addition of the effects of the impulse with the continuous noise component). Given that combinations of noise are common in industrial settings, kurtosis analysis of noise is a very promising metric to quantify the traumatic potential of an exposure. 3) Noise exposures often occur in the context of other environmental challenges to hearing (i.e. heat, chemicals, drugs). Interaction of noise with these factors can increase the hearing loss associated with a given noise exposure. 4) Recent research has shown that high-level noise exposure causes a dangerous increase in toxic free radicals in the cochlea, and that hair cells die primarily through apoptosis. These two insights have led to a number of drugs to prevent or treat noise-induced hearing loss.

#### **470 Genetic Susceptibility to Noise Induced Hearing Loss in Humans**

**Guy Van Camp<sup>1</sup>**, Annelies Konings<sup>1</sup>, Malgorzata Pawelczyk<sup>2</sup>, Per-Inge Carlsson<sup>3</sup>, Erik Borg<sup>3</sup>, Mariola Sliwiska-Kowalska<sup>2</sup>, Lut Van Laer<sup>1</sup>

<sup>1</sup>*Department of Medical Genetics, University of Antwerp, Belgium*, <sup>2</sup>*Department of Audiology and Phoniatrics, Nofer Institute of Occupational Medicine, Lodz, Poland*, <sup>3</sup>*Ahl  n Research Institute,   rebro University Hospital, 701 85   rebro, Sweden*

Noise-Induced Hearing Loss (NIHL) is one of the most important occupational diseases. NIHL is a complex disease caused by an interaction between genetic and environmental factors. Although firm evidence for the genetic basis in humans is still lacking, the involvement of genes in NIHL became clear through various animal studies. We have initiated a study that aimed at the identification of the genetic factors that are involved in human NIHL. In a first phase we have analysed variants (Single Nucleotide Polymorphisms, SNPs) in candidate genes on 2 different sets of noise-exposed samples using association studies. In a second phase, we have screened for association between NIHL and genetic variation on the whole genome level using the same sample sets. These studies resulted in the identification of the first NIHL susceptibility genes.

#### **471 Molecular Basis of Noise-Induced Hearing Loss in the Rat Cochlea.**

**Tzy-Wen Gong<sup>1</sup>**, Gary A. Dootz<sup>1</sup>, David F. Dolan<sup>1</sup>, Margare I. Lomax<sup>1</sup>

<sup>1</sup>*The University of Michigan*

Intense noise causes irreversible damage to the cochlea, resulting in cell death and permanent threshold shift (PTS), whereas mild noise leads to a temporary threshold shift (TTS), without significant cell death. To develop strategies for protecting the cochlea from noise overstimulation, we need to better understand the molecular mechanisms that distinguish these two responses. We exposed rats to broad band noise (2-20 kHz) for 90 minutes at 103dB SPL to produce TTS, and at 120dB to produce PTS. Total RNA was isolated from rat whole cochleae dissected at 2.5 hr after TTS and PTS noise exposure (3 RNA pools per condition), and from non-exposed controls. Levels of gene expression were assessed with Affymetrix RAE230A GeneChips, which contained 7817 unique probe sets, and analyzed by RMA. Of these, 543 genes were differentially expressed following noise. Patterns of gene expression and pathway predictions were determined with Ingenuity Pathways Analysis. Many immediate early genes and heat shock proteins were induced by the PTS noise; a subset of these genes was also induced by the TTS noise. TTS and PTS noise also affected gene expression of proteins implicated in free radical scavenging, programmed cell death, and inflammation. Interestingly, genes for several caspases, for many proteins implicated in nucleic acid binding, and proteins involved in mitochondria function were down-regulated by both TTS and PTS noise. We are currently examining genes differentially expressed between TTS and PTS noise conditions to identify key factors that over-rule protective mechanisms and thus lead to permanent hearing loss. (Supported by grants from GM/UAW, NOHR (TWG), and NIH P30 DC05188)

#### **472 Degeneration of Cochlear Sensorineural Cells: From Molecular Mechanisms to Pharmacological Strategies**

**Jean-Luc Puel<sup>1</sup>**, Jing Wang<sup>1</sup>

<sup>1</sup>*Inserm-UMR 583 and Universit   de Montpellier 1, 80, rue Augustin Fliche, 34295 Montpellier, France.*

In industrial countries, hearing impairment affects approximately 10% of the population and increases in frequency four-fold with aging. Hearing deficits are often caused by loss of sensory hair cells due to a variety of factors including ototoxic drugs, noise, and aging. In mammals, auditory hair cells do not regenerate and loss of hair cells results in irreversible deafness. The concept that, in some instances, sensory hair cell death may be preventable has provided an exciting and novel route to frustrate the degenerative process.

This review outlines some of what is known about the mechanisms of sensorineural cell death and the pharmacological strategies that have been experimented in animal to protect the cochlea from ototoxic and noise exposure, or prevent age-related hearing impairment. Knowledge of the intimate molecular mechanisms involved in cellular degeneration reveals that sensorineural cells

have evolved a complex system of enzymes and other proteins which preserve or destroy these cells during the lifespan of the individual. Ototoxic drugs, damaging levels of sound or age-related sensorineural hearing loss recruit most of the standard apoptotic pathways (e.g. caspase-dependent programmed cell death, caspase-independent programmed cell death), but also several additional enzymatic pathways (calpain-dependent, autophagic programmed cell death) which eventually result in cell death. Many of the pathways interact with each other and so researchers face challenges when attempting to elucidate the pathways involved in response to any given stress stimulus. Better understanding of the molecular mechanisms of sensorineural cell death allows the identification therapeutic targets and the development of pharmacological strategies to prevent cochlear sensory cell and hearing loss. Based on animal experiments, we discuss the efficiency of the new pharmacologic agents such peptide inhibitors of JNK, caspases, calpains or free radical scavengers., and the choice of drug administration modes (systemic versus trans-tympanic) compatible with clinical practice.

#### **[473] Clinical Measures of Susceptibility to Noise-Induced Hearing Loss Using Otoacoustic Emissions**

**Lynne Marshall<sup>1</sup>, Judi Lapsley Miller<sup>1</sup>**

<sup>1</sup>*Naval Submarine Medical Research Laboratory*

Controlled studies show that otoacoustic emissions (OAEs) can indicate preclinical inner-ear damage and susceptibility to noise-induced hearing loss (NIHL) in humans. But before using OAEs for clinical diagnostics, laboratory findings need to be assessed with clinical diagnostics in mind. Our overarching aim is to take the latest science about OAEs and see which methods hold up as potential clinical tests. Our findings over three field studies show that for groups of people, OAEs are more sensitive to noise-induced inner-ear changes than audiograms; however, using small changes in OAEs in individual ears to indicate preclinical inner-ear damage is fraught with difficulty. On the other hand, we found that individual normal-hearing ears with low-level OAEs were more likely to get subsequent permanent threshold shift after a six-month deployment on an aircraft carrier (continuous noise, overlaid with impact noise) and after marine recruit basic training (weapons fire). Various studies by others have indicated that the auditory efferent reflex (measured with OAEs) can be a predictor for NIHL in animals. to be a useful clinical measure, reflex magnitude must vary over a wide range in the population, and reliability must be good. We report an initial exploration on the statistical usefulness of two OAE types for measuring the auditory efferent reflex in humans. This information is essential in helping choose the best measurement techniques and parameters for expensive longitudinal field testing.

#### **[474] Antioxidant Mechanisms for Prevention of Noise-Induced Hearing Loss**

**Colleen Le Prell<sup>1</sup>, Josef Miller<sup>2</sup>**

<sup>1</sup>*University of Florida*, <sup>2</sup>*University of Michigan*

Numerous laboratories have conducted basic and translational studies on molecules that may provide protection against noise-induced hearing loss (NIHL), which is a major unmet medical problem. Antioxidant agents have perhaps proven to be the most effective agents to date, at least in animal models. Recent evidence suggests that combinations of agents may ultimately be the most effective strategy. Translation of agents that reduce NIHL from animal models to human trials is essential in defining the potential clinical utility of antioxidant strategies for prevention of human acquired hearing loss. General steps required to translate the use of these agents from animal models to human trials include identification of appropriate human populations, resolution of all ethical considerations regarding exposure to noise during the course of the trial, approval of the agents and procedures by all relevant regulatory bodies (including for example, IRB boards and, in some cases, the FDA), human subject safety monitoring, data management, and public education. Publication of results such that they are readily accessible to clinicians and others who can implement an effective intervention is also critical. Several antioxidant agents that have proven effective in animal models are in various stages of this process of translation from animal to man; some are now in human clinical trials. These will be discussed. Other potential interventions that may have future clinical utility will also be described. Supported by NIH-NIDCD DC04058 and P30-DC05188.

#### **[475] Noise-Induced Hearing Loss and Military Populations**

**Michael E. Hoffer**

#### **[476] Effects of Sodium Pentobarbital On Neural Responses in the Inferior Colliculus of the Rabbit**

**Shigeyuki Kuwada<sup>1</sup>, Ranjan Batra<sup>2</sup>, Douglas Fitzpatrick<sup>3</sup>**

<sup>1</sup>*University of Connecticut Health Center*, <sup>2</sup>*Univeristy of Mississippi Medical School*, <sup>3</sup>*Univeristy of North Carolina Medical School*

We compared the responses of the same neurons in the inferior colliculus to monaural and binaural sounds when the animal was awake and when it was injected intravenously with a subsurgical dose of sodium pentobarbital. Almost universally, pentobarbital substantially reduced the response rate. This reduction in response rate was accompanied by changes in latency and discharge pattern. Sensitivity to interaural time disparities could also be dramatically altered. Finally, pentobarbital anesthesia changed the response properties over time making it difficult to identify a steady response feature. in the auditory cortex, the ability of a neuron to follow dynamic changes in interaural time disparities was markedly attenuated under barbiturate anesthesia.

#### **477 Do Anesthetics Affect the Processing of Auditory Signals in the Midbrain?**

Luis Populin<sup>1</sup>

<sup>1</sup>*U of Wisconsin*

The inferior and superior colliculi of the midbrain are known to play a fundamental role in the processing of auditory signals and the generation and control of spatial auditory-guided behavior. Recent studies have revealed that the state of the preparation (anesthetized vs behaving) results in large differences in the physiology of these structures. In the inferior colliculus our single unit results show that the recovery of the response to the lagging component of precedence effect stimuli is much shorter in the awake than in the barbiturate anesthetized preparation, which correlates closely with the behavior of the cat. In the superior colliculus the injection of anesthetics during single unit recordings revealed a plethora of dose-dependent and nonlinear changes in the magnitude of the evoked responses, receptive field properties, first spike latency, and bimodal (auditory and visual) integration. Overall, the results challenge a fundamental tenet of sensory physiology, that anesthesia, while decreasing single unit responsiveness, leaves basic physiological properties unaltered.

#### **478 Effect of Anesthesia On Temporal Coding: Implications for the Study of Development**

Dan Sanes<sup>1</sup>, Merri Rosen<sup>1</sup>, Maria Ter-Mikaelian<sup>1</sup>, Malcolm Semple<sup>1</sup>

<sup>1</sup>*New York University*

The emergence of mature temporal processing is essential for a broad range of auditory tasks, from sound localization to animal communication. Surprisingly, development of the neuron coding properties that support these percepts has never been assessed in awake animals. Thus, the extent to which anesthetics factor in to our understanding of functional development remains unclear. A comparison of single neuron temporal coding properties in awake-restrained versus anesthetized adult gerbil auditory cortex (ACx) revealed significant effect on the trial-to-trial variability and temporal precision of discharge to both tones and sinusoidally amplitude-modulated (sAM) stimuli. We have now recorded from single neurons in the ACx of animals prior to sexual maturation (P30-38), and found that immature neurons displayed a lower response strength than did adult neurons, suggesting delayed rate-coding to sAM stimuli. For example, an analysis of modulation depth at slow (1-5Hz) AM frequencies showed that mature ACx cells exhibited higher firing rates as modulation depth increased as compared to young cells, but showed no difference in vector strength. In fact, single neuron detection thresholds for modulation depth displayed higher rate thresholds in young animals, but no maturational difference for synchrony thresholds. In contrast to these findings for sAM, the dynamic range for rate-level functions obtained with static stimuli did not differ between young and adult animals. These data invite a reassessment of published developmental physiology with

the goal of identifying which findings are independent of anesthetic effects.

#### **479 Frequency-Modulation Coding in Primary Auditory Cortex of Awake and Anesthetized New World Monkeys**

Christoph Schreiner<sup>1</sup>, Marc Heiser<sup>1</sup>, Ralph Beitel<sup>1</sup>, Craig Atencio<sup>1</sup>

<sup>1</sup>*University of California San Francisco*

Frequency-modulated (FM) sweeps are important components of animal communication sounds including human speech. The response selectivity for FM sweep parameters of single neurons in primary auditory cortex (AI) shows some differences and some similarities between awake squirrel and owl monkeys and anesthetized squirrel monkeys. Overall, FM responses for phasically responding neurons were congruent between species and awake versus anesthetized states. However, in awake animals, sustained neurons had FM sweep response durations that were longer and, thus, may provide an additional means to encode FM properties. To determine the discriminative power of single neurons we calculated ideal observer performance and the mutual information between neuronal responses and FM sweep parameters. Spike timing and spike rate both carry information about the speed and direction of frequency sweep stimuli. For individual neurons, there is an inverse relation between information carried by spike count and spike timing. This tradeoff suggests that information in AI responses lies on a continuum between rate and temporal codes.

Supported by NIH DC02260 and NIH MH077970

#### **480 Task Dependent Modulation of Spatial Tuning in the Auditory Cortex**

John Middlebrooks<sup>1</sup>, Chen-Chung Lee<sup>1</sup>, Ewan Macpherson<sup>1</sup>, Brian Mickey<sup>1</sup>

<sup>1</sup>*University of Michigan*

We are comparing the effects of an animal's behavioral state on the spatial sensitivity of units in the cat's auditory cortex. In the anesthetized condition, most cortical responses are limited to a burst of spikes at sound onset. In the absence of anesthesia, temporal firing patterns of neurons are more complex, often showing stimulus-dependent modulation of onset, sustained, and/or offset responses. Spatial sensitivity is enhanced in the unanesthetized condition, primarily because firing rates can be modulated above or below ongoing spontaneous rates as a function of sound-source location. We have compared spatial sensitivity in three awake-behaving conditions. The three task states are compared within single 1-1/2 hour sessions. Spatial selectivity is significantly sharper and cortical responses are more deeply modulated by sound-source location when the cat is participating in a localization task than when it is doing a simple auditory discrimination task or is idle. These effects are substantially more robust in the Dorsal Zone of the auditory belt than in the primary auditory cortex.

Supported by NIH grant RO1-DC04312

#### **481 When is Behavior Critical for Understanding Auditory Processing?**

**Shihab Shamma<sup>1</sup>**

<sup>1</sup>*University of Maryland*

is a behaving animal the gold-standard of auditory physiology, or is it an added experimental complication to be avoided? Behavior is the context in which auditory responses are measured, and its value is ultimately judged by the insights it offers relative to the functions being studied. In general, top-down influences likely exceed bottom-up inputs by several times, and have been noted at all stages in the auditory pathway. Thus, cochlear filters, midbrain spatial receptive fields, and cortical spectrotemporal response fields may all change significantly in different behavioral tasks. Nevertheless, in our experience, measurements from the naïve awake or anesthetized animal remain the gold-baseline against which the behavioral effects can be appreciated. Indeed, it remains a rare occurrence that fundamental conclusions about auditory processing had to be revamped because of the effects of behavior. More likely, they are simply refined and improved.

#### **482 Cortical Transformations of Time-Varying Signals Observed in Awake Condition**

**Xiaoqin Wang<sup>1</sup>**

<sup>1</sup>*Johns Hopkins University*

It has long been known that cortical responses to time-varying signals are altered by anesthesia, though the nature of such alterations has not been fully understood. Our studies in marmoset auditory cortex have revealed some important differences in cortical responses to time-varying signals between awake and anesthetized conditions. The upper limit of stimulus-synchronized discharges appears to be higher in awake than in anesthetized condition. More importantly, while auditory cortex neurons of both anesthetized and awake marmosets synchronize to slowly varying signals, only neurons in awake condition are responsive to rapidly varying signals, but without exhibiting stimulus-synchronized discharges. Our recent experiments have also shown that such non-synchronized discharges are also used by a subpopulation of auditory cortex neurons to encode slowly varying signals in the range of acoustic flutter. The sustained and non-synchronized responses to long duration stimuli observed in the auditory cortex of awake marmosets are largely absent in barbiturate- or ketamine-anesthetized animals. These observations show that auditory cortex neurons in awake condition have a greater capacity to dynamically encode time-varying complex sounds and suggest that anesthesia disrupts the neural processing that leads to the non-synchronized cortical responses. In a broader sense, these observations indicate that response properties of auditory cortex observed in anesthetized condition could be observed in awake condition, albeit differing quantitatively. However, the opposite is not necessarily true. In other words, certain response properties observed in awake condition might not be observable in anesthetized condition. The non-

synchronized response to time-varying signals is one of many such examples. Therefore, it is crucial to look for novel neural coding principles in conducting experiments in awake and behaving conditions.

#### **483 Regulation of Pou4f3 Gene Expression in Hair Cells**

**Allen F Ryan<sup>1</sup>, Kwang Pak<sup>1</sup>, Eduardo Chavez<sup>1</sup>, Lina M Mullen<sup>1</sup>**

<sup>1</sup>*ENT, UCSD School of Medicine, La Jolla, CA*

The transcription factor (TF) POU4F3 is expressed by hair cells (HCs) from the time of fate commitment to death. We have shown that, in transgenic mice, 8.5 kb of 5' POU4F3 DNA supports reporter gene expression in HCs. Deletion analysis revealed that while expression in other cells is controlled close to the transcription start site, expression in HCs is regulated in a region 6.5-8.5 kb upstream.

To further evaluate POU4F3 regulation, bioinformatic analysis was used to identify sequences and TF binding sites in the POU4F3 gene that are conserved across mammalian species. A highly conserved element in the proximal promoter includes binding sites for the TF Sp1. A second highly conserved element, within the 6.5-8.5 kb 5' region, contains E-box motifs to which Atoh1 can bind, and motifs that support binding of E2A family TFs, GATA1-3 and Sp1. A third element still further upstream contains motifs for POU4F3, Lhx3 and Gfi1.

To assess the potential for TFs to regulate POU4F3, cells were transfected with the 8.5 kb of 5' POU4F3 DNA linked to GFP, in combination with expression constructs for human Atoh1, E47, Sp1, GATA-3, Lhx3, Gfi1 or POU4F3. Atoh1, Sp1 and Gfi1 transfection produced high levels of reporter gene expression, while GATA3 and E47 produced more modest enhancement and Lhx3 did not change expression. POU4F3 itself also had no effect. While the 8.5 kb reporter construct shows evidence of positive autoregulation on a POU4F3-null background, this regulation may therefore be indirect.

The results are consistent with co-regulation of the POU4F3 gene by a number of TFs, including Atoh1, Sp1 and Gfi1, acting at several sites. Since these TFs support expression of multiple genes in many cell types, they presumably act in specific combinations to regulate expression of genes in HCs. Unlocking these combinatorial codes should help to understand the molecular biology of this cell type.

(Supported by NIH/NIDCD grant DC00139 and by the Research Service of the VA.)

#### **484 The Hair Cell Transcription Factor POU4F3 (Brn-3c) is a Transcriptional Activator of the orphan Steroid/Thyroid Nuclear Receptor NR2F2**

**Chrysostomos Tornari<sup>1</sup>, Emily Towers<sup>1</sup>, Jonathan Gale<sup>1</sup>, Sally Dawson<sup>1</sup>**

<sup>1</sup>*UCL Ear Institute*

The transcription factor POU4F3 (Brn-3c) is exclusively expressed in hair cells in the inner ear and is known to be required for their maturation and survival. In order to

elucidate the mechanism by which POU4F3 loss causes hair cell immaturity and death, a subtractive hybridization was carried out in an inner ear sensory epithelium derived cell line (OC-2) which was manipulated to over- or under-express POU4F3. This analysis returned a number of candidate POU4F3 target genes including nuclear receptor subfamily 2 group F member 2 (NR2F2). NR2F2 is an orphan steroid/thyroid nuclear receptor essential for normal embryonic angiogenesis and heart development<sup>1</sup>. It is expressed in the developing inner ear<sup>2</sup> but its regulation and function in the ear remains uncharacterised. NR2F2 transcription and translation was confirmed in undifferentiated OC-2 cells – which constitutively express POU4F3 – by reverse transcriptase PCR, western blot and immunofluorescence. Potential POU4F3 binding sites in the NR2F2 promoter were identified using Genomatix software. Electrophoretic mobility shift assay analysis confirmed binding of POU4F3 to the two predicted sites with greatest sequence similarity to the POU4F3 consensus. the effect of POU4F3 on NR2F2 transcription was investigated using reporter gene assays. POU4F3 increased NR2F2 promoter activity greater than five fold and this regulation was dependent on functional POU4F3 expression; mutated POU4F3 only increased NR2F2 promoter activity by 50%. Furthermore, the POU4F3 binding sites identified in the NR2F2 promoter were able to confer POU4F3 regulation on a heterologous promoter. The above data confirm that NR2F2 is a direct target of POU4F3. Homozygous NR2F2 knockout mice are embryonic lethal and so alternative approaches are required to elucidate its contribution to hair cell maturation and survival.

1. Pereira et al. (1999) *Genes & Dev.*, 13, p1037

2. Tang et al. (2005) *Gene Expr. Patterns*, 5, p587

#### **[485] Deafness of Trbeta-Deficient Mice is Caused by Tectorial Membrane Malformation Rather Than Retarded Expression of BK Channels in Ihcs**

Harald Winter<sup>1</sup>, Lukas Rüttiger<sup>1</sup>, Marcus Müller<sup>1</sup>, Niels Brandt<sup>1</sup>, Stephanie Kuhn<sup>1</sup>, Ulrike Zimmermann<sup>1</sup>, Matthias Sausbier<sup>1</sup>, Peter Ruth<sup>1</sup>, Bernhard Hirt<sup>1</sup>, Frédéric Flamant<sup>2</sup>, Laure Quignodon<sup>2</sup>, Yong Tian<sup>3</sup>, Jian Zuo<sup>3</sup>, Susanne Feil<sup>1</sup>, Robert Feil<sup>1</sup>, **Jutta Engel<sup>1</sup>**, Marlies Knipper<sup>1</sup>

<sup>1</sup>University of Tuebingen, <sup>2</sup>Ecole Normale Supérieure de Lyon, <sup>3</sup>St. Jude Children's Research Hospital Memphis

Thyroid hormone is essential for the development of hearing. in the cochlea, it acts through thyroid hormone receptors TRalpha and TRbeta. Studies in mice deficient for these receptors revealed that TRbeta, but not TRalpha, is necessary for final differentiation of the cochlea and/or central auditory pathway (Rusch et al. PNAS 1998, Rusch et al. J NSci 2001). Due to the lack of severe cochlear malformation, the hearing defect in TRbeta-/- mice was attributed to delayed expression of the inner hair cells' fast activating BK current, causing a delay in functional maturation. Our analysis of mice with a deletion of the BKalpha subunit revealed normal ABR thresholds in young mice followed by progressive hearing loss due to OHC degeneration (Rüttiger et al. PNAS 2004) ruling out the

possibility that delayed expression of BK channels causes deafness. to analyze reasons for deafness of TRbeta-/- mice, a mouse model with a hair-cell specific deletion of TRbeta (TRbeta-/lox x PCre (Cre recombinase under a prestin promotor, Tian et al. Dev Dyn 2004)) was examined. Cre recombinase was shown to activate before P11 as tested with Rosa26 reporter mice and BKalpha-/lox mice. TRbeta-/lox x PCre mice showed a slight delay in IHC BK expression but had hardly any threshold shift, indicating hearing loss caused by TRbeta deletion is manifested before P11 or is of extra-hair cell origin. in TRbeta-/- IHCs, Ca2+ currents and exocytosis were normal at P20. CAP thresholds were elevated; their waveform did not indicate retrocochlear defects. Surprisingly, DPOAEs and microphonics were reduced, although nearly normal nonlinear capacitances and transducer currents of OHCs have been reported (Rusch et al 1998). Histological analysis revealed a morphological defect of the tectorial membrane supporting the hypothesis that hearing loss in constitutive TRbeta-/- mice might be due to a reduced mechanical performance of the cochlea.

#### **[486] Developmental Acquisition of Sensory Transduction in Mouse Cochlear Hair Cells**

**Andrea Lelli<sup>1</sup>**, Yukako Asai<sup>1</sup>, Jeffrey R. Holt<sup>1</sup>, Gwenaëlle S.G. Geleoc<sup>1</sup>

<sup>1</sup>University of Virginia

To characterize the spatiotemporal pattern of transduction acquisition we examined outer hair cells from acutely excised mouse (CD-1) cochlea at various developmental stages. We charted uptake of FM1-43, which permeates hair cell transduction channels, recorded mechanotransduction currents evoked by rapid bundle deflections (step rise time  $\approx 20 \mu\text{sec}$ ) and examined expression of putative components of the transduction complex as a function of developmental stage and position along the cochlea. organ of Corti whole mounts were imaged five minutes after a 10 sec exposure to  $5 \mu\text{M}$  FM1-43. Uptake of the dye was first detected in the basal portion of the cochlea at P0. Over the first postnatal week we found that uptake progressed towards the apex such that by P8 FM1-43 fluorescence was robust and continuous along the entire length of the cochlea.

To examine the onset of mechanotransduction we recorded from 234 outer hair cells from four cochlear regions, base to apex at stages between E17 and P8. Our data showed a tight correlation between the pattern of FM1-43 uptake and the acquisition of mechanotransduction. We were unable to detect transduction currents before P0. However, we noted rapid acquisition of mechanosensitivity in the basal quarter beginning at P0. within 24 hours 100% of basal outer hair cells in our sample were mechanosensitive. Acquisition of mechanotransduction progressed along the length of the cochlea toward the apex with all of the cells transducing by P6.

We used quantitative RT-PCR with tissue harvested from the four quarters of the developing mouse cochlea (E17-P8) to examine the spatiotemporal expression pattern of Myosin 7a, Myosin 1c, Cadherin 23 and Protocadherin 15.

We found that the onset of Myosin 7a, Myosin 1c and Cadherin 23 expression preceded the acquisition of transduction and that the expression pattern of Protocadherin 15 paralleled the onset of transduction. (Supported by NIH/NIDCD Grant # R01 DC008853)

#### **487 Sensory Transduction and Adaptation in Inner and Outer Hair Cells of the Mouse Auditory System**

**Eric A. Stauffer<sup>1</sup>**, Jeffrey R. Holt<sup>1</sup>

<sup>1</sup>*University of Virginia*

We sought to systematically compare mechanotransduction and adaptation in inner and outer hair cells of the mouse cochlea. We recorded transduction currents from hair cells located at the apical end of acutely excised cochleae from P6 – P8 CD1 and BL6 mice. Cochlear hair cells were stimulated using a stiff glass probe with an angled and forged tip shaped to fit into the concave side of the hair bundle. Step displacements of the probe were driven by a PICMA chip piezo actuator (62  $\mu$ sec rise time). the whole-cell, tight-seal technique was used to record mechanotransduction currents at -64 mV. Outer hair cells had average maximal transduction currents of  $-311 \pm 69$  pA (max. -580 pA,  $n = 11$ ) and an operating range of  $0.44 \pm 0.12$   $\mu$ m while inner hair cells had a broader operating range of  $0.86 \pm 0.17$   $\mu$ m and maximal transduction currents of  $-324 \pm 118$  pA (max. -418 pA,  $n = 16$ ). the similar amplitude was surprising given the difference in the number of stereocilia, 81 for outer hair cells and 48 for inner hair cells, but may be reconciled by a difference in single channel conductance. Morphological differences may account for some of the difference in operating range.

The inferred-shift method (Shepherd and Corey, 1994) allowed us to separate the fast and slow components of adaptation. the fast component accounted for 41% and 43% of the total extent of adaptation in inner and outer hair cells, respectively. the slow component also accounted for a significant fraction: 29% and 31%, respectively.

Surprisingly, the rate of the slow component, up to 13  $\mu$ m/sec at  $P_o=0.5$ , was similar to that of vestibular hair cells. the rate of the fast component was similar among inner (162  $\mu$ m/sec) and outer (156  $\mu$ m/sec) hair cells. Several properties of fast adaptation were consistent with a model that proposes calcium-dependent release of tension allows transduction channel closure. (Supported by NIH/NIDCD Grant #R01-DC005439)

#### **488 Myosin-Xva is Required for Fast Adaptation of Mechano-Electrical Transduction in Inner But Not Outer Cochlear Hair Cells**

**Ruben Stepanyan<sup>1</sup>**, **Gregory Frolenkov<sup>1</sup>**

<sup>1</sup>*Dept. Physiology, University of Kentucky*

In the sensory hair cells of the inner ear, activation of mechanically gated transduction channels is followed by rapid  $Ca^{2+}$ -dependent deactivation. This "fast adaptation" may be linked to cochlear amplification that is required for sensitive hearing. Here we studied fast adaptation in the cochlear hair cells of young postnatal shaker 2 mice

(*Myo15<sup>sh2/sh2</sup>*) that have no functional myosin-XVa. in *Myo15<sup>sh2/sh2</sup>* inner hair cells (IHCs), fast adaptation was absent despite "wild type" nanoampere-scale amplitude and ultra-fast activation kinetics of transduction current as well as normal concentration of cytosolic  $Ca^{2+}$ . However, we observed apparently normal fast adaptation in *Myo15<sup>sh2/sh2</sup>* outer hair cells (OHCs) that also have no functional myosin-XVa. Consistent with the current models, mechanotransduction in *Myo15<sup>sh2/sh2</sup>* OHCs was found to require extracellular "tip-link" filaments interconnecting sensory stereocilia. in contrast to OHCs, *Myo15<sup>sh2/sh2</sup>* IHCs do not have tip links and their mechanosensitivity depends exclusively on "top-to-top" links. Since the lack of functional myosin-XVa does not affect fast adaptation in *Myo15<sup>sh2/sh2</sup>* OHCs, we concluded that myosin-XVa does not contribute directly to fast adaptation machinery. However, a critical component of this machinery is apparently affected by the profound changes of stereocilia link morphology in *Myo15<sup>sh2/sh2</sup>* IHCs. Taken together, our data favors "tension release" model of fast adaptation over "channel re-closure" model. Supported by the Deafness Research Foundation and the University of Kentucky.

#### **489 Molecular Composition, Structure, and Function of the Tip Link in Hair Cells: Implications for Genetic Diseases That Cause Deafness**

**Ulrich Mueller<sup>1</sup>**, Piotr Kazmierczak<sup>1</sup>, Hirofumi Sakaguchi<sup>2</sup>, Martin Schwander<sup>1</sup>, Joshua Tokita<sup>2</sup>, Anna Reynolds<sup>1</sup>, Nicolas Grillet<sup>1</sup>, Wei Xiong<sup>1</sup>, Elizabeth Wilson-Kubalek<sup>1</sup>, Ron Milligan<sup>1</sup>, Bechara Kachar<sup>2</sup>

<sup>1</sup>*The Scripps Research Institute*, <sup>2</sup>*National Institute of Deafness and Communicative Disorders, NIH*

Tip-link filaments that connect the stereocilia of a hair cell in the direction of mechanical sensitivity of the hair bundle are thought to gate mechanoelectrical transduction channels in hair cells. However, reports on the composition, properties and function of tip links have been conflicting. We now demonstrate that two cadherins that are linked to inherited forms of deafness in humans interact to form tip links. Immunohistochemical studies show that cadherin 23 (CDH23) and protocadherin 15 (PCDH15) localize to the upper and lower part of tip links, respectively. the N-termini of the two cadherins co-localize on tip-link filaments. Biochemical experiments show that CDH23 homodimers interact in trans with PCDH15 homodimers to form a filament with structural similarity to tip links. Ions that affect tip-link integrity and a point mutation in the N-terminal part of PCDH15 that causes a recessive form of deafness disrupt interactions between CDH23 and PCDH15. Other mutations in CDH23 and PCDH15 that are associated with deafness in humans do not affect interactions between the two cadherins and likely affect tip link function. Consistent with this model, mice that carry mutations resembling the human mutations show defects that affect hair cell function in mechanotransduction. Collectively, our finding define essential components of the tip link in hair cells and provide strong evidence that some forms of human deafness are caused by defects in tip links.

#### **490 Effects of Exposure to Different Concentrations of Extracellular Calcium on Tip-Link Dimensions**

David Furness<sup>1</sup>, B Nirmal Kumar<sup>2</sup>, Yukio Katori<sup>3</sup>, Carole Hackney<sup>4</sup>

<sup>1</sup>Keele University, <sup>2</sup>Royal Albert Edward Infirmary, <sup>3</sup>Tohoku University School of Medicine, <sup>4</sup>University of Cambridge

The tip link between stereocilia may represent a gating spring coupled to the mechanoelectrical transduction (MET) channel. Excitatory deflections of the stereocilia which stretch the tip link are thought to open the METs and allow both  $\text{Ca}^{2+}$  and  $\text{K}^{+}$  to enter depolarising the membrane. the extracellular  $[\text{Ca}^{2+}]$  concentration affects the characteristics of transduction with very low  $[\text{Ca}^{2+}]_E$  causing both the tip links and transduction to be lost. It has been reported that the tip link is composed of protocadherin 15 (PCDH15) and cadherin 23 (CDH23); the combined length of these molecules might be 170 - 180 nm. CDH23 appears to be a double-stranded helix whose folding depends on the presence of calcium ions (Kazmierczak et al., 2007; Nature 449: 87-92).

Tip link lengths were investigated to compare with that of PCDH15 and CDH23. Lengths were measured in ultrathin sections of guinea-pig cochlea using transmission electron microscopy (TEM). the effects of changing  $[\text{Ca}^{2+}]_E$  were determined by exposing cochlear spirals for 10 min to either 1 mM, 50  $\mu\text{M}$  or 1  $\mu\text{M}$   $[\text{Ca}^{2+}]$  in Hank's buffered salt solution, fixing, embedding for TEM and measuring as before.

Tip-link length ranged from 90 nm to 190 nm, with a mean of  $150 \pm 20$  nm. in 1 mM  $[\text{Ca}^{2+}]_E$ , the tip links were  $164.4 \pm 57$  nm long. After exposure to 50  $\mu\text{M}$   $[\text{Ca}^{2+}]_E$ , tip links were longer,  $185.8 \pm 38$  nm. in 1  $\mu\text{M}$   $[\text{Ca}^{2+}]_E$ , tip links were absent as expected but the dense attachment plaques remained separated by a distance of  $209.7 \pm 39$  nm.

The data show that tip-link length may vary substantially and is affected by the external concentration of calcium ions. the best fit with the predicted length was in 50  $\mu\text{M}$   $[\text{Ca}^{2+}]_E$ , close to the likely calcium concentration in endolymph. One model of the length change compatible with the suggested structure is that the two strands of CDH23 unfold with decreasing  $[\text{Ca}^{2+}]_E$ .

Supported by Deafness Research UK and the Midlands Institute of Otology.

#### **491 Electron Tomography of Hair Bundle Linkers**

Manfred Auer<sup>1</sup>

<sup>1</sup>Lawrence Berkeley Laboratory

We have examined the molecular 3D organization of ankle links, kinociliary links and tip links of frog sacculus sensory epithelia hair bundles using 2D TEM and 3D electron tomographic imaging, and have obtained their respective lengths with nanometer precision.

Ankle links ranged from ~75 nm to ~270 nm and often appear to be paired. Kinociliary links are ~115-120 nm long and consist of single individual strands that only rarely interact with other strands. Tip links were found to our surprise to come in two distinct lengths, they are either

~110-120 nm or ~170 nm. Such distribution can also be seen in published images of the tip link and the large number of 2D projection images that we have collected. Furthermore tip links of either length have a tendency to curl up when no longer attached. in addition to the primary link, we found evidence of an auxiliary link that originates from the main link and independently links to the membrane. It displays dimensions comparable to the tip link, and which also has a tendency to curl up upon detachment. the tendency of the tip link to curl up is in conflict with the current model of a rigid link based on cadherin 23 and protocadherin 15. We will propose an alternative tip link model that is based on fibronectin-dimers attached by their N-terminus to lipid rafts on stereocilia. This model predicts that N-terminal fragments of fibronectin will interfere with tip link recovery after BAPTA treatment, which was indeed observed by imaging Di-Asp uptake into zebrafish neuromast hair cells.

#### **492 Analysis and Functional Evaluation of the Hair-Cell Transcriptome**

Brian McDermott<sup>1</sup>, Jessica Baucom<sup>2</sup>, A. J. Hudspeth<sup>2</sup>

<sup>1</sup>Case Western Reserve University, <sup>2</sup>Howard Hughes Medical Institute and the Rockefeller University

An understanding of the morphogenesis and operation of hair cells requires identification of the genes expressed in these cells and of the functions of the cognate proteins. As an initial step towards this goal, we have used DNA-microarray technology to identify the transcripts present in hair cells of the adult zebrafish. After isolating pure populations of hair cells from the lagena of the inner ear, we amplified and labeled RNA and hybridized the resultant probes to oligonucleotide microarrays. to exclude genes expressed ubiquitously in epithelial cells, we conducted parallel experiments with hepatocytes and disregarded the genes that they expressed. the hair-cell transcriptome of the zebrafish includes genes involved in vesicle fusion, transcriptional regulation, and transmembrane ion movement; among these are homologs of genes that, when mutated, produce deafness in humans and mice. Additional genes encode proteins that are involved in cytoskeletal function, and might therefore contribute to the formation and maintenance of the hair bundle. These components include actin-binding and -capping proteins as well as constituents of the intraflagellar transport system. Finally, the transcriptional profile encompasses numerous genes of undetermined function. Using the molecular-biological techniques applicable to the zebrafish, we have begun to investigate the roles that some of these genes' products play in hair-cell development and function. Two of the genes identified in the screen have already proven necessary for the proper development of hair bundles.

This research was supported by National Institute of Health grants DC00241 and DC006539 from the National Institutes of Health and the 2006 Annenberg Foundation Grant in Auditory Science from the National organization for Hearing Research Foundation.



#### **493 Monoclonal Antibodies Against Highly Purified Stereocilia Membrane Antigens**

Clive Morgan<sup>1</sup>, Peter Gillespie<sup>1</sup>

<sup>1</sup>OHSU

Mechanotransduction and adaptation are key to the detection of sound with the auditory organ and motion with the vestibular organs. the surface of these organs are covered with hair bundles, and stereocilia are the fine processes of the hair bundle where mechanotransduction takes place. the Gillespie lab pioneered the use of the twist-off technique for isolating stereocilia from bullfrog and has recently adapted this technique for analyzing the protein complement of chicken stereocilia using mass spectrometry. We have now developed an alternative bundle isolation technique using density centrifugation and lectin affinity-based isolation. This new method allows the routine analysis of several thousand organs and makes additional downstream fractionation relatively simple. We have used this new technique to raise monoclonal antibodies against bundle membrane proteins. the membrane fraction of bundles from 2000 chicken vestibular and auditory organs were prepared and used to immunize two mice. Fusions were made and 1700 hybridoma supernatants were screened for bundle-specific staining patterns using immuno-cytochemistry. Currently we are examining 18 promising clones in more detail. Antibodies reveal antigen localization falling into three broad categories: 1) kinocilium-like staining above the tallest stereocilia as well as on the tips of the stereocilia - similar to the tip-link antigen staining, 2) punctate labeling restricted to the tips of the stereocilia, and 3) labeling over the entire bundle.

We aim to identify interesting antigens and ultimately uncover components of the transduction apparatus.

#### **494 New Insight into Localization and Function of $\gamma$ -Actin in Hair Cell Stereocilia**

Inna A. Belyantseva<sup>1</sup>, Mei Zhu<sup>2</sup>, Ruben Stepanyan<sup>3</sup>, Benjamin J. Perrin<sup>4</sup>, Gregory I. Frolenkov<sup>3</sup>, James M. Ervasti<sup>4</sup>, Thomas B. Friedman<sup>1</sup>, Karen H. Friderici<sup>2</sup>

<sup>1</sup>Laboratory of Molecular Genetics, Section on Human Genetics, NIDCD/NIH, Rockville, MD 20850, <sup>2</sup>Department of Microbiology and Molecular Genetics, Michigan State University, East Lansing, MI 48824, <sup>3</sup>Department of Physiology, University of Kentucky, Lexington, KY 40536, <sup>4</sup>Department of Biochemistry, Molecular Biology & Biophysics, University of Minnesota, Minneapolis, MN

Nonmuscle  $\beta$ - and  $\gamma$ -actin differ only by four amino acids at their N-termini and in many instances are localized to the same structures such as hair cell stereocilia (Hofer et al. 1997; Furness et al. 2005). Vertebrate conservation of two genes encoding very similar actins suggests that they may perform distinct functions. Data from a muscle specific  $\gamma$ -actin KO show that  $\beta$ -actin does not fully compensate for the loss of  $\gamma$ -actin (Sonnemann et al. 2006). *ACTB* and *ACTG1* encode  $\beta$ - and  $\gamma$ -actin, respectively. Several missense mutations of *ACTG1* are associated with dominant nonsyndromic progressive hearing loss (Zhu et al. 2003; Van Wijk et al. 2003; Rendtorff et al. 2006) while a dominant missense mutation in *ACTB* causes

developmental malformations, deafness, and dystonia (Procaccio et al. 2006). Using  $\gamma$ -actin specific antibodies validated in *ACTG1*<sup>-/-</sup> cochleae and a commercially available FITC-conjugated  $\beta$ -actin antibody, we found that during embryonic development  $\beta$ -actin appears in mouse hair cell stereocilia earlier than  $\gamma$ -actin, which accumulates first in supporting cells and later appears in hair cells. in many cell types of the organ of Corti including hair cells,  $\beta$ -actin overlaps with rhodamine-phalloidin staining, while  $\gamma$ -actin shows a different pattern. After gene-gun-mediated transfection, GFP- $\gamma$ -actin first appears at the tips of hair cell stereocilia similar to the targeting of GFP- $\beta$ -actin, but the time course of GFP- $\gamma$ -actin incorporation into stereocilia along their length varied from cell to cell. After *In Vivo* noise exposure, we observed accumulation of  $\gamma$ -actin in damaged stereocilia. Taking into account the variable onset and progressive character of hearing loss due to mutations of human *ACTG1*, as well as the expression pattern of  $\gamma$ -actin in the auditory hair cells of control and noise treated rodent cochleae, we propose that  $\gamma$ -actin is important for maintenance of cytoskeletal structures, and particularly for remodeling and repair in adult hair cells.

#### **495 ACTG1-Null Mice Develop Progressive Hearing Loss**

Benjamin Perrin<sup>1</sup>, Kevin Sonnemann<sup>1</sup>, Kurt Prins<sup>1</sup>, Megan Korte<sup>2</sup>, JoEllen Boche<sup>2</sup>, JoAnn McGee<sup>2</sup>, Edward Walsh<sup>2</sup>, James Ervasti<sup>1</sup>

<sup>1</sup>University of Minnesota, <sup>2</sup>Boys Town National Research Hospital

Actin is one of the most abundant proteins in nature and plays essential roles in almost every cellular function including muscle contraction, cell migration, vesicle trafficking, and polarized growth. Two cytoplasmic actin isoforms,  $\beta_{\text{cyto}}$ - and  $\gamma_{\text{cyto}}$ -actin, are ubiquitously expressed. Although encoded by separate genes, these cytoplasmic actin isoforms vary at only 4 of 375 amino acid residues; however, these small sequence differences are well conserved through evolution, suggesting that  $\beta_{\text{cyto}}$ - and  $\gamma_{\text{cyto}}$ -actin have distinct cellular functions. Consistent with this idea, the localization of  $\beta_{\text{cyto}}$ - and  $\gamma_{\text{cyto}}$ -actin differs in many cells, including inner-ear hair cells. Additionally, some mutations in the human *ACTG1* gene encoding  $\gamma_{\text{cyto}}$ -actin lead to progressive deafness, indicating an essential cellular role for this isoform that cannot be completely filled by  $\beta_{\text{cyto}}$ -actin. to further characterize the role of  $\gamma_{\text{cyto}}$ -actin in the inner ear, we generated a  $\gamma_{\text{cyto}}$ -actin deficient mouse and found that auditory function and stereocilia morphology were normal in young animals. However, as mutant mice aged, progressive auditory deficits similar to those of the human mutant *ACTG1* deafness phenotype were observed. Further, auditory deficits in  $\gamma_{\text{cyto}}$ -actin null mice of intermediate age correlate with defects in hair cell stereocilia morphology. in older mice with profound hearing deficits, the organ of Corti exhibits degeneration and loss of sensory and support cells. Together, these data suggest a role for  $\gamma_{\text{cyto}}$ -actin in stabilizing or maintaining hair cells in the inner ear.

**496 Genetic, Cell Biological and Physiological Analyses of a Mouse Model for DFNB28 Deafness**

**Shin-ichiro Kitajiri**<sup>1</sup>, Ruben Stepanyan<sup>2</sup>, Richard Goodyear<sup>3</sup>, Guy Richardson<sup>3</sup>, Zubair Ahmed<sup>1</sup>, Gregory Frolenkov<sup>2</sup>, Andrew Griffith<sup>1</sup>, Thomas Friedman<sup>1</sup>

<sup>1</sup>NIDCD/NIH, <sup>2</sup>University of Kentucky, <sup>3</sup>University of Sussex

Mutations of the actin-binding protein TRIOBP were identified as the cause of human hereditary deafness DFNB28. Novel alternative splice isoforms of TRIOBP (TRIOBP4 and TRIOBP5) were identified and RT-PCR showed their expression in inner ear, retina and brain. All currently known DFNB28 mutations involve only exon 6 (Riazuddin et al., 2006; Shahin et al., 2006). Since the initially identified and ubiquitously expressed isoform TRIOBP1 (Seipel et al, 2001) does not contain the amino acid sequence encoded by exon 6, TRIOBP1 is likely not to be affected by these mutations. On the other hand, TRIOBP4 and TRIOBP5 isoforms are truncated by DFNB28 pathogenic mutations and are likely to be necessary for hearing. We generated isoform specific antibodies and confirmed that the TRIOBP5 isoform is localized at the rootlets of stereocilia from late embryonic stages to adulthood, and is also localized transiently at the tips of stereocilia until postnatal day 16. a mouse that is null for both TRIOBP4 and TRIOBP5 isoforms were generated by gene targeting. organ of Corti hair cells from this null mouse show near normal morphology and also have a wild type mechanotransduction current at postnatal days 2-8. However, by postnatal day 25, this null mouse is profoundly deaf. the functions of TRIOBP in hair cell stereocilia are under investigation.

**497 Does WASP Play a Role in Formation of Stereocilia Branches in Myosin VI-Deficient Hair Cells?**

**Agnieszka K Rzadzinska**<sup>1</sup>, Karen P. Steel<sup>1</sup>

<sup>1</sup>Wellcome Trust Sanger Institute, Wellcome Trust Genome Campus, Hinxton, Cambridge CB10 1SA, UK

Hearing and balance depend upon the function of hair cells that are equipped with highly ordered bundles of mechano-sensory stereocilia. Each stereocilium is supported by a paracrystalline actin core formed by hundreds of parallel, uniformly polarized and tightly cross-linked actin filaments, which undergo continuous turnover. the formation and maintenance of the stereocilia bundle is dependent upon several known inner ear proteins, including several unconventional myosins. the detailed scanning electron microscopy analysis of inner ear epithelia harvested from two myosin VI mutant mice, namely Snell's waltzer and tailchaser, show unusual branches on the stereocilia, indicating role for myosin VI in the maintenance of parallel actin bundles. Here we investigated the involvement of several actin-binding proteins in the formation of stereocilia branches by testing their immunoreactivity within control and mutant inner ear epithelia. We found that members of the ARP2/3 complex are present in control epithelia and moreover, they localize to stereocilia from early postnatal stages onwards. in

contrast, WASP can be found only in mature hair cells. the stereocilia localization of the ARP2/3 complex, and the levels of ARP 2/3-specific immunoreactivity, were not affected by myosin VI deficiency. However, we were able to detect WASP-specific staining in developing hair cells lacking myosin VI, at the stage when normal hair cells show no WASP labelling.

**498 Measurement of Anisotropic Mechanical Properties of Cochlear Tectorial Membrane**

**Nuria Gavara**<sup>1</sup>, Richard Chadwick<sup>1</sup>

<sup>1</sup>NIDCD

**BACKGROUND:** the tectorial membrane (TM) is an anisotropic matrix composed of oriented collagen fibers that overlays the inner and outer hair cells of the inner ear. Despite the fundamental role of the TM in proper hearing, little quantitative knowledge of its anisotropic mechanical properties is known. **AIM:** to measure the elastic moduli of the TM (fiber modulus and shear moduli normal and perpendicular to the fiber direction). **METHODS:** Samples of TM isolated from guinea pigs (N=9 animals) were attached to coverslips and fluorescent microbeads (1µm diam.) were deposited on the surface of the TM. an AFM (Bioscope II) tip was used to exert controlled point-like forces onto the surface of the TM in the x, y, and z directions, and a CCD camera was employed to measure bead displacements. Measurements were performed at multiple bead-tip distances. Elastic moduli values were computed using a Boussinesq-like solution for an anisotropic half space by fitting the relationship between applied forces and resulting displacements for different bead-tip distances. **RESULTS:** Fiber modulus was  $2.2 \pm 0.5$  MPa whereas shear moduli parallel and perpendicular to the fiber were  $251 \pm 158$  Pa and  $170 \pm 110$  Pa, respectively. **CONCLUSIONS:** These measurements provide evidence of the anisotropic mechanical properties of TM. Moreover, incorporation of the elastic moduli data into quantitative models of cochlear mechanics will help understand the underlying mechanisms of hearing.

This work is supported by the NIDCD intramural program project Z01-DC000033-10.

**499 Mechanical Tuning of the Tectorial Membrane Response in the Frog Basilar Papilla**

**Richard LM Schoffelen**<sup>1</sup>, Johannes M Segenhout<sup>1</sup>, Pim Van Dijk<sup>1</sup>

<sup>1</sup>Dpt. of Otorhinolaryngology, University Medical Center Groningen, the Netherlands

The frog's inner ear has a unique anatomy among vertebrates: it contains two dedicated auditory end organs, the basilar papilla (BP) and the amphibian papilla. Both of them lack a basilar membrane (BM). the BP covers the upper part of the frog's auditory frequency range and appears to be a 'simple' auditory detector from an anatomical and physiological point of view. Due to the lack of a BM in the BP, any frequency selectivity in this organ must be due to the electrical and mechanical properties of

the hair cells, the tectorial membrane (TM) or associated structures. We investigated whether there is a mechanical basis for the frequency selectivity in the BP.

The inner ears were excised from freshly terminated northern leopard frogs (*Rana pipiens pipiens*). Exposing the round window allowed observation of the BP through a light microscope without damaging the endolymphatic space in which it is contained. a piezo-electric stimulator was applied to the oval window in order to provide a sinusoidal stimulus to the specimen. Stimulus frequencies ranged from 0.5kHz to 3kHz, in 0.5kHz steps.

Using a stroboscopic illumination pattern, the membrane was imaged at different phases of the stimulation wave with a high-resolution digital camera. by additionally moving the microscope's focal plane through the membrane, a 3D image of the membrane in motion was created. the image was subsequently analyzed using optical-flow detection algorithms.

The response of the TM showed a distinctive frequency selectivity within this range. the maximum response was recorded at 2kHz. This result is consistent with the neural response recorded in auditory nerve fibers innervating the BP, the otoacoustic emission measurements in frog species from this family, and the frequency-selective mechanical response observed in the BP's contact membrane. the results presented here provide evidence for a mechanical basis of the frequency selectivity of the frog basilar papilla.

## **500 Stiffness & Longitudinal Coupling in the Cochlea**

**Nneka Eze<sup>1</sup>**, Elizabeth Olson<sup>1</sup>

<sup>1</sup>*Columbia university*

Longitudinal coupling of the cochlear partition is a mechanical property that will influence the travelling wave. Many models only consider the transverse arrangement of the BM fibres so assign no longitudinal coupling. This does not fit with the anatomical picture, which includes the pillar cells that are tightly connected at their heads. the pillar cells have been demonstrated to be an important anatomical factor in the overall stiffness of the cochlear partition, and are likely to also introduce significant longitudinal coupling. The main aim of our experiment is to explore how longitudinal coupling of the cochlear partition shapes the passive substrate of cochlear mechanics. The first part of the experiment is to severely damage the organ of Corti with topical neomycin such that the pillar cells are missing or severely disrupted. Secondly, using the laser interferometer, mechanical measurements from the damaged cochleae, in particular basilar membrane motion measurements, will be compared with normal controls.

Ototoxicity to neomycin was observed after intratympanic injection with cochlear damage that increased in a time dependent manner. the pillar cells appear extremely robust and were very resistant to ototoxic damage in the gerbil. However, in preliminary data, 6 months post-application there was complete loss of all hair cells and normal supporting cells at the base of the cochlea.

in our preliminary motion data, changes occurred that were consistent with reduced stiffness and longitudinal coupling.

in the phase-vs-frequency data, the treated cochlea showed increased phase accumulation (as expected with reduced longitudinal coupling) and a shift to lower frequencies (as expected with lower stiffness).

## **501 Differential Measurement of Basilar Membrane Transfer Functions in Living Cochleae**

**Tianying Ren<sup>1</sup>**, Wenxuan He<sup>1</sup>

<sup>1</sup>*Oregon Health & Science University*

The transfer function (TF) of basilar membrane vibration has been used to characterize the mechanical properties of the cochlear partition. the cochlear amplifier gain has been measured as the magnitude difference of TFs under sensitive and insensitive cochlear conditions near the best frequency (BF). the magnitude TF is commonly measured as the ratio of basilar membrane vibration magnitude to that of stapes vibration. Since the stapes vibration has to be converted into fluid displacement to vibrate the cochlear partition the conventional TF is determined by the stapes-to-basilar membrane conversional mechanism and the transfer function of the basilar membrane. to characterize mechanical properties of a given length of the cochlear partition, the basilar membrane vibrations were measured at two longitudinal locations using a laser interferometer in living cochleae. the magnitude TF between two locations was measured as the ratio of the vibration at the apical location to that at the basal location. the phase TF was obtained by subtracting basal phase from the apical phase. It was found that, at low and intermediate sound pressure levels, the differential magnitude TF showed a small peak at frequencies lower than BF, which is conceptually consistent with the current speculation that the vibration is amplified at a cochlear location basal to the BF. in contrast to the conventional TF, the differential TF revealed a large notch (negative gain) at frequencies near the BF. Differential phase TF showed that the vibration traveled from the basal to apical end through the observed location. Thus, the current data indicate that the cochlea achieves its sharp tuning and nonlinearity through amplifying and attenuating basal membrane vibration.

Supported by NIH-NIDCD.

## **502 Phase Modulation in Basilar Membrane Onset Vibrations**

**anders Fridberger<sup>1</sup>**, Jiefu Zheng<sup>2</sup>, Tianying Ren<sup>2</sup>, **Alfred Nuttall<sup>2</sup>**

<sup>1</sup>*Karolinska Institutet*, <sup>2</sup>*Oregon Health & Science University*

Sound moves the basilar membrane. While many studies investigated the properties of these vibrations once they reached their final level, few studies have examined events at the onset. It is generally accepted that basilar membrane vibrations at low stimulus levels are governed by an as yet ill-defined mechanism, the cochlear amplifier, which increases the sensitivity and frequency resolution of the ear. Our hypothesis is that a close examination of onset responses would allow us to determine important functional properties of the amplifier, such as its speed. We therefore performed a series of experiments in living anaesthetized guinea pigs, where basilar membrane

vibrations were measured in response to single-frequency stimulation near the characteristic frequency of the basal turn recording location. Electrical responses were measured in the same animals using electrodes placed inside the organ of Corti. a consistent pattern of phase change emerged, where basilar membrane vibrations acquired a large phase lag over the first few cycles of the response. the implications of these results are discussed.

### **[503] Mechanical Preprocessing of Amplitude Modulated Sounds in the Apex of the Cochlea**

**Nigel Cooper<sup>1</sup>**

<sup>1</sup>*Keele University*

A displacement-sensitive laser interferometer was used to record the sound-evoked vibrations of individual Hensen's cells in the apical turns of living guinea-pig cochleae. the mechanical responses to amplitude modulated (AM) tones were investigated, and are shown to be physiologically vulnerable. in healthy cochleae, the AM responses are demodulated strongly at both moderate and high sound pressure levels (e.g. 60-80dB SPL). in less healthy and post-mortem cochleae, AM demodulation is weaker and is only seen at high stimulus levels (e.g 85-90dB SPL). the physiologically vulnerable component of the demodulation is considered to be an analogue of the baseline position shifts that can be seen in the apical cochlea's responses to pure-tone stimuli. the simplified computational model of Cooper & Dong (2003) is used to support a suggestion that both the baseline position shifts and the AM demodulation (i) originate from an asymmetry in the outer hair cells' mechano-electrical transduction process and (ii) are put into effect via a voltage-dependent electro-mechanical transduction process such as the somatic motility (but not the hair-bundle motility) of the outer hair cells.

Acknowledgements: Supported by the Royal Society and by Deafness Research UK.

References: Cooper, N.P. and Dong, W (2003) Baseline position shifts and mechanical compression in the apical turns of the cochlea. In: Gummer, A.W. (ed.) the Biophysics of the Cochlea: Molecules to Models. Singapore: World Scientific, pp. 261-270.

### **[504] Is Stereocilia Velocity or Displacement Feedback Used in the Cochlear Amplifier?**

**Shan Lu<sup>1</sup>, David Mountain<sup>1</sup>, Allyn Hubbard<sup>1</sup>**

<sup>1</sup>*Boston University*

Outer hair cells (OHC) likely play an important role in cochlear amplification. the OHC senses stereocilia motion and creates a force feedback to the organ of Corti. It is largely accepted that the stereocilia displacement drives the OHC apical conductance change, which, in turn, drives OHC somatic motility.

Recent research shows that the tension gated OHC current exhibits fast adaptation in response to stereocilia displacement [Kennedy, H. J., M. G. Evans, A. C. Crawford and R. Fettiplace (2003). "Fast adaptation of mechanoelectrical transducer channels in mammalian

cochlear hair cells." *Nature Neuroscience* 6(8): 832-6.]. Such an adaptation process resembles a high-pass filter or differentiator, at least for the inward current. Since velocity is the derivative of displacement, fast adaptation may indicate that it is the stereocilia velocity, rather than displacement that drives the OHC apical conductance.

We changed our multi-compartment, piezo-electro-mechanical model to sense stereocilia velocity rather than displacement. This new model can well match measured basilar membrane velocity data [Ren, T. and Nuttall, A. (2001). Basilar membrane vibration in the basal turn of the sensitive gerbil cochlea, *Hearing Research* 151: 48-60.] and our own cochlear microphonic data. the model, although it is one-dimensional, can approximately fit measured ST pressure data obtained around 300 micrometers above the basilar membrane [Olson, E. S. (1999). "Direct measurement of intra-cochlear pressure waves." *Nature* 402(6761): 526-9.].

[Funded by NIDCD grant R01-DC29]

### **[505] Mechanical Effects of Diametric Expansion of Outer Hair Cells On Cochlear Transduction and Parametric Amplification of Traveling Waves Over the Basilar Membrane in the Inner Ear**

**Amitava Biswas<sup>1</sup>**

<sup>1</sup>*University of Texas at El Paso*

This study compares some of the common models of cochlear mechanics and underscores the discrepancies that arise when some of basic laws of motion appear to be in conflict under the commonly adopted configurations of the cochlear mechanism, particularly the prevailing mechanistic models to explain the phenomenon of enhancement of the travelling waves in the basilar membrane by synchronized co-contraction in the length of outer hair cells (OHCs) and consequential impact on signal transduction in the inner hair cells. Although it is unrealistic that any OHC would contract in length without expanding in diameter, the prevailing models have so far incorporated the longitudinal contraction of OHCs only, assuming that the impact of any diametric expansion of OHCs would be relatively trivial. This analytical study shows that the basilar membrane could behave like a composite Beam-Column system, which may be significantly influenced by the diametric expansion of OHCs. Furthermore, prevailing models of cochlear mechanics do not inherently exhibit any cubic distortion like the real cochlea, whereas the proposed mechanism inherently presents a cubic distortion product according to its geometric construction.

### **[506] Change of Cochlea Mechanics and Auditory Brainstem Response in Animal Model of Otitis Media with Effusion**

**Chenkai Dai<sup>1</sup>, Rong Gan<sup>1</sup>**

<sup>1</sup>*Bioengineering Center & School of Aerospace and Mechanical Engineering, University of Oklahoma*

Otitis media with effusion (OME) is an inflammatory disease of the middle ear and the previous studies in human cadaver ears show that the middle ear function

was impaired by effusion and pressure in the cavity. Recently, it was reported that auditory brainstem response (ABR) measures in childhood were significantly altered with children's experiences of OME. As the critical source of ABR, cochlea mechanics change is related to ABR changes. In this paper, an animal OME model was created by inducing lipopolysaccharide into middle ear of guinea pigs. The vibration of the basilar membrane at apex and basal turn were measured in both control and experimental ears by a laser Doppler vibrometer after 3 days and 14 days of inoculation. The amplitude and latency of ABR in response to click and pure tone sound at selected frequencies were measured in the control and experimental ears. The results show that the displacements of basilar membrane at apex and basal turn in response to 80 dB sound input in the ear canal decreased across frequency range of 200~40k Hz. The amplitude of ABR signal was reduced and the latency increased at 500, 1k, 2k, 4k, 8k, 16k and 32k Hz. The basilar membrane mobility and ABR measured in two experiment groups show different responses induced by OME at early and chronic stages. The cochlea mechanics-ABR coupled analysis suggests that the cochlea function change is related to the ABR change in the animal OME model. This study gives us a better understanding of the relationship between cochlea function and ABR change in the middle ear disease. (Work supported by OCAST HR06-036 and NIH/NIDCD R01DC006632)

### **[507] The Relationship Between Outer Hair Cell Loss and Hearing Loss in Rats Exposed to Styrene**

**Guang-Di Chen<sup>1</sup>**, Chiemi Tanaka<sup>1</sup>, Donald Henderson<sup>1</sup>

<sup>1</sup>*SUNY at Buffalo*

Outer hair cells (OHCs) are known to contribute to the cochlear amplifier. However, the relationship between cochlear amplification and number of OHC is still unclear. There are examples of normal thresholds with missing OHCs and conversely, elevated thresholds with a normal population of OHCs. Styrene targets OHCs starting from the third row, resulting in apoptotic cell death of the targeted cells. However, the remaining OHCs and IHCs appeared intact. IHC death did not occur until all 3 rows of OHCs were missing. Thus, the styrene-injured cochlea may be a good model for study of the relationship between cochlear amplification and OHC number. Our results showed that loss of OHCs up to 1/3 caused only a slight permanent threshold shift (PTS). In some cases, 1/3 of OHCs were missing without any observable biological consequences, indicating that normal cochlear amplification does not require a complete set of OHCs and 2/3 of normally functioning OHCs are sufficient to maintain normal cochlear sensitivity. When OHC loss increased from 1/3 to 2/3, PTS increased gradually to about 40 dB. The hearing loss did not continue to increase with OHC loss in the range from 2/3 to 100%. The data indicate that the gain of the cochlear amplifier is not all or none. In a certain range (1/3 to 2/3 OHC loss), the gain is OHC number dependent.

This study was supported by NIOSH grant 1R01OH008113-01A1

### **[508] Modulation of the Endothelial Barrier**

#### **Permeability**

**Fitz-Roy Curry<sup>1</sup>**

<sup>1</sup>*University of California, Davis*

The permeability properties of microvascular barriers in the ear lie between those of the tight blood brain barrier and the more leaky endothelial barriers in peripheral tissues including muscle and mesentery. This review is based mainly on investigations in individually perfused microvessels from mammalian mesentery. The approach enables measurement of microvessel permeability under conditions where ultrastructure of the vessel wall, signaling pathways in endothelial cells, and organization of the cytoskeleton and cell adhesion complexes are directly measured. The aim is to stimulate ideas for new approaches to understand regulation of the microvascular barriers in the ear. The permeability to macromolecules is determined by a quasi-ordered surface glycocalyx which restricts access of plasma proteins to the endothelial cell surface, the inter-endothelial cleft, and entrance to caveolae. Loss of ordering in the glycocalyx may be one of the earliest events in endothelial barrier dysfunction, increasing macromolecule permeability and adhesion of inflammatory cells to the endothelial cell surface. The cleft pathway between adjacent endothelial cells regulates water and small solute permeability through selective pores or channels within tight junction strands and infrequent breaks in these strands. The integrity of this pathway is determined by a balance between cell-cell adhesion and resting tension within the endothelial cell. Acute increases in permeability result from decreased adhesion without additional tension development. In contrast, endothelial cells in microvessels exposed to sustained inflammatory states express a phenotype with upregulated contractile mechanisms. Some cultured endothelial cell monolayers express a similar contractile phenotype. Microvascular beds of the ear exposed to repeated low level injury (transient hypoxia or loud noise) may develop a similar inflammatory phenotype.

Supported by: NIH HL28607 and HL44485

### **[509] Cochlear Blood Flow and Loud Sound Damage to the Lateral Wall: a Tribute to**

**Merle Lawrence**

**Alfred Nuttall<sup>1</sup>**

<sup>1</sup>*Oregon Health & Science University*

Lateral wall blood flow of the cochlea has a critical role in maintaining cochlear fluid homeostasis and oxygenation. The natural functions of endothelial cells, pericytes and smooth muscle cells are to form the blood/lymph barrier and adjust blood flow. Cochlear microcirculation can be impaired through exposure to intense sound; such impairments include increase in vascular permeability, reduction in circulation (ischemia), aggregation of leukocytes and injury to endothelial cells. The high-energy use of the cochlea requires adequate blood circulation but also enhances the vulnerability of lateral wall cells via oxidative stress. Subsequently, lateral wall inflammation is a resulting hallmark of the sound damage, including the expression of vascular adhesion molecules and the

transmigration of leukocytes across the blood/perilymph barrier. Cytokines such as tumor necrosis factor are initiators of the inflammation and signaling molecules. Nitric oxide is significantly involved both in vascular regulation and cell pathology. Taking Merle Lawrence's cochlear circulation studies as a starting point, this presentation will touch on some of the current data and relevant issues of the cochlear microcirculation in relation to cochlear physiology and the mechanisms of loud sound damage. Supported by NIH NIDCD DC000105

### **[510] Sensitivity of Blood Labyrinth Barrier to Circulating Immune Factors**

**Dennis Trune<sup>1</sup>**

<sup>1</sup>*Oregon Health & Science University*

The endothelial cells of the blood-labyrinth barrier are exposed to circulating immune factors that can affect cochlear function. These include antibodies, antigen-antibody complexes, viruses, bacteria, and other inflammatory cytokines that are toxic to inner ear tissues. Experimental studies suggest the barrier is compromised by these inflammatory mediators, leading to leakage of immunoglobulin and other serum factors into cochlear extracapillary spaces. This causes lateral wall activation of NF- $\kappa$ B, a major transcription factor in inflammation, and the production of nitric oxide. These mechanisms of tissue damage may explain the sensitivity of the inner ear to systemic infections and immune disorders.

### **[511] Unique Inner Ear Intercellular Tight Junctions**

**Bechara Kachar, MD**

*NIDCD, National Institutes of Health*

in the inner ear, tight junctions harboring multiple claudins, occludin, tricellulin, and the zonula occludens family of proteins are widespread and essential for maintaining well-sealed compartments and securing hair cells in the vibrating structures of the ear. Recent studies reveal junctions with quite unique structural organization and molecular composition. One such example is the claudin 9/14 hybrid tight-adherens junctions between outer hair cells and Deiters' cells. Another important aspect of intercellular junctions that is now beginning to be explored is how the hair cells reconcile the robustness and relative stability of their organization with the ability to rearrange and reseal upon hair cell loss.

### **[512] Gap Junction Intercellular Channel Systems in the Inner Ear: Cellular Distribution, Molecular Assembly and Functional Studies**

**Wenxue Tang<sup>1</sup>, Qing Chang<sup>1</sup>, Shueb Ahmad<sup>1</sup>, Xi Lin<sup>1</sup>**

<sup>1</sup>*Emory University School of Medicine*

Gap junctions (GJ) are membrane channels facilitating exchanges of intercellular biochemical and electrochemical signals. Connexins (Cxs) are a family of 20 protein subunits constituting the building blocks of GJs. Twelve compatible Cx subunits assemble together to form GJs. the importance of Cxs in hearing has been revealed by

genetic studies showing that at least four Cx subtypes (Cxs 26, 30, 31 & 43) are essential for normal cochlear functions in human. Mutations in these Cxs account for a significant portion (20-50%) of prelingual non-syndromic deafness.

Most GJs in the cochlea are assembled heteromerically from Cx26 and Cx30. the two Cxs display almost identical cellular expression patterns, both in the developing and in matured cochlea. From birth to postnatal day 10 (P10), GJs in the lateral wall were found to be concentrated between basal cells and fibrocytes surrounding the stria vascularis. More cells in the cochlea were connected by GJs after P12 when hearing starts to mature in mice. Cochlear Schwann cells also express Cx29 and Cx32. Although Cxs are not found in spiral ganglion neurons, they express both pannexin1 and pannexin2. Null mutations of either Cx26 or Cx30, which don't eliminate GJs in the cochlea, result in deficit in forming the endolymphatic potential (EP) and severe hearing loss at early development stages. Interestingly, hair cell loss happened at a much later time, indicating that HC death was not the direct cause of deafness in Cx mutant mice. Using a non-hydrolyzable fluorescent analogue of D-glucose (2-NBDG) to study GJ-mediated biochemical coupling, we found that both the rate and extent of the dye diffusion were significantly decreased in Cx30<sup>-/-</sup> mice. Compromise in GJ-mediated intercellular diffusion of glucose analogue suggested that biochemical coupling important for metabolic activities in the cochlea is affected in the mutant mice, which may be responsible for dysfunction of mitochondria suggested by our microarray and proteomics analyses. Our studies also identified a possible direct link between the loss of EP in the mutant mice and a significant reduction in expressions of KCNQ1 and KCNE1 before the establishment of EP (e.g., P10), since both K<sup>+</sup> channels are known to be required for generating EP.

Our data suggested that deficits in gap junction (GJ) facilitated biochemical coupling in early postnatal development, which are essential for the full expressions of KCNE1 and KCNQ1 and the initial establishment of EP, is directly responsible for deafness found in the Cx mutant mice.

### **[513] Supporting Cells Initiate Spontaneous Activity in the Developing Cochlea**

**Nicolas Tritsch<sup>1</sup>, Eunyoung Yi<sup>1</sup>, Jonathan Gale<sup>2</sup>, Elisabeth Glowatzki<sup>1</sup>, Dwight Bergles<sup>1</sup>**

<sup>1</sup>*Johns Hopkins University*, <sup>2</sup>*University College London*

Spontaneous activity in developing sensory systems has been shown to be important for the growth and survival of projection neurons, as well as the establishment, refinement and maintenance of sensory maps in the brain. in the developing cochlea, bursts of action potentials occur in primary afferent neurons prior to the onset of hearing. This activity is thought to originate within the cochlea, but the mechanisms responsible for initiating auditory nerve firing in the absence of sound are poorly understood. Here we show that supporting cells within Kölliker's organ of the developing mammalian cochlea spontaneously release adenosine 5'-triphosphate (ATP), which triggers large

current oscillations and widespread intracellular  $\text{Ca}^{2+}$  waves by activating purinergic autoreceptors. Moreover, this spontaneous release of ATP causes neighboring inner hair cells to depolarize and release glutamate, triggering discrete bursts of action potentials in primary auditory neurons. This endogenous purinergic signaling synchronizes the output of neighboring inner hair cells, which may help refine tonotopic maps in the brain. Spontaneous ATP-dependent signaling rapidly subsides after the onset of hearing, thereby preventing this experience-independent activity from interfering with accurate encoding of sound. These data indicate that supporting cells in the organ of Corti initiate electrical activity in auditory nerves before hearing, pointing to an essential role for peripheral, non-sensory cells in the development of central auditory pathways.

#### **514 Cell-Cell Communication in the organ of Corti**

Fabio Anselmi<sup>1</sup>, Fabio Mammano<sup>1</sup>

<sup>1</sup>Foundation for Advanced Biomedical Research

In cochlear organotypic cultures obtained from newborn rats and mice, pharmacological dissection indicates that ATP, acting through a highly sensitive purinergic/ $\text{InsP}_3$ -mediated signaling pathway, is the principal paracrine mediator implicated in the long-range propagation of  $\text{Ca}^{2+}$  waves through supporting and epithelial cells of the organ of Corti [1, 2]. In these cultures,  $\text{Ca}^{2+}$  waves generated by mechanical stimulation of hair cells, mimicking *In Vitro* the effects of sound over-stimulation, are identical to  $\text{Ca}^{2+}$  waves evoked by brief (50–200 ms) application of low doses of ATP (4–1  $\mu\text{M}$ ) from a puff pipette. The extraordinary sensitivity to ATP suggests that spreading of calcium signals through the epithelial network is an essential component for the perception of sound and is potentially involved in sound induced gene expression [3]. A fundamental step is ATP release at the endolymphatic surface of the epithelium, which triggers adjacent cell responses. Our experiments with cochlear cultures derived from KO mice lacking either purinergic P2X7 receptors or pannexin 1 (Px1) channel constituents indicate that neither is an essential component of the ATP release mechanism in the organ of Corti. Instead, the pharmacological sensitivity profile is compatible with release of ATP from connexin hemichannels formed by connexin 26 (Cx26) and connexin 30 (Cx30). Supporting cells in the organ of Corti, which abundantly express these two connexin isoforms, also exploit a parallel short-range signaling pathway based on local diffusion of  $\text{InsP}_3$  through Cx26/Cx30 gap junction channels.  $\text{InsP}_3$  biosensors that transduce concentration changes into changes of Förster resonance energy transfer (FRET) permit now to estimate the permeability of single gap junction channels to this and other key second messengers, such as cAMP, implicated in connexin-based hereditary disorders [4].

1. Piazza, V., et al., Purinergic signalling and intercellular  $\text{Ca}^{2+}$  wave propagation in the organ of Corti. *Cell Calcium*, 2006.

2. Beltramello, M., et al., Impaired permeability to  $\text{Ins}(1,4,5)\text{P}_3$  in a mutant connexin underlies recessive hereditary deafness. *Nat Cell Biol*, 2005. 7(1): p. 63-9.
3. Gale, J.E., et al., A mechanism for sensing noise damage in the inner ear. *Curr Biol*, 2004. 14(6): p. 526-9.
4. Hernandez, V., et al., Unitary permeability of gap junction channels to second messengers measured by FRET microscopy. *Nat Methods*, 2007. 4(4):p. 353-8.

Supported by grants from Telethon Italy (GGP05131) and the European commission FP6 Integrated Project EuroHear (LSHG-CT-20054-512063) under the Sixth Research Frame Program of the European Union.

#### **515 Normal Variation in Audiometric Threshold is Associated with Behavioural and Neurodevelopmental Factors**

David Welch<sup>1</sup>, Patrick Dawes<sup>2</sup>

<sup>1</sup>University of Otago, <sup>2</sup>Dept ORL,HNS; Medical and Surgical Sciences, University of Otago

Aim: to investigate whether variation in audiometric thresholds in people with normal hearing predicts behavioural and developmental factors.

Method: the Dunedin Multidisciplinary Health and Development Study, a large cohort based longitudinal study in New Zealand, measured audiometric thresholds at ages 5, 7, 9, and 11 in 1000 people. A single measure of hearing level was established by calculating the binaural 0.5, 1, and 2 kHz average across ages. Hearing levels measured under abnormal middle-ear conditions, and those poorer than 15 dB HL, were excluded. We investigated associations between hearing level, speech in noise recognition, neurocognitive ability, linguistic ability, and behavioural problems to age 15. To test the hypothesis of a neurodevelopmental mechanism underlying the observed associations, we investigated the relationship between hearing and growth rates through the lifecourse to age 32.

Results: Speech in noise recognition, neurocognitive, and language ability were better in those with the very best hearing, and effects were stronger in girls. Girls with the very best hearing had fewer behavioural problems than other girls, while behavioural problems were not associated with hearing in boys. Growth rates during infancy and late adolescence were higher in those with the best hearing.

Conclusions: 1. People with the very best hearing have better behavioural and language outcomes among those with normal hearing. 2. The associations between hearing level and growth rate are strongest at ages when serum insulin-like growth factor 1 (IGF-1) levels are higher. These two findings support the theory that expression of IGF-1 may lead to both improved hearing and development throughout the nervous system, thereby leading to the observed relations between hearing and behaviour.



## **516 Tests of Spatial Listening for Preschool Children**

**Rosemary Lovett<sup>1</sup>**, Quentin Summerfield<sup>1</sup>

<sup>1</sup>University of York

We have measured the age at which normally hearing children can complete performance tests of spatial listening. the tests will be used in a randomised trial comparing children with unilateral and bilateral cochlear implants.

in the *Left-Right Discrimination Test*, a speech stimulus is presented from 60° to the left or right of straight ahead. a head turn towards the source is rewarded by a cartoon video at that location. the *Localisation Toy Test* uses five loudspeakers positioned above five video screens, with each screen displaying a different toy. a speech stimulus is presented from one loudspeaker. the child must localise the stimulus and identify the toy displayed at that location. the loudspeakers are separated by 30°, reduced to 15° on later trials.

in the *Movement Tracking Test*, stimuli are presented sequentially from 13 loudspeakers, giving an illusion of movement. Test sessions are recorded on DVD; an independent observer then rates in which order four patterns of movement had been presented, based on the child's behaviour.

in the *Toy Discrimination Test*, speech stimuli are presented from straight ahead accompanied by pink noise from 90° to the left, straight ahead, or 90° to the right. the noise level is varied adaptively to estimate the speech-reception threshold: the speech-to-noise ratio at which the child is 71% correct in identifying the spoken toy name.

The tests have been attempted by 37 normally-hearing children aged between 18 months and seven years. There are clear age boundaries, after which all children could complete a test. All children completed at least 17 trials of the *Left-Right Discrimination Test* and could sit still for the *Movement Tracking Test*. Children aged three and over completed 30 trials of the *Localisation Toy Test*. Children aged three and a half and over completed three runs of the *Toy Discrimination Test*. the tests are suitable for use with children of the same age as those who will participate in the randomised trial.

## **517 Factors Predicting Auditory Development in Young Children with Hearing Loss**

**Yvonne Sininger<sup>1</sup>**, Laurie Eisenberg<sup>2</sup>, Elizabeth Christensen<sup>1</sup>, Amy Martinez<sup>2</sup>, Alison Grimes<sup>1</sup>, Jasmine Hu<sup>1</sup>

<sup>1</sup>UCLA, <sup>2</sup>House Ear Institute

A multi-center, prospective study "Auditory Development in Early Amplified Children" has investigated auditory skills (speech perception and production and spoken language) in children with hearing loss and documented factors that may influence these skills to determine the relationships. Sixty four children with bilateral sensorineural hearing loss ranging in degree from mild to profound have been evaluated. Factors (independent variables) documented by formal testing, parent or educator inventories or audiologic records include age at diagnosis, age at fitting

of amplification, degree and stability of hearing loss, the adequacy of amplification fitting, cognitive capacity (measured by Leiter International Performance Scale-R or Bayley Scales of Infant Development), parent-child interactions (NCAST Teaching Scales), socio economic status, educational intervention and hearing aid use. These factors are summarized and used as independent variables in a multivariate regression analysis. Speech perception and production and spoken language data from this longitudinal study were obtained when the children reached three years of age and beyond. Specifically, outcome measures include the Imitative Test of Speech Pattern Contrast Perception- On Line (IMSPAC-ol), Pediatric Speech Intelligibility Test, Lexical Neighborhood Test and the Multisyllabic Lexical Neighborhood Test and Arizona Articulation Proficiency Scale, Third Revision. a revision of the Ling Schedules of Development has also been administered to parents. Formal language measures include the Macarthur-Bates Communicative Development Inventory and the Reynell Developmental Language Scales. These measures are combined to provide descriptions of auditory skills on each subject serving as dependent variables in the regression analyses. the relationships between the independent (predictor) variables and primary auditory outcomes will be elucidated by the multivariate regression analyses. This study was supported by NIDCD (R01 DC04433).

## **518 The Influence of Audibility and Cognitive Factors On Auditory Processing and Speech Perception in Children with Mild Sensorineural Hearing Loss**

**Kerri Millward<sup>1</sup>**, Lorna Halliday<sup>1</sup>, Melanie Ferguson<sup>1</sup>, David Moore<sup>1</sup>

<sup>1</sup>MRC Institute of Hearing Research

The aim of this study was to examine the controversial role of audibility and cognitive factors on a variety of speech perception and auditory processing tasks in children with mild sensorineural hearing loss (SNHL). Fifteen children aged 6- to 13-years who had mild (average hearing threshold level (AHTL) across .25-4 kHz: 20-40 dB HL) SNHL were tested on a battery that included audiological, speech perception (sentence and vowel-consonant-vowel (VCV) in quiet, 20-talker (babble) and one-male talker modulated speech noise (ICRA 5)) and auditory processing (spectral, temporal and binaural) tests performed using a 3I-3AFC adaptive paradigm. Cognitive tests included nonverbal IQ (NVIQ), memory (digit span), and visual and auditory attention. a Control group of normally-hearing children matched for age and NVIQ were also tested. the SNHL group performed significantly more poorly than the Control group on all speech perception measures, frequency resolution and temporal integration. None of the auditory processing tasks correlated with AHTL in either the SNHL or the control group. Nevertheless, there were significant correlations between AHTL and sentences-in-quiet, sentences-in-ICRA 5, VCV-in-quiet and VCV-in-ICRA 5 within the SNHL and control groups. for both sentences-in-noise tasks there were correlations with auditory attention test reaction time in the

SNHL group. These results imply that audibility is a factor in quieter (easier) listening environments. However, in noisy (difficult) listening environments higher-level factors may play more of a role.

### **519 A 1-Year Follow Up Study of Cognitive Functions in Deaf Children After Cochlear Implant**

**Min-Sup Shin<sup>1</sup>**, Sang-Sun Kim<sup>2</sup>, Soo-Kyoung Kim<sup>2</sup>, Min-Hyun Park<sup>2</sup>, Seung-Ha Oh<sup>1</sup>, Chong-Sun Kim<sup>1</sup>

<sup>1</sup>*Seoul National University College of Medicine*, <sup>2</sup>*Seoul National University Hospital*

**Objectives :** This study was conducted to examine improvements in cognitive abilities after cochlear implant in congenital deaf children.

**Methods :** Twenty deaf children (mean age: 6 years 4 months) participated in this study. They were administered a neuropsychological test battery before cochlear implant and reassessed by the same test at 6-months and 1-year follow up. the neuropsychological test battery was composed of nonverbal tests to assess cognitive functions, including general intelligence, working memory, attention, and motor coordination. It included Korean Pictorial Test of Intelligence, Leiter International Performance Scale-Revised, Korean version of computerized visual attention test, Grooved Pegboard Test, and Rey Complex Figure Test.

**Results :** the deaf children showed marked improvement in visual organization ability after cochlear implant. Their cognitive functions measured by non-verbal tests such as form discrimination and visual short-term memory were found to have significantly improved. However, their performances on Information, Comprehension, Similarity, and Mathematics subtests which require verbal comprehension abilities were not significantly changed. Deaf children's working memory improved significantly after cochlear implant. Interestingly, although they showed higher omission errors in visual attention test at 6-months follow up than before cochlear implant, while their attentional ability improved up to near normal range at 1-year follow up.

**Conclusion :** At 1-year follow up after cochlear implant, deaf children showed marked improvement in nonverbal cognitive functions, working memory, and visual attention. However, their verbal abilities did not significantly change. It is thereby suggested that cognitive rehabilitation for language acquisition after cochlear implant need the long-time beyond 1 year.

**Key word:** Deaf child, Cochlear Implant, Nonverbal Cognitive functions, Visual attention

### **520 Is there More to Auditory Processing Disorder (APD) Than Just Poor Auditory Processing?**

**Melanie A Ferguson<sup>1</sup>**, Alison Riley<sup>1</sup>, Sonia Ratib<sup>1</sup>, David R Moore<sup>1</sup>

<sup>1</sup>*MRC Institute of Hearing Research*

There are currently no standardised and scientifically validated tests to diagnose auditory processing disorder

(APD). to address this, we are currently undertaking a large, multi-centre population study that aims to (i) ascertain population norms for AP tests, (ii) identify profiles of children with poor AP, (iii) estimate the prevalence of APD, and (iv) establish a validated test battery to diagnose APD. We aim to test 1600 normally-hearing children aged 6-11 y.o., stratified for age, sex and social class with a one-hour test battery over a one-year period (ending 05/08). the battery comprises tests of auditory processing (spectral and temporal), speech intelligibility, cognitive function (non-verbal IQ (NVIQ), memory, repetition of nonsense words, literacy and attention) and hearing sensitivity (1 and 4kHz). All testing is done in a quiet room within schools. in addition, the Children's Communication Checklist (CCC-2) is completed by parents. Data collection is ongoing and interim results are reported here from 205 children with normal hearing threshold levels (<25 dB HL at 1 and 4kHz bilaterally). Poor AP performers (thresholds greater than mean + 2 SD on at least one AP test) had poorer NVIQ and literacy ( $p < 0.05$ ) than typical performers. On tests of sustained attention these poor AP performers had significantly slower reaction times in an auditory task ( $p < 0.01$ ), but not in a visual task ( $p > 0.05$ ), suggesting specifically poorer sustained auditory attention. Poor performers also had a significantly higher social interaction deviation score on the CCC-2, without a difference for general communication, suggesting a tendency towards poorer language abilities. These preliminary results suggest that poor auditory processing may be associated with poorer NVIQ, literacy, auditory attention and language, in line with anecdotal clinical reports of APD.

### **521 Two Classes of Auditory Processing Disorder (APD) in Children**

**David Moore<sup>1</sup>**, Melanie Ferguson<sup>1</sup>, Alison Riley<sup>1</sup>

<sup>1</sup>*MRC Institute of Hearing Research*

Building on definitions of APD that suggest problems in the perception and awareness of basic sound comparisons (e.g. temporal and spectral resolution and discrimination), we have examined the ability of large samples of 6-11 year old children to perform relatively simple audiological, auditory processing (AP), speech-in-noise and cognitive tasks. Children who perform poorly on one or more AP tasks usually respond inconsistently to test items, but their performance on small segments of trials is often within the range typical for their age. the proportion of these inconsistent, 'non-compliant' (NC) performances decreases dramatically with increasing age. by a metric based on performance deviation from the standard during a single AP task (adaptive frequency discrimination task), 30% of 6-7 y.o., 16% of 8-9 y.o. and 7% of 10-11 y.o. threshold determinations ( $N = 185$ ) were of this type. a second, smaller proportion of children (0%, 1.5%, 9.0%, respectively) are 'genuine poor performers' (GPP). They respond consistently, but at a level that is outside the range ( $> 2$  s.d.) appropriate for their age. Their proportion increases with age, possibly due to falling variability. Poor AP performers overall also perform poorly on cognitive tasks (IQ and literacy), although literacy and IQ account for only a small proportion of the variance ( $< 5\%$ ) on AP tasks. in a focus on attention, we have found significant relations

between 'intrinsic' (AP performance variability) and 'extrinsic' (reaction time measures of sustained attention) attention and AP thresholds, but no relation between measures of auditory and visual attention on either type of task. We therefore suggest that unimodal, auditory attention contributes at least to NC-type APD behaviour. We are currently gathering further data from a national study of AP in children (N = 1600) to identify other cases of GPP and we are examining the performance of both these groups of children on other tasks, including various measures of spatial hearing, speech intelligibility and communication skills. Preliminary analysis found that GPP-type children have much poorer mean scores on the carer-completed Children's Communication Checklist than NC-type children, suggesting that GPPs present a scientifically strong case for the existence of APD.

## **522 Frequency Weighting of Speech Information in School-Aged Children and Adults**

**Rose Eapen<sup>1</sup>, Emily Buss<sup>1</sup>, John Grose<sup>1</sup>, Joseph Hall<sup>1</sup>**

<sup>1</sup>*University of North Carolina, Chapel Hill*

The aim of this study was to examine developmental effects in frequency weighting for the perception of speech in noise. the method used to explore this question involved the filtering of BKB sentences into three narrow frequency bands and then presenting all three bands or selectively removing one of the bands. the bands were roughly centered on 1000 Hz (Low), 2000 Hz (Mid), and 4000 Hz (High). We assumed that the frequency weight associated with a particular frequency region was inversely related to the percent correct obtained when the band associated with that region was removed. Listeners with a history of normal hearing were tested on their ability to identify key words in the filtered sentences presented in a speech-shaped noise masker. Initial testing involved adaptive runs where the speech-shaped masker was held at a constant level and the level of the speech with all bands present was varied. Once a level corresponding to 85-90% correct was identified, 50 sentences were then presented at this signal-to-noise ratio in fixed block runs, with all bands present, or with one of the three bands omitted. for both adults and children, removing any one of the three bands resulted in a reduction in performance, with the reduction being slightly less for the High band. Compared to adults, children showed a larger reduction in performance when the Low or Mid band was removed, and about the same reduction in performance when the High band was removed. a possible interpretation of this result is that children weighted the Low and Mid bands relatively more than adults. However, because the High band appeared to carry less information than the Low or Mid bands for both adults and children, a competing interpretation is that children show relatively greater decreases in performance when highly informative bands are removed, regardless of their frequency region. Ongoing research is aimed at differentiating between these interpretations.

## **523 Evaluation of SPATS: Speech Perception Assessment and Training System**

**Charles Watson<sup>1</sup>, James D. Miller<sup>1</sup>, Diane Kewley-Port<sup>1</sup>, Frederic Wightman<sup>2</sup>, Doris Kistler<sup>2</sup>**

<sup>1</sup>*Communication Disorders Technology, Inc.*, <sup>2</sup>*University of Louisville*

The SPATS system for speech perception training has been developed as a means of teaching users of hearing aids (HAs) and cochlear implants (CIs) to learn the bottom-up skills of attending to the essential audible details of English syllable constituents (onsets, nuclei and codas). This system also trains the users to apply these skills in the combined bottom-up and top-down recognition of words in meaningful sentences. Speech samples were recorded by ten adult talkers: male, female, young and old. Training is conducted in the quiet and in the presence of conversational babble. During training sessions the listeners spend about 70% of their time on constituent training and 30% on sentence recognition. Constituent training employs a unique adaptive algorithm that concentrates the training on constituents that are currently of intermediate difficulty. Sentence training utilizes 1000 four-to-seven-word sentences in an adaptive recognition task that evaluates both speed and accuracy. the system was evaluated by 11 HA users and 13 CI users to whom a battery of tests was administered before and after 0, 12, or 24 hours of training. Tests included the HINT, CNC, W22, Cox's CDT, parts of Gatehouse's SSQ, plus measures obtained with SPATS. for HA users performance improved on all of these tests, by an average of about nine percent correct. Performance was a strong function of the amount of training. Similar improvements were observed for CI users although their overall performance was below that of the HA users. These results, together with those recently reported for other speech training systems, suggest that some HA and CI users can derive major benefits from focused speech-perception training. It appears, however, that to achieve significant benefits training must be conducted for a minimum of 2-3 hours per week, over a period of at least 7-10 weeks. Work supported by NIH/NIDCD Grant 44DC006338.

## **524 Auditory Steady State Responses (ASSR) As an Objective Technique to Evaluate Speech Perception: Preliminary Data**

**Venkata Damarla<sup>1</sup>, Gerald, Armstrong-,Bednall<sup>2</sup>, Mohammed Ayub<sup>2</sup>**

<sup>1</sup>*De Monfort University*, <sup>2</sup>*De Montfort University*

The present project aimed at evaluating supra-threshold speech perception abilities in hearing impaired population and in aided hearing using auditory steady state responses (ASSR). the initial experiments consist of a sample study to establish an innovative stimulus derived from original speech. the stimulus was created using a CV syllable /da/. the AM/FM components used to measure ASSR were calculated from the Long Term Average Speech Spectrum of the syllable. the auditory brainstem response (ABR) to the same stimuli (/da/) was also recorded, which reflects the initial stages of speech

processing at the brainstem level. Ten normal hearing subjects, age ranged 20-26 years, participated in the study. Both measurements (ASSR and ABR) were recorded at a stimulus intensity of 70 dB SPL presented through a loudspeaker in a free-field environment. Initial results show good ASSR responses recognized as statistically significant from the background noise. the ABR waveform consists of transient and sustained, periodic components, much like the speech signal itself. Wave V has good amplitude with high test-retest reliability. Further experiments are focused towards extracting the AM/FM component from the original speech signal to use for ASSR measurements.

## **[525] Direct Electrical Stimulation for Gap Evoked Cortical Responses**

**Ming Zhang<sup>1</sup>**, Steven Zupancic<sup>1</sup>, Dwayne Paschall<sup>1</sup>, Joe Hassin Cordero<sup>1</sup>

<sup>1</sup>*Texas Tech University Health Sciences Center*

Electric hearing, i.e. electrically evoked hearing, has become an important topic in modern hearing science. Two types of responses, i.e. behavioral and physiological, can be electrically evoked, i.e. evoked by electrical stimulation. for physiological responses, electrically evoked compound action potentials have been used to assess electric hearing at the peripheral level. to assess electric hearing at the perception level, electrically evoked cortical responses may be used. Gap detection is generally accepted as one of the most sensitive indicators of speech recognition abilities. Combining three notions of electric hearing, physiological response, and gap detection, electrically evoked gap cortical responses may be developed. However, little is known about such responses. We have performed two lines of studies. One was to use indirect electrical stimulations (IDESs), with earphone-generated acoustic signals to the microphone of a stand-alone cochlear implant speech processor (CISP). the signals were processed via a CISP map before being transmitted to the internal device worn by the CI users. the other was to use direct electrical stimulations (DESSs), with computer-generated electrical signals to the CISP directly via a programming cable. the signals were not processed via the CISP map before being transmitted to the internal device worn by the CI users. with IDESSs and acoustic stimulations, the gap-evoked cortical responses (P300) were recorded and previously reported, both in regards to the responses obtained from CI users and normal hearing subjects (Abst ARO 29:433, 2006) and the effect of the carrier frequencies on the cortical responses (Abst ARO 29:432, 2006). the carrier refers to a signal which contains a gap. in this report, we show that the gap-evoked cortical responses (P300) can also be recorded by using DESSs. with DESSs, a specific intracochlear electrode can be selected and a specific carrier pulse rate, i.e. pulses per second (PPS), can be assigned to the selected electrode. the specific electrode is a stimulation electrode located at a specific place along the cochlea. the effects of both the specific carrier pulse rates (such as 1000 PPS or 2000 PPS) and the specific electrodes (such as located at 1000-Hz or 2000-Hz place) on the cortical responses (P300) will be discussed.

We thank Dr. Qian-Ji Fu for his support to this study.

## **[526] Standard Clinical and Wideband Estimates of Ipsilateral Middle Ear Muscle Reflex Thresholds**

**Kim Schairer<sup>1</sup>**, Marin Almer<sup>1</sup>, Cynthia Fowler<sup>1</sup>, Erica Stenberg<sup>1</sup>, Sarah Chipman<sup>1</sup>

<sup>1</sup>*University of Wisconsin*

Ipsilateral middle ear muscle reflex (MEMR) thresholds in response to 1-kHz, 2-kHz, and broadband noise activators were estimated in 38 normal-hearing adult ears using standard clinical and wideband acoustic transfer function (WATF) measures. in a previous study (Schairer et al., 2007, JASA, 121, 3607-3616), it was demonstrated that MEMR thresholds were lower when estimated with the WATF than with the clinical system. However, a fixed range of activator levels was presented, and the lower end of the stimulus range was high enough that reflexes were often obtained at the lowest stimulus level, suggesting that some of those responses may have been above threshold. in the current study, the lower limit was extended to determine if a greater difference between thresholds estimated on the two systems could be observed. Reflexes were elicited at the lower levels presented in the current study, particularly for the BBN activator. However, the differences in threshold estimated by the two systems were similar to differences observed previously, and ranged from 2.8 dB higher to 5.2 dB lower on the WATF system, depending on the measure (admittance or reflectance) and activator. in this study, although an ANOVA was used to determine the presence of the MEMR at each activator level, additional rules were applied to determine threshold offline. the process could be improved by using a correlation or other morphology test along with the ANOVA to determine threshold online, as suggested by other investigators. WATF measures provide comparable estimates of MEMR threshold in comparison to clinical measures, and have benefits including potential for adaptive activator level presentation and objective reflex detection. WATF-MEMR measures could be included in newborn and preschool hearing screenings, and could be used to investigate the integrity of the auditory system through the lower brainstem in patients with suspected auditory processing difficulties.

## **[527] A Previously Undescribed Feature of the Distal Incus**

**Clarinda Northrop<sup>1</sup>**, Stephen Levine<sup>1</sup>, Collin Karmody<sup>2</sup>

<sup>1</sup>*Temporal Bone Foundation*, <sup>2</sup>*Tufts University School of Medicine*

Goal: to describe a prominent indentation in the antero-medial surface of the distal end of the long process of the incus. Previous observations on images of dissected, histologically sectioned, or radiologically enhanced material have not demonstrated this feature.

Methods: Serial sections (20 microns thick, celloidin embedded, H & E stained) of four human temporal bones and one cat were scanned into a computer and aligned manually in Photoshop. for each section in the incudostapedial joint region bone areas of incus and

stapes were manually outlined and segmented to form separate, bone only files, which were combined into a virtual, 3D, surface image, using Amira and Maya Software.

Results: in each of the five, 3D images a clear indentation occurs on the antero-medial surface near the extreme distal long process of the incus. Dimensions of the indentation were calculated using the 3D images. As these dimensions are a sizable fraction of the long process at its inferior extremity the indentation is relatively a prominent feature. In the original sections this indentation is filled with fibers of the incudostapedial ligament capsule; the fibers appear to attach to the concave surface of this indentation. The anterior fibers of the capsule therefore extend further laterally than the posterior fibers, which produces an anterior-posterior asymmetry.

Conclusion: the insertion of the tendon of the stapedius muscle on the posterior side of the head creates an obvious asymmetry to the mechanics of the stapes. Now it seems that this is somewhat counterbalanced by an asymmetrical attachment of the ligament fibers on the anterior side of the distal incus. These two asymmetries probably interact because it has been reported (in cat ears) that contractions of the stapedius muscle move the stapes head posteriorly, without moving the incus. This mechanical feature should allow the effect of the stapes' contraction to be localized to the stapes. Our concept is that the asymmetry of ligamentous attachments stabilizes the functional axis of the incudostapedial joint.

## **[528] The Curved Shape of the Tympanic Membrane Results From the Minimization of its Internal Energy During Morphogenesis**

**Willem Decraemer<sup>1</sup>, Joris Dirckx<sup>1</sup>, Robert Funnell<sup>2</sup>, Hanif Ladak<sup>3</sup>**

<sup>1</sup>University of Antwerp, <sup>2</sup>McGill University Montreal,

<sup>3</sup>Robarts Institute, London, Ontario, Canada

Our research led us to measure the eardrum shape in human and animals such as cat, gerbil and rabbit. These membranes were conical -as if the membrane was pulled in by the manubrium- with convex outward curved sides. From shape measurements on a series of human eardrums during their early development we learned that the umbo grows gradually out of the annulus plane. In an earlier ARO presentation (Decraemer et al. 2000) we hypothesized that this causes a tension in the developing thin membrane and that the drum adopts an equilibrium shape that minimizes the internal elastic energy. Assuming a constant energy per surface area, the total energy is proportional to the total surface area and the equilibrium surface of the drum must be a "minimal-surface", the surface that has the minimal area of all surfaces spanning the given fixed annulus and manubrium boundaries. The eardrum is later somehow "frozen" in this shape so that no tension – nor an overpressure in the middle ear cavity - is required to keep it in this shape. Dipping a wire frame mimicking the manubrium and annulus border in a soap solution one gets a soap film that takes the shape of a minimal surface under the action of surface tension. The soap film resembles closely a tympanic membrane; in particular it presents the curvature we find in the eardrum.

Minimal surfaces for soap film models can also be calculated making use of the freeware Surface Evolver (<http://www.susqu.edu/brakke/>). In this paper we compared the measured eardrum shape with the calculated minimal surface shape for human, cat and gerbil and found differences mainly concentrated in a small zone around the tip of the umbo. A real eardrum has an anisotropic internal structure, a not uniform thickness and bending stiffness, hence some differences were to be expected. Introducing the measured thickness in a mathematical thin-shell finite-element model and calculating the surface shape after pulling the manubrium out of the annulus plane we could relieve the discrepancies. Our main conclusion remains nevertheless that the peculiar shape of the tympanic membrane is caused by internal stress during its growth that forces the membrane into an equilibrium shape that is close to the minimal surface. Modelers can on this basis e.g. calculate a good approximation for the eardrum in an ear model when no measured shape is available.

## **[529] Distribution of Collagens in Healthy Human Tympanic Membranes**

**Magnus Von Unge<sup>1</sup>, Johan Knutsson<sup>1</sup>**

<sup>1</sup>Karolinska Institute

Objective:

We have previously studied the histological distribution of collagens in the pars tensa and the fibrous annulus of the tympanic membrane in healthy Sprague-Dawley rats (accepted for publication). The objective of this study was to investigate the histological distribution of collagens in the healthy human tympanic membrane and compare with results from the rats.

Design:

Immunohistochemical analysis of collagen type I, II, III and IV in a unique material consisting of seven healthy human tympanic membranes. The tympanic membranes were fixated immediately after being taken out from patients undergoing translabryntic surgery for vestibular Schwannomas. The immunohistochemical staining was analysed by light microscopy.

Results:

Preliminary results (collagen type I, III and IV; analysis for collagen type II will soon be performed) are showing a different pattern in the staining of the fibrous annulus compared to the rat. The most striking difference is that the staining of the human specimen shows presence of collagen type I in the fibrous annulus.

The staining of the pars tensa shows clear evidence of collagen type III but not collagen type I in the lamina propria. Collagen type IV is present in the basal membrane of the pars tensa.

Conclusions:

Collagen type I is present in the human fibrous annulus. Collagen type IV can be found in the basal membrane of the pars tensa. There is presence of collagen type III in the lamina propria of the human tympanic membrane.

### **530 Mostly Malleus: Low-Frequency Specialization in the Golden Mole Middle Ear**

**Peter Narins<sup>1</sup>**, Urban Willi<sup>1</sup>

<sup>1</sup>*Dept. of Physiological Science, UCLA, Los Angeles, CA 90095 USA*

Golden moles, found exclusively in sub-Saharan Africa, are nocturnal, surface-foraging omnivores with rudimentary vision. Several species possess massively hypertrophied mallei that presumably confer low-frequency, substrate-vibration sensitivity through inertial bone conduction. When foraging, the Namib Desert golden mole, *Eremitalpa granti namibensis* moves between sand mounds containing most of the living biomass in the Namib Desert. Foraging trails are punctuated with characteristic sand disturbances called "head dips", discrete locations where the animal is thought to obtain a seismic "fix" on the next mound to be visited. Geophone recordings from the mounds reveal spectral peaks centered at ca. 300 Hz, ca. 15 dB greater in amplitude than those from the flats. Moreover, the mallei of the golden moles in the genera *Chrysochloris* and *Eremitalpa* are massively hypertrophied. In fact, out of the 117 species for which data are available, these golden moles are among those with the greatest ossicular mass relative to body size. Laser Doppler vibrometric measurements of the malleus head in response to seismic stimuli in *Chrysochloris* reveals peak sensitivity to frequencies below 300 Hz. Moreover, the orientation of the rotatory axis of the malleus is frequency-dependent. Functionally, these animals appear to be low-frequency specialists, and it is likely that golden moles hear through substrate conduction. Supported by NIH grant DC00222 to PMN.

### **531 Active Modulation of the Auditory Input Through Eustachian Tube Closure in Frogs**

**Marcos Gridi-Papp<sup>1</sup>**, Albert Feng<sup>2</sup>, Zu-Lin Yu<sup>3</sup>, Jun-Xian Shen<sup>3</sup>, Peter Narins<sup>4</sup>

<sup>1</sup>*Dept. of Physiological Science, UCLA*, <sup>2</sup>*Dept. of Molecular and Integrative Physiology and Beckman Inst., University of Illinois*, <sup>3</sup>*State Key Lab. of Brain and Cognitive Science, Inst. of Biophysics, Chinese Academy of Sciences*, <sup>4</sup>*Dept. of Physiological Science and Dept. of Ecology and Evolutionary Biology, UCLA*

Middle ear muscles modulate the auditory input in most vertebrates by restraining the movement of vibrating auditory elements. The result is dampening of the acoustic input, mostly at low frequencies. We found that the Chinese frog *Odorrana tormota* (Ranidae) can actively close its Eustachian tubes (ET) and alter the acoustic input at the middle ear. Closure is produced by pivoting the anterior hyoid horn, which delimits the caudal edge of the ET, at its attachment to the skull. Such movement is promoted by contraction of the submaxillar and of the petrohyoid muscles. ET closure reduces tympanic membrane (TM) vibration in response to low-frequency sound (3-10 kHz) and increases TM vibration in response to high-frequency sound (15-25 kHz). Such shift in TM vibration spectrum is likely to be biologically relevant as *O. tormota* is known to respond to ultrasound up to 32 kHz.

ET closure reduces the volume of the middle ear cavity, which should reduce cavity compliance and stiffen the TM, shifting its vibration spectrum. Unlike other mechanisms of auditory input modulation found in vertebrates, ET closure does not involve direct muscular restraint of the vibrating elements and can produce a real shift in the hearing spectrum, as opposed to frequency-selective attenuation.

### **532 Cetacean Middle Ear and Basilar Membrane Mechanics**

**David Mountain<sup>1</sup>**, Aleks Zosuls<sup>1</sup>, Seth Newburg<sup>1</sup>, Darlene Ketten<sup>2</sup>

<sup>1</sup>*Boston University*, <sup>2</sup>*Woods Hole Oceanographic Institution*

Our ability to predict the impact of sound on marine mammals is limited by our lack of knowledge about the audiogram for many species of interest. Hearing range in mammals depends on a combination of middle ear and cochlear properties. The low-frequency portion of the audiogram is dominated by the middle-ear transfer function while the high-frequency limit is determined by the cochlear frequency-place map. As a first step towards developing computational models of cetacean hearing, we have been measuring the mechanical properties of the middle ear and the basilar membrane in temporal bones harvested from stranded animals.

Middle ear and basilar membrane stiffness measurements are made using piezoelectric force probes similar to those described by Miller et al. (IEEE J. Oceanic Eng. 31:87-94) and Naidu & Mountain (Hear. Res. 124: 124-131). Preliminary results from three species indicate that, as is the case for terrestrial mammals, cetacean middle ear stiffness is lower for species with better low frequency hearing. Experiments in which the middle ear ossicles were disrupted indicate that the cetacean middle ear stiffness is dominated by the bony process which connects the malleus to the bulla.

Our preliminary data for basilar membrane stiffness suggest that basilar membrane stiffness is a good predictor for high frequency hearing. In the basal turn, the basilar membrane stiffness in the bottlenose dolphin (a high-frequency echolocator) is significantly higher than in the minke whale, a non-echolocating species.

[Funded by NIH, ONR, and the International Association of Oil and Gas Producers]

### **533 Measurements of Middle-Ear Pressure Gain and Cochlear Input Impedance in the Chinchilla**

**Michael Slama<sup>1</sup>**, Michael Ravicz<sup>2</sup>, Heidi Nakajima<sup>2</sup>, Wei Dong<sup>3</sup>, John Rosowski<sup>2</sup>

<sup>1</sup>*Harvard-MIT Program in Speech and Hearing Bioscience and Technology*, <sup>2</sup>*Massachusetts Eye and Ear Infirmary, Eaton-Peabody Laboratory*, <sup>3</sup>*Columbia University, Fowler Memorial Laboratory*

Measurements of middle-ear conducted sound pressure in the cochlear vestibule  $P_v$  have only been performed in a few individuals from a few animal species. Simultaneous measurements of sound-induced stapes velocity  $V_s$  are

even more rare. We have performed preliminary measurements of Vs and Pv in chinchillas. the Vs measurements are done using single-beam laser-Doppler vibrometry; Pv is measured with fiber-optic pressure sensors like those described by Olson [JASA 1998; 103: 3445-63]. Accurate *In-Vivo* measurements of Pv are limited by anatomical access to the vestibule, the relative sizes of the sensor and vestibule, and damage to the cochlea when inserting the measurement device. the small size (170  $\mu\text{m}$  diameter) of the fiber-optic microphones helps overcome these three constraints.

Pressure sensors were fabricated following the techniques of Olson (1998). the sensors were calibrated in air by comparing their response in a sound field with a known reference microphone, and in water using a vibrating water column. the sensors were placed into the vestibule of chinchillas, through a small (~220  $\mu\text{m}$  diameter) hole just posterior to the footplate. Cochlear potentials were measured before and after sensor placement to determine the effect of the hole and sensor placement on cochlear health. Pv and Vs were measured in several animals, and the middle-ear pressure gain (ratio of Pv to the sound pressure in the ear canal) and the cochlear input impedance (ratio of Pv to the product of Vs and area of the footplate) were computed. Preliminary results demonstrate (a) we can place the sensor in the vestibule while maintaining cochlear sensitivity; (b) our measurements of middle-ear pressure gain and cochlear input impedance are similar to previous estimates in chinchilla with stimulus frequencies of 500 to 4000 Hz, but are different from the published data at frequencies below 500 Hz. the cause of these differences is being investigated. [Supported by NIDCD]

### **534 Development of an Optoelectronic Holographic Oscope for Characterization of Sound-Induced Displacements in Tympanic Membranes**

**Cosme Furlong<sup>1</sup>**, Maria Hernandez-Montes<sup>1</sup>, Nesim Hulli<sup>1</sup>, Chris Wester<sup>1</sup>, Jeffrey T Cheng<sup>2</sup>, Ellery Harrington<sup>1</sup>, Michael Ravicz<sup>2</sup>, John Rosowski<sup>2</sup>  
<sup>1</sup>*Worcester Polytechnic Institute*, <sup>2</sup>*Massachusetts Eye and Ear Infirmary*

We describe our developments of an optoelectronic holographic (OEH) otoscope for the characterization of nanometer scale motions in tympanic membranes (TMs). OEH systems can provide full-field-of-view information, at video rates, of the sound-induced displacements of the entire surface of the TM, allowing rapid quantitative descriptions of the mechanical response to sound of complete normal or pathological TMs.

Preliminary measurements of TM motion in cadaveric animals helped constrain the optical design parameters for the OEH, including: image contrast, the modulation transfer function (MTF) of the images, system depth of field (DOF), laser power, the working distance (WD) between the interferometer and the TM, magnification, and field of view (FOV). in addition, laser-tissue interaction, laser wavelength, and speckle size were also taken into

consideration. Good contrast required coating the TMs with a water-based white paint.

Advanced imaging software was used in selecting and synthesizing major components. Several prototypes were constructed and characterized. the present configuration has an MTF with a resolution of 28.5 line pairs/mm, DOF of 5 mm, FOV of 9  $\times$  9 mm<sup>2</sup>, and a 473 nm laser with an illumination power of 1.5 mW. the OEH otoscope system includes a high-speed, computer controlled, digital camera, a fiber optic subsystem for the transmission and modulation of laser light, and an optomechanical system for illumination and observation of the TM.

The OEH system can be used in 'time-averaged' mode for fast characterization of the frequency dependence of TM modal patterns, or in a stroboscopic 'double-exposure' mode that allows determination of the magnitude and phase of motion of the entire surface of the membrane. the quality of the preliminary holography images indicates the suitability of our system for testing TM mechanics. Future works include further miniaturization of the system and live-animal measurements.

[Work supported by NIDCD]

### **535 Analysis of Time-Average Holograms of the Displacement of the Tympanic Membrane At Frequencies From 200 to 17500 Hz**

**Jeffrey Tao Cheng<sup>1</sup>**, Michael Ravicz<sup>1</sup>, Nesim Hulli<sup>2</sup>, Maria Hernandez-Montes<sup>2</sup>, Cosme Furlong<sup>2</sup>, John Rosowski<sup>1</sup>  
<sup>1</sup>*Massachusetts Eye and Ear Infirmary, Harvard Medical School*, <sup>2</sup>*Worcester Polytechnic Institute*

Computer-assisted time-averaged holography was used to measure the sound-induced tympanic membrane (TM) motion in post-mortem Chinchillas. the stimuli were tones of 90 to 110 dB SPL and frequencies of 200 to 17500 Hz. At frequencies below 600 Hz the modal displacement patterns are 'simple', with 1 to 4 modal peaks. Between 600 and 4000 Hz the modal patterns are 'complex', with multiple peaks. Above 4000 Hz the patterns are 'ordered' with radial and circumferential arrangements of peaks surrounded by troughs. the troughs are generally deeper between the radially arranged maxima. This ordered displacement indicates a two-dimensional standing wave pattern on the TM with wavelengths equal to twice the spacing of peaks. From these patterns, we calculated velocities of the surface waves along both radial and circumferential directions. the results show: (1) the wave velocities in both directions increased with frequency, suggesting the TM is a viscoelastic material with a complex modulus of elasticity. (2) the wave velocities vary with location and tend to decrease at locations further away from the umbo, suggesting the TM is an inhomogeneous material with greater mass or less stiffness at the TM edge. (3) the wave velocity along the circumferential direction is about 2 times higher than that along the radial direction, consistent with TM anisotropy. (4) the wave velocity estimates vary between 5 and 20 m/s, slower than other estimates of TM wave velocity in the literature. (5) the wavelengths appear similar in frequency and location dependence in the radial and circumferential directions. (6) the standing waves indicate



reflections produced by impedance mismatches at the TM boundaries. Future work will: (a) Investigate the wave patterns in live ears. (b) Calculate standing wave ratio from local peaks and troughs. (c) Correlate vibration patterns of the TM from 200 to 17500 Hz range with the unique multi-layer fiber structure of the TM.

[Work supported by NIDCD]

### **[536] Tympanic Membrane Collagen Fibers: Optical Second Harmonic Generation and Immunofluorescence Microscopy in Human Cadavers**

**Ryan Patrick Jackson**<sup>1,2</sup>, Cara Chlebicki<sup>3</sup>, Yoshitaka Shimizu<sup>1,2</sup>, Tatiana Krasieva<sup>3</sup>, Sunil Puria<sup>1,4</sup>

<sup>1</sup>Stanford University, Department of Otolaryngology, <sup>2</sup>Palo Alto Veterans Affairs, <sup>3</sup>Beckman Laser Institute, University of California, Irvine, <sup>4</sup>Department of Mechanical Engineering

Improved knowledge of the biomechanical properties of the tympanic membrane (TM) may lead to better techniques for surgical and tissue engineering approaches to the repair of TMs. the lamina propria segment of the TM is composed of several types of collagen, which are arranged in radial, circular, and parabolic patterns (Lim 1968), which provide skeletal support to the TM. Electron microscopy, immunohistology, and immunofluorescence (IF) imaging studies have examined collagen types I, II, III, and IV in the TM. However, these studies have drawn incomplete and sometimes conflicting conclusions regarding the distribution, volume fraction and attachment locations of each of these collagen types as a function of radial position in the TM. to address these questions, we are utilizing an imaging technique called Optical Second Harmonic Generation (OSHG) microscopy. OSHG generates images of fibrillar collagen, such as type I collagen, without necessitating the addition of contrast agents or other modifications to TM samples. to help distinguish the collagen types in our images, we are using IF with fluorescently labeled antibodies specific to each collagen type. the resolution of these imaging modalities, 0.2  $\mu\text{m}$  x 0.2  $\mu\text{m}$  in-plane and 0.5  $\mu\text{m}$  out-of-plane, allows for direct visualization of collagen fibers and potentially larger collagen fibrils. by combining OSHG and IF images, three-dimensional reconstructions may be generated that give a more detailed picture of the TM lamina propria. Our data may help us determine the mechanical importance of each of these collagen types in mathematical models of TM motion.

[This work received funding from the National Institutes of Health Grants: T32 MSTP (to R.P.J.), LAMMP P41 RR01192 (to T.K.), and DC05960 (to S.P.).]

### **[537] Estimating a Reverse Transfer Function of the Eardrum From Vibration Otoacoustic Emissions**

**Ernst Dalhoff**<sup>1</sup>, Diana Turcanu<sup>1</sup>, Anthony W. Gummer<sup>1</sup>

<sup>1</sup>University Tübingen, Section of Physiological Acoustics and Communication

Recently, using a custom built ultrasensitive laser Doppler vibrometer (LDV), we have shown that distortion product otoacoustic emissions (DPOAE) can be measured as vibration of the human eardrum in vivo, and proposed to use this parameter in order to support a differential diagnosis of middle- and inner-ear pathologies (Dalhoff, Turcanu, Zenner, Gummer, PNAS 2007). Here, we show measurements of the transfer function of the ear-canal pressure to umbo velocity in the guinea pig when driven in reverse by OAEs. Normal and hearing-impaired guinea pigs were anaesthetized and their pinna together with the cartilaginous part of the ear canal was removed. the tip of a probe microphone was glued within 2-4 mm to the tympanic membrane. Acoustic stimulation was delivered free-field. for the vibration measurements, we mounted our LDV (Dalhoff et al., PNAS 2007) onto an operating microscope. for an averaging time of 40 s, we typically achieved noise levels of 0.2 pm for frequencies higher than 1.5 kHz. Using a multitone stimulus, the forward transfer function of umbo velocity relative to ear canal pressure was acquired. Using two-tone stimulation with a frequency ratio of  $f_2/f_1=1.2$ , we determined the corresponding reverse transfer function at frequencies ranging from 1-10 kHz.

The reverse transfer function showed a bandpass characteristic with maximum of 1  $\text{m}^3/\text{kNs}$  at 3-4 kHz, and  $Q_{10\text{dB}}\sim 0.7$ . Published lumped-circuit models show reasonable agreement with the data up to about 5 kHz, suggesting that they need to be improved at higher frequencies.

Under certain assumptions, it should now be possible to use the reverse transfer function to estimate the eardrum transfer matrix and, thus, estimate the input impedance of the ossicular chain. This procedure would then open up possibilities for a differential diagnosis of middle- and inner-ear pathologies.

Supported by DFG Gu 194/8-1.

### **[538] Stapes Biomechanics: is There an Optimal Stimulus Axis?**

**Minyong Shin**<sup>1,2</sup>, Jong Dae Baek<sup>2,3</sup>, Charles Steele<sup>3</sup>, Sunil Puria<sup>3,4</sup>

<sup>1</sup>Department of Aeronautics and Astronautics, Stanford University, <sup>2</sup>Palo Alto Veterans Affairs, Palo Alto,

<sup>3</sup>Department of Mechanical Engineering, Stanford University, <sup>4</sup>Department of Otolaryngology-HNS, Stanford University

In both forward and reverse sound transmission, the stapes is the interface between incus vibrations and cochlear fluid pressures. an approach towards development of a model of human stapes is tested and then applied to other species. the modeling approach incorporates stapes morphometry and measurements of stapes impedance. for the stapes morphometry, micro-CT

scans were obtained at resolution of 10.5  $\mu\text{m}$ . From the 3D reconstruction of the bony stapes, the mass, the center of mass, and principal axes of inertia were calculated. the annular ligament is sub-divided into elements with each element modeled as three stiffness and three damping terms corresponding to its local coordinates. Equations of motion are solved with the same force vector as one that used in the experiment. of particular interest is the stapes impedance. We report measurements of stapes impedances in 4 human cadaver temporal bones, which is similar to M3 in Puria (2003; JASA) but with the incudo-stapedial joint separated. the stiffness and damping parameters are estimated by minimizing the mean-squared error between the model and measured impedance. the results indicate a ligament stiffness of 0.5-1 kN/m and damping of 0.02-0.06 N/m-s for the piston like motion component. for the shear modulus we estimate a range of 33-77 kN/m<sup>2</sup>. These parameters are used to calculate the response of the stapes with a force vector from different axes directions, which include the anatomical axis, principal inertia axis, and principal stiffness axis. As for the human, the mass, center of mass, and moments of inertia were also obtained for cat, gerbil, guinea pig, and chinchilla bony stapes using micro-CT imaging. the material properties estimated for human annular ligament were applied to the segmented annular ligament of each animal. Comparisons will be made for the three axes of stimulation to determine the optimal axis for sound transmission. [Work supported by grant no. DC05960 from the NIDCD of NIH.]

### **[539] Human Malleus Lever: Relation to Anatomic Axis of Ossicular Rotation**

**N Wendell Todd<sup>1</sup>**

<sup>1</sup>Emory

Background: Most assume that human manubria perpendicularly meet the anatomic axis of ossicular rotation, as an optimally positioned lever. However, such angular relationships have rarely been measured. the orientation of both the manubrium (as viewed through the external ear canal) and the anatomic axis of rotation (as sited in the skull) vary over wide ranges (about 45 and 30 degrees, respectively).

Hypotheses: Manubrium lever angulations are quite variable from ear to ear, and commonly are not perpendicular. Lever angulations are unrelated to both clinical manubrium orientation and the extent of mastoid pneumatization, but are bilaterally symmetrical.

Methods: 41 bequeathed adult human cranial base specimens (82 temporal bones) were studied. the ears were clinically normal. in a custom cephalostat, landmarks were orthogonally registered.

Results: On average, the malleus levers met the axes of orientations perpendicularly, but the range was wide (from 36 degrees anterior, to 33 degrees posterior). Bilateral symmetry was suggested. No convincing correlation was found with either the clinical orientation of the manubrium or the extent of mastoid pneumatization.

Conclusion: These human malleus levers were, on average, perpendicular to the anatomic axes of ossicular rotation. the wide range of angles (at least 69 degrees)

was not associated with either clinical orientation of manubria or mastoid size.

### **[540] Mechanical Stimulation of Complex Stapes Motions in Guinea Pig Ears**

Michail Chatzimichalis<sup>1</sup>, Jae Hoon Sim<sup>1</sup>, Albrecht Eiber<sup>2</sup>, Michael Lauxmann<sup>2</sup>, **Alexander Huber<sup>1</sup>**

<sup>1</sup>University Hospital Zurich, <sup>2</sup>University Stuttgart

According to the current hypothesis of hearing, the pressure difference between the round and oval window is the effective stimulus to the cochlea. in an ongoing study, we test this hypothesis by measuring cochlear activation in response to complex motions of the stapes. If the rotational components of the stapes have an effect on cochlear activation, the current hypothesis has to be expanded. in our measurement setup, it is desired to activate the stapes mechanically in its elementary motion patterns (e.g. translational motion, rotation around the short and the long axis of the footplate). in a biologic system, however, it is not possible to elicit pure elementary motions. Small amounts of other than the desired motions will always be contained in the induced vibrations. It was the goal of this study to optimize the mechanical stimulation setup to reduce the amount of undesired motions, to quantify such motions with high accuracy, to optimize frequency range of the stimulator, and to calculate error boundaries.

The purpose of this study is to test appropriate devices for spatial stimulation of the stapes and to assess the coupling properties between the actuator and the stapes. to generate the appropriate stimulus, a computer driven closed system feedback loop was used and the actual movement of the stapes was measured by a 3D Laser Doppler interferometer. Results of the study will be given at the meeting.

### **[541] Measurement of Physiological Motions of the Stapes in Guinea Pig Ears**

Jae Hoon Sim<sup>1</sup>, Michail Chatzimichalis<sup>1</sup>, Albrecht Eiber<sup>2</sup>, Michael Lauxmann<sup>2</sup>, **Alex Huber<sup>1</sup>**

<sup>1</sup>University Hospital Zurich, <sup>2</sup>University Stuttgart

It has been reported that the motion of the stapes in response to a natural acoustic stimulation is mainly piston-like along the longitudinal axis of the stapes at low frequencies. At higher frequencies, it contains rocking motions around the long and short axes of the footplate in the human and animal ear. This was not systematically tested in guinea pigs as a response to physiological sound stimuli. the goal of this study is to find an optimal method for quantitatively assessing the complex motion of the stapes and its error boundaries. to describe motions of the stapes, a motion component in a specific direction is measured at multiple points on the footplate using a scanning Laser Doppler vibrometer system and one translational and two rotational motion components of the stapes are calculated. the direction of the laser beam in the footplate plane is calculated by correlation between the measurement frame and a stapes-fixed frame, which is obtained by relating coordinates of reference points in both

frames. the coordinates in the stapes-fixed frame are measured from micro-CT scan.

Alternatively, all 3D motion components of a point of the stapes superstructure are measured using a 3D Laser Doppler vibrometer system and the motion components of the stapes are calculated with coordinates of the measurement point obtained from a micro-CT scan. the results from these two methods are compared to validate the accuracy of the methods.

#### **542 Scanning LDV Comparison of Ossicular Dynamic Modes Under Acoustic and Mechanical Stimulation**

**James Easter**<sup>1</sup>, Vikrant Palan<sup>2</sup>, Marco Ayala<sup>3</sup>, Ben Balough<sup>3</sup>

<sup>1</sup>Otologics, LLC, <sup>2</sup>Polytec, Inc., <sup>3</sup>Naval Medical Center San Diego

A scanning Laser Doppler Vibrometer (LDV), Polytec model PSV-400, was used to characterize modes of ossicular vibration in human temporal bones. Stimulation was applied both by acoustic excitation through the EAC, and by mechanical excitation of the ossicular chain using an implantable middle ear transducer (MET, Otologics, LLC). Ossicular vibration was characterized for both types of stimulation by imaging a portion of the ossicular chain while driving it over a range of frequencies and equivalent sound pressure levels. Dynamic modes for acoustic and mechanical stimulation are compared, and possible avenues for improvement of performance in implantable hearing systems are discussed.

#### **543 The Effect of Angulations of the Middle Ear Floating Mass Transducer On the Movement of the Stapes**

**Genevieve Rogers**<sup>1</sup>, Dan Jiang<sup>1</sup>, Athanasios Bibas<sup>2</sup>, Alec Fitzgerald O'Connor<sup>1</sup>

<sup>1</sup>Auditory Implantation Centre, Guy's and St. Thomas Hospitals, London, UK, <sup>2</sup>Dept. of Otolaryngology Head & Neck Surgery, Hippokrateion Hospital, University of Athens, Greece

Background: Implantable middle ear hearing devices such as the Vibrant Soundbridge have been used as an alternative to conventional hearing aids for the rehabilitation of sensorineural hearing loss. the majority of such devices are designed to facilitate stapes movement along its vibrating axis. Such a principle is not always achievable during surgery due to confined middle ear space. Sometimes the device has to be placed with an angle between its designed vibrating axis and that of the stapes. the effect of such angled placement on stapes movement is unknown.

Aim: the current study is to evaluate the frequency response of the stapes driven by the floating mass transducer (FMT), when placed at different angles to the stapes vibration axis.

Method: Three cadaver temporal bones were used. Stapes displacement was measured using laser Doppler vibrometry. the Vibrant Soundbridge FMT was crimped to the long process of the incus. the FMT was driven by a

digitally synthesized sinusoidal signal with a peak to peak voltage input ranging from 0.02 to 0.1V. Measurements were made at frequencies between 0.1 and 10 kHz. Angles between the vibrating axis of the FMT and that of stapes were set at 0° and 45°. the FMT driven responses were compared with the sound derived middle ear transfer function.

Results: Stapes displacement driven by the FMT has a peak at around 2 kHz which was similar to that of sound derived middle ear transfer function. the FMT driven stapes displacement attenuated at frequencies below 700 Hz and above 3 kHz. Changing the FMT angle from 0° to 45° produced a less than 5 dB drop of the peak stapes displacement, but an increase in the displacement at those frequencies above 3 kHz. the magnitude of the increase varied from bone to bone.

Conclusion: Placing the FMT at 45° to the vibrating axis of the stapes results in only a small attenuation to the peak value of the stapes displacement. At such angle, the stapes displacement increases at high frequencies.

#### **544 Characterization of Performance for an Implantable Hearing Device in Human Temporal Bones**

**Rong Gan**<sup>1</sup>, Chenkai Dai<sup>1</sup>, Don Nakmali<sup>2</sup>, Mark Wood<sup>2</sup>

<sup>1</sup>University of Oklahoma, <sup>2</sup>Hough Ear Institute

Middle ear implantable hearing devices as an emerging and effective technology can offer significant advantages to the individuals with mild to moderately severe sensorineural hearing loss. Several devices equipped with piezoelectric or electromagnetic transducers have been developed in the US. Recently, a totally implantable hearing system (TIHS) consisting of a subcutaneous sound processor or sound amplifier, microphone, and electromagnetic transducer is under investigation in Oklahoma (P.I.: Rong Z. Gan). the design of the TIHS has incorporated the bioengineering approaches based on a 3D finite element (FE) computational model of the human ear and the FE analysis of electromagnetic coupling of the transducer. in this paper, we report the experimental measurements in human temporal bones with the TIHS prototype by using laser Doppler interferometry. a series of tests were conducted on the device to characterize its performance for driving the stapes over auditory frequency range. These tests include: 1) mass loading effect on residual hearing with the passive implant, 2) effectivity of the electromagnetic coupling between implanted coil and magnet, and 3) function characterization of whole unit in response to acoustic input across the skin. the results indicate that the TIHS prototype tested in human cadaver ears or temporal bones shows satisfactory performance of the system. the data obtained from those experiments will be further used for clinical trials of the TIHS. (Supported by Oklahoma Center for Advancement of Science & Technology)

#### **545 Hearing Aid Using Cartilage Conduction**

**Takefumi Sakaguchi<sup>1</sup>, Osamu Saito<sup>1</sup>, Hiroshi Hosoi<sup>1</sup>**

<sup>1</sup>*Nara Medical University*

Although bone conduction hearing aid is considered to be better to compensate the hearing loss of the patients who has atresia auris or perforation of tympanic membrane, some of these patients tend to wear air conduction hearing aid because of the feeling of tightness when wearing bone conduction hearing aid. We expected cartilage conduction would reduce feeling of tightness compared to bone conduction, and improve compensation compared to air conduction. In this study, we report the result of the basic studies we performed to evaluate the usefulness of cartilage conduction hearing aid.

Two groups of patients participated in the hearing tests. One had atresia auris, and another had perforated tympanic membrane. Stimuli were presented to the subjects by means of two types of transmitter. One was piezoelectric transducer placed on antilobium, another one was insertion earphone.

We found that the hearing threshold of the patient with atresia auris improved about 25 dB or greater and also found that the hearing threshold of the patients with perforation of tympanic membrane slightly improved when the transducer was located on antilobium compared to the result when insertion earphone was used.

These results suggest that the cartilage conduction hearing aid can be an option of the hearing aid for the patients that have atresia auris or perforation of tympanic membrane.

#### **546 Wideband Acoustic Ear-Canal Reflectance, Including Wideband Tympanometry and Acoustic-Reflex Thresholds: System Development and Results On Children with Middle-Ear Fluid and Adults**

**Yi-Wen Liu<sup>1</sup>, Edward Cohn<sup>1</sup>, John Ellison<sup>1</sup>, Denis Fitzpatrick<sup>1</sup>, Michael Gorga<sup>1</sup>, Michele Gortemaker<sup>1</sup>, Chris Sanford<sup>1</sup>, Douglas Keefe<sup>2</sup>**

<sup>1</sup>*Boys Town National Research Hospital*, <sup>2</sup>*Sonicom, Inc.*

A computerized system has been developed to measure acoustic ear-canal reflectance. The system delivers two stimulus channels to receivers in an ear probe and records a probe-microphone response simultaneously. Static pressure in the ear canal is software monitored and controlled using a pump. Responses to wideband (0.226-8 kHz) clicks are analyzed, acoustic artifacts are rejected, and reflectance and admittance are calculated. In one demonstration of its usefulness, experiments were conducted on 25 children with surgically confirmed middle-ear effusion (MEE) and an age-matched control group with normal findings from pneumatic otoscopy. Results showed that wideband reflectance measured at ambient pressure predicts MEE with an area of 0.93 under the relative operating characteristic (ROC) curve. Experiments are currently being conducted to obtain normative data from adults for wideband tympanometry and middle-ear muscle reflex (MEMR) threshold.

Wideband tympanometry may reveal aspects of middle-ear functioning not evident in either reflectance at ambient pressure or single-frequency tympanograms. A MEMR procedure uses an interleaved temporal sequence of activator pulses to evoke the MEMR and clicks to detect any MEMR shift. Results may be useful in objectively determining MEMR thresholds in infants and adults at lower activator levels than in current clinical testing.

Research supported by NIH grants DC006607 and DC004662.

#### **547 Dynamics of Vestibular Hair Cell Regeneration and Re-Innervation**

**Susanna Pfannenstiel<sup>1</sup>, Douglas E. Brough<sup>2</sup>, Mark Praetorius<sup>1</sup>, Hinrich Staecker<sup>3</sup>**

<sup>1</sup>*University of Heidelberg*, <sup>2</sup>*GenVec Inc.*, <sup>3</sup>*KU School of Medicine*

Delivery of *atoh1* has been demonstrated to result in the generation of hair cells after aminoglycoside damage. To study the dynamics of hair cell regeneration after atonal delivery we treated adult mice with low or high doses of aminoglycosides. At differing time periods post aminoglycoside treatment, animals were injected via the posterior semi circular canal with an advanced generation adenovector carrying *math1* the glial fibrillary acidic protein promoter. At one month post vector delivery the animal's temporal bones were removed, fixed, decalcified and embedded in agar. Thirty micron sections were cut and immunostained for total hair cells, striolar hair cells, supporting cells and innervation. Hair cell counts and supporting cell counts for the macular organs and cristae were derived. Controls consisted of mice treated with aminoglycosides and injected with a green fluorescent protein containing vector.

#### **548 Gene Transfer with Bovine Adeno-Associated Virus Efficiently Transduces the Cochlea of Guinea Pigs in Vivo**

**Seiji B. Shibata<sup>1</sup>, Giovanni Di Pasquale<sup>2</sup>, John A. Chiorini<sup>2</sup>, Yehoash Raphael<sup>1</sup>**

<sup>1</sup>*Kresge Hearing Research Institute, Univ. of MI*, <sup>2</sup>*Gene Therapy and Therapeutics Branch, National Institute of Dental and Craniofacial Research*

Bovine adeno-associated virus (BAAV) has been previously described to show cell tropism and transduction in the neuroepithelial cells of cultured rat inner ear epithelia *In Vitro* (Di Pasquale et al., 2005). In this study we aimed to assess the transgene expression of BAAV with  $\beta$ -actin-GFP as a reporter gene. We used two different routes to inoculate the guinea pig cochlea: scala media (SM) or scala tympani (ST). For SM inoculation, BAAV (5  $\mu$ l) was injected into the endolymph through a fenestra in the 2<sup>nd</sup> turn of the left cochlea via a microcannula (Ishimoto et al., 2002). For ST inoculation, BAAV (5  $\mu$ l) was delivered into the perilymph of the basal turn via a cochleostomy in the left cochlea. This volume of inoculated viral vector delivers  $3.0 \times 10^{10}$  DNase Resistant Particles into the receiving ear. The right ear served as a control in both groups. Fourteen days after the injection, cochleae were assessed histologically.

Immunohistochemistry by GFP antibody and rhodamine-phalloidin were used to enhance GFP signal and to label actin, respectively. Epifluorescence showed that BAAV transduced Hensen cells, pillar cells, inner sulcus cells, interdental cells and a few Deiters cells by both SM and ST inoculations. ABR assessments were done prior to inoculation, 7 days post inoculation and immediately prior to sacrifice. ABR results showed a larger threshold shift in the SM group than the ST group, which is consistent with reports using adenovirus vector inoculation. Transgene expression in the membranous labyrinth by ST is an important outcome because ST is more feasible than SM as an inoculation route for future clinical application. In this first report of BAAV-mediated transgene expression *in vivo*, we demonstrate efficient transduction of the membranous labyrinth epithelium, which suggests that this vector may become clinically applicable for inner ear gene therapy.

Supported by NIH/NIDCD grants T32 DC005356 and RO1-DC001634.

#### **549 Targeting Adenoviral Gene Expression in the Mouse Inner Ear**

**Clifford Hume<sup>1</sup>**, Debbie Bratt<sup>1</sup>, Ming Xiao<sup>1</sup>, Hsin-Pin Lin<sup>1</sup>, Amanda Ogle<sup>1</sup>, Fukuichiro Iguchi<sup>1</sup>

<sup>1</sup>*University of Washington*

Gene therapy for hearing loss and balance disorders will require delivery vehicles that can efficiently and specifically target the appropriate cell types in the inner ear. In other organ systems, this has required careful matching of non-replicating, non-disease causing viruses with gene control elements active only in the target cells. This "double-targeting" maximizes the safety and specificity of each therapy. For each particular molecular or cellular defect, the required temporal and spatial specificity of gene expression will be unique. Because of the availability of models of human hearing loss, we have focused on identifying the cellular targets of viral infection in the mouse inner ear. We are testing the ability of different transcriptional control elements (eg Brn3c vs hCMV) to target gene expression of Type 5 Adenovirus (E1-/E3-/polymerase-) *In Vitro* and *In Vivo* in normal hearing mice. *In Vitro* cultures are established from neonatal Swiss Webster mice (P0-P5), infected with viruses after one day of culture, and analyzed after three days. For the *In Vivo* studies, viruses are injected into the inner ears of adult Swiss Webster mice either through a posterior semicircular canalostomy or a basal turn cochleostomy. Two weeks after injection, ears are analyzed by frozen section immunohistochemistry. Using GFP reporters, we will describe the effects of variation of transcriptional control elements on gene expression in the inner ear.

#### **550 Hyperbranched Polylysines As Novel Drug Carrier are Detectable in Inner Ear Tissue**

**Timo Stoeve<sup>1</sup>**, Melanie Wolf<sup>1</sup>, Verena Scheper<sup>1</sup>, Markus Scholl<sup>2</sup>, Zuzana Kadlecova<sup>2</sup>, Harm-Anton Klok<sup>2</sup>, Thomas Lenarz<sup>1</sup>

<sup>1</sup>*Hannover Medical School*, <sup>2</sup>*EPF Lausanne*

Inner ear deafness is based on hair cell loss, degradation of spiral ganglion cells or dysfunction of the stria vascularis. Treatment of these cell types with genes, plasmids, neurotrophic factors or different drugs has been shown to be effective in therapy of deafness.

A novel generation of multi-functional drug delivery vehicles which are targetable to selected cell populations, biodegradable, traceable *In Vivo* and equipped with controlled drug release for therapy of inner ear tissue would advance the current application methods. First step on this way was to examine if hyperbranched polylysine nanoparticles are detectable *in vivo*.

FITC labeled hyperbranched polylysine nanoparticles with an approximate hydrodynamic radius of 10 nm were dissolved in PBS (pH 7.4) at a ratio of 1:100. A volume of 5 µl of this solution was injected in the scala tympani of guinea pigs via a cochleostomy. 48 hours after treatment cochleae were harvested, the bony capsules were removed and the tissue was dyed in rhodamine-phalloidin. Subsequently the basilar membrane and the stria vascularis were dissected, stained with DAPI and coverslipped. The embedded tissue was examined with a confocal laser scanning microscope. Sequential excitation for the three dyes was performed to detect the nanoparticles, the cell-nuclei and the actin filaments of the cells in the tissue.

The hyperbranched polylysines were detectable in cells of the basilar membrane as well as of the stria vascularis. These findings are supporting the hypothesis that nanoparticles may be used for future therapy strategies for inner ear diseases.

Further research has to be done concerning the extent of NP internalization depending on the concentration and the exposition time, the toxicity, the drug payload and release and the bioefficiency.

Acknowledgment: This study is part of the NanoEar project and received financial support by the European Union under contract number NMP4-CT-2006-026556.

#### **551 Differences in Proliferative Capacity Between the Utricles of Chickens and Mice are Determined, in Part, by Cellular Resistance to Shape Change**

**M. Sol Collado<sup>1</sup>**, Joseph C. Burns<sup>2</sup>, Christopher Magnus<sup>1</sup>, Jeffrey T. Corwin<sup>1</sup>

<sup>1</sup>*Department of Neuroscience, University of Virginia School of Medicine*, <sup>2</sup>*Department of Biomedical Engineering, University of Virginia*

In mammalian utricular sensory epithelia, cell proliferation correlates with a capacity for cellular shape change that declines with age (Davies et al., 2007; Meyers and Corwin, 2007). Here, we have investigated age-dependent cellular

shape change and cell production in utricular epithelia from chickens and mice under two experimental situations. First, we compared outward spreading and BrdU labeling in sheets of utricular sensory epithelia cultured on rigid substrates. in contrast to mammals, 33 sheets of sensory epithelium from chickens that ranged in age from P0 to P180 all spread and proliferated extensively. the increase in sheet area resulted from supporting cell spreading and occurred even when proliferation was blocked by aphidicolin. Next, we measured cellular shape change and proliferation after making excision wounds in the sensory epithelium of chicken and mouse utricles in organ culture. Wounds in the utricles of P0 to P365 chickens all closed in ~24 h, independent of age. in mice, wounds in neonatal utricles closed in < 24 h while wounds in the utricles from adults closed in ~72 h, with 5 times as many BrdU-positive cells in the healed wounds of the neonatal utricles. in utricles from young mice and all chickens, wound closure resulted in shape changes in the cells at the former edge of healed wounds. Closure also resulted in changes in the shape of cells beyond the former wound edge that progressively decrease with distance from the center of the closed wound. in older mice, wound closure results in greater shape changes for cells at the former wound edge, but the cells beyond the edge of the healed wound exhibited little shape change or migration. Together with findings reported at this meeting by Burns et al., our results support the hypothesis that an age-dependent increase in resistance to cellular shape change partly accounts for the limited proliferation that occurs in mature mammalian vestibular epithelia.

## **[552] Cortical Actin Band Thickness May Explain the Difference in Regenerative Capacities of Balance Epithelia in Birds and Mammals**

**Joseph Burns<sup>1</sup>**, Jared Christophel<sup>2</sup>, Jeffrey T. Corwin<sup>3</sup>

<sup>1</sup>*Department of Biomedical Engineering, University of Virginia,* <sup>2</sup>*Department of Otolaryngology-Head and Neck Surgery, University of Virginia, School of Medicine,*

<sup>3</sup>*Department of Neuroscience, University of Virginia, School of Medicine*

Age-dependent restrictions in cellular shape change correlate with a decreased capacity for cell replacement in utricular hair cell epithelia from mice (Davies et al., 2007; Meyers and Corwin, 2007). Since the cytoskeleton regulates cell shape and proliferation, we fixed utricles *In Vivo* and tested the hypothesis that the thickness of cortical actin bands in supporting cells would correlate with the different regenerative capacities of balance epithelia from birds and mammals. Using phalloidin-labeling and confocal microscopy we measured the thickness of >1,500 apical junction regions (AJRs, defined as the junction and cortical actin bands) of adjacent supporting cells in 56 utricles from mice at ages E18 to P83. the full-width half-maximal thickness of the AJR closely followed an age-related logistic growth curve (thickness in  $\mu\text{m}$  =  $2.99 - [2.02 + 0.19(\text{age in days})^{0.89}]$ ,  $r^2 = 0.986$ ). AJR thickness increased from  $0.823 \pm 0.065 \mu\text{m}$  at a rate of ~91.4 nm/day as mice aged from E18 to P10, but the growth

slowed to ~9.8 nm/day between P10 and P83. At P83, AJR thickness was  $2.77 \pm 0.12 \mu\text{m}$ , ~350% greater than at E18. Confocal and TEM imaging provided evidence that increased AJR thickness resulted from cortical actin band reinforcement. in contrast, as chickens aged from P0 to P365, AJR thickness remained relatively constant at  $0.632 \pm 84 \mu\text{m}$ , ~23% thinner than AJRs from E18 mice. of potential importance, AJRs from limited samples of adult human utricles resembled AJRs in adult mice. Together with findings reported at this meeting by Collado et al., our results reveal strong parallels between cortical actin band thickness and the capacity for supporting cells to change shape and proliferate. These results are consistent with the hypothesis that highly reinforced cytoskeletal elements are partly responsible for the permanence of hair cell deficits in mammals; the results also provide a plausible mechanistic explanation for the occurrence of hair cell regeneration in birds.

## **[553] Temporal Differences in Cell Fates During Hair Cell Regeneration in the Chick Cochlea**

**Andrew J. Kamien<sup>1</sup>**, Brittany J. Chapman<sup>1</sup>, Christina L. Kaiser<sup>1</sup>, Douglas A. Cotanche<sup>1</sup>

<sup>1</sup>*Department of Otolaryngology, Children's Hospital, Boston, MA 02115, USA*

Noise exposure, aminoglycoside antibiotic administration, or the aging process can damage hair cells in the inner ear. These agents can permanently kill mammalian cochlear hair cells. However, avian species can replace lost cochlear hair cells. These new hair cells are generated from cochlear supporting cells by one of two distinct mechanisms: direct transdifferentiation (DT) or cell division. in DT, a supporting cell directly changes its phenotype to become a hair cell; in cell division, normally quiescent supporting cells re-enter the mitotic cycle and divide to produce new supporting cells and hair cells. Little is known about the fate of these proliferating cells, in particular, if the time-point during regeneration at which they are produced will effect the eventual phenotype of the cell. the purpose of this study is to determine if cell proliferation during early and late regeneration produces different cell fates.

To induce hair cell loss, ten-day old chicks were given a single injection of gentamicin. At 72, 96, or 120h after gentamicin injection, birds were given a single injection of bromodeoxyuridine (BrdU) and then sacrificed 10 days after gentamicin treatment. Cochleae were dissected and labeled with antibodies against BrdU (to label dividing cells) and myosin VIIa (to label hair cells). Preliminary results indicate that the number of BrdU-labeled cells was greatest after a 72h injection, with fewer BrdU-labeled cells seen after the 96h and 120h injection. the percentage of paired BrdU-labeled nuclei was greatest after the 120h injection, while the percentage of BrdU and myosin VIIa co-labeled cells (i.e., hair cells) was greatest after the 72h injection. These results suggest that cell divisions early in the regeneration process give rise to a higher proportion of new hair cells, while those in later regeneration give rise to mostly supporting cells in order to repopulate the cell field.

### **554 Characterization of Math1 Positive Cells in the Regenerating Avian Cochlea: Creating a Timeline for Math1 Upregulation After Gentamicin Treatment *in Vivo***

**Brittany J. Chapman<sup>1</sup>**, Christina L. Kaiser<sup>1</sup>, Douglas A. Cotanche<sup>1</sup>

<sup>1</sup>*Department of Otolaryngology, Children's Hospital, Boston, MA 02115, USA*

Math1, a basic helix-loop-helix (bHLH) transcription factor, has been identified as playing a critical role in hair cell development, differentiation, and regeneration. Embryonic *Math1*-null mice fail to generate cochlear and vestibular hair cells; misexpression of *Math1* in the developing auditory system induces nonsensory cells to become hair cells. While previous studies have shown Math1 expression in the avian cochlea 15 hours (h) after gentamicin injection, earlier time points of Math1 expression were not studied (Cafaro et al., 2007. *Dev. Dyn.* 236(1): 156-70). the purpose of this study is to determine the earliest point of Math1 expression after gentamicin injection and to create a subsequent timeline detailing Math1 labeling.

To test this, 1-2 week old chicks were given a single gentamicin injection and sacrificed 6, 9, 12, 15, 24, or 48h after injection (AI). Cochleae were dissected and labeled with antibodies against Math1 and co-labeled with phalloidin in order to visualize hair cells and to identify cochlear damage. Initial results show that Math1 expression begins between 9h and 12h AI, before visible signs of hair cell death are evident. Many Math1-labeled supporting cells are present along the inferior cochlear edge at 12, 15, 24, and 48h AI, but no Math1-positive cells are seen in control cochleae or 6h AI. However, primary qualitative results indicate a greater number of Math1 positive cells at 12h and 15h AI than in the 24h and 48h samples. More studies are needed to better characterize Math1 labeling in the avian cochlea after gentamicin treatment and how this leads to hair cell regeneration.

Supported by NIH NIDCD grants DC01689 (DAC) and DC008235 (CLK) and the Sarah Fuller Fund (DAC).

### **555 Hearing Recovery Via Direct Transdifferentiation in an Avian Model**

**Vincent Lin<sup>1</sup>**, Gi Soo Lee<sup>1</sup>, Edwin Rubel<sup>1</sup>, Jennifer Stone<sup>1</sup>

<sup>1</sup>*Virginia Merrill Bloedel Hearing Research Center, University of Washington*

Birds have the ability to regenerate auditory hair cells through either mitosis or direct transdifferentiation of non-sensory supporting cells. Recently studies in mammals demonstrate that direct transdifferentiation of supporting cells into hair cells is triggered by virally mediated misexpression of the nuclear transcription factor, Atoh1. One question that is raised is the degree to which direct transdifferentiation in mammals can restore hearing function. We will address this question in birds by examining the magnitude and rate of hearing recovery that occurs in birds in which direct transdifferentiation is the

only method of hair cell regeneration. We have developed a method in our laboratory to implant birds with Alzet osmotic mini-pumps that deliver cytarabine (Ara-C) directly into the labyrinth. Ara-C is a direct inhibitor of DNA polymerase and kills rapidly dividing cells. in *In Vitro* experiments, we confirm that all supporting cells that enter the cell cycle in chick basilar papillae treated with Ara-C (1-10  $\mu$ M) after streptomycin lesioning undergo apoptosis. Nevertheless, hair cells continue to be regenerated. New hair cells excluded bromodeoxyuridine and were therefore formed via direct transdifferentiation. *In Vivo* delivery of Ara-C (0.5%) using an osmotic mini-pump caused similar apoptosis of dividing supporting cells. Immunohistochemistry with phosphohistone-3, which labels cells in M phase, confirms that supporting cells fail to reach M phase of the cell cycle. Nonetheless, hair cells continue to be regenerated. Preliminary ABR results indicate that birds treated with 0.5% Ara-C begin to demonstrate hearing recovery at approximately 28 days after gentamicin lesioning. Long term testing is currently ongoing to determine the maximum level and stability of hearing recovery after non-mitotic regeneration.

Supported by AOSF, NIH DC 03696 (JSS), NIH DC 04661

### **556 Downregulation of GFP Reporter Gene Expression in Inner Ear Cell Types and it's Implication On Stem Cell Transplantation Research**

**C. Eduardo Corrales<sup>1</sup>**, Kazuo Oshima<sup>1</sup>, Pascal Senn<sup>1</sup>, Rodrigo Martinez<sup>2</sup>, Albert Edge<sup>2</sup>, Stefan Heller<sup>1</sup>

<sup>1</sup>*Stanford University Medical Center, Otolaryngology HNS,*

<sup>2</sup>*Harvard Medical School, Tillotson Lab for Cell Biology of the Inner Ear, MEEI*

Hearing loss is nearly epidemic in proportions, affecting approximately one third of individuals over the age of 65 years. Given its prevalence, it is one of the most common neurodegenerative disorders. in the mammalian inner ear, the mechanosensory receptor cells (hair cells) and their associated spiral ganglion neurons do not regenerate. Over time and with a variety of insults such as ototoxic substances, noise trauma and genetically determined susceptibility to degeneration, these critical sensory cells are lost. Recent experiments have raised hope that stem cell transplantation has the potential to restore function in organ systems that have poor regenerative capacity. Some of these experiments utilize green fluorescent protein (GFP) and related isoforms in form of transgenic reporters to identify transplanted cells in a non-transgenic host organism. Here we report the analysis of inner ear GFP expression in three widely used transgenic mouse lines that were generated by using the ubiquitous chicken beta-actin/CMV promoter allowing the transgenic GFP allele to be expressed in every cell. We noted that the expression of GFP in the inner ear varied from strain to strain, but more importantly it left some cochlear cell types entirely unlabeled. More specifically, we observed an absence of fluorescence in mature cochlear hair cells and spiral ganglion neurons. We detected a decreasing intensity of GFP expression as the cells differentiated and matured, to the point of completely lacking the reporter



protein. We further analyzed embryonic stem cells (developed using the same promoter technology) and observed decrease in GFP expression in differentiated cell types, most noticeably in neurons. These findings suggest that there is an intrinsic downregulation of GFP in some maturing hair cell types and spiral ganglion neurons. The time course and the extent of loss of GFP expression varied with each transgenic mouse line. Our results indicate that stem cells or progenitor cells obtained from commonly used ubiquitous GFP reporter mouse lines may not be suitable for cellular detection in transplantation studies aimed to regenerate hair cells or spiral ganglion neurons.

### **[557] Progenitor Cells in the Human Embryonic Inner Ear - Characterisation and Potential Therapeutic Use**

**Beata Kostyszyn<sup>1</sup>, Mats Ulfendahl<sup>2</sup>**

<sup>1</sup>*Center for Hearing and Communication Research,*

<sup>2</sup>*Center for Hearing and Communication Research, Karolinska Institutet*

Sensorineural hearing loss is characterized by loss of sensory hair cells and /or damage to the associated spiral ganglion neurons. These cells are incapable of regeneration in mammals, including humans. At the present, treatment options for individuals with severe to profound sensorineural hearing loss include hearing aids or cochlear implantation. One of the new approaches that are being investigated to improve the survival or replacement of the damaged hair and neuronal cells is the implantation of embryonic stem or progenitor cells into the inner ear. One possible source of suitable cells for transplantation would be human cell lines derived from fetal cochlea. There is a significant need for a self-renewal able human *In Vitro* system that could be a feasible experimental tool for therapeutic purposes. In order to define suitable tissue for isolation from the embryonic/fetal inner ear we first isolated human cochlea anlage (9 gestational weeks). Tissue was decalcified, fixed in paraformaldehyde and cryosectioned into 10 µm thin slices. Immunohistochemistry with primary antibodies against β-tubulin (neuron specific marker) and Nestin (neural precursor marker) was applied to characterize the developing auditory precursors. Myosin VII a (hair cell marker) and p27 kip1 (cyclin dependent kinase inhibitor) were used to study the onset of differentiation within sensory epithelia. Antibodies against tyrosine kinase B and C receptors were applied to investigate if the differentiating neurons within spiral ganglia could express those proteins in response to neurotrophic factors, such as neurotrophin-3 (NT-3) and brain derived neurotrophic factor (BDNF). A large number of immature Nestin positive neural precursors were detected from gestational week 5 within spiral ganglia. The expression of Nestin gradually declined after gestational week 9, and most of the differentiating neurons within spiral ganglia and neuritis which interspersed the forming sensory epithelia were β-tubulin positive. Expression of p27 kip1 was upregulated from gestational week 7 and concurrently the first differentiating hair cells could be detected with Myosin VII a antibody.

strong immunoreactivity for tyrosine kinase receptor B (expressed in developing spiral ganglia) and C (expressed in spiral ganglia and in the nerve endings contacting sensory epithelia) was seen from gestational week 6, which might be an indication of functional maturation of differentiating neurons during development of the human inner ear.

Given all that information we conclude that isolation of human embryonic/fetal inner ear tissue before gestational week 8 would provide us with largest population of progenitor cells for further *In Vitro* expansion.

### **[558] Retrieval of Stem Cells From Co-Cultured Otocysts**

**Mark Parker<sup>1</sup>, Albert Edge<sup>1</sup>**

<sup>1</sup>*Massachusetts Eye & Ear Infirmary*

Recent studies have suggested that both mesenchymal (Jeon, et al., 2007) and neural stem cells (Parker et. al., 2007) maintain the potential to differentiate into cochlear hair cells. However, in both cases the incidence of hair cell genesis is low. Therefore, the overall goal of this work is to increase the number of hair cells generated by stem cell differentiation. Unfortunately, the specific signaling pathways responsible for stem cell-hair cell transdifferentiation remain undefined. In this abstract, we present an experimental model that examines the initial signaling events that lead mesenchymal stem cells (MSCs) to develop along a cochlear pathway. We injected human MSCs encoding a DsRed neo cassette into the developing murine otocyst, co-cultured them for three days, and recovered the MSC by selection for the neo resistance gene. The recovered MSCs can then be assayed for otocyst-induced changes in MSC gene expression. This model represents proof of principle that MSCs can be retrieved from the developing otocyst and the influence of the inner ear on MSC differentiation may be analyzed.

### **[559] Engraftment of Human Hematopoietic Stem Cells in the Inner Ear of a Humanized Mouse Model**

**Hainan Lang<sup>1</sup>, Bradley a Schulte<sup>1</sup>, Kiyoshi ando<sup>2</sup>, Makio Ogawa<sup>1</sup>, Richard a Schmiedt<sup>3</sup>**

<sup>1</sup>*Department of Pathology and Laboratory Medicine, Medical University of South Carolina,* <sup>2</sup>*Research Center of Regenerative Medicine, Tokai University School of Medicine,* <sup>3</sup>*Department of Otolaryngology – Head & Neck Surgery, Medical University of South Carolina*

Unlike auditory hair cells that are unable to regenerate, non-sensory cells, such as fibrocytes in the spiral ligament of the cochlear lateral wall, are able to repopulate themselves after injury, although their regenerative ability seems to decline with age. The mechanism whereby these non-sensory cells are able to repair themselves remains unknown. Our previous studies have documented that fibrocytes in the spiral ligament and glia-like cells in the auditory nerve of the adult mouse can be derived from hematopoietic stem cells (HSCs) (Lang et al., J Comp Neurol 496: 187-201, 2006). Here, we examine whether certain human inner ear cells are also derived from HSCs.

The ability to perform studies of human HSCs *In Vivo* is severely limited by ethical and technical constraints. To overcome these limitations, we can use human-mouse transplantation models (humanized mice) based on immunodeficient mice to perform *In Vivo* studies of human HSCs in the inner ear. We have transplanted CD 34<sup>+</sup> cells isolated from human cord blood into immunodeficient mice via an intravenous route. Successful engraftment of human cells was found in recipient mice four months after transplantation. The percentage of human cells in the bone marrow of the recipient mice ranged between 26.5% and 60.19%. Engrafted human cells were also present in non-hematopoietic organs including the inner ears of all the recipient mice. Specifically, human cells were present in the cochlear lateral wall including the type I and IV fibrocyte regions. Human cells were also found in the limbus, spiral ganglia and in the connective tissue of the vestibular organs. Supported by NIH DC7506 (H.L.); NIH AG14748 (R.A.S.); NIH DC00713 (B.A.S.); NIH HL69123 (M.O.).

#### **560 Identification of Tissue Specific Stem/Progenitor Cells in Auditory Pathway**

**Hisashi Ooka<sup>1</sup>**, Seiji Kanda<sup>2</sup>, Hiroko Suzuki<sup>2</sup>, Toshimasa Nishiyama<sup>2</sup>, Toshio Yamashita<sup>1</sup>

<sup>1</sup>Dept. of Otolaryngology, Kansai Medical University,

<sup>2</sup>Dept. of Public Health, Kansai Medical University

**Objects:** Recently, in the region of regenerative medicine, it focused on the tissue specific stem/progenitor cells such as neural stem cells in adult brain that has multipotency and identified these cells in various organs. The treatment for the deaf patients that have the auditory damages has been tried, however it was difficult to heal completely. In this research, in order to find out the keys of treatments for these patients by using regenerative medicine, we tried to isolate stem cells from auditory pathway and identify the cell characterization and gene expressions. **Methods and Results:** 3 days age of mice were injected BrdU to the hypodermic at 2 times/day for 3 days continuously, and sacrificed after 16 weeks to identify the slow-cycling cells suggesting the possibility of stem cells. The results of immunohistochemistry showed that a few cells were identified as BrdU<sup>+</sup> and ABCG2<sup>+</sup> double positive cells in the section of cochlear nuclei in auditory pathway. Furthermore, we assumed that it was possible to purify stem cells as side population (SP) cells. Cochlear nuclei cells were isolated from 6 weeks age of mice and stained with Hoechst 33342. After staining, SP cells were sorted as a negative fraction. The population of SP cells was about 1% of total cells of cochlear nuclei. Furthermore, in order to analyze the gene expression of these cells, we used microarray techniques by Mouse oligo Microarray (Agilent technologies). The results showed that the upregulated genes in SP cells were included some specific markers of stem/progenitor cells, such as ABCG2, Sca-1, notch1, and notch4.etc. These cells also had the sphere forming ability. Now we are going to study whether these cells have the multipotency as stem/progenitor cells, and analyze the gene function of the cochlear nuclei specific genes that identified by microarray analysis.

#### **561 Phoenix is Required for Efficient Hair Cell Regeneration in the Zebrafish Lateral Line**

Martine Behra<sup>1</sup>, John Bradsher<sup>2</sup>, Rachid Sougrat<sup>3</sup>, **Shawn Burgess<sup>1</sup>**

<sup>1</sup>NHGRI/NIH, <sup>2</sup>NCI/NIH, <sup>3</sup>NICHD/NIH

The lateral line in fish is a sensory organ used to detect water movements, and is closely linked in structure and function to the vertebrate inner ear. Unlike mammals, amphibians, birds and fish have kept the capability to regenerate damaged hair cells by triggering the division of the supporting cells, a stem cell population in neuroepithelia. We have set up an *In Vivo* assay, which examines the regeneration process in hair cells of the lateral line of living larvae, to take advantage of the easy accessibility of the lateral line and the ease of generating genetic mutations in zebrafish. We have isolated a zebrafish mutation, *phoenix* (*pho*) which is deficient specifically in regeneration of the lateral line hair cells. In contrast, regeneration of the tailfin is unaffected. *Phoenix* mutant larvae develop normally and display a morphologically intact and functional lateral line. However, after destroying the hair cells by exposure to neomycin, the regeneration response in *pho* mutants is severely reduced. Repeated cycles of neomycin exposure demonstrated further that the long-term regenerative capacity of the supporting cells was compromised. We show that the mitotic rate in the supporting cells is decreased and can account for the reduction in the number of newly formed hair cells in the regenerating *pho* mutant. The retroviral integration linked to the phenotype is in a novel gene with no known homologs, defining a new class of proteins with a hair cell regeneration-specific function.

#### **562 Identification of Essential Pathways for Hair Cell Regeneration**

**Sang Goo Lee<sup>1</sup>**, Mingqian Huang<sup>1</sup>, Jerema Malicki<sup>2</sup>, Douglas Cotanche<sup>3</sup>, Zheng-Yi Chen<sup>1</sup>

<sup>1</sup>Neurology Service, Massachusetts General Hospital and Harvard Medical School, <sup>2</sup>Department of Ophthalmology, Massachusetts Eye & Ear Infirmary, <sup>3</sup>Boston Children's Hospital, Harvard Medical School

Hair cells (HC) in lower vertebrate inner ear can regenerate, yet the genes and pathways key to the regeneration are virtually unknown. To identify the essential genes and pathways, we used microarray to study expression profiles of regenerating chick inner ear (basilar papilla) after gentamicin induced HC death. We showed that the proliferation pathway is the most prominently upregulated whereas pathways involved in cell-to-cell contact are the most severely downregulated during chick HC regeneration. *In Situ* hybridization confirmed the general conclusion.

To establish functional roles of the genes and pathways identified, we used zebrafish model where lateral line neuromast hair cells can be rapidly regenerated after damage. We showed that the same pathways are altered in zebrafish after HC damage by neomycin, demonstrating conserved mechanisms underlying zebrafish and chick HC

regeneration. We studied in detail the pathways involved in Fgf and c-Myc, both of which have been implicated in regeneration of other tissues.

Small chemical inhibitors of the Fgf pathway and c-Myc significantly suppressed zebrafish neuromast HC regeneration, and the inhibition is dose-dependent and reversible. to further demonstrate the essential roles of the Fgf pathway in HC regeneration, we studied a heat-shock inducible dominant-negative Fgf zebrafish model in which the Fgf pathway is genetically blocked by heat-shock. Upon block of the Fgf pathway by heat shock, neuromast HC regeneration was severely impaired (~70%), confirming the essential role of the Fgf pathway. We showed that one of the mechanisms involved in suppression of regeneration is inhibition of cell-cycle re-entry. Suppression of HC regeneration is pathway specific, as no effect was observed with control inhibitors.

We have identified essential pathways in HC regeneration, and established a platform by which other pathways can be efficiently studied. Some of the pathways may be important in mammalian HC regeneration.

### **563 Comparative Analysis Between Auditory Stem Cells Isolated From Human and Mouse Fetal Cochleae: the Search for 'Auditory Stemness'**

Marta Milo<sup>1</sup>, Amanda L. Naylor<sup>1</sup>, Objoon Trachoo<sup>1</sup>, Wei Chen<sup>1</sup>, Nopporn Jongkamoniwat<sup>1</sup>, **Marcelo N. Rivolta<sup>1</sup>**

<sup>1</sup>Centre for Stem Cell Biology and Department of Biomedical Sciences, University of Sheffield

Our laboratory has recently isolated populations of fetal auditory stem cells from the human cochlea (hFASCs). Besides their potential therapeutic applications, they are a useful model to study the molecular events involved in auditory cell differentiation in humans. Work on embryonic stem cells has highlighted basic differences in the biology of human stem cells when compared to those from other species. to explore the degree of homology between human and mouse FASCs we have established two lines from the mouse embryonic cochlea from an equivalent stage of development to that employed for the isolation of the human counterpart and using exactly the same protocol for derivation. Human and mouse lines shared similar markers (SOX2, PAX2 and GATA3) and responded to the same protocols employed to induce neuronal and hair cell differentiation. However, differences were detected when their transcriptomes were analysed by oligonucleotide microarrays. From a total of more than 21,500 genes represented in both human and mouse arrays, about 89 (0.4%) were upregulated in hFASCs while 262 (1.2%) were primarily expressed by the mFASCs, when compared using a stringent filtering system setting a 4-fold change threshold. to search for common expression, human and mouse fibroblast genes were subtracted in silico from hFASCs and mFASC. After the subtraction, we produced a subset list that included 1437 genes that shared gene symbols and title. We calculated the fold change (hFASC vs mFASC) and selected genes that were in the range of  $-1 < FC < 1$ . in doing so, 590 candidates were

selected from which 135 have a high absolute expression ( $\log_2 > 4$ ).

These genes shared by auditory stem cells from both species are likely to be highly relevant for stem cell behavior in the inner ear. On the other hand, the 351 differentially expressed genes shows the differences between species and highlights the importance of studying events in the appropriate background.

### **564 Differences and Similarities On the Roles of Rbl1 and Rbl2 in the organ of Corti**

**Sonia M. S. Rocha-Sanchez<sup>1</sup>**, Joseph M. Miller,<sup>1</sup> Erin E. Levesque<sup>1</sup>, Andrew P. Deaver<sup>1</sup>

<sup>1</sup>Creighton University, Omaha, NE 68178 USA

in vivo studies of the pocket proteins (pRBs) Rbl1 (p107) and Rbl2 (p130) function have revealed extensive overlap with one another and with Rb1. in addition, analysis of mice deficient in these proteins (KO) show that individual members of this family harbor distinct functions that are, presently, poorly understood. Rb1 is known to play an essential role in HCs and SCs cell cycle and survival. However, nothing is known on the remaining pRBs. Wild type and KO mice lacking Rbl1 and Rbl2 proteins have been analyzed for the pattern of expression of the pocket proteins, as well as the inner ear phenotype in the KO mice. Unlike RB1, KO mice for either p107 or p130 are viable. Microarray analysis suggests Rb1 and Rbl1 as the predominant pocket proteins in the post-mitotic cells of the OC; whereas Rbl2 levels seem to be lower. *In Situ* hybridization and immunohistochemistry showed that all three pRBs have overlapping expression early in the ear development. However from E18 onwards, differences were found, with Rb1 and Rbl1 transcript and protein being observed in the neurons and HCs, while Rbl2 expression is mainly detected in the SCs. Both p107<sup>-/-</sup> and p130<sup>-/-</sup> animals show abnormal innervation pattern and variation in the number of OHCs and SCs, which is more conspicuous in the apical and middle turns, but not in the basal turn of the cochlea. Overall four rows of OHCs are observed in p107<sup>-/-</sup> mice, while six rows of these cells are counted in p130<sup>-/-</sup> animals. Additionally, p107, but not p130, seems to affect the cytoarchitecture of the OC, as hypothesized from the presence of supernumerary SOX2 positive cells in the inner and outer pillar cells region, as well as in the tunnel of Corti. These results highlight some of the differences and similarities on the role of the pocket proteins in the inner ear and open another potential venue for their utilization on restoration of lost HCs.

This study was supported in part by NIH/COBRE/NCRR P20 RR018788 and a faculty development grant from HFF.

## **565 Prospective Identification and Purification of Cochlear Side Population Stem/Progenitor Cells**

Etienne Savary<sup>1</sup>, Jean Philippe Hugnot<sup>2</sup>, Christian Chabbert<sup>2</sup>, Alain Uziel<sup>3</sup>, **Azel Zine**<sup>1</sup>

<sup>1</sup>*Institute for Research in Biotherapy, Montpellier, France,*

<sup>2</sup>*Institute of Neuroscience, Montpellier, France,* <sup>3</sup>*Service ORL, CHU Gui de Chauliac, 34295 Montpellier, France*

In mammals, permanence of hearing loss is due mostly to the inability of the cochlea to replace lost auditory hair cells (HCs). Generation of new HCs from a renewable source of progenitor cells is a principal requirement for developing a restorative cell therapy within damaged auditory sensory epithelium. a subset of stem cells, termed 'side population cells' (SP) has been identified in several tissues of mammals. the ATP-binding cassette transporter Abcg2/Bcrp1 contributes to the specification of the SP cell phenotype and is proposed as a universal marker for stem/progenitor cells. Here, we demonstrate that Abcg2 transporter is expressed along with two other stem/progenitor cell markers (i.e. Nestin and Musashi1) in distinct and overlapping domains by the supporting cells within the postnatal cochlea.

We have developed and describe a FACS technique that enables the purification of a discrete subpopulation of SP-supporting cells from early postnatal mouse cochleae based on their ability to exclude Hoechst dye.

These FACS purified SP-cells can divide and express stem cell markers such as Abcg2 (a determinant of the SP-cell phenotype) and Musashi1 (a neural stem cell marker). These markers identify cells that divide and then differentiate expressing markers for inner ear HCs (e.g. atoh-1) and supporting cells (e.g. p27Kip1). These results demonstrate that isolated and purified cochlear SP-cells are capable of differentiating into HCs *In Vitro*. This finding implies a possible use for such a purified population of SP-stem/progenitor cells, e. g. a source for the replacement of lost HCs within a damaged organ of Corti.

## **566 Epithelial Transitions Appear to Regulate Supporting Cell Proliferation and Can Be Used to Produce Bona Fide Hair Cells Entirely *In Vitro***

Zhengqing Hu<sup>1</sup>, Jared Christophel<sup>1</sup>, Joseph Burns<sup>1</sup>, Maria Sol Collado<sup>1</sup>, Christopher Magnus<sup>1</sup>, **Jeffrey Corwin**<sup>1</sup>

<sup>1</sup>*University of Virginia*

Sensory hair cell loss contributes to often permanent hearing and balance deficits in humans and other mammals, but non-mammals can regenerate lost hair cells when supporting cells return to the cell cycle and produce progeny that can differentiate as supporting cells and replacement hair cells. Here we will describe investigations of developmental changes in the cytoskeletons and cell-cell junctions of vestibular supporting cells that restrict cellular shape change, limit proliferation, and appear to leave mammals vulnerable to permanent hair cell deficits. We will then relate those findings to new methods that have allowed us to culture avian inner ear cells for months, so that they can be frozen, thawed, expanded to large numbers in flasks, and

used to make substantial numbers of hair cells while entirely *In Vitro*. At any point from passage 6 up to at least passage 23, these cultures can be induced to undergo a mesenchymal-to-epithelial transition that reliably yields new polarized sensory epithelia that develop supporting cells and numerous hair cells, which are crowned by hair bundles comprised of a single kinocilium and an asymmetric array of stereocilia. These hair cells exhibit rapid permeance to FM1-43 and are the only cells in those epithelia that do so. Since a vial of these frozen cells can now provide the capacity to produce bona fide hair cells completely *In Vitro* these results may contribute to accelerated research on hair cells and open new approaches to the biology of hair cells and inner ear disorders, while contributing to a mechanistic understanding of the capacities and limitations that influence regeneration in the hair cell epithelia of mammals and non-mammals.

(Supported by R01-DC00200 and R01- DC006182 from the NIDCD, NIH)

## **567 Regulation of Supporting Cell Proliferation in the Mouse Cochlea**

**Patricia White**<sup>1</sup>, Andy Groves<sup>1</sup>, Neil Segil<sup>1</sup>

<sup>1</sup>*House Ear Institute*

in the normal mouse cochlea, sensory hair cells and their adjacent supporting cells exit mitosis during fetal development and remain postmitotic for the lifetime of the animal. If excessive noise exposure or ototoxic drugs kill the sensory hair cells, the surviving supporting cells do not divide or regenerate the tissue, resulting in permanent deafness. Non-mammalian vertebrates, in contrast, do regenerate lost sensory hair cells through a proliferative mechanism. We have previously shown that purified neonatal, supporting cells are able to reenter the cell cycle and differentiate into sensory hair cells in an *In Vitro* system. While some capacity to transdifferentiate may persist, the capacity to reenter the cell cycle diminishes rapidly during the first two postnatal weeks. Purified neonatal supporting cells readily re-enter the cell cycle *In Vitro*, but purified juvenile supporting cells do not, at least in part because they are unable to down-regulate the cyclin-dependent kinase inhibitor Cdkn1b (p27Kip1).

in this report we investigate the signals that positively regulate the proliferation of purified supporting cells *In Vitro*. Following dissociation, purification, and plating without the addition of a feeder layer, 20 -30% of neonatal supporting cells re-enter the cell cycle within 24 hours. in contrast, although there are similar levels of survival, less than 8% of juvenile supporting cells reenter the cell cycle.

Unlike juvenile supporting cells, neonatal supporting cells express the EGF-receptor, and this correlates with a significant reduction in neonatal supporting cell cycle reentry if EGF is not added to the cultures. in contrast, juvenile cultures are unaffected by the presence or absence of EGF. We use specific inhibitors to second messengers downstream from the EGFR to begin to identify the signaling pathway through which EGF may be acting in neonatal supporting cells.

## **568 Ionic Gradient Mediated Cultures of the Adult Avian Sensory Epithelium *In Vitro***

**Nathaniel Spencer<sup>1</sup>**, Catherine Klapperich<sup>1</sup>, Douglas Cotanche<sup>2</sup>

<sup>1</sup>*Boston University*, <sup>2</sup>*Children's Hospital of Boston*

Hair cell regeneration occurs in the adult avian sensory epithelium *in vivo*, predominantly between 72h and 144h after the onset of a noise or drug insult. Hair cells are situated between a potassium-rich endolymph to the apex and a sodium-rich perilymph to the base. Many papers have demonstrated that artificial perilymph (AP)-based culture systems of the avian adult sensory epithelium lose their effectiveness by 72h. We hypothesize that hair cell survival will be prolonged by culturing the organ in the presence of artificial endolymph (AE) at the apex of hair cells and AP at the base of supporting cells.

To test this hypothesis, we develop a dual chamber culture system for the adult avian sensory epithelium. 6 well Transwell chamber inserts are affixed to Zeonex plates containing a 500  $\mu$ m by 2 mm rectangular hole, and the cartilaginous plates are glued around the hole using a medical grade cyanoacrylate/industrial grade silicone mixture. 1 mL of phenol red-colored AE is added over the hair cells, and the well is placed over 5 mL of clearly-colored AP. Spectrophotometry was used to assess whether the AE/AP gradient was maintained, or whether it "collapsed". "Anchored" and "floating" in AP or AE controls were conducted. the organs were fixed after 72h and 144h, and the F-actin and nuclear morphologies were assessed at 20x and 40x/3x-zoom magnifications. Hair cell density was counted.

Our data suggest that employing an ionic gradient across the epithelium prolongs the viability and preserves the morphology of adult avian hair cells. in the anchored cultures with AE at the apex of hair cells, broad sheets of hair cells with roundly packed hair cell bundles were obtained. This was not the case for the floating, AP anchored, or collapsed controls. Additionally, hair cell densities were significantly highest ( $p < 0.05$ ) at both the 72h and 144 time points for the cultures in which AE was to the apex. Finally, no drop-off in hair cell density between 72h and 144h was observed in the gradient condition. These techniques might be used to prolong cultures of mammalian adult hair cells, or study hair cell regeneration in birds *In Vitro*.

## **569 Inactivation of Notch Signaling Promotes Non-Mitotic Regeneration in Adult Mouse Utricles**

**Vincent Lin<sup>1</sup>**, Elizabeth Oesterle<sup>1</sup>, Jennifer Stone<sup>1</sup>

<sup>1</sup>*Virginia Merrill Bloedel Hearing Research Center, University of Washington*

Adult mammals have a limited capacity for hair cell regeneration in the utricular macula. However, findings by Forge et al. suggest new hair cells are formed in the adult guinea pig utricle via non-mitotic regeneration after *In Vivo* drug damage. Here, we explore the capacity for the adult mouse utricle to undergo hair cell regeneration after *In Vitro* damage. Using organ cultures, we examined whether inhibition of signaling through the Notch receptor

promotes non-mitotic regeneration, which entails direct transdifferentiation of supporting cells into hair cells without mitosis. Adult mouse utricles were treated for 1 day with 1 mM Neomycin, which triggers hair cell death, then for 4 days with 50  $\mu$ M DAPT, which blocks Notch signaling by preventing receptor cleavage. Controls were treated with vehicle only. Immunolabeling revealed significant upregulation of the early hair cell marker Atoh1 in supporting cell nuclei in DAPT-treated utricles but not in vehicle controls. When maintained for two additional days in culture, DAPT-treated utricles showed increased numbers of Atoh1-positive nuclei and co-labeling of Atoh1-positive cells with a later hair cell marker, Myosin VIIa. Atoh1/Myosin VIIa-positive cells had morphologies similar to developing hair cells. in DAPT-treated cultures, Atoh1 expression was significantly downregulated by 8 days *In Vitro*. Cumulative labeling with the proliferation marker, BrdU, showed supporting cell mitosis was rare in DAPT-treated utricles. in vehicle controls, Atoh1-positive nuclei were seldom seen, and supporting cell division was rare, after damage. These data suggest that inhibition of Notch signaling after hair cell damage in the adult mouse utricle promotes non-mitotic regeneration of hair cells. Current studies are exploring whether Notch inhibition promotes hair cell repair and whether larger hair cell lesions produce similar results.

Supported by NIH DC 03696 (JSS), NIH DC 04661

## **570 Inhibition of Notch Signaling Increases Differentiation of Stem Cells to Hair Cells Through Upregulation of Math1**

**Sang-Jun Jeon<sup>1</sup>**, Masato Fujioka<sup>1</sup>, Albert Edge<sup>1</sup>

<sup>1</sup>*Department of Otolaryngology, Harvard Medical School, Massachusetts Eye and Ear infirmary*

in an attempt to increase the conversion of stem cells to hair cells we tested the effect of inhibiting the Notch pathway on the differentiation of stem cells derived from bone marrow and from the inner ear. Culture of murine bone marrow-derived mesenchymal stem cells (MSC) with an inhibitor of gamma-secretase, followed by medium containing bFGF for 4 days and medium containing neurotrophins but no FGF for 10 days, resulted in a 2 fold increase in Math1 expression as measured by real time RT-PCR. Expression of hair cell markers, myosin VIIa and espin, was found after treatment of MSCs with the gamma-secretase inhibitor, whereas no expression of hair cells markers was seen when the cells were cultured under the same conditions for the same time interval without the gamma-secretase inhibitor.

Treatment of utricular stem cells with the gamma-secretase inhibitor increased Math1 expression 6 fold. When these stem cells were isolated from a mouse with a nuclear GFP reporter under the control of a Math1 regulatory region, an increased number of nGFP-positive cells was found and an increased number of the nGFP-positive cells also expressed myosin VIIa. This increase was prevented by treatment of the stem cells with an siRNA that silenced Math1 but not by treatment with a noncoding siRNA. the expression of hair cells markers after treatment of these progenitors with gamma-secretase

inhibitors suggests that they might be used for increasing stem cell conversion to hair cells *in vivo*.

Supported by NIDCD grants DC007174 and DC05209

### **[571] Initiation of Hair Cell Phenotype by Atoh1 Gene Delivery in Cultured Postnatal Mouse organ of Corti**

**Mark Crumling<sup>1</sup>**, Matthew Johnson<sup>1</sup>, R. Keith Duncan<sup>1</sup>, Yehoash Raphael<sup>1</sup>

<sup>1</sup>University of Michigan

Delivery of the pro-hair cell gene, *Atoh1*, to the organ of Corti of rats (*in vitro*) and guinea pigs (*in vivo*) has previously been shown to induce the formation of new hair cells. In order to take advantage of genetic techniques in exploring and enhancing mammalian hair cell regeneration, it is useful to determine if the differentiated mouse auditory epithelium also responds to exogenous *Atoh1* with the production of new hair cells. For this purpose, we cultured postnatal mouse organ of Corti explants and treated them with an adenoviral vector containing or lacking the *Atoh1* gene. Each vector carried *GFP* as a reporter gene. Following culture, explants were fixed, processed for immunohistochemical detection of the hair cell marker, myosin VIIa, and stained with fluorescently-tagged phalloidin. Observation of GFP fluorescence revealed that the adenoviral vectors transduced various cell types throughout the explants, including supporting cells and hair cells, as has been published previously for mouse explants. GFP-positive cells that coexpressed myosin VIIa were found both lateral and medial to the normal location of hair cells. Most of these cells were located toward the lateral edges of the explants and appeared to be fibroblasts, based on their spindle shape. Visualization of f-actin with fluorescently-tagged phalloidin indicated that some of these cells may have had rudimentary hair bundles. The observations were comparable in cultures treated with 1mM gentamicin to kill hair cells before treatment with virus. Similar myosin VIIa/GFP-positive cells in ectopic locations were lacking in cultures treated with virus containing only *GFP*. The results suggest that *Atoh1* can initiate hair cell production in the postnatal mouse organ of Corti and that cochlear fibroblasts may be of potential use in studies of hair cell regeneration.

Supported by GenVec and by NIH grants F32-DC008050, R01-DC01634, and P30-DC05188.

### **[572] Expression of Pou3f3/ Brn1 and it's Possible Epigenetic Regulation in the Developing Mammalian Cochlea**

**Hideki Mutai<sup>1</sup>**, Masato Fujii<sup>1</sup>, Tatsuo Matsunaga<sup>1</sup>

<sup>1</sup>National Institute of Sensory organs, National Tokyo Medical Center

Rodents start hearing at approximately 2 weeks after birth, despite the fact that all the hair cells are already generated before birth. Functional differentiation and/or maturation of the cells in the cochlea are considered to cause the delay. Epigenetic regulation of genes typically marked by cytosine methylation of the genomic DNA has important

roles in cell type-specific gene expression as well as imprinting and early embryogenesis. We attempted to see if epigenetic regulation is also involved during postnatal development of auditory epithelium.

Genomic DNA of cochlear epithelia from inbred rats at postnatal day 1 (P1), P7, and P14 were subjected to amplification of inter-methylated sites (AIMS)-PCR (2002 Nuc Acid Res 30: e28) modified by digesting DNA with methylation-sensitive restriction enzyme HpaII. One of the PCR products specifically amplified at P1 was identified as a 3'-flanking region of a transcription factor Pou3f3/Brn1. Bisulfite sequencing revealed that the genomic DNA of Pou3f3 was slightly methylated during development, raising the possibility that transcription of Pou3f3 in the small portion of the epithelium is epigenetically repressed during postnatal development.

Immunohistochemical study revealed that Pou3f3 was expressed in the supporting cells but not in the hair cells, Hensen's cells, and Claudius cells. Pou3f3 was also expressed in the mesenchymal cells, such as spiral ligament fibrocytes and tympanic covering layer. Distribution of the molecule did not match those of other POU family genes, Pou3f4/Brn4 and Pou4f3/Brn3.1. Pou3f3 deficient mice did not exhibit any morphological abnormalities of the cochlea. There was no difference in the activities of otosphere formation from the auditory epithelia or differentiation to hair cells and neuronal cells by the absence of the gene. Pou3f3 may play a role in functional differentiation of supporting cells and mesenchymal cells in the cochlea, rather than developmental morphogenesis.

### **[573] Expression of the IGFII Mrna Binding Protein (Imp2) in the Developing Mouse Inner Ear**

**Androulla Economou<sup>1</sup>**, Mark Maconochie<sup>1</sup>

<sup>1</sup>University of Sussex

Signalling via the insulin-like growth factors (IGFs) is important for normal inner ear development. The two major IGF ligands, IGF1 and IGFII signal through the IGF1 receptor. IGF1 is required for survival, proliferation and differentiation of otic neuroblasts, and both IGF1 and IGFII have been shown to stimulate proliferation of otic epithelia in culture. The functional requirements for IGF signalling *In Vivo* in the inner ear, were demonstrated following reports of sensorineural deafness in a patient carrying an IGF1 mutation. Furthermore, IGF1 mutant mice demonstrate defects in the normal development of cochlear innervation. However, how IGF activity might be controlled in the inner ear is unknown.

Previously we isolated the Imp2 gene from an otic vesicle subtractive screen against adult liver cDNA. Imp2 is a member of a highly conserved group of three related proteins (Imp1-3), which are able to bind the IGFII mRNA. Imp2 binding may control translation and/or localise the IGFII mRNA, thereby offering a regulatory mechanism for controlling the availability of the ligand for IGF signal transduction. In order to investigate the involvement of Imp2 in inner ear development, we are first characterising the spatial and temporal pattern of Imp2 expression in the inner ear during mouse embryogenesis.

## **574 Dynamic Expression of Rdh10 During Inner Ear Development**

Raymond Romand<sup>1</sup>, Angela B. Thompson<sup>2</sup>, Takako Kondo<sup>2</sup>, Pascal Dolle<sup>1</sup>, Eri Hashino<sup>2</sup>

<sup>1</sup>IGBMC, <sup>2</sup>Indiana University School of Medicine

Retinoic acid (RA), a non-peptidic signalling molecule derived from vitamin A, is synthesized from maternal retinol by two oxidative reactions involving alcohol/retinol dehydrogenases (ADH/RDHs) and retinaldehyde dehydrogenases (RALDHs). the activity of RALDHs is known to be crucial for RA synthesis; however, a recent study revealed that retinol dehydrogenase 10 (RDH10) represents a new limiting factor in this synthesis. to elucidate the role for this novel enzyme in RA metabolism during mouse inner ear development, we investigated the spatiotemporal expression pattern of the Rdh10 gene using qRT-PCR and *In Situ* hybridization. Rdh10 expression was detectable as early as E9.5, reached its peak at E10.5, remained at high levels up to E14.5 and was down-regulated by E18.5. Consistent with this temporal expression pattern, a high level of Rdh10 transcripts was observed at E9.5 in the rostro-medial region of the otocyst. by E12.5, strong Rdh10 expression was detected in the endolymphatic sac and the endolymphatic duct, while no signal was observed in the sensory epithelia. At E14.5-18.5, the two components of the endolymphatic system remained distinctively labelled, whereas Rdh10 transcripts were also observed in the presumptive stria vascularis in the cochlea. Together, the early onset and high levels of Rdh10 expression in the embryonic ear suggest an essential role for this enzyme in RA synthesis in this organ. in addition, the highest expression domain of Rdh10 in the endolymphatic system, a structure involved in fluid metabolism and secretion, suggests that RA may be circulated in the ear structure during embryonic development through the endolymphatic system. the Rdh10 expression domain overlaps with the Raldh2 expression domain, which is consistent with a role of this enzyme in generating region-specific pools of retinaldehyde that is subsequently used by various RALDHs to generate RA.

## **575 Function of the Cyclin-Dependent Kinase Inhibitor P27kip1 in the Developing Mouse Utricle**

Tao Kwan<sup>1</sup>, andy Groves<sup>1</sup>, Neil Segil<sup>1</sup>

<sup>1</sup>House Ear Institute

We have examined the function of cyclin-dependent kinase inhibitor p27kip1 in the regulation of cell cycle exit and hair cell differentiation in the developing vestibular system. in the organ of Corti, cell cycle exit is separated temporally from differentiation. Conversely, in the developing mouse utricular macula, cell cycle exit and differentiation overlap both spatially and temporally. Previous studies have shown that p27kip1 is expressed when sensory progenitor cells exit the cell cycle in the developing cochlea and is required for regulating the normal timing of cell cycle exit in the organ of Corti (Chen and Segil, 1999). p27kip1 is also expressed in the utricular

macula. However, the expression pattern of p27kip1 differs from that of the cochlea during development. Similar to that of organ of Corti, supernumerary hair cells (32%,  $p<0.0001$ ) were observed in the utricle of p27kip1 knock out mouse, while reduced hair cell numbers (28%,  $p<0.0001$ ) were seen in mice that over-express p27kip1. Compared to the wildtype utricular maculae, the timing of cell cycle exit is prolonged in the p27kip1 knock out mice and shortened in p27kip1 over-expressing mice. Unlike the cochlea, the timing and expression of p27kip1 is closely coupled with differentiation. This reflects the contrasting patterns of hair cell and supporting cell differentiation in cochlea and utricle. Taken together, our results indicate that as in the organ of Corti, p27kip1 is involved in coordinating progenitor cell cycle exit with sensory patterning in the utricular macula. However, differences in the mechanisms governing differentiation and patterning in utricle contrast with those in the cochlea. These are paralleled by changes in p27kip1 expression and cell cycle exit that regulate the generation of sensory precursors.

## **576 Generation and Characterization of Otopetrin 1 Knockout Mice**

Euysoo Kim<sup>1</sup>, Yunxia Lundberg<sup>2</sup>, Felipe Salles<sup>3</sup>, Bechara Kachar<sup>3</sup>, Mark Warchol<sup>1</sup>, David ornitz<sup>1</sup>

<sup>1</sup>Washington University, <sup>2</sup>Boys Town National Research Hospital, <sup>3</sup>NIH

Otoconia are dense calcium carbonate particles that are required for sensation of gravity. Otopetrin 1 (OTOP1) is a multitransmembrane domain protein that is required for the development of otoconia. Two mouse mutants of Otop1, *tit* and *mlh*, show a severe balance defect due to nonsyndromic otoconial agenesis. Recently, overexpression of Otop1 was shown to have a profound effect on cellular calcium regulation, suggesting a direct role of OTOP1 in the calcification of otoconial particles. to understand whether missense mutations in *tit* and *mlh* are functionally equivalent to a null allele, we generated a knockout for Otop1. the Otop1 gene was targeted by the insertion of a b-galactosidase gene in a way to inactivate all alternative splice forms. the homozygous Otop1 knockout mice lacked otoconia, and showed no major histological abnormalities in the sensory epithelia. Analysis of the b-gal expression pattern revealed that Otop1 is expressed in the supporting (precursor) and hair cells of the maculae as early as embryonic day E13.5 and a positive lacZ signal was observed as late as P30. Immunohistochemistry with antibodies against Otop1 showed that the protein is localized to the apical side of supporting cells. Localization of the protein in other cell types is currently being examined. These results indicate that OTOP1 is expressed early enough in the maculae to participate in calcification and growth of otoconia and the persistent expression in adult stages suggests a possible function in the maintenance of otoconia.



## **577 Exploring the Roles of DRAGON**

### **(Rgmb), a BMP Co-Receptor, in the Ear**

Cynthia Hsu<sup>1</sup>, Joshua Murtie<sup>1</sup>, Hisashi Tokano<sup>2</sup>, Tarek Samad<sup>3</sup>, Clifford Woolf<sup>3</sup>, Silvia Arber<sup>4</sup>, Albert Edge<sup>2</sup>, Gabriel Corfas<sup>1</sup>

<sup>1</sup>Harvard Medical School / Childrens' Hospital Boston,

<sup>2</sup>Harvard Medical School / MEEI, <sup>3</sup>Harvard Medical School / MGH, <sup>4</sup>Biozentrum, University of Basel

Defective bone development or remodeling is a significant contributor to congenital conductive hearing loss. Identifying molecules that regulate middle ear bone development should provide insights into the basis of these diseases and potential diagnostic and treatment tools.

We recently found that DRAGON (aka RGMb), a Bone Morphogenetic Protein (BMP) co-receptor, is strongly expressed in the embryonic ear, suggesting that it could play a role in inner ear development. To test the roles of this molecule we studied DRAGON KO mice. At their time of death at P14, DRAGON KO homozygous mice have a distinct thickening of the bulla, indicating that, like other TGF $\beta$  superfamily members, DRAGON may have a role in controlling the precise balance of bone growth and resorption. Interestingly, although middle ears of heterozygotes appeared quite normal morphologically, hearing tests of adult animals performed by measurements of acoustic brainstem responses showed greater variability in threshold ranges compared to their wild type counterparts, indicating that DRAGON hypo-function may result in subtle alterations in hearing.

In addition to its role as a BMP co-receptor, DRAGON binds to neogenin, a receptor expressed on axonal growth cones, and the interaction between DRAGON and neogenin plays a role in axonal guidance in other tissues. To explore whether defective axonal guidance in the ear could contribute to the altered hearing phenotype, we examined the innervation of the cochlea in the DRAGON KO mice. No gross abnormalities in afferent innervation were observed, suggesting that the BMP co-receptor function is the major contributor to the ear phenotype seen in the DRAGON KO mouse.

## **578 Hedgehog Signaling in the Developing Inner Ear**

Dorothy Frenz<sup>1</sup>, Wei Liu<sup>1</sup>, Edward Lee<sup>1</sup>, Alan Shanske<sup>1</sup>

<sup>1</sup>Albert Einstein College of Medicine

Sonic hedgehog (Shh) is a critical regulator of inner ear development. Absence of Shh produces severe inner ear anomalies consistent with congenital deafness and balance disorders. These anomalies include the otic capsule, which is less affected phenotypically than other structures in the inner ear. This observation suggests that removal of Shh may not abolish all hedgehog signaling, i.e. the inner ear may express another hedgehog protein that influences otic capsule development. This study demonstrates that loss of Shh is accompanied by maintenance of hedgehog pathway activity and that this activity is putatively due to Indian hedgehog (Ihh). We show that antisense blockade of Ihh compromises otic capsule chondrogenesis *In Vitro*, while exogenous Ihh

peptide leads to stimulation of the chondrogenic process. Supplementation of Shh-deficient cultures with exogenous Ihh can functionally compensate for Shh and rescue the chondrogenic suppression evoked by diminished Shh. Furthermore, we provide evidence that loss of Ihh function in the developing mouse inner ear produces compromised otic capsule chondrogenic differentiation. Our findings support a role for Ihh in the developing otic capsule, and suggest that disruption in Ihh signaling may contribute to Shh loss-of-function-mediated capsular defects.

## **579 Discovery of FGF-Regulated Genes Involved in Otic Placode Induction**

Lisa Urness<sup>1</sup>, Suzanne Mansour<sup>1</sup>

<sup>1</sup>University of Utah

The inner ear, with its precisely ordered array of sensory, non-sensory and neuronal cell types, is derived almost in its entirety from a small patch of head ectoderm known as the otic placode. Once induced, the placode invaginates to form a vesicle, which subsequently undergoes morphogenesis and cell-type specification generating the elaborate cochlear and vestibular structures. Fibroblast growth factor (FGF) signals originating in periotic tissues are required redundantly to initiate placodogenesis. Studies of mutant mice revealed that FGF signals are required not only for the initial induction of the placode, but also for otic vesicle morphogenesis and cell type differentiation in the organ of Corti. With this myriad of roles, it is not surprising that several human hearing loss syndromes are caused by mutations affecting the FGF signaling pathway, yet we know little about the transcriptional response to FGF signals during any of these developmental stages.

We showed that mice lacking both *Fgf3* and *Fgf10* fail to initiate inner ear development, and that the role of FGF signaling in this case is to specify the appropriate patterns of gene expression within the prospective otic placode. To identify otic placode genes up- or down-regulated in response to inductive FGF3/10 signals, we isolated RNA from the otic placode and a small portion of the overlying neuroectoderm of 4-8 somite-stage *Fgf3*<sup>-/-</sup>/*Fgf10*<sup>-/-</sup> and control embryos. Conventional and gene-trap microarray comparisons of these RNAs will reveal the global transcriptional response to FGF otic inducing signals in mouse embryos. We expect that the target genes will likely be regulated by FGF signals during otic morphogenesis and differentiation as well, and will therefore be excellent candidates for genes that cause or modify human hearing loss. We will present the results of our microarray analyses and preliminary studies of the expression patterns of highly regulated genes. Supported by AHRF, DRF and NIDCD.

### **580 Genomic Analysis of the Function of the Transcription Factor Gata3 During Development of the Mammalian Inner Ear**

Marta Milo<sup>1</sup>, Marcelo Rivolta<sup>2</sup>, Mahesan Niranjan<sup>2</sup>, Matthew Holley<sup>1</sup>

<sup>1</sup>Department of Biomedical Science, University of Sheffield, UK, <sup>2</sup>University of Sheffield

A major challenge in our understanding of development is to elucidate the diverse functions of key regulatory genes. Such functional information can provide critical insights into potential regenerative therapies. the transcription factor Gata3 is crucial for setting up the early signaling events in ear development and haploinsufficiency causes hypoparathyroidism, deafness and renal anomaly syndrome. to explore the function of Gata3 we used microarrays, generating temporal profiles of gene expression during differentiation of conditionally immortal cell lines that model specific cells and stages in auditory development. We applied a novel statistical method to analyse expression profiles and produced an unbiased list of 26 genes clustered to Gata3 in three different auditory neuronal and epithelial cell lines. Seven genes in this list were linked to IGF-signalling, including the serine/threonine kinase Akt2/PKB $\beta$ . Gata3 was co-expressed with Akt2/PKB $\beta$  in all cells and the protein products shared similar expression patterns in vivo. in heterozygous Gata3 null mice the expression of Gata3 was correlated with high levels of activated Akt/PKB in the ear, eye and central nervous system. RNAi of Gata3 *In Vitro* led to some down-regulation of Akt2/PKB $\beta$ , upregulation of Akt1/PKB $\alpha$  and down regulation of the cyclin-dependent kinase inhibitor p27kip1, a known target of Akt activation. It also led to a dramatic change in the localization of both isoforms of Akt/PKB from the nucleus to the cytoplasm. the nuclear to cytoplasmic translocation of Akt/PKB plays a major role in regulating its activity and consequently in the regulation of cellular responses to a range of growth factors, including IGF. It can explain the diverse function of Gata3 in coordinating the behaviour of different epithelial, neural and connective tissues during the early development of the inner ear.

### **581 Expression Patterns of Mirna in the Developing Inner Ear**

Rosalie Sacheli<sup>1</sup>, Laurent Nguyen<sup>1</sup>, Laurence borgs<sup>1</sup>, Renaud Vandenbosch<sup>1</sup>, Morgan Bodson<sup>1</sup>, philippe Lefebvre<sup>1</sup>, **Brigitte Malgrange<sup>1</sup>**

<sup>1</sup>Center for cellular and Molecular Neuroscience, University of Liege

MicroRNAs (miRNAs) are small conserved RNA molecules of 21-22 nucleotides which negatively modulate gene expression, primarily through base pairing to the 3' untranslated region (UTR) of target mRNAs. Although they have been found to regulate developmental and physiological processes in several organs and tissues, their role in the inner ear transcriptome is completely unknown. in this report, we systematically examined, the temporal and spatial expression of three miRNAs (mir-96, mir-182 and mir-183) that are believed to arise from a single precursor RNA, during development and maturation

of the cochlea. Both mir-96, mir-182 and mir-183 were expressed in the developing otic vesicle.

Collectively, the expression of the three miRNA mir-96, mir182 and mir183 is dynamic during cochlea development, particularly during patterning and differentiation of the cochlear structures.

### **582 Transgenic Misexpression of Inner Ear Neurosensory Micrnas in Glial Cell Types in FVB/N Mice**

Michael D. Weston<sup>1</sup>, Marsha L. Pierce<sup>1</sup>, Lane H. Beisel<sup>1</sup>, Garrett A. Soukup<sup>1</sup>

<sup>1</sup>Creighton University

Recent studies have demonstrated that microRNA (miRNA) function is required for normal development of the vertebrate inner ear, and that inner ear "neurosensory miRNAs" (i.e. miR-183, -96, and -182) are highly conserved and expressed among neurosensory organs. Moreover, mutations in miR-96 appear to be responsible for genetic hearing loss in both man and mouse. the coordinated temporospatial expression of neurosensory miRNAs in ganglia and hair cells of the mouse inner ear suggests these regulatory RNAs might enforce neuronal and sensory cell fate/function by repressing glial cell programs. to test this hypothesis, we have generated transgenic (Tg) FVB/N mice that drive ectopic neurosensory miRNA misexpression using the core promoter of glial fibrillary acidic protein (GFAP). of 3 transgenic founder lines, one segregated a severe ataxia phenotype with cataracts. Morphologic and immunohistologic assessments of cerebella from P21 Tg+ and Tg- mice indicate that misexpression of these miRNAs likely affects cerebellar function. in particular, Purkinje cells appear to be affected by misexpression of the neurosensory miRNAs in golgi epithelial cells (Bergmann glia). Quantitative RT-PCR demonstrates a ~35 fold increase in neurosensory miRNAs in Tg+ cerebella compared to those of Tg- littermate controls. Surprisingly, no difference in inner ear expression of the neurosensory miRNAs was observed between Tg+ and Tg- littermates despite reports of GFAP expression in glial supporting cell types. Nonetheless, this *In Vivo* model of neurosensory miRNA misexpression demonstrates the potency of specific mammalian miRNAs and will be used to discover/validate neurosensory miRNA target genes. the elucidation of specific miRNA-regulated cellular pathways that intersect normal ear development and hearing disease etiologies may provide novel avenues for future therapeutic intervention. This work is supported by NIH/NCRR P20RR018788 (GAS) and NIH/NIDCD F32DC008253 (MDW).

### **583 Gfi1-Cre Knock-in Mouse Line: a Tool for Hair Cell-Specific Gene Deletion**

Xiaoling Xie<sup>1</sup>, Min Deng<sup>1</sup>, Lin Gan<sup>1</sup>

<sup>1</sup>University of Rochester

Conventional deletion of developmentally essential genes in mice often results in embryonic and neonatal lethality, thus, preventing the functional study of genes during later embryonic development and in adult. the Cre/loxP

recombination system allows the disruption of genes in a tissue-specific manner to circumvent embryonic and neonatal lethality. Since the inner ear hair cells are not essential for mouse survival, hair cell-specific Cre recombinase deleter mouse strains offer a powerful tool for the study of gene function both in the developing and mature hair cells. Here, we have generated a Gfi1-Cre mouse line by knocking-in Cre coding region sequences into Gfi1 locus and inactivating the endogenous Gfi1. Similar to conventional Gfi1 knockout mice, the heterozygous Gfi1-Cre (Gfi1<sup>cre/+</sup>) mice were viable and displayed no discernible defects. by crossing the Gfi1-Cre line with the R26R-lacZ reporter line, we analyzed the Cre recombination efficiency and specificity *in vivo*. the Cre activity of this Gfi1-Cre line was revealed by lacZ expression and was detectable in both nascent and mature hair cells in the cochlea and vestibule. Interestingly, in contrast to the previously reported Gfi1 expression in the inner ear neurons, we did not detect the expression of lacZ reporter in neurons. Thus, the Gfi1-Cre knock-in mouse line provides a powerful tool for generating hair cell-specific knockout mouse lines to study gene function in the developing inner ear hair cells.

#### **584 Cell-Specific Inducible Gene Recombination in Postnatal Inner Ear Supporting Cells and Glia**

**Maria Gomez-Casati<sup>1</sup>**, Joshua Murtie<sup>1</sup>, Gabriel Corfas<sup>1</sup>

<sup>1</sup>*Children's Hospital Boston. Harvard Medical School*

Recent studies indicate that inner ear supporting cells (SCs) and glia play important roles in inner ear development, function and regeneration after injury, but the molecular mechanisms underlying these processes remain poorly understood. Gene KO or over-expression of candidate molecules could be used to study their roles in the inner ear, but since most molecules play roles at different stages and in many tissues and cell types, having the ability to alter their expression at any given time only in supporting and glial cells would be very useful.

Here we tested the effectiveness and cell-specificity of inducible Cre-mediated gene recombination in the postnatal inner ear. We used mice that express an inducible form of Cre (CreERT) under the transcriptional control of the proteolipid protein (PLP) promoter. PLP encodes for a myelin protein that is also expressed by SCs of the inner ear (Morris et al, 2006). in these mice, CreERT is expressed in all cells in which the PLP promoter is active, but remains inactive until mice are injected with tamoxifen. Only then does Cre move into the nucleus and produces loxP-mediated recombination of the target gene.

To assess the activity of the CreERT protein following tamoxifen treatment, we used the ROSA26 LacZ reporter mouse line, in which the  $\beta$ -galactosidase ( $\beta$ -gal) gene is expressed only after Cre-mediated excision of a LoxP-flanked stop cassette. PLP-CreERT::Rosa26 double transgenic mice were injected with tamoxifen at various ages for different number of days and  $\beta$ -gal expression was then studied by an histochemical reaction. Recombination was detected in Schwann cells, satellite cells in the ganglia and in a specific group of SCs, i.e.

cochlear inner phalangeal cells and SCs surrounding both type I and II hair cells in vestibular maculae. Importantly, signal was undetectable in untreated mice. These results show that PLP-CreERT mice are a powerful tool to dissect gene function in inner ear SCs and glia.

#### **585 Ultrasound-Guided Microinjection Into the Nascent Mouse Otocyst *in Utero***

**Philip Zald<sup>1</sup>**, John Brigande<sup>1</sup>

<sup>1</sup>*Oregon Health & Science University, Oregon Hearing Research Center, Portland, OR 97239*

The inaccessibility of the developing mammalian inner ear *in utero* has hampered efforts to understand the molecular mechanisms underlying morphogenesis and cell fate specification. Our goal is to define experimental embryological approaches to gain access to the mouse inner ear *in utero* and reliably manipulate gene expression. Bioactive reagents can be presented to otic epithelial progenitors by fiber-optic-guided transuterine microinjection into the embryonic day 11.5 (E11.5) mouse otocyst. the maternally-derived decidual tissues prevent bright field illumination of anatomical landmarks that enable accurate targeting to the otocyst earlier than E11.5. the current study validates the use of high frequency ultrasonic imaging to visualize the nascent mouse otocyst. Mouse embryos were imaged in the transverse plane *in utero* at E9.5 (n=46) and E10.5 (n=56) using the VEVO660 Ultrasound Biomicroscope and a 40MHz transducer. the otocyst presented as an intensely echogenic epithelial rim delimiting the fluid-filled vesicle. the average maximal otocyst diameter was  $0.14 \pm 0.04$  mm ( $\pm$ SD; n=83) at E9.5 and  $0.30 \pm 0.06$  mm (n=101) at E10.5. Embryos were harvested immediately after imaging and somite pairs were counted as an independent developmental measure of embryonic age. Otocyst diameter loosely correlated with somite number ( $R^2=0.74$ ) as there was some overlap in diameter measures at the two ages. the nominal resolution of the 40MHz scan head likely contributes to this variability. We show that ultrasound biomicroscopy is a rapid and reproducible method for visualization of the early mouse otocyst *in utero* and provides an ideal image for targeting reagents to the developing mouse inner ear by microinjection. Our initial efforts to transfect otic epithelial progenitors with bioactive reagents at early otocyst stages will be discussed.

Supported by the NIDCD-NIH and the McKnight Fund for Neuroscience

#### **586 Analysis of Multicolor Neuronal Profiling Using Novel Lipophilic Dyes**

**Heather Jensen-Smith<sup>1</sup>**, Brian Grey<sup>2</sup>, Katharine Muirhead<sup>3</sup>, Betsy Ohlsson-Wilhelm<sup>4</sup>, Bernd Fritzsche<sup>1</sup>

<sup>1</sup>*Creighton University*, <sup>2</sup>*Molecular Targeting Technologies, Inc.*, <sup>3</sup>*SciGro, Inc./Midwest office*, <sup>4</sup>*SciGro, Inc./Northeast office*

Dissecting development of neuronal connections is critical for understanding neuronal function in both normal and diseased states. Although progress is being made utilizing various mutants and/or genetic constructs expressing fluorescent proteins like GFP, characterization of the

development and final location of neuronal pathways remains a difficult task. Furthermore, antibodies can not specifically label the vast majority of developing neurons in mutant and wildtype animals. Fluorescent lipophilic dyes have proven useful for overcoming such difficulties. These dyes diffuse laterally along nerve cell membranes in fixed preparations, allowing tracing of the position of a given neuron within the neuronal network in murine mutants fixed at various stages of development. Until recently, however, most evaluations have been limited to one or at most two color analyses. Here we describe a standardized test system developed to allow comparison of candidate dyes and its use to evaluate a series of 488 nm-excited green-emitting lipophilic dyes. the best of these, NV Jade, has spectral properties well matched to NV Red and NV Maroon, better solubility in DMF than DiO or DiA, improved thermostability compared with NV Emerald, and the ability to fill neuronal profiles at rates of 1 mm per day for periods of at least 5 days. Use of NV Jade in combination with NV Red and NV Maroon substantially improves the efficiency of connectional analysis in complex mutants and transgenic models where limited numbers of specimens are available. We here show how triple labeling can be used to analyze developing inner ear neuronal connections in wildtype and mutant mice.

### **[587] MR Microscopy in Studying the Development of the Embryonic Chick Inner Ear**

**Jerod Rasmussen<sup>1</sup>, Vinod Kaimal<sup>1</sup>, Jaye Ward<sup>1</sup>, Ronald Pratt<sup>1</sup>, Scott Holland<sup>1</sup>, Daniel Choo<sup>1</sup>**

<sup>1</sup>*Cincinnati Children's Hospital*

Advancing our understanding of inner ear morphogenesis is essential to our comprehension of and strategies for managing congenital hearing loss. This study investigates the feasibility of visualizing development through embryological time points using MR microscopy as a non-invasive and non-terminal imaging modality.

*in ovo* proton images were acquired on a Bruker 7T BioSpec 30/70 scanner using an in-house designed single loop coil, 44 mm in diameter. 3D spin echo (RARE) and steady state (FISP) imaging sequences were utilized in order to investigate the spatial and temporal resolution limits respectively. T2-weighted RARE imaging consisted of TR/TE=1500/100 ms and a nearly isotropic resolution of 100 microns. T2/T1-weighted FISP protocols consisted of TR/TE=4/2 ms and an isotropic resolution of 200 microns. the high spatial resolution images were obtained using deceased *in ovo* embryos at varying embryonic stages (E4,7,10,14-18,20,21) to simulate a longitudinal study. a single embryo (E18) was imaged to examine range of motion at high temporal resolution *in vivo*.

Microstructures become resolvable as early as E7 using RARE imaging. As maturation progresses, many identifiable inner ear structures are clearly visible, including the ampulla, sacculus, lagenae, cochlear duct, and the lateral, posterior and superior semicircular canals. *In Vivo* FISP imaging, though more susceptible to motion artifact and reduced spatial resolution, was able to resolve the inner ear structures faster than the rate of gross

motion. the feasibility of performing a longitudinal study of inner ear development in the chick embryo has been demonstrated. RARE imaging is not optimal for *In Vivo* imaging due to motion sensitivity during the long TRs necessary. FISP imaging is adequate for *In Vivo* studies, but will likely benefit from motion reduction via sedation or other means.

### **[588] Estimating Auditory Frequency Range of Birds Based On Transducer Channel Re-Closure**

**Bora Sul<sup>1</sup>, Kuni Iwasa<sup>1</sup>**

<sup>1</sup>*Section on Biophysics/NIDCD/NIH*

Sensitivity of the ear depends on a reverse transduction process that modulates mechanical stimulation. Here, we attempt to explain the auditory range of birds based on hair bundle motility by making three assumptions: [1] Fast adaptation of the bundles is based on channel re-closure (twitch) due to Ca entry during channel opening. [2] the energy generated by twitch must be enough to counteract viscous loss in the gap between the tectorial membrane and the papilla. [3] the mechanical stimulation is a continuous sinusoid with infinitesimal amplitude.

With these assumptions, the limiting frequency is expressed by  $f_{lim} = \beta N F_g^2 \alpha / (2\pi^2 \gamma)$ . Here  $\beta$  is Boltzmann factor, N number of tip links,  $F_g$  gating force per channel, and  $\alpha$  phase factor determined by channel kinetics. Damping coefficient  $\gamma$  is proportional to the area per hair cell and inversely to the gap, approximated by the hair bundle height.

Transition rates of the channel are determined to maximize  $\alpha$  in a 4-state model. Values for number of tip links, bundle height, and hair cell area are taken from literature (Tilney & Tilney, 1988; Manley et al., 1996).

If we use 40fN for gating force  $F_g$  for cultured chicken hair cells (Zhao et al.1996), the limiting frequency is ~ 200Hz. However this value is less than 1/10 of those in other animals, including mice (van Netten & Kros, 2000), bullfrogs (Howard & Hudspeth, 1988; Le Goff et al., 2005), and turtles (Ricci et al., 2002). If we use these values, the limiting frequency increases more than 100-fold and exceeds the auditory range of birds (mostly up to ~ 4 kHz).

Our results show that gating force is a key factor in determining the auditory frequency range. the value available for the chicken is singular. It is unclear whether or not cultured hair cells have less gating force than hair cells *in vivo*. If this value is indeed valid *in vivo*, the avian hair cells may need a unique mechanism for fast adaptation.

### **[589] On the No-Slip Boundary Condition in the Subtectorial Space**

**Arun Palghat Udayashankar<sup>1</sup>, Anthony W. Gummer<sup>1</sup>**

<sup>1</sup>*University Tübingen, Section Physiological Acoustics and Communication*

Recent studies have suggested that slip at a fluid-solid interface could have some significance for fluid flow in confined biological systems (Craig et al., Phys. Rev. Lett. 2001). This necessitated an investigation into the

boundary condition assumed at the interface of the tectorial membrane (TM) and endolymph in the context of an analytical model for fluid flow in the subreticular space. Reliable experiments at the interface of water and phospholipid bilayers have pegged the slip length ( $b$ ) in these systems at a few tens of nm. When slip lengths of this magnitude were plugged into the expressions for radial velocity in the subreticular space, it was found that the velocity obtained assuming the slip boundary condition (s.v.) deviated from the velocity obtained assuming the no-slip boundary condition (n.s.v.) only very close to the boundary ( $< 1 \mu\text{m}$  from the TM). Furthermore, in the third turn of the cochlea ( $\sim 800 \text{ Hz}$ ), near the supposed channel locations (tops of the shortest and middle stereocilia), the deviation of the magnitude of n.s.v./s.v. from unity was  $< 3\%$  for  $b=100 \text{ nm}$ . This deviation increases with decrease in separation between the reticular lamina and the TM and increase in frequency (up to  $5\%$  at  $3 \text{ kHz}$  in the first turn). Slip lengths greater than  $100 \text{ nm}$  have not been reported in ideal solutions. If the endolymph is thought of as an ideal solution, its physical properties (relevant for slip) are unlikely to give rise to higher slip lengths. It is well known that  $b$  matters only if it is comparable to the length scale over which velocity changes. Our analysis quantifies this statement in the context of fluid flow in the subreticular space.

In conclusion, although there might be some fluid slip at the interface of the TM and endolymph, it is not large enough to alter significantly the physical picture obtained using a no-slip boundary condition.

Supported by DFG Gu 194/7-1.

## **[590] A Distributed Impedance Model of Tectorial Membrane Traveling Waves**

**A.J. Aranyosi<sup>1</sup>, Roozbeh Ghaffari<sup>1</sup>, Dennis Freeman<sup>1</sup>**

<sup>1</sup>MIT

Radial displacements applied to one end of an isolated tectorial membrane (TM) launch traveling waves on the tissue (see accompanying poster). We have developed a transmission-line model of the TM that accounts for these waves. In the model, the TM is divided into a series of masses connected by springs and dashpots. The mass of each section was determined by assuming that the TM has the density of water. The values for the springs and dashpots were determined from a least-squares fit to measured wave motion. The resulting shear moduli were  $17 \pm 5$  and  $47 \pm 12 \text{ kPa}$  for apical and basal TM segments respectively. The shear viscosities were  $0.15 \pm 0.04$  and  $0.19 \pm 0.07 \text{ Pa-s}$  for apical and basal segments, respectively. The hair bundles and limbal attachment were each modeled as springs between the TM and stationary ground. Incorporating these springs into the model caused a modest increase in space constants at low frequencies, with little change at high frequencies. Adding subreticular damping reduced the extent of wave propagation at low frequencies for gap sizes on the order of  $1 \mu\text{m}$ . However, these gap sizes occur only in the basal high-frequency region of the cochlea. Therefore subreticular damping did not significantly affect TM wave propagation near the best frequency at any location. These effects were small because the mass, stiffness, and viscosity of the TM are

comparable to those of the entire cochlear partition. Thus even in the presence of subreticular damping and loaded by hair bundles and the limbal attachment, a traveling wave on the TM can propagate in vivo. This simple model can be coupled to models of the BM traveling wave to investigate how the interaction of two traveling waves affects cochlear tuning.

## **[591] Obvious and 'Hidden' Waves in the Cochlea**

**Egbert de Boer<sup>1</sup>, Alfred L. Nuttall<sup>2</sup>, Jiefu Zheng<sup>2</sup>**

<sup>1</sup>Academic Medical Center, <sup>2</sup>Oregon Health and Science University

According to the 'classical' view of cochlear mechanics, outer hair cells (OHCs) produce an additional pressure in the fluid which causes the cochlear wave to be (selectively) amplified. The assembly of OHC-generated pressure sources can be imagined to give rise to a wave, this wave we have given the name 'hidden wave'. On two occasions we have found that this hidden wave deviates in its properties from what 'classical' cochlear mechanics dictates. The first instance is with the presentation of two tones where 'hidden waves' are generated with Distortion-Product (DP) frequencies. When the two frequencies are close together, the cochlear DP wave travels near the overlap region in the 'wrong' direction: it does not travel basalward but apicalward. A paper about this finding (we call this effect Inverted Direction of Wave Propagation, or IDWP) has been submitted.

We have extended our search to the case of single tones. Our analysis of responses to tones with various degrees of compression has revealed a 'hidden wave' that travels slower than the main cochlear wave. In both cases these waves are generated by the OHCs, at least according to the above-mentioned 'classical' view. We are currently studying the relation between these two manifestations.

To here: 200 words.

## **[592] Amplification by Spatial Feed-Forward and Feed-Backward Forces in a String Model of the Cochlear Traveling Wave**

**Annalisa M. Pawlosky<sup>1</sup>, Christopher A. Shera<sup>2</sup>**

<sup>1</sup>Speech & Hearing Biosciences and Technology Program, MIT, Cambridge, MA, <sup>2</sup>Eaton-Peabody Laboratory, Harvard Medical School, Boston, MA

The mechanisms of traveling-wave amplification in the cochlea are not well understood. Several recent papers suggest that amplification involves spatial feed-forward and/or feed-backward forces along the cochlear partition (e.g., due to the tilted orientation of the outer hair cells and/or the phalangeal processes of the Deiters' cells). We analyze this amplification mechanism using a simple string model of the cochlear traveling wave. In the string model, every segment of string experiences inertial, tensile, and viscous forces. In addition to these local forces, each segment is driven by forces proportional to the string's displacement at two other nearby locations, one on the basal side (the feed-forward force) and the other on the

apical side (the feed-backward force). We discuss (1) asymmetries in amplification/attenuation for forward- and reverse-traveling waves; (2) the conditions needed to achieve maximal wave amplification, their relationship to negative damping, and whether they are realized in the cochlea; and (3) possible implications for the generation of otoacoustic emissions.

(Supported by NIH grants T32 DC00038 and R01 DC03687.)

### **593 Simulation of a Cochlear Model As a Descriptive Tool for Normal and Abnormal Auditory Functioning**

**Miriam Furst<sup>1</sup>**

<sup>1</sup>*Tel Aviv University*

Recently we have developed a comprehensive ear model that is composed of the middle ear, cochlear fluid dynamics and outer hair cell (OHC) motility and nonlinearity. the model was solved in the time domain as a response to any type of acoustic stimulation. the basilar membrane velocity was derived as a function of both time and distance from the stapes. Otoacoustic emissions (OAE) were obtained at the ear canal. Audiograms were calculated on basis of the basilar motion. OHC loss was studied by the model, and demonstrated threshold shift, loss of OAE, and loss of frequency tuning.

Our purpose is to present the simulation of the model as a useful tool to describe normal and abnormal cochlear functioning. Pure tone thresholds, types of otoacoustic emissions and responses to noisy speech signals will be presented. Visual presentation of the simulated cochlear responses will help in understanding the function of the ear. to mention a few examples: (1) the relation between pure-tone threshold and existence of otoacoustic emissions; (2) the relation between abnormal threshold and speech sounds representation in noisy background; (3) the effect of hearing aids on speech representation.

### **594 A Large Scale 3-D Computational Model for Global Cochlear Current Calculations**

**Pavel Mistrik<sup>1</sup>, Fabio Mammano<sup>2</sup>, Jonathan Ashmore<sup>1</sup>**

<sup>1</sup>*University College London*, <sup>2</sup>*Venetian Institute for Molecular Medicine*

Although many models of cochlear function suggest that potassium recirculation is critical for cochlear function, the contribution of any individual component of the loop is hard to determine. Many of the molecules involved in the cochlear potassium (K<sup>+</sup>) homeostasis are now known yet their precise contribution to normal hearing and its disturbance remains obscure. to clarify contributions we have constructed a large scale quantitative model of cochlear K<sup>+</sup> recirculation using circuit elements in a programmable grid. the 3300 element values, representing cells with realistic ion channels, co-transporters and gap junctions, are based on the guinea pig experimental data. We have used macroscopic cochlear mechanics as input to the mechanotransducer gating. the model can easily be reconfigured to compute, in realistic times, the current flow around 11 circuit elements per section for 300 cochlear

sections. in agreement with a wide variety of empirical data, the model predicts the attenuation of receptor potential in the cochlear sensory cells (inner and outer hair cells, IHC and OHC respectively). Furthermore, the model predicts several essential differences in high frequency behaviour between networked and isolated hair cells. Firstly, the effective corner frequency of the IHC receptor potential is shifted to higher frequencies (from 60 to 450 Hz) when in a network. Secondly, the tonotopic variation in the OHC conductance normally overlooked is found essential to maintain the attenuation of OHC receptor potential at a relatively low level (-5 dB/decade in the 200 Hz-30 kHz range). Thirdly, the model shows the exponential decay of extracellular longitudinal current spread consistent with estimates from cochlear microphonic measurements. the model predicts, in addition, that the OHC amplification could be driven by the transmembrane receptor potential controlling cell motility over the entire hearing range. Supported by EuroHear Grant LSHG-CT-2004-512063.

### **595 Mathematical Modeling of the I/V Relation of Vascular Smooth Muscle Cells of Guinea Pig Spiral Modiolar Artery**

**Zhi-Gen Jiang<sup>1</sup>, Fang-Yi Chen<sup>1</sup>, Bing-Cai Guan<sup>1</sup>, Ket-Tao Ma<sup>1</sup>**

<sup>1</sup>*Oregon Hearing Research Center, Oregon Health & Science University*

The resting membrane potential (RP), a key vasotone regulator, of the smooth muscle cells (SMC) results from persistent ion currents via ionic conductances (G<sub>x</sub>) and Na-K-ATP pump current. Based on electrophysiological theory, we developed a mathematical function that modeled the whole-cell I/V relation, and also compiled a computer program that could use this function to fit to ramp command-generated whole-cell I/V curves recorded from a SMC. the fitting results yielded measurements of multiple ion conductances including maximum conductance (G<sub>MAX</sub>) of each channel type, and the half activation voltage (V<sub>0.5</sub>) and slope factor (*k*) of each voltage (V<sub>m</sub>)-dependent channel. Based on our data and others', the SMC normally has three V<sub>m</sub>-dependent and four nearly V<sub>m</sub>-independent conductance types: (1) the delayed rectifier K<sup>+</sup> (G<sub>Kdr</sub>), (2) the inward rectifier K<sup>+</sup> (G<sub>Kir</sub>), (3) the G<sub>Ca</sub>, (4) the gap junction coupling conductance (G<sub>gap</sub>, applicable only in the case of *In Situ* cells), (5) the non-inactivating V<sub>m</sub>-independent K<sup>+</sup> (G-K<sub>non-v</sub>, including K<sub>ATP</sub>), (6) the non-selective cation conductance (G<sub>cat</sub>, including ohmic leak, TRP channels, etc.) and (7) the Na-K-pump (G<sub>P</sub>). in mathematical terms, to obtain the total membrane current we have:  $I_{tot} = I_{Kdr} + I_{Kir} + I_{Ca} + I_{gap} + I_{Knon-v} + I_{cat} + I_P$ . to obtain the  $I_{tot}$  as the function of membrane potential (*x*), we have:

- (1)  $I_{Kdr} = (x - E_K) * (G_{MAX-Kdr} - G_{MAX-Kdr} / (1 + \exp((x - V_{0.5Kdr}) / k_{Kdr})))$ ;
- (2)  $I_{Kir} = (x - E_K) * G_{MAX-Kir} / (1 + \exp((x - V_{0.5Kir}) / k_{Kir}))$ ;
- (3)  $I_{Ca} = (x - E_{Ca}) * (G_{MAX-Ca} - G_{MAX-Ca} / (1 + \exp((x - V_{0.5Ca}) / k_{Ca})))$ ;
- (4)  $I_{gap} = (x - RP) * G_{gap}$ ; (5)  $I_{Knon-v} = (x - E_K) * G_{Knon-v}$ ; (6)  $I_{cat} = (x - E_{cat}) * G_{cat}$  and (7)  $I_P = (x - V_{r-p}) * G_P$ .

The starting and bound values of all the parameters for computer fitting were estimated from current- and voltage-clamp experiments on SMCs and Boltzmann equation

fitting to the isolated  $V_m$ -dependent current, e.g., equation (1) to 10 mM TEA-sensitive current I/V curve for  $G_{Kdr}$  and equation (2) to 100  $\mu$ M  $Ba^{2+}$ -sensitive net current I/V curve for  $G_{Kir}$ , etc. Results showed that the parameter values of the main conductances given by the modeling fit to high quality I/V records were very consistent with those from isolated current measurements in both dispersed and *In Situ* SMCs. We conclude that this modeling method could efficiently detect membrane conductances that simultaneously contribute to the whole-cell I/V relation. Supported by NIH NIDCD DC 004716 and P30 DC005983

## **[596] Modeling of the Bimodal Distribution of Resting Membrane Potentials of Guinea Pig Cochlear Arteriolar Cells**

**Fang-Yi Chen<sup>1</sup>, Zhi-Gen Jiang<sup>1</sup>**

<sup>1</sup>*Oregon Hearing Research Center, Oregon Health & Science University*

Cells in the spiral modiolar artery (SMA) normally show bi-stable resting potentials (RP) of  $\sim -40$  mV and  $\sim -75$  mV, called low and high RP cells (Jiang et al., 2001). We hypothesize that the bimodal RP phenomenon results from summation between the current of inward rectifier  $K^+$ -channel and all the other persistent membrane currents. We recently proposed a mathematical model of whole-cell I/V relation (Jiang et al., 2008), that is mainly composed of five voltage dependent and independent persistent currents via the inward rectifier  $K^+$  channel ( $K_{ir}$ ), the delayed rectifier  $K^+$  channel ( $K_{dr}$ ), the non-inactivating voltage-independent  $K^+$  channel ( $K_{non-v}$ ), the non-selective cation channel (Cat) and the Na-K-ATP-pump (pump). Based on this model, we computed the RP according to Goldman-Hodgkin-Katz equation zero current derivative (Bae et al., 1999; Hille, 2001):

$$V_m(RP) = (E_K * G_{Kir} + E_K * G_{Kdr} + E_K * G_{Knon-v} + E_{Cat} * G_{Cat} + E_{pump} * G_{pump}) / (G_{Kir} + G_{Kdr} + G_{Knon-v} + G_{Cat} + G_{pump}).$$

Equ.(1)

Where,  $G_{Knon-v}$ ,  $G_{Cat}$  &  $G_{pump}$  are nearly voltage-independent but,  $G_{Kir} = G_{maxKir} / (1 + \exp((V_m - V_{0.5Kir}) / k_{Kir}))$ ,

Equ.(2)

$$\text{and } G_{Kdr} = G_{maxKdr} - G_{maxKdr} / (1 + \exp((V_m - V_{0.5Kdr}) / k_{Kdr})).$$

Equ.(3)

According to the above equations, a computational program was composed in MATLAB (Mathworks, Natick, MA) to search for the RP value. After input of an initial  $V_m$  value to equations (2) and (3), the  $G_{Kir}$  and  $G_{Kdr}$  were calculated and fed to equation (1) for a new value of  $V_m$ . This new  $V_m$  was used by an iteration process for newer and newer  $G_{Kir}$ ,  $G_{Kdr}$  and  $V_m$  until a stable  $V_m$  was reached. This stable  $V_m$  was identified as the RP since it satisfies zero net transmembrane current.

When we applied random values ( $n \geq 50,000$ ) of normal distribution of the  $G_{maxKir}$  and one or more of other conductances' random values, whose mean values were estimated from our whole-cell recordings of the SMA vascular smooth muscle cells, the modeling program successfully produced a bimodal distribution of RPs peaked at  $-75$  and  $-40$  mV with a boundary near the  $V_{0.5Kir}$  value. an enhanced  $G_{maxKir}$  caused mainly an increase of high RP population and a hyperpolarizing shift of the peak

of the high RP population, and vice versa. Minimizing  $G_{maxKir}$  to 0.1% of the control value resulted in a skewed single summit distribution, peaked at  $\sim -40$  mV. the RP distribution is relatively insensitive to  $K_{dr}$  changes. Application of an enhanced and reduced  $G_{Knon-v}$  (e.g.,  $K_{ATP}$  changed by NO production) caused a reduction and increase of low RP counts, respectively, without change of the boundary.  $G_{Cat}$  had an opposite effect. in conclusion, this modeling reproduced the bimodal distribution of the RP observed in the SMA and graphically depicted the effects of altered  $K_{ir}$  and other currents on the RP generation and, in the case of mass population, the RP distribution. Supported by NIH NIDCD DC 004716 and P30 DC005983

## **[597] Improving the Intelligibility of Speech in Noise with a Model of Medial Efferent Suppression**

**Robert Ferry<sup>1</sup>, Ray Meddis<sup>1</sup>, Guy Brown<sup>2</sup>**

<sup>1</sup>*University of Essex*, <sup>2</sup>*University of Sheffield*

A computer model of the auditory periphery has been modified to include the effect of stimulating the medial efferent system. the model implements the effect of medial efferent stimulation by attenuating the nonlinear pathway of a dual-resonance nonlinear (DRNL) basilar membrane model. We have previously demonstrated (Ferry and Meddis, in press) that this attenuation is sufficient to reliably simulate the physiological data for basilar membrane displacement and auditory nerve firing rate, with and without the effect of stimulating the medial efferent system. We have used this model to simulate the compound action potential (CAP) data of Dolan and Nuttall (1988). They showed that efferent stimulation suppresses the CAP in response to a tone presented in quiet. However, when a tone is presented in noise, the effect of efferent stimulation is to *increase* the CAP, reversing the masking effect of the noise and 'unmasking' the tone. We investigated this unmasking effect by coupling the auditory model with a hidden Markov model-based automatic speech recogniser. Speech stimuli from the AURORA 2.0 speaker-independent connected digit corpus were presented to the model in the presence of pink noise at various signal-to-noise ratios. the auditory model was evaluated with and without the effect of efferent suppression. Speech recognition accuracy was used to quantify the benefit to intelligibility provided by efferent stimulation. the best recognition performance was obtained when using the version of the model that used efferent suppression.

## **References**

Dolan, D. F., and Nuttall, A. L. (1988). "Masked cochlear whole-nerve response intensity functions altered by electrical stimulation of the crossed olivocochlear bundle," J., Acoust. Soc. Am. **83**, 1081–1086.



## **598 Lizards That Hear Higher Than Birds**

Johanna Kraus<sup>1</sup>, Geoffrey Manley<sup>1</sup>

<sup>1</sup>*Technische Universitaet Muenchen*

in general, lizard hearing ability was thought to be confined to frequencies below about 5kHz (Manley, *Peripheral hearing mechanisms in reptiles and bird*, Springer-Verlag, 1990). Recently, however, spontaneous otoacoustic emissions were reported for some lizards at 7.7kHz (*Anolis sagrei*, Manley and Gallo, 1997, JASA 102: 1049-1055) and 8.25kHz (*Delma haroldi*; Manley et al., Abstract 810, 30th ARO meeting, 2007), implying higher upper frequency limits in some species.

We undertook a field study of legless lizards of the Australian family Pygopodidae, which are derived evolutionarily from the diplodactyline subfamily of geckos. Lizards were released again after study. Freshly-caught Pygopods *Lialis* and *Delma* were lightly gas anesthetized and a silver-wire electrode inserted deep into the mouth to record CAP responses from the auditory nerve. the electrode position was optimized for maximal CAP amplitudes. Sound delivery and CAP recording was under the control of a laptop computer using Labview software and a PCMCIA card as interface. CAP thresholds were 1.5µV between N1 and P1. Assumed neural thresholds, using a correction derived from CAP and neural thresholds from other species) were 30dB below CAP thresholds. Due to the very small number of nerve fibers involved (estimated to be ~1000) and the tiny maximal CAP (~5µV) this correction is likely to be an underestimate.

We compared CAP audiograms from two genera of pygopods, *Lialis* (here Burton's snake lizard *Lialis burtonis*) and *Delma* (*Delma pax* and *Delma borea*) with those from related geckos of the genus *Diplodactylus*. the derived neural audiograms show sensitive responses for *Diplodactylus* from 0.5 to 5.5kHz and for *Lialis* from 1.0 to 8.0kHz. the *Delma* species, however, showed a remarkable second peak of sensitivity centered at 11kHz and 30dB SPL. the upper limit of hearing in *Delma* thus exceeds that of other lizards by far and even virtually all birds (exception: the highly specialized barn owl). At present no behavioral correlates for this high-frequency hearing are known.

Supported by a grant to GAM from the Deutsche Forschungsgemeinschaft. We thank Don Robertson of Physiology, University of W. Australia for cooperation and patient administrative help, DEC of W.A. for permission to work in National Parks and the owners of the Pilbara cattle stations Anna Plains and Pardoo for friendly assistance.

## **599 Quantitative Analysis of the Regularity of a Cellular Mosaic: Comparisons of Cell Spacing and orientation in the Guinea Pig organ of Corti**

Donald Swiderski<sup>1</sup>, Masahiko Izumikawa<sup>1</sup>, Yehoash Raphael<sup>1</sup>

<sup>1</sup>*University of Michigan*

A hallmark of the mammalian organ of Corti is the arrangement of functionally differentiated cell types (inner and outer hair cells, pillar and Deiters' cells) in distinct

rows. Previous quantitative analysis focused on large scale gradients (e.g., cell length from cochlear apex to base) and their possible functional correlates. in this study, we focus instead on the regularity of the cellular matrix (i.e., the local deviations from the general trends). the complex morphologies of the hair cells and supporting cells provide a rich parameter space of potentially independent, informative variables that could be used to describe the organization of the organ of Corti, and quantitative analysis of the regularity of this matrix has potential to reveal subtle effects of mutation, trauma and disease. in experimental studies, it could also serve as a measure of efficacy of treatment. in addition, data from these quantitative analyses may also lead to greater understanding of developmental/epigenetic mechanisms that organize this cellular matrix. to address these issues, we have begun to explore the utility of several measures of local variation in cell shape and orientation and also measures of the distribution of variation (e.g., skewness and kurtosis). Preliminary results indicate that distances between stereociliary bundles of successive cells of a row of outer hair cells are both smaller and less variable in control animals than in experimental animals. This result is obtained even when there are no obvious gaps indicative of a missing hair cell. the direction of the vector connecting comparable points in successive cells is also more variable in experimental animals, indicating poorer alignment of the cells. These results confirm that the manipulations do have quantifiable effects on organ of Corti organization, and suggest that effects of milder treatments may also be detected with more refined methods.

## **600 ATP-Mediated Humoral Inhibition of Sound Transduction Supplants Neural Efferent Inhibition At High Sound Levels As the Mechanism for Expanding the Dynamic Range of Hearing**

Gary D. Housley<sup>1</sup>, Peter R. Thorne<sup>2</sup>, Srdjan M. Vljakovic<sup>2</sup>, Rachel T. Morton-Jones<sup>2</sup>, Baljit S. Khakh<sup>3</sup>, Debra A. Cockayne<sup>4</sup>, Allen F. Ryan<sup>5</sup>

<sup>1</sup>*University of New South Wales*, <sup>2</sup>*University of Auckland*,

<sup>3</sup>*University of California, Los Angeles*, <sup>4</sup>*Roche, Palo Alto*,

<sup>5</sup>*University of California, San Diego*

ATP-gated ion channels are assembled from P2X receptor subunits. There is a high level of expression of the P2X<sub>2</sub> subunit by cells lining the cochlear partition, particularly the hair cells. Loud sound is known to elevate ATP in the cochlear fluids and produce a shunt conductance which reduces hearing sensitivity (Thorne et al. JARO, 2004). We examined the functional significance of P2X<sub>2</sub> receptor expression to hearing by comparing ATP-activated conductance properties in the epithelial cells of the cochlear partition between transgenic mice lacking the P2X<sub>2</sub> receptor and wildtype controls. Voltage-clamped Reissner's membrane epithelial cells from knockout mice exhibited significantly attenuated current responses to ATP compared with the WT controls. the knockout mice therefore have reduced purinergic shunt conductance across the cochlear partition. When these mice were

exposed to transient high sound levels (90 dB white noise, 8 kHz – 16 kHz, 30 minutes), they exhibited significantly less temporary threshold shift (TTS) than the WT controls, using ABR click thresholds. These experiments indicate that noise-induced ATP acts via P2X<sub>2</sub> receptor signalling to reduce sound transduction sensitivity. These findings provide strong evidence that ATP acts as a humoral inhibitory regulator of sound transduction that supplants the saturated efferent inhibition at high sound levels, extending the dynamic range of hearing.

Support: Health Research Council of New Zealand, U.S. Dept of Veterans Affairs – Medical Research Service, Marsden Fund and James Cook Fellowship (Royal Society NZ), NIH grant DC00139.

### **601 Inner Ear Function in Fourteen Inbred Mouse Strains Identifies A/J As an Otoconia-Deficient Strain**

**Sherri Jones<sup>1</sup>, Bruce Mock<sup>1</sup>, David Bergstrom<sup>2</sup>**

<sup>1</sup>East Carolina University, <sup>2</sup>The Jackson Laboratory

Screening tests previously identified 3 inbred mouse strains with early onset gravity receptor dysfunction and normal hearing: MRL/MpJ, CE/J and SJL/J (Jones et al. 2006, Brain Res. 1091, 40-46). the purpose of this study was to complete detailed evaluation of auditory and vestibular function at various ages in these strains and to screen function in additional strains. Auditory brainstem responses (ABR) and vestibular evoked potentials (VsEPs) were collected for MRL/MpJ (n = 70) and SJL/J (n=68) at 1 to 10 months and for CE/J at 1 to 15 months (n=80). the following strains were tested at 2 to 3 months (n): A/HeJ (2); A/J (10); LG/J (6); P/J (4); PL/J (9); SM/J (4); AKR/J (6), FVB/NJ (6); SWR/J (6); RBF/DNJ (6); CAST/EiJ (4). Morphology was examined with SEM. Young C57BL/6J and CBA/CaJ mice were controls. Results demonstrated robust VsEPs for MRL/MpJ, CE/J and SJL/J strains up to 8 months with VsEP thresholds averaging -8.5 dB re: 1.0g/ms, which was similar to young cohorts from the tested strains and to young control mice (averaging -10.8 dB re: 1.0g/ms). Beyond 10 months, CE/J showed progressively higher VsEP thresholds. SJL/J mice demonstrated normal ABR thresholds up to the oldest ages tested; MRL/MpJ mice showed progressive high frequency hearing loss and CE/J mice demonstrated high frequency hearing loss at 1 month which progressively worsened to severe to profound loss by 15 months. of the additional strains tested, A/J demonstrated the most interesting results. VsEPs showed reduced amplitudes and elevated thresholds while SEM revealed very few, large otoconia in the maculae. Detailed studies completed here do not support the previous screening results and demonstrate essentially normal gravity receptor function for MRL/MpJ and SJL/J. CE/J does lose gravity receptor function beyond 10 months of age. Hearing is quite varied among the strains tested. Finally, these data are the first to identify A/J as an otoconia-deficient strain. Support: NIH R01DC006443.

### **602 Glucocorticoid Regulation of Sodium Transport Gene Expression in Reissner's Membrane**

**Sung Huhn Kim<sup>1</sup>, Nithya N. Raveendran<sup>1</sup>, Kyunghye Kim<sup>1</sup>, Donald G. Harbidge<sup>1</sup>, Joel D. Sanneman<sup>1</sup>, Daniel C. Marcus<sup>1</sup>**

<sup>1</sup>Kansas State University

Reissner's membrane (RM) epithelium forms much of the barrier that sustains the large ionic differences between cochlear endolymph and perilymph. We reported that RM contributes to normal cochlear function by absorption of Na<sup>+</sup> from endolymph via the epithelial sodium channel (ENaC) in gerbil inner ear [Lee et al, *Neuroscience*, 2003]. We also reported that glucocorticoids increase glucocorticoid receptor (GR)-dependent vectorial Na<sup>+</sup> transport in primary cultures of rat semicircular canal epithelium [Pondugula et al, *Am J Physiol Renal Physiol*, 2004] and demonstrated the genes involved in the pathway [Pondugula et al, *Physiol Genomics*, 2005].

in the present study, we sought in mouse RM 1) to determine the presence of genes involved in the Na<sup>+</sup> transport pathway, 2) to determine whether their level of expression was regulated by corticosteroids using quantitative RT-PCR and 3) to obtain functional evidence for these genes by pharmacologic and electrophysiologic means. Transcripts were present for the transport channel  $\alpha$ -,  $\beta$ -,  $\gamma$ -subunits of ENaC; the steroid receptors GR and MR (mineralocorticoid receptor); the GR agonist-controller 11 $\beta$ -HSD1; Na<sup>+</sup> transport control components Sgk1 and Nedd4-2. Expression of the MR agonist-controller 11 $\beta$ -HSD2 was near the lower limit of detection. Dexamethasone upregulated transcript expression of  $\alpha$ - and  $\beta$ -subunits of ENaC (~6 and ~3 fold). Currents directed into the endolymphatic face of RM were sensitive to amiloride and benzamil, but not EIPA. the currents were also inhibited by ouabain and K<sup>+</sup>-channel blockers.

These molecular and functional observations are consistent with Na<sup>+</sup> absorption by RM in the mouse that is mediated by apical ENaC, basolateral Na<sup>+</sup>-pump and K<sup>+</sup> channels, and that is under the control of glucocorticoids but not mineralocorticoids. These results provide an understanding and molecular definition of one possible mode of therapeutic action of glucocorticoids in the treatment of Meniere's disease.

Supported by NIH grants R01-DC00212, P20-PR017686.

### **603 Gap Junction Hemichannel-Mediated Inositol 1, 4, 5-Trisphosphate (IP3) Release in the Cochlear Sensory Epithelium**

**David G Gossman<sup>1</sup>, Hong-Bo Zhao<sup>1</sup>**

<sup>1</sup>Dept. of Surgery - Otolaryngology, University of Kentucky Medical Center, Lexington, KY, 40536

Inositol 1, 4, 5-trisphosphate (IP3) is an important second messenger that can perform intercellular signaling between cells via gap junctional coupling. It has been reported that defectiveness of this intercellular signaling in the cochlea is associated with some gap junction connexin mutants' induced hearing loss. However, its mechanism remains unclear. a gap junctional channel is composed of

two hemichannels, allowing transfer of ions and molecules up to 1 kDa. Here, we report that hemichannels in the cochlear sensory epithelium can release IP<sub>3</sub> under normal physiological conditions. Using a fluorescence polarization technique to directly measure IP<sub>3</sub> concentration, we found that IP<sub>3</sub> release was increased by a reduction of extracellular Ca<sup>2+</sup> concentration or increase in membrane tension. the release increased about 3-5 fold as extracellular Ca<sup>2+</sup> decreased from 2 mM to 0 mM, and could be blocked by gap junctional blockers. However, the release could not be blocked by purinergic P<sub>2</sub> receptor antagonists. Verapamil (Verap) is a selective P-glycoprotein inhibitor and can inhibit the ATP-binding cassette (ABC) transporters also could not block this IP<sub>3</sub> release. Fluorescent dye uptake assays showed that supporting cells in the cochlear sensory epithelium had uptake of Lucifer yellow, which is analogous to IP<sub>3</sub> in size and charge; whereas hair cells, which have no connexin expressions, had no dye uptake. the data indicate that cochlear gap junctional channels are permeable to IP<sub>3</sub>. Connexin mutations may directly impair IP<sub>3</sub> permeability in the cochlea to induce hearing loss. the data also suggest that IP<sub>3</sub> can pass through hemichannels to participate in intercellular signaling via an extracellular pathway, which may play an important role in long-distance intercellular communication in the cochlea.

Supported by NIDCD (R01) DC-05989

#### **604 Evidence for Cochlear Hypothyroidism in a Pendred Syndrome Mouse Model**

Sara Billings<sup>1</sup>, Christa Linsenmeyer<sup>1</sup>, Philine Wangemann<sup>1</sup>

<sup>1</sup>Kansas State University

Pendred syndrome is a disease that entails congenital childhood deafness and post-puberty goiter. It is caused by mutations in the gene *Slc26a4*, which is expressed in the inner ear and the thyroid. Since hypothyroidism has been shown to cause deafness, the possibility that hearing loss in Pendred syndrome is at least partially secondary to the thyroid phenotype has long been considered. Although no overt hypothyroidism was found in adult *Slc26a4*<sup>-/-</sup> mice, recent results from our lab demonstrating luminal acidification and oxidative stress in the *Slc26a4*<sup>-/-</sup> thyroid has led us to hypothesize an interaction between thyroid hormone homeostasis and inner ear development in *Slc26a4*<sup>-/-</sup> mice. This study examines *Slc26a4*<sup>-/-</sup> mice for evidence of hypothyroidism. Body weights of sex-matched littermates were obtained to check for retardation of overall growth. organ of Corti whole mounts and cochlea sections were evaluated with histological and immunohistochemical techniques for evidence of hypothyroidism. the following indications of hypothyroidism were found: 1) Pre-weaning *Slc26a4*<sup>-/-</sup> mice weighed ~10% less than their sex-matched *Slc26a4*<sup>+/+</sup> littermates. 2) Opening of the tunnel of Corti was delayed by ~1 day. 3) Efferent innervation to the outer hair cells was similarly delayed. 4) Tectorial membranes of *Slc26a4*<sup>-/-</sup> mice showed evidence of hypertrophy and disorganization. 5) BK K<sup>+</sup> channels were not present on inner hair cells in P12 or P15 *Slc26a4*<sup>-/-</sup> mice. in conclusion, there are characteristic signs of a modest thyroid hormone deficiency in the inner ear of

*Slc26a4*<sup>-/-</sup> mice, which may contribute to hearing loss in Pendred syndrome. Supported by NIH R01-DC01098.

#### **605 Olivocochlear Function is Dramatically Increased in Mice with a Point Mutation (L9'T) of the $\alpha 9$ Nicotinic Ach Receptor**

Stéphane F. Maison<sup>1</sup>, Juliàn Taranda<sup>2</sup>, Jimena A. Ballester<sup>2</sup>, Eleonora Katz<sup>2</sup>, Jim Boulter<sup>3</sup>, Paul A. Fuchs<sup>4</sup>, Douglas E. Vetter<sup>5</sup>, A. Belén Elgoyhen<sup>2</sup>, M. Charles Liberman<sup>1</sup>

<sup>1</sup>Dept of Otolaryngology & Laryngology, Harvard Medical School; Eaton-Peabody Lab, MA Eye & Ear Infirmary, <sup>2</sup>Instituto de Investigaciones en Ingeniería Genética y Biología Molecular, CONICET-UBA, <sup>3</sup>University of California, Los Angeles, <sup>4</sup>Dept of Otolaryngology, Head and Neck Surgery, Johns Hopkins University, <sup>5</sup>Dept of Neuroscience, Tufts University School of Medicine

Acetylcholine (ACh) is the major neurotransmitter of olivocochlear (OC) efferents. the OC-mediated suppression of outer hair cell (OHC) function and associated cochlear threshold elevation are mediated by  $\alpha 9/\alpha 10$  nicotinic ACh receptors (nAChRs). This study investigates the *In Vivo* effects of a point mutation (L9'T) in the pore region of the  $\alpha 9$  subunit designed to increase the strength of OC effects by decreasing the desensitization of the channel in the presence of ACh [Plazas et al., British J Pharmacol, 2005].

Cochlear sensitivity in mutants was characterized by measuring 1) ABRs at 7 log-spaced frequencies from 5.6 to 45.2 kHz, 2) DPOAEs evoked by primaries with  $f_2$  at the same 7 frequencies, and 3) the magnitude of DPOAE suppression evoked by electric stimulation of the OC bundle. Groups of mice homozygous and heterozygous for the mutation were compared with wildtype littermates.

Both ABR and DPOAE thresholds in homozygous knock-ins were elevated by 5-15 dB across all test frequencies re wildtype suggesting OHC dysfunction. Systemic injection of strychnine [30 mg/kg], a potent blocker of the  $\alpha 9$  nAChR, produced a partial rescue of the threshold-shift phenotype, suggesting that baseline OC-mediated suppression was at least partially responsible for the baseline threshold elevation. Correspondingly, the magnitude and time course of OC suppressive effects induced by electric stimulation of the OC bundle were dramatically affected with slower and larger suppression observed in mutants.

Given that OC effects are dramatically larger in mutants and OC efferents protect the ear from acoustic injury, this mutation could prove useful in enhancing resistance to acoustic injury.

## **606 Targeted Deletion of $\beta 2$ or $\alpha 7$ Nicotinic Ach Receptors: Effects On Cochlear Thresholds and Resistance to Acoustic Injury**

**Stéphane F. Maison<sup>1</sup>, M. Charles Liberman<sup>1</sup>**

<sup>1</sup>*Dept of Otolaryngology & Laryngology, Harvard Medical School; Eaton-Peabody Lab, MA Eye & Ear Infirmary*

Cholinergic terminals from medial and lateral olivocochlear (OC) efferents synapse with hair cells and cochlear afferents in both inner and outer hair cell areas. OC effects on hair cells via  $\alpha 9/\alpha 10$  nicotinic ACh receptors (nAChRs) are well studied. However, cochlear neurons express a number of other nAChRs [Bao et al, J Neurosci 25:3041, 2005], including  $\beta 2$  and  $\alpha 7$ . to gain insight into the functional role of these other receptors, we are studying the cochlear phenotype of  $\alpha 7$ - and  $\beta 2$ -nAChR-null mice.

Cochlear phenotype in mutants was characterized by measuring 1) amplitude vs level functions for ABRs and DPOAEs in 7 frequency regions, 2) the magnitude of DPOAE suppression evoked by electric stimulation of the OC bundle and 3) temporary and permanent threshold shifts following overexposure to noise.

No cochlear abnormality was seen in  $\alpha 7$ -null mice compared with wildtype controls. in  $\beta 2$ -nulls, both ABR and DPOAE thresholds were elevated by as much as 40 dB at test frequencies above 16 kHz, suggesting OHC dysfunction. Shock-evoked OC suppression of cochlear responses was unaffected in both mutant lines. However,  $\beta 2$ -nulls showed increased resistance to temporary acoustic injury, with mean threshold shifts by both ABRs and DPOAEs from 15-30 dB smaller than wildtypes after exposure to 8-16 kHz noise at 94 dB for 15 min.

Apparent OHC dysfunction is surprising given that 1) RT-PCR and *In Situ* hybridization fail to reveal nAChRs besides  $\alpha 9/\alpha 10$  in OHCs [Morley et al, Mol Brain Res 53: 78, 1998] and 2) no ACh-induced currents are seen in isolated hair cells after  $\alpha 9/\alpha 10$  blockade [Verbitsky et al. Neuropharm 39: 2515, 2000]. However, OC terminals synapse on OHC afferents, and "afferent" synapses with OHCs appear reciprocal in nature [Nadol, Ann ORL 90:12, 1981], thereby providing an indirect route for OC effects on OHCs.

## **607 A Point Mutation in the Hair Cell Nicotinic Receptor Alters Structure and Function of the Medial Efferent-Hair Cell Synapse**

**Julián Taranda<sup>1</sup>, Jimena Ballesterro<sup>1</sup>, Eleonora Katz<sup>1</sup>, Stéphane F Maison<sup>2</sup>, Charles M Liberman<sup>2</sup>, Douglas E Vetter<sup>3</sup>, Jim Boulter<sup>4</sup>, Paul a Fuchs<sup>5</sup>, a Belén Elgoyhen<sup>1</sup>**

<sup>1</sup>*Inst. Inv. Ingeniería Genética y Biología Molecular, CONICET,* <sup>2</sup>*Eaton Peabody Lab, MEEI, Harvard Medical School,* <sup>3</sup>*Dept. of Neuroscience, Tufts Univ. School of Medicine,* <sup>4</sup>*Department of Psychiatry and Biobehavioral Sciences, UCLA,* <sup>5</sup>*Otolaryngology- Head and Neck Surgery, Johns Hopkins University School of Medicine*

A nicotinic receptor (nAChR) composed of the  $\alpha 9$  and  $\alpha 10$  subunits mediates synaptic transmission between medial efferent olivocochlear (OC) fibers and hair cells. a mouse with targeted deletion of the  $\alpha 9$  gene has demonstrated that this subunit is necessary for classic

suppressive effects of OC activation on cochlear responses. to complement the knock-out, we have generated mice with a gain-of-function mutation in the  $\alpha 9$  subunit by homologous recombination. a threonine for leucine change was introduced at position 9' (L9'T) of the second transmembrane domain of the  $\alpha 9$  protein. Responses to acetylcholine (ACh) recorded in voltage-clamp from P 8-P13 inner hair cells of acutely excised organs of Corti of L9'T knock-in (ki) mice showed a significant increase in sensitivity to exogenously applied ACh (EC50, 63.9 $\pm$ 8.3  $\mu$ M, n=5, wt; 38.9 $\pm$ 6.3  $\mu$ M, n=6, ki). in addition, responses to ACh desensitized more slowly in the ki (I30/Imax 25 $\pm$ 3%, n=12, wt; 53 $\pm$ 7%, n=8, ki). Spontaneous and electrically evoked postsynaptic currents also decayed much more slowly in the ki ( $\tau$ = 61.8 $\pm$ 2.4 ms, wt and 241.9 $\pm$ 16.7 ms, ki). Cochlear histology was normal, as assessed by light-microscopic evaluation of plastic embedded sections. However, synaptophysin immunostaining of the middle cochlear turn in adults revealed an increase in the mean number of efferent terminals per outer hair cell (2.9  $\pm$  0.4, ki; 2.0 $\pm$ 0.4, wt; p<0.02), with as many as 6 terminals found on ki outer hair cells the present results indicate that a point mutation in the  $\alpha 9$  nAChR subunit leads to changes in postsynaptic response and presynaptic structure of contacts between medial efferent neurons and cochlear hair cells. Supported by NIDCD R01DC001508 to PAF and ABE and HHMI, ANPCyT and UBA to ABE, NIDCD RO1 00188 to MCL and DC6258 to DEV.

## **608 Expression of CTL2 (SLC44A2) and Vesicular Markers in Guinea Pig Inner Ear**

**Pavan Kommarreddi<sup>1</sup>, Thankam Nair<sup>1</sup>, Yehoash Raphael<sup>1</sup>, Thomas Carey<sup>1</sup>**

<sup>1</sup>*Kresge hearing research institute*

Choline transporter-like protein 2 (CTL2) has been identified as a target antigen in antibody mediated hearing loss. CTL2 protein is a predicted transporter and belongs to the solute carrier (SLC) family of proteins. the CTL family proteins are now called SLC44A. the function of the SLC44A subfamily is still unknown; however, some members of the SLC family are known to function via vesicular transport. CTL2 is a multi-transmembrane N-glycosylated protein now designated as SLC44A2 is highly expressed in the inner ear. the expression of SLC44A2 is observed in both the membrane and in punctate cytoplasmic vesicles. to investigate the possible role of SLC44A2 in trafficking through the endocytic pathway we have used antibodies to several vesicular markers (CHT1, Rab5, caveolin, and clathrin). Here we show that the expression of SLC44A2 is abundant in the supporting cells of organ of corti, spiral limbus, inner and outer sulcus, stria vascularis, spiral ganglion and the spiral vessels. Choline transporter 1 (CHT1) is expressed only at the base of inner and outer hair cells in guinea pig inner ear. Rab5 is highly expressed in the organ of corti, spiral limbus, spiral ligament and the spiral ganglion cells. Although clathrin is highly expressed in the inner ear, it was most abundant in the inner hair cell. Clathrin is also expressed in the outer hair cells, supporting cells in the organ of Corti, and with a unique punctate staining pattern in the spiral ganglion cells. Caveolin is expressed in the vessels of stria

vascularis and spiral ligament. Although CHT1 and caveolin are expressed in the inner ear they do not co-localize with SLC44A2 while clathrin and Rab5 are expressed abundantly in the inner ear and exhibit a distribution pattern similar to that of SLC44A2. Current studies are developing transfected cell culture models to examine co-localization in sub-cellular compartments. Supported by the Townsend Fund, NIH R01 DC03686, NIH T32 DC00011, and NIH P30 DC05188

## **[609] Hearing Loss in $\alpha$ -Tectorin C1509G Transgenic Mouse**

Anping Xia<sup>1</sup>, Fred Pereira<sup>1</sup>, Markus Pfister<sup>2</sup>, John Oghalai<sup>1</sup>

<sup>1</sup>Baylor College of Medicine, <sup>2</sup>University of Tübingen, Germany

The tectorial membrane (TM) is an extracellular matrix that attaches to the stereocilia of OHCs and guides mechanoelectrical transduction.  $\alpha$ -tectorin is a glycoprotein that is thought to be involved in cross-linking collagen and possibly other glycoproteins within TM. We created a transgenic mouse that has a cysteine to glycine mutation at the 1509 codon in  $\alpha$ -tectorin that has been found to cause autosomal dominant sensorineural hearing loss in humans. We performed histological and physiological studies to determine the consequences of this mutation.

Light microscopy demonstrated that the TM was shortened in heterozygotes and bulbous in homozygotes. Immunostaining demonstrated that wild-type, heterozygote, and homozygote mice all contained  $\alpha$ -tectorin,  $\beta$ -tectorin, and otogelin within their TMs. Transmission electron microscopy of the TM revealed that the marginal band, Kimura's membrane, and the covernet bundles had reduced staining density in heterozygotes. These effects were even more pronounced in homozygotes.

ABR measurements identified a 40 dB threshold elevation in heterozygotes and a 60 dB threshold elevation in homozygotes relative to wild-type littermates. DPOAE measurements revealed that heterozygotes had a 10-20 dB threshold elevation and homozygotes had a 40 dB threshold elevation. the cochlear microphonic amplitude was moderately reduced in heterozygotes and severely reduced in homozygotes below stimulus levels of 90 dB SPL. the cochlear microphonic was in phase with the stimulus in wild-type mice but led the stimulus by 90 degrees in homozygote mice. in heterozygotes, the cochlear microphonic was in phase with the stimulus at lower intensity levels, but progressively shifted to lead the stimulus as the intensity was increased.

These findings indicate that the  $\alpha$ -tectorin C1509G mutation alters the structure of the TM so that its interactions with the OHC stereocilia vary according to genotype. These data are consistent with a model whereby all OHCs are stimulated by the TM in wild-type mice, some OHCs are stimulated by the TM in heterozygote mice, and no OHCs are stimulated by the TM in homozygote mice.

Supported by grants NIH-NIDCD grants K08 DC006671 (to JSO) and DC00354 and DC008134, and NSF BES-0522862 (to FAP)

## **[610] Deafness in Pendred Syndrome Mouse Model is Due to Free Radical Stress Mediated Loss of Kcnj10 Protein Expression**

Ruchira Singh<sup>1</sup>, Philine Wangemann<sup>1</sup>

<sup>1</sup>Kansas State University

Pendred syndrome is due to loss-of-function mutations of *Slc26a4*, which codes for the HCO<sub>3</sub><sup>-</sup> transporter pendrin. Loss of pendrin causes deafness via a loss of the K<sup>+</sup> channel *Kcnj10* in stria vascularis and consequent loss of the endocochlear potential. Pendrin and *Kcnj10* are expressed in different cell types. Here we report that free radical stress provides a link between the loss of *Kcnj10* and the loss of pendrin. Studies were performed using native and cultured stria vascularis from *Slc26a4*<sup>+/-</sup> and *Slc26a4*<sup>-/-</sup> mice as well as CHO-K1 cells. *Kcnj10*, oxidized proteins and proteins involved in iron metabolism were quantified by Western blotting. Nitrated proteins were quantified by ELISA. Total iron was measured by ferrozine spectrophotometry and gene expression was quantified by qRT-PCR. At postnatal day 10 (P10), stria vascularis from *Slc26a4*<sup>+/-</sup> and *Slc26a4*<sup>-/-</sup> mice expressed similar amounts of *Kcnj10*. *Slc26a4*<sup>-/-</sup> mice lost *Kcnj10* expression during the next 5 days of development. in contrast, stria vascularis, obtained from P10 *Slc26a4*<sup>-/-</sup> mice and kept in culture for 5 days, maintained *Kcnj10* expression. Stria vascularis from *Slc26a4*<sup>-/-</sup> mice was found to suffer from free radical stress evident by elevated amounts of oxidized and nitrated proteins and other changes in protein and gene expression. Free radical stress induced by 3-morpholiniosydnonimine-N-ethylcarbamide (SIN-1) was found to be sufficient to reduce *Kcnj10* expression in CHO-K1 cells. These data demonstrate that free radical stress provides a link between loss of pendrin and loss of *Kcnj10* in *Slc26a4*<sup>-/-</sup> mice and possibly in human patients suffering from Pendred syndrome.

## **[611] Hair Cell Loss in Connexin 30 Deficient Mice is Accompanied by Anomalous Epithelial Repair Patterns**

Andrew Forge<sup>1</sup>, Ruth Taylor<sup>1</sup>, Regina Nickel<sup>1</sup>, Daniel Jagger<sup>1</sup>, Shoeb Ahmad<sup>2</sup>, Wenxue Tang<sup>2</sup>, Xi Lin<sup>2</sup>

<sup>1</sup>University College London, <sup>2</sup>Emory University School of Medicine

Connexin (cx)30, together with cx26, comprises gap junctions that connect supporting cells in the organ of Corti. Cx30 and cx26 are also both present between cells in the spiral ligament and in the stria vascularis. in mice with targeted disruption of cx30, endocochlear potential fails to develop, possibly due to effects that result in defective sealing of the tight junctions between stria capillary endothelial cells (Cohen-Salmon et al., 2007: PNAS 104, 6229). However, cx30 deficiency also results in loss of hair cells suggesting effects upon the organ of Corti itself. We have examined in detail the organ of Corti of cx30<sup>-/-</sup> mice at various ages from 17 – 174 days old. Thin sections revealed localised separations of adjacent plasma

membranes in the cell body regions of Deiters' cells at the sites where large gap junctions are seen in the organ of Corti of normal animals. At 17d of age there was scattered loss of outer hair cells (OHC) in the basal coil but all hair cells were present more apically. OHC loss increased with age and progressed apically, but loss of inner hair cells was evident only in samples taken at 174d when OHC loss was almost complete. Loss of OHC was accompanied by repair of the sensory epithelium by supporting cells, but features of this repair differed from the stereotypical pattern usually observed after conditions that induce acquired hearing loss. In many cases individual hair cells were replaced by the heads of only one supporting cell, and, unusually, inner pillar cells often replaced first row OHC at the reticular lamina. The phalangeal processes of Deiters' cells also failed to expand when OHC were lost. Lack of cx30 may therefore restrict co-ordination of repair responses by Deiters' cells.

## **[612] Drugs Enter the Perilymph of Guinea Pigs Through the Bony Otic Capsule**

**Anthony A. Mikulec<sup>1</sup>**, Stefan K. Plontke<sup>2</sup>, Jared J. Hartsock<sup>3</sup>, Alec N. Salt<sup>3</sup>

<sup>1</sup>St. Louis University School of Medicine, <sup>2</sup>University of Tübingen, <sup>3</sup>Washington University School of Medicine

In prior studies, we quantified the spread of markers and drugs from the middle ear into cochlear perilymph through the round window membrane (RWM). In those studies, the drug or marker was irrigated across the RWM, with absorbent wicks used to minimize fluid accumulation in the bulla. The application protocol produced a drug gradient along the cochlea, with highest levels at the base and low levels at the apex. In the present study, we have found that when drug or marker was applied by filling the bulla, a completely different distribution of drug is generated. Experiments were performed in which solutions containing the marker TMPA or gentamicin were administered by completely filling the bulla. After a 2 hour application period, the cochlea was rinsed and sequential 1 µL samples of perilymph were taken from the apex. In most cases, the TMPA or gentamicin concentration of the first sample (originating from apical turns) was substantially higher than that of the fourth sample (originating from the basal turn), showing that drug levels at the apex were greater than those at the base. In separate experiments, a TMPA-sensitive microelectrode was sealed into perilymph of the third cochlear turn and the bulla was filled with solution containing TMPA. The measured TMPA concentration started rising within 5 min of TMPA application, which is far faster than could occur by diffusion from the base. These results can be accounted for by TMPA and gentamicin entering perilymph through the bone in the apical regions of the cochlea. The rate of entry is presently being quantified by mathematical simulations of the experiments. These observations raise concerns that the distribution and effectiveness of drugs given transtympanically in guinea pigs, or other species in which the cochlea protrudes into the bulla, may not be comparable to that likely to occur in the human, where entry through the bone will be substantially lower.

Support: NIDCD grant DC01368 (AS); AOS (AM).

## **[613] Functional Changes Associated with "One-Shot" Intracochlear Injections Through the Round Window Membrane.**

**Alec N. Salt<sup>1</sup>**, Jared J. Hartsock<sup>1</sup>, Ruth M. Gill<sup>1</sup>

<sup>1</sup>Washington University School of Medicine

We have previously reported that intracochlear injections produce more consistent perilymphatic drug levels compared to applications to the round window (RW) membrane. In the present study, the functional consequences of intracochlear injections have been compared following intracochlear injections of sodium salicylate or control procedures in guinea pigs. Cochlear sensitivity was monitored before and at various times (0.5, 1, 1.5, 2, 3, 4 hrs) following a single intracochlear injection. Action potential (AP) thresholds (1 to 22 kHz in ¼ octave steps), distortion product otoacoustic emissions (DPOAE) (f1:0.5 to 16 kHz in ¼ octave steps, 70 dB SPL), DPOAE thresholds (f1:1 to 16 kHz in ¼ octave steps) and operating point analysis of the cochlear microphonic (0.5 kHz, 70 to 100 dB SPL) were used to assess cochlear status. Solutions were injected through the RW membrane using a glass pipette, beveled to a tip diameter of 20 µm, attached to a WPI Ultrapump. Sodium salicylate (10 or 20 mM in artificial perilymph) or artificial perilymph alone was injected through the RW membrane at a rate of 100 nl/min for 20 min (2 µL total). Injections were performed either with or without Healon (hyaluronate gel) present in the RW niche, which was used to control drug leakage. Salicylate injections produced a reversible elevation of high-frequency AP and DPOAE thresholds, the magnitude of which was more consistent when Healon was present in the RW niche. Fluid (leaking from around the injection pipette) or Healon in the RW niche caused an elevation of low-frequency thresholds by approximately 10 dB. These results demonstrate that single intracochlear drug injections can be performed in a non-traumatic manner, using techniques that minimize the loss of drug from the injection site. The method may be appropriate for long-term studies in animals where a single drug injection is required.

This study supported by NIH/NIDCD grant DC01368.

## **[614] Development of a Three-Dimensional Model for Calculation of Substance Distribution in the Inner Ear After Round Window Application Based On a Realistic Geometry of the Guinea Pig Inner Ear**

Norbert Siedow<sup>1</sup>, Martin Hering-Bertram<sup>1</sup>, Ruth Gill<sup>2</sup>, Alec Salt<sup>2</sup>, **Stefan Plontke<sup>3</sup>**

<sup>1</sup>Fraunhofer-Institute Kaiserslautern, <sup>2</sup>Washington University in St. Louis, <sup>3</sup>University of Tübingen

The local delivery of drugs to the inner ear is a promising alternative to systemic therapy. Direct measurements of drug concentration time courses in the animal are technically challenging and in the human inner ear are rarely possible. Computer simulations provide a valuable tool for planning and interpreting animal experiments and for estimating drug concentrations in the larger inner ears of humans. A previous, limited 3D-Model clearly

demonstrated the importance of accurate 3D anatomical studies to predict drug movements accurately.

Data sets for reconstruction of the 3D anatomy of the guinea pig inner ear were obtained from computed tomography (CT) and orthogonal plane fluorescence optical sectioning (OPFOS). Fluid spaces of the inner ear were segmented in Amira software and the 3D volume data transferred to a finite-element computer package (ANSYS®, ANSYS Inc., Canonsburg, PA, USA) creating 117.773 and 586.674 tetrahedrons. the data sets were tagged with respect to different anatomical structures, thus allowing the calculation of substance diffusion across the round window membrane and within and between the perilymphatic and endolymphatic spaces of the cochlea and of the labyrinth, the organ of Corti, and the spiral ligament.

Initial simulation results with the model incorporating the new geometry reveal a number of critical issues that must be considered, such as the site at which drug clearance from the inner ear to blood takes place. Clearance occurring from the spiral ligament gives markedly different results compared to clearance from the modiolus. the model demonstrates the necessity for the identification of transport and permeability properties of tissue boundaries based on measurements in animal experiments.

Other goals are to reduce simulation times through dimensionality reduction of the model and to create an interactive model for identification of relevant pharmacokinetic parameters.

Supported by grants BMBF 0313844 to SKP and NIDCD DC01368 to ANS.

### **615 Mechanism by Which High-Dose of Salicylate Induces Tinnitus**

Jérôme Ruel<sup>1</sup>, Christian Chabbert<sup>1</sup>, Régis Nouvian<sup>1</sup>, Rim Bendris<sup>1</sup>, Michel Eybalin<sup>1</sup>, Claude Louis Leger<sup>2</sup>, Jérôme Bourien<sup>1</sup>, Marcel Mersel<sup>1</sup>, **Jean Luc Puel<sup>1</sup>**

<sup>1</sup>Inserm-UMR 583, <sup>2</sup>Laboratoire de Nutrition Humaine et Athérogénèse

Currently many millions of people treated for various pains receive high-doses of salicylate. Consequently, understanding the mechanisms by which high-doses of salicylate induce tinnitus is an important issue for the medical research community. Behavioral testing in rats showed that tinnitus induced by salicylate or mefenamate (another cyclooxygenase blocker) are mediated by cochlear N-Methyl-D-Aspartate (NMDA) receptors. Here, we report that auditory nerve endings of cochlear spiral ganglion neurons expressed NMDA receptors. Patch-clamp recordings and two-photon calcium imaging on cochlear slices demonstrate that salicylate and arachidonate (a substrate of cyclooxygenase) potentiate NMDA responses of cochlear spiral ganglion neurons. Together with the measurement of cochlear arachidonate content *in vivo*, single unit recordings of auditory nerve fibers suggest that salicylate-induced neural excitation is due to the activation of cochlear arachidonate-sensitive NMDA receptors. This new pharmacological profile of salicylate provides a molecular mechanism for the

generation of tinnitus at the periphery of the auditory system.

### **616 Role of Vesicular Glutamate Transporters in the Cochlea**

Rebecca Seal<sup>1</sup>, Omar Akil<sup>2</sup>, Christopher Weber<sup>2</sup>, Eunyoung Yi<sup>3</sup>, Lisa Grant<sup>3</sup>, Amanda Clause<sup>4</sup>, Karl Kandler<sup>4</sup>, Elisabeth Glowatzki<sup>3</sup>, Lawrence Lustig<sup>2</sup>, Robert Edwards<sup>1</sup>

<sup>1</sup>Dept. Neurology, UCSF School of Medicine, <sup>2</sup>Dept. Oto/HNS, UCSF School of Medicine, <sup>3</sup>Dept. Oto/HNS, Johns Hopkins School of Medicine, <sup>4</sup>Dept. of Neurobiology, University of Pittsburgh

The regulated exocytotic release of glutamate requires its packaging into secretory vesicles, a process catalyzed by the vesicular glutamate transporters (VGLUTs). the three VGLUT isoforms exhibit largely non-overlapping expression patterns within the mammalian brain, suggesting a distinct role for each protein. VGLUTs 1 and 2 are the most abundant isoforms that together include essentially all neurons previously shown to release glutamate as a transmitter. in contrast, VGLUT3 is expressed by neurons that are usually associated with the release of a different classical transmitter. for example during development, VGLUT3 is expressed by MNTB neurons that project to the LSO and release GABA and glycine.

Inner hair cells of the cochlea use glutamate as a neurotransmitter and have been shown to express VGLUT1. However, the precise role of VGLUT1 and a potential role for the other two VGLUT isoforms in the cochlea have not yet been demonstrated. in this study, we use immunohistochemistry and RT-PCR to evaluate the expression pattern of VGLUT isoforms within the cochlea. in addition, we employ physiological measurements of cochlear function (e.g. auditory brainstem response and otoacoustic emissions) in VGLUT knock-out mice to elucidate the role of these transporters in hearing.

### **617 Chronic Intra-Cochlear Delivery of CGRP (8-37), a CGRP Receptor Antagonist, Does Not Reliably Influence Auditory Nerve Activity**

Colleen Le Prell<sup>1</sup>, Lindsey Willis<sup>1</sup>, David Dolan<sup>2</sup>, Karin Halsey<sup>2</sup>, Larry Hughes<sup>3</sup>

<sup>1</sup>University of Florida, <sup>2</sup>University of Michigan, <sup>3</sup>Southern Illinois University Medical School

The lateral olivocochlear (LOC) neurons project from the auditory brainstem to the cochlea, where they synapse on radial dendrites of auditory nerve (AN) fibers. Calcitonin-gene-related peptide (CGRP) is an LOC transmitter. Depression of sound-driven auditory brainstem response amplitude in CGRP-null mice suggests the potential for endogenous CGRP release to upregulate spontaneous and/or sound-driven activity. Consistent with this, chronic infusion of 200  $\mu$ M CGRP into the guinea pig cochlea enhanced the amplitude of both round window noise (a measure of ensemble spontaneous activity) and the synchronous whole-nerve response to sound (compound action potential, CAP). When CAP was assessed in the



presence of broadband noise (500-20 kHz; 8, 16, 24, or 32 dB SPL), we observed a level-dependant reduction in CAP amplitude (i.e., as the noise level was increased, CAP amplitude decreased). There was a reliable interaction between the effects of CGRP and the effects of the background noise, leading us to suggest that release of CGRP by the LOC neurons has the potential to enhance afferent activity in quiet and in the presence of a noise background. to determine if endogenous CGRP modulates auditory nerve activity in an equivalent manner, we chronically infused the CGRP receptor antagonist CGRP (8-37; 250 ?M) into the guinea pig cochlea. Preliminary data from two animals indicated that CGRP antagonists reduced both round window noise and CAP amplitude as after manipulations that broadly disrupt the LOC system; however, reliable functional changes have not been observed in a larger sample (N=7 additional animals) infused with the same antagonist concentration. Taken together, the data do not provide compelling evidence that tonic and/or sound-driven release of CGRP by the LOC neurons significantly influences AN activity in the guinea pig. Supported by R03-DC007342 (CGL) and P30-DC05188.

#### **[618] Vasopressin-Induced Enlargement of the Intrastrial Space in the Stria Vascularis**

**Akinobu Kakigi<sup>1</sup>, Masahiko Nishimura<sup>1</sup>, Taizo Takeda<sup>1</sup>, Teruhiko Okada<sup>2</sup>**

<sup>1</sup>*Department of Otolaryngology, Kochi Medical School,*

<sup>2</sup>*Department of Anatomy, Kochi Medical School*

Recently, many lines of evidence have supported the possibilities that vasopressin (VP) is closely linked to the formation of endolymphatic hydrops in Meniere's disease. Water flux is thought to occur through the stria vascularis (SV), and the endolymph is hyper osmotic to perilymph by 11-40 mOsmol/kg H<sub>2</sub>O. in the basal cells, the existence of aquaporin2 (AQP2), which facilitates the osmotic movement of water molecules and is regulated its expression by vasopressin, has been reported. Efflux of water from the basal cells to the intrastrial space may occur. in the present study, Wistar rats were used to examine whether the acute administration of VP might induce enlargement of the intrastrial space. One µg/ml of VP (50ml/kg) was injected intraperitoneally. the SV was harvested 1 hour after VP injection, then observed by transmission electron microscopy (TEM). It was also examined whether pre-administration of an antagonist of VP type 2 receptor (V2R) might reduce the effect of VP administration. One hundred mg/kg of OPC-31260, which is V2R antagonist, was administered orally 1 hour before the VP injection. the SV was harvested 1 hour after the VP injection, then observed by TEM. the intrastrial spaces were remarkably enlarged in the VP injection study. the enlargement of intrastrial space was reduced by administration of OPC-31260 before the VP injection. These findings suggest that VP increases the efflux of water from the basal cells to the intrastrial space via AQP2, causing the formation of endolymphatic hydrops.

#### **[619] Expression and Localization of Voltage-Gated K<sup>+</sup> (Kv) Channel Kv2.1 and it's Modulatory Subunit Kv6.3 in the Guinea Pig Cochlea**

**Paula Mannström<sup>1</sup>, Zhe Jin<sup>2</sup>, GuiHua Liang<sup>1</sup>, Leif Järleback<sup>3</sup>, Mats Ulfendahl<sup>1</sup>**

<sup>1</sup>*Center for Hearing and Communication Research, Karolinska Institutet, Sweden,* <sup>2</sup>*Department of Clinical Science, Lund University, Sweden,* <sup>3</sup>*The Swedish Research Council - Medicine, Stockholm, Sweden*

The voltage-gated K<sup>+</sup> (Kv) channel Kv2.1 belongs to the Shab voltage-gated delayed rectifier family. This functional channel plays a prominent role in controlling the excitability in neurons, and regulating secretion, as well as regulating electrical function in muscle cells. the Kv6.3 subunit belongs to a subfamily of silent subunits, which do not form any functional channels by themselves but modulate the activity of functional channels. the Kv6.3 subunit has been reported to modulate the Kv2.1 channel and change its electrophysiological properties.

in this study, we have explored the expression and localization of Kv2.1 and Kv6.3 in the adult guinea pig cochlea. Cochleas were micro-dissected into three parts: the lateral wall, organ of Corti, and modiolus (including spiral ganglion neurons). the expression of Kv2.1 and Kv6.3 mRNA transcripts and proteins were investigated using RT-PCR and Western blot. Their respective subunit localization in the guinea pig cochlea was examined using immunohistochemistry. Both Kv2.1 and Kv6.3 mRNA transcripts were expressed in all dissected cochlear tissues: most prominently in the organ of Corti and for Kv2.1 also in the modiolus. Kv2.1 and Kv6.3 protein expression was detected in the adult guinea pig cochlea, and the localization has to be further explored using immunohistochemistry.

Our findings suggest that the assembly of Kv2.1 and Kv6.3 in the cochlea may be important in the sensation of hearing and possibly plays a role in the tuning mechanism of the inner ear.

#### **[620] Heterogeneous Expression of Inward Rectifier K<sup>+</sup>-Channels (Kir) May Contribute to Distinct Modes of Resting Membrane Potentials Among the Cochlear, Brain and Mesenteric Arterioles**

**Ke-Tao Ma<sup>1</sup>, Yu-Qin Yang<sup>1</sup>, Bing-Cai Guan<sup>1</sup>, Takatoshi Karasawa<sup>1</sup>, Xiao-Rui Shi<sup>1</sup>, Zhi-Gen Jiang<sup>1</sup>**

<sup>1</sup>*Oregon Hearing Research Center, Oregon Health & Science University*

Our data show that resting membrane potentials (RP) of the spiral modiolar artery (SMA) cells exhibit a prominent bimodal distribution peaked near -75 and -40 mV, whereas the cells of brain artery (BA) showed a bimodal RP distribution with a dominating population around the peak of -77 mV, and the mesenteric arterial (MA) cells exhibited a skewed single peak distribution around -72 mV. We hypothesize that the heterogeneous K<sub>ir</sub> expression and thus its properties play a role in generating the distinct RP modes among these three vascular beds. Using

intracellular and whole-cell recording, vessel diameter tracking methods, immuno-cytochemical, RT-PCR and Western blotting detection of Kir2.x gene expression, we tested the hypothesis and found that: 1) a solution of 10 mM K<sup>+</sup> caused a -7.1, 6.7 and 9.8 mV membrane potential change; 2) 20 mM K<sup>+</sup> usually caused a dilation, biphasic dilation followed by a constriction, and a constriction only in the SMA, BA and MA, respectively. 3) Ba<sup>2+</sup> caused a concentration-dependent depolarization in high RP cells with an EC<sub>50</sub> of 89, 158 and 201  $\mu$ M for the SMA, BA and MA, respectively. 4) Whole-cell recording analysis showed that Kir currents at -120 mV in 60 mM external K<sup>+</sup> was suppressed by Ba<sup>2+</sup> with an IC<sub>50</sub> of 561 $\pm$ 73, 446 $\pm$ 30 and 811 $\pm$ 49 nM for the SMA, BA and MA, respectively. 5) Immunocytochemical staining found Kir2.1 signal only in VSMC of all the vessels. Western blotting data revealed that the SMA, BA and MA express Kir2.1 protein at a ratio of 1:1.08:0.83. 6) Semi-quantitative RT-PCR analysis found the four Kir2.x family members all have mRNA transcripts in the three vessels but Kir2.3 was higher in BA and MA than SMA, whereas Kir2.4 exhibited higher expression in SMA compared to BA and MA. We conclude that heterogeneous expression of Kir2.x isoforms may form different heteromeric channels in the three vessels with different conductance and voltage dependency, thus contributing to the distinct RP distribution modes. Supported by NIH NIDCD DC 004716 (ZGJ)

## **[621] Estimation of the Stability of Cochlear Gap Junctions Comprised of Homomeric and Heteromeric Configurations**

**Shoeb Ahmad<sup>1</sup>, Qing Chang<sup>1</sup>, Wenxue Tang<sup>1</sup>, Xi Lin<sup>1</sup>**

<sup>1</sup>*Dept of Otolaryngology / Cell Biology, Emory University School of Medicine*

In the rodent cochlea, connexin26 (Cx26) and Cx30 are co-expressed in most gap junction (GJ) plaques to form heteromeric GJ intercellular channels. Genetic studies have shown that targeted gene deletion of any one of the co-assembly partner (Cx26 or Cx30) in mice causes deafness, despite continuing expression of the partner Cx capable of forming homomeric GJs. It is not known why in the absence of the co-assembly partner, the remaining homomeric GJs are not able to maintain cochlear homeostasis required for normal hearing. Recently, we showed that in Cx30 knockout (KO) mice, the expression level of Cx26 is also significantly reduced from the wild type (wt) levels. Apparently the remaining Cx26 homomeric GJs become less stable in the absence of heteromeric assembly partner, thereby affecting the overall capacity of GJ mediated intercellular communication resulting in deafness. to test this hypothesis, we first utilized an *In Vitro* system of HEK293 cells stably expressing homomeric GJs of either Cx26-EGFP or Cx30-mCherry. Standard pulse-chase approach involving metabolic labeling of proteins with 35S-methionine and 35S-cysteine followed by chase in the non-radioactive media was employed. Both Cx26 and Cx30 in homomeric configuration were found to have similar half-lives of ~4-4.5h. We are in the process of measuring half-lives of heteromeric GJs *In Vitro* (cells permanently expressing

both Cx26-EGFP and Cx30-mCherry). Future work will also include comparing half-lives of cochlear GJs between wt (heteromeric GJs consisting of Cx26&Cx30) and Cx30KO (homomeric GJs) mice. Our preliminary data suggested that cochlear homomeric GJs have half-lives shorter than average half lives of most other integral membrane proteins (about 24h). Better understanding of Cx turnover mechanism in the cochlea can help designing approaches to stabilize Cx protein in the cochlea, which may potentially have therapeutic effects in treating patients carrying monogenic Cx mutations as suggested by our recent work (Ahmad et al., 2007).

## **[622] Basement Membrane Pathology Influences Stria Metabolism**

**Charles Askew<sup>1</sup>, Michael Anne Gratton<sup>1</sup>**

<sup>1</sup>*Dept. of Otorhinolaryngology, Head and Neck Surgery, University of Pennsylvania, Philadelphia*

Dysregulation of molecular mechanisms governing basement membrane synthesis/degradation has been observed in mice modeling Alport syndrome, a disease caused by mutation of type IV collagen. in the inner ear, altered basement membrane homeostasis results in accumulation of basement membrane proteins that ensheath capillaries in the stria vascularis. the relationship between basement membrane thickness and cochlear function has been assessed in earlier studies using measurements of the endocochlear potential (EP). Exposure to physiological stress, in the form of moderate noise stimulation, resulted in a significant decrease in the EP of Alport mice while that of their wild-type littermates was normal. Susceptibility to noise-induced hearing loss suggests that stria capillary basement membrane pathology may change filtration characteristics for energy substrate and oxygen from the blood to stria tissue. This study examines Na,K-ATPase activity in the stria of wild type and Alport mice. Na,K-ATPase activity, the driving force for K<sup>+</sup> secretion in the stria, was quantified individually through a colorimetric enzyme assay. Results show significantly less Na,K-ATPase specific activity after moderate noise exposure in the stria of Alport mice as compared with their wild type littermates. the stria of wild type and Alport mice exhibited the same amounts of Na,K-ATPase activity when not stressed by noise. Previous studies have shown the stria in Alport mice to be a hypoxic microenvironment, and hypoxia is known to inhibit ATP production in mitochondria of non-muscular tissue. the present study suggests that the amount of energy substrate and/or oxygen available in the stria vascularis of Alport and wild type mice differs as a result of basement membrane thickness and this difference is exacerbated when mice are physiologically stressed by exposure to moderate levels of noise.

Supported by NIDCD grant DC-006442

## **623 Developmental Change of Na<sup>+</sup>-Absorptive Function in the Epithelial Cells of Reissner's Membrane**

**Jun-Ho Lee**<sup>1</sup>, Hye-Young Kim<sup>1</sup>, Hyoung-Mi Kim<sup>1</sup>, Ja-Won Koo<sup>2</sup>, Young-Ho Kim<sup>3</sup>, Sun-O Chang<sup>1</sup>, Chong-Sun Kim<sup>2</sup>

<sup>1</sup>Seoul National University Hospital, <sup>2</sup>Seoul National University Bundang Hospital, <sup>3</sup>Boramae Hospital

The epithelial cells of Reissner's membrane (RM) form most of the boundary of the cochlear duct and are known to be capable of transporting Na<sup>+</sup> out of cochlear endolymph via epithelial Na<sup>+</sup> channels (ENaC) (Lee and Marcus, 2003). However, little is known in developing age. the purpose of this study is to investigate the developmental change of the ion transport in RM using voltage-sensitive vibrating probe technique. Rats were used at the age of postnatal day (PND) 1, 3, 5, 7, 14, and 21. After the cochlear lateral wall was dissected from the apical turn of the cochlea, the stria vascularis was removed. the attached portion of RM was folded over the suprastrial portion of the spiral ligament and perfused at 37°C. the vibrating probe technique was chosen to measure transepithelial currents under short circuit conditions due to the small extent of the RM epithelial domain.

Results showed that the short-circuit current (I<sub>sc</sub>) toward apical to basolateral direction in the physiologic saline gradually increased during early neonatal development. the amiloride-sensitive ENaC current also increased from PND 1 to PND 7, when the endolymphatic Na<sup>+</sup> concentration is known to reach the lowest level like in adult. the I<sub>sc</sub> decreased by application of UTP at early neonatal ages. the response to UTP was not inhibited by 100 μM suramin or PPADS at any age. the suramin is a potent blocker of rat P2Y<sub>2</sub>, but not of P2Y<sub>4</sub>. PPADS is an antagonist of rat P2X<sub>1</sub>, P2X<sub>2</sub>, P2X<sub>3</sub>, P2X<sub>5</sub>, P2X<sub>7</sub>, and P2Y<sub>1</sub>, and of human and mouse P2Y<sub>6</sub>. These criteria applied to the present results point to the P2Y purinergic receptor in developing RM as the P2Y<sub>4</sub> subtype. However, the cellular localization of P2Y<sub>4</sub> and its functional role should be determined further. in summary, our results support that the RM is responsible for the maintenance of the endolymphatic low Na<sup>+</sup> concentration. P2Y<sub>4</sub> receptor is expressed in neonatal RM, but its role is uncertain as yet.

## **624 Progesterone Receptors in the Inner Ear of Rat**

**Rusana Simonoska**<sup>1</sup>, Annika Stenberg<sup>1</sup>, Lena Sahlin<sup>2</sup>, Malou Hultcrantz<sup>1</sup>

<sup>1</sup>Inst. Clinical Neuroscience, Dept. of Otorhinolaryngology, <sup>2</sup>Dept. of Woman and Child Health

Background: Hearing loss appears to be more profound in elderly males than females. There are also well-known sex differences in the ABR, where women have shorter latencies than men. in addition, women with Turner syndrome (45,X), who are biologically estrogen deficient, have longer auditory brainstem response (ABR) latencies and early rapid aging of the ear (presbycusis). There are case reports that hormone replacement therapy and oral contraceptive use can lead to hearing loss, but of another

type, the acute sudden deafness. Such contradictory aspects of the estrogen action are commonly found and may spring from the fact that there are two estrogen receptors, alfa and beta, both of which we have earlier shown to be present in the inner ear of mouse, rat and humans or it could be due to the action of another female sex hormone, progesterone. So far, there have not been any published studies on whether there are any progesterone receptors in the inner ear.

Aim: are there any progesterone receptors (PR) in the inner ear? Localization?

Methods: Immunohistochemical staining for progesterone receptors in the inner ear of Sprague Dawley rats was performed.

Results: We found that progesterone receptor B was indeed present in the inner ear, in the large cells of the spiral ganglion.

## **625 The Actions of Dopamine Receptor Subtypes within the Guinea Pig Cochlea**

**Andrew Garrett**<sup>1</sup>, Don Robertson<sup>1</sup>, Wilhelmina Mulders<sup>1</sup>

<sup>1</sup>University of Western Australia

Controversy exists on whether the lateral olivocochlear system (LOCS), an efferent system that synapses onto the afferent dendrites contacting the inner hair cells, exerts excitatory or inhibitory effects in the mammalian cochlea. One of the neurotransmitters of the LOCS is dopamine, which in the central nervous system can exert both excitatory and inhibitory effects, depending on the receptor subtypes present. It is therefore possible that dopamine mediates both inhibitory and excitatory actions of the LOCS via different receptor subtypes.

To address this question, we investigated the effects of cochlear perfusion of highly specific D<sub>1</sub>, D<sub>2</sub> and D<sub>3</sub> receptor subtype agonists and antagonists on sound-evoked and spontaneous cochlear nerve activity in anaesthetized guinea pigs, measured using the amplitude of the compound action potential (CAP) and summating potential (SP) as well as the spectrum of the spontaneous neural noise (SNN), respectively. Activating either D<sub>1</sub> (SKF 81297), D<sub>2</sub> ((+)-PHNO) or D<sub>3</sub> (PD 1289087) receptors significantly reduced CAP amplitudes at all intensities (36-90dB SPL). in addition, PD 128907 reduced SP amplitudes. Blocking D<sub>1</sub> (SCH 23390) or D<sub>2</sub> (L741,626) receptors also reduced CAP amplitudes whereas the D<sub>3</sub> antagonist U99194A did not have any effect. the SP amplitude was decreased by both D<sub>2</sub> and D<sub>3</sub> antagonists, but increased with the D<sub>1</sub> antagonist. the SNN was inhibited in the presence of the D<sub>2</sub> agonist but neither the D<sub>1</sub> or D<sub>3</sub> agonists nor the antagonists had any effect on the SNN. the agonist data support an inhibitory role for dopamine on auditory nerve activity, possibly via D<sub>2</sub> receptors. However, the antagonist data suggest that dopamine has an excitatory effect on auditory responses via the D<sub>1</sub> and D<sub>2</sub> receptors. the changes observed in SP amplitudes have not been before reported and suggest that dopamine may influence the sound-evoked depolarisation of the inner hair cells, either directly, or via an action on outer hair cells.

**626 Hypoxic Environment Created by Thickened Strial Capillary Basement Membranes Involves Cytokine Upregulation**

Lara Dunn<sup>1</sup>, Dominic Cosgrove<sup>2</sup>, Michael Anne Gratton<sup>1</sup>

<sup>1</sup>University of Pennsylvania, <sup>2</sup>BoysTown National Research Hospital

Alport syndrome, an inherited disease due to a type IV collagen mutation, causes renal failure and deafness. Cochleae of 9 week old Alport mice have thickened strial capillary basement membranes (SCBM) and show an upregulation of HIF-1 $\alpha$ . Hypoxic environments can upregulate cytokines, such as TNF $\alpha$  and IL-1 $\beta$ . These cytokines contribute to the amplification of MMPs, which degrade basement membranes and therefore, disrupt the homeostasis of the SCBM. Specifically, TNF $\alpha$  induces MMP-2 and MMP-9 expression, while IL-1 $\beta$  enhances MMP-2 and MMP-3 expression - all type IV collagenases. TNF $\alpha$  has also been shown to enhance MMP-14 expression, which also increases MMP-2 production. These MMPs have all been shown to be upregulated in Alport mice compared to their wild-type counterparts.

in this study, it was hypothesized that Alport mice would show greater TNF $\alpha$  and IL-1 $\beta$  expression compared to wild-type mice. a greater difference in expression was expected between wild-type and Alport mice following noise exposure. the stress of noise should place a greater metabolic demand on the stria, which should increase the level of hypoxia in the tissue and, therefore increase cytokine expression. the expression of TNF $\alpha$  and IL-1 $\beta$  was evaluated in the following subsets of 9 week old mice: wild-type mice, Alport mice, wild-type mice with noise exposure, Alport mice with noise exposure, and wild-type mice with hypoxia exposure. Immunohistochemistry confirmed that the Alport mouse has an enhanced expression of TNF $\alpha$  and IL-1 $\beta$ , and that the differential between the wild-type and Alport mouse is maintained when comparing those exposed to noise. in addition, cytokine expression in the wild-type mouse exposed to hypoxia mimicked the expression observed in the Alport mouse. It is concluded that the thickened SCBM creates a hypoxic environment that leads to a cascade of cytokine and MMP production that disrupts homeostasis within the cochlea.

Supported by NIDCD grant DC006442

**627 Techniques of Celloidin Removal From Temporal Bone Sections**

Jennifer O'Malley<sup>1</sup>, Saumil Merchant<sup>1</sup>, Barbara Burgess<sup>1</sup>, Diane Jones<sup>1</sup>, Joe Adams<sup>1</sup>

<sup>1</sup>Massachusetts Eye and Ear Infirmary

There are over 10,000 human temporal bone specimens contained within various laboratories in the United States. the majority of these specimens are embedded in celloidin. Unstained sections are generally stored in 80% ethanol. These sections represent the best preserved specimens of human ears that exist. Celloidin embedding produces superior morphology for light microscopy. These sections provide a rich anatomical resource and potentially represent a rich immunohistochemical resource as well.

for years, researchers have tried, with sporadic success, to remove the celloidin and immunohistochemically stain such sections. Various organic solvents have been tested including acetone, ether alcohol, clove oil, and sodium methoxide. in this study, we systematically evaluated each of these removal techniques on optimally fixed mouse temporal bones perfused with 10% formalin and 1% acetic acid embedded in celloidin. the bones were sectioned at 20 microns. the celloidin sections were firmly adhered to subbed glass slides with albumin and formalin and allowed to dry. the sections were then subjected to acetone, ether alcohol, clove oil, or sodium methoxide. Once the celloidin was removed, the sections were stained with six different antibodies (Aqp1, CTGF, NaKATPase, PGDS, Tubulin, and NF) to determine the best and most reproducible method for immunostaining celloidin embedded tissue. the acetone, ether alcohol, and clove oil sections all looked similar. There was celloidin still evident on the slides, the immunostaining was not selective, and overall, there was a brown background in all of these sections. We found sodium methoxide was the best and most reproducible method for removing the celloidin and thus gave the cleanest, most selective, and reproducible results with the six antibodies tried.

Supported by NIDCD

**628 Development of a Thin-Sheet Laser Imaging Microscope for Optical Sectioning of the Mouse Cochlea and Brain**

Peter Santi<sup>1</sup>, Tiffany Glass<sup>1</sup>, Shane Johnson<sup>1</sup>, Patrick GrandPre<sup>1</sup>, Alex Strachota<sup>1</sup>, David Hultman<sup>2</sup>, James Leger<sup>2</sup>

<sup>1</sup>Department of Otolaryngology, University of Minnesota,

<sup>2</sup>Electrical and Computer Engineering, University of Minnesota

The ability to selectively visualize biological structures in three-dimensions (3D) is useful for understanding structure/function relationships in complex organs such as the cochlea. a prerequisite for 3D reconstruction is the creation of a well-aligned, z-stack of serial sections from a whole cochlea. a z-stack of images can be obtained by nondestructive, optical sectioning using a thin sheet of light directed through a whole cochlea that has been fixed, decalcified, dehydrated, and cleared to transparency. This procedure has been previously reported by Voie et al. (J Microsc. 170, 229-36; 1993), and was called orthogonal plane fluorescence optical microscopy (OPFOS). Subsequent to their publication, a number of other investigators have made improvements in thin-sheet, optical sectioning of thick tissues. However, a thin-sheet optical sectioning instrument is not yet commercially available, which has hindered development of this important, new imaging technology. the purpose of this presentation is to describe development of a thin-sheet laser-imaging microscope (T-SLIM), which combines improvements made by other investigators, and to describe the instrument in sufficient detail so that other investigators may construct it. T-SLIM uses dual beam illumination with a thin sheet of light produced by solid-state, green (532 nm) laser. Dual beam illumination

provides even illumination across the specimen, and minimizes horizontal shadow artifacts produced by single beam OPFOS. In addition, we have also added a feature developed by Buytaert and Dirckx (J. Biomed. Optics., 12, 014039; 2007) which significantly improves image resolution by collecting images only from that portion of the specimen which is illuminated by thinnest region (beam waist) of the light sheet. Our results indicate that dual beam optical sectioning, and beam waist image scanning, produces excellent optical sections for large specimens such as the mouse brain with attached cochleas. Construction of a T-SLIM system by other investigators would encourage further development of this new imaging technology and determine its capabilities and limitations.

Supported by grants to P. Santi from the Digital Technology Center (UM), Capita Foundation, and the NIDCD

## **[629] Multiphoton Imaging of Motion Patterns in the Intact Organ of Corti**

**Eric Scarfone**<sup>1</sup>, Miriam von Tiedemann<sup>2</sup>, anders Fridberger<sup>2</sup>, Mats Ulfendahl<sup>2</sup>

<sup>1</sup>CNRS and Karolinska Institutet, <sup>2</sup>Karolinska Institutet

The inner ear in general and the organ of Corti in particular are convoluted organs comprising large extracellular spaces and extensive epithelial surfaces (ie the reticular lamina). Hair Bundles, the large membraneous expansions of the sensory cells that protrude into those extracellular spaces and interacting with acellular structures (i.e. tectorial membrane, cupula). Under the reticular lamina, intercellular spaces are extensive too; hence outer hair cells and supporting cells stand out in a unique manner, their lateral wall free of cellular contact, in the tunnel of Corti and in connected fluid spaces. Nearly the entire structure lies on the basilar membrane, which separates the two comparatively large fluid spaces of Scala media and tympani. Hence, most of the organ of Corti relies on cellular cytoskeleton and on the relative pressure of the various fluid compartments to achieve its structural stability and its response to the tiny pressure changes of sound. the resulting visco-elastic properties of the whole organ resemble an engineer's nightmare and it is little wonder if motion at the molecular level (hair bundles, prestin) will be resolved long before motion of the whole organ is understood.

We seek to bring some information to the question of dynamic patterns of motion in the organ of Corti by applying static pressure changes to the Scala tympani in a functional *In Vitro* preparation of the Guinea pig ear. a combination of fluorescent dyes was used for positive and negative cellular labelling thus enabling us to visualize independently cells, extracellular spaces and accessory structures. Multiphoton laser scanning microscopy (Bio-Rad Microscience MRC1024ES) was used to acquire serial optical sections (xy) along the optical axis of the microscope (z). This method of image acquisition enabled us to achieve a much better signal to noise ratio in areas of the sample where no images could be acquired using standard confocal microscopy. We have thus been able to acquire images along the entire extent of a turn of the cochlea, starting at the reissner's membrane and ending at

levels below the basilar membrane. Deconvolution of images (Huygens, SVI and custom developed software) and 3-dimensional reconstruction (Imaris, Bitplane) have been used to image and compare volumes at different pressure levels. We will show motion of cellular and acellular structures as well as of fluid volumes.

## **[630] Cochlear Soft Tissue Displacement Can Be Visualized in a Closed Cochlea with Hard X-Rays**

**andrew Fishman**<sup>1</sup>, Christoph Rau<sup>2</sup>, Lixin Fan<sup>1</sup>, Claus-Peter Richter<sup>1</sup>

<sup>1</sup>Northwestern University, <sup>2</sup>Diamond Light Source

Micromechanical events in the cochlea represent the combined motions of all elements that convey vibrations from the basilar membrane to the stereocilia bundles of the inner hair cells, the sensory receptors of the mammalian cochlea. Because of the difficulty of visualizing the organ of Corti, experimental data on micromechanics are extremely limited. the present experiments will introduce a novel imaging method to visualize cochlear soft tissues without opening the cochlear wall. an in-line phase contrast imaging method using hard X-rays have been successfully used to image cochlear tissues including the basilar membrane the organ of Corti and the tectorial membrane. Furthermore, in the present experiments it was possible to image soft tissue displacements in the cochlea without opening the cochlear wall.

Experiments were made at the Advanced Photon Source (APS), Argonne National Laboratory. the APS is a synchrotron radiation source of the third generation, for which the particular characteristic is the highly coherent X-ray radiation. X-rays are generated with an undulator, inserted in a straight section of the storage ring. Images taken with hard X-rays at full field. a video flow algorithm by Lucas and Kanade was used to determine and quantify cochlear soft tissue displacements.

The results show that displacements as low as 100 nm could be visualized.

The UNICAT facility at the Advanced Photon Source is supported by the U.S. DOE under Award No. DEFG02-91ER45439, through the Frederick Seitz Materials Research Laboratory at the University of Illinois at Urbana-Champaign, the ORNL (U.S. DOE contract DE-AC05-00OR22725 with UT-Battelle LLC), the NIST (U.S. Department of Commerce) and UOP LLC. the APS is supported by the U.S. DOE, Basic Energy Sciences, office of Science under contract No. W-31-109-ENG-38. CPR is supported by a grant from the NSF (IBN-0415901).

**631 Cochlear Scala Areas and Basilar Membrane (BM) Width with the Straight and the Bent Modiolus Axis Using Micro Computed Tomography ( $\mu$ CT) Imaging**

Namkeun Kim<sup>1,2</sup>, Yong-Jin Yoon<sup>1</sup>, Charles R. Steele<sup>1</sup>, Sunil Puria<sup>1,3</sup>

<sup>1</sup>Mechanical Engineering, Stanford University, <sup>2</sup>Veterans Affairs Palo Alto, <sup>3</sup>Otolaryngology-HNS, Stanford University

Three gerbil and one chinchilla cadaver temporal bones were scanned using the  $\mu$ CT imaging, segmented, and their 3D anatomy reconstructed. the scala vestibuli (SV) which includes the scala media (SM) and the scala tympany (ST) fluid spaces are calculated along the cochlea spiral from the oval window and the round window respectively. the spiral is wound around a rotation axis through the modiolus. the axis starts at the center of the modiolus in the apical turn. the radius for the SV and the ST is considered as the distance from the rotation axis to the center of each fluid space. Particularly, the axis for rotation of cochlea spiral is not straight but bent near the basal part. Previous approaches such as magnetic resonance microscopy (MRM) imaging (Thorne et al., 1999) have not considered the bend in the basal turn. to compensate the spiral lengths and the SV area due to the bent axis, geometrical calculations were performed to transform variables such as angle and distance from the bent axis to the straight axis. Assuming that spiral starts at the same location, areas from  $\mu$ CT and MRM agree qualitatively, which provides a validation of the  $\mu$ CT method. From this  $\mu$ CT method, scala fluid spaces along the spiral length at the basal part are obtained.

Another cochlear structure of interest is the morphometry of the primary and secondary osseous spiral laminae with  $\mu$ CT imaging. in small animals where the cochlea is not surrounded by a significant amount of surrounding bone (gerbil and guinea pig), we can calculate the basilar membrane (BM) width by measuring the gap between the primary and secondary osseous spiral lamina edges. Compared to Naidu et al. (2006) using histological methods, our results are typically about 20% wider. This is likely due to the fact that the cartilaginous portion visible in histology is not imaged well in  $\mu$ CT. These morphometry measurements are important for the development of anatomically based 3D mathematical models of the cochlea.

**632 3-D Structure of Human Endolymphatic Duct and Sac: Possible Role of Gravity and Endocytosis in Transmission and Absorption of Endolymphatic Particulate and Macromolecular Material**

Leslie Michaels<sup>1</sup>, Sava Soucek<sup>2</sup>

<sup>1</sup>University College London, <sup>2</sup>St. Mary's Hospital, London

A 3-D study of the human endolymphatic duct and sac was carried out in horizontal step sections of a series of normal human temporal bones. a 3-D model of a human temporal bone published on the Internet by the Mass. Eye & Ear Hospital, Harvard, was used as a template. the narrow,

proximal region of the endolymphatic duct contains large papillary ingrowths. Beyond this region, as the sac, it widens from medial to lateral side and remains wide for the rest of its course, which is downward. it's anteroposterior extent is narrow, however, and in the extraosseous portion the two walls are usually in contact. Papillary ingrowths are frequent in the intraosseous portion. Active epithelial tubular outgrowths occupy a large part of the intraosseous sac lumen and project a short distance into the extraosseous sac. the epithelium of the tubules is often multilayered and shows granular protrusions into the lumina. Large vacuoles protrude from the surface cells and numerous macrophages, often showing apoptotic features, and eosinophilic fluid are seen in the lumina. Psammoma bodies and hyaline fibrous projections are present in older subjects.

The endolymphatic sac lies inferiorly to both the superior division (utricle and semicircular canals) and inferior division (sacculle and cochlear duct) in the endolymphatic system. There is good evidence, substantiated by the success of Epley's maneuver in the treatment of benign positional paroxysmal vertigo, that, under pathologic conditions, particulate material can be deposited by gravity in the posterior ampulla, the lowest part of the superior division of the endolymphatic system. a similar mechanism may explain the normal transmission of particulate material and also macromolecules in endolymph solution to the sac. Appearances indicate that the mode of absorption of this material may be one of endocytosis, as has been already described in the endolymphatic sac of guinea pigs by Fukazawa et al. (Anat. Rec. 1991;230:425-433).

**633 Computed Two Dimensional Reconstruction of the Human Cochlea Based On Histopathology Input**

Ophir Handzel<sup>1</sup>, Amir A. Handzel<sup>2</sup>, Darren M Whiten<sup>1</sup>, Joseph B. Nadol, Jr.<sup>1</sup>

<sup>1</sup>Massachusetts Eye and Ear Infirmary, Harvard School of Medicine, <sup>2</sup>Rahway, NJ

Computed two dimensional reconstruction of the human cochlea based on histopathology input

Two dimensional reconstruction of the cochlea is an essential tool for the study of the inner ear. Guild introduced a method for a 2-dimensional reconstruction in 1921 that has been used since to study histological sectioned by microscopy. After obtaining the pertinent data from temporal bone sections, one plots the graph using a compass and French-curve ruler. Manual drawing of the reconstructed graph is both time-consuming and adds an unnecessary inaccuracy to the reconstruction.

We developed a computerized reconstruction application is based on the MatLab software. MatLab was chosen due to its graphic capabilities, affordability and widespread availability. the input for the program is the same as for manual reconstruction: tangential points of the organ of Corti or the spiral ganglion seen in horizontal sections and the measured distances between the hook and basal cochlear regions. the output is a 2-dimensional reconstruction of the cochlea and Rosenthal's canal

projected on a scaled grid with the histological sections numbered along the y-axis. Marks at one millimeter intervals are placed along the graphs and the length of the cochlear duct and Rosenthal's canal are computed precisely.

Computerizing the reconstruction process may improve the accuracy of the graphs and expedite its plotting. the length of the cochlea, for example, is calculated based on the actual section coordinates rather than measured by marking the reconstructed graph with a compass. a computer reconstruction is readily available for corrections, presentation and incorporation into other computer-based documents. a computerized graph is potentially amendable to various types of comparison and manipulation such as superimposing mirror images in order to compare left and right sided cochlear reconstructions and for statistical analysis.

### **[634] Circumferential Filaments and the SSC: Electron Tomography of the Outer Hair Cell Lateral Wall**

**William Triffo**<sup>1</sup>, Hildur Palsdottir<sup>2</sup>, Kent McDonald<sup>3</sup>, Manfred Auer<sup>2</sup>, Robert Raphael<sup>1</sup>

<sup>1</sup>Rice University, <sup>2</sup>Lawrence Berkeley National Laboratory,

<sup>3</sup>University of California at Berkeley

A complete understanding of outer hair cell (OHC) mechanics depends on precise knowledge of intracellular structure, and efforts to model OHC physiology are likewise limited to the fidelity of known intracellular geometry. Previous studies have localized the mechanism of OHC electromotility to the cortex of the OHC, referred to as the lateral wall. the lateral wall can be viewed as a trilaminar composite made up of (1) the plasma membrane (PM), (2) a network of actin and spectrin termed the cortical lattice, and (3) lamellar stacks known as the subsurface cisternae (SSC). 3D study of lateral wall components in intact cells augments the existing model, which relies in part on 2D data obtained from partially extracted cell preparations. Because of the variability of internal membrane morphology under aldehyde EM preparation protocols, we have pursued high-pressure freezing (HPF) and freeze-substitution (FS) to preserve the SSC. Using HPF/FS cochlear samples from mouse and guinea pig, we have employed electron tomography (ET) to study the 3D structural relationship of the PM, cortical lattice, and SSC. ET utilizes a series of transmission electron microscopy projections from a tilted sample to reconstruct a volume density map, allowing us to visualize macromolecular assemblies in their native cellular context. We observe physical connections between the circumferential actin filaments and the SSC. Preliminary evidence suggests that the circumferential filaments closely follow the curvature of the SSC, even in cases where the SSC and plasma membrane curvatures differ. Combined with the pillar proteins that join the plasma membrane and cortical lattice, these actin-SSC connections provide mechanical coupling between the PM and underlying SSC, which has direct implications for current models of OHC motility.

### **[635] Immunohistochemical Localization of Ubiquitin A-52 Protein in the Mouse Inner Ear**

**Ryosuke Kitoh**<sup>1</sup>, Aki Oshima<sup>1</sup>, Nobuyoshi Suzuki<sup>1</sup>, Shigenari Hashimoto<sup>1</sup>, Yutaka Takumi<sup>1</sup>, Shin-ichi Usami<sup>1</sup>

<sup>1</sup>Shinshu University School of Medicine

Through cDNA microarray analysis of gene expression in the cochlea and vestibule, a number of genes that are highly expressed specifically in auditory tissues have been detected. Also, screening for genetic alterations in these genes has identified several possible disease-causing mutations. the ubiquitin A-52 residue ribosomal protein fusion product 1 (UbA52) gene is one of those genes highly expressed specifically in the cochlea and vestibule. This suggests that UbA52 potentially has a crucial functional role in the inner ear and may have relevance to hearing disorders. Through cellular localization we immunocytochemically investigated its function in the inner ear. in the adult mouse, UbA52 protein was distributed in the stria marginal cells and vestibular dark cells, which regulate the endolymphatic ion homeostasis. in the developing mouse cochlea, no significant staining was observed from birth to postnatal day 3, whereas after postnatal day 6, strong UbA52-immunoreactivities were observed in stria marginal cells. Endolymphatic K<sup>+</sup> concentration is elevated between postnatal days 3 to 8, therefore our results indicate that UbA52 may have a functional role in regulation of ion secretion in the inner ear. in the inner ear, the proteins of ubiquitination targets or enzymes are still unknown, and further study of those proteins may provide new pathological models of inner ear disorders.

### **[636] Vascular Gap Junction Protein Expression in the Cochlear Lateral Wall**

**Xiaorui Shi**<sup>1</sup>, Hiroshi Yamamoto<sup>1</sup>, Christopher Stauffer<sup>1</sup>, Alfred Nuttall<sup>1</sup>

<sup>1</sup>Oregon Health and Science University

The essence of vascular function is cellular coordination (Figuroa et al., 2004, *Microvasc Res*; de Wit et al., 2006, *Biol Chem*). in particular, cell-to-cell communication through gap junctions is important for many biological processes including rapid transmission of electrical signals and the intercellular propagation and synchronization of physiological processes between adjacent cells within a tissue. in this study, using the immunohistochemistry combined with confocal microscopy technique and western blot analysis, we found that pericytes on the vessels of the spiral ligament have Connexin 40 (Cx 40) and Connexin 37 (Cx 37). in particular, Cx 40 was abundantly expressed in both endothelial cells and pericytes of the vessel of the spiral ligament. Also Cx 40 was intensively expressed in the intermediate-like cells of the stria vascularis. There was no Cx 37 and Cx 40 signal in the endothelial cells and the pericytes of the stria vascularis vasculature. Also no detectable Connexin (Cx 43) was found in the vessels of the spiral ligament and the stria vascularis. Our results are different from studies that assessed Connexin expression in the retinal or brain pericytes which do express Cx 43. the variation of Connexin expression in the different vasculatures may have important consequences for the



difference of coordination and propagation of vascular signals and responses. the regional expression heterogeneity of Cx 40 and Cx 37 indicates functional and structural heterogeneity of pericytes in the vessels of the spiral ligament and the stria vascularis.

Supported by NIH NIDCD DC 000105, DC 005983

### **[637] Exposure of the Ultrastructural Components of Amphibian and Mammalian Inner Ear Sensory Epithelia**

**Ruth Taylor<sup>1</sup>, Andrew Forge<sup>1</sup>**

<sup>1</sup>*University College London*

organisation of the cytoskeletal components contribute to the overall architecture in inner ear sensory epithelia that allows for the efficient transduction of sound and vibration to the central processing regions. Mutations in genes responsible for these components result in deafness. the aim of this study is to examine the ultrastructure of the cytoskeleton through high resolution visualisation of the cells of the inner ear sensory epithelia by SEM. Following incubation with detergent to demembranate tissue, filamentous structures are revealed at the apical surface of supporting cells. At the level of tight junctions microfilament networks are connected to the plasma membrane via crosslinks in both supporting cells and hair cells. in newt inner ear epithelia, microfilaments can be seen within stereocilia together with connecting crosslinks. in addition to visualising structural components immunogold labelling can be utilised to localise elements at a molecular level. Here we show the microtubules of pillar cells labelled with immunogold using back-scatter detection in SEM. These methods allow the examination of three dimensional relationship between ultrastructural components not only in the normal tissue but also enable the changes that occur during repair and regeneration to be determined.

### **[638] PKC Beta II Expression in the Rat organ of Corti**

**Sabine Ladrech<sup>1</sup>, Jing Wang<sup>1</sup>, Hassan Boukhaddaoui<sup>1</sup>, Jean-Luc Puel<sup>2</sup>, Michel Eybalin<sup>1</sup>, Marc Lenoir<sup>1</sup>**

<sup>1</sup>*INSERM 583 - INM, <sup>2</sup>INSERM 583 - INM and University Montpellier I*

Several phosphorylation pathways (among others: Dulon et al., 1990, *J. Neurosci.*, **10**, 1388-1397; Szonyi et al., 1999, *Hear. Res.*, **137**, 29-42; Zhang et al., 2003, *J. Biol. Chem.*, **278**, 35644-35650) are thought to mediate the regulation of OHC slow and fast motility. Moreover, Protein kinase C (PKC) is believed to be involved in repair and protection of spiral ganglion neurons (Lerner-Natoli et al., 1997, *Brain Res.*, **749**, 109-119; Lallmend et al., 2005, *J. Cell Sci.*, **118**, 4511-4525) and hair cells (Chung et al., 2006, *J. Assoc. Res. Otolaryngol.*, **7**, 373-382) in various stress conditions. Here, we studied the expression of the calcium dependant PKC beta II isoform in the rat organ of Corti at different postnatal ages using immunocytochemistry.

PKC beta II was expressed as early as postnatal day (PND) 5 in efferent axons running in the inner spiral bundle, in efferents targeting outer hair cells (OHCs) and

in Hensen cells. At PND 8, a slight expression of PKC beta II was also seen at the OHC synaptic pole in the basal and middle cochlear turns. At PND 12, PKC beta II expression declined in the efferent fibres contacting OHCs whereas expression concentrated at the postsynaptic membrane. the adult-like pattern of PKC beta II distribution was observed at PND 20. Throughout the cochlea, we found PKC beta II expression at the OHC postsynaptic membrane facing the medial efferent endings, in lateral efferent terminals of the inner spiral bundle and in the Hensen cells. in the apical cochlear region, PKC beta II was additionally expressed at the lateral cell membrane of Deiters and Claudius cells. the data suggest an involvement of PKC beta II in both cochlear efferent neurotransmission and ion homeostasis.

### **[639] FXYP6, a Novel Cochlear Regulator of Na,K-ATPase**

**Benjamin Delprat<sup>1</sup>, Jean-Luc Puel<sup>1</sup>, Kaethi Geering<sup>2</sup>**

<sup>1</sup>*Inserm-UMR 583 and Université de Montpellier 1, 80, rue Augustin Fliche, 34295 Montpellier, France, <sup>2</sup>Department of Pharmacology and Toxicology, Rue du Bugnon 27, 1005 Lausanne, Switzerland*

The family of mammalian FXYP proteins contains 7 members, 6 of which have been identified as regulators of Na,K-ATPase. Each FXYP protein modulates the transport properties of Na,K-ATPase e.g. its Na<sup>+</sup> and/or its K<sup>+</sup> affinity in a distinct way which is adapted to the physiological needs of the tissue in which it is expressed.

We have characterized FXYP6, the last FXYP protein of unknown function. After expression in *Xenopus* oocytes, FXYP6 associate with alpha1-beta1, alpha2-beta1, alpha3-beta1 isozymes. Either in non differentiated or differentiated PC12 cells, FXYP6 can be co-immunoprecipitated with Na,K-ATPase. in *xenopus* oocytes, FXYP6 decreases the apparent K<sup>+</sup> affinity of Na,K-ATPase over the more positive membrane potentials and also decrease the apparent Na<sup>+</sup> affinity. FXYP6 is mainly expressed in the brain. Interestingly, the protein is found in the cochlea where it is expressed in various epithelial cells bording the endolymph and in the auditory neurons. Moreover, FXYP6 colocalizes with Na,K-ATPase in stria vascularis and is co-immunoprecipitates with Na,K-ATPase. These results suggest a role of FXYP6 in endolymph homeostasis.

So in conclusion, our studies show that FXYP6 protein is a tissue-specific modulator of Na,K-ATPase. However, we cannot exclude that FXYP6 protein may have other functions which need to be determined.

### **[640] Relative Time Course of Degeneration of Lateral Wall Fibrocytes and organ of Corti in the CD-1 Mouse Model of Presbycusis**

**David Furness<sup>1</sup>, Emma Blake<sup>1</sup>, Shanthini**

**Mahendrasingam<sup>1</sup>**

<sup>1</sup>*Keele University*

Five distinct types of fibrocyte (I – V) occur in the cochlear lateral wall and are important in homeostasis and maintenance of the endocochlear potential. Fibrocyte degeneration precedes hair-cell loss in some animal models of presbycusis and underlies hereditary deafness

in DFN3 (Minowa et al., 1999; Science 285, 1408-1411). Replacement with stem cells or stimulating fibrocyte regeneration may thus be a means of preventing or ameliorating presbycusis. In this study we are evaluating the CD-1 mouse as a model for intervention in fibrocyte degeneration. To determine the time course of degeneration, cochleae from 3 to 20 week-old mice were glutaraldehyde and osmium fixed and embedded for transmission electron microscopy (TEM). The relative role of different fibrocytes was also assessed: (i) to examine mitochondrial function cochleae were fixed for 15 min in paraformaldehyde (pfa), incubated in DAB for 3 hours, postfixed and prepared for TEM; (ii) to quantify distributions of Na<sup>+</sup>/K<sup>+</sup>ATPase, cochleae were fixed in pfa (2 h), embedded in LR White and sectioned for post-embedding immunogold labelling. At 5 weeks, the organ of Corti was intact whilst there was evidence of cellular degeneration in all fibrocytes, such as mitochondrial swelling, cytoplasmic and nuclear disruption which progressed with age. Cellular disruption was noted in hair cells at 10 weeks, and became progressively more significant, but lagged behind changes in the fibrocytes. Fibrocyte types V and II showed the greatest mitochondrial activity and the strongest labeling for Na<sup>+</sup>/K<sup>+</sup>ATPase. These data suggest that fibrocyte degeneration and homeostatic failure could lead to hair-cell degeneration in CD-1 mice, making this a suitable model for exploring prevention of presbycusis by fibrocyte restoration. They also identify the type V and II fibrocytes as those that may make the greatest contribution to homeostasis, and thus the most appropriate types to attempt to replace. Supported by Deafness Research UK.

#### **[641] Age-Associated Microvascular Disease and Endocochlear Potential (EP) Reduction in NOD.NON-H2<sup>nb1</sup> Mice**

**Kevin K. Ohlemiller<sup>1</sup>**, Patricia M. Gagnon<sup>1</sup>

<sup>1</sup>*Washington University School of Medicine*

Microvascular disease and autoimmunity are proposed as a basis for some strial age-related hearing loss (ARHL). In a survey of aging inbred mouse strains, we noted that some NOD.NON-H2<sup>nb1</sup> mice show EP reduction after 6 mos. These mice are congenic to NOD/ShiLtJ, which show polygenic autoimmune pathology, and are used as a model of autoimmune-based Type I diabetes. The NOD.NON-H2<sup>nb1</sup> line was created by crossing NOD/ShiLtJ mice to NON/LtJ mice to incorporate the H2<sup>nb1</sup> allele. The congenics retain autoimmune tendencies, but are not diabetic; However, they carry both Cdh23<sup>ah1</sup> and Ahl2, and show progressive hearing loss from an early age (Johnson and Zheng 2002; Johnson et al., 2000). We sought to identify the cellular correlates of EP reduction in the congenic line, and to determine whether EP decline may be independent of Cdh23<sup>ah1</sup> and Ahl2.

22 mice (mixed M/F) aged 2-26 mos were examined. Few outer hair cells remained after 6 mos, and few inner hair cells (IHCs) remained after 1 yr. The time course of afferent neuronal loss was similar to that for IHCs, so that neuronal loss appeared secondary to IHC loss. Average basal turn EP fell from 110 mV at 2 mos to 63 mV after 6 mos. EPs measured at 6-24 mos ranged from 27-102 mV. The clear

anatomical correlate of EP reduction was strial degeneration, beginning in the cochlear base and apex. Strial loss was preceded by loss of capillaries; Avascular segments of stria and densely stained capillary debris were frequently observed. Within the modiolus, fibrocytes surrounding the spiral modiolar artery showed patches of dense staining resembling those seen in Palmerston North (lupus) mice (Trune et al., 1991).

NOD.NON-H2<sup>nb1</sup> mice do not show outward autoimmune disease, but undergo strial degeneration suggestive of immune attack on strial vessels. We speculate that this pathology is genetically influenced, but independent of Cdh23<sup>ah1</sup> and Ahl2. These mice may model strial ARHL arising from otherwise subclinical immune dysfunction.

#### **[642] Endocochlear Potential (EP) Reduction in Albino Coisogenics to C57BL/6 Inbred Mice After 24 Months of Age**

**Kevin K. Ohlemiller<sup>1</sup>**, Patricia M. Gagnon<sup>1</sup>

<sup>1</sup>*Washington University School of Medicine*

Strial age-related hearing loss (ARHL) represents a mix of environmental and genetic factors. To date, the best animal models are gerbils (Spicer and Schulte 2005), and BALB/c (Bagg albino) mice (Ohlemiller and Gagnon 2006), both of which show age-related EP reduction tied to degeneration of strial marginal cells. While no candidate loci for strial ARHL have been identified, genes that affect the production of melanin pigment are of interest. Melanin may act as an antioxidant, and also binds toxins and Ca<sup>2+</sup>. To our knowledge, no well-controlled study of the effect of melanin's absence has been performed. This requires comparison of subjects differing only in melanin production. We compared cochlear basal turn EP and strial appearance in C57BL/6 (B6; n=121) mice and coisogenic C57BL/6-Tyr<sup>c-2J</sup> (B6 albino; n=86) mice at ages ranging 2-30 mos.

Mean EPs were similar in 2 mo albino B6 (110.3 mV) and B6 (110.6 mV). EP decline was noted only in B6 albinos after 24 mos of age. Mean EP in old albinos (94.2 mV; range: 47-113 mV) was significantly lower than in young albinos, or in old B6 (103.9 mV). Only 6 of 21 (29%) of old albinos showed an EP below 90 mV. No effect of gender was apparent. Morphometric analysis of the upper basal turn in 21 albino cochleas revealed no cell or strial loss that predicted EP decline.

B6 albino coisogenic mice may show late-life EP decline not seen in pigmented B6 mice. Loss of protective actions of melanin may magnify environmental or stochastic influences, such that ~30% of albinos show EP reduction after 24 mos. Thus genes that impact the form, concentration, or distribution of melanin may participate in the appearance of strial ARHL. B6 albinos join BALB/c as mouse models displaying late-life EP decline. However, the two strains show key differences in that 1) Young BALBs show lower EPs than B6; and 2) EP decline in BALBs can be predicted by marginal cell loss. Thus the present results in B6 albinos do not explain EP decline in BALB/c mice.

### **643 The Role of Caveolin; is It New Molecular Target for Modulation of Aging Process in Cochlear Hair Cells ?**

**Yoon-Gun Jung**<sup>1</sup>, Kyu Sung Kim<sup>1</sup>, Seung Ho Lee<sup>1</sup>, Dong-Youl Lee<sup>1</sup>, Hoseok Choi<sup>1</sup>

<sup>1</sup>*Department of Otorhinolaryngology, Inha University College of Medicine*

According to the gate theory, certain biomolecules such as caveolins, amphipysins, G proteins, and integrins play decisive roles in determining the senescent phenotype and thus provide targets for modulating the aging process. Among these molecules, caveolin can associate with a variety of regulatory and structural molecules via their scaffolding domains and thereby influence a broad spectrum of biological phenomena including both the physiology and morphology of the senescent cells.

If caveolin may be a component on the deterministic nature on aging, we think that also in cochlear hair cells it become molecular target for modulation of aging process. First we investigated the basal expression of caveolin-1, caveolin-2, caveolin-3, NOS and SOD in UB/OC-1 cells (cochlear hair cells). and then with the use of RNA interference technique, we wanted to know whether down-regulation of caveolin influence telomerase activity and reactive oxygen species (ROS) production in cochlear hair cells.

The result was that there was presence of caveolin-1 chiefly in UB/OC-1 hair cells and down-regulation of Caveolin-1 reduced protein kinase a (PKA) activity. Telomerase was activated by caveolin down-regulation and caveolin down-regulation inhibits oxidative stress in mitochondrial level.

in conclusion, down-regulation of caveolin-1 reduces oxidative stress in mitochondrial level.

and down-regulation of caveolin-1 induces decrease of PKA activity. Telomerase activity is increased by down-regulating caveolin-1 or by PKA inhibitor, thus caveolin-1 may have anti-aging effect in cochlear cells with or without relation to PKA.

### **644 Phosphoinositide Signaling in Age-Related Hearing Loss**

**Su-Hua Sha**<sup>1</sup>, Fu-Quan Chen<sup>1</sup>, andra Talaska<sup>1</sup>, Jochen Schacht<sup>1</sup>

<sup>1</sup>*Kresge Hearing Research Institute*

The mechanisms responsible for age-related hearing loss are multi-factorial and largely unknown. However, it has become clear from studies in aging tissues including the cochlea that oxidant stress can lead to compromised redox-homeostasis. an initial reaction of the cells is to restore and maintain their balance via the activation of homeostatic signaling pathways. Phosphoinositide signaling is a well characterized stress-induced response, controlling diverse processes including cytoskeletal organization, cell survival and cell death pathways.

Phosphatidylinositol 4,5-bisphosphate (PIP<sub>2</sub>) and phosphatidylinositol 3,4,5-trisphosphate (PIP<sub>3</sub>) are the major signaling molecules, interconvertible by phosphorylation (PI3-kinase) and dephosphorylation

(PTEN phosphatase). We have previously shown that shifting the balance between PIP<sub>2</sub> and PIP<sub>3</sub> with aminoglycoside antibiotics affects downstream pathways of cell survival mediated by p-Akt and gene expression mediated by histone acetylation (Jiang et al., 2006). in this study, we investigate changes in phosphoinositide signaling with age in the cochlea of CBA/J mice. a PIP<sub>2</sub>/PIP<sub>3</sub> imbalance may arise from an increase in PTEN activity from 3 months to 18 months. Akt and p-Akt decrease with age, indicating compromised homeostatic pathways. in addition, histone acetylation was diminished from 3 months to 23 months, suggesting an impact of these age-related changes on gene transcription. the sum of these data indicates that phosphoinositide signaling in the aged inner ear may contribute to the death of outer hair cells in presbycusis.

This study was supported by program project grant AG-025164 from the National Institute of Aging and core grant P30 DC-05188 from the National Institute on Deafness and Other Communication Disorders, NIH.

### **645 Reduction of OHC Motor Protein (Prestin) in Aged Rats**

**Guang-Di Chen**<sup>1</sup>, Man-Na Li<sup>1</sup>, Eric Bielefeld<sup>1</sup>, Chiemi Tanaka<sup>1</sup>, Donald Henderson<sup>1</sup>

<sup>1</sup>*SUNY at Buffalo*

Twenty-four month old Fischer 344 rats typically have a 20-40-dB threshold shift in the frequency range of 2 to 40 kHz compared to the Fischer rats at an age of 3 months (young rats). Previous research (Bielefeld et al., 2008) showed that the aged rats may have an up to 10% outer hair cell (OHC) loss in the cochlear region of 20-90% from the apex, but without significant inner hair cell (IHC) loss. the limited OHC loss can not explain the magnitude of the hearing loss. OHCs are known to contribute to the cochlear sensitivity via their motile activity (electromotility). We hypothesize that some of the surviving OHCs are dysfunctional in the cochlear active process, leading to a loss of cochlear amplification. This experiment measured OHC motor protein, prestin, in the surviving OHCs. the results showed that many surviving OHCs had reduced prestin level, most likely indicating a loss or reduction of OHC electromotility. the data suggest that degradation of OHC motor protein may be one of the contributors to age-related hearing loss.

This study was supported by NIH grant 1R01DC00686201A1

### **646 Cellular and Molecular Mechanisms of Presbycusis**

**Jing Wang**<sup>1</sup>, ladrech Sabine<sup>1</sup>, Julien MENARDO<sup>1</sup>, Jérôme Ruel<sup>1</sup>, Guy Rebillard<sup>1</sup>, Michel Eybalin<sup>1</sup>, Marc Lenoir<sup>1</sup>, Jean-Luc Puel<sup>1</sup>

<sup>1</sup>*INSERM U583*

Presbycusis, an age related hearing loss has been attributed to degeneration of the sensory hair cells, the stria vascularis, and/or the ganglion neurons. This loss of cochlear cells can be due to environmental factors such as ototoxic drugs (aminoglycosides, quinine, and cisplatin) or

overexposure to noise, as well as genetic factors. Once lost, the sensory hair cell or the ganglion neurons are not replaced by new ones, making hearing loss irreversible. Thus, any strategy to protect the stria vascularis, sensory hair cells and/or ganglion neurons from environmental-related and/or genetic-related progressive hearing loss may contribute to the development of treatment against presbycusis.

The aim of this study is to investigate the cellular and molecular mechanisms of degeneration of the stria vascularis, sensory hair cells and ganglion neurons in a well-known mouse model of senescence, the senescence-accelerated prone mouse strain 8 (SAM-P8) and resistant 1 (SAM-R1), these mouse strains have proven useful in elucidating aspects of aging processes. Results obtained with these mice are compared with those obtained with C57/BL6J mice, an early onset age-related hearing loss mouse model.

Our results indicate that the progressive hearing loss is a complex phenomenon involving various cochlear structures: sensory cells, neural cells and strial cells and that some important cell death signalling pathways are involved in the degeneration of cochlear cells in both SAM-P8 and C57/BL6J strains.

Well understanding molecular cascades involved in the progressive deterioration of the auditory function is important to develop pharmacological strategies targeted to each type of progressive deafness.

#### **647 The Expression of Heat Shock Proteins in the Cochlea of DBA/2J Mice**

Kazuma Sugahara<sup>1</sup>, Takefumi Mikuriya<sup>1</sup>, Yoshinobu Hirose<sup>1</sup>, Yuji Miyauchi<sup>1</sup>, Makoto Hashimoto<sup>1</sup>, Hiroaki Shimogori<sup>1</sup>, Hiroshi Yamashita<sup>1</sup>

<sup>1</sup>*Department of Otolaryngology, Yamaguchi University, Graduate School of Medicine*

In the previous meeting, we reported that the heat shock proteins play the great role in the protection of the hair cells against the stress. in many kinds of cells, the heat shock proteins prevent the cell death against the stresses. DBA/2J mice were well-known as the animal model of age-related hearing loss. It was reported that the expression of heat shock proteins was suppressed in the cell death regarding aging. in the present study, we investigated the expression of heat shock proteins in the cochlea of DBA/2J mice. CBA/N mice were used for control. DBA/2J and CBA/N mice were sacrificed at 1, 3, 6, 9 months after birth. the expression of hsp110, hsp90, hsp70, hsp60, hsp40, and hsp27 were assayed with western-blot analysis. the expression of hsp90, 60, 40, 27 were reduced in both of aged DBA/2J and aged CBA/N mice. in contrast, the expression of hsp70 was not suppressed in aged CBA mice. the results suggest that hsp70 may affect the progress of age-related hearing loss.

#### **648 Age-Related Hearing Loss: Aquaporin 4 Gene Expression Changes in the Mouse Cochlea and Auditory Midbrain**

Nathan Christensen<sup>1</sup>, Mary D'Souza<sup>1</sup>, Xiaoxia Zhu<sup>1</sup>, Martha Zettel<sup>1</sup>, Robert Frisina<sup>1</sup>

<sup>1</sup>*Univ. Rochester Medical School*

Aquaporins comprise a family of proteins composing cell membrane channels or pores that play the important role of regulating water flow in the body, including rapid transport of water molecules through the cell membrane. They are particularly involved in central nervous system homeostasis, cerebrospinal fluid formation, and responses to traumatic brain injury. in addition, aquaporins—and specifically Aqp4—play an important role in the maintenance of normal hearing function. the present investigation aimed at exploring gene expression changes for Aqp4 in the cochlea and auditory midbrain – inferior colliculus. Four groups of CBA mice were defined based upon their age and hearing levels (as determined by ABR thresholds and DPOAE amplitudes): 1) Young controls, 2) Middle-aged with good hearing, 3) Old with mild presbycusis, and 4) Old with severe presbycusis. DNA-Microarray RMA normalized data yielded Aqp4 gene expression changes with the M430A Microarray GeneChip. Log Signal Ratios (LSR) from the probe-sets were subjected to the following statistical analyses: 1) One-way ANOVA, 2) Linear Regression of LSR vs. ABR or DPOAE, and 3) Fold changes in microarray gene expression. by gene microarray analysis and quantitative real-time PCR verification, Aqp4 is seen to be **down-regulated** in the mouse auditory midbrain as the mouse ages, with a subsequent **up-regulation** with the development of severe presbycusis. in addition, Aqp4 expression is **down-regulated** in the mouse cochlea with the progression of presbycusis from middle age to old age. Much work remains to be done to thoroughly understand the causal chain of events underlying the pathogenesis of presbycusis, but the changes seen here in Aqp4 gene expression likely play an important role in K<sup>+</sup> recycling deficits in the course of presbycusis, in a mouse model of age-related hearing loss.

[Supported by NIH: NIA, NIDCD]

#### **649 Sources and Variability of Noise in Rodent Vivariums: an Uncontrolled Variable with Implications for Studies of Age-Related Hearing Loss**

Amanda Lauer<sup>1</sup>, Bradford May<sup>1</sup>, Julie Watson<sup>1</sup>

<sup>1</sup>*Johns Hopkins University*

Modern rodent housing facilities are designed for meticulous control and monitoring of environmental variables such as lighting, temperature and humidity, ventilation, and infection control in order to enhance animal health and decrease extraneous factors that may affect experimental outcomes. However, the amount of noise in these facilities is rarely monitored or controlled. Many studies have identified behavioral and physiological effects of noise on laboratory animals. Multiple studies have shown that minor variations in an animal's

environment can affect the outcome of various phenotyping measures. We monitored sound levels in three different rodent housing facilities to provide an extensive characterization of the variability and sources of noise within these facilities. We show that sound levels can vary markedly across different housing facilities within the same institution. Rooms with microisolation cages with ventilation motors located inside the animal room showed the highest sound levels. Levels were relatively low in a room with static filter-top cages. Levels were intermediate in rooms with microisolation cages with ventilation motors located outside the animal room. Animal care activities, biosafety cabinets, and experimenter traffic within the animal rooms produced a significant amount of noise in addition to noise associated with air exchange systems. Uncontrolled acoustic environments in rodent housing facilities may introduce unwanted variability, particularly in studies of age-related hearing loss. the timecourse of hearing loss may be accelerated in some mice when chronically exposed to moderate to high noise levels.

#### **[650] CL4 Epithelial Cells: a Model System for Examining the Targeting, Interactions and Activities of the Hair Cell Proteins Cadherin 23, Harmonin, Whirlin, Myosin Xva, Espin, Prestin and TRPML3**

Lili Zheng<sup>1</sup>, Jing Zheng<sup>1</sup>, Donna Whitton<sup>1</sup>, Jaime Garcia-Anoveros<sup>1</sup>, **James Bartles<sup>1</sup>**

<sup>1</sup>*Northwestern University*

We are using LLC-PK1-CL4 epithelial cells (CL4 cells) as an experimental system in which to reconstitute selected aspects of hair cell structure and function and examine the effects of deafness mutations. These cells readily establish apical-basolateral plasma membrane polarity when cultured on glass coverslips and are easy to transfect with multiple constructs. Upon transfection with espins, the short brush border microvilli of CL4 cells elongate to yield structures reminiscent of stereocilia, vastly improving spatial resolution for confocal microscopy. Here, we have used this system to examine the targeting, interactions or activities of proteins required for normal hearing: cadherin 23 (cdh23), harmonin, whirlin, myosin XVa, espin, prestin and TRPML3. When expressed in CL4 cells, FLAG-cdh 23 was efficiently targeted to the microvillar (apical) plasma membrane. GFP-harmonin was detected in the cytoplasm and nucleus, but became efficiently targeted to microvilli when co-expressed with FLAG-cdh23. Mutagenesis revealed that the harmonin PDZ1 domain was necessary and sufficient for binding to cdh23 and ascribed the binding site for the harmonin PDZ1 domain to a peptide in the central region of the cdh23 tail. When co-expressed with untagged myosin XVa and espin, GFP-whirlin was efficiently targeted to the tips of espin-elongated microvilli. When expressed in CL4 cells, prestin was targeted to the basolateral domain, whereas pendrin, a different member of the SLC26 family of multifunctional anion exchangers, was targeted to the microvillar plasma membrane. Through comparisons of pendrin-prestin chimeras we identified a dominant basolateral targeting signal in the cytoplasmic tail of prestin. When co-expressed with

untagged espin, TRPML3-GFP was targeted to the espin-elongated microvilli and to cytoplasmic vesicles. Interestingly, TRPML3-GFP bearing the varitint-waddler (Va) A419P deafness mutation caused CL4 cells to be extruded from the epithelial monolayer and die.

#### **[651] Apical Targeting of Tecta and Tectb in CL4 Epithelial Cells**

P. Kevin Legan<sup>1</sup>, Kelli R. Phillips<sup>2</sup>, Richard J. Goodyear<sup>1</sup>, Lindsey J. Welstead<sup>1</sup>, Lili Zheng<sup>3</sup>, James R. Bartles<sup>3</sup>, Janet L. Cyr<sup>2</sup>, **Guy P. Richardson<sup>1</sup>**

<sup>1</sup>*University of Sussex*, <sup>2</sup>*West Virginia University School of Medicine*, <sup>3</sup>*Northwestern University School of Medicine*

Tecta (alpha-tectorin) and Tectb (beta-tectorin) are major non-collagenous components of the tectorial and otoconial membranes of the inner ear. Both molecules are glycoproteins that are secreted from the apical surfaces of supporting cells during inner ear development. Tecta (~250 kDa) is composed of several modules: a C-terminal zona pellucida (ZP) domain, a central region comprising three full and two partial von Willebrand Type D repeats and an N-terminal region with homology to the G1 domain of entactin. Tectb (~45 kDa) contains a single ZP domain. the predicted amino acid sequences of the tectorins indicate that both are expressed as membrane-bound, glycosyl phosphatidyl inositol (GPI)-linked precursors that are targeted to the apical surfaces of supporting cells by virtue of their GPI tails and released from secretory vesicle membranes by the action of a furin-like endo-proteinase that recognizes a tetrabasic cleavage site located adjacent to the site of GPI addition.

Full-length cDNA clones encoding either Tecta or Tectb were transfected into CL4 epithelial cells together with GFP-tagged espin, which promotes the formation of elongated microvilli at the apical surface of the cells. Cells were fixed at 24-, 48- and 72-hours posttransfection, immunolabelled for Tecta or Tectb, and examined by confocal microscopy. At 24- and 48- hours posttransfection, strong expression of Tecta and Tectb was observed associated with the espin-induced elongated microvilli. Moreover, discrete punctae of tectorin labeling were often observed at the tips of the elongated microvilli. Surface labeling levels decreased substantially as a function of time, suggesting that the tectorins may be secreted into the medium. These results suggest the CL4 cell line is a valuable tool for studying the expression and targeting of the tectorin proteins *In Vitro*.

This work is supported by the Wellcome Trust (GPR) and NIH/NIDCD grants R01DC6402 (JLC) and R01DC004314 (JRB).

#### **[652] Expression of EGFP-Tagged Inositol Phospholipid Reporters in Early Postnatal Cochlear Hair Cells**

**Gowri Nayak<sup>1</sup>**, Richard Goodyear<sup>1</sup>, Guy Richardson<sup>1</sup>

<sup>1</sup>*University of Sussex, United Kingdom*

Inositol phospholipids are key components of many signalling pathways, including those that regulate the actin cytoskeleton. the hair-cell antigen/Ptprq is a receptor-like

inositol lipid phosphatase that is expressed in the sensory hair bundle (Oganesian et al., 2003; Goodyear et al., 2003). In hair cells of the frog sacculus, immunofluorescence studies have shown that Ptpqr and phosphatidyl inositol (4, 5) biphosphate (PI-4,5 P<sub>2</sub>) are distributed in a reciprocal fashion, with PI-4,5 P<sub>2</sub> being absent from the basal regions of the hair bundle where Ptpqr is expressed at high levels (Hirono et al., 2004). In this study, EGFP-tagged reporters were used to examine the distribution of inositol phospholipids in the hair cells of the early postnatal mouse cochlea.

Reporters for PI-4 P (the pleckstrin-homology [PH] domain of FAPP1), PI-4,5 P<sub>2</sub> (PH domain of PLC  $\beta$ 1), PI-3,4 P<sub>2</sub> (PH domain of TAPP1) and PI-3,4,5 P<sub>3</sub> (PH domains of GRP1 and PKB) all label the sensory hair bundle. Reporters for PI-3 P (PEPP1 and TAFF1) did not label the hair bundle. PEPP1 labelled the basolateral membrane and the tight-adherens junction, whereas TAFF1 labelled cytoplasmic granules thought to be part of the endosomal system. Strong labelling of the basolateral membrane was also observed with the EGFP-tagged PLC  $\beta$ 1-PH domain. Reporter distribution in the hair bundles of mice homozygous for a deletion of the catalytic domain of Ptpqr was similar to that observed in heterozygous or wild type mice suggesting other inositol phospholipids, e.g., PI-5 P or PtdIns 3,5 P<sub>2</sub>, may be substrates for Ptpqr.

Supported by the RNID and the Wellcome Trust.

### **653 The Role of PTPRQ and Myosin VI in Maintaining the Shape of Stereocilia**

**Hirofumi Sakaguchi**<sup>1</sup>, Joshua Tokita<sup>2</sup>, Moshe Naoz<sup>3</sup>, Daniel Bowen-Pope<sup>4</sup>, Nir S. Gov<sup>3</sup>, Bechara Kachar<sup>2</sup>

<sup>1</sup>Kyoto Prefectural University of Medicine, <sup>2</sup>NIDCD/NIH,

<sup>3</sup>The Weizmann Institute of Science, <sup>4</sup>University of Washington

Stereocilia are specialized microvilli, which have a unique structural feature at the base known as the tapered base. Little is known about how disassembly of actin filaments is regulated and how membrane constriction is achieved at the base. Based on the localization of PTPRQ and myosin VI in the tapered base, and the similarities in stereocilia phenotypes in the mutant mice for these proteins, we postulate that these two proteins participate in a common molecular system at the stereocilia base. In our model, myosin VI cross-links the underlying cytoskeleton to the plasma membrane by interacting with the cytoplasmic domain of PTPRQ. The extracellular domain of PTPRQ maintains the membrane curvature and the PIPase activity of PTPRQ influences actin depolymerization. The concerted action of these two proteins molds the base of the stereocilia into its characteristic tapered shape. Using immunohistochemistry, we confirmed that both ectodomain and cytodomain of PTPRQ are localized to the base of stereocilia. In the myosin VI mutant Snell's waltzer mice, PTPRQ was distributed along the stereocilia shaft and not restricted to the base. SEM studies demonstrate that PTPRQ-KO mice lack the tapered base, similar to the Snell's waltzer mice. We evaluated the possible interaction of PTPRQ and myosin VI using *In Vitro* cotransfection assays in COS-7 cells. Colocalization of the Catalytic domain of PTPRQ and GFP-myosin VI raised the

possibility that these proteins could form a functional complex. We also observed that overexpression of PTPRQ could induce elongation of microvilli on the surface of supporting cells as well as the formation of filopodia in COS-7 cells. Elongation of the actin protrusions was induced by PTPRQ with cytodomain-deleted mutation, suggesting that the ectodomain of PTPRQ may contribute to stabilization or promotion of the actin protrusion.

### **654 Position of Calcium Entry Into the Outer Hair Cell Stereocilia**

**Csaba Harasztosi**<sup>1</sup>, Anthony W. Gummer<sup>1</sup>

<sup>1</sup>University Tübingen, Section of Physiological Acoustics and Communication

Crucial steps involved in the mechanoelectrical transduction (MET) process still remain obscure. It is well known that Ca<sup>2+</sup> is involved in the process, regulating fast and slow adaptation. In an attempt to locate the positions of the MET channels, here we examine dynamics of free Ca<sup>2+</sup> concentration change that occurs upon stereocilia (SC) deflection. This is achieved by fluorescence recording of the free Ca<sup>2+</sup> concentration in the hair bundle of outer hair cells (OHCs).

OHCs were mechanically isolated from the adult guinea-pig cochlea. Ca<sup>2+</sup> transients were evoked by fluid-jet stimuli. To facilitate Ca<sup>2+</sup> entry into the hair bundle, Ca<sup>2+</sup> concentration in the fluid-jet solution was 4 mM (extracellular 100  $\mu$ M). The Ca<sup>2+</sup> concentration changes were monitored using the acetoxymethyl ester form of the fluo-3 dye and confocal laser-scanning microscopy.

Mechanical stimulation evoked exponential increase of intracellular Ca<sup>2+</sup> concentration in the SC. The time constant ( $\tau$ ) was shortest in the top region of the middle SC ( $\tau=37\pm2$  ms).  $\tau$  increased with distance along the SC towards the cuticular plate (CP) amounting to a factor of about 6. The time constant for the top region ( $\tau=313\pm54$  ms) of the longest SC was approximately independent of position along the SC. The fluorescence signal in the CP also increased exponentially, with  $\tau=207\pm23$  ms of the same order as that in the longest SC. A MET channel blocker (10  $\mu$ M Gd<sup>3+</sup>) increased the time constant in the shorter but not the longest SC; the increase was ten fold, thus yielding a value similar to that seen in controls for the longest SC.

The experimental data suggest that Ca<sup>2+</sup> enters the shorter SC locally from the extracellular fluid through the MET channels. Using a model of Ca<sup>2+</sup> dynamics (see poster: A. Srinivasan et al.), we suggest that the slow Ca<sup>2+</sup> signal recorded in the longest SC is the result of passive Ca<sup>2+</sup> diffusion from the CP. Therefore, we conclude that the MET channels are located at the lower end of the tip links.

### **655 Modelling of the Dynamics of $\text{Ca}^{2+}$ Concentration in Outer Hair Cell Stereocilia**

Arunkumar Srinivasan<sup>1</sup>, Csaba Harasztosi<sup>1</sup>, Anthony W. Gummer<sup>1</sup>

<sup>1</sup>University Tübingen, Section of Physiological Acoustics and Communication

$\text{Ca}^{2+}$  plays important regulatory roles in the stereocilia (SC). the concentration of  $\text{Ca}^{2+}$  in the SC must be tightly controlled by different mechanisms. the relative contributions of the different mechanisms can be better understood with the help of a mathematical model. a model of  $\text{Ca}^{2+}$  homeostasis in non-mammalian SC has been developed by Lumpkin and Hudspeth (1997). Their model incorporates four  $\text{Ca}^{2+}$  clearance mechanisms across the compartments within a single SC.

Here, we have adapted their model to mammalian outer hair cells (OHC) and, in addition, allowed for the possibility of passive diffusion from the middle SC through the cuticular plate (CP) into the longest SC. the dimensions (length of the different rows and diameter) of the SC were modified to fit that of the guinea-pig OHC. the simulation was set to run with a 5-s long stimulus.

The simulation results were compared with the fluorescence signal from a  $\text{Ca}^{2+}$  indicator dye fluo-3 recorded in SC from OHCs isolated from the guinea-pig cochlea (see poster: Harasztosi & Gummer: Position of Calcium Entry into Outer Hair Cell Stereocilia). the model reproduces the dynamics of the  $\text{Ca}^{2+}$  transients in both the longest and middle SC. in accordance with the fluorescence data, the model predicts that  $\text{Ca}^{2+}$  dynamics are faster at the top of the middle SC than in the longest SC ( $\tau=59\pm 1$  ms compared with  $\tau=265\pm 5$  ms).

The matching of experimental and model data supports the possibility of passive diffusion from the middle to the longest SC via the CP. Then, the data suggest that the MET channels are only located at the lower end of the tip link.

### **656 Tip-Link Stretching During Inner Hair Cell Stereocilia Bundle Deflection**

Sonya Smith<sup>1</sup>, Richard Chadwick<sup>2</sup>

<sup>1</sup>Howard University & NIDCD, <sup>2</sup>NIDCD

Stretching and contracting of IHC tip-links activates gated ion channels on individual stereocilia and thus directly affects mechano-transduction. Understanding the physical mechanisms involved this process is important. We have developed a computational model of IHC stereocilia bundle deflection using the immersed boundary method that includes tip links. We present results that show the effect of fluid flow stimulus on the deflection and the associated tip-link stretching of a three-row stereocilia bundle at various locations of the cochlea. At low frequencies, the model results agree with those of Fridberger[1] in which their time-resolved confocal imaging results indicate that IHC deflection, at least in the apical turn, is out of phase with the maximum displacement of the reticular lamina. This suggests an additional influence other than interaction with the surrounding oscillatory flow. Hensen's stripe may play a role altering the fluid flow in

this region due to the close proximity of IHC stereocilia to this part of the tectorial membrane. However, convection and bending in simple fluid shear can also explain this displacement pattern of the IHC bundle. Additionally our results show an apparent frequency doubling in the tip-link stretching at low frequencies that is in qualitative agreement with Russel et al.[2] This doubling results from differential distortion in the stretching of the two rows of tip-links.

References:

[1] Fridberger, A., et al. Imaging hair cell transduction at the speed of sound: Dynamic behavior of mammalian stereocilia. *PNAS* 103:1918-1923, (2006)

[2] Russel, I. and M. Kossel. "Modulation of Hair Cell Voltage Responses to Tones by Low-Frequency Biasing of the Basilar Membrane in the Guinea Pig Cochlea." *J. Neuroscience* 12: 1587-1601 (1992).

This work is supported by the NIDCD intramural program project Z01-DC0000033-10

### **657 Membrane Flexoelectricity and the Power Stroke of Hair Bundle Motility**

Richard Rabbitt<sup>1</sup>, Kathryn Breneman<sup>1</sup>, William Brownell<sup>2</sup>

<sup>1</sup>University of Utah, <sup>2</sup>Baylor College of Medicine

It has recently been shown that membrane tethers pulled from hair cells are electromotile and generate tensile forces when the cell is depolarized. This effect appears to have flexoelectric origins, where the curvature-induced electric dipole of the tether membrane interacts with the electric field to generate a piezoelectric-like force. We hypothesize that this same mechanism is at play in hair cell stereocilia and contributes significantly to fast forces and electrical events observed during mechano-electrical transduction (MET). to investigate this idea, we formulated a model of the stereocilia from first principles of physics that includes MET current and the membrane-based flexoelectric effect. Key physical parameters include the stereocilia dimensions and the flexoelectric coefficient of lipid membranes. Model results indicate that the flexoelectric effect may underlie the power-stroke of fast hair bundle motility, negative stiffness, and fast adaptation – events triggered by and dependent upon the MET current. If true, the hypothesis suggests a role for the staircase architecture of the hair bundle and might also explain the strong correlation between frequency sensitivity and hair bundle length across organs and species. Supported by NIDCD R01 DC04928 (Rabbitt) and RO1 DC00384 (Brownell).

### **658 Effect of Calcium On Channel-Based Adaptation in Mammalian Cochlear Hair Cells**

Jong-Hoon Nam<sup>1</sup>, Robert Fettiplace<sup>1</sup>

<sup>1</sup>University of Wisconsin-Madison

There is a dilemma in current mechanotransduction (MT) theories of the mammalian auditory hair cell. the prevailing view is that myosin motors play a crucial role to the hair cell adaptation and the amplification of the external stimuli. There are two hallmarks of the myosin-based hair cell adaptation. First, the adaptive recovery: at the removal of



a large negative stimulus, there follows a considerable current spike. Second, the adaptive shift: for a sustained stimulus, the hair cell shifts its operating range according to the magnitude of the maintained stimulus. At least in bullfrog sacculus hair cells, these two observations were elegantly explained by the myosin-based adaptation theory. the dilemma is that these two facets of slow adaptation are observed in mammalian auditor hair cells on a millisecond time scale. for myosin-based adaptation to hold on this time frame requires myosin climbing speeds more than a hundred times faster than measured values. to explore this problem, we combined a channel kinetics model with a 3-D finite element (FE) model of the OHC bundle. in the model the MT channel has ten states—five closed and five open depending on the number of calcium ions bound. the mechanical properties of the FE model were chosen to match the experimental results. the simulation could reproduce the experimental results of the calcium effects on the bundle mechanics. Further we suggest a solution to the myosin dilemma by introducing new channel kinetics. in our model, we used the climbing speed reported for myosin and still saw the two hallmarks of the myosin-based adaptation but within a millisecond time frame. These were largely unaffected by removing the contribution of the myosin motors. We do not argue that the myosin-based adaptation is unnecessary in the hair cell MT, but that the role of myosin-motors to the mammalian auditory hair cell adaptation is limited to providing the resting tension of the gating spring and does not significantly contribute to the response dynamics on a millisecond time scale. (Grant R01 DC01362 from NIDCD)

### **659 Potential Roles of Pkd1 in Mechanotransduction of Mouse Cochlear Hair Cells**

**Katherine Steigelman**<sup>1</sup>, Xudong Wu<sup>2</sup>, Jiangang Gao<sup>1</sup>, Feng Qian<sup>3</sup>, KB Piontek<sup>3</sup>, Gregory Germino<sup>3</sup>, Jian Zuo<sup>1</sup>  
<sup>1</sup>St. Jude Children's Research Hospital, <sup>2</sup>Harvard Medical School, <sup>3</sup>Johns Hopkins University School of Medicine

The components of the mechanotransduction (MET) channel in the hair cells of the cochlea are still unknown. We hypothesize that as a member of the TRP family, polycystic kidney disease (Pkd1) is part of the MET channel in the hair cells because Pkd1 may play a role in fluid-flow sensation and Ca<sup>2+</sup> ion uptake in kidney cilia. It may also form cation channels with conduction similar to that of MET channels. We created and analyzed two mutant mouse models with two independent alleles of *Pkd1*, a knockin model (*Pkd1*<sup>T3041V</sup>) that disrupts the normal cleavage of the protein and a hair cell specific conditional knockout model.

in wildtype cochleae, we have localized the mRNA of Pkd1 to both the inner and outer hair cells through RT-PCR from laser-captured individual hair cells and the protein to the hair bundle/cuticular plate of IHCs and OHCs through immunohistochemistry. in the *Pkd1*<sup>T3041V</sup> model, click auditory brainstem response (ABR) tests revealed a 25dB hearing loss compared to wild type littermates. SEM imaging displayed abnormal hair cell morphology in *Pkd1*<sup>T3041V</sup> mice. However, FM1-43 dye uptake experiments show similar results to the wildtype.

Our second mouse model uses a hair cell specific inducible Cre, Math1CreER, and a floxed Pkd1 allele to conditionally knockout the gene specifically in postnatal cochlear hair cells. Based on preliminary results these mice show an average threshold elevation of 25-30 dB at various frequencies compared to wildtype littermates. These results demonstrate that the hearing loss is due specifically to a phenotype in the hair cells and not other cell types of the cochlea.

We plan further analysis of the *Pkd1*<sup>T3041V</sup> allele and conditional knockout allele of *Pkd1* to provide *In Vivo* evidence that Pkd1 is a component of the MET channel in the hair cells and determine the roles of Pkd1 in the inner ear.

This work is supported in part by ALSAC, the Hartwell Foundation, DC06471, CA023944, CA21765, DK062199 and DK48006.

### **660 Rapid Uptake of the Styryl Dye AM1-43 in Hair Cells is Inhibited by P2X Antagonists**

**Krista Aschenbach**<sup>1</sup>, Mark Crumling<sup>2</sup>, Mingjie Tong<sup>2</sup>, R. Keith Duncan<sup>2</sup>

<sup>1</sup>Calvin College, <sup>2</sup>University of Michigan

Amphipathic styryl dyes like FM1-43 rapidly enter sensory hair cells, presumably through the transduction channels located at the tips of the stereocilia. Compelling evidence for this route of entry into hair cells was described by Meyers et al. (J. Neurosci., 2003, 23:4054-4065). Those authors also showed that FM1-43 could enter cells via P2X2 receptor activation, though it was argued that this was not the dominant route of entry into hair cells. However, the question remains whether dye uptake can be attributed to transduction channels alone, P2X receptors, or both. Our objective was to determine if entry of the fixable styryl dye AM1-43 could be blocked by P2X2 receptor antagonists. Chick basilar papillae were acutely dissected and immersed in a Hanks' balanced salt solution with 50 μM CaCl<sub>2</sub>. After 5 min of pre-incubation in this solution, the epithelium was exposed to AM1-43 for 1 min, followed by a series of 30 sec washes in Advasep-7 to remove unincorporated dye. Other tissue samples followed a similar protocol with a P2X blocker in the pre-incubation and dye solutions. Blockers included 100 μM suramin, 100 μM PPADS, and 100 μM TNP-ATP, all of which effectively block P2X2 receptors. Fluorescence was quantified under constant exposure settings to compare dye uptake in the various conditions. Each blocker significantly reduced dye uptake. We were unable to further excite dye entry by adding ATP, suggesting that activation of P2X receptors from endogenous ATP release had already saturated receptor activation. Some of the agents used are competitive antagonists of ATP binding to P2X receptors, rather than pore blockers. Therefore, we believe the blockers inhibited dye entry into hair cells by acting on P2X receptors, as opposed to nonspecifically blocking transduction channels. Consequently, caution should be exercised when using rapid dye uptake as an assay for transduction channel function. (Supported by NIH P30-DC05188 and F32-DC008050)

## **661 Protocadherin 15 is Necessary for the Coordinated Maturation of Apical Cell Components in Developing Hair Cell**

Yayoi Kikkawa<sup>1</sup>, Karen Pawlowski<sup>1</sup>, Charles Wright<sup>2</sup>, Kumar Alagramam<sup>3</sup>

<sup>1</sup>Otolaryngology-HNS, UT Southwestern Medical Center,

<sup>2</sup>Callier Center, Behavior and Brain Sciences, UT Southwestern Medical Center, <sup>3</sup>Otolaryngology-HNS, Case Western Reserve University

The Ames waltzer (av) mouse mutant harbors a mutation in the protocadherin 15 gene (Pcdh15) and is a model for deafness in Usher syndrome 1F and non-syndromic deafness DFNB23. Since we identified Pcdh15 in 2001, we have systematically accumulated genetic evidence by investigating various alleles of av to demonstrate that Pcdh15 is necessary for stereocilia morphogenesis and bundle polarity. Recent reports from other investigators show that Pcdh15 is expressed in the stereocilia and it is a component of the tip-link. The present study focused on early outer hair cell (OHC) development in the av3J, a presumptive null allele of Pcdh15. Here, we followed the development of cellular components of the outer hair cell (OHC) apex during the establishment of polarity of the stereocilia bundle. Three different methods were utilized in this study; scanning electron microscopy (SEM), transmission electron microscopy (TEM), and confocal microscopy to examine structural maturation of outer hair cells in av3J mice with emphasis on the fonticulus, basal body/centriole complex, actin mesh, and the microtubule network during initiation of bundle organization, which occurs in control mice between embryonic day 16.5 (E16.5) and postnatal day 5 (P5). We found dramatic ultrastructural rearrangements near the hair cell surface in av3J mice. Earliest changes were in kinocilia, basal body and stereocilia positioning and microtubule arrangement once the kinocilia had lateralized to the side of the cell (between E 16.5 and P0, prior to cuticular plate formation and stereocilia elongation). By P0, the developing fonticulus in av mice appeared enlarged, with a normal vesicle density. Stereocilia bundle disorganization increased after P0, with disruptions of the actin mesh within the cuticular plate. These observations support the hypothesis that mutations in Pcdh15 in av3J mice adversely affect coordinated maturation of apical cell components, resulting in disturbed hair cell polarity in av mice. These results show that Pcdh15 plays multiple roles in hair cell biology and how central it is to hearing.

This research was supported by the NIDCD Grant DC05385 to KA and a Deafness Research Foundation Grant to YK.

## **662 Analysis of CD3 Domain Containing Isoforms of Protocadherin 15 in Zebrafish.**

John Heaphy<sup>1</sup>, Daniel Chen<sup>1</sup>, Brian McDermott<sup>1</sup>, Kumar Alagramam<sup>1</sup>

<sup>1</sup>Otolaryngology-HNS, Case Western Reserve University School of Medicine

Mutations in the protocadherin 15 (PCDH15) gene are linked to human syndromic (USH1F) and nonsyndromic (DFNB23) deafness. It has been shown that two zebrafish

pcdh15 paralogs are required for proper receptor-cell function and morphology in the ear (pcdh15a) and eye (pcdh15b). Recent studies in the mouse indicate that a protein product of an alternatively spliced form of Pcdh15, which encodes a domain containing the cytoplasmic domain CD3, may be associated with the hair cell tip-link complex, and that ectodomains of Pcdh15 and cadherin 23 (Cdh23) may interact to form the tip link. These localization and biochemical studies suggest that Pcdh15 may have a direct role in mechanotransduction and that specific isoforms may have different functions in the hair cell. Conservation of the CD3 isoform sequence across species and the availability of zebrafish or mice harboring mutations affecting the expression of specific isoforms would provide genetic evidence for this hypothesis. We show here that zebrafish express pcdh15a and pcdh15b splice variants with significant sequence similarity to the murine CD3 domain. Morphological and functional analysis in zebrafish hair cells using a reverse genetic approach is underway.

## **663 EHD4 is a Potential Interacting Partner of CDH23**

Soma Sengupta<sup>1</sup>, Katharine Miller<sup>1</sup>, Manju George<sup>1</sup>, Khurram Naik<sup>1</sup>, Jonathan Chou<sup>1</sup>, MaryAnn Cheatham<sup>1</sup>, Peter Dallos<sup>1</sup>, Hamid Band<sup>1</sup>, Jing Zheng<sup>1</sup>

<sup>1</sup>Northwestern University

Hair cells located in the inner ear change mechanical signals related to sound into electrical signals that facilitate neurotransmitter release onto auditory neurons. The key element in the transformation process is the mechano-electric transducer (MET) apparatus located near the top of stereocilia. Cadherin 23 (CDH23) is found to be the tip-link of the MET apparatus and mutations in the gene encoding CDH23 causes deafness. This important discovery leads us to search the composition of MET apparatus as well as CDH23-associated proteins.

A membrane-based yeast two-hybrid system was used to identify CDH23-associated proteins in an outer hair cell library using the transmembrane region and cytoplasmic tail of CDH23 as the bait. Several proteins were identified as potential CDH23 associated protein including a newly discovered protein EHD4, a member of the EHD protein family. Several EHD-binding proteins have been identified recently and despite their possible role in endocytic recycling of different receptors, little is known about their function in cells. In order to study the interaction of these two proteins, CDH23 and EHD4 have been co-transfected into mammalian cells. Their expression pattern was investigated by immunohistochemistry. Our data showed that co-localization occurred between CDH23 and EHD4. These results indicate that there might be a direct interaction between CDH23 and EHD4. This assumption has been proved by co-immunoprecipitation experiments where direct interaction between EHD4 and CDH23 was established. Additional experiments will be done to determine if this interaction has any effect in hearing through *In Vivo* physiology analysis of EHD4 knockout mouse model. This work is supported by NIH grants DC 006412 (to J. Zheng)

## **664 Identification of a De Novo Protein in Hair Cells**

**Katharine Miller<sup>1</sup>**, MaryAnn Cheatham<sup>1</sup>, Peter Dallos<sup>1</sup>, Jing Zheng<sup>1</sup>

<sup>1</sup>*Northwestern University*

The mechano-electrical transducer (MET) apparatus found in hair cells is responsible for transforming mechanical into electrical signals. Key proteins in the MET apparatus are the MET channel and tip-link. Although the MET channel remains unknown, the tip link is composed partly by Cadherin 23 (Cdh23) homodimers. Identifying proteins associated with Cdh23 could greatly enhance our understanding of tip-link function and of the MET complex as well.

Through a membrane-based yeast two-hybrid approach using a cDNA library built from OHCs, we identified a de novo protein associated with Cdh23-bait. the de novo protein belongs to CEACAM (Carcinoembryonic antigen-related cell-cell adhesion molecule) family, a group of glycoproteins with diverse functions ranging from tissue homeostasis, cell growth and differentiation to angiogenesis and tumor suppression. the CEA family has low sequence similarity between genes and varied domain organization. Many of the 22 ceacam genes found in mice were identified through bioinformatics analysis. the de novo protein identified in our study is one of only five known CEACAM proteins that are conserved among mice, rats, and humans. it's domain organization is also distinctive within the CEACAM families. Additional experiments are performed in order to determine whether or not this protein plays an important role in cochlear hair cells. This work is supported by NIH grants DC 006412 (to J. Zheng)

## **665 MAGI-1 Binds to Cadherin 23 and Localizes At Hair-Cell Bundles**

**Zhigang Xu<sup>1</sup>**, Anthony Peng<sup>1</sup>, Kazuo Oshima<sup>1</sup>, Sabine Mann<sup>1</sup>, Stefan Heller<sup>1</sup>

<sup>1</sup>*Stanford University School of Medicine*

In search of proteins that interact with Cdh23, we performed yeast two-hybrid screens of a chicken cochlear cDNA library and we isolated a clone encoding MAGI-1c. MAGI-1 is a member of the membrane-associated guanylate kinase (MAGUK) protein family. It contains 6 (PDZ) domains, 2 WW domains, and 1 guanylate kinase-like (GuK) domain, making it an ideal scaffold for organizing multiple proteins into a protein complex. MAGUK proteins usually localize beneath the plasma membrane at regions of cell-cell adhesion in polarized epithelial cells and neurons. There they play central scaffolding roles assembling multiple proteins into a complex. MAGIs have an inverted domain organization when compared with other MAGUKs, which is reflected in the name MAGI: MAGUKs with Inverted orientation. the MAGI-1 gene gives rise to three splice variants encoding MAGI-1a, 1b, and 1c, which have different carboxyl termini. with RT-PCR we determined that MAGI-1a and MAGI-1c are expressed in the inner ear. with immunocytochemistry, we localized MAGI-1 in hair-cell bundles. the interaction between MAGI-1 and Cdh23 was

confirmed by co-immunoprecipitation. Our present data suggest that MAGI-1 is an ideal candidate for organizing different proteins into protein complexes in hair bundles.

## **666 Cadherin 23 in an Ancestral Hair Bundle**

**Glen Watson<sup>1</sup>**, Erin Graugnard<sup>1</sup>, Lankhanh Pham<sup>1</sup>, Patricia Mire<sup>1</sup>

<sup>1</sup>*University of Louisiana at Lafayette*

Tip links in hair bundles of mammals are likely composed of cadherin 23 and protocadherin 15 (P. Kazmierczak, H. Sakaguchi, J. Tokita, E.M. Wilson-Kubalek, R.A. Milligan, U. Muller, B. Kachar, *Nature* vol 449:87-91, 2007). We identified a homolog of cadherin 23 in sea anemones, sessile marine invertebrates related to corals and jellyfish. Anemones employ hair bundle mechanoreceptors on their tentacles to detect the swimming movements of prey. the anemone cadherin 23 comprises 6074 residues including 44 cadherin domains. the protein is predicted to have three membrane-spanning alpha helices: one near the N terminus; and the other two positioned closely together at the C-terminus. Thus, anemone cadherin 23 features a large exoplasmic loop that includes the 44 cadherin domains. Beginning with the 19<sup>th</sup> cadherin domain, a quadruple repeat pattern emerges that persists through the 43<sup>rd</sup> cadherin domain. Sequence identity is high among cadherins belonging to the same group (e.g., the first position of the quad repeat) but low among cadherins belonging to different groups. Antibodies raised to an exoplasmic peptide of anemone cadherin 23 produces punctate labeling of hair bundles at the immunofluorescent level. Immunoelectron microscopy shows clusters of immunogold particles at the tips of stereocilia. It may be possible that anemone cadherin 23, with its large loop, forms a component of tip links as a monomer (i.e., without first forming a cis homodimer). Supported by NSF IOB542574.

## **667 Glucose Transporter 5 is Not Required for Cochlear Amplification But Necessary for Male Fertility**

Xudong Wu<sup>1</sup>, **Yiling Yu<sup>1</sup>**, Xiang Wang<sup>2</sup>, Tetsuji Yamashita<sup>1</sup>, John Swift<sup>1</sup>, Jing Zheng<sup>3</sup>, Jiangang Gao<sup>1</sup>, Carl Duccummon<sup>4</sup>, Raymond Ke<sup>5</sup>, Peter Dallos<sup>3</sup>, David He<sup>2</sup>, MaryAnn Cheatham<sup>3</sup>, Jian Zuo<sup>1</sup>

<sup>1</sup>*St. Jude Children's Research Hospital*, <sup>2</sup>*Creighton University*, <sup>3</sup>*Northwestern University*, <sup>4</sup>*Fertility Associates of Memphis*, <sup>5</sup>*University of Tennessee*

Glucose transporter 5 (Glut5 or SLC2A5), a high-affinity fructose transporter, has been proposed to be a part of motor protein complex in outer hair cells (OHCs) required for cochlear amplification. While it is also highly expressed in the sperm of testis and epididymis, its function in these cells *In Vivo* is unknown. Here we show that Glut5-deficient mice display normal OHC morphology and motor function (i.e., nonlinear capacitance and electromotility) and normal cochlear amplification (i.e., CAP thresholds). in contrast to previous reports, we find that Glut5 is undetectable in wildtype OHCs. We therefore conclude that Glut5 is not required for OHC motility and/or cochlear amplification. in contrast to previous reports, we find that

Glut5 is predominantly localized to the principal region of the sperm tail. Our results indicate that Glut5-deficient mice exhibit reduced litter size and a decreased number of sperm which has an intact acrosome whereas the *In Vitro* fertilization appears normal. Sperm motility, structural stability and viability are also reduced, whereas sperm flagellum length and ultrastructure are normal. Glut5-deficient sperm also display normal mitochondrial function, distribution of a key glycolytic enzyme (GAPDS), as well as two major motor proteins (dynein and kinesin ATPases). Finally, Glut5-deficient sperm phenotypes are not compensated by an increase of Glut2 but are associated with a concurrent decrease of Glut3. Our results highlight the importance of fructose-transport mediated glycolysis in sperm motility and structural integrity, and acrosomal activation in fertilization. Glut5 is, therefore, a potential therapeutic target for male contraception and mutations or environmental factors that disrupt Glut5 could lead to reduced male fertility in humans.

This work is supported in part by ALSAC, the Hartwell Foundation, the Hugh Knowles Center and by NIH grants DC00089 (to P. D.), DC06471, CA023944, and CA21765 (to J. Zuo), DC 006496 (to D.Z.Z.H.), DC006412 (to J. Zheng).

#### **668 Characterization of OHC Motor Protein in 293 Stable Cell Lines**

**Shu Min Bian**<sup>1</sup>, Jun-Ping Bai<sup>1</sup>, Joseph Santos-Sacchi<sup>1</sup>, Dhasakumar Navaratnam<sup>1</sup>

<sup>1</sup>*Yale University*

Prestin is a member of the SLC26 family of anion transporters that gives rise to OHC electromotility. Since its initial identification however attempts at making cell lines that would allow better characterization of the protein have not been especially successful. We have established HEK293 and 293T cell lines stably expressing the outer hair cell prestin. We characterized both wild type gerbil prestin and its YFP-tagged version by western blotting and by fluorescence imaging. Functional studies were carried out by measuring the non-linear capacitance (NLC) in patch-clamp experiments. the amplitude of NLC is around 0.5-1.5 pF, close to that of the transiently transfected cells. for prestin turnover and maturation studies, we also established tetracycline-inducible prestin cell lines. We hope these cell lines will be valuable in studying different aspects of the molecular, biochemical, and physiological properties of prestin.

Supported by NIH grants R01 DC 007894 (DSN)  
R01 DC 008130 (JSS)

#### **669 Prestin-Associated Charge Movement in HEK 293 Cells**

Mathew J. Volk<sup>1</sup>, Lavanya Rajagopalan<sup>1</sup>, Haiying Liu<sup>1</sup>, William E. Brownell<sup>1</sup>, **Fred A. Pereira**<sup>1</sup>

<sup>1</sup>*Baylor College of Medicine*

Prestin is an important component of the membrane-based motor that enhances electromotility in outer hair cells (OHC). it's ability to greatly increase charge movement

into and out of the OHC lateral wall plasma membrane can be easily measured and has been described as a non-linear capacitance (NLC). Previous experiments have shown that the expression of prestin in the cell membrane of a human embryonic kidney (HEK 293) cell can induce NLC. No studies have fully characterized the time course and concentration-dependence of prestin NLC onset and progression in HEK 293 cells. We performed capacitance recordings of isolated HEK 293 cells at time points between 6 and 48 hours post-transfection, and the prestin-associated charge density was calculated. All transfected cells, identified by fluorescence from an independently produced GFP encoded in the prestin construct, showed the characteristic bell-shaped NLC. Charge density increased with time post-transfection from a mean of 12.6 fC/pF between 10-16 hours after transfection to 25.0 fC/pF between 36-48 hours after transfection ( $p < 0.001$ ). We have additionally created a Tet-on inducible expression system to further control the expression of prestin-mGFP and will describe our results of NLC measures at the earliest stages when prestin first localizes at the plasma membrane. Development of a regulated prestin expression system allows for a more precise evaluation of prestin membrane expression and contribution to prestin-associated charge movements.

This work is supported by grants from the W. M. Keck Center for Interdisciplinary Bioscience Training (LR), DC00354 (WEB, FAP), DC008134 and NSF BES-0522862 (FAP).

#### **670 Heterologous Expression of the Outer Hair Cell Motor Protein Prestin in Sf9 Cells**

**Takashi Tadenuma**<sup>1</sup>, Koji Iida<sup>1</sup>, Michio Murakoshi<sup>1</sup>, Shun Kumano<sup>1</sup>, Kouhei Tsumoto<sup>2</sup>, Katsuhisa Ikeda<sup>3</sup>, Izumi Kumagai<sup>1</sup>, Toshimitsu Kobayashi<sup>1</sup>, Hiroshi Wada<sup>1</sup>

<sup>1</sup>*Tohoku University*, <sup>2</sup>*The University of Tokyo*, <sup>3</sup>*Juntendo University*

Cochlear amplification is responsible for the wide dynamic range and sharp frequency selectivity of the mammalian hearing. the basis of this amplification is thought to be the elongation and contraction of outer hair cells (OHCs) in response to the change of their membrane potential. This cell length change is believed to be based on voltage-dependent conformational change of the motor protein prestin distributed over the lateral membrane of the OHCs. Although prestin has been attracting attention in recent years and has been extensively studied, its structure and function have not yet been revealed. to obtain the knowledge on the structure and function of prestin, research at the molecular level is necessary, thus a method of obtaining prestin molecules is required. with regard to wild-type prestin, an expression system was constructed with CHO cells (Iida et al., 2005). Using the prestin molecules from prestin-expressing CHO cells, wild-type prestin has been studied at the molecular level. However, to obtain further knowledge of prestin, mutational analysis at the molecular level needs to be carried out. in order to do this, a method to obtain mutant prestin molecules is also required. However, generation of CHO cell lines expressing new target prestin mutants is difficult because it takes 2-3 months. Thus, establishment

of an alternative to the CHO expression system is needed. In this study, an attempt was made to express functional prestin in Sf9 cells using the baculovirus expression system, which requires only 2-3 weeks for construction. Prestin cDNA was introduced into Sf9 cells with recombinant baculovirus, and the expression of prestin was confirmed by Western blotting and immunofluorescence analysis. By patch-clamp measurements, it was verified that the prestin expressed in Sf9 was functional. Furthermore, it was revealed that approximately 700  $\mu\text{g}$  of prestin molecules could be obtained from one liter of culture.

### **[671] Immune Atomic Force Microscopy of the Plasma Membrane of Prestin-Transfected Chinese Hamster Ovary Cells Using Quantum Dots**

**Michio Murakoshi<sup>1</sup>**, Koji Iida<sup>1</sup>, Shun Kumano<sup>1</sup>, Hiroshi Wada<sup>1</sup>

<sup>1</sup>*Tohoku University*

Prestin, a membrane protein of the outer hair cells (OHCs), is known to be the motor which drives somatic electromotility of the OHCs. By using cytoplasmic anions as extrinsic voltage sensors, this protein is thought to operate at microsecond rates and to cause reciprocal movement of OHCs in their longitudinal direction. Due to this motility, the basilar membrane is subjected to force, resulting in cochlear amplification and thus leading to the high sensitivity of mammalian hearing. Previous morphological studies of OHCs using an electron microscope showed the lateral membrane of the OHCs to be densely covered with particles about 10 nm in diameter, these particles being believed to be a motor protein. Imaging by atomic force microscopy (AFM) of prestin-transfected Chinese hamster ovary (CHO) cells revealed particle-like structures 8-12 nm in diameter to possibly be prestin. However, since there are many kinds of intrinsic membrane proteins other than prestin in the plasma membranes of OHCs and CHO cells, it was impossible to clarify which structures observed in such membranes were prestin. In the present study, an experimental approach combining AFM with quantum dots (QDs), used as topographic surface markers, was carried out to detect individual prestin molecules. The inside-out plasma membranes were isolated from the prestin-transfected and untransfected CHO cells. Such membranes were then incubated with anti-prestin primary antibodies and QD-conjugated secondary antibodies. Fluorescence labeling of the prestin-transfected CHO cells but not of the untransfected CHO cells was confirmed. The plasma membranes of both types of CHO cells were subsequently scanned by AFM. QDs, about 8 nm in height, were clearly seen in the prestin-transfected CHO cells and structures possibly corresponding to prestin molecules were observed in the vicinity of the QDs. The QDs were not seen in the AFM images of the untransfected CHO cells.

### **[672] The Mechanism of Chloride Flux Across the Outer Hair Cell Membrane**

**Xiantao Li<sup>1</sup>**, Joseph Santos-Sacchi<sup>1</sup>

<sup>1</sup>*Yale University*

The discovery of prestin's intracellular Cl<sup>-</sup> sensitivity revealed the importance of anion control of outer hair cell (OHC) electromotility. Though we know that electromotility can be modulated by flux of chloride across the OHC membrane *In Vitro* (Rybalchenko and Santos-Sacchi, 2003; Song et al., 2005) and *In Vivo* (Santos-Sacchi et al., 2006), so far there are few data about the molecular mechanisms involved in intracellular Cl<sup>-</sup> regulation. To elucidate on the question, whole cell and single channel recording were employed on guinea pig OHCs in search of chloride conductances. We found an outward current that was inhibited when extracellular Cl<sup>-</sup> level was switched from 140 mM to 0 mM. Under symmetric [Cl<sup>-</sup>], with cationic currents blocked, there remain outward and inward currents. 100  $\mu\text{M}$  DIDS inhibited an outwardly rectifying component of the outward current. 1 second hyperpolarizing steps activate an inwardly rectifying current and 500  $\mu\text{M}$  cadmium partially inhibited this inward current. The outward and inward Cl<sup>-</sup> currents were similar to I<sub>Cl.vol</sub> and I<sub>Cl.ir</sub> respectively. We also identify an I<sub>Cl.vol</sub>-like Cl<sup>-</sup> channel in single channel recordings from the OHC lateral membrane.

(Supported by NIDCD DC 000273 to JSS)

### **[673] Modulation of Prestin's State Dependent Chloride Binding**

**Lei Song<sup>1</sup>**, Joseph Santos-Sacchi<sup>1</sup>

<sup>1</sup>*Yale University*

Somatic motility of the mammalian outer hair cell (OHC) is achieved through the conformational changes of the membrane motor protein prestin. Prestin's conformation is voltage dependent and its associated charge movement can be characterized as a nonlinear capacitance (NLC). The voltage at peak NLC (V<sub>pkcm</sub>) is sensitive to a number of perturbations including membrane tension, temperature, and membrane holding potential. The latter phenomenon involves a shift in the state probability of prestin along the voltage axis with prolonged holding potential, hyperpolarizing voltage shifting V<sub>pkcm</sub> in the positive direction and visa versa. Recently, an important role for intracellular Cl has been demonstrated (Oliver et al, 2001; Rybalchenko and Santos-Sacchi, 2003; Song et al., 2005). Indeed, we have shown that motor conformation at a fixed voltage depends on binding of this intracellular anion; i.e., chloride shifts V<sub>pkcm</sub>. Since Cl<sup>-</sup> is crucial to prestin's function, modulation of prestin's Cl<sup>-</sup> binding will ultimately lead to the modulation of cochlear amplification.

Here we manipulate membrane holding potential and intracellular Cl<sup>-</sup> concentration to see how these two perturbations influence each other. At 140 mM intracellular Cl<sup>-</sup>, negative holding potentials are most efficacious in shifting the NLC curves, whereas at 1 mM intracellular Cl<sup>-</sup> level, positive holding potential dominates the response. At 10 mM intracellular Cl<sup>-</sup> level, a concentration close to the native state (Song et al., 2005; Santos-Sacchi et al., 2006), there is a balanced response from both positive and

negative holding potentials. This newly identified heightened sensitivity of motor state under physiological chloride concentrations suggests that the OHC efferent transmitters, ACh and GABA, could interactively impact OHC motor function. Such investigations are underway.

(This research is supported by NIH NIDCD grant DC 000273 to JSS)

### **674 The Role of Cysteine Residues in Prestin**

**Jun-Ping Bai**<sup>1</sup>, Alexei Surguchev<sup>2</sup>, Joseph Santos-Sacchi<sup>2</sup>, Dhasakumar Navaratnam<sup>1</sup>

<sup>1</sup>*Yale Medical School, Dept. of Neurology*, <sup>2</sup>*Yale Medical School, Dept. of Surgery*

Prestin is an slc26 anion transporter family member that is integral to the generation of electromotility. Mammalian prestin contains 9 cysteine residues of which 7 lie in the hypothetical transmembrane region. Previous evidence has shown that mutation of individual cysteine residues within the protein did not adversely affect its function (McGuire R et al., 2007). Other groups have argued that cysteine residues in the transmembrane are important to its forming multimers and in its function (Zheng J et al., 2006). Here we show that in keeping with prior data mutation of individual residues resulted in a functional protein. However, mutating all the cysteine residues together resulted in a non functional protein. These data suggest that particular cysteine residues could compensate for the loss of other specific cysteine residues. We have tried to identify these residues by generating random combinations of individual cysteine residues. Our data suggests that while the combination of C192S and C196S and separately C395S resulted in a functional protein, mutating all three residues in combination resulted in a non-functional protein. Separately mutating C381S resulted in a functional protein although combining C381S with C192S and C196S resulted in a non-functional protein. (Supported by R01 DC 007894 and R01 DC 008130)

### **675 Effects of Cysteine Mutations On Prestin Function and Oligomerization**

**Ryan McGuire**<sup>1</sup>, Fred Pereira<sup>2</sup>, Robert Raphael<sup>1</sup>

<sup>1</sup>*Rice University*, <sup>2</sup>*Baylor College of Medicine*

The solute carrier membrane protein prestin (Slc26a5) is a required and sufficient component of the motor mechanism that drives electromechanical transduction in cochlear outer hair cells. Prestin interactions have been measured biochemically using Western blot, optically through fluorescence resonance energy transfer (FRET), and verified *In Vivo* through yeast two-hybrid assay. Monomer, dimer, trimer, and tetramer prestin populations are commonly observed, but the nature of or purpose for these interactions is not currently understood. Since disulfide bonding might be involved in assembly of the higher order states, we have studied isosteric serine replacement of single cysteine residues throughout prestin in order to investigate whether these mutants have concurrent changes in NLC and the distribution among oligomeric states. the mutations were introduced into a gerbil prestin-

eGFP fusion, the constructs expressed in HEK cells, and function (NLC) tested 24-48 hours post-transfection. Whole-cell patch clamping of the serine replacement mutants revealed three distinct classes of altered NLC: 1) a shift in V1/2 to depolarizing potentials, 2) tightening of the NLC curve, reflective of increased valance of charge movement, and 3) decreased area under the NLC curve, representing reduced charge movement. Most interestingly, the reduced charge density mutants had lower levels of monomer than wild type prestin as measured through Western blot analysis. Mutants exhibiting other types of functional changes did not show systematic changes to the distribution of oligomerization states. These results indicate that cysteine residues in prestin mediate important molecular interactions and that the monomer is important for full charge transfer.

### **676 Dynamic Conformational Features of Prestin's C-Terminus**

**Michael Podgorski**<sup>1</sup>, Christopher Philpott<sup>2</sup>, Amanda Nourse<sup>1</sup>, Richard Kriwacki<sup>1</sup>, Stephen White<sup>1</sup>, Jian Zuo<sup>1</sup>

<sup>1</sup>*St. Jude Children's Research Hospital*, <sup>2</sup>*University of Bath, UK*

Functional studies of full-length Prestin have linked its C-terminus to the apparent conformational flexibility that accompanies membrane voltage changes. Using limited proteolysis, NMR spectroscopy, and analytical ultracentrifugation (AUC), we have characterized the size, shape, and stability of the Prestin C-terminus (residues 499-744; Prestin-C). Sequence analysis suggested that a 60-70 residue loop divides the STAS domain within Prestin-C into two discrete parts. Based on these results, we hypothesize that Prestin-C consists of a folded STAS domain flanked by intrinsically unstructured segments. We studied recombinant Prestin-C as well as a series of proteins with N-terminal, C-terminal, or internal deletions. Our results show the Prestin-C adopts a range of extended conformations that undergo structural re-arrangements. AUC data suggests that Prestin-C conformers interconvert on a fast time-scale, while chromatographic studies imply that each conformer exhibits different charge traits. Our continuing studies are focused on understanding the role of these conformational dynamics relative to Prestin's function as an electrochemical "rheostat". These structural rearrangements we have observed may be related to the unique properties of Prestin within the SLC26 protein family.

This work is supported in part by ALSAC, the Hartwell Foundation, and by NIH grants

DC06471 and CA21765.

### **677 A Computational Analysis of Tether Pulling Experiments: Probing Membrane-Cytoskeleton Interaction**

**Kristopher Schumacher**<sup>1</sup>, Aleksander Popel<sup>1</sup>, Bahman Anvari<sup>2</sup>, William Brownell<sup>3</sup>, Alexander Spector<sup>1</sup>

<sup>1</sup>*Johns Hopkins University*, <sup>2</sup>*University of California-Riverside*, <sup>3</sup>*Baylor College of Medicine*

Prestin is necessary for normal hearing, and it is a critical component of the membrane motor complex in the active outer hair cell (OHC). Other cells such as human embryonic kidney (HEK) and Chinese hamster ovary (CHO) cells can be transfected with prestin and used to study this protein's contribution. Membrane tethers pulled from OHCs, prestin transfected HEKs, and wild-type CHO cells provide a means to characterize the mechanical and/or electromechanical properties of the cell membrane, including the interactions between the cell membrane and the underlying cytoskeleton. We propose a computational method aimed at the interpretation and design of tether pulling experiments in OHC, HEK, and CHO cells. Our model accounts for the significant membrane-cytoskeleton interactions by considering the detailed information on the topology of bonds connecting the plasma membrane and the cytoskeleton. OHCs have a special system of pillars connecting the membrane and the cytoskeleton, and HEK and CHO cells have a bond arrangement via PIP2 bonds which is common to many other cells. We compute the force-dependent piecewise membrane deflection and bending as well as modes of stored energy in three major regions of the system: body of the tether, membrane-cytoskeleton attachment zone, and the transition zone between the two. a validation of our model is presented based on recent experimental data on CHO cells. the proposed method can be an effective tool in the analyses of experiments to probe membranes of electromotile cells.

### **678 Computational Analysis of the Lateral Diffusion Phenomenon in Outer Hair Cells**

**Kristopher Schumacher**<sup>1</sup>, William Brownell<sup>2</sup>, Alexander Spector<sup>1</sup>

<sup>1</sup>*Johns Hopkins University*, <sup>2</sup>*Baylor College of Medicine*

The cochlear outer hair cell's (OHC's) plasma membrane is the site of prestin, the motor protein responsible for this cell's active properties critical for normal hearing. in response to shifts in transmembrane potential, prestin is capable of conformational changes that alter its in-plane surface area and are coupled to the membrane's net thermodynamic properties (e.g., tension). Recent OHC fluorescence recovery after photobleaching (FRAP) experiments have shown that the macroscopically observed diffusion rate of an inert, fluorescent, lipid tracer, located within the lateral plasma membrane, is anisotropic and depends on the cell's polarization. the membrane fluidity (as measured by tracer diffusion rate) may be an important contributor to lipid-protein interactions that lead to the cell's active properties. to better understand this phenomenon, we develop a random-walk model (i.e., Monte-Carlo simulations) that includes estimates of the substructural details of the OHC's plasma membrane. for example, the discrete protein and cytoskeletal interaction

sites in the membrane, as well as the geometric and thermodynamic effects of prestin protein conformational changes, are included in the model. the results of this computational analysis in conjunction with FRAP experiments helps to characterize the lateral diffusion phenomenon in OHCs.

### **679 Amphipath-Induced Nanoscale Curvature in the Outer Hair Cell Plasma Membrane**

**Jennifer Greeson**<sup>1</sup>, Robert Raphael<sup>1</sup>

<sup>1</sup>*Rice University*

The outer hair cell is a unique sensory cell capable of transducing changes in transmembrane potential into whole cell deformations. This electromotile process is believed to endow the mammalian auditory system with its enhanced frequency sensitivity and selectivity. At the molecular level, it is manifested through the action of the transmembrane protein prestin, and the accepted electrical signature is a measured nonlinear capacitance (NLC). Several agents are capable of altering the NLC operating range including the amphipathic compounds salicylate, chlorpromazine and trinitrophenol. These compounds are known to preferentially intercalate into one bilayer leaflet altering membrane curvature. Though the mechanism by which these agents modulate NLC is not fully understood, it is reasonable to speculate their effects on membrane architecture play an important role; however, the magnitude of OHC membrane curvature changes is not large enough to visualize using conventional microscopy. As such, we developed an extension of fluorescence polarization microscopy (FPM) suitable for the cylindrical OHC. FPM is capable of measuring the orientation of a fluorophore in the membrane, and here we utilize it to assess the orientation of di-8-ANEPPS in the OHC. Our results indicate that in untreated cells, di-8-ANEPPS orients at 26° with respect to the membrane. Following treatment with salicylate (10 mM), chlorpromazine (0.1 mM), or trinitrophenol (0.1 mM), this orientation shifts 9-15°. These orientations are consistent with nanoscale changes in membrane curvature. the membrane bending induced by trinitrophenol is reversible by the simultaneous application of CPZ; however, the membrane bending induced by salicylate is not. These results suggest that TNP and CPZ exert their effects on OHC NLC via a purely membrane-mediated effect, whereas salicylate's interaction with the plasma membrane is more complicated and may result from the compound's direct interaction with prestin.

### **680 Membrane Cholesterol Concentration Affects the Lateral Mobility of Outer Hair Cell Plasma Membrane Constituents**

**Louise organ**<sup>1</sup>, Robert Raphael<sup>1</sup>

<sup>1</sup>*Rice University*

Mammalian hearing exhibits exquisite sensitivity and frequency selectivity which is attributed to the unique electromotile properties of outer hair cells (OHCs). the OHC transmembrane protein prestin functions as both a voltage sensor and mechanical motor, converting changes



in membrane potential into axial, cellular deformations. Recent studies suggest that manipulations in membrane cholesterol levels shift the membrane microdomain distribution of prestin, modulate prestin oligomerization states, and alter prestin function. Thus, we hypothesize that OHC plasma membrane cholesterol levels may regulate electromotility either through microdomain-mediated mechanisms that cluster or segregate prestin molecules or via alterations in the material properties of the membrane, which in turn affect the resident proteins. Using fluorescence recovery after photobleaching (FRAP) in HEK cells, we show both the immobile fraction (*IF*) and effective diffusion coefficient (*D*) of prestin-mGFP are affected by membrane cholesterol concentration. Depletion of cholesterol with m $\beta$ CD causes a significant increase in *IF*, but no change in *D*. However, overloading the plasma membrane with cholesterol significantly increases *D* as does serial loading and depletion, regardless of application order. Preliminary work also suggests that lipid lateral mobility varies among the three regions of the OHC and that diffusion in individual regions is sensitive to alterations in cholesterol concentration. Cumulatively, these results demonstrate the complexity of prestin-membrane interactions and highlight the importance of their inclusion in models of prestin function.

### **[681] Modulating Prestin Function Through Alterations in Membrane Lipid Content**

**John Sfondouris<sup>1</sup>, Haiying Liu<sup>1</sup>, Lavanya Rajagopalan<sup>1</sup>, Fred Pereira<sup>1</sup>, William Brownell<sup>1</sup>**

<sup>1</sup>*Baylor College of Medicine*

The lateral membrane of the cochlear outer hair cell (OHC) is home to a membrane-based motor that powers OHC electromotility, enabling amplification and fine tuning of auditory signals. the OHC membrane protein prestin plays a central role in this process by greatly increasing the charge movement into and out of the membrane. We have previously shown that membrane cholesterol modulates prestin function in OHCs and in prestin-transfected human embryonic kidney (HEK) 293 cells. These observations suggest that other changes in membrane lipid composition could also alter prestin function. the present study explores the effects of membrane cholesterol and docosahexaenoic acid (DHA) content on prestin function in prestin-transfected HEK 293 cells using a whole-cell voltage-clamp to measure prestin-associated charge movement. Increasing membrane cholesterol results in a large hyperpolarizing shift in the peak voltage of the NLC ( $V_{pkc}$ ). After a few minutes, there is a decrease in the total charge moved even though little or no change is observed initially after the voltage shift. Both the voltage shift and the decrease in total charge demonstrate a clear saturating concentration dependence. Incubation of cholesterol-loaded cells in cholesterol-free media reduces the shift in  $V_{pkc}$  but has no effect on the total charge movement. in contrast, decreasing membrane cholesterol results in a large depolarizing shift in  $V_{pkc}$  which is reduced upon incubation in cholesterol-free media but there is no change in the amount of charge moved. Lastly, increasing membrane DHA results in a hyperpolarizing shift in  $V_{pkc}$  accompanied by an increase in

total charge movement, compared to untreated cells. Our results indicate the importance of membrane lipid composition as a modulator of prestin function and provide new insights into the mechanism of prestin-associated charge movement in OHC electromotility.

Research supported by NIH/NIDCD research grant RO1-00354.

### **[682] Modulation of Membrane Motor of Outer Hair Cells by Phospholipids**

**Jie Fang<sup>1</sup>, Kuni Iwasa<sup>1</sup>**

<sup>1</sup>*NIDCD*

Prestin-based electromotility is critical for the sensitivity and frequency-selectivity of the mammalian ear. This motility is based on coupling between movement of electric charge across the membrane and membrane area. It therefore can be monitored not only by the length of these cylinder-shaped cells but also as nonlinear capacitance with bell-shaped voltage dependence. Despite recent progress, our current understanding of electromotility remains still phenomenological and not quite physical. To obtain more molecular understanding, we examined the effect of membrane thickness on electromotility by incorporating phospholipids of various chain lengths using gamma-cyclodextrin. the experiment was performed in the whole-cell mode of patch clamp using channel blockers in both internal and external media. Phospholipid-loaded 5mM gamma-cyclodextrin was perfused from a perfusion pipette. the concentration of the lipids was 100microM. We found that short phospholipid PC10:0 induces large positive shifts (>100mV) in the voltage dependence but makes the membrane leaky, leading to breakage. PC12:0 also shifts the voltage dependence positively by more than 100mV without decreasing the membrane resistance. PC14:0, however, induced a positive shift of ~15 mV. for PC22:0, the shift was ~30mV.

Our results demonstrate that the length of phospholipids in the plasma membrane is an extremely sensitive factor for electromotility. We interpret that hydrophobic mismatch is the most likely mechanism for these shifts that exceed 100mV. Large shifts for short chain PCs can be explained if the motor molecule takes the thinner conformation at more negative membrane potential. Because the volume of the membrane protein must conserve, the thinner conformation would correspond to larger membrane area and contributes to the elongation of the cell. This interpretation is therefore consistent with the area motor model for electromotility.

### **[683] The Direct Effects of Cholesterol and M $\beta$ cd On Outer Hair Cell Motility and Capacitance**

**Rei Kitani<sup>1</sup>, Seiji Takehata<sup>1</sup>, Michio Murakoshi<sup>2</sup>, Hiroshi Wada<sup>2</sup>, Shin-ichiro Maruya<sup>1</sup>, Takahisa Abe<sup>1</sup>, Hideichi Shinkawa<sup>1</sup>**

<sup>1</sup>*Hirosaki University School of Medicine*, <sup>2</sup>*Tohoku University*

Hearing in mammals owes its preciseness to the amplification by electromotility of outer hair cells (OHCs), arising from conformational changes of nanoparticles that

are densely packed in the lateral wall. Since the discovery of prestin, putative motor protein, much attention has been paid to it with lesser attention to the surrounding lipids in the investigation of the OHC electromotility. Cholesterol is a necessary component of biological membranes and regulates their fluidity and rigidity. Although the relationship between hearing acuity and circulating cholesterol level has been discussed, the mechanism is still controversial. Here, we examined the direct effects of cholesterol loading and depleting on the OHC electromotility and voltage-dependent capacitance using water-soluble cholesterol and methyl-beta-cyclodextrin (M $\beta$ CD). Atomic force microscopy revealed that cholesterol loading remarkably increased Young's modulus of the lateral wall in a concentration dependent manner. a continuous video image analysis demonstrated that exogenous cholesterol compressed the maximal amplitude of the electromotility, although the charge movement induced by voltage change was not affected. Depleting cholesterol in the plasma membrane using M $\beta$ CD increased the maximal amplitude of the electromotility, while also shifting a peak membrane capacitance voltage to the depolarized direction with reduction of the peak capacitance. Our results indicate that cholesterol alters the OHC electromotility directly via regulating the rigidity of the membrane-cytoskeleton complex, suggesting that not only modification of prestin but also of the surrounding lipid in the membrane affects cochlear amplification and hearing acuity.

#### **684 Exploring the Generation of Low Frequency Cochlear Microphonic Distortion**

Jiefu Zheng<sup>1</sup>, Tianying Ren<sup>1</sup>, Alfred Nuttall<sup>1</sup>

<sup>1</sup>Oregon Health & Science University

We previously reported the distortion of the low frequency cochlear microphonic (CM) recorded via the round window electrode at low to moderate sound levels (ARO abstract #502, 2007). the mechanisms underlying the generation of this particular distortion are complex, and more experiments are needed to gain a better understanding. to determine if the observed distortion is a contamination from the neurophonic responses, neural inhibitors such as TTX, quinine, CNQX and AP5 were used to block the action potentials as well as the post synaptic potentials of the cochlear afferent fibers. CAP threshold was elevated by at least 40 dB by the application of these chemicals into the cochlea, but both the primary and second harmonic of the low frequency CM were not affected at a significant degree. Recordings from a glass microelectrode in the scala tympani, scala media and within the organ of Corti were made to learn if the distortion is associated with the hair cell nonlinearity. Although the distortion was observed in the recording within the organ of Corti, the relative magnitude of the distortion to that of the primary is smaller than those with the scala tympani and scala media recordings. These results suggest that the auditory nerve does not contribute to the observed distortion significantly, and that the harmonic distortion products might be generated by hair cells from cochlear locations different from the basal turn. Supported by NIH/NIDCD 00141

#### **685 Accuracy of Vibration Distortion Product Otoacoustic Emissions for Estimating Hearing Threshold**

Diana Turcanu<sup>1</sup>, Ernst Dalhoff<sup>1</sup>, Marcus Müller<sup>2</sup>, Hans-Peter Zenner<sup>2</sup>, Anthony W. Gummer<sup>1</sup>

<sup>1</sup>University Tübingen, Section of Physiological Acoustics and Communication, <sup>2</sup>University Tübingen, Department Otolaryngology

Growth functions of the cubic component of the distortion product otoacoustic emission (DPOAE) in response to two tones have been successfully used to estimate hearing thresholds in humans (Boege and Janssen, JASA 2002). Recently, we have extended this technique to DPOAEs measured as vibration of the umbo (Dalhoff, Turcanu et al., PNAS 2007). This was achieved with a custom-made ultrasensitive laser Doppler vibrometer (LDV) with a noise floor of less than 1 pm. Here, we investigate the inherent accuracy of the vibration DPOAE to estimate threshold. This is achieved by using animal experiments, because in animals the reference thresholds can be more accurately determined and readily manipulated.

Guinea pigs were anaesthetized with Ketavet (50 mg/kg) and Rompun (8 mg/kg). Thresholds were determined from the compound action potential (CAP) in response to tone pips. Umbo vibration was measured with our custom-made LDV, without using a reflector. Sound pressure was recorded in the ear canal with a probe-tube microphone with tip situated 2–3 mm from the umbo. for DPOAEs, the stimulus was  $f_2/f_1 = 1.2$  and  $f_2 = 5\text{--}15$  kHz;  $L_2 = 25\text{--}65$  dB SPL and  $L_1 = 0.46L_2 + 41$  dB. the estimated distortion product threshold (EDPT) was derived from up to nine I/O functions of the vibration DPOAE. Experiments were performed in normal and hearing impaired (ossicular chain fixation and furosemide) animals.

For CAP thresholds spanning a range of 40 dB at any one frequency, the EDPT correlated significantly ( $p < 0.05$ ) with the CAP threshold. the standard deviation of the estimated threshold was 6 dB. Since the error in estimating threshold from the CAP is very small (about 1 dB across experimenters), this standard deviation of 6 dB yields an expected upper limit for the accuracy of the distortion product threshold as an objective estimator of hearing threshold. Nevertheless, the accuracy might be improved by a still more sensitive LDV and fine-structure suppression.

Supported by DFG Gu 194/8-1.

#### **686 Hearing Threshold Estimation in Humans Using Distortion Product Otoacoustic Emissions Measured with a Pulsed Paradigm**

Ales Vetesnik<sup>1</sup>, Diana Turcanu<sup>2</sup>, Ernst Dalhoff<sup>2</sup>, Anthony W. Gummer<sup>2</sup>

<sup>1</sup>Czech Technical University Prague, Department of Nuclear Chemistry, <sup>2</sup>University Tübingen, Section of Physiological Acoustics and Communication

Hearing threshold estimation in humans by means of extrapolation of the input-output (I/O) function of the cubic distortion product of otoacoustic emissions (DPOAE) is

strongly influenced by the DPOAE generation mechanism; this involves basically two generators. the primary generator is assumed to be based on the nonlinear interaction of the basilar-membrane responses to the primary tones and the secondary generator on a local perturbation at the distortion product characteristic frequency site. It is assumed that the secondary generator is partially responsible for deficiencies encountered in the threshold estimation method.

Using normal hearing subjects, we investigate the possibility of separating the primary source from the secondary source contribution in the time domain during the DPOAE amplitude onset period. for this purpose, a pulsed  $f_2$  primary paradigm is used. It is shown that the DPOAE primary source is built up just before the interference with the secondary source significantly alters the DPOAE amplitude. Hearing threshold is subsequently estimated for the same frequency region by extrapolating DPOAE I/O functions constructed from time resolved DPOAE amplitudes. Comparison is made between the pulsed  $f_2$  primary paradigm method and the spectral smoothing of the DP-grams obtained with the conventional continuous primary tones paradigm in the frequency region 1.5–2.5 kHz. We show that the estimated threshold mirrors the audiometrical threshold and that the number of I/O-functions included in the analysis improves from 70% (Dalhoff, Turcanu et al., PNAS 2007) to better than 90%. Supported by DFG Gu 194/8-1.

### **[687] Distortion Product Otoacoustic Emissions (DPOAE) Behavior and Growth Rate in Tinnitus Subjects with Normal Audiograms**

**Leah Acker**<sup>1</sup>, Christopher Shera<sup>2</sup>, Jennifer Melcher<sup>2</sup>

<sup>1</sup>*Speech and Hearing Bioscience and Technology, MIT,*

<sup>2</sup>*Eaton Peabody Laboratory, Harvard Medical School*

Tinnitus disrupts the daily life of 1 out of every 200 adults, yet its physiological basis remains largely a mystery. a fundamental, but unanswered, question is whether cochlear pathology is always a prerequisite for developing tinnitus. While tinnitus and hearing loss (as measured by elevated pure tone thresholds) commonly co-occur, they are far from perfectly correlated with one another. the present study took a fresh look at the status of the auditory periphery in people with tinnitus using DPOAEs. We specifically studied people with normal audiograms so any abnormal findings would not be attributable to large-scale hair cell damage. We tested 4 tinnitus and 6 non-tinnitus subjects with normal audiograms ( $\leq 25$  dB HL at 125 - 8000 Hz) and one tinnitus subject with a slight loss at 8000 Hz (30 - 35 dB HL). DPOAE magnitudes were measured for a set of 52 frequencies ( $500 \text{ Hz} \leq f_2 \leq 8 \text{ kHz}$ , with  $f_2/f_1=1.2$ ) and nine intensities ( $20 \text{ dB} \leq L_2 \leq 60 \text{ dB}$ , with  $L_1 = 39 + 0.4 \cdot L_2$ ). We found that tinnitus subjects had higher DPOAE levels than control subjects between 1 kHz and 2 kHz at the highest intensity tested ( $L_2 = 60 \text{ dB}$ ). Additionally, we found that at both high and moderate intensities ( $L_2 = 60$  and  $40 \text{ dB}$ ), tinnitus subjects had larger DPOAEs than control subjects for frequencies above 4 kHz. Finally, trends indicate that the growth rate of

DPOAEs in tinnitus subjects is larger than the growth rate seen in control subjects between 1.5 kHz and 2 kHz. These data suggest peripheral auditory malfunction in tinnitus subjects with normal audiograms.

### **[688] The Effect of Ear Canal Volume On Oaes: Can It Explain Gender Differences?**

**Bradford Backus**<sup>1</sup>, Ann Hickox<sup>1</sup>, Fatimah Jilani<sup>1</sup>

<sup>1</sup>*University College London*

Women are known to have larger and more numerous otoacoustic emissions (OAEs) than men. One explanation for this suggests that hormonal events during prenatal masculinisation play a role (McFadden et al, 2002). Although females are known to have smaller ear canal volumes (ECVs), the extent of this factor's contribution to the observed gender differences has not been well-explored. We measured transiently evoked (TE) OAEs in 46 ears from 23 normal-hearing subjects (15 female; 8 male, mean age = 22.1) in conjunction with their ECVs. the mean TEOAE response level for females was  $4.8 \text{ dB SPL} \pm 0.430$  and for males it was  $2.72 \text{ dB SPL} \pm 0.5313$ . This difference was statistically significant using the t-test for unequal groups ( $P=0.02$ ). Mean ECV for males (16 ears) was  $1.135 \text{ ml} \pm 0.274$  and for females (22 ears) was  $0.995 \text{ ml} \pm 0.286$ . This difference was significant ( $P=0.0485$ ) when a female outlier was removed. an ANOVA analysis over the factors: "Gender" and "ECV", indicated that ECV was the dominant factor in determining mean response level (Gender p-value = 0.1318; ECV p-value = 0.001, interaction p-value = 0.0253). a second investigation that artificially changed ECV by using different sized ear tips during OAE measurements suggests that the effect of ECV on OAEs depends upon (1) absolute ECV and (2) the frequency band of TEOAE. the effect is strongest at 2 and 3 kHz. We conclude that ECV is a significant contributor to observed gender differences in OAE response level.

### **[689] Inter-Aural Analysis of Normal Neonatal Teoaes**

**Erik Berninger**<sup>1</sup>, Kjell-Erik Israelsson<sup>2</sup>, Åke Olofsson<sup>3</sup>

<sup>1</sup>*Karolinska Institutet, Karolinska University Hospital,*

*Stockholm, Sweden,* <sup>2</sup>*Mälar Hospital, Eskilstuna, Sweden,*

<sup>3</sup>*Karolinska Institutet, Stockholm, Sweden*

Transient-evoked otoacoustic emissions (TEOAEs) were recorded from more than 30,000 newborns over a 6 year period. Analysis was performed on all TEOAEs recorded from newborns that passed the bedside universal hearing screen on both ears, at the same test occasion, in order to characterize the normal left/right ear relationship of neonatal TEOAEs. Although distinct, and highly significant, mean lateral asymmetries (right ear > left ear) existed in entire TEOAE level (1.1 dB), and at all half-octave frequencies ( $\leq 1.2 \text{ dB}$ , 700-4,000 Hz), the cumulative distribution of, e.g., inter-aural difference in entire TEOAE revealed that no more than 62% of the newborns exhibited higher TEOAEs in the right ear compared to the left ear, thereby illustrating the large variability in TEOAEs, at birth. Linear regression analysis on paired data revealed modest correlation between entire TEOAE level in right (dB SPL,

y) vs. left ear (dB SPL, x):  $y = 6.5 + 0.71x$  ( $r=0.71$ ,  $p < 0.0000$ ,  $n=21,560$ ). the corresponding half-octave correlations were highly frequency-dependent. the correlation coefficient varied from 0.16 at 700 Hz, to 0.68 at 4,000 Hz. All slopes of regression lines were significantly different from zero. Further analysis on the relationship between left/right ear TEOAE waveforms will be discussed.

#### **[690] Measurement of Distortion Product Otoacoustic Emissions (Dpoaes) in Neonatal GJB2 Transgenic Mice and gjb2 Knockout Mice**

Akira Minekawa<sup>1</sup>, Yuya Narui<sup>1</sup>, Ayako Inoshita<sup>1</sup>, Takashi Iizuka<sup>1</sup>, Takuji Koike<sup>2</sup>, Katsuhisa Ikeda<sup>1</sup>

<sup>1</sup>Department of Otorhinolaryngology, Juntendo University Graduate School of Medicine, Tokyo, <sup>2</sup>Department of Mech. Eng. and Intelligent Systems of University of Electro-Communications, Tokyo

Hereditary deafness affects about 1 in 2000 children and mutations in the *GJB2* gene are the major cause in various ethnic groups. *GJB2* encodes connexin26, a putative channel component in cochlear gap junction. However, the pathogenesis of hearing loss caused by the *GJB2* mutations remains obscure. We generated transgenic mice expressing a mutant connexin26 with R75W mutation that was identified in a deaf family with autosomal-dominant inheritance. in 2-week-old transgenic mice, sensory hair cells were present in the cochlea. However, deformity of the cell shapes together with presumed increase of the cytoplasm in the supporting cells appeared to diminish the extracellular fluid space surrounding the outer hair cells and the tunnel of Corti space. and the auditory brainstem response (ABR) revealed that the mice at 2 weeks old showed severe to profound hearing impairment. Furthermore we generated targeted disruption of *gjb2* using Cre recombinase controlled by P0. It was desirable to measure DPOAEs in addition to ABR for researching inner ear functions (outer hair cell functions). However in small animals such as mice, their external auditory canal is very narrow and their auditory frequency threshold level is very high. in the previous study, we could measure DPOAEs in neonatal mice precisely with our newly developed system. in this study we measured DPOAEs in neonatal *GJB2* transgenic mice and *gjb2* knockout mice with our newly developed system. in 2-week-old transgenic mice, most of DPOAEs was not detected in spite of the presence of OHC in the electron microscopical observation. the function of OHC is important for the appearance of DPOAEs. It is suspected that DPOAEs did not appear because of dysfunction of OHC.

#### **[691] Strain-Dependence of Age-Related Hearing Loss in Wild and Domesticated Mongolian Gerbils**

Bernhard Gaese<sup>1</sup>, Tobias Eckrich<sup>1</sup>, Elisabeth Foeller<sup>1</sup>, Ingo Stuermer<sup>2</sup>, Manfred Koessl<sup>1</sup>

<sup>1</sup>J.W. Goethe-University, Frankfurt, <sup>2</sup>Georg-August University of Goettingen

The Mongolian gerbil (*Meriones unguiculatus*) is one of the animal models in auditory research that has been used in several studies on age-related hearing loss. the standard laboratory strain originated from a group of 20 founders caught in 1935; the strain is now domesticated as it was bred in captivity for more than 70 years. Recently, several anatomical and physiological adaptations have been described that might be related to inbreeding and domestication. Here, we determined properties of distortion product otoacoustic emissions (DPOAEs) in different age groups of domesticated gerbils and compared them with measurements in wild-type gerbils from F6-F7 generations of a strain originating from animals trapped in Central Asia in 1995.

DPOAE thresholds were comparable between both strains up to an age of 9 months. Until then, thresholds were below 10 dB SPL for f2 frequencies between 4 and 44 kHz. in older domesticated animals, the thresholds were increased by up to 12 dB. Significant increases were found at stimulus frequencies of 2 kHz, 12 - 20 kHz, and 56 - 60 kHz. the best frequency ratio f2/f1 to evoke maximum DPOAE amplitude was larger in domesticated animals at the age of 9 months or older. While these data show that there is a deterioration of cochlear sensitivity in domesticated animals, the magnitude of the described changes is comparably small. Thus, the general suitability of domesticated gerbils for auditory research seems not to be affected.

#### **[692] Attention and Contralateral Suppression of Teoae**

Angela Garinis<sup>1</sup>, Theodore Glattke<sup>1</sup>, Barbara Cone-Wesson<sup>1</sup>

<sup>1</sup>University of Arizona

Reduction of transient ototacoustic emission (TEOAE) amplitude coincident with the presentation of broadband noise (BBN) to the contralateral ear has been termed contralateral suppression and is believed to be byproduct of the activity of the auditory efferent system. the interaction of attention and laterality was investigated using a contralateral TEOAE suppression paradigm. the aims of this investigation were to: 1) test the hypothesis that cortical processes, such as attention, may alter the amount of contralateral suppression and 2) describe the amount of suppression for right versus left ear stimuli and noise (i.e., laterality). TEOAEs were evoked by 60 dB peSPL clicks in 15 normally hearing adults in 4 test conditions for each ear: 1) quiet (no noise); 2) 60 dB SPL contralateral BBN; 3) words (at -3 dB SNR) embedded in 60 dB SPL contralateral BBN while subjects classified words as animal versus food items; 4) words from condition #3 played backwards and embedded in 60 dB SPL contralateral BBN. Results suggest a right ear

advantage for all conditions, with greater suppression when TEOAE was recorded from the right ear (noise presented left) than for noise right-TEOAE left. the words-in-noise attention condition resulted in less suppression compared to noise alone ( $t_{11}=2.71$ ,  $p=.0078$ ) but no differences were found for the noise alone vs. the noise with words backwards condition. These results suggest that cortical attention processes have an impact on efferent suppression.

### **693 Does Language Experience Sensitize Olivocochlear Reflexes that are Evoked by Stimuli that Vary in Pitch?**

Shaum Bhagat<sup>1</sup>, Jingjing Xu<sup>1</sup>

<sup>1</sup>The University of Memphis

Neuroimaging and evoked potential studies have demonstrated differences between native Mandarin and native English speakers in the auditory processing of lexical tones. These differences in pitch encoding are evident for linguistic and nonlinguistic contexts at the level of the rostral brainstem [Krishnan et al., 2005; Krishnan et al., 2006]. the aim of this study was to examine if linguistic experience modulates olivocochlear activity evoked by pitch-varying stimuli when measured via the contralateral suppression paradigm. Transient-evoked otoacoustic emissions (TEOAEs) were recorded from the right ear of normal-hearing adults in conditions with and without a contralateral suppressor. the TEOAE stimuli consisted of a series of linear clicks presented at 65 dB peSPL. Three types of 70 dB SPL contralateral suppressors (white noise, Mandarin tones, and tone glides) were utilized. Our initial results indicate that white noise elicits greater amounts of TEOAE suppression compared to Mandarin tones or tone glides in both native Mandarin and English speakers. However, the Mandarin tones evoke more TEOAE suppression in native Mandarin speakers than in native English speakers. These preliminary findings suggest that the pitch-encoding neural mechanisms shaped by linguistic experience may influence neural control of cochlear micromechanics.

### **694 Role of HSF1 in Induction of Heat Shock Proteins Following Heat Shock or Noise Stress**

Tzy-Wen L. Gong<sup>1</sup>, Lynne Fullarton<sup>1</sup>, Gary A. Dootz<sup>1</sup>, Ivor J. Benjamin<sup>2</sup>, David C. Kohrman<sup>1</sup>, David F. Dolan<sup>1</sup>, Richard A. Altschuler<sup>1</sup>, Margaret I. Lomax<sup>1</sup>

<sup>1</sup>University of Michigan Kresge Hearing Research Institute,

<sup>2</sup>University of Utah

Diverse cellular and environmental stressors activate the heat shock response and induce heat shock proteins. Stress activates the transcription factor heat shock factor 1 (HSF1), which binds to heat shock elements in the genes for heat shock proteins, leading to rapid induction. We used an Hsf1-/- knockout mouse model to evaluate the role of HSF1 in the cochlea following heat and noise stress. Heat shock rapidly induced expression of Hsp25, Hsp47, Hsp70.1, Hsp70.3, Hsp84, Hsp86, and Hsp110 in the cochlea of wild-type or Hsf1+/- heterozygotes, but not in Hsf1-/- null mice. Exposure to broad band noise (2-20

KHz) at 106 dB SPL for 2 hr also induced genes for heat shock proteins. Maximal induction of all Hsps occurred 4 hr after the noise exposure. in contrast, noise stress produced lower levels of mRNA for Hsp25, Hsp70.1, Hsp70.3, and Hsp86 in Hsf1+/-heterozygotes. Induction of heat shock proteins was attenuated, but not eliminated, in Hsf1-/- mice, suggesting that signaling pathways controlled by additional transcriptional regulators contribute to induction of heat shock proteins following noise stress. We also developed a new Hsf1 knockout mouse model for aging studies by crossing CBA/CaJ with the Hsf1 knockout strain. in a small cohort of this new mouse model, preliminary analysis of auditory thresholds with age suggest that HSF1 protects against age-related hearing loss at high frequencies (48kHz). Supported by NIH grants P01 AG025164, P30 DCO5188, and the Margaret G. Bertsch Research Endowment

### **695 Noise Induced Stress Responses of the Cochlear Lateral Wall**

Joe Adams<sup>1</sup>

<sup>1</sup>Mass. Eye & Ear Infirmary

The unfolded protein response is a stress response wherein the presence of unfolded proteins in the endoplasmic reticulum triggers a halt of translation of more proteins until the backlog of unfolded proteins is resolved. a key player in this stress response is glucose responsive protein78 (GRP78). it's presence has been widely used as an indicator of stress following a variety of inducing factors. Immunostaining for GRP78 in the cochlea of unstressed CBA mice shows low level staining in ganglion cells and inner hair cells, with more robust staining of Deiters cells. the levels of staining in these cells or other cells within the organ of Corti do not change following 8-16 kHz noise exposures but cells within the lateral wall of the cochlea respond with increased immunoreactivity for GRP78 shortly following noise exposures. On hour following a two hour 92 dB SPL noise exposure type IV fibrocytes in the upper basal turn show GRP78 reactivity. with increasing sound levels the region of reactive type IV cells expands basally and apically. Following 94 dB exposures type I fibrocytes begin to show GRP78 immunoreactivity and at 97 dB marginal cells of the stria vascularis begin to show GRP78 immunoreactivity. These results show that following noise exposures connective tissue cells and stria marginal cells utilize stress response pathways that are not used by ganglion cells or by cells in the organ of Corti and that for some cells the stress responses are easily detected at exposure levels far below those previously found to cause damage. the unfolded protein response may account for reduced immunostaining for other proteins following noise exposures. Previous work has indicated that cells of the spiral ligament play a role in protecting sensory cells from acoustic trauma. It is expected that the present results will provide means for further exploration of interactions of epithelial and connective tissue cells.

**696 Hensen Cell Proteomics and Anti-Inflammatory Responses in the Mammalian Cochlea**

Anastasiya Maricle<sup>1</sup>, Gilda Kalinec<sup>1</sup>, Debbie Guerrero<sup>2</sup>, Buddahadeb Mallik<sup>3</sup>, Bulbul Chakravarti<sup>3</sup>, Deb Chakravarti<sup>3</sup>, Paul Webster<sup>2</sup>, **Federico Kalinec<sup>1</sup>**

<sup>1</sup>Gonda Department of Cell and Molecular Biology, House Ear Institute, Los Angeles, CA 90057, <sup>2</sup>Ahmanson Advanced Electron Microscopy and Imaging Center, House Ear Institute, Los Angeles, CA 90057, <sup>3</sup>Proteomics Center, Keck Graduate Institute of Applied Life Sciences, Claremont, CA 91711

Hensen cells are amongst the most prominent and abundant supporting cells in the organ of Corti, but little is known about their functional and structural roles. It has been suggested that immature Hensen cells would be able to differentiate into either Deiters' or outer hair cells, and it is currently acknowledged that they might be important for K<sup>+</sup> recycling in the mammalian cochlea. Hensen cells could also be part of mechanisms aimed at protecting auditory sensory cells from noise trauma, in particular that known as "sound conditioning" or "toughening", but no conclusive evidence has been presented yet. Generation of a data set containing lists of proteins normally expressed by these cells, and the proteins whose abundance or post-translational modification status is altered after noise stimulation, could be an invaluable resource for investigators in the Hearing Research field. We have adopted a two-step approach for this purpose that consists of: (1) high-throughput proteome identification based on in-gel or in-solution trypsin digestion followed by liquid chromatography/electrospray ionization/tandem mass spectrometry (LC-ESI-MS/MS), and (2) determination of the physiological functions of some of the major proteins identified using a combination of bioinformatics, microscopic imaging, biophysical, pharmacological and molecular biology approaches. Ongoing proteome mapping studies have provided evidence that proteins known to be important mediators of anti-inflammatory responses are expressed in Hensen cells. by using confocal and transmission electron microscopy we have investigated the cellular and intracellular distribution of these protein both in guinea pig cochleae as well as in isolated Hensen cells. Our experimental findings suggest that Hensen cells could be a central component of the anti-inflammatory system in the mammalian cochlea. We believe that in the near future, our ongoing proteomic study will provide further evidence to support this novel role as well as other unknown functions of cochlear Hensen cells at the level of individual protein molecules.

**697 Mitochondrial Dysfunction Disrupts Trafficking of Kir4.1 in Spiral Ganglion Satellite Cells and Causes Hearing Loss**

Jing Zou<sup>1</sup>, Ya Zhang<sup>1</sup>, Shankai Yin<sup>2</sup>, Hao Wu<sup>1</sup>, Ilmari Pyykko<sup>3</sup>

<sup>1</sup>Department of Otolaryng H&N Surg, Shanghai Jiaotong University School of Medicine, Xinhua Hospital, <sup>2</sup>The Affiliated Sixth People's Hospital, Otolaryngology Institute of Shanghai Jiaotong University, <sup>3</sup>Department of Otolaryngology, Medical School, University of Tampere

Kir4.1 is responsible for 1) pumping K<sup>+</sup> ions from excited OHCs and the intrastrial space of the stria vascularis, to both set the resting membrane potential and maintain endolymph potential, and 2) buffering extracellular K<sup>+</sup> in SGCs to restore neural excitability. BKCa plays a key role in phase locking signals in the mammalian inner ear. to evaluate the role of these channels and mitochondrial dysfunction in SNHL, 3-nitropropionic acid (3-NP) was administered to the rat round window membrane for 30 min. ABR was measured before and 2 h after 3-NP administration. Bulla was processed for confocal microscopy to measure Kir4.1 and BKCa channel expression and trafficking. 23 (±4.4 SE) dB and 58 (±6.7 SE) dB hearing loss developed in the rats treated with 0.3 mol/liter 3-NP and 0.5 mol/liter 3-NP respectively. BK was visualized in the cellular membrane and cytoplasm in the apical neck and the middle region of IHCs, but not altered by 3-NP treatment. Kir4.1 was detected in the immediate cells of stria vascularis, Deiter's cells of organ of Corti, and spiral ganglion satellite cells (SGSCs). Disrupted Kir4.1 trafficking was noticed in SGSCs 2 h post 3-NP treatment. the altered Kir4.1 trafficking in SGSCs partly contributes to SNHL.

**698 Cochlear Protein Expression At an Early Stage of Cisplatin Ototoxicity**

Samson Jamesdaniel<sup>1</sup>, Dalian Ding<sup>1</sup>, Richard Salvi<sup>1</sup>, Donald Coling<sup>1</sup>

<sup>1</sup>Center for Hearing and Deafness, University at Buffalo

Cisplatin-induced changes in cochlear protein expression at an early stage of the ototoxic pathway were analysed using antibody microarrays. 725 proteins were investigated 48 h after intraperitoneal administration of cisplatin (12mg/kg). Cochlear proteins from control and cisplatin injected rats were labeled with Cy3 or Cy5 using a dye-swapping paradigm. Four male Wistars and four female Fischer-344 rats were compared to identify proteins involved in cisplatin ototoxicity, irrespective of sex and strain variation. ABR for stimuli at 2.5, 5, 10, 20, 40 kHz and for clicks indicated threshold shifts ranging from 4–28 dB. DPOAEs (cubic distortion product) showed either no change or a small, approximately 10 dB decrease at 8 and 16 kHz (Wistars only). Cochleograms indicated minimal hair cell loss reflecting the early stage of ototoxicity. However, cisplatin did induce remarkable changes in the expression of 19 proteins independent of sex and strain. 15 proteins showed an increase in both strains by 1.5 fold and more, while 4 proteins were decreased by 0.6 fold or less. All of these proteins have been reported to be involved in cell death, cell survival, or progression through

the cell cycle. However, only 4 have been reported in previous studies in the cochlea (proteins immunoreactive with antibodies against myosin VI, neurofilament 68, active caspase 3, epidermal growth factor), while 6 proteins have been investigated in other tissues in studies involving the effect of cisplatin. 15 are novel to the study of inner ear function or pathology. the results of this proteomic analysis reflect the commencement of ototoxic and cell survival responses even before the observation of a significant functional or anatomical loss. Further investigation of these proteins and their pathways may lead to identification of molecules that initiate or have a vital role in apoptosis or cellular survival. We acknowledge support from Deafness Research Foundation (DC) and NIH (R01DC00630, RS).

### **699 Role of NADPH-Oxidases (Noxs) in Cisplatin-Induced Ototoxicity**

**HyungJin Kim<sup>1</sup>**, Hongseob So<sup>1</sup>, Channy Park<sup>1</sup>, JeongHan Lee<sup>1</sup>, Raekil Park<sup>1</sup>

<sup>1</sup>*Wonkwang University School of Medicine*

In our previous study, we clearly demonstrated the roles of pro-inflammatory cytokines and subsequent ROS generation on cisplatin ototoxicity *In Vitro* and *in vivo*. However, the roles of NADPH oxidase on ROS generation and ototoxicity by cisplatin have not been fully elucidated. Herein, immunohistochemical studies demonstrated that treatment of HEI-OC1 auditory cells with cisplatin induced the expression of NADPH oxidase isoforms, Nox-1 and Nox-4, in mice cochlea. mRNA expression of Nox-1, Nox-4, NOXO1, p22-phox, and p67-phox was also increased in cisplatin-treated cells. Inhibition of NADPH oxidase with diphenylen iodonium chloride (DPI) and apocynin abolished the pro-inflammatory cytokine production, ROS production and the subsequent apoptotic death in cisplatin-treated cells. Furthermore, suppression of NOX1 and NOX4 expression by siRNA transfection markedly abolished the cytotoxic effect and ROS generation of cisplatin. Taken together, our data suggest that ROS generated, in part, through the activation of NADPH oxidase plays an essential role in cisplatin-ototoxicity.

This work was supported by the Korea Science & Engineering Foundation (KOSEF) through the Vestibulocochlear Research Center (VCRC) at Wonkwang University in 2007.

### **700 Rapid Cochlear Inner Hair Cell Death Induced by Gentamicin**

**Emmy Wu<sup>1</sup>**, Jean Paul Font<sup>2</sup>, Tomoko Makishima<sup>2</sup>

<sup>1</sup>*University of Texas Medical Branch*, <sup>2</sup>*Department of Otolaryngology, University of Texas Medical Branch*

Gentamicin (GM) has been widely known for its ototoxicity, especially in relationship with hair cell death in the inner ear. We observed that the cochlear inner hair cells selectively and rapidly disappear within 24 hours in an *In Vitro* mouse inner ear explant culture system after GM administration. in this study, we have investigated the timing of cell death, and the involvement of Caspase-3, an apoptosis marker, in this process.

Inner ear explants (cochlear duct, utricle, saccule, cristae ampullares) were prepared from C57BL/6J mice at

postnatal day 4 (P4) – P6. the explants were incubated either with or without 0.03% GM, and harvested at 6, 12, 18, 24 and 48 hours. the tissue was fixed and labeled with anti-active Caspase-3 antibody, Phalloidin and Hoechst33342, incubated with fluorescent secondary antibodies, and whole mount explants were visualized under fluorescent microscopy.

in the cochlear explants, significant loss of inner hair cells, without damage to the outer hair cells was observed as early as 6 hours, and was prominent at 24 and 48 hours of GM incubation. Inner hair cell death was determined when Phalloidin-labeled hair cell stereocilia and Hoechst-labeled nuclei were both absent adjacent to the corresponding row of intact outer hair cells. There was no significant hair cell loss in the vestibular explants. Caspase-3 activation was seen in the cochlear hair cells, especially at the site of hair cell loss, as early as 6 hours, and was most significant around 18 hours of GM incubation.

Our results indicate that this rapid inner hair cell death induced by GM may involve the apoptotic pathway, as shown by Caspase-3 activation. We plan to determine whether Caspase-3 activation is necessary for this phenomenon, by using tissue deficient of Caspase-3. the rapid and selective induction of cell death in this system can be used as a tool to search for methods to prevent cell death in the inner ear.

### **701 Gentamicin Uptake Ability Determines the Cytotoxic Susceptibility of Cochlea Turns**

**JeongHan Lee<sup>1</sup>**, Channy Park<sup>1</sup>, Myung-Ja Youn<sup>1</sup>, Sang-Heon Lee<sup>1</sup>, Hongseob So<sup>1</sup>, Raekil Park<sup>1</sup>

<sup>1</sup>*Wonkwang University School of Medicine*

Although gentamicin (GM) is extremely effective antimicrobial agent, it often causes severe sensorineural hearing loss and balance disturbance due to ototoxic effect on inner ear hair cells (HCs). Hair cell loss by GM begins in the basal, the high-frequency region of the cochlea, and progresses towards the apex consistent with the pattern of hearing loss. However, GM uptake ability of hair cells from each turn on hearing loss remains to be elucidated. in this study, we hypothesized that the difference of each turn on GM uptake may determine the severity of hair cell damages. We examined *In Vitro* and *In Vivo* GM ototoxicity by a whole cochlear explant culture from neonatal SD rat injected GTTR (Texas Red conjugated-GM). in *In Vitro* experiment of whole cochlear explants, GM induced hair cell death in a time- and dose-dependent manner. HCs in basal turn are more susceptible to GM-mediated cytotoxicity than those in apical turn. in addition, after injection of GTTR into neonatal SD rats, weakly diffused fluorescence was observed in the cell bodies of both IHCs and OHCs in apical turn. However, diffusely punctuated GTTR fluorescence was obviously increased in HCs from basal turn. Taken together, these results suggest that the amount of GM uptake by HCs from each turn is varying and this difference in uptake ability determines the cytotoxic susceptibility of GM on hair cells of cochlea turns. This work was supported by the Korea Science & Engineering Foundation (KOSEF) through the Vestibulocochlear Research Center (VCRC) at Wonkwang University in 2007.



## **702 Proteomic Analysis of the Protein Expression in the Cochlea of Noise-Exposed Mice**

**Nam-Kyung Yeo<sup>1</sup>**, Hun Hee Kang<sup>2</sup>, Joong Ho Ahn<sup>1</sup>, Jong Woo Chung<sup>1</sup>

<sup>1</sup>*Department of Otolaryngology, Asan Medical Center, University of Ulsan College of Medicine,* <sup>2</sup>*Asan Institute for Life Science*

Proteomics is a powerful tool for protein analysis, providing valuable information on biochemical processes involved in diseases, monitoring of cellular processes, and characterizing the protein expression levels. We tried to find the proteins that are associated with pathophysiology of the noise-induced hearing loss and mechanisms of the disease by proteomic approach. BALB/C male mice were used. Control group was placed in noise booth without noise and experimental groups were exposed to noise (120 dB SPL broad band white noise) for 3 hours daily for 3 consecutive days. the hearing level was determined by ABR measurement. Total protein of cochlea was isolated and separated into numerous spots by two-dimensional electrophoresis. Protein spots that were highly detected in the only noise exposed cochleas were selected and subsequently analyzed with matrix-assisted laser desorption/ionization time of flight mass spectrometry (MALDI-TOF MS). About 286 protein spots were detected in noise group. Selected spots were analyzed, and various proteins were identified. These included angiopoietin-like 1, heat shock protein, and apoptosis regulator Bcl-2. We should need more studies to confirm the relationship between these proteins and noise induced ototoxicity. These proteins may help us in understanding the mechanisms of pathogenesis of noise-induced hearing loss.

## **703 Expression Patterns of KCNJ10 K+ Channel in the Cochlear Lateral Wall After Acoustic Trauma**

**Yong Ho Park<sup>1</sup>**, Jae Yong Park<sup>1</sup>

<sup>1</sup>*Chungnam National University*

**Background and Objectives:** It is well known that noise induced hearing loss is due to sensory hair cell loss and other neuronal damage. But recently noise exposure also could damage lateral wall of cochlea such as stria vascularis and spiral ligament. K<sup>+</sup> is the major cation in endolymph and important to maintain homeostasis within the cochlea. We have investigated the expression patterns of K<sup>+</sup>(KCNJ10) channel in noise -induced cochlear damage. **Materials and Method:** Twenty adult male guinea pigs(300~350 g) were included in this study. in experimental group (n=16), acoustic trauma was induced by continous broad band noise for 2 hr to 115 dB SPL and broad band noise for 6 hr to 120 dB SPL with 3 consecutive days. After noise exposure, auditory brainstem response threshold shift and hair cell loss were evaluated. a study for KCNJ10 K<sup>+</sup> channel expression was examined by immunohistochemical staining. **Results:** After noise exposure, auditory brainstem response showed transient threshold shift and permanent threshold shift in

accordance with noise exposure. and the expression patterns of KCNJ10 K<sup>+</sup> channel were changeable in TTS group. But there were no change of expression patterns in PTS group. **conclusion:** in the cochlear lateral wall, KCNJ10 K<sup>+</sup> channel expressions were affected with noise exposure and these change might be associated with maintain the homeostasis in the cochlea.

## **704 Oxidative Status Regulates the Cell Death Propensity Toward Apoptosis or Necrosis of Hcs Following Exposure to Intense Noise**

**Guiliang Zheng<sup>1</sup>**, Bohua Hu<sup>2</sup>

<sup>1</sup>*State University of New York at Buffalo; Institute of Otolaryngology, Chinese PLA General Hospital,* <sup>2</sup>*State University of New York at Buffalo*

Two modes of hair cell (HC) death, apoptosis and necrosis, are involved in the pathogenesis of HC lesions following exposure to intense noise. It is known that generation of HC apoptosis is associated with overproduction of oxidative stress in the cochlea. Thus, we hypothesized that the decision of a cell to die via apoptosis or necrosis is regulated by the level of the oxidative stress in HCs. to test the hypothesis, we manipulated the antioxidant capacity of the cochlea using local application of buthionine sulfoximine (BSO), a selective inhibitor of glutathione synthetase, and observed the effect of the glutathione reduction on generation of apoptosis and necrosis in the cochlea. Chinchillas received cochlear perfusion of the BSO solution (10 &#181;l, 60 mM in artificial perilymph) in one ear. the contralateral ears of the animals received artificial perilymph perfusion (served as controls). Four hours after the BSO application, the animals were exposed a 4 kHz narrow band noise at 110 dB for 2 hours. Auditory brainstem responses (ABR), elicited by tone bursts at frequencies of 1, 2, 4, 8 and 16 kHz, were measured before and 1 hour after the BSO application, as well as before and 1 hour after the noise exposure. Upon the completion of the final ABR testing, the animals were sacrificed and the cochleae were collected for pathological examination to determine the cell death pathways incurred. the results showed that following the noise exposure, the ratio of the numbers of necrotic to apoptotic HCs was significantly increased in the BSO-treated ears as compared with that observed in the control ears. Surprisingly, the overall level of HC damage, as indicated by the sum of apoptotic, necrotic and missing HCs, appeared to be reduced in the BSO treated ears, although pre-noise hearing testing revealed no significant difference of ABR thresholds between the BSO treated and the perilymph treated control ears. the results suggest that reduction of the GSH level in HCs creates a microenvironment that is favored for the generation of necrotic cell death.

## **705 Exposure to Intense Noise Causes Paracellular Permeability of Supporting Cells in the Organ of Corti**

Bo Hua Hu<sup>1</sup>, Gui-Liang Zheng<sup>2</sup>

<sup>1</sup>State University of NY at Buffalo, <sup>2</sup>State University of NY at Buffalo and Institute of Otolaryngology, Chinese PLA General Hospital

Exposure to intense noise traumatizes the cochlear structures, leading to the death of hair cells (HCs) and supporting cells. As a sign of structural defects, the presence of macromolecular markers in HCs with the compromised plasma membrane has been observed in noise-traumatized cochleae. Although the presence of the fluorescence markers in the HCs is an indicator of the structural failure of the reticular lamina, it is not clear whether the macromolecular tracers could reach HCs through the compromised basilar membrane and the extracellular connection between supporting cells. In the current study, we observed the paracellular permeability of the basilar membrane in normal and noise-exposed cochleae with a fluorescent marker, fluorescein isothiocyanate-dextran with graded molecular weights. Chinchillas were exposed to 75 pairs of impulses at 155 dB pSPL. Immediately after the noise exposure, the animals were anesthetized, and the compartment of the scala tympani of the cochlea was perfused with the FITC-dextran solution. The cell viability was assessed with a propidium iodide assay. In the normal cochleae without acoustic trauma, there was no dextran fluorescence in the organ of Corti. Following the noise exposure, the fluorescence of the 3 and 40 kD FITC-dextran was observed in several paracellular spaces including the reticular lamina between HCs and the phalangeal process of Deiters cells, as well as around Deiters and Hensen cells. In addition, there was strong dextran fluorescence in the cytoplasm of dying HCs. Since HCs are not directly accessible to the perfused dextran solution, the presence of the dextran fluorescence in the dying HCs suggests the passage of the dextrans through the paracellular pathway of supporting cells. Moreover, the current study demonstrated that the level of paracellular permeability was limited in noise-damaged cochleae because there was no FITC-dextran fluorescence in the cochleae stained with large molecular weights of FITC-dextrans (500 kD or 2,000 kD). Collectively, the results of the current study suggest the occurrence of mechanical injury to cell-cell junctions of supporting cells. Study of the biological role of this structural defect of the supporting cell attachment in induction of HC death seems imperative.

## **706 Relation of Focal Hair-Cell Lesions to Noise-Exposure Parameters**

Gary W. Harding<sup>1</sup>, Barbara A. Bohne<sup>1</sup>

<sup>1</sup>Washington University School of Medicine

Previously, we examined the relation between total energy in the noise exposure & percentage losses of outer (OHC) & inner (IHC) hair cells in the apical & basal halves of 607 chinchilla cochleae (Harding & Bohne, JASA 115, 2004). The animals had been exposed continuously to either a 4-kHz octave band of noise (OBN) at 47-108 dB SPL for 0.5

hr-36 days, or a 0.5-kHz OBN at 65-128 dB SPL for 3.5 hr-433 days. Interrupted exposures were also employed for both OBNs. Post-exposure recovery times ranged from 0-913 days. Cluster analysis was used to separate the data into 3 magnitudes of damage. The data were also separated into recovery times of 0 days (acute) & > 0 days (chronic). It was found that moderate-level, moderate-duration exposures produced OHC & IHC losses that were related to total energy, while hair-cell losses from high-level, short-duration exposures were not related to total energy. A substantial part of the hair-cell losses occurred in focal lesions (i.e.,  $\geq 50\%$  loss of IHCs, OHCs or both cell types over a distance of  $\geq 0.03$  mm). This abstract describes, within the same 3 clusters, the apex-to-base distribution of 1820 lesions found in 468 of 660 noise-exposed cochleae. In these cochleae, organ-of-Corti (OC) length in mm was converted to % distance from the apex. The data were analyzed to determine % distance from the apex and size (mm) of the lesions. In 55 of 140 non-noise-exposed OCs, there were 186 lesions, the characteristics of which were also determined. Focal lesions involved IHCs only, OHCs only or combined OHCs & IHCs. The OHC only and combined lesions were grouped for the analysis. The distributions of lesion location were tallied in 2 %-distance bins. In controls, focal lesions were uniformly distributed from apex to base & 70% of them were pure IHC lesions. In cochleae exposed to the 4-kHz OBN, lesions were distributed in the basal half of the OC. In cochleae exposed to the 0.5-kHz OBN, lesions occurred in both halves of the OC. With continuous exposures, 74% of the lesions were pure OHC or combined lesions. With interrupted exposures, 48% of the lesions were pure IHC lesions. Lesion size was larger in the chronic compared to acute cochleae with similar exposures. There was a minimum total energy at which focal lesions began to appear & slightly higher energies resulted in nearly all exposed cochleae having focal lesions.

## **707 Phosphorylation of Nuclear Factor-Kappa B in the Inner Ear by Loud Sound Stimulation**

Hiroshi Yamamoto<sup>1</sup>, Xiaorui Shi<sup>1</sup>, Irina Omelchenko<sup>1</sup>, Alfred Nuttall<sup>1</sup>

<sup>1</sup>Oregon Health and Science University

Nuclear factor-kappa B (NF- $\kappa$ B) plays an essential role in the regulation of genes involved in various biological processes, such as inflammation, immune responses, neuronal development, and cellular apoptosis. NF- $\kappa$ B activation can be achieved through two main pathways. The canonical (classical) pathway is known to be involved in the response of various cell types to pathogen associated molecules as well as proinflammatory cytokines, such as tumor necrosis factor alpha (TNF- $\alpha$ ) and interleukin-1 (IL-1). The noncanonical (alternative) is activated by a different specific set of stimuli, including B-cell activating factor (BAFF), lymphotoxin  $\beta$ , and CD40L.

In this study, using immunohistochemistry and immunoblot analysis, we determined whether one or both NF- $\kappa$ B pathways, canonical (classical) or noncanonical (alternative), were involved in the loud sound-induced

cellular damage mechanisms in guinea pig cochlea. in control (non-sound stimulated) condition, we found that there was no detectable phosphorlated P65 in canonical pathway or P100 in the noncanonical pathway in both organ of Corti and cochlear lateral wall. However, NF- $\kappa$ B activation related P65 phosphorylation was detected in the inner ear immediately following loud sound exposure at 120dB SPL/3hr for a day. There was no phosphorylation of P100 at any time period following loud sound stimulation. These results suggest that loud sound stress activates NF- $\kappa$ B dependent on P65 (canonical) pathway but not P100 (non-canonical) pathway in the response to loud sound-induced cellular damage. Supported by NIH/NIDCD DC 000105 and DC 04716

### **708 Gadd45 $\beta$ is a Pro-Survival Factor Induced by Noise-Overexposure in the Membranous Labyrinth of 129 Mice Highly Resistant to Noise Damage**

Michael Anne Gratton<sup>1</sup>, Anna Eleftheriadou<sup>2</sup>, Ana Vazquez<sup>3</sup>

<sup>1</sup>University of Pennsylvania, Philadelphia PA, USA, <sup>2</sup>G. Gennimatas Hospital Athens, Greece, <sup>3</sup>University of California Davis

Stress-activated pathways and the induction of apoptosis have been implicated in noise-induced hair cell damage. Specifically, interfering with the Jun N-terminal kinase (JNK) pathway was demonstrated to confer significant protection from noise-induced hearing loss (NIHL). Additionally, GADD45 $\beta$  can suppress JNK apoptotic signaling (De Smaele et al. 2001). GADD45 $\beta$  expression was compared in control and noise-exposed groups of NIHL resistant 129Sv mice. the "noise" groups were exposed to a 1-h, 105-dB SPL, 10-kHz centered octave band of noise. a significant upregulation of GADD45 $\beta$  transcript level occurred post-noise. Furthermore, GADD45 $\beta$  protein expression was studied. GADD45 $\beta$  immunoreactivity was evident in cochlea from 129 mice that had been exposed to noise and sacrificed 6 h postexposure. in contrast, virtually no immunoreactivity was detected in the cochleae of sham-exposed control mice. GADD45 $\beta$  immunofluorescence was localized to the stria vascularis of noise-exposed 129 mice. Specifically, GADD45 $\beta$  immunofluorescence appeared to be associated with the cell nuclei. Enhanced GADD45 $\beta$  immunoreactivity following noise exposure was also evident in the inner and outer hair cells and in some supporting cells of the organ of Corti as well as fibrocytes of the spiral limbus. Additionally, very strong immunofluorescence was observed in 8th cranial nerve fibers post-noise exposure when compared to corresponding sections from sham-exposed control mice where virtually no such immunofluorescence was detected. Although the implications of the upregulation of GADD45 $\beta$  in the cochlea are not yet understood there is strong evidence for antiapoptotic roles for GADD45 $\beta$ . Increased expression of GADD45 $\beta$  may contribute to the resistance to NIHL observed in 129Sv mice. Together, the findings could provide a rational basis of designing novel interventions against NIHL using endogenous protective mechanisms

known to interfere with the cell death pathways. This work was supported by NIDCD R21-DC04990 to AEV.

### **709 Sensors for Real-Time Monitoring of Reactive Oxygen Species for Study of Noise-Induced Hearing Loss**

Rebekah Wilson<sup>1</sup>, Alexander Scheeline<sup>1</sup>, Edward T. Chainani<sup>1</sup>, Jonathan H. Siegel<sup>2</sup>

<sup>1</sup>University of Illinois at Urbana-Champaign, <sup>2</sup>Northwestern University

Noise induced hearing loss (NIHL) affects 28 million Americans and with the growing population, this number will only increase. Being able to investigate important species that may be present during loud noise exposure will help to build better preventative measures and may even help reverse the damage. We are developing two types of amperometric sensors to detect reactive oxygen species (ROS) in the inner ear of Mongolian gerbils during noise exposure. the sensors are assembled on a flexible Kapton<sup>®</sup> substrate. One style of sensor employs a three electrode setup, with Ir/IrO<sub>x</sub> pseudo-reference electrode, polypyrrole counter electrode and superoxide dismutase (SOD) or peroxidases on the working electrode (with the enzyme anchored to the substrate via a thiol linker). These can be created on one or both sides of the sensor substrate to optimize fabrication. the other style is a two electrode setup where both sensors are coated with SOD via a thiol linker.

A second type of sensor is being fabricated to monitor ion concentration using bipolar pulse conductance, with the main targets being K<sup>+</sup>, Na<sup>+</sup>, Ca<sup>2+</sup>, Mg<sup>2+</sup>, and Cl<sup>-</sup>. We report sensor fabrication and modification along with sensitivity, reproducibility, and interference studies for such sensors, with possible preliminary data on excised cochlea.

### **710 Individual Susceptibility to Noise-Induced Hearing Loss: Inner Ear Control Seems to Be a Key Factor**

Ann-Cathrine Lindblad<sup>1</sup>, Åke Olofsson<sup>1</sup>

<sup>1</sup>Karolinska Institutet

In a project regarding noise susceptibility about 200 Swedish conscripts had tests of the inner ear at the start and at the end of service (7-11 months). an unexposed control group was tested with the same interval. the hearing of conscripts from armoured personal carriers, APCs, and from army orchestras were most affected by the noise but in entirely different ways. the APC group had many incidents with impulse noise, and we learnt to identify the characteristic pattern caused by impulse noise, which suggests impaired ipsilateral control.

in a second project former subjects came for a follow-up about 4.5 years later. Hearing thresholds, otoacoustic emissions, and thresholds for very short tones in modulated noise, were measured again on 73 former conscripts and controls. Since the music group was found to be vulnerable because of less use of protection also 23 students from the Royal College of Music were tested 3 times with one-year intervals. "Long-term" predictors have been sought.

Deteriorating hearing thresholds after noise exposure could be predicted from certain results in the very first measurement of all groups. the only results useful for prediction for all groups, i.e. for all types of exposure, already for a time span of 1 year or less were the thresholds for brief tones in intensity-modulated noise. Other predictors like contralateral suppression of TEOAEs were suggested but with different frequency bands for the groups.

For the longer time spans 5-6 years as well as 2 years also the variability in DPOAEs (individual st. dev. for 20 consecutive measurements at 1 or 2 kHz) is a good predictor. Large variability in results can be recorded for responses near to noise level, but also when responses are strong due to weak restraining control. Thus our two best predictors for "long-term" exposure of young people concern the quality of the ipsilateral control of the inner ear. an intriguing figure regarding the larger vulnerability of the left ear will be shown.

### **711 Neuroprotective Effects of T-817MA Against Noise-Induced Hearing Loss**

Daisuke Yamashita<sup>1</sup>, Akihiro Shiotani<sup>2</sup>, Sho Kanzaki<sup>3</sup>, Kaoru Ogawa<sup>3</sup>

<sup>1</sup>Department of Otolaryngology, National Tokyo Medical Center, Tokyo, Japan, <sup>2</sup>Department of Otolaryngology, National Defense Medical College, Saitama, Japan, <sup>3</sup>Department of Otolaryngology, Keio University Hospital, Tokyo, Japan

Oxidative stress, including reactive oxygen species and other free radicals, is thought to play an important role in neuronal cell death, including noise-induced hearing loss. 1-{3-[2-(1-Benzothiophen-5-yl)Ethoxy]propyl}azetidin-3-ol maleate (T-817MA), a novel neurotrophic agent, protects against oxidative stress-induced neurotoxicity. This study examines the effects of T-817MA in noise-induced ototoxicity in the cochlea. Guinea pigs received treatment with T-817MA-enhanced water (0.2 mg/ml, 0.7 mg/ml) or untreated water (control) beginning 10 days prior to noise exposure and continuing through this study. All subjects were exposed to 4-kHz octave-band noise at 120-dB SPL for 5h. Auditory thresholds were assessed by sound-evoked auditory brainstem response at 4, 8, and 16 kHz, prior to and 10 days following noise exposure. Hair cell damage was analyzed by quantitative histology. T-817MA significantly reduced threshold deficits and hair cell death. These results suggest T-817MA reduces noise-induced hearing loss and cochlear damage, suggesting functional and morphological protection.

### **712 Bcl-2 Prevents Hearing Loss in a Mouse Model of Sound Trauma**

Susanna Pfannenstiel<sup>1</sup>, Mark Praetorius<sup>2</sup>, Peter-K. Plinkert<sup>2</sup>, Douglas E Brough<sup>3</sup>, Hinrich Staecker<sup>1</sup>

<sup>1</sup>Dept. Otolaryngology Head and Neck Surgery, Univ. Kansas School of Medicine, KS U.S.A., <sup>2</sup>Dept. Otolaryngology, Univ. Heidelberg, Heidelberg Germany, <sup>3</sup>GenVec Inc. Gaithersburg, MD U.S.A.

Overexpression of bcl-2 has been demonstrated to prevent hair cell death in an *In Vitro* and in an *In Vivo* ototoxicity

model. to determine if the mechanisms of injury influences the protective effects of bcl-2 we have developed a mouse model of bcl-2 delivery after sound trauma. Adult C57Bl/6 mice were anesthetized and measured by auditory brain stem response (ABR) and distortion products of otoacoustic emissions (DPOAEs). After evaluation of the hearing threshold mice underwent a sound exposure of 16 kHz and 115 dB for two hours. ABR and DPOAEs were evaluated ten days and 24 days after sound exposure. Finally, the cochleae were removed and the inner ear examined by thick serial sections under confocal microscopy to establish the degree of hair cell loss. After evaluation of pre treatment hearing thresholds, a second group of mice was pretreated with an advanced generation adenovector expressing human bcl-2 driven by the CMV promoter delivered via the posterior semicircular canal. Seventy two hours after vector delivery mice were exposed to sound. Hearing thresholds were evaluated ten and 24 days post sound trauma and histology was evaluated 24 days post sound trauma. Bcl-2 gene therapy was found to protect hair cells from sound trauma.

### **713 Protective Effect of Exogenous GM-1 Ganglioside On Acoustic Injury of the Cochlea**

Shuho Tanaka<sup>1</sup>, Keiji Tabuchi<sup>1</sup>, Akira Hara<sup>1</sup>

<sup>1</sup>University of Tsukuba

GM-1 ganglioside, a glycosphingolipid with an attached monosialic acid moiety, is found in high concentrations embedded in the external lipid layer of neuronal membranes. It was found as one of the neuronotrophic agents, and then the actions in the central nervous system have been most studied. the concentration of such endogenous GM-1 ganglioside increases in the brain tissue after injury, and GM-1 ganglioside prevents neuronal degeneration following various central and/or peripheral nervous system lesions. Because of its neuroprotective and neurorestorative properties, GM-1 ganglioside has been clinically administered to patients with spinal cord injury, Alzheimer's disease and so on. the purpose of this study was to evaluate the effects of GM-1 ganglioside on acoustic injury of cochlea. Mice were exposed to a 4 kHz pure tone of 128 dB SPL for 4 hours. GM-1 ganglioside was intraperitoneally administered immediately before the onset of acoustic overexposure. the threshold shift of the auditory brainstem response (ABR) and hair cell loss were then evaluated one and two weeks after acoustic overexposure. GM-1 ganglioside significantly decreased ABR threshold shift and protect the cochlea against acoustic injury. This finding indicated a protective role of GM-1 ganglioside against acoustic injury of the cochlea.

## **714 Priming with Low Dose Systemic Lipopolysaccharide Protects Against Acoustic Trauma in the Murine Cochlea**

**H.Elizabeth Shick<sup>1</sup>**, Eisuke Sato<sup>1</sup>, Keiko Hirose<sup>2</sup>

<sup>1</sup>Neuroinflammation Research Center, Lerner Research Institute, Cleveland Clinic, <sup>2</sup>Head and Neck Institute, Cleveland Clinic

We have previously shown that mononuclear phagocytes accumulate in the mouse cochlea after acoustic injury. We questioned whether these phagocytic cells could be primed to play a protective role. Previous studies in the central nervous system have demonstrated that low dose systemic lipopolysaccharide (LPS) can be protective prior to ischemic insult. Systemic LPS results in microglial activation and subsequent neuronal protection.

in these experiments, we preconditioned mice with 1 mg/kg LPS injected IP for two consecutive days and determined that (1) LPS at this dose caused minimal threshold elevation and no cochlear damage that could be perceived on light microscopy (2) LPS preconditioning was associated with massive influx of cochlear macrophages that was detected 24 hours after the first dose of LPS and remained elevated to 21 days after LPS injection (3) LPS priming performed 24 hours prior to 100 dB octave band noise resulted in protection against both transient threshold shift and permanent threshold shift. Based on these findings, it appears that preconditioning of cochlear macrophages with mediators of systemic inflammation can result in protection of the cochlea against subsequent injury by acoustic trauma.

## **715 The Effect of Anti-Interleukin-6 Receptor Antibody in Noise Induced Damaged Cochlea**

**Kenichiro Wakabayashi<sup>1</sup>**, Masato Fujioka<sup>2</sup>, Sho Kanzaki<sup>1</sup>, Masatsugu Masuda<sup>3</sup>, Daisuke Yamashita<sup>1</sup>, Hiroataka James Okano<sup>4</sup>, Hideyuki Okano<sup>4</sup>, Kaoru Ogawa<sup>1</sup>

<sup>1</sup>Department of Otolaryngology, Head and Neck Surgery, Keio University School of Medicine, <sup>2</sup>Eaton-Peabody Lab. Massachusetts Eye and Ear Infirmary, <sup>3</sup>Department of Surgery, Otolaryngology, University of California School of Medicine, <sup>4</sup>Department of Physiology, Keio University School of Medicine

Back grounds : Recent studies have shown that inflammatory responses occur in inner ear under various damaging conditions including noise-overstimulation. We reported that proinflammatory cytokine interleukin-6 (IL-6) increased at 3 hr after noise exposure in rat model (Fujioka M et al. J. Neuroscience Res. 2007). to investigate the effect of the inhibition of IL-6 by anti-interleukin-6 receptor antibody (MR16-1) for hearing loss model animal, we gave MR16-1 to noise exposed mice and evaluated its effect in noise induced damaged cochlea.

Purpose: Evaluation of the effect of MR16-1 in noise induced damaged cochlea

Methods: C57BL6 mice were given noise exposure (4kHz octave band noise, 124dB SPL, 2hr), and immediately we injected mice intraperitoneally with a single dose of MR16-1 (100  $\mu$ g/g body weight) or rat IgG for a control group.

We evaluated hearing function using acoustic brain stem response (ABR) and pathological changes using plastic sections, frozen sections, and transmission electron microscope.

Results: At 3 weeks after noise exposure, there is functional improvement in 4kHz with ABR in the group of MR16-1 comparing with the control group. Pathological changes in lateral walls and stria vascularis were protected in the group of MR16-1, but not in the control group.

Discussion: MR16-1 had protective effect for noise induced damage in inner ear both functionally and pathologically. We will investigate other proinflammatory cytokines with the same assay and extend these results to the primate model.

## **716 The Effect of Phospholipase A2 Inhibitors On Acoustic Injury of the Cochlea**

**Uemaetomari Isao<sup>1</sup>**, Keiji Tabuchi<sup>1</sup>, Nakamagoe Mariko<sup>1</sup>, Hara Akira<sup>1</sup>

<sup>1</sup>University of Tsukuba

The protective mechanism of steroidal hormones against acoustic injury has not been clarified yet. Steroidal hormones block cascades of arachidonic acid (AA) via phospholipase A2 (PLA2) inhibition. the PLA2 family consists of two subtypes: the secretory PLA2 (s-PLA2) and the cytosolic PLA2 (c-PLA2). PLA2 is a family of phospholipid hydrolyzing enzymes that are involved in diverse pathological process and plays an important role in production of prostaglandins and leukotrienes. the purpose of the present study was to examine the protective effect of two types of PLA2 inhibitors in acoustic injury. Female ddY mice of 8 weeks of age were used in this study. Animals were subjected to a 4 kHz pure tone of 128 dB SPL for 4 hours through an open field system inside a sound-exposure box. Auditory brainstem response (ABR) was examined before, one and two weeks after acoustic overexposure. After final ABR measurements at two weeks after acoustic overexposure, whole mounts of organ of Corti were stained for the nucleus with propidium iodine, and missing hair cells (missing of staining with propidium iodide) were counted every 0.33 mm segments. c-PLA2 inhibitor significantly improved the ABR threshold shifts and decreased hair cell loss two weeks after acoustic overexposure when it was administered before acoustic overexposure. However s-PLA2 inhibitor did not exhibited a protective effect. the present findings suggest that c-PLA2 inhibitor have protective effects against acoustic injury of the cochlea.

## **717 Therapeutic Effects of Combinations of 4-OHPBN and Other Antioxidant Drugs On Noise-Induced Hearing Loss**

**Chul-Hee Choi<sup>1</sup>**, Kejian Chen<sup>1</sup>, Angelica Vasquez-Weldon<sup>2</sup>, Ronald Jackson<sup>3</sup>, Robert Floyd<sup>2</sup>, Richard Kopke<sup>1</sup>

<sup>1</sup>Hough Ear Institute, <sup>2</sup>Oklahoma Medical Research Foundation, <sup>3</sup>Naval Medical Center

Sensorineural hearing loss caused by acute acoustic trauma (AAT) results from oxidative stress leading to excessive production of reactive oxygen, nitrogen, and other free radical species in the cochlea. Oxidative stress

may occur through different mechanisms such as mitochondrial injury, excessive glutamate release, and depletion of glutathione. Antioxidants such as N-acetyl-L-cysteine (NAC), a glutathione prodrug, acetyl-L-carnitine (ALCAR), a mitochondrial biogenesis agent, and hydroxylated alpha-phenyl-tert-butyl nitrone (4-OHPBN), a nitron-based free radical trap, have been used to reduce noise-induced hearing loss. This study tested the effects of 4-OHPBN plus NAC and 4-OHPBN plus NAC and ALCAR on noise-induced hearing loss.

Chinchillas were randomly assigned to three groups, exposed to a 105 dB narrow-band noise centered at 4 kHz for 6 hours, and administered different drug combinations with different doses: 1) administered carrier solution only; 2) administered 4-OHPBN (50mg/kg) + NAC (100mg/kg); 3) administered 4-OHPBN (20mg/kg) + NAC (50mg/kg) + ALCAR (20mg/kg). Carrier solutions or drugs were intraperitoneally injected four hours after noise exposure with the same injections twice daily for the next two days. Threshold shifts in auditory brainstem responses compared between before and 3 weeks after noise exposure were calculated at 0.5, 1, 2, 4, 6, and 8 kHz. Missing outer hair cells (OHC) in the percent distance from the cochlear apex were also obtained. These data were analyzed with ANOVA.

Both drug combinations reduced permanent threshold shifts and OHC loss and showed a synergistic effect in the treatment of AAT. the drug combinations had greater efficacy with lower dosage than those of each antioxidant drug alone. the results demonstrate that combinations of antioxidants can effectively treat acute acoustic trauma and decrease the required medication doses.

Supported by the office of Naval Research and INTEGRIS Baptist Medical Center

### **718 The Effectiveness of N-Acetyl-L-Cysteine (L-NAC) in the Treatment of Noise-Induced Hearing Loss**

**Bob Davis<sup>1</sup>**, Roger Hamernik<sup>1</sup>, Wei Qiu<sup>1</sup>

<sup>1</sup>SUNY Plattsburgh

Three groups of chinchillas were exposed to a nonGaussian continuous broadband noise at an Leq = 105 dB SPL, 8 h/d for 5 d. One group (N = 6) received only the noise. a second group (N = 6) received the noise and was additionally treated with L-NAC (325 mg/kg, i.p.). Treatment was administered twice daily for two days prior to exposure and for two days following the exposure. During exposure the animals received the L-NAC just prior to and immediately after each daily exposure. the third group (N = 4) was exposed to the noise and received saline injections on the same schedule as the L-NAC treated animals. Auditory evoked potential recordings from the inferior colliculus were used to estimate pure tone thresholds and surface preparations of the organ of Corti quantified the sensory cell population. in all three groups permanent threshold shift exceeded 50 dB at 2.0 kHz and above with severe sensory cell loss in the basal half of the cochlea. There was no statistically significant difference among the three groups in all measures of noise-induced trauma. Thus, treatment with L-NAC did not reduce the

trauma produced by a high-level, long duration, broadband noise exposure.

### **719 Auditory Toughening Induced by Low Level Sound in Rats**

**Pawel J Jastreboff<sup>1</sup>**, Cynthia a DeMots<sup>2</sup>, Jamie L Moran<sup>2</sup>, Jianrong Shi<sup>2</sup>, Margaret M Jastreboff<sup>2</sup>

<sup>1</sup>Emory University, <sup>2</sup>Towson University

**Introduction:** Auditory toughening, i.e., conditioning an animal to a low-level intermittent sound prior to a traumatic noise exposure, has been shown to protect the cochlea from damaging levels of sound. Past results were restricted to conditioning to high-level sound, above 80 dB SPL. the aims of this study were to evaluate whether: 1) a lower level of conditioning sound is effective and 2) the outer hair cells (OHC) system is involvement in this process.

**Methods:** 21 male pigmented rats were divided into 3 groups: control, exposed to 47 dBA SPL ambient background (n=6) and two toughening groups exposed to broad band noise (5 days, 12 h/day) with intensities of 60 dBA SPL(n=8) and 72 dBA SPL (n=7). 48 hours following toughening (or waiting for the control group) rats were exposed under Nembutal anesthesia to traumatic pure tone (7.8 kHz, 110 dB SPL, 20 min, left ear). Auditory Brainstem Response (ABR) and Distortion Product Otoacoustic Emission (DPOAE) measurements were performed at the beginning of experiment, after toughening (or waiting for control group), immediately following the traumatic exposure, and 12 days later.

**Results:** Traumatic sound exposure resulted in a shift of about 40 dB for ABR and about 30 dB for DPOAE. There were no significant differences between groups. Statistically significant recovery was observed for both ABR and DPOAE 12 days later, with the extent of recovery significantly correlated to the level of background noise (P<0.001).

**Conclusions:** Auditory toughening at 60 or 72 dBA significantly improves recovery after 12 days of hearing threshold and of OHC function while it did not offer a protective effect on cochlear function immediately following a traumatic sound exposure. This suggests that protective mechanisms involve long term survival and recovery of hair cells. the minimal sound level for the protective effect may be below 60 dBA SPL.

### **720 Detection of Highly-Reactive Oxygen Species (Hros) in Rat Organ of Corti Treated with Gentamicin**

**Yun-Hoon Choung<sup>1</sup>**, Akiko Taura<sup>2</sup>, Kwang Pak<sup>2</sup>, Eduardo Chavez<sup>2</sup>, Masatsugu Masuda<sup>2</sup>, Allen F. Ryan<sup>2</sup>

<sup>1</sup>UCSD School of Medicine and VA Medical Center, Ajou University School of Medicine, <sup>2</sup>UCSD School of Medicine and VA Medical Center

**Background and Objectives:** Reactive oxygen species (ROS) are thought to be involved in aminoglycoside-induced hair cell (HC) loss. Two new probes, aminophenyl fluorescein (APF) and hydroxyphenyl fluorescein (HPF) are selective dyes for the detection of hROS (OH, ONOO<sup>-</sup>,

OCI) in living cells. These probes were used to detect hROS in the cells of neonatal rat organ of Corti (oC) after gentamicin exposure *In Vitro* and to examine the relationship between cell death and the formation of hROS. **Materials and Methods:** hROS formation was examined in two conditions. in the first, explants of basal, middle or apical turn oC from p3 Sprague-Dawley rats were maintained in Dulbecco's modified Eagle's medium (DMEM) and exposed to gentamicin (50  $\mu$ M) for 24, 48, or 72 hours. the explants were concurrently treated with APF (15  $\mu$ M) or HPF (7.5  $\mu$ M) and their fluorescence was documented. in the second experiment, explants were exposed to higher levels of gentamicin (0.5 and 1 mM), and observed at 0, 2, 10, 20, 40, 60 and 80 minutes. Formation of hROS was compared with HC loss across cochlear turns by co-labeling with phalloidin and DAPI after fixation. the sensitivity of HPF and APF for the detection of hROS was compared by analysis of cell number and fluorescence intensity.

**Results:** in the first study, hROS formation was initially detected in HCs of the basal and middle turn oC exposed to 50  $\mu$ M gentamicin at 48 hours, with an increase in hROS at 72 hours. the formation of hROS at 48 hours was restricted to outer HCs (OHCs), and occurred before the loss of HC stereocilia. At 72 hours, OHCs that had lost their stereocilia showed hROS, and formation of hROS in a few inner HCs (IHCs) was noted. Very little formation of hROS was observed in apical turn explants, even at 72 hours. in the second experiment, formation of hROS was first detected at 10 minutes primarily in first row OHCs and IHCs, and remained constant for 80 minutes. No HC loss was observed by 80 minutes. in both experiments, APF was more sensitive than HPF in detecting hROS.

**Conclusion:** the generation of hROS appears to be an important initial step in gentamicin-induced hair cell death. the differential sensitivity of basal and middle turn HCs appears to be related to differences in hROS formation, with very little formation in apical HCs. Low dose gentamicin *In Vitro* produce patterns of hROS formation that are similar to HC loss produced by gentamicin *in vivo*. the effects of antioxidants on hROS formation in HCs, as well as *In Vivo* studies, are in progress.

(Supported by NIH grant DC00139, the Research Service of the VA, and the Korea Research Foundation Grant funded by the Korean Government (MOEHRD, Basic Research Promotion Fund) (KRF-2006-E00081))

## **721 Novel Aminoglycoside-Interacting Proteins**

**Pavan Kommareddi<sup>1</sup>**, Jochen Schacht<sup>1</sup>

<sup>1</sup>*Kresge hearing research institute, University of Michigan, Ann Arbor*

The mechanisms of aminoglycoside toxicity are a complex series of events from entry into cells to intracellular distribution and modulation of signaling pathways. Recent focus has largely been on uptake processes, and the overall effect of these drugs on redox balance and apoptotic pathways. Less is known about specific intracellular binding sites and the consequence of such interactions on the initiation and overall expression of toxicity. Early research had suggested phosphoinositides

as receptor-like sites for aminoglycosides, and association with RNA has been suggested in analogy to the antibacterial action of the drugs. in bacteria aminoglycosides bind to 30S or 50S ribosomal subunits RNA and block initiation of protein synthesis, translation and misreading of mRNA followed by misincorporation of amino acids. Aminoglycoside-protein interactions have received attention mostly in connection with putative transporters such as megalin but have remained relatively unexplored for intracellular targets.

We investigated specific aminoglycoside-protein interactions in order to gain further insight into the mechanism of aminoglycoside toxicity. a phage display technique was developed using mouse kidney mRNA with both oligo dT and random primers to create a T7 phage display library. Kanamycin was immobilized on polystyrene beads to serve as a substrate for biopanning for kanamycin-binding proteins displayed on phages. Isolated phages were used to infect BLT5403 bacteria for amplification. Amplified phages were used in another round of biopanning for a total of four cycles to enhance binding specificity. Individual phage were isolated by a plaque assay, subjected to PCR and sequenced. Expressed proteins were identified through BLAST and DNASTar. We found fourteen unique proteins interacting with kanamycin. the proteins identified are involved in ribosome biogenesis, mitochondrial respiratory chain and transcription.

This study was supported by research grant DC-03685 and core grant P30 DC-05188 from the National Institute on Deafness and Other Communication Disorders.

## **722 Role of Gap Junctions and Gap Junctional Coupling in Aminoglycoside Ototoxicity**

Nilesh Shah<sup>1</sup>, Jim Pearson<sup>1</sup>, Yufei Yu<sup>2</sup>, Michele Gandolfini<sup>2</sup>, Renato Rozental<sup>2</sup>, **Ana Kim<sup>1</sup>**

<sup>1</sup>*New York Eye and Ear Infirmary,* <sup>2</sup>*New York Medical College*

Hair cells are the mechanoreceptors in the cochlear and vestibular system, playing the crucial role of transducing sound and motion signals from the periphery to the central nervous system. Majority of disorders causing hearing loss and balance disorders are thought to be due to degeneration of these hair cells. Hearing loss may occur in up to about 20% of patients, and balance dysfunction in about 15% from aminoglycoside use. Currently, there is no treatment to replace the lost hair cells. Gap junctions are sites of direct communication between adjacent cells, allowing passage of small metabolites, ions, and second messengers, thereby coupling cells electrically and chemically. a proposed mechanism of aminoglycoside ototoxicity is through the inhibition of intercellular coupling by free radical formation. We previously presented data on our well established animal model of streptomycin ototoxicity, where by 2 weeks after streptomycin injection through the oval window, SEM studies showed complete hair cell loss within the vestibular epithelia. Vestibulo-collic testing showed reduced gain and phase leads consistent with vestibular dysfunction compared to the control group



( $p=0.00$ ). Using this established animal model, this current study focuses on the role of gap junctions and gap junctional coupling in mediating aminoglycoside-induced ototoxicity.

This work was supported by the Triological Society Career Development Award and Children's Hearing Institute.

### **723 Do Gap Junctions Enable Intercellular Aminoglycoside Trafficking?**

**Anna Stagner<sup>1</sup>, Qi Wang<sup>1</sup>, Takatoshi Karasawa<sup>1</sup>, Peter Steyger<sup>1</sup>**

<sup>1</sup>*Oregon Health & Science University*

Trans-tympanic membrane injection of aminoglycosides enables these drugs to resolve clinical vestibular disorders. In animals, trans-tympanic administration of aminoglycosides also traffics throughout the basal coil of the cochlea, and are localized in fibrocytes in the lateral wall radial to the stria vascularis. Can aminoglycosides traffic through cells via gap junctions composed of connexin (Cx) Cx26 or Cx43?

Fluorescently-tagged gentamicin (GTTR) microinjected into MDCK cells passes into neighboring cells, presumably via Cx43 gap junctions. To determine if Cx26 gap junctions also allow GTTR trafficking, communication-deficient HeLa cells were transfected with GFP-tagged Cx26, which formed gap junctions permeable to Alexa-488. We also used HeLa-TetOn cells stably transfected with Cx26 under the control of a tetracycline-response element; Cx26 localizes at the cell membrane after 48 hours doxycycline treatment. Microinjection of anionic Alexa-488 shows dye coupling in both transient and doxycycline-induced Cx26 expressing cells; this coupling is not seen with injection of GTTR or Texas Red alone. Cx26-expressing HeLa cells showed greater uptake of extracellular GTTR compared to non-expressing cells. In doxycycline-induced Cx26-expressing HeLa cells, GTTR uptake was decreased by treatment with 18 $\alpha$ -glycyrrhetic acid, a non-specific gap junction blocker. These data were verified using unconjugated gentamicin and subsequent immunocytochemistry.

The data suggest that gap junctions may play a role in aminoglycoside trafficking in the lateral wall of the inner ear.

*Funded by DC004555 (PSS), T32 DC005945 (AS) and F32 DC008465 (TK)*

### **724 Gentamicin Trafficking in the Cochlea**

**Qi Wang<sup>1</sup>, Chun-Fu Dai<sup>2</sup>, Peter Steyger<sup>1</sup>**

<sup>1</sup>*Oregon Health & Science University*, <sup>2</sup>*Fudan University*

Systemic administration of aminoglycosides is essential for treating bacterial sepsis in premature infants, children and adults, yet has serious nephrotoxic and ototoxic side effects. The mechanism(s) by which aminoglycosides enter the cochlea remain poorly understood. To identify potential transport routes aminoglycosides use to pass from the vasculature into endolymph, we injected purified Texas Red-conjugated gentamicin (GTTR) into mice, prior to transcardiac perfusion fixation at several subsequent timepoints. Cochleae were excised and cryostat-sectioned, or the stria vascularis whole-mounted, for confocal

microscopy. We observed rapid and preferential uptake of GTTR in marginal cells of the stria vascularis compared to neighboring cell types, and verified by gentamicin immunocytochemistry.

To elucidate which mechanisms may be involved, we co-administered increasing molar ratios of gentamicin:GTTR (150-900 mg/kg), each dose containing 1.7 mg/kg GTTR. Three hours later, cochleae were fixed and examined by confocal microscopy. Increasing molar dilution of GTTR by gentamicin led to decreased GTTR fluorescence in hair cells and marginal cells, but not in intra-strial tissues nor strial capillaries. Thus, GTTR uptake in marginal cells is competitively inhibited by gentamicin, suggesting that a regulatable barrier for gentamicin entry into endolymph exists at the interface between marginal and intermediate cells. Preferential loading of the stria vascularis by systemically-administered aminoglycosides could facilitate aminoglycoside entry from endolymph into hair cells via (i) apical endocytosis, and/or (ii) non-selective cation channels, including mechanoelectrical transduction channels.

*Funded by NIDCD DC004555 (PSS), and Educational Ministry of China (NCET 06-0369; CFD).*

### **725 Identification of Gentamicin-Binding Proteins in the Inner Ear**

**Takatoshi Karasawa<sup>1</sup>, Qi Wang<sup>1</sup>, Larry David<sup>1</sup>, Peter Steyger<sup>1</sup>**

<sup>1</sup>*Oregon Health & Science University*

Inner ear sensory hair cells and kidney proximal tubule cells are the two cell types that retain aminoglycosides and are prone to aminoglycoside-induced cytotoxicity. Although there are a number of cell death mechanisms that are induced by aminoglycosides, we still have little understanding of how these drugs induce cytotoxicity. We hypothesize that aminoglycosides bind specific proteins in kidney proximal tubule cells and hair cells to trigger cell death mechanisms. As a first step to identify gentamicin-binding proteins (GBPs) in the inner ear, we identified proximal tubule-specific GBPs that are not present in distal tubule cells, since these GBPs may contribute to gentamicin-induced cytotoxicity in proximal tubule cells and inner ear sensory hair cells. We developed proximal and distal tubule cell lines from murine kidney primary cultures by spontaneous immortalization. We used gentamicin-agarose conjugates to pull-down GBPs from whole cell lysate of these cell lines, and resolved these GBPs by SDS-polyacrylamide gel electrophoresis. Several proximal tubule-specific GBPs were identified using mass spectrometry, including calreticulin, a known GBP (Horibe et al., 2004). We have determined the cochlear distribution of calreticulin by immunohistochemistry using murine cochleae. Calreticulin was localized in hair cell stereocilia, near the luminal surface of marginal cells in the stria vascularis, and lateral wall fibrocytes. We will also determine protein localization for the other GBPs. Future studies will determine whether gentamicin binding to GBPs induces cell death mechanisms, or inhibits GBPs' interactions with their physiological binding molecules/proteins.

## **726 CX3CR1 Expression in Cochlear Macrophages Down-Regulates Kanamycin Ototoxicity**

**Eisuke Sato**<sup>1</sup>, H.Elizabeth Shick<sup>1</sup>, Richard M. Ransohoff<sup>1</sup>, Keiko Hirose<sup>2</sup>

<sup>1</sup>Department of Neurosciences, Lerner Research Institute, Cleveland Clinic, <sup>2</sup>Head and Neck Institute, Cleveland Clinic

We have previously shown that resident macrophages are present in the murine cochlea. After injury, these macrophages increase in number. Cochlear leukocytes are identified by CD45 and 90% of these cells express CX3CR1+. CX3CL1 is the only known ligand for CX3CR1, and this ligand/receptor pair are necessary for signaling between neurons and microglia in the CNS. After kanamycin ototoxicity, CX3CR1null mice demonstrate more robust macrophage migration, more severe threshold elevation and more hair cell damage when compared to wild type and heterozygous mice.

We investigated how CX3CR1 on circulating leukocytes contributes to hearing loss and hair cell death after aminoglycoside by generating the following bone marrow chimeras: CX3CR1<sup>+/+</sup>→WT recipients; CX3CR1<sup>+/GFP</sup>→WT recipients; and CX3CR1<sup>GFP/GFP</sup>→WT recipients. Chimerized mice were treated with 800mg/kg kanamycin IP twice daily for 15 days. 2 weeks after treatment, ABR and histologic analysis were done. No difference in the average of the number of cochlear macrophages, ABR, or hair cell death were seen among the three chimeras. Additionally, all irradiated mice showed increased rates of monocyte migration when compared to non-irradiated kanamycin-treated animals.

Interestingly, a strong correlation was found between numbers of cochlear macrophages and hair cell death in CX3CR1<sup>GFP/GFP</sup>→WT mice, but not CX3CR1<sup>+/+</sup>→WT or CX3CR1<sup>+/GFP</sup>→WT animals. Our data suggest that: (1) Circulating CX3CR1-deficient macrophages exert a toxic effect on the cochlea after kanamycin exposure, while circulating macrophages that express CX3CR1 do not have the toxic phenotype; (2) in CX3CR1<sup>GFP/GFP</sup> mice, monocyte migration is more robust than in wild type or heterozygous mice; (3) the migration of circulating monocytes into the cochlea is enhanced by radiation. CX3CR1 may play a role in regulating monocyte trafficking in the cochlea and modulates toxic effects of these inflammatory cells after aminoglycoside exposure.

## **727 Cisplatin-Induced Gene Expression in the Rat Cochlea**

**Mette Kirkegaard**<sup>1</sup>, Åsa Skjönsberg<sup>1</sup>, Violeta Bucinskaite<sup>2</sup>, Göran Laurell<sup>3</sup>, Mats Ulfendahl<sup>1</sup>

<sup>1</sup>Center for Hearing and Communication Research, Karolinska Institutet, <sup>2</sup>Department of Physiology and Pharmacology, Karolinska Institutet, <sup>3</sup>ENT Research Laboratory, Umeå University

Cisplatin (cis-diaminodichloroplatinum) is a widely used chemotherapeutic agent but unfortunately the use is limited by its ototoxic and nephrotoxic effects. In addition to the DNA-damaging effects, cisplatin induces oxidative stress to cells of the inner ear, leading to mitochondrial damage and activation of cell death pathways. The aim of the present study was to explore the molecular signaling pathways in the cochlea by studying gene regulation at different time points following a cisplatin insult. Female Sprague Dawley rats were anesthetized and injected through the left jugular vein with cisplatin (16 mg/kg). Control animals received equivalent volumes of saline. Auditory brain stem responses were measured before the treatment and at 24, 48 and 96 hours following the cisplatin injection. Cisplatin treatment induced a mean threshold shift of 11 and 46 dB at 48 and 96 hours post treatment. At 24 hours post cisplatin injection there was no effect on the ABR. Following ABR measurements, the animals were sacrificed and the soft tissue of the cochlea, including the organ of Corti, stria vascularis and spiral ganglion, was dissected out and RNA was isolated and used for gene expression analysis. RNA extracted from a single cochlea was used on each microarray in order to identify the biological variation and to be able to correlate the induced threshold shifts to the gene regulation in individual animals. RNA from three control and three cisplatin-treated animals at each time point was hybridized to the GeneChip® Rat Genome 230 2.0 Array (Affymetrix). The statistical significance of differentially expressed genes was tested using a t-test, and the resulting list of genes sorted according to functional category in Gene Ontology. The long-term aim is that this approach will lead to new therapeutic interventions for cisplatin-induced hearing loss. Future therapies could work by blocking cell death pathways or stimulating protective or regenerative pathways.

## **728 Induction of Cisplatin Induced Kidney Injury Molecule 1 (KIM-1) by the NADPH Oxidase Isoform, NOX3, in the Rat Cochlea**

**Debashree Mukherjee**<sup>1</sup>, Sarvesh Jajoo<sup>1</sup>, Leonard Rybak<sup>1</sup>, Vickram q<sup>1</sup>

<sup>1</sup>SIU School of Medicine

Previous data from our laboratories have shown that kidney injury molecule-1 (KIM-1) is expressed in the cochlea and is induced by cisplatin. The induction of this protein by cisplatin was inhibited in animals pretreated with lipoic acid, a scavenger of reactive oxygen species (ROS). Cisplatin also induced the unique cochlear NADPH oxidase, NOX3 isoform, and Rac1 via an ROS-dependent mechanism. Rac1 appears essential for full NOX3 activity. In this study, we determined the roles of NOX3 and Rac1

in cisplatin-mediated upregulation of KIM-1. Using UB/OC-1 cells, we show that transient expression of the dominant negative Rac1 (dnRac1) suppressed cisplatin-mediated ROS generation and KIM-1 expression. However, UB/OC-1 cell over-expressing the wild type Rac1 or transfected with a control plasmid showed a 3-4 fold increase in KIM-1 expression in response to cisplatin, compared to vehicle-treated controls. Similar results were obtained in UB/OC-1 cells transfected with short inhibitory (si) RNA for NOX-3, but not with a scrambled siRNA sequence, and then treated with cisplatin. to determine the signaling pathway(s) activated by ROS in the induction of KIM-1, we focused on the mitogen activated protein kinase (MAPK), and nuclear factor (NF)- $\kappa$ B. Preliminary data indicate a role of extracellular signal regulated kinase (ERK1/2) and NF- $\kappa$ B in the induction of KIM-1. These results, implicate the NADPH oxidase system as a major regulator of KIM-1 expression by cisplatin in the cochlea via different signaling pathways.

## **729 Effects of Bax Inhibiting Peptide, Bcl-XI and Betulinic Acid On Neomycin Induced Outer Hair Cell Deaths**

**Yuji MIYAUCHI<sup>1</sup>**, Kazuma SUGAHARA<sup>1</sup>, Hiroaki SHIMOGORI<sup>1</sup>, Takefumi MIKURIYA<sup>1</sup>, Yoshinobu HIROSE<sup>1</sup>, Hiroshi YAMASHITA<sup>1</sup>

<sup>1</sup>*Yamaguchi University*

**Background:** It is already reported that death signal transduction is involved in the deaths of the outer hair cells. and it is becoming clear that mitochondria plays an important role in the process. in this study we evaluated if we could suppress the deaths of the outer hair cells, by blocking the death signal transduction in the mitochondria.

**Methods:** CBA/N mice aged from 4 to 6 weeks were used. Under deep anesthesia using Pentobarbital, we removed and cultured the utricles under sterile conditions. the deaths of the outer hair cells were induced by adding 1 mM neomycin. Bax inhibiting peptide, or Bcl-xL or betulinic acid were added to the culture medium. After culturing, the utricles were fixed by using 4%paraformaldehyde, and the sensory cells were immunohistochemically labeled by anti-calmodulin antibody and anti-calbindin antibody. the sensory cells were counted under fluorescent microscope.

**Results:** When 1 mM neomycin was added to the culture medium, deaths of about 25% of the outer hair cells were observed by 24 hours. We noticed tendency in inhibition of these deaths, by some of the substances introduced to the culture medium. We will be determining the prime concentration of these substances.

## **730 HSP-70 is Both Necessary and Sufficient to Protect Against Aminoglycoside-Induced Sensory Hair Cell Death**

**Mona Taleb<sup>1</sup>**, Carlene S. Brandon<sup>1</sup>, Lisa L. Cunningham<sup>1</sup>

<sup>1</sup>*Medical University of South Carolina*

Sensory hair cells are sensitive to death from aging, noise trauma, and ototoxic drugs. Induction of heat shock proteins (HSPs) is a highly-conserved stress response that can inhibit apoptosis in a variety of systems. We have previously shown that heat shock results in a robust upregulation of HSPs in the hair cells of the adult mouse utricle *In Vitro*. in addition, heat shock significantly inhibits both cisplatin- and aminoglycoside-induced hair cell death. While heat shock induces several HSPs, the most strongly-induced is HSP-70. Here we have begun to examine the role of HSP-70 in mediating the protective effect of heat shock. in order to determine whether HSP-70 is necessary for the protective effect of heat shock on aminoglycoside-induced hair cell death, we utilized *HSP-70* knockout mice. While heat shock protected wild-type utricles against gentamicin-induced hair cell death, utricles from *HSP-70* knockout mice were not protected. in addition, we have examined the role of HSF-1 in mediating the protective effect of heat shock. HSF-1 is the major transcription factor that induces HSP expression. in order to determine if HSF-1 is necessary for the protective effect of heat shock on aminoglycoside-induced hair cell death, we examined *HSF-1* knockout mice. the protective effect of heat shock on aminoglycoside-induced hair cell death was observed in wild-type mice but not in *HSF-1* knockouts. to determine whether HSP-70 is sufficient to protect hair cells, we utilized transgenic mice that constitutively overexpress rat HSP-70. the *HSP-70* overexpressing utricles were significantly protected against neomycin-induced hair cell death, while utricles from wild-type littermates were not. Taken together, these data indicate that HSP-70 and HSF-1 are both necessary for the protective effect of heat shock against aminoglycoside-induced death. Furthermore, overexpression of HSP-70 alone is sufficient to protect hair cells against aminoglycoside-induced death.

## **731 Histone Deacetylase Inhibitors Rescue Hair Cells From Gentamicin Ototoxicity In Vitro**

**Fuquan Chen<sup>1</sup>**, Su-Hua Sha<sup>1</sup>, Jochen Schacht<sup>1</sup>

<sup>1</sup>*Kresge Hearing Research Institute, University of Michigan, Ann Arbor, MI 48109-0506*

Acetylation (as well as phosphorylation) of histones is an important form of chromatin regulation generally linked to transcriptional activation. Histone acetyltransferase acetylates lysine on histone tails while histone deacetylase (HDAC) removes those acetyl groups and represses gene transcription. Inhibitors of histone deacetylase (HDAC-I) induce hyperacetylation of histones that modulates the chromatin structure and gene expression. Differential effects of HDAC-I on gene expression in different cell types have led to the study of HDAC-I in the treatment of cancer and neurodegenerative diseases.

We have previously shown that kanamycin treatment decreases the acetylation of histone H3 in vivo. We therefore hypothesized that preventing histone deacetylation may rescue hair cells from aminoglycoside ototoxicity. In organotypic culture of the mouse organ of Corti, the acetylation of histone H3 significantly decreased while HDAC1, a class I HDAC, increased after gentamicin stress which causes hair cells loss. Trichostatin (TSA), a HDAC-I, caused hyper-acetylation of histone H3 in hair cells incubated under control conditions. Under gentamicin stress, TSA maintained an almost normal level of acetylation of histone H3 in hair cells and rescued them from ototoxicity. Sodium butyrate, another HDAC-I, likewise rescued hair cells from gentamicin-induced death.

This study was supported by research grant DC-03685 and core grant P30 DC-05188 from the National Institute on Deafness and Other Communication Disorders, National Institutes of Health.

### **732 Protective Effects of GSHe On Cochlear Hair Cells From 4-HNE and Neomycin Ototoxicity**

Xinsheng Gao<sup>1</sup>, Kejian Chen<sup>1</sup>, Richard Kopke<sup>1</sup>

<sup>1</sup>Hough Ear Institute

It is broadly accepted that acute acoustic trauma results in oxidative stress to the cochlea through overproduction of cellular reactive oxygen, nitrogen, and other free radical species. It is suggested that ototoxicity of some antibiotics may also occur through the above mechanisms. 4-hydroxynonenal (4-HNE) is found in higher quantities during oxidative stress. Unlike glutathione (GSH), glutathione ester (GSHe) is cell-permeable and is reported to be effective in antagonizing 4-HNE as well as cisplatin and gentamycin ototoxicity. This study compared the protective effects of GSHe on 4-HNE induced and neomycin induced hair cell damage in cochlear cultures.

organs of Corti from P-3 CD-1 mouse pups were dissected and cultured for 24 hrs before being exposed to 200-400  $\mu$ M 4-HNE or 0.5 mM neomycin for 48 hrs. the experimental groups received 10 mM GSHe as the same time the ototoxic drugs were applied. the cochlear cultures were fixed and stained with phalloidin-TRITC for hair cell counts two days after drug application (day 5 of cochlear culture). Numbers of inner and outer hair cells per unit distance (100  $\mu$ m) of middle and basal turns from the control and treated cochleae were counted and compared.

The results suggest that GSHe protects both inner and outer hair cells from 4-HNE-induced toxicity in both the middle and basal turns and from neomycin-induced toxicity in the basal turn. in conclusion, GSHe is capable of protecting 4-HNE induced and neomycin induced hair cell death.

Supported by INTEGRIS Baptist Medical Center, Oklahoma City

### **733 Non-Anticoagulant Low Molecular Weight Heparin Protects Cochlear Hair Cells From Gentamicin Damage**

Richard Salvi<sup>1</sup>, Dalian Ding<sup>1</sup>, Weidong Qi<sup>1</sup>, Dongzhen Yu<sup>1</sup>, Haiyan Jiang<sup>1</sup>, Shaker Mousa<sup>2</sup>

<sup>1</sup>University at Buffalo, <sup>2</sup>Pharmaceutical Research Institute of Albany

Previous studies suggest that gentamicin-induced ototoxicity is mediated by a number of different factors including free radical injury, activation of calcium-activated protease, and mitochondrial stress pathways all of which are known to contribute to apoptosis. Heparin and its improved version Low Molecular Weight Heparin (LMWH) are known to have polypharmacological actions including anti-thrombotic, anti-inflammatory, and angiogenesis modulating effects via the indirect inhibition of coagulation factors, release of the vascular tissue factor pathway inhibitor, inhibition of NFkB and oxidative stress pathways, inhibition of key matrix-degrading enzymes, selectin and cell adhesion molecule modulation, and other undefined mechanisms. However, heparin/LMWH anticoagulant effects lead to compromised hemostasis and bleeding and hence limiting its expanded use beyond thrombotic disorders. Because of these safety limitations, a novel class of Non-anticoagulant LMWH (NAC-LMWH) maintaining the diverse pharmacological actions of heparin without affecting systemic coagulation and hemostasis was developed. These diverse pharmacological actions without affecting hemostasis suggest that NAC-LMWH might effectively and safely protect cells from gentamicin induced ototoxicity. to test this hypothesis, we tested the effectiveness of a novel NAC-LMWH in suppressing gentamicin ototoxicity in postnatal day 3 rat organotypic cultures. Cochlear organotypic cultures were treated for 24 h with 0.1 mM of gentamicin alone or in combination with NAC-LMWH at concentrations ranging from 10-200  $\mu$ M. the 0.1 mM dose of gentamicin caused extensive hair cell loss; that loss was greatest near the base and progressively decreased towards the apex. Gentamicin alone resulted in the loss of approximately 65% of the hair cells in the base of the cochlea. the addition of NAC-LMWH caused a dose-dependent decrease in hair cell loss. the percentage of missing hair cells declined to about 40% with 10  $\mu$ M, 30% with 100  $\mu$ M, and less than 25% with 200  $\mu$ M NAC-LMWH. Supported in part by NIH grant R01 DC06630-01

### **734 NIM-811, an Inhibitor of Mitochondrial Permeability Transition Pore Opening, Inhibits Aminoglycoside-Induced Hair Cell Death**

Shimon Francis<sup>1</sup>, Lisa Cunningham<sup>1</sup>

<sup>1</sup>Medical University of South Carolina

Changes in mitochondrial function mediate apoptosis in many systems. Several lines of evidence indicate that mitochondrial signaling is involved in aminoglycoside-induced hair cell death. Aminoglycoside exposure results in early disorganization of the mitochondrial inner membrane and cristae in hair cells, as well as increased

intracellular reactive oxygen species (ROS). Overexpression of Bcl-2, a protein that functions to maintain outer mitochondrial membrane integrity, also inhibits aminoglycoside-induced hair cell death. Taken together, these data suggest that mitochondrial membrane permeability transition (MPT) may play a key role in aminoglycoside-induced hair cell death. MPT results when hydrophilic pores are formed by oxidized proteins in the inner mitochondrial membrane. Pore formation leads to loss of mitochondrial membrane potential, uncoupling of oxidative phosphorylation, ROS formation, and matrix swelling, resulting in the release of pro-apoptotic factors. In order to begin investigating the role of mitochondrial function and integrity in aminoglycoside-induced hair cell death, we asked whether inhibition of MPT suppresses neomycin-induced hair cell death in the adult mouse utricle. Cyclosporin A (CsA), an inhibitor of MPT, has been shown to inhibit gentamicin-induced death of guinea pig cochlear hair cells (*Hear Res.* 2002, 169: 47). CsA has additional anti-apoptotic effects, including calcineurin inhibition. We have used NIM 811, a CsA analog that does not inhibit calcineurin, to examine the role of MPT in neomycin-induced hair cell death. Utricles were cultured in 2  $\mu$ M NIM 811 for 2h, and then for 24h in NIM 811 and 2 mM neomycin. Neomycin significantly reduced hair cell viability in both striolar and extrastriolar regions (t-test,  $p < 0.05$ ,  $n = 25$ ). NIM 811 inhibited neomycin-induced hair cell death in both striolar and extrastriolar regions (t-test,  $p < .05$ ,  $n = 14$ ). These data suggest that MPT plays a role in neomycin-induced hair cell death.

### **[735] Melatonin Prevents Gentamicin Induced Ototoxicity in Vestibular Haircell of Rat Utricle**

**Jae-Yun Jung**<sup>1</sup>, Chung-Beom Kim<sup>1</sup>, Jin-Chul Ahn<sup>2</sup>, Hee jun Hwang<sup>2</sup>, Chung-Ku Rhee<sup>1</sup>

<sup>1</sup>Dankook University Hospital, <sup>2</sup>Medical Laser Research Center

**Background and Objectives**° Aminoglycosides, a commonly used antibiotic agent, appear to generate free oxygen radicals within the inner ear, with subsequent permanent damage to sensory cells and neurons, resulting in permanent vestibulo-cochlear toxicity. Melatonin, a pineal secretory product, has properties of both direct and indirect powerful antioxidant. the aim of the present study was to confirm the antioxidant effect of melatonin against gentamicin-induced ototoxicity. **Subjects and Method**°Utricular maculae prepared from postnatal day 2-4 Sprague-Dawley rats were divided into different groups as follows : 1) control, 2) melatonin only, 3) gentamicin only, 4) gentamicin plus melatonin(10, 50, 100  $\mu$ M). for hair cell count, utricles were stained with phalloidin- FITC. Reactive oxygen species (ROS) was assessed using the fluorescent probe, hydrofluorescent diacetate acetyl ester (H2DCFDA). Caspase-3 activity was also examined using the fluorescent caspase-3 substrate and western blot. **Results**°Gentamicin induced loss of utricular hair cells. Melatonin reduced ROS production and caspase-3 activation in gentamicin treated utricular hair cells. **Conclusion**°Melatonin has protective effect in gentamicin-

induced ototoxicity in utricle of rat by inhibiting ROS production and caspase-3 activity.

### **[736] The Potential of Hepatocyte Growth Factor (HGF) for Protection of Cochlear Hair Cells**

**Takatoshi Inaoka**<sup>1</sup>, Yayoi Kikkawa<sup>1</sup>, Takayuki Nakagawa<sup>1</sup>, Yasuhiko Tabata<sup>2</sup>, Hirohito Tsubouchi<sup>3</sup>, Akio Ido<sup>3</sup>, Ryusuke Hori<sup>1</sup>, Kazuya Ono<sup>1</sup>, Juichi Ito<sup>1</sup>

<sup>1</sup>Kyoto University, <sup>2</sup>Institute for Frontier Medical Sciences, Kyoto University, <sup>3</sup>Kagoshima University

Recently, we have established a drug delivery system for the inner ear using biodegradable gelatin hydrogels, which enables sustained delivery of neurotrophins or growth factors to cochlear fluids through the round window membrane (Endo 2005, Iwai 2006, Lee 2007). In addition, the local ethical committee has permitted a phase II and III clinical trial to test the efficacy of local IGF1 application via the gelatin hydrogel for acute, profound hearing loss. Hepatocyte growth factor (HGF) is a paracrine cellular growth and morphogenetic factor, and has been shown to have protective effects of neuronal cells. A previous study has demonstrated that HGF gene transfer to cerebrospinal fluid ameliorates hearing impairment due to aminoglycosides (Oshima 2004). The aim of this study was to examine protective effects of HGF on cochlear hair cells against ototoxic treatment. We used an explant culture system of cochlea sensory epithelia obtained from postnatal day 3 mice. First we investigated a dose-dependent effect of neomycin on hair cell degeneration in explant cultures. Neomycin application caused dose-dependent loss of inner (IHC) and outer hair cells (OHC) in explant cultures. We then examined the effect of supplementation of 20 ng/ml HGF to the culture media. The results demonstrated promotion of the survival of IHC and OHC by HGF application. More relevant effects were found on IHC. These findings indicate that HGF is a promising candidate for local inner ear treatment using biodegradable hydrogels.

### **[737] A Src-Inhibitor Prevents Cisplatin-Induced Hearing Loss**

**Anna Rita Fetoni**<sup>1</sup>, Guang-di Chen<sup>2</sup>, Eric Bielefeld<sup>2</sup>, **Donald Henderson**<sup>2</sup>

<sup>1</sup>Institute of Otolaryngology, Università Cattolica S. Cuore, <sup>2</sup>SUNY at Buffalo

The Src-inhibitor, KX1-004, has been shown to prevent noise-induced hearing loss (NIHL) from continuous and impulse noise when the drug was delivered at the round window or systemically. In this experiment, KX1-004 was used with cisplatin with the goal of evaluating whether the Src inhibitor prevents hair cell loss and hearing loss associated with cisplatin. The controls were Long-Evan rats, dosed with 16 mg/kg of cisplatin delivered IP over a 30 minute period. The experimental group received the same dose of cisplatin, as well as, KX1-004, at a dose of 10 mg/kg, 1 hour before cisplatin and 24 hours later. The control group developed a 40 to 50 dB threshold shift at 10, 20 and 40 kHz by day 5, while the KX1-004 co-treated group developed 10 to 20 dB hearing loss and less than

half the hair cell loss as the controls. in a second set of experiments, Long-Evan rats were treated with cisplatin and cisplatin plus KX1-004, and the cochlear tissue was analyzed 3 days later. the apoptosis related molecule, p53, showed an upregulation with cisplatin that was inhibited with KX1-004. the research from noise and cisplatin suggest that Src is active in apoptosis of cochlear hair cells and inhibition of the Src activity can protect the cochlea from cisplatin and high-level noise.

[Research supported by grant #1R01DC00686201A1]

### **738 Cisplatin-Induced Ototoxicity: Systemic Administration of Thiosulfate Reveals Favorable Kinetics in Scala Tympani Perilymph**

Pernilla Videhult<sup>1</sup>, Cecilia Engmér<sup>2</sup>, Inger Wallin<sup>3</sup>, Göran Laurell<sup>4</sup>, Hans Ehrsson<sup>1</sup>

<sup>1</sup>Karolinska Institutet and Karolinska Pharmacy,

<sup>2</sup>Karolinska Institutet, <sup>3</sup>Karolinska Pharmacy, <sup>4</sup>Umeå University

The chemotherapeutic agent cisplatin is effective against many human tumors, but its use is limited due to a high incidence of ototoxicity. Studies have shown that the sulfurcontaining antioxidant thiosulfate may reduce hearing damage when administered systemically in proximity to cisplatin. Unfortunately, this might also decrease the antitumoral effect. the aim of the present study was to establish to what extent thiosulfate reaches the inner ear after an i.v. injection in the guinea pig. One  $\mu$ l of scala tympani perilymph was aspirated from the basal turn of each cochlea 10, 30, 60, 120, or 180 min after administration of thiosulfate (102 mg/kg b.w.). Blood and CSF samples were also taken. Thiosulfate was quantified by HPLC and fluorescence detection after precolumn derivatization with monobromobimane. the results show that the thiosulfate concentration in perilymph peaked already after 10 min. Due to a more rapid elimination from blood, the perilymph levels exceeded those of the blood towards the end of the experiment. the area under the concentration-time curve for thiosulfate in perilymph and blood was 3100  $\mu$ M $\times$ min and 6300  $\mu$ M $\times$ min, respectively. Further studies are warranted to establish whether systemic delivery of thiosulfate preceding that of cisplatin may protect the inner ear without compromising the antitumoral effect.

### **739 Drug-Enhanced Electrical Responsiveness Despite Reduced Spiral Ganglion Cell Density in the Deafened Guinea Pig Cochlea**

Anette Fransson<sup>1</sup>, Marc Poirot<sup>2</sup>, Philippe De Medina<sup>2</sup>, Mats Ulfendahl<sup>1</sup>

<sup>1</sup>Hearing & Research Communication, <sup>2</sup>INSERM U-563

Using a guinea pig cochlear implant model, it has previously been demonstrated that neurotrophic factor intervention not only enhances spiral ganglion survival but also significantly improves the electrical responsiveness of the system. It has thus been suggested that there is correlation between the efficacy of cochlear prostheses in

humans and the number of remaining spiral ganglion neurons (SGN). the purpose of the present study was to investigate the potential beneficial effects of two new compounds AF0122 and AF0243.

Animals were deafened by intracochlear infusion using 10% neomycin for 48 hours. All animals were treated for four weeks with AF0122, AF0243 or artificial perilymph (AP). After a 4-week treatment period the animals were sacrificed and the cochlea processed for morphological analysis. Electrically-evoked auditory brainstem responses (eABRs) were measured weekly throughout the experiment. Drug treatment significantly enhanced the electrical responsiveness (reduced eABR thresholds). This effect was maintained for at least two weeks after the cessation of the drug treatment. the effect was comparable to what we have previously reported using the neurotrophic factor GDNF. the results of the histological analysis were, however, somewhat unexpected. in the drug treated animals, the spiral ganglion density was much reduced compared to normal animals and only very slightly better than untreated deafened animals. the fact that the electrical responsiveness was so good despite the very reduced number of surviving spiral ganglion neurons clearly indicates that there are additional factors involved in controlling the functional responsiveness of the spiral ganglion and thus the efficacy of cochlear implants.

### **740 Noise-Induced Primary Neuronal Degeneration in Ears with Complete Threshold Recovery**

Sharon G. Kujawa<sup>1</sup>, M. Charles Liberman<sup>1</sup>

<sup>1</sup>Massachusetts Eye and Ear Infirmary

Acute effects of acoustic overexposure include excitotoxic injury to cochlear afferents, characterized by swelling of terminals under inner hair cells (IHCs). Electron microscopic studies suggest peripheral terminals can recover and dendritic contacts regenerate within days of an excitotoxic insult [Pujol and Puel, 1999]. However, recent work in mice (Kujawa and Liberman 2006) shows that exposures producing permanent threshold shifts (PTSs) without hair cell loss cause a slow-onset neuropathy with loss of spiral ganglion cells (SGCs) over 3-6 months. This slow death suggests that terminal regrowth and re-innervation is incomplete or abnormal.

Here we use confocal immunohistochemistry (staining for nerve terminals and synaptic ribbons) and cochlear functional assays (ABRs and DPOAEs) to assess whether this slow-onset SGC loss 1) is preceded by acute loss of peripheral terminals/synapses and subsequent synapse re-formation, and 2) is present even when acute threshold shifts appear reversible. CBA/CaJ mice (6 or 16 wks old) were noise exposed (8-16 kHz, 100 dB SPL, 2 hr) and assessed re: age-matched, unexposed controls at various post-exposure times (1, 3, 7 d; 2, 8, 16, or 32 wk). Both 6 wk and 16 wk animals show large temporary threshold shifts; however, no shifts remain 2 wk post-exposure in the 16 wk animals. in both groups, hair cells remain intact, but SGC numbers ultimately decline by 40-50%. Confocal images from both groups show fewer IHC synapses (up to 50%) and retraction of afferent dendrites by 3 days post exposure. There is no sign of synaptic recovery at later

times. Suprathreshold ABR amplitudes are reduced, even in animals with normal threshold sensitivity. We hypothesize that disruption of neurotrophin signaling caused by the acute retraction of afferent terminals leads, on a slower time scale, to death of the SGC soma and axons. These findings raise important concerns regarding long-term consequences of apparently benign acoustic overexposures.

Research supported by grants from the NIDCD: RO1 DC0188.

#### **741 Electrically Evoked Middle Latency Responses in Awake Guinea Pigs After Cochlear Hair Cell Loss and Temporary Neurotrophic Treatment**

Huib Versnel<sup>1</sup>, Martijn Agterberg<sup>1</sup>, John de Groot<sup>1</sup>, Katja Daamen<sup>1</sup>, Frans Albers<sup>1</sup>, Sjaak Klis<sup>1</sup>

<sup>1</sup>Dept. of Otorhinolaryngology, University Medical Center Utrecht, the Netherlands

Application of exogenous neurotrophins enhances spiral ganglion cell (SGC) survival in deafened animals. Functionally, enhanced sensitivity of the auditory nerve after neurotrophic treatment has been demonstrated by means of electrically evoked brainstem responses. However, it is not clear whether protection of the auditory nerve also leads to improved responsiveness at a cortical level. Here, we study effects of deafening and subsequent neurotrophic treatment on SGC survival and on the cortical responsiveness by means of electrically evoked middle latency responses (eMLRs).

To examine the effect of deafening, female albino guinea pigs were implanted with a multiple-electrode array (Cochlear) and after 6 weeks they were deafened by a combined administration of kanamycin and furosemide. to examine the effect of neurotrophic treatment a second group of guinea pigs was first deafened and after 2 weeks the right cochleas were implanted with an electrode array and a drug-delivery cannula. Brain-derived neurotrophic factor (BDNF; 100 µg/ml) was infused into the cochlea over a period of 4 weeks at a rate of 0.25 µl/hr. Left cochleas served as untreated controls. in all animals, eMLRs were recorded once a week in awake condition. Electrical stimuli were monophasic pulses of 60-400 µA and 20 µs. Animals were sacrificed 2 weeks after cessation of BDNF treatment, and cochleas were processed for histological analysis.

After deafening the eMLR threshold deteriorated but the amplitude at high current levels did not change. After treatment with BDNF the eMLR thresholds and amplitudes remained relatively stable, also in the period after cessation of treatment. SGC survival was significantly larger in treated than in untreated cochleas. in conclusion, the lasting neuroprotective effect of BDNF as demonstrated by the cochlear histology leads to a robust cortical responsiveness. This implies that a temporary neurotrophic treatment might be beneficial for cochlear implant users.

#### **742 Fate of Calretinin-Positive Afferents Following Focal Gentamicin-Induced Lesions to the Vestibular Sensory Epithelia**

David R. Sultemeier<sup>1</sup>, Dylan J. Hirsch-Shell<sup>1</sup>, Augustine Chung<sup>1</sup>, Larry F. Hoffman<sup>1</sup>

<sup>1</sup>Geffen School of Medicine at UCLA

It has recently been shown that small doses of intralabyrinthine-administered gentamicin induce focal lesions of the vestibular sensory epithelia, with type I hair cells exhibiting greater ototoxic sensitivity than type II hair cells. This suggests that such treatments may produce a realistic model for studying the pathophysiology of mild ototoxicity, particularly with respect to the fate of primary afferent neurons that are either wholly (i.e. in the case of calyx-only afferents) or partially (i.e. in the case of dimorphic afferents) deafferented. in this study, we have investigated the dendritic morphologies of afferents that project to the regions of sensory neuroepithelia that exhibit the most dramatic lesions following low gentamicin doses. We have modified the method of intralabyrinthine administration reported by Li et al. (*Acta Otolaryngol.* 2004), in which access to the superior semicircular canals in chinchillas are made through the chronic placement of small caliber cannulae. in our studies, solutions are infused (in HBSS) over finite periods to deliver specific quantities of gentamicin, providing a method of exquisite control over the gentamicin that is locally delivered. the resulting lesions are delineated through immunocytochemistry for calretinin expression in afferent neurons. We found that even the small doses (e.g. 20µg) of gentamicin produce lesions whereby calretinin-positive (CAL+) calyces are conspicuously absent from the central region of the cristae. the full complement of CAL+ calyces is present in surgical and vehicle controls. the lesioned cristae still exhibit CAL+ parent axons within the stroma, projecting to the basement membrane, at 4 days post-administration suggesting that the ototoxic effects of gentamicin do not extend to the primary afferents. We are actively investigating the possibility as to whether the morphology of these dendrites supports the notion that they seek alternative inputs from neighboring viable hair cells.

Supported by NIDCD (to LFH) and the Victor Goodhill Ear Center at UCLA (DRS).

#### **743 Nicotinamide Adenine Dinucleotide Protects Cochlear Hair Cells and Afferent Axons Against Mefloquine Ototoxicity In Vitro**

Dalian Ding<sup>1</sup>, Weidong Qi<sup>1</sup>, Dongzhen Yu<sup>1</sup>, Haiyan Jiang<sup>1</sup>, Richard Salvi<sup>1</sup>

<sup>1</sup>University at Buffalo

Mefloquine hydrochloride is widely used drug for prophylactic or chemotherapeutic treatment of malaria. However, some studies suggest that mefloquine may have neurologic or auditory side effects. Our previous study demonstrated that mefloquine caused a dose-dependent cochlear toxicity in organotypic cultures. the major morphological changes were observed in cochlear hair cells, peripheral auditory nerve fibers and the spiral



ganglion neurons. Cochlear hair cell loss progressed from base to apex. Peripheral axonal degeneration appeared to another unique characteristic of mefloquine injury. Since nicotinamide adenine dinucleotide (NAD) has been found to protect against axonal degeneration caused by various neurotoxic agents, we hypothesized that NAD might protect spiral ganglion axons and hair cells from mefloquine damage. To evaluate this hypothesis, we treated cochlear organotypic cultures with 35  $\mu$ M of mefloquine alone or combined with NAD at concentrations ranging from 5-20 mM. Treatment with 35  $\mu$ M mefloquine for 24 hours caused almost complete destruction of hair cells and auditory nerve fibers in the basal turn; however, most hair cells and nerve fibers in apical turn were intact. In contrast, the auditory nerve fibers in both the basal turn and apical turn were not damaged if the cochlear cultures were treated for 24 h with 35  $\mu$ M mefloquine plus 20 mM NAD. Interestingly, 20 mM NAD also protected many hair cells from mefloquine ototoxicity. Treatment with 35  $\mu$ M mefloquine alone resulted in the destruction of approximately 75% of the hair cells. However, when mefloquine was combined with 20 mM of NAD the hair cell loss declined to 30%. However, treatment with 5 mM NAD did not provide any protection against mefloquine induced ototoxicity. These results indicate that 20 mM NAD may be useful in preventing or delaying hair cell or axonal degeneration induced by mefloquine.

Supported in part by NIH grant R01 DC06630

#### **744 The Effect of 17-Beta Estradiol On Kainic Acid Excitotoxicity in the Guinea Pig Cochlea**

**Keiji Tabuchi<sup>1</sup>**, Shuhei Sakai<sup>1</sup>, Hidekazu Murashita<sup>1</sup>, Akira Hara<sup>1</sup>

<sup>1</sup>*Univ. of Tsukuba*

Previous studies have shown that the application of kainic acid to the round window membrane induces excitotoxicity of afferent dendrites and significantly decreases the amplitude of the compound action potential (CAP). On the other hand, it is known that the 17-beta estradiol is a neuroprotective agent for excitotoxicity in the central nervous systems (CNS). The present study examined whether 17-beta estradiol protected the cochlea against excitotoxicity induced by kainic acid. Albino guinea pigs weighing 250 g to 300 g were used. Kainic acid (10 mM) were applied on the intact round window membrane to induce excitotoxicity of the cochlea. CAP thresholds were examined before, one day after, three days after and 7 days after the drug application. 17-beta estradiol was administered simultaneously with kainic acid. CAP threshold shifts following kainic acid exposure were significantly decreased by 17-beta estradiol. Furthermore, the protective effect of 17-beta estradiol was significantly inhibited by the application of tamoxifen, an estrogen receptor modulator. These results suggest that 17-beta estradiol ameliorated kainic acid excitotoxicity in the cochlea by estrogen receptor activation.

#### **745 Regulation of Jun N-Terminal Kinase (JNK) by Depolarization in Spiral Ganglion Neuron (SGN) Survival and Neurite Outgrowth**

**Jie Huang<sup>1</sup>**, Simrit Sodhi<sup>1</sup>, Steven Green<sup>1</sup>

<sup>1</sup>*University of Iowa*

The JNK-Jun signaling pathway has been implicated in neuronal death under various circumstances. We have previously shown that this pathway is activated during SGN death *In Vitro* after trophic factor deprivation and *In Vivo* after deafening. We have defined a novel signaling pathway by which depolarization inhibits JNKs in cultured neonatal rat SGNs. The key steps in sequence are: Ca<sup>2+</sup> - CaMKII - FAK/PyK2 - PI3K - PKB - inhibition of MLKs (upstream activators of JNK). By expressing dominant negative forms of focal adhesion protein (FAK) and/or proline-rich tyrosine kinase (PyK2), we showed that both FAK and PyK2 contribute to suppression of JNK by depolarization. By using combinations of dominant-negative and constitutively-active mutants of FAK, PyK2, PI3-OH kinase, protein kinase B, JNK1 and JNK3, we could order the steps in the pathway. For example, constitutively active PI3K or PKB suppressed JNK activation downstream of dominant negative FAK. Also, expression of a constitutively-active MKK7-JNK3 fusion blocked suppression of Jun phosphorylation by depolarization, implicating the MLK-MKK-JNK module as the target of suppression by the pathway. MKK7-JNK1 was much weaker than MKK7-JNK3 in phosphorylating Jun, suggesting functional distinction among JNK isoforms. Although JNK inhibitors promote survival, they strongly inhibit neurite growth. However, SGNs from JNK3 null mice show improved survival *In Vitro* (comparable to survival with JNK inhibitors) but their neurite growth is normal, confirming that JNK3 contributes to apoptosis while being dispensable for neurite growth. Presumably, JNK1 and/or JNK2 are the isoforms required for neurite growth, an issue that we are further investigating. Distinguishing isoform-specific actions of JNK is important because any therapy targeting JNK would optimally involve both promotion of SGN survival and maintenance of their peripheral processes.

This study is supported by NIH grant DC002916 (SHG) and American Heart Association Fellowship 0710093Z (JH)

#### **746 Suppression of Jun Phosphorylation by Membrane Depolarization in Neonatal Rat Spiral Ganglion Neurons (Sgns) *In Vitro***

**Damon Fairfield<sup>1</sup>**, Jie Huang<sup>1</sup>, Steven Green<sup>1</sup>

<sup>1</sup>*Depts. of Biological Sciences and Otolaryngology, University of Iowa, Iowa City, IA 52242, USA*

We previously showed that SGNs cultured in the absence of trophic support undergo apoptosis, correlated with increased activity of the pro-apoptotic JNK-Jun signaling pathway. Addition of inhibitors of JNK activity or JNK activation increases survival, establishing a role for the JNK-Jun pathway in regulating SGN apoptosis following trophic withdrawal. Similarly, SGNs from JNK3 null mice

exhibit increased survival in 5K comparable to that obtained by JNK inhibitors, identifying a specific JNK isoform. We also reported that chronic depolarization of SGNs *In Vitro* by 30 mM K<sup>+</sup> (30K), promotes survival, in part, through the activation of Ca<sup>2+</sup>-dependent CaMKII which suppresses Jun phosphorylation. We show here that SGNs cultured for various durations (0-48 h) in non-depolarizing (5 mM K<sup>+</sup>, 5K) medium prior to return to 30K commit gradually to cell death, with commitment occurring mainly between 8-24 h after withdrawal of trophic support. the time course of Jun activation in SGNs deprived of trophic support was examined using antibodies specific for Jun phosphorylated on Ser63 and Ser73 (pJun). Relative to SGNs in 30K, elevated pJun staining was observed by 8 h after culture in 5K, corresponding approximately to the beginning of irreversible commitment to cell death. We also examined the rate at which chronic depolarization suppresses Jun phosphorylation by re-addition of 30K to trophic factor-deprived cultures for various times. Suppression of Jun phosphorylation was observed by 30 min after re-addition, with pJun intensity gradually declining to control non-deprived levels by 12 h. We are currently examining the ability of patterned electrical stimulation to suppress Jun phosphorylation in SGNs both *In Vitro* and *in vivo*. This research was supported by NIDCD R01 DC002961 (SHG), NRSA F32 DC007270 (DAF) and AHA pre-doctoral fellowship 07100930 (JH).

#### **747 Role of JNK3 Activity in Spiral Ganglion Neuron Death After Hair Cell Loss in JNK 3 Null Mice**

Il-Woo Lee<sup>1</sup>, Catherine Kane<sup>2</sup>, Steven Green<sup>2</sup>

<sup>1</sup>Department of Biological Sciences & Otolaryngology, University of Iowa and Pusan National University,

<sup>2</sup>Department of Biological Sciences and Otolaryngology, University of Iowa

We have previously shown that the JNK-Jun signaling pathway is activated in apoptotic spiral ganglion neurons (SGNs) *In Vivo* after deafening and *In Vitro* after trophic factor deprivation. There are multiple JNK isoforms, JNK1-3, of which JNK3 has been most closely associated with apoptosis of neurons deprived of trophic support or subjected to certain neurotoxic agents *In Vivo* and *In Vitro*. Because the JNK isoforms are involved not only in apoptosis but in many aspects of cell and neuronal function, including stress responses and neurite growth, targeting specific isoforms may be an attractive means for improving SGN survival and preserving function. We have shown that SGNs from JNK3 null mice have improved survival following trophic factor deprivation. We ask here whether JNK3 specifically is required for SGN death *In Vivo* after hair cell loss. JNK3 null mice were obtained from Dr. Alex Kuan (Cincinnati Children's Hospital Research Foundation) and established on a CBA/CaJ background by ten generations of backcrossing. Homozygous 30 day old JNK3 null mice and wild-type littermates were unilaterally deafened by application of neomycin powder on gelfoam in the round window niche. Deafening was verified by ABR and by loss of myosin 6 immunoreactivity in sections from the cochleae. We counted SGNs in cochleae from mice euthanized 2, 4, or 6 weeks post-deafening. SGN numbers

in the deafened and control contralateral cochleae of JNK3 null mice were similar, indicating that JNK3 is required for SGN death after hair cell loss in the mouse.

#### **748 The Effects of Neurotrophic Factors On Peripheral and Central Neuritogenesis in Rat Spiral Ganglion Explant Cultures**

Kenji Kondo<sup>1</sup>, Kwang Pak<sup>2</sup>, Eduardo Chavez<sup>2</sup>, Yulian Jin<sup>1</sup>, Kimitaka Kaga<sup>1</sup>, Tatsuya Yamasoba<sup>1</sup>, Allen Ryan<sup>2</sup>

<sup>1</sup>University of Tokyo, Graduate School of Medicine,

<sup>2</sup>University of California, San Diego School of Medicine, and Veterans Administration Medical Center

Spiral ganglion neurons (SGNs) are bipolar neurons as are other primary sensory neurons, with a peripheral process that synapses upon hair cells in the organ of Corti, and a central process that projects to the cochlear nucleus of the medulla. Although each process has its own distinct function in auditory signal transduction, the biological difference between the peripheral and the central processes remains largely unclear. In this study, the effects of brain-derived neurotrophic factor (BDNF), neurotrophin-3 (NT-3), and leukemia inhibitory factor (LIF) on the outgrowth and extension of the peripheral and central processes of rat SGNs were evaluated separately using a newly developed explant culture system. SGs (postnatal day 5) were dissected and harvested carefully from a modiolus using microscissors as a thin slice of tissue with the root portions of both peripheral and central processes maintained undamaged. The explants were then cultured on coverslips with the addition of either BDNF, NT-3 or LIF at 1-100 ng/ml and analyzed for the number of peripheral and central processes emanating from the explants, and the average length of maximum neurite extension in peripheral and central processes. Overall, the peripheral side of the explant exhibited more neurite outgrowth than the central side. BDNF was a potent stimulant of the number of peripheral processes (10-100 ng/ml) and central processes (100 ng/ml alone) that exited the explant. The extension of peripheral process length was also more prominent than that of central processes. The former was enhanced by BDNF (1-100 ng/ml), NT-3 (1-100 ng/ml) and LIF (100 ng/ml), while the latter was enhanced by BDNF (1-100 ng/ml), NT-3 (100 ng/ml) and LIF (10 ng/ml). The larger intrinsic capacity of SGNs for growth of peripheral processes than central processes appears to agree with the results of *In Vivo* regeneration studies of other sensory neurons. Our results also suggest that the outgrowth and extension of peripheral and central processes of the SGNs are differentially regulated by neurotrophic factors.

## **749 Developmental Cues in SGN Formation Can Be Replicated in ES Cells to Induce Glutamatergic Neurons for Auditory Nerve Replacement**

**Jeannie Hernandez**<sup>1</sup>, Noel Wys<sup>1</sup>, Diane Prieskorn<sup>1</sup>, Matt Velkey<sup>1</sup>, K. Sue O'Shea<sup>1</sup>, Karolina Wesolowski<sup>1</sup>, Josef Miller<sup>1</sup>, Richard Altschuler<sup>1</sup>

<sup>1</sup>University of Michigan

Inner hair cell (IHC) loss leads to progressive degeneration of the auditory nerve. Cochlear prostheses can bypass IHC function by directly stimulating remaining auditory nerve. for patients in whom little or no auditory nerve remains, replacement of the auditory nerve spiral ganglion neurons (SGNs) could be a key step to restore hearing. Use of embryonic stem cells (ESCs) to replace auditory nerve is addressed in this study. Previous reports have found that undifferentiated ESCs implanted into the cochlea predominantly differentiate into a glial cell phenotype. We hypothesized that differentiation into a neuronal phenotype may be improved by exogenously reproducing the endogenous cues that guide SGN differentiation during normal development. This was assessed both *In Vivo* and *In Vitro* using the proneural transcription factor Neurogenin-1 (Ngn1), which activates a downstream cascade necessary for normal SGN differentiation, migration, and survival. *In Vitro* results showed that 48h of forced Ngn1 expression induced a neuronal phenotype. Addition of the neurotrophic factors BDNF and GDNF increased the number reaching the target phenotype, with approximately 50% of ESCs becoming neuronal and glutamatergic (TUJ1 and VGLUT positive). Forced expression of Ngn1 initially repressed differentiation into glia, but after turning off Ngn1 expression, approximately 30% of ESCs then reached a glial phenotype (GFAP positive). *in vivo*, mESCs implanted into the scala tympani/modiolar region of 5 weeks deafened guinea pig cochleae underwent similar treatment, with Ngn1 expression induced for 48h followed by 26 days of BDNF/GDNF infusion. We found *In Vivo* results were highly comparable to *In Vitro*, with approximately 60% of mESCs differentiating into a neuronal, glutamatergic phenotype. This study demonstrates that developmental signals guiding auditory nerve differentiation can be replicated in ES cells to effectively push them toward an SGN-like phenotype.

## **750 Tonotopic Neurotrophin Release: a Key Regulator of Pre- and Post-Synaptic Protein Distribution in Spiral Ganglion Neurons**

**Jacqueline Flores-Otero**<sup>1</sup>, Hui Zhong Xue<sup>2</sup>, Robin L. Davis<sup>2</sup>

<sup>1</sup>Rutgers University and UMDNJ, <sup>2</sup>Rutgers University

Previous work from our laboratory has revealed a 'yin-yang' regulation of spiral ganglion neuron (SGN) phenotype by neurotrophins (Adamson, et al., *J. Neurosci.* 2002). Exogenous application of neurotrophin-3 (NT-3) or brain derived neurotrophic factor (BDNF) can reproduce apical or basal SGN electrophysiological properties, respectively, along with up- or down-regulation of the appropriate voltage-gated ion channels and

electrophysiologically relevant proteins. This suggests that NT-3 and BDNF are released preferentially in apical and basal regions of the cochlea. Consistent with this hypothesis, others have shown that NT-3 expression levels are indeed higher in the apex of the cochlea (Fritzsche et al., *J Neurosci.* 1997; Sugawara et al., *JCN* 2007), yet very little is currently known about BDNF expression patterns in postnatal and adult cochleae.

To examine this issue, we developed a functional assay of neurotrophin action by co-culturing micro-isolates from the organ of Corti with spiral ganglion neuron explants, each from known tonotopic regions. This approach allowed us to mix-and-match cochlear regions with different populations of spiral ganglion neurons to assess their impact on neuronal phenotype. Immunocytochemical analysis of the resultant distribution of pre- and post-synaptic proteins showed results consistent with our predictions that could be reversed with function blocking anti-NT-3 and anti-BDNF antibodies.

in conclusion, the functional assay that we developed indicates that NT-3 is preferentially released by apical cochlear micro-isolates whereas BDNF is preferentially released by basal cochlear micro-isolates. Further studies will examine the protein distributions of these two neurotrophins in the organ of Corti using an immunocytochemical approach.

Supported by NIH RO1 DC01856 (RLD) and Gates Millennium Scholarship (JFO).

## **751 P75<sup>NTR</sup> Expression in Spiral Ganglion Schwann Cells Following Deafness**

**Matthew Provenzano**<sup>1</sup>, Kaitlin Zander<sup>1</sup>, Amanda Nymon<sup>1</sup>, Ningyong Xu<sup>1</sup>, Jason Clark<sup>1</sup>, Steven Green<sup>1</sup>, Marlan Hansen<sup>1</sup>

<sup>1</sup>University of Iowa

Spiral ganglion Schwann cells (SGSCs) myelinate spiral ganglion neurons (SGNs) and are a potential source of neurotrophic support for SGNs. Successful efforts to maintain or regenerate a functional auditory nerve may require viable SGSCs. SGNs gradually die following deafening, functionally denervating the SGSCs. Previous studies of sciatic nerve have shown that SCs upregulate the neurotrophin receptor p75<sup>NTR</sup> after denervation. Proneurotrophins (proNTs) can induce apoptosis via p75<sup>NTR</sup>. p75<sup>NTR</sup> is upregulated in SGSCs following deafening (kanamycin injection). p75<sup>NTR</sup>-positive cells co-labeled with anti-S100 antibody (a Schwann cell marker), but not anti-neurofilament. SGSCs also expressed the proNT co-receptor sortilin. p75<sup>NTR</sup> upregulation in SGSCs in the spiral lamina and in the ganglion was concomitant with degeneration of SGN peripheral processes and SGN death. Also concomitant with p75<sup>NTR</sup> upregulation in SGSCs was appearance of apoptotic (TUNEL-positive) SGSCs and proliferating (assessed by BrdU uptake) SGSCs. Cultured SGSCs express p75<sup>NTR</sup> and sortilin. Treatment of cultured SGSCs with proNGF or proBDNF causes apoptosis. in culture and *In Vivo* in deafened rats, SGSCs re-enter the cell cycle. in dividing (BrdU-positive) SGNs, p75<sup>NTR</sup> is cleaved: the extracellular domain is lost, evidenced by loss of immunoreactivity of an extracellular

epitope, while the intracellular domain (ICD) is translocated to the nucleus. These results indicate that p75<sup>NTR</sup> contributes to the proliferative and apoptotic response of SGSCs to deafening and identify a novel mitogenic signaling pathway involving nuclear translocation of the p75<sup>NTR</sup> ICD. Further definition of these mechanisms will contribute to understanding Schwann cell responses and function following deafferentation by hair cell loss.

## **[752] Endoplasmic Reticulum-Targeted Bcl-2 Promotes Spiral Ganglion Neuron (SGN) Survival While Mitochondrially-Targeted Bcl-2 Causes SGN Death in Prosurvival Conditions**

**John Renton<sup>1</sup>**, Ningyong Xu<sup>1</sup>, Marlan Hansen<sup>1</sup>

<sup>1</sup>*Department of Otolaryngology, University of Iowa*

Survival of deafferented spiral ganglion neurons (SGNs) and regeneration of the peripheral axons will likely enhance the efficacy of cochlear implants. In cultured SGNs, over-expression of Bcl-2 prevents SGN death but inhibits neurite growth. Classically, Bcl-2 is felt to act at the mitochondria to promote cell survival. However, recent studies suggest that Bcl-2 also acts at the endoplasmic reticulum (ER) to promote survival. This study assesses the effects of Bcl-2 targeted to either the mitochondria (GFP-Bcl-2-Maob) or ER (GFP-Bcl-2-Cb5) on SGN survival and neurite growth. Additionally, we evaluated the effects of MAP/ERK kinase (MEK) and phosphatidylinositol 3-kinase (PI3K) activity on SGN survival and neurite length.

Dissociated spiral ganglion cultures, prepared from P5 rat pups, were transfected with GFP-Bcl-2-Maob or GFP-Bcl-2-Cb5 in the presence or absence of neurotrophic factors. Subsets of cultures were transfected with constitutively active MEK (MEKEE) or constitutively active PI3K (P110). Appropriate targeting of Bcl-2 to subcellular compartments was verified and SGN survival and neurite length were determined for each condition.

Expression of GFP-Bcl-2-Cb5 promotes SGN survival to a greater extent than either wild type GFP-Bcl-2 or GFP-Bcl-2-Maob. In the presence of prosurvival stimuli, such as neurotrophin-3 (NT-3) or depolarization, expression of GFP-Bcl-2-Maob paradoxically results in SGN death. MEKEE and P110 also promote SGN survival while P110 promotes neurite growth to a greater extent than NT-3 or MEKEE. As with wild-type GFP-Bcl-2, GFP-Bcl-2-Cb5 and GFP-Bcl-2-Maob inhibit neurite growth even in the presence of NT-3, MEKEE, or P110.

Historically, prosurvival Bcl-2 has been thought to act primarily at the mitochondria. However, our data show that Bcl-2 targeted to the ER is more effective at rescuing SGNs in the absence of trophic factors. Additionally, Bcl-2 targeted to the mitochondria results in SGN death in the presence of trophic factors.

## **[753] Trkb Receptor Trafficking in Spiral Ganglion Neurons**

**Pamela Roehm<sup>1</sup>**, Katrin Deinhardt<sup>1</sup>, Moses Chao<sup>1</sup>

<sup>1</sup>*New York University School of Medicine*

Spiral ganglion neurons (SGNs) are first order sensory neurons that convey information from the peripheral sensory system to central auditory pathways. SGNs require neurotrophins (NTFs) for development, survival and neurite outgrowth, and express trkB and trkC receptors which bind to brain-derived neurotrophic factor (BDNF) and neurotrophin-3 (NT3) respectively. These NTFs are expressed at different concentrations in a gradient from the apex to the base of the cochlea in a developmentally-specific fashion. Exposure of SGNs to the NTF found at higher concentrations in the opposite ends of the cochlea leads to profound changes in their firing patterns (Adamson, 2002). To cause these profoundly different effects in SGNs, NTFs are first internalized and then they or their effectors are transported to the site of action. Previous studies of tetanus toxin trafficking in motor neurons have shown that it is transported by retrograde axonal transport to the cell soma via a Rab5 and Rab7 dependent process, and suggested that BDNF and trkB using this same pathway (Deinhardt, 2006). This pathway has not been previously studied in SGNs. Using live imaging supplemented by images of timed fixed cultures, we have studied the process of BDNF/trkB receptor trafficking in SGNs. Our studies reveal that both local slow transport as well as rapid longer range motion (at rates comparable to active transport processes) occur in these neurons. Surface labeling of trkB reveals that it colocalizes with the Rab5 GTPase in early endosomes after 20 minutes. These basic trafficking events underlie the proper functioning of BDNF in SGNs. Strategies utilizing BDNF and other NTFs to improve SGN survival and neurite outgrowth intrinsically depend on proper uptake and localization of NTF/receptor complexes within these specialized cells; thus improved understanding of these processes will allow more rational use of NTFs for these purposes.

## **[754] Regrowing Neurites in Dissociated Cultures of Newborn Mouse Spiral Ganglia Preferentially Associate with Schwann Cells**

**Donna S. Whitlon<sup>1</sup>**, David Tieu<sup>2</sup>, Mary Grover<sup>2</sup>, Brian Reilly<sup>2</sup>, May T. Coulson<sup>2</sup>

<sup>1</sup>*Dept. Otolaryngology and Hugh Knowles Center, Northwestern University*, <sup>2</sup>*Dept. Otolaryngology, Northwestern University*

Evidence from developmental and regeneration studies of the cochlea and other neuronal tissues give reason to hypothesize a role for non-neural cells in the growth and regeneration of spiral ganglion nerve fibers. We examined the associations of regrowing neurites and non-neural cells in dissociated cultures of newborn mouse spiral ganglia. In cultures maintained for 7 days, regrowing neurites formed non-random patterns atop a confluent bed of non-neural cells that were similar to those formed by endogenously expressed laminin and entactin but not fibronectin or tenascin. In 42 hour cultures maintained in three different

growth media, regrowing neurites were preferentially associated with spindle-shaped non-neural cells and did not grow directly on laminin, fibronectin, or tenascin coated culture dishes. the spindle shaped cells incorporated BrDU in culture, and were immunoreactive for the proteins sox10, P75 and connexin29, but not GFAP. the spindle shaped cells existed in the culture within a much larger, general population of fibronectin positive cells, but were themselves distinctly fibronectin negative. Nerve fibers grew in association with the fibronectin negative cells while avoiding fibronectin positive cells. Immunolabeling of fixed cochleas from neonatal mice localized sox10, P75 and connexin29, but not GFAP, to Schwann cells. These observations identify the spindle shaped cells as belonging to the Schwann cell lineage and raise the possibility that interactions between spiral ganglion neurons and Schwann cells may provide a permissive growth environment for spiral ganglion neurites. (Supported by NIH grant#DC00653, the Hugh Knowles Center and the Department of Otolaryngology, Northwestern University).

### **[755] Activation of Phosphatidylinositol 3-Kinase Partially Overcomes the Inhibition of Neurite Growth by Protein Kinase a in Spiral Ganglion Neurons**

**Ningyong Xu<sup>1</sup>**, Jonathan Engbers<sup>1</sup>, Steven Green<sup>2</sup>, Marlan Hansen<sup>1</sup>

<sup>1</sup>*Department of Otolaryngology, University of Iowa,*

<sup>2</sup>*Department of Biological Sciences and Otolaryngology, University of Iowa*

Regrowth of spiral ganglion neuron (SGN) peripheral axons to more closely approximate the stimulating electrodes of a cochlear implant would likely allow for more refined stimulation and improved patient outcomes. Cyclic-AMP (cAMP)-dependent protein kinase a (PKA) regulates axon growth in many neurons and is an activity dependent prosurvival signal in SGNs. We have begun investigating the effects of cAMP and PKA activity on SGN neurite growth using dissociated SG cultures from P5 rats. Treatment of SG cultures with 1 mM of the cell permeant cAMP analog, cpt-cAMP, promotes SGN neurite growth while 10 mM cpt-cAMP inhibits neurite growth, suggesting a biphasic response of SGN neurites to elevated cAMP. Expression of a constitutively active PKA isoform tagged with green fluorescent protein (GFP, GPKA) targeted to the nucleus or cytoplasm strongly inhibits SGN neurite growth, even in the presence of neurotrophic factors. Neurite length inversely correlates with the expression level of GPKA ( $r=-0.50$ ,  $p<0.05$ ) further suggesting that higher levels of PKA activity lead to diminished neurite growth. Neurotrophins promote SGN neurite growth likely via activation of phosphatidylinositol 3-kinase (PI3K), Ras-MEK-extracellular regulated kinase (ERK), and c-Jun N-terminal kinases (JNK). We attempted to overcome the inhibition of neurite growth by PKA by overexpressing constitutively active isoforms of JNK-1, JNK-3, MEK, and PI3K in the presence of GPKA. Constitutively active JNK-3 promotes cell death even in the presence of PKA and NT3. While constitutively active JNK-1 does not promote cell death, it is also not sufficient to overcome the inhibition of

neurite growth by PKA nor is constitutively active MEK. Conversely, constitutively active PI3K partially rescues neurite growth in SGNs co-transfected with GPKA suggesting that the reduction in SGN neurite growth by PKA may be due, in part, to inhibition of PI3K activity.

### **[756] Splice-Isoforms of the Actin-Cytoskeletal Protein Espin Expressed in Type-I Spiral Ganglion Neurons are Present in the Nucleus and Contain a Functional Nuclear Localization Signal**

**Gabriella Sekerkova<sup>1</sup>**, Lili Zheng<sup>1</sup>, Enrico Mugnaini<sup>1</sup>, James Bartles<sup>1</sup>

<sup>1</sup>*Northwestern University*

The espins are multifunctional actin-cytoskeletal proteins that are produced in several isoforms from a single gene. Espins bundle F-actin with high affinity, cause the elongation of parallel actin bundles and can bind actin monomer via a WASP homology 2 domain and profilins via proline-rich peptides. Espins are enriched in the stereocilia of inner-ear hair cells, but are also found in the actin-rich specializations of some neurons, e.g., the microvilli of the vomeronasal neurons and the dendritic spines of Purkinje cells. Here, we report a novel localization of espins to a subset of spiral ganglion (SG) neurons in the rat and mouse. Affinity purified espin antibody labeled a subset of type-I SG neurons, including their central projections innervating root neurons and octopus cells in the cochlear nucleus. the labeling was specific because SG staining was absent in SG neurons of homozygous jerker mutant mice, which lack espin protein because of a point mutation in the espin gene. Western blot analysis showed that espin 3 and espin 4 were the major espin isoforms in SG neurons. Remarkably, the espin antibody labeled both the cytoplasm and nucleus of SG neurons. We determined that this nuclear immunolabeling reflected the presence of espin splice-isoforms that contain a functional nuclear localization signal. RT-PCR analysis of SG indicated that roughly one-third of the espin transcripts in SG encode espin proteins that include this additional, short peptide, which is enriched in positively charged amino acids. Consistent with the function of a nuclear localization signal, this short peptide proved to be necessary and sufficient to target espin proteins to the nucleus in heterologous expression systems. Our discovery of espin isoforms containing a functional nuclear localization signal in SG neurons suggests novel roles for espins in actin-cytoskeletal regulation in the nucleus. (Support: NIH DC004314 to JRB)

### **[757] Non-Invasive Strategy to Characterize the Impact of Gestational Iron Deficiency on Auditory Nerve Myelination**

**Camelia Mihaila<sup>1</sup>**, Jordan Schramm<sup>1</sup>, Anne Luebke<sup>1</sup>, Margot Mayer-Proschel<sup>1</sup>

<sup>1</sup>*University of Rochester Medical Center, Rochester, NY 14642*

Iron deficiency represents the most common nutritional disorder, affecting more than 2 billion people around the world. Even in developed countries such as the US, it has

been estimated that 35-58% of healthy women show some degree of iron deficiency, with a higher prevalence during pregnancy. Iron deficient infants show long-term cognitive abnormalities, language learning impairments, and increases in the latency of auditory brainstem responses (ABRs). Some of these impairments have been linked to aberrant development of glial cells, resulting in hypomyelination. We recently discovered that iron deficiency disrupts glial precursor cell function during embryogenesis as early as E13.5, a developmental window that had not been considered previously on the possible causes of dysmyelination associated with iron deficiency. We provide data showing that the iron deficiency prior to mating, and in the 1st trimester (E7), results in embryonic brain iron deficiency. In addition, we show that offspring from iron deficient rat dams at these timepoints exhibited significantly slower conduction velocities as assessed by ABR latency measures. Interestingly, offspring from rat dams iron deficient in the 2<sup>nd</sup> and 3<sup>rd</sup> trimesters (>E14) exhibited normal auditory nerve conduction velocities.

In summary, our data for the first time show a tight association between myelin protein expression and auditory nerve conduction velocities. Our approach offers a unique opportunity to define the developmental window of vulnerability and allows us to determine strategies for myelination repair.

(Supported by NIH DC003086, NS044374, TL1-RR024135)

## **[758] Impaired Innervation and Synapse Formation in a Genetic Model of Secondary Hypothyroidism**

Qing Fang<sup>1</sup>, R. Keith Duncan<sup>1</sup>, Lisa Beyer<sup>1</sup>, David Dolan<sup>1</sup>, Tzy-wen Gong<sup>1</sup>, Yehoash Raphael<sup>1</sup>, Margaret Lomax<sup>1</sup>, Sally Camper<sup>1</sup>, **Mirna Mustapha<sup>1</sup>**

<sup>1</sup>University of Michigan

The developing organ of Corti is highly sensitive to thyroid hormone. In mice axonal growth and synaptogenesis take place in the first two postnatal weeks, during the thyroid hormone critical period. Maturation involves coordination of a massive rearrangement of afferent and efferent fibers and synapses. Here we report the characterization of a mouse model of secondary hypothyroidism (*Pit1<sup>dw</sup>*) that has no detectable circulating thyroid hormone and profound hearing impairment. This model has advantages over other hypothyroid mutants because of the severity of hearing impairment, long-term viability of the animals, and ease of thyroid hormone replacement. Physiological tests of peripheral hearing indicate that inner and outer hair cell innervation and function are impaired. Morphological analysis reveals abnormalities in the pattern of synapses and ribbon formation in outer and inner hair cells, respectively. Immunostaining for presynaptic and postsynaptic markers confirms abnormal synaptogenesis at the basal aspect of both inner and outer hair cells. This study reveals permanently reduced and unorganized efferent synapses with outer hair cells and immature afferent ribbon formation at inner hair cells in adult *Pit1<sup>dw</sup>* mutants. Comparison of the cochlear transcriptome of adult *Pit1<sup>dw</sup>* mutant and wild-type littermates using

microarray analysis of gene expression reveals differential expression of genes that are involved in neurotransmitter release. *Pit1<sup>dw</sup>* mice exhibit a substantial reduction in otoferlin, a protein required for synaptic release. We hypothesize that the efficiency of calcium-mediated exocytosis is permanently reduced in *Pit1<sup>dw</sup>* mice. This defect is likely a major contributor to the loss of the compound action potential and to the profound deafness exhibited by these mutants. We are in the process of evaluating the contribution of individual gene expression deficiencies to the innervation and synapse defects. These studies will enhance our understanding of neuronal development in the cochlea as well as the mechanism of action of thyroid hormone on cochlear maturation.

Supported by NIDCD: DC05188, DC02982, DC05401, DC05053, and NOHR

## **[759] Mechanisms of Depression At the Mouse Endbulb of Held**

Hua Yang<sup>1</sup>, Matthew Xu-Friedman<sup>1</sup>

<sup>1</sup>Department of Biological Sciences, State University of New York at Buffalo

Synapses are subject to a number of activity-dependent changes during repetitive use. To get a better understanding the functional role of plasticity, we study the synapses formed by auditory nerve fibers onto bushy cells in the mouse anteroventral cochlear nucleus ("the endbulb of Held"). The most prominent form of plasticity at the endbulb is depression. A number of mechanisms have been proposed to underlie depression, including vesicle depletion, and postsynaptic receptor saturation and desensitization. We evaluated the importance of these mechanisms using voltage-clamp recordings in brain slices at near-physiological temperatures. For pairs of closely spaced pulses, depression of both AMPA and NMDA components of the second EPSC showed two distinct phases of recovery. The fast component of depression for the AMPA EPSC was eliminated in the presence of cyclothiazide, suggesting it results from desensitization. The fast component of depression for the NMDA EPSC was reduced in the presence of the low-affinity antagonist L-AP5, suggesting it results from saturation. The remaining depression for both AMPA and NMDA EPSCs was highly similar, suggesting a presynaptic source, such as vesicle depletion. We developed a simple model of depression that could account for the paired-pulse data of the AMPA EPSC. However, the model predicts significantly greater depression during trains than is observed, suggesting there are activity-dependent forms of recovery. We tested this possibility using EGTA-AM to reduce calcium-dependent forms of recovery, and found that train-induced depression was significantly slowed. Adding activity-dependent recovery to the model allowed it to account for EPSC amplitude under a wide range of conditions.

## **760 Pharmacological Modulations of Endolymphatic K<sup>+</sup> Concentration in Cultured Mouse Utricle**

Sylvain Bartolami<sup>1</sup>, Melanie Cavalier<sup>1</sup>, Sophie Gaboyard<sup>1</sup>, Christian Chabbert<sup>1</sup>

<sup>1</sup>INSERM

The high K<sup>+</sup> concentration in the endolymph is required for hair cells to transduce balance stimuli. the maintenance of this high K<sup>+</sup> concentration partly depends on K<sup>+</sup> recycling: Once hair cells are depolarized following K<sup>+</sup> influx through stereocilia transducer channels, basolateral outward currents are activated to extrude K<sup>+</sup> in the perilymph. Then, a connective tissue network of gap junction presumably conveys K<sup>+</sup> towards dark cells which are in charge to secrete K<sup>+</sup> back into the endolymph. Recently, we developed a murine organotypic model of utricle able to regenerate its endolymphatic compartment (called cyst) in order to investigate the regulation of endolymph homeostasis. Utricles dissected from neonate mice were grown in 3D matrix. After 2 days *In Vitro* (div), utricles regenerate the cysts, easily recognizable under a dissecting microscope. Electrophysiological recordings show that an intracystic potential is maintained between -1.5 and -3.5 mV during the first 9 div. Afterwards, potential values become less steady. Using K<sup>+</sup> selective electrodes, K<sup>+</sup> accumulation was then estimated within cysts. K<sup>+</sup> accumulates from div 2 to 5 where its concentration reaches 82.8 +/- 4.2 mM and remains fairly high for the following 6 div (level range: 60.1 +/- 8.8 to 95.0 +/- 7.7 mM). Bath application of 1 mM ouabaine (a selective Na<sup>+</sup> K<sup>+</sup> ATPase blocker) induces a decrease in K<sup>+</sup> endocystic concentration, in a time-dependent fashion: a significant 34.4 % inhibition is obtained after a 15 min treatment, which further reaches 70.8 % at 40 min. Conversely, bath application of gentamicin (1 mM), amikacin (1 mM) and FM1.43 (5µM) increase the K<sup>+</sup> endocystic concentration: 90 min treatments induce, respectively, 27.7 +/- 2.4 mM, 37.5 +/- 3.8 mM and 15.0 +/- 3.7 mM significant rises of [K<sup>+</sup>], with respect to a 71.7 +/- 3.8 mM control level. Since (1) ouabaine is known to inhibit the ability of dark cell to secrete K<sup>+</sup> in the endolymph and (2) gentamicin, amikacin and FM1.43 are blockers of the transduction channel, hence obliterating transduction currents mediated by the influx of K<sup>+</sup> from endolymph to hair cells, then the present data suggest that functional K<sup>+</sup> recycling pathway does exist in this vestibular organotypic model.

Key words: vestibule, utricle, endolymph, potassium recycling, aminoglycoside, FM 1.43, ouabaine

## **761 Megalin is Transported in the Endolymphatic Sac**

Maki Arai<sup>1</sup>, Kunihiro Mizuta<sup>1</sup>, Akihiko Saito<sup>2</sup>, Yasuyuki Hashimoto<sup>1</sup>, Satoshi Iwasaki<sup>1</sup>

<sup>1</sup>Hamamatsu University School of Medicine, <sup>2</sup>Niigata University Graduate School of Medical and Dental Sciences

Megalin is an endocytic receptor predominantly expressed in the kidney proximal tubule cells and in the inner ear. in the present study, we examined immunohistochemical

localization of megalin in the rat endolymphatic sac with light- and electron microscopy. Under light microscopy, we found that the endolymphatic space included strongly stained components. the cytoplasm of some epithelial cells were moderately stained, and other cells were faintly stained. to study this unusual staining pattern, we used electron microscopy and compared the labeling of endocytic vacuoles in epithelial cells of the endolymphatic sac with the labeling of endocytic vacuoles in the kidney proximal tubule cells. Firstly, in the endolymphatic sac, stained vacuoles were observed not only immediately beneath the luminal side, but also near the basolateral membrane, whereas in kidney proximal tubule cells, staining was detected only on the luminal side. Secondly, in the epithelial cells of the endolymphatic sac, diffuse labeling was observed on material in the vacuole, whereas in the kidney proximal tubule cells, labeling was limited mostly to the endocytic membrane. in some cells, labeling was continuous from the cytoplasm to the endolymphatic space, with no labeling of the vacuole. in summary, megalin immunoreactivity was present in both kidney proximal tubule cells and epithelial cells of the endolymphatic sac. However, the different staining patterns in these cells suggest that endocytic mechanisms appear to differ in the endolymphatic sac and in the proximal tubule. We have previously reported that megalin was located in the microvilli of epithelial cell of endolymphatic sac (ARO Midwinter Meeting Abstract, 2005). However, our recent data presented here made us conjecture that megalin is secreted from a certain type of epithelial cells in the endolymphatic sac into the endolymphatic space, and is then taken up by another type of epithelial cells for endolymphatic sac homeostasis.

## **762 Ultrastructural Co-Localization of Cochlin and Type II Collagen in the Rat Semicircular Canal**

Kunihiro Mizuta<sup>1</sup>, Tetsuo Ikezono<sup>2</sup>, Maki Arai<sup>1</sup>, Yasuyuki Hashimoto<sup>1</sup>, Satoshi Iwasaki<sup>1</sup>

<sup>1</sup>Hamamatsu University School of Medicine, <sup>2</sup>Nippon Medical School

Cochlin, a major constituent of the inner ear extracellular matrix, is encoded by COCH gene whose mutations are associated with an autosomal dominant progressive sensorineural hearing loss and vestibular disorder at the DFNA9 locus. it's isoforms are classified into three subgroups. Type II collagen is also an extracellular matrix material in the acellular structures and subepithelial connective tissue of the inner ear. We recently localized cochlin in the same areas of the inner ear as type II collagen with light microscopy using a polyclonal antibody against bovine cochlin. Here we extended our immunocytochemical study to an ultrastructural level.

the rabbit polyclonal antibody used in this study was raised against vWFA like domain 1 of cochlin. This antibody recognized all three cochlin isoforms. Antibody against type II collagen was purchased commercially. an electron microscopic analysis was performed with these antibodies using the post embedding immunogold method.

Immunolabeling for cochlin was detected in the fibrillar substance underlying the supporting epithelium of the



sensory cells and beneath the epithelial cells facing the endolymph in the semicircular canals. Immunolabeling for type II collagen was observed in the same fibrillar substance in the subepithelial area. Their co-localization was clear in thin fibers of several microns long.

Based on these observations, we suggest that cochlin works together with type II collagen in structural homeostasis in the inner ear.

### **763 Effects of Recombinant Otoconin90 and Otoconin22 Upon Calcite Crystal Growth *In Vitro***

Wenfu Lu<sup>1</sup>, Dan Zhou<sup>2</sup>, John J Freeman<sup>3</sup>, Isolde Thalmann<sup>1</sup>, David ornitz<sup>4</sup>, Ruediger Thalmann<sup>1</sup>

<sup>1</sup>Washington University Medical School, Department of Otolaryngology, St. Louis, MO 63110, <sup>2</sup>University of Missouri - St. Louis, Center for Nanoscience, St. Louis, MO 63121, <sup>3</sup>Washington University, Department of Earth & Planetary Sciences, St. Louis, MO 63130, <sup>4</sup>Washington University Medical School, Department of Molecular Biology and Pharmacology

Otoconia are minute biomineral particles which enhance perception of gravity and maintenance of balance. Specialized biomacromolecules, typically acidic glycoproteins, play an essential role in controlling crystal nucleation, size, shape and mechanical properties. Otoconin90 (OC90), the principal soluble matrix protein of mammalian otoconia, is a homolog of secretory phospholipase A2. Sequence analysis indicates numerous anionic and hydrogen-bonding acceptor-donor clusters, which are believed, respectively, to facilitate interaction of calcium with the calcite crystal lattice and of the protein with carbonate ions. to test the modulatory effects of OC90 upon calcite crystal growth *In Vitro*, we generated significant quantities of the recombinant protein using a stable HEK293 cell line. OC90 (0.01 to 5  $\mu$ M) added to the growth solution, resulted in a dramatic increase of nucleation density of calcite in a concentration-dependent manner, whereas crystal size was markedly decreased. the rhombohedral morphology of pure calcite crystals underwent marked changes at higher OC90 concentrations resulting in marked rounding of the acute edges of each of the (104) faces. Together with a progressive lengthening in direction of the c-axis, the modified calcite crystal assumed a shape similar to mammalian otoconia. Corresponding experimentation with otoconin22 (OC22), the principal soluble matrix protein of aragonitic amphibian otoconia, resulted in only a minor increase of nucleation density and decrease of crystal size. However, morphologic changes resembled those induced by OC90. Significantly, as in the case with the aragonitogenic protein AP8 of the mollusk nacre, only calcite and no aragonite (verified by Raman spectrometry) was nucleated. This situation is analogous to other aragonitogenic proteins, where aragonite is expressed only in combination with major changes in the microenvironment. [Supported by NIDCD DC02236 (DMO) & DC01414 (IT)]

### **764 Osteopontin is Not Critical for Otoconia Formation or Balance Function**

Xing Zhao<sup>1</sup>, Yesha Lundberg<sup>1</sup>

<sup>1</sup>BTNRH

Unlike the structural and mechanic role of bone crystals, the inertial mass of otoconia crystals provides a shearing force to stimulate the mechanoreceptors of the utricle and saccule (the gravity receptor organ). It is not clear whether otoconia, composed primarily of CaCO<sub>3</sub> and glycoproteins, go through similar calcification processes as bone. We have recently shown that otoconin-90 (Oc90) regulates the growth of otoconia crystals as osteopontin does bone crystals. Here we analyzed the role of this non-collagenous bone matrix protein, osteopontin, in otoconia formation and balance function utilizing its knockout mice, whose inner ear phenotype has not been examined. Despite the presence of the protein in wildtype otoconia and vestibular hair cells, morphological, ultrastructural and protein composition analyses of osteopontin null otoconia show that the protein is not needed for crystal formation and no evidence of compensatory protein deposition is found. Employment of a wide spectrum of balance tests including reaching and air-righting reflexes, gait, beam-crossing, swimming and rotorod tests demonstrates that the protein is not critical for balance function either. When compared with findings on other otoconins, the data manifest a hierarchy of importance of proteins in crystallization and indicate mechanistic similarities and differences between bone and otoconia calcification.

### **765 Oc90 Deletion Leads to Imbalance But Normal Hearing: a Comparison with Other Otoconia Mutants**

Xing Zhao<sup>1</sup>, Sherri Jones<sup>2</sup>, Ebenezer Yamoah<sup>3</sup>, Yunxia Lundberg<sup>1</sup>

<sup>1</sup>Boys Town National Research Hospital, <sup>2</sup>East Carolina University, <sup>3</sup>University of California at Davis

Our sense of gravitation and linear acceleration is mediated by stimulation of vestibular hair cells through displacement of otoconia in the utricle and saccule. Otoconia abnormalities lead to imbalance. Utilizing our recently generated knockout mouse model for otoconin-90/95 (Oc90), we have demonstrated that the protein is essential to form the organic matrix of otoconia by specifically recruiting other matrix components. We have then determined the extent to which the giant otoconia in the Oc90 null mice affect balance and compared with mutants possessing various degrees of otoconia deficiencies using a wide spectrum of balance behavioral tests and vestibular evoked potentials (VsEPs). Despite the somewhat different aspects of balance and coordination that are evaluated by these methods, overall the tests have consistently ranked the order of imbalance as (from worst to best) Nox3<sup>het</sup> < otopetrin<sup>tt</sup> < Oc90 null < otogelin<sup>wt</sup> < Oc90 wt and C57Bl/6 mice using either the frequency of occurrence or the severity of abnormal functions. This order coincides with the degree of otoconia deficiencies. Notably, all mice (except Nox3<sup>het</sup>) show remarkable learned compensation of vestibular functions by staying on the rotating rod longer in each successive

trial, and such learned improvements rank the same order as their initial balance ability. Despite the vestibular morbidity, most of these mutants have normal hearing. the study demonstrates that otoconial proteins regulate crystal growth and morphology, that the otoconia mass has a proportional impact on the amount of stimulus relayed to vestibular ganglia by the sensory epithelium and that the combined outcome from a series of behavioral tests and direct measures can detect and evaluate imbalance severity. the data also provide a scientific rationale for vestibular exercises for patients with related balance disorders.

## **766 Estrogen Receptors in the Rat Vestibular Periphery**

*Withdrawn*

## **767 Distribution of Metabotropic Glutamate Receptors in the Adult Rat Vestibular Periphery**

**P. Ashley Wackym**<sup>1</sup>, Juman Kubba<sup>2</sup>, Christy Erbe<sup>1</sup>, Alexandra Lerch-Gaggl<sup>1</sup>, Paul Popper<sup>1</sup>

<sup>1</sup>Medical College of Wisconsin, <sup>2</sup>American University UAE

Metabotropic glutamate receptors (mGluRs) mediate the effects of glutamate on neuronal excitability and on feedback regulation of neuropeptide release. Molecular cloning has revealed eight mGluRs, classified into three subgroups based on their sequence similarities, preferred signal transduction mechanisms and pharmacology. Group I includes mGluR1 and mGluR5, which are coupled to phosphoinositid hydrolysis. Group II includes mGluR2 and mGluR3, which are negatively coupled to adenylate cyclase. in addition, group I and group II mediate the rapid, membrane effects of estradiol. Since glutamate is the main neurotransmitter in the vestibular epithelia, these receptors may be important in the physiology of the vestibular periphery. We investigated the expression and distribution of group I mGluRs in the vestibular ganglion and crista ampullaris.

RT-PCR of vestibular ganglia RNA revealed that both mGluR1 and mGluR5 are expressed in the vestibular ganglia. mGluR1 immunoreactivity was detected in mostly the small neurons of the vestibular ganglia and in nerve terminals in the crista ampullaris. Similarly, mGluR5 immunoreactivity was detected in neuronal somata of the vestibular ganglion and in nerve terminals. Further studies elucidating the localization of these receptors relative to neuropeptides and their receptors in the vestibular epithelia are in progress. Supported by NIDCD grants DC02971 and DC006571.

## **768 Supporting Cells Regulate Synaptogenesis in the Vestibular System**

**Joshua Murtie**<sup>1</sup>, Konstantina Stankovic<sup>2</sup>, M. Charles Liberman<sup>2</sup>, Gabriel Corfas<sup>1</sup>

<sup>1</sup>Children's Hospital Boston, <sup>2</sup>Mass Eye and Ear Infirmary

Supporting cells (SCs) of the mature vestibular epithelia are closely associated with hair cells and afferent nerve terminals, making them likely contributors to the development and function of hair cell-afferent synapses, however this remains to be demonstrated. to explore this potential role of vestibular SCs we used transgenic mice in which erbB receptor signaling in these cells is blocked by expression of a dominant-negative erbB receptor (DN-erbB4). We focused on this signaling pathway because a) sensory neurons express the erbB ligand NRG1 while SCs express erbB receptors and b) we have previously shown that SC erbB signaling is important for survival of cochlear sensory neurons.

At P21, DN-erbB4 mice displayed behaviors consistent with vestibular dysfunction including ataxia, spinning behavior, and inability to swim. Evoked potential recordings also showed that vestibular function was severely affected at P21, even though macular epithelia were normal in size and general structure. FM1-43 dye uptake and NF200 staining were also normal in mutant mice, indicating that hair cell mechano-transduction and afferent innervation were unaffected. However, synaptic site numbers (defined as the colocalization of RIBEYE and GluR2/3 staining) were dramatically reduced at P21, suggesting that a synaptic defect could be the cause of the phenotype. Comparison between the time-course of synapse development showed that synapse number increases more than 4-fold between P0 and P21 in wild type maculae while they fail to do so in the mutants. Interestingly, the synaptic alterations were accompanied by a dramatic reduction in BDNF expression in SCs. Together these results indicate that SCs play a critical role in synaptogenesis in the vestibular epithelia and that this may be mediated by NRG1-erbB and BDNF-TrkB signaling.

## **769 Developmental Expression of Inward Rectifier K<sup>+</sup> Currents in Vestibular Afferent Neurons of the Rat**

**Enrique Soto**<sup>1</sup>, Rosario Vega<sup>1</sup>, Enoch Luis<sup>1</sup>

<sup>1</sup>Universidad Autónoma de Puebla

Vestibular afferent neurons of rodents have been shown to express various ionic channels including two inward rectifying currents  $I_{K1}$  and  $I_h$ . Preliminary observations indicate that inward rectifying currents show a significant increase in their magnitude during maturation of rat vestibular afferent neurons from early postnatal to young stages. Our experiments were aimed to characterize inward K<sup>+</sup> currents and to define if there are an increase in the inward current density during development and which type of inward current increased if any.

Experiments were made on early postnatal C2 rats (postnatal days (P) 7 – 10) and in young P28 rats, all of them supplied by the "Claude Bernard" animal house of the University of Puebla. Inner ear was dissected and

isolated afferent neurons placed in primary culture as previously described (Soto et al., 2002; Limón et al., 2005). Cultured neurons were recorded with the use of the patch-clamp technique in the whole-cell voltage-clamp configuration. In some of the experiments, cells were also recorded in current-clamp to study their membrane potential ( $V_m$ ) and their responses to current injection and drug application.

P23-26 neurons showed a large hyperpolarization-activated inward current, which was not so evident in P7-10 rats. The mean inward current density in neurons from young P7-10 rats was  $11.3 \pm 6.5$  pA/pF ( $n = 14$ ) whereas that in neurons from P28 rats was  $25.6 \pm 16.5$  pA/pF ( $n = 9$ ). Difference in inward current density was significant with a  $P = 0.008$ . To elucidate which type of inward current increased its expression the effect of  $Ba^{2+}$ ,  $Cs^+$  and zatebradine was studied. The use of  $Ba^{2+}$  and zatebradine ( $I_{K,1}$  blockers) allowed us to show that no significant change of  $I_h$  between P28 and P7-10 takes place. Thus indicating that the increase in inward current expression was mainly due to an increase in  $I_{K,1}$ .

These data coincide with an increase in the action potential threshold in afferent neurons between P7-10 and P23-26. Probably indicating that current maturation in this cells implies a decrease in their excitability.

This work was supported by grant from CONACYT 46511 and VIEP-BUAP grant 2007, EL is a PIFI fellowship recipient and CP is CONACYT fellowship recipient (185855).

## **770 Potassium Currents and Action Potential Shaping in Vestibular Calyx Terminals**

Katie Rennie<sup>1</sup>, Ritu Dhawan<sup>1</sup>

<sup>1</sup>University of Colorado HSC

In the peripheral vestibular system afferent neurons make terminal synapses with hair cells and have a resting discharge that is modulated by hair bundle deflection. Calyx neurons contact type I hair cells and have an irregular discharge of action potentials. We have made whole cell patch-clamp recordings from calyx terminals isolated together with their presynaptic type I hair cells from the semicircular canals of Mongolian gerbils to investigate ionic conductances underlying action potential firing.

In voltage clamp  $Na^+$  currents were blocked by tetrodotoxin or by replacement of external  $Na^+$  with choline. Calyx terminals showed minimal current at the mean zero-current potential of  $-59.1 \pm 1.1$  mV (mean  $\pm$  SEM,  $n = 39$ ), but three types of  $K^+$  currents were identified at potentials above  $-50$  mV. A rapidly activating and inactivating  $K^+$  current was blocked by 4-aminopyridine (4-AP, 0.3-2.5 mM). A second more slowly activating, slowly inactivating current was sensitive to tetraethylammonium (TEA). The block was maximal at  $\sim 30$  mM TEA. The TEA-sensitive current showed steady-state inactivation with a mean half inactivation of  $-95$  mV following 500 ms conditioning pulses. Removal of extracellular calcium also reduced outward currents suggesting the presence of a  $Ca^{2+}$ -activated  $K^+$  current. The outward  $K^+$  currents were

blocked by replacing  $K^+$  in the patch electrode solution with  $Cs^+$ , revealing a sustained inward  $Ca^{2+}$  current at potentials above  $-40$  mV.

In current clamp repetitive firing was not observed, but single  $Na^+$ -dependent action potentials ( $\sim 65$  mV in amplitude) were evoked following hyperpolarization to potentials more negative than  $-60$  mV. Action potentials were followed by an afterhyperpolarization that was altered by both 4-AP and TEA.

Supported by NIDCD R01 DC008297 and NOHRF

## **771 Localization of Initial Segments in Calyx and Dimorphic Vestibular Afferents in the Rat** Anna Lysakowski<sup>1</sup>, Steven D. Price<sup>1</sup>, Jay M. Goldberg<sup>2</sup>

<sup>1</sup>University of Illinois at Chicago, <sup>2</sup>University of Chicago

Synaptic currents in calyx endings could be severely attenuated if they needed to reach the heminode to trigger an action potential (Goldberg, J. Neurophysiol. 76:1942-57, 1996). This led us to speculate that the initial segment (IS) may be located closer to synaptic sites. To study the location of the IS, we used well-characterized antibodies to several markers of ISs and nodes of Ranvier (Hedstrom and Rasband, J. Neurochem. 98:1345-52, 2006), including  $Na$  channels ( $\text{pan-}Na_v$ ), ankyrinG,  $\beta IV$  spectrin and neurofascin (NF) 186. Calretinin distinguished calyx and dimorphic fibers, whereas myelin was marked by myelin basic protein (MBP). In both the cristae and the maculae, IS markers were found at the heminode.  $\beta IV$  spectrin and NF 186 were localized to the heminode.  $\text{Pan-}Na_v$  and ankyrinG, were densely present at the heminode; labeling diminished upwards along the calyx outer face. In dimorphic fibers, the end of the myelin and the heminode occur below the basal lamina. In calyx fibers, the heminode, marked by MBP and IS markers, is found at the basal lamina or above, even deep within the neuroepithelium, reminiscent of the "M fibers" of Ross et al. (Acta Otolaryngol. 102:75-86, 1986). We suggest that synaptic currents can travel effectively from the calyx inner face to the heminode because they are enhanced by  $Na$  conductances found on the calyx outer face.  $Na_v 1.5$ , previously localized ultrastructurally to the calyx inner face (Lysakowski et al., ARO, 2006) may also be involved, although the inner face was not labeled by IS antibodies. It will be important to characterize the specific  $Na_v$  channels localized at the heminode and the calyx ending. In the crista, the first full node is typically found at the base of the stroma, about  $100 \mu m$  from the basal lamina.

Supported by NIH DC-02521 (AL) and NIH DC-02058 (JMG).

## **772 Efferent Cholinergic Receptors in the Turtle Posterior Crista**

Joseph Holt<sup>1</sup>, Marcin Klapczynski<sup>2</sup>, Steve Price<sup>2</sup>, J. Michael McIntosh<sup>3</sup>, Jay Goldberg<sup>4</sup>, Anna Lysakowski<sup>2</sup>

<sup>1</sup>University of Texas Medical Branch (UTMB), <sup>2</sup>University of Illinois at Chicago (UIC), <sup>3</sup>University of Utah, <sup>4</sup>University of Chicago

In the turtle posterior crista, electrical stimulation of efferent fibers results in an inhibition of synaptic release from hair cells in the torus region and a direct excitation of afferent fibers, including calyx-bearing (CD) and bouton (B) fibers (Holt et al., J. Neurosci. 26: 13180-13193, 2006). As in other hair cell systems, our pharmacology suggests that  $\alpha 9/\alpha 10$  nicotinic acetylcholine receptors (nAChRs), linked to small-conductance, calcium-activated potassium channels, mediate the hair-cell inhibition. But the direct excitation of afferent fibers is only modestly antagonized by  $\alpha 9/\alpha 10$  blockers suggesting that different nAChRs are involved. This distinction has now been confirmed with  $\alpha$ -conotoxin RglA, a selective  $\alpha 9/\alpha 10$  nAChR antagonist (Ellison et al., Biochem. 45: 1511-1517, 2006). to identify the molecular basis for these pharmacological differences, we are now studying other nAChR subunits. to this end we cloned the  $\alpha 9$  nAChR subunit in the turtle (Cameron et al., ARO, 2005), from which an antibody and *In-Situ* probes were made. the antibody stained hair cells sporadically, but *In-Situ* hybridization stained virtually all hair cells near the torus, where efferent inhibition is seen. in an attempt to identify other nAChRs, we used commercially available antibodies against rat  $\alpha 4$  and  $\beta 2$  nAChR subunits. Both antibodies stained boutons in the torus region (where postsynaptic excitation as well as hair-cell inhibition is seen), as well as calyx endings (which only show postsynaptic excitation). Because the specificity of several nAChR antibodies has recently been questioned (N. Moser et al., J. Neurochem. 102:479-92, 2007), we confirmed the presence of  $\alpha 4$  and  $\beta 2$  nAChR subunits in the turtle inner ear by sequencing RT-PCR products. to continue the analysis, we plan to do *In-Situ* hybridization in the vestibular ganglion and neuroepithelia with  $\alpha 4$  and  $\beta 2$  probes. Supported by NIH DC-02058 (JMG), NIH DC-02521 (AL).

## **773 Kinocilium Mechanical Properties**

Corrie Spoon<sup>1</sup>, Wally Grant<sup>1</sup>

<sup>1</sup>VA Tech

**INTRODUCTION:** Hair cell bundles located in the medial extrastriolar section of the utricle of the red-eared turtle have long kinocilium (10-40  $\mu\text{m}$ ) and short stereocilia (2-5  $\mu\text{m}$ ). the exposed long section of kinocilium (8-30  $\mu\text{m}$ ) was used for these experiments. **EXPERIMENT:** the base of the kinocilium was backed up with a solid glass pipette, mechanically fixing its base so that when it was deflected in the excitatory direction only the kinocilium bent in flexure. This allowed for measurement of mechanical properties of the exposed kinocilium. Two techniques were used for measurement: (1) the tip of a flexible glass whisker of known stiffness, was placed in contact with the tip of the kinocilium. the base of the glass whisker is displaced a known amount and the displacement of the end

in contact with the kinocilium was measured with a double diode device. the stiffness of the kinocilium was calculated using this information. (2) the tip of the kinocilium was displaced with a rigid pipette and released to travel through the suspending solution, back to its equilibrium position. This motion was recorded using high-speed video (7 frames/millisecond). Using frame-by-frame analysis of the tip position, a time constant for this return to equilibrium was calculated. From the time constant and fluid drag formulation of motion through the solution, the flexural rigidity (EI) was calculated. the fluid drag was calculated using Oseen's drag formulation for a cylinder at Reynolds numbers that were used in the experiment. Validity of this technique was confirmed using a test glass whisker that was substituted for the kinocilium. This substitute glass whisker had a constant diameter (like a kinocilium). the constant diameter allowed for calculation of the fluid drag and stiffness. the stiffness of the test glass whisker was also measured to confirm the calculated stiffness value. **RESULTS:** Measured values of the flexural rigidity (EI) were average, and these and the standard deviations were: (1) glass whisker  $EI=2578 \text{ pN-}\mu\text{m}^2$  ( $\sigma=673$ ,  $n=11$ ), (2) high-speed video  $EI=3512 \text{ pN-}\mu\text{m}^2$  ( $\sigma=1312$ ,  $n=13$ ). Stiffness values ( $k=F/\delta$ ) are easily calculated however they vary with height.

## **774 The Influence of Glycogen Synthase Kinase 3 On Cell Proliferation in the Murine Vestibular Sensory Epithelium**

Zhenjie Lu<sup>1</sup>, Jeffrey Corwin<sup>1</sup>

<sup>1</sup>Department of Neuroscience, University of Virginia School of Medicine, Charlottesville, VA 22908

Regenerative replacement allows non-mammalian vertebrates to recover from sensory hair cell loss within a matter of weeks to months, while such losses lead to permanent hearing and balance deficits in humans and other mammals. the vestibular organs of mammals exhibit modest forms of repair, but their potential for effective hair cell regeneration is limited by an early postnatal decrease in the capacity for cell proliferation within the sensory epithelium. We have investigated the developmental decline of proliferative capacity in the hair cell epithelium of the murine utricle and have assessed its potential regulation by glycogen synthase kinase-3 (GSK3). Western blots of sensory epithelium demonstrated that two active forms of GSK3 increase postnatally and are mirrored by decreasing levels of inactive GSK3 $\beta$ , suggesting that GSK3 may be influential in limiting the capacity for hair cell regeneration in mammals. Across postnatal ages, pharmacological inhibition of GSK3 by either LiCl or SB-216763 resulted in increased cell proliferation in cultured sheets of pure utricular sensory epithelium. the inhibition of GSK3 also stabilized  $\beta$ -catenin and Snail, and resulted in decreased E-cadherin expression. Transfection of cultured sensory epithelium with a dominant-negative GSK3 $\beta$  enhanced cell proliferation in a cell autonomous manner, while overexpression of wild-type GSK3 $\beta$  reduced proliferation. the results indicate that the balance of active and inactive GSK3 can influence the proliferation of vestibular supporting cells during the neonatal decline in cell

replacement capacity that appears to leave mammalian vestibular epithelia vulnerable to permanent hair cell deficits. Therefore, investigations of GSK3-mediated pathways may be of value for understanding and perhaps overcoming the limits to effective cell replacement in mammalian ears.

(Supported by NIDCD awards R01-DC00200 and R01-DC-06182)

### **775 Immunohistochemical Localization of Ephb2 in the Human Vestibular Crista Ampullaris**

Ivan Lopez<sup>1</sup>, Gail Ishiyama<sup>2</sup>, Christopher Geiger<sup>1</sup>, Akira Ishiyama<sup>1</sup>

<sup>1</sup>*Surgery Department UCLA School of Medicine,*

<sup>2</sup>*Neurology Department UCLA School of Medicine*

Recent studies on the expression of EphB2 and Ephrin-B2 in the vestibular apparatus suggest that these molecules play an important role in the production of endolymph and ionic homeostasis (Cowan et al., *Neuron*, 26, 417-30, 2000; Dravis et al, *Hear Res* 223, 93-104, 2007). in mice vestibule, EphB2 is located in dark cells, whereas Ephrin-B2 is located in transitional and supporting cells. There are no previous studies on EphB2 localization in normal or Meniere's disease human cristae ampullaris (CA). for this purpose vestibular endorgans were microdissected from human temporal bones 3-5 hours post-mortem from individuals with no history of vestibular problems (from 84-96 years old; n=4), CA obtained from ablative surgery from patients diagnosed with Meniere's disease were also used (n=3). Cryostat sections were incubated with a goat antibody against EphB2 (1: 200 in PBS, Santa Cruz, California, USA) and analyzed using light and fluorescent microscopy. in cross sections of normal and Meniere's CA, EphB2 immunoreactivity was selectively localized to vestibular dark cells. Hair cells and supporting cells were non-immunoreactive. the similar expression of EphB2 in dark cells of the human CA and mice (Dravis et al, 2007) suggests that EphB2 may play a similar role in the regulation inner ear ionic and fluid homeostasis.

Funded by NIDCD-NIH grants DC005028-05, DC008635-02, and DC005187-05.

### **776 Inactivation of Ephb2 Kinase Activity Results in Vestibular Dysfunction**

Kenneth Lee<sup>1</sup>, Mark Henkemeyer<sup>2</sup>

<sup>1</sup>*Otolaryngology-Head & Neck Surgery, UT Southwestern & Children's Medical Center Dallas,* <sup>2</sup>*Center for Developmental Biology, UT Southwestern Medical Center at Dallas*

Normal vestibular function is dependent on maintenance of proper ionic homeostasis of the endolymph. Previously, our laboratory has shown that EphB2 is expressed in the K<sup>+</sup> secreting dark cells in mouse vestibular cristae. Studies with null mice have shown that mutation of EphB2 or an associated ligand ephrin-B2, expressed in the adjacent transitional cells, result in rapid head bobbing and circling. Accompanying these behavioral phenotypes, knock out mice demonstrate semicircular canals with reduced bony and membranous volumes as well as lower

endolymphatic potentials and K<sup>+</sup> concentrations. EphB2 is a member of the largest known family of receptor tyrosine kinases, and contains an intracellular kinase domain and a C-terminal PDZ binding motif, both implicated in the propagation of signal within the cell. We have generated a mouse with a point mutation that produces a full length EphB2 protein but with an inactive kinase domain. This mouse also demonstrates head bobbing and circling behavior. Bony and membranous semicircular canal morphology are analyzed and quantified in these mice to determine the anatomical result of blocking kinase but maintaining PDZ binding function of EphB2. the results provide a more precise understanding of the mechanism by which EphB2 signaling into the endolymph-producing dark cells is involved in normal development and function of the vestibular system.

### **777 Microrna-21 Overexpression May Contribute to Tumor Growth in Vestibular Schwannomas**

Joseph Cioffi<sup>1</sup>, Sabrina Mendolia-Loffredo<sup>1</sup>, Becky Massey<sup>1</sup>, P. Ashley Wackym<sup>1</sup>

<sup>1</sup>*Department of Otolaryngology and Communication Sciences, Medical College of Wisconsin*

Vestibular schwannomas are benign tumors that arise from Schwann cells of the vestibular portion of the eighth cranial nerve predominantly as a result of mutations in the *nf2* gene which encodes the tumor suppressor merlin. the pathways by which defective merlin promotes tumor growth are poorly understood. MicroRNAs are a family of small, noncoding RNAs that modulate protein expression by binding to messenger RNAs and either interfere with translation or facilitate cleavage of the message. They have been shown to play regulatory roles in cell proliferation, differentiation and apoptosis, and evidence suggesting a role in cancer development is emerging. Therefore, we examined microRNA expression profiles in vestibular schwannomas using microarrays. We demonstrated consistent overexpression of microRNA-21 (miR-21) in human vestibular schwannomas when compared to normal vestibular and facial nerves. These results have been confirmed using real-time RT-PCR assays. PTEN, a known target of miR-21 and regulator of the PI3K signaling pathway, was examined and found to be expressed in all normal nerve and vestibular schwannoma tissues by RT-PCR but absent or barely detectable in 3 out of 4 vestibular schwannomas by Western blot analysis. Since the gene encoding miR-21 is known to contain Stat3 enhancer sites, and because merlin has been shown to inhibit STAT activation through its interaction with HRS, we examined the expression of several cytokines and receptors known to activate Stat3. These data suggest that overexpression of microRNA-21, possibly resulting from enhanced Stat3 activation, may lead to down regulation of PTEN thereby reducing its inhibitory effect on the PI3K/AKT signaling pathway resulting in increased cell proliferation and tumor growth. These findings suggest that miR-21 may be a suitable molecular target for therapies aimed at specifically blocking the growth of vestibular schwannomas.

## **778 Substance P May Act On Vestibular Endorgan As an Excitatory Factor**

**Hiroshi Orita<sup>1</sup>**, Hiroaki Shimogori<sup>1</sup>, Yoshinobu Hirose<sup>1</sup>, Takefumi Mikuriya<sup>1</sup>, Makoto Hashimoto<sup>1</sup>, Kazuma Sugahara<sup>1</sup>, Hiroshi Yamashita<sup>1</sup>

<sup>1</sup>*Yamaguchi University School of Medicine*

Substance P (SP) is an undecapeptide belonging to a class of neuropeptides, entitled tachykinins. in the inner ear, though many previous studies concerning localization of SP were reported in the nineteen-nineties, showing that SP exists abundantly in the vestibular endorgans, functional role of SP in the inner ear is still unknown. SP often acts as a neuromodulator in the CNS and can directly influenced the neuronal excitability. We hypothesized that SP may influence the neuronal excitability in vestibular periphery. the aim of the present study was to investigate the influence of SP, locally applied in guinea pig unilateral inner ear, using sinusoidal rotation test.

Hartley white guinea pigs with normal tympanic membranes and normal Preyer reflexes were used in this study. in each animal, a tiny hole was made adjacent to the round window in the right ear, and SP (10-4 M), SP (10-3 M), SP antagonist, or SP (10-3 M) + SP antagonist was infused through this hole by osmotic pump. Rotation tests were performed before treatment and 12 h and 24 h after treatment, and VOR gains were calculated.

Animals administered with SP (10-3 M) showed significant increase of VOR gains 12 h after treatment, which was disappeared 24 h after treatment. Furthermore, this increase disappeared by simultaneous administration of SP antagonist. Animals administered with SP (10-4 M), SP antagonist only showed no obvious changes in VOR gains. These results indicate the possibility that SP may act on vestibular endorgan as an excitatory factor via NK1 receptors.

## **779 Detection of P-CREB in the Guinea Pig Vestibular Ganglion Cells After Peripheral Vestibular Disorder**

**Hiroaki Shimogori<sup>1</sup>**, Kazuma Sugahara<sup>1</sup>, Makoto Hashimoto<sup>1</sup>, Yoshinobu Hirose<sup>1</sup>, Takefumi Mikuriya<sup>1</sup>, Hiroshi Yamashita<sup>1</sup>

<sup>1</sup>*Yamaguchi University Graduate School of Medicine*

Phosphorylation of the transcription factor cAMP responsive element-binding protein (CREB) is thought to play a key role in synaptic plasticity and long-term memory. in a previous report, phosphorylated form of CREB (p-CREB) -like immunoreactivities were observed in bilateral vestibular nuclei 1 h after unilateral vestibular labyrinthectomy, indicating that the activation of the p-CREB play a role in the initial events of vestibular compensation. While, under hypergravity, p-CREB-like immunoreactivities were observed in vestibular ganglion cells. These results show that vestibular periphery also has a potential of neuronal plasticity. the aim of this study was to detect the p-CREB-like immunoreactivity in vestibular ganglion cells after various kinds of peripheral vestibular disorders.

Hartley white guinea pigs with normal tympanic membranes and normal Preyer reflexes were used in this study. Animals were divided into three groups. in the first group, animals were received surgical labyrinthectomy in the right ear. in the second group, a tiny hole was made adjacent to the round window in the right ear, and TTX was infused through this hole by osmotic pump. in the third group, animals were received lateral semicircular canal transection in the right ear. One, 4 and 24 h after treatment, each animal was anesthetized deeply and was decapitated immediately. the temporal bone was dissected and vestibular ganglion was examined immunohistochemically for p-CREB.

In all groups, we observed p-CREB-like immunoreactivities in vestibular ganglion cells, which were disappeared within 24 h. But changes of p-CREB-like immunoreactivity in each group were different according to the method of peripheral vestibular lesions.

These data indicate the possibility that vestibular periphery may possess a potential of neuronal plasticity and show an appropriate response to peripheral vestibular disorder.

## **780 Efferent Control of the Afferent Discharge in the Axolotl Vestibular Endorgans**

**Rosario Vega<sup>1</sup>**, Hortencia Chávez<sup>2</sup>, Enrique Soto<sup>1</sup>

<sup>1</sup>*Instituto de Fisiología, Universidad Autónoma de Puebla, México*, <sup>2</sup>*Fac. Estomatología, Universidad Autónoma de Puebla, México*

The vestibular efferent system is thought to mediate both excitatory and inhibitory influences on the afferent discharge. However it is not still clear the mechanisms that determines either response type. the inner ear of the axolotl (*Ambystoma tigrinum*) with only type-II hair cells and a single efferent innervation constitute a model to study efferent control mechanisms. in this work we developed two kinds of experimental preparations: one in which the efferent system remains intact and vestibular endorgans remain in connection with the brain (vestibule-brain); and one in which the vestibular system was completely isolated and efferent system sectioned (isolated vestibule). the action of cholinergic (ACh) drugs on the electrical activity of afferent neurons of the semicircular canals, utricle and saccule were studied in both preparations.

Recording of the semicircular canal afferent neurons in the isolated vestibule preparation shown that perfusion of ACh antagonists atropine and d-tubocurarine (d-TC) did not have any effect after about 15 min of nerve sectioning. Although perfusion of acetylcholine (in the presence of eserine) and carbachol produced a significant excitatory effect that is slightly reduced by d-TC (28 %) and completely eliminated by 10 µM atropine. Strychnine have non significant effects on the basal discharge nor on the excitatory effect of carbachol. the nicotinic agonist 1-dimethyl-4-phenyl-piperazinium (DMPP) (10 µM to 1 mM, n = 14), did not have any significant effect.

in the vestibule-brain preparation atropine and d-TC (both at 10 -100 µM; n = 10 each) significantly reduced the afferent discharge, independently of the time after the

preparation was obtained. ACh agonists have a very mild or no effect in this preparation. Notably resection of the brain connection, produced a 50% reduction of the afferent activity. Recordings from utricular afferents shown a very similar -mainly muscarinic- pharmacology to that of the semicircular canals. in contrast, in the saccular afferents the selective nicotinic agonist DMPP produced a significant excitatory effect.

These results indicate that in the axolotl vestibular system the efferent system has a mainly excitatory influence which is responsible for about 50% of the afferent activity. in the semicircular canals and the utricle pharmacology is mainly muscarinic , in the saccule a mixed muscarinic nicotinic activity is present, and no expression of the  $\alpha 9-\alpha 10$  seems to take place in our system.

Financed by VIEP20/SAL/06-G grant to RV

### **781 The Effect of Efferent Stimulation on an Afferent's Response to Sinusoidal Indentation in the Turtle Posterior Crista** **Joseph Holt<sup>1</sup>**

<sup>1</sup>University of Texas Medical Branch (UTMB)

In the turtle posterior crista, an afferent's response to efferent stimulation can be related to the location of its ending in the neuroepithelium: Bouton units near the planum (BP) are weakly excited whereas bouton afferents near the torus (BT) are strongly inhibited. Bouton units more medially-located (BM) show mixed inhibitory-excitatory responses, and calyx/dimorphic (CD) afferents show a large excitation often consisting of both fast and slow components. Most of these responses can be attributed to the actions of two pharmacologically-distinct nicotinic ACh receptors (nAChRs), one on hair cells and the other on afferents.

My lab has been studying the effects of efferent stimulation on the response of posterior crista afferents to sinusoidal indentation of the canal duct. in BT, BM, and CD units, the addition of efferent stimulation can significantly reduce the afferent's sensitivity (i.e. gain) to a 0.3-Hz indenter stimulus. in BT/BM units, this reduction is observed at efferent shock frequencies as low as 5-Hz whereas higher shock counts (50-100 Hz) often completely block the afferent's response to indentation. in these units, the effects of efferent stimulation are asymmetrical in that the gain reduction comes predominantly from a graded loss of responsiveness during the excitatory phase of indentation whereas peak inhibition is only modestly reduced. Conversely, the indenter response in CD afferents is not as affected by efferent stimulation at lower shock frequencies, and the gain reduction at higher shock frequencies appears to be a product of reducing the magnitude of inhibition with peak excitation remaining relatively unchanged. Interestingly, the efferent-mediated slow excitation in CD units may give rise to a gain enhancement during sinusoidal indentation. We are currently pharmacologically dissecting out the role of each nAChR in these effects and describing how efferent stimulation impacts afferent responses to indentation at higher frequencies.

### **782 Bullfrog Horizontal Semicircular Canal Afferents Responding to Sinusoidal Rotational Stimuli Do Not Show an Increase in Phase Lead Re: Velocity with Increasing Stimulus Frequency**

**Dylan Hirsch-Shell<sup>1</sup>, Larry Hoffman<sup>1</sup>**

<sup>1</sup>University of California, Los Angeles

In toadfish, chinchillas and rhesus macaque monkeys, most horizontal semicircular canal afferents show increases in both sensitivity and phase lead of their responses relative to head angular velocity with increasing stimulus frequency over the range from 2-20 Hz. in contrast, pigeon afferents appear to have a different overall behavior: irregular afferents respond with increasing sensitivity over the same frequency range and are eventually driven to a phase-locking mode of firing where only one spike is elicited per stimulus cycle; however, regular and intermediate afferents have sensitivities that initially rise but then begin to decrease until no modulation of the discharge rate is observed; none of the afferents have responses with the prominent increases in phase lead with increasing stimulus frequency seen in the previously mentioned species. in order to gain a broader perspective on possible adaptive advantages, ethological explanations, or biological bases for these two contrasting afferent population characteristics, we studied the responses of semicircular canal afferents in an amphibian species (American bullfrog, *Rana catesbeiana*) to rotational stimuli in the frequency range from 0.4-12.8 Hz. in the limited sample of data collected so far, it appears that bullfrog afferents respond similarly to pigeon afferents. Namely, irregular afferents show increasing sensitivity with frequency and tend to be quickly driven to a phase-locking mode in which only one or two spikes occur within each stimulus cycle, while their phase leads begin to show a decline at ~6-12 Hz. Meanwhile, regular afferents show low sensitivities and phase leads (or even lags) at 0.4 Hz, which continue to decrease with increasing stimulus frequency. the absence of increasing phase leads in bullfrog afferent responses indicates that this characteristic is not a general consequence to high frequency coding in hair cell/afferent systems. Rather, this observation suggests that it represents a specific adaptation to neuroethologic demands.

### **783 Diversity in the Intrinsic Firing Patterns of Primary Vestibular Afferent Neurons**

**Radha Kalluri<sup>1</sup>, Jingbing Xue<sup>1</sup>, Ruth Anne Eatock<sup>1</sup>**

<sup>1</sup>Eaton-Peabody Laboratory, Massachusetts Eye and Ear Infirmary & Harvard Medical School

In mammalian vestibular afferent neurons, spike timing ranges from highly irregular to remarkably regular (Goldberg 2000). Regular firing patterns may enhance information transmission at low stimulus frequencies (Sadeghi et al. 2007). the somata of vestibular afferents are reported to express diverse ion conductances, which may shape firing regularity (Highstein and Politoff 1978; Smith and Goldberg 1986). to study how intrinsic membrane properties affect excitability, we use the perforated-patch whole-cell method to record from



neuronal somata from rats and mice in the first two postnatal weeks. the somata are either dissociated or in semi-intact preparations of ganglion plus attached utricle. Results in rats and mice are qualitatively similar. in current-clamp mode, we see three classes of response to current steps: a single initial spike; multiple spikes; and one or more spikes followed by voltage oscillations, which may be an immature variant of multiple spiking. Voltage-gated currents are qualitatively similar in fully dissociated and semi-intact preparations; space clamp is better in the former, while spontaneous spiking, driven by synaptic activity, is evident in the latter. Compared to single-spikers, multiple-spikers have larger current densities; faster transient outward currents; smaller resting potentials:  $-46 \pm 5.7$  mV (SE; 10 cells) vs.  $-55 \pm -3.6$  mV (10); higher spike thresholds:  $-27 \pm 1.5$  mV vs.  $-35 \pm 1.5$  mV; and a more prominent afterhyperpolarization following spikes and depolarizing current steps. to examine the influence of intrinsic membrane properties on firing regularity, we drive spiking in isolated somata with simulated epscs. Preliminary results suggest that following each spike, multiple-spikers integrate multiple pseudo-epses, producing a gradual rise to spike threshold. We speculate that intrinsic conductances play a role in firing regularity in vivo, with multiple spikers corresponding to more regular afferents and single spikers to more irregular afferents.

Supported by DC002290.

#### **[784] Effects of a GABA-B1 Receptor Antagonist On the Rotational Responses of Mouse Semicircular Canal Vestibular Afferents**

**Timothy Hullar<sup>1</sup>**, Aizhen Yang<sup>1</sup>, Gay Holstein<sup>2</sup>, Richard Rabbitt<sup>3</sup>, Stephen Highstein<sup>1</sup>

<sup>1</sup>Washington University in St. Louis, <sup>2</sup>Mt. Sinai School of Medicine, <sup>3</sup>University of Utah

GABA has been shown to be an inhibitory transmitter in the vestibular epithelium of the toadfish *Opsanus tau* and to shape the responses of its canal afferents in response to sinusoidal head rotations. to investigate this further, we examined the responses of horizontal semicircular canal afferents in C57BL/6J mice before and after administration of CGP, a GABA-B1 receptor antagonist. the control population consisted of 78 fibers (39 regular, 20 irregular, 19 phase-led irregular) and the treated population consisted of 26 afferents from 22 mice. the mean interspike interval (ISI) was 0.024 s in the pre-treatment group and 0.031 s in the post-treatment group ( $p = 0.09$ ). the mean coefficient of variation of ISI (CV) increased from 0.22 before to 0.41 after treatment ( $p = 0.0008$ ). the normalized coefficient of variation (CV\*) increased from 0.16 pretreatment to 0.30 posttreatment ( $p = 0.00095$ ). These data indicate that blocking the GABA-B1 receptor decreases the rate and regularity of spontaneous afferent activity. These effects are likely due to both pre- and post-synaptic actions of the receptor, as previously described in toadfish.

Supported in part by NIDCD grants DC006869 and DC006677

#### **[785] Comparison of Sinusoidal Responses to Externally Applied Currents and Angular Head Movements in the Vestibular Nerve of the Chinchilla**

Kyu-Sung Kim<sup>1</sup>, **David Lasker<sup>2</sup>**, Lloyd Minor<sup>2</sup>

<sup>1</sup>Department of Otolaryngology-Head and Neck Surgery, Inha University, <sup>2</sup>Department of Otolaryngology-Head and Neck Surgery, Johns Hopkins University

Extracellular recordings were made from 65 afferents innervating the semicircular canals in 8 adult, barbiturate-anesthetized chinchillas. Responses to sinusoidal stimuli (rotations and externally applied galvanic currents to the middle ear) were measured. Afferents were divided into three groups: bouton and dimorphic regular (R), dimorphic irregular (D) and calyx-only irregular(C) afferents based upon their discharge regularity and sensitivity to head movements at 2 Hz. the frequency of applied current ranged from 0.1 to 20 Hz with peak amplitude from 10-100uA. the rotational frequency varied from 2 to 16 Hz. Because of variability in the amount of current stimulation from animal to animal, we calculated a normalized measure of galvanic sensitivity at 2 Hz based upon the discharge regularity. As reported in Baird et al.(1988), this current sensitivity increased logarithmically with increasing CV\*. Transfer functions were fit to the sensitivity and phase across the frequency spectrum for each group of afferents. Phase lead at 20 Hz to externally applied currents measured  $29 \pm 13^\circ$ (R),  $32 \pm 12^\circ$ (D),  $26 \pm 9^\circ$ (C) ( $p > 0.1$ ). in contrast, phase at 16 Hz in response to head velocity measured  $31 \pm 25^\circ$ (R),  $57 \pm 6^\circ$ (D),  $83 \pm 22^\circ$ (C) ( $p < 0.01$ ). Externally applied galvanic currents act directly on vestibular nerve afferent. Comparison of rotational and galvanic responses allowed us to compute the relative contributions of synaptic and post-synaptic mechanisms. One conclusion emerging from this analysis is that the dynamics of the type I hair cell synapse are associated with an acceleration-sensitive component at higher frequencies. (Supported by NIH R01DC02390)

#### **[786] Kv1.1 and Kv.1.2 Immunolabeling in Vestibular Nucleus Neurons After Unilateral Vestibular Ganglionectomy**

**Anastas Popratiloff<sup>1</sup>**, Jenny Yi<sup>1</sup>, andrew Lerner<sup>1</sup>, Kenna Peusner<sup>1</sup>

<sup>1</sup>George Washington University Medical Center

Vestibular compensation is a popular model for studying brain plasticity. Usually, the static symptoms disappear about a week after unilateral vestibular ganglionectomy (UVG), but in some cases compensation is poor. in chickens, the tangential nucleus is a major vestibular nucleus whose principal cells (PCs) participate in the vestibular reflexes that are affected severely by UVG. From patch-clamp recordings in brain slices of uncompensated seven day old hatchlings (H7), which underwent UVG three days earlier, we found that increased numbers of PCs fired spontaneous spikes on the lesion side, while PCs on the intact side lacked spontaneous spike activity. in addition, the amplitude of IDS, a dendrotoxin (DTX)-sensitive potassium (K) current, increased in PCs on the lesion side, and more so on the

intact side compared to controls. During development, immunolabeling studies have shown that DTX-sensitive K channel subunits, Kv1.1 and Kv1.2, are down-regulated in PC bodies, and become differentially localized in cellular compartments. After hatching, Kv1.1 clustered at cell body surfaces, while Kv1.2 was detected in synaptic terminals. Using immunolabeling and confocal imaging, here we tested Kv1.1 and Kv1.2 expression in PCs of H7 chickens which underwent UVG at H4, but did not compensate. Sections were double-immunolabeled for Kv1.1 and MAP2, or Kv1.2 and synaptotagmin. Kv1.1 expression in PC bodies increased significantly on the lesion and intact sides compared to controls. Also, line scans showed that PCs on the lesion and intact sides had significantly higher Kv1.1 surface expression than controls, with stronger signal on the intact side. the ratio for Kv1.1 surface/cytoplasmic labeling in PCs on the intact side was significantly higher than in PCs on the lesion side and controls. Kv1.2 expression in synaptotagmin-positive profiles on PC bodies decreased bilaterally compared to controls. These results suggest that Kv1.1 immunolabeling of PCs from lesion and intact sides of uncompensated hatchlings was governed by different mechanisms, since PCs on the intact side exhibited a higher proportion of surface/cytoplasmic expression than PCs on the lesion side or controls. Decreased Kv1.2 expression in synaptic terminals contacting PC bodies suggests that the terminals themselves undergo changes after UVG.

#### **787 Regional Distribution of Serotonin and Melatonin Receptor Subtypes in Rat Vestibular Nuclei**

Carey Balaban<sup>1</sup>, Seong-Ki Ahn<sup>1</sup>

<sup>1</sup>University of Pittsburgh

Vestibular disorders, anxiety and motion sickness are frequently co-morbid with migraine and disordered sleep, particularly after mild traumatic brain injury. the serotonergic (5-HT) and melatonin (MT) systems likely contribute to these co-morbidity conditions because 5-HT is a precursor for MT synthesis (Tryptophan → hydroxytryptophan → 5-HT → N-acetyl-5-HT → MT). This study examines the differential distribution of 5-HT and MT receptors in vestibular nuclei (VN). Frozen sections of brains from 10 adult male Long-Evans rats (260-400 g), perfused transcardially with phosphate-buffered saline and paraformaldehyde-lysine-periodate fixative, were stained immunocytochemically for 5-HT or MT receptors with polyclonal anti-5-HT1A (Immunostar), anti-5-HT1B (Chemicon), anti-5-HT1D (Imgenex), anti-MT1 or anti-MT2 polyclonal antibodies (Chemicon), biotinylated secondary antibody and standard ABC-peroxidase methods. the 5-HT1A, 1B and 1D receptors were expressed differentially in VN. Fine varicose axons in the periventricular plexus (PP) showed intense 5-HT1A receptor expression in medial VN (MVN) and extended into superior VN (SVN). the PP axons did not express 5-HT1B receptors. Rather, 5-HT1B positive somata and processes were dense in rostral MVN, dorsal SVN and ventral nucleus prepositus hypoglossi. Dense expression was restricted to the dorsolateral aspect of caudal MVN; it declined ventrally, laterally and caudally. Only somata and dendrites of some

neurons expressed 5-HT1B receptors in lateral and inferior VN. 5-HT1D receptors appeared as puncta on neuronal somata scattered throughout VN. the MT1 receptors were expressed widely on somata and dendrites throughout VN, while MT2 receptors were expressed by varicose axons in localized regions of SVN and LVN. These studies suggest that 5-HT and MT interactions vary regionally in VN and that 5-HT/MT regulation may contribute to co-morbid migraine, anxiety and balance disorders.

#### **788 Acute and Chronic Compensatory Changes in Contralesional Vestibular Nucleus Following Unilateral Labyrinthectomy in Alert Macaque**

Soroush Sadeghi<sup>1</sup>, Lloyd Minor<sup>2</sup>, Kathleen Cullen<sup>1</sup>

<sup>1</sup>Dept of Physiology, McGill University, <sup>2</sup>Dept of Otolaryngology - Head and Neck Surgery, Johns Hopkins University

Previous studies following unilateral lesions have shown that the sensitivity of contralesional vestibular nuclei (VN) cells decreases acutely and does not recover. While there is less agreement on the changes in resting discharge acutely, chronically all studies show a return to normal values (e.g., Newlands and Perachio 1990, Ris and Godaux 1998, Smith and Curthoys 1988). Nevertheless, there are certain shortcomings in these previous studies. for example, most were conducted on anesthetised rodents and neurons were not characterized in terms of their physiological discharge properties or central projections. Recordings were made from type I position-vestibular-pause (PVP) and vestibular-only (VO) neurons in one rhesus monkey before and after unilateral labyrinthectomy from contralesional VN (days 1-40). Vestibular and neck sensitivities were assessed using 0.5 Hz sinusoidal rotations of the whole body (WBR) and body under head (BUH), respectively. *Resting Discharge*: On days 1 and 2 after lesion, the resting rates were normal for PVP (n=13, 81.42±5.7 vs. 89±12 in normal animals, p=0.3) and VO (n=12, 48.2±6.1 vs. 46.9±6.6, p=0.7) neurons. *Vestibular sensitivities*: the sensitivities of neurons were significantly suppressed at day 1: VOs (~50%) and PVPs (~60%) and increased up to day 40 to ~70% of normal values. *Neck sensitivities*: Acutely ~30% of PVP and VO cells showed modulation in response to BUH rotations, with gains of 0.05-0.2 (spk/s)/(°/s). Notably, this modulation was not always complementary to the vestibular response, so that it resulted in its cancellation during head-on-body rotations in some of the cells. Interestingly, none of the neurons showed sensitivity to BUH rotations after day 14. *Conclusion*: 1) the acute decrease in the sensitivity of type I contralesional PVPs and its recovery later on corresponds with the ~60% acute decrease in the vestibulo-ocular reflex gain and its recovery in one month. 2) Because of the absence of cervico-ocular reflex following unilateral lesions, the neck sensitivities that we saw are not sufficient to produce an eye movement, but they might play a role in restoring the resting discharge of contralesional VN neurons in the acute stage (see also Newlands and Perachio 1991).

This work was supported by the Canadian Institutes of Health Research (CIHR) and NIH R01 DC02390.

## **789 Canal-Otolith Integration in the Vestibuloocular Reflex**

**Kimberly McArthur<sup>1</sup>, J. David Dickman<sup>1</sup>**

<sup>1</sup>*Washington University School of Medicine*

Previous studies indicate that both canal and otolith signals make significant contributions to the vestibuloocular reflex (VOR). In the pigeon (*Columba livia*), we have previously reported that a dynamic otolith signal improves the phase of the rotational VOR during low frequency earth-horizontal axis rotations. In the current study, we continue our examination of otolith contributions to the rotational VOR, using combinations of tilt and translation stimuli to test a simple model of canal-otolith integration. We also report a small but consistent eye movement response component that may constitute the pigeon's translational VOR. We describe its properties and discuss implications for central processing of otolith signals in these animals. *Support contributed by NIH DC006913 & DC007618 and T32 GM008151 Systems & Molecular Neurobiology Training Grant.*

## **790 Dependence of the Vestibulo-Ocular Reflex On Eye Position During Passive Translation**

**Min Wei<sup>1</sup>, Nan Lin<sup>1</sup>, Shawn Newlands<sup>1</sup>**

<sup>1</sup>*University of Texas Medical Branch*

Compensatory eye movements during translational motion maintain visual acuity on the fovea at the expense of image slip on the peripheral retina. The geometry of this stabilization requires the velocity of each eye during motion to scale proportionally to the inverse of target-to-eye distance and the eye position. To investigate which eye positional signal (the proprioceptive information of the ocular plant or the motor corollary discharge) modulates eye movements during the translational motion, monkeys were trained to fixate a near target and moved rightwards or leftwards in darkness. Before motion onset, the target was turned off and monkey's left eye was brought to a new position by micro-stimulating the left abducens nerve while the right eye kept in normal fixation position as a comparison. We found that the translational vestibulo-ocular reflex (TVOR) is unaffected in responses of both eyes when the left eye position is moved by the micro-stimulation. This result suggests that the central corollary discharge or high-level motor command, rather than the proprioceptive information of the ocular plant, is the origin of the positional signal to modulate the TVOR.

This study was supported by funding from NIH R01 – DC006429.

## **791 The 3D Vestibulo-Ocular Reflex: a Comparison Between C57BL6 and TS65DN Mice**

**Americo Migliaccio<sup>1</sup>, Robert Meierhofer<sup>1</sup>, Charles Della Santina<sup>1</sup>, Roger Reeves<sup>1</sup>**

<sup>1</sup>*Johns Hopkins University*

We hypothesize that the known cerebellar Purkinje and granular cell deficiencies of Ts65Dn mice will manifest as abnormal 3-dimensional angular vestibulo-ocular reflex

(3D aVOR) function during head rotations. In monkeys, injury to the cerebellar nodulus or uvula causes a change in the vestibular time constant (Tc) of post-rotatory nystagmus (hor Tc increases, ver/tor Tc decreases). This finding suggests that vestibulo-cerebellar circuits in the nodulus and uvula mediate post-rotatory nystagmus by perseverating vestibular sensory signals for a period longer than that predicted by the cupular time constant alone. This mechanism is known as 'velocity storage'. In mice, however, there is evidence suggesting that the vestibular time constant is shorter than the cupular time constant, thus the mouse aVOR may adopt a form of 'velocity dumping'. We hypothesize that vestibulo-cerebellar input is required to regulate the amount of velocity dumping during the mouse 3D aVOR.

In this study we compared the 3D aVOR of C57Bl6 (n=4) and Ts65Dn (n=3) mice in response to sinusoidal rotations across frequencies ranging from 0.02 to 5Hz (peak velocity 50°/s). Binocular 3D eye position was measured using a video-oculography (VOG) technique we previously described. We calculated the 3D aVOR gain (eye/head velocity) and phase (positive indicates a phase lead) in head coordinates. Across all rotation planes, at frequencies <0.5Hz, the Ts65Dn aVOR gain was ~30% lower than the C57Bl6 mouse (P<0.05), whereas at higher frequencies the gains were similar. Ts65Dn aVOR phase was typically more positive than C57Bl6 phase across frequencies, however, this difference was not statistically significant (P=0.21).

Our data suggest that the vestibular time constant of the Ts65Dn is shorter than the C57Bl6 time constant. This result suggests that in the mouse, vestibulo-cerebellar circuits act to increase the vestibular time constant.

## **792 An Electroanatomical/Neuromorphic Model to Guide Electrode Design for a Multichannel Vestibular Prosthesis**

**Russell Hayden<sup>1</sup>, Susumu Mori<sup>1</sup>, Charles Della Santina<sup>1</sup>**

<sup>1</sup>*Johns Hopkins University*

We developed a multichannel vestibular prosthesis to return semicircular canal function via electrical stimulation of ampullary nerves. The device partially restores the 3D vestibulo-ocular reflex in bilaterally lesioned chinchillas. Increasing stimulation selectivity and electrode-nerve coupling will be key to optimizing *In Vivo* performance.

We created an electroanatomical/neuromorphic (EA/NM) model of the implanted labyrinth to facilitate design of electrodes with optimal selectivity and coupling. *In Situ* electrode location was determined for 4 implanted chinchillas using  $\mu$ CT scans (36  $\mu$ m voxels) which were coregistered to a standard anatomy derived from  $\mu$ MRI scans (30  $\mu$ m voxels) and  $\mu$ CT (12  $\mu$ m voxels) of a normal chinchilla. We used Amira software for segmentation and generation of a tetrahedral mesh and finite element solvers from COMSOL Multiphysics to predict the voltage potential field, which then served as input to a neuromorphic (NM) model of 450 afferent axons in each branch of the vestibular nerve. Each axon was simulated using *spatially extended nonlinear node* models incorporating afterhyperpolarization dynamics into the distal heminode.

EA/NM predictions of relative ampullary nerve activation (and thus eye rotation axis) were compared against an existing model that assumes ampullary nerve activity scales directly with relative axial current densities (RACD). Both models were evaluated against 3D video-oculographic recordings of the 4 implanted chinchillas. Each performed well, predicting eye rotation axes within an error (mean  $\pm$  SD) of  $20 \pm 9^\circ$  (RACD) and  $23 \pm 14^\circ$  (EA/NM). the EA/NM model also allowed investigation of temporal dynamics, revealing a modest performance improvement for pseudo-monophasic biphasic stimuli. *Supported by NIH/NIDCD K08 DC006216 (CCDS).*

### **793 VOR Adaptation to Active Head Impulses**

**Michael Schubert<sup>1</sup>**, Mark Shelhamer<sup>1</sup>, Charles Della Santina<sup>1</sup>

<sup>1</sup>*Johns Hopkins University*

In healthy subjects, the gain of the angular vestibulo-ocular reflex (aVOR) can be increased to a greater amount when the error signal driving the change is gradually increased, compared with an error signal that demands a sudden, large change. We sought to determine whether the same is true in people with unilateral vestibular hypofunction (UVH). Scleral search coil was used to measure horizontal aVOR gains before, during, and after aVOR adaptation in five UVH subjects exposed to an incremental aVOR task (INCR) and a times-2 aVOR task (x2). the training sessions were separated by two weeks and consisted of subjects fixating a visual target during ~300 self-generated (active) transient yaw head impulses. in the INCR paradigm, the target velocity progressively increased by 10% of head velocity until the aVOR gain demand reached 2.0. in the x2 paradigm, the target velocity was equal but opposite head velocity for a constant aVOR gain demand of 2.0. Pre- and post-training aVOR gains were measured in complete darkness for both active and passive head rotations. Active head accelerations ( $784 \pm 311$  deg/sec/sec) were lower than passive head accelerations ( $3402 \pm 527$  d/s/s),  $p = 1.5 \times 10^{-8}$ . Both paradigms elicited increases in aVOR gain during the training compared with baseline; however, only the INCR paradigm led to aVOR gain change for active head impulses at the post training measure ( $n=5$ ,  $18.2 \pm 9.3\%$  vs.  $-5.8 \pm -3.8\%$ ,  $p = 0.001$ ). in contrast, we found mixed results between the two paradigms for increasing aVOR gains to passive head rotations; INCR ( $n=2/5$ , INCR 52% and 20% vs. x2 30% and -6% respectively,  $p < 0.05$ ) and x2 ( $n=2/5$ , 417% and 25% vs. -12% and 14% respectively  $p < 0.05$ ). One individual showed no change in aVOR gain during passive head rotations. Our data indicate incremental error signals are better for aVOR gain adaptation to active head impulses than error signals requiring a large change in the aVOR gain in people with UVH.

### **794 Effect of Vestibular Rehabilitation On Passive Dynamic Visual Acuity**

**Matthew Scherer<sup>1</sup>**, Americo Migliaccio<sup>2</sup>, Michael Schubert<sup>2</sup>

<sup>1</sup>*University of Maryland*, <sup>2</sup>*Johns Hopkins University*

Computerized dynamic visual acuity (DVA) during passive head impulses is a functional measure of gaze stability and has been shown to identify semicircular canal hypofunction. Active DVA has been shown to improve with gaze stabilization exercises. We sought to determine whether DVA during passive head impulses (pDVA) would also improve following vestibular rehabilitation (VR) in patients with unilateral and bilateral vestibular hypofunction. VR consisted of gaze and gait stabilization exercises done as a home exercise program. When DVA improved for active head rotations, the post pDVA measure was administered. We used scleral search coil technique to characterize the angular vestibulo-ocular reflex (aVOR) gain and other eye responses. Mean duration of VR was  $66 \pm 24$  days, over a total of  $5 \pm 1.4$  outpatient visits. Two of three subjects showed improvements in pDVA with a mean reduction of 43% (LogMAR 0.58 to 0.398 and 0.92 to 0.40). However, aVOR gain increased only in the former (0.53 to 0.75,  $p=4.4 \times 10^{-8}$ ). Each subject used compensatory saccades (CS) in the direction of the deficient aVOR for ipsilesional head rotations. Position ( $p = 0.08$ ) and velocity ( $p = 0.07$ ) of the CS trended downward for ipsilesional head impulses. Accelerations of the CS during ipsilesional head impulses were reduced after VR in 2 of 3 subjects (mean  $11389 \pm 7870$  and  $1954 \pm 3161$  respectively,  $p < 0.05$ ). Our data suggest VR can improve DVA during passive head impulses, in some individuals.

### **795 Vergence-Mediated Modulation of the Human Vestibulo-Ocular Reflex During Galvanic Stimulation**

**Americo Migliaccio<sup>1</sup>**, Charles Della Santina<sup>1</sup>, John Carey<sup>1</sup>

<sup>1</sup>*Johns Hopkins University*

Vergence is one of several conditions requiring angular vestibular-ocular reflex (AVOR) gain modulation. an animal study found that the vergence-mediated gain rise of the AVOR was attenuated by 64% when bilateral, anodal currents were delivered to each labyrinth. This finding was interpreted as indicating that gating of irregular afferent inputs (presumably at the level of central vestibular neurons) is responsible for the rapid change in AVOR gain that accompanies near viewing. We sought to determine if there was similar evidence implicating a role for irregular afferents in the vergence-mediated gain rise in the human AVOR. Our study is based upon analysis of the AVOR evoked by head rotations, delivered passively while subjects viewed a near or far target and applying galvanic stimulation via surface electrodes.

We tested 12 subjects during 1-3 sessions each. Vestibular stimuli consisted of passive head rotations from 0.02-4Hz ( $12-25^\circ/s$ ) and head impulses (whole-body [peak~ $15^\circ$ ,  $50^\circ/s$ ,  $350^\circ/s^2$ ] and head-on-body [peak~ $30^\circ$ ,  $150^\circ/s$ ,  $3000^\circ/s^2$ ]). the galvanic stimulus was on for 10s every 20s. All polarity combinations were considered with

emphasis on uni- and bi-lateral anodic inhibition. the average current stimulus was  $5.9 \pm 1.6$  mA (range: 3-9.5mA), vergence angle (during near-viewing) was  $23.6 \pm 6.3^\circ$  and slow phase eye velocity caused by left anode current stimulation (head-fixed) was  $-1.4 \pm 1.1^\circ/\text{s}$ ,  $-0.2 \pm 0.6^\circ/\text{s}$  and  $1.5 \pm 1.4^\circ/\text{s}$  (torsion, vertical, horizontal). Galvanic stimulation did not alter the vergence-mediated AVOR gain across all head rotational frequencies and velocities examined. Nystagmus induced by galvanic stimulation offset the slow-phase baseline during sinusoidal head rotations, but did not affect the VOR gain (eye/head velocity amplitude). We hypothesize that the transmastoid galvanic stimuli did not effectively silence irregular afferents and that external currents of  $\sim 15\text{-}30\text{mA}$  are likely needed to reproduce the animal results.

## **796 Establishment of Primary Vestibular Schwannoma Cultures From Patients with Unilateral**

Hartmut Hahn<sup>1</sup>, Hubert Kalbacher<sup>2</sup>

<sup>1</sup>Dept. of Otorhinolaryngology Head and Neck Surgery, Tübingen Hearing Res. Center, Univ. of Tübingen,

<sup>2</sup>University of Tübingen

Acoustic neuroma is a benign tumor originating from the Schwann cells of the [vestibulocochlear nerve](#). a considerable number of new cases is diagnosed each year with a prevalence of about 1 in 100,000 worldwide. Therapies include conservative treatment, microneurosurgery and gamma knife radiosurgery. the bilateral acoustic neuroma results from genetic mutations in the neurofibromatosis gene (NF2). the cause of unilateral acoustic neuroma is widely unknown. There is a lack of animal models for the study of acoustic neuroma. Cell cultures derived from tumors could therefore be useful to understand signaling pathways causing tumor origin. Schwann cells from unilateral tumors were obtained by an explant technique from tumor surgery autopsies. Immunocytochemistry was used to demonstrate Schwann cell origin of the cultures. Transfection assays were established for targeted interventions *In Vitro* to analyze signaling pathways causing cellular proliferation. We conclude that cells derived from unilateral acoustic neuroma may provide a useful model system for the study of the pathogenesis of the disease.

Support: fortune programme of the University of Tübingen, project no. 1309-0-0

## **797 Effect of Adaptation On Auditory Nerve Response to Electric Stimulation:**

### **Computational Modeling Approach**

Jihwan Woo<sup>1</sup>, Charles Miller<sup>1</sup>, Paul Abbas<sup>2</sup>

<sup>1</sup>Department of Otolaryngology, University of Iowa Hospitals and Clinics, <sup>2</sup>Department of Speech Pathology and Audiology, University of Iowa

Auditory nerve adaptation to electrical stimulation has recently been described (Zhang et al., 2007, JARO) and may be significant to performance with a cochlear prosthesis. the subject of this presentation is the development of a biophysical computational model that incorporates adaptation effects. Our long-term goal is to refine this model so that it will allow us to predict auditory

nerve fiber (ANF) response to a wide range of proposed electric stimuli, something not feasible with real ANFs due to contact-time constraints. Our Hodgkin-Huxley type model incorporates dynamic changes in extracellular potassium that could plausibly lead to changes in ANF resting potential that can give rise to adaptation-like response patterns. of interest to us, therefore, are the parameters that influence extracellular potassium such as initial concentration and rates of change concomitant with neural activity. This presentation will report on the progress of this model development, using data sets obtained from cat ANFs as means of comparisons. the results include descriptions of the effects of adaptation across onset response rate and the function describing recovery from adaptation due to prior excitation. We will also demonstrate responses to more complex stimuli, such as speech-like stimuli. Responses will be described in terms of the interval histogram, spike-rate decrement, Fano factor, and vector strength, as well as stimulus level. Main effects observed to date include level-dependent rate adaptation and temporal features (such as desynchronization) that are modified by the inclusion of adaptation. Indeed, a feature of this model approach is the ability to "turn off" adaptation in order to ascribe features of ANF temporal responses to the property of adaptation. We will also describe how adaptation influences the overall response of an ensemble of simulated fibers.

Supported by NIH grant 5-R01-DC006478 and KRF-2006-352-H00007.

## **798 Temporal Response Properties of Auditory Nerve Fibers to Modulated High Frequency Electric Pulse Trains**

Ning Hu<sup>1</sup>, Charles A. Miller<sup>2</sup>, Paul J. Abbas<sup>2</sup>, Barbara K. Robinson<sup>1</sup>, Ji Hwan Woo<sup>1</sup>

<sup>1</sup>Department of Otolaryngology-HNS, University of Iowa Hospitals and Clinics, <sup>2</sup>Department of Otolaryngology-HNS, Department of Speech Pathology and Audiology, University of Iowa

We have been conducting a series of auditory nerve fiber (ANF) studies to determine how their responses change over the duration of electric pulse-train stimuli. We first examined how spike rate and spike amplitude varied with level, pulse rate, and time (Zhang et al., 2007, JARO) and recently determined how temporal properties (e.g., vector strength, interval statistics) varied across pulse-train duration (Miller et al., 2007, CIAP). This study examined responses of ANF to sinusoidally amplitude modulated (SAM) electric pulse trains. Although Litvak et al. (2001, JASA) have examined steady-state responses to such stimuli, we have been focusing on ANF response changes across the duration of such stimuli. Our general hypothesis is that adaptation and refractory effects will modify SAM pulse-train responses over time intervals similar to the duration of speech tokens. Using acutely deafened cats, the nerve was stimulated using 400 ms long, 5000 pulse/s, trains of current pulses delivered through an intracochlear electrode. This high-rate carrier was modulated by 10, 20, 50, 100, and 500 Hz sinusoids and five modulation depths (0, 5, 10, 20, and 50%). Different stimulus levels were also explored in order to examine dynamic-range effects.

Vector strength (VS) for both the carrier and modulator were measured. Preliminary findings of ongoing work are as follows. VS to the carrier (VSc) underwent relatively small decreases, while VS to the modulator (VSm) underwent large increases, in some cases by almost an order of magnitude. VSm changes were also sensitive to changes in stimulus level, with the largest changes observed for low-level stimuli. As could be predicted, VSm increased with upward changes in modulation depth. Phase delay (analyzed relative to the modulation period) also changed across time, stimulus level, and modulation depth. in some cases, phase increased over time, consistent with an instantaneous decrease in frequency (as represented by spike intervals) over the duration of the pulse train. We are also assessing VS and phase-delay trends as a function of modulation frequency; these data will also be reported. We attribute these temporal changes to the effects of refractoriness and adaptation and suggest that these effects should be incorporated into realistic models of the auditory nerve's response to electric stimuli.

Support provided by the NIH R01-DC006478-02.

### **799 Ih and IKLT Act Synergistically in a Stochastic Hodgkin-Huxley Model of the Auditory Nerve**

**Mohamed Negm<sup>1</sup>, Ian Bruce<sup>1</sup>**

<sup>1</sup>*McMaster University*

Development of an accurate model for mammalian auditory nerve fibers will help in the understanding and improvement of cochlear implant (CI) functionality. Previous studies have shown that the original Hodgkin-Huxley (1952) model (with kinetics adjusted for mammalian body temperature) may be better at describing nodes of Ranvier in auditory nerve fibers than models for other mammalian axon types. However, the HH model is still unable to explain a number of phenomena observed in auditory nerve responses to CI stimulation such as long-term accommodation, adaptation and the time-course of relative refractoriness. Recent physiological investigations of spiral ganglion cells have shown the presence of a number of ion channel types not considered in the previous modeling studies, including low-threshold potassium (IKLT) channels and hyperpolarization-activated cation (Ih) channels. in this study, we looked at the effects of including these channel types in a stochastic HH-model. Simulation results show that inclusion of these channel types can affect membrane properties such as the mean spike threshold and the variability of threshold fluctuations. Moreover, Ih and IKLT exhibit synergistic effects on the membrane behavior, consistent with results found in other cells containing these channel types.

### **800 Factors Affecting Neural Response Telemetry Recordings in the Chronically Stimulated Cat**

**James Fallon<sup>1</sup>, Andrew Wise<sup>1</sup>, Robert Shepherd<sup>1</sup>**

<sup>1</sup>*Bionic Ear Institute*

There is now overwhelming evidence that for the best outcomes in congenitally deaf patients they should receive effective auditory stimulation, via a cochlear implant, as early as possible. However, ensuring effective stimulation in very young patients requires the objective determination of the threshold and maximum comfortable levels of stimulation. to this end, systems to record the electrically evoked compound action potential (ECAP) have been developed, including Neural Response Telemetry (NRT) by Cochlear Ltd. Many factors affect the ability of these systems to record ECAPs, including electrode impedance, electrode location, and evoked auditory brainstem response (EABR) threshold. Two months after neonatal deafening, profoundly deaf cats were implanted with banded multi-channel scalar tympani electrode arrays and received unilateral ES to a restricted section of the basal turn from a Nucleus<sup>®</sup> CI24 cochlear implant and Nucleus<sup>®</sup> ESPrit 3G speech processor. Daily monitoring of the electrode voltage waveforms in response to 100  $\mu$ A stimuli allowed for detailed assessment of electrode impedances. Additionally, Custom Sound EP<sup>®</sup> clinical software and Nucleus<sup>®</sup> Freedom<sup>™</sup> implants and speech processors were used to monitor electrode impedance and record NRT every two weeks. Finally, EABRs were recorded every month. a total of 56 electrodes were implanted in 8 animals, from which it was possible to record EABRs from 49 electrodes (87%) and NRTs from 28 electrodes (50%). When both an EABR and NRT could be recorded from the same electrode there was no significant difference between the threshold for EABR and NRT (Student T-test;  $p = 0.342$ ). for some electrodes ( $n = 21$ ; 37%) it was possible to record an EABR but not an NRT. When compared to electrodes for which it was possible to record both EABRs and NRTs, these electrodes did not have significantly different electrode impedances (Student T-test; Access Resistance:  $p = 0.403$ ; Total Impedance:  $p = 0.705$ ), EABR thresholds (Student T-test;  $p = 0.130$ ) nor were they located within different regions of the cochlear (Chi-square;  $p = 0.720$ ). in no case was it possible to record an NRT but not an EABR. These results indicate that it is possible to record NRTs in only 57% of cases where there is known to be a response, but that electrode impedance, electrode location, and threshold are not contributing factors. Improvements in the ability to objectively determine threshold and maximum comfortable levels of stimulation are still required as they may contribute to an improved clinical performance among subjects implanted at a very young age. Work funded by NIDCD (NO1-DC-3-1005), Garnett Passe and Rodney Williams Memorial Foundation, the Bionic Ear Institute & the Victorian State Government.



### **801 Electrical Field Measurement and Loudness: Estimating the Effective Stimulus for Complex Electrode Configurations**

**Carlo Berenstein<sup>1</sup>, Lucas Mens<sup>1</sup>, Jef Mulder<sup>1</sup>, Filiep Vanpoucke<sup>2</sup>**

<sup>1</sup>*Radboud University Nijmegen Medical Centre, <sup>2</sup>Advanced Bionics*

Complex electrode configurations, such as Bipoles (BP) and Tripoles (TP), using multiple poles inside the cochlea have been investigated as a means to reduce channel interaction compared to monopolar (MP) stimulation. These complex configurations invariably require higher current levels to achieve sufficient loudness growth than a monopole. This study tests whether direct measures of the electrical field created by various stimulus configurations can predict loudness growth for these configurations in individual patients.

We have measured highly accurate intracochlear electrical fields using MP, BP and TP electrode configurations. These fields are specific to each subject. We can show that the measured BP/TP field corresponds accurately to the linear combination of the individual electrical fields generated by each electrode.

We hypothesize that the peak of the BP/TP electrical field is the main determinant for the perceived loudness. Therefore we can make a subject-specific prediction of the BP/TP loudness derived from the MP field measurement. This hypothesis was tested by establishing supra-threshold levels by loudness balancing in an adaptive psychophysical procedure.

Earlier, we found that loudness growth predicted from the electrical fields almost perfectly matched, or strongly deviated the behavioral loudness, a trend that was subject-specific and constant per electrode number across all electrode configurations. This suggested a relation with the location of the electrode array in the cochlea, possibly influenced by the contribution of the near-field component of the electrical field. We will show the results of a more in-depth analysis to validate these findings.

This method may provide fundamental insight in the electrical stimulation of the auditory nerve or more practically, a valuable predictor for fitting complex electrode configurations, enabling the adoption of these configurations in future clinical practice.

### **802 Excitation Patterns for Physical Electrode and Simultaneous Dual-Electrode Stimulation Measured Using Neural Response Imaging (NRI)**

**Aniket Saoji<sup>1</sup>, Leonid Litvak<sup>1</sup>**

<sup>1</sup>*Advanced Bionics*

In a cochlear implant (CI), an intra-cochlear electrode array is used to stimulate the auditory neurons. In addition to delivering stimulation to the physical electrodes, simultaneous dual-electrode stimulation can be used to generate intermediate pitches between two adjacent electrodes. However, it is unclear if the peripheral neural excitation produced by simultaneous dual-electrode stimulation is similar to excitation patterns produced by stimulating the physical electrodes.

In this study, a modified masker-probe paradigm (Abbas et al., 2004, *Audiol Neuro Otol.* 9, 203-213) was used to assess the spread of excitation produced by physical electrode and simultaneous dual-electrode stimulation in four Advanced Bionics CI users. The masker was a single biphasic pulse (32  $\mu$ s/phase) presented on either electrode EL, or simultaneously on EL-1 and EL+1. Intracochlear evoked responses elicited by probes delivered to either EL-2, EL, EL+1, EL+2, or EL+4 were recorded on Electrodes EL-1 and EL+3 using NRI. The loudness level ( $\mu$ A) of the probe was balanced to the masker level which was set at the most comfortable level. The masker-probe interval was 500 msec.

For these four CI users, evoked response measurements revealed similar patterns of peripheral excitation for physical electrode and simultaneous dual-electrode stimulation. Both conditions exhibited a peak near the middle electrode (EL), and the peaks were of comparable width. However, substantial variability was observed in the spread of excitation produced by physical electrode and simultaneous dual-electrode stimulation across the four CI listeners.

### **803 Fast Recovery Amplifier for Multichannel Neural Recording Using High Rate Electrical Stimulation**

**Matthew Schoenecker<sup>1</sup>, Olga Stakhovskaya<sup>1</sup>, Russell Snyder<sup>1</sup>, Ben Bonham<sup>1</sup>, Patricia Leake<sup>1</sup>**

<sup>1</sup>*University of California San Francisco*

In neurophysiological studies of neural prostheses, it is often desirable to measure neural responses to electrical pulse trains at relatively high carrier rates. However, long amplifier recovery times following electrical artifacts typically limit usable carrier frequencies to a few hundred pulses per second (pps), especially for monopolar stimulation. We have developed a fast-recovery recording system that can be used to record central responses to intracochlear stimuli at carrier rates above 1000 pps. The amplifier is relatively simple and is designed to be a component in an implantable multichannel recording device.

We successfully validated function of the system by recording data from the central nucleus of the inferior colliculus (ICC) in anesthetized guinea pigs while stimulating the cochlea with unmodulated or sinusoidally amplitude-modulated pulse trains. We recorded data from multiple locations in the guinea pig ICC while applying monopolar intracochlear electrical stimuli at 1000 pps. After artifact removal, regions of the ICC with appropriate tonotopic tuning showed evoked neural activity while other regions showed no evoked activity despite comparable or larger stimulus artifacts. Comparison of pre- and postmortem data confirm that the waveforms are of biological origin and not merely electrical artifacts.

To highlight a potential application for this system, we measured threshold vs. depth functions (spatial tuning curves) for sustained responses to 1000-pps pulse trains. We also measured the modulation index of responses to these same pulse trains amplitude-modulated at 100 Hz.

The system presented here will enable us to study interactions among multiple cochlear implant channels



during interleaved stimulation at relatively high rates. Furthermore, the system is simple to implement and may be useful in a variety of multichannel recording devices, both for neuroprosthesis and basic neuroscience applications.

Supported by NIH-NIDCD Contract N01-3-DC-1006.

## **[804] A Frequency Position Function for Cochlear Implants**

**Daniel Taft<sup>1</sup>**, David Grayden<sup>1</sup>, Anthony Burkitt<sup>2</sup>

<sup>1</sup>The University of Melbourne, <sup>2</sup>The Bionic Ear Institute

Greenwood's equation [1] specifies frequency as a function of position on the cochlear basilar membrane. However this does not readily apply to cochlear implants, which bypass the organ of Corti (OC) and stimulate spiral ganglion (SG) cell somata directly in Rosenthal's canal. These auditory neurons would normally have received acoustic input from dendrites radiating from the modiolus apically to a point of lower characteristic frequency.

Investigating this discrepancy is of interest since cochlear implants primarily exploit the place coding of pitch. Fiber trajectories in surface preparations of human cadaveric cochleae have been used to derive SG position as a function of OC position [2]. This suggests a correction could be applied to the position variable in Greenwood's equation, adapting it for cochlear implants. the assumption, however, is that the array's current path predictably targets neighboring SG cells.

This study sought to validate the OC-SG histology equation [2] with psychophysical data. Cochlear implant recipients were sought with residual hearing in their non-implanted ear (70 dB HL thresholds, 250 Hz up to 1 kHz). a pitch-matching procedure was used, where subjects manually adjust the frequency of a pure tone to match the pitch of an electric pulse train (monopolar mode). the resulting data was compared to predicted values based on X-ray derived electrode OC position, corrected for SG stimulation before calculating Greenwood's frequency.

We found that the OC-SG correction improves Greenwood's equation for cochlear implants. Mean squared error was reduced by 89% (n=4). We also confirm an overall linear electrode-pitch relationship [3] for apical electrodes in Nucleus implants. Whereas Greenwood's equation always overestimated the perceived pitch for each electrode, the SG-OC correction removed this bias. However, the characteristic frequency associated with electrically stimulated neurons cannot yet be reliably predicted in individual subjects.

[1] Greenwood, D. D. "A Cochlear Frequency-Position Function for Several Species - 29 Years Later.", JASA, 87, 1990.

[2] Sridhar, D., O. Stakhovskaya, O., Leake, P. A., "A Frequency-Position Function for the Human Cochlear Spiral Ganglion." Audiol Neurotol, 11, 2006.

[3] Baumann, U. and Nobbe, A. "The cochlear implant electrode-pitch function." Hear Res, 213, 2006.

## **[805] Frequency-Place Mapping and Speech Intelligibility: Implications for a Cochlear Implant Localization Strategy**

**Piotr Majdak<sup>1</sup>**, Matthew Goupell<sup>1</sup>, Bernhard Laback<sup>1</sup>, Wolf-Dieter Baumgartner<sup>2</sup>

<sup>1</sup>Austrian Academy of Sciences, <sup>2</sup>Vienna General Hospital

The effect of the frequency-place mapping on speech intelligibility was investigated in seven cochlear implant (CI) and six normal hearing listeners. in the first experiment the Oldenburger sentence test was used to test acute speech intelligibility in quiet and at several different signal-to-noise ratios (SNR). the upper frequency boundary (M) and the number of electrodes or channels (N) were varied systematically including both "matched" frequency-place conditions (M = N) and "unmatched" frequency-place conditions (M ≠ N). the lower frequency boundary of the speech was always fixed while the upper frequency boundary was varied. in a second experiment the perceptual learning of three conditions was investigated.

The data show that for the matched conditions the number of channels can be decreased from twelve to eight or ten (depending on the SNR) without significantly affecting the speech intelligibility. It was also found that for the unmatched conditions speech intelligibility was insensitive to small spectral changes (±0.77 octaves for the most basal electrode). Generally, four different frequency-place mappings were found to provide similar speech understanding as the clinical CI mapping. the results of the learning experiment show that the subjects could learn expanded and matched maps but not compressed.

The results have implications for new stimulation strategies for CI listeners. a sound localization strategy requires an implementation of both interaural cues (for horizontal plane localization) and spectral cues (for vertical plane localization). Overlapping the spectral cues with the normal speech spectrum might be detrimental to speech understanding in CIs. the results indicate that it would be possible to provide additional spatial information in future stimulation strategies for CI listeners without significant degradation of the speech perception.

Supported by the Austrian Science Fund, FWF, project number P18401-B15.

## **[806] A Novel Cochlear Implant Coating Attracts Neurons**

**Jennifer a Chikar<sup>1</sup>**, Jeffrey L Hendricks<sup>1</sup>, David C Martin<sup>1</sup>, Bryan E Pfingst<sup>1</sup>, Yehoash Raphael<sup>1</sup>

<sup>1</sup>University of Michigan

The peripheral processes and cell bodies of the auditory nerve often degenerate following damage to cochlear hair cells. It is possible to promote survival of the nerve after hair cell loss by introducing neurotrophic factors into the cochlea. Supporting the survival of ganglion cell bodies has been shown to decrease thresholds for cochlear implant stimulation; however, the cell body remains relatively far from the stimulation source. Decreasing the distance between the nerve and the implant may provide a further reduction in thresholds and an increased number of independent channels. in the current study we assessed

the feasibility of attracting auditory nerve fibers onto the cochlear-implant electrodes in vivo. We used an implant coated with a hydrogel to provide an extracellular matrix around the implant, a conducting polymer poly(3,4-ethylenedioxythiophene) (PEDOT) to extend the effective area of the electrodes, and a growth factor to act as a chemoattractant for neuronal growth. Guinea pigs were deafened and implanted with either a bare or a coated implant, and sacrificed 7 to 28 days later. the implant remained within the cochlea during tissue processing, allowing visualization of the relationship between neurite growth and the implant. Using neurofilament stain and fluorescence stereoscopy, we observed nerve fibers growing in the direction of the implant within the scala tympani of cochleae that received a coated implant. We did not observe any nerve fibers in the scala tympani of cochleae that received a bare implant. Supporting data for the tropic effects of this implant coating are being collected by culturing ganglion cell explants in the presence of the coating. These data indicate that it is possible to support nerve processes growth within the scala tympani and that this cochlear implant coating can specifically attract this growth. Supported by the Williams Professorship, NIH/NIDCD Grants F31-DC009134, T32-DC00011, P30-DC05188 and Biotectix LLC.

### **807 Effect of BDNF and Electrical Stimulation On the Size and Number of Spiral Ganglion Cells**

**Olga Stakhovskaya<sup>1</sup>**, Gary Hradek<sup>1</sup>, Alexander Hetherington<sup>1</sup>, Patricia Leake<sup>1</sup>

<sup>1</sup>*University of California San Francisco*

The postnatal development and ongoing survival of spiral ganglion (SG) neurons are dependent upon both neural activity and neurotrophic (NT) factors expressed by SG neurons and supporting cells. We have demonstrated in previous studies that electrical stimulation promotes SG survival *In Vivo* in animals deafened early in life; however, SG density was still significantly below normal. in the present study we explored the combined effect of electrical stimulation and administration of the neurotrophic factor (BDNF) in cats. Kittens were deafened at 30 days of age by systemic administration of neomycin. After deafness was confirmed, an intracochlear electrode was inserted with an attached osmotic pump, which infused BDNF throughout the entire period of electrical stimulation (6-13 weeks).

Previously, we analyzed the effects of electrical stimulation using an area fraction method, which allows unbiased measurement of the area of the Rosenthal's canal occupied by the neurons. Measurements of cell size showed little or no difference in the cell size between deafened and stimulated ears, leaving an increase in cell number as the major factor underlying the observed differences in area fraction. Combined administration of BDNF and electrical stimulation promoted a marked increase in SG cell size, preventing the reduction in cell size caused by deafness in the non-implanted ears. Due to the resulting significant difference in SG cell size, a new method (physical disector) was required to estimate the number of surviving SG cells. Results showed a significant

effect of the BDNF in the basal part of the cochlea with considerably smaller or no difference in cell number in more apical regions. Data will also be compared with cell number estimations determined with several different methods that have been applied previously in the literature to evaluate cell numbers when a significant difference in cell size has been observed.

Work supported by NIDCD Contract N01-DC-3-1006.

### **808 Effect of Instrument Timbre on Cochlear Implant Listeners' Music Perception**

**John Galvin<sup>1</sup>**, Qian-jie Fu<sup>1</sup>

<sup>1</sup>*House Ear Institute*

Different musical instruments exhibit different acoustic properties ("timbre"), even for the same fundamental frequency. for cochlear implant (CI) users, musical pitch perception may be influenced by instrument timbre, due to interactions with CI signal processing (e.g., frequency-to-electrode mapping, compression settings, etc.) and patients' functional auditory resolution (e.g., spectral resolution, pitch range, modulation sensitivity, etc.). in the present study, we measured the effect of instrument timbre on CI users' melodic contour identification [or MCI; method described in Galvin and Fu (2007), *Ear and Hearing* 28(3): 302-319]. in Experiment 1, MCI was measured using samples of 7 instruments (3-tone complex, clarinet, glockenspiel, organ, piano, trumpet, violin). Results for 8 CI subjects showed that instrument timbre significantly affected MCI performance. There was great inter-subject variability in terms of the size of timbre effects, as well as instrument preference; musical experience before and after implantation seemed to play a strong role in performance. in general, subjects performed best with the 3-tone complex and the organ, and worst with the piano. Experiment 2, the effect of MCI training was studied in 4 CI subjects, using methods described in Galvin and Fu (2007). After training with only the piano samples, CI subjects' MCI performance across instruments significantly improved after training. These results indicate that instrument timbre may affect CI users' melodic pitch perception; CI signal processing may be better optimized to improve pitch perception with different instruments (e.g., alternate frequency allocations, "simplification" of the music input, etc.). the results also suggest that music experience and training may allow CI users to better extract musical pitch from a variety of instrument sources, even with the limited spectro-temporal resolution provided by the implant device.

### **809 Cochlear Implant-Mediated Perception of Non-Linguistic Sounds**

**Yell Inverso<sup>1</sup>**, Charles Limb<sup>2</sup>

<sup>1</sup>*Gallaudet University/PCO School of Audiology/Johns Hopkins*, <sup>2</sup>*Johns Hopkins Medical Institutions*

The overwhelming majority of test measures to assess cochlear implant (CI) candidacy, efficacy, and progress are based on speech perception. Non-linguistic sounds (NLS), by comparison, have received comparatively little attention, despite their importance for daily living and environmental sound awareness. We tested 22

postlingually-deafened cochlear implant users (mean age  $59.4 \pm 10$  years) at the Johns Hopkins Listening Center in Baltimore, MD using a Non-Linguistic Sounds Test (NLST) that was developed for this study. the NLST consists of 50 non-linguistic sound tokens distributed over five categories (animal, human non-speech, mechanical/alerting, nature, and musical instruments). Prior to testing in CI users, the NLST was presented to ten normal hearing individuals, and any tokens not properly identified were excluded from the test. to account for the potentially wide range of performance in the CI population, the NLST contains both closed-set (category identification) and open-set (token identification) features. CI subjects were asked to identify the source of the presented stimuli, as well as the proper category from the above five choices. Results indicated overall poor performance of CI users to recognize NLS ( $49\% \pm 13.5$  identification of NLS,  $71\% \pm 11.5$  categorization) as compared with speech perception measures ( $88\% \pm 22.8$  HINT). an overall score of less than 50% correct identification was obtained across all five categories inspected. Furthermore, a significant association between speech perception and accuracy of NLS was identified ( $p < .05$ ). the results suggest that NLS is a difficult category of complex sound for CI users to perceive, and should receive greater attention during post-implant rehabilitation. the NLST may be a useful clinical test to measure CI performance and progress, particularly in patients for whom language acquisition remains problematic.

#### **[810] Hybrid and Long-Electrode Implant Users Show Similar Changes in Speech Recognition Performance As the Number of Active Electrodes is Varied**

**Lina Reiss<sup>1</sup>, Christopher Turner<sup>1</sup>, Sue Karsten<sup>1</sup>, Sheryl Erenberg<sup>1</sup>, Bruce Gantz<sup>1</sup>**

<sup>1</sup>University of Iowa

The Hybrid (short-electrode) cochlear implant is designed to provide high-frequency information while preserving residual low-frequency acoustic hearing. One question of interest is whether the current Hybrid device, with just 6 electrodes along the apical 4 mm length of a 10 mm array, is sufficient for speech recognition in the cases where significant residual hearing is lost. If not, would increasing the number of channels or device length improve performance with the Hybrid alone?

We compared consonant recognition using the implant alone in 8 Hybrid subjects and 2 long-electrode subjects. Hybrid subjects were tested with a speech processor providing 6, 5, 4, 3, 2, or 1 channels (active electrodes) over a frequency range of 1063-7938 Hz. Long-electrode subjects with an equivalent internal device (N24) were tested with 22, 8, 6, 5, 4, 3, 2, or 1 channels over a frequency range of 188-7938 Hz. Both groups were tested in quiet and in background noise at 0 dB SNR.

On average, Hybrid subjects benefited from no more than 3 channels. However, when the results were broken down by peak score, the best users with peak scores of 60-70% peaked at 4 channels in both quiet and 0 dB SNR. the two long-electrode users (good performers relative to the

overall pool with peak scores of 50-60%) showed similar results to Hybrids, and are consistent with previous studies of long-electrode users (Shannon et al., 1995; Fu et al., 1998; Friesen et al., 2001). Hence, the Hybrid device shows a better channel benefit/length ratio of 3-4 channels/4mm compared to 4-5 channels/14.5mm for the long electrode device. Therefore, electrode interactions may not be the major limiting factor for channel benefit, at least for consonant recognition and with the N24 device.

Funding for this research was provided by NIDCD grants RO1DC000377 and 2P50 DC00242 and GCRC/NCRR grant RR00059.

#### **[811] Perception of Speech and Environmental Sounds by Normal Hearing Listeners and Cochlear Implant Users**

**Jeremy Loebach<sup>1</sup>, Tessa Bent<sup>1</sup>, Nathan Peterson<sup>2</sup>, Marcia Hay-McCutcheon<sup>2</sup>, David Pisoni<sup>1</sup>**

<sup>1</sup>Indiana University Bloomington, <sup>2</sup>Indiana University School of Medicine

Over the past decade, research utilizing cochlear implant (CI) simulations in normal hearing (NH) listeners has become increasingly common. Although previous research has demonstrated that the closed-set recognition of consonants and vowels is comparable for CI users and NH subjects listening to 6-channel vocoded versions of the stimuli (Dorman & Loizou, 1998), the validity of the vocoder as a model for cochlear implants has not been sufficiently tested. the present study assessed the open-set recognition of speech (words, meaningful sentences and anomalous sentences) and environmental sounds in postlingually deafened CI users and compared their performance with NH subjects listening to 8-channel sinewave vocoded versions of the stimuli. Although wide variability was observed among CI users, on average they performed comparably to NH subjects on the open-set recognition of isolated words and meaningful sentences. However, CI users performed more poorly than NH listeners on the open-set recognition of anomalous sentences and environmental sounds. Since both anomalous sentences and environmental sounds showed significant benefits from training in the NH listeners, these data suggest that additional training for CI users may improve their performance on these materials. Moreover, training with anomalous sentences may enhance the flexibility of cognitive resources that mediate sentence processing, providing an additional benefit when listening to speech in noise. Additionally, training on environmental sounds may help to focus the listener's attention on important spectro-temporal information in the signal providing an additional benefit for speech recognition in noise. Taken together, these findings suggest that acoustic models of cochlear implants using sinewave vocoders provide accurate estimates of the performance of postlingually deafened CI users.

Research supported by NIH-NIDCD grants T32-DC00012 and R01-DC00111.

## **812 The Relationship Between Electrically Evoked Compound Action Potential and Speech Perception in Hybrid Cochlear Implant Users**

**Jae-Ryong Kim**<sup>1</sup>, Paul Abbas<sup>2</sup>, Christine Etler<sup>1</sup>, Sara O'Brien<sup>1</sup>, Carolyn Brown<sup>2</sup>

<sup>1</sup>*Department of Otolaryngology-Head and Neck Surgery, University of Iowa Hospitals and Clinics,* <sup>2</sup>*Department of Speech Pathology and Audiology, University of Iowa, Iowa city, IA, 52246, USA*

Several studies have examined the relationship between physiological and/or psychophysical measures and auditory nerve survival in animal subjects. Some have shown a relationship between the growth of response and nerve survival. More recently, Prado-Guitierrez et al. (2006) showed a relationship between the current differences using two inter-phase gaps (IPGs) and nerve survival. One may hypothesize that nerve survival in a cochlear implant may be related to the effectiveness of the implant and consequently to individual scores on speech perception tests. Studies relating physiological measures such as ECAP and EABR threshold and growth have not shown clear relationships to speech perception abilities.

We revisited this question in users of the Nucleus hybrid implant. Our hypothesis was that with a short electrode array, there would be more uniformity in the response properties across electrodes within an individual. In that way, there might be more across subject differences and physiological measures may better characterize the individual subject. We measured ECAP growth functions to biphasic pulses with two IPGs in twelve hybrid implant users. We then calculated 1) the current difference (the change in current level required to record ECAPs with the same amplitude) using two IPGs of 8 and 45  $\mu$ s, and 2) the slope of the growth function. For each subject, these measures were compared with performance on tests of word recognition.

The current differences using two IPGs showed no correlation with results of word recognition test. In contrast, relatively strong correlations ( $r=0.7822$ ) have been found between the slope of ECAP growth functions and performance on word recognition test.

Effectiveness of the hybrid implant can be quite variable. These results show that ECAP measures may be useful in developing a test to predict outcomes with the implant.

## **813 Integration of Fundamental Frequency and Duration Cues in Lexical Tone Recognition by Cochlear Implant Recipients and Listeners with Normal Hearing**

**Shu-Chen Peng**<sup>1</sup>, Ryan Yung-Song Lin<sup>2</sup>, Monita Chatterjee<sup>1</sup>

<sup>1</sup>*University of Maryland -- College Park,* <sup>2</sup>*Chi-Mei Medical Center, Taipei Medical School*

This study examined the integration of multiple sources of acoustic cues in lexical tone recognition by prelingually deafened, pediatric cochlear implant (CI) recipients, as well as their normal-hearing (NH) peers listening to spectrally and temporally degraded stimuli. Acoustic cues

for lexical tones, including fundamental frequency and duration patterns were manipulated orthogonally between the high level tone (Tone 1) and the high-falling tone (Tone 4) of a disyllabic word, *yan-jing*. In a single-interval, two-alternative forced-choice task, CI and NH participants identified whether each stimulus sounded like *yan3-jing1* ("eye") or *yan3-jing4* ("eyeglasses") with the unprocessed stimuli. Each NH listener also identified stimuli that were noise-vocoded. Consistent with previous findings with speech intonation recognition by CI and NH native speakers of American English, the preliminary results indicated that: (a) CI listeners' weighting of fundamental frequency was less pronounced than that of NH listeners; (b) unlike NH listeners who showed little reliance upon the duration cues in identifying unprocessed stimuli, CI users demonstrated systematic utilization of duration cues in identifying the same set of stimuli; and (c) with noise-vocoded (spectrally and temporally degraded) stimuli, NH listeners' identification exhibited weighting patterns for duration cues in a way similar to that of CI listeners. Implications for the processing of multi-dimensional acoustic cues for lexical tone and intonation recognition in acoustic and electrical hearing will be discussed. [Supported by Chi-Mei Medical Center Research Foundation & NIDCD-R01DC04786]

## **814 Concurrent Vowel and Tone Recognition in Acoustic and Simulated Electric Hearing**

**Xin Luo**<sup>1</sup>, Qian-Jie Fu<sup>1</sup>

<sup>1</sup>*Department of Auditory Implants and Perception, House Ear Institute*

Fundamental frequency (F0) cues are important for tonal languages, as well as for segregating competing talkers. The present study investigated normal hearing listeners' ability to recognize concurrent Chinese vowels and tones. Four Chinese vowels (/a/, /u/, /i/, /e/), each produced by a male and a female talker according to four lexical tones, were duration- and amplitude-normalized. The concurrent syllables were constructed by summing two single-vowel syllables from the male and female talkers (male-female condition) or from the same male talker (male-male condition). Subjects were tested while listening to the original, unprocessed speech, as well as speech processed by 4- and 8-channel acoustic cochlear implant (CI) simulations. Concurrent syllable recognition was measured using a 16-alternative, forced-choice paradigm. Subjects were asked to identify the two syllables, and responses were scored as the percentage that both syllables, vowels, or tones were correctly identified. The results showed that syllable, vowel, and tone recognition significantly worsened with the 4- or 8-channel CI simulations, but was not significantly different between the male-female and male-male talker conditions. With the CI simulations, tone and syllable recognition was significantly better when the tones of the two syllables were the same; vowel recognition was not significantly affected by the tone pairs. Vowel and syllable recognition was significantly better for some vowel pairs (e.g., /u/-/u/) than for others (e.g., /a/-/u/), while tone recognition was not significantly affected by the vowel pairs. These results suggest that CI

speech processing strongly limits listeners' ability to segregate concurrent vowels and tones. Differences in F0 between the two talkers, and differences in the F0 contours between the two syllables did not aid in source segregation, most likely due to the weak F0 coding in the CI simulations.

### **815 Loudness Adaptation Occurs with Modulated Stimuli**

David Landsberger<sup>1</sup>, Robert Shannon<sup>1</sup>

<sup>1</sup>House Ear Institute

It is well known that when a fixed-level stimulus is presented electrically for several seconds, the perceived loudness of the signal fades. It has been assumed that the fading only occurs when the stimulus is at a fixed-level and that the complicated stimuli of a speech processing strategy prevent the loudness fading. Previous measures of loudness adaptation generally require a subject to report loudness ratings, which are highly subjective.

A quantitative procedure for measuring loudness adaptation was developed using the method of constant stimuli. In each trial, a bipolar stimulus was presented at the apical portion of an electrode array for 30 seconds. After 30 seconds, a 500 ms. fixed-level bipolar pulse train was presented in the medial portion of the electrode array. The subject's task was to report if the 500 ms. tone was louder or quieter than the end of the 30-second tone. The current of the 500 ms. stimulus varied from trial to trial. Using the psychometric function derived from the data, the amount of current required to make the medial stimulus equally loud as the end of the 30-second apical stimulus can be calculated. The 500 ms. medial stimulus with the calculated current was then loudness balanced to a 500 ms. version of the original 30-second stimulus using a double staircase method. If the measured current of the 500 ms. apical stimulus was lower than the current of the original 30-second apical stimulus, then loudness adaptation had occurred.

Results have shown that loudness adaptation is observed in CI patients in most situations. Stimuli that were unmodulated, modulated at 100Hz or with uniform random deviated noise created loudness adaptation. Preliminary data suggests that loudness adaptation also occurs when the modulations are at 10Hz. These results have shown that it is not simply the presence of amplitude modulations that prevents speech processing strategies from providing stimulation that perceptually fades.

### **816 Electrophysiological and Behavioral Indices of Sound Change Detection in Late-Implanted Prelingually Deafened Children**

Elizabeth Dinces<sup>1</sup>, Janie Chobot - Rodd<sup>1</sup>, Sanjay Parikh<sup>1</sup>, Elyse Sussman<sup>1</sup>

<sup>1</sup>Albert Einstein College of Medicine

Nature and advanced clinical technology have provided in the deaf person who receives a cochlear implant (CI) a unique opportunity to explore neural plasticity of the auditory system following sensory deprivation. Scalp-recorded auditory evoked potentials (AEPs) provide a non-invasive measure of cortical brain activity that has been shown to reflect the neurophysiological changes occurring

during cortical maturation in childhood. Although it is optimal to implant children as early as possible, it is not always possible to do so. Therefore, it is important to evaluate the efficacy of implantation at various stages of human development. The purpose of the current study was to determine the time course after implantation that stimulus features (frequency, intensity, and tone duration) can be automatically discriminated by the brain (with no task and without attention focused on the sounds) compared to the time course for active behavioral discrimination demonstrated by subject performance. A longitudinal design was used in which we recorded AEPs in three 11 year-old new CI users with severe to profound congenital deafness the day the implant was turned on (approx. 4 weeks post-surgery), then both behavioral and electrophysiology at one-, three-, and six-months following. We found different outcomes in behavioral and electrophysiological sound-feature processing abilities among the study participants. The best user showed rapid development of neurophysiologic indices of change detection along with improvement in behavioral and real-world auditory skills. In contrast, the AEPs of the poorer CI user indexed only sound onset detection and there was little change in behavioral outcomes. The results provide evidence of rapid neurophysiological changes in some late-implanted users.

### **817 Combined Use of Monopolar and Bipolar Stimulation for Speech Coding in Cochlear Implants**

Joseph Schmutz<sup>1</sup>, Bomjun Kwon<sup>2</sup>

<sup>1</sup>University of Utah School of Medicine, Salt Lake City, UT 84132, <sup>2</sup>Department of Communication Sciences and Disorders, University of Utah, Salt Lake City, UT 84112

In Nucleus 24 or Freedom cochlear implant systems monopolar (MP) stimulation mode is used for speech processing, where current flow is generated between the electrodes inside and outside the cochlea. Bipolar (BP) stimulation uses two electrodes inside the cochlea in proximity, targeting a narrower neural population, and may create a different sound percept from that of MP stimulation. We hypothesized that CI users may receive speech information through BP stimulation that is not conveyed by MP stimulation. By interleaving monopolar and bipolar stimulation nonsimultaneously, we attempted to give implant users a more complete set of information by which they could perceive speech. Because we observed that MP and BP stimulation create different pitch percepts, it was necessary to establish pitch relations between them. Vowel sounds were used for the electrode-frequency adjustment of BP channels. Without a good understanding of the BP pitch space, we explored BP pitches using only a limited range of electrodes (for example, when MP and BP maps were used together in the full range without an adjustment, the intelligibility of vowel sounds was mostly lost). The subjects listened to the word 'heed' in a MP map, plus a few BP channels mostly in the basal range to encode the second formant (F2) information. According to our observation with 5 subjects so far, in order to maintain the vowel identity, a shift in electrode-frequency allocation was necessary in BP

stimulation, by 4 electrodes. for example, if the F2 was represented by MP electrodes E10 through E8, then BP channels (6,8) through (4,6) should be used to produce similar vowel identity. Generally the sound percept of the combined modes of stimulation appeared to be different from that of their usual MP map, and it is to be examined whether this different sound percept leads to an improvement in performance (better speech recognition in quiet and in noise). [Supported by NOHR]

### **818 Learning Effects in Simulated Electric-Acoustic Hearing**

**Christopher A. Brown<sup>1</sup>**, Sid P. Bacon<sup>1</sup>

<sup>1</sup>*Arizona State University*

Individuals with residual hearing restricted to low frequencies are candidates for electric-acoustic stimulation (EAS). When low-frequency acoustic information is added to either real or simulated high-frequency electric stimulation, speech recognition often improves dramatically. Recently, we simulated EAS, and replaced the low-frequency acoustic speech with a tone that was modulated in frequency (fm) to track the target talker's fundamental frequency and in amplitude (am) with the amplitude envelope of the low-pass speech. While the addition of the modulated tone ( $T_{fm/am}$ ) provided significant benefit in speech intelligibility over vocoder only, the level of performance did not reach that observed when low-pass speech was present. On the other hand, pilot data with EAS patients indicated that in some cases, the addition of  $T_{fm/am}$  was as beneficial as the addition of speech in the low-frequency region. We hypothesized that the difference could be due to differences in experience combining higher frequency electric (or simulated electric) stimulation with lower frequency acoustic stimulation. to test this hypothesis, normal-hearing subjects listened to pre-recorded radio broadcasts under simulated EAS (a vocoder with 4 bands between 750 and 5500 Hz combined with 500-Hz low-pass speech) for 1.5 hours per day for three weeks. At weekly intervals, they were tested in three conditions: vocoder only, vocoder plus low-pass speech, and vocoder plus  $T_{fm/am}$ . Performance in vocoder only remained relatively low, whereas performance in vocoder plus low-pass speech was high and showed little change. Interestingly, performance in vocoder plus  $T_{fm/am}$  improved considerably over time, despite the fact that subjects were not exposed to this condition. This suggests that experience combining (simulated) electric stimulation with (low-pass) speech can influence the ability to combine novel acoustic cues in the low-frequency region (e.g.,  $T_{fm/am}$ ) with (simulated) electric stimulation.

### **819 Multidimensional Characterization and Differentiation of Neurons in the Anteroventral Cochlear Nucleus**

**Marei Typlt<sup>1</sup>**, Susanne Dehmel<sup>1</sup>, Bernhard Englitz<sup>2</sup>, Cornelia Kopp-Scheinpflug<sup>1</sup>, Rudolf Rübsamen<sup>1</sup>

<sup>1</sup>*University of Leipzig*, <sup>2</sup>*MPI MIS*

Multiple parallel pathways ascend from the cochlear nucleus. It is generally accepted that the origin of these pathways are distinct groups of neurons which differ in

their physiological properties. Typically, units recorded *In Vivo* are classified according to their peri-stimulus-time-histogram (PSTH), in the anteroventral cochlear nucleus (AVCN) these are primarylike, primarylike notch, and different chopper patterns. Units showing a specific PSTH also share other physiological characteristics, e.g. spontaneous rates, response bandwidth etc. Intracellular labelling of single cells after recording support the idea of a congruence between PSTH-types and morphologically defined neuron types. in the AVCN primary like patterns are attributed to spherical bushy cells, primarylike notch patterns to globular bushy cells, and chopper patterns to stellate or multipolar cells. Still, studies suggesting the respective physio-morphological correlation also report non-consistent cases. Other physiological characteristics like divergent organization of synaptic input and membrane properties might be decisive in determining the units' discharge patterns as well. Thus, a classification based on PSTH exclusively might not be the best choice for.

The present study attempts to classify AVCN units based on a cluster analysis of a multitude of physiological properties. We reappraised the PSTH-classification and searched for alternative ways of grouping AVCN units employing extracellularly recorded *In Vivo* data. Spontaneous rates, frequency tuning curves, responses to pure tones at the characteristic frequency, responses to sinusoidally amplitude modulated stimuli, and signal waveforms were evaluated. Establishing a classification of AVCN units under consideration of a larger breadth of physiological characteristics might help to expose the functional organization of the AVCN and to make out the relevant physiological characteristics identifying neuron types.

### **820 Spike Waveforms in the Anteroventral Cochlear Nucleus Revisited**

**Arkadiusz Stasiak<sup>1</sup>**, Mark Sayles<sup>1</sup>, Ian Winter<sup>1</sup>

<sup>1</sup>*University of Cambridge*

Action potentials recorded extracellularly from the anteroventral cochlear nucleus (AVCN) are often characterised by waveforms with three distinct components; a small, positive going (P) potential that occurs approximately 0.5 ms before the second negative going (A) potential and a third, larger (B) potential (Pfeiffer, 1966, *Science*, 154: 667-668). the initial P component is thought to arise from the large end-bulbs of Held present in the rostral pole of the AVCN and is thus a pre-synaptic potential. the 'A' component is hypothesized to arise from the initial segment (IS) while the third, 'B' component, is thought to arise from the soma-dendritic complex (SD). the presence of a 'P' potential has been associated with units which show a Primary-like temporal adaptation pattern and a Type I receptive field. Some reports, however, show units with a 'P' potential characterised by what appears to be strong inhibition (e.g. Winter and Palmer, 1990, *Hear. Res.*, 44, 161-178; Kopp-Scheinpflug et al., 2002, *J. Neurosci.* 11004-11018). by analysing the 'P' potential and post-synaptic component separately for these units it might be possible to obtain an input-output function for these units (e.g. Kopp-Scheinpflug et al., *Ibid.*). We are

interested in applying this technique to the representation of complex sounds and have begun by recording the shape of spontaneous action potentials from the rostral pole of the AVCN. Recording from units with 'P' potentials in the anaesthetised guinea pig the SD component could be absent in as many as 95% of waveforms, however, the IS component was tightly coupled to the presumed prepotential. in agreement with previous studies, when triggering off the SD component the PSTH shape and receptive field are much altered. in contrast when triggering off the IS component the PSTH shape and receptive fields are Primary-like and type I respectively. It is crucial, therefore, to report the component of the waveform being triggered.

## **821 Temporal Responses of Cochlear Nucleus Units and the Dominance Region of Pitch**

**William Shofner<sup>1</sup>**

<sup>1</sup>*Indiana University*

Iterated rippled noise (IRN) is generated when wideband noise (WBN) is delayed, attenuated and added to the original WBN. the pitch evoked is at the reciprocal of the delay. a spectral dominance region has been described for pitch discrimination of IRN in human listeners (Leek and Summers, 2001 JASA 109:2944) as well as for the discrimination of IRN from WBN in chinchillas (Shofner and Yost, 1997 Hear Res 110:15). These studies indicate that the region most effective in generating the pitch is around the 3rd-5th harmonic peaks of IRN. Physiological correlates of spectral dominance for tone complexes have been described for the frequency following response recorded from humans (Greenberg et al, 1987 Hear Res 25:91) and for auditory-nerve fibers in cats using interspike intervals (Cariani and Delgutte, 1996 J Neurophysiol 76:1717).

In the present study, single unit responses to IRNs and WBN were recorded from the cochlear nucleus of anesthetized chinchillas. IRNs had a fixed delay of 4 ms; the fundamental frequency of these IRNs was 250 Hz (i.e. 1/ 4 ms). Stimuli were presented at 20 dB above threshold, and temporal discharge properties were analyzed using all-order interspike-interval histograms. Responses to IRNs were compared to WBN responses, and differences were quantified using a measure based on the 4th moment of the histogram. Similar to the bandpass filtering used in the above psychophysical studies, unit responses were averaged in one-octave bands centered at best frequencies of  $N/4$  ms, where  $N$  is harmonic number. Averaged responses of chopper/regular units show no indication of a dominance region. Averaged responses of primarylike/prepotential units show a maximum around the 3rd harmonic indicating the existence of a dominance region. the results suggest that, in addition to stellate cells, the contribution of bushy cells in processing pitch-related information should not be ignored.

Supported by NIDCD R01 DC005596

## **822 The Effect of F0 Modulation Rate On the Temporal Representation of the F0 of Complex Sounds in Reverberant Spaces**

**Mark Sayles<sup>1</sup>, Ian Winter<sup>1</sup>**

<sup>1</sup>*University of Cambridge*

Reverberation is known to reduce the intelligibility of speech. the physical effects of reverberation are to smear spectral transitions, and to disrupt temporal envelope periodicity. We have studied the effects of reverberation on the temporal representation of harmonic complex sounds with modulated fundamental frequency (F0) contours from single units in the ventral cochlear nucleus. Stimuli were harmonic complexes containing harmonics 1-20 of an octave wide linear frequency sweep between F0min and F0max. Sweeps were either up-going or down-going, with components summed in either cosine, or alternating sine-cosine phase. F0min was varied between 100 and 400 Hz. Reverberation was added by time-domain convolution with impulse responses recorded in a corridor at source-to-receiver (S-R) distances of .32, .63, 1.25, 2.5, 5, 10m (Courtesy of Tony Watkins). in a subset of units the F0 sweep rate was varied [0, 0.5, 1, 2, 4 oct/s] at S-R distances of .63, 2.5 and 10 m. the interspike-interval distribution as a function of time shows a strong representation of the modulated F0 in the dry condition across BF. in the phase locking range of BFs there is also a strong representation of the fine structure. Increasing S-R distance degraded the representation of F0. Increasing the harmonic spacing decreases the effects of reverberation on the representation of the F0. Higher modulation rates result in greater degradation of the temporal representation of F0. for up-going sweeps the main peak in the summary correlation function is shifted towards lower frequencies, and for down-going sweeps towards higher frequencies with increasing S-R distance. This indicates a response to the indirect sound components in reverberation.

## **823 Spatio-Temporal Representation of the Pitch of Complex Tones in the Auditory Nerve and Cochlear Nucleus**

**Grace Wang<sup>1</sup>, Bertrand Delgutte<sup>2</sup>**

<sup>1</sup>*Department of Electrical Engineering and Computer Science, MIT,* <sup>2</sup>*Eaton Peabody Laboratory, Massachusetts Eye and Ear Infirmary*

Traditional models for pitch processing have relied on either a purely spatial representation based on the tonotopic mapping in the cochlea, or a purely temporal representation dependent on neural phase locking. the cochlear traveling wave also introduces spatio-temporal phase cues to the resolved harmonics of a complex tone that might be used in pitch extraction. in the auditory nerve (AN), these cues are robust with stimulus level and are more consistent with psychophysical data than the traditional rate-place or temporal cues. This study aims to evaluate whether the spatio-temporal cues are extracted in cochlear nucleus (CN) neurons.

Our results are based on single unit recordings from AN fibers and CN neurons in anesthetized cats in response to acoustic stimuli. We used transient complex stimuli



("Huffman sequences") designed to manipulate the relative timing between AN fibers tuned to neighboring frequencies (Carney J Neurophys 64:437). CN neurons were said to be phase-sensitive (PS) if their rate responses changed more with Huffman phase manipulations than did AN fibers at the same stimulus levels. Even though most CN units were not PS, several primary-like-with-notches, onsets, and a few phase-locked low-frequency units were PS in the direction consistent with cross-frequency coincidence detection. the few primary-like and chopper units that were PS tended to be sensitive in the opposite direction.

We also recorded responses of CN units to harmonic complex tones with missing fundamentals. We hypothesized that PS CN neurons would either have rate representations of pitch similar to spatio-temporal representations in the AN, or show an enhancement of the spatio-temporal phase cues. While we found a few units that maintained salient pitch cues at high stimulus levels, there was no obvious correlation between spatio-temporal sensitivity and robust rate cues to pitch.

Supported by an NDSEG fellowship and NIH grants RO1 DC002258 and P30 DC005209.

## **824 Responses of Cochlear Nucleus Neurons to Harmonic and Mistuned Complex Tones**

**Donal Sinex<sup>1</sup>**, Albert Zhou<sup>1</sup>

<sup>1</sup>Utah State University

Responses of chinchilla cochlear nucleus (CN) neurons to single harmonic tones, harmonic tones with mistuned components, and double harmonic tones with different fundamental frequencies were measured. Neurons in the CN exhibited several qualitatively-different discharge patterns in response to these complex tones. in general, primarylike neurons synchronized to a few individual stimulus components, without regard to whether the stimulus was a single harmonic tone, a tone with a mistuned component, or double harmonic tone. Not surprisingly, this pattern was similar to what has been observed in auditory nerve fibers. Chopper neurons tended to respond with the periodicity of simple envelopes produced by interactions between adjacent stimulus components, but they exhibited little or no response synchronized to individual stimulus components. These discharge patterns also did not depend strongly on the type of stimulus presented. in a small subset of CN neurons, double harmonic tones and mistuned tones elicited discharge patterns that were qualitatively different from the same neurons' responses to single harmonic tones. These responses strongly resembled the complex modulated discharge patterns that are observed in a large proportion of neurons in the inferior colliculus (IC). We had previously hypothesized that the distinctive discharge patterns elicited from IC neurons by double and mistuned tones are created in the IC by wideband integration; that hypothesis was not entirely supported by the present results. However, a possible alternative hypothesis, that the complex modulated responses observed in the IC are simply relayed from CN, was also not supported. Supported by DC00341.

## **825 Re-Evaluating Ventral Cochlear Nucleus Chopper Unit Responses to Amplitude-Modulated Tones**

**Jonathan Laudanski<sup>1</sup>**, Stephen Coombes<sup>1</sup>, Alan Palmer<sup>2</sup>, Christian Sumner<sup>2</sup>

<sup>1</sup>School of Mathematical Sciences, University of Nottingham, UK, <sup>2</sup>MRC Institute of Hearing Research, Nottingham, UK

Responses to amplitude-modulated pure tones have been used extensively to assess temporal properties of neurons at all levels of the auditory system. the synchronisation to the modulation frequency has often been quantified by the vector strength, which is based on the distribution of spikes within the period of modulation.

Here we show that a generalised description of temporal responses ("mode-locking", from the theory of forced non-linear systems) applies to the firing of chopper neurons. We demonstrate that, in response to amplitude-modulated tones, even chopper neurons that do not yield high vector strength values, for some stimulus conditions (e.g. 5 spikes per 2 cycles of the modulation period) exhibit complex yet temporally precise discharge patterns. Choppers are often modelled as simple integrate-and-fire neurons. These be analysed using the powerful techniques of non-linear dynamical systems theory, and such analysis of these models predicts mode-locking behaviour. We show that such models can account for the complex temporal of responses in chopper units, can even give good fits to detailed spike timing in individual neurons. These results show that simple measures of temporal coding, such as vector strength, can be misleading. in VCN chopper units vector strength can underestimate the precision of temporal coding. to our knowledge, this is the first time that the higher order temporal codes predicted by mode-locking theory have been observed in real neurons.

## **826 Extraction of Temporal Envelope Information From Spike Times**

**Sharba Bandyopadhyay<sup>1</sup>**, Eric Young<sup>2</sup>

<sup>1</sup>University of Maryland, College Park, <sup>2</sup>Johns Hopkins University, Baltimore

Representation of coding properties of neurons based on spike times, like modulation transfer functions (MTFs), spectro-temporal receptive fields (STRFs) and spike triggered averages (STAs) are biologically useful if the later stage neurons are capable of reading that information. within the above framework, this study investigates coding and extraction of temporal envelope information in responses of dorsal cochlear nucleus (DCN) principal neurons to random temporal shape (RTS) stimuli. Coding of temporal envelopes has been traditionally studied using modulation transfer functions based on vector strength, which provides a representation of a neuron's temporal envelope filtering properties. Recently, a number of studies have used other spike time based distance metrics, namely ones proposed by Van Rossum (VR-metric) and Victor and Purpura (VP-metric) to quantify the information in responses about stimuli based on spike times. Such methods have been rarely applied to the study of coding of temporal envelopes. Both the above metrics

imply a decoder that implements these metrics biologically as a later stage neuron. We compare the performance of the above metrics, with other biologically plausible ways of extracting spike time based information like excitation followed by inhibition and coincidence detection. (Supported by NIH grant DC00115)

## **827 Response-Gain Change in DCN Principal Cells Produced by Somatosensory Inputs**

**Wei-Li Ma<sup>1</sup>**, Eric D. Young<sup>1</sup>

<sup>1</sup>*Johns Hopkins University*

In cat, dorsal cochlear nucleus (DCN) likely serves as the site of integration for complex auditory spectral information and other information including pinna orientation. DCN principal cell basal dendrites receive auditory information via auditory nerve fibers, while the parallel fiber network carries auditory feedback and a variety of other inputs to the apical dendrites. the manner by which these streams of information are integrated, however, is not well understood. Stimulation of one of the input domains, dorsal column somatosensory nucleus (DoCSN), elicits a stereotyped inhibition of DCN principal cell spontaneous activity.

We examined the effect of DoCSN stimulation on principal cell representations of auditory stimuli. Single neuron responses were recorded from decerebrate cat DCN under simultaneous auditory and DoCSN stimulation. Stimuli were 200 repetitions of sound alone interleaved with 200 repetitions of sound plus DoCSN stimulation delivered in a four-pulse paradigm. Acoustic stimuli were 200 ms of tones or broadband noise. Responses were tested against two alternate hypotheses: DoCSN stimulation alters sound driven responses in a 1) subtractive- or 2) divisive-fashion. the first hypothesis suggests that the effect is consistent with standard inhibition while the second hypothesis posits that input from the parallel fiber network mediates increases in somatic conductances, which short excitatory current input to the basal dendrites in a voltage-divider fashion. Both effects are observed although neither hypothesis completely describes the results. This research provides insight into the mechanisms of multisensory integration in DCN.

This research was funded by the 2007 Louise and Alan Reed Grant in Auditory Neuroscience from the NOHR and by NIH grant DC00109.

## **828 Optical Imaging of the Dorsal Cochlear Nucleus Using the Voltage Sensitive Dye, Di-2-ANEPEQ**

**James Kaltenbach<sup>1</sup>**, Frank Licari<sup>1</sup>

<sup>1</sup>*Wayne State University*

Optical imaging, in combination with voltage sensitive dyes, can provide a useful approach to the study of stimulus-driven activity in the auditory system. Thus far, optical imaging of the auditory system has been limited to the auditory cortex. the usefulness of this method for studies of subcortical auditory structures is therefore unknown. This laboratory has been investigating optical

imaging for *In Vivo* studies of the dynamics of stimulus-driven activity in the dorsal cochlear nucleus (DCN) of hamsters. We have employed the voltage sensitive dye, Di-2-ANEPEQ, because it is water soluble and can be applied to surface structures without the toxic effects inherent in the use of most other dyes, which must be dissolved in aromatic solvents. to establish a foundation for future studies, this presentation examines the optical responses of the DCN to simple sounds, such as tones and broadband noise. We varied the parameters of stimulation systematically to establish the relationship of response magnitude to specific stimulus parameters such as frequency, intensity and duration. We also examined the dynamics of the responses to tones modulated in frequency over short time intervals (1-16 sec). Some of the results show that the patterns of responses are very much in line with what is predicted based on the known tonotopic organization of the DCN and the temporal properties of its neurons. Tones typically elicited oval spots or bands of activation that approximated the isofrequency bands of the DCN. Shifts in frequency caused systematic shifts in the locations of the bands. the band of activity was observed to migrate systematically toward the high frequency end of the tonotopic gradient when the stimulus frequency was increased and toward the low frequency end when stimulus frequency was decreased. Other features are more difficult to reconcile with the known properties of DCN neurons. for example, the electrophysiological responses of many DCN neurons show either chopper patterns or buildup patterns that saturate within a few hundred milliseconds of stimulation. in contrast, the optical responses continued to buildup throughout the duration of the stimulus, even when the duration of the stimulus was several seconds. Other distinctions of the optical responses will be compared and contrasted with electrophysiological responses. Representative movies of both steady state and dynamic activation patterns will also be presented. (This work was supported by NIH grant R21 DC006041).

## **829 Effect of MK-801 Treatment On the Induction of Hyperactivity in the Dorsal Cochlear Nucleus by Intense Sound Exposure**

**Michael Criddle<sup>1</sup>**, James Kaltenbach<sup>1</sup>

<sup>1</sup>*Wayne State University*

Numerous lines of evidence support the hypothesis that DCN hyperactivity, characterized by an increase in spontaneous activity, is an important neural correlate of some forms of tinnitus. for example, both tinnitus and DCN hyperactivity develop in animals following intense noise exposure and there is a significant relationship between the behavioral evidence of tinnitus and the degree of hyperactivity in the DCN (Kaltenbach et al., 2004). Moreover, the tonotopic profile of activity and numerous features of its behavior correlate with similar features in psychophysically defined tinnitus in human subjects (Kaltenbach, 2006).The present study was carried out in an effort to explore the mechanism by which hyperactivity emerges in the DCN following intense noise exposure. We

hypothesized that hyperactivity involves plasticity in the NMDA receptor pathway, because the NMDA receptor is found in the superficial layer of the DCN where it affects the activity of fusiform cells, which have been shown previously to be generators of hyperactivity. to test this hypothesis, we examined the effect of blocking NMDA receptors on the level of hyperactivity that develops in the DCN. Comparisons of DCN activity were performed in three groups of hamsters. the first group consisted of animals exposed to intense sound (10 kHz, 115 dB SPL, 4 hrs) while a second group served as unexposed controls. a third group of animals was exposed to sound after being pretreated with the NMDA receptor antagonist, MK-801. the control group received a sham injection of 0.9% saline. All groups were allowed a recovery period of 30-40 days following exposure or control treatment. Each was then studied electrophysiologically by recording levels of spontaneous activity as a function of location along the tonotopic axis of the DCN. the results showed that intense tone exposure caused a significant increase in spontaneous activity in the DCN relative to those in control animals, similar to those observed in previous studies. in contrast, the exposed animals treated with MK-801 displayed a consistent decrease in spontaneous activity across the entire DCN. These findings suggest that NMDA receptor blockade may play an important role in the generation of hyperactivity in the DCN. the possible circuit elements involved in the induction of hyperactivity will be discussed. (This work was supported by R01 DC003258).

### **[830] Auditory Cortex Stimulation to Suppress Tinnitus Related Activity**

**Jinsheng Zhang<sup>1</sup>**, Zhenlong Guan<sup>2</sup>, Virginia Ramachandran<sup>1</sup>, Jonathan Dunford<sup>1</sup>, Michael Seidman<sup>3</sup>, Susan Bowyer<sup>3</sup>, Quan Jiang<sup>3</sup>, Kost Elisevich<sup>3</sup>

<sup>1</sup>Wayne State University, <sup>2</sup>Hebei Normal University, <sup>3</sup>Henry Ford Health System

Auditory cortex stimulation (ACS) through rTMS or direct cortical electrical stimulation has recently been used to treat tinnitus. However, the obtained benefit varies greatly across individual patients and is sometimes short-lived. to improve the efficacy of tinnitus treatment, search has been made for optimal stimulation strategies including selection of effective stimulation sites in the auditory cortex and parameters. However, these efforts are hampered by lack of full understanding of the underlying mechanisms of ACS-induced suppression of tinnitus. We electrically stimulated the primary AC to investigate the modulatory effects of cortical electrical stimulation (CES) on neural activity in the dorsal cochlear nucleus (DCN) and inferior colliculus (IC), where neural correlates of tinnitus have been previously reported. Adult rats and Syrian hamsters previously exposed to a loud sound (16 kHz band noise, 115 dB SPL, 6 hours) were used. Behavioral testing was conducted to evaluate tinnitus and hearing loss. Electrical stimulation and electrophysiology were then performed. a 4-shank, 16-channel NeuroNexus electrode array was inserted in the right primary AC for electrical stimulation. for recording, two 16-channel probes were inserted into the left DCN and right IC, respectively. the stimuli were single charge-balanced biphasic electrical pulses (40  $\mu$ s

wide), delivered at intensities of 0-50  $\mu$ A and at a rate of 100 pps. Our preliminary results from behavioral testing showed that sound exposure induced both tinnitus and hearing loss. Electrophysiological results indicated that CES induced both suppression and excitation of spontaneous firing rates in the DCN and IC. Among the induced responses, there were higher proportion and degree of suppressive than excitatory effects. Such effects were found to be more potent in noise-exposed animals than unexposed controls. the results suggest that stimulation of certain areas of the auditory cortex may cause modulatory effects on tinnitus-related neural activity at the brainstem level.

### **[831] Can the Multi-Channel Surface Microelectrode Distinguish the Cochlear Nucleus in Guinea Pigs?**

**Kiyoshi Oda<sup>1</sup>**, Daisuke Yamauchi<sup>1</sup>, Tetsuaki Kawase<sup>1</sup>, Tosimitsu Kobayashi<sup>1</sup>

<sup>1</sup>Tohoku university

Auditory brainstem implant (ABI) is a prosthesis which directly stimulate the cochlear nucleus to restore the "hearing" in to patients with bilateral deafness due to the cochlear nerve pathology, such as bilateral vestibular schwannomas(neurofibromatosis type2). As for the positioning of the ABI, since the full surface of the cochlear nucleus is not visible, electrophysiological guidance is very important to identify the site of cochlear nucleus and the optimal placement of the ABI device. the auditory potentials in response to the electrical stimulation on the cochlear nucleus using the multi-channel surface microelectrode, in which inter-electrode distance is 100 $\mu$ m, were examined in the guinea pigs. the stimulating electrode was placed on the cochlear nucleus, which was exposed after the partial removal of the temporal bone. Bipolar stimulation of two of these 64 electrode(usually nearest two electrode) was gradually increased up to 3000uA. Even in using the surface bipolar stimulations with this very short separation of two electrodes, the unequivocal waves of electrically evoked auditory brainstem responses(EABR), which increased in amplitude with increasing stimulation current, were constantly derived. It would be suggested that the more precise electrophysiological mapping may be possible –based on the EABR threshold distribution using the bipolar stimulations with very short separation.

Key words: multi-channel surface microelectrode; electrically evoked auditory brainstem responses(EABR); electrophysiological mapping

### **[832] A Morphologic Study of Fluorogold-Labeled Tensor Tympani Motoneurons in Mice**

**Sudeep Mukerji<sup>1</sup>**, M. Christian Brown<sup>1</sup>, Daniel J. Lee<sup>1</sup>

<sup>1</sup>Eaton-Peabody Laboratory, Massachusetts Eye and Ear Infirmary

The tensor tympani is one of two middle ear muscles that regulates the transmission of sound through the middle ear. the number and distribution of tensor tympani motoneurons (TTM) is known for some species but not yet

for mice, despite the mouse becoming a common animal model for hearing research. Compared to larger species, mice are known to have shorter basilar membranes, fewer auditory nerve fibers, and fewer olivocochlear (efferent) neurons. Our hypothesis is that they would also have fewer TTMs. We investigated the number and morphology of TTMs in mice using Flourogold, a retrograde neuronal tracer. After a 7-9 day survival period, a column of labeled TTMs was identified ventral and ventrolateral to the ipsilateral trigeminal nucleus. Incidentally, there was also extensive visceral labeling at the level of the seventh motor nucleus, a finding consistent with earlier work on rats (Spangler et al, 1982). the labeled TTMs exhibited different shapes varying from fusiform, octopus to stellate. They formed sparsely branched, radiating dendrites, some greater than 300 micrometers, that appeared to be longer for those oriented in the medial direction. the number of mouse TTMs from each case (n=9) ranged from 30-90 (mean=56) and the soma size (minor axis) ranged from 12-17 micrometres (mean=15). Compared with studies of TTMs in the cat and rat, mouse TTMs were both smaller and fewer in number. Supported by NIDCD RO1 DC01089, KO8 DC06285, and the Norwegian State Lending Agency

### **833 Ultrastructural Features of Inputs to Tensor Tympani Motoneurons in the Rat**

**Thane E. Benson<sup>1</sup>**, M. Christian Brown<sup>2</sup>, Daniel J. Lee<sup>2</sup>

<sup>1</sup>*Eaton Peabody Laboratory, Massachusetts Eye and Ear Infirmary,* <sup>2</sup>*Department of Otolaryngology and Laryngology, Harvard Medical School*

The tensor tympani (TT) muscle is one of two middle ear muscles that regulate sound transmission through the middle ear. in animals, the TT may contract in response to sound to prevent overstimulation from self-generated vocalization, swallowing and chewing. the central inputs to motoneurons controlling the TT have not been fully identified. in this first study of their ultrastructure, we used electron microscopy to analyze synaptic terminals on TT motoneurons (TTMs) labeled with horseradish peroxidase in rats. Retrogradely labeled TTMs found amidst large axons lateral to the trigeminal nucleus ranged in size from 10 to 22 µm in diameter (minor axis) and varied in the number of dendrites and dendritic orientation. Three were selected for ultrastructural analysis. the percentage of terminal coverage on the soma ranged from 9 to 17%; that on proximal dendrites from 26 to 29%. Inputs on TTMs were categorized by synaptic vesicle size and shape. the three major types were those with 1) large round, 2) small round, or 3) pleomorphic vesicles, and they occurred in a ratio of 1:1.25:1 (n = 53 terminals of which 20 gave rise to one or more synapses). Single examples of other terminal types were also found. the major terminal types on TTMs were morphologically similar to synapses on stapedius motoneurons but were found in more equal proportions (Benson et al, ARO 2007). the relatively high number of pleomorphic terminals suggests significant inhibitory input to TTMs. Dendritic input may be significant to TTM function given a relative paucity of somatic input.

Supported by: NIDCD RO1 DC01089 and KO8 DC06285

### **834 The Role of the Cochlear Root Nucleus in the Modulation of the Acoustic Startle Reflex by Sounds**

**Ricardo Gómez-Nieto<sup>1</sup>**, Nathan Maltezos<sup>1</sup>, Donal G. Sinex<sup>2</sup>, María E. Rubio<sup>1</sup>, Dolores E. López<sup>3</sup>

<sup>1</sup>*University of Connecticut, Department of Psychology and Neurobiology, Storrs, CT 06269-3156,* <sup>2</sup>*Utah State University, Department of Psychology, Logan, UT 84322-2810,* <sup>3</sup>*Universidad de Salamanca, INCYL. 37007 Salamanca, Spain*

Cochlear root neurons (CRNs) play a crucial role in mediating the acoustic startle response in rats. They project directly to the caudal pontine reticular nucleus, eliciting the acoustic startle, but they also receive descending cholinergic inputs from the ventral nucleus of the trapezoid body which may modulate acoustic startle. One prominent acoustic startle modulation is the prepulse inhibition where a weaker stimulus (prepulse) presented prior to the intense stimulus inhibits the subsequent startle response. Several studies have reported that this inhibition occurs in reticulospinal neurons by activation of muscarinic receptors M2 and M4. Here we present electrophysiological and anatomical evidences that this inhibition also occurs at the level of CRNs. We obtained extracellular recordings *In Vivo* from single CRNs to test the effects of auditory prepulses on their neural activity. Our electrophysiological data indicate that CRNs responses are strongly inhibited by auditory prepulses. Furthermore, CRNs responses depended on parameters of the auditory prepulse such as intensity and interpulse interval, showing their strongest inhibition at high intensity level and short interpulse intervals. to determine whether muscarinic receptors were expressed in CRNs, we performed immunocytochemistry at light microscopy. Our data showed that M2 and M4 muscarinic cholinergic receptor types are expressed in the cochlear root nucleus. Collectively, the present findings support the idea that the cochlear root nucleus might be the first interface in the modulation of the acoustic startle reflex by sounds.

Grant sponsors: PROFIT: #CIT-390000-2005-4, #BFU2006-00811and JCyL-FSE: #SA-007C05, to D.E.L; DC00341 from NIDCD to D.G.S.; DC006881 from NIDCD to M.E.R.

### **835 Medial Olivocochlear (MOC) Efferent Acoustic Reflexes in Humans are Widely Tuned and Have Their Biggest Effects At Frequencies Above That of the Eliciting Sound**

**Wattjana Lilaonitkul<sup>1</sup>**, John Guinan, Jr<sup>2</sup>

<sup>1</sup>*Massachusetts Institute of Technology,* <sup>2</sup>*Mass. Eye & Ear Infirmary*

It has been assumed that the MOC acoustic reflex provides negative feedback that is focused narrowly on the frequency region of a sound that elicits the MOC activity. This picture is based on data showing that MOC fibers (1) have V-shaped tuning curves slightly wider than those of auditory-nerve fibers, and (2) project to a cochlear region with a characteristic frequency (CF) similar to the MOC

fiber's CF. to determine if this picture applies under physiologic conditions, we measured sound-elicited MOC effects on stimulus frequency otoacoustic emissions (SFOAEs) in awake humans. SFOAEs were evoked by 40 dB SPL tones near 1 kHz. MOC activity was elicited by tones or by half-octave bands of noise that were ipsilateral, contralateral or binaural (re the test ear), at levels (typically 60 dB SPL) that did not elicit middle-ear-muscle activity as shown by suppressed-SFOAE tests. for SFOAEs near 1 kHz, significant inhibition of SFOAEs was seen with noise bands centered over a five-octave range, with greater effects for noise centered below than above the test frequency, and the greatest effect for contralateral noise bands centered 0.5-1 octave below the test frequency and for ipsilateral or binaural noise bands centered at the test frequency. a similar picture was found for tones except that the response was more skewed with frequencies below the test frequency far more effective than frequencies at, or above, the test frequency. Similar patterns were found for elicitors at lower sound levels, and for ipsilateral, contralateral and binaural elicitors, although when the elicitor was in the ipsilateral ear, the effects were partly obscured by direct elicitor suppression of the SFOAE. the results indicate that the MOC acoustic reflex is not narrowly tuned, and that the greatest MOC effect near 1 kHz is produced by sounds at frequencies lower than 1 kHz. This reflex organization may help overcome the upward spread of masking. (Supported by NIH RO1DC005977 & P30DC005209)

### **[836] Contralateral Sound Evokes Slow Suppression of Ipsilateral Cochlear Responses**

**Erik Larsen<sup>1</sup>**, Charles Liberman<sup>2</sup>

<sup>1</sup>*Speech and Hearing Bioscience and Technology, Harvard-MIT Division of Health Sciences and Technology,*

<sup>2</sup>*Eaton-Peabody Laboratory, Massachusetts Eye & Ear Infirmary*

Activation of medial olivocochlear (MOC) efferents to outer hair cells can suppress cochlear responses on both slow and fast timescales, and the slow effect component has been implicated in protection from acoustic injury. When MOC activity is shock-evoked, slow suppression has an onset time constant of ~10 sec and is seen only in responses to high frequency tones (>10 kHz) [Sridhar et al., J. Neurosci, 15:3667, 1995]. Sound-evoked slow effects from contralateral noise have been reported, however only round window (RW) noise was measured and possible contributions of other feedback systems, e.g. the lateral OC pathway, were not excluded [Lima da Costa et al., J. Neurophysiol. 78:1826, 1997].

Here we examine sound-evoked slow and fast effects in the anesthetized guinea pig. a 5-min epoch of contralateral noise at ~70 dB SPL evokes a slow-onset, slow-offset suppression of ipsilateral CAP, DPOAEs, and RW noise, without a robust fast component. Onset and offset time constants are variable, but mean suppression peaks ~3 min post contra-noise onset. Mean magnitude of this slow effect on response amplitude is 2 dB on CAP, 3 dB on DPOAE and 2 dB on RW noise. Suppression magnitude

decreases markedly with increased ipsilateral stimulus level, as expected for an MOC effect. However, the relatively large RW noise effects are unexpected for the MOC; furthermore, in contrast to shock-evoked slow effects, there is no frequency dependence in effect magnitude in the 4-22 kHz range. Systemic gentamicin reduced the slow suppression, consistent with MOC system involvement. Lack of change in ipsilateral ear-canal sound pressures during the contralateral noise suggests lack of involvement of middle ear muscles and loss of the effect following contralateral cochlear destruction eliminates crosstalk as a possibility. Lesion experiments are in progress to verify the contributions of the OC pathways.

Research supported by grants from the NIDCD: RO1 DC0188 and T32 DC00032.

### **[837] Efferent Modulation of the Responses of Cochlear Nucleus Neurons to Tones in Noise**

**Wilhelmina Mulders<sup>1</sup>**, Donald Robertson<sup>1</sup>

<sup>1</sup>*University of Western Australia*

The detection of salient signals amidst background noise is an important function of the auditory system. Behavioural studies have suggested a role for the medial olivocochlear (MOC) system in this function. This efferent system originates in the brainstem and synapses directly onto the outer hair cells in the cochlea. When the MOC system is activated whilst recording input-output (I/O) functions of auditory primary afferent fibres in a continuous background noise, the result is a decompression of the I/O functions. This process is called unmasking and improves the dynamic range of the fibres. However, it is as yet not known how the unmasking effects observed in the auditory periphery are translated into higher auditory brain centres, where intrinsic circuitry could modulate effects. in this study we have investigated the effects of continuous background noise on responses of different neuron types to pure tones in the ventral cochlear nucleus of guinea pigs, without and with MOC system activation. Results show that the unmasking effects of MOC system activation on tone responses in continuous background noise can still be observed in the cochlear nucleus. These unmasking effects manifest themselves as decompression of input-output functions as well as an improved slope, which results in an improvement in the range of intensity discrimination of the tones. the data show however, that the strength of the unmasking effects of MOC system activation varies between the different neuronal types, which suggests further modulation of the effects by intrinsic circuitry in the cochlear nucleus. Unmasking was not detected in onset chopper neurons, despite its demonstrable presence in other neuronal types in the same animals. These observations firstly show that the neural substrate for unmasking by MOC stimulation is present beyond the primary afferent level. Secondly, the data may reflect the level of involvement of different neuronal types in intensity discrimination.

### **838 Effects of Acute Noise Exposure On Synaptic Activity in the Central Auditory Pathway -A Manganese-Enhanced MRI Study**

**Dietmar Basta<sup>1</sup>, Moritz Groeschel<sup>2</sup>, Susanne Mueller<sup>3</sup>, Romy Goetze<sup>2</sup>, Randolph Klingebiel<sup>3</sup>, Arne Ernst<sup>1</sup>**

<sup>1</sup>University of Berlin, Dept. of ENT at ukb, <sup>2</sup>Inst. of Biology, Humboldt University of Berlin, <sup>3</sup>Charité Medical School Berlin

It is well known that noise exposure besides cochlear hair cell loss leads to profound long term changes within the central auditory pathway. a modified spontaneous activity, changes in neuronal cell density and neurotransmitter action were reported for several central auditory structures. However, it is not possible yet to distinguish between the changes based on the reduced input from the noise-damaged organ of corti (deprivation) and neuronal changes which are directly related to the auditory overstimulation. for understanding the noise induced functional disabilities (reduced speech recognition or discrimination ability), it seems to be highly important to clarify the influence of these two mechanisms.

The time between the noise exposure and the investigation seems to be crucial for central effects. It has been shown that hair cell loss and therefore deafferentation appears slowly in the early days after the treatment. Therefore it should be possible to study direct effects on central structures immediately after an acoustic overstimulation.

To test this hypothesis normal hearing mice were noise-exposed (3h, 115 dB SPL, white band noise 10-20 kHz) under anesthesia. At the end of the treatment a manganese chloride solution was injected intraperitoneally (i.p.). This procedure was earlier described to monitor synaptic activity by using the MRI-technique (replacement of calcium influx by manganese). After the manganese ions reached their highest intracellular level (24 h post injection), 7-Tesla MRI-scanning with a resolution of (100 µm x 100 µm x 150µm) was performed. the signal strength in calibrated images (muscle was used as reference) of the dorsal and the ventral cochlear nucleus, the olivary complex, the inferior colliculus and the medial geniculate body were measured and compared with normal hearing controls (same anesthesia and manganese treatment as in the experimental group).

The noise exposure slightly increased the synaptic activity in all the investigated structures of the auditory pathway. Statistical significant effects could be observed in the dorsal and ventral cochlear nucleus. No changes occurred in the non-auditory control area (periaqueductal gray).

The results demonstrate that acoustic overstimulation influence directly the neuronal network within the central auditory pathway. Acute noise exposure seems to affect more the lower auditory pathway i.e. the cochlear nucleus. Long term effects should be studied to estimate additional effects caused by the loss of cochlear afferent signals.

### **839 Neural Representation of Pitch in the Human Brainstem: Sine Versus Alternating Phase Stimuli**

**Ananthanarayan Krishnan<sup>1</sup>, Christopher Plack<sup>2</sup>**

<sup>1</sup>Purdue University, <sup>2</sup>Lancaster University

Pitch-matching experiments have shown that the pitch of ALT-phase stimuli, relative to SINE-phase stimuli, is the same when the harmonics are resolved and increases by an octave when the harmonics are unresolved. the implication is that when the harmonics are resolved (lower harmonic numbers), the phase relationship between them is irrelevant since the harmonics do not interact significantly in the cochlea. However, when three or more harmonics excite the same place on the BM (i.e., are unresolved), the resulting pattern of vibration will reflect the phase relationship between them. the aim of this study was to see if these differences in pitch for SINE and ALT are reflected in the scalp recorded human frequency following response (FFR). FFRs were recorded from 13 normal-hearing subjects using SINE (F0=90; and 180 Hz) and ALT (F0=90 Hz) stimuli presented monaurally at 80 dB SPL. the seven harmonics of each stimulus was placed in 4 spectral regions (360-900 Hz; 720-1260 Hz; 1080-1620 Hz; and 1440-1980 Hz) and low pass noise was used to eliminate distortion products from contributing to the response. Both spectral and autocorrelation (AC) analysis of the response waveforms showed that for the SINE 90 and 180 stimuli the FFR spectral peaks and autocorrelation peaks corresponded to the F0. for the ALT 90 stimulus, the FFR spectral data and the AC analysis showed clear peaks corresponding to 90 Hz when the stimulus spectral content was restricted to the two lowest regions but the FFR peaks shifted to 180 Hz in response to stimuli whose spectral content was restricted to the two highest frequency regions (1080-1620 Hz and 1440-1980 Hz). These results are strikingly similar to perceptual results and suggest that the human FFR preserves pitch relevant information related to processing of resolved and unresolved components.

### **840 Human Frequency Following Responses to Sinusoidal Amplitude Modulated Tones**

**Ananthanarayan Krishnan<sup>1</sup>, Vidya Ganesh<sup>1</sup>, Jayaganesh Swaminathan<sup>1</sup>**

<sup>1</sup>Purdue University

The temporal modulation transfer function (TMTF) characterizes the threshold of detection as a function of modulation rate and has a characteristic low-pass shape, depicting a decrease in sensitivity to high modulation rates. Previous psychoacoustical experiments have shown a cut-off frequency at around 50 Hz. Physiological experiments have established that the cut-off frequency decreases as we ascend the auditory system, from the auditory nerve (around 1 kHz) to the auditory cortex (around 16 Hz). the objective of this study was to examine the effects of modulation rate and depth of a 4000 Hz sinusoidal amplitude modulated (SAM) tone on the frequency following response (FFR) in subjects with normal hearing. in the first experiment, modulation

frequency was varied from 100 to 800 Hz in steps of 100 Hz. in the second experiment, modulation depth was varied from 0 to 100 %, in steps of 20, keeping the modulation frequency constant at 100 Hz. Preliminary results showed a TMTF with a low-pass shape, with a cut-off frequency around 400 Hz. These estimates based on phase-locked activity in a population of brainstem neurons are much higher in comparison to those obtained from single units in the inferior colliculus in rats, which are around 200 Hz. As expected, the degree of phase locking improves with an increase in the modulation depth, as shown by an increase in the autocorrelation magnitude of the FFR. These results suggest that the FFR may be utilized to evaluate certain aspects of temporal processing in the human brainstem in normal and hearing impaired individuals.

#### **841 Brainstem Frequency Following Responses in Adults Who Stutter**

**Ananthanarayan Krishnan<sup>1</sup>**, Amanda Hampton<sup>1</sup>, Christine Weber-Fox<sup>1</sup>

<sup>1</sup>*Purdue University*

Auditory processing has long been thought to be one of many factors involved in stuttering (Hall & Jerger, 1978; Rosenfield & Jerger, 1984). Previous research of auditory processing in stuttering has examined behavior (Blood, 1996; Kramer, Green, & Guitar, 1987; Toscher & Rupp, 1978; and others) and activity in the cortex (Biermann-Ruben, Salmelin, & Schnitzler, 2005; Morgan, Cranford, & Burk, 1997; Salmelin et al., 1998). the limited research on auditory processing in stuttering using the auditory brainstem response (ABR) has been inconsistent, with some studies finding no differences (Stager, 1990), while others showing differences (Blood & Blood, 1984; Deitrich, Barry, & Parker, 1995) between adults who stutter (AWS) and normally fluent speakers (NFS). The sustained phase-locked neural activity reflected in the human frequency following responses (FFR) provides for a convenient analytic tool to evaluate the ability of the auditory neurons in the rostral brainstem to follow rapid frequency changes over time early in the auditory processing system. Degraded representation at the brainstem level has been correlated with degraded processing at the cortical level. the current study measured the integrity of temporal processing at the level of the brainstem in AWS compared to NFS. AWS and age- and education-matched fluent speakers were presented non-speech sounds synthesized from sine-wave stimuli. FFRs were recorded in response to 8 tonal glides, four up-sweeps and four down-sweeps with the rate of frequency change varied systematically. Preliminary results show that the representation of frequency change is degraded (amplitude reduction as well as poor tracking of the frequency change) in some but not all AWS. These results suggest a brainstem temporal processing disruption which could adversely affect processing at the level of the cortex.

#### **842 Experience-Dependent Enhancement of Pitch Representation in the Brainstem is Not Speech Specific**

**Jayaganesh Swaminathan<sup>1</sup>**, Ananthanarayan Krishnan<sup>1</sup>, Jackson Gandour<sup>1</sup>

<sup>1</sup>*Purdue University*

Neural representation of pitch at the level of the brainstem is influenced by language experience. the aim of this paper is to determine whether this language experience-dependent plasticity for pitch representation in the brainstem is speech specific. Brainstem frequency following responses (FFR) were recorded from Chinese and English participants in response to four Mandarin tonal contours presented in a nonspeech context in the form of iterated rippled noise (IRN). by using iterated rippled noise (IRN) stimuli, we were able to remove any potential confound of lexical-semantic information. IRN stimuli were made up of broad band noise with temporal regularities that can yield a pitch percept. Pitch strength (whole contour, 250ms; 40ms segments) and pitch tracking accuracy (whole contour) were extracted from the FFRs using autocorrelation algorithms. Narrow band spectrograms were used to extract spectral information. Results showed that the Chinese group exhibits stronger pitch representation and smoother pitch tracking than the English group. Moreover, crosslanguage comparisons of pitch strength of individual segments revealed that the Chinese group exhibits relatively more robust pitch representation of those segments containing rapidly-changing pitch. a discriminant analysis of three 40 ms f0 frames at large (level, rising, falling) maximally differentiated on the basis of acceleration suggests that sensitivity of the FFR to rising f0 trajectories is heavily weighted in separating listeners on the basis of language experience. FFR spectral data was complementary showing that the Chinese group exhibits stronger representation of multiple pitch-relevant harmonics relative to the English group across all four tones. These findings support the view that at early preattentive stages of subcortical processing, neural mechanisms underlying pitch representation are shaped by particular features or dimensions of the auditory stream rather than speech per se. Adopting a temporal correlation analysis scheme for pitch encoding, we propose that long-term experience sharpens the tuning characteristics of neurons along the pitch axis with enhanced sensitivity to linguistically relevant, rapidly-changing portions of a pitch contour.

#### **843 Brainstem Evoked Potentials in Lizards**

**Beth Brittan-Powell<sup>1</sup>**, Jakob Christensen-Dalsgaard<sup>2</sup>, Yezhong Tang<sup>1</sup>, Catherine Carr<sup>1</sup>, Robert Dooling<sup>1</sup>

<sup>1</sup>*University of Maryland*, <sup>2</sup>*University of Southern Denmark*

Tokay geckos (*Gekko gecko*) are nocturnal animals found in Southeast Asia and known for their loud vocalizations. This aim of this study was to determine hearing sensitivity in the Tokay gecko and to compare hearing sensitivity of a vocal lizard to a non-vocal lizard, the green anole (*Anolis carolinensis*).

Hearing sensitivity was measured in 5 geckos and 7 anoles using the auditory brainstem response (ABR).



Animals were sedated with isoflurane and ABRs were measured at levels of 1 and 3% isoflurane. Platinum electrodes were inserted just under the skin at the vertex, behind the stimulated ear and grounded at the other side of the head. Responses to brief tone bursts emitted through a coupler sealed over the eardrum were evoked at frequencies between 0.1-10 kHz and intensity levels of 5 to 90 dB SPL.

The typical ABR waveform showed two to three prominent peaks occurring within 6 ms of the stimulus onset. Based on the ABR, geckos and anoles were most sensitive between 1.6-2 kHz and had similar hearing sensitivity up to about 5 kHz (thresholds typically 20-50 dB SPL). Above 5 kHz, anoles were about 20 dB more sensitive than geckos based on ABR thresholds. As far as we know, this is the first comparative study of the ABR in lizards. Generally, absolute thresholds from ABR audiograms were comparable to what has been found in small birds. Best hearing sensitivity, however, extended over a larger frequency range in the lizards than most bird species, with lizards showing better low frequency (below 500 Hz) hearing.

*This work was supported in part by training grant DC-00046 to RJD and by DC-000436 to CEC from the National Institute of Deafness and Communicative Disorders of the National Institutes of Health.*

#### **844 How Secure is the Calyx of Held?**

**Myles Mc Laughlin<sup>1</sup>**, Marcel van der Heijden<sup>1</sup>, Philip Joris<sup>1</sup>

<sup>1</sup>Laboratory of Auditory Neurophysiology, K.U.Leuven, Belgium

The medial nucleus of the trapezoid body (MNTB) plays a key role in the sensitivity of the lateral superior olive (LSO) to interaural level differences, an important cue for sound localization. It receives excitatory input via a giant presynaptic terminal, the calyx of Held, and acts as a sign inverter giving inhibitory input to the LSO. However, a recent study in the gerbil by Kopp-Scheinpflug et al. in 2003 (KS) challenged the view of MNTB as a simple and reliable sign inverter.

Typical extracellular recordings from MNTB neurons show a complex spike (A) consisting of a prepotential (A1) followed by a biphasic action potential (A2). A1 is presumably generated by synaptic currents following a presynaptic spike at the calyx of Held. A2 is a postsynaptic action potential generated by the MNTB neuron triggered by A1. KS observed a second event (B) - a small unipolar potential resembling event A1 in shape, but not followed by A2. They interpreted B as originating from the same structure as A1 and termed it an "isolated prepotential," i.e. a presynaptic event failing to elicit a postsynaptic spike.

We propose an alternative "two-unit" hypothesis, in which A and B reflect the potentials of two uncoupled neurons. Like KS we assume that A is a complex spike generated by an MNTB "unit" i.e. a calyx of Held and its associated MNTB neuron. But we propose that B is a spike arising from a different fiber or neuron and that the resemblance between events B and A1 is fortuitous.

Interspike intervals (ISIs) are critical to distinguish between the two hypotheses. In the one-unit hypothesis events A1

and B arise from one unit and therefore, the ISI between all occurrences of events A1 and B will respect the refractory period (RP). In the two-unit hypothesis A1 and B arise from different neurons and the ISI will not necessarily respect the RP.

Using frequency sweeps at different levels (stimuli similar to those used by KS) we made 147 recordings from 28 units with complex spikes in the MNTB of 5 cats. Using spike sorting techniques we found 22 units (80 recordings) where event B was also present in the recording. Examining the ISI of events A1 and B showed that for 21 units (55 recordings) events A1 and B must arise from separate neurons. We therefore conclude that in the cat MNTB presynaptic action potentials are reliably transmitted through the calyx of Held resulting in a postsynaptic action potential.

Supported by FWO (G.0392.05) and Research Fund KUL (OT/05/57)

#### **845 Efficacy of Transmission At the Giant Synapses of Held *in Vivo***

**Bernhard Englitz<sup>1</sup>**, Sandra Tolnai<sup>2</sup>, Marei Typlt<sup>2</sup>, Cornelia Kopp-Scheinpflug<sup>2</sup>, Juergen Jost<sup>1</sup>, Rudolf Ruebsamen<sup>2</sup>

<sup>1</sup>MPI MIS, <sup>2</sup>University of Leipzig, Institute of Biology II

The giant synapses of Held play an important role in high-fidelity auditory processing and provide a model system for synaptic transmission at central synapses. Recent studies have suggested that signal transmission frequently fails at both synapses under various *In Vitro* and *In Vivo* conditions.

In this study we introduce a novel approach for detecting the incidences of failed transmission *in vivo*. It provides a noise-tolerant, statistical test for the presence of transmission failures by considering the potentials preceding postsynaptic APs. Using simulated recordings its performance could be assessed and it was verified to provide a high level of accuracy in detecting transmission failures.

Applied to *In Vivo* recordings of spontaneous, excited and inhibited/suppressed neuronal discharges, contrasting results were obtained for AVCN spherical bushy cells (SBCs) and MNTB principal cells. In accordance with previous studies of SBCs, failures of AP transmission were detected in a substantial fraction of units, peaking at 80 % for inhibitory/suppressive conditions. In the MNTB, failures were detected in only a small fraction (~5 %) of spontaneous responses and never in the other conditions, contrasting with previous findings. Based on our method's accuracy these results indicate that under the studied conditions (1) transmission in the MNTB fails scarcely and (2) transmission in the AVCN fails to substantial and condition-dependent degrees. The condition-dependence indicates the local action of inhibition, which renders SBCs an interesting system for studying the integration of excitation and inhibition *in vivo*. The present approach should prove instrumental in further studies of transmission at the giant synapses of Held.

## **846 Rapid Maturation of MNTB Neurons Before the Onset of Hearing**

Brian Hoffpauir<sup>1</sup>, George Spirou<sup>1</sup>

<sup>1</sup>WVU School of Medicine, Sensory Neuroscience Research Center

We have previously shown that, in mice, calyces of Held grow rapidly from P2-P4, at which time they can cover 40% of the somatic surface area of the postsynaptic MNTB neurons and produce evoked EPSCs greater than 10 nA. Although most studies describing calyx and MNTB maturation focus on ages around and after the onset of hearing, we hypothesize that MNTB neurons must mature during earlier stages of development to compensate for the rapid growth in synaptic input. To test this, we have measured basic biophysical properties of MNTB neurons in brain slices at near physiological temperatures from P0-P6, P8, and P14. Input resistance values decrease from  $876 \pm 51 \text{ M}\Omega$  to  $320 \pm 49 \text{ M}\Omega$  between P0-P4, then further decrease to  $231 \pm 39 \text{ M}\Omega$  by P14. MNTB cells fire trains of action potentials during single current steps from P0-P3. An increasing fraction of cells transition to the adult-like phenotype until P6, when most cells fire only 1-2 spikes. The resting membrane potential shifts from  $-62.8 \pm 1.3 \text{ mV}$  to  $-72.0 \pm 3.0 \text{ mV}$  over P0-P4, with little change thereafter. Spike amplitudes grow steadily from 25 to 40 mV over P0-P5, and then decrease to 30 mV by P14. Spike rise times and half-widths decrease rapidly from P0-P4 and continue to decline slowly thereafter. The current injection thresholds for action potential generation gradually increase from  $33 \pm 3.5 \text{ pA}$  to  $63 \pm 8.6 \text{ pA}$  over P0-P3, but jump to  $167 \pm 38 \text{ pA}$  at P4 before reaching an asymptote near 250 pA from P6-P14. Evoked EPSCs at P0-P1 typically measure 0.06-0.1 nA, equal to 1-2X the amplitude of spontaneous minis. Surprisingly, these small currents are capable of evoking action potentials, suggesting that spontaneous activity can drive action potentials in MNTB neurons at early ages, before the presynaptic calyces of Held begin to form. Together, these data indicate that MNTB neurons undergo significant biophysical maturation in the absence of auditory stimuli, with most properties achieving near adult values by P8.

## **847 Glutamate Release at Developing, GABA/Glycinergic MNTB-LSO Synapses Elicits Dendritic Ca<sup>2+</sup> Influx Via NMDA Receptors**

Abigail Kalmbach<sup>1</sup>, Karl Kandler<sup>1</sup>

<sup>1</sup>University of Pittsburgh

Before hearing onset, synapses in the inhibitory pathway from the medial nucleus of the trapezoid body (MNTB) to the lateral superior olive (LSO) not only release GABA and glycine but also glutamate (Gillespie et al 2005). This transient glutamate release from nominally inhibitory synapses coincides with the period in which the MNTB-LSO pathway is tonotopically refined. We hypothesize that by releasing glutamate, developing MNTB-LSO synapses can elicit NMDA-R mediated calcium influx, which has been shown to underlie the refinement of excitatory topographic maps.

To test this hypothesis, we combined 2-photon microscopy with whole-cell patch clamp recordings in slices from postnatal mice (P3-P7). Patch electrodes contained 60 mM chloride ( $E_{\text{Cl}} = -20 \text{ mV}$ ), the sodium channel antagonist QX-314 (5mM), and the calcium indicator Oregon Green BAPTA (100uM). Under these conditions, electrical stimulation of the MNTB-LSO pathway (3-5 stimuli at 10Hz) consistently elicited local Ca<sup>2+</sup> transients in LSO dendrites. Application of the NMDA-R antagonist DL-APV (100uM) reduced dendritic Ca<sup>2+</sup> responses by 35% (control peak  $\Delta F/F = 0.24 \pm 0.024$ ; +APV  $\Delta F/F = 0.16 \pm 0.016$ ;  $p = 0.0001$ , paired ttest;  $n = 18$  cells). Despite their significant contribution to MNTB-elicited dendritic Ca<sup>2+</sup> responses, NMDA-Rs did not contribute to somatically recorded electrical responses. APV had no effect on the peak amplitudes or the time courses of MNTB-elicited synaptic potentials ( $p = 0.8$ , paired ttests).

Together, these results indicate that activation of NMDA-Rs by MNTB terminals plays an important role in eliciting dendritic Ca<sup>2+</sup> responses in developing LSO neurons during the time of topographic map refinement. In contrast, NMDA-Rs at MNTB-LSO synapses appear to play no role in the somatic integration of synaptic potentials.

Supported by DC008938 (AK) and DC004199 (KK).

## **848 Functional Effects of Kv1 Channel Density and Location in MSO Neurons**

Pablo Jercog<sup>1</sup>, Paul Mathews<sup>2</sup>, Nace Golding<sup>2</sup>, John Rinzel<sup>1,2</sup> New York University, <sup>2</sup>University of Texas at Austin

In order for neurons in the medial superior olive (MSO) to be sensitive to interaural time differences, they precisely detect the coincident arrival of dendritic inputs that originate from each ear. *In Vitro* and computational studies have shown that the Kv1 family of low voltage-activated potassium channels significantly contributes to precise temporal processing in MSO neurons. However, little is known about the possible role these channels play in dendritic integration: where are the Kv1 channels concentrated and what does it matter? Based on our kinetic analysis of Kv1 using voltage clamp and dual somatic and dendritic current clamp recordings we have developed a multi-compartmental model of these bipolar neurons. With the model, we account for observations that subthreshold EPSPs of dendritic origin undergo significant temporal sharpening (half width decreasing with increasing intensity) and with little or no broadening during propagation to the soma. We highlight the significance of Kv1 dynamics by demonstrating the model neuron's loss of temporal precision when the conductance of Kv1 current is frozen at resting levels. Moreover, our model suggests that a significantly higher density of Kv1 channels exists in the axo-somatic compartment than in more distal dendrites. Such a distribution, as compared with a uniform or higher dendritic density, preserves temporal precision of EPSPs and avoids disadvantaging EPSPs that would suffer considerable shunting when generated in distal dendrites soon after EPSPs were generated more proximally along the same path to the soma.

### **[849] Dominant Role of N-Type $\text{Ca}^{2+}$ Channels in Triggering Synaptic Transmission in Nucleus Laminaris of the Chick**

Yong Lu<sup>1</sup>, Hongxiang Gao<sup>1</sup>

<sup>1</sup>*Northeastern Ohio Universities College of Medicine*

Neurons of the chicken nucleus laminaris (NL), the third-order auditory neurons involved in azimuth sound localization, receive bilaterally segregated glutamatergic excitation from the cochlear nucleus magnocellularis, and GABAergic inhibition from the superior olivary nucleus. We investigated voltage-gated calcium channels (VGCCs) triggering the excitatory and the inhibitory transmission in NL. Whole-cell voltage clamp recordings were performed in acute brainstem slice preparations. We have three main findings. 1) the excitatory transmission was predominantly mediated by N-type VGCCs, because  $\omega$ -conotoxin GVIA (1-2.5  $\mu\text{M}$ ), a specific N-type blocker, inhibited excitatory postsynaptic currents (EPSCs) by >90%, while blockers for other types (L-, P/Q-, and R-type) each produced little or no inhibition. 2) the VGCCs mediating the two segregated excitatory inputs were symmetrical, as seen by the nearly identical percent blockade of the two EPSCs elicited by partially independent electrical stimulations, with the same blocker in the same cell. 3) the inhibitory transmission in NL neurons was also predominantly mediated by N-type VGCCs;  $\omega$ -conotoxin GVIA (1  $\mu\text{M}$ ) produced >90% reduction of inhibitory postsynaptic currents. Our results demonstrate that N-type VGCCs play a dominant role in triggering both the excitatory and the inhibitory transmission in NL, and suggest that these channels are the primary targets modulated by metabotropic receptors. Furthermore, the symmetry in VGCCs mediating the bilaterally segregated excitatory inputs may be optimal for coincidence detection of the two inputs. Supported by startup funds from NEOUCOM.

### **[850] Time Course of Inhibition in the Chick Auditory Brainstem: Distinct Roles for GABA and Glycine**

Sidney Kuo<sup>1</sup>, Larry Trussell<sup>1</sup>

<sup>1</sup>*OHSU*

The processing of interaural sound intensity and timing cues is believed to be initiated in separate divisions of the avian cochlear nucleus, the nucleus angularis (NA) and nucleus magnocellularis (NM). Axons of bilateral NM neurons converge bilaterally onto their target cells in nucleus laminaris (NL). All three regions receive a common GABAergic input from the same ipsilateral source, the superior olivary nucleus (SON). SON in turn receives excitatory input from NA and NL. Given the distinct functions of NM, NL and NA in sound processing, as well as the very divergent morphology and physiology of their respective cells, we asked if the properties of inhibition within each region may also be distinct. Recordings were made in NM, NL and NA neurons of embryonic chick brainstem slices (E17-19) using whole-cell voltage clamp. Electrically evoked inhibitory postsynaptic currents (IPSCs), recorded in the presence of glutamate receptor blockers (20  $\mu\text{M}$  DNQX, 40-100  $\mu\text{M}$  DL-APV) in NL and NM ranged from 300 pA to 4 nA when

using maximal stimuli. IPSCs decayed > two-fold faster in NL than NM (weighted time constants  $8.2 \pm 2.9$  ms vs.  $27.0 \pm 9.7$  ms, respectively). As IPSCs in both regions were blocked by GABAzine (SR95531), these results are consistent with the idea that GABA receptor channel gating properties are different in the two brain regions. Evoked IPSCs recorded from NA neurons were smaller in amplitude than in NM/NL, ranging from 60 to 500 pA. These exhibited a slow component of decay resembling IPSCs in NL and NM; accordingly this component was blocked by GABAzine. Surprisingly, block of GABA<sub>A</sub> receptors did not fully eliminate the IPSC in NA neurons. the remaining current decayed quite rapidly, with a weighted time constant of  $3.0 \pm 0.4$  ms. This fast component was eliminated by the addition of 500 nM strychnine, an antagonist of glycine receptors. Thus, inhibition differs between the primary regions of the chick auditory brainstem both in kinetics and in transmitters.

Support: NIH grant DC004450.

### **[851] Topography and Morphology of Superior Olivary Nucleus Projections Upon Nucleus Laminaris in Chicken**

Kathryn Tabor<sup>1</sup>, Edwin Rubel<sup>2</sup>

<sup>1</sup>*Neurobiol & Behav Prog, Virginia Merrill Bloedel Hearing Research Center, University of Washington*, <sup>2</sup>*Dept of Oto-HNS, Virginia Merrill Bloedel Hearing Research Center, University of Washington*

Auditory coincidence-detector neurons in avian nucleus laminaris (NL) are involved in the computation of interaural time delays resulting from the azimuthal position of a sound source. NL in chick is composed of a compact monolayer of bitufted neurons with dendritic arbors oriented dorsoventrally. the sensitivity of NL neurons to coincident inputs is modulated by inhibitory feedback from the superior olivary nucleus (SON), which receives excitatory input from NL and n. angularis (NA). to better understand the mechanism underlying this modulation and its significance in coincidence detection, we used *In Vitro* tract tracing to determine the topographical organization of the projection from SON to NL, and the morphology of SON axonal terminals within the NL. Intact brainstems of E21 chicken embryos containing the cochlear nuclei, NL and SON were dissected in chilled ACSF. a solution containing 10% tetramethylrhodamine biotinylated dextran amine was injected through glass pipettes into the SON using a combination of pressure injection and electroporation. Injection sites were restricted to a fifth of the SON. Retrogradely labeled neurons were widely distributed across the NL. Anterogradely labeled SON axonal terminals were found throughout the NL as well. SON terminals form wide arborizations with extremely dense boutons around the cell bodies and the proximal portion of both dorsal and ventral dendrites of NL neurons. Sparse terminations were also detected in the regions of the distal dendrites. Interestingly, the distribution of the densest termination exhibited a topographical relationship to the injection site within the SON. the densest terminations were found in caudal NL following injections into caudal SON, while injections into rostral SON

produced the densest termination in rostral NL, suggesting some topographical organization of the projections from SON to NL. These terminations arborize across the lateral-medial axis of NL.

Supported by grants DC04661, DC03829, DC05361 from NIH/NIDCD

### **852 The Shape of Laminaris**

**David Harris<sup>1</sup>, Armin Seidl<sup>1</sup>, Edwin Rubel<sup>1</sup>**

<sup>1</sup>*University of Washington*

Nucleus laminaris (NL) is a sheet of about 1200 bipolar neurons in the avian auditory brainstem pathway. It is arranged tonotopically with low frequency sensitivity in the posterior-lateral end and high frequencies at the anterior-medial end. the entire plane is twisted in the shape of a potato chip. Dorsal NL dendrites receive afferent innervation from the ipsilateral ear via the adjacent N magnocellularis (NM) and ventral dendrites receive input from the contralateral NM via the crossed dorsal acoustic tract (XDAT). orthogonal to the frequency axis is the anatomical "delay line." Along this axis individual neurons can compare arrival times of specific spectral components from each ear implying that NL cells function as "coincidence detectors." Since precise convergence of ipsilateral and contralateral input is an essential element of this model, we decided to measure the exact 3-dimensional shape of these nuclei and the lengths of the interconnecting pathways. Chicks (P1-P14) were perfused with paraformaldehyde plus methylene blue to vitally stain nuclei. As frozen sections were taken through the brainstem, 10 Mpix digital images were taken of the cut surface. the stack of stained and aligned images was processed with Nikon Capture 6, Photoshop 7.0 and Amira 4.1 software. Measurements of the length of the XDAT present two anomalies. (1) the ipsilateral projection is about one half the length of the contralateral projection. for NL cells to detect coincidences we must hypothesize precise differences in conduction velocities. (2) the XDAT connecting high frequency portions of NL is significantly shorter (2.1 mm) than the low frequency connection (3.5 mm) with a linear gradient between. There is a similar CF-length function for the ipsilateral projection. This gradient either introduces a frequency-dependent group delay into the circuit, or it is counterbalanced by a concomitant gradient in conduction velocities.

Supported by NIH-NIDCD DC003829, DC004661, DC008042.

### **853 Interaural Time Difference Processing in the Medial Superior Olive of the Gerbil: Invariance to Changes in Absolute Intensity**

**Michael Pecka<sup>1</sup>, Benedikt Grothe<sup>1</sup>**

<sup>1</sup>*Biocenter of the Ludwig-Maximilians-University Munich, Department Neurobiology, Planegg-Martinsried*

The dominant cue for localization of low-frequency sounds are microsecond differences in the time-of-arrival of sounds at the two ears (interaural time difference, ITD). in mammals, ITD sensitivity is established in the medial superior olive (MSO) by coincidence detection of excitatory inputs from both ears. MSO neurons typically exhibit peak

firing rates, hence coincidence of their excitatory inputs, for particular ITDs outside the behaviorally relevant range of ITDs, while displaying a monotonic modulation in their firing rate in response to ITDs within the relevant range. This distinctive positioning of the peak and slope of the ITD-functions was shown to be related to additional inhibitory MSO inputs and ensures maximal ITD sensitivity for ITDs within the behaviorally relevant range. However, ITD-functions are typically obtained at a fixed intensity and it is unknown how absolute intensity influences the coincidence detection mechanism and, hence, the tuning of single cells to ITD. We recorded extracellularly from MSO single cells *In Vivo* and obtained ITD-functions to tones over a wide range of absolute binaural intensities (35 dB; no interaural intensity differences). We found that the ITD tuning of MSO neurons was remarkably invariant to changes in absolute intensity. On average, neurons exhibited significant ITD sensitivity over a range of >25 dB. Furthermore, the positions of both the peak and the slope of the ITD-functions were mostly unaffected by changing absolute intensity. Most notably, firing rates at unfavorable ITDs remained disproportionately low with increasing intensities, thereby assuring a large modulation in firing rate over the behaviorally relevant range of ITDs at all intensities. These results demonstrate that the coincidence detection mechanism of the MSO is highly robust to changes in absolute intensity, a feature potentially related to the inhibitory MSO inputs and/or to high concentrations of low-threshold K<sup>+</sup> channels in MSO neurons.

### **854 Phasic and Tonic Inhibition in the Lateral Superior Olive**

**Jason Mikiel-Hunter<sup>1</sup>, Roberta Donato<sup>1</sup>, David McAlpine<sup>1</sup>**

<sup>1</sup>*UCL - Ear Institute*

The principal cells of the lateral superior olive (pLSO cells) present a minor conundrum in the auditory brain stem as they are sensitive to both interaural level differences (ILDs) and interaural time differences (ITDs). for the pLSO cells to display this ITD sensitivity, low frequency amplitude modulations must be concealed in carrier signals on account of their inability to extract information from the fine structure of high-frequency stimuli. the range of suitable modulation frequencies is limited to hundreds of Hertz which demarcates them from the principal cells of the medial superior olive (pMSO cells) whose specialized synaptic and electrophysiological adaptations allow them to process ITDs at frequencies as high as several thousand Hertz. Nevertheless recent studies have suggested that pLSO neurons in the lateral section of the nucleus exhibit properties similar to their pMSO counterparts. in the present study we investigate the possibility that this similarity may extend to the mechanisms involved in integrating incidental synaptic information at a cellular level. a brain stem preparation has been implemented for two different species, the rat and guinea pig: a selection based upon the animals' auditory preference for different frequency ranges. This may affect how any relationship between the two main nuclei of the superior olive complex develops such that adaptations may exist in their LSO to promote its ITD sensitivity. pLSO cells have been patched in whole-cell

configuration whilst bundle tracts originating in the AVCN were electrically stimulated in control or in the presence of the glycine receptor-antagonist strychnine. This allowed us to determine the impact of inhibition on synaptic integration. Initial data from the guinea pig points towards a contralateral excitatory pathway which is evoked concurrently with a fast precisely-timed contralateral inhibition which at room temperature can be entrained at frequencies up to 100Hz. At higher stimulation rates (up to 1KHz) the timing of the response is not degraded by a tonic contribution though the responses are clearly no longer entrained. How the precise timing of inhibitory response might underlay LSO ITD sensitivity to amplitude modulated sounds observed *In Vivo* is discussed in the conclusions.

### **[855] Response Properties of Single Units in the Lateral Superior Olive of Decerebrate Cats**

**Nathaniel Greene<sup>1</sup>, Oleg Lomakin<sup>1</sup>, Kevin Davis<sup>1</sup>**

<sup>1</sup>*University of Rochester*

Neurons in the central nucleus of the inferior colliculus (ICC) of decerebrate cats show three major response patterns when tones of different frequencies and sound pressure levels are presented to the contralateral ear. the frequency response maps of type I units are uniquely defined by a narrow V-shaped excitatory area at best frequency (BF) and flanking inhibition at higher and lower frequencies. Units that produce type I maps typically have a high BF (>3 kHz), a high rate of spontaneous activity (~10 spikes/s), and monotonic rate-level curves for BF tones and noise. These units receive ipsilateral inhibition, and display binaural excitatory/inhibitory (EI) interactions. Given this constellation of properties, it has been hypothesized that the contralateral lateral superior olive (LSO) provides the dominant excitatory input to type I units. Most previous studies of the LSO have been made in anesthetized preparations; here, we report on the monaural and binaural response properties of single units in the LSO of decerebrate cats. Monaural responses were classified in the response map scheme, and binaural classification was based on sensitivity to interaural level differences (ILDs). the results reveal that LSO units form a relatively homogeneous population. the response maps of LSO units show V-shaped excitatory tuning and flanking inhibition (in units with spontaneous activity). LSO units have high BFs, low spontaneous rates (< 1 spike/s), monotonic rate-level curves for BF tones and noise, and exhibit IE binaural response properties. These results are largely consistent with prior observations, and support the conjecture that a crossed LSO projection is the primary source of excitation for type I units. Quantitative comparisons between the LSO and ICC unit types suggest that additional excitatory and inhibitory inputs sharpen the tuning and enhance the ILD sensitivity of type I units. Supported by NIDCD grant R01 DC 05161-07.

### **[856] A Model for Responses of Neurons in the Auditory Brainstem to Bilateral Electrical Stimulation of the Cochlear Nerve**

**Yoojin Chung<sup>1</sup>, H. Steven Colburn<sup>1</sup>**

<sup>1</sup>*Boston University*

Increasing numbers of patients are provided with cochlear implants in bilateral configurations with the goal of achieving binaural benefits as in normal hearing (NH) listeners; however, Bilateral Cochlear Implant (BiCI) listeners' sensitivity to interaural time differences (ITD) is not as good as seen in NH listeners and the neural mechanism for interaural time difference (ITD) processing in BiCI listening is not clear. It has been reported that single neurons in the binaural pathway can tune to the ITDs of electric stimulation in a narrow range of conditions. in this study, we are developing models for predicting responses of individual ITD-sensitive neurons to electrical stimulation.

A descriptive model of ANF response to electric and acoustic stimuli is developed as an input to a model of binaural processing in the ascending auditory pathway. This model, an extension of the model of Bruce et al. (IEEE Trans Biomed Eng, 1999) and Nourski et al. (NIH contract 15th QPR, 2006), predicts the firing rate and temporal discharge patterns of the ANF response. Specifically, this model describes 1) how the amplitude and stimulation rate of the electric stimulus affect the firing rate and temporal discharge patterns of the ANF response, and 2) how the firing rate and temporal discharge patterns change over time from the onset of acoustic and electrical stimulation. Spike times from this ANF model are used as the input to a network of cochlea-nucleus, medial-superior-olive, and inferior-colliculus models that were developed for the normal auditory pathway.

The response patterns of the IC model neurons with ANF inputs corresponding to electrical stimulation show many characteristics of the empirical data (Smith and Delgutte, 2007). in particular, the narrow dynamic range of ANF responses makes the IC more sensitive to stimulus intensity so that sharp ITD tuning is only observed in a narrow range of parameters. in addition, the rapid adaptation of ANF response to electric stimuli leads to the large effects of stimulus pulse rate and of amplitude modulation with higher pulse rates. These effects can be complex because the IC model also includes an adaptation mechanism.

### **[857] Naturalistic Input Causes Slow Adaptation of Firing Rate and Phase-Locking in Neurons of the Chick Nucleus Magnocellularis**

**Marina Kuznetsova<sup>1</sup>, William Spain<sup>2</sup>**

<sup>1</sup>*Neurobiology and Behavior, University of Washington,*

<sup>2</sup>*Physiology and Biophysics, University of Washington, VAPSHCS*

In the auditory system *in vivo*, adaptation of firing rate to sound over several seconds has been observed at the level of the inferior colliculus and above. We previously observed adaptation over a similar time scale *In Vitro* in the avian Nucleus Magnocellularis (NM), which contains

first-order central neurons of the circuit that uses the interaural time difference (ITD) to localize sound. Because of their high internal chloride concentration, NM neurons are depolarized by GABAergic as well as glutamatergic synaptic input. NM neurons respond to noisy depolarizing current injections with a slow ( $\tau \sim 10$  s) increase in firing rate ( $Ad_{slo}$ ) accompanied by an increase in spike jitter.  $Ad_{slo}$  is mediated by slow inactivation of low-threshold, voltage-activated Kv1 channels, and requires sustained depolarization but is independent of firing rate. In this study we used dynamic clamp to determine whether natural patterns of synaptic input can elicit  $Ad_{slo}$  in NM neurons, using the chick brain slice preparation (E21-P1).  $Ad_{slo}$  was elicited by simulated 8<sup>th</sup> nerve synaptic inputs phase-locked to 1000 and 1500 Hz sine waves, but not by 500 Hz input. Adding jitter and increasing the firing rate of the simulated 8<sup>th</sup> nerve fibers had little effect on  $Ad_{slo}$ . In contrast, addition of simulated GABAergic input increased  $Ad_{slo}$  for every excitatory stimulus tested. These data support the hypothesis that NM neurons can exhibit  $Ad_{slo}$  *in vivo*. We hypothesize that while  $Ad_{slo}$  increases the output of NM neurons, it may reduce the sound localization signal at the next level of processing in Nucleus Laminaris (NL). NL neurons modulate their firing rate as a function of ITD, by detecting simultaneous arrival of inputs from the ipsilateral and contralateral NM. Increase in spike jitter due to  $Ad_{slo}$  could desynchronize NM inputs across NL and reduce its firing rate modulation to ITD during a long lasting sound, allowing for better localization of novel stimuli.

### **[858] Suppression of Transient Response Facilitates Localization of Brief Sounds in Owl's Auditory System**

Go Ashida<sup>1</sup>, Kazuo Funabiki<sup>1</sup>

<sup>1</sup>Kyoto University / Osaka Bioscience Institute

Owls can catch prey in total darkness by locating rustling sounds. These sounds typically consist of broadband noise bursts of durations of a few tens of milliseconds. In the avian auditory system, neurons in the nucleus laminaris (NL), receiving bilateral inputs from axons of the nucleus magnocellularis (NM), form circuits involved in the computation of interaural time differences (ITD), which are used to detect the azimuth of the sound source. Single unit recordings of NM and NL cells of the barn owl *In Vivo* have revealed that spiking activities of the neurons from both nuclei gradually decrease with time after the onset of the sound stimulus. However, NL neurons showed faster decay in activity than NM neurons. The firing rate curve of an NL neuron plotted against ITD shows clear peaks and troughs if the duration over which spike rate is counted exceeds 10 milliseconds. This time scale corresponds to the minimum length of sound to compute its direction measured behaviorally in owls (Konishi, 1973). To investigate the relationship between the fast decay seen in the PSTH and the efficiency of ITD coding in a very short time window, we performed numerical simulation using an NL neuron model. Our results indicate that the large transient component of the input after the onset lessens the ITD modulation. Therefore suppressing the transient input into NL may serve to facilitate ITD detection.

Possible mechanisms enabling this suppression will also be discussed.

### **[859] Psychophysical and Physiological Evidence for Fast Binaural Processing**

Ida Siveke<sup>1</sup>, Stephan Ewert<sup>2</sup>, Benedikt Grothe<sup>1</sup>, Lutz Wiegand<sup>1</sup>

<sup>1</sup>Ludwig-Maximilians-Universität, <sup>2</sup>Carl von Ossietzky Universität

In mammals, the auditory system is the temporally most precise sensory modality. To localize low-frequency sounds in space, it is capable to resolve differences in sound arrival times at the ears with microsecond precision. Considering that the duration of an action potential is around 50 times longer than the minimal just noticeable interaural time differences, this acuity is a biological feat. In contrast, the binaural system has been described to be very sluggish in updating dynamically changing interaural time differences as they arise for example from a low-frequency sound source moving along the horizontal plane.

This study aims to investigate the temporal resolution of monaural and binaural processing and to directly link electrophysiological recordings from the gerbil's dorsal nucleus of the lateral lemniscus to human psychophysical results. In combination with already established stimuli a newly designed binaural stimulus that transmits very rapid and plausible auditory motion was used. The neuronal responses to binaural stimuli under increasing masking noise, the same setting as used in the psychophysical experiments, were investigated and the neuronal performance estimated using a receiver operating characteristics analysis.

Using this newly designed stimulus, the binaural psychophysical detection performance in humans was much faster than reported previously, and comparable to the monaural performance for detecting temporal modulations in amplitude. The electrophysiological data showed that neural encoding at the level of the DNLL is very fast. Moreover the neuronal performance reflected the observed improved psychophysical performance. Thus, the current data provide both psychophysical and physiological evidence against a general, hard-wired binaural sluggishness.

### **[860] Binaural Sensitivity to Interaural Time Differences At High Speeds in Cat Midbrain**

Philip Joris<sup>1</sup>

<sup>1</sup>Lab. of Auditory Neurophysiology, K.U.Leuven, Belgium, and Dept. of Physiology, U.W.-Madison

Relative motion between our surroundings and receptor organs yields information to the outside world. Selectivity to motion is pervasive in vision but is controversial in hearing. Low-frequency interaural time differences (ITDs) are an important source of auditory spatial information in humans. Sensitivity to ITDs first arises in the brainstem and is based on a mechanism of coincidence detection. In the midbrain, neurons show a dynamic sensitivity to tones rocking back and forth in ITD, roughly corresponding to sound sources oscillating in azimuthal position. This

sensitivity is to changes in ITD rather than to the instantaneous ITD, and has been interpreted as sensitivity to motion.

I recorded responses in the inferior colliculus of the cat to broadband noise swept in ITD. Comparison to static and moving ITDs was performed in 64 neurons. In most neurons, ITD-sensitivity to static noise and to noise moving at moderate speeds (100 to 1000  $\mu$ s/s) was well-matched. Surprisingly, the ITD-sensitivity was preserved even at unnaturally high speeds (highest speed tested was 128 ms/s). The response is not invariant with speed: compared to slow speeds, the response at high speeds can show an onset component; in- or decreases in instantaneous firing rate; and an apparent shift along the ITD axis. These changes, however, are trivial consequences of the adaptation properties and neural latency of midbrain neurons. Thus, despite the integrative properties of the midbrain, instantaneous ITD is exquisitely coded at this level, even at unnaturally high speeds. This remarkable tolerance for speed is explained by the physics of the stimulus and the process of coincidence detection.

Supported by the Fund for Scientific Research – Flanders (F.W.O. G.0392.05), Research Fund K.U.Leuven (OT/05/57), and NIH DC-00116 to T.C.T. Yin.

### **861 Transformation of Neural Representation of the Auditory Space Along the Collicular Pathway**

**Shigeto Furukawa<sup>1</sup>, Katuhiro Maki<sup>1</sup>**

<sup>1</sup>NTT Communication Science Labs

In the nervous system, sensory information can be represented in the form of neural spike timing as well as spike count. This study examines the changes in the form of the auditory space representation along the pathway from the central nucleus of the inferior colliculus (ICc), through the external nucleus (ICx), to the superior colliculus (SC). Specifically, the relative importance of spike count and timing was evaluated in terms of *transmitted information* (TI), an information-theoretic measure, which indicates the amount of azimuth-related information carried by spike patterns. Single unit responses were recorded from the three nuclei of anesthetized gerbils. The stimuli were 50-ms wide-band noise bursts at various sound levels that varied in terms of the azimuth on the horizontal plane in a virtual acoustic space. The neural responses were classified by using a radial basis function algorithm to derive the azimuth-related TI for each unit. Two types of spike density function (SDF) were tested as inputs to the classification algorithm. One was a vector representing spike occurrence as a function of post-stimulus time, which contained both spike count- and timing-based information ( $SDF_{\text{Count+Time}}$ ). The other had the same vector format as  $SDF_{\text{Count+Time}}$ , but the spike timing-based information was eliminated by shuffling the spike times when calculating the vector ( $SDF_{\text{Count}}$ ). The difference between TIs derived for  $SDF_{\text{Count+Time}}$  and  $SDF_{\text{Count}}$  can be regarded as indicating the relative importance of the spike timing-based information. Generally in the ICc, the TI for  $SDF_{\text{Count}}$  was substantially smaller than the TI for  $SDF_{\text{Count+Time}}$ . The difference was

smaller in the ICx and was smallest in the SC. This result indicates that the representation of azimuth information was transformed progressively from spike timing-based to spike rate-based codes along the collicular pathway.

### **862 Localization and Extraction of Frog Calls From a Chorus Using an Acoustic Beamformer**

**Douglas L. Jones<sup>1</sup>, Margaret L. Jones<sup>2</sup>, Rama Ratnam<sup>3</sup>**

<sup>1</sup>University of Illinois at Urbana-Champaign, <sup>2</sup>University of Chicago, <sup>3</sup>University of Texas at San Antonio

Male frogs and toads congregate in dense choruses around bodies of water and vocalize to attract conspecific females. This study uses a microphone array and state-of-the-art signal processing techniques (acoustic beamforming) to map the spatial distribution of frogs and toads in a chorus and determine the temporal interactions between vocalizing individuals. Spatial locations of calling individuals were determined from acoustic recordings using an array of microphones positioned around a spawning area (a marsh) in Texas. The multi-channel data was first partitioned into frequency bands distinct to each species to prevent species overlap. Next, within each of these (wide) frequency bands, the location of the strongest source was estimated using inter-microphone arrival time delays. These were averaged over the desired band to generate a wideband estimate of the location. Resolutions better than 10 cm were achieved for an array size of 9 m x 9 m. Broadly, the algorithm was able to accurately localize non-overlapping conspecific individuals. Localization was equally accurate for pulsatile broad-band callers (cricket frogs, *Acris crepitans*) as for tonal narrow-band callers (Gulf coast toads, *Bufo valliceps*) suggesting that robust localization is possible utilizing a time-frequency trade-off. Once the location of a calling individual was determined, a minimum variance distortionless response (MVDR) beamformer extracted the voice of the individual while suppressing all other callers. The voice of each located individual was recovered in this manner. A temporal overlap matrix of the callers was constructed from the recovered voices. For cricket frogs (density ranging from 7-9 frogs per 50 sq. m.) the temporal overlap was less than 6% for all pairs of individuals. This research demonstrates that beamforming techniques for monitoring a chorusing population is feasible, and holds promise for research in ecology, ethology, and neuroethology.

### **863 The End of Localization Dominance in the Barn Owl**

**Brian Nelson<sup>1</sup>, Terry Takahashi<sup>1</sup>**

<sup>1</sup>University of Oregon

Barn owls, like humans, localize sounds that arrive directly from a source and are less influenced by reflections that follow after a short delay – a phenomenon known as localization dominance. We measured head-saccades evoked by two correlated noisebursts from different loci presented in rapid succession with a variable delay. As the delays were shorter than the sounds' durations, the stimuli had brief segments when the lead or lag was present alone, flanking a segment when both sounds were



present. the lead- or lag-alone segments could be independently lengthened or shortened. When the lag-alone segment was lengthened at any given delay, the number of lag-directed saccades increased, suggesting that the salience of the echo depends on the duration of the lag-alone segment. the proportion of saccades toward each speaker did not vary with the duration of the lead-alone segment when the duration of the lag-alone segment was held constant. Neural responses in the auditory space map of the owl's inferior colliculus increased when lead-alone and lag-alone segments were lengthened, but the relative strengths of these two responses does not correlate well with the relative proportion of saccades to the lead and lag sources. Furthermore, the response evoked by the lead-alone segment had no influence on the response evoked by the lag-alone segment. We propose the alternative view that localization dominance in the owl occurs at short delays because a short lead-alone segment is more likely to evoke a supra-threshold response on the map than would a short lag-alone segment. Localization dominance ends when both segments are equally likely to evoke a supra-threshold response.

Supported by grants from the NIDCD F32-DC008267 and RO1-DC03925.

#### **[864] Effects of Amplitude Modulation On the Localization of Direct Sounds and Reflections with Synchronized Onsets and Offsets in the Barn Owl**

Brian Nelson<sup>1</sup>, Terry Takahashi<sup>1</sup>

<sup>1</sup>University of Oregon

Humans and owls can localize sounds under echoic conditions. This capacity persists even when the transient time disparities at the onset and offset of a lead/lag sound pair are removed, suggesting that time disparities between the corresponding features of each envelope may define the lead/lag relationship. We measured the head-saccades of barn owls to lead/lag pairs having only ongoing envelope disparities (OEDs) while varying envelope modulation (EM) depth. for short OEDs and deep EMs, the owls localized the leading source preferentially; the proportion of saccades to the leading sound increased at a short OED. Turns to either source were equally likely with shallow envelopes suggesting that lead/lag relationships are ambiguous without EMs. Saccades to both sources were as precise as those to single sources when EM was deep. Localization precision diminished, however, when EM depth was reduced or when saccades were made to the lag at a short OED. Recordings in the owl's auditory space-map revealed possible explanations. When two sources emit uncorrelated noises, the binaural cues are averages of each location's values weighted by each sound's momentary amplitude. Space map cells are therefore synchronized in their firing to the sound in their spatial receptive field. Responses to lagging sounds were weaker and less well synchronized at a short OED, which could bias the bird towards the leading source. Responses also weaken as EM depth decreases, which possibly leads to the ambiguity in localization behavior.

Supported by grants from the NIDCD F32-DC008267 and RO1-DC03925.

#### **[865] The Precedence Effect in Mice, Demonstrated in the Inhibitory Effect of Reversing the order of Clicks within Pairs From Two Speakers On the Startle Reflex**

James Ison<sup>1</sup>, Nathaniel Housel<sup>1</sup>, Stephanie Yee<sup>1</sup>, Colleen Zenczak<sup>1</sup>, Paul Allen<sup>1</sup>, Anita Karcz<sup>2</sup>, Conny Kopp-Scheinflug<sup>2</sup>

<sup>1</sup>University of Rochester, <sup>2</sup>University of Leipzig

Almost all acoustic environments are complicated because of echoes, but these are rarely noticed because the perceptual environment is simplified by neural echo-suppression mechanisms. This "precedence effect" (PE) has been demonstrated in humans, other mammals, birds and some insects, but not yet in mice. This species is an attractive target of a precedence study, first because the mouse depends largely on IID to locate sounds, and second, it is the now favored model to study physiological/genetic mechanisms of hearing. the CBA/CAJ mouse (3 mo. old males, n = 9) was confined in a small test cage facing two speakers 90 degrees apart. Each speaker provided a 100 micro-sec click with an inter-speaker interval (ICI) of 1 ms, right then left, the pair repeated every 10 ms throughout the experiment. Startle noise bursts were presented about every 20 sec. On control trials the burst was coincident with the first click of the repetitive series, or 1, 2, 3, 5, 7, or 10 ms later, and on PE trials the order of the pair was reversed (L then R) and the burst presented at 0, 1, 2, 3, 5, 7, or 10 ms or 100, 101, 102, 103, 104, 105, 107, or 110 ms later. to the human the "buzz" from the right hand speaker switched to the left after the reversal. the ASR was not affected by the reversal within the first 10 ms, but 100 ms later the ASR was inhibited by about 40%. Other studies then showed that this "behavioral PE" increased as the ICI increased, from 0 to .25, .50, 1.0 and 2.0 ms; and also increased as the interval between the reversal and the startle pulse increased from 10 up to about 60 ms, and was then maintained out to at least 300 ms: a "real" switch of click pairs from the right to the left reached an earlier peak and decayed more rapidly. (Supported by NIH, AG095247 and DC05409, and the Schmitt Foundation)

#### **[866] Unambiguous Lateralization of Ambiguous Binaural Sounds**

Richard Freyman<sup>1</sup>, Uma Balakrishnan<sup>1</sup>, Patrick Zurek<sup>2</sup>

<sup>1</sup>University of Massachusetts, <sup>2</sup>Sensimetrics Corporation

The lateralization of 250-ms trains of brief noise bursts was explored using an acoustic pointing technique. Successive binaural pairs of 1-ms broadband noise bursts alternated in interaural time delay (ITD) between left-leading and right-leading, with ITD's ranging from 100 to 600 microseconds. This alternating ITD pattern was repeated every 4 ms. Correlation of the bursts with one another was manipulated both within and across the binaural pairs. the onsets and offsets were either abrupt or gated with a long rise-fall time. the ITD of the pointer, a 50-ms burst of noise, was adjusted by the listeners to

match the lateral position of the target. Although the long-term cross correlation functions of the alternating stimuli were symmetrical about the midline, most of the tested signals were easily and consistently lateralized to one side or the other. for burst tokens that were frozen for the entire train, the determining factor for the abrupt-onset stimuli was the ITD of the very first burst pair. for stimuli in which burst tokens changed after each set of two alternating binaural burst pairs, lateralization was controlled by the ITD of the first pair in each alternating set. This control was maintained even with the imposition of 125-ms rise-fall times, and even when one extra binaural noise pair was added at the beginning such that the ITD of the first pair was opposite that of the first ITD in the alternating sets. These results reinforce a view of the precedence effect that depends not only on the interaural cues at the beginning of a sound, but also on temporal relationships within an ongoing sound [Work supported by NIH DC01625]

### **867 Adaptation to Room Acoustics and the Effect on Speech Intelligibility**

**Eugene Brandewie<sup>1</sup>, Pavel Zahorik<sup>1</sup>**

<sup>1</sup>*University of Louisville*

Although the negative effects of reverberant sound on speech intelligibility have been well documented, the extent to which prior exposure in a reverberant space may improve speech intelligibility is unknown. Here we demonstrate that speech intelligibility can be improved though listening experience in reverberant environments, presumably by a process of adaptive echo suppression. Using virtual acoustic techniques, three rooms were simulated. These rooms were identical in size and shape, but varied by their reverberant characteristics. Target signals from the Coordinated Response Measure (CRM) speech corpus were simulated in each room at a location of 1.4 meters directly in front of the subject (0 degrees azimuth). a competing broadband noise source was presented opposite the listener's right ear (90 degrees azimuth) in the same room as the signal, 1.4 meters away. the listener's task was to correctly identify the color/number target (i.e. green / 3) presented in the CRM phrase. Two conditions were tested. in the first condition, signals consisted of only color/number pairs (without a carrier phrase) presented in one of the three rooms selected at random from trial to trial. in the second condition, CRM sentences were extended using two phrases and presented in the same room. the listener was instructed to respond to the color/number target in the second ('Baron') phrase in this condition. Each condition was presented in blocks to normal hearing subjects over 9 signal-to-ratios. Results show a difference in performance threshold for the three rooms as expected from a decrease in the better-ear advantage as reverberant energy increased in the listener's better (left) ear. an effect of adaptation was also found, consistent with a buildup of echo suppression resulting from prior listening exposure in the room.

### **868 Effects of Reverberation on Neuronal Sensitivity to Fine Time Structure and Envelope ITD in the Inferior Colliculus of Awake Rabbit**

**Sasha Devore<sup>1</sup>, Bertrand Delgutte<sup>2</sup>**

<sup>1</sup>*Speech and Hearing Bioscience and Technology Program, Harvard-MIT Division of Health Sci. and Tech.,*

<sup>2</sup>*Eaton-Peabody Laboratory, Massachusetts Eye and Ear Infirmary*

In reverberant rooms, the superposition of acoustic reflections on the direct wavefront results in temporal fluctuations in the interaural time difference (ITD) and decorrelation of the ear-input signals. in the mammalian inferior colliculus (IC), low characteristic frequency (CF) neurons are typically sensitive to ITD in the fine time structure (ITD<sub>fs</sub>) of sounds, while high-CF neurons are sensitive to ITD in the envelopes (ITD<sub>env</sub>) of broadband noise induced by cochlear filtering. in an effort to improve our understanding of the neural basis of sound localization in reverberant environments, we characterized the effects of reverberation on ITD<sub>fs</sub>- and ITD<sub>env</sub>-sensitivity of neurons in the IC with a wide range of CFs.

We simulated anechoic and reverberant binaural room impulse responses (BRIRs) that contained ITD but not interaural level difference cues. Acoustic stimuli consisted of 400-ms bursts of Gaussian noise filtered with the BRIRs. We measured responses as a function of virtual azimuth for single units in the IC of awake Dutch-belted rabbits. to assess the effects of reverberation on each unit's ITD-sensitivity, we computed the mutual information (MI) between stimulus azimuth and spike count separately for anechoic and reverberant conditions. for the anechoic condition, MI did not obviously depend on CF over the range 250-8500 Hz. However, reverberation led to a greater reduction in MI in high-CF neurons than in low-CF neurons. Therefore, at the level of the IC, ITD<sub>fs</sub>-sensitive units more accurately encode stimulus azimuth than ITD<sub>env</sub>-sensitive units in reverberation. Preliminary analysis of our stimuli with a peripheral auditory model indicates that the effects of reverberation on both fine time structure and stimulus envelope are more severe with increasing CF, suggesting that our IC results may be a consequence of the frequency-dependent nature of ITD<sub>fs</sub>- and ITD<sub>env</sub>-sensitivity in the auditory pathway.

Supported by NIH grants DC002258 and DC005209.

### **869 Tuning of Inferior Colliculus Neurons to Amplitude-Modulation Frequency of Tone and Noise Carriers and to the Frequency of Click Trains**

**Laurel H. Carney<sup>1</sup>**

<sup>1</sup>*University of Rochester*

Tuning of inferior colliculus (IC) neurons to amplitude modulation (AM) frequency has been demonstrated based on changes in average discharge rate, synchrony to the envelope, or both (synchronized rate) as a function of modulation frequency. Approximately 50% of IC neurons have bandpass tuning for AM frequency, and this tuning plays an essential part in recent psychophysical models for

AM sensitivity in response to complex sounds. Several models for the tuning of IC cells to AM frequency have been proposed; these models have been developed based on the responses of IC cells and other auditory neurons in the ascending pathway to AM tones. Responses in the IC to stimuli with temporal fluctuations other than AM tones provide important tests for these models and shed light on the neural mechanisms underlying AM tuning. the results of the present study show that IC cells in awake rabbit that had bandpass tuning for AM tones also had bandpass tuning for AM wideband noise, and individual cells had similar best modulation frequencies for these two carriers. in addition, the same neurons were studied using click trains with click frequencies that matched the range of AM frequencies tested. IC neurons with bandpass tuning for AM tones and noise also had bandpass tuning to click rate, with the highest rates being elicited by click trains with frequencies that matched the best modulation frequency in response to tones and noise. the implications of these physiological results for models of AM tuning will be discussed.

### **[870] Separating the Impact of Non-Linearity and Parameter Change on Stimulus-Dependent Adaptation**

**Phillipp Hehrmann<sup>1</sup>**, Isabel Dean<sup>2</sup>, Misha Ahrens<sup>1</sup>, Nicol Harper<sup>2</sup>, David McAlpine<sup>2</sup>, Maneesh Sahani<sup>1</sup>

<sup>1</sup>*Gatsby Computational Neuroscience Unit, University College London, London WC1N 3AR, UK, <sup>2</sup>Department of Physiology and the Ear Institute, University College London, London WC1E 6BT, UK*

Neurons in the inferior colliculus (IC) of anaesthetized guinea pigs have been observed to adapt their response characteristics to the sound level distribution of the stimulus. More specifically, the rate-level functions of these neurons seem to change in a way that improves the population coding accuracy around the most commonly occurring stimulus sound levels. However, the neural mechanisms underlying this effect are unclear. Recent work has demonstrated that non-linear systems can exhibit apparent stimulus adaptation when the distribution of probing stimuli is changed, even though the parameters of the underlying system remain constant. We wanted to investigate to what degree the observed adaptive effects can be explained purely by changes in the probing stimuli. Using a non-parametric model of neural firing rate as a function of both the current and immediately preceding sound level, we found that changes in the stimulus could indeed account for a substantial degree of the observed adaptation in the cells studied.

We then studied a parametric model originally proposed to characterize the response of A1 neurons to short amplitude transients. This model combines a spectrotemporal-receptive-field-like summation mechanism, with dynamic non-linearities at both the input and the output stage. the longest time constants are on the order of 10ms and thus provide no mechanism for longer-term adaptive effects. We found that the rate-level functions obtained from this model were sensitive to the stimulus statistics in a way that matched several key characteristics of the changes observed in IC, despite the

lack of an explicit adaptive mechanism. However, it is known that responses of IC neurons adapt on a time scale of seconds. We are thus currently extending the model in order to also capture these slow processes.

### **[871] The Corticofugal System to the Inferior Colliculus Separately Modulates the Responses to Inputs from the Two Ears**

**Kyle Nakamoto<sup>1</sup>**, Trevor Shackleton<sup>1</sup>, Alan Palmer<sup>1</sup>

<sup>1</sup>*MRC-Institute of Hearing Research*

Previously, we showed that deactivation of the auditory cortex can alter the interaural level difference sensitivity of neurons in the inferior colliculus (IC). This could serve to separate the responses to stimuli based upon their laterality. to study this, we used two harmonic complexes in different dichotic combinations. Responses were measured in the IC of anaesthetised guinea pigs before, during and after cortical deactivation by a cooling loop. Two fundamental frequencies (F0s) 125 Hz and 145 Hz, were presented in three conditions: (1) both monaurally to the contralateral ear; (2) one monaurally to the contralateral ear, the other monaurally to the ipsilateral ear; (3) both stimuli to both ears. the relative contributions of each harmonic complex was determined from the Fourier magnitude of the response at each F0. in ~30% of cells cortical cooling substantially reduced IC responses, so phase locking was insignificant. in a further ~20% of cells the corticofugal system appeared to be gating the response to ipsilateral stimuli. Before cortical deactivation phase locking to the ipsilateral harmonic complex was insignificant, during cooling it became significant. This occurred both with and without any effect of cooling on the spike rate. This suggests that the descending system to the IC is not simply modulating inhibition or excitation, but rather separately altering the effectiveness of the ipsilateral and contralateral inputs by gating or altering the gain of the input from each ear. Non-focal deactivation of auditory cortex, including both primary and secondary areas, can have large effects on both the phase locking and rate response of IC neurons, even in an anesthetized preparation.

### **[872] FM Sweep Direction Selectivity in the Inferior Colliculus of the Mexican Freetailed Bat is Inherited**

**Josh Gittelman<sup>1</sup>**, Na Li<sup>1</sup>, Le Wang<sup>2</sup>, H. Steven Colburn<sup>2</sup>, George Pollak<sup>1</sup>

<sup>1</sup>*School of Biological Sciences, Section of Neurobiology, UT Austin, <sup>2</sup>Biomedical Engineering and Hearing Research Center, Boston University*

The Mexican Freetailed bat preferentially uses downward frequency modulations (FMs) for both echolocation and communication. in the inferior colliculus (IC), most neurons that exhibit direction selectivity (DS) for FMs prefer downward sweeps, consistent with the preponderance of downward FMs in the bat's vocalizations.

DS in the IC could be created, inherited or both. Where DS is created, up- and downward FMs evoke synaptic inputs of equal magnitude, but in a different temporal order; the temporal arrangement of the inputs determines the

magnitude of the post-synaptic potential and thus the number of spikes. Alternatively, if up- and downward FMs evoke synaptic inputs of different magnitude, then DS is inherited; the pre-synaptic cells must themselves be directionally selective. These two mechanisms could work together. Extracellular recordings show that when inhibition is blocked, DS is reduced or eliminated, suggesting that inhibition helps to create DS in the IC.

We made whole-cell patch-clamp recordings in the IC of awake bats to test these hypotheses, and used a model to explore the effects of blocking inhibition. Specifically, we examined the magnitude and timing of FM-evoked inputs. In most cells that exhibited DS, the magnitude of the evoked inputs was strongly affected by sweep direction, whereas the temporal arrangement was not. The preferred FM evoked larger excitatory inputs compared to the non-preferred FM. In some cells, the preferred FM also evoked larger inhibitory inputs. The increase in inhibition was smaller than the increase in excitation, so that the preferred sweep evoked a larger depolarization. In a model where DS is contained entirely in the excitatory inputs, blocking inhibition still alters selectivity, consistent with previous extracellular results. Since the input magnitudes changed strongly with sweep direction, we suggest that DS in the IC is largely inherited from lower nuclei that are themselves directionally selective.

### **873 Changes in Inferior Colliculus Activity of the Rat Related to Tinnitus**

**Didier Depireux<sup>1</sup>**, Elizabeth Powell<sup>1</sup>, Yadong Ji<sup>1</sup>, Barak Shechter<sup>1</sup>

<sup>1</sup>*U of Md Medical School*

Pharmacological, cognitive, and behavioral approaches are used to treat tinnitus, but all have limited success due to the poor understanding of the etiology of tinnitus and the difficulty in consistently and objectively measuring its symptoms. We have developed a rat model of noise-trauma induced tinnitus, which enables us to measure neurophysiological changes induced by tinnitus and their reversal by treatment (e.g., drug treatment or other manipulations). For instance, lidocaine is known to temporarily suppress tinnitus resulting from noise trauma. We use an awake, behaving rat with a chronic multi-electrode array implanted in inferior colliculus with which we measure neural activity before, immediately after, and several weeks after noise trauma-induced tinnitus and after intravenous injection of lidocaine. These animals are also subject to behavioral diagnostics for tinnitus. We perform post-mortem characterization of molecular changes in tinnitus correlated with CREB, phosphorylated-CREB, and GABA immuno-reactivity. Once this model is validated, we will be able to use it to screen other potential drugs for tinnitus treatment, evaluating their effectiveness, best course of treatment as well as potential side-effects.

Supported in part by a grant from the American Tinnitus Association

### **874 Spectral and Temporal Interactions in Cat Inferior Colliculus of Combined Electric and Acoustic Stimulation of the Hearing Cochlea**

**Maïke Vollmer<sup>1</sup>**, Ben H. Bonham<sup>2</sup>, Jochen Tillein<sup>3</sup>

<sup>1</sup>*University Hospital Wuerzburg*, <sup>2</sup>*University of California, San Francisco*, <sup>3</sup>*University Hospital Frankfurt/Main*

The present study determined spectral and temporal response patterns of inferior colliculus (IC) neurons to combined electric and acoustic stimulation (EAS) of the hearing cochlea. Normal hearing cats were implanted with scala tympani electrodes, and an earphone was sealed to the ipsilateral auditory meatus for acoustic stimulation. Unmodulated and sinusoidally amplitude modulated (SAM) acoustic tones and electric sinusoids were presented to the implanted ear. Responses were recorded along the tonotopic axis of the contralateral IC using a 16-channel silicon electrode array.

Electrical stimulation of the hearing cochlea evoked both electroneural and electrophonic responses. Electrophonic responses had lower thresholds (up to 34 dB difference), longer latencies and larger dynamic ranges than electroneural responses. Using a forward-masking paradigm (acoustic maskers of varying frequencies and intensities were followed by an electric probe of a fixed frequency/intensity combination), the CF of the masked electroneural probe response typically corresponded to the CF of the acoustic masker, independent of the electric probe intensity and frequency. In contrast, the characteristic frequency (CF) of the masked electrophonic probe response corresponded to the frequency of the probe at low probe intensities; at higher probe intensities it corresponded to the CF of the preceding masker. Similar intensity-dependent CF-shifts of the masked probe responses were observed if the acoustic maskers were followed by an acoustic probe (acoustic two-tone masking). The results underscore the similarity between electrophonic and acoustic responses.

Using simultaneous-masking, the intensity of and the phase relationship between the electric and acoustic SAM signals strongly affected (increased or decreased) neuronal discharge rates and the degree of phase-locking to EAS.

The results demonstrate that the spectral and temporal stimulus characteristics of electric stimulation and combined EAS of the hearing cochlea lead to complex interactions in the central auditory system. It is not yet clear to what extent such interactions influence speech perception in EAS users with residual hearing.

(Supported by NOHR, NIH N01 DC-3-1006, NIH N01 DC-2-1006 and MedEl)

**875 Auditory Midbrain Implant in NF2 Patients: Safety of Surgical Approach and Electrical Stimulation of Midbrain with AMI.**

Minoo Lenarz<sup>1</sup>, Hubert Lim<sup>1</sup>, Gert Josef<sup>1</sup>, Amir Samii<sup>2</sup>, Thomas Lenarz<sup>1</sup>

<sup>1</sup>Otolaryngology Department of Medical University of Hannover, <sup>2</sup>Neurosurgical department of International Neuroscience Institute Hannover

The auditory midbrain implant (AMI) is a new hearing prosthesis designed for stimulation of the auditory midbrain, particularly the inferior colliculus central nucleus (ICC). We have begun clinical trials in which three NF2 patients have been implanted with the AMI array. the removal of acoustic neuromas and AMI implantation was performed safely in a single surgical setting using the modified lateral suboccipital approach with a supracerebellar infratentorial extension for device implantation. None of the patients developed any complications either due to tumor removal or device implantation. Although the intended target was the ICC, we achieved proper placement in one patient while in the other two patients the array was implanted into the dorsal nucleus of the inferior colliculus and surface of the lateral lemniscus, respectively. Stimulation of these different regions elicited different auditory and non-auditory percepts which gives us more insight to the electrophysiology of the human midbrain. All three patients obtained various pitch, temporal, loudness, and directional percepts with stimulation of their AMI sites. the non-auditory percepts due to AMI stimulation were usually in form of paresthesia in the extremities or trunk. the only motor side effect observed in one of our patients was contra-lateral facial nerve stimulation. None of the patients experienced pain or vegetative side effects due to AMI stimulation. the sites which elicited non-auditory percepts were turned off at the end of the first fitting session. Overall, our combined surgical approach enabled safe tumor removal and simultaneous device implantation with no complications and electrical stimulation of the midbrain with AMI did not elicit any serious side effects in our patients. AMI is a safe alternative for hearing restoration in NF2 patients.

**876 Auditory Localisation Ability is Decreased by Cutting the Olivocochlear Bundle**

Samuel Irving<sup>1</sup>, M. Charles Liberman<sup>2</sup>, Christian J. Sumner<sup>1</sup>, David R. Moore<sup>1</sup>

<sup>1</sup>MRC Institute of Hearing Research, Nottingham, UK,

<sup>2</sup>Eaton Peabody Laboratory, Boston, MA, USA

Unilateral and asymmetric conductive hearing losses lead to immediate impairments in the ability to localise sound. However, impaired azimuthal localisation caused by a unilateral earplug improves with subsequent training in ferrets (Kacelnik et al., PLoS Biology, 2006). It has been suggested that efferent pathways from the higher auditory system to the periphery may be implicated in plasticity of this sort. Because the final common efferent pathway to the cochlea is the olivocochlear bundle (OCB), in this study we cut the OCB in ferrets to ascertain its

involvement in localisation plasticity. Ferrets were trained in a localisation task where they were required to approach a speaker to collect a water reward. Experimental animals had their OCB cut and localisation performance was then tested before and after insertion of a unilateral earplug. the OCB cut caused a decrease in localisation performance to sounds originating on the side of the cut. This detriment was further exacerbated by insertion of an earplug, regardless of which ear was plugged. Control animals carried out the same behavioural task as experimental animals but did not have their OCB cut. Over 10 days of further training, a small but significant improvement occurred for a 1s, but not for a 40ms stimulus. Based on the (unlesioned) results of Kacelnik and colleagues, we suggested (ARO, 2007) that an OCB lesion may abolish earplug-induced localisation plasticity. However, we found here that lesioned animals do not differ from controls in improved localisation following earplugging. We conclude that (i) lesioning the OCB impairs localisation, particularly when binaural cues are disrupted, and (ii) the OCB does not have a role in the slow, training-dependent improvement in localisation following unilateral earplugging.

**877 Kcna1 Null Mutant Mice, with Known Temporal Processing Deficits in the Auditory Brainstem Show Spatial-Location Behavioral Deficits Under Both Monaural and Binaural Conditions**

Anita Karcz<sup>1</sup>, Paul Allen<sup>2</sup>, Conny Kopp-Scheinflug<sup>1</sup>, James Ison<sup>2</sup>

<sup>1</sup>University of Leipzig, <sup>2</sup>University of Rochester

in vitro as well as *In Vivo* studies in the auditory brainstem show an important contribution of the Kv1.1 potassium channel subunit to precise action potential timing and the control of neuronal excitability. Sound localization using interaural intensity differences (IIDs) is believed to depend on both the strength and the temporal acuity of the bilateral input into the lateral superior olive (LSO). Neurons in the medial nucleus of the trapezoid body (MNTB) in *Kcna1* null mutant (-/-) mice show increased latency and jitter that may be expected to degrade and delay the inhibitory input into the LSO and also to impair binaural sensory behaviors. Corroborating these hypotheses, we have found that -/- LSO neurons are insensitive to IIDs corresponding to the contralateral hemifield, and behavioral experiments have shown that -/- mice are less able to detect a change in sound position from one location to another. Using Prepulse Inhibition (PPI) of the Acoustic Startle Response generated by a switch from broadband noise from one location to another we examine the performance in sound source discrimination under both binaural and monaural conditions, with the hypothesis that if their deficit is restricted to binaural hearing, then under less favorable monaural conditions the -/- mice should be no different from the wild-type +/+ mouse. in fact, the performance of -/- mice was not further degraded by this manipulation, while the PPI of +/+ mice was diminished by up to 24% (90° speaker separation) compared to the binaural condition. However, even in the monaural

condition +/- mice were able to detect the change of sound location better than the -/- mice (90°: +/- monaural: 28% PPI; -/- binaural: 11% PPI), suggesting the hypothesis that the deletion of the *Kcna1* gene must affect monaural processing of spatial cues as well as binaural processing.

### **[878] Azimuthal Sound Localization and Spatial Unmasking in the Mongolian Gerbil (*Meriones Unguiculatus*)**

**Andrea Lingner<sup>1</sup>, Teresa Kindermann<sup>1</sup>, Lutz Wiegrebe<sup>1</sup>, Benedikt Grothe<sup>1</sup>**

<sup>1</sup>*Ludwig-Maximilians-University, Munich*

Arrival time differences of sounds at the two ears (Interaural Time Differences, ITDs) are the main cue to localize low-frequency sound sources. Recent electrophysiological studies in the Mongolian gerbil (*Meriones unguiculatus*) have revealed the importance of glycinergic, inhibitory inputs in the MSO for the processing of ITDs. In the first part of this study we conducted two psychophysical experiments examining azimuthal sound localization and spatial unmasking in adult gerbils. First, we quantified the azimuthal sound localization of gerbils in a six-alternative-forced-choice (6AFC) paradigm with variable angles between the sound sources. Stimuli were low-frequency tones, bandpass (1000Hz  $\pm$ 10%) noise, and broadband noise. Overall localization performance ranged between 15° and 19°, significantly better than previously reported. In the spatial unmasking experiment, we quantified the signal-to-noise ratio (SNR) required to detect a low-pass noise signal at one of the six speakers when the masking low-pass noise, presented from all speakers, was either uncorrelated or correlated. The speakers were separated by 35°. With the uncorrelated masker, all animals required a significantly lower SNR to detect the signal, a clear demonstration of spatial unmasking in gerbils. In the ongoing second part of this study we examine the effect of juvenile noise exposure on the sound localization ability and spatial unmasking. A recent anatomical study in gerbils showed a developmental maturation of the inhibitory inputs in the MSO cells after hearing onset. Omnidirectional noise exposure between P10 and P25 leads to a disturbed refinement process of the inhibitory synapses, causing shifts in the ITD sensitivity. Thus, we focus on differences between noise- and normally-reared gerbils.

### **[879] Localization of High Pass, Low Pass, and Narrow Band Sounds by Cats**

**Janet Ruhland<sup>1</sup>, Tom Yin<sup>1</sup>**

<sup>1</sup>*University of Wisconsin-Madison*

Localization along the azimuthal dimension depends on interaural time and level disparities, while localization in elevation depends on the broadband power spectra at each ear resulting from the filtering properties of the head and pinnae at high frequencies. We hypothesized that localization of broadband (BB) noise would be superior to localization of high pass (HP) noise, and HP noise superior to low pass (LP) noise for targets in elevation, but nearly equivalent for targets in azimuth, and localization of narrow

band (NB) and pure tones should be much more accurate in azimuth. In addition, we expected that cats would localize tones and NB noise at idiosyncratic elevations depending upon frequency, as in some human studies.

We trained cats using operant conditioning to indicate the apparent locations of sounds via gaze shift. Targets consisted of BB, HP or LP noise, tones from .5 to 14 kHz and 1/6 octave NB noise with center frequencies from 6 to 16 kHz. For each sound type, localization performance was summarized by the slope of the regression relating localization responses to target positions. Overall localization accuracy for all sounds was better in azimuth than in elevation, in some cases by a wide margin. Gaze shifts to targets in azimuth were most accurate to BB, only slightly less accurate for HP, LP and NB sounds and quite a bit less accurate for tones. In elevation, cats were most accurate in localizing BB, somewhat less accurate to HP, and less yet to LP noise, though still with slopes about 0.60, but they localized NB noise much worse and were unable to localize tones. For NB or tones in elevation, cats did not have unique responses at different frequencies but appeared to respond with a "default" location at all frequencies. Deterioration of localization as bandwidth narrows is consistent with the hypothesis that spectral information is critical for sound localization in elevation.

Supported by DC02840 and DC07177.

### **[880] The Acoustical Cues to Sound Location in the Adult Chinchilla: Measurements of Directional Transfer Functions (DTFs)**

**Kanthaiah Koka<sup>1</sup>, Heath Jones<sup>1</sup>, J Lupo<sup>1</sup>, Daniel Tollin<sup>1</sup>**

<sup>1</sup>*Univ of Colorado Hlth Sci Ctr*

The acoustical cues for sound location are generated by the spatial- and frequency-dependent filtering of the propagating sound waves by the head and external ears. There are three main cues to sound location: interaural differences in time (ITD) and level (ILD) and monaural spectral shape cues. Although the chinchilla has been used for decades to study the anatomy, physiology, and psychophysics of binaural and spatial hearing, little is actually known about the localization cues available to them. Here, we measured the directional transfer functions (DTFs), the directional components of the head-related transfer functions, for 4 adult chinchillas. The mean weight, head diameter, and the length and width of the pinnae for the chinchillas were 670  $\pm$ 114 g, 35.5  $\pm$ 0.8 mm, 51.8  $\pm$ 1.5 mm and 27.8  $\pm$ 1.7 mm, respectively. DTFs were measured at both ears from 325 locations, with steps of 7.5° in both azimuth and elevation. The resultant localization cues were computed from the DTFs. In the frontal hemisphere, spectral notches were present for frequencies from ~6-13 kHz; in general, the frequency corresponding to the notch increased with increases in source elevation and in azimuth towards the ipsilateral ear. The mean maximum ITD observed across the chinchillas was 244  $\pm$ 14  $\mu$ s. Interaural level differences (ILD) depended strongly on source azimuth and frequency. In general, maximum ILDs were < 10 dB for frequencies <5 kHz, and ranged from 10-30 dB for the frequencies from 5-

15 kHz. ILDs for frequencies > ~15 kHz varied with azimuth in complicated ways.

Support: NIDCD R01-DC6865

### **881 The Effects of Experimentally-Induced Conductive Hearing Loss On Spectral and Temporal Aspects of Sound Transmission Through the Ear**

**J. Eric Lupo<sup>1</sup>**, Kanthaiiah Koka<sup>1</sup>, Daniel J. Tollin<sup>1</sup>

<sup>1</sup>*Department of Physiology and Biophys, University of Colorado Health Sciences Center, Aurora, CO USA*

Conductive hearing loss (CHL) is known to produce hearing deficits, including sound localization ability. the differences in sound intensities and timing experienced between the two tympanic membranes are important cues to sound localization. Although much is known about the effect of CHL on hearing level, little investigation has been done into the effects on timing and subsequent effects on the cues to location. This study investigated effects of earplugs on cochlear microphonic (CM) amplitude and timing and their corresponding effect on two localization cues, interaural level difference (ILD) and interaural time difference (ITD). Acoustic and CM measurements were made in 5 chinchillas before, after earplug insertion and after earplug removal using pure tones (500 Hz to 24 kHz). Occlusion resulted in a variable mild hearing loss of 20-33 dB (mean 27 ±4.9 dB) depending on frequency. in the normal and occluded situation, ILDs increased with increasing frequency (5.1 dB and 26 dB at 500 Hz and 20 kHz, respectively). Across all positions in azimuth, with the ear occluded, ILD magnitude was increased. At 0°, with the ear occluded, timing delays varied from -400 to -1500 µs (mean -800 ±0.5 µs) with 500 Hz demonstrating the greatest delays. ITDs in the normal and occluded cases decreased with increasing frequency across all positions in azimuth. ITD magnitude with the ear occluded increased as a result of conduction delays at the occluded ear. CHL leads to substantial changes in the magnitudes of both the ITD and ILD cues to sound location, which results in a shifted auditory space. This may be the basis for the difficulties in sound localization seen in patients with CHLs. Support: NIDCD R01-DC6865

### **882 Temporal Weighting of Cues for Vertical-Plane Sound Localization**

**Ewan A. Macpherson<sup>1</sup>**, Marnie L. Wagner<sup>1</sup>

<sup>1</sup>*Kresge Hearing Research Institute, University of Michigan* Human listeners localize sound in the vertical dimension using directionally dependent spectral cues. Vertical-plane localization of brief sounds is degraded at high sound levels, but localization of intense sounds improves as durations are lengthened [e.g. Vliegen & Van Opstal, JASA 115:1705-1713 (2004)]. the *adaptation hypothesis* proposes that short intense stimuli distort the peripheral representation of spectral cues and that accurate localization of long intense sounds is due to adaptation by the auditory system over the course of those stimuli. That hypothesis predicts that the auditory system extracts more information from later portions of intense stimuli than from the same portions of less-intense sounds.

We tested the adaptation hypothesis by measuring human listeners' temporal weighting of spectral cues in low- (30 dB SPL) and high- (70 dB SPL) level trains of noise bursts. Each train consisted of three 33-ms bursts or ten 10-ms bursts. Each individual burst was presented from a different randomly selected location in the vertical plane. Stimuli were presented in virtual auditory space, and listeners responded by orienting the head toward the perceived direction of each burst train. Weights were assigned to each burst position in a train by computing across trials a multiple linear regression between localization judgements and the actual locations of the bursts making up each stimulus.

For three-burst trains, the weights for all bursts were approximately equal at 30 dB, but at 70 dB the weight for the final burst was much larger than for the preceding bursts. for ten-burst trains, the first burst carried the largest weight at 30 dB, but at 70 dB the largest weight shifted to the second burst and the weight carried by the final burst increased. These results are consistent with the adaptation hypothesis and also parallel the effects of burst rate on the temporal weighting of cues in horizontal-plane localization [Stecker & Hafter, JASA 111:2355 (2002)].

### **883 A Physiologically-Based Model of ITD Discrimination in a Bilateral Cochlear Implant Subject**

**Kenneth Hancock<sup>1</sup>**, Victor Noel<sup>1</sup>

<sup>1</sup>*Massachusetts Eye & Ear Infirmary*

Principal cells of the medial superior olive are sensitive to the relative arrival times of inputs originating at each ear, and hence encode interaural time differences (ITDs). the net internal interaural delay determines the best ITD (BD) of each neuron, and consists of mechanical and neural components. the mechanical component is the net cochlear traveling wave delay resulting from mismatches in characteristic frequency between the ears. the neural component comprises axonal propagation delays and the influence of inhibitory synapses.

Mean BD decreases with increasing best frequency (BF), such that the rising slopes of neural rate-ITD curves tend to occur on the midline. As a consequence, ITD acuity is finest on the midline and systematically worsens as reference ITD increases (moves away from the midline). It is uncertain to what extent mechanical and neural delays each contribute to this system of organization. Bilateral cochlear implants bypass the mechanical delays and thus provide insight to the relative importance of the neural component.

ITD acuity was measured as a function of ITD in a bilaterally-implanted human subject using low-rate pulse trains and a two-alternative forced choice procedure. Just noticeable differences in ITD increased with reference ITD in a similar manner to the normal hearing condition. to account for these data quantitatively, a model of ITD discrimination was derived from published physiological recordings of ITD-sensitive neurons in inferior colliculus of bilaterally-implanted cats. the model predicts the data only if the rising slopes of the rate-ITD curves tend to occur on the midline irrespective of rate-ITD curve halfwidth.



Together, the results show that normal ITD coding is at least partially the result of systematic biases in the neural delay component, and emphasize that alignment of rate-ITD slopes on the midline is a fundamental feature of the ITD code.

### **884 Trading of Interaural Time and Level Differences in Modulated High-Frequency Stimuli**

**G Christopher Stecker<sup>1</sup>**

<sup>1</sup>*University of Washington*

Several recent studies have demonstrated that binaural sensitivity at high carrier frequencies is reduced at modulation rates above 100-200 Hz or interclick intervals (ICI) shorter than 5-10 ms. Consequently, lateralization of high-rate, high-frequency stimuli is dominated by interaural information contained in the sound onset. Several investigators have argued for this rate-limitation to occur at the level of monaural input to binaural processing, and thus to affect interaural differences of time (ITD) and level (ILD) equivalently.

Recent data from our lab [ARO Abs 30:910] indicates significant onset dominance when detecting dynamic ITD, but not ILD, in high-rate (< 5 ms ICI) 4000 Hz click trains. This result suggests that the two cues are not subject to equivalent rate limitation, and further predicts that when the two cues are presented in combination, their relative perceptual weighting (the ITD/ILD "trading ratio," TR) must vary with ICI.

The current study presented combinations of ITD and ILD in 4000 Hz Gaussian click trains to estimate TR by two different procedures: a "closed-loop" procedure in which subjects adjusted the ILD of a target click train to counteract the effects of an imposed ITD, and an "open-loop" procedure in which subjects indicated the lateral position of click trains containing independent combinations of ITD and ILD. Preliminary results indicate that TR, expressed in microseconds per dB, increased significantly as ICI decreased from 10 to 2 ms, thus revealing a greater influence of ILD at high modulation rates where ongoing envelope ITD sensitivity becomes impaired. One exception was an experienced subject whose TR values were lower than all other subjects (indicating greater weighting of ITD) and did not change with ICI. Overall, the results lend support to theories that evaluate the relative reliability of interaural cues prior to weighted combination in support of sound localization.

### **885 Coding of Interaural Time and Level Differences in the Human Brain: Adaptation and Interactions?**

**Julia Maier<sup>1</sup>, David McAlpine<sup>2</sup>, Georg Klump<sup>1</sup>, Daniel Pressnitzer<sup>3</sup>**

<sup>1</sup>*Zoophysiology and Behaviour Group, Carl-von-Ossietzky University Oldenburg, Oldenburg, Germany,* <sup>2</sup>*UCL Ear Institute, London, United Kingdom,* <sup>3</sup>*Laboratoire Psychologie de la Perception, CNRS-Université Paris Descartes, Paris, France*

Interaural time and level differences (ITDs and ILDs, respectively) are the main cues enabling mammals to

localise the source of a sound in the azimuthal plane. Single-neuron recordings in the guinea pig have demonstrated that responses of ITD-sensitive neurons in the inferior colliculus adapt to the most commonly occurring ITDs in a distribution, when the distribution is restricted to the ecologically-relevant range (Maier et al 2007). Here, we investigate, using a psychophysical paradigm, the extent to which human listeners show similar adaptive behaviour. Discriminability ( $d'$ ) was measured for ITDs and ILDs with and without preceding adaptation to ITDs. Stimuli were lateralized with reference ITDs of 0 and  $\pm 400 \mu s$ , and equivalent ILDs measured beforehand in a matching procedure. the ITD or ILD to be discriminated from the reference was a fixed number of just-noticeable differences corresponding to a  $d'$  of 2 for the non-adapted condition at all reference positions, as measured in preceding experiments. All stimuli were bands of noise 800Hz wide, centred at 500Hz and 400ms in duration. the ITD adaptor was 1s or 2s in duration, selected randomly. Stimuli were presented over headphones. Stimulus parameters were chosen so as to match as closely as possible the experimental paradigm employed in the neural recordings. by examining potential interactions between ITDs and ILDs, in terms of the adaptor-indicator relationship, we hope to determine the extent to which the cue (ITD, ILD) *per se*, or higher, perceptual processing, influences the perceived location of the sound source.

Maier, J.K., Harper, Dean, I., N.S., Klump, G.M. and McAlpine D., 2007: Dynamics of ITD sensitivity in the IC: Adaptive coding? Abstr. Assoc. Res. Otolaryngol. 418, 145. Supported by MRC, the SFB/TRR31 "Aktives Gehör" and the graduate school "Neurosensory Science, Systems and Applications", Oldenburg, Germany.

### **886 Misalignment of Ilds and Itds Induces Recalibration of Itds by More Informative Ilds?**

**Peter Keating<sup>1</sup>, Aimee Brighton<sup>1</sup>, Jan Schnupp<sup>1</sup>, Andrew King<sup>1</sup>**

<sup>1</sup>*University of Oxford*

Spatial hearing involves the integration of various acoustical cues, including interaural time and intensity differences (ITDs and ILDs). to facilitate such integration, however, the auditory system must align these cues in an appropriate manner. Crossmodal studies indicate that misalignment of two spatial cues is resolved through recalibration of the less informative cue. to address whether the same is true within the auditory system, misalignment was induced between a dominant ILD cue and a less informative ITD cue. Human subjects lateralised sinusoidally amplitude modulated (SAM) tones of 500 ms duration, with a 3500 Hz carrier frequency, 64 Hz modulation rate, and varying ITDs. Psychometric ITD functions were assessed in this way before and after a conditioning period during which ITDs were paired with ILDs that were systematically offset by 20° either to the left or the right. in 6 out of 7 subjects, this conditioning protocol shifted ITD functions in the predicted directions. the magnitude of this effect, however, exhibited substantial

variability across individuals. Although the effects in 2 subjects were found to be significant using bootstrap tests, data pooled across all subjects approached but just failed to reach significance ( $P = 0.063$ ). Although these data are broadly consistent with recalibration, possible effects of ITD-adaptation cannot yet be ruled out.

### **887 Learning New Pinna Cues for Sound Locations Inside and Outside the Audio-Visual Region of Space**

**Simon Carlile<sup>1</sup>**, Toby Blackman<sup>1</sup>, Joel Cooper<sup>1</sup>

<sup>1</sup>*Auditory Neuroscience Laboratory, University of Sydney*

The spectral cues to sound location are dependent on the precise morphology of the outer ear. Modifying the shape of the pinna and the subsequent spectral cues degrades localisation performance on the cone-of-confusion. for locations in the audio-visual (AV) region of space, listeners adapt to chronic modification within 30 days (Hofman et al 1998 Nat. Neurosci. 1:417-21). This experiment compares this adaptation to sound locations outside the AV region. Eight subjects wore pinnae moulds for up to 62 days during which localization performance was repeatedly measured for 76 locations surrounding the listener. Initially, there was a significant increase in cone-of-confusion errors and performance improved over the accommodation period but remained above pre-mould control. Performance for locations within the AV region of space ( $\pm 70^\circ$  from the frontal midline) was compared with locations outside. Consistent with previous studies, sound localisation was generally more accurate for frontal locations and the overall errors were larger in the non-AV region. There was, however, no relative difference in the cone-of-confusion errors between the AV and non-AV regions throughout the accommodation period. These data indicate that, despite the lack of direct visual information for the non-AV region, there is similar adaptation as in the AV region. Furthermore, the lack of difference in relative performance and rates of accommodation suggest a single underlying process for accommodation. Vision per se may not provide a direct teacher signal to drive this accommodation but some other process(es) relying on visual input may play a role.

### **888 Visual Calibration of Auditory Spatial Perception in Humans and Monkeys**

**Norbert Kopco<sup>1</sup>**, I-Fan Lin<sup>2</sup>, Barbara Shinn-Cunningham<sup>2</sup>, Jennifer Groh<sup>3</sup>

<sup>1</sup>*Technical University of Kosice, Slovakia*, <sup>2</sup>*Boston University*, <sup>3</sup>*Duke University*

At the early stages of auditory and visual processing, space is represented in different coordinate frames: the location of auditory stimuli is detected relative to the orientation of the head, while visual stimuli are detected relative to the orientation of the eyes. Since visual signals are known to help calibrate auditory spatial perception, the two modalities must align at some processing stage. Following up on previous results [Lin et al., JASA 121, 3095, 2007, and Kopco et al. SFN Abstract # 662.4, 2007], this study investigated the influence of visual spatial cues on auditory localization to determine the frame of

reference in which the visually-guided auditory calibration occurs.

Visually-guided shifts in sound localization were induced in seven human subjects and two monkeys who made eye saccades to auditory or audio-visual stimuli. On the audio-visual (training) trials, the visual component of the targets was displaced laterally by  $5^\circ$  to  $6^\circ$ . Interleaved auditory-only (probe) trials served to evaluate the effect of experience with mismatched visual stimuli on auditory localization. to dissociate head- from eye-centered reference frames, the initial fixation position of the eyes in the auditory-only trials either differed from or equaled the location used during the audio-visual training trials.

in both the humans and the monkeys, the displaced visual stimuli shifted the endpoints of saccades on the probe trials by 30 to 50%. the shifts were induced in a mixture of head- and eye-centered coordinate frames and at multiple temporal scales. These findings suggest that the neural mechanisms underlying spatial plasticity are not strictly head-centered but incorporate information about eye position, possibly at distinct processing stages. This is reminiscent of demonstrations of eye-position-dependent modulation of neural responses in the auditory pathway of non-human primates [e.g. Groh et al., Neuron, 29:509-518, 2001].

[Supported by NIH and VEGA]

### **889 Eye-Position and Cross-Sensory Learning Both Contribute to Prism Adaptation of Auditory Space**

**Qi N. Cui<sup>1</sup>**, William E. O'Neill<sup>1</sup>, Gary D. Paige<sup>1</sup>

<sup>1</sup>*University of Rochester, Rochester, NY USA*

Optical prisms shift visual space, and through adaptation over time, generate a compensatory realignment of sensory-motor reference frames. in humans, prism-induced lateral shifts of visual space produce a corresponding shift in sound localization. We recently reported that sound localization shifts toward eccentric eye position, approaching  $\sim 40\%$  of gaze over several minutes. Given that eye position affects sound localization directly, prism adaptation may well reflect contributions of both eye position and cross-sensory plasticity. Specifically, as the visual world is shifted by prisms, so too must eye position shift to fixate the same field of targets. Over time, average eye position will shift in kind, and this alone, apart from potential cross-sensory plasticity, will presumably cause a corresponding shift in sound localization. to test this new concept of prism adaptation, young (18-26yo) subjects were studied in a dark echo-attenuated room with their heads fixed, facing the center of a cylindrical screen at 2m. a non-visible speaker on a robotic arm behind the screen presented auditory targets in a random sequence across the frontal field ( $\pm 50^\circ$  Az x  $\pm 25^\circ$  El). Subjects localized targets using a laser pointer before and after 4 hr of adaptation to base-R or base-L prisms that induced an  $11.4^\circ$  visual shift L or R, respectively. in separate sessions subjects were exposed to: 1) natural binaural hearing; 2) diotic hearing devoid of meaningful spatial cues; or 3) attenuated hearing to simulate hearing loss. Results suggest that the prism adaptation of auditory space is

dependent upon two independent influences: 1) the effect of displaced mean eye position induced by the prisms, which occurs without cross-sensory experience; and 2) true cross-sensory learning in response to an imposed offset between auditory and visual space.

Supp. by NIH grants F30-DC009372, R01-AG16319, P30-DC05409, & T32-GM07356.

## **[890] Influence of Auditory and Visual Distraction On Spatial Localization**

**Marina Dobрева<sup>1</sup>, William O'Neill<sup>1</sup>, Gary Paige<sup>1</sup>**

<sup>1</sup>*University of Rochester School of Medicine & Dentistry*

We investigated the effect of spatial and non-spatial distraction on auditory and visual localization and whether distraction interferes selectively with the encoding, consolidation, or memory of target location. Human subjects were tested in a dark echo-attenuated room with their heads restrained, facing the center of a speaker-cloth screen at 2 m distance. a robotic arm with a speaker and LED presented auditory and visual targets from behind the screen in a random sequence of locations across frontal space. in a 'baseline' task, subjects first matched their eyes and a manually-guided laser pointer to a central fixation spot. a target was then presented as a 1 s train of broadband noise bursts or LED flashes (150 ms at 5 Hz). Subjects fixated the central spot until it was extinguished 6 s after target offset and then localized (with laser and eyes) the memorized target position and recorded their response with a key press. in a 'distraction' task, distracters (three 300 ms presentations; 1 s total) occurred with target presentation ("encoding"), immediately after ("consolidation"), or 1 s into the "memory" period. *Spatial* distracters included pure tones (880 Hz) or green LED flashes, presented in a random sequence of three horizontal locations. *Non-spatial* distracters included a sequence of pure tones (220-880 Hz), varying in pitch. Subjects reported (key press) the location or pitch of the last distracter with respect to the previous one, while continuing to look and point toward the central fixation spot before localizing the target.

Baseline sound localization was accurate (spatial gain, SG= ~1.0) in azimuth and <1 in elevation. SG of sound localization increased ~10% in azimuth with *auditory pitch (non-spatial)* or *visual (spatial)* distraction, regardless of timing, while visual localization was unmodified by distraction. We conclude that sound localization is generally more susceptible to distraction than its visual counterpart.

## **[891] Anterior Ventral Insula and Caudolateral Frontal Operculum As a Brain for Vocalization**

**Hiroko Kosaki<sup>1</sup>, Masashi Waga<sup>2</sup>, Mortimer Mishkin<sup>2</sup>**

<sup>1</sup>*National Printing Bureau Hospital*, <sup>2</sup>*NIMH*

Auditory-vocal interaction plays a significant role in communication. Motor theory of speech perception describes auditory sensor involves motor function, when it recognizes the sound of speech. Recent articles on insular aphasia suggested that there is significant insular contribution in both speech perception and production

(Drunkers, 1996). Revisiting of structure of insula may indicate the possible relationship between sensory perception and motor function on language and communication. to understand the mechanism of insula involvement in motor theory of speech, cortex of rhesus macaque was examined. Ventral part of anterior Insula (ProS) may be the area for sensory integration by cortico-cortical projection, except visual and olfactory modality (Chippolini and Pandya, 1999). Our former report on 1-core-5 rings structure of macaque auditory cortex (Kosaki, et al, 2003, and 2005) indicated that this ProS might be one of three pole-like areas, which are the place for integration of various sensory modalities. ProS also has the reciprocal connection with caudo-ventral part of frontal operculum (ProM), which are supposed to be a supplementary motor cortex or premotor cortex for laryngeal and mouth movement. ProS and ProM not only have a direct connection between them, but also both are connected to the cortical area, which are homologue for human Broca area. These cortical connections may be the basis for neuronal network to explain motor theory of speech.

### **REFERENCES**

- Chippolini PB and Pandua, DN. Cortical Connections of the oroparietal Opercular Areas in the Rhesus Monkey. *J. Comp. Neurol.* 1999; 403:431-438  
Dronkers NF. a new brain region for coordinating speech articulation. *Nature.* 1996 ;384:159-61  
Kosaki, H, Saunders, R.C., and Mishkin, M. Concentric scheme of monkey auditory cortex. *JASA.* 2308 , 2003  
Kosaki, H :1-core-5-rings scheme of auditory cortex. *IEICE Technical Report TL2005-8*, 1-4, 2005

## **[892] Gamma Oscillations During an Auditory Target-Discrimination Task Reflect Matches with Short-Term Memory – a Parallel Study in Humans and Rodents**

**Marcus Jeschke<sup>1</sup>, Daniel Lenz<sup>2</sup>, Christoph S. Herrmann<sup>2</sup>, Frank W. Ohl<sup>3</sup>**

<sup>1</sup>*Leibniz Institute for Neurobiology*, <sup>2</sup>*Department of Biological Psychology, Otto-von-Guericke University Magdeburg*, <sup>3</sup>*Leibniz Institute for Neurobiology & Institute for Biology, Otto-von-Guericke University Magdeburg*

Gamma-band oscillations have been implicated in a variety of cognitive functions as well as more basic stimulus-related aspects of neuronal activity. in an effort to combine a large body of these findings it has recently been proposed that gamma-band oscillations reflect the interaction of incoming sensory information with information about past stimuli stored in memory.

Here we investigated the prediction of this 'match-and-utilization' model that the strength of gamma oscillations depends on the similarity of present stimuli with stored memory templates. We employed an auditory target-discrimination task in which the subjects had to respond to one out of four frequency-modulated tones that varied with respect to two stimulus dimensions, viz. "spectral content" and "modulation direction". We conducted the study in rodents and in humans to exploit the complementary advantages of both paradigms, viz. easy intracerebral

recording from primary sensory cortex and monitoring of learning-effects in the rodent experiment, and whole scalp accessibility of EEG signals and straightforward instruction of subjects in the human experiment.

in both species, we found that the early, evoked gamma-band activity did not show task- or learning-related modulations, indicating that it reflects aspects of the physical nature of the stimuli. in contrast, the late, induced gamma-band activity was significantly influenced by the task. in both paradigms the target always elicited the strongest gamma-band response, while partial matches with the target resulted in intermediate response strengths. Assigning the role of the target to different stimuli led to the same result in the human subjects. in the animal subjects, the dependence of the gamma-band response strength on the similarity with the target developed with learning and was not found in naïve animals. in combination, our results add further support for the general validity of the match-and-utilization model of gamma-band oscillations.

### **[893] Encoding the Functional Meaning of Sound - Recognition and Representation of Auditory Targets in Ferret Frontal Cortex**

**Jonathan Fritz<sup>1</sup>, Stephen David<sup>1</sup>, Pingbo Yin<sup>1</sup>, Shihab Shamma<sup>1</sup>**

<sup>1</sup>*University of Maryland*

Frontal cortex (FC) has been conjectured to play an important role in auditory attention. Top-down projections from FC to auditory cortex, enhanced to attended acoustic stimuli, may play a role in adaptive reshaping of A1 receptive fields during behavior (Fritz et al., 2007). Before it is possible to decode the information conveyed by such top-down signals, it is essential to understand the representation of sound in the FC. We recorded from over 400 neurons in FC of behaving ferrets, trained on multiple auditory detection and discrimination tasks. They learned to detect variable tonal, tone-in-noise or click targets against a discontinuous background of rippled noise stimuli, using conditioned avoidance techniques. They also learned tonal discrimination and click rate discrimination tasks. Performance on each task in a given session required selective attention to different salient spectral frequency cues or temporal click rate cues. We recorded neuronal responses to acoustic stimuli in orbital and anterior sigmoidal cortex of FC in three ferrets during quiescent states and also while the animals were performing a sequence of multiple auditory tasks. in behavioral contexts, we observed a variety of neural patterns of “recognition” responses, ranging widely in onset latency and duration, which categorically distinguished between acoustic background and foreground stimuli. We compared target responses in the same frontal neurons during multiple successive task conditions with different acoustic targets. Responses to targets were often, but not always, independent of the acoustic identity of the target and thus could encode an abstract representation of the category of target stimuli. However, responses of some frontal cells also included sensory, motor, reward and also “rule-based” components. We discuss neural encoding of target stimuli in the frontal

cortex in terms of target recognition and functional representation of task-salient sounds during behavior.

### **[894] Neural Responses Evoked by Harmonic and Inharmonic Tones in Monkey Auditory Cortex**

**Mitchell Steinschneider<sup>1</sup>, Yonatan Fishman<sup>1</sup>**

<sup>1</sup>*Albert Einstein College of Medicine*

Inharmonicity is an important feature of auditory scene analysis. Complex tones whose components are harmonically related are perceived as a single sound object. in contrast, two sound objects are perceived when a single, resolved component of a harmonic complex is sufficiently mistuned: one corresponding to the harmonic complex and the other to the mistuned tone (e.g., Moore et al., 1986). When high, unresolved harmonics are mistuned, inharmonicity is detected by the perception of “beats” produced by amplitude fluctuations in the waveform temporal envelope. We are investigating neural responses involved in the detection of inharmonicity by examining auditory evoked potentials (AEPs) and multiunit activity (MUA) evoked by harmonic and mistuned tone complexes in monkey auditory cortex. Inharmonicity was produced by mistuning either the 3rd (resolved) or 9th (unresolved) harmonic while maintaining a constant f0 of the complex, or by shifting the f0 and maintaining a constant frequency of the 3rd or 9th harmonic. the 3rd and 9th harmonics were placed at or near the best frequency of the recording site. AEPs evoked by complexes with mistuned 3rd harmonics show enhanced negativities relative to harmonic sounds similar to AEPs recorded in humans under comparable listening conditions (e.g., McDonald and Alain, 2005). MUA evoked by inharmonic complexes may be augmented or suppressed relative to that evoked by harmonic complexes based upon a complex interaction between the spectral sensitivity of recording sites and the spectral composition of the sounds. MUA obtained for the 9th harmonic condition reveal both changes in response strength and phase-locking to “beat” frequencies of the inharmonic complexes. the relevance of these response modulations for perceptual “pop-out” of mistuned resolved harmonics and detection of inharmonicity for unresolved harmonics continues to be explored.

Supported by DC00657.

### **[895] Multi-Second Adaptation of Neural Responses to Tone Sequences in the Avian Forebrain and it's Relationship with the Build-Up of Auditory Streaming.**

**Christophe Michey<sup>1</sup>, Mark Bee<sup>1</sup>, Andrew Oxenham<sup>1</sup>, Georg Klump<sup>2</sup>**

<sup>1</sup>*University of Minnesota*, <sup>2</sup>*University of Oldenburg*

Many ecologically relevant sounds occur as part of sequences, which typically unfold over the course of a few seconds or more. Bird songs and human speech are two examples. Because natural environments typically contain multiple sound sources, sequences produced by concurrent sources may overlap. the ability to parse such

concurrent sequences into separate auditory "streams", which correspond to individual sources and can be attended selectively, is likely to be a key component of adaptation to diverse ecological environments. Recent studies have revealed that neural responses to tones in the primary auditory cortex (A1) of cats and macaques show adaptation over the course of several seconds, not just milliseconds. It has been suggested that this multi-second adaptation could explain the build-up of auditory stream segregation, i.e., the fact that the perceptual segregation of a sound sequence into separate streams typically requires a few seconds in order to occur. Here, we extend these findings by demonstrating multi-second adaptation to tone sequences in the forebrain of European starling (*Sturnus vulgaris*). We document how multi-second adaptation in field L2 (the avian homologue of mammalian A1) depends on the spectral and temporal parameters of the sequence, including tone duration and inter-tone interval. Finally, we show that this adaptation can account for various rates of build-up, depending not only on stimulus parameters such as frequency separation and stimulation rate, but also on the listener's intention, thus providing a flexible dynamic auditory-scene-analysis mechanism. [Work supported by NIDCD RO107657 (CM and AO), NSF INT-0107304 (MAB), and DFG GK 306 (GMK)].

#### **[896] Dynamics of Rapid Plasticity During Positively and Negatively Reinforced Behavior in Auditory Cortex**

**Stephen David<sup>1</sup>, Jonathan Fritiz<sup>1</sup>, Shihab Shamma<sup>1</sup>**

<sup>1</sup>*University of Maryland*

As behavioral conditions change, neurons in primary auditory cortex (A1) adjust their tuning properties in a way that may optimize responses to behaviorally important stimuli. a previous study in our laboratory found that when a pure tone is associated with a negative reinforcer, A1 neurons selectively increase their response to the frequency of the tone. However, it is unclear what information is encoded by this narrowband gain change. It could reflect a general enhanced response to any important stimulus, but it could also encode information about stimulus reward value. to study this issue, we measured the effects of a positive reinforcement task that used the same stimuli but reversed their reward value. Ferrets were trained to ignore (by not licking) a sequence of reference stimuli, composed of 1-4 temporally orthogonal ripple combinations (TORCs) and to respond (by licking) 100-1000 ms after the onset of a pure tone target following the TORCs. Hits were rewarded with a small quantity of water (~0.1 ml). Early licks and misses were punished by a timeout.

We recorded extracellular data from 70 isolated A1 neurons of two animals performing the tone detection task. Data were also recorded during passive presentation of the task stimuli before and after behavior. We compared spectro-temporal receptive fields (STRFs) estimated from TORCs before, during and after behavior. Across the entire set of neurons, the average STRF slightly decreased its gain at the target frequency during the first

half of the behavioral session. However, the gain then rebounded, and after behavior the average gain at the target frequency increased to 10% above the original level. Neurons were more likely to change their tuning if the target elicited a sustained response rather than a transient or suppressive response. the fact that gain increases for both positively and negatively reinforced stimuli suggests that plasticity in A1 signals important stimuli, regardless of their reward value.

#### **[897] Representation of the Chutter Call in the Guinea Pig Primary Auditory Cortex**

**Mark Wallace<sup>1</sup>, Alan Palmer<sup>1</sup>**

<sup>1</sup>*MRC, Institute of Hearing Research, Nottingham, UK*

Some communication calls contain a mixture of complex harmonic tones, frequency modulated ramps and noise bursts separated by brief periods of silence. One such call is the guinea pig chutter which we used to study the representation of thalamic input in the low-frequency end of the primary auditory cortex - AI(LF). a single exemplar of this chutter call, along with pure tones, was presented to anaesthetised guinea pigs via a closed sound system. the chutter contained 10 sequential components or elements which were each capable of producing an increase in firing among forebrain neurones. Out of the 264 cortical units in AI(LF) there were 48 different response combinations to the 10 information bearing elements within the chutter call. Some of these response combinations were much more common than others. the upper layers of AI were organized into clusters or modules where the cells had similar response latencies and similar temporal response properties to the chutter. We also recorded from 46 low-frequency units in the medial geniculate body and they gave the same response combinations as occurred in the cortex. Thus, while most cortical responses seemed likely to have been directly inherited from the thalamic input, there were a few examples of constructive convergence. We conclude that the upper layers of AI are organised into clusters where the cells have similar response latencies and generally respond to a unique combination of elements present within a complex vocalization like the chutter.

#### **[898] Guinea Pig Primary Auditory Cortex Neurons Discriminate Between Vocalizations From Animals of Different Ages Using a Rate Code**

**Jasmine M S Bailey<sup>1</sup>, Alan R Palmer<sup>1</sup>, Mark N Wallace<sup>1</sup>**

<sup>1</sup>*MRC Institute of Hearing Research, Nottingham, United Kingdom.*

As animals increase in size, the pitch of their vocalizations generally becomes lower, probably as a result in changes in their vocal tract length. the fundamental frequency (F0) of the guinea pig (GP) short *purr* call was found to decrease from 476-261 Hz as the animal's size increased between 8-100 days of age. One short *purr* call was adapted so that its F0s corresponded to calls from animals aged 8, 12, 44, and 100 days old. the responses of single units to these four *purrs* were compared. Mean rate

differences between the responses to the four stimuli were considered to show selectivity if the firing rate changed monotonically by more than 20% between the calls with the lowest and highest F0. If the response to the purr calls with intermediate F0s was the largest or smallest (by a minimum of 20% relative to adjacent F0 values) the response was considered to be selective but non-monotonic. Of the cells that responded to the purrs in the primary auditory cortex (A1) a large proportion, 36/54 (67%) showed call selectivity using these mean rate criteria. The majority, 23/36 (64%) gave monotonic responses (mean change 300%, range 24-1516%) and 13/36 (36%) gave non-monotonic responses (mean change 97%, range 20-552%). All of the monotonic sensitivity to the purrs and most of the non selectivity could be explained by features of the frequency response areas in response to pure tones. However, the response selectivity of the non-monotonic group could not be predicted by frequency response areas. Although the frequency response area of a purr responsive cell has a strong predictive value for indicating which example of the purr call will produce the highest firing rate, spectral sensitivity is not the only factor involved in determining the response.

### **[899] Pitch is Represented by a Rate-Latency Code in Monkey Primary Auditory Cortex**

**Yonatan Fishman<sup>1</sup>, Mitchell Steinschneider<sup>1</sup>**

<sup>1</sup>*Albert Einstein College of Medicine*

Many natural sounds are characterized by a harmonic spectrum and elicit a pitch matched to their fundamental frequency (f0), even when spectral energy at the f0 is absent, a phenomenon known as "virtual pitch" (VP). While auditory cortex has been implicated in VP perception, precisely how VP is represented at the cortical level remains unclear. Here we report data suggesting how the pitch of pure tones and harmonic complex tones may be co-represented in primate primary auditory cortex (A1). Using pure tones and harmonic complexes missing the f0 and with spectra overlapping the excitatory frequency response area of the neural populations, we find that the lower the pitch of the sound, the greater the proportion of later, sustained multiunit activity (MUA) in macaque A1. Pitch is represented by the temporal distribution of activity in A1: sounds of higher and lower pitch evoke activity concentrated in earlier and later portions of the neural response, respectively. Pure tones and harmonic complexes with the same pitch evoke a similar amount of sustained neural activity, which exceeds that evoked by the individual components of the harmonic complexes. These response patterns are scale-invariant, persisting when MUA is normalized to the total or maximal evoked activity. The latency and duration of the N1 component of the auditory evoked potential concurrently recorded in laminae 1-2 correlate with the f0-related MUA response patterns. These findings suggest that the pitch of pure tones and complex tones is represented by a common, scale-invariant rate-latency code in A1.

### **[900] Cortical Network Plasticity to Communication Sounds in Awake Mice**

**Edgar Galindo-Leon<sup>1</sup>, Robert Liu<sup>1</sup>**

<sup>1</sup>*Emory University*

An important question in the neurobiology of communication perception concerns the neural changes associated with the learning of behaviorally relevant sounds. The mouse is developing into a promising model to address this issue: it features a well-characterized ultrasound communication system between pups and adults; it holds the potential for genetic dissection of underlying mechanisms; and, as we demonstrate in this presentation, electrophysiological studies in awake animals are feasible. We investigate the encoding of natural mouse pup ultrasound calls in the auditory cortex of awake, restrained animals that recognize the calls' behavioral significance (mothers), as well as those who do not (virgins). Local field potentials (LFP) and well-isolated single units (SU) are recorded from the high-frequency region of the left mouse auditory cortex. We introduce the novel concept of trial-by-trial LFP 'phase reliability' (PR) as a useful method to differentiate neural network activity. The largest differences in PR between mothers and virgins are found at sites whose best frequencies (BF) are more than ~20 kHz below the frequency of the ultrasound calls. Moreover, the percentage of tone-excited SU's that respond to pup calls is significantly increased in mothers, regardless of whether the BF is near or far from the call frequency. We discuss the possibility that our results demonstrate plasticity in either the high frequency synaptic input to low BF sites, and/or the synchronization of spiking activity within the local neural population. Support provided by NIH R01 DC008343 and the NSF Center for Behavioral Neuroscience.

### **[901] A Comparison of Binaural Sensitivity in the Onset- and offset-Responses of Primary Auditory Cortex Neurons in Ketamine-Anaesthetised Ferrets**

**Douglas Hartley<sup>1</sup>, Jan Schnupp<sup>1</sup>, Johannes Dahmen<sup>1</sup>, Andrew King<sup>1</sup>**

<sup>1</sup>*Oxford University, UK*

Onset responses are the dominant neuronal response type recorded under barbiturate anesthesia in primary auditory cortex (A1). In contrast, neurons with paired onset- and offset-responses, have been described in A1 of both ketamine- and halothane-anesthetized and awake animals. Furthermore, in monaurally-stimulated awake cats, cortical onset- and offset-frequency-receptive fields (FRFs) usually cover different frequency ranges in a given cell.

Sensitivity to binaural cues has also been seen in the onset responses of A1 neurons, including sensitivity to interaural time differences (ITDs) and, in separate studies, sensitivity to interaural level differences (ILDs). In order to characterize further the binaural properties of A1 neurons, we investigated the sensitivity of neurons to ITDs and ILDs in both the onset- and offset-responses of ketamine-anaesthetised ferrets. Recordings were made using multichannel recording electrodes in response to i) ILDs

over a range of average binaural levels in unmodulated broadband noise, and ii) envelope ITDs in sinusoidally amplitude-modulated broadband noise. In the same recordings, we also assessed binaural frequency tuning and fine-structure ITD sensitivity using pure-tone stimuli. Earlier psychophysical experiments in humans suggest there is a minimum integration period of between 100-150 ms for the resolution of spatial information. Thus, to investigate neural correlates of this phenomenon, ILD and ITD sensitivity was assessed in response to 500, 100 and 20 ms stimuli. It was common to see both onset- and offset-responses to binaural stimuli of >100 ms in duration, whereas at shorter stimulus durations (20 ms), distinct onset- and offset-responses could not be distinguished. Single units were commonly sensitive to both ILDs and ITDs in the envelope and/or fine-structure of the stimulus. Sensitivity to both binaural cues as well as the FRFs often changed significantly from the onset- to the offset-response in the same units.

## **[902] Natural Wideband Acoustic Stimuli Reveal Complex Spectral Integration in Auditory Cortex**

**Paul Watkins<sup>1</sup>, Dennis Barbour<sup>1</sup>**

<sup>1</sup>*Washington University in St Louis*

Sensory neurons typically vary their action potential spiking patterns when presented with stimuli containing energy distributed over a relatively small, compact region of the sensory epithelium. This region of sensitivity is referred to as the classical receptive field (cRF). Neural responses to the cRF in primary visual cortex can be modified by stimulus energy in a surrounding region, the non-classical receptive field (ncRF); however, stimuli with energy confined only to the ncRF do not alter spiking behavior by themselves. Previous studies in auditory cortex have demonstrated the possibility that many auditory neurons contain inputs from an extremely wide frequency range, even though the auditory cRF is often relatively compact in frequency. This finding together with studies demonstrating increased receptive field complexity under experimental conditions of lessened inhibition imply that these subthreshold (i.e., ncRF) inputs may be actively involved in coding stimuli under natural conditions where inhibitory inputs are modulated by sensory stimulation. Understanding the spectral integration of auditory neurons will be important for understanding how such neurons process natural wideband stimuli, particularly species-specific vocalizations such as human speech. We measured cRFs of well-isolated single neurons in the primary auditory cortex of awake marmosets using stationary, parameterized, wideband random spectral stimuli (RSS) to create an optimal linear stimulus (OLS)—the wideband stimulus matching the best linear estimate of the neuron's frequency response. We then recorded the neuron's response to filtered versions of the OLS and of species-specific vocalizations. We identified frequencies outside of the cRF but which induced significant changes in spiking patterns elicited by the filtered OLS and vocalizations. The majority of neurons sampled demonstrated changes in spiking patterns from at least one non-classical frequency. Such non-classical

frequencies were often scattered over a large bandwidth. Filtered vocalizations typically revealed a larger bandwidth of spectral integration than filtered OLS in the same neuron. We also found evidence for a correlation between the number of frequencies contributing to the ncRF and the response of the neuron to wideband spectral contrast—a feature potentially important for encoding vocalizations in noise.

## **[903] Non-Classical Effects and Nonlinear Coding Schemes in Primary Auditory Cortex of the Awake Ferret**

**Barak Shechter<sup>1</sup>, Didier Depireux<sup>1</sup>**

<sup>1</sup>*University of Maryland School of Medicine*

Neural computation in sensory systems is often modeled as a first order linear system. This first order approximation is computed by reverse correlating a stimulus with the spike train it evokes. Methods have been developed generalizing this procedure to multi-dimensional stimuli. The spectro-temporal receptive field (STRF) is an example of a two-dimensional linear characterization of processing in the auditory pathway. This first order approximation often falls short because neural output is inherently nonlinear (e.g. discrete events and non-negative spiking rates). We examine the degree of nonlinearity by using both spectrally and temporally modulated auditory gratings. We have also developed nonlinear methods of extending the STRF model which we apply to the same cortical responses. With these new methods, we analyze the higher order nonlinearity both within the classical receptive field and in its surround, and show non-classical effects such as complex spectral enhancement.

## **[904] Intracortical Auditory Evoked Potentials to Frequency Deviants in an Oddball Paradigm in the Awake Rat Auditory Cortex**

**Wolfger von der Behrens<sup>1</sup>, Bernhard Gaese<sup>1</sup>**

<sup>1</sup>*J.W. Goethe-University, Frankfurt*

Neuronal representation of auditory stimuli depends significantly on the history of auditory events preceding a stimulus. This dependency is discussed as a neuronal basis for detecting behaviourally relevant changes in the auditory environment. A neural correlate of this in human EEG is the well described change detection process of mismatch negativity (Näätänen et al., *Trends in Neuroscience*, 24:283, 2001). It has been shown for single neurons that responses in the auditory cortex adapt to repetitive tones over time while representing rarely and randomly occurring deviants veridically (Ulanovsky et al. *Nature Neuroscience*, 6:391, 2003).

Auditory event-related potentials (ERP) evoked by a repetitive standard tone were compared to a rarely occurring deviant. Recordings were performed intracortically in the awake rat auditory cortex using four chronically implanted tungsten electrodes. Pure tone stimuli (200 ms duration) were presented with a repetition rate of 1 Hz at 50 dB SPL. Standard and deviant stimuli differed in frequency (0.25 or 0.5 octave). The probability of the deviant was either 10% or 30%.



Basically, intracortical evoked responses to pure tones consisted of one fast positive wave with a short latency in the range of 25 ms and a negative wave with a latency of around 100 ms. a reliable and consistent difference in the amplitude of this negative component was found between standard and deviant. the magnitude of the difference increased with decreasing probability of the deviant and increasing frequency separation. the strongest effect was found for a low probable deviant (10%) and a frequency separation of 0.5 octaves. This response pattern in the 100-ms ERP-component correlated well to spike responses of single neurons at much shorter latencies (around 15 ms). Thus two different approaches for measuring neuronal adaptation could be matched: fast single neuron spike responses with slower evoked negative potentials.

### **[905] Functional organization of the Auditory Cortex Fields in the Rat**

Oliver Profant<sup>1</sup>, Jana Burianova<sup>1</sup>, Jolana Grecova<sup>1</sup>, **Josef Syka<sup>1</sup>**

<sup>1</sup>*Institute of Experimental Medicine ASCR, Prague, Czech Rep.*

The study was aimed at understanding functional organization of individual fields of the auditory cortex (AC) in Long Evans rats. Fields were characterized on the basis of the neuronal responses to simple acoustical stimuli - broad band noise (BBN) and pure tone bursts. Neuronal activity was recorded in ketamine-xylazin anaesthetised rats under acoustical stimulation in the free field conditions. a 16-channel multielectrode was inserted perpendicularly to the surface of the AC allowing simultaneous recording of the neuronal activity from multiple neurons in different cortical layers. Five fields were distinguished on the basis of neuronal response pattern: primary auditory field (AI), anterior auditory field (AAF), suprarhinal auditory field (SRAF), posterior auditory field (PAF) and belt area. Neurons in the AI, AAF and SRAF typically responded to both pure tones and BBN stimulation and demonstrated tonotopic organization. in contrast to this neurons located in the belt reacted only to BBN stimulation. the tonotopic organization was not observed in the PAF. Individual fields were characterized by tonotopic organization, response latency, pattern, duration and strength. the onset response pattern was dominant in all fields, however, the occurrence of the pattern differed from field to field. Neurons in AI demonstrated among all fields the shortest latency and also the highest response strength to BBN stimulation. a depth profile of the latency of neuronal responses was constructed within six layers of the AC. the shortest response latency was found in neurons of the layer IV whereas the longest latency demonstrated neurons of the layers I and II. Our results confirmed existence of several fields of the AC in rat based on different features of the neuronal responses. This information may be useful in finding out the principles of processing of different types of complex, behaviorally relevant sounds in the AC.

Supported by: GACR 309/07/1336, IGA NR 8113-4, LC 554.

### **[906] Neuronal Responses to Vocalization Signals in the Auditory Cortex of the Guinea Pig**

**Daniel Suta<sup>1</sup>**, Jiri Popelar<sup>1</sup>, Jana Burianova<sup>1</sup>, Josef Syka<sup>1</sup>

<sup>1</sup>*Institute of Experimental Medicine ASCR, Prague, Czech Republic*

Responses of neurons in the auditory cortex (AC) to typical guinea pig vocalizations (whistle, purr, chatter, chirp) were recorded in ketamine-xylazine anesthetized guinea pigs using multichannel electrodes (4 shanks, each with 4 recording sites) advanced orthogonally to the cortical surface. Neurons were localized in the primary AC (AI), dorsocaudal field (DC) and in the ventral and dorsal belt areas of the AC. Acoustical stimuli were presented in free field conditions. Majority of neurons responded to several calls. There were no significant differences between neuronal responses to vocalizations in the AI and DC fields. the responses in the AI and DC were characterized by a short latency and temporally precise reflection of the fundamental acoustical features of the guinea pig vocalization sounds. Response patterns were typically highly correlated in case of neurons recorded at the same shank (i.e. within the same cortical column) whereas lower correlation between response patterns was found in case of neurons recorded from separate shanks. Neuronal responses to calls consisting of several phrases (purr, chatter) demonstrated increasing synchronization in the ventro-dorsal direction. Long-lasting call whistle evoked various types of the response pattern - from a sustained type to segmented types with one or more short peaks in the peristimulus time histogram. in contrast to the core areas (AI, DC), less structured responses were present in the belt areas with a more sustained and less temporally precise pattern. the results show frequent occurrence of the phasic type of neuronal responses in the auditory cortex similar to data reported previously in the medial geniculate body (Suta et al., Exp Brain Res, 2007). in addition, the data point at non homogeneity of neuronal responses not only among individual fields but also within particular fields of the auditory cortex.

Supported by GACR 309/07/1336, IGA NR/8113-4, AVOZ50390512 and LC 554.

### **[907] Dynamic Auditory Representation in Ferret Frontal Cortex During Passive Listening and During Performance of an Auditory Categorization Task**

**Pingbo Yin<sup>1</sup>**, Jonathan Fritz<sup>1</sup>, Shihab Shamma<sup>1</sup>

<sup>1</sup>*Institute for System Research, University of Maryland, College Park, MD 20742*

The frontal cortex plays a central role in the selection and control of behavior, and by top-down projections, contributes to dynamic gating of salient sensory input. Through some frontal neurons may exhibit substantial selectivity with regard to physical parameters of the stimulus, the responses are often highly adaptive and the sensory inputs to frontal units are modulated by previous experience or training, motivation, behavioral goals and internal state. in the present experiments, we explored the

neuronal mechanisms underlying such modulation of auditory inputs. Ferrets were trained on an auditory categorization task, in which the animals learned to identify a falling 2-tone contour from a rising 2-tone contour, irrespective of tone frequency and the frequency interval between the two tones (Yin et al., 2007). Single units were recorded from frontal cortex during task performance and also during passive listening to the standard stimulus set before and after the task. the standard stimulus set included 50 stimuli and spanned 5 acoustic categories (broadband modulated noise, ferret vocalizations, tone pips, 2-tone upward and downward contours). the broadband modulated noises and ferret vocalizations were appeared as irrelevant background sound during the delay periods of the task trials. Our preliminary data indicate: 1) neuronal responses during passive listening before the task performance were based upon the five acoustic categories; 2) during task performance, neuronal responses to auditory stimuli were highly dependent on the functional role they played in the behavioral task, such as 'sample', 'match', or 'non-match' sounds; 3) this adaptive response modulation by task meaning persisted during passive listening to the same auditory stimuli after task performance.

### **[908] Modulation Rate Tuning in Core and Belt of Macaque: Effects of Carrier Duty Cycle**

**C.R. Camalier**<sup>1</sup>, William R. D'Angelo<sup>1</sup>, Susanne J. Sterbing-D'Angelo<sup>1</sup>, Troy A. Hackett<sup>2</sup>

<sup>1</sup>*Ctr Integrative and Cognitive Neuroscience, Dept Psychology; Vanderbilt Univ.*, <sup>2</sup>*Dept Speech and Hearing Sciences; Vanderbilt Univ*

According to our working model of the primate auditory cortex, information is processed in serial/parallel by a network of areas distributed among three different regions: core, belt, and parabelt. Anatomical and physiological findings suggest that the projections of neurons in the core region converge upon the belt region in a manner that produces temporal and spectral integration. This convergence results in wider frequency tuning functions in belt, and would presumably lead to lower entrainment rates for temporally modulated stimuli. However, few studies have characterized temporal tuning in the auditory cortex of the awake primate (e.g. Liang et al 2002, Malone et al. 2007). This study characterizes tuning curves to temporally modulated stimuli in caudal auditory core and belt. We recorded responses from single neurons in the awake, passive listening macaque to a battery of stimuli with modulation rates ranging from 3 to 957 Hz: Three different carrier waveforms were used: sinusoidal amplitude modulated Gaussian noise, trains of clicks, and Gaussian noise modulated by transposed sine waves (see Bernstein and Trahiotis 2002). Rate and temporal modulation transfer functions were compared for these different carriers from single units across caudal auditory cortex, primarily A1, CM, CL, and ML. Comparing tuning properties across carrier type allows for a comparison of duty cycles where the temporal frequencies are constant. Thus, this allows us to evaluate whether cortical neurons across core and belt act as temporal modulation rate

detectors and/or are also responding to other features, such as envelope shape.

### **[909] Spectral Density Discrimination**

**Christophe Stoelinga**<sup>1</sup>, Robert Lutfi<sup>1</sup>

<sup>1</sup>*Auditory Behavioral Research Lab, Univ. of Wisconsin - Madison*

Spectral density (D), defined as the number of partials comprising a sound divided by its bandwidth, has been suggested as cue for the identification of the size and geometry of sound sources.<sup>1</sup> Little data is available, however, regarding how well human listeners are able to discriminate differences in spectral density. in a cued, single-interval, forced-choice procedure with feedback, three highly-practiced listeners discriminated differences in the spectral density of multitone complexes varying in bandwidth and frequency. within a block of trials the bandwidth and the number of tones comprising the cue was fixed; the comparison had the same bandwidth, but either a greater or lesser number of tones than the cue on any trial. the listener's task was to indicate whether the number of tones comprising the comparison was greater or less than that of the cue. to reduce extraneous cues for discrimination the overall level of complexes was roved and the frequencies were drawn at random uniformly over bandwidth on each presentation. a family of psychometric functions was obtained relating percent correct discrimination to the number of tones in the comparison for each number of tones comprising the cue (N = 6, 11, 21 or 31). the slope and intercept of the functions varied systematically with N in a manner consistent with Weber's Law (constant Weber fraction of  $\Delta D/D \approx 0.3$ ). the upper asymptote, moreover, decreased with N as expected based on known limits in the ear's ability to resolve closely spaced frequencies. the results are considered in terms of their implications for the identification of sound source properties based on spectral density. [Research supported by NIDCD grant 5R01DC006875-02].

<sup>1</sup> Lutfi, R.A. (2007). Human Sound Source Identification. in Springer Handbook of Auditory Research: Auditory Perception of Sound Sources Edited by W.A. Yost. and A.N Popper (Springer-Verlag, New York), in press.

### **[910] Level Dominance in Source Identification From Synthesized Impact Sounds**

**Robert Lutfi**<sup>1</sup>, Christophe Stoelinga<sup>1</sup>, Ching-Ju Liu<sup>1</sup>

<sup>1</sup>*Auditory Behavioral Research Lab, Univ. of Wisconsin - Madison*

Impact sounds were synthesized according to standard textbook equations given for the motion of loosely-suspended, metal plates. in a two-interval, forced-choice procedure highly-practiced listeners identified from these sounds a predefined class of target plates based on their particular material and geometric properties. the effects of two factors on identification were examined: the relative level of partials comprising the sounds (reL) and the relative amount of information each partial provided for identification (reH). in different conditions one factor was

fixed while the other either increased or decreased with frequency. the effect on listener identification in each case was determined from a discriminant analysis of trial-by-trial responses, yielding a vector of listener decision weights on the frequency and decay of individual partials. the decision weights increased proportionally with reL, but were largely uninfluenced by reH – a result exactly opposite to expectations based on the behavior of a maximum-likelihood observer. the results are compared to similar results obtained recently for the discrimination of arbitrary tone sequences [Lutfi and Jesteadt (2006) JASA 120(6), 3853-3860]. [Research supported by NIDCD grant 5R01DC006875-02].

### **[911] The Effect of Onset Asynchrony On Relative Weights in Profile Analysis**

Jinyu Qian<sup>1</sup>, Virginia Richards<sup>1</sup>

<sup>1</sup>University of Pennsylvania

Relative weights were derived to explore the effect of onset asynchrony on decision strategies in profile analysis. Subjects detected an intensity increment in the 1000-Hz signal component of multi-tone complexes using a two-alternative forced-choice procedure. the frequency components ranged from 200 to 5000 Hz and were equally spaced on a logarithm scale. to derive relative weights, normally distributed random perturbations (with zero-mean and a standard deviation of 1 dB) were added in phase to each component of the spectrum. Six conditions were tested depending on the number of frequency components (either 5 or 15 tones) and the onsets of the signal relative to the non-signal components. the signal component either had the same onset as the non-signal components (simultaneous conditions) or started earlier than the non-signal components by either 100 ms (leading-100 conditions) or 300 ms (leading-300 conditions). the non-signal components were 200 ms in duration. All components had the same offset. the overall level of the stimulus was randomly chosen on each interval. Relative weights were derived for the overall level randomization and each frequency component in the multi-tone complex. Thresholds and relative weights were compared across conditions. Consistent with earlier studies, the thresholds were lowest in the simultaneous conditions and highest in the leading-300 conditions [e.g. D. M. Green and H. Dai, Auditory Physiology and Perception, 471–477 (1992)]. Across conditions, the relative weights for overall level randomization increased almost linearly with the thresholds. One possible explanation is that in the leading conditions, due to the segregation of the signal away from the non-signal components, subjects relied more on the level of the signal component alone (intensity discrimination) than on across-frequency level comparisons. [Supported by NIH RO1 DC002012]

### **[912] Speaker Size Discrimination for Acoustically Scaled Versions of Naturally Spoken Words**

Yoshie Aoki<sup>1</sup>, Toshio Irino<sup>1</sup>, Hideki Kawahara<sup>1</sup>, Roy D. Patterson<sup>2</sup>

<sup>1</sup>Faculty of Systems Engineering, Wakayama University,

<sup>2</sup>CNBH, Dept. of Physiology, Development, and Neuroscience, Cambridge University

The sounds that convey words from speaker to listener contain information about the length of the speaker's vocal tract as well as its shape (the message). Humans can extract the message from the voices of men, women, and children without being confused by the size information, and they can extract the size information without being confused by the message. This suggests that the auditory system can extract and separate information about vocal tract shape from information about vocal tract length (VTL) (strictly speaking, acoustic scale). It has been hypothesized that the auditory system applies a scale transform to sounds to accomplish the segregation [Irino and Patterson, Speech Commun. 36, 181-203 (2002)]. Smith et al. [J. Acoust. Soc. Am. 117(1), 305-318 (2005)] and Ives et al. [J. Acoust. Soc. Am. 118(6), 3816-3822 (2005)] performed discrimination experiments with acoustically scaled vowels and syllables, respectively, and demonstrated that the ability to discriminate speaker size extends beyond the normal range of speaker sizes. We extended the size discrimination experiments to naturally spoken, four-mora Japanese words (i.e. four syllable words) to demonstrate that size perception is robust to the rigors of naturally spoken words. Size discrimination was measured in a 2AFC experiment with five reference combinations of VTL and glottal pulse rate (GPR) as in Ives et al. 2006. Just Noticeable Differences (JNDs) for VTL were calculated from the psychometric functions and averaged about 6%. the variability across subjects and VTL-GPR combinations was relatively small. the value, 6%, is a little greater than the 5% observed in the syllable experiment (Ives et al., 2005) and a little smaller than the 8% observed in the vowel experiment (Smith et al., 2005). the JND for loudness and duration is typically 10% or a little more. the results suggest that size perception is robust to the variation in naturally spoken speech.

### **[913] The Speech Critical Band for Vowels: Frequency Resolution is Governed by Attributes of the Acoustic Speech Signal**

Eric W Healy<sup>1</sup>, Kimberlee a Crass<sup>1</sup>

<sup>1</sup>University of South Carolina

The hypothesis tested was that the frequency resolution employed during the reception of some speech materials is limited or governed by attributes of the acoustic speech signal, rather than attributes of the physiological auditory system. English vowels in /hud/ context were filtered to bands just wide enough to provide recognition in three frequency regions (low, mid, and high). the frequency resolution of the acoustic signal within each region was controlled using a vocoder simulation. As the number of vocoder sub-bands increased, the bandwidth of each decreased, increasing acoustic resolution. Performance of

18 normal-hearing (NH) listeners improved and reached asymptote as the frequency resolution within each separately-presented region increased. the signal resolution at performance asymptote, a measure of the resolution employed by listeners to process the speech, was found to be lower than would be predicted by psychophysical tuning. This Speech Critical Band (S-CB) for vowels was found to be 1.6 times the width of the psychophysical Critical Band (CB, measured in ERBs) in the low-frequency region, and 1.8 times the CB in the mid and high regions. Thus, the frequency resolution employed by NH listeners when processing these materials appears to be limited by the sparse spectral content of the acoustic speech signal and does not make use of the full resolving power of the auditory system. These results suggest that a "tolerable broadening" may exist, in which reception of English vowels is unaffected up to a limit. These findings have implications for both sensorineural hearing impairment and cochlear implants, for which frequency resolution can be poorer than normal.

#### **914 Spectral Shape Discrimination for Various Stimulus Paradigms**

**Mini Shrivastav<sup>1</sup>, David Eddins<sup>2</sup>**

<sup>1</sup>University of Florida, <sup>2</sup>University of Rochester

Spectral shape is an important cue for the perception of speech and non-speech stimuli. Spectral shape discrimination has been studied using a variety of tasks and stimulus conditions including multi-tonal complexes and broadband noise. There is evidence to show that spectral shape discrimination thresholds vary with the task at hand and the nature of the stimuli used. Hence, it is difficult to compare findings across different experiments that use these various stimulus paradigms. the present study aims at measuring spectral shape discrimination thresholds within the same set of listeners for two different stimulus paradigms. Thresholds will be measured for a group of 10 young normal hearing listeners for the following stimulus paradigms: 1) detecting an increment in a equal-amplitude random phase multi-tonal complex, and 2) detecting a peak in a shaped broadband noise. the overall bandwidth of the stimuli (250-4200 Hz) and the spectral location of the peak (920 Hz) will be the same for both paradigms. the data will provide information on how spectral shape discrimination within the same group of listeners varies as a function of the stimulus paradigm used to measure it.

#### **915 Training Induced Improvements in the Ability to Detect Spectral Modulation**

**Andrew T. Sabin<sup>1</sup>, Cara L. DePalma<sup>1</sup>, David A. Eddins<sup>2</sup>, Beverly A. Wright<sup>1</sup>**

<sup>1</sup>Northwestern University, Department of Communication Sciences and Disorders, <sup>2</sup>University of Rochester, Department of Otolaryngology

The pattern of peaks and valleys of sound level spread across audio frequency is one of the primary acoustical cues used to distinguish speech sounds, musical timbres, and sound locations in the vertical plane. to date there has been little investigation into whether the ability to detect

such spectral patterns can be improved through practice. Here we examined this possibility by training normal-hearing listeners on a spectral modulation detection task. the listeners had to distinguish a noise carrier with a flat spectrum from one with a sinusoidal spectral modulation, and the modulation depth was varied adaptively to determine the spectral modulation detection threshold. Ten trained listeners practiced spectral modulation detection 1 hr/day for 7 days using a 100-ms stimulus spanning 200-1600 Hz with a spectral modulation frequency of 1 cycle/octave. Thresholds on the trained condition improved significantly more in these trained listeners (from 10.5 to 7.6 dB) than in ten control listeners who only participated in pre- and post-training sessions (from 9.8 to 9.3 dB). Interestingly, the trained listeners did not show more improvement than controls on two untrained spectral modulation frequencies (0.5 and 2 cyc/oct; 200-1600 Hz) or on an untrained range of audio frequencies (1 cyc/oct; 1600-12800 Hz). Thus the training-induced improvements were specific to the trained spectral modulation frequency and range of audio frequencies. This specificity to the trained stimulus provides some support for the hypothesis that the auditory system analyzes spectral shape via channels tuned to both spectral modulation and audio frequency. Further, the demonstration that the ability to detect spectral modulation improves with practice suggests that training might help normal-hearing listeners improve on real-world tasks that require fine spectral shape perception, and hearing-impaired individuals compensate for their degraded internal representation of spectral contrast. (Supported by NIH/NIDCD)

#### **916 The Minimum Audible Difference in Direct-To-Reverberant Energy Ratio and it's Relationship to Room Acoustics**

**Erik Larsen<sup>1</sup>, Nandini Iyer<sup>2</sup>, Charissa Lansing<sup>3</sup>, Albert Feng<sup>3</sup>**

<sup>1</sup>Harvard-MIT Division of Health Sciences and Technology,

<sup>2</sup>Wright-Patterson AFB, <sup>3</sup>University of Illinois at Urbana-Champaign

Direct-to-reverberant energy ratio (D/R) decreases monotonically with increasing source-to-receiver distance. We found that changes in D/R are discriminated primarily using spectral cues, and that temporal cues may be used but only when spectral cues are diminished or not available. Further, sensitivity to interaural cross-correlation is too low to be useful in typical listening conditions. These findings are based on acoustic analysis of these variables in an auditorium and two psychophysical experiments. the first experiment involved determination of D/R JND at -10, 0, 10 and 20 dB D/R using wideband noise with two values for on- and offset time. We found JNDs of 2-3 dB at 0 and 10 dB D/R, which is substantially lower (higher sensitivity) than has been reported previously. JNDs at -10 at 20 dB D/R are at least 6-8 dB. the second experiment consisted of three parts where specific cues to D/R were reduced or removed. We found that monaural JNDs are as good as binaural JNDs but that eliminating nearly all spectral cues leads to an increase in JND of about 3 dB. Insofar as auditory distance perception relies on D/R, these results suggest that sensitivity to changes in distance is best

within 30 – 100% of critical distance, and should be largely insensitive to the temporal aspects of sounds. Finally, our results provide an explanation for the 'auditory horizon effect'.

### **917 Dynamic Aspects of Auditory Spatial Attention**

**Erol Ozmeral<sup>1</sup>**, Virginia Best<sup>1</sup>, Norbert Kopco<sup>1</sup>, Christine Mason<sup>1</sup>, Gerald Kidd Jr<sup>1</sup>, Barbara Shinn-Cunningham<sup>1</sup>

<sup>1</sup>*Boston University*

Spatial attention plays an important role when listening in complex auditory environments and can, for example, enhance the identification of a speech target embedded in a mixture. However, little is known about the dynamics of auditory spatial attention. In this study, we examined the impact of relatively rapid changes in target location on speech identification in a mixture.

Stimuli were presented from a five-loudspeaker array. On each trial, the listener's task was to identify a sequence of four spoken digits that was presented either from a single location (fixed condition) or from a location that changed randomly from digit to digit (switching condition). For each position in the sequence, interfering digits occurred simultaneously at the other four locations, and a visual cue indicated where the target was located. The rate of presentation was varied by inserting silent delays between digits of 0, 250, 500 or 1000 ms.

Performance in the switching condition was always poorer than in the fixed condition, as a result of at least two factors: (1) a cost associated with switching locations at rapid rates of presentation, and (2) a loss of refinement of selectivity throughout the sequence that is observed when the location is fixed.

### **918 An Investigation of the Factors Responsible for Spatial Release From Masking**

**Gerald Kidd Jr.<sup>1</sup>**, Christine R. Mason<sup>1</sup>, Virginia Best<sup>1</sup>, Nicole L. Marrone<sup>1</sup>, Nathaniel I. Durlach<sup>1</sup>

<sup>1</sup>*Boston University*

Spatial release from masking was examined for the task of speech identification. One goal was to determine the factors responsible for a large release from masking found when two speech maskers were symmetrically placed around the speech target location. This configuration may severely reduce the effectiveness of a "better-ear listening" strategy as well as pose challenges for traditional binaural-unmasking models. In the current experiments, the target was a talker uttering sentences from the Coordinate Response Measure test in the presence of one or two concurrent maskers. The primary experimental variables were the type of masker (energetic or informational) and the frequency content of the target and/or maskers (e.g., low-pass, high-pass or bandpass filtered). The results indicated that spatial release from masking is a complex process based on interaural differences that support the actions of both lower-level and higher-level mechanisms. In symmetric masking conditions, the presence of a high degree of informational masking appears to be important

for obtaining a large spatial release, which is due primarily, we believe, to perceptual segregation of sources and the focus of attention at a point along the spatial dimension. [Supported by AFOSR and NIH/NIDCD]

### **919 The Effects of Interaural Place Mismatches On Interaural Time Difference Detection with Sinusoidally Amplitude Modulated and Transposed Stimuli**

**Richard Rutkowski<sup>1</sup>**, Mark Lutman<sup>1</sup>

<sup>1</sup>*Institute of Sound and Vibration Research, University of Southampton*

Recent studies have indicated advantages with bilateral cochlear implantation, particularly in the provision of localisation cues such as interaural time differences (ITD). However, this may be compromised by interaural place mismatches (IPM) in electrode position and shallow insertion depth, leading to stimulation of mainly high-frequency channels where ITD information is ambiguous. In normally-hearing listeners, high-frequency ITD detection is possible through envelope cues of sinusoidally amplitude modulated (SAM) stimuli. Recent work has also demonstrated significantly improved ITD sensitivity with 'transposed' stimuli, which provide timing cues associated with the peripheral processing of low-frequency signals to high-frequency channels. This might offer a useful strategy for bilaterally implanted patients; however, the robustness of these stimuli to IPM has not been investigated. The present study examined this issue by measuring just noticeable differences in ITD (ITD-JNDs) for SAM and transposed stimuli from 11 normally-hearing listeners. For each stimulus, carrier frequencies centred at 3 kHz and 5 kHz were presented across a range of interaural mismatches similar to IPMs observed in implant patients. Overall, consistently lower ITD-JNDs were found for transposed compared to SAM stimuli in both experienced and inexperienced listeners at relatively quiet and louder levels. Significant reductions in ITD-JND were observed at specific mismatches, but were mainly restricted to carrier frequencies centred at 3 kHz. In experienced listeners, bandwidths measured from ITD-JND vs. IPM functions at around 3 kHz were also significantly broader for transposed compared to SAM stimuli. These results indicate that transposed stimuli enhance ITD discrimination and show less vulnerability to interaural discrepancies in carrier frequency, lending support to future work investigating implant processing strategies that aim to model the auditory periphery more effectively.

### **920 A New Phenomenon: Binaural Loudness Constancy**

**Mary Florentine<sup>1</sup>**, Michael Epstein<sup>1</sup>

<sup>1</sup>*Northeastern University*

ABSTRACT: (1792/2000 characters with spaces)

Does expectation of loudness from a visible speaker play a role in reducing the loudness difference between monaural and binaural presentation? Results of the present experiment suggest that it does. We call this new phenomenon, Binaural Loudness Constancy. Motivation

for the present experiment came from the observation that classroom demonstrations of binaural loudness summation for speech in a sound field never yielded the magnitude of the effect that was reported in the literature for tones presented via headphones. Therefore, this study examined whether binaural loudness summation differs between live-voice speech and recorded speech and/or tones. Monitored live voice spondees, recorded spondees, and tones were presented monaurally and binaurally via earphones and via loudspeakers in an audiometric booth. Eight young listeners with normal hearing judged the loudness of the stimuli across a wide range of levels using magnitude estimation. a repeated-measures ANOVA indicated that both stimulus type and presentation mode were significant factors in the amount of binaural summation. Pair wise comparisons of the stimulus types indicate that the monitored live voice spondees yielded significantly different binaural-to-monaural ratios than tones ( $p=0.03$ ) and recorded spondees ( $p=0.03$ ). Tones and recorded spondees did not differ significantly ( $p>0.05$ ). Results show significantly less binaural loudness summation with a visually present speaker than with recorded speech or tones—consistent with Binaural Loudness Constancy. This new phenomenon seems similar to loudness constancy [Zahorik and Wightman, *Nature Neuroscience* 4, 78-83 (2001)] and reminds us of the importance of cognitive factors in the judgment of loudness. [Work supported by NIH-NICDC grant R01DC02241].

## **[921] Dynamic Itds Underlie Binaural Detection of Low-Frequency Tones in Wideband Noise**

**Marcel van der Heijden<sup>1</sup>**, Philip Joris<sup>2</sup>

<sup>1</sup>*Erasmus MC, Rotterdam, Netherlands*, <sup>2</sup>*K.U.Leuven, Leuven, Belgium*

Binaural detection in an NoS $\pi$  task relies on interaural disparities introduced by adding an antiphasic signal to diotic noise. What metric of interaural disparity best predicts performance? Some models use interaural correlation; other differentiate between dynamic interaural time differences (ITDs) and interaural level differences (ILDs) of the effective stimulus.

We used a novel signal processing technique that selectively degrades different aspects (potential cues) of binaural stimuli (e.g., only ITDs are scrambled). Degrading a particular cue affects performance only if that cue is relevant to binaural processing. We applied this selective-scrambling technique to the stimuli of a classic NoS $\pi$  task (500-Hz signal; wideband noise masker).

We obtained data from 5 listeners and found:

- 1) selective scrambling of ILDs had little effect on binaural detection;
- 2) selective scrambling of ITDs significantly degraded detection;
- 3) combined scrambling of ILDs and ITDs had the same effect as exclusive scrambling of ITDs.

We conclude that, at least for this binaural detection task:

- 1) dynamic ITDs dominates detection performance;
- 2) ILDs are largely irrelevant.
- 3) interaural correlation is a poor predictor of detection.

A one-parameter detection model that uses ITD variance as detection criterion described all binaural aspects of the data quite well. Our findings vindicate Jeffress' 1956 proposition that binaural detection can be reduced to detection of dynamic ITDs.

## **[922] Continuous Versus Discrete Frequency Changes: Different Detection Mechanisms?**

**Catherine Semal<sup>1</sup>**, **Laurent Demany<sup>1</sup>**

<sup>1</sup>*CNRS and Universite Bordeaux 2*

It has been suggested that continuous frequency changes (glides) can be detected by a specific auditory mechanism, which is not activated by a frequency change between two steady tones separated by a silent interval, and is not sensitive to the direction (ascending vs. descending) of a glide (Sek & Moore, *JASA* 1999; Lyzenga, Carlyon & Moore, *JASA* 2004). This suggestion is mainly based on the finding of larger frequency JNDs for tones separated by a silent interval than for tones smoothly connected by a frequency glide. in the present study, we confirmed this previous finding using 250-ms pure tones which were either separated by a 250-ms silent interval (condition "S") or smoothly connected by a 250-ms glide (condition "G"). However, performance was also better in condition G than in condition S when the task was no longer to detect frequency changes but to identify the direction of barely detectable frequency changes (using the psychophysical paradigm described by Semal & Demany, *JASA* 2006). This is inconsistent with the idea that the hypothetical "glide detectors" are insensitive to the direction of a glide. Moreover, when the glides used in condition G were no longer smoothly connected to the neighboring frequency plateaux but were instead bounded by 10-ms cosinusoidal amplitude ramps, which were also imposed at each extremity of the plateaux, performance was no longer significantly better than in condition S. the latter result indicates that the advantage provided by the glides in condition G did not stem from the existence of glide detectors but from the sole fact that the glides produced a continuous transition between the neighboring steady tones. in condition G as well as condition S, therefore, frequency changes were presumably detected by means of comparisons between temporally non-contiguous frequency samples or "snapshots".

## **[923] Acoustic Fmri Noise Reduction: a Perceived Loudness Approach**

**Carlos Vicente Rizzo Sierra<sup>1</sup>**, Dimitri Vrehen<sup>2</sup>, Hendrikus Duifhuis<sup>3</sup>

<sup>1</sup>*BME NIC | University of Groningen*, <sup>2</sup>*Dept A.I., University of Groningen*, <sup>3</sup>*University of Groningen*

Functional magnetic resonance imaging (fMRI) enables sites of brain activation to be localized in human subjects. for auditory system studies, however, the acoustic noise generated by the scanner tends to affect the activation significantly. the present study aims at a quantitative approach of noise reduction; we want to obtain physical and subjective magnitude measures of the acoustic scanner noise.

This is achieved by performing a psychophysical matching experiment between an echo planar imaging (EPI) sequence and a 1/3 octave band of pink noise, centered at 1 KHz. Simulated EPI noise from x, y and z gradient coil direction was also matched with the 1/3 octave band of pink noise. In six subjects with normal hearing we found that the perceived loudness (in sones) and perceived loudness level (in phons) of this EPI sequence does not increase linearly with the sound pressure level (SPL).

Perceived loudness in sones appears to give a better estimate of subjective noise strength and it suggests that total EPI noise is equivalent to adding up intensities per gradient coil noise (x, y and z direction). This study supports our working hypothesis that as long as we do not have a full understanding of the relation between the acoustic properties of EPI noise and its subjective percept, its characterization and the estimated subjective effects should consist of both (physical and subjective) measures.

The implication is that for development of an effective fMRI acoustic noise reduction technique the perceived loudness characteristics of this noise should be more extensively studied and combined with well known physical magnitudes given by current sound analyzer technology.

#### **924 Active Noise Cancellation System (ANC) Reduces the Perceived Noise During Functional Magnetic Resonance Imaging (fMRI)**

**Deborah Hall<sup>1</sup>, John Chambers<sup>1</sup>, Michael Akeroyd<sup>1</sup>, Alan Palmer<sup>1</sup>**

<sup>1</sup>*Medical Research Council*

One of the main challenges for auditory fMRI concerns the intense acoustic noise (up to 115 dB) generated during scanning. Although this can be attenuated by about 30 dB with ear defenders, there is considerable scope for additional benefit. We took advantage of two features of the noise: i) its predictable temporal onset, and ii) its fixed power spectrum (which is dominated by intense components at low frequencies) to engineer an ANC system to achieve further acoustic reduction. Here, we evaluated the perceptual and neurophysiological benefits of cancellation using a scanning sequence that was dominated by a peak at 600 Hz, with two major subsidiary components at 150 and 300 Hz.

We first measured detection thresholds for a signal masked by the scanner noise, with and without ANC. The target signal was a narrowband (50 Hz) noise centred on 600 Hz. The ANC system was allowed to continually adjust the cancellation parameters and it was shown to improve detection thresholds by 20 dB (stdev=1 dB, N=4). Next we examined the benefits across frequency (N=4). The target signals were centred at each of three major frequencies of 150, 300, and 600 Hz, plus 450 Hz (chosen because the acoustic measurements did not demonstrate any benefit from ANC at that frequency). In this experiment, the cancellation parameters were frozen at the start. Detection thresholds were improved by 4, 11, 15 dB at 150, 300 and 600 Hz respectively. Even at 450 Hz, the benefit of ANC was 10 dB; due to a release from masking. We conclude that ANC offers substantial benefits for audibility. The better

results from Experiment 1 (20 vs 15 dB at 600 Hz) are a consequence of using the error microphone signal to adjust the cancellation signal throughout the scanning run for optimum noise reduction.

Additional fMRI data also demonstrate that ANC improves the statistical detection of sound-evoked activation in the primary auditory cortex, without interfering with image quality.

#### **925 Professional Applications for Soundcards for Research and Education**

**Frank Endler<sup>1</sup>, Hermann Wagner<sup>1</sup>**

<sup>1</sup>*RWTH Aachen University*

Modern soundcards are highly sophisticated hardware components, designed to add sound capability to a computer. Apart from its capability to produce or record sounds, a soundcard can also be regarded as a digital-to-analog (DA) and analog-to-digital (AD) input/output (IO) interface. Modern soundcards support high sampling rates up to 192 kHz and high bit resolutions up to 24 Bit. Analog waveforms, e.g. extracellular recordings, can be captured very precisely. Thanks to high sampling rates also supersonic stimuli can be presented with a soundcard. Soundcards with eight input and output channels are available below 300 € which could make high quality multi-channel recording and playback extremely well-priced. If more than eight channels are required, it is possible to cascade soundcards to achieve even more channels.

Despite the fact that it is technically possible to use soundcards in research and education, the use of soundcards is still an exception. The lack of appropriate software is probably the main drawback. Although Software Development Kits for addressing soundcards are available, building a software application from the beginning can be very time consuming.

Here I present software solutions for research and education which support soundcards as IO device. These software solutions are not restricted to a special kind of soundcard, which makes them very flexible and scalable. Beside multi-channel recording and playback these applications provide a signal generator and stimulus interface which simplifies the presentation of auditory signals. Additional auditory stimuli, not included in the stimulus interface, can be applied as wav-files. An interface to MatLab will enable users to apply scripts for stimulus generation and data analysis. Thus, the programs can be upgraded for e.g. spike detection or plotting functionality. By this way these solutions are easy to use and at the same time flexible for professional requirements.

#### **926 The Pupillary Dilation Response: a Tool for Assessing Sensory Performance in Humans**

**Avinash Deep Bala<sup>1</sup>, Laci Helmhout<sup>1</sup>, Paul Dassonville<sup>1</sup>, Terry Takahashi<sup>1</sup>**

<sup>1</sup>*University of Oregon*

The pupillary dilation response (PDR) is a sensitive and reliable measure of auditory performance in the barn owl.



At higher SPLs, the owl PDR is all-or-none, habituates quickly, and recovers upon presentation of novel stimuli. This property is used to assay discrimination. At lower SPLs, the PDR becomes graded and resists habituation. Thus, at perithreshold SPLs, the PDR is used to assay detection.

We evaluated the PDR as a tool for assessing human auditory performance. the pupil size of human subjects was tracked (Eyelink1000, SR Research) using an IR-sensitive camera, while they fixated a small dot on a monitor. Head position was maintained using chin and forehead rests. Post-trial, the fixation point was replaced by a "?"; subjects then pressed one of two keys to indicate whether or not they heard the sound. Thus, we simultaneously acquired pupil size data and key press data.

Initial characterization of the PDR was done using stimuli at moderate levels (35-60 dB SPL), which elicited a reliable and reproducible PDR. the response habituated quickly upon stimulus repetition, reaching a steady state after about 40 trials, as in owls. the habituated response was recovered by increasing or decreasing SPL, or by varying the pitch of the stimulus. Following this initial characterization, the PDR was evaluated as an audiometric tool, comparing it to key-presses in each individual trial.

As in owls, we found that the human PDR is graded at low SPLs, and resists habituation. a series of gammatones spanning 6 octaves, with center frequencies from 250 Hz to 8 kHz, were presented at increments of 3, 5, or 10 dB to probe detection. After each trial, subjects indicated by key press whether or not they detected the gammatone. Thresholds derived from PDR or key-presses fell within the 3 dB resolution of our stimuli. This data suggests that at least in measuring detection thresholds, the PDR approaches the sensitivity of traditional audiometric tests. (Supported by grant DC03925)

## **927 Overshoot Measured Psychophysically and Physiologically in the Same Ears**

**Kyle Walsh<sup>1</sup>, Edward Pasanen<sup>1</sup>, Dennis McFadden<sup>1</sup>**

<sup>1</sup>University of Texas at Austin

For normal-hearing listeners, the detectability of a brief tonal signal is often worse when the signal is presented at the onset of a long-duration masker than when the signal is delayed by about 150 msec after masker onset, a phenomenon known as overshoot. Overshoot is maximal when the masker is moderate in level. Also, overshoot can be reduced or eliminated by aspirin or noise exposure, or as the result of cochlear hearing loss (detectability at masker onset paradoxically improves even though hearing sensitivity is reduced). These facts suggest that the cochlear amplifiers play a role in overshoot. If so, then transient-evoked otoacoustic emissions (TEOAEs) to a brief tonal signal might be weaker if the signal is presented near the onset of a masking noise than if delayed relative to masker onset.

Both psychophysical data and TEOAEs were collected from eight normal-hearing males using essentially the same stimulus waveforms and methods of presentation. a

brief signal (10 msec) was presented 2 msec (short-delay) or 225 msec (long-delay) following the onset of a broadband masker (350 ms) that was symmetrically-notched (0, 10, 20, or 40% of the signal frequency at 1800 Hz). Psychophysically, the psychometric functions were shallower for the short-delay condition than for the long-delay condition, and that was true across subjects and notch widths. Psychophysically, overshoot magnitude averaged about 18 dB across subjects and conditions. Physiologically, no subject exhibited an overshoot-like difference in the strength of TEOAEs measured for short and long delays. the implications include: (1) the mechanisms contributing to overshoot operate after the mechanisms responsible for TEOAEs; (2) TEOAEs can be used to determine how much of certain psychophysical phenomena is contributed by cochlear micromechanics.

(Supported by NIDCD grant DC 00153).

## **928 Acoustic Overstimulation and Noise-Induced Tinnitus Assessed with Gap Prepulse Inhibition of Acoustic Startle in Rats**

**Edward Lobarinas<sup>1</sup>, Wei Sun<sup>1</sup>, Krishna Sarbadhikari<sup>1</sup>, Richard Salvi<sup>1</sup>**

<sup>1</sup>University at Buffalo

Humans exposed to high level noise often develop temporary or permanent hearing loss. in some cases the hearing loss is accompanied by an immediate onset tinnitus, but in other cases tinnitus onset may begin days or weeks later. the percentage of animals that develop tinnitus following acoustic trauma is poorly understood, but preliminary results suggest that the percentage increases with the duration and intensity of the exposure and that tinnitus begins shortly after exposure. to address these issues, we used gap prepulse inhibition of acoustic startle (GPIAS) to determine the percentage of rats that develop noise-induced tinnitus and the time of tinnitus onset. Rats were unilaterally exposed to a narrow band noise (12 kHz, 1000 Hz BW) at 123 or 126 dB SPL for 2 h and allowed to recover from anesthesia for 2 h. Each rat was then tested for tinnitus and tinnitus pitch at several post-exposure times. GPIAS testing consisted of 40 trials containing a 115 dB SPL noise burst (20 ms) presented in a 60 dB SPL background noise centered at 6, 12, 16, 20 or 24 kHz (100 Hz BW). On 20 trials the background noise was on continuously (no-gap) and on 20 trials a 50ms silent gap (pre-pulse) was inserted in the background noise 100 ms before the startle stimulus. During baseline, detection of the silent gap inhibited startle amplitudes by 20-80% relative to the no-gap condition. Failure of the silent gap to inhibit the startle reflex was interpreted as evidence of tinnitus at the test frequency. When rats were exposed to unilateral 123 dB SPL noise trauma 33% showed results consistent with the presence of tinnitus. Increasing the intensity of the noise exposure to 126 dB SPL increased the percent of animals with tinnitus like behavior to over 70%. GPIAS was impaired at multiple frequencies immediately after the exposure; however, after 48 h tinnitus-like behavior was mainly observed at 12 and 16 kHz. the results suggest that noise-exposure induces tinnitus in a subset of animals and the likelihood of

inducing tinnitus increases with exposure level. In some cases, the tinnitus is transient and in other animals it is persistent. When persistent tinnitus is observed after a 12 kHz narrow band exposure, the putative pitch is typically at 12 or 16 kHz.

Supported in part by grants from the American Tinnitus Association, Tinnitus Research Consortium, NIH 1R01DC009091 and Auris Medical

**929 Pitfalls in Behavioral Estimates of Basilar-Membrane Compression in Humans**  
**Magdalena Wojtczak<sup>1</sup>, Andrew J. Oxenham<sup>1</sup>**

<sup>1</sup>University of Minnesota

Estimates of basilar-membrane (BM) compression in human listeners have been obtained mainly from psychophysical experiments measuring recovery from forward masking for two masker frequencies, one equal to the signal frequency (on-frequency masker), and the other about an octave below the signal frequency (off-frequency masker). The psychophysical methods use an assumption that recovery functions measured with on- and off-frequency maskers should be identical provided that masker levels are chosen to yield the same excitation at the signal-frequency place. Our recent data suggest that this assumption may not be correct, especially when the off-frequency masker is presented at a very high level (90 dB and above). A 4-kHz masker and a 2.4-kHz masker were set to levels that produced the same amount of forward masking of a brief 4-kHz signal at a 0-ms delay. For those masker levels, masked thresholds were measured for delays extending between 0 and 115 ms. Listeners showed slower recovery for the 2.4-kHz masker, when the masker was presented at a level of 92 dB SPL. For lower masker levels, the difference between the rates of recovery for an off-frequency masker and the equally effective (at a 0-ms delay) on-frequency masker decreased or completely disappeared. The data were used to estimate an error made by deriving BM compression using an assumption that the recovery rates are identical for the on- and off-frequency forward masker. Our analysis suggests that for most listeners the assumption of equal recovery rates may lead to substantial overestimation of BM compression. [Supported by NIH grant R01DC03909].

**930 Does Norwich's Entropy Theory of Perception Derive the Weber Fraction for Audition?**

**Iftikhar Nizami<sup>1</sup>**

<sup>1</sup>1312 Grayson Place, Decatur, GA 30030

The just-noticeable intensity change,  $\Delta I$  at intensity  $I$ , corresponds to a sensation change,  $\Delta F$  at sensation  $F$ .  $F(I)$ , an equation relating  $F$  to  $I$ , was derived by Norwich et al. (Norwich, in *Percept Psychophys* **35**, 1984, and **42**, 1987; Norwich & McConville, *J Comp Physiol* **A168**, 1991; Wong & Norwich, *J Acoust Soc Am* **97**, 1995; Norwich & Wong, *Percept Psychophys* **59**, 1997) from "a mathematical function similar to Shannon's informational entropy function" (Norwich, *Acta Biotheor* **53**, 2005, p 176). Norwich et al. took  $dF(I)/dI$ , replaced  $d$ 's by  $\Delta$ 's, and reordered terms to obtain the Weber fraction  $\Delta I/I$  as a

function of  $\Delta F$  and 3 free parameters. That equation could not describe data because  $\Delta F$  "depends only on the arbitrary scale of measurement of subjective magnitudes" (1984, p 271) and hence was unknowable. Therefore, Norwich et al. removed  $\Delta F$  by setting it to 1. Was  $\Delta F=1$  justified? If the change in  $F$  for  $\Delta I$  is a fixed span along the sensation axis, then having an arbitrary scaling factor for sensation gives two different rules:  $\Delta F=\text{constant}$  for a linear sensation axis, or  $\Delta F/F=\text{constant}$  for a logarithmic one. These rules are untestable, but Weber's Law,  $\Delta I/I=\text{constant}$ , is approximated for >25 dB SL for many frequency/duration pairs, and for white noise. Weber's Law underlies the Weber-Fechner Law,  $F=c \ln I +k$ , when  $\Delta F=\text{constant}$ , and underlies Stevens' Law,  $F=EI^n$ , when  $\Delta F/F=\text{constant}$ . Thus, whether  $\Delta F$  or  $\Delta F/F$  is probably constant depends on whether the Weber-Fechner or Stevens' law best fits empirical loudness estimates. Curvefitting by least-squares assumes constant variance of estimates across intensities. In fact, loudness estimates show more change in variance across intensities than do their logarithms. Log-loudnesses from 31 published plots of loudness vs. intensity were fitted to the log forms of the aforementioned Laws. Stevens' Law fitted best 29 times, implying that  $\Delta F$  is not constant, i.e. that Norwich et al. have not derived the Weber fraction for audition.

**931 Rare Event Theory and Absolute Thresholds**

**Raymond Meddis<sup>1</sup>, Wendy Lecluyse<sup>1</sup>**

<sup>1</sup>University of Essex

Rare event theory offers a simple explanation of the sigmoidal shape of the psychometric function observed at absolute threshold as well as the relationship between absolute threshold and stimulus duration. The explanation does not require a hypothetical noise source (as in signal detection theory) nor does it require a hypothetical temporal integrator. Instead, the detection of a stimulus is linked to the occurrence of a stochastic event that has a low probability of occurrence when the intensity of the stimulus is itself low. Under these circumstances, the event may or may not occur before the stimulus ends and, as a result, the event may (or may not) be detected. A simple application of the binomial theorem allows us to derive the familiar shape of the psychometric function. Further analysis explains the shape of the function relating absolute threshold to the duration of the stimulus. 'Rare-event' theory has the advantage that it can be more easily associated with physiological processes occurring in the auditory system. Moreover, it has the potential to be used as a diagnostic indicator distinguishing sub-types of hearing impairment.

**932 Accuracy of Threshold Estimates in a Single Interval Procedure**

**Wendy Lecluyse<sup>1</sup>, Ray Meddis<sup>1</sup>**

<sup>1</sup>University of Essex

In psychoacoustic experiments a number of different procedures are used when making threshold estimates. Most commonly used is a forced-choice paradigm combined with the transformed up-down staircase

procedure (Levitt, 1971), where a number of peaks and troughs are used to estimate a final threshold value. However, a Single Interval (yes-no) procedure where a psychometric function is fitted to the responses (e.g. Green's maximum likelihood procedure, 1993), enables us to make a continuous assessment of the mean threshold and makes the stop time of a threshold run completely arbitrary. Moreover, it allows us to measure accuracy as a function of the number of trials used in a run. the stop rule of a run can then be decided as a fixed number of trials related to a particular level of accuracy. Since the accuracy requirement might be different in different settings, e.g. clinical setting versus laboratory setting, Single Interval procedures offer flexibility on this issue.

in this study we look at accuracy as a function of a) the number of trials in a run, b) the slope of the psychometric function and c) the number of runs used to estimate the threshold. Computer simulations presented alongside empirical data from human listeners show that the number of required trials can be prescribed if the desired level of accuracy is specified before starting the measurements.

#### References:

- Green, D.M. (1993). "Maximum-likelihood procedure for estimation thresholds in a yes-no task," *J. Acoust. Soc. Am.* 93, 2096-2105.
- Levitt, H. (1971). "Transformed up-down methods in psychoacoustics," *J. Acoust. Soc. Am.* 49, 467-477.

### **933 CBA/Caj Mouse Audiograms Using the Psychophysical Method of Constant Stimuli**

**Kelly E. Radziwon<sup>1</sup>**, Daniel J. Stolzberg<sup>1</sup>, Micheal L. Dent<sup>1</sup>  
<sup>1</sup>SUNY, University at Buffalo

Using operant conditioning and the Method of Constant Stimuli (MOCS), audiograms were constructed for five normal hearing CBA/Caj mice. the psychophysical MOCS involves the presentation of stimuli both below and well above threshold throughout each experimental session. Trials are presented in a random order, making it impossible for the mouse to anticipate the next stimulus. Klink et al. (2006) found that MOCS procedures produced audiograms in NMRI mice with lower thresholds than when other procedures, such as adaptive tracking, were used. in this study, hearing thresholds were obtained for eight frequencies ranging from 1 kHz to 42 kHz. for each frequency, seven attenuation values were presented: five values above threshold, one value at threshold, and one value below threshold. Catch trials were also randomly presented to determine the false alarm rate and to calculate the animals' biases. Thresholds were calculated using signal detection theory and a criterion of  $d' = 1.5$ . in general, we found that the MOCS procedures yielded lower thresholds than previous studies that used methods such as the galvanic skin response (Berlin, 1963) and the descending method of limits (Birch et al., 1968).

### **934 A New Approach for Measuring Spectral-Ripple Discrimination**

**Jong Ho Won<sup>1</sup>**, Seeyoun Kwon<sup>2</sup>, Christopher Clinard<sup>3</sup>, Ward Drennan<sup>1</sup>, Vasant Dasika<sup>1</sup>, Kelly Tremblay<sup>3</sup>, Jay Rubinstein<sup>1</sup>

<sup>1</sup>VM Bloedel Hearing Research Center, University of Washington, <sup>2</sup>Department of Biomedical Engineering, Hanyang University, <sup>3</sup>Department of Speech and Hearing Science, University of Washington

Previous studies have found a significant correlation between spectral-ripple discrimination and speech perception in quiet and in noise (Henry et al. 2005; Won et al. 2007). the present study investigated the relationship between two types of behavioral threshold measurements, using spectral-ripple stimuli, in adult cochlear implant (CI) users. the new single-interval method was suitably designed 1) to test the physiological response to spectral changes; and 2) to later modify this method into an observer-based procedure for prelingual CI users. Physiological and observer-based approaches to determine spectral discrimination ability will improve the evaluation of the hearing capabilities of young children and infants. It is therefore necessary to determine if results obtained using the proposed discrimination paradigm are similar to the previously established method which uses a 3-interval forced-choice paradigm. Using the old method, subjects were asked to identify the interval containing the test stimulus (i.e. the inverted ripple sound), which differ from the other two intervals containing the reference stimulus (the standard ripple sound). the new method uses a 1-interval, 2-alternative forced-choice paradigm. Stimuli are four seconds in duration; the first 2 seconds consist of a standard ripple and the last 2 seconds contain either an inverted (spectral-ripple phase inversed) or a standard ripple (no change). the ability to behaviorally detect the changed stimulus is then measured. Results showed: 1) good agreement between the two approaches; and 2) good correlations between single-interval ripple thresholds and psychophysical measurements such as speech in quiet and in noise. a future direction will be to use the new single-interval method to determine if behavioral and electrophysiological ripple discrimination thresholds can predict speech perception in quiet and noise in infants and toddlers. [Supported by R01-DC007525, R01-DC007705, and KRF-2006-612-D00106]

Key words: spectral resolution, cochlear implant

### **935 Temporal Resolution and the High-Frequency Limit of Hearing**

**Milind Kunchur<sup>1</sup>**

<sup>1</sup>Univ. of South Carolina

In linear systems, the characteristic response time  $\tau$  and the upper frequency limit  $f_{\max}$  go hand in hand, and typically  $\tau \sim 1/\omega_{\max} = 1/2\pi f_{\max}$ . the complexities of auditory neurophysiology negate this simple reciprocal relationship and a preliminary estimation suggests that threshold  $\tau$  may well underceed the nominally expected  $9 \mu s (= [2\pi 18kHz]^{-1})$  for certain stimuli. Typical instrumentation used in psychoacoustic research lacks the temporal speed and fidelity to reveal this potentially acute temporal resolution

of hearing. in this work, experiments using special ultrahigh-fidelity equipment confirmed discernment at timescales of around 5  $\mu$ s (microseconds), which are shorter than found previously.

### **936 Temporal Masking in Adolescents with Language-Based Learning Impairments**

**Craig Formby**<sup>1</sup>, Regina Cicci<sup>2</sup>, Kimberly Block<sup>3</sup>, Lauren Wawroski<sup>3</sup>, Monica Hawley<sup>2</sup>

<sup>1</sup>University of Alabama, <sup>2</sup>University of Maryland School of Medicine, <sup>3</sup>University of Maryland College Park

Among the most compelling findings in psychoacoustics over the past decade are backward-masking deficits reported for persons with language-based learning problems (LPs). Ostensibly, this deficit is a temporal-processing disorder that contributes to the LPs. This controversial interpretation of backward-masking deficits has been influential in shaping language-based treatments. Alternative explanations for the backward-masking and language deficits are considered in this report; namely, that attentional processes and cognitive demand are greater for the backward-masking condition than for other temporal-masking conditions. Backward-, simultaneous-, and forward-masking conditions, originally reported by Wright et al. (1997), were evaluated in 10 adolescents with LPs and 10 controls. All participants were provided intensive practice and familiarization for the masking tasks. They also were provided an auditory cue to aid them in attending to the signal in the masker. Adolescents with LPs had a small, but significant overall increase (~4 dB) in their masked thresholds across all temporal masking conditions compared with the masked thresholds for the Control group. LP performance for the backward-masking condition was significantly poorer than performance for the Controls, but was not dramatically poorer than that measured for other temporal masking conditions. Auditory cuing did not significantly improve masked detection for either group of adolescents nor for any measurement condition. with appropriate training and familiarization of temporal-masking tasks, adolescents with LPs in this study performed similarly, although slightly worse, than age-matched Controls.

### **937 Speech Identification Based On Temporal Fine Structure Cues in Normal-Hearing and Hearing-Impaired Listeners : Comparison of Two Speech-Coding Schemes**

**Marine Ardoint**<sup>1</sup>, Stanley Sheft<sup>2</sup>, Christian Lorenzi<sup>1</sup>

<sup>1</sup>Laboratoire de Psychologie de la Perception; CNRS - Université Paris Descartes; ENS - DEC, <sup>2</sup>Parmlly Hearing Institute; Loyola University Chicago

The contribution of temporal fine structure (TFS) cues to consonant identification was assessed in normal-hearing and hearing-impaired listeners with two speech-processing schemes designed to remove temporal envelope (E) cues. Stimuli were processed vowel-consonant-vowel speech tokens. Derived from the analytic signal, carrier signals were extracted from the output of a bank of analysis filters. the "PM" and "FM" processing schemes estimated a phase- and frequency modulation function, respectively, of

each carrier signal and applied them to a sinusoidal carrier at the analysis-filter center frequency. to evaluate TFS processing *per se*, stimulus manipulations were designed to control the extent of E reconstruction subsequent to peripheral auditory filtering of TFS signals. a third scheme retaining only E cues from each band was used for comparison. for normal-hearing listeners, stimuli processed with the PM and FM schemes were found to be highly intelligible (50-80% correct identification with 6.25% correct representing chance performance). Analysis of confusions between consonants showed that TFS and E cues differentially transmitted information regarding manner and place. Taken together, these results indicate that TFS cues convey important phonetic information that is not solely a consequence of E reconstruction. Hearing-impaired listeners with a nearly flat hearing loss performed at or close to chance level with the PM and FM schemes. These results suggest that hearing-impaired listeners cannot use the TFS information preserved in the processed-speech stimuli.

### **938 Behavioral Thresholds to Amplitude Modulation Following Developmental Conductive Hearing Loss.**

**Merri Rosen**<sup>1</sup>, Emma Sarro<sup>1</sup>, Jack Kelly<sup>2</sup>, Dan Sanes<sup>1</sup>

<sup>1</sup>New York University, <sup>2</sup>Carleton University

The development of brain circuitry is susceptible to experience. in children, even mild to moderate hearing loss during maturation can interfere with temporal discrimination tasks and may ultimately disrupt language acquisition. CNS synaptic physiology is altered by conductive hearing loss (CHL; Xu et al '07), but the relationship between these cellular alterations, central auditory computations, and sensory perception are unknown. We assessed behavioral performance on a sinusoidal amplitude modulation (SAM) detection task following CHL in P10 gerbils. Beginning at P60, animals were tested with 5 Hz SAM stimuli using either a noise or a 4 kHz tone carrier. Detection thresholds were higher for CHL animals when assessed with a descending limits paradigm. Control and CHL animals each displayed improved performance over several sessions. However, a preliminary assessment suggests that CHL adults are more susceptible to different training procedures, where increased task difficulty early in training differentially impairs final performance. Current experiments are testing how behavioral thresholds for fast (100 Hz) modulations are affected by early-onset CHL, and further investigating the differential effect of training paradigm. to examine neural correlates of SAM detection thresholds, we recorded AI responses to SAM stimuli in a separate set of awake adult gerbils. This obtained threshold tuning curves for modulation depth detection based on both firing rate (FR) and synchrony (vector strength, VS). in normal adults, the cumulative population histogram of the FR but not the VS tuning curve is well-matched to the perceptual SAM tuning curve. Future experiments will be conducted in CHL adults. a similar correlation would strengthen the likelihood of firing rate as an important parameter in SAM encoding. (Support: NIH DC6864 to DHS, NIH DC9165 and NOHR Research Award to MJR)

### **939 Towards the Clinical Applicability of Temporal Masking Procedures**

**Frederick Gallun<sup>1</sup>**, Sarah Melamed<sup>1</sup>, Michelle Molis<sup>1</sup>, Marjorie Leek<sup>1</sup>, Matthew Makashay<sup>2</sup>, Van Summers<sup>2</sup>

<sup>1</sup>*National Center for Rehabilitative Auditory Research,*

<sup>2</sup>*Walter Reed Army Medical Center*

Increasingly, non-simultaneous masking procedures have been emphasized in obtaining cochlear tuning functions and estimates of compression. As part of a larger study, two groups of listeners, one with impaired hearing (HI) and one with hearing in the normal range (NH), were tested with a temporal masking procedure aimed at characterizing the cochlear functioning of individual listeners. the target to be detected was a 20-ms tone presented at 10 dB SL. Forward-masked thresholds were obtained adaptively (3 down/1 up) in a two-interval forced choice task for four target frequencies (.5, 1, 2, 4 kHz) across a range of delays (masker offset to target onset) between 10 and 100 ms (in 10 ms steps). the 108-ms masking tone was presented either at the same frequency as the target or at the target frequency multiplied by .55 (e.g., 550 Hz for a 1000 Hz target). Minimal practice preceded the testing and two estimates of threshold were obtained for each masker frequency and delay. a third estimate was obtained if the two thresholds differed by more than 4 dB. Surprisingly, on-frequency masking functions expressed as target-to-masker ratio were very similar for the NH and HI groups. Equally unexpected was that the differences in compression as estimated from the ratios of the slopes (linear best-fit to all points collected) for the on- and off-frequency maskers were less extreme than expected from the literature (Rosengard et al, JASA, 117, 3028-3041), except for the 4 kHz targets. the implications of these results will be discussed in light of the prospects of using such a measure in a clinical setting. [Work supported by the Oticon Foundation].

### **940 Common Aspects of Temporal and Spatial Processing Across Normal Hearing and Cochlear Implant Listening**

**J. Brandon Laflen<sup>1</sup>**, Eric Healy<sup>2</sup>, Preeti Parikh<sup>1</sup>, Mario Svirsky<sup>1</sup>

<sup>1</sup>*New York University,* <sup>2</sup>*University of South Carolina*

Aspects of auditory processing that are common across normal-hearing (NH) and cochlear-implant (CI) individuals were investigated by modeling fundamental frequency (F0) discrimination data. the three-parameter model was based upon neural activation patterns (NAPs). These represent the probability of neural spikes, as a function of time and spatial distance along the cochlea, in the acoustically- or electrically-stimulated auditory nerve. Difference NAPs (dNAPs) were calculated based on the difference between the NAPs corresponding to the standard stimulus and the increment stimulus at each increment level. the model estimated the probability that the difference between the standard and increment was detectable, based on the dNAP. it's three parameters involved (1) temporal smoothing, achieved by filtering the temporal dimension of the dNAP with a lowpass filter, (2) spatial smoothing, achieved by filtering the spatial dimension of the dNAP

with a lowpass filter, and (3) scaling the dNAP, by raising each entry to a parameterized power (*i.e.*, a  $p$ -norm distance function).

Even though F0 just-noticeable-differences were lower for the NH group than for the CI group, the best fit to both datasets was observed when temporal smoothing was below 300 cycles/sec (approx. 3 msec), spatial smoothing was below 300 cycles/meter (approx. 3 mm along the basilar membrane), and scaling power was significantly greater than unity. Interestingly, these temporal, spatial, and scaling characteristics were observed independently when modeling the NH and the CI data, suggesting that these aspects of auditory processing are common to both acoustic and electric stimulation of the auditory nerve. These processes may therefore reflect more central aspects shared by both groups.

### **941 Disruption of the Consolidation of Learning On an Auditory Temporal-Interval Discrimination Task**

**Beverly A. Wright<sup>1</sup>**, Andrew T. Sabin<sup>1</sup>, Roselyn M. Wilson<sup>1</sup>

<sup>1</sup>*Dept. of Communication Sciences and Disorders, Northwestern University*

For training to have a long lasting effect, the influence of practice must be transferred from short- to long-term memory through a process called consolidation. in perceptual learning, consolidation has been shown primarily on visual tasks, often by demonstrations that improvement on a target condition is disrupted by the subsequent training of a non-target condition within a limited time window. Here we report the disruption of learning on a basic auditory discrimination task by the training of a non-target auditory task, and show that this interference occurs regardless of the training order of the two tasks. We trained different groups of listeners either only on temporal-interval discrimination (360 trials/day), or on both temporal-interval and frequency discrimination (each for 360 trials/day) in each of 7 daily training sessions, using the same standard stimulus for both tasks (100 ms, 1 kHz). Listeners who practiced only the target temporal-interval task improved significantly more on that task than an untrained control group. However, no such learning was evident when the temporal-interval training was immediately followed by the frequency training, indicating retrograde interference. Surprisingly, there was also no improvement on the temporal-interval task when the training on it occurred either immediately after, or even 4 hours after, training on the frequency task, suggesting anterograde interference. These data thus demonstrate that learning on auditory temporal-interval discrimination can be disrupted by practicing frequency discrimination either before, or after, practicing the interval task each day, and that this disruption can occur over at least a 4-hour time period. This observation is consistent with the idea that auditory perceptual learning requires consolidation, and that the consolidation process depends on mechanisms whose states can be altered by events that occur hours before training on the target task.

[Supported by NIH/NIDCD.]

## **942 Using Psychoacoustics to Explore Cochlear Function: Basic Mechanisms and Applications to Hearing Aids**

**Brian C.J. Moore<sup>1</sup>**, Brian C.J. Moore<sup>1</sup>

<sup>1</sup>*University of Cambridge*

Over the last two decades there has been a dramatic increase in understanding of cochlear physiology and of the distinct roles of the inner and outer hair cells. In this lecture, I will start by giving an overview of these roles in terms of their influence on auditory perception. Hearing loss often involves reduced functioning of the inner and outer hair cells. I will describe the perceptual consequences of this, including loss of frequency selectivity, loss of suppression, loss of sensitivity to temporal fine structure, and loudness recruitment, and I will present simulations of some of these effects. Specific psychoacoustic tests now exist for measuring cochlear compression, for assessing sensitivity to temporal fine structure and for diagnosing "dead regions" in the cochlea. I will describe a variety of applications of psychoacoustic tests and models to the design and fitting of hearing aids, and will discuss possible future developments.

## **943 Multiquantal Neurotransmitter Release by Afferent Synapses of the Bullfrog's Amphibian Papilla**

**A. J. Hudspeth<sup>1</sup>**, Erica C. Keen<sup>1</sup>, Daniel Andor-Ardó<sup>1</sup>

<sup>1</sup>*The Rockefeller University*

The ribbon synapses of hair cells release neurotransmitter with exceptional voltage sensitivity, temporal fidelity, and persistence. The bullfrog's amphibian papilla provides a useful preparation for study of the release process, for it is possible to make whole-cell, tight-seal recordings both from afferent nerve terminals and from the hair cells they innervate. When an afferent terminal is held at -90 mV, depolarization of an associated hair cell elicits glutamatergic excitatory postsynaptic currents ranging in amplitude from about -20 pA to more than -300 pA. Over the range of membrane potentials in which signaling ordinarily occurs, the magnitude of the postsynaptic response scales linearly with the presynaptic  $\text{Ca}^{2+}$  current. The iontophoretic application of glutamate confirms that postsynaptic receptors respond linearly to neurotransmitter and are not saturated by even the largest hair-cell signals. Postsynaptic receptors also show little trial-to-trial variability in their response to the application of a constant glutamate concentration, suggesting that the broad distribution of postsynaptic current amplitudes arises primarily from variation in the concentration of glutamate in the synaptic cleft. Although amplitude histograms suggest that the large events represent multiples of a quantal response averaging about -50 pA, it has not been possible to make unambiguous fits of the data with a binomial statistical model. We have developed a maximum-entropy deconvolution algorithm with which to distinguish the individual components of a complex excitatory postsynaptic current as well as a maximum-likelihood algorithm for aligning and scaling individual events. These tools indicate that excitatory postsynaptic currents of all sizes are kinetically similar within a

resolution of 150  $\mu\text{s}$ , so the multiquantal release process involves a high degree of synchrony.

This research was supported by NIH grant DC00241.

## **944 Synaptic Specializations in Turtle Auditory Hair Cells**

**Michael Schnee<sup>1</sup>**, Timothy Benke<sup>2</sup>, Anthony Ricci<sup>1</sup>

<sup>1</sup>*Stanford University*, <sup>2</sup>*University of Colorado Health Sciences Center*

Presynaptic specializations in auditory hair cells; such as number of synapses and synaptic vesicle density, are involved in the ability of synapses to operate across frequency ranges. Vesicular release via capacitance measurements has demonstrated three kinetic components of release that correlate with synaptic vesicle populations near dense bodies. A linear relationship between calcium entry and release did not vary between cells with different characteristic frequencies. The effect of calcium buffers on size and rates of release of different vesicle pools was investigated and a simple model of vesicle transport was capable of reproducing the observed results. Paired pulse stimulations and release rates at the hair cell's resting potential were also investigated. No evidence of facilitation was observed, the increased capacitance of the second pulse could be accounted for by the increased calcium load due to the slow rate of calcium clearance. No depletion of fast pools was observed with the paired pulse experiments either. Supported by NIDCD 03896.

## **945 Modulation of Transmitter Release At the IHC Ribbon Synapse by the Presynaptic Resting Potential**

**Juan Goutman<sup>1</sup>**, Elisabeth Glowatzki<sup>1</sup>

<sup>1</sup>*Johns Hopkins School of Medicine*

Synaptic transmission at the inner hair cell (IHC) afferent synapse requires high precision in order to code for sound signals. Here we describe a mechanism by which precision of transmitter release at this synapse might be improved.

Simultaneous whole cell patch clamp recordings were performed from IHCs and contacting afferent dendrites in excised organs of Corti from postnatal rats (P9-P11). The afferent synaptic response was studied while manipulating IHC membrane potential and calcium influx. Using this approach, we previously have characterized the voltage dependence of release with a maximum at  $\sim -30$  mV. In response to steady IHC depolarizations, the afferent fiber response showed synaptic depression (Goutman and Glowatzki, 2007).

When IHCs were depolarized from a hyperpolarized potential, -89 mV, to -29 mV for a brief period of time (2 ms), a high failure rate for release was found. Successful responses showed a wide range of EPSC amplitudes and also long ( $\sim 4$  ms) and varying delays from the onset of the presynaptic depolarization. If a conditioning step to an intermediate potential ( $\sim -50$  mV) was applied to the IHC before the test pulse, a significant increase in the probability of release was observed. Additionally, the delay of the response was shorter ( $\sim 2$  ms) and less variable.

Similar results were found when conditioning was induced with a paired pulse protocol.

These results suggest that release at the IHC ribbon synapse can be modulated by the presynaptic membrane potential in a way that resembles facilitation in the CNS. Under physiological conditions, the IHC may have a resting potential positive enough to allow for continuous calcium influx and transmitter release, resulting in spontaneous activity in auditory nerve fibers. Our results show that at this IHC resting potential the synapse may be conditioned and therefore activate release with shorter delays and less variability.

This work was supported by NIDCD DC006476 and HFSP RGY12/2004 grants to EG.

#### **[946] The Source of Regularly Timed Background Neural Activity in the Frog Sacculus**

**Mark Rutherford<sup>1</sup>, William Roberts<sup>1</sup>**

<sup>1</sup>*University of Oregon*

The frog sacculus is an inner ear organ with auditory and vestibular function, sensitive to seismic vibrations as well as head tilt and airborne sound (J. Lannou and L. Cazin, 1976). Studies of anesthetized frogs have shown that in the absence of any applied sound or seismic stimulus many saccular afferent axons fire action potentials with a uniform interspike interval (H. Koyama et. al., 1982). to investigate the source of this "resting discharge" we recorded from postsynaptic afferent neurites and hair cells in the sensory epithelium of the isolated frog sacculus, with mechanoelectrical transduction blocked and no enzymatic treatment. Similar to previous *In Vivo* recordings, we observed regularly spaced afferent action potentials in the 4-30 Hz range, in both extracellular and intracellular recordings. Whole-cell recordings showed that afferent axons do not fire rhythmically in this frequency range in response to constant current injection, but are instead driven by regularly-spaced bursts of CNQX-sensitive synaptic potentials from hair cells. Whole-cell recordings from hair cells revealed that those of the tall-thin morphology have large (up to 60 mV) membrane potential oscillations in the 4-30 Hz range, which we believe to be the source of the regular resting discharge of afferent axons. These oscillations have an asymmetric spike-like shape, were sensitive to extracellular calcium, were abolished by the L-type calcium channel blocker nifedipine, and promoted by blockade of calcium-activated (BK) potassium channels with iberiotoxin. Oscillations were ongoing with no applied current, as well as during a small steady depolarizing current to mimic the normal resting transduction current. the frequency of the hair cell voltage oscillation increased to a new, stable frequency in response to increasing levels of depolarizing current. We speculate that the tall-skinny hair cells in the saccular periphery signal a rate code for head tilt.

#### **[947] Synaptic Transmission Between the Type I Hair Cell and the Calyx Afferent – a Bit of a Mystery**

**Joseph Holt<sup>1</sup>, Anna Lysakowski<sup>2</sup>, Jay Goldberg<sup>3</sup>**

<sup>1</sup>*University of Texas Medical Branch (UTMB)*, <sup>2</sup>*University of Illinois at Chicago (UIC)*, <sup>3</sup>*University of Chicago*

The peculiar structure and distinctive physiology of type I hair cells and their calyx endings raise questions as to the mechanisms of synaptic transmission between these structures. Both the type I hair cell and its calyx ending express some prominent potassium conductances that should impede conventional chemical transmission. Furthermore, accumulation of potassium and glutamate within the synaptic cleft of the calyx ending may also be unfavorable for effective synaptic transmission. Intracellular recordings from calyx-bearing afferents in the turtle, however, reveal that indeed synaptic transmission does occur. This talk will focus on characterizing synaptic transmission at the type I hair cell synapse, comparing it to that at other hair cell synapses, and discussing how the potential anatomical and physiological impediments may be handled.

#### **[948] The Molecular Machinery for Exocytosis At IHC Ribbon Synapses**

**Isabelle Roux<sup>1</sup>, Regis Nouvian<sup>2</sup>, Amel Behloul<sup>3</sup>, Marylin Beurg<sup>4</sup>, Didier Dulon<sup>4</sup>, Tobias Moser<sup>2</sup>, Christine Petit<sup>3</sup>, Saaid Safieddine<sup>5</sup>**

<sup>1</sup>*John Hopkins University*, <sup>2</sup>*Goettingen University Medical School*, <sup>3</sup>*Pasteur Institute/INSERM*, <sup>4</sup>*INSERM*, <sup>5</sup>*Pasteur Institute/INSERM, Paris*

The inner hair cell (IHC) ribbon synapse signals sound stimulus to the central nervous system (CNS) with high temporal precision and over a wide range of stimulus intensities. in addition to keeping the CNS constantly informed about surrounding sounds, the IHC synapse is specialized in maintaining a high level of tonic neurotransmitter release over long periods of time, even in a quiet environment. When compared to the CNS synapses, the IHC ribbon synapse presents several striking differences, which are likely to be involved in its unique functional characteristics: i) the  $\text{Ca}^{2+}$  invasion of the ribbon synapse active zone upon cell depolarization occurs through L-type  $\text{Ca}^{2+}$  channels (instead of P/Q channels at the CNS synapses); ii) otoferlin is proposed to be the major calcium sensor (instead of synaptotagmin I at the CNS synapses); iii) the unique molecular constituent of the ribbon synapse, RIBEYE, is essential for synaptic ribbon component assembly. Despite significant progress in elucidating the molecular composition of the presynaptic active zone of the IHC ribbon synapse, we are still far from understanding the basic mechanisms underlying the functioning of this synapse. in my presentation, I will briefly discuss what is current knowledge about the function of the SNARE proteins and their protein regulators at the CNS synapse. I will highlight the recent discoveries of molecular and cell biological processes that shed new light on how vesicle fusion at the ribbon synapse may occur. the molecular mechanisms by which otoferlin may be functionally integrated into the fusion machinery of the



ribbon synapse with respect to the CNS synapse will also be discussed.

#### **[949] SNARE Dependence At the Inner Hair Cell Afferent Synapse**

Régis Nouvian<sup>1</sup>, Thomas Binz<sup>2</sup>, Tobias Moser<sup>1</sup>

<sup>1</sup>University of Goettingen, <sup>2</sup>Hannover University Medical School

During exocytosis in most synapses, a four-helical coiled coil protein complex is formed, between the three SNARE proteins syntaxin 1, synaptobrevin 2 and SNAP-25, bridging synaptic vesicle and plasma membrane. This SNARE complex is essential for priming and fusion of synaptic vesicles and is probably also present in inner hair cells. However, the SNARE functions at a ribbon synapse are still unknown. By taking advantage of clostridial neurotoxins light chains, which cleave the SNARE proteins and by examining a synaptobrevin mouse mutant, I will present insights about SNARE complex on inner hair cell exocytosis, probed by patch-clamp recordings of membrane capacitance changes upon depolarization and flash photolysis of caged calcium.

#### **[950] The Role of Synaptic Ribbons in Neural Coding in the Auditory System – Insights From Mutant Mice Lacking the Ribbon-Anchoring Protein Bassoon**

Nicola Strenzke<sup>1</sup>, Bradley N. Buran<sup>2</sup>, Darina Khimich<sup>3</sup>, M. Charles Liberman<sup>1</sup>, Tobias Moser<sup>3</sup>

<sup>1</sup>Eaton-Peabody Laboratory, Harvard Medical School, Boston, MA, <sup>2</sup>Harvard-MIT Division of Health Sciences and Technology, Cambridge, MA, <sup>3</sup>Inner Ear Lab, Dept. of Otolaryngology, University of Göttingen, and CMPB Göttingen, Germany

Bassoon-knockout mice are deficient in morphologically intact synaptic ribbons. Electrophysiological studies in inner hair cells have shown a significant reduction of the fast component of exocytotic vesicle release (Khimich et al, Nature 2005). This has been attributed mostly to a reduction of the readily releasable pool in the absence of intact ribbons. Here, we further investigated stimulus-secretion coupling in the Bassoon-deficient IHCs. Using immunolabelling and confocal microscopy we found Ca<sub>v</sub>1.3 channels to be clustered also in the absence of the ribbon. Still, an impaired Ca<sup>2+</sup> influx – exocytosis coupling was indicated by an out of proportion inhibition of exocytosis by the slow Ca<sup>2+</sup> chelator EGTA. We then used *In Vivo* recordings from single auditory nerve fibers to explore the effects of the presynaptic defect on auditory coding. Sound-stimulated and spontaneous action potential rates in single neurons of the auditory nerve were decreased. Forward masking effects were enhanced, but the time course of recovery from masking was normal. The temporal precision of auditory nerve fiber responses to transposed tones was not impaired. Thus, the reduction of amplitudes in auditory brainstem responses and auditory steady state responses (Pauli-Magnus et al., Neuroscience 2007) appears to be a consequence of quantitatively reduced activation of auditory nerve fibers rather than dys-synchrony.

#### **[951] The Reliability and Precision of Auditory Nerve Responses**

Michael Avissar<sup>1</sup>, Adam C. Furman<sup>1</sup>, James C. Saunders<sup>1</sup>, Thomas D. Parsons<sup>1</sup>

<sup>1</sup>University of Pennsylvania

The cochlear hair cell-afferent fiber synapse converts a graded potential into a discrete signal of all-or-none action potentials, or spikes. Therefore, the reliability of spike counts and the precision of spike timing reflect the limits of synaptic function. We quantify the limitations of rate and temporal coding by measuring the reliability and precision of auditory nerve responses *in vivo*. We relate the results to both synaptic function and the ability of the auditory nerve to transmit information.

This research was supported by awards from the NIDCD (DC000710 - JCS, DC003783 - TDP), the Pennsylvania Lions Hearing Research Foundation (JCS, TDP).

#### **[952] From the Tilted Mouse to the Otopetrin Gene Family: Molecular Insights Into Otoconia Formation**

David Ornitz<sup>1</sup>, Inna Hughes<sup>1</sup>, Euysoo Kim<sup>1</sup>, Mark Warchol<sup>1</sup>, Belen Hurle<sup>2</sup>, Mitsuyoshi Saito<sup>1</sup>, Paul Schlesinger<sup>1</sup>, Ruediger Thalmann<sup>1</sup>

<sup>1</sup>Washington University, <sup>2</sup>National Human Genome Research Institute

Problems with balance are a leading cause of injury in elderly populations. Otoconia are complex calcium carbonate (CaCO<sub>3</sub>) biominerals that are required for the sensation of gravity. Degeneration of otoconia is thought to contribute significantly to balance disorders and to the displacement or ectopic formation of otoconia that occur in patients suffering from benign paroxysmal vertigo (BPV). In addition, commonly used aminoglycoside antibiotics can lead to disruption of otoconial structure and function. Despite the prevalence of balance disorders, little is known about the mechanisms regulating the development and pathology of the vestibular mechanosensory apparatus.

*Tilted* mice have a severe balance disorder due to the congenital absence of otoconia. By positional cloning we identified mutations in *Otopetrin 1* (*Otop1*) as the genetic etiology of the *tilted* mouse phenotype. OTOP1 is a multi-transmembrane domain protein required for the formation of otoconia in the vertebrate inner ear. Examination of the phenotypes of animals with mutations or deficiencies in *Otop1* suggests a direct role for OTOP1 in the initiation of extracellular biomineralization, possibly through the regulation of intracellular Ca<sup>2+</sup>.

Here, we demonstrate that OTOP1 can modulate purinergic mediated Ca<sup>2+</sup> homeostasis in cell lines and in macular epithelial cells. These studies define a unique set of biochemical activities of OTOP1 including depletion of endoplasmic reticulum Ca<sup>2+</sup> stores, specific inhibition of the purinergic receptor, P2Y, and regulation of the influx of extracellular Ca<sup>2+</sup> in response to ATP, ADP and UDP. These activities can be inhibited by the polyanion suramin in a rapidly reversible manner. This first characterization of the consequences of OTOP1 overexpression indicates a

profound effect on cellular  $\text{Ca}^{2+}$  regulation. in a physiologic setting, these activities could direct the formation and growth of otoconia and regulate other biomineralization processes.

### **953 Effects of Fetuina and Osteopontin Upon Calcite Crystal Growth *In Vitro***

**Ruediger Thalmann**<sup>1</sup>, Dan Zhou<sup>2</sup>, John J Freeman<sup>3</sup>, David M Ornitz<sup>4</sup>, Isolde Thalmann<sup>1</sup>, Wenfu Lu<sup>1</sup>

<sup>1</sup>Washington University Medical School, Department of Otolaryngology, St. Louis, MO 63110, <sup>2</sup>University of Missouri - St. Louis, Center for Nanoscience, St. Louis, Mo 63121, <sup>3</sup>Washington University, Department of Earth & Planetary Sciences, St. Louis, MO 63130, <sup>4</sup>Washington University Medical School, Dept. of Molecular Biology and Pharmacology

In addition to otoconin90 (OC90) several minor otoconins have recently been identified, including osteopontin (OPN) and FetuinA. Both proteins are enriched in the mineral phase of bone and teeth. OPN is a sialoprotein containing polyaspartic acid and serine phosphorylation sites which regulate mineral binding, as well as a conserved arg-gly-asp motif, which mediates cell attachment and signaling. FetuinA, an acidic serum glycoprotein, contains two conserved cystatin domains. in addition to their functional role in bone and teeth, the two proteins are powerful inhibitors of unwanted ectopic calcification with hydroxyapatite. Loss of these inhibitors in severe renal deficiency causes widespread ectopic calcification of vasculature, heart and kidney. the role of these proteins in  $\text{CaCO}_3$  mineralization is not known. Therefore we tested potential modulatory effects of OPN and FetuinA upon calcite crystal growth *In Vitro*. OPN added to the growth solution induced no changes of nucleation density or crystal size. However, calcite crystal morphology was strongly modified by rounding of the acute edges of the (104) faces and elongation parallel to the C-axis, resulting in a shape resembling calcitic otoconia. in contrast to OPN, FetuinA (10-500 ug/ml) caused a marked increase of nucleation density and corresponding reduction in crystal size as a function of protein concentration. Moreover, significant crystal aggregation was noticeable at higher concentrations. Changes in crystal morphology were analogous to those induced by OPN and OC90, but less pronounced. It is significant for the interpretation of these *In Vitro* experiments, that reportedly mice deficient in OPN (OPN  $-/-$ ) and FetuinA (FetuinA  $-/-$ ) do not exhibit a behavioral phenotype suggesting vestibular impairment. More extensive *In Vitro* and *In Vivo* studies will be required if we hope to elucidate the functional significance of these minor otoconins. [Supported by NIDCD DC02236 (DMO) & DC01414 (IT)]

### **954 Identification of a Serpin Homolog As a Constituent Protein of Fish Otoliths**

Hidekazu Tohse<sup>1</sup>, Young-Jin Kang<sup>1</sup>, Amy Stevenson<sup>1</sup>, Peter Yau<sup>1</sup>, **Richard Kollmar**<sup>1</sup>

<sup>1</sup>University of Illinois at Urbana-Champaign

Otoliths and otoconia couple linear accelerations, including gravity, to sensory hair cells in the inner ears of fishes and higher vertebrates. Their sizes and shapes are tightly regulated, but little is known about the molecular mechanisms that govern their growth. Both consist of more than 95%  $\text{CaCO}_3$ , the balance being mostly protein; unlike teeth or bones, they are completely acellular. in analogy to other biominerals, it has been proposed that the constituent proteins of otoliths and otoconia control the deposition of the inorganic ions. So far, only a handful of such proteins, including members of the extracellular matrix, have been described in different species. We set out to systematically identify otolith proteins by taking advantage of technical advances in proteomics in recent years. First, we compared the complement of otolith proteins in a broad range of species by denaturing gel electrophoresis. We observed similar band patterns that suggested an upper limit of about two dozen different otolith proteins. Next, we sequenced tryptic peptides from abundant commercial species de novo by tandem mass spectrometry and queried sequence databases with a customized search algorithm. One protein that had so far not been described in otoliths was identified as a homolog of the mammalian serpins, a family of serine protease inhibitors. Some serpins have also been shown to associate with collagens or be involved in blood clotting. to confirm the serpin's expression in the inner ear, we isolated a cDNA of the ortholog from the zebrafish (*Danio rerio*) and conducted *In Situ* hybridizations. the cognate mRNA was detectable as early as 24 hours post fertilization in the developing otic vesicle, when otoliths begin to grow. On the basis of its biochemical localization and the expression pattern of its mRNA, we propose that this serpin homolog is involved in otolith morphogenesis, a hypothesis that is testable in zebrafish by using antisense morpholino technology.

### **955 Oncomodulin Identifies Unique Hair Cell Types in Vestibular Sensory Organs**

**Dwayne Simmons**<sup>1</sup>, Benton Tong<sup>2</sup>, Aubrey Hawkes<sup>1</sup>, Angela Schrader<sup>2</sup>

<sup>1</sup>University of California, Los Angeles, <sup>2</sup>Washington University

The tight regulation of calcium is essential to inner ear function. in adults, oncomodulin (OCM) is a major calcium binding protein (CPB) in the inner ear, however, its function remains elusive. Given that OCM is a CBP and a member of the parvalbumin family, its role in the regulation of calcium concentration may be very important to hair cell function. Studies of OCM in the inner ear have been mostly limited to the cochlea, and consequently, little is known about its expression in vestibular hair cells. in the cochlea, OCM is expressed at both young and older adult ages. Although expressed robustly at younger ages, OCM expression is substantially reduced in vestibular tissues at

older adult ages. in the cochlea, OCM is found only in outer hair cells (OHCs) and can be localized preferentially near the OHC membrane. in vestibular organs, OCM is also only found in a subset of hair cells, but has a more diffuse localization throughout the hair cell body. in cochlear OHCs, OCM expression may overlap with calretinin and calbindin developmentally, but does not overlap with either calbindin or  $\alpha$ -parvalbumin expression in adult tissues. in vestibular organs, we did not observe any overlapping expression in hair cells between OCM and calbindin, calretinin, or  $\alpha$ -parvalbumin in adult tissues. Further in vestibular organs, we found OCM immunoreactivity restricted to hair cells found either in striolar regions of the utricle and saccule or in apical regions of the cristae. within the utricle or saccule, OCM was expressed mostly in type I hair cells. These data suggest that OCM may have distinct functional roles in cochlear and vestibular hair cells.

### **956 Post-Injury Repair and Functional Restoration in Mammal Vestibular Endorgans**

Aurore Brugeaud<sup>1</sup>, Cecile Travo<sup>1</sup>, Gilles Desmadryl<sup>1</sup>, Christian Chabbert<sup>1</sup>

<sup>1</sup>INSERM

Because of their direct interaction with our environment, the inner ear sensory cells are particularly exposed to traumatic or ototoxic injuries. Upon such aggressions, the nerve terminals that contact the sensory cells will directly be affected by excitotoxic damages, leading to transient or permanent impairments of the auditory or vestibular functions. with the ultimate aim to bring concrete therapeutic solutions for the neuroprotection of synaptic contacts, or the functional restoration of damaged synapses, we attempted for several years, to identify the cellular elements involved in the vestibular synaptogenesis in the developing mammal (Chabbert et al. 2003), and in the post-injury repair of mature synaptic contacts (Brugeaud et al. 2007). Using *In Situ* approaches, we demonstrated that this last process involved cellular mechanisms common to those previously used during the setting of the vestibular sensory network. Since that, we carried on that study trying to determine whether the efferents were involved in the synaptic repair process, and whether neurotrophines were also involved as in the neonatal period. We will present the last results of these studies together with those obtained using the organotypic cultures models we recently developed to study in detail the functional restoration ability of the vestibular sensory network.

Chabbert et al. (2003) *J. Physiol. Lond.* 553:113-123

Brugeaud et al. (2007) *J. Neurosci.* 27: 3503-3511

### **957 Immunolocalization of Connexin 26 and 30 in Postmortem Human Vestibular**

#### **Endorgans**

Andrew McCall<sup>1</sup>, Ivan Lopez<sup>1</sup>, Gail Ishiyama<sup>2</sup>, Akira Ishiyama<sup>1</sup>

<sup>1</sup>UCLA School of Medicine, Division of Otolaryngology -- Head and Neck Surgery, <sup>2</sup>UCLA School of Medicine, Department of Neurology

Connexins are the protein subunits of gap junctions which permit diffusion of water, ions, and small molecules between cells. Although genetic mutations in connexin 26 and 30 are best known for their role in human hearing loss, vestibular abnormalities associated with connexin 26 mutations have also been reported (Todt et al., 2005). Animal studies in multiple rodent species have immunolocalized connexin 26 and 30 to vestibular supporting cells (Forge et al., 2003). Connexion 26 has been immunolocalized to gap junctions between melanocytes in the human vestibular dark cell area (Masuda et al., 2001). However, there are no previous reports on connexion 30 localization in the human vestibular periphery, nor reports on immunolocalization of connexin 26 in the human vestibular sensory epithelia. Vestibular endorgans were microdissected from subjects with documented normal auditory and vestibular function during life (n = 4). Cryostat sections were incubated with antibodies against connexin 26, 1:500 in PBS (ADI, San Antonio, TX) or against connexin 30, 1:500 in PBS (Zymed, San Francisco, CA). Immunolocalization was evaluated under the fluorescence microscope.

Connexin 26 and 30 immunolocalized to the supporting cells in the vestibular periphery in the human. in addition, connexin 26 immunoreactivity was present in the stroma immediately adjacent to the bony labyrinth and connexin 30 demonstrated strong immunoreactivity throughout the stroma of the human vestibular periphery. the presence of connexin 26 and 30 in the vestibular periphery supporting cells mirrors previous findings in rodents. in contrast, the finding of connexin 26 and 30 in the stroma of the human vestibular periphery was not demonstrated in previous animal studies. the presence of connexin 26 and 30 in the supporting cells and stroma of the human vestibular periphery strongly suggests that connexins have an important functional role such as ionic homeostasis in the human vestibular system.

### **958 Immunolocalization of Basement Membrane Proteins in Human Vestibular Endorgans in Meniere's Disease, Acoustic Neuroma, and Normal**

Sarah Mowry<sup>1</sup>, Ivan Lopez<sup>1</sup>, Gail Ishiyama<sup>2</sup>, Akira Ishiyama<sup>1</sup>

<sup>1</sup>UCLA Division of Otolaryngology-Head and Neck Surgery, <sup>2</sup>UCLA Department of Neurology

Basement membranes (BM) are layers of extracellular macromolecules at the boundary between cells and connective tissues. the BM may contribute a significant role to fluid and electrolyte composition and likely plays a role in endolymph homeostasis. in the present study, we applied immunohistochemistry to evaluate the expression

of collagen IVA2, nidogen and laminin  $\beta 2$  in the human vestibular basement membrane (BM). We used vestibular endorgans microdissected from postmortem temporal bones from subjects with documented normal auditory and vestibular function during life ( $n = 5$ ). Also, we used surgically acquired vestibular endorgans from patients undergoing ablative surgery for intractable Meniere's disease ( $n = 3$ ) and for acoustic neuroma resection ( $n = 2$ ). Fluorescent immunohistochemistry using antibodies directed at collagen IVA2, nidogen, and laminin  $\beta 2$  was applied to serially sectioned cristae ampullaris, utricular and saccular maculae. the distribution of these BM proteins in the perivascular and perineural stromal BMs was similar in the normals, acoustic neuroma and Meniere's disease. Collagen IVA2 and nidogen co-localized within the BM underlying the neuroepithelium throughout the utricular macula and crista ampullaris from postmortem normals. Collagen IVA2 and nidogen expression appeared to be decreased in acoustic neuroma specimens and increased in the Meniere's disease specimens throughout the crista ampullaris BM when compared to normals. Regionally, the utricular macula BM in Meniere's disease appeared to show decreased collagen IVA2 and nidogen expression in the central regions when compared to autopsy specimens. Laminin  $\beta 2$  was present, although not uniformly distributed, within the BM of the neuroepithelium of the crista ampullaris and the utricular macula of autopsy specimens. Laminin  $\beta 2$  expression appeared to be increased in the saccular BM beneath the neuroepithelium from Meniere's disease. These findings may contribute to our understanding of the pathogenesis of Meniere's disease and acoustic neuroma. Funded by NIDCD-NIH grants DC005028-05 and DC008635-02..

### **[959] Branching Patterns of Physiologically Characterized Semicircular Canal Afferents in the Toadfish, *Opsanus Tau*: Contacts with Two Types of Hair Cell**

Victor L. Friedrich, Jr.<sup>1</sup>, Giorgio P. Martinelli<sup>1</sup>, Stephen M. Highstein<sup>2</sup>, Suhrud Rajguru<sup>2</sup>, Richard D. Rabbitt<sup>3</sup>, **Gay Holstein<sup>1</sup>**

<sup>1</sup>Mount Sinai School of Medicine, <sup>2</sup>Washington University St. Louis, <sup>3</sup>University of Utah

Immunoreactivity for both GABA and glutamate have been demonstrated in separate populations of crista hair cells. to aid in understanding the physiological significance of this, arborization patterns of physiologically characterized vestibular horizontal canal afferent processes receiving GABAergic hair cell input were examined. Following fixation, epithelia containing injected afferents were processed for two-color fluorescence for biocytin and GABA, and whole mounts were imaged by two-photon microscopy.

1. Overall, two groups of hair cells can be distinguished on the basis of their vertical extent in the epithelium. Most hair cells span the entire thickness of the epithelium, while others extend only from the apical surface to an intermediate level and are not present basally. Both groups include GABAergic cells.

2. Afferent fibers differ widely in the location and profuseness of their terminal arbors. Axons entering the sensory epithelium emit a variable number of branches that remain, with further branching, near the basal surface of the epithelium. Focal swellings of this basal arbor, en passant and terminal, represent likely sites of synaptic contact. Vertically-oriented spicules emit from the basal arbor and ascend through a substantial thickness of the epithelium. These spicules, which are abundant on some arbors and absent on others, represent the only apparent mechanism for synaptic sampling of the shorter hair cells, and could serve as a mechanism for afferents to sample different apical-basal levels of individual hair cells.

Intracellularly labeled arbors having direct contact with GABAergic hair cells exhibit a range of morphologies and include both simple and highly complex arbors containing variable numbers of synaptic swellings and vertically-oriented spicules. These data suggest that afferents sampling GABAergic hair cells may present a variety of response patterns and do not represent a homogeneous population. Supported by NIDCD grant DC006677. Twophoton microscopy was performed at the MSSM MicroSRF, supported in part with a HHMI-BRSP award.

### **[960] Ligand-Gated Purinergic Receptors (P2X) Demonstrate Heterogeneous Subunit Characteristics in Rat Vestibular Ganglion Neurons**

**Ken ITO<sup>1</sup>**, Yasuhiro CHIHARA<sup>1</sup>, Shinichi IWASAKI<sup>1</sup>, Yoshinori SAHARA<sup>2</sup>

<sup>1</sup>University of Tokyo, <sup>2</sup>Tsurumi University

The present study demonstrates, for the first time, the expression of purinergic receptors (P2X) on rat vestibular ganglion neurons (VGNs) using the whole-cell patch-clamp recording. Under the whole-cell voltage-clamp recording condition, application of adenosine 5'-triphosphate (ATP; 100 microM) evoked desensitizing inward currents in VGNs at a holding potential of -60 mV. the dose-response study showed an EC<sub>50</sub> of 11.0 microM and a Hill's coefficient of 0.82. Suramin (100 microM) reversibly inhibited ATP-evoked inward currents. Alpha,beta-methylene ATP (100 microM), a P2X-specific agonist, evoked inward currents but had a lower potency than ATP. Application of adenosine 5'-diphosphate (ADP; 100 microM) also evoked similar, but much smaller currents. the current-voltage relationship of the ATP-evoked conductance demonstrated pronounced inward rectification with the reversal potential more positive than 0 mV, suggesting a cation non-selective conductance. However, the channel was not permeable to a large cation (N-methyl-D-glucamine) and acidification (pH 6.3) had little effect on the ATP-evoked conductance. the intermediate decay time constant of ATP-evoked currents (2-3 s), a value between those of rapidly desensitizing subgroups (P2X1 and P2X3) and slowly desensitizing subgroups (P2X2, P2X4, etc.), suggested heterogeneous expression of P2X receptors in rat VGNs. Expression of P2X1-X6 receptor subunits were confirmed by the RT-PCR. the physiological implication of P2X receptors includes modulation of excitability at the synapse between hair cells and dendrites and/or trophic support (or also

neuromodulation) from supporting cells surrounding the VGNs.

## **961 Heritability of Semicircular Canal Orientation**

**Hilary Brazeal<sup>1</sup>**, James Cheverud<sup>1</sup>, Timothy Hullar<sup>1</sup>

<sup>1</sup>*Washington University School of Medicine*

Anatomic abnormalities of the inner ear can cause deafness and imbalance, health issues which affect a substantial portion of the population. Some abnormalities are linked to single gene mutations, but others may be determined polygenically. As an initial step towards identifying groups of genes involved in the determination of labyrinthine anatomy, we investigated the heritability of semicircular canal orientation. the data set consisted of sixteen genetically distinct mouse strains, each strain represented by two individuals. MicroCT scanning provided images of the semicircular canals and custom Matlab programs were used to measure the canals' geometry. the angles among the semicircular canals were used as a quantitative measure of anatomic variability. the data were analyzed using ANOVA.

The angles among ipsilateral semicircular canals have an average broad-sense heritability of 0.557, indicating a moderate to high level of heritability. the angle between the left posterior and left lateral canals (LP-LL angle) had a genetic correlation (Rg) of 0.97 with the angle between the left anterior and left lateral canals (LA-LL angle). a similarly high Rg (1.00) was seen for the RP-RL angle and the RA-RL angle. Rg values were also significant for the LP-LA angle and the RP-RA angle (1.00) and for the LA-LL angle and the RA-RL angle (1.00). These data indicate that variation in semicircular canal orientation is genetically controlled. a larger data set combined with molecular scoring will allow us to map quantitative trait loci (QTLs) affecting semicircular canal development. Further analysis of each of these loci will be necessary to determine their possible role in normal and pathologic inner ear development.

Supported in part by NIDCD grant DC006869

## **962 A Comparison of the Vestibulotoxic Effects of Gentamicin and Co-Administration of Kanamycin and Furosemide in Guinea Pigs**

**Hendrik Bremer<sup>1</sup>**, John de Groot<sup>1</sup>, Huib Versnel<sup>1</sup>, Frans Albers<sup>1</sup>, Sjaak Klis<sup>1</sup>

<sup>1</sup>*Dept. of Otorhinolaryngology, University Medical Center Utrecht, the Netherlands*

The aim of our study was to investigate the immediate effect of co-administration of kanamycin and furosemide upon the vestibular system and to compare it to the vestibulotoxic effect of chronic gentamicin administration. Fifteen albino guinea pigs were used in this study. Five animals were injected with a single dose of both kanamycin (400 mg/kg, im) and furosemide (100 mg/kg, iv), 5 animals received daily gentamicin injections (100 mg/kg/day, ip) for 10 consecutive days, and 5 untreated animals served as a control group. Cochlear function was assessed by recording auditory brainstem responses

(ABRs) and vestibular function by measuring vestibular short-latency evoked potentials (VsEPs).

There was hardly any effect of gentamicin upon cochlear function: ABR thresholds in the gentamicin group were comparable to those in the normal group. Combined kanamycin and furosemide administration resulted in a severe hearing loss (60 dB). There was a significant effect of gentamicin on vestibular function: VsEP thresholds were elevated and VsEP amplitudes showed a decrease. Co-administration of kanamycin and furosemide had no significant effect on the VsEPs. in addition to these finished physiological results, a histological investigation of both the cochlea and the otolith organs of the three experimental groups will be performed.

Conclusion: Kanamycin/furosemide co-administration as applied here has mainly a cochleotoxic effect, whereas chronic gentamicin administration has a vestibulotoxic effect.

## **963 Recovery of Gaze Stability During Vestibular Regeneration**

**Asim Haque<sup>1</sup>**, **J. David Dickman<sup>1</sup>**

<sup>1</sup>*Washington University*

Many motion related behaviors, such as gaze stabilization, balance, orientation, and navigation largely depend upon a properly functioning vestibular system. Following vestibular insult, many of these responses are compromised, but can return during the regeneration of vestibular receptors and afferents that is known to occur in birds, reptiles and amphibians. Here, we characterize gaze stability in response to rotational motion during vestibular regenerative recovery in pigeons. Ototoxic agents were used to produce a complete vestibular receptor loss. Immediate post-lesion effects included severe head oscillations, postural ataxia, and total lack of gaze control. We found that these abnormal behaviors gradually subsided and gaze stability slowly returned to normal function according to a temporal sequence that lasted several months. We also found that the dynamic recovery of gaze function during regeneration was not homogeneous for all types of motion. Instead, high frequency motion stability was first achieved, followed much later by slow movement stability, forcing us to refute our original hypothesis. in addition, we found that initial gaze stability was established using almost exclusive head response components, with little eye movement contribution. However, that trend reversed as recovery progressed so that when gaze stability was complete, the eye component had increased and the head response had decreased to levels significantly different from that in normal birds. This was true even though the head-fixed VOR response recovered normally. Recovery of gaze stability coincided well with the three stage temporal sequence of morphologic regeneration previously described by our laboratory.

## **964 Vestibular Difference Between Blast and Blunt Head Trauma**

**Michael Hoffer<sup>1</sup>**, Kim Gottshall<sup>1</sup>, Ben Balough<sup>1</sup>, Carey Balaban<sup>1</sup>

<sup>1</sup>*Spatial orientation Center*

Introduction: Traumatic brain injury (TBI) can be caused by traditional head impact injuries or by blast trauma. Many investigators have asserted that these injury patterns produce identical clinical outcomes and ultimately result from the same pathophysiologic mechanisms, whereas other groups have asserted that the two injury patterns are dramatically different. In this work, we present evidence supporting this latter viewpoint. We identified 34 patients who had experienced closed head injury alone without a blast component (CHI group) and 21 patients who had experienced pure blast injury (blast group). Each group underwent a detailed history and auditory/vestibular test battery.

Results: Both groups were composed of males with an average age of 26. In the CHI group, 59%(20/34) had post-traumatic migraine associated dizziness, 6% (2/34) had post traumatic exercised induced dizziness (PTEID), and 35% (12/34) post traumatic spatial disorientation.. the expression of balance disorders in the blast population differed dramatically from the CHI group. Headaches and constant unsteadiness were uniformly present, with one subgroup of patients also complaining of episodes of true vertigo. These conditions, termed post-blast instability with or without vertigo were present in 29% (6/21) and 48% (10/21) of the patients respectively. the PTIED seen after blast differs from the closed head injury because the blast patients complain of headaches and dizziness that begins during exercise as opposed to after exercise. This was present in 24% (5/21) individuals. In addition, the blast group had significantly more individuals with hearing loss and neuro-cognitive disorders when compared to the CHI group.

Conclusion: the work presented here provides significant evidence that the profile of blast-related TBI differs markedly from the profile in closed head injury. In this work we examine pathophysiologic differences between these two disorders that might explain these differences.

## **965 Estrogen Receptors and Implications for Neuroprotection in the Auditory System**

Inna Meltser<sup>1</sup>, Yeasmin Tahera<sup>1</sup>, Konstantina Charitidi<sup>1</sup>, Jan-Åke Gustafsson<sup>1</sup>, **Barbara Canlon<sup>1</sup>**

<sup>1</sup>*Karolinska Institutet*

Estrogen acts through estrogen receptors which are ligand-activated transcription factors belonging to the nuclear hormone receptor superfamily. Estrogens have numerous effects on the central nervous system throughout life in both males and females. The actions of estrogen are mediated by two distinct estrogen receptors (ER) ER alpha (ER alpha) and ER beta (ER beta). These two receptors are the products of two distinct genes that are believed to have unique functions in the body. They may be simultaneously present in some organs and tissues whereas in other organs one of the receptor types dominates over the other. At present there is limited knowledge as to how each receptor type affects the

function of the auditory system, or if there are gender-related facets in the inner ear. Understanding the mechanisms of estrogen receptor actions in the auditory system is important for improving hormone replacement therapy against hearing loss, especially during aging. Can specific ligands to the alpha and beta receptors be successfully used as hormone therapy to protect against degeneration of the auditory system? These questions remain unanswered, as are the reasons for the well-known sex differences in the auditory system throughout life. This review will discuss how estrogen receptors participate in hearing and how these receptors and their specific ligands can be used to preserve hearing.

## **966 Hormone Replacement Therapy Can Negatively Affect Hearing in Aged Women and Female Mice**

**Robert Frisina<sup>1</sup>**

<sup>1</sup>*Univ. Rochester Medical School*

Recent research underscores the significant effects that sex hormones can have on the development, plasticity and aging changes of the peripheral and central auditory systems. For example, we compared the hearing abilities of aged women (N=124) who had taken hormone replacement therapy (HRT) with otherwise healthy age-matched controls. We found that the women who had taken combination HRT (estrogen+progestin) had significantly worse hearing than those taking estrogen HRT alone, and those that had never taken HRT, as measured by audiograms, distortion-product otoacoustic emissions (DPOAEs), speech-perception in background noise, and spatial processing (hearing-in-noise test, HINT). Animal studies in middle age perimenopausal CBA mice, receiving subcutaneous pellets of HRT to model some aspects of the human clinical condition, show similar hearing deficits as measured with auditory brainstem response (ABR) thresholds and DPOAE amplitudes. In conclusion, combination HRT involving progestin appears to have a negative effect on hearing, relative to estrogen alone.

[Supported by NIH: NIA, NIDCD]

## **967 What Do Sex, Twins, Spotted Hyenas, Adhd, and Sexual orientation Have in Common?**

**Dennis McFadden<sup>1</sup>**

<sup>1</sup>*University of Texas, Austin*

A series of studies suggests that the human peripheral auditory system is changed by the processes of masculinization that operate during prenatal development. Those studies involved measurements of otoacoustic emissions (OAEs) and auditory evoked potentials (AEPs). Among the points to be covered in this talk are: OAEs and some AEPs show marked sex differences; OAEs show large individual differences, but also appear to be reasonably stable traits through life; the OAEs of females having male co-twins are shifted in the direction of males; female spotted hyenas are highly masculinized from birth, and their OAEs are not stronger than those of males; boys

diagnosed with one form of attention-deficit/hyperactivity disorder (ADHD) have hypermasculinized OAEs; the OAEs and certain AEP measures of homosexual and bisexual females are shifted in the direction of males. Various facts suggest that these group differences in human OAEs and AEPs are not attributable to differential hearing loss or drug use (including oral contraceptives), or to differences in other obvious lifestyle factors. Under reasonable assumptions, our results suggest that exposure to high levels of androgens during prenatal development push OAEs and AEPs in the male direction. Unknown is exactly which cochlear elements are affected by this prenatal androgen exposure, but some suggestions will be offered.

[Supported by National Institute on Deafness and Other Communication Disorders.]

## **[968] Steroid-Dependent Auditory Plasticity for the Enhancement of Acoustic Communication**

**Joseph Sisneros<sup>1</sup>**

<sup>1</sup>*University of Washington*

The plainfin midshipman fish, *Porichthys notatus*, has become an excellent model to investigate mechanisms of auditory reception, neural encoding, and vocal production shared by vertebrates. the reproductive success of the plainfin midshipman is highly dependent on this species ability to detect and locate conspecific vocal signals produced during the breeding season for intraspecific social communication. Midshipman fish, like other teleost fish, use the saccule as the main acoustic end organ for hearing. Recent work shows that the frequency sensitivity of the auditory saccular afferents changes seasonally with female reproductive state such that summer reproductive females become better suited than winter non-reproductive females to encode the higher harmonics of the male's advertisement call. Approximately one month before the spring/summer breeding season, female midshipman show peaks in circulating plasma levels of testosterone and 17Beta-estradiol, which are now known to induce the female's summer reproductive auditory phenotype and enhance the female's sensitivity to the dominant higher harmonic components of the male's mate call. Furthermore, midshipman-specific estrogen receptor alpha and androgen receptor have been identified in the saccule which provides support for a direct steroid effect on the inner ear. in this talk, I will present additional physiological evidence that saccular hair cell receptors are prime candidate sites for this novel form of steroid-dependent auditory plasticity. in addition I will discuss why this plasticity may represent an adaptation to enhance the acquisition of auditory information needed for social and reproductive-related behaviors.

## **[969] Hearing Loss and Estrogen Receptors in Turner Syndrome**

**Malou Hultcrantz<sup>1</sup>**, Malou Hultcrantz<sup>1</sup>

<sup>1</sup>*Dept Otorhinolaryngology, Karolinska Universityhospital, Sweden*

**Aim:** is the female sex steroid estrogen the key to preserved hearing in the aging human? This question still remains unanswered, but hearing loss is more profound in elderly males than females. There are also well-known sex differences in the auditory brainstem response (ABR), where women have shorter latencies than men. Moreover women with Turner syndrome (45,X), who are biologically estrogen deficient, show longer ABR latencies and an early presbycusis. These findings are also supported by animal experiments. in apparent contradiction, there are case reports that hormone replacement therapy and oral contraceptive use can lead to hearing loss, but of another type, the acute sudden deafness. Such contradictory aspects may spring from the fact that there are two estrogen receptors, alfa and beta, both of which are present in the inner ear of mouse, rat and humans. Knowing how sex steroids can alter the hearing abilities might give us important clues as to how estrogen can preserve hearing in humans.

**Methods:** 344 females with Turner's syndrome, diagnosed by chromosomal analysis, were tested audiometrically. Air and bone conduction thresholds were measured for 10 different frequencies, as well as testing of speech discrimination. Mean values were calculated and compared to age-matched controls. Onehundredfortyfive females in menopause, in the normal population, were tested for hearing in three groups: premenopausal, postmenopausal and postmenopausal with estrogen substitution.

**Results:** Estrogen deficiency due to streak ovaries is the dominant problem in Turner's syndrome (loss of one X chromosome) affecting 1:2000 newborn girls. Ear and hearing problems affect outer, middle and inner ear. Younger women with Turner's syndrome showed a typical sensorineural dip in the midfrequencies that progressed over time and gave severe social hearing problems over the age of 40, when a premature degenerative process started in the high frequency region. Hearing aids were common over the age of 40.

in the cohort of menopausal females, females with substitution of estrogen showed a different hearing pattern. **Conclusion:** with increasing age a progressive high frequency sensorineural hearing loss is found among females with Turner syndrome and females substituted during menopause show a different hearing pattern.

## **[970] Long-Term Estrogen Treatment Induces a Hearing Loss in Guinea Pigs**

**Kathleen Horner<sup>1</sup>**

<sup>1</sup>*CNRS UMR 6153*

Our current research is based on our earlier observation in the clinic of high incidence of hyperprolactinemia amongst patients presenting symptoms of Ménière's disease (Horner et al. 2002, Falkenius et al. 2005). These intriguing observations led us to investigate the effect of



hyperprolactinemia on the inner ear. Hyperprolactinemia was induced via estrogen implants in guinea pigs. Hyperprolactinemia was confirmed together with high levels of estrogen.

First, we observed a bone-related pathology of the otic capsule. Recent data show that bone cell function is regulated by the receptor activator of NF- $\kappa$ B (RANKL), its receptor RANK and decoy receptor osteoprotegerin (OPG) which can inhibit the effects of RANKL (Hadjidakis & Androulakis, 2006). OPG is highly expressed in the cochlear spiral ligament and is found in high concentrations in the perilymph (Zehnder et al. 2005). Disturbance of the balance RANKL-RANK-OPG could be a major etiological factor in otosclerosis (Mc Kenna & Kristiansen, 2007). Since the expression RANKL is dependent on prolactin, as shown for the mammary gland, (Srivastava et al. 2003) hyperprolactinemia might facilitate the development of bone-related pathology.

Second: There was some hearing loss in guinea pigs which was more substantial in males than females. Estrogen seems to be protective for the cochlea but estrogen together with progestin can negatively affect hearing (Guimaraes et al., 2006). Interestingly estrogen-progesterone synergy can result in hyperprolactinemia (Williams et al. 1985).

The relative protection in females might be related to gender difference in cortisone. Cortisone was not assayed in animals, but in patients high levels of prolactin were positively correlated with cortisol in females and not males (Horner & Cazals, 2005). Glucocorticoids provide protection of the inner ear from noise exposure and are considered to regulate auditory sensitivity by acting on its downstream transcription factor NF- $\kappa$ B (Review, Canlon, 2007).

### **[971] Using Vibrotactile Stimulation to Enhance Mandarin Tone Recognition in Normal-Hearing and Cochlear-Implant Subjects**

**Juan Huang<sup>1</sup>, Janice Chang<sup>1</sup>, Fan-Gang Zeng<sup>1</sup>**

<sup>1</sup>*University of California Irvine*

Low-frequency acoustic stimulation (<500 Hz) can enhance cochlear-implant (CI) performance in noise and in pitch-related tasks, but it is not available to most cochlear implant users. Touch sensation operates in this low frequency range and may be used to enhance CI performance. Here we tested this hypothesis by measuring Mandarin Tone recognition under auditory-only, vibrotactile-only, or combined auditory-vibrotactile condition in quiet and in noise. Mandarin tones were presented to normal-hearing listeners via acoustic simulations of CI or to CI users directly. Fundamental frequency (F0) was extracted from the Mandarin tones and presented to the normal-hearing or CI subjects through a vibrotactile stimulator attached to the subject's fingertip. Percent correct scores were obtained as the outcome measures. Preliminary data showed that F0 via vibrotactile stimulation significantly enhanced auditory Mandarin Tone recognition in both quiet and in noise. The amount of enhancement depended on F0 extraction, tone patterns,

and subject variables. Historically, vibrotactile stimulation has been used to aid speech communication in the deaf but was abandoned due to superior performance by cochlear implants. The present results suggest that combined vibrotactile and auditory stimulation can enhance cochlear-implant performance. These results may not only rekindle the interest in vibrotactile stimulation in particular but also stimulate a new research direction exploring multi-sensory integration in general.

### **[972] Stimulation of the Auditory Nerve Using Optical Radiation**

**Claus-Peter Richter<sup>1</sup>, Rodrigo Bayon<sup>1</sup>, Margarete Otting<sup>1</sup>, Eul Suh<sup>1</sup>, Sheila Goyal<sup>1</sup>, Jeffrey Hotelling<sup>1</sup>, Agnella Izzo<sup>1</sup>, Joseph Walsh Jr.<sup>1</sup>**

<sup>1</sup>*Northwestern University*

Cochlear implants bypass damaged hair cells in the auditory system and directly electrically stimulate the auditory nerve. Stimulating discrete spiral ganglion cell populations in cochlear implant users' ears is similar to the encoding of small acoustic frequency bands in a normal-hearing person's ear. In contemporary cochlear implants, however, the injected electric current is spread widely along the scala tympani and across turns. We have shown that extreme spatially selective stimulation of the cochlea is possible using light (Izzo et al. 2007, JBO, Vol. 12, 021008). Here, we review the basic optical parameters required to stimulate the auditory nerve and present the correlation between surviving spiral ganglion cells after longterm deafening and neural stimulation with optical radiation.

Pre-deafening acoustic thresholds were obtained in gerbils and stimulation with optical radiation was made with various pulse durations, energy levels and repetition rates. For longterm deafening the animals received 25, 50, 75, and 100 mM Neomycin transtympanically and were allowed to survive for several weeks during which neural degeneration occurred. Deafness was confirmed by measuring acoustically evoked compound action potentials. Optically evoked compound action potentials were determined for different radiation conditions. After completion of the experiment, each animal was euthanized and cochleae harvested for histology.

Thresholds for acoustic compound action potentials were significantly elevated after neomycin application. Thresholds and amplitudes of the compound action potential amplitudes depended on the number of surviving spiral ganglion cells.

This project has been funded with federal funds from the National Institute on Deafness and Other Communication Disorders, National Institutes of Health, Department of Health and Human Services, under Contract No. HHSN260-2006-00006-C / NIH No. N01-DC-6-0006.

### **973 Auditory Nerve Adaptation and Recovery in Response to Electric Pulse Trains**

**Charles Miller<sup>1</sup>**, Ning Hu<sup>1</sup>, Fawen Zhang<sup>2</sup>, Paul Abbas<sup>1</sup>, Barbara Robinson<sup>1</sup>, Jihwan Woo<sup>1</sup>

<sup>1</sup>University of Iowa, <sup>2</sup>University of Cincinnati

The adaptation of auditory nerve fibers (ANFs) to ongoing electric stimuli (such as pulse trains) has only recently been systematically described. We assessed how mammalian ANFs respond to electric trains presented at rates of 250, 1000, and 5000 pulse/s (Zhang et al., 2007, JARO 8, 356-72). Measures from deafened cats demonstrated that both "rapid" and "short term" components of spike rate adaptation can exist without the action of hair-cell physiology. These results will be presented along with new data describing how temporal response properties (i.e., vector strength (VS), fano factor, and spike interval statistics) vary across the duration of 300 ms long pulse trains. Responses to the lowest- and highest-rate trains were compared across a wide range of ANF response rates. VS was relatively constant across time and primarily dependent upon response rate. However, fano factor and median spike intervals both demonstrated increases - in some cases, large - over the first 100 ms of the pulse-train response. the limits of high-rate "desynchronization" will also be presented. Finally, an ongoing project has been examining how ANFs recover from adaptation. This study employs a high-rate conditioning ("masker") pulse train, followed by a low-rate series of probe pulses used to assess recovery from the conditioning stimulus. We will present data showing the nature of recovery from conditioner-evoked spike activity as well as the influence of sub-threshold conditioners (i.e., high-rate trains that produce little or no spike activity) on the subsequent ANF responses. the data indicate that rate recovery follows a time course greater than that expected from refractory effects (e.g., Miller et al., 2001, JARO 2, 216-32). in addition to rate recovery, changes in temporal properties will also be examined.

Research supported through NIH grant R01-DC006478.

### **974 Topography of Auditory Nerve Projections to the Cochlear Nucleus in Cats After Neonatal Deafness and Electrical Stimulation by a Cochlear Implant**

**Patricia Leake<sup>1</sup>**, Gary Hradek<sup>1</sup>, Ben Bonham<sup>1</sup>, Russell Snyder<sup>1</sup>

<sup>1</sup>University of California San Francisco

We previously reported that auditory nerve projections from the spiral ganglion (SG) to the cochlear nucleus (CN) exhibit clear cochleotopic organization in adult cats deafened as neonates prior to hearing onset. However, the topographic specificity of projections in deafened animals was proportionately broader (less precise relative to the CN frequency gradient) than in normal controls.

This study examined SG-to-CN projections in adult cats that were deafened neonatally by ototoxic drug injections and received a unilateral cochlear implant at 6-8 wks. of age. After ~8 months of intracochlear electrical stimulation,

SG projections from implanted cochleae were compared to projections from contralateral non-implanted ears. the cochleotopic organization of the SG projections into frequency-band laminae was clearly evident in deafened animals despite severe auditory deprivation during postnatal development. When normalized for the smaller CN size after deafness, AVCN, PVCN and DCN projections from the stimulated ears were broader by 32%, 34% and 53%, respectively, than projections in normal animals. Further, there was no significant difference between projections from the stimulated and contralateral non-stimulated cochleae. Deafened animals examined at 8 wks. of age (age of implantation of older group) showed similar broadening of projections.

Our findings suggest that early normal auditory experience is essential for normal development (and/or subsequent maintenance) of the CN and the topographic specificity of SG-to-CN projections. After early deafness, the CN is smaller than normal, and the topographic precision of the neural projections that underlie frequency resolution in the normal central auditory system is significantly reduced. Several months of applied electrical stimulation from a cochlear implant introduced at 6-8 wks. of age failed to ameliorate, reverse or to exacerbate these degenerative changes.

Work supported by NIH-NIDCD Grant R01DC-000160 and Contract N01-DC-3-1006.

### **975 Binaural Jitter Improves Sound Lateralization in Electric and Acoustic Hearing**

**Bernhard Laback<sup>1</sup>**, Matthew Goupell<sup>1</sup>, Piotr Majdak<sup>1</sup>

<sup>1</sup>Austrian Academy of Sciences

There is evidence that interaural time differences (ITD) in the fine structure of a sound are most important for sound localization and for understanding speech in noise. Cochlear implant (CI) listeners have been shown to be often sensitive to fine structure ITD at low pulse rates, but their sensitivity declines at higher pulse rates which are required for speech coding. We hypothesized that this limitation is at least partially due to binaural adaptation associated with periodic stimulation. with five CI listeners, we tested the effect of introducing binaurally-synchronized jitter (binaural jitter) in the stimulation timing, assuming that this reduces the periodicity in the neural response and thus avoids binaural adaptation. the range of tested pulse rates was 400 to 1515 pulses per second (pps). in addition, we performed a similar experiment with normal hearing (NH) listeners using bandpass-filtered acoustic pulse trains and testing the pulse rates 600 and 1200 pps. a background noise was added to minimize the audibility of spectral changes introduced by the jitter.

Consistent with the hypothesis, the CI listeners showed large improvements in ITD sensitivity from binaural jitter at high pulse rates (800 - 1515 pps), but not at 400 pps. the NH listeners also showed large improvements from binaural jitter at both rates tested. Comparison between the results for the jittered condition at high rates and the unjittered condition at lower rates indicates that both subject groups did not simply rely on the long interpulse-intervals to improve performance.

It is concluded that random temporal variation reactivates the adapted binaural auditory system. Thus, binaurally-jittered stimulation improves the access of bilateral CI listeners to ITD information.

*Work supported by the Austrian Academy of Sciences and the Austrian Science Fund, FWF, project number P18401-B15*

## **[976] The Effect of Competing Noise On Spoken Word Recognition in Toddlers Who Use Unilateral or Bilateral Cochlear Implants**

**Tina M. Grieco-Calub<sup>1</sup>, Jenny R. Saffran<sup>2</sup>, Ruth Y. Litovsky<sup>3</sup>**

<sup>1</sup>*University of Wisconsin-Madison, <sup>2</sup>Psychology Department, University of Wisconsin-Madison,*

<sup>3</sup>*Department of Communicative Disorders, University of Wisconsin-Madison*

Recognizing speech in the presence of competing noise is known to be challenging. for congenitally-deaf children who learn oral language through the use of cochlear implants (CIs), this task may be especially hard due to the degraded signal that CIs provide. in this study, we measured spoken word recognition abilities in young children who use CIs at an age in which language learning is exponential. Participants were 20 congenitally-deaf toddlers who use unilateral or bilateral CIs (mean age=31 mo.) and 20 age-matched toddlers with normal hearing (NH). Word recognition was evaluated in quiet and in the presence of competing speech (two-talker babble, +10 dB signal-to-noise ratio) using a 2-AFC looking-preference paradigm. offline frame-by-frame analysis of session videos was used to calculate *accuracy* (recognition of a visual target object after hearing an auditory label) and *latency* (amount of time it takes to identify the target object). Results show that NH toddlers are highly accurate at identifying target objects in quiet. in the presence of competing speech, their overall accuracy is reduced and the latency is increased. Comparisons between groups suggest that, although toddlers who use CIs identify target objects significantly above chance, their overall accuracy is poorer than that of NH toddlers. in addition, the latency is significantly longer in toddlers who use CIs than NH toddlers, both in quiet and in the presence of competing speech. Consistent with previous work with older children, these data show that competing speech reduces word recognition abilities in NH toddlers and, to a greater extent, in toddlers who use CIs. More importantly, results from this study suggest that toddlers who are fitted with CIs at a young age are nonetheless slower at integrating a visual target object and its auditory label, regardless of the presence of noise competitors. These data may provide insight into the language-learning mechanisms in young children who use CIs.

## **[977] Binaural Benefits in Children with Bilateral Cochlear Implants**

**Lieselot Van Deun<sup>1</sup>, Astrid van Wieringen<sup>1</sup>, Fanny Scherf<sup>2</sup>, Ingeborg Dhooge<sup>3</sup>, Naïma Deggouj<sup>4</sup>, Christian Desloovere<sup>5</sup>, Erwin offeciers<sup>6</sup>, Paul Van de Heyning<sup>2</sup>, Leo De Raeve<sup>7</sup>, Jan Wouters<sup>1</sup>**

<sup>1</sup>*ExpORL, Dept. Neurosciences, K.U.Leuven, Belgium,*

<sup>2</sup>*Univ.Dept.ORL, Antwerp University Hospital, University of Antwerp, Belgium,* <sup>3</sup>*Dept. ORL, UGent, Belgium,* <sup>4</sup>*Service ORL, Clinique St-Luc-UCL, Bruxelles, Belgium,* <sup>5</sup>*Dept. ORL, UZLeuven, Belgium,* <sup>6</sup>*Dept. ORL, AZ St Augustinus, Wilrijk, Belgium,* <sup>7</sup>*CORA-CI, Hasselt, Belgium*

Several studies have shown that bilaterally implanted adults seem to be able to exploit head shadow and summation effects. Although binaural squelch effects have been established in some adult CI users, they often are small. in view of the plasticity of the brain, it is hypothesized that children, implanted bilaterally at a young age, may experience larger binaural benefits.

in Belgium a group of 42 children with bilateral cochlear implants participates in a study aimed at documenting bilateral and binaural benefits. of this group 27 children, between 4 and 15 years of age, participated in a sound localization test in free field with their clinical processors. Some of them showed very accurate localization ability, with mean absolute errors around 10°, whereas others were not able to localize sounds reliably. Presently, age at implantation of the first CI seems to be the most important determinant of children's localization capacity. in addition, the processing of binaural cues is investigated using a setup with synchronized experimental CI processors. Binaural masking level differences are measured to determine whether children with bilateral CI are capable of exploiting interaural time differences during the detection of signals in noise. a child-friendly test procedure, adapted to their interest and attention span, is used.

This research is funded by the Research Foundation – Flanders (FWO Vlaanderen).

## **[978] The Effect of Duration On Multi-Rate Pitch Perception in Cochlear Implants**

**Joshua Stohl<sup>1</sup>, Chandra Throckmorton<sup>1</sup>, Leslie Collins<sup>1</sup>**

<sup>1</sup>*Duke University*

Multi-rate sound processing strategies have been proposed as a means of transmitting more spectral information to cochlear implants (Nie et al., 2005; Throckmorton et al., 2006). the goal of these strategies is to improve speech recognition in noise and music perception. As suggested by Throckmorton et al. (2006) and supported by Stohl et al. (2007), subject-specific tuning of a multi-rate strategy may be necessary to provide maximum benefit to the user. in this study, psychophysics will be used to investigate the effect of duration on the place and rate-pitch percepts under a variety of conditions. a pitch ranking task was first used to determine the influence that stimulus duration had on the overall pitch structure due to place. a rate discrimination task was implemented to obtain baseline difference limens (DL) with respect to 200 pulses per second. for the remaining experiments, an ABA stimulus pattern was used, where B

was a higher pulse rate than A. the rate discrimination was repeated with the ABA stimuli. Following the discrimination task, a detection task was implemented in which subjects were asked to identify the interval containing the ABA stimulus. in the detection experiment, the pulse rate assigned to B was discriminable from A, and the duration was adaptive. the data obtained from these psychophysical experiments indicate that embedded rate DLs are higher than DLs obtained from stimuli in isolation, and that some minimum duration is required to obtain a rate-pitch percept from an embedded rate change. the variability between subjects supports the need to tune multi-rate strategies, and the inclusion of this type of data may be necessary for subjects to gain some benefit from multi-rate strategies.

## **[979] Upper Limit of Rate Pitch in Cochlear Implant Users**

**Robert Carlyon**<sup>1</sup>, John Deeks<sup>1</sup>, Ying-Yee Kong<sup>2</sup>, Christopher Long<sup>3</sup>, Colette McKay<sup>4</sup>

<sup>1</sup>Medical Research Council, <sup>2</sup>Northeastern University,

<sup>3</sup>Cochlear Americas, <sup>4</sup>University of Manchester

A number of studies indicate that cochlear implant users can rarely discriminate changes in the rate of a pulse train applied to a single electrode, once that rate exceeds about 300 pps. Expt 1 investigated the idea that this "upper limit" is due to modulations in the pattern of electrically evoked compound action potentials (ECAPs) in the response to high-rate pulse trains. Rate discrimination by Nucleus CI24 listeners was measured with base rates of 100, 200, 300, 400 and 500 pps, all mixed within each block of trials. in each trial subjects indicated which of two sounds had the higher pitch. Most listeners showed a breakdown in performance above 200-300 pps. Manipulations predicted to reduce ECAP modulation, including the addition of 5000-pps "desynchronizing" pulse trains, the introduction of gradual onset/offset ramps, or requiring listeners to detect changes in the frequency of AM imposed on a 5000-pps pulse train, all failed to markedly alter the pattern of results.

Expt 2 obtained pitch rankings from CI24 users for stimuli having rates between 112.5-1800 pps, to investigate a recent suggestion that the upper limit is increased when multiple electrodes are stimulated concurrently. Contrary to the prediction, pitch ranks increased monotonically only up to about 300 pps, both for single- and multiple-electrode stimulation.

Expt 3 studied the upper limit in two "star" MedEl C40+ users, who showed monotonically increasing pitch ranks for rates up to at least 840 pps. Four rates between 500-840 pps were presented separately on three adjacent electrodes. Multi-dimensional scaling revealed separate perceptual dimensions for electrode and rate.

in conclusion, when the upper limit is 200-300 pps, it is impervious to a wide range of manipulations expected to alter the pattern of auditory nerve activity. in contrast, for subjects showing a higher upper limit, pitch increases monotonically over a wide range, and this increase is not due to incidental "place" cues.

## **[980] Understanding and Utilization of Pitch Perception in Electric Hearing**

**Qing Tang**<sup>1</sup>, Fan-Gang Zeng<sup>1</sup>

<sup>1</sup>Departments of Anatomy and Neurobiology, Biomedical Engineering, University of California, Irvine

Poor pitch perception remains an unsolved issue in electric hearing and contributes to poor speech recognition in noise and music appreciation. Here we conducted three experiments to quantify pitch perception in electric hearing and to improve melody recognition in cochlear implant subjects. Experiment 1 matched acoustic pitch to electric pitch in two unique subjects who had a cochlear implant on one side and substantial acoustic hearing on the other side. Frequency-to-place maps were constructed as a function of electrode position at different stimulation rates (100, 200, 1653, or 2900 Hz). Experiment 2 ranked pitch of virtual channels against single electrode stimulation in 5 Clarion implant subjects. the virtual channels were constructed to have different centroids, or apical edges, or basal edges in the excitation pattern with the spacing between virtual channels being varied from 1 electrode to 10 electrodes. Experiment 3 encoded pitch of twelve familiar melodies using (1) stimulate rate on a single electrode, (2) the electric frequency-to-place map derived from Experiment 1, or (3) virtual channels derived from pitch ranking data in Experiment 2. Melody recognition was obtained as the outcome measure of the functional electric pitch encoded by these 3 methods.

Similar to previous studies (Boex et al., 2006; Dorman et al., 2007), Experiment 1 showed a similar electric frequency-to-place map at high stimulation rates, but a much shallower frequency-to-place map at low stimulation rates. Experiment 2 found that both the centroid and the apical edge of excitation pattern affected electric pitch, while the basal edge did not. Preliminary data from Experiment 3 showed that both stimulate rate and electrode place affected melody recognition. Furthermore, even when electric pitch was "properly" encoded by the matched frequency-to-place map, relative low melody recognition was still obtained presumably due to low pitch salience in electric hearing. Melody recognition data using different virtual channels are being collected and will be reported at the meeting.

(Supported by NIH RO1 DC002267)

## **[981] Evaluation of Singing in Children with Cochlear Implants**

**Li Xu**<sup>1</sup>, Ning Zhou<sup>1</sup>

<sup>1</sup>Ohio University

Cochlear implant users receive limited pitch information through the current implant devices. the coarse pitch information might hinder the development of singing in the prelingually-deaf children who have received cochlear implants. the purpose of the present study was to investigate the proficiency of singing in those children. Eight prelingually-deaf children with cochlear implants (age: 5 to 9 years old) participated in the study. Each of the children sang one of the songs that was the most familiar to him or her. the number of notes of the songs varied from 10 to 45. a normal-hearing adult sang the

same songs to provide references for comparison. the F0 contour of each note in all the songs was extracted using an autocorrelation method. the following metrics were computed and then compared between the children with cochlear implants and the normal-hearing adult singer: (1) F0 direction of any adjacent notes, (2) F0 range of the entire song, and (3) mean deviation of the normalized F0 across the notes between the children and the adult singer. On average, the F0 direction for the children with cochlear implants was only 60% correct (chance performance = 50% correct). the F0 ranges for the children with cochlear implants showed grossly compressed patterns. Their F0 ranges were on average 8 semitones smaller than those for the normal-hearing adult singer. the mean deviation of normalized F0 across notes for all children with cochlear implants was 2–3 semitones depending on the melodies of the songs. These results indicate that prelingually-deaf children with cochlear implants have significant deficits in singing due to their inability to manipulate pitch variation in correct directions and to produce accurate pitch height, both of which are important for good singing.

## **[982] Effect of Pulse Width and Rate On Speech Perception and CI Programming Parameters**

**Jeroen Brijaire<sup>1</sup>**, Raymond Bonnet<sup>1</sup>, Peter-Paul Boermans<sup>1</sup>, Johan Frijns<sup>1</sup>

<sup>1</sup>*Leiden University Medical Center*

The availability of new cochlear implant speech processors has led to an increase in stimulation rate, shortening of the pulses and the introduction of paired pulsatile strategies (PPS). These higher rates should provide for better temporal information and improved speech perception. the present study systematically investigates the effect of stimulation rate (967-3868 pps/channel), pulse width (PW, 11-43  $\mu$ s/phase) and paired pulsatile stimulation (PPS) versus continuous interleaved sampling (CIS) on speech perception, T-levels, M-levels and dynamic range. During 3 non-consecutive days, 27 post-lingually deafened patients, implanted with either a CII or a HiRes90K with a HiFocus electrode, were fitted with nine 12-channel strategies following a Latin-square design. After one hour of customization, speech recognition was tested with CVC-words in quiet and in speech-shaped noise (65 dB SPL, SNR = +10dB). No strategy turned out to be significantly better for the group. Individual patients' best scores were obtained with a number of strategies, with no clear optimal pulse width or rate. All PPS strategies yielded significantly worse scores than their CIS counterparts. PW and rate influenced the T- and M-levels in a systematic way, the T-levels decreased by 1.8 dB per doubling of the pulse rate, while the M-levels were considerably less influenced (0.15 dB per doubling of the rate). the change in T-levels was -6.4 dB per doubling of pulse width, with an associated change in M-levels of -5.4 dB. Changing from CIS to PPS led to a reduction of 1.3 dB and 1.9 dB for T- and M-levels respectively. This reduction is superimposed on the changes caused by doubling the rate, inherent to the PPS paradigm.

It is concluded that PW, rate and paired stimulation have predictable and independent effects on both T- and M-levels for all strategies tested. Speech understanding with CIS is generally better than with PPS, but no CIS strategy outperforms the other ones.

## **[983] Neural Tonotopy in CI: an Evaluation in Unilateral CI Patients with Contralateral Normal Hearing**

**Katrien Vermeire<sup>1</sup>**, Peter Schleich<sup>2</sup>, Peter Nopp<sup>2</sup>, andrea Nobbe<sup>2</sup>, Ernst Aschbacher<sup>2</sup>, Maurits Voormolen<sup>1</sup>, Paul Van de Heyning<sup>1</sup>

<sup>1</sup>*University Hospital Antwerp*, <sup>2</sup>*MED-EL headquarters*

**Objectives:** in actual cochlear implant systems the signal is filtered into different frequency bands and transmitted to electrodes along the cochlea which elicit different pitch perceptions. in this study the frequency-place map for electric hearing was investigated as a means to possibly improve current speech coding strategies by delivering spectral information to the appropriate cochlear place. **Methods:** Fourteen subjects with near to normal hearing in the contra-lateral ear have been provided with a MED-EL cochlear implant in the deaf ear in order to reduce intractable tinnitus. Pitch scaling experiments were performed using twelve single-electrode stimuli in the implanted ear and twelve acoustic sinusoids logarithmically spaced between 100 and 8500 Hz in the contra-lateral ear. the frequency-place function was calculated according to the exact electrode position in the cochlea obtained by postoperative skull radiographs by means of a cochlear view and were compared to Greenwood's frequency-place function in normal hearing. **Results:** Electrical stimulation with a constant stimulation rate elicited a low pitch perception in the apical region of the cochlea, and shifting the stimulating electrode towards the basal region of the cochlea elicited an increasingly higher pitch perception. the frequency-place function obtained with our subjects did not show a significant shift relative to Greenwood's frequency-position function.

**Conclusions:** Electrical stimulation of the cochlea in patients with a unilateral cochlear implant and with near to normal hearing at the non-implanted ear, provided a specific frequency-position function consistent with Greenwood's function.

## **[984] Spectral Analysis of Spontaneous and Evoked Activity in Rat Auditory Cortex**

**Michael Rummel<sup>1</sup>**, Sneha Shrestha<sup>1</sup>, Bryan Baxter<sup>1</sup>, **Matthew Banks<sup>1</sup>**

<sup>1</sup>*University of Wisconsin-Madison*

**Abstract**

The frequency spectrum of cortical field potentials represents synchronous network activity over wide spatial and temporal scales. in primary auditory cortex, activity in the gamma (30 – 80 Hz) and high gamma bands (80 – 200 Hz) has been linked to perception and level of consciousness. in somatosensory cortex, transient oscillations at even higher frequency (~600 Hz) are triggered at short latency by sensory stimuli. We investigated the incidence of such high frequency activity

in auditory cortex of awake rats. Local field potentials were recorded using chronically implanted epidural electrodes. Stimuli consisted of frequency modulated tone sweeps (250 msec, 10 – 20 kHz). Wavelet transforms were used to perform time-frequency analysis of spontaneous and evoked activity over the frequency range 20 – 1900 Hz. Mean pre-stimulus (spontaneous) power spectra fell off as  $1/f^2$ , with prominent 'shoulders' or deviations from this line occurring at ~50 and ~740 Hz. Auditory stimuli evoked activity across the analyzed frequency range, but activity persisted after stimulus offset primarily at frequencies above 200 Hz. In single trial responses these late, high frequency components were variable in their incidence, amplitude and latency. We found no correlation between power at a particular frequency prior to the stimulus and the power of that frequency component of the evoked response. Computation of the spectral comodulation revealed significant trial-by-trial correlation in power between the highest frequency ( $f > 200$  Hz) components, but no interactions between low ( $f < 100$  Hz) and high frequency components. These data indicate that activity at frequencies  $> 200$  Hz is prominent in auditory cortex and may represent a general feature of primary sensory cortex. The variable and prolonged latency of these components suggest that the activity represents intra-cortical stimulus processing.

**985 Differential Effects of Iontophoretic Application of the GABA<sub>A</sub>-Antagonists Bicuculline and Gabazine On Tone-Evoked Local Field Potentials in Primary Auditory Cortex: Interaction with Ketamine Anesthesia**

Simone Kurt<sup>1</sup>, Christoph Moeller<sup>2</sup>, Marcus Jeschke<sup>3</sup>, Holger Schulze<sup>4</sup>

<sup>1</sup>*Institute for Neurobiology, University of Ulm, Germany,*

<sup>2</sup>*Leibniz Institute for Neurobiology, Magdeburg, Germany,*

<sup>3</sup>*The Johns Hopkins School of Medicine, Laboratory for Auditory Neurophysiology, Baltimore, USA,* <sup>4</sup>*University of Erlangen-Nuremberg, Experimental Otolaryngology, Erlangen, Germany*

Gamma-aminobutyric acid (GABA) is one of the main inhibitory transmitters in the central nervous system. In a recent study (Kurt et al., *Hear. Res.*, 2006) we have demonstrated differential effects of two iontophoretically applied GABA<sub>A</sub>-blockers, bicuculline (BIC) and gabazine (SR 95531), on neuronal responses in primary auditory cortex (AI). Whereas the only effect of gabazine was to block GABA<sub>A</sub>-mediated inhibition, BIC-application additionally induced dose-dependent side-effects, probably on calcium-dependent potassium channels. Here we investigated the effects of the two drugs on pure tone evoked local field potentials (LFPs) in AI. In contrast to spiking activity, which reflects neuronal output, LFPs are believed to mainly reflect dendritic activity and therefore neuronal input.

LFPs were recorded from the left AI of anaesthetized and unanaesthetized Mongolian gerbils before, during and after microiontophoretic application of BIC and gabazine using multi-barrel glass electrodes. After the application of

both drugs, a significant increase of the amplitude of the N1-component of the LFP was observed in both anaesthetized and unanaesthetized animals, but this increase was significantly more pronounced after BIC than after gabazine application, a result which corresponds to the effects on neuronal discharge rate reported earlier. In contrast, the effects of BIC and gabazine on LFP duration and LFP spectral tuning were affected by ketamine anesthesia, an effect that was not seen in the spiking data.

**986 Involvement of "Limbic" Brain Centers in Humans During the Perception of Sounds Without Emotional Content**

Dave Langers<sup>1</sup>, Jennifer Melcher<sup>1</sup>

<sup>1</sup>*Massachusetts Eye and Ear Infirmary*

Sounds that lack behavioral relevance (e.g., tones, noise) generally evoke little activation outside the classical auditory pathway, despite many connections that link auditory centers to other non-auditory brain areas (like the amygdala). We demonstrate that this absence of activation may be due to limitations of common neuroimaging analysis methods and that, in fact, non-auditory centers (including those commonly termed limbic/paralimbic) may be recruited even during simple auditory paradigms without emotional content.

Functional magnetic resonance imaging was performed on 14 healthy subjects. 32-s broadband noise fragments were presented and activated brain areas were detected using [i] conventional regression analysis to extract signal variations with similar periodicity as the stimulus on/off cycles, and [ii] independent component analysis (ICA) to identify brain networks without prior assumptions about the presented stimuli. Connectivity analysis was performed to determine partial temporal correlations (i.e., effective connectivity) between brain areas.

One ICA component comprised major centers throughout the auditory pathway, including those identified with the conventional analysis: inferior colliculi, medial geniculate bodies, and auditory cortices. In contrast to the conventional analysis, ICA also identified other components with stimulus-related signal time courses. One included the amygdala and hippocampus, and overlapped the auditory component in the medial geniculate body; others included the striatum, cingulate cortex, insula and orbitofrontal cortex. Connectivity analysis confirmed strong functional connections between the medial geniculate body and both classical auditory and mediotemporal limbic centers.

Our results suggest that brain structures mediating emotion may interact directly with basic sensory processing and that the medial geniculate body is a nexus for this interaction.

### **987 Tracking the Neuromagnetic Response in Auditory Cortex As the Repetition Rate of a Sound is Varied Across the Lower Limit of Melodic Pitch**

**Andre Rupp<sup>1</sup>**, Banu Soenmez<sup>1</sup>, Alexander Gutschalk<sup>1</sup>, Roy D. Patterson<sup>2</sup>

<sup>1</sup>*Section of Biomagnetism, Department of Neurology, University Hospital Heidelberg*, <sup>2</sup>*CNBH Dept Physiology University of Cambridge*

The lower limit of melodic pitch (LLMP) is around 32 Hz [Pressnitzer et al., J. Acoust. Soc. Am. 109, 2074-2084 (2001)]. the current study used MEG (magnetoencephalography) to measure the pitch onset response (POR) evoked by temporally regular sounds, as the repetition rate (RR) changed from well below the LLMP (8 Hz) up to the LLMP (32 Hz) and well beyond it (128 Hz). the sounds were click trains (CTs), regular interval noise (RIN) created with a delay-and-add network, and damped and ramped sinusoids. Continuous stimuli were created by concatenating 1-s segments of each RR, for each of the four stimulus types. Auditory evoked fields were recorded in 19 subjects. Spatio-temporal source analysis revealed two separate sources in auditory cortex in each hemisphere. the anterior generator, located in lateral Heschl's gyrus, was particularly sensitive to the pitch changes associated with the changes in RR. the source waveforms exhibited a substantial POR that peaked about 100 ms after the transition from 8 Hz to 32 Hz, and a larger POR just after the transition from 32 Hz to 128 Hz. the click trains evoked particularly large sustained fields (SF) in the anterior source which increased with RR, as did the damped and ramped sinusoids. the posterior source, located in the Planum temporale was more sensitive to changes in intensity. the results were similar when the stimuli were reversed and the RR decreased from 128, to 32 and then 8 Hz. the ramped sinusoids produced larger PORs and SFs than the damped sinusoids echoing the temporal asymmetries observed psychophysically [Patterson and Irino J. Acoust. Soc. Am. 104, 2967-2979 (1998)]. the results show that the pitch responses (POR and SF) observed in the anterior source on Heschl's gyrus can be observed all the way down to the LLMP, and they can be separated from the intensity response in the posterior source.

### **988 Selective Attention to Spatial and Non-Spatial Sound Features Studied with Fmri**

**Aspasia E. Paltoglou<sup>1</sup>**, Deborah A. Hall<sup>1</sup>

<sup>1</sup>*MRC Institute of Hearing Research*

This study investigates the hypothesis that selectively attending to frequency modulation (FM) and spatial motion enhances activity in auditory cortical areas that are sensitive to those attended features. Previous evidence shows enhancement, but only in the spatial domain. However, spatial and non-spatial tasks were not matched for difficulty. It is possible that the easier non-spatial task failed to show attentional enhancement for this reason. In this study, we matched FM and motion parameters for difficulty across individual listeners. Sound sequences consisted of 18 harmonic-complex tones ( $F_0 = 400$  Hz, harmonics 1-5, 400 ms duration, 50 ms ISI). Tones were

frequency modulated (5 Hz rate, 12.5% depth) and/or varied in inter-aural time difference (150  $\mu$ s steps) to generate a percept that swept back and forth in the azimuthal plane. There were three sound conditions; moving FM, stationary FM and moving steady state. Listeners received three different instructions: i) 'just listen', ii) 'detect FM targets' defined by a shallower modulation depth, and iii) 'detect motion targets' defined by a jump in the opposite direction. This abstract reports results from six listeners, using a 3T MR scanner (32-slices, 3 mm<sup>3</sup>, TR=10 s). Behavioral performance was not significantly different for any one particular condition ( $p > 0.05$ ). the location of FM- and motion-related activation (consistent across two comparisons, passive listening and controlling for attention) was broadly compatible with previous research. So far, we have found some evidence for enhancement when attending to FM in the regions of lateral Heschl's gyrus responsive to FM. This provides partial support for attentional enhancement within auditory regions that are sensitive to non-spatial acoustic features. We were surprised to see that this finding was extended to the motion-sensitive regions too, but analysis using a larger group of listeners (N=18) will test whether these preliminary findings are robust.

### **989 Beyond What and Where: Auditory Cortical Encoding of Pitch, Timbre and Location Cues**

**Jennifer Bizley<sup>1</sup>**, Kerry Walker<sup>1</sup>, Andrew King<sup>1</sup>, Jan Schnupp<sup>1</sup>

<sup>1</sup>*University of Oxford*

We have investigated the cortical encoding of complex sounds in the ferret using band-pass filtered click trains ("artificial vowels"). the band-pass filters imposed peaks ("formants") in the energy spectrum of the stimuli, which determined the stimulus timbre. the click rate determined the pitch of the sound, and virtual acoustic space was used to reproduce sound-source location cues. Our stimulus set included 64 artificial vowels, which covered a 3-dimensional parameter matrix of 4 pitches, 4 timbres and 4 spatial locations. These sounds were presented over earphones to 5 anesthetized ferrets, and extracellular spike responses were recorded in 5 auditory cortical fields. The responses were subjected to a variance decomposition analysis by summing spike counts into 20 ms bins and performing a 2-way ANOVA with time bin and stimulus as factors. We then calculated the proportion of stimulus-induced variance that could be attributed to azimuth, pitch and timbre for each unit. Many units showed sensitivity for two, or more, of these sound parameters. Neurons in A1 showed the greatest sensitivity to stimulus location. Pitch sensitivity was restricted mainly to low frequency areas where the primary and non primary tonotopic fields meet. in contrast, timbre sensitivity was found throughout both primary fields, A1 and AAF, and, additionally, in the posterior fields. the total amount of variance that could be explained by the stimulus-time interactions decreased in higher-order cortical areas. However, responses in the higher-order fields tended to have a greater proportion of their variance accounted for by interactions between two of the stimulus parameters,



which suggests that neurons in these areas are more selective for specific combinations of stimulus features. In conclusion, while there is a degree of functional specialization, we do not find evidence for a clear separation of discrete “what” and “where” processing streams within the 5 cortical areas studied.

### **990 Responses to Alternating Tones in Auditory Cortex of Anaesthetized Guinea Pigs and Ferrets**

**Chris Scholes<sup>1</sup>**, Alan Palmer<sup>1</sup>, Chris Sumner<sup>1</sup>

<sup>1</sup>*MRC Institute of Hearing Research*

Alternating tones are heard as one or two streams depending on their frequency difference (FD) and presentation rates (PRs). Stream segregation builds up and is dependent on the attentional state. Neural activity in response to tone sequences, from the auditory cortex of awake macaque and starling, has revealed a possible neural correlate of stream segregation (Fishman et al., 2004, *J Acoust Soc Am* 116:1656-1670; Bee and Klump, 2005, *Brain Behav Evol* 66:197-214), including the ‘build-up’ (Micheyl et al., 2005, *Neuron* 48:139-148). These studies did not address the role of single units in any depth, and the role of attention was unclear. We have recorded unit responses to alternating tones in the cortex of anaesthetized guinea-pigs and ferrets, thus eliminating effects of attention, revealing more about the contribution of single units versus population codes, and confirming the findings in a wider range of species. We have also examined ‘build-up’ across a wider range of presentation rates than previous studies.

The response of the majority of A1 neurons in ferrets and guinea pigs, assessed using peak amplitude and spikecount measures, was consistent with previous findings. At low PRs or low FDs many single neurons responded as well to both tones. At larger FDs, the response to one tone reduced as it fell out of the receptive field. Sometimes, the response to the remaining tone increased. At high PRs, the response to both tones reduced, but more so for the tone further from characteristic frequency. These effects were attributable to the adaptation of firing rate. The effects of PR, FD and build-up were evident in single units as well as in the population. In some units, locking to the tones was poor at higher PRs. A more reliable measure was based on the first 2 components in the FFT of a histogram locked to the repetition period of the tones. This showed consistent changes in representation of the alternating tones even when phase locking was poor.

### **991 Identification of Auditory Cortical Areas Using Current-Source-Density Analysis**

**Poppy Crum<sup>1</sup>**, Elias Issa<sup>1</sup>, Xiaoqin Wang<sup>1</sup>

<sup>1</sup>*Johns Hopkins School of Medicine*

Anatomical studies of human and non-human primates show the auditory cortex is divided into hierarchically connected core, belt, and parabelt regions (Hackett & Kass, 1998). These divisions are distinguished by both thalamocortical and corticocortical connections. Despite observable differences in neural response properties, to date no reliable physiological method has been

established to identify the boundaries between these areas, in particular the boundary between the belt and parabelt regions. In this study, we tested the feasibility that Current-Source-Density (CSD) may offer a predictable measure for identifying the location of recorded neural response in the auditory system as originating from a particular cortical division. Measurement of CSD across the laminae of primary sensory cortices demonstrates a characteristic current sink in layer IV indicative of the local depolarizing currents of cells in response to lemniscal thalamic input. Anatomical studies of auditory cortex have shown stark differentiation in the proportion of input from the lemniscal pathway (MGBv) received by the core, belt, and parabelt regions. Therefore, it was predicted the presence of the layer IV sink and characteristic pattern of CSD should change across these areas as the relative thalamic input changes. We made recordings of the CSD across the medial-to-lateral surface of the awake marmoset auditory cortex and showed a clear correlation between the presence of a layer IV sink and the medial-to-lateral position. The local-field-potential (LFP) was measured at 100µ steps orthogonal to the laminar striations and used to compute the CSD for an individual recording track. Single-units responsive to auditory stimuli were also characterized for penetrations across the medial-to-lateral dimension to compare with changes in the pattern of the CSD. The observed changes in the pattern of CSD were then correlated with observable anatomical boundaries along the medial-to-lateral dimension based on histological staining of auditory cortex (PV, SMI-32, AChE, and Nissl). Establishing a means of registering cellular location as belonging within a cortical region offers many possibilities for future study of single neurons outside of primary-auditory-cortex (A1).

### **992 GABA Shapes a Systematic Map of IID Selectivity in the Auditory Cortex**

**Khaleel Razak<sup>1</sup>**, Zoltan Fuzessery<sup>2</sup>

<sup>1</sup>*Univ. California, Riverside*, <sup>2</sup>*Univ. Wyoming*

We present evidence for a systematic map of interaural intensity difference (IID) sensitivity in the auditory cortex. We also show that IID sensitivity is shaped locally by intracortical GABA. The auditory cortex is involved in sound localization behaviors. But how the cortex codes for sound locations remains a topic of debate. There is no evidence of a systematic representation of sound locations in the cortex. A consistent organizational feature is a clustered organization of binaural cues that underlie sound localization. However, it is unclear how the clustered organization leads to a representation of auditory space. Here we show that a systematic map of interaural intensity difference (IID) sensitivity exists within a binaural cluster in the auditory cortex of the pallid bat. The pallid bat listens passively to prey-generated noise to localize prey. Its auditory cortex contains a region selective for low-frequency noise. Within this low-frequency region, two clusters of binaural properties are present. One cluster consists of binaurally inhibited (EO/I) neurons. The second cluster contains neurons with predominantly binaural (OO/FI) interactions. We show here that the preferred IID of OO/FI neurons shifts systematically within the OO/FI

cluster. the map is relatively stable with increasing absolute intensity. Binaural selectivity is sharper for noise than tones, and the systematic representation is observed only when noise is used as stimuli. Interestingly, there is a correlation between best-frequency and IID sensitivity. Iontophoretic application of GABA-A receptor antagonists (bicuculline/gabazine) converts OO/FI neurons to EO/I neurons, suggesting that a cluster of OO/FI neurons is sculpted out of a larger cluster of EI neurons using GABA. How the IID map may be integrated with frequency tuning and external ear directionality to give rise to a population code of sound locations is discussed.

### **[993] Task-Dependence of Spatial Sensitivity in Cat Auditory Cortex: Area A1 V.S. DZ.**

**Chen-Chung Lee<sup>1</sup>**, Ewan Macpherson<sup>1</sup>, John Middlebrooks<sup>1</sup>

<sup>1</sup>*Kresge Hearing Research Institute, University of Michigan*

Previous studies from our lab have shown that neurons in cortical area DZ have higher spatial sensitivity than neurons in A1 of anesthetized cats. Moreover, the spatial sensitivity of many DZ units sharpens when a cat is engaged in a sound-localization task. in the current study we compared the task dependence of spatial sensitivity between cortical area DZ and A1. We recorded extracellular spike activity with chronically implanted 16-channel probes. in all conditions, probe stimuli were 80 ms broadband noise bursts from free field speakers in the horizontal plane, spaced in 20 degree increments. We compared neuronal responses under three behavioral conditions: 1) Idle: exposed to probe stimuli without engaging in behavior tasks. 2) Discrimination: detect a change from the probe stimulus to a click train, regardless of the location of the sound. 3) Localization: distinguish a shift in stimulus elevation to 40 degree above horizontal plane. Overall, task-dependent modulation of responses was more common in DZ than in A1. Spike patterns usually were modulated differently between A1 and DZ across behavioral conditions. A1 neurons usually showed task-dependent modulations only in their phasic responses whereas DZ neurons showed task-dependent modulations of both phasic and tonic responses. the enhanced selectivity usually resulted from increased suppression of responses to non-favored locations. These task-dependent changes in spatial sensitivity observed here may be interpreted as a top-down modulation of the spatial sensitivity of auditory cortical neurons. Different modulation patterns shown in A1 and DZ might suggest their distinct functions in processing auditory spatial information.

Supported by RO1-DC-00420

### **[994] Adrenergic Modulation Reveals Two Functionally Different Inhibitory Pathways in the Auditory Cortex of the Rat**

**Humberto Salgado<sup>1</sup>**, Ankur Patel<sup>1</sup>, Justin Nichols<sup>1</sup>, Mitali Bose<sup>2</sup>, Marco Atzori<sup>3</sup>

<sup>1</sup>UTD, <sup>2</sup>UTSW, <sup>3</sup>University of Texas at Dallas

Sensory cortices receive noradrenergic terminals from the brainstem whose function is not completely understood. We studied the effect of norepinephrine on the properties of pharmacologically isolated inhibitory GABAAR-mediated inhibitory postsynaptic currents (IPSCs) on layer 2/3 neurons of the rat auditory cortex using voltage-clamp recording in a thin-slice preparation.

in order to evoke IPSCs we used pairs or trains of extracellular stimuli at various interpulse delays (20-200 ms). the effects of adrenergic agonists and antagonists and their combinations have been tested on two afferent pathways by placing the stimulating electrode either in the superficial layer 1, or in layer 2/3, at no less than 150 microns from the recording electrode.

Application of norepinephrine, beta-, or alfa2-agonists produced a large, sustained and fully reversible increase in the amplitude of the evoked IPSCs (70% of the control amplitude), accompanied by a decrease in pair pulse ratio, defined as the ratio between the second and the first responses, and an increase in miniature IPSC frequency in the presence of the Na-channel blocker tetrodotoxin, indicating a presynaptic locus for the action of norepinephrine. On the contrary application of norepinephrine or alfa1 agonists produced a decrease in evoked IPSC amplitude of about 30% of the control amplitude.

Application of norepinephrine in the presence of adrenergic beta and alfa2 blockers produced a decrease in the IPSC evoked by stimulation of layer 2/3, suggesting that beta and alfa2 receptor mediated IPSC amplitude increase masked a background of alfa1 receptor mediated IPSC depression.

Although the physiological significance of the differential modulation of inhibitory inputs is not clear yet, we speculate that a decrease inhibition from layer 1 might promote alertness through enhancement of the non-specific auditory thalamo-cortical pathway, while increased inhibition in perigranular layers might promote synchronization of modality-specific input.

### **[995] Human Auditory Cortical Responses to Self-Vocalization with and Without Altered Auditory Feedback**

**Jeremy Greenlee<sup>1</sup>**, Fangxiang Chen<sup>1</sup>, Hiroyuki Oya<sup>1</sup>, Charles Larson<sup>2</sup>, Hiroto Kawasaki<sup>1</sup>, Haiming Chen<sup>1</sup>, Matthew Howard<sup>1</sup>

<sup>1</sup>University of Iowa, <sup>2</sup>Northwestern University

Self-vocalization is known to alter firing rates of auditory cortical neurons in non-human primates in a predominantly suppressive manner. Imaging studies in humans show excitation of temporal cortices during vocalization but to a lesser degree than that seen during listening. the mechanisms responsible for these findings remain unclear. We have investigated 5 patients undergoing surgical treatment of epilepsy to examine the influence of self-

vocalization on auditory cortex. Recordings were taken from intracranial electrode arrays positioned on the pial-surface over secondary auditory fields and stereotactically implanted into primary auditory fields on Heschl's gyrus (HG). We recorded brain activity simultaneously while subjects performed the following tasks: self-vocalization with normal auditory feedback, self-vocalization with time or frequency altered feedback (2 patients), playback of the subject's own voice, and playback of a different speaker's voice. Recordings were analyzed offline and average evoked potentials (AEPs) and time-frequency power analyses were examined for each condition.

Compared to both playback conditions, self-vocalization produced differences in evoked and induced activity in all patients compared to playback. Differences were seen on both posterior superior temporal gyrus (STG) and HG auditory fields, although more differences were seen on STG. Marked attenuation or complete abolition of AEPs was observed at some contacts while others showed preservation of AEPs. Adding delayed or pitch-shifted feedback during vocalization produced further changes in the pattern of self-vocalization responses, also in a regional pattern. Power analyses and AEPs showed similar regional differences in auditory cortical responses. These findings suggest that self-vocalization influences auditory cortex in an auditory field-specific manner.

#### **[996] Horizontal Connections and Their Functions in the Primary Auditory Cortex**

**Kazuo Imaizumi**<sup>1</sup>, Robert Froemke<sup>1</sup>, Jeffery Winer<sup>2</sup>, Benedicte Philibert<sup>1</sup>, Christoph Schreiner<sup>1</sup>

<sup>1</sup>UC San Francisco, <sup>2</sup>UC Berkeley

A conspicuous anatomical feature in the neocortex is the presence of horizontal connections between neuron clusters with similar receptive field properties. In the mid-frequency region of cat primary auditory cortex (AI), neuron clusters with different spectral bandwidths (frequency extent of the tuning curve) are alternately organized. Here we compare differences in the connectivity pattern and their neural functions between the narrow- (NB) and broad-band (BB) regions. We injected different retrograde tracers in the NB and BB regions. Labeled neurons forming isolated patches often occurred at functionally similar locations regarding frequency and bandwidth. However, patches connecting to the BB region were skewed toward higher frequency regions and showed some overlap with NB regions. Double labeled neurons connecting to both the NB and BB regions were rare. Near the injection sites, extension of connections across the frequency bands was almost equal for the NB and BB regions, suggesting invariant cortical integration distance within AI. To examine the contribution of local circuits, we also applied intracortical microstimulation techniques in the same bandwidth module across different frequency bands. For the BB region, best frequencies shifted toward electrically stimulated frequencies, suggesting dominant excitatory connections. For the NB region, by contrast, best frequencies shifted either toward or away from the stimulated frequencies, suggesting robust inhibitory connections. Currently, we are examining contribution of local inhibitory circuits in the modules by application of

GABA antagonists. Overall, a complex network of connectivity pattern appears to be largely function-specific, and is likely shaped by specific local inhibitory circuitry. Our results suggest the existence of parallel spectral processing schemes within AI.

Supported by NIDCD R01DC2260 and NS34835 (CES), R01DC2319 (JAW), and Jane Coffin Childs Foundation (RCF)

#### **[997] Results of the First High Density Whole Genome Association Study for Age-Related Hearing Impairment**

Rick Friedman<sup>1</sup>, **Lut Van Laer**<sup>2</sup>, Sonal Sheth<sup>1</sup>, Els Van Eyken<sup>2</sup>, Sarah Bonneux<sup>2</sup>, Erik Fransen<sup>2</sup>, Ilmari Pyykko<sup>3</sup>, Cor W.R.J. Cremers<sup>4</sup>, Hannie Kremer<sup>4</sup>, Ingeborg Dhooge<sup>5</sup>, Dafydd Stephens<sup>6</sup>, Eva Orzan<sup>7</sup>, Markus Pfister<sup>8</sup>, Michael Bille<sup>9</sup>, Agnete Parving<sup>9</sup>, Martti Sorri<sup>10</sup>, Paul H. Van de Heyning<sup>11</sup>, Dietrich Stephan<sup>12</sup>, Matthew J. Huentelman<sup>12</sup>, Guy Van Camp<sup>2</sup>

<sup>1</sup>House Ear Institute, <sup>2</sup>Department of Medical Genetics, University of Antwerp, <sup>3</sup>Department of Otorhinolaryngology, University of Tampere, <sup>4</sup>Department of Otorhinolaryngology, Radboud University Nijmegen Medical Centre, <sup>5</sup>Department of Otorhinolaryngology, University Hospital of Ghent, <sup>6</sup>Welsh Hearing Institute, Cardiff University, <sup>7</sup>Department of Otorhinolaryngology, University Hospital Padova, <sup>8</sup>Department of Otorhinolaryngology, University of Tübingen, <sup>9</sup>Department of Audiology, Bispebjerg Hospital, <sup>10</sup>Department of Otorhinolaryngology, University of Oulu, <sup>11</sup>Department of Otorhinolaryngology, University Hospital of Antwerp, <sup>12</sup>Neurogenomics Division, the Translational Genomics Research Institute

Age-Related Hearing Impairment (ARHI), or presbycusis, is the most prevalent sensory impairment in the elderly. Approximately 50 % of 80-year-olds suffer from a significant hearing loss (25 dB or more). ARHI is a complex disease caused by an interaction between environmental and genetic factors. The contribution of various environmental factors has been extensively studied. In contrast, investigations to identify the genetic risk factors have only recently been initiated. So far only 3 susceptibility genes have been reported. Here we describe the results of a whole genome association study based on a pooling approach using 1692 ARHI samples derived from 8 centres from 6 European countries. Based on an age- and sex-independent measure of hearing loss (Z-score), the samples were combined into good and bad hearing pools for each centre separately. Each DNA pool was genotyped in triplicate on the GeneChip® Human Mapping 500K array pair from Affymetrix and allelic differences were calculated based on previously optimised ranking algorithms (GenePool; Pearson et al., 2007, Am. J. Hum. Genet. 80, 126-139). The 252 top-ranked SNPs identified in the general European population group were confirmed using individual genotyping. Subsequently, the 20 most interesting SNPs, based on significance values as well as on functional considerations, were genotyped in a replication cohort. This resulted in a highly significant SNP (surviving 1 million permutations) located in a gene that previously had not been shown to be involved in monogenic hearing loss. Finemapping genotyping

experiments could position the association peak within a 150 kb region surrounding exon 2 of the gene. Functional studies showed that this new putative ARHI susceptibility gene is expressed in the inner and outer hair cells and in spiral ganglion cells of the inner ear.

#### **[998] Mutations of a Novel Gene are Responsible for Recessively Inherited Nonsyndromic Hearing Loss, *DFNB63***

**Zubair Ahmed**<sup>1</sup>, Saber Masmoudi<sup>2</sup>, Ersan Kalay<sup>3</sup>, Inna Belyantseva<sup>1</sup>, Mohammed Mosrati<sup>2</sup>, Rob Collin<sup>4</sup>, Saima Riazuddin<sup>1</sup>, Mounira Hmani-Aifa<sup>2</sup>, Hanka Venzelaar<sup>5</sup>, Mayya Kavar<sup>1</sup>, Tlili Abdelaziz<sup>2</sup>, Bert van der Zwaag<sup>6</sup>, Shahid Khan<sup>7</sup>, L Ayadi<sup>8</sup>, Sheikh a Riazuddin<sup>7</sup>, I Charfedine<sup>9</sup>, Refik Caylan<sup>10</sup>, Jaap Oostrik<sup>4</sup>, Ghorbel Abdelmonem<sup>9</sup>, Sheikh Riazuddin<sup>7</sup>, Thomas B Friedman<sup>1</sup>, Hammadi Ayadi<sup>2</sup>, Hannie Kremer<sup>3</sup>

<sup>1</sup>National Institute on Deafness and Other Communication Disorders, National Institutes of Health, <sup>2</sup>Laboratoire de Génétique Moléculaire Humaine, Faculté de Médecine de Sfax, Tunisie, <sup>3</sup>Dept of Human Genetics, and Dept of Otorhinolaryngology, Radboud University Nijmegen Medical Centre, <sup>4</sup>Department of Otorhinolaryngology, Radboud University Nijmegen Medical Centre, Nijmegen, <sup>5</sup>Center for Molecular and Biomolecular Informatics, Radboud University Nijmegen, Nijmegen, <sup>6</sup>Dept of Pharmacology & Anatomy, Rudolf Magnus Institute of Neuroscience, U Medical Center Utrecht, <sup>7</sup>National Centre of Excellence in Molecular Biology, University of the Punjab, Lahore, Pakistan, <sup>8</sup>Unité Cibles Diagnostique et Thérapeutique des Pathologies Humaines, Centre de Biotechnologie de Sfax, <sup>9</sup>Service d'O.R.L., C.H.U. Habib Bourguiba de Sfax, Tunisie., <sup>10</sup>Dept of Otorhinolaryngology, Faculty of Medicine, Karadeniz Technical University, Trabzon, Turkey

Approximately one-half of all cases of pre-lingual hearing loss are caused by genetic factors. Identification of the genes causing deafness is one strategy to uncover molecular components necessary for the function of the auditory system. Families from Pakistan, Turkey and Tunisia segregating deafness as an autosomal recessive trait were ascertained and a novel locus for nonsyndromic deafness *DFNB63* was mapped in a 4.8 cM interval on human chromosome 11q13.3-q13.4 (Khan et al., 2007; Kalay et al., 2007; Tlili et al., 2007). Enrollment of additional family members and *DFNB63* families helped to refine the reported critical interval to less than 1 cM. There are 30 known and predicted genes in the *DFNB63* linked region. Sequence analyses of all 30 genes were carried out using DNA samples of affected individuals of these *DFNB63* families. Mutational screening revealed three missense mutations and one splice site mutation co-segregating with *DFNB63* deafness. RT-PCR analysis of 17 different human and mouse tissues revealed a wide pattern of expression of *DFNB63*. *In Situ* analysis using a probe designed from the unique 3'UTR of *DFNB63* showed expression in the inner ear. We also used RT-PCR and Northern and Western blot analyses to study the molecular evolution of the structure of the *DFNB63* gene in the rat, mouse, the lemur, baboon, rhesus, chimp and humans. Further studies are in progress to determine the

sub-cellular localization and function of the protein encoded by *DFNB63*.

#### **[999] Identification of a Candidate Mutation for a Rare Auditory Neuropathy Through Combined Linkage and Gene Expression Analysis**

Cynthia J. Schoen<sup>1</sup>, Sarah B. Emery<sup>2</sup>, Katy Downs<sup>2</sup>, Margit Burmeister<sup>1</sup>, **Marci M. Lesperance**<sup>2</sup>

<sup>1</sup>University of Michigan, Department of Human Genetics,

<sup>2</sup>University of Michigan, Department of Otolaryngology-Head & Neck Surgery

We are investigating a rare large pedigree with an autosomal dominant form of auditory neuropathy. While true dominance can rarely be documented in human genetic disorders, in this family, two affected homozygotes appear to have the same phenotype as the heterozygotes. the locus, *AUNA1*, was previously mapped to 13q14-21 using linkage analysis (Kim et al. 2004). Since the expression of a mutated gene product is often dysregulated, we used whole genome expression arrays (Illumina Human-6 v2 Expression BeadChip), consisting of 48,000 probes, to determine global expression changes in order to identify candidate genes. RNA was obtained from lymphoblastoid cell lines (LCLs) from affected heterozygotes, homozygotes, and age- and sex-matched controls. of the ten probes exhibiting the most significant up- or downregulation, the only two mapping to the non-recombinant *AUNA1* interval were from the *DIAPH3* gene. Compared to controls, there appeared to be a two-fold increase in expression in both homozygotes and heterozygotes alike, which was confirmed by quantitative RT-PCR with probes against exons 5-6. Sequencing of *DIAPH3* revealed a mutation in the 5' untranslated region (UTR), which segregated with deafness and was absent in 318 control chromosomes. We hypothesize that the changes in expression observed in other genes signify downstream effects of the *DIAPH3* mutation. This strategy represents a novel method to both confirm and identify candidate genes while simultaneously elucidating genetic pathways. the finding of gene overexpression is consistent with a dominant negative mechanism of deafness as would be expected with true dominance. Furthermore, these findings represent the first demonstration of a mutation in the 5' UTR causing human nonsyndromic deafness. Still remaining to be determined is whether the deafness results from simple overexpression of the wild-type transcript or from expression of an aberrant transcript yet to be identified.

#### **[1000] The Search for Biological Networks of Hearing: Combining Genomic, Proteomic and Microrna Characterization**

**Karen B. Avraham**<sup>1</sup>, Tal Elkan<sup>1</sup>, Ginat Toren<sup>1</sup>, Ronna Hertzano<sup>1</sup>, Amiel Dror<sup>1</sup>, Rani Elkan<sup>1</sup>, Takunori Satoh<sup>2</sup>, Martin Irmeler<sup>3</sup>, Johannes Beckers<sup>3</sup>, Eran Hornstein<sup>4</sup>, Donna M. Fekete<sup>2</sup>, Lilach M. Friedman<sup>1</sup>

<sup>1</sup>Dept. of Human Molecular Genetics & Biochemistry, Tel Aviv University, Tel Aviv, Israel, <sup>2</sup>Biological Sciences, Purdue University, West Lafayette, Indiana, USA, <sup>3</sup>GSF-

National Research Center for Environment and Health, GmbH, Neuherberg, Germany, <sup>4</sup>Dept. of Human Molecular Genetics, Weizmann Institute of Science, Rehovot, Israel  
Systems biology involves studying the interaction and interplay of many levels of biological information. We have combined transcriptomic and proteomic analyses of a comparison of early post-natal cochlear and vestibular sensory epithelia to identify networks of genes and proteins essential for the development and function of these inner ear organs. We further identified microRNAs (miRNAs) that are uniquely expressed in these sensory epithelia using bioinformatics and experimental approaches, including microarray profiling and *In Situ* hybridization.

miRNAs are recognized as important regulators of gene expression at the post-transcriptional level. to understand the biological roles of miRNAs, their targets need to be identified. However, bioinformatics tools predict 100s, if not 1000s, of targets for each miRNA. in order to narrow down the prediction results to targets with greater potential, we have used our integrated transcriptomic and proteomic expression data sets. We reduced the number of potential targets by a significant number. These targets are now being investigated to discover whether they are indeed true biological targets. Finally, for a number of miRNAs, morpholino experiments in zebrafish demonstrated abnormalities in inner ear development and/or structure.

Expression profiling of vestibular and cochlear sensory epithelia using Affymetrix microarrays and proteomics analysis using the Q-TOF mass spectrometer with ITRAQ labeling has led to the identification of genes and protein networks. a network analysis was applied to find proteins of interest that are physically connected, pointing to some common function/pathway/complex. Two major sub-networks emerged from the integrated clusters, indicating multiple interactions between proteins expressed in the cochlear and vestibular systems.

Support: EUROHEAR LSHG-CT-20054-512063, NIH RO1 DC005641, Israel Science Foundation. R.H. present address: Department of Otorhinolaryngology, University of Maryland, Baltimore, MD.

#### **1001 Relation Between Renin-Angiotensin-Aldosterone System and Otosclerosis: a Genetic Association and *In Vitro* Study**

Yutaka Imauchi<sup>1</sup>, Xavier Jeunmaître<sup>2</sup>, Magali Boussion<sup>2</sup>, Evelyne Ferrary<sup>1</sup>, Olivier Sterkers<sup>1</sup>, Alexis Bozorg Grayeli<sup>1</sup>

<sup>1</sup>Inserm, UNIT-M 867, APHP Hopital Beaujon, University Paris 7, France, <sup>2</sup>AP-HP, Department of Genetics, Hopital Européen Georges Pompidou; Inserm, U772, Paris, France

Introduction: Angiotensin II (Ang II) may be implicated in the regulation of bone remodeling and its activity is related to several gene polymorphisms including AGT M235T for plasmatic and tissular concentrations of angiotensinogen (AGT), ACE I/D for the angiotensin converting enzyme activity, and AT1R A/C1166 for the Ang II receptor function. the objective of this study was to investigate the implication of this hormone in otosclerosis.

Materials and Methods: the above-mentioned polymorphisms were investigated in 186 patients with otosclerosis and 526 healthy controls, both groups originated from the French Caucasian population. Primary cell cultures of stapedial bone from patients with otosclerosis (n=6) and control subjects (n=5) were investigated for the mRNA expressions of Ang II receptors (type 1 and 2) and cellular AGT, and the effect of Ang II (10<sup>-7</sup> M, 24H) on the alkaline phosphatase activity and the interleukin-6 (IL-6) secretion in the culture media.

Results: a significant association was found between otosclerosis and the AGT M235T and the ACE I/D polymorphisms. Higher proportions of TT (29 vs 16%, p<0.01) and DD (50 vs 38%, p<0.05) genotypes were observed in cases vs controls. No association was found between the AT1R A/C1166 polymorphism and otosclerosis. Ang II receptor types 1 and 2 and AGT were detected in the cultures. Ang II increased the *In Vitro* secretion of IL-6 and decreased the alkaline phosphatase activity only in otosclerotic cells.

Conclusions: These observations suggest a relation between the local renin angiotensin system activity and otosclerosis opening new therapeutic insights.

#### **1002 Genetic Pathways for Chronic Otitis Media – Identification of Mouse Models and Characterisation of the Underlying Genes**

Rachel Hardisty-Hughes<sup>1</sup>, Nick Parkinson<sup>1</sup>, Jiewu Yang<sup>1</sup>, Hilda Tateossian<sup>1</sup>, Sue Morse<sup>1</sup>, Rosario Romero<sup>1</sup>, Michael Cheeseman<sup>1</sup>, **Steve Brown<sup>1</sup>**

<sup>1</sup>MRC Mammalian Genetics Unit, Harwell, UK

Otitis media (OM), inflammation of the middle ear, is the most common cause of hearing impairment and surgery in children. Recurrent (ROM) and chronic (COME) forms of otitis media are known to have a strong genetic component, but nothing is known of the underlying genes involved in the human population. From a deafness screen as part of the mouse mutagenesis programme we have identified two novel dominant mutants, *Jeff* and *Junbo*, which develop a conductive deafness due to a chronic suppurative otitis media. Both these mutants represent models for chronic forms of middle ear inflammatory disease in humans. the *Jeff* mutant carries a mutation in an F-box gene, *Fbxo11*, a member of a large family of proteins that are specificity factors for the SCF E3 ubiquitin ligase complex (Hardisty-Hughes R. et al. 2006 *Hum. Mol. Genet.* 15, 1-7). *Fbxo11* is expressed in the mucin secreting cells of the middle ear epithelia during the period at which otitis media develops in *Jeff*. Initial studies of *FBXO11* SNPs in human OM families have uncovered nominal evidence of association, indicating the genetic involvement of human *FBXO11* in chronic otitis media with effusion and recurrent otitis media (Segade et al., 2006). *Jeff* homozygotes show cleft palate, facial clefting and perinatal lethality and *Fbxo11* is also expressed in the epithelial palatal shelves during development. *Junbo* carries a mutation in the *Evi1* transcription factor (Parkinson et al. 2006 *PLoS Genetics* 2: e149), a gene previously implicated in myeloid leukaemia. *Evi1* represses the TGF- $\beta$  signalling pathway by the binding of *Smad3*. the *Junbo* mutation provides *In Vivo* evidence implicating

this pathway in the development of OM. Interestingly, we have investigated interacting partners to *Fbxo11* and find that it interacts with spectrin beta II that itself is known to interact with *Smad3* to mediate the effects of TGF- $\beta$  signalling. The evidence suggests that both *Fbxo11* and *Evi1* cause OM through effects on signalling via *Smad3* and provide a common mechanistic route for the development of chronic OM. *Fbxo11* and *Evi1* are two of the first molecules to be identified contributing to the genetic etiology of otitis media.

### **1003 A Missense Mutation in the Conserved C2B Domain of Otoferlin Causes Deafness in a New Mouse Model of DFNB9**

Chantal Longo-Guess<sup>1</sup>, Leona Gagnon<sup>1</sup>, David Bergstrom<sup>1</sup>, Kenneth Johnson<sup>1</sup>

<sup>1</sup>The Jackson Laboratory

The otoferlin gene has previously been shown to be important in the auditory process for both mice and humans. Mutations in the otoferlin gene have been shown to underlie deafness disorders in both species, and characterization of targeted knockout mice has demonstrated a role for otoferlin protein in vesicle exocytosis at the inner hair cell afferent synapse. Here we describe a new ENU-induced mutation of the mouse otoferlin gene that we have named *deaf5Jcs* (*Otof*<sup>*deaf5Jcs*</sup>). The mutation is a T to a substitution in exon 10 of *Otof*, which causes a non-conservative amino acid change from isoleucine to asparagine in the C2B domain of the protein. Using an otoferlin specific antibody, we detected strong expression of the protein in cochlear hair cells of control mice, but saw no expression in mutant mice, indicating that the mutated base is necessary for the stability of this protein. Otoferlin has been shown to be highly expressed in vestibular hair cells, but the vestibular phenotype and vestibular evoked potentials (VsEPs) of *deaf5Jcs* mutant mice were not different from those of wild type mice, indicating that otoferlin is not necessary for proper vestibular function. Mice homozygous for the *deaf5Jcs* mutation were shown to be profoundly deaf by auditory brainstem response (ABR) testing, confirming an essential role for otoferlin in inner hair cell neurotransmission.

### **1004 A Targeted *Coch* Missense Mutation: a Knock-in Mouse Model for DFNA9 Late-Onset Hearing Loss and Vestibular Dysfunction**

Nahid Robertson<sup>1</sup>, Sherri Jones<sup>2</sup>, Theru Sivakumaran<sup>1</sup>, Anne Giersch<sup>1</sup>, Sara Jurado<sup>1</sup>, Linda Call<sup>1</sup>, Constance Miller<sup>3</sup>, Stéphane Maison<sup>3</sup>, M. Charles Liberman<sup>3</sup>, Cynthia Morton<sup>1</sup>

<sup>1</sup>Brigham & Women's Hospital, Harvard Medical School, Boston, MA, USA, <sup>2</sup>East Carolina University, Greenville, NC, USA, <sup>3</sup>Harvard Medical School, Eaton-Peabody Laboratory, Massachusetts Eye & Ear Infirmary, Boston, MA, USA

Mutations in *COCH* (coagulation factor C homology), expressed at high levels in the inner ear, are etiologic for the late-onset, progressive, sensorineural hearing loss and vestibular dysfunction at the DFNA9 locus. To date, 12

mutations (11 missense and one in-frame deletion) have been found in *COCH*. We introduced the G88E mutation by gene targeting into the mouse and have created a *Coch*<sup>G88E/G88E</sup> knock-in mouse model for the study of DFNA9 pathogenesis and cochlin function. RT/PCR and immunohistochemistry confirmed successful transcription and translation of the mutated *Coch* RNA and protein products. Vestibular evoked potential (VsEP) thresholds were analyzed using a two factor ANOVA (Age X Genotype). At all ages tested (11, 13, 17, 19, and 21 months), VsEP thresholds were elevated compared to wild-type littermates. At the oldest ages, 2 *Coch*<sup>G88E/G88E</sup> mice had no measurable VsEP. Age-related changes were also observed for both wild-type and affected mice; however, the affected homozygotes clearly showed elevated thresholds at every timepoint tested. Auditory brainstem response (ABR) thresholds for *Coch*<sup>G88E/G88E</sup> mice were substantially elevated at 21 months but not at the younger ages tested. At 21 months, 4 of 8 *Coch*<sup>G88E/G88E</sup> mice and 2 of 3 *Coch*<sup>G88E/+</sup> mice had absent ABRs. DPOAE amplitudes of *Coch*<sup>G88E/G88E</sup> mice were substantially lower than wild-type and absent in the same homozygotes with absent ABRs. These results suggest that vestibular function is affected beginning as early as 11 months when cochlear function appears to be normal, and dysfunction increases with age. Hearing loss declines substantially at 21 months of age and progresses to profound hearing loss at some to all frequencies tested. This is the only mouse model developed to date where hearing loss begins at such an advanced age, providing an opportunity to study both progressive age-related hearing loss and possible interventional therapies.

### **1005 A Lack of Espin Proteins Causes Dramatic Defects in Stereocilium Length and Width: Scanning Electron Microscopic Analysis of Hair Cells in Jerker Mice of the CBA/Caj Background**

Gabriella Sekerkova<sup>1</sup>, Eul Suh<sup>1</sup>, Lili Zheng<sup>1</sup>, Enrico Mugnaini<sup>1</sup>, Claus-Peter Richter<sup>1</sup>, James Bartles<sup>1</sup>

<sup>1</sup>Northwestern University

We discovered and are characterizing the espins. These actin-bundling proteins of hair cell (HC) stereocilia are the target of deafness mutations in mice and humans. Espins bundle actin filaments and cause parallel-actin-bundle elongation. Previously, we mapped the jerker deafness mutation to the mouse espin gene and showed that jerker homozygotes lack espin protein. Earlier studies examining jerker homozygotes in an uncharacterized genetic background found evidence for stereociliary and HC degeneration. A similar pattern of degeneration, accompanied by increased auditory brainstem response (ABR) threshold, was noted in jerker heterozygotes, but with later onset. While working with jerker mice obtained from the Jackson Laboratory (strain JE/LeJ), we noticed several problems in the background strain. To circumvent these problems, we prepared a new congenic jerker mouse line by backcrossing for 13 generations into the CBA/CaJ strain, which experiences little age-related hearing loss. Scanning electron microscopic analysis of CBA/CaJ jerker homozygotes revealed that a lack of espin

proteins results in stereocilia that are abnormally short and thin. in the cochlea, thin stereocilia precursors failed to undergo postnatal elongation to produce a staircase. by P15, most had shrunk and disappeared. the vestibular HCs of jerker homozygotes retained their collections of short stereocilia for longer periods of time. Length differences were especially pronounced for the peripheral zone of cristae (< 8  $\mu$ m vs. > 25  $\mu$ m in wild-type). Vestibular stereocilia were also uneven in thickness and became very thin and wavy near their tip. the cochlea of aged CBA/CaJ jerker heterozygotes showed few abnormalities. ABR threshold measurements on 13-month CBA/CaJ jerker heterozygotes differed little from wild-type controls. Thus, the degeneration noted previously in jerker heterozygotes was likely the result of age-related hearing loss. (Support: NIH DC004314 to JRB)

### **1006 Hearing Loss in the Caveolin-1 Knockout Mouse**

**R. Keith Duncan<sup>1</sup>**, Jennifer Benson<sup>1</sup>, David Dolan<sup>1</sup>, Richard Altschuler<sup>1</sup>

<sup>1</sup>University of Michigan

Lipid microdomains are central elements in cell signaling. These microdomains are divided into at least two categories, the cholesterol and ganglioside rich lipid rafts and caveolae. the caveolae subset is typically identified as large invaginations in the cell membrane due to oligomerization of caveolin proteins along the inner leaflet of the lipid bilayer. Previously, we reported the expression of three caveolin genes in the chick basilar papilla and demonstrated the presence of discrete caveolin-rich clusters at the synaptic pole of hair cells (Chen et al., ARO, 2007). These data suggested a potential role for lipid microdomains in hair cell function. Our objective in the current study was to determine whether genetic knockout of caveolin-1 (Cav1KO) leads to hearing impairment. Auditory brainstem responses (ABR) were measured for pure tones at 12, 24, and 48 kHz in control (JAX identifier) and Cav1KO (JAX identifier) mice 12-14 weeks of age. Mutant mice exhibited higher ABR thresholds at all test frequencies, compared with age-matched controls. Distortion product otoacoustic emissions (DPOAE) were measured to determine whether the hearing loss in Cav1KO was associated with deficits in the cochlear amplifier. Abnormal DPOAEs were recorded for test frequencies centered at 12 and 24 kHz (2f<sub>1</sub> – f<sub>2</sub>), revealing a 20 to 30 dB shift in sensitivity for mutant mice compared with controls. Cytocochleograms revealed no significant inner hair cells loss at any point along the tonotopic axis of Cav1KO or control mice. However, knockout animals exhibited significant outer hair cell (OHC) loss at the base, potentially contributing to abnormal DPOAEs at 24 kHz. in contrast, reduced DPOAE amplitude at 12 kHz was not due to outer hair cell loss in mutants, since the percent loss of OHCs at this tonotopic location was <2%, similar to control animals. Both observations suggest that caveolin-1 plays an important role in outer hair cell function. (Supported by NIH P30 DC05188)

### **1007 Hypothyroidism-Induced Deafness is Associated with Poor Innervation, Reduced Potassium Channel Gene Expression, and Genetic Modifiers**

**Qing Fang<sup>1</sup>**, Mirna Mustapha<sup>1</sup>, Sally Camper<sup>1</sup>, David Dolan<sup>1</sup>, R. Keith Duncan<sup>1</sup>, Tzy-wen Gong<sup>1</sup>, Margaret Lomax<sup>1</sup>, Yehoash Raphael<sup>1</sup>, Kenneth Johnson<sup>2</sup>

<sup>1</sup>University of Michigan, <sup>2</sup>The Jackson Laboratory

Congenital hypothyroidism causes permanent hearing deficits in humans and mice, but the underlying mechanism is poorly understood. the *Pou1f1*<sup>dw</sup>(*Pit1*<sup>dw</sup>) mutant mice are deficient in pituitary thyrotropin (TSH), with no measurable thyroid hormone (TH), and exhibit profound deafness as assessed by auditory brainstem response (ABR). Although developmentally delayed, the morphology of the organ of Corti and expression of the outer hair cell motor protein prestin are nearly indistinguishable in six-week old mutants and normal littermates. the expression of two potassium channel proteins, KCNQ4 and KCNJ10, is permanently reduced in mutant cochlea, which may explain the absence of otoacoustic emissions and reduction of the endocochlear potential in these mutants. in addition, abnormalities in hair cell innervations are apparent in *Pou1f1*<sup>dw</sup> mutants, which could be the major contributor to the profound deafness observed in this hypothyroid strain. Genetic background affects the risk of hearing impairment in hypothyroid mice. to determine the complexity of the protective effects, an F1xF1 intercross was generated between *Pou1f1*<sup>dw</sup> carriers and an inbred strain of *Mus castaneus*. Approximately 16% of the mutant progeny exhibited ABR thresholds indicative of good hearing. a genome scan of these individuals revealed that a locus on Chromosome 2 can rescue hearing despite persistent hypothyroidism. Microarray analysis identified cochlear gene expression changes caused by hypothyroidism in *Pou1f1*<sup>dw</sup> mice. Some of these are positional candidates for the modifier genes. We expect that identification of the modifier genes will enhance our understanding of the mechanisms of hypothyroidism-induced hearing impairment.

Supported by NIDCD: DC05188, DC02982, DC05401, DC05053; and NOHR.

### **1008 Modifier Factors Modulate the Phenotypic Expression of Deafness-Associated Mitochondrial DNA Mutations**

**Min-Xin Guan<sup>1</sup>**

<sup>1</sup>Cincinnati Children's Hospital Medical Center

Mutations in the mitochondrial DNA are one of the most important causes of hearing loss. of those, the homoplasmic A1555G and C1494T mutations at a highly conserved decoding region of in the 12S rRNA have been associated with aminoglycoside-induced and non-syndromic hearing loss in many families worldwide. the A1555G or C1494T mutation is expected to form novel 1494C-G1555 or 1494U-A1555 base-pair at the highly conserved A-site of 12S rRNA. These transitions make the secondary structure of this RNA more closely resemble the



corresponding region of bacterial 16S rRNA. Thus, the new U–A or G–C pair in 12S rRNA created by the C1494T or A1555G transition facilitates the binding of aminoglycosides, thereby accounting for the fact that the exposure to aminoglycosides can induce or worsen hearing loss in individuals carrying these mutations. Furthermore, the growth defect and impairment of mitochondrial translation were observed in cell lines carrying the A1555G or C1494T mutation in the presence of high concentration of aminoglycosides. In addition, nuclear modifier genes and mitochondrial haplotypes modulate the phenotypic manifestation of the A1555G and C1494T mutations. These observations provide the direct genetic and biochemical evidences that the A1555G or C1494T mutation is a pathogenic mtDNA mutation associated with aminoglycoside-induced and nonsyndromic hearing loss. Therefore, these data have been providing valuable information and technology to predict which individuals are at risk for ototoxicity, to improve the safety of aminoglycoside antibiotic therapy, and eventually to decrease the incidence of deafness.

# Author Index (Indexed by abstract number)

- Aarnisalo, Antti, 163  
 Abbas, Paul, 229, 797, 798, 812, 973  
 Abdala, Carolina, 190  
 Abdelaziz, Tlili, 998  
 Abdelmonem, Ghorbel, 998  
 Abe, Satoko, 44  
 Abe, Takahisa, 683  
 Abel, Rebekah, 190  
 Abaira, Victoria E., 436  
 Abrams, Harvey, 395, 396  
 Abu-Hamdan, Maher D., 215  
 Acker, Leah, 687  
 Ackley, R. Steven, 242  
 Acosta, Edward, 74  
 Adachi, Osamu, 39, 159  
 Adams, Joe, 39, 159, 627, 695  
 Adelstein, Robert, 445  
 Adler, Henry, 166  
 Aftab, Saba, 47  
 Agrawal, Smita, 286  
 Agterberg, Martijn, 741  
 Ahmad, Shueb, 40, 41, 512, 611, 621  
 Ahmed, Zubair, 54, 496, 998  
 Ahn, Jin-Chul, 735  
 Ahn, Joong Ho, 146, 271, 296, 358, 702  
 Ahn, Seong-Ki, 787  
 Ahrens, Misha, 870  
 Akeroyd, Michael, 924  
 Akil, Omar, 43, 214, 616  
 Akira, Hara, 716  
 Alagramam, Kumar, 36, 45, 47, 661, 662  
 Alain, Claude, 403  
 Alaniz, Jesse, 425  
 Albers, Frans, 741, 962  
 Alho, Kimmo, 374  
 Allen, Paul, 363, 365, 865, 877  
 Allred, Dax, 24  
 Almer, Marin, 526  
 Altschuler, Richard, 132, 694, 749, 1006  
 Alvarado, David, 8  
 Alvarez, Rafael, 408  
 Amitay, Sygal, 457  
 Anderson, Charles T., 142  
 Anderson, Nick, 419  
 Ando, Kiyoshi, 559  
 Andor-Ardó, Daniel, 207, 943  
 Andrew, Jacqueline, 454  
 Anselmi, Fabio, 514  
 Anvari, Bahman, 677  
 Aoki, Yoshie, 912  
 Appler, Jessica, 446  
 Arai, Maki, 761, 762  
 Aranyosi, A. J., 175, 590  
 Arber, Silvia, 577  
 Ardeshirpour, Farhad, 347  
 Ardoint, Marine, 937  
 Armstrong-Bednall, Gerald, 524  
 Arts, Alexander, 38  
 Asai, Yukako, 97, 486  
 Asako, Mikiya, 307  
 Aschbacher, Ernst, 983  
 Aschenbach, Krista, 660  
 Ashida, Go, 858  
 Ashmore, Jonathan, 594  
 Askew, Charles, 46, 622  
 Atencio, Craig, 479  
 Atkin, Graham, 93  
 Atzori, Marco, 355, 994  
 Auer, Manfred, 491, 634  
 Autti, Taina, 374  
 Avan, Paul, 13  
 Avissar, Michael, 223, 226, 951  
 Avraham, Karen B., 66, 1000  
 Ayadi, Hammad, 998  
 Ayadi, L., 998  
 Ayala, Marco, 275, 542  
 Ayub, Mohammed, 524  
 Babus, Janice, 66  
 Backus, Bradford, 688  
 Bacon, Sid P., 818  
 Bae, Jae Woong, 51  
 Baek, Jong Dae, 538  
 Bai, Jun-Ping, 139, 668, 674  
 Bailey, Jasmine M. S., 898  
 Bailey, Peter J., 409, 421  
 Bal, Ramazan, 309  
 Bala, Avinash Deep, 462, 926  
 Balaban, Carey, 2, 264, 787, 964  
 Balakrishnan, Uma, 866  
 Balk, Marja, 374  
 Balkany, Thomas, 78, 161, 269  
 Ballesterio, Jimena A., 605, 607  
 Baloh, Robert, 245  
 Balough, Ben, 250, 275, 542, 964  
 Banakis, Renee, 195  
 Bance, Manohar, 150  
 Band, Hamid, 663  
 Bandyopadhyay, Sharba, 826  
 Banks, Matthew, 337, 984  
 Barbour, Dennis, 383, 419, 902  
 Barsz, Kathy, 363  
 Bartke, Andrzej, 366  
 Bartles, James, 90, 650, 651, 756, 1005  
 Bartolami, Sylvain, 760  
 Basappa, Johnvesly, 212  
 Basch, Martin, 442  
 Basta, Dietmar, 838  
 Basura, Gregory, 356  
 Batra, Ranjan, 476  
 Battey, James F., 5  
 Battmer, Rolf-Dieter, 278  
 Batts, Shelley, 165, 272  
 Baucom, Jessica, 492  
 Baumgartner, Wolf-Dieter, 288, 805  
 Baxter, Bryan, 984  
 Baydas, Giyasettin, 309  
 Bayon, Rodrigo, 672  
 Beckers, Johannes, 66, 1000  
 Bee, Mark, 414, 895  
 Behloul, Amel, 948  
 Behra, Martine, 561  
 Beineke, Andreas, 30  
 Beisel, Kirk, 85, 138  
 Beisel, Lane H., 582  
 Beitel, Ralph, 479  
 Beltran-Parrazal, Luis, 243  
 Belyantseva, Inna, 494, 998  
 Bendris, Rim, 615  
 Benjamin, Ivor J., 694  
 Benke, Timothy, 944  
 Benson, Jennifer, 1006  
 Benson, Thane E., 833  
 Bent, Tessa, 811  
 Bentancor, Claudia, 329  
 Berenstein, Carlo, 801  
 Bergevin, Christopher, 194  
 Bergles, Dwight, 198, 513  
 Bergstrom, David, 601, 1003  
 Berk, Richard, 25  
 Berkingali, Nurdanat, 131  
 Bermingham-McDonogh, Olivia, 105, 440  
 Bernhardt, Virna, 394  
 Berninger, Erik, 689  
 Bernstein, Leslie, 460  
 Best, Virginia, 405, 459, 917, 918  
 Beurg, Maryline, 205, 948  
 Beyer, Lisa, 64, 447, 758  
 Bhagat, Shaum, 693  
 Bhattacharya, Aparajita, 416  
 Bhinder, Munir A., 54  
 Bian, Lin, 189  
 Bian, Shu Min, 668  
 Bibas, Athanasios, 543  
 Bielefeld, Eric, 156, 357, 645, 737  
 Bien, Alex, 95  
 Bierer, Julie, 289  
 Bierer, Steven M., 289  
 Bille, Michael, 997  
 Billings, Sara, 604  
 Bilyk, Michael, 226  
 Binz, Thomas, 949  
 Bird, Jonathan, 273  
 Biswas, Amitava, 505  
 Bizley, Jennifer, 989  
 Blackman, Toby, 887  
 Blake, Emma, 640  
 Blanz, Judith, 35  
 Bledsoe, Sanford, 307  
 Block, Kimberly, 936  
 Boche, Joellen, 495  
 Bodson, Morgan, 108, 581  
 Boermans, Peter-Paul, 982  
 Bohne, Barbara A., 706  
 Bok, Jinwoong, 435  
 Bonham, Ben, 328, 803, 874, 974  
 Bonko, Julie, 241  
 Bonkowski, Michael S., 366  
 Bonnet, Raymond, 982  
 Bonneux, Sarah, 997  
 Bootz, Friedrich, 21  
 Borenstein, Jeffrey, 455  
 Borg, Erik, 470  
 Borgs, Laurence, 581  
 Bose, Mitali, 994  
 Botta, Laura, 91  
 Boukhaddaoui, Hassan, 638  
 Boulter, Jim, 605, 607  
 Bourien, Jérôme, 615  
 Bourne, David, 453  
 Boussion, Magali, 1001  
 Bova, Frank, 290  
 Bowen-Pope, Daniel, 653  
 Bowyer, Susan, 830  
 Bradsher, John, 561  
 Braid, Louis D., 399  
 Bramer, Tobias, 72  
 Brandewie, Eugene, 867  
 Brandon, Carlene S., 730  
 Brandt, Niels, 485  
 Bratt, Debbie, 549  
 Brazeal, Hilary, 961  
 Bremer, Hendrik, 962  
 Breneman, Kathryn, 657  
 Breuskin, Ingrid, 108  
 Brey, Robert, 248  
 Briaire, Jeroen, 982  
 Brigande, John, 585  
 Brighton, Aimee, 886  
 Brignell, Christopher, 373  
 Brill, Oliver, 193  
 Brimjoin, William O., 362, 364  
 Brittan-Powell, Beth, 843  
 Brosch, Michael, 348  
 Brough, Douglas E., 547, 712  
 Brown, Carolyn, 812  
 Brown, Christopher A., 818  
 Brown, Daniel J., 232  
 Brown, Guy, 597  
 Brown, M. Christian, 832, 833  
 Brown, Steve, 1002  
 Brown, Trecia, 343  
 Brownell, William, 657, 669, 677, 678, 681  
 Brozoski, Thomas J., 302  
 Bruce, Ian, 799  
 Brugeaud, Aurore, 956  
 Brugge, John, 379  
 Brungart, Douglas, 463  
 Buchman, Vladimir, 214  
 Bucinskaite, Violeta, 727  
 Budinger, Eike, 348  
 Bulkin, David, 17  
 Buran, Bradley N., 950  
 Burgess, Barbara, 627  
 Burgess, Shawn, 127, 561  
 Burianova, Jana, 905, 906  
 Burkholder-Juhasz, Rose, 295  
 Burkitt, Anthony, 804  
 Burmeister, Margit, 999  
 Burns, Joseph, 551, 552, 566  
 Buss, Emily, 522  
 Byrum, Katherine, 439  
 Byun, Jae Yong, 237  
 Cadge, Barbara, 57  
 Call, Linda, 1004  
 Camalier, C. R., 908  
 Camper, Sally, 758, 1007  
 Canlon, Barbara, 965  
 Cano, Joel, 310  
 Cao, Xiang, 411  
 Cao, Xiao-Jie, 313  
 Cardwell, Lydia, 66  
 Carey, John, 239, 244, 795  
 Carey, Thomas, 38, 608  
 Carlile, Simon, 887  
 Carlsson, Per-Inge, 470  
 Carlyon, Robert, 413, 979  
 Carney, Laurel H., 869  
 Carr, Catherine, 314, 843  
 Carter, Joseph, 241  
 Carter, Olivia, 403  
 Carzoli, Kathryn, 298  
 Caspary, Donald M., 302  
 Castiglioni, Andrew, 90  
 Cavalier, Melanie, 760  
 Caylan, Refik, 998  
 Cespedes, Paola, 416  
 Cha, Chang Il, 237, 359  
 Chabbert, Christian, 565, 615, 760, 956  
 Chadwick, Richard, 498, 656  
 Chainani, Edward T., 709  
 Chakravarti, Bulbul, 696  
 Chakravarti, Deb, 696  
 Chambers, John, 924  
 Chan, Kenny H., 99  
 Chance, Mark, 36  
 Chandrasekaran, Bharath, 420  
 Chang, Andrew, 73  
 Chang, Janice, 971  
 Chang, Qing, 40, 41, 512, 621  
 Chang, Sun-O, 623  
 Chao, Moses, 753  
 Chapman, Brittany J., 169, 553, 554  
 Charfedine, I., 998  
 Charitidi, Konstantina, 965  
 Chatterjee, Monita, 292, 813  
 Chatzimichalis, Michail, 540, 541  
 Chavez, Eduardo, 98, 483, 720, 748  
 Chávez, Hortencia, 780  
 Cheah, Kathryn, 107  
 Cheatham, Maryann, 141, 142, 195, 663, 664, 667  
 Cheeseman, Michael, 1002  
 Chen, Daniel, 36, 662  
 Chen, Fangxiang, 995  
 Chen, Fang-Yi, 595, 596  
 Chen, Fuquan, 147, 644, 731  
 Chen, Guang-Di, 155, 156, 357, 507, 645, 737  
 Chen, Haiming, 995  
 Chen, Kejian, 453, 717, 732  
 Chen, Lei, 82  
 Chen, Lin, 324  
 Chen, Ping, 444  
 Chen, Shihong, 161, 269  
 Chen, Shixiong, 184, 189  
 Chen, Thomas L., 383  
 Chen, Wei, 221, 563  
 Chen, Zheng-Yi, 562  
 Chen, Zhiqiang, 455  
 Cheng, Jeffrey Tao, 534, 535  
 Cheng, Katherine, 447  
 Cheng, Wendy, 141  
 Cherian, Neil, 31, 260  
 Chertoff, Mark, 228, 233  
 Cheverud, James, 961  
 Chiaradia, Caio, 176  
 Chihara, Yasuhiro, 960  
 Chikar, Jennifer A., 806  
 Chintanpalli, Ananthakrishna, 418  
 Chiorini, John A., 548  
 Chipman, Sarah, 526  
 Chiu, Lynn, 452  
 Chlebecki, Cara, 536  
 Cho, Jin-Ho, 274  
 Chobot-Rodd, Janie, 816  
 Choi, Byung Yoon, 54  
 Choi, Chul-Hee, 717  
 Choi, Hoseok, 148, 643  
 Choi, Soo Young, 51  
 Choi, Yong-Sun, 186  
 Choo, Daniel, 74, 587  
 Chou, Jonathan, 663  
 Choung, Yun-Hoon, 98, 720  
 Christensen, Elizabeth, 517  
 Christensen, Lisa, 25  
 Christensen, Nathan, 648  
 Christensen-Dalsgaard, Jakob, 843  
 Christon, Joseph, 438  
 Christophel, Jared, 552, 566  
 Chung, Augustine, 742  
 Chung, Chun Kee, 382  
 Chung, Jong Woo, 146, 271, 296, 358, 702  
 Chung, Yoojin, 856  
 Cicci, Regina, 936  
 Cioffi, Joseph, 321, 777  
 Clark, Jason, 48, 751  
 Clause, Amanda, 616  
 Clinard, Christopher, 934  
 Cockayne, Debra A., 600  
 Coco, Anne, 454  
 Coffin, Allison, 267  
 Cognet, Laurent, 133  
 Cohn, Edward, 546  
 Colburn, H. Steven, 856, 872  
 Colburn, Steve, 417  
 Colesa, Deborah J., 293

- Coling, Donald, 357, 698  
Collado, Maria Sol, 551, 566  
Collin, Rob, 998  
Collins, Leslie, 978  
Cone-Wesson, Barbara, 692  
Conn, Brian, 275  
Coombes, Stephen, 825  
Cooper, Joel, 887  
Cooper, Nigel, 503  
Cordero, Joehassin, 525  
Corfas, Gabriel, 577, 584, 768  
Corrales, C. Eduardo, 556  
Cortez, Ana, 33  
Corwin, Jeffrey, 551, 552, 566, 774  
Cosgrove, Dominic, 37, 46, 50, 626  
Cotanche, Douglas, 169, 553, 554, 562, 568  
Coticchia, James, 25  
Coulson, May T., 754  
Crane, Benjamin, 245  
Crass, Kimberlee A., 913  
Creedon, Thomas, 395  
Cremers, Cor W. R. J., 997  
Criddle, Michael, 829  
Crosson, Jillian, 433  
Crum, Poppy, 991  
Crumling, Mark, 165, 571, 660  
Cui, Guiying, 201  
Cui, Qi N., 889  
Cui, Yilei, 304  
Cullen, Kathleen, 788  
Cunningham, Lisa, 730, 734  
Cureoglu, Sebahattin, 26  
Curry, Fitz-Roy, 508  
Cyr, Janet L., 651  
D'Souza, Mary, 69, 70, 648  
Daamen, Katja, 741  
Dabdoub, Alain, 12, 106, 443  
Dahmen, Johannes, 281, 901  
Dai, Chenkai, 506, 544  
Dai, Chunfu, 389, 724  
Dailey, Michael E., 350  
Dalhoff, Ernst, 537, 685, 686  
Dallos, Peter, 141, 142, 195, 663, 664, 667  
Dalmay, Tamas, 11  
Daly, Kathleen, 24  
Damarla, Venkata, 524  
D'Angelo, William R., 908  
Dasika, Vasant, 934  
Dassonville, Paul, 926  
Daudet, Nicolas, 273  
David, Larry, 725  
David, Stephen, 893, 896  
Davis, Bob, 718  
Davis, Kevin, 855  
Davis, Matthew, 422  
Davis, Robin, 221, 222, 750  
Dawes, Patrick, 515  
Dawson, Sally, 57, 261, 484  
De Angelis, Martin Hrabé, 11  
De Boer, Egbert, 591  
De Groot, John, 741, 962  
De Kleine, Emile, 370  
De Medina, Philippe, 739  
De Raeve, Leo, 977  
De San Martin, Javier Zorrilla, 209  
Dean, Isabel, 870  
Deaver, Andrew P., 564  
Deaville, Rob, 30  
Decraemer, Willem, 528  
Deeks, John, 979  
Degagne, Jacqueline, 29  
Deggouj, Naïma, 977  
Dehmel, Susanne, 819  
Deinhardt, Katrin, 753  
Delgutte, Bertrand, 823, 868  
Della Santina, Charles, 79, 244, 791, 792, 793, 795  
Deliano, Mathias, 280  
Delprat, Benjamin, 639  
Demany, Laurent, 922  
Demer, Joseph, 245  
Demots, Cynthia A., 719  
Deng, Min, 111, 583  
Dent, Micheal, 426, 933  
Depalma, Cara L., 915  
Depireux, Didier, 66, 873, 903  
Desloovere, Christian, 977  
Desmadryl, Gilles, 956  
Devore, Sasha, 868  
Dhar, Sumitrajit, 190  
Dhawan, Ritu, 770  
Dhooge, Ingeborg, 977, 997  
Di Pasquale, Giovanni, 548  
Dickman, J. David, 789, 963  
Dierking, Darcia, 191, 192  
Dimitrijevic, Andrew, 385  
Dinces, Elizabeth, 816  
Ding, Dalian, 153, 154, 157, 158, 301, 698, 733, 743  
Dinh, Christine, 161, 269  
Dirckx, Joris, 528  
Divenyi, Pierre, 424  
Dobrev, Marina, 890  
Doetzlhofer, Angelika, 442  
Doherty, Joni, 34  
Doi, Katsumi, 104, 349  
Dolan, David, 471, 617, 694, 758, 1006, 1007  
Dolle, Pascal, 574  
Donaldson, Kevin, 344  
Donato, Roberta, 854  
Dong, Wei, 177, 178, 533  
Dooling, Robert, 843  
Dootz, Gary A., 471, 694  
Dormer, Kenneth, 453  
Dosch, Hans Guenter, 369  
Dahmen, Johannes, 281, 901  
Drennan, Ward, 433, 934  
Drescher, Dennis G., 88, 203, 204, 215  
Drescher, Marian J., 88, 203, 204, 215  
Drexler, Daniel, 394  
Driver, Elizabeth, 12  
Dror, Amiel, 1000  
Du, Li Lin, 53, 58  
Ducummon, Carl, 667  
Duifhuis, Hendrikus, 923  
Dulon, Didier, 205, 948  
Duncan, R. Keith, 81, 571, 660, 758, 1006, 1007  
Dunford, Jonathan, 830  
Dunn, Lara, 626  
Durham, Dianne, 228, 297  
Durlach, Nathaniel I., 918  
Eapen, Rose, 522  
Earl, Brian, 228  
Easter, James, 275, 542  
Eatock, Ruth Anne, 783  
Eckrich, Tobias, 179, 691  
Economou, Androulla, 573  
Eddins, David A., 56, 364, 367, 914, 915  
Edge, Albert, 116, 556, 558, 570, 577  
Edsman, Katarina, 72  
Edwards, Robert, 616  
Eernisse, Rebecca, 321  
Eggers, Scott, 248  
Egner, Alexander, 197  
Ehret, Guenter, 335  
Ehrlich, Garth D., 25  
Ehrsson, Hans, 738  
Eiber, Albrecht, 540, 541  
Eichhammer, Peter, 259  
Eisenberg, Laurie, 517  
El Ouardi, Abdessamad, 202  
El Seady, Ragad, 129  
El-Amraoui, Aziz, 136  
Eleftheriadou, Anna, 708  
Elgoyhen, A. Belén, 209, 605, 607  
Elisevich, Kost, 830  
Elkan, Rani, 1000  
Elkan, Tal, 1000  
Elkashlan, Hussam, 38  
Elkon, Rani, 66  
Ellison, John, 546  
Emery, Sarah B., 999  
Endler, Frank, 925  
Engbers, Jonathan, 755  
Engel, Jutta, 202, 485  
Engineer, Crystal, 425  
Englitz, Bernhard, 819, 845  
Engmer, Cecilia, 72, 738  
Enniful, George, 10  
Enomoto, Keisuke, 349  
Enright, Anton, 11  
Epstein, Michael, 920  
Erbe, Christy, 766, 767  
Erenberg, Sheryl, 810  
Erickson, Christopher, 437  
Ernst, Arne, 838  
Ertmer, Wolfgang, 277  
Ervasti, James, 494, 495  
Escabi, Monty, 333  
Eshraghi, Adrien, 78, 161, 269  
Esterberg, Robert, 444  
Etler, Christine, 812  
Euteneuer, Sara, 217  
Ewert, Stephan, 859  
Eybalin, Michel, 615, 638, 646  
Eze, Nneka, 500  
Fahey, Paul, 182, 183  
Fairfield, Damon, 746  
Fallon, James, 281, 800  
Fan, Lixin, 630  
Fang, Jie, 682  
Fang, Qing, 758, 1007  
Farahbaksh, Nasser, 92  
Fayad, Jose, 33  
Feil, Robert, 485  
Feil, Susanne, 485  
Fekete, Donna, 439, 1000  
Feng, Albert, 531, 916  
Ferguson, Melanie, 518, 520, 521  
Ferrary, Evelynne, 77, 1001  
Ferry, Robert, 597  
Fetoni, Anna Rita, 737  
Fettiplace, Robert, 658  
Fiering, Jason, 455  
Finley, Charles C., 290  
Fisher, Daniel J., 119  
Fishman, Andrew, 630  
Fishman, Yonatan, 894, 899  
Fitzpatrick, Denis, 546  
Fitzpatrick, Douglas, 347, 476  
Flamant, Frédéric, 485  
Fleck, Terry, 182  
Florentine, Mary, 920  
Flores-Otero, Jacqueline, 750  
Floyd, Robert, 717  
Foeller, Elisabeth, 691  
Folmer, Robert, 396  
Font, Jean Paul, 700  
Forge, Andrew, 611, 637  
Formby, Craig, 936  
Fowler, Cynthia, 526  
Fraenkel, Ernest, 7  
Francis, Nikolas A., 173  
Francis, Shimon, 734  
Fransen, Erik, 997  
Fransson, Anette, 739  
Frederick, Eric, 395  
Freeman, Dennis, 175, 590  
Freeman, John J., 763, 953  
Frenz, Dorothy, 578  
Freyman, Richard, 866  
Fridberger, Anders, 502, 629  
Friderici, Karen H., 494  
Friedland, David, 321  
Friedman, Lilach M., 1000  
Friedman, Rick, 65, 997  
Friedman, Thomas, 54, 86, 494, 496, 998  
Friedrich, Victor L., 959  
Frijns, Johan, 129, 982  
Frisina, Robert, 56, 69, 70, 70, 360, 361, 367, 648, 966  
Frisina, Susan, 56  
Fritz, Andreas, 444  
Fritz, Jonathan, 344, 893, 896, 907  
Fritzsch, Bernd, 10, 101, 107, 437, 448, 449, 586  
Froemke, Robert, 996  
Frolenkov, Gregory, 86, 488, 494, 496  
Fu, Qian-Jie, 808, 814  
Fuchs, Helmut, 11  
Fuchs, Paul, 209, 210, 605, 607  
Fujii, Masato, 170, 219, 263, 572  
Fujimoto, Yasuko, 130  
Fujinami, Yoshiaki, 263  
Fujioka, Masato, 116, 263, 570, 715  
Fukuoka, Hisakuni, 55  
Fullarton, Lynne, 694  
Funabiki, Kazuo, 858  
Funayama, Manabu, 52  
Funnell, Robert, 528  
Furlong, Cosme, 534, 535  
Furman, Adam C., 223, 951  
Furman, Joseph, 246, 247  
Furness, David, 490, 640  
Furst, Miriam, 593  
Furukawa, Masayuki, 393  
Furukawa, Shigeto, 861  
Fuzessery, Zoltan, 992  
Fyk-Kolodziej, Bozena, 299, 306, 307  
Gaboyard, Sophie, 760  
Gaese, Bernhard, 691, 904  
Gagnon, Leona, 1003  
Gagnon, Patricia M., 641, 642  
Galazyuk, Alexander, 332  
Gale, Jonathan, 198, 261, 273, 484, 513  
Galindo-Leon, Edgar, 900  
Gallun, Frederick, 939  
Galvin, John, 808  
Gan, Lin, 111, 583  
Gan, Rong, 506, 544  
Gandolfini, Michele, 722  
Gandour, Jackson, 420, 842  
Ganesh, Vidya, 840  
Gans, Donald, 18  
Gantz, Bruce, 810  
Gao, Hongxiang, 849  
Gao, Jiangang, 141, 659, 667  
Gao, Tingting, 443  
Gao, Wei, 112  
Gao, Xinsheng, 453, 732  
Garadat, Soha, 287  
Garcia-Anoveros, Jaime, 90, 650  
Garige, Suneetha, 46  
Garinis, Angela, 692  
Garrett, Andrew, 625  
Gastaldi, Giulia, 91  
Gavara, Nuria, 498  
Gburcik, Valentina, 261  
Geering, Kaethi, 639  
Geiger, Christopher, 775  
Geisler, Hynsoon, 258  
Geleoc, Gwenaëlle S.G., 97, 486  
Gellibolian, Robert, 20, 27, 33  
George, Manju, 663  
German, Sarah, 101  
Germino, Gregory, 659  
Ghaffari, Roozbeh, 175, 590  
Giersch, Anne, 1004  
Gill, Ruth, 613, 614  
Gillespie, Peter, 493  
Girod, Doug, 297  
Gittelman, Josh, 872  
Glass, Tiffany, 628  
Glatke, Theodore, 692  
Glowatzki, Elisabeth, 198, 220, 513, 616, 945  
Glueckert, Rudolf, 132  
Gnansia, Dan, 415  
Goebel, Joel, 248  
Goetze, Romy, 838  
Goldberg, Jay, 771, 772, 947  
Golding, Nace, 848  
Gomez-Casati, Maria, 584  
Gomez-Nieto, Ricardo, 315  
Gómez-Nieto, Ricardo, 834  
Gong, Neng, 324  
Gong, Qin, 184  
Gong, Tzy-Wen, 471, 694, 758, 1007  
Goodrich, Lisa, 436, 446  
Goodyear, Richard, 13, 496, 651, 652  
Gooler, David, 334  
Gopal, Kamakshi, 392  
Gopen, Quinton, 255  
Gordin, Arie, 364  
Gordon, Karen, 283, 375  
Gorga, Michael, 191, 192, 546  
Gortemaker, Michele, 546  
Gossman, David G., 603  
Gottshall, Kim, 250, 964  
Goupell, Matthew, 288, 805, 975  
Goutman, Juan, 945  
Gov, Nir S., 653  
Goyal, Sheila, 972  
Grady, Brian, 453  
Graham, Christine, 218  
Grandpre, Patrick, 628  
Grant, Lisa, 616  
Grant, Wally, 773  
Gratton, Michael Anne, 46, 622, 626, 708  
Graugnard, Erin, 666  
Grayden, David, 804  
Grayeli, Alexis Bozorg, 77, 236, 1001  
Grecova, Jolana, 905  
Green, Gary, 376  
Green, Steven, 270, 350, 745, 746, 747, 751, 755  
Greene, Nathaniel, 855  
Greenlee, Jeremy, 995  
Greeson, Jennifer, 679  
Gregory, Frederick, 201  
Grey, Brian, 586  
Gridi-Papp, Marcos, 531  
Grieco-Calub, Tina M., 976  
Griest, Susan, 395, 396  
Griffith, Andrew, 54, 67, 496  
Griffiths, Timothy, 380  
Grillet, Nicolas, 489  
Grimes, Alison, 517  
Groenenboom, Kristin, 191, 192  
Groeschel, Moritz, 838  
Groh, Jennifer, 17, 888  
Grose, John, 522  
Groß, Susanne, 398  
Gburcik, Valentina, 853, 859, 878  
Grover, Mary, 113, 114, 754  
Groves, Andy, 103, 442, 567, 575  
Grushko, Julia, 372

- Gu, Chunling, 45  
Gu, Jianwen, 336  
Gu, Rende, 123  
Guan, Bing-Cai, 595, 620  
Guan, Min-Xin, 1008  
Guan, Zhenlong, 830  
Gudsnuk, Kathryn, 303  
Guerrero, Debbie, 696  
Guinan, John, 173, 240, 835  
Gumenyuk, Valia, 372  
Gummer, Anthony, 176, 179, 537, 589, 654, 655, 685, 686  
Gustafsson, Jan-Åke, 965  
Gutschalk, Alexander, 987  
Haake, Scott, 161, 269  
Hackett, Alyssa, 112  
Hackett, Troy A., 908  
Hackney, Carole, 490  
Haeseleer, Françoise, 201  
Hahn, Hartmut, 796  
Hajak, Goeran, 259  
Hall, Deborah, 373, 924, 988  
Hall, Ian, 327  
Hall, Joseph, 522  
Halliday, Lorna, 456, 457, 518  
Hall-Stoodley, Luanne, 25  
Hallworth, Richard, 95, 138  
Halpin, Chris, 336  
Halsey, Karin, 617  
Hamernik, Roger, 718  
Hampton, Amanda, 841  
Hancock, Kenneth, 883  
Handzel, Amir A., 633  
Handzel, Ophir, 633  
Hannon, Erin, 403  
Hansen, Marlan, 48, 751, 752, 755  
Hansen, Volkert, 202  
Happel, Max, F.K., 280  
Haque, Asim, 963  
Hara, Akira, 109, 713, 744  
Hara, Hirotaka, 251  
Harasztosi, Csaba, 179, 654, 655  
Harbidge, Donald G., 602  
Hardelin, Jean-Pierre, 13  
Harding, Gary W., 706  
Hardisty-Hughes, Rachel, 1002  
Harper, Nicol, 870  
Harrington, Ellery, 534  
Harris, David, 852  
Harris, Julie, 76  
Harris, Stephen, 102  
Harrison, Robert, 343, 375  
Hartley, Douglas, 281, 901  
Hartman, Byron H., 105  
Hartmann, Rainer, 282  
Hartsock, Jared J., 612, 613  
Harvey, Margaret, 82  
Harvey, Natasha, 448  
Hashimoto, Makoto, 151, 152, 235, 647, 778, 779  
Hashimoto, Shigenari, 44, 635  
Hashimoto, Yasuyuki, 761, 762  
Hashino, Eri, 100, 119, 120, 574  
Hatazawa, Jun, 349  
Hatfield, James S., 215  
Hattori, Nobutaka, 52  
Hausman, Fran, 162  
Hawkes, Aubrey, 955  
Hawley, Monica, 936  
Hayashi, Chieri, 52, 393  
Hayashi, Toshinori, 440  
Hayden, Russell, 792  
Hay-McCutcheon, Marcia, 811  
Haywood, Nick, 404  
He, David, 138, 141, 142, 667  
He, Jiao, 78  
He, Wenxuan, 174, 501  
Healy, Eric, 913, 940  
Heaphy, John, 662  
Hederstierna, Christina, 32  
Hehrmann, Philipp, 870  
Heid, Silvia, 282  
Heijden, Marcel V. D., 188  
Heil, Peter, 224  
Heinz, Michael, 225, 418  
Heiser, Marc, 479  
Heller, Stefan, 451, 556, 665  
Helmhout, Laci, 926  
Heman-Ackah, Selena, 28, 71  
Hemmert, Werner, 208  
Henderson, Donald, 155, 156, 357, 469, 507, 645, 737  
Hendricks, Jeffrey L., 806  
Henkemeyer, Mark, 776  
Henry, James, 395, 396  
Henson, Miriam M., 290  
Henson, O. W., 290  
Hering-Bertram, Martin, 614  
Hernandez, Jeannie, 749  
Hernandez, Michelle, 21  
Hernandez-Montes, Maria, 534, 535  
Herrington, Richard, 392  
Herrmann, Barbara S., 240  
Herrmann, Christoph S., 892  
Hertzano, Ronna, 66, 1000  
Hervais-Adelman, Alexis, 378, 422  
Hetherington, Alexander, 807  
Hickox, Ann, 688  
Highstein, Stephen, 784, 959  
Higuchi, Hitomi, 253, 254  
Hill, Gerhard W., 186  
Hillman, Dean, 93  
Hiraumi, Harukazu, 130  
Hirose, Keiko, 714, 726  
Hirose, Yoshinobu, 151, 152, 647, 729, 778, 779  
Hirsch-Shell, Dylan, 742, 782  
Hirt, Bernhard, 485  
Hmani-Aifa, Mounira, 998  
Hoa, Michael, 25  
Hoang, Kimberly, 161  
Hoffer, Michael, 250, 475, 964  
Hoffman, Larry, 742, 782  
Hoffpauir, Brian, 846  
Hoidis, Silvi, 216  
Holland, Scott, 587  
Holley, Matthew, 580  
Holstein, Gay, 784, 959  
Holt, Avril Genene, 299, 306, 307  
Holt, Jeffrey R., 87, 97, 486, 487  
Holt, Joseph, 772, 781, 947  
Hom, David, 28, 71  
Hong, Seok Min, 359  
Hori, Ryusuke, 130, 168, 736  
Horie, Rie, 75, 130  
Horii, Arata, 104  
Horner, Kathleen, 970  
Hornstein, Eran, 1000  
Horwitz, Barry, 371  
Horwitz, Geoffrey C., 87  
Hoshino, Tomofumi, 109  
Hosoi, Hiroshi, 545  
Hosoya, Makoto, 116  
Hotaling, Jeffrey, 972  
Housel, Nathaniel, 365, 865  
Housley, Gary D., 217, 600  
Howard, Mary, 377  
Howard, Matthew, 379, 995  
Hoya, Noriyuki, 263  
Hradek, Gary, 807, 974  
Hsu, Cynthia, 577  
Hsu, Will C., 316  
Hu, Bohua, 704, 705  
Hu, Jasmine, 517  
Hu, Ning, 229, 798, 973  
Hu, Zhengqing, 566  
Huang, Jie, 745, 746  
Huang, Juan, 971  
Huang, Mingqian, 562  
Hubbard, Allyn, 181, 504  
Huber, Alex, 540, 541  
Hubka, Peter, 282  
Hübner, Christian, 35  
Hudspeth, A. J., 207, 492, 943  
Huentelman, Matthew J., 997  
Hughes, Inna, 952  
Hughes, Larry, 302, 366, 617  
Hugnot, Jean Philippe, 565  
Huisman, Margriet, 129  
Hullar, Timothy, 784, 961  
Hulli, Nesim, 534, 535  
Hultcrantz, Malou, 32, 624, 969  
Hultman, David, 628  
Hume, Clifford, 549  
Hunker, Kristina L., 64  
Hurd, Elizabeth A., 447  
Hurle, Belen, 952  
Hurley, Laura, 15, 327  
Husain, Fatima, 371  
Husnain, Tayyab, 54  
Huyck, Julia Jones, 458  
Hwang, Chanho, 102  
Hwang, Hee Jun, 735  
Hyson, Richard, 298  
Ido, Akio, 736  
Idrizbegovic, Esma, 391  
Iguchi, Fukuichiro, 76, 549  
Ihlefeld, Antje, 413  
Iida, Koji, 137, 670, 671  
Iizuka, Takashi, 42, 49, 393, 690  
Ikeda, Katsuhisa, 42, 49, 52, 137, 393, 670, 690  
Ikeda, Takuo, 235  
Ikeya, Makoto, 103  
Ikezono, Tetsuo, 762  
Imaizumi, Kazuo, 996  
Imauchi, Yutaka, 1001  
Inaoka, Takatoshi, 130, 736  
Ingham, Neil, 62  
Inoshita, Ayako, 42, 49, 393, 690  
Inverso, Yell, 809  
Iosub, Radu, 211  
Irina, Toshio, 912  
Irmiler, Martin, 66, 1000  
Irving, Samuel, 876  
Isaiah, Amal, 281  
Isao, Uemaetomari, 716  
Ishikawa, Kazuo, 390  
Ishiyama, Akira, 243, 775, 957, 958  
Ishiyama, Gail, 243, 775, 957, 958  
Ison, James, 365, 865, 877  
Israelsson, Kjell-Erik, 689  
Issa, Elias, 991  
Itasaka, Yoshiaki, 390  
Itatani, Naoya, 398  
Ithari, Yukiko, 393  
Ito, Juichi, 75, 122, 130, 149, 168, 736  
Ito, Ken, 960  
Ives, Timothy, 378  
Iwaki, Takako, 349  
Iwasa, Kuni, 143, 588, 682  
Iwasaki, Satoshi, 761, 762  
Iwasaki, Shinichi, 960  
Iyer, Nandini, 463, 916  
Izumikawa, Masahiko, 124, 165, 599  
Izzo, Agnella, 231, 276, 972  
Jackson, Ronald, 717  
Jackson, Ryan Patrick, 536  
Jacob, Howard J., 6  
Jacobson, Dana, 228  
Jacobson, Samuel G., 53  
Jacques, Bonnie, 441  
Jagger, Daniel, 611  
Jajoo, Sarvesh, 728  
Jakkamsetti, Vikram, 355  
James, Eric, 766  
Jamesdaniel, Samson, 698  
Järleback, Leif, 619  
Jastreboff, Margaret M., 719  
Jastreboff, Pawel J., 719  
Jeng, Fu-Cherng, 229  
Jenkins, Herman, 275  
Jennings, Richard, 247, 368  
Jensen-Smith, Heather, 586  
Jentsch, Thomas, 35  
Jeon, Sang-Jun, 116, 570  
Jepson, Paul D., 30  
Jercog, Pablo, 848  
Jero, Jussi, 163  
Jeschke, Marcus, 280, 892, 985  
Jeung, Changmo, 187  
Jeunmaitre, Xavier, 1001  
Ji, Weiqing, 345, 346  
Ji, Yadong, 873  
Jia, Shuping, 142  
Jiang, Dan, 543  
Jiang, Haiyan, 153, 158, 733, 743  
Jiang, Quan, 830  
Jiang, Zhi-Gen, 89, 595, 596, 620  
Jianzhong, Lu, 341  
Jilani, Fatimah, 688  
Jin, Huijun, 184  
Jin, Yulian, 748  
Jin, Zhe, 619  
John, Earnest O., 99  
Johnson, Kenneth, 1003, 1007  
Johnson, Matthew, 571  
Johnson, Shane, 628  
Johnson, Stuart, 199, 200  
Johnsrude, Ingrid, 378, 422  
Jolkowski, Kristin, 191, 192  
Jones, Diane, 627  
Jones, Douglas L., 862  
Jones, Gary, 284  
Jones, Heath, 880  
Jones, Jennifer, 110  
Jones, Margaret L., 862  
Jones, Sherri, 601, 765, 1004  
Jongkamonwiwat, Nopporn, 563  
Joris, Philip, 844, 860, 921  
Josef, Gert, 875  
Joseph, Debbie, 78  
Joseph, Gert, 278  
Jost, Juergen, 845  
Juhn, Steven, 26  
Juiz, Jose, 310  
Jung, Eui-Sung, 274  
Jung, Jae-Yun, 735  
Jung, Timothy T. K., 99, 167  
Jung, Yoon-Gun, 148, 643  
Jurado, Sara, 1004  
Kachar, Bechara, 489, 511, 576, 653  
Kada, Shinpei, 130, 149  
Kadlecova, Zuzana, 550  
Kaga, Kimitaka, 263, 748  
Kageyama, Ryoichiro, 104  
Kaimal, Vinod, 587  
Kaiser, Christina L., 169, 553, 554  
Kajimoto, Katsufumi, 349  
Kakehata, Seiji, 683  
Kakigi, Akinobu, 618  
Kalay, Ersan, 998  
Kalbacher, Hubert, 796  
Kale, Sushrut, 225  
Kalinec, Federico, 696  
Kalinec, Gilda, 696  
Kallman, Jeremy, 60  
Kalluri, Radha, 194, 783  
Kalmbach, Abigail, 847  
Kaltenbach, James, 828, 829  
Kamar, Ramsey, 133  
Kamien, Andrew J., 553  
Kamiya, Kazusaku, 263  
Kanda, Seiji, 560  
Kandler, Karl, 616, 847  
Kane, Catherine, 270, 747  
Kang, Hun Hee, 271, 358, 702  
Kang, Robert, 433  
Kang, Stephen Y., 293  
Kang, Young-Jin, 954  
Kanzaki, Sho, 42, 711, 715  
Karasawa, Takatoshi, 620, 723, 725  
Karcz, Anita, 865, 877  
Karmody, Collin, 527  
Karnes, Hope, 297  
Karsten, Sue, 810  
Kasai, Misato, 393  
Kashino, Makio, 407  
Kasperek, Sylvia, 202  
Kathiresan, Thandavaryan, 82  
Katori, Yukio, 490  
Katz, Eleonora, 209, 605, 607  
Kawahara, Hideki, 912  
Kawamoto, Kohei, 124  
Kawano, Atsushi, 52  
Kawar, Mayya, 998  
Kawasaki, Hiroto, 379, 995  
Kawase, Tetsuaki, 831  
Kawauchi, Takeshi, 122  
Kazmierczak, Piotr, 489  
Ke, Raymond, 667  
Keating, Peter, 886  
Keebler, Michael V., 400  
Keefe, Douglas, 546  
Keegan, Mark, 455  
Keen, Erica, 207, 943  
Kelley, Matthew, 12, 66, 106, 441, 443, 445  
Kelly, Jack, 326, 938  
Kemp, David, 193  
Kempton, Beth, 22, 29, 162  
Kenna, Margaret, 255  
Kennedy, Helen J., 211  
Kennedy, Kirin S., 226  
Kent-Taylor, Anne, 11  
Kerschner, Joseph, 23  
Ketten, Darlene, 532  
Kewley-Port, Diane, 523  
Kkhk, Baljit S., 600  
Khampang, Pawjai, 23  
Khan, Shahid, 998  
Khimich, Darina, 197, 950  
Kidd, Gerald, 405, 918  
Kikkawa, Yayoi, 75, 130, 168, 661, 736  
Kil, Jonathan, 123, 268  
Kilgard, Michael, 355, 425  
Kim, Ana, 722  
Kim, Chong-Sun, 382, 519, 623  
Kim, Chung-Beom, 735  
Kim, Duck O., 186  
Kim, Eun-Hee, 437  
Kim, Eunsook, 266  
Kim, Euysoo, 576, 952  
Kim, Hye-Young, 623  
Kim, Hyoung-Mi, 623  
Kim, Hyungjin, 265, 266, 699  
Kim, Ja Hyun, 382  
Kim, Jae-Ryong, 812  
Kim, Jong Yang, 271  
Kim, June Sic, 382  
Kim, Kyu Sung, 643, 785  
Kim, Kyunghye, 602

- Kim, Min-Woo, 274  
Kim, Namkeun, 631  
Kim, Sang-Sun, 519  
Kim, Soo-Kyoung, 519  
Kim, Sung Hee, 51  
Kim, Sung Huhn, 602  
Kim, Un Kyung, 51  
Kim, Woosung, 419  
Kim, Yoon Hwan, 99, 167  
Kim, You Hyun, 99, 167  
Kim, Young Ho, 171, 623  
Kim, Yunha, 265, 266  
Kimura, Yasuyuki, 349  
Kindermann, Teresa, 878  
King, Andrew, 281, 886, 901, 989  
King, Ericka, 59  
Kingsley, Emily, 25  
Kirby, Alana E., 291  
Kirkegaard, Mette, 727  
Kisley, Lauren, 47  
Kistler, Doris, 523  
Kitagawa, Youko, 160  
Kitajiri, Shin-Ichiro, 496  
Kitani, Rei, 683  
Kitoh, Ryosuke, 635  
Kitterick, P. T., 409, 421  
Klapczynski, Marcin, 772  
Klapperich, Catherine, 568  
Klein, Reinhild, 164  
Kleinjung, Tobias, 259  
Klinge, Astrid, 397  
Klingebiel, Randolph, 838  
Klinger, Matthias, 217  
Klis, Sjaak, 230, 741, 962  
Klok, Harm-Anton, 550  
Kloosterman, Wigard, 439  
Klump, Georg, 397, 398, 885, 895  
Knipper, Marlies, 258, 485  
Knowles, E. E. M., 409  
Knutsson, Johan, 529  
Kobayashi, Toshimitsu, 137, 670, 831  
Koessler, Manfred, 691  
Kohrman, David C., 64, 694  
Koike, Takuji, 690  
Koistinen, Sonja, 374  
Kojima, Ken, 122  
Koka, Kanthaiah, 880, 881  
Kollmar, Richard, 954  
Kommareddi, Pavan, 38, 608, 721  
Kondo, Kenji, 748  
Kondo, Takako, 119, 120, 574  
Kong, Ying-Yee, 979  
Konings, Annelies, 470  
Koo, Ja-Won, 623  
Kopco, Norbert, 888, 917  
Kopke, Richard, 453, 717, 732  
Kopitz, Michelle, 56  
Kopp-Scheinpflug, Conny, 865, 877  
Kopp-Scheinpflug, Cornelia, 819, 845  
Kopun, Judy, 191, 192  
Korneluk, Robert, 150  
Korte, Megan, 495  
Kosaki, Hiroko, 891  
Kostyszyn, Beata, 557  
Kotak, Vibhakar, 351  
Koterski, Sandra, 113, 114  
Kouike, Hiroko, 170, 263  
Koundakjian, Edmund, 446  
Kral, Andrej, 282  
Krasieva, Tatiana, 536  
Kraus, Johanna, 598  
Kraus, Suzanne, 157, 301  
Kremer, Hanne, 997, 998  
Krishnan, Ananthanarayan, 420, 839, 840, 841, 842  
Kristiansen, Arthur G., 39, 159  
Kriwacki, Richard, 676  
Kubba, Juman, 767  
Kubo, Takeshi, 349  
Kuenzel, Thomas, 312  
Kuhn, Stephanie, 485  
Kujawa, Sharon, 39, 240, 455, 740  
Kulesza, Randy, 305  
Kumagai, Izumi, 137, 670  
Kumano, Shun, 137, 670, 671  
Kumar, B. Nirmal, 490  
Kunchur, Milind, 935  
Kuo, Sidney, 850  
Kurt, Simone, 335, 985  
Kuwada, Shigeyuki, 476  
Kuznetsova, Marina, 857  
Kwan, Tao, 575  
Kwon, Bomjun, 817  
Kwon, Seeyoun, 934  
Laback, Bernhard, 288, 805, 975  
Labay, Valentina, 67  
Lacko, Joseph, 246  
Ladak, Hanif, 528  
Ladrech, Sabine, 638  
Lafren, J. Brandon, 940  
Laforenza, Umberto, 91  
Lagasse, James, 123  
Lagasse, Jim, 268  
Lagziel, Ayala, 86  
Lahtinen, Lisa, 180  
Lalwani, Anil, 61, 93  
Lammert, Adam, 424  
Landgrebe, Michael, 259  
Landsberger, David, 815  
Lang, Hainan, 559  
Langers, Dave, 986  
Langford, Cordelia, 11  
Langguth, Berthold, 259, 384  
Lansing, Charissa, 916  
Lanting, Cris, 370  
Larrain, Barbara, 162  
Larsen, Erik, 836, 916  
Larson, Charles, 995  
Lasker, David, 785  
Laudanski, Jonathan, 825  
Lauer, Amanda, 649  
Laundrie, Erin, 339, 341  
Laurell, Goran, 72, 727, 738  
Lauxmann, Michael, 540, 541  
Lawson, Katharine, 372  
Layton, Maria, 68  
Lazaridis, Evelyn, 226  
Le Prell, Colleen, 474, 617  
Leake, Patricia, 803, 807, 974  
Lecluyse, Wendy, 931, 932  
Lee, Adrian K.C., 410  
Lee, Amy, 201  
Lee, Chao-Yang, 423  
Lee, Chen-Chung, 480, 993  
Lee, Daniel J., 832, 833  
Lee, Dong-Youl, 643  
Lee, Edward, 578  
Lee, Gi Soo, 555  
Lee, Haa-Yung, 20, 27  
Lee, Hae Jin, 51  
Lee, Ho Sun, 382  
Lee, Hye Mi, 146  
Lee, Hyo Jeong, 382  
Lee, Il-Woo, 747  
Lee, Jennifer, 93  
Lee, Jeonghan, 699, 701  
Lee, Jin Hee, 382  
Lee, Jun-Ho, 623  
Lee, Kang-Min, 266  
Lee, Kenneth, 776  
Lee, Kwang-Sun, 296  
Lee, Kyu Yup, 51, 130  
Lee, Sang Goo, 562  
Lee, Sang Heun, 51, 701  
Lee, Seung Ho, 643  
Lee, Thomas, 412  
Leek, Marjorie, 401, 939  
Lefebvre, Philippe, 108, 581  
Lefèvre, Gaëlle, 13  
Legan, P. Kevin, 651  
Legendre, Kirian, 136  
Leger, Claude Louis, 615  
Leger, James, 628  
Legout, Jordan D., 100  
Leibold, Lori, 466  
Leibovici, Michel, 13  
Leichtle, Anke, 21  
Lelli, Andrea, 486  
Lenarz, Minoo, 278, 875  
Lenarz, Thomas, 131, 234, 277, 278, 550, 875  
Lenoir, Marc, 638, 646  
Lenz, Daniel, 892  
Leong, U-Cheng, 363  
Lerch-Gaggl, Alexandra, 767  
Lerner, Andrew, 786  
Lesperance, Marci M., 999  
Leung, Keith, 107  
Leuthardt, Eric C., 419  
Levesque, Erin E., 564  
Levine, Robert, 256, 257, 336, 387  
Levine, Stephen, 527  
Lewis, Morag, 11  
Li, Geng-Lin, 207  
Li, Haiqiong, 439  
Li, Man-Na, 156, 357, 645, 872  
Li, Shuangding, 444  
Li, Xiantao, 672  
Li, Yan, 61  
Li, Yuanzhe, 52  
Li, Yuhua, 41  
Liang, Guihua, 619  
Liang, I-Chi, 270  
Liang, Jin, 127  
Libby, Patricia, 56  
Liberman, M. Charles, 605, 606, 607, 740, 768, 836, 876, 950, 1004  
Liberman, Tamara, 329  
Licari, Frank, 828  
Lichtenhan, Jeffery, 233  
Liebold, Candace, 145  
Lies, Sarah M., 63  
Lilaonitkul, Watjana, 835  
Lim, David, 20, 27  
Lim, Hubert, 277, 278, 875  
Lim, Sangkyun, 238  
Limb, Charles, 429, 430, 809  
Lin, Hsin-Pin, 549  
Lin, I-Fan, 888  
Lin, Jizhen, 28, 71  
Lin, Nan, 790  
Lin, Ryan Yung-Song, 813  
Lin, Vincent, 96, 555, 569  
Lin, Xi, 40, 41, 512, 611, 621  
Lindblad, Ann-Cathrine, 710  
Ling, Lynne, 302  
Lingner, Andrea, 878  
Linsenmeyer, Christa, 604  
Linthicum, Fred, 33  
Litovsky, Ruth, 284, 285, 286, 287, 976  
Litvak, Leonid, 802  
Liu, Ching-Ju, 910  
Liu, Dong, 438  
Liu, Haiying, 128, 669, 681  
Liu, Hesheng, 387  
Liu, Qing, 222  
Liu, Robert, 900  
Liu, Shuqing, 36, 45  
Liu, Wei, 578  
Liu, Xue Zhong, 53, 58  
Liu, Yi-Wen, 546  
Lobarinas, Edward, 340, 341, 384, 928  
Loeb, Gerald E., 290  
Loebach, Jeremy, 811  
Lolli, Brenda, 385  
Lomakin, Oleg, 855  
Lomax, Margaret, 471, 694, 758, 1007  
Long, Christopher, 979  
Long, Glenis, 180, 187  
Longo-Guess, Chantal, 1003  
Lonsbury-Martin, Brenda, 182  
López, Dolores E., 834  
Lopez, Ivan, 243, 775, 957, 958  
Lorenzi, Christian, 415, 937  
Losh, Joe, 350  
Lovell-Badge, Robin, 107  
Lovett, Michael, 8  
Lovett, Rosemary, 516  
Lu, Jianzhong, 338, 339, 340, 384  
Lu, Shan, 504  
Lu, Thomas, 285  
Lu, Wenfu, 763, 953  
Lu, Yong, 849  
Lu, Zhenjie, 774  
Luebke, Anne, 80, 757  
Luis, Enoch, 769  
Lujan, Rafael, 310  
Luksch, Harald, 312  
Lundberg, Yesha, 764  
Lundberg, Yunxia, 576, 765  
Luo, Xin, 814  
Lupo, J., 880, 881  
Lustig, Lawrence, 43, 214, 616  
Lutfi, Robert, 909, 910  
Lutman, Mark, 919  
Lv, Ping, 85  
Lynch, Eric, 123, 268  
Lysakowski, Anna, 771, 772, 947  
Ma, Eva, 117  
Ma, Ke-Tao, 595, 620  
Ma, Wei-Li, 827  
Ma, Xiaofeng, 331  
Maat, Bert, 185  
Macarthur, Carol, 22, 29  
Macleod, Katrina, 314  
Maconochie, Mark, 573  
Macpherson, Ewan, 480, 882, 993  
Madathany, Thomas, 90  
Maddox, Ross, 408  
Maekawa, Hitoshi, 160  
Magnus, Christopher, 551, 566  
Mahendrasingam, Shanthini, 640  
Maier, Hannes, 35  
Maier, Julia, 885  
Maison, Stéphane F., 605, 606, 607, 1004  
Majdak, Piotr, 288, 805, 975  
Majdani, Omid, 234  
Makashay, Matthew, 939  
Maki, Katuhiro, 861  
Makishima, Tomoko, 67, 700  
Makmura, Linna, 65  
Malgrange, Brigitte, 108, 581  
Malicki, Jerema, 562  
Mallik, Buddhadeb, 696  
Maltezos, Nathan, 315, 834  
Mammano, Fabio, 514, 594  
Manis, Paul, 318, 356  
Manix, Marc, 212  
Manley, Geoffrey, 598  
Mann, Sabine, 665  
Mannström, Paula, 619  
Mansour, Suzanne, 579  
Mapes, Frances, 56  
Marcotti, Walter, 199, 200  
Marcus, Daniel C., 602  
Marcus, Keith A., 64  
Maricich, Stephen, 449  
Maricle, Anastasiya, 696  
Mariko, Nakamagoe, 716  
Marion, Miranda, 24  
Marquardt, Meg, 95  
Marrone, Nicole L., 918  
Marshall, Lynne, 473  
Marslen-Wilson, William, 378  
Martin, David C., 806  
Martin, Donna M., 447  
Martin, Dusan, 99, 167  
Martin, Glen, 182, 183  
Martin, William, 395, 396  
Martinelli, Giorgio P., 959  
Martinez, Amy, 517  
Martinez, Rodrigo, 556  
Maruya, Shin-Ichiro, 683  
Masetto, Sergio, 199  
Masmodi, Saber, 998  
Mason, Christine R., 405, 917, 918  
Massey, Becky, 777  
Massow, Ole, 277  
Masuda, Masatsugu, 98, 715, 720  
Masuda, Yukihiro, 160  
Mathews, Paul, 848  
Mathias, S. R., 409  
Matsubara, Atsushi, 44  
Matsumoto, Masahiro, 122, 130  
Matsunaga, Tatsuo, 170, 219, 263, 572  
Matsunaga, Yoshiko, 168  
Matsunobu, Takeshi, 160  
Matsushita, Yuichiro, 168  
May, Bradford, 649  
Mayer-Proschel, Margot, 757  
McAlpine, David, 380, 854, 870, 885  
McArdle, Rachel, 395, 396  
McArthur, Kimberly, 789  
McCall, Andrew, 957  
McCleish, Stephen, 138  
McCullar, Jennifer, 125  
McDermott, Brian, 492, 662  
McDermott, Josh H., 468  
McDonald, Kent, 634  
McFadden, Dennis, 927, 967  
McGee, Joann, 495  
McGowan, Kathleen, 70  
McGuire, Ryan, 675  
McIntosh, J. Michael, 772  
McKay, Colette, 979  
McKenna, Michael J., 39, 159, 455  
McLaughlin, Myles, 844  
Meddis, Ray, 597, 932  
Meddis, Raymond, 931  
Meenderink, Sebastiaan, 188  
Megerian, Cliff, 47  
Meierhofer, Robert, 791  
Meikle, Mary, 395, 396  
Melamed, Sarah, 401, 939  
Melcher, Jennifer, 256, 257, 336, 387, 687, 986  
Meltser, Inna, 965  
Melvin, Thuy-Anh, 79, 244  
Menardo, Julien, 646  
Mendolia-Loffredo, Sabrina, 777  
Mens, Lucas, 801  
Merchant, Saamil, 177, 627  
Merriam, Elliott, 337  
Mersel, Marcel, 615  
Mescher, Mark, 455  
Metea, Monica, 249  
Mey, Jörg, 312  
Meyer, Alexander, 197  
Mhatre, Anand, 61, 93  
Michaels, Leslie, 632

- Michalewski, Henry, 385  
Michalski, Nicolas, 13  
Michel, Vincent, 13  
Micheyl, Christophe, 402, 895  
Mickey, Brian, 480  
Middlebrooks, John, 289, 291, 480, 993  
Migliaccio, Americo, 244, 791, 794, 795  
Mihaila, Camelia, 757  
Mikiel-Hunter, Jason, 854  
Mikulec, Anthony A., 612  
Mikuriya, Takefumi, 151, 152, 647, 729, 778, 779  
Millen, Kathleen, 101  
Miller, Charles, 229, 797, 798, 973  
Miller, Constance, 1004  
Miller, James D., 523  
Miller, Josef, 132, 474, 749  
Miller, Joseph M., 564  
Miller, Judi Lapsley, 473  
Miller, Justin, 69, 70  
Miller, Katharine, 663, 664  
Miller, Todd, 167  
Milligan, Ron, 489  
Millman, Rebecca, 376  
Millward, Kerri, 456, 518  
Milo, Marta, 563, 580  
Minami, Shujiro, 263  
Minekawa, Akira, 690  
Minoda, Ryosei, 124  
Minor, Lloyd, 239, 785, 788  
Minowa, Osamu, 42  
Mire, Patricia, 666  
Mishkin, Mortimer, 891  
Mistrik, Pavel, 594  
Miyauchi, Yuji, 647, 729  
Miyazawa, Toru, 165  
Mizuta, Kunihiro, 761, 762  
Mizutari, Kunio, 219, 263  
Mock, Bruce, 601  
Moeller, Christoph, 985  
Molis, Michelle, 401, 939  
Montcouquiol, Mireille, 118  
Montemayor, Celina, 128  
Montgomery, Ruth, 431  
Moon, Sung, 20, 27  
Moore, Brian C.J., 942  
Moore, Craig, 150  
Moore, David, 456, 457, 518, 520, 521, 876  
Moore, Robert, 250  
Moradoghli-Haftevam, Emma, 416  
Moran, Jamie L., 719  
Morell, Robert, 86  
Morgan, Clive, 493  
Mori, Susumu, 792  
Morizono, Testuo, 254  
Morizono, Tetsuo, 253  
Morris, David, 150  
Morse, Sue, 1002  
Morton, Cynthia, 1004  
Morton-Jones, Rachel T., 600  
Moser, Markus, 335  
Moser, Tobias, 197, 948, 949, 950  
Mosrati, Mohammed, 998  
Motts, Susan D., 14  
Mountain, David, 181, 504, 532  
Mousa, Shaker, 733  
Mowry, Sarah, 958  
Mueller, Marcus, 216  
Mueller, Susanne, 838  
Mueller, Ulrich, 489  
Mugnaini, Enrico, 756, 1005  
Muirhead, Katharine, 586  
Mukerji, Sudeep, 832  
Mukherjee, Debashree, 728  
Mulder, Jef, 801  
Mulders, Wilhelmina, 625, 837  
Mullen, Lina M., 483  
Müller, Marcus, 485, 685  
Muller, Martijn, 368  
Münkner, Stefan, 202  
Münscher, Adrian, 35  
Murakoshi, Michio, 137, 670, 671, 683  
Murashita, Hidekazu, 744  
Murata, Junko, 104  
Murphy, Brian, 455  
Murtie, Joshua, 577, 584, 768  
Mustapha, Mirna, 758, 1007  
Mutai, Hideki, 219, 263, 572  
Myers, Paula, 395, 396  
Myers, Steven F., 203  
Nadol, Joseph B., 633  
Nagashima, Reiko, 263  
Nagata, Keiichi, 90  
Naik, Khurram, 142, 663  
Nair, Thankam, 38, 608  
Nakagawa, Susumu, 219  
Nakagawa, Takashi, 253, 254  
Nakagawa, Takayuki, 75, 122, 130, 149, 168, 736  
Nakai, Akira, 151  
Nakajima, Heidi, 533  
Nakajima, Hideko, 177  
Nakamoto, Kyle, 871  
Nakmali, Don, 544  
Nam, Eui-Cheol, 256, 257, 336  
Nam, Jong-Hoon, 658  
Nam, Sung Il, 94  
Nannapaneni, Nishant, 300  
Naoz, Moshe, 653  
Narins, Peter, 92, 530, 531  
Narui, Yuya, 690  
Navaratnam, Dhasakumar, 134, 139, 668, 674  
Nayak, Gowri, 652  
Naylor, Amanda L., 563  
Neely, Stephen, 191, 192  
Negm, Mohamed, 799  
Nelson, Brian, 462, 863, 864  
Neubauer, Heinrich, 224  
Nevel, Adam, 276  
Newburg, Seth, 532  
Newlands, Shawn, 790  
Newman, Craig, 395, 396  
Newman, Dina, 56  
Nguyen, Laurent, 581  
Nguyen, Yann, 77  
Nichols, David, 101, 448  
Nichols, Justin, 355, 994  
Nichols, Michael, 95  
Nickel, Regina, 611  
Nie, Kaibao, 433  
Nie, Liping, 85  
Niedermeier, Kay, 260  
Niranjan, Mahesan, 580  
Nishimura, Hiroshi, 349  
Nishimura, Masahiko, 618  
Nishiyama, Toshimasa, 560  
Niu, Haoru, 65  
Nizami, Iftikhar, 930  
Nobbe, Andrea, 983  
Noda, Tetsuo, 42  
Noel, Victor, 883  
Nolan, Lisa, 57  
Nong, Xiaoyun, 269  
Nopp, Peter, 983  
Norris, Dennis, 378  
Northrop, Clarinda, 527  
Nourse, Amanda, 676  
Nourski, Kirill, 229, 379  
Nouvian, Regis, 615, 948, 949  
Nowotny, Manuela, 176, 179  
Nutt, Robert C., 367  
Nuttall, Alfred, 83, 84, 89, 502, 509, 591, 636, 684, 707  
Nymon, Amanda, 751  
O'Brien, Sara, 812  
Oba, Sandra, 190  
O'Beirne, Greg A., 172  
O'Connor, Alec Fitzgerald, 543  
Oda, Kiyoshi, 831  
Oertel, Donata, 311, 313  
Oesterle, Elizabeth, 125, 569  
Officiers, Erwin, 977  
Ogawa, Kaoru, 42, 219, 263, 711, 715  
Ogawa, Makio, 559  
Oghalai, John, 449, 609  
Ogita, Hideaki, 130  
Ogle, Amanda, 549  
Ogura, Masami, 160  
Oh, Seung Ha, 382  
Oh, Seung-Ha, 519  
Oh, Soo Hee, 296  
Ohl, Frank W., 280, 892  
Ohlsmiller, Kevin K., 641, 642  
Ohlsson-Wilhelm, Betsy, 586  
Ohtsuka, Toshiyuki, 104  
Ohyama, Takahiro, 103  
Okada, Minae, 407  
Okada, Teruhiko, 618  
Okamoto, Yasuhide, 263  
Okamura, Hiro-Ok, 49  
Okano, Hideyuki, 104, 116, 715  
Okano, Hirotaka James, 715  
Okano, Takayuki, 168  
Okoruwa, Oseremen, 138  
Oku, Naohiko, 349  
O'Leary, Stephen, 73  
Oliver, Guillermo, 448  
Olivier, Michael, 59  
Olney, Daniel, 360, 361  
Olofsson, Åke, 689, 710  
Olson, Elizabeth, 177, 178, 500  
O'Malley, Jennifer, 627  
Omelchenko, Irina, 707  
O'Neill, William, 889, 890  
Ono, Kazuya, 75, 122, 130, 168, 736  
Onozato, Kaoru, 160  
Ooka, Hisashi, 560  
Oostrik, Jaap, 998  
Organ, Louise, 680  
Orita, Hiroshi, 778  
Ornitz, David, 576, 763, 952, 953  
Oron, Yahav, 256  
Orzan, Eva, 997  
Osaki, Yasuhiro, 349  
O'Shea, K. Sue, 749  
Oshima, Aki, 44, 635  
Oshima, Kazuo, 556, 665  
Oswald, Anne-Marie M., 342  
Otting, Margarete, 972  
Ou, Henry, 96, 267, 452  
Ouyang, Xiaomei, 53, 58  
Owens, Kelly, 262, 267  
Oxenham, Andrew, 400, 402, 468, 895, 929  
Oya, Hiroyuki, 379, 995  
Ozdemir, Elif, 387  
Ozmeral, Erol, 917  
Paasche, Gerrit, 131, 234  
Paige, Gary, 889, 890  
Paisley, Mara, 158  
Pajor, Nathan, 371  
Pak, Kwang, 21, 98, 483, 720, 748  
Palan, Vikrant, 275, 542  
Palmer, Alan, 227, 825, 871, 897, 898, 924, 990  
Palsdottir, Hildur, 634  
Paltoglou, Aspasia E., 988  
Pan, Huiqi, 20, 27  
Pan, Ling, 111  
Pan, Zhuo-Hua, 307  
Panford-Walsh, Rama, 258  
Pang, Jiaqing, 22  
Papaioannou, Virginia E., 100  
Paparella, Michael, 26  
Papsin, Blake C., 283  
Parham, Kourosh, 186  
Pariikh, Preeti, 940  
Pariikh, Sanjay, 816  
Park, Channy, 265, 699, 701  
Park, Dong Choon, 359  
Park, Hongju, 238  
Park, Hun Yi, 148  
Park, Il-Yong, 274  
Park, Jae Yong, 703  
Park, Jhang Ho, 146  
Park, Keehyun, 148  
Park, Min-Hyun, 382, 519  
Park, Moon Seo, 237  
Park, Raekil, 265, 266, 699, 701  
Park, Shi-Nae, 43, 214  
Park, Soo-Kyung, 358  
Park, Soon Hyung, 94  
Park, Sun Ho, 94  
Park, Yong Ho, 703  
Park, Youn Ho, 94  
Parker, Mark, 558  
Parkinson, Nick, 1002  
Parrish, Jennifer L., 302, 366  
Parsons, Thomas D., 223, 951  
Parving, Agnete, 997  
Pasanen, Edward, 927  
Paschall, Dwayne, 525  
Patel, Andrew, 34  
Patel, Ankur, 994  
Patterson, D. Michael, 53  
Patterson, Roy, 378, 912, 987  
Patuzzi, Robert, 172, 232  
Paul, Isabella, 421  
Pawelczyk, Malgorzata, 470  
Pawlosky, Annalisa M., 592  
Pawlowski, Karen, 47, 661  
Pearce, Jacqueline, 392  
Pearson, Jim, 722  
Pecka, Jason, 138  
Pecka, Michael, 853  
Pedemonte, Marisa, 329, 394  
Pelling, Anna, 107  
Peng, Anthony, 665  
Peng, Shu-Chen, 813  
Peng, You-Wei, 37, 46  
Peppi, Marcello, 455  
Pereira, Fred, 128, 609, 669, 675, 681  
Perez-Gonzalez, David, 322  
Perin, Paola, 91  
Perlegas, Peter, 24  
Perrin, Benjamin, 494, 495  
Peters, Linda, 86  
Peterson, Diana, 18  
Peterson, Nathan, 811  
Petit, Christine, 13, 136, 205, 948  
Pettingill, Lisa, 454  
Peusner, Kenna, 786  
Pevny, Larysa, 106  
Pfannenstiel, Susanna, 547, 712  
Pflingst, Bryan, 293, 295, 806  
Pfister, Markus, 609, 997  
Pham, Lankhanh, 666  
Philibert, Benedicte, 996  
Philippon, Bertrand, 415  
Phillips, Kelli R., 651  
Philpott, Christopher, 676  
Pierce, Marsha, 10, 582  
Pietola, Laura, 163  
Pietsch, Markus, 234  
Pillers, De-Ann, 22  
Piontek, Kb, 659  
Pisoni, David, 811  
Plack, Christopher, 373, 839  
Plasterk, Ronald, 439  
Plinkert, Peter K., 164  
Plinkert, Peter-K., 712  
Pliss, Lioudmila, 317  
Plontke, Stefan, 612, 614  
Podgorski, Michael, 676  
Poeppel, David, 377, 386  
Poirot, Marc, 739  
Pol-Fernandes, David, 394  
Pollak, George, 872  
Polley, Daniel, 353  
Popel, Aleksander, 677  
Popelar, Jiri, 906  
Popescu, Maria, 353  
Popper, Paul, 766, 767  
Popratiloff, Anastas, 786  
Populin, Luis, 477  
Porter, Benjamin, 425  
Porter, Kristin, 17  
Post, J. Christopher, 3, 25  
Poulsen, David, 80  
Powell, Elizabeth, 873  
Praetorius, Mark, 164, 547, 712  
Prahl, Susanne, 30  
Prakash, S. R., 240  
Pratt, Ronald, 587  
Pressnitzer, Daniel, 406, 885  
Price, Steve, 771, 772  
Prieskorn, Diane, 132, 749  
Prieve, Beth, 180  
Prijs, Vera, 230  
Prins, Kurt, 495  
Profant, Oliver, 905  
Provenzano, Matthew, 48, 751  
Puel, Jean Luc, 615  
Puel, Jean-Luc, 472, 638, 639, 646  
Puligilla, Chandrakala, 12, 66, 106, 443  
Puria, Sunil, 536, 538, 631  
Pyle, Mark, 248  
Pyykko, Ilmari, 697, 997  
Q, Vickram, 728  
Qazi, Taha, 165  
Qi, Weidong, 733, 743  
Qian, Feng, 659  
Qian, Jinyu, 911  
Qiu, Wei, 718  
Quignodon, Laure, 485  
Quinlan, Elizabeth, 344  
Quint, Elizabeth, 11  
Rabbits, Richard, 144, 657, 784, 959  
Radziwon, Kelly E., 933  
Raible, David, 117, 262, 267, 452  
Rajagopalan, Lavanya, 669, 681  
Rajguru, Suhrud, 959  
Rajon, Didier A., 290  
Ramachandran, Virginia, 830  
Ramakrishnan, Neeliyath A., 204  
Ransohoff, Richard M., 726  
Rao, Deepti, 356  
Raphael, Robert, 133, 634, 675, 679, 680  
Raphael, Yehoash, 64, 124, 165, 171, 272, 293, 447, 548, 571, 599, 608, 758, 806, 1007  
Rasmussen, Jerod, 587  
Ratib, Sonia, 520  
Ratnam, Rama, 196, 862  
Ratnanather, J. Tilak, 429  
Ratzlaff, Kerstin, 164

- Rau, Christoph, 630  
Rau, Thomas, 234  
Rauch, Steven D., 4, 240  
Raveendran, Nithya N., 602  
Ravicz, Michael, 177, 533, 534, 535  
Rawn, Caitlin, 466  
Rawool, Vishakha, 388  
Ray, Catherine, 440  
Raz, Yael, 112  
Razak, Khaleel, 992  
Read, Heather, 333  
Rebillard, Guy, 646  
Redfern, Mark, 246, 247, 368  
Redshaw, Nick, 11  
Reece, Alisa, 74  
Reed, Charlotte M., 399  
Reed, Richard, 432  
Rees, Adrian, 322  
Reeves, Roger, 791  
Reh, Thomas, 105, 440  
Reich, Uta, 277  
Reid, Errold, 381  
Reilly, Brian, 754  
Reinhart, Katherine, 262  
Reiss, Lina, 810  
Ren, Tianying, 174, 501, 502, 684  
Renaud, Gabriel, 127  
Rennie, Katie, 770  
Renton, John, 752  
Reuter, Günter, 277  
Reuveni, Marissa, 86  
Reyes, Alex D., 342  
Reynolds, Anna, 489  
Rhee, Chung-Ku, 735  
Riazuddin, Saima, 54, 998  
Riazuddin, Sheikh, 54, 998, 998  
Ricci, Anthony, 944  
Rich, Stephen, 24  
Richards, Virginia, 411, 412, 465, 911  
Richardson, Guy, 13, 496, 651, 652  
Richter, Claus-Peter, 231, 276, 630, 972, 1005  
Riley, Alison, 520, 521  
Rinne, Teemu, 374  
Rinzel, John, 848  
Ritter, Steffen, 369  
Rivolta, Marcelo, 563, 580  
Rizk, Joseph, 306  
Roberts, Brian, 404  
Roberts, Brock, 262  
Roberts, Michael, 319  
Roberts, William, 206, 946  
Robertson, Donald, 68, 625, 837  
Robertson, George, 150  
Robertson, Nahid, 1004  
Robinson, Barbara, 229, 798, 973  
Rocca, Christine, 434  
Rocha-Sanchez, Sonia M. S., 564  
Rodger, Jenny, 68  
Rodio, Silvana, 394  
Roehm, Pamela, 753  
Rogers, Genevieve, 543  
Rogers, Mike, 62  
Rohbock, Karin, 258  
Romand, Raymond, 574  
Romero, Rosario, 1002  
Roof, Bryan, 355  
Rosen, Merri, 478, 938  
Rosenhall, Ulf, 32  
Rosowski, John, 177, 533, 534, 535  
Roth, Yehudah, 256  
Roux, Isabelle, 220, 948  
Rova, Cherokee, 80  
Rowe, Kelly, 270  
Rozental, Renato, 722  
Rubel, Edwin, 76, 96, 117, 262, 267, 452, 555, 851, 852  
Ruben, Robert, 19  
Rubinstein, Jay, 433, 934  
Rubio, Maria, 303, 315, 320, 834  
Rudic, Milan, 77  
Ruebsamen, Rudolf, 819, 845  
Ruel, Jérôme, 615, 646  
Ruettiger, Lukas, 258  
Ruhland, Janet, 879  
Ruiz, Fernanda R., 128  
Rummel, Michael, 984  
Runge-Samuelson, Christina, 59  
Rupp, Andre, 369, 987  
Ruth, Peter, 485  
Rutherford, Mark, 206, 946  
Rutkowski, Richard, 919  
Rüttiger, Lukas, 485  
Ryan, Allen, 21, 98, 217, 483, 600, 720, 748  
Ryan, Amy B., 97  
Rybak, Leonard, 728  
Rybalchenko, Volodya, 140  
Ryugo, David, 303  
Rzadzinska, Agnieszka, 11, 497  
Saber, Amanj, 72  
Sabin, Andrew T., 915, 941  
Sabine, Ladrech, 646  
Sacheli, Rosalie, 581  
Sadeghi, Soroush, 788  
Saffiedine, Saaid, 205  
Saffran, Jenny R., 976  
Safieddine, Saaid, 136, 948  
Sahani, Maneesh, 870  
Sahara, Yoshinori, 960  
Sahlin, Lena, 624  
Saito, Akihiko, 761  
Saito, Mitsuyoshi, 952  
Saito, Osamu, 545  
Sajan, Samin, 8  
Sakaguchi, Hirofumi, 489, 653  
Sakaguchi, Takefumi, 545  
Sakai, Shuhei, 744  
Sakai, Yoko, 393  
Sakamoto, Tatsunori, 75, 130, 168  
Sakata, Motomichi, 290  
Sale, Michele, 24  
Salgado, Humberto, 355, 994  
Salles, Felipe, 576  
Salloum, Claire A., 283  
Salminen, Marjo, 163  
Salt, Alec, 612, 613, 614  
Saltzman, Mark, 450  
Salvi, Richard, 153, 154, 157, 158, 301, 338, 340, 341, 384, 698, 733, 743, 928  
Samad, Tarek, 577  
Samii, Amir, 875  
Sams, Mikko, 374  
Sanchez, Jason, 330  
Sandridge, Sharon, 395, 396  
Sanes, Dan, 351, 478, 938  
Sanford, Chris, 546  
Sanneman, Joel D., 602  
Santi, Peter, 628  
Santos, Felipe, 267, 452  
Santos-Sacchi, Joseph, 89, 134, 139, 140, 668, 672, 673, 674  
Saoji, Aniket, 802  
Sarbadhikari, Krishna, 928  
Sarro, Emma, 938  
Sasai, Yoshiki, 103  
Sasaki, Akira, 44  
Sato, Eisuke, 714, 726  
Sato, Teruyuki, 390  
Satoh, Takunori, 1000  
Saunders, James C., 223, 226, 951  
Sausbier, Matthias, 485  
Savary, Etienne, 565  
Sawusch, James, 426  
Sayles, Mark, 820, 822  
Scarfone, Eric, 629  
Schachern, Patricia, 26  
Schacht, Jochen, 145, 147, 644, 721, 731  
Schachtele, Scott, 350  
Schairer, Kim, 526  
Schalk, Gerwin, 419  
Scheeline, Alexander, 709  
Scheich, Henning, 348  
Scheper, Verena, 550  
Scherer, Marc, 179  
Scherer, Matthew, 794  
Scherf, Fanny, 977  
Schiemann, Dorrit, 282  
Schlecker, Christina, 164  
Schlee, Winfried, 338  
Schleich, Peter, 983  
Schlesinger, Paul, 952  
Schmiedt, Richard A., 559  
Schmutz, Joseph, 817  
Schnee, Michael, 944  
Schneider, Glenn, 69, 70  
Schnupp, Jan, 281, 886, 901, 989  
Schoen, Cynthia J., 999  
Schoenecker, Matthew, 328, 803  
Schoffelen, Richard Lm, 499  
Schofield, Brett R., 14  
Scholes, Chris, 990  
Scholl, Ben, 352  
Scholl, Markus, 550  
Schrader, Angela, 955  
Schramm, Jordan, 757  
Schreiner, Christoph, 354, 479, 996  
Schrott-Fischer, Anneliese, 132  
Schubert, Michael, 793, 794  
Schuck, Julie, 126  
Schulte, Bradley A., 559  
Schulze, Holger, 258, 985  
Schumacher, Kristopher, 677, 678  
Schvartz, Kara, 292  
Schwander, Martin, 489  
Schwartz, Andrew, 464  
Schweizer, Michaela, 35  
Scrabble, Heidi, 97  
Seal, Rebecca, 616  
Segade, Fernando, 24  
Segenhout, Johannes M., 499  
Segil, Neil, 442, 567, 575  
Seidl, Armin, 852  
Seidman, Michael, 830  
Sekerova, Gabriella, 756, 1005  
Seki, Makiko, 393  
Selezneva, Elena, 348  
Sellick, Peter, 68  
Selvakumar, Dakshnamurthy, 88  
Semaan, Maroun, 47  
Semal, Catherine, 922  
Semple, Malcolm, 478  
Sengupta, Soma, 141, 663  
Senn, Pascal, 556  
Seong, Ki-Woong, 274  
Sewell, William, 455  
Sfondouris, John, 681  
Sha, Su-Hua, 145, 147, 644, 731  
Shackleton, Trevor, 227, 871  
Shah, Nilesh, 722  
Shahzad, Mohsin, 54  
Shamma, Shihab, 344, 481, 893, 896, 907  
Shang, Jailin, 125  
Shannon, Robert, 279, 815  
Shanske, Alan, 578  
Shatadal, Shalini, 311  
Shechter, Barak, 873, 903  
Sheft, Stanley, 937  
Shelhamer, Mark, 793  
Shen, Jun-Xian, 531  
Shepherd, Robert, 281, 294, 454, 800  
Shera, Christopher, 194, 592, 687  
Sheth, Sonal, 997  
Sheykholeslami, Kianoush, 241  
Shi, Jianrong, 719  
Shi, Xiaorui, 89, 620, 636, 707  
Shi, Yongbing, 252  
Shibata, Seiji B., 548  
Shick, H. Elizabeth, 714, 726  
Shim, Hyun Joon, 358, 359  
Shimano, Takashi, 299, 306, 307  
Shimizu, Ritsuko, 109  
Shimizu, Yoshitaka, 536  
Shimogori, Hiroaki, 151, 152, 235, 647, 729, 778, 779  
Shin, Hyangae, 238  
Shin, Jung-Eun, 146, 238  
Shin, Min-Sup, 519  
Shin, Minyong, 538  
Shinden, Seiichi, 263  
Shinkawa, Hideichi, 683  
Shinn-Cunningham, Barbara, 408, 410, 424, 459, 464, 888  
Shinn-Cunningham, Gerald, 917  
Shiotani, Akihiro, 160, 711  
Shiroya, Tsutomu, 168  
Shofner, William, 821  
Shomron, Noam, 9  
Shore, Susan, 16, 300, 304  
Shrestha, Sneha, 984  
Shrivastav, Mini, 914  
Shub, Daniel E., 465  
Siebeneich, Wolfgang, 766  
Siebert, Ursula, 30  
Siedow, Norbert, 614  
Siegel, Jonathan, 195, 709  
Sierra, Carlos Vicente Rizzo, 923  
Sim, Jae Hoon, 540, 541  
Simmons, Dwayne, 955  
Simon, Jonathan Z., 386  
Simon, Julian, 452  
Simoncelli, Eero P., 468  
Simonoska, Rusana, 624  
Simpson, Brian, 463  
Sinex, Donal, 824, 834  
Singer, Wibke, 258  
Singh, Ruchira, 610  
Sininger, Yvonne, 517  
Sinks, Belinda, 248  
Sisneros, Joseph, 968  
Sisson, Joseph, 50  
Sivakumaran, Theru, 1004  
Sivaramakrishnan, Shobhana, 325, 330  
Siveke, Ida, 859  
Skinner, Kim, 249  
Skjongsberg, Åsa, 727  
Sklare, Daniel, 427  
Slama, Michael, 533  
Slattery, Eric, 121  
Sliwiska-Kowalska, Mariola, 470  
Smith, David W., 290  
Smith, Michael, 126  
Smith, Sonya, 656  
Smith, Yoland, 303  
Smolders, Jean, 216  
Snyder, Joel, 403  
Snyder, Russell, 328, 803, 974  
So, Hongseob, 265, 266, 699, 701  
Sodhi, Simrit, 745  
Soenmez, Banu, 987  
Sokolowski, Bernd, 82  
Song, Lei, 89, 140, 673  
Song, Weiming, 184  
Sonnemann, Kevin, 495  
Sorri, Martti, 997  
Soto, Enrique, 769, 780  
Soucek, Sava, 632  
Sougrat, Rachid, 561  
Soukup, Garrett, 10, 582  
Spain, William, 857  
Sparto, Patrick, 246  
Specht, Hans-Joachim, 369  
Speck, Judy, 121  
Spector, Alexander, 677, 678  
Spencer, Nathaniel, 568  
Spirou, George, 846  
Spoon, Corrie, 773  
Srinivasan, Arthi, 279  
Srinivasan, Arunkumar, 655  
Srinivasan, Satish, 448  
Staecker, Hinrich, 547, 712  
Staffaroni, Laura, 372, 381  
Stagner, Anna, 723  
Stagner, Barden, 182, 183  
Stakhovskaya, Olga, 328, 803, 807  
Stankovic, Konstantina, 39, 159, 768  
Starr, Arnold, 385  
Stasiak, Arkadiusz, 820  
Stauffer, Christopher, 636  
Stauffer, Eric A., 487  
Stecker, G. Christopher, 884  
Steel, Karen, 11, 62, 497  
Steele, Charles, 538, 631  
Steigelman, Katherine, 659  
Steinschneider, Mitchell, 372, 381, 894, 899  
Stenberg, Annika, 624  
Stenberg, Erica, 526  
Stepanyan, Ruben, 488, 494, 496  
Stephan, Dietrich, 997  
Stephens, Dafydd, 997  
Sterbing-D'Angelo, Susanne J., 908  
Sterkers, Olivier, 77, 236, 1001  
Stevenson, Amy, 954  
Stewart, Barbara, 395, 396  
Steyger, Peter, 723, 724, 725  
Stick, Melissa, 427  
Stiegemann, Bettina, 191, 192  
Stoelinga, Christophe, 909, 910  
Stoever, Timo, 131, 234, 550  
Stohl, Joshua, 978  
Stolzberg, Daniel, 338, 340, 341, 933  
Stone, Jennifer, 555, 569  
Stoodley, Paul, 25  
Strachota, Alex, 628  
Streckert, Joachim, 202  
Street, Valerie, 60  
Streeter, Tim, 408  
Strenzke, Nicola, 950  
Strome, Scott E., 66  
Stronks, Christiaan, 230  
Strutz, Juergen, 259  
Stuermer, Ingo, 691  
Su, Gina L., 293  
Suga, Nobuo, 331, 345, 346  
Sugahara, Kazuma, 151, 152, 235, 251, 647, 729, 778, 779



- Sugamura, Mayumi, 253, 254  
 Suh, Eul, 231, 972, 1005  
 Suh, Myung-Whan, 382  
 Sul, Bora, 143, 588  
 Sultermeyer, David R., 742  
 Summerfield, A. Quentin, 409, 421, 516  
 Summers, Van, 939  
 Sumner, Christian, 825, 876, 990  
 Sun, Guangwei, 170, 263  
 Sun, Hongyu, 323  
 Sun, Ming-Zhong, 36, 45  
 Sun, Wei, 338, 339, 340, 341, 384, 928  
 Sun, Yu, 312  
 Surguchev, Alexei, 134, 139, 674  
 Sussman, Elyse, 372, 381, 816  
 Suta, Daniel, 906  
 Suzuki, Hiroaki, 44  
 Suzuki, Hiroko, 560  
 Suzuki, Mamoru, 52  
 Suzuki, Nobuyoshi, 44, 635  
 Svirsky, Mario, 940  
 Swaminathan, Jayaganesh, 840, 842  
 Swan, Erin, 455  
 Swiderski, Donald, 165, 599  
 Swift, John, 667  
 Syed, Emilie, 282  
 Syka, Josef, 905, 906  
 Tabata, Yasuhiko, 75, 736  
 Tabor, Kathryn, 851  
 Tabuchi, Keiji, 109, 713, 716, 744  
 Tadenuma, Takashi, 670  
 Taft, Daniel, 804  
 Tahera, Yeasmin, 965  
 Takahashi, Shin, 390  
 Takahashi, Terry, 462, 863, 864, 926  
 Takeda, Taizo, 618  
 Takemoto, Tsuyoshi, 251  
 Takesian, Anne, 351  
 Takiguchi, Youichiro, 263  
 Takumi, Yutaka, 44, 635  
 Talaska, Andra, 145, 644  
 Taleb, Mona, 730  
 Talmadge, Carrick, 180, 187  
 Tamaki, Chizuko, 242  
 Tamura, Manabu, 104  
 Tan, Hongyang, 191, 192  
 Tan, Justin, 294  
 Tan, Xiaotong, 138  
 Tanabe, Tetsuya, 160  
 Tanaka, Chiemi, 155, 156, 357, 507, 645  
 Tanaka, Shuho, 713  
 Tang, Qing, 980  
 Tang, Shan, 79  
 Tang, Wenxue, 40, 41, 512, 611, 621  
 Tang, Yezhong, 843  
 Taranda, Julián, 605, 607  
 Tateossian, Hilda, 1002  
 Taura, Akiko, 98, 720  
 Taura, Kojiro, 98  
 Taylor, Jenny, 456, 457  
 Taylor, Ruth, 611, 637  
 Telian, Steven, 38  
 Tempel, Bruce L., 63  
 Ter-Mikaelian, Maria, 478  
 Thalmann, Isolde, 763, 953  
 Thalmann, Ruediger, 763, 952, 953  
 Thelen, Nicolas, 108  
 Thiry, Marc, 108  
 Thompson, Angela B., 100, 119, 574  
 Thompson, Ann, 115  
 Thompson, Sarah, 380  
 Thompson, Scott, 360, 361  
 Thorne, Peter R., 600  
 Throckmorton, Chandra, 978  
 Tian, Junru, 245  
 Tian, Yong, 485  
 Tiede, Leann, 95  
 Tieu, David, 113, 114, 754  
 Tillein, Jochen, 282, 874  
 Todd, N. Wendell, 539  
 Tohse, Hidekazu, 954  
 Tokano, Hisashi, 577  
 Tokita, Joshua, 489, 653  
 Tokunaga, Akinori, 104  
 Tollin, Daniel, 880, 881  
 Tolnai, Sandra, 845  
 Tong, Benton, 955  
 Tong, Mingjie, 81, 660  
 Toren, Ginat, 1000  
 Tornari, Chrysostomos, 484  
 Toupet, Michel, 236  
 Towers, Emily, 261, 484  
 Trachoo, Objoon, 563  
 Trahiotis, Constantine, 460  
 Tran, Huy, 123  
 Travo, Cecile, 956  
 Treadway, Corey K., 203  
 Tremblay, Kelly, 934  
 Triffo, William, 634  
 Tritsch, Nicolas, 198, 513  
 Tritto, Simona, 91  
 Trune, Dennis, 22, 29, 162, 510  
 Trussell, Larry, 319, 850  
 Tsubouchi, Hirohito, 736  
 Tsuda, Hitoshi, 160  
 Tsumoto, Kouhei, 137, 670  
 Tsuprun, Vladimir, 26  
 Tucker, Andrew F., 436  
 Turcan, Sevin, 213  
 Turcanu, Diana, 537, 685, 686  
 Turk, Dennis, 395, 396  
 Turner, Christopher, 810  
 Turner, Jeremy G., 302, 366  
 Ty, Sidya, 125  
 Typlt, Marei, 819, 845  
 Tzounopoulos, Thanos, 320  
 Udayashankar, Arun Palghat, 589  
 Ueno, Tetsuko, 253, 254  
 Ulfendahl, Mats, 72, 557, 619, 629, 727, 739  
 Urness, Lisa, 579  
 Usami, Shin-Ichi, 44, 55, 635  
 Uziel, Alain, 565  
 Valentino, Orlando, 33  
 Valero, Jerome, 283  
 Valero, Michelle D., 196  
 Valli, Paolo, 91  
 Vallurupalli, Mounica, 38  
 Van Camp, Guy, 470, 997  
 Van De Heyning, Paul, 977, 983, 997  
 Van De Water, Thomas, 78, 161, 269  
 Van Der Heijden, Marcel, 844, 921  
 Van Der Zwaag, Bert, 998  
 Van Deun, Lieselot, 977  
 Van Dijk, Pim, 185, 370, 499  
 Van Doersten, Peter, 80  
 Van Dongen, Stijn, 11  
 Van Eyken, Els, 997  
 Van Hoesel, Richard, 283, 284, 286  
 Van Laer, Lut, 470, 997  
 Van Wieringen, Astrid, 977  
 Vandenbosch, Renaud, 581  
 Vanpoucke, Filiep, 801  
 Vasilyeva, Olga, 360  
 Vasquez-Weldon, Angelica, 453, 717  
 Vaupel, Kristina, 335  
 Vazquez, Ana, 708  
 Vega, Rosario, 769, 780  
 Velez, Alejandro, 414  
 Velkey, Matt, 749  
 Velluti, Ricardo A., 329  
 Venzelaar, Hanka, 998  
 Vermeire, Katrien, 983  
 Verpy, Elisabeth, 13  
 Versnel, Huib, 230, 741, 962  
 Vetesnik, Ales, 686  
 Vetter, Douglas, 212, 213, 218, 605, 607  
 Videhult, Pernilla, 738  
 Vielsmeier, Veronika, 259  
 Vincent, Couloigner, 77  
 Vivero, Richard, 78  
 Vojkovic, Srdjan M., 600  
 Volk, Mathew J., 669  
 Vollmer, Maïke, 874  
 Von Der Behrens, Wolfer, 904  
 Von Gersdorff, Henrique, 207  
 Von Kriegstein, Katharina, 380  
 Von Tiedemann, Miriam, 629  
 Von Unge, Magnus, 529  
 Vonthein, Reinhard, 202  
 Voormolen, Maurits, 983  
 Voytenko, Sergiy, 332  
 Vrehen, Dimitri, 923  
 Wackym, P. Ashley, 1, 59, 766, 767, 777  
 Wada, Hiroshi, 137, 670, 671, 683  
 Waga, Masashi, 891  
 Wagner, Hermann, 312, 925  
 Wagner, Marnie L., 882  
 Wagoner, Jessica, 305  
 Wakabayashi, Kenichiro, 715  
 Walker, Claire J., 63  
 Walker, Kerry, 989  
 Wall, Eric, 270  
 Wallace, Mark, 897, 898  
 Wallin, Inger, 738  
 Walsh, Edward, 495  
 Walsh, Joseph, 231, 276, 972  
 Walsh, Kyle, 927  
 Walton, Joseph, 362, 363, 364  
 Wang, Grace, 823  
 Wang, Guang-Hui, 324  
 Wang, Hongning, 302  
 Wang, Huan, 208  
 Wang, Jian, 150  
 Wang, Jing, 472, 638, 646  
 Wang, Le, 872  
 Wang, Qi, 723, 724, 725  
 Wang, Qiong, 270  
 Wang, Weimin, 37  
 Wang, Wenjun, 381  
 Wang, Xiang, 138, 142, 667  
 Wang, Xiaoqin, 482, 991  
 Wang, Youdan, 453  
 Wangemann, Philine, 604, 610  
 Warchol, Mark, 8, 110, 118, 121, 273, 576, 952  
 Ward, Bryan K., 247  
 Ward, Jaye, 587  
 Ward, Jonette, 74  
 Warnecke, Athanasia, 131  
 Wasserman, Stephen I., 21  
 Watkins, Paul, 383, 902  
 Watson, Bracie, 428  
 Watson, Charles, 523  
 Watson, Glen, 666  
 Watson, Julie, 649  
 Wawroski, Lauren, 936  
 Weber, Christopher, 43, 214, 616  
 Weber-Fox, Christine, 841  
 Webster, Paul, 696  
 Wedemeyer, Carolina, 209  
 Wehr, Mike, 352  
 Wei, Dongguang, 85  
 Wei, Min, 790  
 Weil, Dominique, 13  
 Weisz, Nathan, 338  
 Wenzelaar, Hanka, 998  
 Welch, David, 515  
 Welch, Thomas, 426  
 Welgampola, Miriam, 239  
 Welstead, Lindsey J., 651  
 Wenstrup, Jeffrey, 18, 308  
 Wenzel, Gentiana I., 277  
 Werner, Lynne, 467  
 Wesolowski, Karolina, 749  
 Wester, Chris, 534  
 Westerfield, Monte, 438  
 Weston, Michael, 10, 582  
 Whitchurch, Elizabeth, 462  
 White, Patricia, 567  
 White, Stephen, 676  
 Whiten, Darren M., 633  
 Whitton, Donna, 113, 114, 650, 754  
 Whitney, Susan, 246  
 Widjaja, Sandra, 294  
 Wiegrebe, Lutz, 859, 878  
 Wightman, Frederic, 523  
 Wild, Conor, 422  
 Willi, Urban, 530  
 Willis, Lindsey, 617  
 Willis, Marie, 233  
 Wilson, E. Courtenay, 399  
 Wilson, Rebekah, 709  
 Wilson, Roselyn M., 941  
 Wilson-Kubalek, Elizabeth, 489  
 Winer, Jeffery, 354, 996  
 Winter, Harald, 485  
 Winter, Ian, 820, 822  
 Wise, Andrew, 454, 800  
 Witton, Caroline, 373  
 Wojtczak, Magdalena, 929  
 Wolf, Eric, 270  
 Wolf, Melanie, 550  
 Wolfsberg, Tyra, 127  
 Wolfson, Aaron, 417  
 Won, Jong Ho, 433, 934  
 Wong, Daniel, 375  
 Woo, Jeong-Im, 20, 27  
 Woo, Jihwan, 797, 798, 973  
 Wood, Mark, 544  
 Woodson, Erika A., 48  
 Woolf, Clifford, 577  
 Wouters, Jan, 977  
 Wright, Beverly A., 458, 461, 915, 941  
 Wright, Charles, 47, 661  
 Wu, Doris, 102, 435  
 Wu, Emmy, 700  
 Wu, Hao, 697  
 Wu, Shu Hui, 323  
 Wu, Tao, 83, 84, 89  
 Wu, Xudong, 141, 659, 667  
 Wys, Noel, 749  
 Xia, Anping, 449, 609  
 Xia, Jing, 459  
 Xiang, Juanjuan, 386  
 Xiao, Ming, 549  
 Xiao, Ying, 325  
 Xie, Ruili, 318  
 Xie, Xiaoling, 111, 583  
 Xiong, Wei, 489  
 Xu, Jin, 294  
 Xu, Jingjing, 693  
 Xu, Li, 423, 981  
 Xu, Ningyong, 48, 751, 752, 755  
 Xu, Pin-Xian, 437  
 Xu, Tian-Le, 324  
 Xu, Tonghui, 85  
 Xu, Zhigang, 665  
 Xue, Hui Zhong, 750  
 Xue, Jingbing, 783  
 Xuefei, Ma, 445  
 Xu-Friedman, Matthew, 316, 317, 759  
 Yamamoto, Hiroshi, 636, 707  
 Yamamoto, Masayuki, 109  
 Yamamoto, Norio, 12, 445  
 Yamano, Takafumi, 253, 254  
 Yamasaki, Aigo, 251  
 Yamashita, Daisuke, 263, 711, 715  
 Yamashita, Hiroshi, 151, 152, 235, 251, 647, 729, 778, 779  
 Yamashita, Tetsuji, 667  
 Yamashita, Toshio, 560  
 Yamasoba, Tatsuya, 748  
 Yamauchi, Daisuke, 831  
 Yamoah, Ebenezer, 85, 765  
 Yan, Denise, 53, 58  
 Yang, Aizhen, 784  
 Yang, Hua, 759  
 Yang, Jiewu, 1002  
 Yang, Shiguang, 428  
 Yang, Yu-Qin, 620  
 Yarin, Yury, 197  
 Yau, Peter, 954  
 Yavuzoglu, Asuman, 308  
 Yee, Stephanie, 365, 865  
 Yeo, Nam-Kyung, 702  
 Yeo, Seung Geun, 237, 359  
 Yi, Eunyoung, 198, 220, 513, 616  
 Yi, Jenny, 786  
 Yin, Pingbo, 893, 907  
 Yin, Shankai, 697  
 Yin, Tom, 879  
 Ying, Yu-Lan Mary, 264  
 Yokoi, Hidenori, 393  
 Yokoi, Naoko, 393  
 Yoo, Lawrence, 245  
 Yoon, Yong-Jin, 631  
 Youn, Myung-Ja, 701  
 Young, Eric, 826, 827  
 Yu, Dongzhen, 154, 158, 733, 743  
 Yu, Heping, 45  
 Yu, Ning, 135  
 Yu, Yiling, 667  
 Yu, Yufei, 722  
 Yu, Zhiping, 150  
 Yu, Zu-Lin, 531  
 Yuan, Kexin, 354  
 Yuhas, Ward, 210  
 Zahorik, Pavel, 867  
 Zald, Philip, 585  
 Zallocchi, Marisa, 37, 46, 50  
 Zampini, Valeria, 199  
 Zander, Kaitlin, 751  
 Zapala, David, 248  
 Zenczak, Colleen, 365, 865  
 Zeng, Chunhua, 300  
 Zeng, Fan-Gang, 285, 287, 385, 416, 971, 980  
 Zenner, Hans-Peter, 685  
 Zettel, Martha, 648  
 Zhang, Fawen, 973  
 Zhang, Hui, 124  
 Zhang, Huiming, 326  
 Zhang, Jinsheng, 830  
 Zhang, Min, 324  
 Zhang, Ming, 525  
 Zhang, Xuedong, 181  
 Zhang, Ya, 697  
 Zhang, Yuxuan, 461  
 Zhao, Hong-Bo, 135, 603  
 Zhao, Xing, 764, 765  
 Zhao, Yanjun, 320  
 Zheng, Gui-Liang, 704, 705  
 Zheng, Jiefu, 502, 591, 684  
 Zheng, Jing, 141, 142, 650, 663, 664, 667  
 Zheng, Lili, 90, 650, 651, 756, 1005  
 Zheng, Qing, 36, 45, 47

Zheng, Yi, 333  
Zhou, Albert, 824  
Zhou, Dan, 437, 763, 953  
Zhou, Guangwei, 255  
Zhou, Jianxun, 300  
Zhou, Ning, 423, 981  
Zhou, Yide, 157, 301  
Zhu, Mei, 494  
Zhu, Xiaoxia, 360, 361, 648  
Zimmermann, Ulrike, 258, 485  
Zine, Azel, 565  
Zoghbi, Huda, 449  
Zosuls, Aleks, 532  
Zou, Jing, 697  
Zuo, Jian, 141, 142, 485, 659,  
667, 676  
Zupancic, Steven, 525  
Zurek, Patrick, 866